

DEVELOPMENT OF NICKEL-CATALYZED ASYMMETRIC  
CROSS-COUPLING REACTIONS

Thesis by  
Travis Jon DeLano

In Partial Fulfillment of the Requirements  
for the Degree of  
Doctor of Philosophy

CALIFORNIA INSTITUTE OF TECHNOLOGY  
Pasadena, California

2022  
(Defended April 18<sup>th</sup>, 2022)

© 2022

Travis Jon DeLano

ORCID: 0000-0002-2052-611X

All Rights Reserved

*For Zippy*

## ACKNOWLEDGEMENTS

My graduate school experience has been filled with scientific growth, amazing colleagues, and many experiences that I will remember for years to come. When I began college, grad school was never in my plans. I am only here thanks to the many incredibly talented scientists and kind people I worked with while at Northeastern University who helped develop my skills and passion for research, eventually resulting in this thesis. I am thankful to Professor Michael Pollastri for allowing me to join his lab as a young undergraduate. Mike, along with Dr. Dana Klug and Dr. Lori Ferrins, taught me the fundamentals of practical organic chemistry and the importance of doing chemistry that matters; I truly do not know what my life would look like without them. While at Northeastern, I also had the pleasure of completing two six-month co-ops at companies in the Boston area. I would like to thank Rachel Gershman and all my coworkers at Millennium Pharmaceuticals for teaching me so much and fostering a welcoming environment. My second co-op experience, at Vertex Pharmaceuticals, was the highlight of my career to date, in large part due to my wonderful manager Mike Boyd and all my coworkers on the chemistry team, including Simon Giroux, Nathan Waal, and Philip Collier. My time at Vertex sparked my interest in methodology development for my graduate studies, and I am very excited to return next month.

One of the highlights of my time at Caltech is the incredible scientists I have had the pleasure of working with. I would like to thank my advisor, Professor Sarah Reisman for giving me the opportunity to join her laboratory. Sarah has helped me become a better scientist and has assembled such a skilled and passionate team of chemists in her lab. I'm especially thankful for Sarah's support in encouraging me to venture into a new area of

research for our lab, electrochemistry, when I was a first-year graduate student. Sarah's scientific ideas, skill at writing, and aesthetic eye for figure-making will have a lasting impact on my work. I look forward to following all the new directions of her group after I've left.

I would also like to thank the other members of my committee, Professors Max Robb, Kim See, and Brian Stoltz. I've had the pleasure of taking classes taught by each of them and was uniformly impressed with their passion and compassion. As committee members, I'm grateful for their questions and insight, as well as their prompt replies to my (many) scheduling emails. I've also enjoyed interacting with their groups, whether through assistance analyzing polymers that I (accidentally) made, involvement in the Center for Synthetic Organic Electrochemistry, or our Monday night joint group meetings with the Stoltz lab.

I would like to thank the many amazing collaborators I've had the opportunity to work with over the past five years. My research on the  $\alpha$ -chloroester project would not have been possible without the pioneering work of Dr. Kelsey Poremba and Dr. Leah Cleary. I was lucky to later be joined on the project by both Sara Dibrell and Dr. Caitlin Lacker, who helped immensely with ideas and completion of the project. This project also allowed us to collaborate with Prof. Matt Sigman and a talented graduate student in his lab, Adam Pancoast, who was a delight to work with and continued to answer my questions and run calculations for me long after the project was over. I also had the opportunity to collaborate again with my friend Dr. Caitlin Lacker and several talented and thoughtful researchers at Merck, Dr. Tiffany Piou, Kevin Belyk, and Dr. Jongrock Kong, on an

interesting Ni/photoredox project. This has been a great group of people to work with, and I think we've discovered some compelling chemistry together.

Whether I've directly worked on projects with them or not, I have thoroughly enjoyed collaborating with every member of Team Nickel that I have overlapped with: Dr. Julie Hofstra, Dr. Kelsey Poremba, Dr. Chris Lavoie, Dr. Marco Brandstätter, Dr. David Hill, Dr. David Charboneau, Dr. Caitlin Lacker, Alex Shimosono, Sara Dibrell, Ray Turro, Jaron Tong, Emily Chen, Daniel Chang, Cedric Lozano, Ángel Hernández-Mejías, Ciara Ordner, and Dana Gephart. I'm consistently impressed by the knowledge and ideas that everyone brings to the team, and especially grateful for how much time everyone spends thinking about other peoples' projects. In particular, I have had countless conversations with Julie, Ray, Alex, and Emily about nickel and more, both as colleagues and friends.

One of the most unexpected and rewarding collaborative research experiences of my time at Caltech was my involvement with our CMS 273 team, Dr. Mike Maser, Dr. Serim Ryou, and Alex Cui. Coming into the course with no background in machine learning, I learned so much from all of them and was delighted that we continued to collaborate long after the end of the course. I still look back fondly on our weekly team meetings and am very proud of the research we conducted. I'd also like to thank Professors Yisong Yue and Pietro Perona for their helpful ideas and input on our ML research.

None of my research at Caltech would have been possible without the incredible instrumentation facilities and support staff in our division. I would like to thank Dr. Scott Virgil for keeping all the instrumentation in the Catalysis Center in excellent condition, and for being great to TA for. Additionally, Scott and Silva's annual holiday parties will be some of my fondest memories from my time at Caltech. I would like to thank Dr. Dave

VanderVelde and Dr. Mona Shahgholi for running the NMR and mass spectrometry facilities, and especially for keeping everything running smoothly during pandemic disruptions. I would also like to thank Joe Drew and Alison Ross for everything they do for CCE, as well as Armando Villasenor and Gregory Rolette for making sure all our packages get to us. Additionally, I would like to thank Jeff Hitchcock at M. Braun; for much of my Ph.D., I was one of the people in charge of our group glovebox, and I truly could not have navigated many of the glovebox emergencies without the patient help of Jeff.

All of us on the 3<sup>rd</sup> floor of Schlinger have been fortunate to have such dedicated people working to support us over my time at Caltech. Our administrative assistants, Beth Marshall, Veronica Triay, and Lynne Martinez have all been very helpful in scheduling meetings, booking rooms, and keeping everything running smoothly. I would also like to express my appreciation to Leslie and Tony for helping to keep our lab clean, keeping up with all the trash we generate, and being lovely people to chat with.

I feel lucky to have overlapped with so many wonderful people and chemists in the Reisman group. My entering class, Karli Holman, Alex Shimozone, and Dr. Mike Maser are some of the best people and most inquisitive scientists I've had the pleasure of working with. I'll always remember late nights in the lab with Alex listening to Soulja Boy and all our great times living together on Cordova. I'm consistently impressed with his generosity and perseverance. Mike and I worked next to each other for our first few years of grad school, and I had the privilege to collaborate with him as he transitioned towards machine learning as his primary research focus. Mike has been a great friend and colleague, and he has definitely been missed in the lab since he graduated.

I would like to thank Drs. Julie Hofstra, Denise Grünenfelder, and Nick Cowper for being so welcoming and helpful during my first year in the Reisman lab. I always felt that I could ask them for help with anything, big or small. I would especially like to thank Julie for teaching me everything I needed to know to get my first project up and running and being such a patient and inspiring mentor and good friend.

The class above me have served as great role models, both as chemists and people. Their experience and wisdom were always so helpful when going through candidacy and the other hurdles of grad school. I want to thank Dr. Caitlin Lacker for her unending patience when four first-year grad students all got placed in her bay. I feel so fortunate to have collaborated on several projects with her and I have thoroughly enjoyed our friendship. Dr. Skyler Mendoza is one of the most social and welcoming people I've met; it was a pleasure to work with him, and I especially enjoyed hanging out with him at our group socials and camping trips. Nick Fastuca has been a great friend and bay-mate; I have many fond memories of cookouts at his house, beach parties, and adventures enjoying good beer. Importantly, I'll so fondly remember ice skating with everyone in this class at Lunch Bunch.

In my second year of grad school, we were joined by a wonderful group of new students who have consistently impressed me and become some of my closest friends. Jeff Kerkovius is an exceedingly creative chemist who conducts reactions on vastly larger scale than I've ever attempted. I will miss his unending puns and hospitality after I leave Caltech. Yujia Tao is one of the funniest people I've worked with and can get more reactions and information out of a single milligram of material than anyone I know. Sara Dibrell is such a passionate chemist who makes the nicest slides and figures, and is one of the best writers



I've ever had the pleasure of working with. Ray Turro impresses me so much with his creativity, dedication, and kindness. I feel so fortunate to have met and interacted with all of them and hope to remain friends long after I leave. It has also been a pleasure to work with Jaron Tong, Andrea Stegner, Jordan Thompson, Cedric Lozano, Emily Chen, and Ángel Hernández-Mejías. They've all been delightful additions to our group and their futures are so bright.

Outside of lab, I am fortunate to have many amazing friends who have helped me through the hardest parts of grad school and helped me celebrate the successes along the way. I am so grateful for my friendship with Rachael Heiss and am so lucky that she moved out to California from Boston when I was in my first year. Rachael is such a kind, funny, fun, and thoughtful presence in my life and my first year of grad school wouldn't have been the same without frequent trips out to Manhattan Beach to visit her, TJ Parekh, Daniel Blake, and Sequoia. Being able to disconnect from Caltech and enjoy their company and the beach was much needed. In more recent years, dining and hanging out with Rachael and Daniel Garza have been a highlight for Karli and me. I would also like to thank my wonderful roommates from grad school, Ethan Williams, Alex Shimosono, Sarah Bevilacqua, Ailiena Maggiolo, Alex Phillips, and Karli Holman. I particularly loved my time living in the blue house on Cordova and celebrating Halloween with door decorations.

My family has served as such a wonderful source of support, love, and humor for my entire life, and I am so grateful for them. I've enjoyed all my phone calls home to my parents while I've been at Caltech, and I'm thrilled that they were able to come visit Pasadena to celebrate Thanksgiving several times. My brother Nate has long been a role model of mine and it has been so nice to keep in touch about our lives and our science

while playing Xbox together over the last few years. There are so many people from before my time in graduate school who I would like to thank for their friendship and positive impact on my life, including Amy and Sean Buckley, my college roommates Rachael Heiss, Rose Leopold, Dan Russotto, Eric Holland, Alex Kavourias, Liam Quinn, and Tyson, and my colleagues at David's 388, Bo Byrne, Carlos Tirado, and Dylan Leddy.

Most importantly, I would like to thank my partner Karli Holman. I certainly did not enter grad school intending to fall in love with my lab mate, but I couldn't be more lucky or happy that I did. Karli is the best person I have met, and I would absolutely not have made it through grad school without her by my side. She is infinitely kind, funny, loving, empathetic, witty, and smart. I am so grateful to have spent nearly every day of the last several years with her. We've shared so many memorable times, including 16 oz. cold brews at the turtle pond, going to concerts, camping in Big Sur, and our trip to Thailand. One of the greatest pleasures of my life is that we had the privilege to love our incredible dog Zippy together. Although she passed away far too soon, Zippy was the sweetest, cuddliest, most perfect dog I have ever known; she taught me so much and was such a brindle baby. She brought out the best in everyone she knew and is dearly missed. Karli is the best, most selfless dog mom, and I will always be grateful that we got to take care of Zippy, and our foster dog Daisy, together. We've had some amazing times over the last few years, and I am beyond excited to begin the next chapter of our life together in Boston.

## ABSTRACT

Asymmetric cross-coupling reactions have emerged in recent decades as powerful tools for the formation of valuable carbon–carbon bonds in the synthesis of enantioenriched small molecules. Nickel catalysis in particular has proven to be an especially powerful tool for the formation of C(sp<sup>2</sup>)–C(sp<sup>3</sup>) bonds in part due to the propensity of nickel catalysts to access odd oxidation states and interact with radical intermediates. Application of asymmetric nickel catalysis to a variety of radical precursors has resulted in the development of a broad range of stereoconvergent reductive and redox-neutral cross coupling reactions, allowing for the highly enantioselective formation of many synthetically useful and biologically relevant molecules.

Herein we describe our recent efforts in the development of new nickel-catalyzed enantioselective cross-coupling reactions. First, an enantioselective reductive cross-coupling of alkenyl and benzyl halides was rendered electroreductive. Careful electrochemical cell design proved critical for this reaction, which represents the first report of an enantioselective nickel-catalyzed electroreductive cross coupling reaction. We next discuss our development of an enantioselective reductive cross coupling of  $\alpha$ -chloroesters with aryl iodides. This reaction proceeds with especially high ee when  $\beta$ -branched substrates are employed, prompting the development of a multivariate linear regression model to probe the origin of the observed enantioselectivity trends. Finally, a redox-neutral nickel/photoredox co-catalyzed coupling of  $\alpha$ -*N*-heterocyclic potassium alkyl trifluoroborates and aryl bromides is reported. This reaction, developed in collaboration with researchers at Merck, provides rapid enantioselective access to motifs commonly found in bioactive molecules.

## PUBLISHED CONTENT AND CONTRIBUTIONS

Portions of the work described herein were disclosed in the following communications:

DeLano, T. J.; Reisman, S. E. *ACS Catal.* **2019**, *9*, 6751–6754.

DOI: 10.1021/acscatal.9b01785. Copyright © 2019 American Chemical Society

T.J.D. conducted all reaction development and screening, compilation of data, evaluation of substrates, and characterization of products. T.J.D. contributed to the conception of the project and preparation of the manuscript.

DeLano, T. J.; Dibrell, S. E.; Lacker, C. R.; Pancoast, A. R.; Poremba, K. E.; Cleary, L.;

Sigman, M. S.; Reisman, S. E. *Chem. Sci.* **2021**, *12*, 7758–7762.

DOI: 10.1039/D1SC00822F. Copyright © 2021 Royal Society of Chemistry

T.J.D. contributed to reaction screening, preparation and evaluation of substrates, compilation of data, characterization of products, and preparation of the manuscript.

**TABLE OF CONTENTS**

<b>CHAPTER 1</b>	<b>1</b>
Enantioselective Electroreductive Cross-Coupling of Alkenyl and Benzyl Halides via Nickel Catalysis	
1.1 INTRODUCTION .....	1
1.1.1 Motivation.....	1
1.1.2 Early Nickel-Catalyzed Electroreductive Couplings.....	2
1.1.3 Modern Nickel-Catalyzed Electroreductive Cross-Couplings.....	11
1.2 DEVELOPMENT OF AN ASYMMETRIC NICKEL-CATALYZED ELECTROREDUCTIVE CROSS-COUPPLING.....	14
1.2.1 Initial Considerations and Cell Design .....	14
1.2.2 Reaction Optimization .....	17
1.2.3 Reaction Scope.....	23
1.2.4 Preliminary Kinetic Studies .....	26
1.2.5 Attempts to Expand Reactivity .....	38
1.3 CONCLUDING REMARKS.....	43
1.4 EXPERIMENTAL SECTION .....	43
1.4.1 Materials and Methods.....	43
1.4.2 Construction of Electrochemical Cell for 0.6 mm Scale Reactions.....	45
1.4.3 Construction of Electrochemical Cell for 6.0 mm Scale Reactions.....	47
1.4.4 Substrate Preparation .....	49

	xiv
1.4.5 Electroreductive Cross-Couplings .....	53
1.4.6 Characterization of Reaction Products.....	57
1.4.7 SFC Traces of Racemic and Enantioenriched Products .....	80
1.5 NOTES AND REFERENCES .....	104
<b>APPENDIX 1</b>	<b>112</b>
Spectra Relevant to Chapter 1	
<b>CHAPTER 2</b>	<b>165</b>
Nickel-Catalyzed Asymmetric Reductive Cross-Coupling of $\alpha$ -Chloroesters with Aryl Iodides	
2.1 INTRODUCTION .....	165
2.2 REACTION OPTIMIZATION.....	167
2.3 REACTION SCOPE.....	170
2.3.1 Scope of Aryl Iodides .....	170
2.3.2 Scope of $\alpha$ -Chloroesters.....	172
2.4 MULTIVARIATE LINEAR REGRESSION MODELING.....	177
2.4.1 Introduction.....	177
2.4.2 Dataset Generation.....	177
2.4.3 Conformational Optimization and Parameter Acquisition .....	178
2.4.4 Multivariate Correlation Analysis.....	180
2.5 MECHANISTIC STUDIES.....	182
2.5.1 Introduction.....	182
2.5.2 Manganese Enolate Studies .....	184

2.5.3 Radical Trapping Experiments .....	185
2.5.4 Stoichiometric Studies .....	187
2.6 CONCLUDING REMARKS.....	187
2.7 EXPERIMENTAL SECTION.....	188
2.7.1 Materials and Methods.....	188
2.7.2 Substrate Preparation .....	189
2.7.3 General Procedure for Reductive Cross-Coupling .....	206
2.7.4 Characterization of Reaction Products.....	207
2.7.5 Mechanistic Experiments.....	232
2.7.6 Dataset Generation for Statistical Modeling.....	238
2.7.7 Computational Methods.....	239
2.7.8 SFC Traces of Racemic and Enantioenriched Products .....	242
2.8 NOTES AND REFERENCES.....	272
 <b>APPENDIX 2</b> .....	<b>277</b>
Cartesian Coordinates of Substrate and Ligand Conformers	
 <b>APPENDIX 3</b> .....	<b>359</b>
Spectra Relevant to Chapter 2	
 <b>CHAPTER 3</b> .....	<b>432</b>
Enantioselective Synthesis of <i>N</i> -Benzylic Heterocycles by Nickel/Photoredox Dual Catalysis	
3.1 INTRODUCTION .....	432

3.2 REACTION OPTIMIZATION.....	436
3.3 REACTION SCOPE.....	442
3.4 PRELIMINARY MECHANISTIC EXPERIMENTS .....	449
3.5 CONCLUDING REMARKS.....	455
3.6 EXPERIMENTAL SECTION .....	455
3.6.1 Materials and Methods.....	455
3.6.2 Ligand Preparation.....	457
3.6.3 Optimization of Reaction Parameters .....	457
3.6.4 Substrate Preparation .....	463
3.6.5 Enantioselective Cross-Coupling.....	470
3.6.6 Characterization of Reaction Products.....	471
3.6.7 SFC Traces of Racemic and Enantioenriched Products .....	502
3.7 NOTES AND REFERENCES.....	531
 <b>APPENDIX 4</b>	<b>535</b>
Spectra Relevant to Chapter 3	
 <b>ABOUT THE AUTHOR</b>	<b>619</b>



**LIST OF ABBREVIATIONS**

$[\alpha]_D$	angle of optical rotation of plane-polarized light
Å	angstrom(s)
Ar	aryl or argon
atm	atmosphere(s)
BiIM	biimidazole
BiOX	bioxazoline
Bn	benzyl
Bn <sub>2</sub> O	dibenzyl ether
Boc	<i>tert</i> -butoxycarbonyl
bpy	2,2'-bipyridine
Bz	benzoate
<sup>13</sup> C	carbon-13 isotope
°C	degrees Celsius
C <sub>6</sub> H <sub>6</sub>	benzene
calc'd	calculated
CH <sub>2</sub> Cl <sub>2</sub>	dichloromethane
<i>cis</i>	on the same side
cm <sup>-1</sup>	wavenumber(s)
conv.	Conversion
Cy	cyclohexyl
CyanoBOX	cyanobis(oxazoline)

$\delta$	chemical shift in ppm
d	doublet
<i>d</i>	deutero
D	deuterium
DEMS	diethoxymethylsilane
diglyme	diethylene glycol dimethyl ether
dme	dimethoxyethane
DMF	<i>N,N</i> -dimethylformamide
DMPU	<i>N,N</i> -dimethylpropyleneurea
DMSO	dimethyl sulfoxide
dppe	1,2-bis(diphenylphosphino)ethane
dr	diastereomeric ratio
D'BAD	di- <i>tert</i> -butyl azodicarboxylate
dtbbpy	4,4'-di- <i>tert</i> -butyl-2-2'-dipyridyl
<i>ee</i>	enantiomeric excess
<i>E</i>	<i>trans</i> (entgegen) olefin geometry
EDG	electron-donating group
EI	electron impact
equiv	equivalent(s)
ESI	electrospray ionization
Et	ethyl
Et <sub>3</sub> N	triethylamine
EtOAc	ethyl acetate

EtOH	ethanol
EWG	electron-withdrawing group
FAB	fast atom bombardment
FTIR	Fourier transform infrared spectroscopy
g	gram(s)
GC	gas chromatography
h	hour(s)
$^1\text{H}$	proton
$h\nu$	irradiation with light
HFIP	1,1,1,3,3,3-hexafluoro-2-propanol
HMPA	hexamethylphosphoramide
HMPT	tris(dimethylamino)phosphine
HRMS	high resolution mass spectrometry
Hz	hertz
I	current
<i>in situ</i>	in the reaction mixture
$^i\text{Pr}$	<i>iso</i> -propyl
<i>iso</i>	isomeric
$J$	coupling constant in Hz
kcal	kilocalorie(s)
L	liter or ligand
m	multiplet or meter(s)
M	molar or molecular ion

<i>m</i>	<i>meta</i>
μ	micro
MeCN	acetonitrile
MeNO <sub>2</sub>	nitromethane
2-MeTHF	2-methyl tetrahydrofuran
mg	milligram(s)
MHz	megahertz
min	minute(s)
mL	milliliter(s)
MLR	multivariate linear regression
mol	mole(s)
<i>m/z</i>	mass-to-charge ratio
N	normality
ND	not determined
nm	nanometer(s)
NMR	nuclear magnetic resonance
NSAID	non-steroidal anti-inflammatory drug
<i>o</i>	<i>ortho</i>
<i>p</i>	<i>para</i>
PC	propylene carbonate
Ph	phenyl
pH	hydrogen ion concentration in aqueous solution
PhBr	bromobenzene

PhCl	chlorobenzene
PhH	benzene
PhI	iodobenzene
PhMe	toluene
Pin	pinacol
PITU	<i>N</i> -hydroxyphthalimide tetramethyluronium hexafluorophosphate
PPh <sub>3</sub>	triphenylphosphine
ppm	parts per million
psi	pounds per square inch
Py	pyridine
PyOX	pyridine-oxazoline
q	quartet
Q	charge passed
R	generic (alkyl) group
<i>R</i>	rectus
<i>R<sub>f</sub></i>	retention factor
rt	room temperature
RVC	reticulated vitreous carbon
s	singlet or seconds
<i>S</i>	sinister
sat.	saturated
SET	single electron transfer
SFC	supercritical fluid chromatography

SS	stainless steel
t	triplet
TBAI	tetra- <i>n</i> -butylammonium iodide
TBAPF <sub>6</sub>	tetra- <i>n</i> -butylammonium hexafluorophosphate
TBME	<i>tert</i> -butyl methyl ether
TDAE	tetrakis(dimethylamino)ethylene
temp	temperature
TEMPO	2,2,6,6-tetramethylpiperidine 1-oxyl
TFA	trifluoroacetic acid
TFSI	bis(trifluoromethane)sulfonimide
THF	tetrahydrofuran
THP	tetrahydropyran
TLC	thin layer chromatography
TMS	trimethylsilyl
TOF	time-of-flight
<i>trans</i>	on the opposite side
UV	ultraviolet
<i>vide infra</i>	see below
VTNA	variable time normalization analysis
Z	<i>cis</i> (zusammen) olefin geometry

## ***Chapter 1***

### *Enantioselective Electroreductive Cross-Coupling of Alkenyl and Benzyl*

### *Halides via Nickel Catalysis<sup>†</sup>*

## **1.1 INTRODUCTION**

### **1.1.1 Motivation**

Over the past decade, the Reisman group has developed a number of nickel-catalyzed enantioselective reductive cross-coupling reactions.<sup>2</sup> In the course of developing reductive cross-couplings, our group and others have observed several challenges presented by the use of superstoichiometric metal powder reductants. The heterogeneous nature of these reactions can complicate mechanistic experiments, and precise control of

---

<sup>†</sup> Portions of this chapter have been reproduced from published studies and the supporting information found therein.<sup>1</sup> Fellowship support was provided by the National Science Foundation (Graduate Research Fellowship, T.J.D., Grant No. DGE-1144469). Financial support from the NIH (R35GM118191-01) is gratefully acknowledge. Portions of this work were supported by the National Science Foundation Center for Synthetic Organic Electrochemistry (CHE-2002158).

vial and stir bar size have proven critical for effective stirring and reproducibility.<sup>2,3</sup> Substantial variabilities in reaction yield, conversion, enantioselectivity, and reproducibility were observed depending on the vendor, batch, mesh size, storage conditions, and activation method of the metal powder. Additionally, these reactions produced significant amounts of metal waste, which could hinder their adoption in industrial settings.<sup>4</sup> Alternative strategies for reductive catalyst turnover could improve the utility of these reactions and enable mechanistic experiments that could facilitate the development of additional reductive cross-coupling methodologies.

Several approaches have been explored for conducting nickel-catalyzed reductive cross-couplings without superstoichiometric metal powder reductants. Our group and others have employed tetrakis(dimethylamino)ethylene (TDAE) and related reagents as soluble reductants for the coupling of C(sp<sup>2</sup>) and C(sp<sup>3</sup>) electrophiles.<sup>3,5,6</sup> The Gong group has reported the use of B<sub>2</sub>pin<sub>2</sub> as a soluble reductant for the coupling of unactivated primary and secondary alkyl bromides, providing evidence suggesting that the reactions do not proceed through in situ-generated organoboron species.<sup>7</sup> Metallaphotoredox approaches employing Ir photocatalysts have been reported by MacMillan, Lei, and Vannucci, employing (TMS)<sub>3</sub>SiH, Et<sub>3</sub>N, and triethanolamine as soluble terminal reductants, respectively.<sup>8-11</sup> After publication of the work reported herein, Walsh and Mao reported an enantioselective Ni/Ir cross coupling employing Hantzsch ester as an organic reductant.<sup>12</sup>

### **1.1.2 Early Nickel-Catalyzed Electroreductive Couplings**

Electrochemical catalyst turnover has also been harnessed to effect nickel-catalyzed reductive cross-couplings in the absence of metal powders. Electrochemical



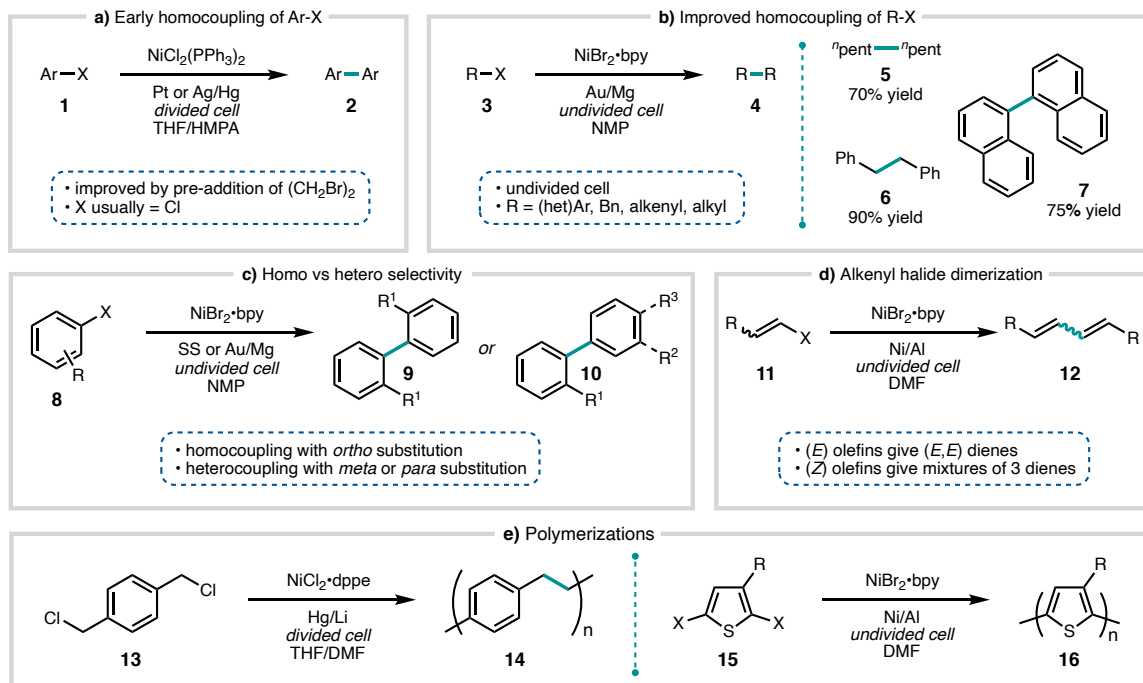
approaches are especially attractive because they are inherently efficient, allow for precise control over the desired reduction, and can be readily scaled.<sup>13</sup> Seminal reports of electroreductive nickel-catalyzed cross-couplings came from the groups of Amatore, Durandetti, Jutand, Nédélec, and Périchon, beginning in the 1980s. These works, as well as the works of others, focused on four major challenges: 1) homocoupling of organic halides, 2) cross-coupling of organic halides, 3) addition of organic halides to unsaturated groups, and 4) carboxylation of organic molecules. These early efforts will be thoroughly outlined, followed by a discussion of recent advances in the field.

The homocoupling of organic halides was an especially attractive area for the early development of electroreductive nickel-catalyzed couplings because the challenge of cross-selectivity could be avoided. Initial reports utilized phosphine-ligated nickel complexes, which were electrolyzed in a divided cell before addition of the aryl halide (Figure 1.1a).<sup>14,15</sup> Interestingly, Périchon and coworkers observed that addition of alkyl bromides during the electrolysis significantly improved yields and reduced catalyst deactivation, presumably by reacting with a  $\text{Ar}_2\text{NiL}_2$  species. It was also found that the decomposition of  $\text{NiCl}_2$  to Ni metal or  $\text{Ni}(\text{OH})_2$  were the primary modes of catalyst death.<sup>16</sup>

Further development of this electroreductive homocoupling procedure allowed for a variety of organic halides to be effectively coupled in an undivided cell, using a gold mesh cathode and a sacrificial aluminum anode (Figure 1.1b).<sup>17</sup> A variety of substrates could be dimerized, including aryl and alkyl halides. Attempts to apply these conditions to cross-coupling were unsuccessful. When aryl halides with different reactivity were employed, such as PhI and *p*-Me-C<sub>6</sub>H<sub>4</sub>-Br, the more reactive PhI dimerized at early time

points, followed by aryl bromide dimerization at late time points. If similarly reactive aryl halides were employed, a statistical mixture of products was observed.<sup>17</sup> Further reports

**Figure 1.1** Early Ni-catalyzed electroreductive homocoupling of organic halides.



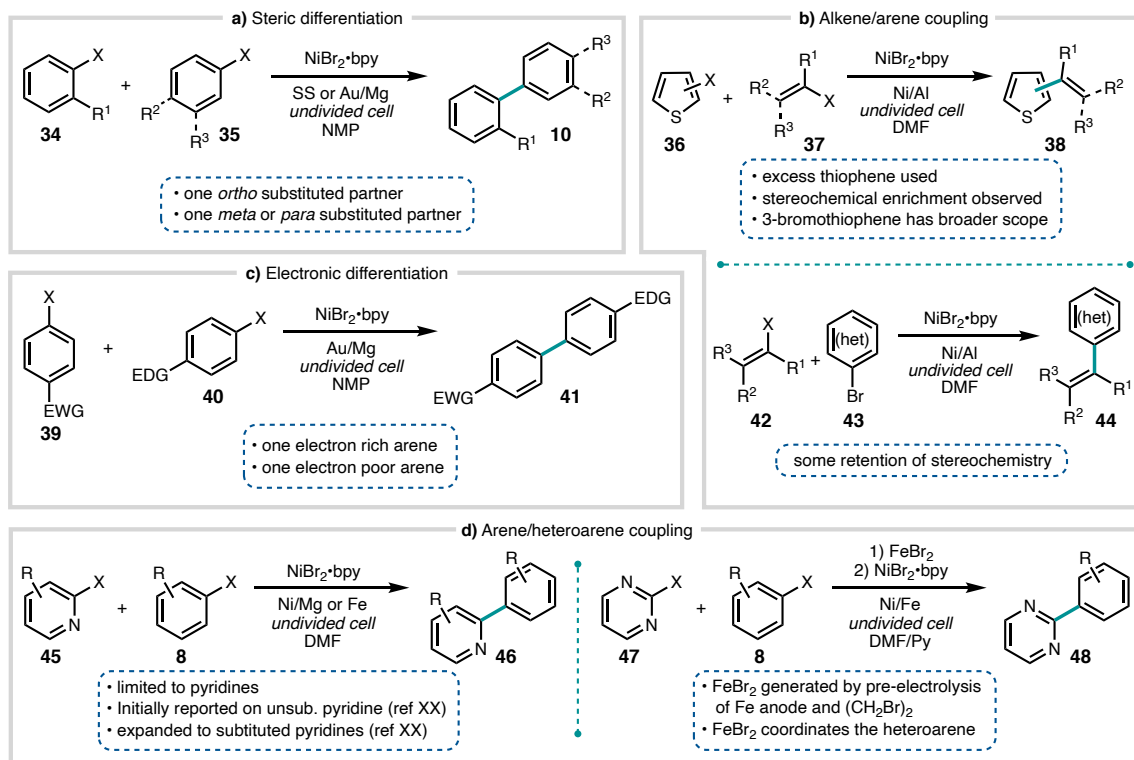
demonstrated that similar reactions could also be run with alcohols or water as solvent.<sup>18,19</sup>

With minor adjustments to reaction conditions, Jutand developed the electroreductive homocoupling of aryl triflates.<sup>20</sup> Périchon also demonstrated that for aryl halides, the substitution relative to the halide could determine whether homo- or cross-coupling was observed (Figure 1.1c).<sup>21</sup> A similar transformation could be conducted with alkenyl halides, at room temperature for bromides and iodides and elevated temperatures for chlorides. When (*E*) alkenyl halides were employed, the resulting (*E,E*) dienes were generally formed in good yields with excellent stereoselectivity. In contrast, when (*Z*) alkenyl halides were used, complex mixtures of (*Z,Z*), (*E,Z*), and (*E,E*) dienes were formed (Figure 1.1d). Preliminary studies could not determine the source of this divergence in

reactivity.<sup>22</sup> Dihalogenated compounds have been employed in a similar manner for electroreductive polymerizations (Figure 1.1e).<sup>23–25</sup> Elegant mechanistic studies from Amatore, Jutand, and Périchon variously implicate radical chain mechanisms as well as Ni<sup>0</sup>, Ni<sup>I</sup>, Ni<sup>II</sup>, and Ni<sup>III</sup> intermediates, through a variety of electrochemical and rate experiments.<sup>26–28</sup>

With well-established methods for homocoupling developed, the field moved towards the more formidable challenge of the electroreductive *cross*-coupling of organic halides. Though simply using an excess of one electrophile can provide good yields of the desired cross-coupled product, avoiding this excess is often desirable. Given the potential for mechanistic differentiation of the two electrophiles during their oxidative additions, many early electroreductive cross-coupling reactions employed one C(sp<sup>2</sup>) electrophile and one C(sp<sup>3</sup>) electrophile. An early report from Jutand, Fauvarque, and Périchon employed a significant excess of aryl halide coupled with an  $\alpha$ -halo ester to afford the  $\alpha$ -arylated esters in good yield, using either Hg or Au anodes (Figure 1.2a).<sup>29</sup> Shortly thereafter, an electroreductive coupling of acyl chlorides with activated halides was reported, giving  $\beta,\gamma$ -unsaturated ketones (Figure 1.2a).<sup>30</sup> This reaction performed best with a carbon cathode in acetonitrile, in contrast to the more commonly-used metal cathodes in amide solvents. Electroanalytical studies on a related system showed that oxidative addition of the generated Ni<sup>0</sup> complex to benzyl chloride was ~10 times faster than oxidative addition to the benzoyl chloride. The resulting Ni(II) complex was then proposed to be reduced to an anionic nickel(0) complex, which selectively reacts with the acyl electrophile via nucleophilic substitution.<sup>31</sup>



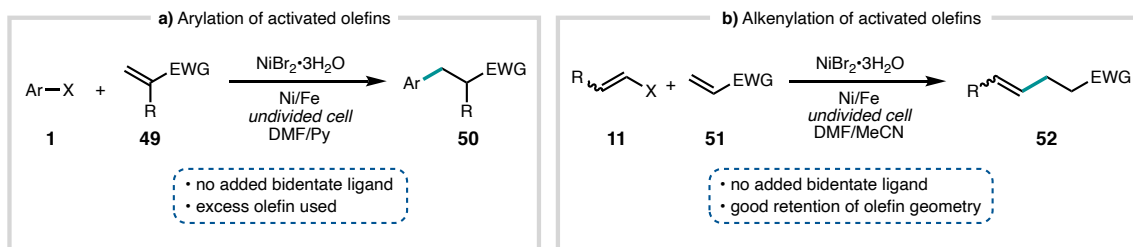
**Figure 1.3** Early Ni-catalyzed electroreductive  $C(sp^2)$ – $C(sp^2)$  cross-couplings.

While the difference in reactivity from hybridization of the  $C(sp^2)$  and  $C(sp^3)$  electrophiles can be harnessed for their cross-coupling, several pioneering groups in the field of nickel-catalyzed electroreductive cross-coupling tackled the perhaps more challenging problem of  $C(sp^2)$ – $C(sp^2)$  cross-electrophile coupling. Seminal work from Périchon leveraged steric differentiation of one *ortho*-substituted arene electrophile and one *meta*- or *para*-substituted coupling partner to afford good yields of cross-coupled biaryls (Figure 1.3a).<sup>21</sup> Electronic differentiation of the arenes has also been used to achieve cross selectivity, by employing one electron-rich and one electron-poor coupling partner (Figure 1.3c).<sup>38</sup> In related works, several alkenyl halides have been shown to couple effectively with heteroaryl halides, although some level of stereochemical scrambling was observed (Figure 1.3b).<sup>22,32,39</sup>

Electroreductive couplings of 2-halo pyridines with a variety of substituted aryl halides were developed, but were ineffective with pyrimidine or pyrazine coupling partners, presumably due to catalyst coordination and deactivation by the aryl halides (Figure 1.3d).<sup>40,41</sup> An ingenious solution to this problem was developed by Gosmini, Nédélec, and Périchon, in which an iron anode was first pre-electrolyzed in the presence of 1,2-dibromoethane to generate FeBr<sub>2</sub>. The coordination of FeBr<sub>2</sub> to the Lewis-basic heteroaryl halides allowed the nickel-catalyzed electroreductive couplings to proceed in good yields (Figure 1.3d).<sup>42</sup>

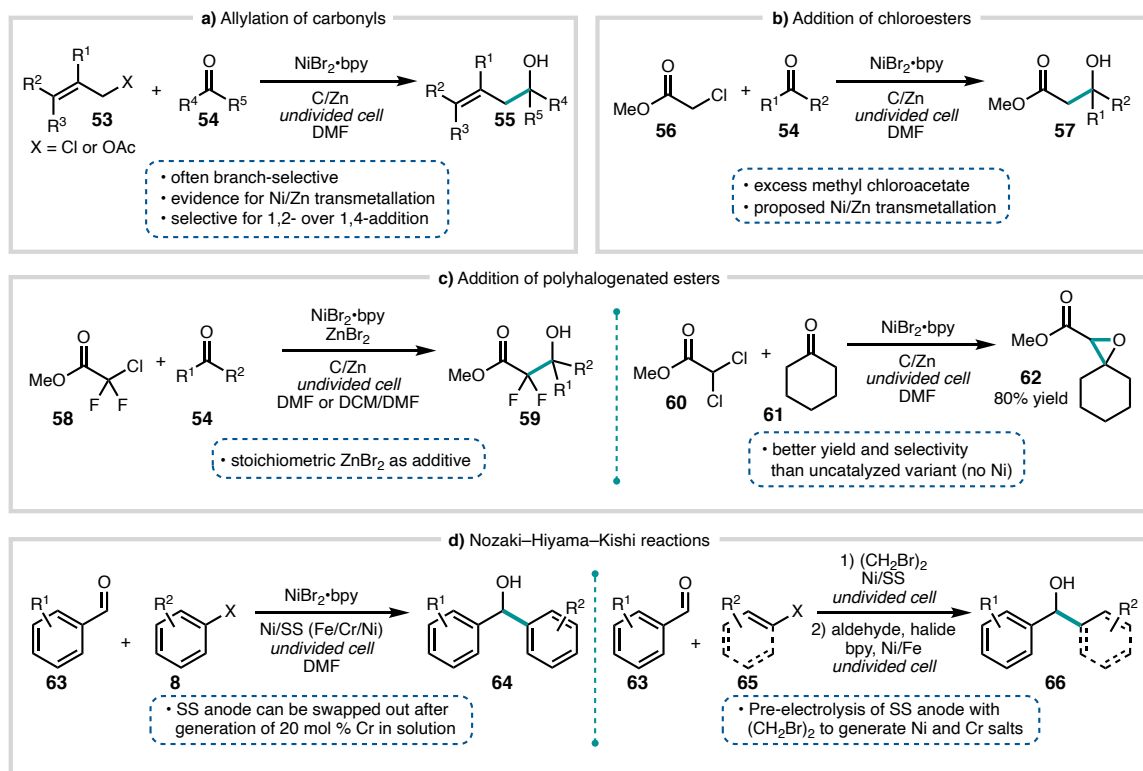
In addition to organic halides, other classes of electrophiles have also been employed in electroreductive nickel catalysis. Nédélec and Périchon showed that electroreductive 1,4-addition of aryl and alkenyl halides to electron-deficient olefins could be achieved (Figure 1.4).<sup>22,43,44</sup> In contrast to previously developed nickel-catalyzed electroreductive cross-coupling reactions, these 1,4-additions did not require the addition of a bidentate ligand to support nickel. No exogenous ligand was required for alkenylations; pyridine was used in arylations, presumably as a ligand. Although acrolein was not a competent coupling partner in this reaction, its diethyl acetal could be smoothly arylated then deprotected to afford the  $\beta$ -arylated aldehyde products.<sup>45</sup>

**Figure 1.4** Early Ni-catalyzed electroreductive couplings of halides with olefins.



Electroreductive nickel catalysis has also been employed for 1,2-addition of a variety of electrophiles to ketones and aldehydes. Allylic electrophiles can selectively undergo 1,2-addition, even to  $\alpha,\beta$ -unsaturated carbonyls (Figure 1.5a).<sup>46–48</sup> Evidence has been presented supporting a key transmetalation from Ni to Zn.  $\alpha$ -Chloro ester **56** has also been used in a similar manner (Figure 1.5b).<sup>46</sup> When methyl 2-chloro-2,2-difluoroacetate **58** was employed, a variety of difluorinated alcohols were formed in good yields (Figure 1.5c).<sup>49</sup> Interestingly, Périchon found that when dichloride **60** was reacted with cyclohexanone **61** under nickel-catalyzed electroreductive conditions, the resulting chlorohydrin cyclized in situ to form epoxide **62** in 80% yield (Figure 1.5c).<sup>46</sup> Electroreductive nickel- and chromium-catalyzed Nozaki–Hiyama–Kishi reactions have

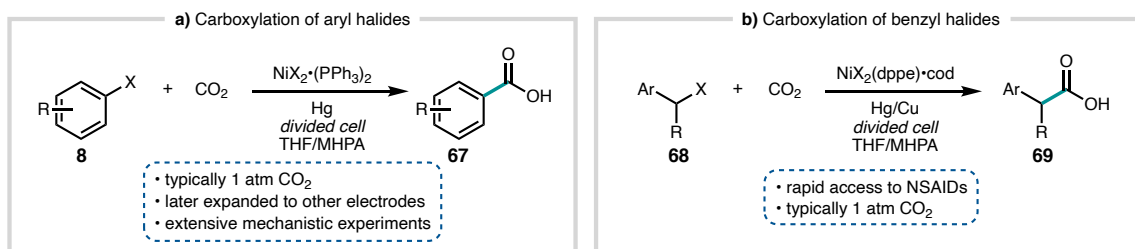
**Figure 1.5** Early Ni-catalyzed electroreductive couplings of halides with carbonyls.



also been developed by Durandetti, Nédélec, and Périchon, generally employing sacrificial chromium-containing stainless steel as the anode (Figure 1.5d).<sup>50,51</sup> Under these conditions, a variety of alkyl and alkenyl halides can be added into aldehydes, even when an iron anode is swapped out for the stainless steel part-way through the reaction.

Pioneering researchers in electroreductive nickel chemistry, in particular Amatore and Jutand, extensively explored the use of CO<sub>2</sub> as an electrophilic coupling partner to afford carboxylic acids. Aryl halides have been employed in divided cells to afford benzoic acid derivatives (Figure 1.6a).<sup>52,53</sup> When benzylic halides were employed as electrophiles in combination with CO<sub>2</sub>, NSAIDs were rapidly and directly formed (Figure 1.6b).<sup>54–57</sup> Interestingly, a variety of reactions at the anode have been coupled with this transformation. Sacrificial anodes can be oxidized, or an inert anode can oxidize either lithium oxalate or a metal powder reductant.<sup>58</sup>

**Figure 1.6** Early Ni-catalyzed electroreductive carboxylation of halides.

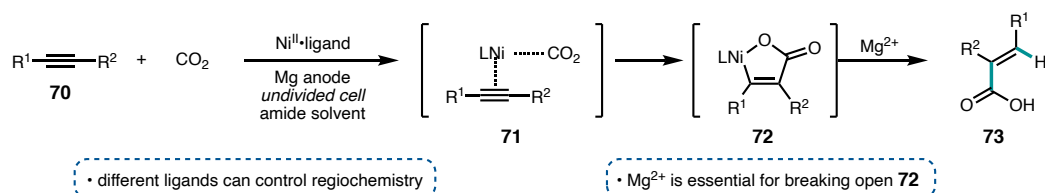


Carbon–carbon multiple bonds have also been employed as electrophiles in nickel-catalyzed electroreductive couplings with CO<sub>2</sub>. A seminal report from Duñach and Périchon described the selective hydrocarboxylation of terminal alkynes, proceeding through **72** (Figure 1.7a).<sup>59</sup> This reactivity has been extended to a variety of substituted alkynes, alkenes, and allenes.<sup>60–69</sup> In all cases, it was found that a magnesium anode was optimal, because Mg<sup>2+</sup> was required to open the cyclic intermediate **72** for catalyst



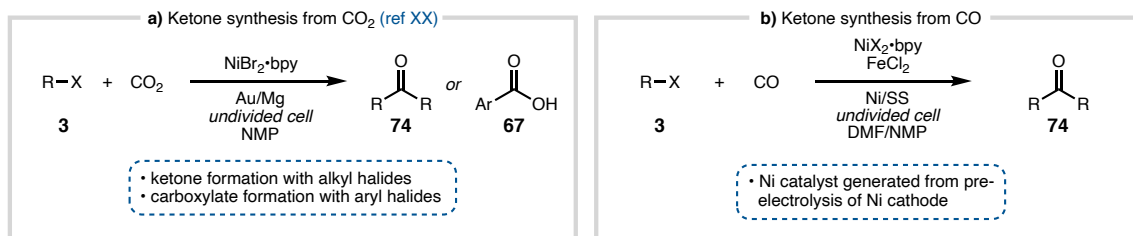
turnover.<sup>66</sup> In the case of disubstituted alkynes, the regioselectivity of the hydrocarboxylation has been controlled by the use of different ligands.<sup>60</sup>

**Figure 1.7** Ni-catalyzed electroreductive carboxylation of C–C multiple bonds.



Gases have been employed as electrophiles in nickel-catalyzed electroreductive couplings for the formation of ketones. Garnier, Rollin, and Périchon found that when alkyl halides were reacted with CO<sub>2</sub> in the presence of a Ni catalyst, symmetric ketones were formed (Figure 1.8a).<sup>70</sup> When aryl halides were employed under the same conditions, the major products were benzoic acid derivatives. Under similar conditions, it was found that carbon monoxide could be employed for the formation of symmetric ketones from both alkyl and aryl halides (Figure 1.8b).<sup>71–74</sup> Symmetric ketones could also be formed by employing stoichiometric metal carbonyl additives as CO sources.<sup>75</sup>

**Figure 1.8** Ni-catalyzed electroreductive ketone synthesis from CO and CO<sub>2</sub>.



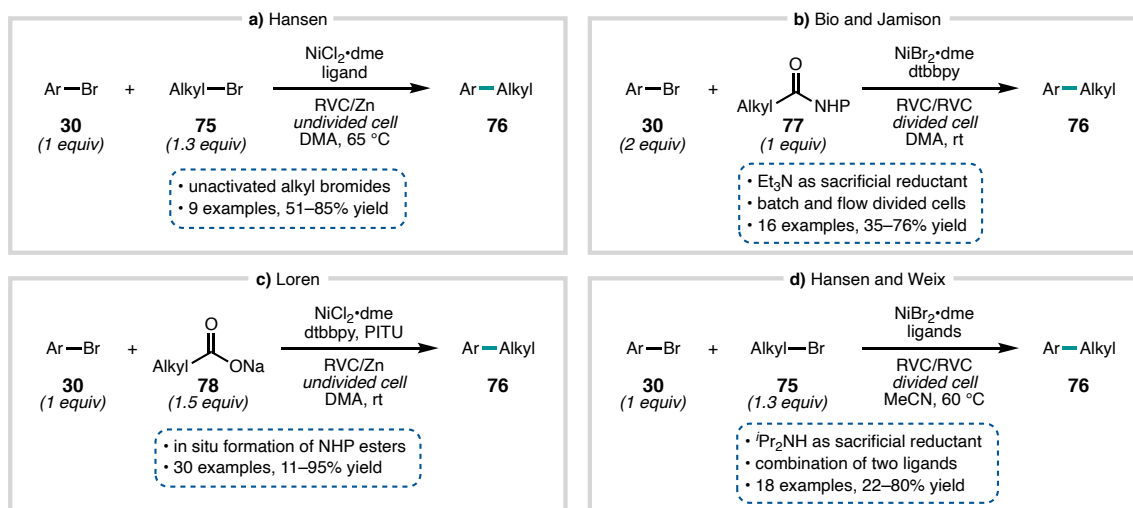
### 1.1.3 Modern Nickel-Catalyzed Electroreductive Cross-Couplings

All of the aforementioned pioneering studies on nickel-catalyzed electroreductive couplings laid a robust foundation for the development of more modern approaches. There

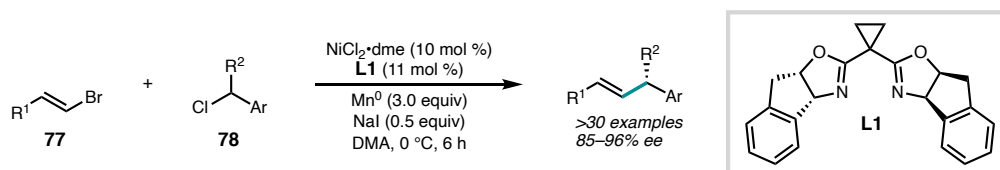
are several key areas of improvement that could be realized with respect to early reports. First, many of the cross-coupling reactions required slow addition of an excess of the more reactive electrophile. Second, many of the alkyl coupling reactions required activated alkyl halides. Third, many of these methodologies required expensive or unwieldy electrode materials, such as gold or mercury. Beginning in the 2010s, there has been renewed interest in the further development of nickel-catalyzed electroreductive cross-coupling reactions, with an emphasis on overcoming some of these key challenges. All these modern methods were enabled by the use of a relatively new electrode material, reticulated vitreous carbon foam (RVC). RVC has a very high surface area as well as remarkable resistance to chemical fouling and adsorption of reaction components.<sup>76</sup>

Using RVC as a cathode, Hansen and coworkers reported the electroreductive coupling of aryl bromides with unactivated alkyl bromides using a sacrificial zinc anode, affording coupled products in good yields (Figure 1.9a).<sup>77</sup> Bio and Jamison then reported the coupling of aryl bromides with alkyl *N*-hydroxyphthalimide (NHP) esters in both batch and flow, using two RVC electrodes and Et<sub>3</sub>N as a homogeneous sacrificial reductant (Figure 1.9b).<sup>78</sup> Loren extended this work by employing in situ-generated alkyl NHP esters from the corresponding sodium carboxylates using *N*-hydroxyphthalimide tetramethyluronium hexafluorophosphate (PITU) (Figure 1.9c).<sup>79</sup> Since the publication of our manuscript, Hansen and Weix reported a divided cell electroreductive coupling employing acetonitrile as solvent and <sup>i</sup>Pr<sub>2</sub>NH as reductant (Figure 1.9d).<sup>80</sup>

Nearly all of the nickel-catalyzed electroreductive cross coupling reactions reported to date employ an excess of one electrophile, and all afford exclusively achiral or racemic products, with the exception of a single diastereoselective method.<sup>36</sup> Given these

**Figure 1.9** Modern Ni-catalyzed electroreductive couplings.

limitations, we hoped to harness the utility of electrochemistry to develop the first asymmetric electrochemical reductive cross-coupling. Specifically, we hoped to translate our previously reported asymmetric coupling of benzylic chlorides and alkenyl bromides, using cyclopropyl indaBOX **L1**, into an electrochemical manifold (Figure 1.10).<sup>81</sup> We hypothesized that this could provide several key advantages to our chemistry, including expanded substrate scope, improved scalability, improved sustainability, and the mitigation of many of the difficulties encountered when using superstoichiometric metal powder reductants.

**Figure 1.10** Non-electrochemical asymmetric reductive coupling of alkenyl and benzyl electrophiles.

## 1.2 DEVELOPMENT OF AN ASYMMETRIC NICKEL-CATALYZED ELECTROREDUCTIVE CROSS-COUPLING

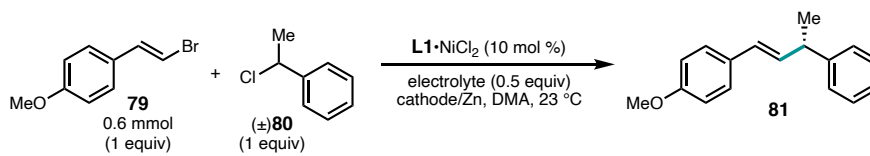
### 1.2.1 *Initial Considerations and Cell Design*

Optimization of an electrochemical reaction involves several key considerations that differ from optimizing a traditional reaction. First, an effective reaction cell must be designed. This begins with the choice of a divided or undivided cell, and requires the geometry, electrode spacing, and controls to keep reactions under inert conditions to be determined. Additionally, the electrode materials must be carefully chosen and optimized to ensure good performance. A suitable electrolyte must also be identified, and a solvent must be chosen that can fully solubilize all reaction components and allow for efficient charge transfer. Finally, the choice must be made to run reactions in a galvanostatic (constant current) or potentiostatic (constant voltage) mode, and the current or voltage of electrolysis must be selected.

Initial cell design and conditions for our asymmetric alkenylation were inspired by those reported by Hansen and coworkers.<sup>77</sup> This cell was constructed from a 3-necked flask, with a 0.25-inch Zn rod and 0.25-inch graphite rod serving as anode and cathode, respectively (Figure 1.11, 1<sup>st</sup> generation cell). The electrodes were inserted through 14/20 septa in the two outer necks of the cell, and the reaction was kept under argon while a current of 5 mA was passed between the electrodes for 12 h. Sodium iodide served as an important reaction additive in our initial report, and was able to also serve as a competent electrolyte in this context. Unfortunately, initial attempts using this cell design with alkenyl bromide **79** and benzyl chloride **80** only produced racemic **81** in 12% yield. (Table 1.1,

entry 1). Gratifyingly, exchanging the graphite cathode for a RVC cathode afforded **81** in 91% ee, albeit in only 2% yield after 12 h (Table 1.1, entry 2).

**Table 1.1** Initial optimization.



Entry	Cathode	Electrolyte	I/V <sup>a</sup>	Time (h)	% Yield <sup>b</sup>	% ee <sup>c</sup>
1	Graphite	Nal	5 mA	12	12	0
2	RVC	Nal	5 mA	12	2	91
3	RVC	TBAPF <sub>6</sub>	5 mA	12	35	72
4	RVC	TBAPF <sub>6</sub>	3.3 V	12	38	78
5	RVC	TBAI	3.3 V	12	40	89
6 <sup>d</sup>	RVC	TBAPF <sub>6</sub>	3.3 V	1	53	68

<sup>a</sup> Unreferenced. <sup>b</sup> Determined by <sup>1</sup>H NMR. <sup>c</sup> Determined by chiral SFC.

<sup>d</sup> Reaction run in vial-based cell (Figure 1.11, 2<sup>nd</sup> gen.)

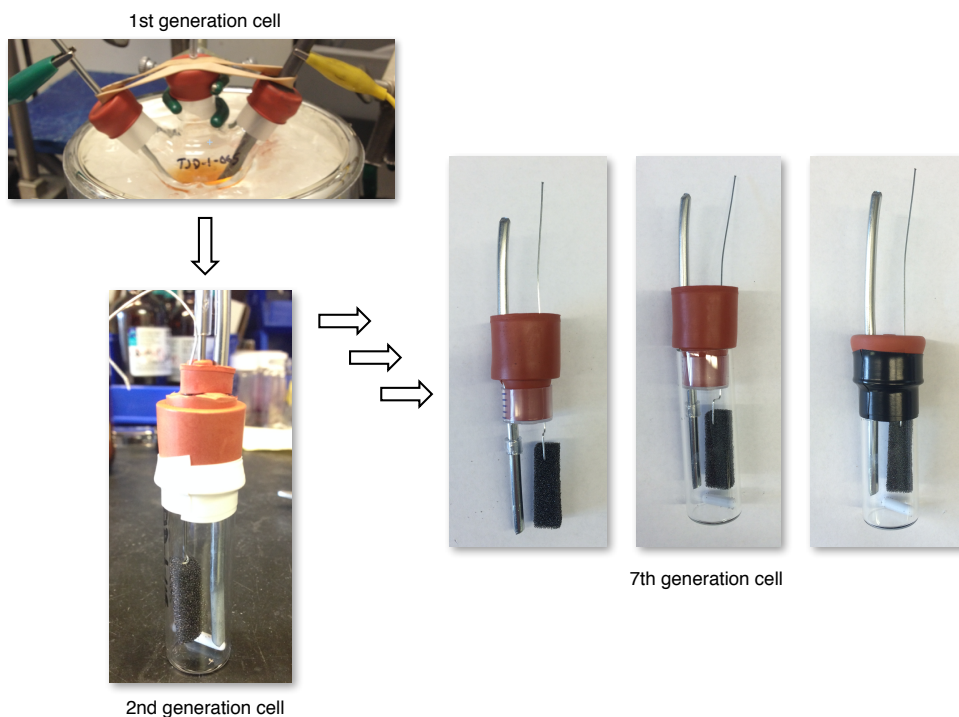
Having observed some level of productive asymmetric catalysis, we wondered if altering the electrolyte could perhaps improve the outcome of the reaction. In this three-necked cell, both tetrabutylammonium hexafluorophosphate (TBAPF<sub>6</sub>) and tetrabutylammonium iodide (TBAI) resulted in significantly better reaction conversion (entries 3–5). In an effort to potentially fine-tune reactivity later in optimization, the reaction setup was switched from galvanostatic to potentiostatic operation at this point.

The three-necked cell used for this portion of the reaction optimization presented several obstacles for efficient catalysis and reproducibility. The electrodes in this cell were only held in place by the rubber septa through which they were punctured. After the wires of the potentiostat were connected to the exposed portions of these electrodes, they exerted significant torque, making it difficult to keep the electrodes consistently placed and spaced within the cell. Additionally, the 3 mL reaction volume in a relatively wide flask resulted

in small surface areas of electrodes submerged within the reaction solution, even when RVC was used as a cathode. A significant improvement in reactivity was observed when a new, more compact cell was designed, affording **81** in 52% yield and 68% ee after only 1 h (entry 6). This new cell, designed around a 2-dram vial (Figure 1.11, 2<sup>nd</sup> generation cell), allowed for significantly greater submerged electrode surface area and much more consistent separation between the electrodes, a key parameter for ensuring reproducibility between experiments.

Given the significant improvements in conversion and reaction rate that were observed upon alteration of the cell design, we decided to complete cell optimization before continuing with optimization of the reaction conditions. After a series of iterative design improvements, a finalized cell was designed (Figure 1.11, 7<sup>th</sup> generation cell). This cell

**Figure 1.11** Evolution of cell design.

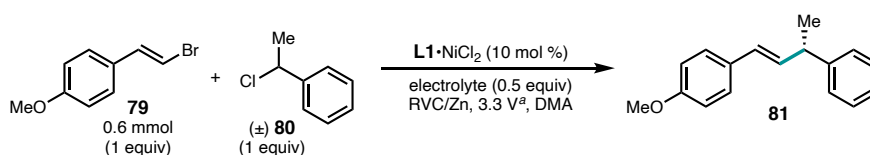


was quick and easy to build from common lab materials, was simple to clean and reuse, kept reactions under sufficiently inert conditions, and maintained the electrodes at a consistent distance from each other (~1.5 mm). Using this cell with TBAI as electrolyte, **81** was obtained in 57% yield and 89% ee, with 12% remaining **80** after 1 h.

## 1.2.2 Reaction Optimization

Cooling the reaction proved beneficial for enantioselectivity, as expected, but also significantly improved the mass balance (Table 1.2, entries 1–4). Additionally, an improvement in cross-selectivity was observed; the reactions run at 0 °C formed only 3% benzyl homodimer, compared to 13% when the reaction was run at room temperature. Unfortunately, attempts to cool the reaction further were fruitless due to water condensing onto the exposed portions of the electrodes. Extending the electrolysis time allowed the reaction to proceed to complete conversion, giving **81** in 77% yield and 85% ee (entry 6).

**Table 1.2** Effects of reaction temperature.



Entry	Electrolyte	Temp. (°C)	Time (h)	% Yield <sup>a</sup>	% ee <sup>c</sup>	% <b>81</b> <sup>b</sup>	% BnBn <sup>b</sup>
1	TBAPF <sub>6</sub>	23	1	45	67	4	13
2	TBAPF <sub>6</sub>	0	1	42	81	40	3
3	TBAI	23	1	57	89	12	13
4	TBAI	0	1	49	94	43	3
5	TBAI	0	2	68	86	8	8
6	TBAI	0	3	77	85	0	8

<sup>a</sup> Unreferenced. <sup>b</sup> Determined by <sup>1</sup>H NMR. <sup>c</sup> Determined by chiral SFC.

Having achieved full reaction conversion, our next goal was to optimize electrochemical parameters in order to further improve the yield and enantioselectivity. Reducing the voltage to 1.5 V or 0.5 V significantly reduced conversion but improved enantioselectivity (Table 1.3, entries 1–3). Further increasing the voltage to 5.0 V produced a much messier reaction profile, and afforded product in lower yield (entry 4). A cleaner reaction profile and improved mass balance were observed when the concentration of supporting electrolyte was increased to 0.2 M (entry 5). Voltages below 0.5 V resulted in very little conversion, which is in accordance with the measured open circuit voltage of 0.46 V.

**Table 1.3** Effect of voltage.



Entry	Equiv TBAI	Voltage (V <sup>a</sup> )	% Yield <sup>b</sup>	% ee <sup>c</sup>	% <b>80</b> <sup>b</sup>	% BnBn <sup>b</sup>
1	0.5	0.5	10	93	63	3
2	0.5	1.5	17	94	48	4
3	0.5	3.3	77	85	0	8
4	0.5	5.0	61	90	27	4
5	1.0	3.3	66	91	26	3

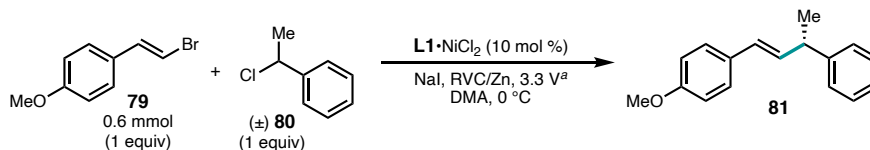
<sup>a</sup> Unreferenced. <sup>b</sup> Determined by <sup>1</sup>H NMR. <sup>c</sup> Determined by chiral SFC.

Given that cell design had proven critical early in the optimization efforts, some conditions that had only been tested in the earliest versions of the cell were revisited. Due to its role in improving yield, conversion, and enantioselectivity in the heterogeneous version of this reaction,<sup>81</sup> and other reports of it enhancing reactivity in reductive cross-couplings,<sup>82–84</sup> we hypothesized that sodium iodide could serve as both a beneficial reaction additive *and* the supporting electrolyte in the optimized cell. When the reaction was



performed at 3.3 V for two hours with 1 equiv NaI, improved yield (70%), improved enantioselectivity (88%), and complete conversion were observed relative to TBAI (Table 1.4, entry 5). Going forward, NaI was used for optimization.

**Table 1.4** Effects of electrolyte concentration.



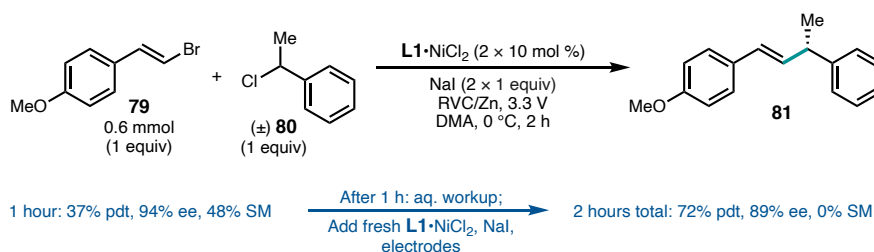
Entry	Equiv NaI	Time (h)	% Yield <sup>b</sup>	% ee <sup>c</sup>	% <b>80</b> <sup>b</sup>	% BnBn <sup>b</sup>
1	0.5	1	61	91	34	2
2	1.0	1	58	93	30	2
3	2.0	1	44	93	36	4
4	0.5	2	70	87	2	8
5	1.0	2	70	88	0	4

<sup>a</sup> Unreferenced. <sup>b</sup> Determined by <sup>1</sup>H NMR. <sup>c</sup> Determined by chiral SFC.

As previously noted, increased reaction conversion led to reduced enantioselectivity across a wide variety of conditions. Several experiments were carried out in order to understand the source of this trend and to find conditions that could maintain high levels of enantioselectivity at full reaction conversion. When enantioenriched product **81** (88% ee) was resubjected to the reaction conditions (NaI,  $L1 \cdot NiCl_2$ , DMA, 3.3 V, 1 h, 0 °C), the product was recovered without any erosion in enantioselectivity, indicating that product racemization was likely not occurring under the reaction conditions. To probe the possibility of ligand and/or catalyst decomposition, a two-stage experiment was conducted (Scheme 1.1). First, the coupling reaction of **79** and **80** was run for one hour. An aqueous workup was conducted, and an aliquot of the reaction was removed for crude <sup>1</sup>H NMR analysis, purification, and SFC. At this point, the reaction had formed 37% of **81** in 94% ee, with 48% remaining **80**. The crude reaction mixture was then re-dissolved in DMA,

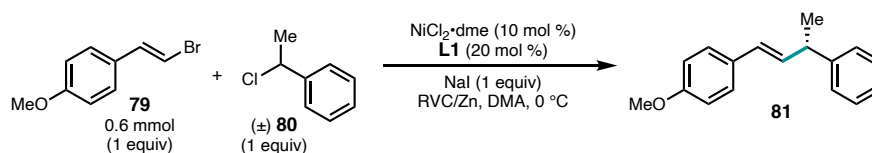
and fresh NaI and **L1**·NiCl<sub>2</sub> were added (these were removed in the aqueous workup). After an additional hour at 3.3 V (with fresh electrodes), a second workup was conducted and the reaction was again analyzed. The reaction went to full conversion, affording **81** in 72% yield but only 89% ee. This was essentially the same result observed without replacing the catalyst midway through the reaction. Catalyst degradation was further ruled out as a cause of diminished ee through same-excess experiments (*vide infra*).

**Scheme 1.1** Two-stage electroreductive coupling.



At this point, it was still unclear what was causing the consistent decrease in enantioselectivity as the electroreductive coupling reactions went to completion. Fortunately, the addition of additional ligand to the reaction (10 mol % NiCl<sub>2</sub>·dme, 20 mol % **L1**) afforded coupled product **81** in 84% yield and 93% ee.

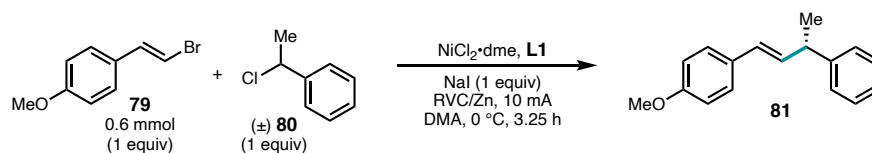
Given our limited success in improving the reaction by precisely tuning the applied potential, we wondered if switching to galvanostatic mode could prove beneficial. Several advantages to running the electrolysis at constant current are: 1) more consistent results between experiments, 2) much safer operation (no spikes to dangerous currents), and 3) more direct control over catalyst turnover rate. Given these advantages, several constant current regimes were tested and compared to the optimized potentiostatic results (Table 1.5).

**Table 1.5** Comparison of constant current and constant voltage reactions.

Entry	I / V	Time (h)	% Yield <sup>b</sup>	% ee <sup>c</sup>	% <b>80</b> <sup>b</sup>	% BnBn <sup>b</sup>
1	3.3 V <sup>a</sup>	2	84	93	0	5
2	5 mA	6.5	61	93	0	8
3	10 mA	3.25	84	94	0	5
4	20 mA	1.63	77	91	1	4

<sup>a</sup> Unreferenced. <sup>b</sup> Determined by <sup>1</sup>H NMR. <sup>c</sup> Determined by chiral SFC.

At all currents tested, the reactions went to full conversion after passing the theoretically required two equivalents of electrons, indicating excellent Faradaic efficiencies. A current of 10 mA was found to afford **81** in optimal yield and enantioselectivity (84% yield, 94% ee), which compared well with our published result obtained with stoichiometric Mn<sup>0</sup> powder as the terminal reductant (91% yield, 93% ee) (Table 1.5, entry 3).<sup>81</sup> With these constant current conditions, we found that nickel and ligand loading could not be lowered without diminishing yield and ee (Table 1.6).

**Table 1.6** Effects of nickel and ligand loading.

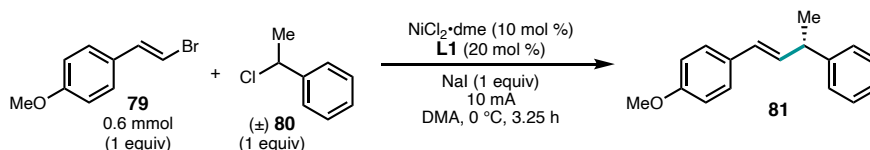
Entry	mol % Ni	mol % L1	% Yield <sup>a</sup>	% ee <sup>b</sup>	% <b>80</b> <sup>a</sup>	% BnBn <sup>a</sup>
1	10	20	84	94	0	5
2	10	15	79	92	0	5
3	10	12	76	92	0	4
4	5	7	24	84	29	9

<sup>a</sup> Determined by <sup>1</sup>H NMR, relative to Bn<sub>2</sub>O as an internal standard. <sup>b</sup> Determined by chiral SFC.

Before exploring the scope of this transformation, we wanted to ensure that the originally optimal electrode materials were still performing best under these newly

optimized conditions. Replacing the RVC cathode with graphite resulted in significantly reduced conversion, yield, enantioselectivity, and mass recovery (Table 1.7, entry 2). Reduced mass recovery with graphite as an electrode has been previously observed by Baran and coworkers.<sup>85</sup> Replacement of the Zn anode with either Al or Mg led to buildup of oxidized species on the anode surface, resulting in a voltage overload before the reactions could go to completion (entries 3, 4). Voltage overload was not observed when an Fe electrode was used; in this case, however, the reaction had not gone to completion after 2 equivalents of electrons had been passed through (entry 5). Doubling the reaction time did result in full conversion of the starting materials, but in lower yield of **81** and worse Faradaic efficiency than when Zn was used as the anode (entry 6).

**Table 1.7** Effects of electrode materials.



Entry	Cathode	Anode	% Yield <sup>a</sup>	% ee <sup>b</sup>	% <b>80</b> <sup>a</sup>	% BnBn <sup>a</sup>
1	RVC	Zn	84	94	0	5
2	Graphite	Zn	14	41	16	7
3	RVC	Al	48	96	27	6
4	RVC	Mg	23	96	46	2
5	RVC	Fe	53	95	28	5
6	RVC	Fe	70 <sup>c</sup>	94	0	6

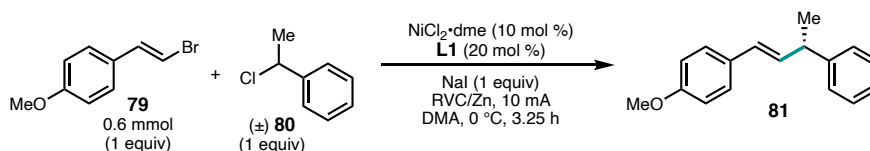
<sup>a</sup> Determined by <sup>1</sup>H NMR, relative to Bn<sub>2</sub>O as an internal standard. <sup>b</sup> Determined by chiral SFC.

<sup>c</sup> Electrolyzed for 6.5 h

Satisfied with Zn and RVC as electrode materials, several control experiments were conducted. Confirming previous results, NaI remained the optimal electrolyte in this system (Table 1.7, entries 2–4). Cooling proved essential for cross selectivity, yield, and enantioselectivity (entry 5). No current could be passed in the absence of NiCl<sub>2</sub>·dme or NaI

(entries 6,8). In the absence of ligand, racemic **81** was obtained in only a 5% yield, indicating a low rate of background reactivity (entry 7). When the reaction was stirred in the cell without passing a current, 2% product was obtained, presumably by direct reduction by the Zn wire (entry 9).

**Table 1.8** Control experiments.



Entry	Deviation from std.	% Yield <sup>a</sup>	% ee <sup>b</sup>	% <b>80</b> <sup>a</sup>	% BnBn <sup>a</sup>
1	None	84	94	0	5
2	TBAI instead of NaI	67	91	0	7
3	TBAPF <sub>6</sub> instead of NaI	59	78	11	4
4	NaPF <sub>6</sub> instead of NaI	24	76	32	5
5	23 °C	49	89	0	15
6	No $\text{NiCl}_2 \cdot \text{dme}$	0	–	71	16
7	No <b>L1</b>	5	0	56	2
8	No NaI	0	–	99	0
9	No current	2	–	98	0

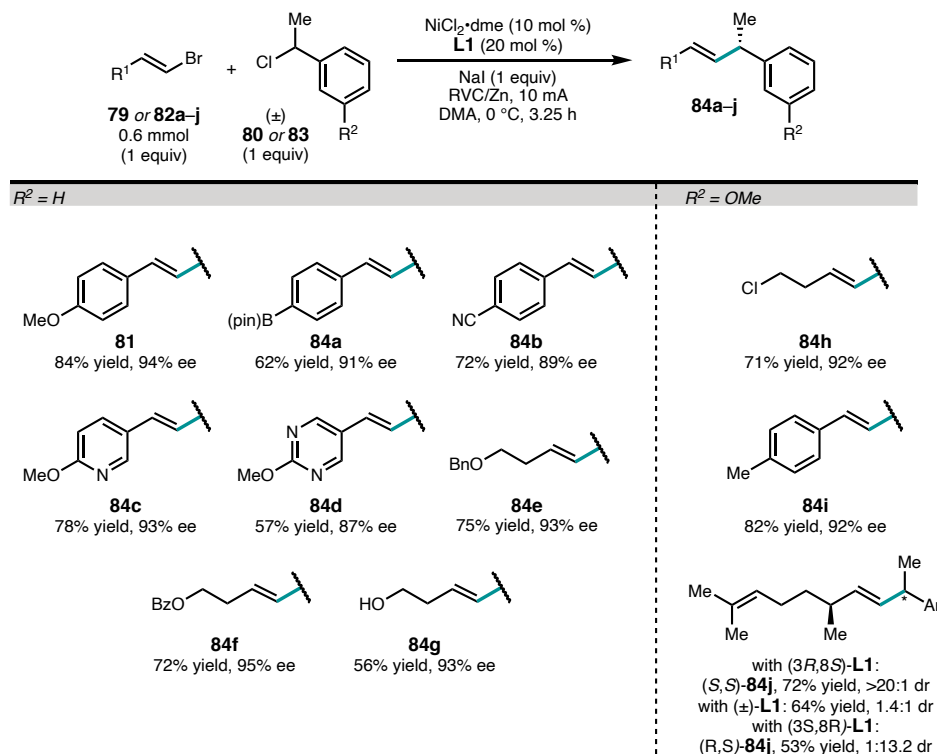
<sup>a</sup> Determined by <sup>1</sup>H NMR, relative to Bn<sub>2</sub>O as an internal standard. <sup>b</sup> Determined by chiral SFC.

### 1.2.3 Reaction Scope

With optimized conditions in hand, the scope of this enantioselective electroreductive cross-coupling was explored. First examining the alkenyl bromide coupling partner, we found that both aryl- and alkyl-substituted alkenyl bromides coupled in high yields and enantioselectivities (Figure 1.12). Aryl groups bearing both electron-withdrawing groups (**82b**) and electron-donating groups (**79**) were well tolerated. Heterocyclic substrates (**82c** and **82d**) were tolerated, as well as both benzyl and benzoyl-protected alcohols (**82e** and **82f**). Aryl boronate **82a**, free alcohol **82g**, and primary alkyl chloride **82h** all coupled successfully to form products poised for direct elaboration (**84a**,

**84g**, and **84h**). Use of either (3*R*, 8*S*)-**L1** or (3*S*, 8*R*)-**L1** enabled the coupling of (–)-citronellal-derived alkenyl bromide **82j** to give either the (*S,S*)- or (*R,S*)-diastereomers of diene **84j**, each with good diastereoselectivity.

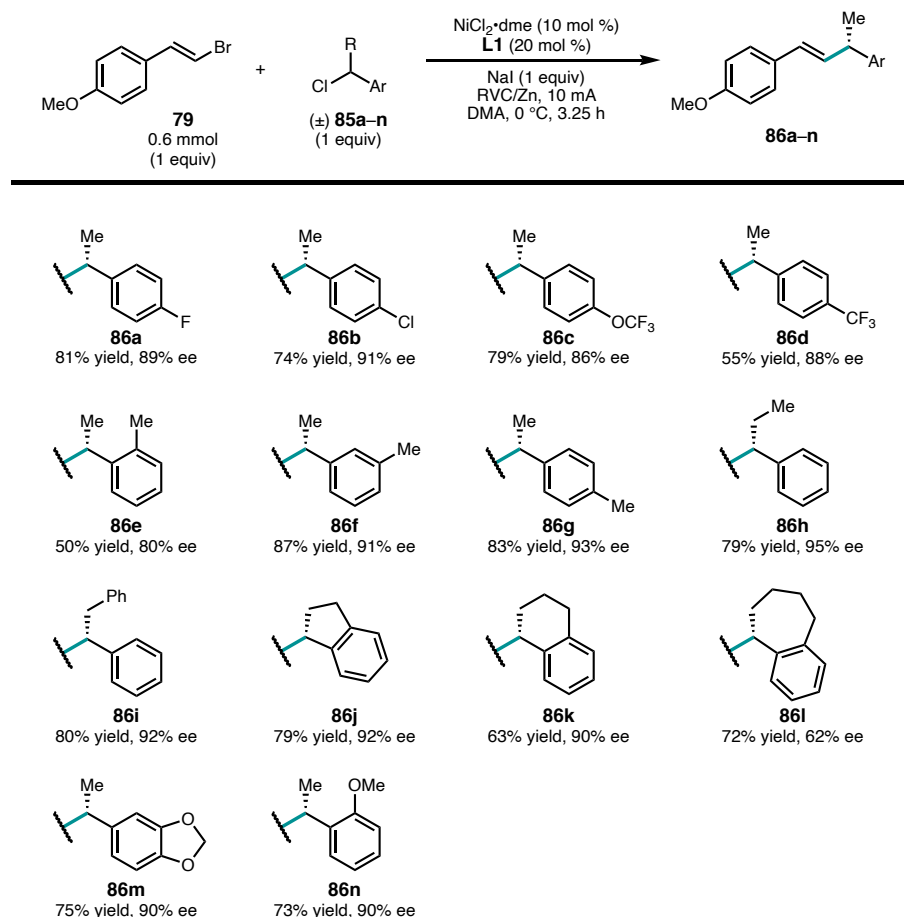
**Figure 1.12** Scope of alkenyl bromides.



A variety of benzylic chlorides also proved to be competent coupling partners (Figure 1.13). Several halogenated arenes (**85a–d**) were tolerated; unfortunately, an aryl bromide-containing substrate suffered from competitive bromide/iodide exchange and protodebromination. Whereas the *o*-methyl product **86e** was obtained in diminished yield and ee, the *o*-methoxy substrate performed significantly better (**85n**). Extending the  $\alpha$ -phenyl alkyl chain from methyl to ethyl gave product **86h** in good yield and excellent ee. Further increasing the steric bulk of this substituent resulted in a slight loss of ee (**85i**). The five- and six-membered ring products **86j** and **86k** were formed with good

enantioselectivity; however, a significant drop in selectivity was observed in the formation of 7-membered ring-containing product **86l**.

**Figure 1.13** Scope of benzylic chlorides.

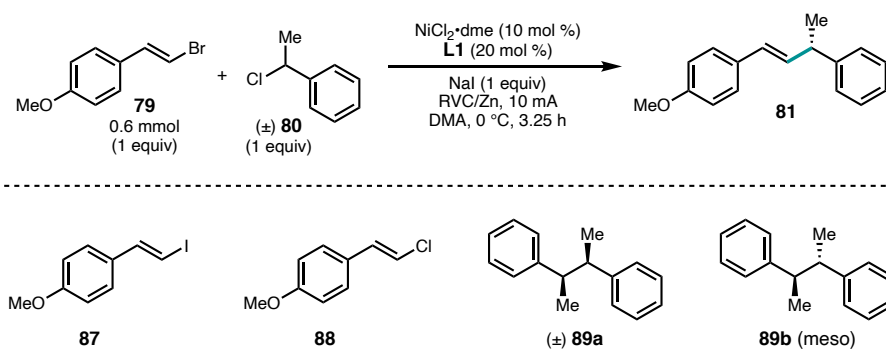


One potential advantage of electrochemical control of this reaction is the ease of scaleup. Gratifyingly, we were able to construct an effective cell for reaction scaleup based on a large test tube, employing a 0.25-inch diameter zinc anode and a RVC cathode. When the coupling of alkenyl bromide **79** and benzylic chloride **80** was conducted on 6.0 mmol scale (the current was scaled from 10 mA to 100 mA), 1.19 g **81** was obtained with only minor reductions in yield and enantioselectivity (83% yield, 91% ee).

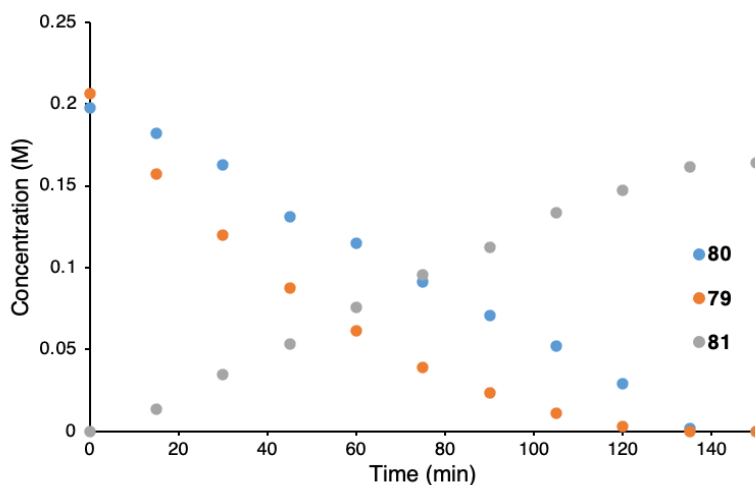
### 1.2.4 Preliminary Kinetic Studies

Having demonstrated the scope of this reaction, we sought to conduct preliminary investigations to probe the reaction's kinetics. Inspired by elegant reports from the Blackmond and Burés groups on visual techniques for kinetic analysis, we next sought to probe the kinetics of our electroreductive alkenylation reaction.<sup>86,87</sup> The first step in conducting our kinetic analysis was monitoring the reaction progress under the standard reaction conditions (Figure 1.14). Using a gas chromatography (GC) assay, we saw that benzyl chloride **80** was consumed in a relatively linear fashion, in contrast to alkenyl bromide **79**. The rate of product (**81**) formation appeared to be relatively constant, until complete consumption of **79** and **80** at late time points (Figure 1.15).

**Figure 1.14** Reaction and observed byproducts.





**Figure 1.15** Reaction profile under standard conditions.

Analysis of the reaction aliquots revealed the presence of several additional species over the course of the reaction, derived from both alkenyl bromide **79** and benzyl chloride **80** (Figure 1.14). Alkenyl halides **87** and **88** arise from redox-neutral halogen exchange of alkenyl bromide **79**. Benzylic chloride **80** can couple with itself under the reaction conditions, giving homodimers **89a** and **89b**, which were observed in a 1:1 ratio, perhaps suggesting the intermediacy of a cage-escaped radical. Homocoupling of the alkenyl bromide was not observed under the reaction conditions.

Tracking alkenyl halides **79**, **87**, and **88** over the course of the reaction shows several interesting trends (Figure 1.16). Alkenyl iodide **79** is formed during the reaction and likely serves as a competent coupling partner in the electroreductive coupling. The concentration of **87** increases at early time points, then slowly drops to 0 M by the time benzyl chloride **80** has been fully consumed (135 min). In contrast, the concentration of alkenyl chloride **88** does not begin to shrink until complete consumption of both alkenyl bromide **79** and benzyl chloride **80**, possibly due to direct electroreduction (Figure 1.17).<sup>88</sup>

Notably, although the consumption of alkenyl bromide **79** was not linear, combining the concentrations of all three alkenyl halide species (**79**, **87**, and **88**) does reveal a linear consumption during the majority of the reaction (Figure 1.16).

**Figure 1.16** Profile of alkenyl species under standard conditions.

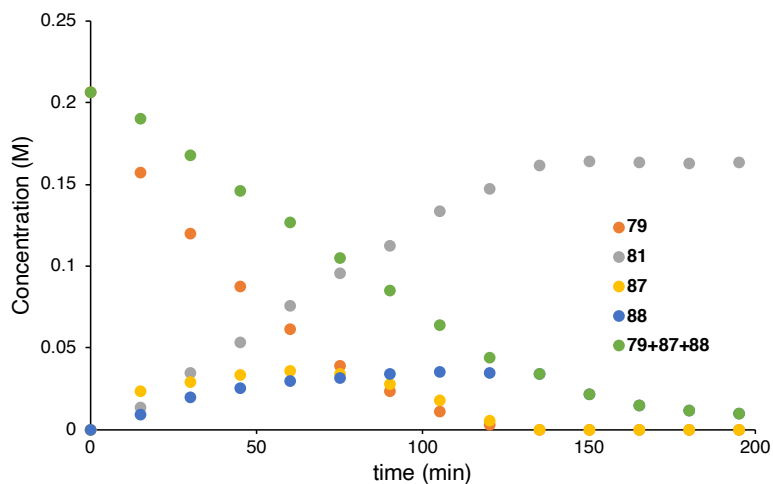
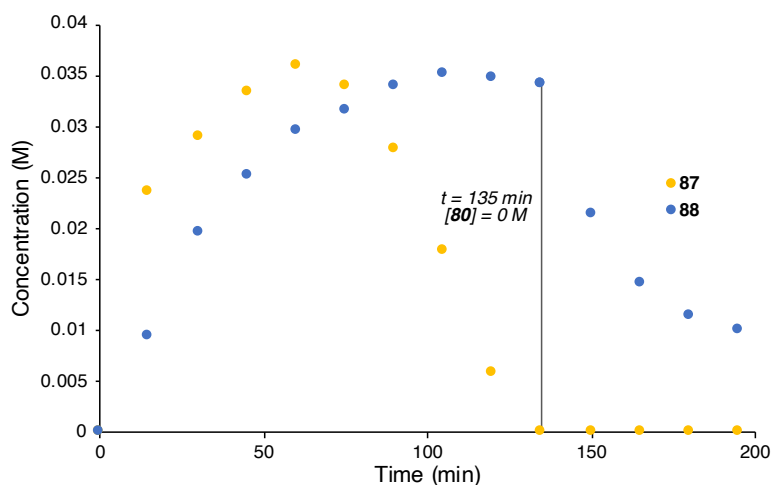


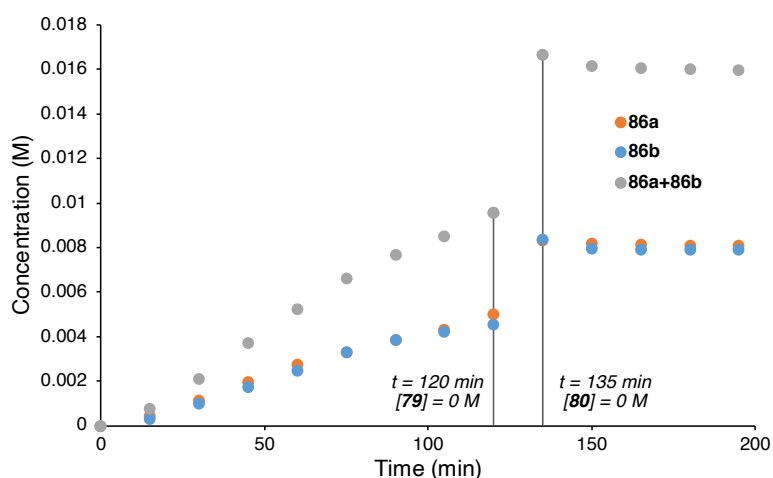
**Figure 1.17** Profile of **87** and **88** under standard conditions.



In addition to forming cross-coupled product **81**, the radical derived from benzyl chloride **80** can homocouple to form both **89a** and **89b** (Figure 1.14). These two species are formed in a nearly 1:1 ratio over the course of the reaction. (Figure 1.18). The

homocoupling products **89a** and **89b** formed steadily over the course of the reaction, until alkenyl bromide **79** was fully consumed (120 min); at this point, the remaining **80** rapidly homocoupled until it was fully consumed (135 min). At the end of the reaction, approximately 16% of **80** had been converted to **89a** and **89b**. A control experiment found that in the absence of **79**, **89a** and **89b** were formed in a combined 89% yield (1:1 ratio).

**Figure 1.18** Profile of **80** homocoupling under standard conditions.

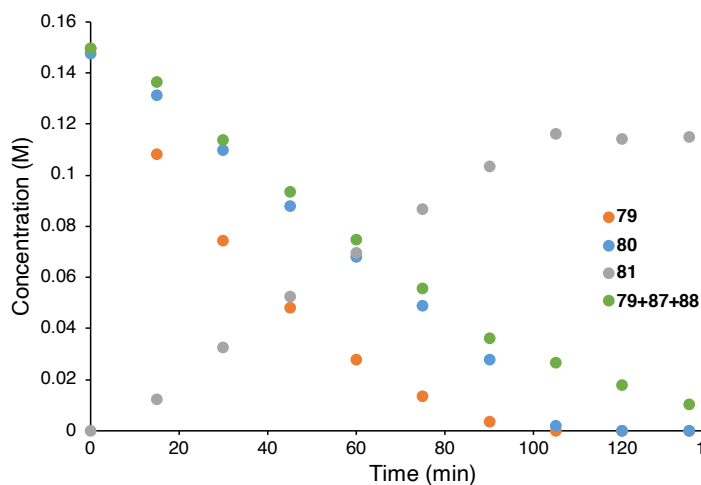


With a solid understanding of the reaction profile under standard conditions, we next sought to interrogate the reaction through graphical kinetic analysis.<sup>86,87</sup> Key to analyzing a reaction using these techniques is understanding the robustness of the reaction with respect to product inhibition and catalyst decomposition. These questions can be simply probed by conducting a “same excess experiment” in which the reaction is run under conditions that mimic the standard reaction after partial conversion. To that end, the reaction was repeated, beginning with lower concentrations (0.15 M) of each of the two coupling partners (Figure 1.19). Importantly, the concentrations of all other reaction components were held constant relative to the standard conditions, allowing us to mimic

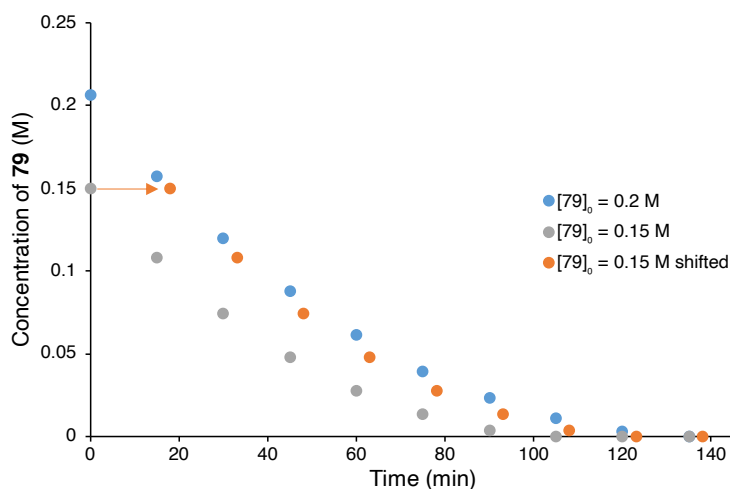
the conditions of the reaction after consumption of 25% of the starting materials.

Qualitatively, the reaction profile looks similar under these conditions.

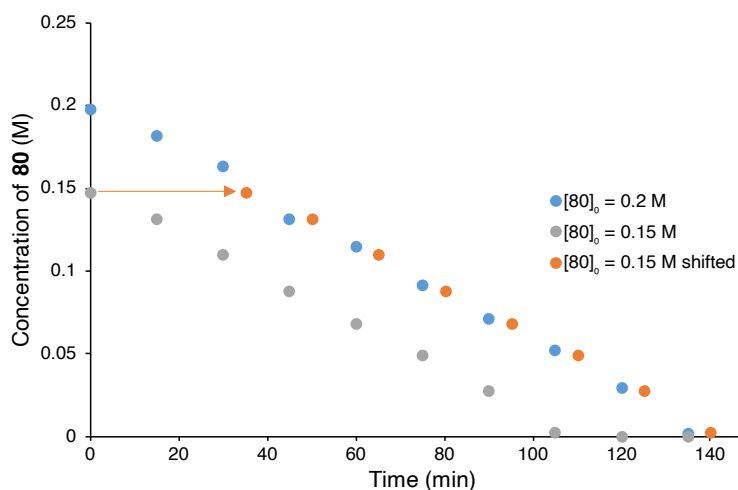
**Figure 1.19** Reaction profile under same excess conditions.

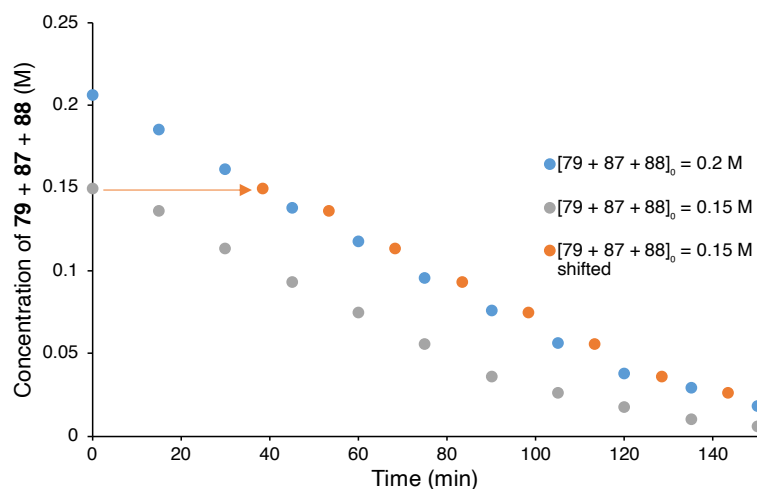


To probe for catalyst death, an induction period, or product inhibition, the same excess experiment can be graphically overlaid with the standard reaction. If the catalytic system is robust, we expect good overlay between the experiments due to a consistent concentration of catalyst, after time-shifting to adjust for concentration. This overlay can be conducted with respect to different species in the reaction. Good overlay is observed with respect to alkenyl bromide **79** when shifting the “same excess” data 18.1 minutes, the amount of time required, under standard conditions, to bring [79] down to 0.15 M (Figure 1.20).

**Figure 1.20** Same excess overlay with respect to **79**.

Similar overlay is seen if the two experiments are overlaid with respect to the benzyl chloride (**80**) or to the summed concentration of alkenyl halides (**79**, **87**, and **88**) in solution (Figures 1.21 and 1.22). Interestingly, the time shifts required for **80** and **79** + **87** + **88** are very similar to each other (35.2 min and 38.3 min, respectively).

**Figure 1.21** Same excess overlay with respect to **80**.

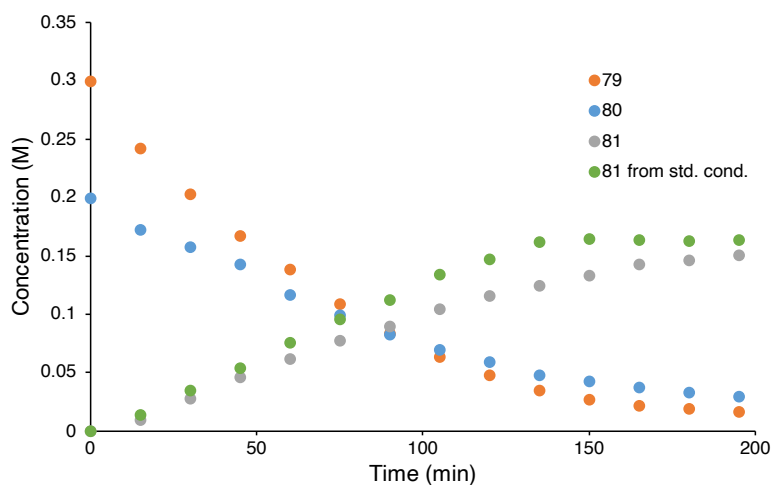
**Figure 1.22** Same excess overlay with respect to **79**+**87**+**88**.

Taken together, the good overlay seen in these same excess experiments suggested that 1) product inhibition was not a major concern, and 2) catalyst decomposition was not a major factor in this reaction, in agreement with previous experiments (Scheme 1.1). Having established the robustness of the reaction, we next sought to probe the kinetics of this transformation using so-called different excess experiments.<sup>87</sup> These experiments involve changing the concentration of one reaction component while holding all others constant. Graphical transformation of the resulting product concentration data can be used to determine the reaction order in each component. As an example, the reaction was run with an initial **79** concentration of 0.3 M, rather than 0.2 M (Figure 1.23).

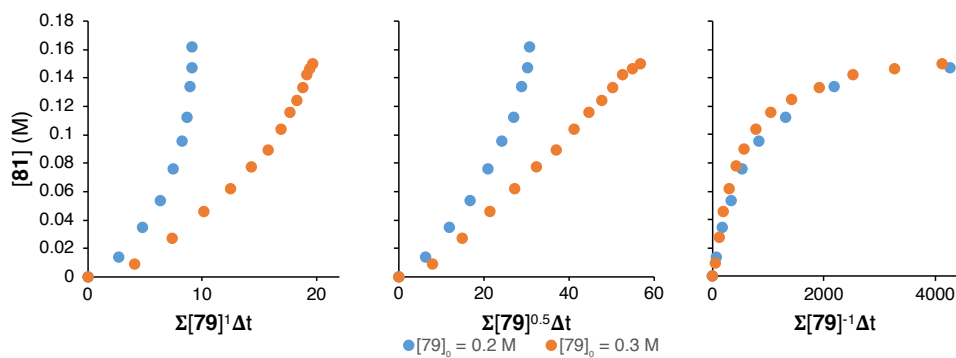
Product formation over time for both the standard reaction conditions and the different excess experiment can be plotted together (Figure 1.23). The lack of overlay between these data indicated that the rate of product formation does depend on the concentration of alkenyl bromide, therefore the reaction does not appear to be 0<sup>th</sup> order in **79**. Variable time normalization of the product concentrations can be used to graphically

determine the reaction order in **79**.<sup>87</sup> The exponent in the variable normalized time axis can be adjusted until good overlay is observed; the exponent that gives good overlay is the apparent order of the reaction in the reaction component that was changed. As shown in Figure 1.24, exponents such as 1, 0.5, and  $-1$  do not give good overlay in this case.

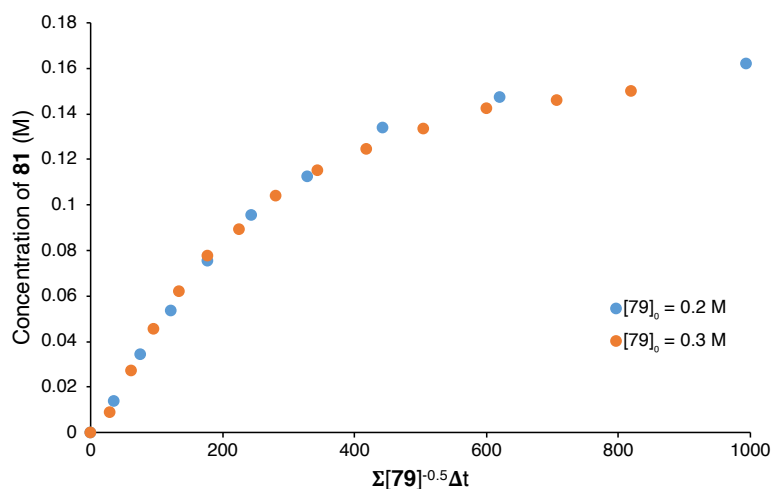
**Figure 1.23** Different Excess:  $[79]_0 = 0.3$  M.



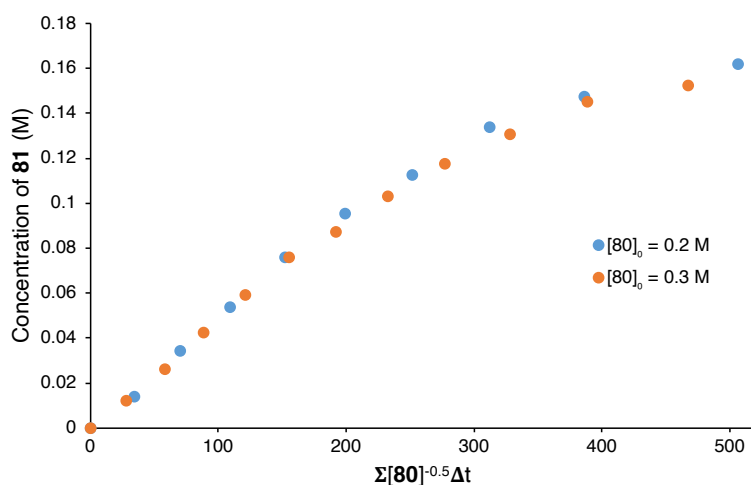
**Figure 1.24** Variable time normalization overlay attempts with respect to **79**.



In contrast, an exponent of  $-0.5$  gives good overlay between the product concentration profiles for the standard reaction conditions and  $[79]_0 = 0.3$  M (Figure 1.25). Given this good overlay, the apparent order of the reaction in **79** is  $-0.5$ .

**Figure 1.25** Variable time normalization overlay with respect to **79**.

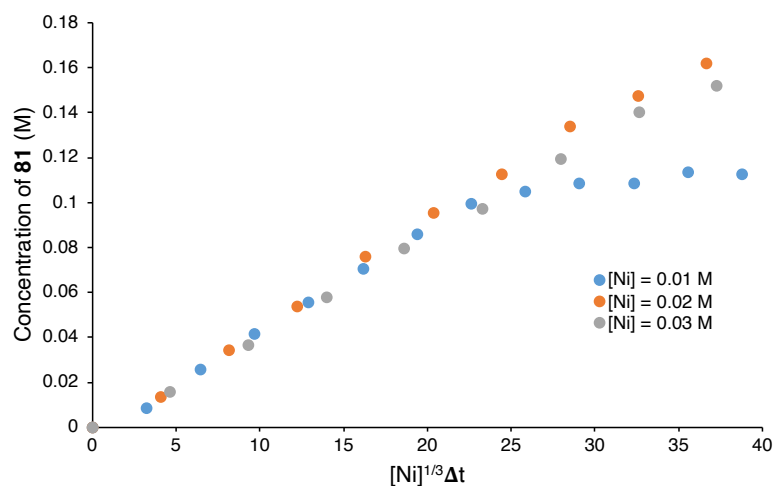
The reaction was next conducted under a separate set of “different excess” conditions by increasing the initial concentration of benzyl chloride **80** to 0.3 M while holding the concentrations of all other reaction components constant. Using the same workflow described above for **79**, variable time normalization analysis was used to find the rate dependence of the reaction on **80**, giving an apparent order of  $-0.5$ , the same that was found for alkenyl bromide **79** (Figure 1.26).

**Figure 1.26** Variable time normalization overlay with respect to **80**.



Having found reaction orders for the two coupling partners, we next sought to determine the reaction order in nickel. Under the standard reaction conditions, the initial concentration of nickel is 0.02 M (10 mol %). Two additional reactions were run, varying the nickel concentration (0.01 M, 0.03 M). In the context of substrates whose concentrations can be measured over the course of the reaction, the variable time normalization transformation takes into account the changing concentration of the species of interest. Because the GC assay cannot quantify the concentration of nickel over the course of the reaction, it is assumed to remain constant for VTNA purposes.<sup>87,89</sup> With this assumption, the three reactions at varied nickel concentrations can be plotted together, and the exponent adjusted until good overlay is seen (Figure 1.27).

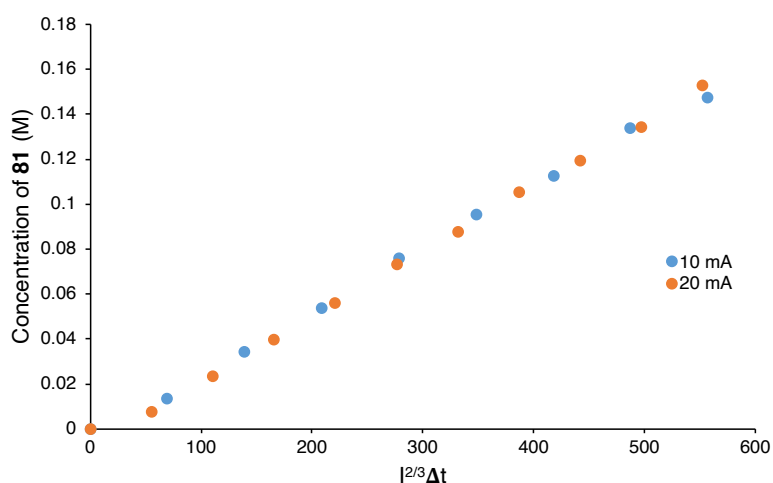
**Figure 1.27** Variable time normalization overlay with respect to Ni.



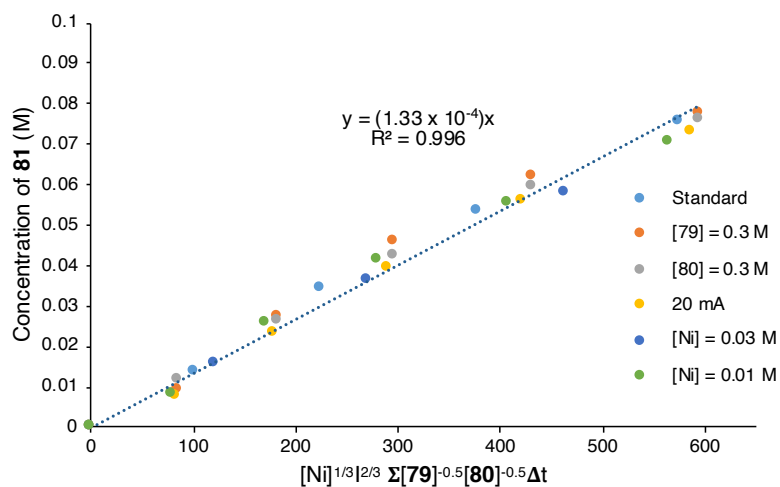
An order of positive  $\frac{1}{3}$  gives excellent overlay at early time points (the first ~100 minutes of the reaction). The higher nickel concentrations (0.02 M and 0.03 M) remain well-overlaid at later time points, suggesting some amount of catalyst decomposition at lower nickel loading.

Given that our reductive cross-coupling reaction is electrochemically driven, we sought to treat current similarly to nickel concentration to identify the dependence of the rate of product formation on current. The reaction was run with the same concentrations as the standard reaction, but a current of 20 mA was applied rather than 10 mA. Once again, VTNA was used to transform the data and uncover the apparent order of the reaction in current (Figure 1.28).

**Figure 1.28** Variable time normalization overlay with respect to current.



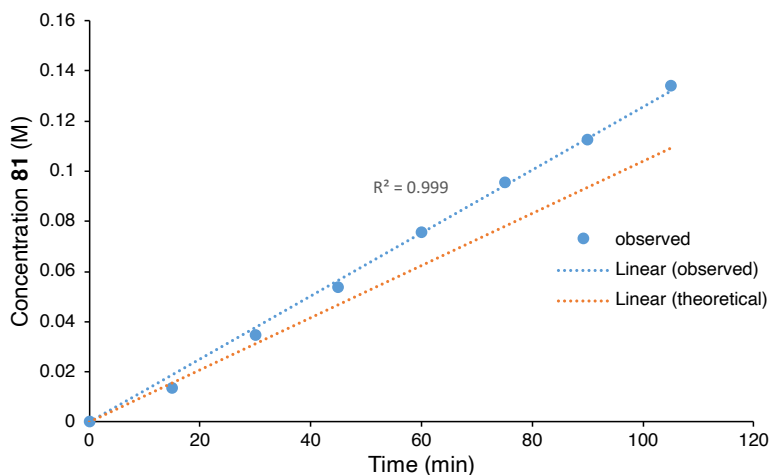
The kinetic parameters extracted from each of the preceding experiments were then combined in an attempt to fully normalize the data. If all important factors were accounted for, we would expect to be able to overlay product concentration data from every experiment by normalizing each data point for current and the concentrations of **79**, **80**, and Ni. Gratifyingly, good overlay was observed when applying the exponents derived from the different excess experiments (**79**:  $-1/2$ ; **80**:  $-1/2$ ; Ni:  $1/3$ ; and I:  $2/3$ ) (Figure 1.29).

**Figure 1.29** Total variable time normalization overlay.

Closer examination of these apparent kinetic orders reveals that there must be confounding factors in this analysis. Namely, we are seeing apparent negative orders in both electrophiles (**79** and **80**) but linear formation of cross-coupled product **81**. VTNA is based on the assumption that we can use the stoichiometry of the reaction to deduce the order of the reaction, but that assumption does not appear to hold true in this case, so the apparent orders that we derived are not the “true” kinetics of the reaction of interest. One complicating factor that could explain some of the confusing kinetics results can be seen by looking at the Faradaic efficiency of the reaction. Under the standard reaction conditions, after 105 minutes the concentration of **81** was 0.134 M (Figure T16). Given that formation of a single molecule of **81** requires two electrons, and that the constant current applied to the reaction is 10 mA, we can calculate the expected yield of product if 100% of the electrons applied to the system went towards product formation. Plotting this theoretical yield against the experimental data reveals that 23% more **81** was formed than would be expected if all the applied current went toward productive reactivity. Given this

discrepancy, there must be some other source of electrons contributing to the observed reactivity.

**Figure 1.30** Observed and expected **81** formation over time.



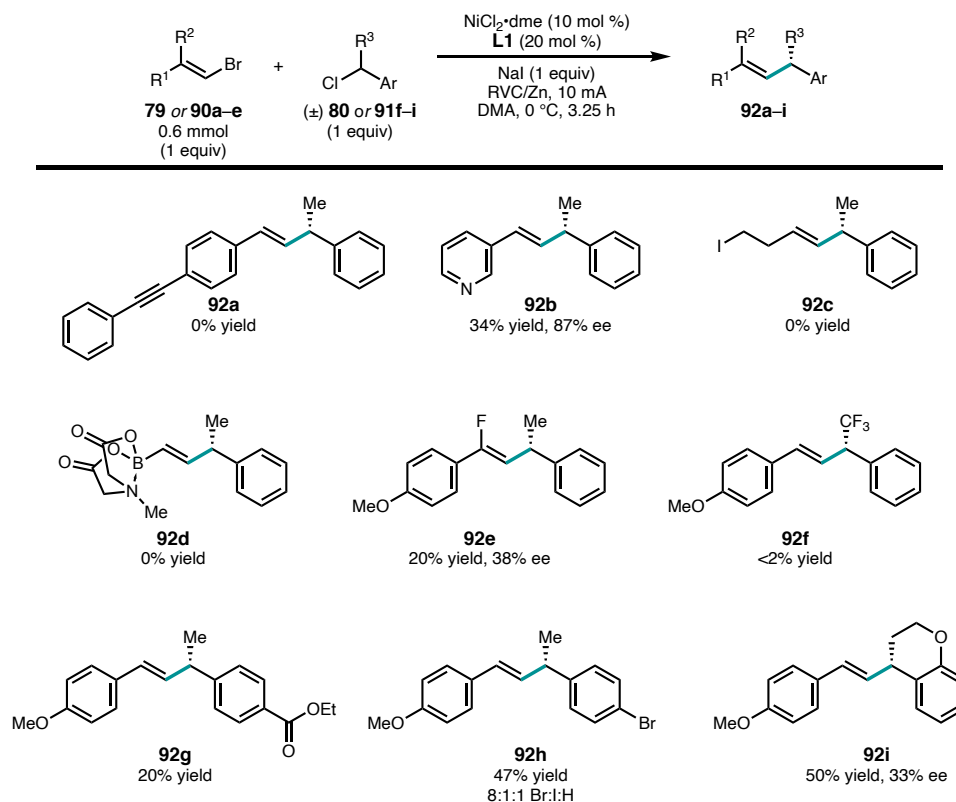
At this point, it is unclear what this source of electrons is, but this alternate reaction pathway could be contributing to the apparent kinetic order of the reaction derived from VTNA studies not aligning with the observed linear product formation. A plausible source of these “excess” electrons is the sacrificial zinc anode: zinc powder can turn this reaction over in the absence of electrochemistry.<sup>81</sup> However, given that the Zn anode is anodically polarized during the reaction, direct reduction of nickel intermediates at the anode seems challenging. Going forward, divided cell experiments could be conducted to probe these possibilities.

### 1.2.5 Attempts to Expand Reactivity

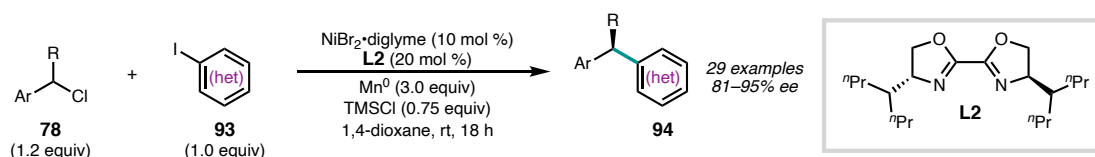
At the outset of this project, it was hypothesized that employing electrochemical turnover would allow for a broader substrate scope than that achieved using

superstoichiometric metal powder reductants. Hansen and coworkers were able to see improved yields electrochemically with certain electron-poor heterocyclic substrates in comparison to  $Zn^0$  conditions.<sup>77</sup> Unfortunately, electrochemical turnover did not expand the substrate scope of our enantioselective electroreductive cross-coupling of alkenyl bromides and benzylic chlorides.

A number of substrates that were tested in this transformation proved unsuccessful. For example, neither the  $Mn^0$  nor electrochemical versions of the reaction have been able to tolerate the presence of basic nitrogen heterocycles without a group adjacent to the nitrogen (Figure 1.31, **90b**). Subjection of alkyne-containing alkenyl bromide **90a** to the reaction conditions resulted in complete decomposition of the starting material and significant formation of benzyl homocoupling. Likewise, primary alkyl iodide **90c** and MIDA-protected boronate ester **90d** decomposed under the reaction conditions without forming any of the desired cross-coupled product. Fluorinated analogues **92e** and **92f** were formed in low yields. The use of ethyl benzoate **91g** resulted in a surprisingly low yield of the cross-coupled product **92g**, with significant amounts of both homocoupled products formed; this reaction performed significantly better with  $Mn^0$  as the terminal reductant, although it is unclear why. Aryl bromide **91h** coupled in reasonable yield but could not be separated from the aryl iodide and protodebrominated contaminants generated during the reaction. Chromane **91i** afforded product in modest yield, but with notably poor enantioselectivity. This same effect was observed when  $Mn^0$  was used as the reductant.

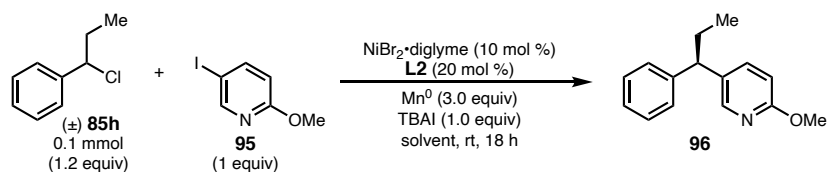
**Figure 1.31** Limitations of substrate scope.

Having shown that one of our group's reductive couplings could be translated into an electrochemical reaction, we sought to expand more of our chemistry in the same way, while testing the scope of this electrochemical manifold. In 2017, our group reported the reductive coupling of heteroaryl iodides with benzyl chlorides, using a  $\text{NiBr}_2\cdot\text{diglyme}/\text{L2}$  catalyst system with superstoichiometric  $\text{Mn}^0$  powder as the reductant (Figure 1.32).<sup>90</sup>

**Figure 1.32** Synthesis of 1,1-diaryllkanes via enantioselective reductive cross-coupling.

Unlike the previously discussed alkenylation reaction, this reaction used 1,4-dioxane as solvent, included TMSCl as an additive, and did not contain any electrolyte. These differences suggested that this reaction may be less readily amenable to an electrochemical manifold; polar solvents and electrolytes are typically required for efficient electron transfer, and corrosive TMSCl could be damaging to the electrodes. Unsurprisingly, initial attempts to couple **95** with **85h** electrochemically did not result in any productive reactivity. The addition of TMSCl to the electrochemical cell resulted in irreversible corrosion of the RVC cathode, so most screening in this system was conducted in the absence of TMSCl. The addition of more polar cosolvents, prestirring, variation in order of addition, heating, variation in electrolytes, nickel/ligand precomplexation, and the addition of redox mediators such as methyl viologen all resulted in immediate voltage overload, with no current passed.

An alternative to 1,4-dioxane was sought due to its low dipole moment, poor solubilizing properties, and limited use in electrochemical applications. Before solvents could be screened, however, a non-interfering electrolyte had to be identified. A broad screen of electrolytes was conducted using 1,4-dioxane as solvent, and both  $Mn^0$  and  $Zn^0$  as reductants. Tetrabutylammonium iodide and lithium bis(trifluoromethanesulfonyl)imide (LiTFSI) were found to be uniquely tolerated in this reaction. Product **96** was obtained in 25% yield and 80% ee using TBAI/ $Mn^0$  and 6% yield and 89% ee using TBAI/ $Zn^0$ . Having identified a suitable electrolyte, a variety of solvents were then surveyed using both reductants with added TBAI (Table 1.9).

**Table 1.9** Solvent screening with metal powder reductants.

Entry	Solvent	Homogeneous?	$\text{Zn}^0$		$\text{Mn}^0$	
			% Yield <sup>a</sup>	% ee <sup>b</sup>	% Yield <sup>a</sup>	% ee <sup>b</sup>
1	DMA	yes	2	49	18	53
2	DMF	yes	0	–	3	50
3	NMP	yes	0	–	0	–
4	MeCN	no	1	10	15	41
5	THF	mostly	10	47	30	70
6	MeOH	yes	0	–	1	54
7	MeNO <sub>2</sub>	mostly	0	–	0	–
8	EtOAc	no	17	55	5	80
9	DCM	mostly	8	35	23	52
10	DMSO	yes	0	–	0	–
11	DMPU	yes	0	–	0	–
12	PhMe	no	5	74	0	–
13	HFIP	yes	0	–	0	–
14	PC	yes	3	63	5	72

<sup>a</sup> Determined by <sup>1</sup>H NMR, relative to  $\text{Bn}_2\text{O}$  as an internal standard. <sup>b</sup> Determined by chiral SFC.

Unfortunately, the solvents that performed best were also those in which the reaction components were the least soluble (except for the metal reductant, which was insoluble in all solvents tested). Perhaps due to these solubility issues, none of the solvents that showed reactivity with the metal powder reductants allowed any current to pass when the reaction was attempted electrochemically. Attempts to translate other asymmetric nickel-catalyzed reductive cross couplings to our electrochemical system showed similar trends. Reactions optimized for amide solvents, such as the coupling of benzylic NHP esters with alkenyl bromides, provided the desired products, albeit with poor selectivity.<sup>5</sup> Reactions optimized for 1,4-dioxane as a solvent, such as the coupling of heteroaryl iodides with  $\alpha$ -chloronitriles, did not allow any current to pass before voltage overload.<sup>91</sup> It appears that our 1,4-dioxane-based asymmetric nickel-catalyzed reductive cross-couplings are not



currently amenable to electrochemical turnover, though the problem could likely be solved with further optimization, perhaps through judicious choice of a cosolvent system.

### 1.3 CONCLUDING REMARKS

Enantioselective cross-electrophile couplings are powerful methods for the synthesis of enantioenriched products from stable and readily accessible racemic precursors. This chemistry, as currently established, has numerous benefits but still suffers from some of the key challenges associated with metal powder reductants. Gratifyingly, translation of a metal powder-mediated reductive coupling into an electrochemical cell allowed for efficient turnover of the nickel catalyst to afford a variety of coupled products in good yields and enantioselectivities. This coupling of alkenyl bromides with benzylic chlorides represents the first example of an electrochemical, enantioselective nickel-catalyzed reductive cross coupling. Notably, the reaction proceeds efficiently without an excess of either coupling partner. The construction of a larger cell allowed for simple reaction scaleup, affording the coupled product on gram scale. Future studies could seek to better understand the mechanism of this transformation and render other enantioselective reductive couplings, especially those run in ethereal solvents, electroreductive.

### 1.4 EXPERIMENTAL SECTION

#### 1.4.1 *Materials and Methods*

Unless otherwise stated, reactions were performed under a N<sub>2</sub> atmosphere using freshly dried solvents. Tetrahydrofuran (THF), diethyl ether (Et<sub>2</sub>O), methylene chloride (CH<sub>2</sub>Cl<sub>2</sub>),

toluene (PhMe), hexanes, and benzene (C<sub>6</sub>H<sub>6</sub>) were dried by passing through activated alumina columns under a positive pressure of argon. Triethylamine (Et<sub>3</sub>N), diisopropylamine (*i*-Pr<sub>2</sub>NH), and trimethylsilyl chloride (TMSCl) were distilled over calcium hydride prior to use. Anhydrous *N,N*-dimethylacetamide (DMA) and anhydrous *N*-methylpyrrolidinone (NMP) were purchased from Sigma-Aldrich and stored under N<sub>2</sub>. **L1** was synthesized using the procedure reported by Reisman and coworkers.<sup>92</sup> Unless otherwise stated, chemicals and reagents were used as received. All reactions were monitored by thin-layer chromatography using EMD/Merck silica gel 60 F254 pre-coated plates (0.25 mm) and were visualized by UV, CAM, or KMnO<sub>4</sub> staining. Flash column chromatography was performed as described by Still et al. using silica gel (230-400 mesh, Silicycle) or 10% AgNO<sub>3</sub> doped silica gel (+230 mesh, Sigma Aldrich).<sup>93</sup> Purified compounds were dried on a high vacuum line (0.2 torr) to remove trace solvent. Optical rotations were measured on a Jasco P-2000 polarimeter using a 100 mm path-length cell at 589 nm. <sup>1</sup>H and <sup>13</sup>C NMR spectra were recorded on a Bruker Avance III HD with Prodigy cryoprobe (at 400 MHz and 101 MHz, respectively), a Varian 400 MR (at 400 MHz and 101 MHz, respectively), or a Varian Inova 500 (at 500 MHz and 126 MHz, respectively). <sup>1</sup>H NMR spectra were also recorded on a Varian Inova 300 (at 300 MHz). NMR data is reported relative to internal CHCl<sub>3</sub> (<sup>1</sup>H, δ = 7.26) and CDCl<sub>3</sub> (<sup>13</sup>C, δ = 77.0) Data for <sup>1</sup>H NMR spectra are reported as follows: chemical shift (δ ppm) (multiplicity, coupling constant (Hz), integration). Multiplicity and qualifier abbreviations are as follows: s = singlet, d = doublet, t = triplet, q = quartet, m = multiplet, br = broad. IR spectra were recorded on a Perkin Elmer Paragon 1000 spectrometer and are reported in frequency of absorption (cm<sup>-1</sup>). Analytical chiral SFC was performed with a Mettler SFC supercritical

CO<sub>2</sub> analytical chromatography system (CO<sub>2</sub> = 1450 psi, column temperature = 40 °C) with Chiralcel AD-H, OD-H, AS-H, OB-H, and OJ-H columns (4.6 mm x 25 cm). HRMS were acquired from the Caltech Mass Spectral Facility using fast-atom bombardment (FAB), electrospray ionization (ESI-TOF), or electron impact.

### **1.4.2 Construction of Electrochemical Cell for 0.6 mmol Scale Reactions**

Using a razor blade, a 5 mL (6 mL) NORM-JECT Luer Centric plastic syringe (**a**) was cut at the 1 mL mark to give a ~9 mm segment (**b**). The Luer tip was cut off (**c**). Using a 16 G (1.6 mm x 40 mm) needle, a ~3 mm in diameter hole was punctured next to the edge of the end of the syringe (**d**). A segment of 1/8" diameter zinc wire (99.9% pure, Rotometals) was pushed through the newly-created hole to widen it slightly (**e**). A 4 mm segment was cut from a rubber septum (for 14/20 joints, Ace Glass) (**f**, **g**). Using the same 16 G needle, several holes were poked through the septum (**h**). These holes were then punctured with the zinc wire (**i**). The septum was pushed into the syringe, with the wire going through side hole in the syringe. A ~4 mm segment was cut from the Luer tip and slid onto the zinc wire ~5 mm from the top (**j**). Directly across from the zinc wire, the syringe and septum were punctured with a 21 G (0.8 mm x 40 mm) needle (**k**). A piece of stainless steel wire was pushed through the needle (**l**). The needle was removed, leaving behind the wire (**m**). The lower end of the wire was bent into a hook shape (**n**). A 6 mm x 6 mm x 2 cm segment of reticulated vitreous carbon foam was cut using a razor blade (ERG Duocel, 100 PPI) (**o**). The RVC foam was punctured with the hook-shaped wire (**p**). The threaded top was cut off a 2-dram glass vial (before and after cutting shown, (**q**)). The electrode assembly was

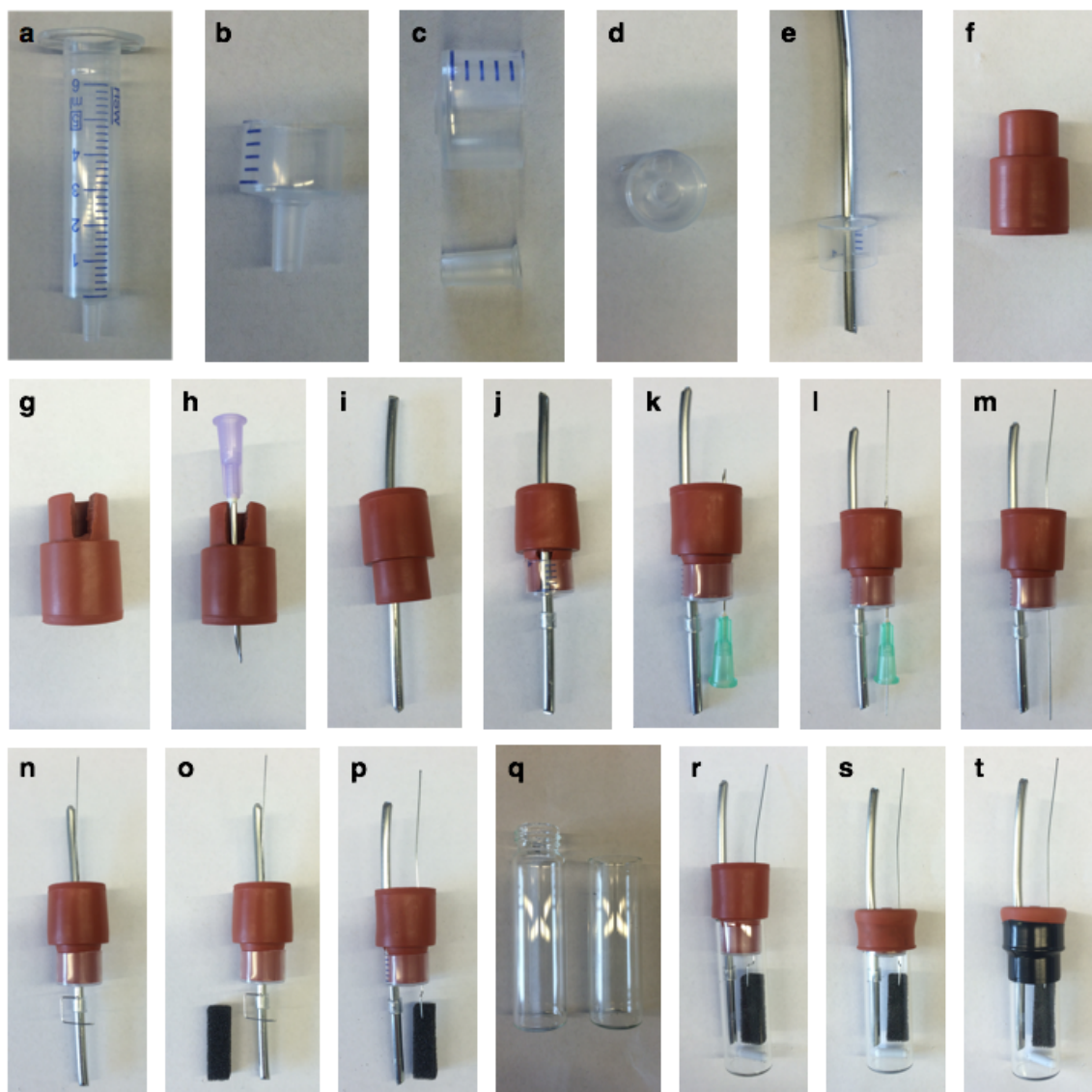
inserted into the vial (r). The septum was folded over the vial (s). The septum was sealed to the vial with electrical tape (t). Note: during operation, alligator clips from the potentiostat are connected directly to the wires. A needle for sparging is inserted through the center of the septum, then through the hole in the plastic (where the Luer tip used to be). The current density for this cell under a current of 10 mA was calculated as follows:

$$6\text{mm} \times 6\text{mm} \times 14\text{mm} = 5.04 \times 10^{-7} \text{m}^3 \text{ (volume of submerged electrode)}$$

$$100 \text{ppi RVC} = 2 \times 10^3 \frac{\text{ft}^2}{\text{ft}^3} = 6560 \frac{\text{m}^2}{\text{m}^3}$$

$$5.04 \times 10^{-7} \text{m}^3 \times 6560 \frac{\text{m}^2}{\text{m}^3} = 3.3 \times 10^{-3} \text{m}^2$$

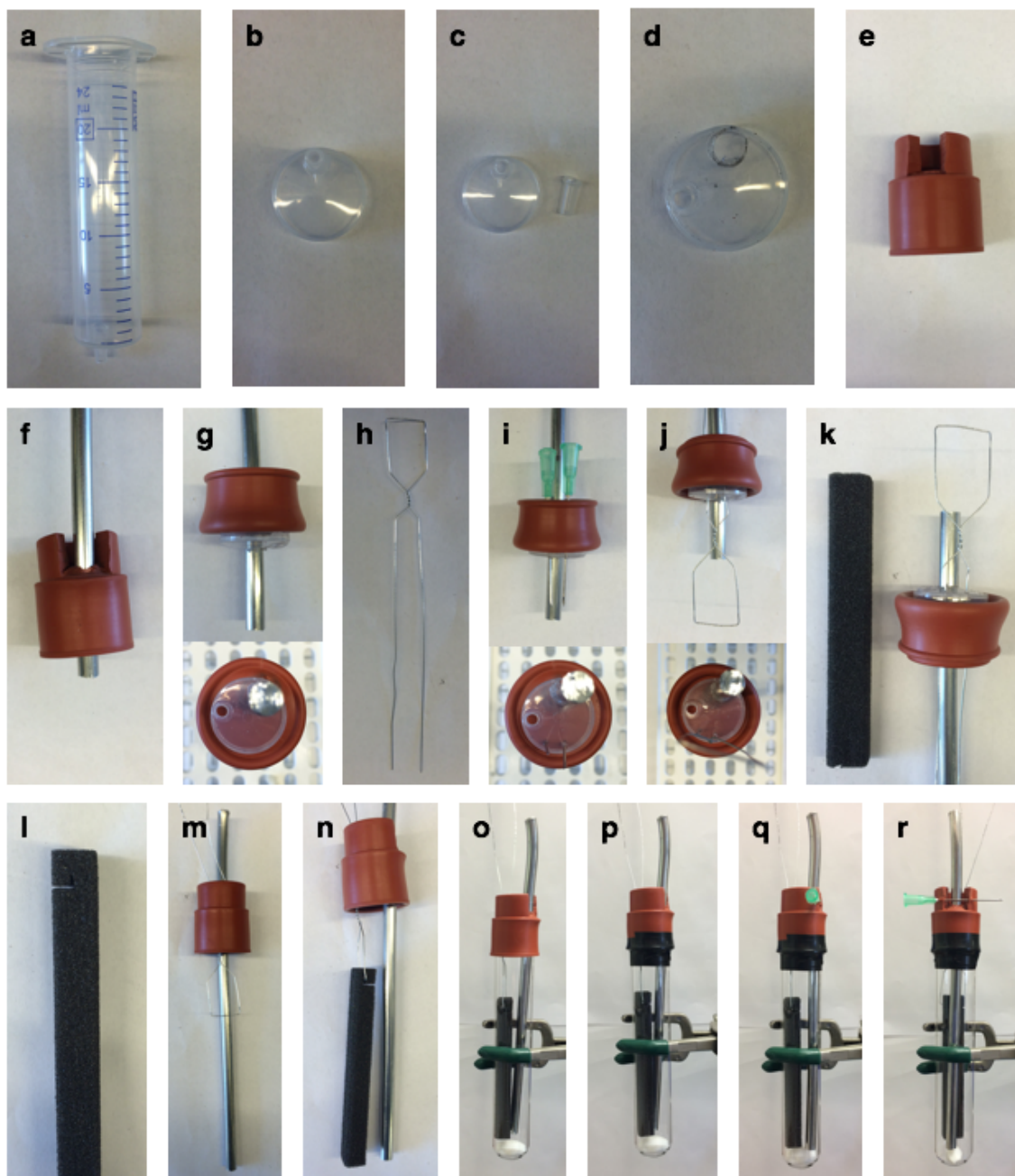
$$\frac{0.01 \text{A}}{3.3 \times 10^{-3} \text{m}^2} = 3.0 \frac{\text{A}}{\text{m}^2}$$



### 1.4.3 Construction of Electrochemical Cell for 6.0 mmol Scale Reactions

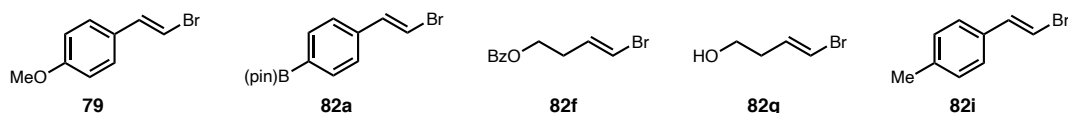
Using a razor blade, a 20 mL (24 mL) NORM-JECT Luer plastic syringe (**a**) was cut at the first marked graduation (**b**). The Luer tip was then cut off (**c**). A 6 mm diameter hole was cut near the edge of the plastic, using a 16 G (1.6 mm x 40 mm) needle (**d**). The hole was

then widened using a segment of 1/4" diameter zinc extruded rod (99.9%, Rotometals). A ~1 cm segment was cut from a rubber septum (for 24/40 joints, Ace Glass) (**e**). Several holes were punctured in the septum using the same 16 G needle (in the newly cut section), then the zinc rod was forced through the holes (**f**). The septum was folded up on itself, then the syringe piece was slid down the zinc rod (**g**, side and top views). A piece of stainless steel wire was bent into the shape shown (**h**) using pliers. Two 21 G (0.8 mm x 40 mm) needles were punctured through the septum and plastic, directly across from the zinc rod and ~5 mm apart from each other (**i**, side and top views). The two ends of the wire were pushed through the needles, then the needles were removed (**j**). A 12 mm x 10 mm x 9 cm segment of reticulated vitreous carbon foam was cut using a razor blade (ERG Duocel, 100 PPI) (**k**). Using a piece of wire, an L-shaped notch was cut through the end of the RVC (**l**). The zinc rod was pushed farther through the septum and plastic (**m**). The RVC electrode was hung from the wire, using the L-shaped notch (**n**). The electrode assembly was lowered into a 25 mm x 150 mm test tube (**o**). The septum was sealed to the tube with electrical tape (**p**). A 21 G (0.8 mm x 40 mm) needle was inserted through the cut edges of the septum, applying pressure to force the zinc rod to the edge of the test tube (**q**, **r**). Note: during operation, alligator clips from the potentiostat are connected directly to the wires, and to the needle that is touching the zinc wire. A needle for sparging is inserted through the septum, then through the hole in the plastic (where the Luer tip used to be).

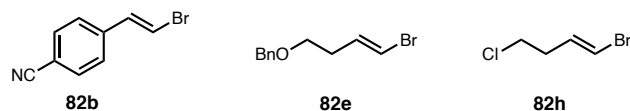


### 1.4.4 Substrate Preparation

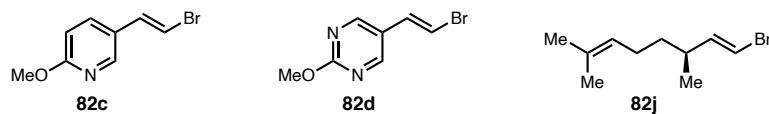
Alkenyl bromides **79**, **82a**, **82f**, **82g**, and **82i** were prepared according to literature procedures reported and referenced by Reisman and coworkers.<sup>81</sup>



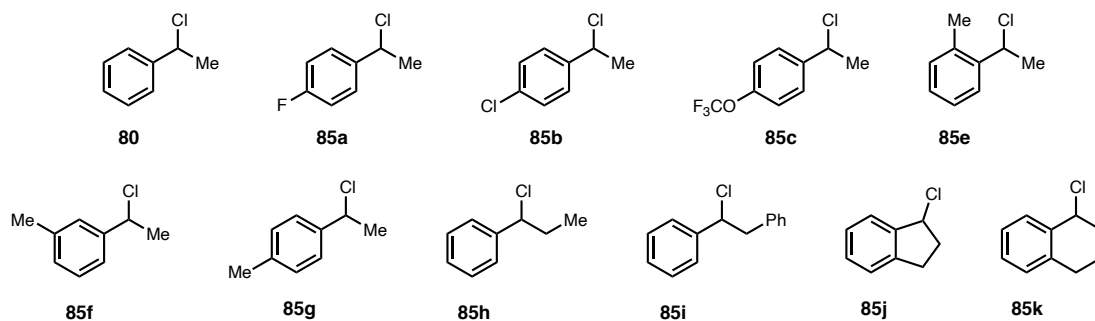
Alkenyl bromides **82b**, **82e**, and **82h** were prepared according to procedures reported and referenced by Reisman and coworkers.<sup>5</sup>



Alkenyl bromides **82c**, **82d**, and **82j** were prepared according to procedures reported and referenced by Reisman and coworkers.<sup>94</sup>

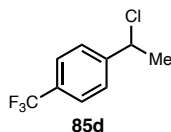


Benzyl Chlorides **80**, **85a–c**, and **85e–k** were prepared according to procedures reported and referenced by Reisman and coworkers.<sup>81</sup>

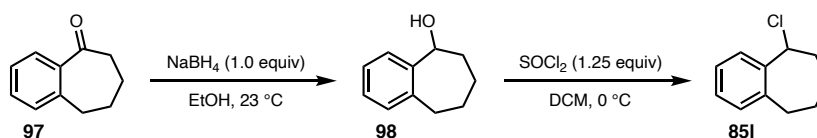




Benzyl chloride **85d** was prepared according to the procedure reported by Reisman and coworkers.<sup>95</sup>



### 5-chloro-6,7,8,9-tetrahydro-5H-benzo[7]annulene (**85i**)

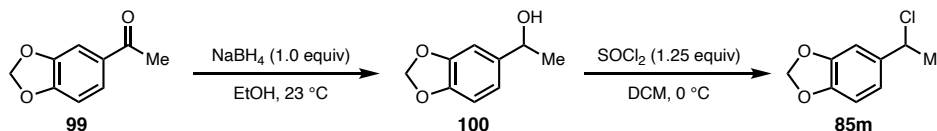


To a 20-mL vial equipped with a cross-shaped stir bar were added 6,7,8,9-tetrahydro-5H-benzo[7]annulen-5-one (**97**, 1.0 g, 6.24 mmol, 1.0 equiv) and absolute ethanol (6.25 mL). NaBH<sub>4</sub> (236 mg, 6.24 mmol, 1.0 equiv) was added in a single portion, and the reaction was allowed to stir at 23 °C under N<sub>2</sub> for 16 h. The reaction was quenched by the addition of 6.25 mL H<sub>2</sub>O and 6.25 mL sat. aq. NaCl. The reaction was extracted four times with EtOAc; combined organics were dried with anhydrous MgSO<sub>4</sub>, filtered, and concentrated to yield 6,7,8,9-tetrahydro-5H-benzo[7]annulen-5-ol (**98**, 962 mg, 95%) as a white amorphous solid. Spectral data matched those reported in the literature.<sup>96</sup>

To an oven-dried 100-mL round-bottomed flask equipped with a Teflon-coated stir bar were added 6,7,8,9-tetrahydro-5H-benzo[7]annulen-5-ol (**98**, 870 mg, 5.36 mmol, 1.0 equiv) and DCM (29 mL), under N<sub>2</sub>. The flask was cooled to 0 °C, then thionyl chloride (797 mg, 486 μL, 6.70 mmol, 1.25 equiv) was added dropwise via syringe over 5 minutes. The reaction was allowed to stir at 0 °C for 1 h, then concentrated on a rotovap. The resulting crude oil was rapidly passed through a short silica plug, eluting with hexanes to yield 5-chloro-6,7,8,9-tetrahydro-5H-benzo[7]annulene (**85i**, 862 mg, 89%) as a colorless

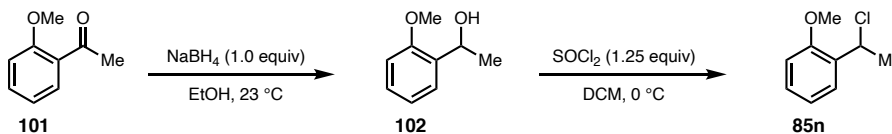
oil. Spectral data matched those reported in the literature, with 5.7 mol % eliminated styrene byproduct.<sup>97</sup>

### 5-(1-chloroethyl)benzo[*d*][1,3]dioxole (**85m**)



To a 20-mL vial equipped with a cross-shaped stir bar were added 1-(benzo[*d*][1,3]dioxol-5-yl)ethan-1-one (**99**, 1.64 g, 10.0 mmol, 1.0 equiv) and absolute ethanol (10 mL). NaBH<sub>4</sub> (378 mg, 10.0 mmol, 1.0 equiv) was added in a single portion, and the reaction was allowed to stir at 23 °C under N<sub>2</sub> for 16 h. The reaction was quenched by the addition of 10 mL H<sub>2</sub>O and 10 mL sat. aq. NaCl. The reaction was extracted four times with EtOAc; combined organics were dried with anhydrous MgSO<sub>4</sub>, filtered, and concentrated to yield 1-(benzo[*d*][1,3]dioxol-5-yl)ethan-1-ol (**100**, 1.60 g, 96%) as a colorless oil. Spectral data matched those reported in the literature.<sup>98</sup>

To an oven-dried 100-mL round-bottomed flask equipped with a Teflon-coated stir bar were added 1-(benzo[*d*][1,3]dioxol-5-yl)ethan-1-ol (**100**, 1.57 g, 9.45 mmol, 1.0 equiv) and DCM (51 mL), under N<sub>2</sub>. The flask was cooled to 0 °C, then thionyl chloride (1.40 g, 857 μL, 11.8 mmol, 1.25 equiv) was added dropwise via syringe over 5 minutes. The reaction was allowed to stir at 0 °C for 1 h, then concentrated on a rotovap. The resulting crude oil was rapidly passed through a short silica plug, eluting with 50% EtOAc/hexanes to yield 5-chloro-6,7,8,9-tetrahydro-5*H*-benzo[7]annulene (**85m**, 1.55 g, 89%) as a colorless oil. Spectral data matched those reported in the literature.<sup>99</sup>

**1-(1-chloroethyl)-2-methoxybenzene (85n)**

To a 20-mL vial equipped with a cross-shaped stir bar were added 1-(2-methoxyphenyl)ethan-1-one (**101**, 1.50 g, 10.0 mmol, 1.0 equiv) and absolute ethanol (10 mL). NaBH<sub>4</sub> (378 mg, 10.0 mmol, 1.0 equiv) was added in a single portion, and the reaction was allowed to stir at 23 °C under N<sub>2</sub> for 16 h. The reaction was quenched by the addition of 10 mL H<sub>2</sub>O and 10 mL sat. aq. NaCl. The reaction was extracted four times with EtOAc; combined organics were dried with anhydrous MgSO<sub>4</sub>, filtered, and concentrated. The resulting crude oil was purified by column chromatography (20% EtOAc/hexanes) to yield 1-(2-methoxyphenyl)ethan-1-ol (**102**, 1.45 g, 95%) as a colorless oil. Spectral data matched those reported in the literature.<sup>100</sup>

To an oven-dried 100-mL round-bottomed flask equipped with a Teflon-coated stir bar were added 1-(2-methoxyphenyl)ethan-1-ol (**102**, 1.44 g, 9.46 mmol, 1.0 equiv) and DCM (51 mL), under N<sub>2</sub>. The flask was cooled to 0 °C, then thionyl chloride (1.41 g, 858 μL, 11.8 mmol, 1.25 equiv) was added dropwise via syringe over 5 minutes. The reaction was allowed to stir at 0 °C for 1 h, then concentrated on a rotovap. The resulting crude oil was rapidly passed through a short silica plug, eluting with 10% Et<sub>2</sub>O/hexanes to yield 1-(1-chloroethyl)-2-methoxybenzene (**85n**, 1.51 g, 93%) as a colorless oil. Spectral data matched those reported in the literature.<sup>101</sup>

### 1.4.5 Electroreductive Cross-Couplings

#### General Procedure 1: Reaction on 0.6 mmol Scale

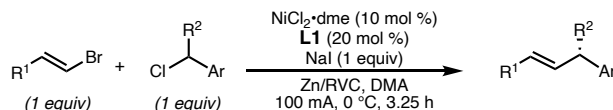


On the bench-top, a 2-dram vial with the threads cut off (see photos in Construction of Electrochemical Cells, above) was equipped with a stir bar, and the alkenyl bromide (0.60 mmol, 1 equiv), **L1** (42.8 mg, 0.12 mmol, 0.20 equiv), NiCl<sub>2</sub>·dme (13.2 mg, 0.06 mmol, 0.10 equiv), and NaI (90.0 mg, 0.60 mmol, 1.0 equiv) were added. The vial was sealed with a septum, then DMA (3.0 mL) was added via syringe, under Ar. The reaction was stirred and sparged with Ar for 3 min. The benzyl chloride (0.60 mmol, 1 equiv) was added via syringe in a single portion. The septum was quickly removed and an RVC cathode and Zn anode (as described in Construction of Electrochemical Cells, above) were inserted into the vial. The new septum was sealed with electrical tape, and the reaction was sparged with argon for an additional 2 min. The reaction was cooled to 0 °C and electrolyzed at 10 mA for 3.25 hours. The electrodes were removed from the cell and rinsed into a separatory funnel with Et<sub>2</sub>O and H<sub>2</sub>O. The reaction was transferred to this separatory funnel and quenched with 2.5 mL 1 N aqueous HCl. The contents were further diluted with Et<sub>2</sub>O and H<sub>2</sub>O; the aqueous layer was then extracted twice more with Et<sub>2</sub>O. Combined organics were washed with 1 M aqueous LiCl, dried with anhydrous MgSO<sub>4</sub>, filtered, and concentrated.

**Notes:** Both electrodes could be reused a significant number of time if cleaned properly. The RVC cathode was immediately rinsed sequentially with acetone, water, acetone, and

*Et*<sub>2</sub>O, before drying with a heat gun. The Zn anode was submerged in 1 M aqueous HCl for ~1 min, until all the black oxide had dissolved (gas evolved). The anode was then rinsed with water, followed by acetone. The vial was washed with sequentially acetone, soapy water, DI water, and acetone, then dried in an oven. Comparable yield and enantioselectivity were obtained if N<sub>2</sub> was used in place of Ar (84% yield, 93% ee for **81**). When the reaction was conducted open to air, **81** was only obtained in 17% yield and 55% ee.

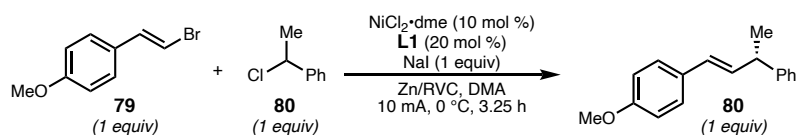
### General Procedure 2: Reaction on 06.0 mmol Scale



A 25 x 150 mm test tube equipped with an oval Teflon-coated stir bar was dried overnight in an oven, sealed with a septum, then cooled under argon. The alkenyl bromide (0.60 mmol, 1 equiv), L1 (428 mg, 1.2 mmol, 0.20 equiv), NiCl<sub>2</sub>·dme (132 mg, 0.060 mmol, 0.10 equiv), and NaI (900 mg, 6.0 mmol, 1.0 equiv) were added. The tube was sealed with a septum and electrical tape, then DMA (30 mL) was added via syringe, under argon. The reaction was sparged with argon while stirring for 10 min. The benzylic chloride (6.0 mmol, 1.0 equiv) was added via syringe in a single portion. The septum was removed and quickly replaced with a septum fit with a Zn anode and RVC cathode (see Construction of Electrochemical Cell, above). This septum was sealed to the tube with electrical tape, then the reaction was sparged with argon for an additional 5 min. The reaction was cooled to 0 °C and electrolyzed at 100 mA for 3.25 hours. *Caution: extreme care must be taken*

*not to touch the electrodes while this dangerous current is flowing.* The electrodes were removed from the cell and rinsed into a separatory funnel with Et<sub>2</sub>O and H<sub>2</sub>O. The reaction was transferred to this separatory funnel and quenched with 15 mL 1 N aqueous HCl. The contents were further diluted with Et<sub>2</sub>O (300 mL) and H<sub>2</sub>O (200 mL); the aqueous layer was then extracted twice more with Et<sub>2</sub>O (2 x 200 mL). Combined organics were washed with 1 M aqueous LiCl (200 mL), dried with anhydrous MgSO<sub>4</sub>, filtered, and concentrated. *Note: These electrodes could be rinsed and reused using the same procedure described above for the 0.6 mmol scale reaction.*

### Procedure for Kinetic Analysis



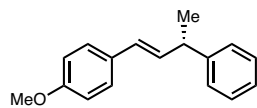
A 5-mL volumetric flask was oven-dried and cooled under nitrogen. To this flask were added (E)-1-(2-bromovinyl)-4-methoxybenzene (**79**, 213 mg, 1.0 mmol), **L1** (71.3 mg, 0.2 mmol), NiCl<sub>2</sub>·dme (22.0 mg, 0.1 mmol), and NaI (150 mg, 1.0 mmol). Anhydrous DMA (1 mL) was added to the flask to reach 5 mL total solution volume. A 5-mL oven-dried IKA Electrasyn vial was sealed with a rubber septum and cooled under nitrogen. 3.0 mL of the reaction stock solution was added to the Electrasyn vial via syringe (0.6 mmol scale reaction). The reaction was sparged with argon for 3 minutes. (1-chloroethyl)benzene (**80**, 84.4 mg, 0.6 mmol) was added to the reaction via syringe. The septum was quickly removed and replaced with an Electrasyn cap fitted with a RVC cathode (6 x 4 x 35 mm) and Zn anode. The reaction was cooled to 0 °C and sparged for an additional 2 minutes

with argon. Dibenzyl ether (29.7 mg, 0.15 mmol) was added via syringe as an internal standard. The reaction was stirred at 600 rpm for an additional minute to homogenize, then an aliquot (~20  $\mu$ L) was removed from the reaction with a hypodermic (1 mL) syringe. Immediately after removing this  $t = 0$  aliquot, the reaction was electrolyzed at 10 mA for 3.25 hours, stirring at 600 rpm and maintaining a 0  $^{\circ}$ C bath for the course of the reaction. An aliquot (~20  $\mu$ L) was removed every 15 minutes via syringe, *taking care to never touch the metal of the syringe*. Each aliquot was processed immediately after removal from the reaction: The aliquot was diluted with 0.4 mL 20% EtOAc/hexanes, then pushed through a ~1 cm silica plug in a pipette, further eluting with 1 mL 20% EtOAc/hexanes.

The aliquots were analyzed by gas chromatography equipped with a flame ionization detector (GC-FID) Helium was used as the carrier gas, with a constant pressure of 25.0 psi. An Agilent HP-1 column was used (30 m length, 0.320 mm diameter, 0.25  $\mu$ m film). The column was held at 50  $^{\circ}$ C for 2 minutes, then ramped to 250  $^{\circ}$ C at a rate of 25  $^{\circ}$ C/min. The temperature was then held at 250  $^{\circ}$ C for 5 min. The temperature of the injector was held at 250  $^{\circ}$ C and the temperature of the detector was held at 300  $^{\circ}$ C.

### 1.4.6 Characterization of Reaction Products

#### (*S,E*)-1-methoxy-4-(3-phenylbut-1-en-1-yl)benzene (**81**)



Prepared from (*E*)-1-(2-bromovinyl)-4-methoxybenzene (**79**, 127.8 mg, 0.6 mmol) and (1-chloroethyl)benzene (**80**, 84.4 mg, 0.6 mmol)

according to General Procedure 1. The crude residue was purified by column

chromatography (silica, 20% toluene/hexanes) to yield **81** (119.7 mg, 84% yield) in 94% ee as a colorless oil.

$R_f = 0.48$  (silica, 30% PhMe/hexanes, UV).

**Chiral SFC:** (OB-H), 2.5 mL/min, 20% IPA in CO<sub>2</sub>,  $\lambda = 280$  nm):  $t_R$  (major) = 6.8 min,  $t_R$  (minor) = 8.0 min.

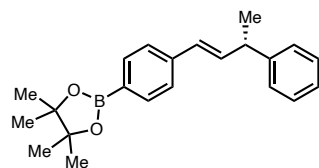
$[\alpha]_D^{23} = -51^\circ$  (c = 1.0, CHCl<sub>3</sub>).

**<sup>1</sup>H NMR (400 MHz, CDCl<sub>3</sub>):**  $\delta$  7.36 – 7.27 (m, 6H), 7.25 – 7.20 (m, 1H), 6.88 – 6.81 (m, 2H), 6.37 (d,  $J = 15.9$  Hz, 1H), 6.26 (dd,  $J = 15.9, 6.6$  Hz, 1H), 3.81 (s, 3H), 3.68 – 3.59 (m, 1H), 1.47 (d,  $J = 7.0$  Hz, 3H).

**<sup>13</sup>C NMR (101 MHz, CDCl<sub>3</sub>):**  $\delta$  158.9, 146.0, 133.3, 130.5, 128.6, 128.0, 127.4, 127.4, 126.3, 114.0, 55.4, 42.7, 21.5.

**Reaction on 6.0 mmol scale.** Prepared from (*E*)-1-(2-bromovinyl)-4-methoxybenzene (**79**, 1.28 g, 6.0 mmol) and (1-chloroethyl)benzene (**80**, 844 mg, 6.0 mmol) according to General Procedure 2. The crude residue was purified by column chromatography (silica, 20% toluene/hexanes) to yield **81** (1.191 g, 83% yield) in 91% ee as a colorless oil.

**(*S,E*)-4,4,5,5-tetramethyl-2-(4-(3-phenylbut-1-en-1-yl)phenyl)-1,3,2-dioxaborolane (**84a**)**



Prepared from (*E*)-2-(4-(2-bromovinyl)phenyl)-4,4,5,5-tetramethyl-1,3,2-dioxaborolane (**82a**, 185.4 mg, 0.6 mmol) and (1-chloroethyl)benzene (**80**, 84.4 mg, 0.6 mmol) according to



General Procedure 1. The crude residue was purified by column chromatography (silica, 20-50% toluene/hexanes) to yield **84a** (123.8 mg, 62% yield) in 91% ee as a white amorphous solid.

$R_f$  = 0.55 (silica, 70% PhMe/hexanes, UV).

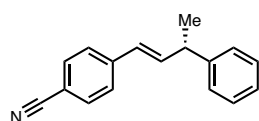
**Chiral SFC:** (OJ-H), 2.5 mL/min, 15% IPA in CO<sub>2</sub>,  $\lambda$  = 254 nm):  $t_R$  (major) = 3.9 min,  $t_R$  (minor) = 7.2 min.

$[\alpha]_D^{23}$  = -38° (c = 1.0, CHCl<sub>3</sub>).

**<sup>1</sup>H NMR (400 MHz, CDCl<sub>3</sub>):**  $\delta$  7.76 – 7.71 (m, 2H), 7.39 – 7.26 (m, 6H), 7.25 – 7.20 (m, 1H), 6.48 (dd,  $J$  = 15.9, 5.8 Hz, 1H), 6.42 (d,  $J$  = 16.0 Hz, 1H), 3.70 – 3.61 (m, 1H), 1.48 (d,  $J$  = 7.0 Hz, 3H), 1.35 (s, 12H).

**<sup>13</sup>C NMR (101 MHz, CDCl<sub>3</sub>):**  $\delta$  145.6, 140.5, 136.5, 135.1, 128.7, 128.6, 127.5, 126.4, 125.6, 83.8, 42.8, 25.0, 21.3.

#### (*S,E*)-4-(3-phenylbut-1-en-1-yl)benzotrile (**84b**)



Prepared from (*E*)-4-(2-bromovinyl)benzotrile (**82b**, 124.8 mg, 0.6 mmol) and (1-chloroethyl)benzene (**80**, 84.4 mg, 0.6 mmol) according to General Procedure 1. The crude residue was purified by column chromatography (silica, 1-3% Et<sub>2</sub>O/hexanes) to yield **84b** (100.3 mg, 72% yield) in 88% ee as a colorless oil.

$R_f$  = 0.40 (silica, 10% EtOAc/hexanes, UV).

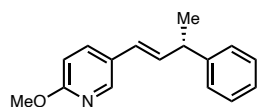
**Chiral SFC:** (OB-H), 2.5 mL/min, 10% IPA in CO<sub>2</sub>,  $\lambda$  = 280 nm):  $t_R$  (minor) = 9.4 min,  $t_R$  (major) = 10.0 min.

$[\alpha]_D^{24} = -51^\circ$  (c = 1.0, CHCl<sub>3</sub>).

**<sup>1</sup>H NMR (400 MHz, CDCl<sub>3</sub>):** δ 7.59 – 7.54 (m, 2H), 7.45 – 7.39 (m, 2H), 7.38 – 7.31 (m, 2H), 7.29 – 7.21 (m, 3H), 6.53 (dd, *J* = 15.9, 6.7 Hz, 1H), 6.41 (dd, *J* = 16.0, 0.5 Hz, 1H), 3.73 – 3.62 (m, 1H), 1.48 (d, *J* = 7.0 Hz, 3H).

**<sup>13</sup>C NMR (101 MHz, CDCl<sub>3</sub>):** δ 144.8, 142.2, 139.5, 132.5, 128.8, 127.4, 127.3, 126.8, 126.7, 119.2, 110.4, 42.8, 21.0.

**(*S,E*)-2-methoxy-5-(3-phenylbut-1-en-1-yl)pyridine (84c)**



Prepared from (*E*)-5-(2-bromovinyl)-2-methoxypyridine (**82c**, 128.4 mg, 0.6 mmol) and (1-chloroethyl)benzene (**80**, 84.4 mg, 0.6 mmol)

according to General Procedure 1. The crude residue was purified by column chromatography (silica, 0-5% Et<sub>2</sub>O/hexanes) to yield **84c** (111.3 mg, 78% yield) in 93% ee as a colorless oil.

**R<sub>f</sub>** = 0.36 (silica, 7% Et<sub>2</sub>O/hexanes, UV).

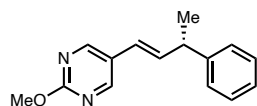
**Chiral SFC:** (OB-H), 2.5 mL/min, 20% IPA in CO<sub>2</sub>, λ = 280 nm): *t<sub>R</sub>* (major) = 3.7 min, *t<sub>R</sub>* (minor) = 5.1 min.

$[\alpha]_D^{23} = -43^\circ$  (c = 1.0, CHCl<sub>3</sub>).

**<sup>1</sup>H NMR (500 MHz, CDCl<sub>3</sub>):** δ 8.07 (d, *J* = 2.4 Hz, 1H), 7.64 (dd, *J* = 8.7, 2.5 Hz, 1H), 7.36 – 7.30 (m, 2H), 7.29 – 7.25 (m, 2H), 7.25 – 7.20 (m, 1H), 6.68 (d, *J* = 8.6 Hz, 1H), 6.35 (dd, *J* = 16.0, 0.5 Hz, 1H), 6.27 (dd, *J* = 15.9, 6.5 Hz, 1H), 3.93 (s, 3H), 3.67 – 3.61 (m, 1H), 1.48 (d, *J* = 7.0 Hz, 3H).

<sup>13</sup>C NMR (126 MHz, CDCl<sub>3</sub>): δ 163.4, 145.6, 145.3, 135.5, 134.8, 128.7, 127.4, 126.8, 126.4, 124.7, 110.9, 53.6, 42.8, 21.3.

**(*S,E*)-2-methoxy-5-(3-phenylbut-1-en-1-yl)pyridine (84d)**



Prepared from (*E*)-5-(2-bromovinyl)-2-methoxypyrimidine (**82d**, 129.0 mg, 0.6 mmol) and (1-chloroethyl)benzene (**80**, 84.4 mg, 0.6

mmol) according to General Procedure 1. The crude residue was purified by column chromatography (silica, 1:1:3 toluene/Et<sub>2</sub>O/hexanes) to yield **84d** (82.0 mg, 57% yield) in 87% ee as a colorless oil.

*R<sub>f</sub>* = 0.32 (silica, 1:1:2 PhMe/Et<sub>2</sub>O/hexanes, UV).

**Chiral SFC:** (OB-H), 2.5 mL/min, 20% IPA in CO<sub>2</sub>, λ = 280 nm): *t<sub>R</sub>* (major) = 5.4 min, *t<sub>R</sub>* (minor) = 6.1 min.

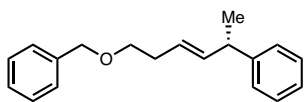
[α]<sub>D</sub><sup>23</sup> = -38° (c = 1.0, CHCl<sub>3</sub>).

<sup>1</sup>H NMR (500 MHz, CDCl<sub>3</sub>): δ 8.48 (s, 2H), 7.36 – 7.31 (m, 2H), 7.28 – 7.21 (m, 3H), 6.38 (dd, *J* = 16.0, 6.6 Hz, 1H), 6.26 (dd, *J* = 16.0, 1.3 Hz, 1H), 4.00 (s, 3H), 3.69 – 3.62 (m, 1H), 1.48 (d, *J* = 7.0 Hz, 3H).

<sup>13</sup>C NMR (126 MHz, CDCl<sub>3</sub>): δ 164.8, 156.7, 144.9, 137.0, 128.8, 127.4, 126.6, 125.2, 121.4, 55.1, 42.9, 21.1.

**FTIR (NaCl, thin film, cm<sup>-1</sup>):** 3025, 2962, 2926, 1592, 1555, 1471, 1455, 1410, 1325, 1045, 1029.

**HRMS (TOF-ESI, *m/z*):** calc'd for C<sub>15</sub>H<sub>17</sub>ON<sub>2</sub> [M+H]<sup>+</sup>: 241.1341; found: 241.1348.

**(*S,E*)-6-(benzyloxy)hex-3-en-2-yl)benzene (84e)**

Prepared from (*E*)-(((4-bromobut-3-en-1-yl)oxy)methyl)-benzene (**82e**, 144.7 mg, 0.6 mmol) and (1-chloroethyl)benzene

(**80**, 84.4 mg, 0.6 mmol) according to General Procedure 1. The crude residue was purified by column chromatography (silica, 2% Et<sub>2</sub>O/hexanes) to yield **84e** (119.6 mg, 75% yield) in 93% ee as a colorless oil.

$R_f$  = 0.44 (silica, 3% Et<sub>2</sub>O/hexanes, KMnO<sub>4</sub>).

**Chiral SFC:** (OD-H), 2.5 mL/min, 5% IPA in CO<sub>2</sub>,  $\lambda$  = 210 nm):  $t_R$  (major) = 8.1 min,  $t_R$  (minor) = 8.9 min.

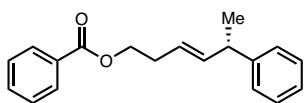
$[\alpha]_D^{24}$  = +6° (c = 1.0, CHCl<sub>3</sub>).

**<sup>1</sup>H NMR (400 MHz, CDCl<sub>3</sub>):**  $\delta$  7.40 – 7.26 (m, 7H), 7.25 – 7.17 (m, 3H), 5.71 (ddt,  $J$  = 15.4, 6.7, 1.4 Hz, 1H), 5.50 (dtd,  $J$  = 15.2, 6.7, 1.3 Hz, 1H), 4.53 (s, 2H), 3.52 (t,  $J$  = 6.8 Hz, 2H), 3.49 – 3.41 (m, 1H), 2.37 (qt,  $J$  = 6.8, 1.1 Hz, 2H), 1.36 (d,  $J$  = 7.0 Hz, 3H).

**<sup>13</sup>C NMR (101 MHz, CDCl<sub>3</sub>):**  $\delta$  146.3, 138.7, 137.2, 128.5, 127.8, 127.6, 127.3, 126.1, 125.4, 73.0, 70.2, 42.4, 33.2, 21.5.

**FTIR (NaCl, thin film, cm<sup>-1</sup>):** 3027, 2964, 2928, 2854, 1493, 1453, 1362, 1100, 969, 735, 698.

**HRMS (TOF-ESI,  $m/z$ ):** calc'd for C<sub>19</sub>H<sub>21</sub>O [M+H-H<sub>2</sub>]<sup>+</sup>: 265.1592; found: 265.1600.

**(*S,E*)-5-phenylhex-3-en-1-yl benzoate (84f)**

Prepared from (*E*)-4-bromobut-3-en-1-yl benzoate (**82f**, 153.1 mg, 0.6 mmol) and (1-chloroethyl)benzene (**80**, 84.4 mg, 0.6

mmol) according to General Procedure 1. The crude residue was purified by column chromatography (silica, 2% Et<sub>2</sub>O/hexanes) to yield **84f** (121.3 mg, 72% yield) in 95% ee as a colorless oil.

$R_f$  = 0.35 (silica, 3% Et<sub>2</sub>O/hexanes, KMnO<sub>4</sub>).

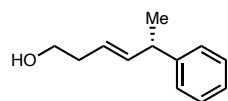
**Chiral SFC:** (OJ-H), 2.5 mL/min, 10% IPA in CO<sub>2</sub>,  $\lambda$  = 280 nm):  $t_R$  (major) = 4.8 min,  $t_R$  (minor) = 5.7 min.

$[\alpha]_D^{24}$  = +3° (c = 1.0, CHCl<sub>3</sub>).

**<sup>1</sup>H NMR (400 MHz, CDCl<sub>3</sub>):**  $\delta$  8.10 – 8.05 (m, 2H), 7.64 – 7.58 (m, 1H), 7.52 – 7.45 (m, 2H), 7.35 – 7.28 (m, 2H), 7.28 – 7.20 (m, 3H), 5.82 (ddt,  $J$  = 15.4, 6.8, 1.4 Hz, 1H), 5.58 (dtd,  $J$  = 15.2, 6.8, 1.3 Hz, 1H), 4.41 (td,  $J$  = 6.7, 1.4 Hz, 2H), 3.56 – 3.46 (m, 1H), 2.55 (qt,  $J$  = 6.8, 1.0 Hz, 2H), 1.40 (d,  $J$  = 7.0 Hz, 3H).

**<sup>13</sup>C NMR (101 MHz, CDCl<sub>3</sub>):**  $\delta$  166.7, 146.0, 138.3, 133.0, 130.5, 129.7, 128.5, 128.4, 127.3, 126.2, 124.3, 64.4, 42.4, 32.2, 21.4.

#### (*S,E*)-5-phenylhex-3-en-1-ol (**84g**)



Prepared from (*E*)-4-bromobut-3-en-1-ol (**82g**, 90.6 mg, 0.6 mmol) and (1-chloroethyl)benzene (**80**, 84.4 mg, 0.6 mmol) according to General

Procedure 1. The crude residue was purified by column chromatography (silica, 10-20% EtOAc/hexanes) to yield **84g** (59.2 mg, 56% yield) in 93% ee as a colorless oil.

$R_f$  = 0.55 (silica, 30% EtOAc/hexanes, KMnO<sub>4</sub>).

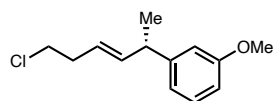
**Chiral SFC:** (OJ-H), 2.5 mL/min, 2% MeOH in CO<sub>2</sub>,  $\lambda$  = 210 nm):  $t_R$  (major) = 10.2 min,  $t_R$  (minor) = 11.4 min.

$[\alpha]_D^{24} = +12^\circ$  (c = 1.0, CHCl<sub>3</sub>).

**<sup>1</sup>H NMR (400 MHz, CDCl<sub>3</sub>):** δ 7.35 – 7.27 (m, 2H), 7.25 – 7.16 (m, 3H), 5.76 (ddt, *J* = 15.4, 6.7, 1.3 Hz, 1H), 5.45 (dtd, *J* = 15.4, 7.0, 1.4 Hz, 1H), 3.65 (t, *J* = 6.3 Hz, 2H), 3.52 – 3.41 (m, 1H), 2.35 – 2.26 (m, 2H), 1.43 (s, 1H), 1.36 (d, *J* = 7.0 Hz, 3H).

**<sup>13</sup>C NMR (101 MHz, CDCl<sub>3</sub>):** δ 146.1, 138.8, 128.6, 127.2, 126.2, 124.8, 62.2, 42.5, 36.1, 21.6.

**(*S,E*)-1-(6-chlorohex-3-en-2-yl)-3-methoxybenzene (84h)**



Prepared from (*E*)-1-bromo-3-chloroprop-1-ene (**82h**, 101.7 mg, 0.6 mmol) and 1-(1-chloroethyl)-3-methoxybenzene (**83**, 102.4 mg,

0.6 mmol) according to General Procedure 1. The crude residue was purified by column chromatography (silica, 10-12% toluene/hexanes) to yield **84h** (95.5 mg, 71% yield) in 92% ee as a colorless oil.

$R_f = 0.35$  (silica, 15% PhMe/hexanes, UV).

**Chiral SFC:** (OJ-H), 2.5 mL/min, 1% IPA in CO<sub>2</sub>, λ = 280 nm): *t*<sub>R</sub> (minor) = 6.7 min, *t*<sub>R</sub> (major) = 7.2 min.

$[\alpha]_D^{24} = +7^\circ$  (c = 1.0, CHCl<sub>3</sub>).

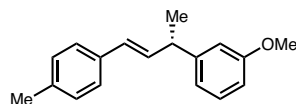
**<sup>1</sup>H NMR (400 MHz, CDCl<sub>3</sub>):** δ 7.25 – 7.20 (m, 1H), 6.84 – 6.73 (m, 3H), 5.73 (ddt, *J* = 15.4, 6.7, 1.3 Hz, 1H), 5.48 (dtd, *J* = 15.2, 6.8, 1.4 Hz, 1H), 3.81 (s, 3H), 3.54 (t, *J* = 7.0 Hz, 2H), 3.48 – 3.39 (m, 1H), 2.49 (qt, *J* = 6.9, 1.0 Hz, 2H), 1.35 (d, *J* = 7.0 Hz, 3H).

**<sup>13</sup>C NMR (101 MHz, CDCl<sub>3</sub>):** δ 159.8, 147.7, 138.3, 129.5, 124.7, 119.7, 113.2, 111.3, 55.3, 44.5, 42.4, 35.9, 21.4.

**FTIR (NaCl, thin film,  $\text{cm}^{-1}$ ):** 2962, 2929, 1600, 1584, 1486, 1454, 1435, 1260, 1151, 1042, 969, 699.

**HRMS (TOF-ESI,  $m/z$ ):** calc'd for  $\text{C}_{13}\text{H}_{17}\text{OCl}$   $[\text{M}+\bullet]^+$ : 224.0968; found: 224.0961.

**(*S,E*)-1-methoxy-3-(4-(*p*-tolyl)but-3-en-2-yl)benzene (**84i**)**



Prepared from (*E*)-1-(2-bromovinyl)-4-methylbenzene (**82i**, 118.3 mg, 0.6 mmol) and 1-(1-chloroethyl)-3-methoxybenzene (**83**, 102.4 mg, 0.6 mmol) according to General Procedure 1. The crude residue was purified by column chromatography (silica, 10-14% toluene/hexanes) to yield **84i** (123.7 mg, 82% yield) in 92% ee as a colorless oil.

$R_f$  = 0.50 (silica, 30% PhMe/hexanes, UV).

**Chiral SFC:** (OJ-H), 2.5 mL/min, 15% IPA in  $\text{CO}_2$ ,  $\lambda$  = 254 nm):  $t_R$  (minor) = 4.9 min,  $t_R$  (major) = 6.2 min.

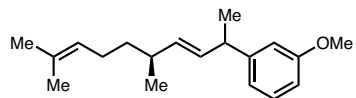
$[\alpha]_D^{24}$  =  $-43^\circ$  ( $c$  = 1.0,  $\text{CHCl}_3$ ).

**$^1\text{H}$  NMR (400 MHz,  $\text{CDCl}_3$ ):**  $\delta$  7.32 – 7.27 (m, 3H), 7.17 – 7.11 (m, 2H), 6.94 – 6.89 (m, 1H), 6.88 – 6.85 (m, 1H), 6.80 (ddd,  $J$  = 8.2, 2.7, 0.9 Hz, 1H), 6.44 (d,  $J$  = 16.0 Hz, 1H), 6.36 (dd,  $J$  = 15.9, 6.3 Hz, 1H), 3.84 (s, 3H), 3.69 – 3.60 (m, 1H), 2.36 (s, 3H), 1.49 (d,  $J$  = 7.0 Hz, 3H).

**$^{13}\text{C}$  NMR (101 MHz,  $\text{CDCl}_3$ ):**  $\delta$  159.8, 147.7, 136.9, 134.9, 134.1, 129.5, 129.3, 128.5, 126.2, 119.9, 113.4, 111.4, 55.3, 42.7, 21.4, 21.3.

**FTIR (NaCl, thin film,  $\text{cm}^{-1}$ ):** 2964, 2924, 1608, 1600, 1584, 1513, 1486, 1454, 1260, 1158, 1045, 968, 802, 699.

**HRMS (TOF-ESI,  $m/z$ ):** calc'd for  $\text{C}_{18}\text{H}_{20}\text{O}$   $[\text{M}+\bullet]^+$ : 252.1514; found: 252.1524.

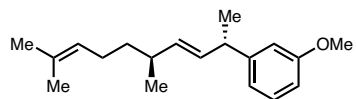
**1-((5*S*,*E*)-5,9-dimethyldeca-3,8-dien-2-yl)-3-methoxybenzene (84j)**

Prepared from (*S*,*E*)-1-bromo-3,7-dimethylocta-1,6-diene (**82j**, 130.3 mg, 0.6 mmol) and 1-(1-chloroethyl)-3-methoxybenzene (**83**, 102.4 mg, 0.6 mmol) according to General Procedure 1, with the exception of racemic **L1** (42.8 mg, 0.12 mmol) in place of (*3R*,*8S*)-**L1**. The crude residue was purified by column chromatography (silica, 5-7.5% toluene/hexanes) to yield (*2-rac*,*5S*)-**84j** (104.8 mg, 64% yield) in 1.4:1 dr (determined by NMR analysis of the purified product) as a colorless oil. Spectral data for each diastereomer are reported below.

$R_f = 0.51$  (silica, 15% PhMe/hexanes,  $\text{KMnO}_4$ ).

$[\alpha]_D^{24} = +22^\circ$  ( $c = 1.0$ ,  $\text{CHCl}_3$ ).

**FTIR (NaCl, thin film,  $\text{cm}^{-1}$ ):** 2963, 2918, 2869, 1600, 1584, 1486, 1454, 1436, 1375, 1260, 1158, 1046, 971, 699.

**1-((2*S*,*5S*,*E*)-5,9-dimethyldeca-3,8-dien-2-yl)-3-methoxybenzene ((*S*,*S*)-84j)**

Prepared from (*S*,*E*)-1-bromo-3,7-dimethylocta-1,6-diene (**82j**, 130.3 mg, 0.6 mmol) and 1-(1-chloroethyl)-3-methoxybenzene (**83**, 102.4 mg, 0.6 mmol) according to General Procedure 1. The crude residue was purified by column chromatography (silica, 5-7.5% toluene/hexanes) to yield (*2S*,*5S*)-**84j** (117.4 mg, 72% yield) in >20:1 dr (determined by NMR analysis of the purified product) as a colorless oil.

$R_f = 0.51$  (silica, 15% PhMe/hexanes,  $\text{KMnO}_4$ ).



$[\alpha]_D^{24} = +28^\circ$  (c = 1.0, CHCl<sub>3</sub>).

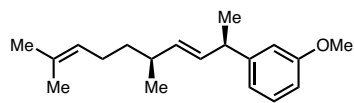
**<sup>1</sup>H NMR (400 MHz, C<sub>6</sub>D<sub>6</sub>):** δ 7.15 – 7.12 (m, 1H), 6.95 – 6.92 (m, 1H), 6.89 – 6.84 (m, 1H), 6.68 (ddd, *J* = 8.2, 2.6, 1.0 Hz, 1H), 5.63 (ddd, *J* = 15.4, 6.7, 1.0 Hz, 1H), 5.34 (ddd, *J* = 15.4, 7.9, 1.3 Hz, 1H), 5.25 – 5.17 (m, 1H), 3.41 – 3.31 (m, 4H), 2.17 – 1.96 (m, 3H), 1.71 – 1.66 (m, 3H), 1.57 (s, 3H), 1.38 – 1.30 (m, 5H), 0.96 (d, *J* = 6.7 Hz, 3H).

**<sup>13</sup>C NMR (101 MHz, CDCl<sub>3</sub>):** δ 159.7, 148.5, 135.3, 133.3, 131.3, 129.4, 124.9, 119.8, 113.2, 111.1, 55.3, 42.4, 37.4, 36.5, 26.1, 25.9, 21.8, 21.0, 17.8.

**FTIR (NaCl, thin film, cm<sup>-1</sup>):** 2963, 2924, 2869, 1600, 1584, 1486, 1454, 1436, 1260, 1158, 1046, 971, 776, 699.

**HRMS (FAB, *m/z*):** calc'd for C<sub>19</sub>H<sub>29</sub>O [M+H]<sup>+</sup>: 273.2218; found: 273.2228.

**1-((2*R*,5*S*,*E*)-5,9-dimethyldeca-3,8-dien-2-yl)-3-methoxybenzene ((*R*,*S*)-**84j**)**



Prepared from (*S*,*E*)-1-bromo-3,7-dimethylocta-1,6-diene (**82j**, 130.3 mg, 0.6 mmol) and 1-(1-chloroethyl)-3-methoxybenzene (**83**, 102.4 mg, 0.6 mmol) according to General Procedure 1, with the exception of the (**3*S*,8*R***)-**L1** ligand (9.7 mg, 0.02 mmol) in place of the (**3*R*,8*S***)-**L1** ligand. The crude residue was purified by column chromatography (silica, 5-7.5% toluene/hexanes) to yield (**2*R*,5*S***)-**84j** (86.3 mg, 53% yield) in 1:13.2 dr (determined by NMR analysis of the purified product) as a colorless oil.

**R<sub>f</sub>** = 0.51 (silica, 15% PhMe/hexanes, KMnO<sub>4</sub>).

$[\alpha]_D^{24} = +20^\circ$  (c = 1.0, CHCl<sub>3</sub>).

**<sup>1</sup>H NMR (400 MHz, C<sub>6</sub>D<sub>6</sub>):** δ 7.15 – 7.12 (m, 1H), 6.93 (t, *J* = 2.1 Hz, 1H), 6.89 – 6.84 (m, 1H), 6.68 (ddd, *J* = 8.2, 2.6, 1.0 Hz, 1H), 5.61 (ddd, *J* = 15.4, 6.8, 1.0 Hz, 1H), 5.34

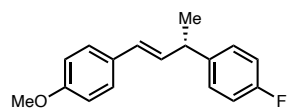
(ddd,  $J = 15.4, 7.9, 1.3$  Hz, 1H), 5.22 – 5.15 (m, 1H), 3.41 – 3.32 (m, 4H), 2.16 – 1.93 (m, 3H), 1.70 – 1.65 (m, 3H), 1.54 (s, 3H), 1.38 – 1.29 (m, 5H), 0.98 (d,  $J = 6.7$  Hz, 3H).

$^{13}\text{C}$  NMR (101 MHz,  $\text{CDCl}_3$ ):  $\delta$  159.7, 148.5, 135.3, 133.3, 131.3, 129.4, 124.9, 119.8, 113.2, 111.1, 55.2, 42.3, 37.4, 36.4, 26.0, 25.9, 21.7, 21.0, 17.8.

FTIR (NaCl, thin film,  $\text{cm}^{-1}$ ): 2963, 2924, 2869, 1600, 1584, 1486, 1453, 1436, 1260, 1158, 1046, 971, 776, 699.

HRMS (FAB,  $m/z$ ): calc'd for  $\text{C}_{19}\text{H}_{29}\text{O}$   $[\text{M}+\text{H}]^+$ : 273.2218; found: 273.2223.

**(*S,E*)-1-fluoro-4-(4-(4-methoxyphenyl)but-3-en-2-yl)benzene (86a)**



Prepared from (*E*)-1-(2-bromovinyl)-4-methoxybenzene (**79**, 127.8 mg, 0.6 mmol) and 1-(1-chloroethyl)-4-fluorobenzene (**85a**, 95.2 mg, 0.6 mmol) according to General Procedure 1. The crude residue was purified by column chromatography (silica, 10% toluene/hexanes) to yield **86a** (124.7 mg, 81% yield) in 89% ee as a white amorphous solid.

$R_f = 0.43$  (silica, 20% PhMe/hexanes, UV).

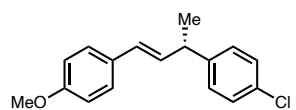
Chiral SFC: (OB-H), 2.5 mL/min, 15% IPA in  $\text{CO}_2$ ,  $\lambda = 280$  nm):  $t_R$  (major) = 5.9 min,  $t_R$  (minor) = 8.0 min.

$[\alpha]_D^{24} = -42^\circ$  ( $c = 1.0$ ,  $\text{CHCl}_3$ ).

$^1\text{H}$  NMR (400 MHz,  $\text{CDCl}_3$ ):  $\delta$  7.32 – 7.27 (m, 2H), 7.25 – 7.19 (m, 2H), 7.04 – 6.97 (m, 2H), 6.87 – 6.82 (m, 2H), 6.34 (dd,  $J = 16.0, 0.4$  Hz, 1H), 6.21 (dd,  $J = 15.9, 6.7$  Hz, 1H), 3.80 (s, 3H), 3.66 – 3.57 (m, 1H), 1.44 (d,  $J = 7.0$  Hz, 3H).

**<sup>13</sup>C NMR (101 MHz, CDCl<sub>3</sub>):**  $\delta$  161.5 (d,  $J_{C-F}$  = 243.8 Hz), 159.0, 141.6, 141.6, 133.0, 130.3, 128.8 (d,  $J_{C-F}$  = 7.8 Hz), 128.1, 127.4, 115.27 (d,  $J_{C-F}$  = 21.2 Hz), 114.1, 55.4, 41.9, 21.6.

**(*S,E*)-1-chloro-4-(4-(4-methoxyphenyl)but-3-en-2-yl)benzene (86b)**



Prepared from (*E*)-1-(2-bromovinyl)-4-methoxybenzene (**79**, 127.8 mg, 0.6 mmol) and 1-chloro-4-(1-chloroethyl)benzene (**85b**, 105.0 mg, 0.6 mmol) according to General Procedure 1. The crude residue was purified by column chromatography (silica, 5-10% toluene/hexanes) to yield **85b** (121.2 mg, 74% yield) in 91% ee as a white amorphous solid.

$R_f$  = 0.42 (silica, 20% PhMe/hexanes, UV).

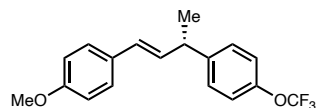
**Chiral SFC:** (OB-H), 2.5 mL/min, 25% IPA in CO<sub>2</sub>,  $\lambda$  = 280 nm):  $t_R$  (major) = 6.0 min,  $t_R$  (minor) = 8.6 min.

$[\alpha]_D^{25}$  = -39° (c = 1.0, CHCl<sub>3</sub>).

**<sup>1</sup>H NMR (400 MHz, CDCl<sub>3</sub>):**  $\delta$  7.31 – 7.26 (m, 4H), 7.22 – 7.17 (m, 2H), 6.86 – 6.81 (m, 2H), 6.34 (dd,  $J$  = 15.9, 0.5 Hz, 1H), 6.19 (dd,  $J$  = 15.9, 6.7 Hz, 1H), 3.80 (s, 3H), 3.64 – 3.55 (m, 1H), 1.43 (d,  $J$  = 7.0 Hz, 3H).

**<sup>13</sup>C NMR (101 MHz, CDCl<sub>3</sub>):**  $\delta$  159.0, 144.5, 132.6, 131.9, 130.3, 128.8, 128.7, 128.4, 127.4, 114.1, 55.4, 42.1, 21.4.

**(*S,E*)-1-methoxy-4-(3-(4-(trifluoromethoxy)phenyl)but-1-en-1-yl)benzene (86c)**



Prepared from (*E*)-1-(2-bromovinyl)-4-methoxybenzene (**79**,

127.8 mg, 0.6 mmol) and 1-(1-chloroethyl)-4-(trifluoromethoxy)benzene (**85c**, 134.8 mg, 0.6 mmol) according to General Procedure 1. The crude residue was purified by column chromatography (silica, 10% toluene/hexanes) to yield **86c** (153.1 mg, 79% yield) in 86% ee as a white amorphous solid.

$R_f = 0.55$  (silica, 30% PhMe/hexanes, UV).

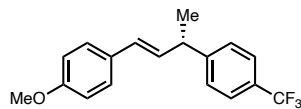
**Chiral SFC:** (AD-H), 2.5 mL/min, 7% IPA in CO<sub>2</sub>,  $\lambda = 254$  nm):  $t_R$  (major) = 7.8 min,  $t_R$  (minor) = 9.0 min.

$[\alpha]_D^{24} = -30^\circ$  (c = 1.0, CHCl<sub>3</sub>).

**<sup>1</sup>H NMR (400 MHz, CDCl<sub>3</sub>):**  $\delta$  7.32 – 7.26 (m, 4H), 7.19 – 7.13 (m, 2H), 6.87 – 6.82 (m, 2H), 6.36 (dd,  $J = 15.9, 0.8$  Hz, 1H), 6.20 (dd,  $J = 15.9, 6.8$  Hz, 1H), 3.80 (s, 3H), 3.68 – 3.59 (m, 1H), 1.45 (d,  $J = 7.0$  Hz, 3H).

**<sup>13</sup>C NMR (101 MHz, CDCl<sub>3</sub>):**  $\delta$  159.1, 147.7, 144.7, 132.5, 130.2, 128.7, 128.5, 127.4, 120.66 (q,  $J_{C-F} = 256.5$  Hz), 121.1, 114.1, 55.4, 42.1, 21.5.

**(*S,E*)-1-methoxy-4-(3-(4-(trifluoromethyl)phenyl)but-1-en-1-yl)benzene (86d)**



Prepared from (*E*)-1-(2-bromovinyl)-4-methoxybenzene (**79**, 127.8 mg, 0.6 mmol) and 1-(1-chloroethyl)-4-(trifluoromethyl)benzene (**85d**, 125.2 mg, 0.6 mmol) according to General Procedure 1.

The crude residue was purified by column chromatography (silica, 10-15% toluene/hexanes) to yield **85d** (100.6 mg, 55% yield) in 88% ee as a white amorphous solid.

$R_f = 0.42$  (silica, 20% PhMe/hexanes, UV).

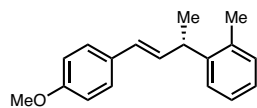
**Chiral SFC:** (OB-H), 2.5 mL/min, 5% IPA in CO<sub>2</sub>,  $\lambda = 280$  nm):  $t_R$  (major) = 6.6 min,  $t_R$  (minor) = 7.5 min.

$[\alpha]_D^{25} = -35^\circ$  (c = 1.0, CHCl<sub>3</sub>).

**<sup>1</sup>H NMR (400 MHz, CDCl<sub>3</sub>):**  $\delta$  7.60 – 7.54 (m, 2H), 7.41 – 7.36 (m, 2H), 7.32 – 7.27 (m, 2H), 6.87 – 6.82 (m, 2H), 6.37 (dd,  $J = 16.0, 0.8$  Hz, 1H), 6.20 (dd,  $J = 15.9, 6.8$  Hz, 1H), 3.80 (s, 3H), 3.73 – 3.64 (m, 1H), 1.47 (d,  $J = 7.0$  Hz, 3H).

**<sup>13</sup>C NMR (101 MHz, CDCl<sub>3</sub>):**  $\delta$  159.2, 150.1 (q,  $J_{C-F} = 1.5$  Hz), 132.0, 130.1, 128.8, 128.6 (q,  $J_{C-F} = 32.3$  Hz), 127.8, 127.4, 125.5 (q,  $J_{C-F} = 3.8$  Hz), 124.5 (q,  $J_{C-F} = 271.8$  Hz), 114.1, 55.4, 42.6, 21.3.

**(*S,E*)-1-(4-(4-methoxyphenyl)but-3-en-2-yl)-2-methylbenzene (86e)**



Prepared from (*E*)-1-(2-bromovinyl)-4-methoxybenzene (**79**, 127.8 mg, 0.6 mmol) and 1-(1-chloroethyl)-2-methylbenzene (**85e**, 92.8 mg, 0.6 mmol) according to General Procedure 1. The crude residue was purified by column chromatography (silica, 5-15% toluene/hexanes) to yield **86e** (75.6 mg, 50% yield) in 80% ee as a white amorphous solid.

$R_f = 0.33$  (silica, 20% PhMe/hexanes, UV).

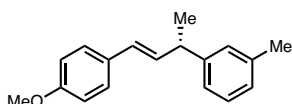
**Chiral SFC:** (OB-H), 2.5 mL/min, 15% IPA in CO<sub>2</sub>,  $\lambda = 280$  nm):  $t_R$  (major) = 7.6 min,  $t_R$  (minor) = 9.5 min.

$[\alpha]_D^{25} = -42^\circ$  (c = 1.0, CHCl<sub>3</sub>).

**<sup>1</sup>H NMR (400 MHz, CDCl<sub>3</sub>):** δ 7.33 – 7.25 (m, 3H), 7.24 – 7.11 (m, 3H), 6.87 – 6.82 (m, 2H), 6.33 (d, *J* = 16.4 Hz, 1H), 6.23 (dd, *J* = 15.9, 6.1 Hz, 1H), 3.90 – 3.79 (m, 4H), 2.39 (s, 3H), 1.45 (d, *J* = 7.0 Hz, 3H).

**<sup>13</sup>C NMR (101 MHz, CDCl<sub>3</sub>):** δ 158.9, 143.9, 135.7, 132.9, 130.6, 130.5, 127.9, 127.3, 126.5, 126.4, 126.1, 114.0, 55.4, 38.1, 20.7, 19.6.

**(*S,E*)-1-(4-(4-methoxyphenyl)but-3-en-2-yl)-3-methylbenzene (86f)**



Prepared from (*E*)-1-(2-bromovinyl)-4-methoxybenzene (**79**, 127.8 mg, 0.6 mmol) and 1-(1-chloroethyl)-3-methylbenzene (**85f**, 92.8 mg, 0.6 mmol) according to General Procedure 1. The crude residue was purified by column chromatography (silica, 10-12% toluene/hexanes) to yield **86f** (131.9 mg, 87% yield) in 91% ee as a colorless oil.

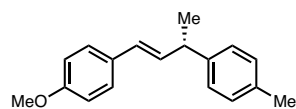
**R<sub>f</sub>** = 0.35 (silica, 20% PhMe/hexanes, UV).

**Chiral SFC:** (OB-H), 2.5 mL/min, 15% IPA in CO<sub>2</sub>, λ = 280 nm): *t<sub>R</sub>* (major) = 7.1 min, *t<sub>R</sub>* (minor) = 8.0 min.

**[α]<sub>D</sub><sup>24</sup>** = -48° (c = 1.0, CHCl<sub>3</sub>).

**<sup>1</sup>H NMR (400 MHz, CDCl<sub>3</sub>):** δ 7.35 – 7.28 (m, 2H), 7.26 – 7.20 (m, 1H), 7.13 – 7.02 (m, 3H), 6.88 – 6.82 (m, 2H), 6.39 (d, *J* = 15.9 Hz, 1H), 6.26 (dd, *J* = 15.9, 6.7 Hz, 1H), 3.81 (s, 3H), 3.65 – 3.55 (m, 1H), 2.36 (s, 3H), 1.46 (d, *J* = 7.1 Hz, 3H).

**<sup>13</sup>C NMR (101 MHz, CDCl<sub>3</sub>):** δ 158.9, 146.0, 138.1, 133.4, 130.6, 128.5, 128.2, 127.8, 127.4, 127.0, 124.4, 114.0, 55.4, 42.6, 21.6, 21.5.

**(*S,E*)-1-methoxy-4-(3-(*p*-tolyl)but-1-en-1-yl)benzene (86g)**

Prepared from (*E*)-1-(2-bromovinyl)-4-methoxybenzene (**79**, 127.8 mg, 0.6 mmol) and 1-(1-chloroethyl)-4-methylbenzene (**85g**, 92.8 mg, 0.6 mmol) according to General Procedure 1. The crude residue was purified by column chromatography (silica, 10-12% toluene/hexanes) to yield **86g** (125.8 mg, 83% yield) in 93% ee as a white amorphous solid.

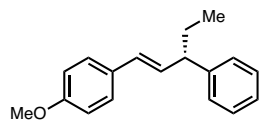
$R_f$  = 0.35 (silica, 20% PhMe/hexanes, UV).

**Chiral SFC:** (OJ-H), 2.5 mL/min, 15% IPA in CO<sub>2</sub>,  $\lambda$  = 254 nm):  $t_R$  (minor) = 5.9 min,  $t_R$  (major) = 6.4 min.

$[\alpha]_D^{24}$  = -43° (c = 1.0, CHCl<sub>3</sub>).

**<sup>1</sup>H NMR (400 MHz, CDCl<sub>3</sub>):**  $\delta$  7.33 – 7.27 (m, 2H), 7.20 – 7.11 (m, 4H), 6.87 – 6.81 (m, 2H), 6.36 (d,  $J$  = 15.9 Hz, 1H), 6.24 (dd,  $J$  = 15.9, 6.7 Hz, 1H), 3.80 (s, 3H), 3.65 – 3.55 (m, 1H), 2.34 (s, 3H), 1.45 (d,  $J$  = 7.0 Hz, 3H).

**<sup>13</sup>C NMR (101 MHz, CDCl<sub>3</sub>):**  $\delta$  158.9, 143.0, 135.8, 133.5, 130.6, 129.3, 127.8, 127.3, 127.3, 114.0, 77.5, 77.2, 76.8, 55.4, 42.3, 21.5, 21.1.

**(*S,E*)-1-methoxy-4-(3-phenylpent-1-en-1-yl)benzene (86h)**

Prepared from (*E*)-1-(2-bromovinyl)-4-methoxybenzene (**79**, 127.8 mg, 0.6 mmol) and (1-chloropropyl)benzene (**85h**, 92.8 mg, 0.6 mmol) according to General Procedure 1. The crude residue was purified by column chromatography (silica, 15% toluene/hexanes) to yield **86h** (119.7 mg, 79% yield) in 95% ee as a white amorphous solid.

$R_f = 0.35$  (silica, 20% PhMe/hexanes, UV).

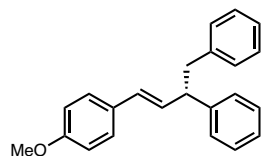
**Chiral SFC:** (OB-H), 2.5 mL/min, 15% IPA in CO<sub>2</sub>,  $\lambda = 254$  nm):  $t_R$  (minor) = 7.8 min,  $t_R$  (major) = 9.8 min.

$[\alpha]_D^{24} = -47^\circ$  (c = 1.0, CHCl<sub>3</sub>).

**<sup>1</sup>H NMR (400 MHz, CDCl<sub>3</sub>):**  $\delta$  7.35 – 7.18 (m, 7H), 6.86 – 6.81 (m, 2H), 6.35 (d,  $J = 15.8$  Hz, 1H), 6.20 (dd,  $J = 15.8, 7.8$  Hz, 1H), 3.80 (s, 3H), 3.33 – 3.26 (m, 1H), 1.89 – 1.77 (m, 2H), 0.92 (t,  $J = 7.3$  Hz, 3H).

**<sup>13</sup>C NMR (101 MHz, CDCl<sub>3</sub>):**  $\delta$  158.9, 144.9, 132.3, 130.6, 128.9, 128.6, 127.8, 127.3, 126.2, 114.0, 55.4, 51.1, 29.0, 12.5.

**(*S,E*)-(4-(4-methoxyphenyl)but-3-ene-1,2-diyl)dibenzene (86i)**



Prepared from (*E*)-1-(2-bromovinyl)-4-methoxybenzene (**79**, 127.8 mg, 0.6 mmol) and (1-chloroethane-1,2-diyl)dibenzene (**85i**, 130.0 mg, 0.6 mmol) according to General Procedure 1. The crude residue

was purified by column chromatography (silica, 15-20% toluene/hexanes) to yield **86i** (151.2 mg, 80% yield) in 92% ee as a white amorphous solid.

$R_f = 0.33$  (silica, 30% PhMe/hexanes, UV).

**Chiral SFC:** (OD-H), 2.5 mL/min, 10% IPA in CO<sub>2</sub>,  $\lambda = 280$  nm):  $t_R$  (minor) = 10.7 min,  $t_R$  (major) = 11.4 min.

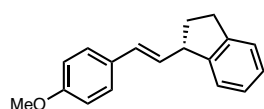
$[\alpha]_D^{24} = +12^\circ$  (c = 1.0, CHCl<sub>3</sub>).



**<sup>1</sup>H NMR (400 MHz, CDCl<sub>3</sub>):** δ 7.32 – 7.27 (m, 2H), 7.25 – 7.19 (m, 7H), 7.19 – 7.12 (m, 1H), 7.11 – 7.06 (m, 2H), 6.84 – 6.79 (m, 2H), 6.26 (dd, *J* = 15.9, 6.2 Hz, 1H), 6.23 (d, *J* = 15.9 Hz, 1H), 3.79 (s, 3H), 3.75 – 3.67 (m, 1H), 3.17 – 3.05 (m, 2H).

**<sup>13</sup>C NMR (101 MHz, CDCl<sub>3</sub>):** δ 159.0, 144.1, 140.2, 131.3, 130.4, 129.5, 129.4, 128.5, 128.2, 128.0, 127.4, 126.4, 126.0, 114.0, 55.4, 51.0, 42.9.

**(*S,E*)-1-(4-methoxystyryl)-2,3-dihydro-1*H*-indene (**86j**)**



Prepared from (*E*)-1-(2-bromovinyl)-4-methoxybenzene (**79**, 127.8 mg, 0.6 mmol) and 1-chloro-2,3-dihydro-1*H*-indene (**85j**, 91.6 mg,

0.6 mmol) according to General Procedure 1. The crude residue was purified by column chromatography (silica, 10-15% toluene/hexanes) to yield **86j** (118.9 mg, 79% yield) in 92% ee as a white amorphous solid.

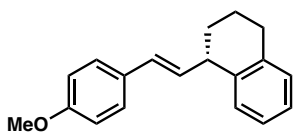
**R<sub>f</sub>** = 0.35 (silica, 20% PhMe/hexanes, UV).

**Chiral SFC:** (OB-H), 2.5 mL/min, 20% IPA in CO<sub>2</sub>, λ = 280 nm): *t<sub>R</sub>* (major) = 4.9 min, *t<sub>R</sub>* (minor) = 7.3 min.

**[α]<sub>D</sub><sup>24</sup>** = -3° (c = 1.0, CHCl<sub>3</sub>).

**<sup>1</sup>H NMR (400 MHz, CDCl<sub>3</sub>):** δ 7.37 – 7.13 (m, 6H), 6.90 – 6.82 (m, 2H), 6.48 (d, *J* = 15.7 Hz, 1H), 6.12 (dd, *J* = 15.7, 8.6 Hz, 1H), 3.94 – 3.86 (m, 1H), 3.81 (s, 3H), 3.04 – 2.86 (m, 2H), 2.41 (dtd, *J* = 12.6, 7.6, 3.6 Hz, 1H), 1.93 (dq, *J* = 12.6, 8.8 Hz, 1H).

**<sup>13</sup>C NMR (101 MHz, CDCl<sub>3</sub>):** δ 159.0, 146.2, 144.1, 131.1, 130.4, 129.8, 127.4, 126.7, 126.4, 124.7, 124.6, 114.1, 55.5, 49.3, 33.8, 31.9.

**(*S,E*)-1-(4-methoxystyryl)-1,2,3,4-tetrahydronaphthalene (86k)**

Prepared from (*E*)-1-(2-bromovinyl)-4-methoxybenzene (**79**, 127.8 mg, 0.6 mmol) and 1-chloro-1,2,3,4-tetrahydronaphthalene (**85k**, 100.0 mg, 0.6 mmol) according to General Procedure 1. The

crude residue was purified by column chromatography (silica, 10-15% toluene/hexanes) to yield **86k** (99.7 mg, 63% yield) in 90% ee as a white amorphous solid.

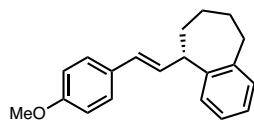
$R_f$  = 0.47 (silica, 30% PhMe/hexanes, UV).

**Chiral SFC:** (OB-H), 2.5 mL/min, 20% IPA in CO<sub>2</sub>,  $\lambda$  = 280 nm):  $t_R$  (major) = 5.4 min,  $t_R$  (minor) = 7.6 min.

$[\alpha]_D^{24}$  = +12° (c = 1.0, CHCl<sub>3</sub>).

**<sup>1</sup>H NMR (500 MHz, CDCl<sub>3</sub>):**  $\delta$  7.33 – 7.29 (m, 2H), 7.23 – 7.19 (m, 1H), 7.15 – 7.08 (m, 3H), 6.87 – 6.82 (m, 2H), 6.37 (d,  $J$  = 15.7 Hz, 1H), 6.14 (dd,  $J$  = 15.7, 8.5 Hz, 1H), 3.81 (s, 3H), 3.64 – 3.57 (m, 1H), 2.90 – 2.76 (m, 2H), 2.08 – 1.90 (m, 2H), 1.84 – 1.72 (m, 2H).

**<sup>13</sup>C NMR (101 MHz, CDCl<sub>3</sub>):**  $\delta$  158.9, 138.8, 137.1, 133.1, 130.5, 129.9, 129.8, 129.3, 127.4, 126.1, 125.7, 114.1, 55.5, 43.1, 30.7, 29.9, 21.1.

**(*S,E*)-5-(4-methoxystyryl)-6,7,8,9-tetrahydro-5H-benzo[7]annulene (86l)**

Prepared from (*E*)-1-(2-bromovinyl)-4-methoxybenzene (**79**, 127.8 mg, 0.6 mmol) and 5-chloro-6,7,8,9-tetrahydro-5H-

benzo[7]annulene (**85l**, 108.4 mg, 0.6 mmol) according to General Procedure 1. The crude residue was purified by column chromatography (silica, 10-16% toluene/hexanes) to yield **86l** (120.3 mg, 72% yield) in 62% ee as a white amorphous solid.

$R_f$  = 0.47 (silica, 30% PhMe/hexanes, UV).

**Chiral SFC:** (AS-H), 2.5 mL/min, 5% IPA in CO<sub>2</sub>,  $\lambda$  = 254 nm):  $t_R$  (major) = 7.8 min,  $t_R$  (minor) = 9.0 min.

$[\alpha]_D^{24}$  = -21° (c = 1.0, CHCl<sub>3</sub>).

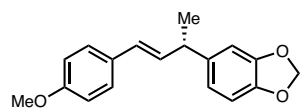
**<sup>1</sup>H NMR (400 MHz, CDCl<sub>3</sub>):**  $\delta$  7.36 – 7.29 (m, 2H), 7.22 – 7.16 (m, 1H), 7.16 – 7.11 (m, 3H), 6.89 – 6.83 (m, 2H), 6.42 (dd,  $J$  = 16.0, 6.7 Hz, 1H), 6.21 (d,  $J$  = 16.0 Hz, 1H), 3.86 – 3.72 (m, 4H), 2.96 – 2.77 (m, 2H), 2.07 – 1.75 (m, 4H), 1.75 – 1.59 (m, 2H).

**<sup>13</sup>C NMR (101 MHz, CDCl<sub>3</sub>):**  $\delta$  158.9, 144.6, 142.9, 131.2, 130.7, 129.9, 129.1, 128.4, 127.3, 126.3, 126.1, 114.1, 55.5, 48.3, 36.4, 34.0, 29.2, 28.1.

**FTIR (NaCl, thin film, cm<sup>-1</sup>):** 2921, 2850, 1607, 1511, 1453, 1442, 1250, 1174, 1036, 756.

**HRMS (TOF-ESI,  $m/z$ ):** calc'd for C<sub>20</sub>H<sub>22</sub>O [M+•]<sup>+</sup>: 278.1671; found: 278.1668.

**(*S,E*)-5-(4-(4-methoxyphenyl)but-3-en-2-yl)benzo[*d*][1,3]dioxole (86m)**



Prepared from (*E*)-1-(2-bromovinyl)-4-methoxybenzene (**79**,

127.8 mg, 0.6 mmol) and 5-(1-chloroethyl)benzo[*d*][1,3]dioxole

(**85m**, 110.8 mg, 0.6 mmol) according to General Procedure 1. The crude residue was purified by column chromatography (silica, 30-35% toluene/hexanes) to yield **86m** (127.3 mg, 91% purity, 68% yield) in 90% ee as a colorless oil. Note: 5m could not be separated from 8.5 mol % **85m** homocoupling.

$R_f$  = 0.49 (silica, 60% PhMe/hexanes, UV).

**Chiral SFC:** (AD-H), 2.5 mL/min, 20% IPA in CO<sub>2</sub>, λ = 280 nm):  $t_R$  (major) = 6.1 min,  $t_R$  (minor) = 6.9 min.

$[\alpha]_D^{24} = -24^\circ$  (c = 1.0, CHCl<sub>3</sub>).

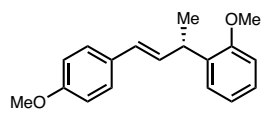
**<sup>1</sup>H NMR (400 MHz, CDCl<sub>3</sub>):** δ 7.33 – 7.27 (m, 2H), 6.88 – 6.81 (m, 2H), 6.80 – 6.70 (m, 3H), 6.34 (d,  $J = 16.3$  Hz, 1H), 6.20 (dd,  $J = 15.9, 6.7$  Hz, 1H), 5.93 (s, 2H), 3.80 (s, 3H), 3.59 – 3.51 (m, 1H), 1.42 (d,  $J = 7.0$  Hz, 3H).

**<sup>13</sup>C NMR (101 MHz, CDCl<sub>3</sub>):** δ 158.9, 147.8, 145.9, 140.1, 133.3, 130.4, 127.9, 127.4, 120.2, 114.0, 108.3, 108.0, 101.0, 55.4, 42.4, 21.6.

**FTIR (NaCl, thin film, cm<sup>-1</sup>):** 2962, 2898, 1607, 1510, 1485, 1438, 1244, 1175, 1037, 937, 807.

**HRMS (TOF-ESI,  $m/z$ ):** calc'd for C<sub>18</sub>H<sub>18</sub>O<sub>3</sub> [M+•]<sup>+</sup>: 282.1256; found: 282.1245.

**(*S,E*)-1-methoxy-2-(4-(4-methoxyphenyl)but-3-en-2-yl)benzene (86n)**



Prepared from (*E*)-1-(2-bromovinyl)-4-methoxybenzene (**79**, 127.8 mg, 0.6 mmol) and 1-(1-chloroethyl)-2-methoxybenzene (**85n**, 102.4 mg, 0.6 mmol) according to General Procedure 1. The crude residue was purified by column chromatography (silica, 30-32.5% toluene/hexanes) to yield **86n** (113.8 mg, 71% yield) in 89% ee as a colorless oil.

$R_f = 0.55$  (silica, 60% PhMe/hexanes, UV).

**Chiral SFC:** (AD-H), 2.5 mL/min, 10% IPA in CO<sub>2</sub>, λ = 280 nm):  $t_R$  (minor) = 9.7 min,  $t_R$  (major) = 10.7 min.

$[\alpha]_D^{24} = -100^\circ$  (c = 1.0, CHCl<sub>3</sub>).

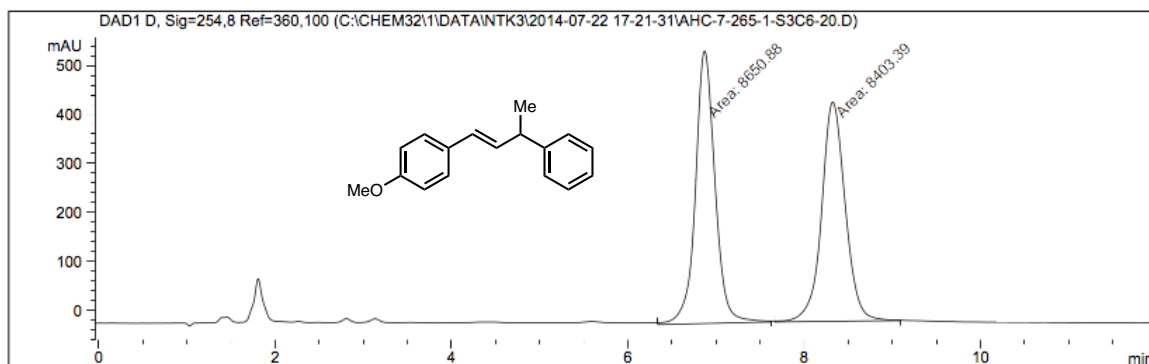
**<sup>1</sup>H NMR (400 MHz, CDCl<sub>3</sub>):** δ 7.34 – 7.28 (m, 2H), 7.25 – 7.17 (m, 2H), 6.94 (td, *J* = 7.5, 1.2 Hz, 1H), 6.89 (dd, *J* = 8.2, 1.2 Hz, 1H), 6.86 – 6.82 (m, 2H), 6.38 (d, *J* = 16.2 Hz, 1H), 6.30 (dd, *J* = 15.9, 5.9 Hz, 1H), 4.12 – 4.04 (m, 1H), 3.86 (s, 3H), 3.80 (s, 3H), 1.42 (d, *J* = 7.1 Hz, 3H).

**<sup>13</sup>C NMR (101 MHz, CDCl<sub>3</sub>):** δ 158.8, 156.8, 134.5, 133.0, 130.9, 127.7, 127.6, 127.3, 127.2, 120.8, 114.0, 110.7, 55.6, 55.4, 35.2, 20.3.

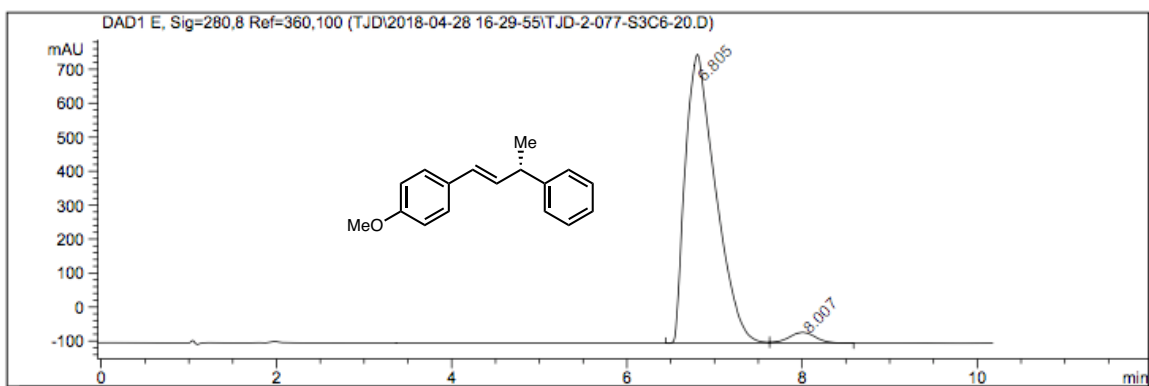
**FTIR (NaCl, thin film, cm<sup>-1</sup>):** 3030, 2960, 2835, 1607, 1510, 1489, 1463, 1456, 1239, 1174, 1032.

**HRMS (TOF-ESI, *m/z*):** calc'd for C<sub>18</sub>H<sub>20</sub>O<sub>2</sub> [M+•]<sup>+</sup>: 268.1463; found: 268.1450.

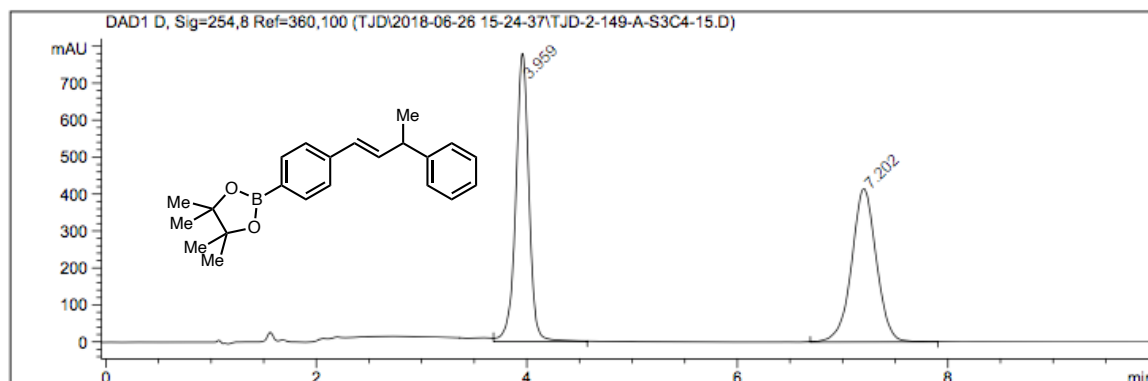
## 1.4.7 SFC Traces of Racemic and Enantioenriched Products

**81: racemic**

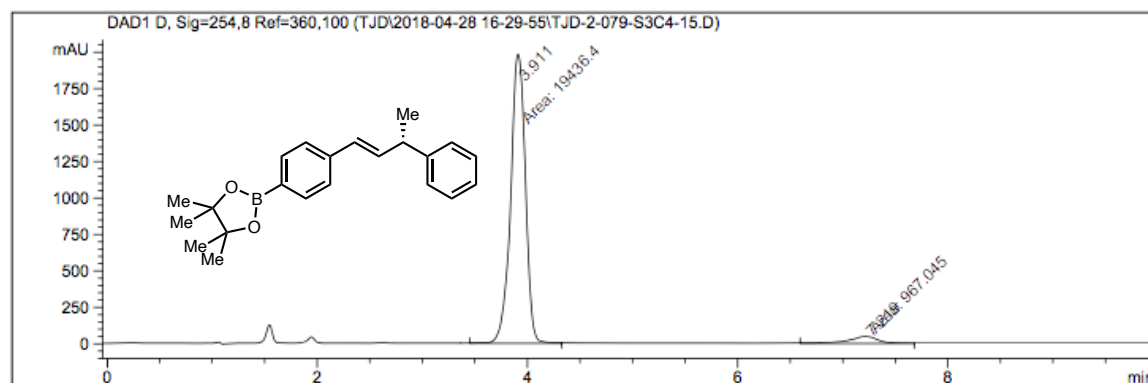
Peak #	RetTime [min]	Type	Width [min]	Area [mAU*s]	Height [mAU]	Area %
1	6.871	MM	0.2583	8650.88281	558.20911	50.7256
2	8.325	MM	0.3119	8403.38672	449.10953	49.2744

**81: enantioenriched (94% ee)**

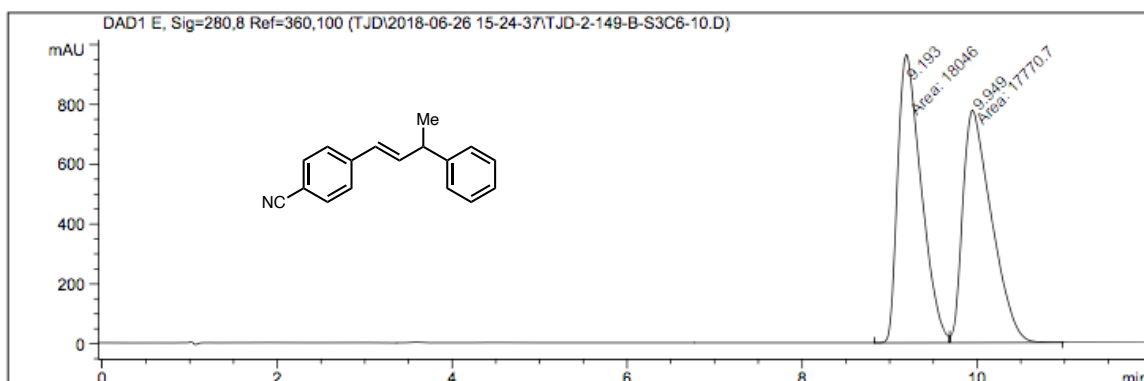
Peak #	RetTime [min]	Type	Width [min]	Area [mAU*s]	Height [mAU]	Area %
1	6.805	BV	0.3649	2.04499e4	849.41632	96.7967
2	8.007	VB	0.3273	676.75940	31.93015	3.2033

**84a:** racemic

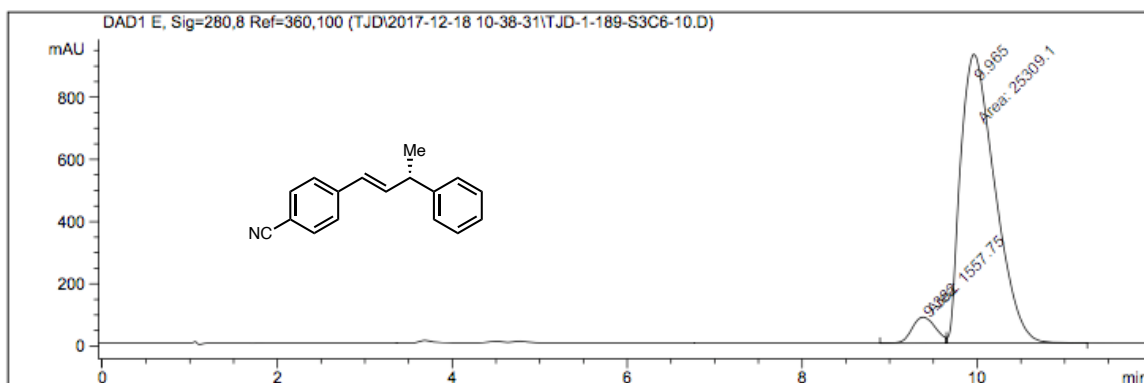
Peak #	RetTime [min]	Type	Width [min]	Area [mAU*s]	Height [mAU]	Area %
1	3.959	VB	0.1339	6802.28711	778.63159	50.0709
2	7.202	BB	0.2507	6783.01904	415.05194	49.9291

**84a:** enantioenriched (91% ee)

Peak #	RetTime [min]	Type	Width [min]	Area [mAU*s]	Height [mAU]	Area %
1	3.911	MM	0.1631	1.94364e4	1986.65588	95.2604
2	7.219	MM	0.3255	967.04510	49.51790	4.7396

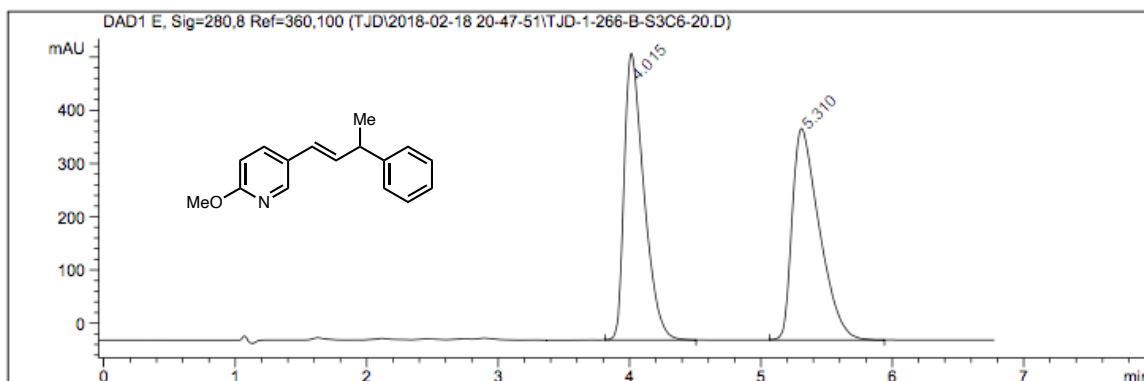
**84b: racemic**

Peak #	RetTime [min]	Type	Width [min]	Area [mAU*s]	Height [mAU]	Area %
1	9.193	MF	0.3119	1.80460e4	964.19104	50.3843
2	9.949	FM	0.3811	1.77707e4	777.22571	49.6157

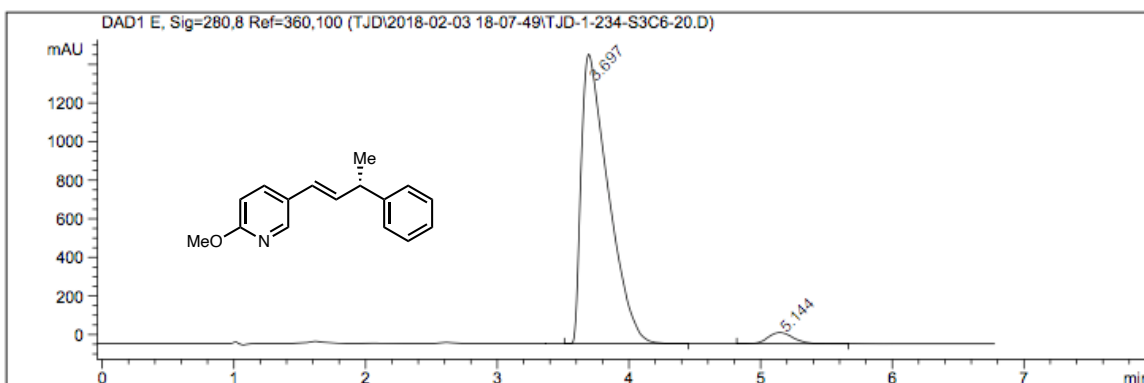
**84b: enantioenriched (88% ee)**

Peak #	RetTime [min]	Type	Width [min]	Area [mAU*s]	Height [mAU]	Area %
1	9.382	MF	0.3101	1557.74841	83.73310	5.7980
2	9.965	FM	0.4540	2.53091e4	929.11011	94.2020

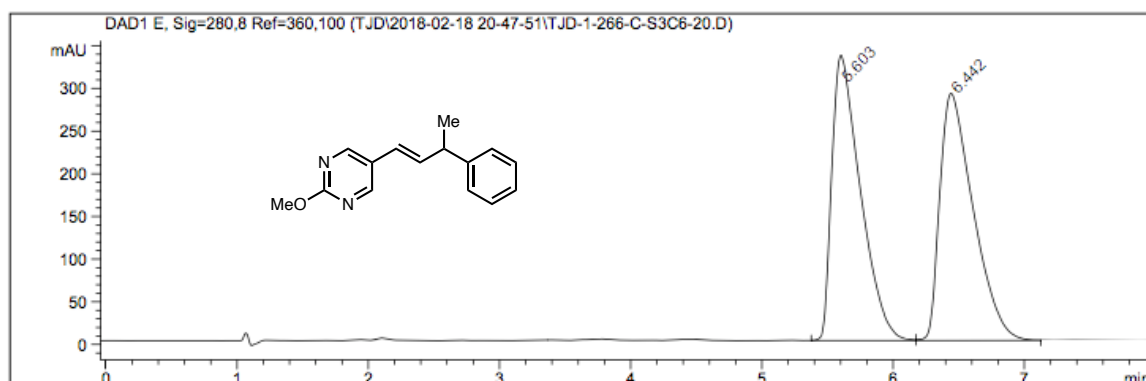


**84c: racemic**

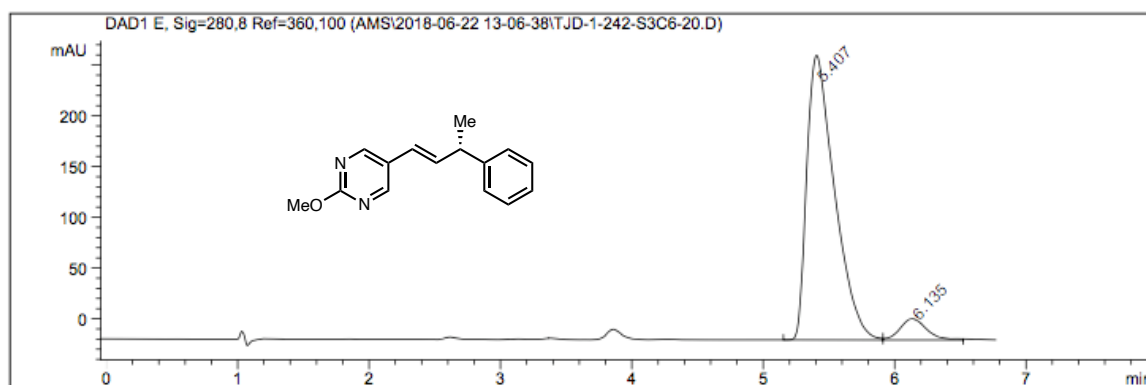
Peak #	RetTime [min]	Type	Width [min]	Area [mAU*s]	Height [mAU]	Area %
1	4.015	BB	0.1577	5620.01318	538.57825	49.5911
2	5.310	BB	0.2157	5712.68408	397.39774	50.4089

**84c: enantioenriched (93% ee)**

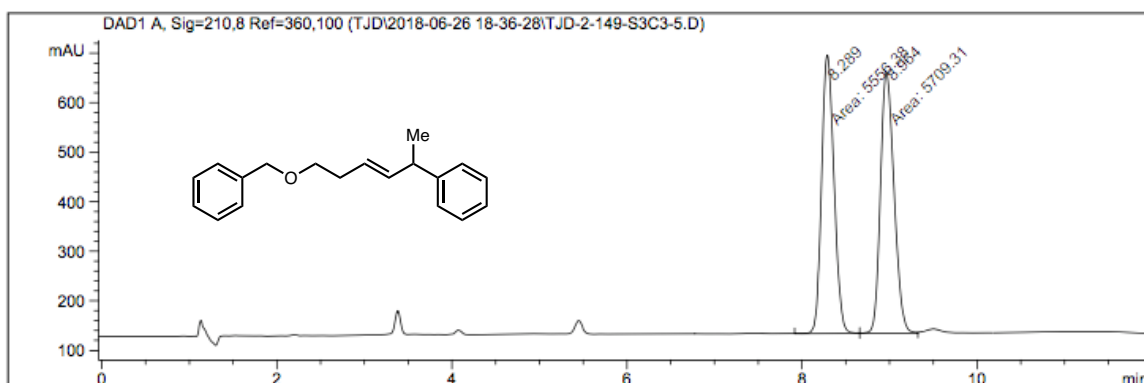
Peak #	RetTime [min]	Type	Width [min]	Area [mAU*s]	Height [mAU]	Area %
1	3.697	BB	0.2107	2.14262e4	1499.87000	96.5123
2	5.144	BB	0.2055	774.28833	58.85278	3.4877

**84d**: racemic

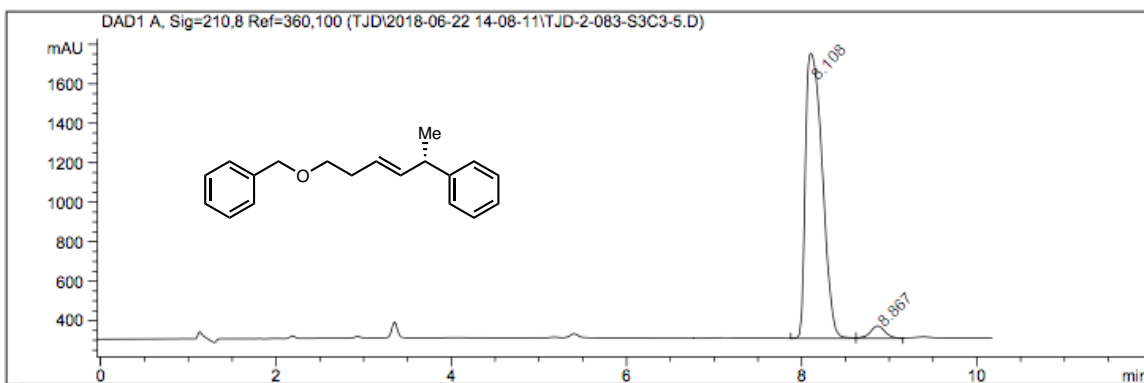
Peak #	RetTime [min]	Type	Width [min]	Area [mAU*s]	Height [mAU]	Area %
1	5.603	BV	0.2265	5057.28418	334.21259	49.7155
2	6.442	VB	0.2682	5115.17090	289.40912	50.2845

**84d**: enantioenriched (87% ee)

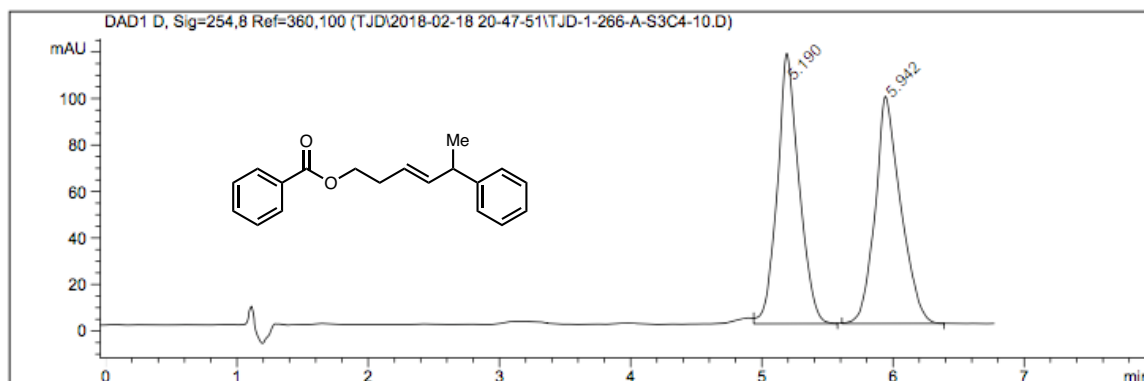
Peak #	RetTime [min]	Type	Width [min]	Area [mAU*s]	Height [mAU]	Area %
1	5.407	BV	0.2196	4124.62549	280.35568	93.3511
2	6.135	VB	0.2157	293.77594	20.94203	6.6489

**84e: racemic**

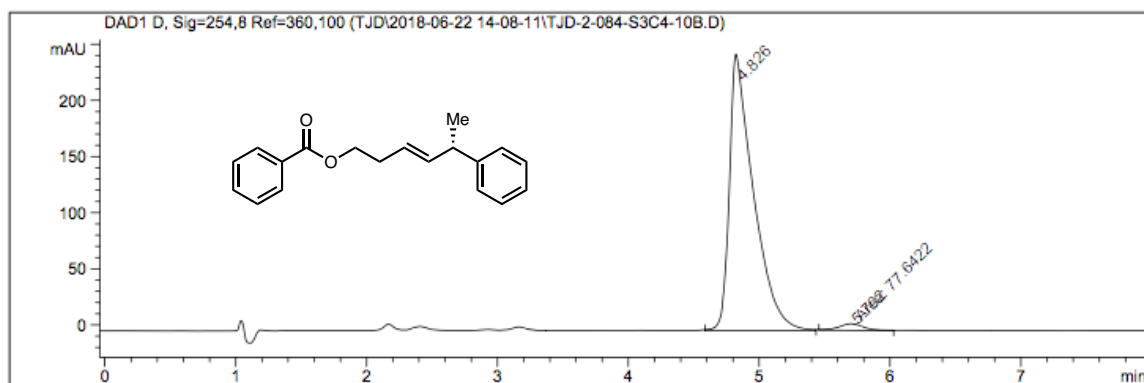
Peak #	RetTime [min]	Type	Width [min]	Area [mAU*s]	Height [mAU]	Area %
1	8.289	MF	0.1643	5556.37646	563.54108	49.3213
2	8.964	FM	0.1804	5709.30518	527.56628	50.6787

**84e: enantioenriched (93% ee)**

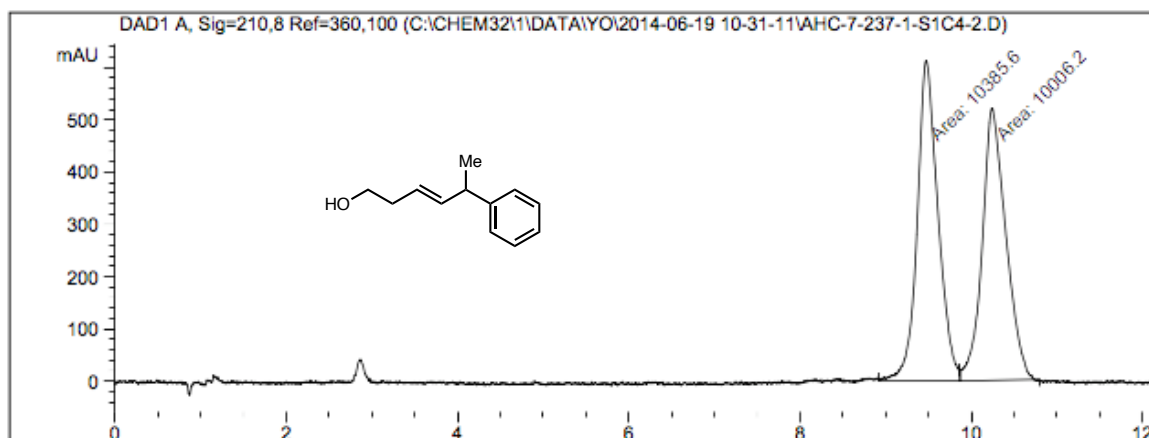
Peak #	RetTime [min]	Type	Width [min]	Area [mAU*s]	Height [mAU]	Area %
1	8.108	VV	0.2199	1.92896e4	1443.39917	96.2996
2	8.867	VV	0.1809	741.21216	63.14388	3.7004

**84f:** racemic

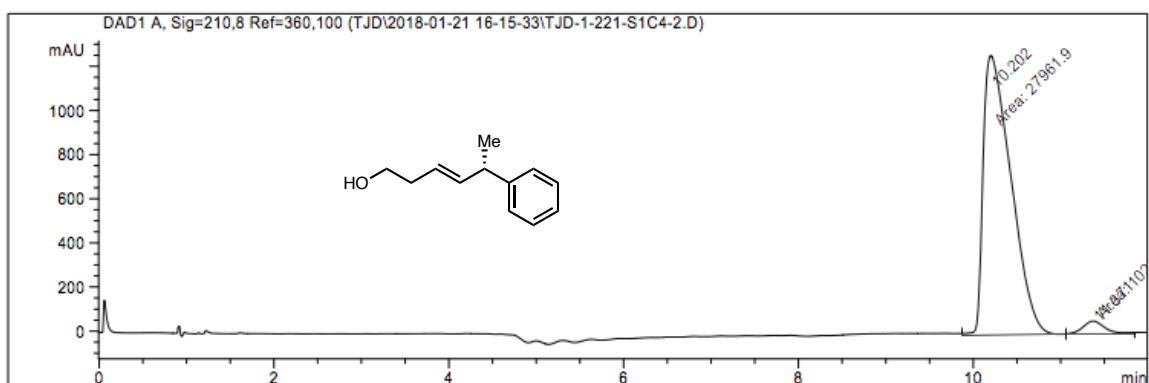
Peak #	RetTime [min]	Type	Width [min]	Area [mAU*s]	Height [mAU]	Area %
1	5.190	VB	0.1605	1341.30066	116.30424	50.3037
2	5.942	BB	0.1881	1325.10693	97.78625	49.6963

**84f:** enantioenriched (95% ee)

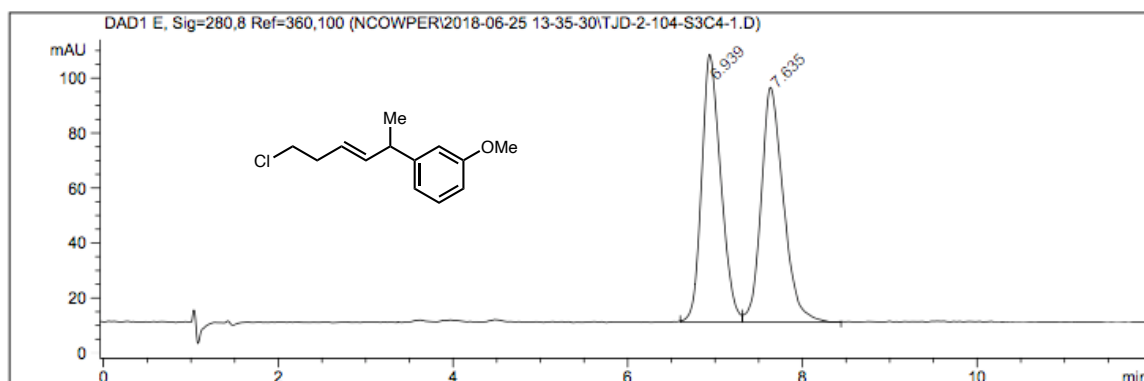
Peak #	RetTime [min]	Type	Width [min]	Area [mAU*s]	Height [mAU]	Area %
1	4.826	BV	0.1773	3139.86328	245.37181	97.5869
2	5.702	MM	0.2128	77.64215	6.08122	2.4131

**84g**: racemic

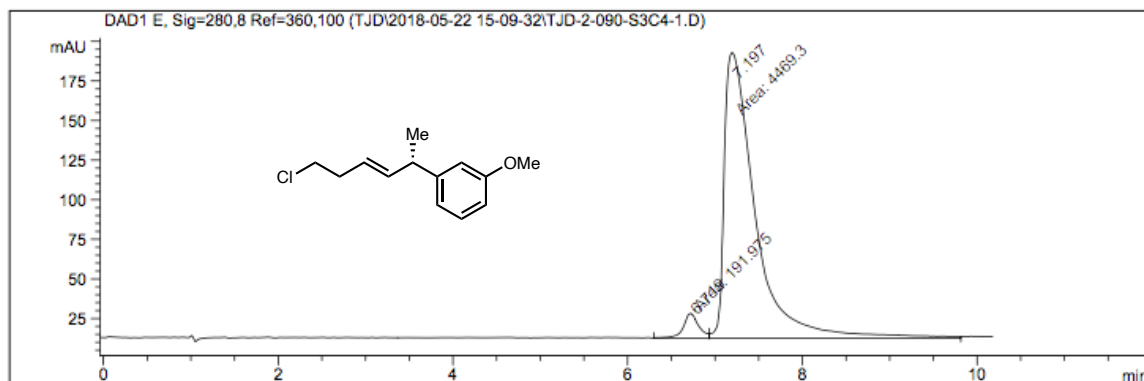
Peak #	RetTime [min]	Type	Width [min]	Area [mAU*s]	Height [mAU]	Area %
1	9.474	MM	0.2823	1.03856e4	613.19647	50.9302
2	10.244	MM	0.3204	1.00062e4	520.49475	49.0698

**84g**: enantioenriched (93% ee)

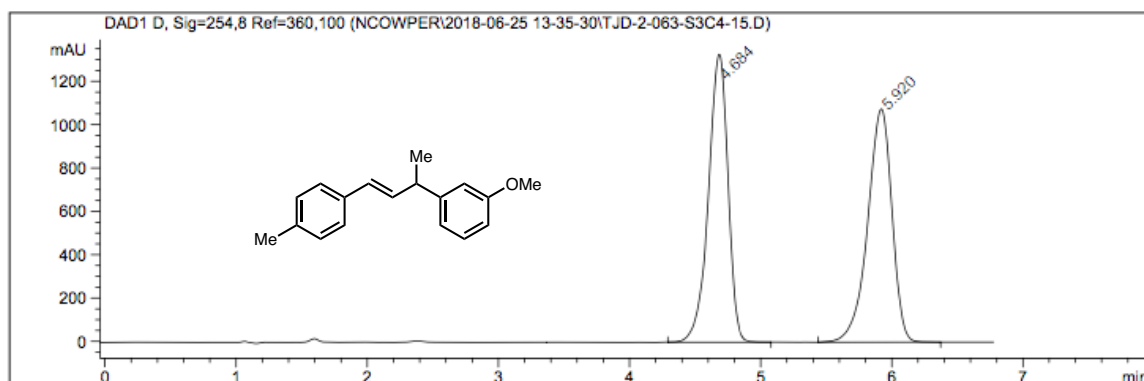
Peak #	RetTime [min]	Type	Width [min]	Area [mAU*s]	Height [mAU]	Area %
1	10.202	MM	0.3677	2.79619e4	1267.29468	96.4629
2	11.371	MM	0.2960	1025.29797	57.73108	3.5371

**84h**: racemic

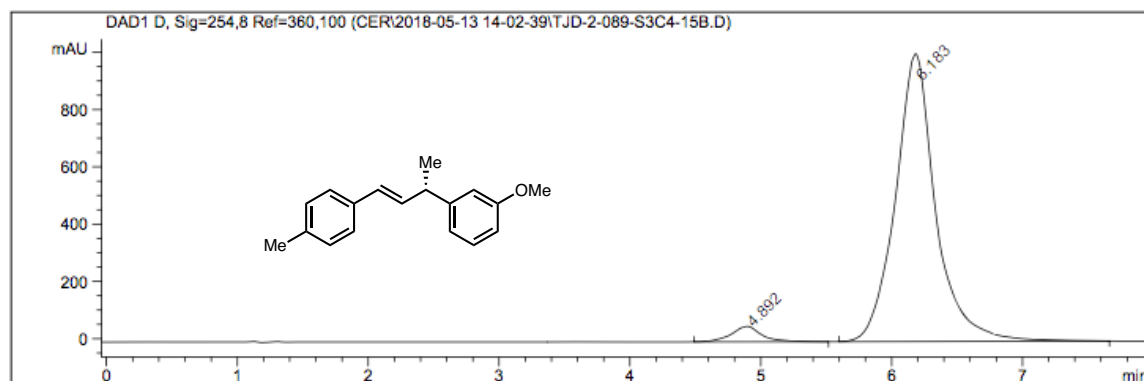
Peak #	RetTime [min]	Type	Width [min]	Area [mAU*s]	Height [mAU]	Area %
1	6.939	BV	0.2294	1479.83264	97.33060	49.5639
2	7.635	VB	0.2578	1505.87402	85.36206	50.4361

**84h**: enantioenriched (92% ee)

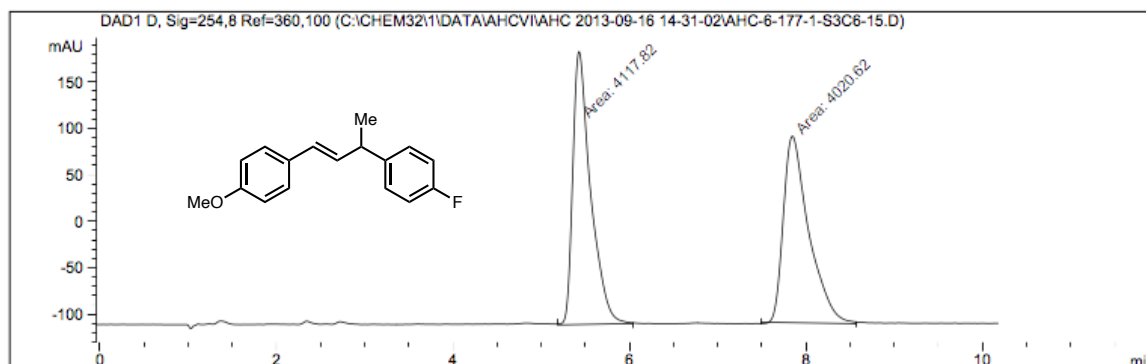
Peak #	RetTime [min]	Type	Width [min]	Area [mAU*s]	Height [mAU]	Area %
1	6.719	MF	0.2020	191.97549	15.84125	4.1185
2	7.197	FM	0.4127	4469.30273	180.50043	95.8815

**84i: racemic**

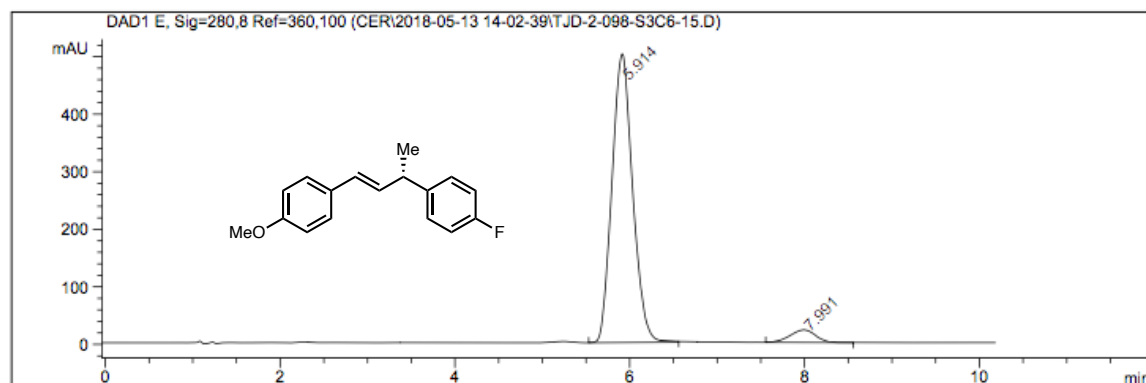
Peak #	RetTime [min]	Type	Width [min]	Area [mAU*s]	Height [mAU]	Area %
1	4.684	BB	0.1616	1.38246e4	1326.30127	49.9185
2	5.920	BB	0.1985	1.38698e4	1075.49414	50.0815

**84i: enantioenriched (92% ee)**

Peak #	RetTime [min]	Type	Width [min]	Area [mAU*s]	Height [mAU]	Area %
1	4.892	BB	0.2309	870.28857	54.32077	3.8869
2	6.183	BB	0.3140	2.15198e4	1004.19073	96.1131

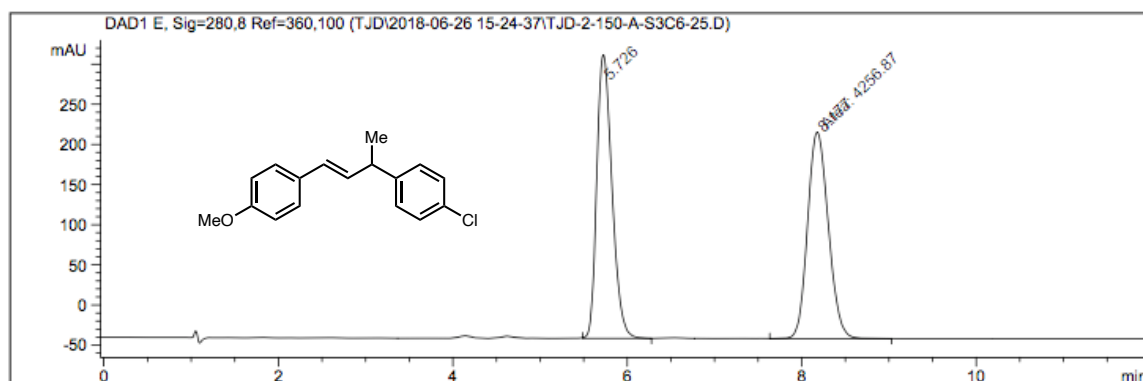
**86a:** racemic

Peak #	RetTime [min]	Type	Width [min]	Area [mAU*s]	Height [mAU]	Area %
1	5.429	MM	0.2337	4117.82129	293.71591	50.5972
2	7.848	MM	0.3339	4020.61816	200.69434	49.4028

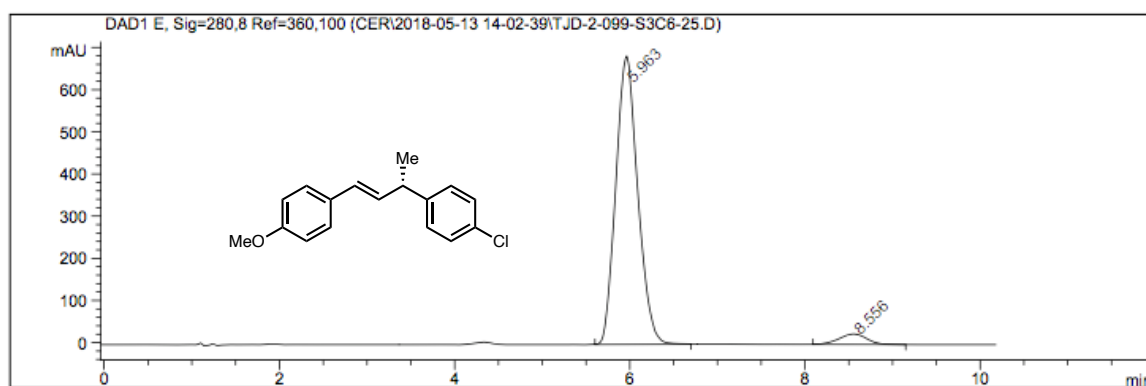
**86a:** enantioenriched (90%ee)

Peak #	RetTime [min]	Type	Width [min]	Area [mAU*s]	Height [mAU]	Area %
1	5.914	VB	0.2477	8243.13574	501.59589	94.9228
2	7.991	BB	0.3186	440.90982	21.92904	5.0772

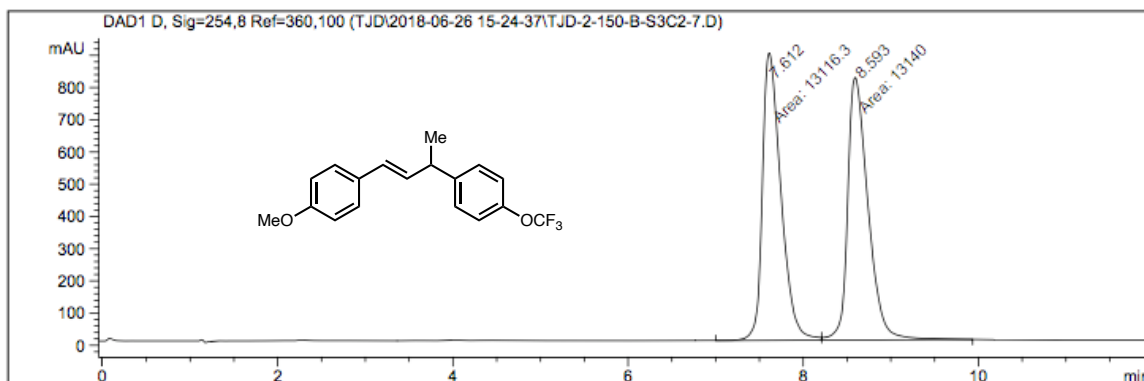


**86b**: racemic

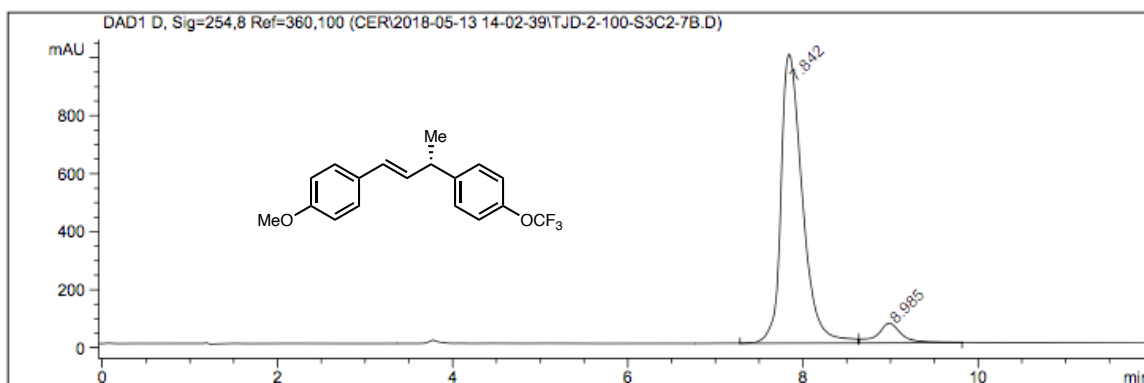
Peak #	RetTime [min]	Type	Width [min]	Area [mAU*s]	Height [mAU]	Area %
1	5.726	BB	0.1895	4279.93555	352.95728	50.1351
2	8.177	MM	0.2757	4256.86816	257.29523	49.8649

**86b**: enantioenriched (91% ee)

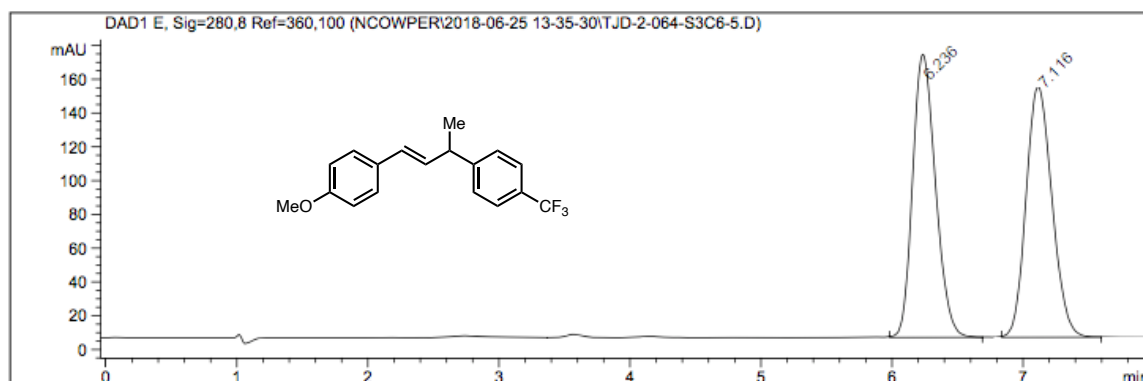
Peak #	RetTime [min]	Type	Width [min]	Area [mAU*s]	Height [mAU]	Area %
1	5.963	BB	0.2633	1.19123e4	683.64136	95.5834
2	8.556	BB	0.3440	550.43402	25.08791	4.4166

**86c: racemic**

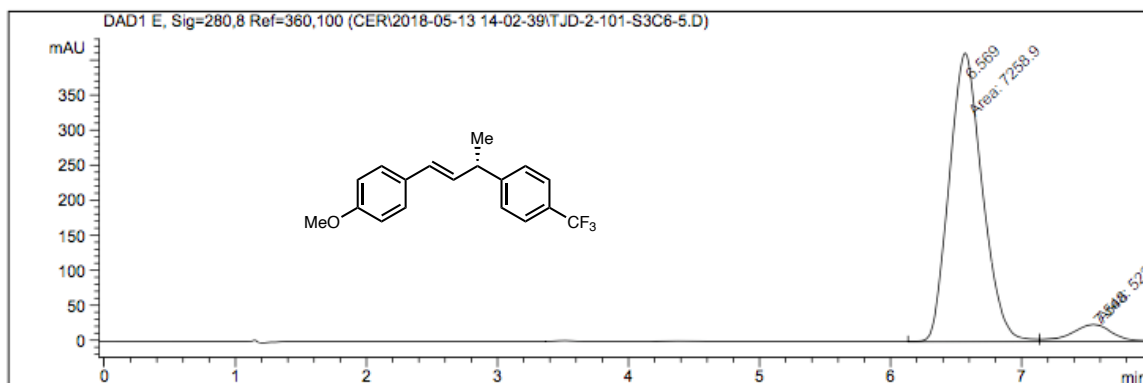
Peak #	RetTime [min]	Type	Width [min]	Area [mAU*s]	Height [mAU]	Area %
1	7.612	MF	0.2448	1.31163e4	893.09790	49.9549
2	8.593	FM	0.2685	1.31400e4	815.61133	50.0451

**86c: enantioenriched (86% ee)**

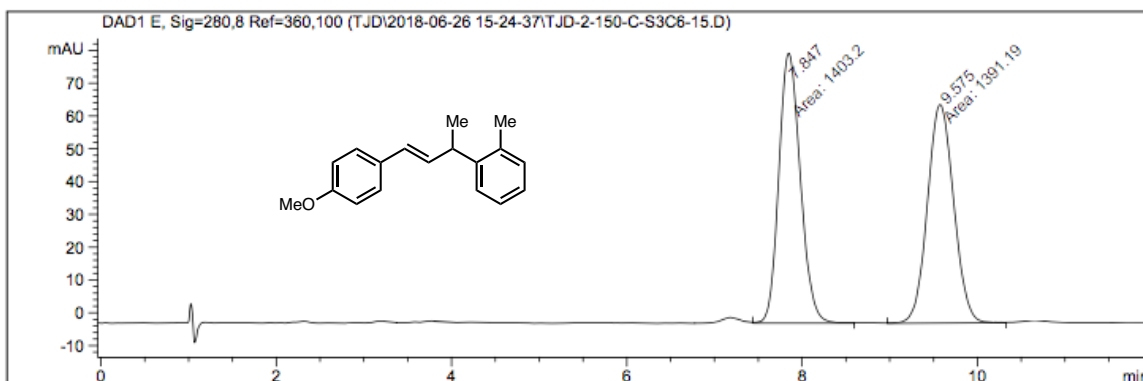
Peak #	RetTime [min]	Type	Width [min]	Area [mAU*s]	Height [mAU]	Area %
1	7.842	VV	0.2592	1.69869e4	995.06494	92.7528
2	8.985	VB	0.2788	1327.27454	68.27623	7.2472

**86d: racemic**

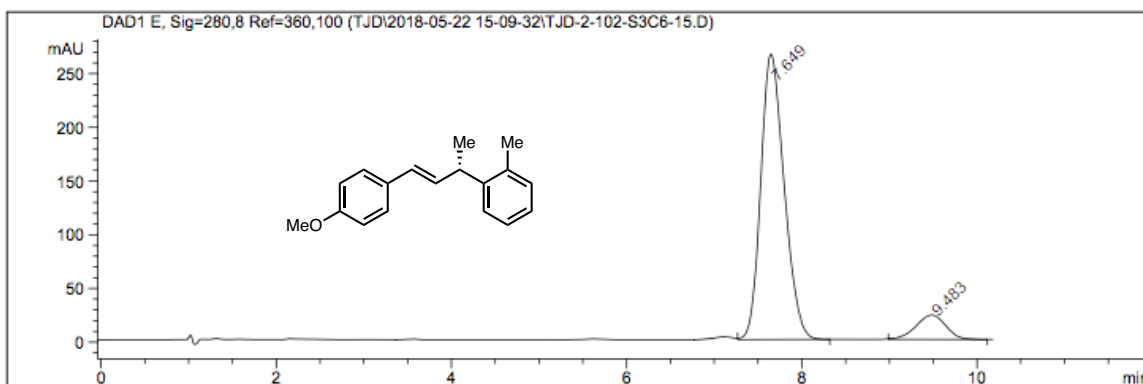
Peak #	RetTime [min]	Type	Width [min]	Area [mAU*s]	Height [mAU]	Area %
1	6.236	BB	0.1900	2037.27722	167.43411	49.9070
2	7.116	BB	0.2167	2044.87195	148.43217	50.0930

**86d: enantioenriched (87% ee)**

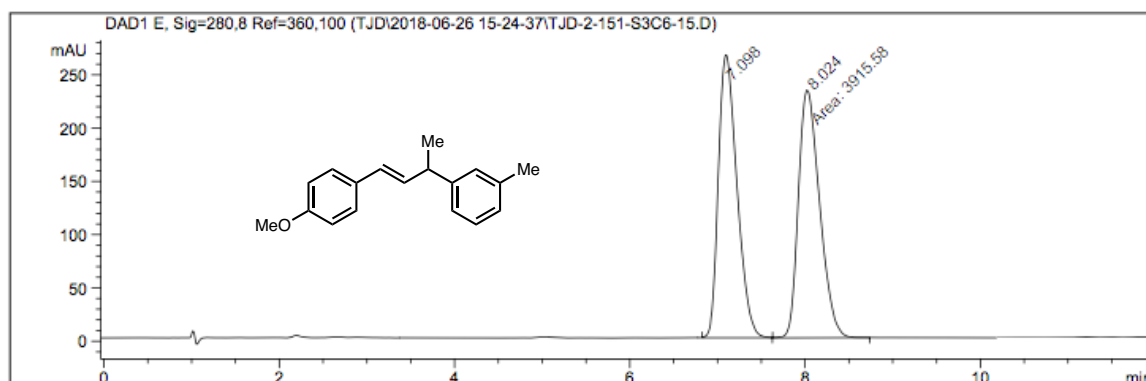
Peak #	RetTime [min]	Type	Width [min]	Area [mAU*s]	Height [mAU]	Area %
1	6.569	MF	0.2935	7258.89746	412.21140	93.2829
2	7.548	FM	0.3567	522.70099	24.42154	6.7171

**86e**: racemic

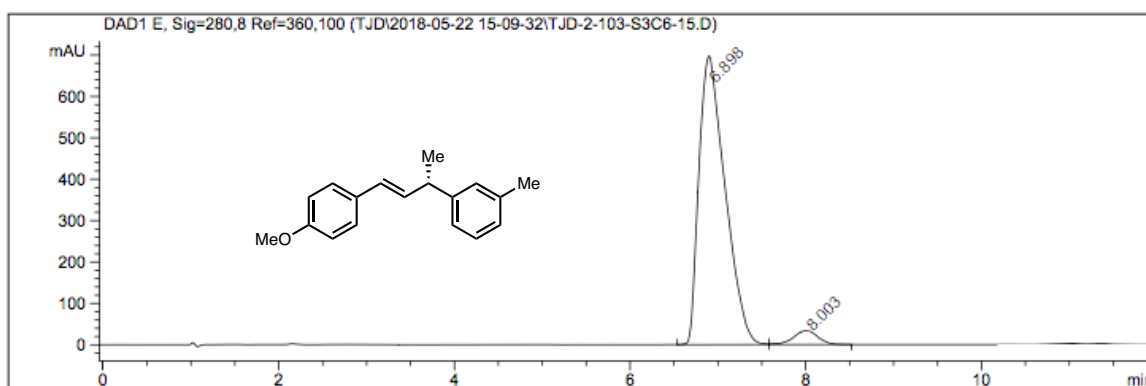
Peak #	RetTime [min]	Type	Width [min]	Area [mAU*s]	Height [mAU]	Area %
1	7.847	MM	0.2841	1403.19934	82.31859	50.2149
2	9.575	MM	0.3476	1391.19177	66.70676	49.7851

**86e**: enantioenriched (80% ee)

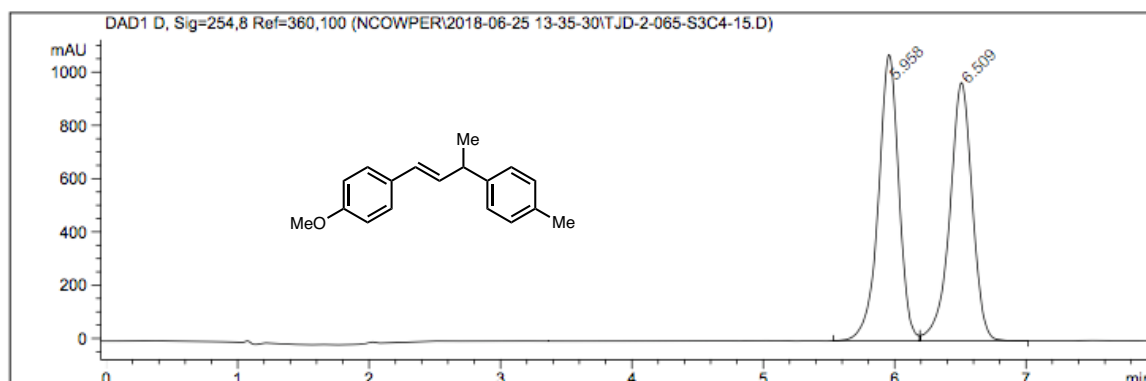
Peak #	RetTime [min]	Type	Width [min]	Area [mAU*s]	Height [mAU]	Area %
1	7.649	VB	0.2844	4928.94092	265.69165	90.1632
2	9.483	BB	0.3633	537.74707	22.79209	9.8368

**86f:** racemic

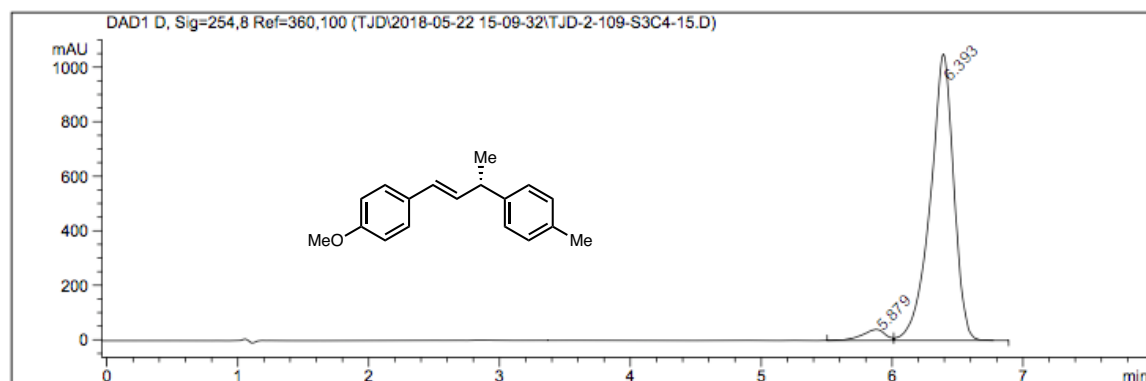
Peak #	RetTime [min]	Type	Width [min]	Area [mAU*s]	Height [mAU]	Area %
1	7.098	BV	0.2284	3922.91309	265.46570	50.0468
2	8.024	MM	0.2804	3915.57642	232.72861	49.9532

**86f:** enantioenriched (91% ee)

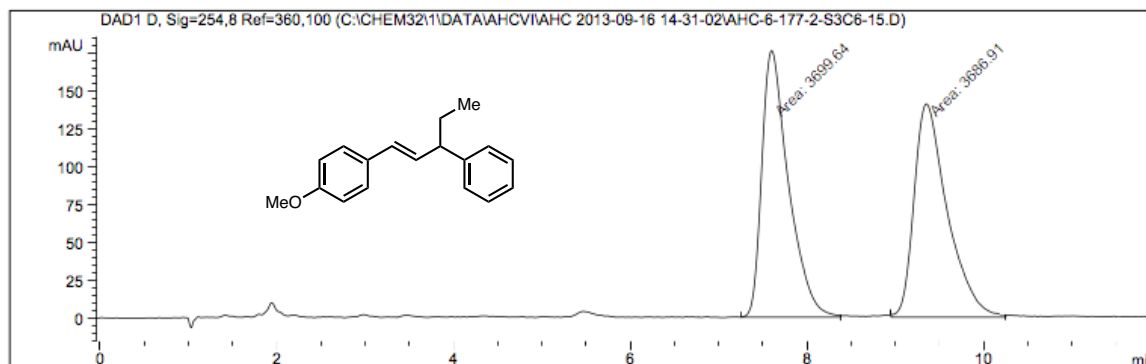
Peak #	RetTime [min]	Type	Width [min]	Area [mAU*s]	Height [mAU]	Area %
1	6.898	BV	0.3132	1.44054e4	696.79517	95.7053
2	8.003	VB	0.2939	646.43817	33.98825	4.2947

**86g**: racemic

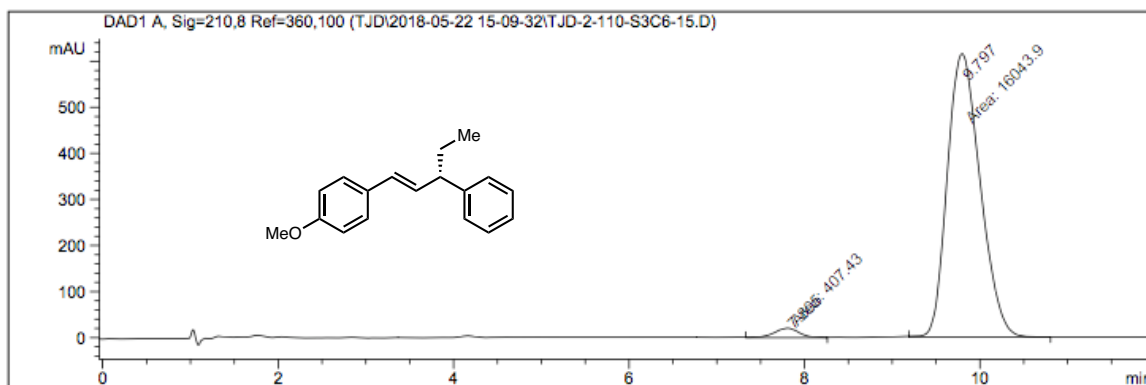
Peak #	RetTime [min]	Type	Width [min]	Area [mAU*s]	Height [mAU]	Area %
1	5.958	BV	0.1622	1.16174e4	1073.94104	50.1090
2	6.509	VB	0.1792	1.15668e4	969.66266	49.8910

**86g**: enantioenriched (93% ee)

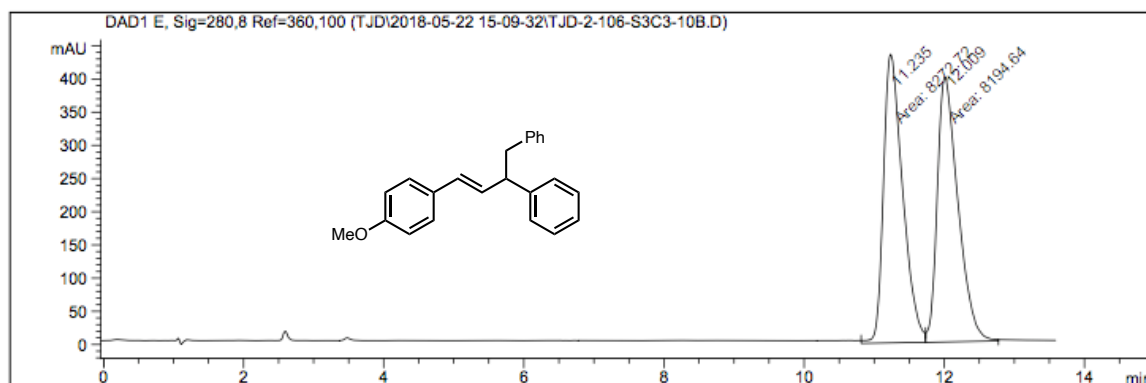
Peak #	RetTime [min]	Type	Width [min]	Area [mAU*s]	Height [mAU]	Area %
1	5.879	BV	0.1761	495.75064	41.28818	3.6415
2	6.393	VB	0.1819	1.31183e4	1048.95959	96.3585

**86h**: racemic

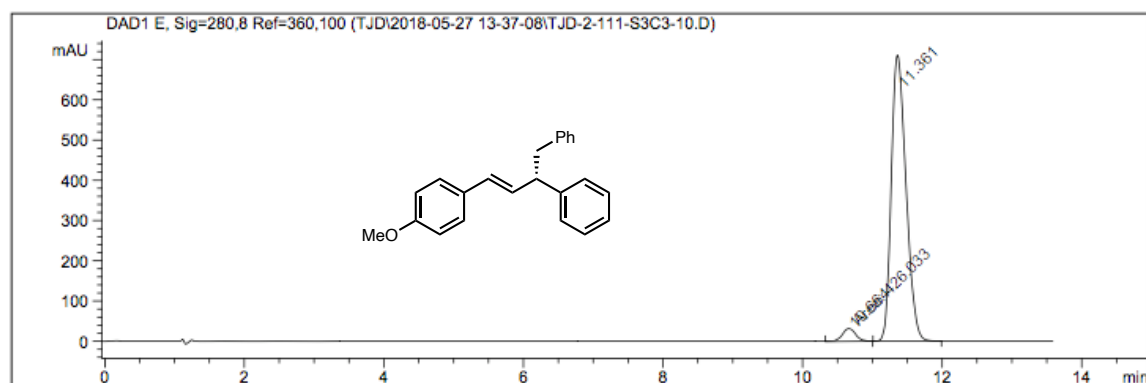
Peak #	RetTime [min]	Type	Width [min]	Area [mAU*s]	Height [mAU]	Area %
1	7.600	MM	0.3500	3699.64233	176.16603	50.0862
2	9.352	MM	0.4361	3686.90503	140.91353	49.9138

**86h**: enantioenriched (95% ee)

Peak #	RetTime [min]	Type	Width [min]	Area [mAU*s]	Height [mAU]	Area %
1	7.805	MM	0.3292	407.43002	20.62672	2.4766
2	9.797	MM	0.4343	1.60439e4	615.66370	97.5234

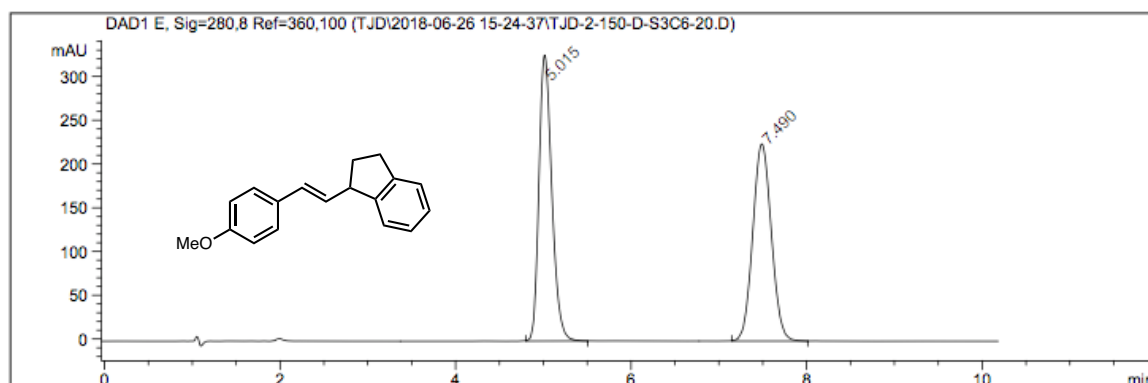
**86i**: racemic

Peak #	RetTime [min]	Type	Width [min]	Area [mAU*s]	Height [mAU]	Area %
1	11.235	MF	0.3171	8272.72363	434.85117	50.2371
2	12.009	FM	0.3425	8194.64453	398.71689	49.7629

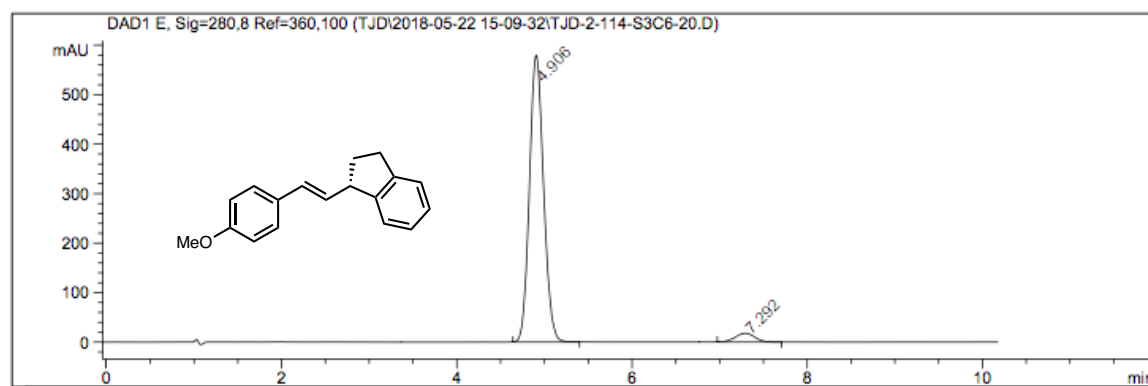
**86i**: enantioenriched (92% ee)

Peak #	RetTime [min]	Type	Width [min]	Area [mAU*s]	Height [mAU]	Area %
1	10.664	MM	0.2189	426.03320	32.44466	3.9344
2	11.361	VB	0.2270	1.04023e4	709.86749	96.0656

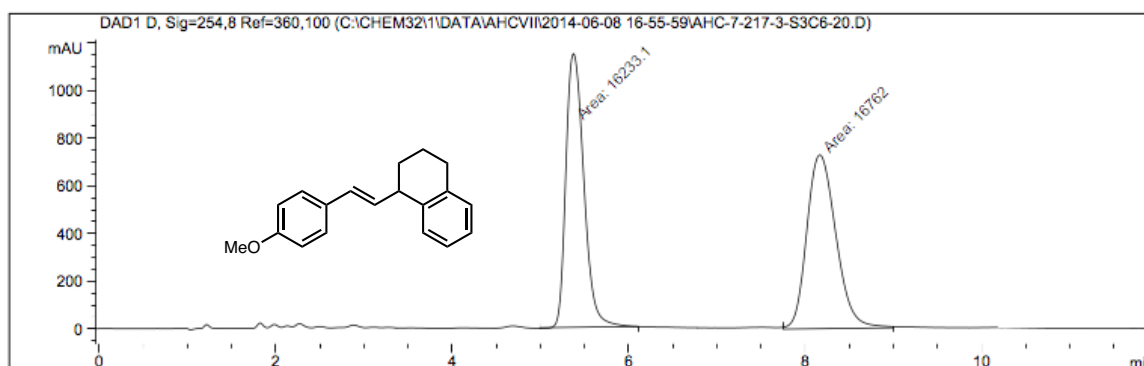


**86j**: racemic

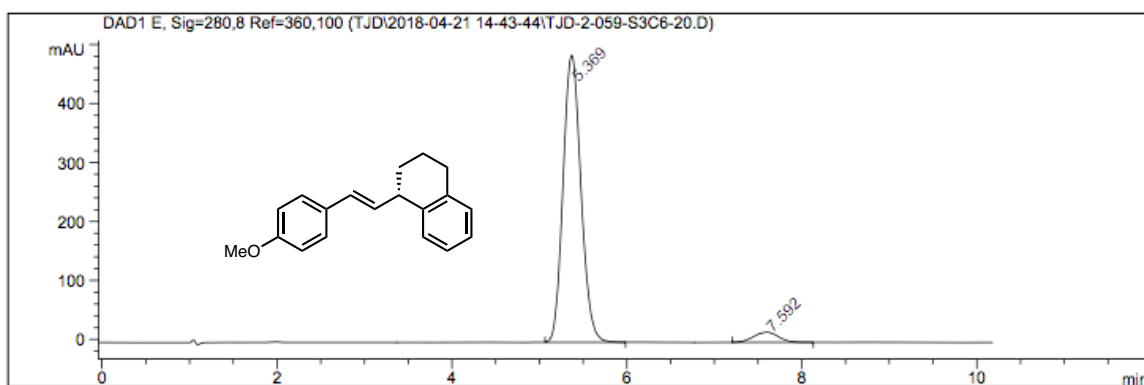
Peak #	RetTime [min]	Type	Width [min]	Area [mAU*s]	Height [mAU]	Area %
1	5.015	BB	0.1591	3332.37524	326.43350	50.1220
2	7.490	BBA	0.2318	3316.15186	225.15051	49.8780

**86j**: enantioenriched (92% ee)

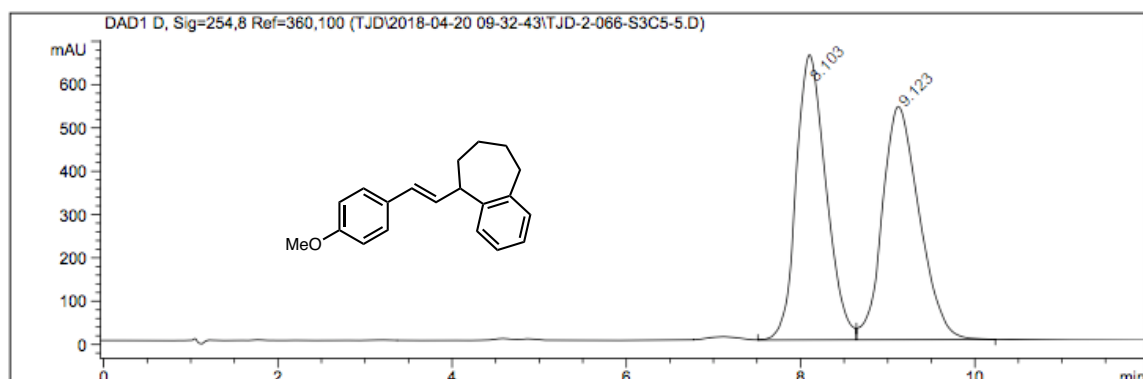
Peak #	RetTime [min]	Type	Width [min]	Area [mAU*s]	Height [mAU]	Area %
1	4.906	BB	0.1748	6491.37842	579.01587	95.8259
2	7.292	BB	0.2432	282.75620	18.00612	4.1741

**86k:** racemic

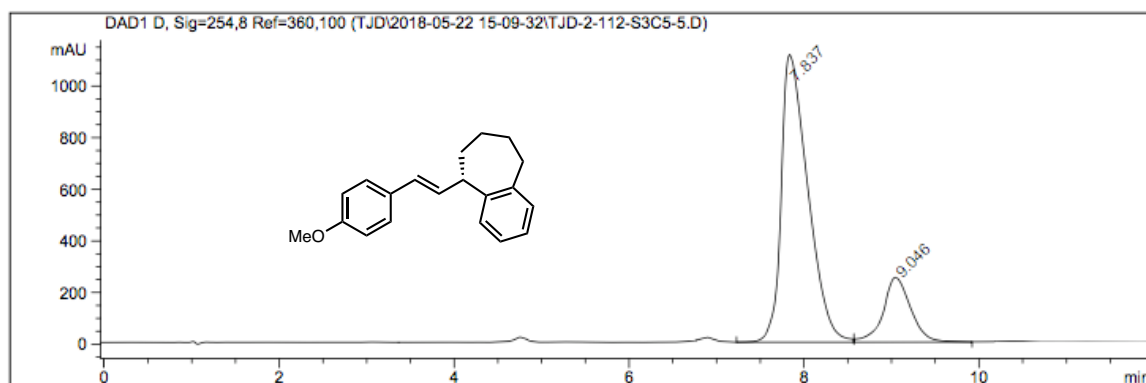
Peak #	RetTime [min]	Type	Width [min]	Area [mAU*s]	Height [mAU]	Area %
1	5.375	MM	0.2355	1.62331e4	1148.88831	49.1985
2	8.167	MM	0.3832	1.67620e4	728.97369	50.8015

**86k:** enantioenriched (91% ee)

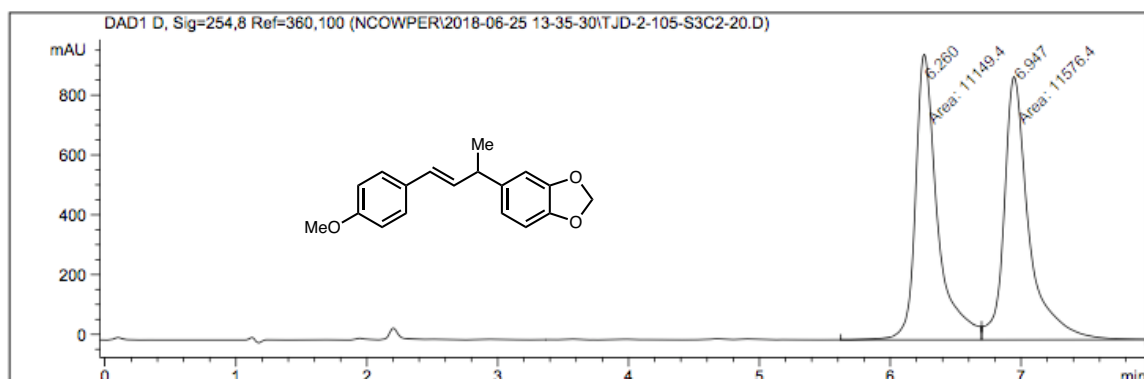
Peak #	RetTime [min]	Type	Width [min]	Area [mAU*s]	Height [mAU]	Area %
1	5.369	BB	0.2220	6926.49170	486.77115	95.2917
2	7.592	BB	0.3063	342.23242	17.64303	4.7083

**86l**: racemic

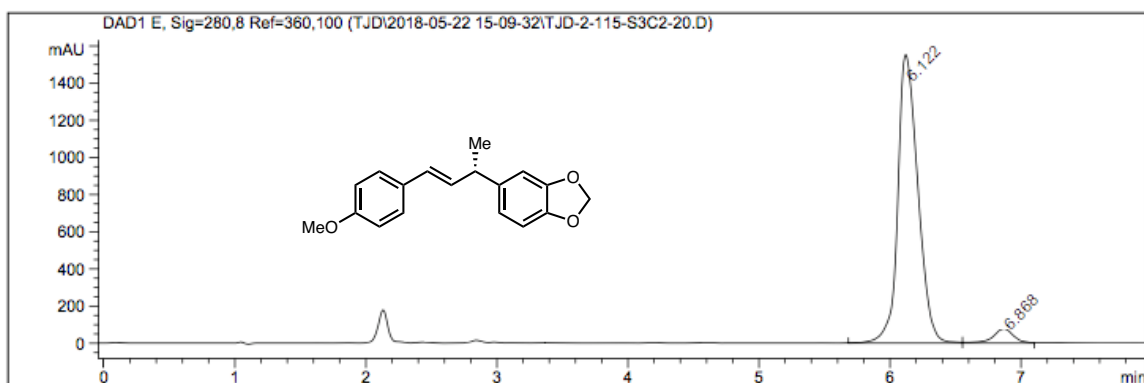
Peak #	RetTime [min]	Type	Width [min]	Area [mAU*s]	Height [mAU]	Area %
1	8.103	VV	0.3745	1.57134e4	658.29962	49.6820
2	9.123	VB	0.4626	1.59146e4	538.73486	50.3180

**86l**: enantioenriched (62% ee)

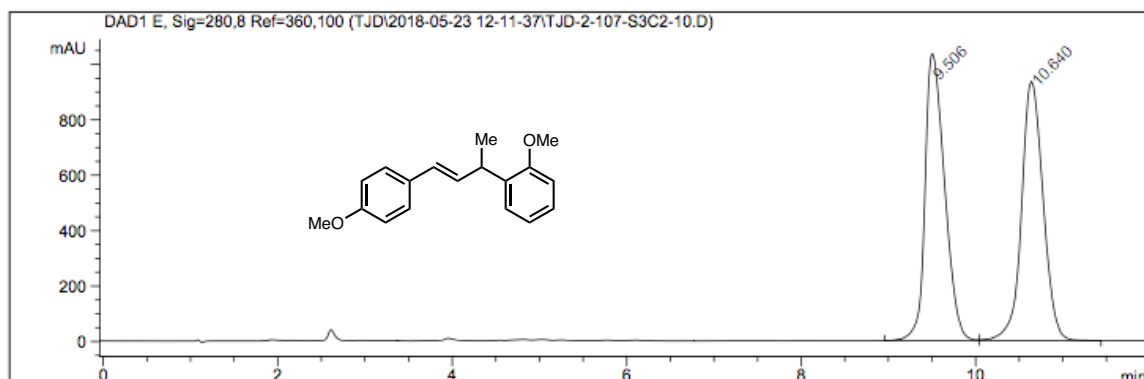
Peak #	RetTime [min]	Type	Width [min]	Area [mAU*s]	Height [mAU]	Area %
1	7.837	VV	0.3237	2.36158e4	1112.40430	81.1648
2	9.046	VB	0.3271	5480.30713	250.64174	18.8352

**86m**: racemic

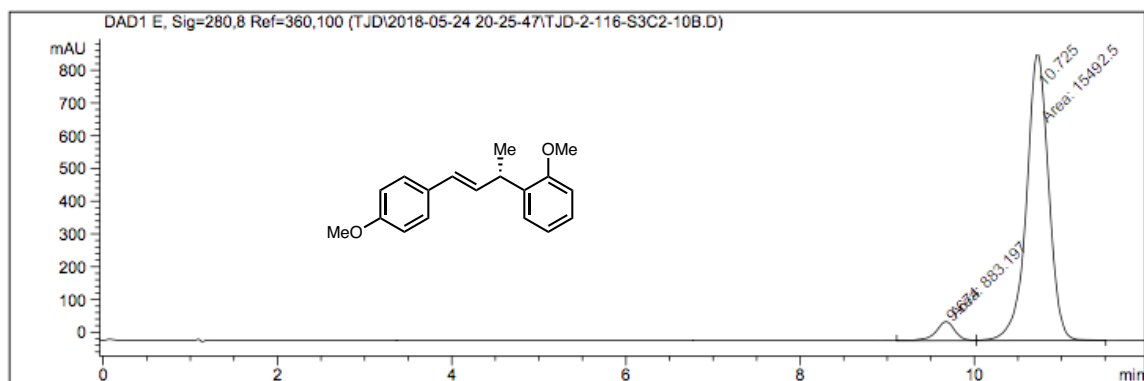
Peak #	RetTime [min]	Type	Width [min]	Area [mAU*s]	Height [mAU]	Area %
1	6.260	MF	0.1943	1.11494e4	956.31140	49.0605
2	6.947	FM	0.2191	1.15764e4	880.54950	50.9395

**86m**: enantioenriched (90% ee)

Peak #	RetTime [min]	Type	Width [min]	Area [mAU*s]	Height [mAU]	Area %
1	6.122	BV	0.1687	1.65625e4	1549.45154	95.1631
2	6.868	VV	0.1624	841.82269	77.71959	4.8369

**86n**: racemic

Peak #	RetTime [min]	Type	Width [min]	Area [mAU*s]	Height [mAU]	Area %
1	9.506	BV	0.2463	1.61926e4	1036.09363	50.0758
2	10.640	VB	0.2694	1.61436e4	935.20160	49.9242

**86n**: enantioenriched (90% ee)

Peak #	RetTime [min]	Type	Width [min]	Area [mAU*s]	Height [mAU]	Area %
1	9.674	MF	0.2520	883.19702	58.40783	5.3934
2	10.725	FM	0.2945	1.54925e4	876.69427	94.6066

## 1.5 NOTES AND REFERENCES

- (1) DeLano, T. J.; Reisman, S. E. *ACS Catal.* **2019**, *9* (8), 6751–6754.
- (2) Poremba, K. E.; Dibrell, S. E.; Reisman, S. E. *ACS Catal.* **2020**, *10* (15), 8237–8246.
- (3) Charboneau, D. J.; Brudvig, G. W.; Hazari, N.; Lant, H. M. C.; Saydjari, A. K. *ACS Catal.* **2019**, *9*, 3228–3241.
- (4) Zhao, W.; Guizzetti, S.; Schwindeman, J. A.; Daniels, D. S. B.; Guerrero, C. A.; Knight, J. *Org. Process Res. Dev.* **2018**, *22* (2), 117–124.
- (5) Suzuki, N.; Hofstra, J. L.; Poremba, K. E.; Reisman, S. E. *Org. Lett.* **2017**, *19* (8), 2150–2153.
- (6) Anka-Lufford, L. L.; Huihui, K. M. M.; Gower, N. J.; Ackerman, L. K. G.; Weix, D. J. *Chem. – Eur. J.* **2016**, *22* (33), 11564–11567.
- (7) Xu, H.; Zhao, C.; Qian, Q.; Deng, W.; Gong, H. *Chem. Sci.* **2013**, *4* (10), 4022–4029.
- (8) Chen, T. Q.; MacMillan, D. W. C. *Angew. Chem. Int. Ed.* **2019**, *58* (41), 14584–14588.
- (9) Duan, Z.; Li, W.; Lei, A. *Org. Lett.* **2016**, *18* (16), 4012–4015.
- (10) Paul, A.; Smith, M. D.; Vannucci, A. K. P. *J. Org. Chem.* **2017**, *82* (4), 1996–2003.
- (11) Zhang, P.; Le, C. “Chip”; MacMillan, D. W. C. *J. Am. Chem. Soc.* **2016**, *138* (26), 8084–8087.
- (12) Guan, H.; Zhang, Q.; Walsh, P. J.; Mao, J. *Angew. Chem. Int. Ed.* **2020**, *59* (13), 5172–5177.

- (13) *Encyclopedia of Applied Electrochemistry*; Kreysa, G., Ota, K., Savinell, R. F., Eds.; Springer New York: New York, NY, 2014.
- (14) Troupel, M.; Rollin, Y.; Sibille, S.; Perichon, J.; Fauvarque, J.-F. *J. Organomet. Chem.* **1980**, *202* (4), 435–446.
- (15) Troupel, M.; Rollin, Y.; Sibille, S.; Fauvarque, J.-F.; Perichon, J. *J. Chem. Res. Synop.* **1980**, No. 1, 26–27.
- (16) Rollin, Y.; Troupel, M.; Perichon, J.; Fauvarque, J.-F. *J. Chem. Res. Synop.* **1981**, No. 10, 322–323.
- (17) Rollin, Y.; Troupel, M.; Tuck, D. G.; Perichon, J. *J. Organomet. Chem.* **1986**, *303* (1), 131–137.
- (18) Courtois, V.; Barhdadi, R.; Troupel, M.; Périchon, J. *Tetrahedron* **1997**, *53* (34), 11569–11576.
- (19) Raynal, F.; Barhdadi, R.; Périchon, J.; Savall, A.; Troupel, M. *Adv. Synth. Catal.* **2002**, *344* (1), 45–49.
- (20) Jutand, A.; Mosleh, A. *J. Org. Chem.* **1997**, *62* (2), 261–274.
- (21) Meyer, G.; Rollin, Y.; Perichon, J. *J. Organomet. Chem.* **1987**, *333* (2), 263–267.
- (22) Cannes, C.; Condon, S.; Durandetti, M.; Périchon, J.; Nédélec, J.-Y. *J. Org. Chem.* **2000**, *65* (15), 4575–4583.
- (23) Amatore, C.; Gaubert, F.; Jutand, A.; Utley, J. H. P. *J. Chem. Soc. Perkin Trans. 2* **1996**, No. 11, 2447–2452.
- (24) Mellah, M.; Labbé, E.; Nédélec, J.-Y.; Périchon, J. *New J. Chem.* **2002**, *26* (2), 207–212.

- (25) Petit, M.-A.; Pfuger, F.; Jutand, A.; Cheurot, C.; Troupe, M. *Makromol. Chem., Rapid Commun.* **1983**, *4*, 455–457.
- (26) Amatore, C.; Jutand, A. *Organometallics* **1988**, *7* (10), 2203–2214.
- (27) Amatore, C.; Jutand, A.; Steffensen, W.; Rømming, C.; Salmén, R.; Tønnesen, H. H.; Tokii, T. *Acta Chem. Scand.* **1990**, *44*, 755–764.
- (28) Amatore, C.; Jutand, A.; Mottier, L. *J. Electroanal. Chem. Interfacial Electrochem.* **1991**, *306* (1), 125–140.
- (29) Folest, J. C.; Périchon, J.; Fauvarque, J. F.; Jutand, A. *J. Organomet. Chem.* **1988**, *342* (2), 259–261.
- (30) Marzouk, H.; Rollin, Y.; Folest, J. C.; Nédélec, J. Y.; Périchon, J. *J. Organomet. Chem.* **1989**, *369* (3), C47–C50.
- (31) Amatore, C.; Jutand, A.; PeÂrichon, J.; Rollin, Y. *Monatshefte für Chemie*, **2000**, *131*, 1293–1304.
- (32) Durandetti, M.; Nédélec, J.-Y.; Périchon, J. N. *J. Org. Chem.* **1996**, *61* (5), 1748–1755.
- (33) Conan, A.; Sibille, S.; d’Incan, E.; Périchon, J. *J. Chem. Soc. Chem. Commun.* **1990**, *1*, 48–49.
- (34) Durandetti, M.; Sibille, S.; Nedelec, J.-Y.; Perichon, J. *Synth. Commun.* **1994**, *24* (2), 145–151.
- (35) Durandetti, M.; Périchon, J. *Synthesis* **2004**, *2004* (18), 3079–3083.
- (36) Durandetti, M.; Périchon, J.; Nédélec, J.-Y. *J. Org. Chem.* **1997**, *62* (23), 7914–7915.
- (37) Durandetti, M.; Lachaise, I.; Nedelec, J. Y.; Perichon, J. FR2765246 (A1), 1998.



- (38) Meyer, G.; Troupel, M.; Périchon, J. *J. Organomet. Chem.* **1990**, *393* (1), 137–142.
- (39) Durandetti, M.; Périchon, J.; Nédélec, J.-Y. *Tetrahedron Lett.* **1997**, *38* (50), 8683–8686.
- (40) Gosmini, C.; Lasry, S.; Nédélec, J.-Y.; Périchon, J. *Tetrahedron* **1998**, *54* (7), 1289–1298.
- (41) Gosmini, C.; Nédélec, J. Y.; Périchon, J. *Tetrahedron Lett.* **2000**, *41* (26), 5039–5042.
- (42) Gosmini, C.; Nédélec, J. Y.; Périchon, J. *Tetrahedron Lett.* **2000**, *41* (2), 201–203.
- (43) Condon-Gueugnot, S.; Leonel, E.; Nédélec, J.-Y.; Périchon, J. *J. Org. Chem.* **1995**, *60* (23), 7684–7686.
- (44) Condon-Gueugnot, S.; Dupré, D.; Nédélec, J.-Y.; Périchon, J. *Synthesis* **1997**, *1997* (12), 1457–1460.
- (45) Condon, S.; Dupré, D.; Nédélec, J. Y. *Org. Lett.* **2003**, *5* (24), 4701–4703.
- (46) Sibille, S.; d’Incan, E.; Leport, L.; Massebiau, M.-C.; Périchon, J. *Tetrahedron Lett.* **1987**, *28* (1), 55–58.
- (47) Durandetti, S.; Sibille, S.; Périchon, J. *J. Org. Chem.* **1989**, *54* (9), 2198–2204.
- (48) Sibille, S.; Nédélec, J.-Y.; Périchon, J. *Electroorg. Synth. Festschr. Man. M Baizer* **1991**, 361–367.
- (49) Mcharek, S.; Sibille, S.; Nédélec, J.-Y.; Périchon, J. *J. Organomet. Chem.* **1991**, *401* (1), 211–215.
- (50) Durandetti, M.; Périchon, J.; Nédélec, J.-Y. *Tetrahedron Lett.* **1999**, *40* (51), 9009–9013.
- (51) Durandetti, M.; Nédélec, J.-Y.; Périchon, J. *Org. Lett.* **2001**, *3* (13), 2073–2076.

- (52) Troupe, M.; Rollin, Y.; Perichon, J. *Nouv. J. Chim.* **1981**, 5 (12), 621–625.
- (53) Fauvarque, J. F.; Chevrot, C.; Jutand, A.; François, M.; Perichon, J. *J. Organomet. Chem.* **1984**, 264 (1), 273–281.
- (54) Fauvarque, J. F.; Jutand, A.; François, M. *Nouv. J. Chim.* **1986**, 10 (2).
- (55) Fauvarque, J. F.; Jutand, A.; François, M. *J. Appl. Electrochem.* **1988**, 18 (1), 109–115.
- (56) Fauvarque, J. F.; Jutand, A.; François, M.; Petit, M. A. *J. Appl. Electrochem.* **1988**, 18 (1), 116–119.
- (57) Fauvarque, J.-F.; Jutand, A.; Chevrot, C.; Pfluger, F.; Troupel, M. P. FR2530266 (A1), 1982.
- (58) Fauvarque, J. F.; De Zelicourt, Y.; Amatore, C.; Jutand, A. *J. Appl. Electrochem.* **1990**, 20 (2), 338–340.
- (59) Duñach, E.; Périchon, J. *J. Organomet. Chem.* **1988**, 352 (1), 239–246.
- (60) Labbé, E.; Duñach, E.; Périchon, J. *J. Organomet. Chem.* **1988**, 353 (3), C51–C56.
- (61) Duñach, E.; Dérien, S.; Périchon, J. *J. Organomet. Chem.* **1989**, 364 (3), C33–C36.
- (62) Dérien, S.; Clinet, J.-C.; Duñach, E.; Périchon, J. C. *Synlett* **1990**, 1990 (06), 361–364.
- (63) Duñach, E.; Périchon, J. N. *Synlett* **1990**, 1990 (03), 143–145.
- (64) Dérien, S.; Duñach, E.; Périchon, J. *J. Organomet. Chem.* **1990**, 385 (3), C43–C46.
- (65) Dérien, S.; Clinet, J.-C.; Duñach, E.; Périchon, J. F. *J. Chem. Soc. Chem. Commun.* **1991**, 8, 549–550.
- (66) Dérien, S.; Dunach, E.; Perichon, J. *J. Am. Chem. Soc.* **1991**, 113 (22), 8447–8454.

- (67) Dérien, S.; Clinet, J.-C.; Duñach, E.; Périchon, J. *Tetrahedron* **1992**, *48* (25), 5235–5248.
- (68) Dérien, S.; Clinet, J.-C.; Duñach, E.; Périchon, J. *J. Organomet. Chem.* **1992**, *424* (2), 213–224.
- (69) Dérien, S.; Clinet, J. C.; Dunach, E.; Perichon, J. *J. Org. Chem.* **1993**, *58* (9), 2578–2588.
- (70) Garnier, L.; Rollin, Y.; Périchon, J. *J. Organomet. Chem.* **1989**, *367* (3), 347–358.
- (71) Oçafrain, M.; Devaud, M.; Troupel, M.; Périchon, J. *J. Chem. Soc. Chem. Commun.* **1995**, *22*, 2331–2332.
- (72) Oçafrain, M.; Devaud, M.; Nédélec, J. Y.; Troupel, M. *J. Organomet. Chem.* **1998**, *560* (1), 103–107.
- (73) Oçafrain, M.; Dolhem, E.; Nédélec, J. Y.; Troupel, M. *J. Organomet. Chem.* **1998**, *571* (1), 37–42.
- (74) Garnier, L.; Rollin, Y.; Perichon, J. EP0323300 (A1), 1988.
- (75) Dolhem, E.; Oçafrain, M.; Nédélec, J. Y.; Troupel, M. *Tetrahedron* **1997**, *53* (50), 17089–17096.
- (76) Friedrich, J. M.; Ponce-de-León, C.; Reade, G. W.; Walsh, F. C. *J. Electroanal. Chem.* **2004**, *561*, 203–217.
- (77) Perkins, R. J.; Pedro, D. J.; Hansen, E. C. *Org. Lett.* **2017**, *19* (14), 3755–3758.
- (78) Li, H.; Breen, C. P.; Seo, H.; Jamison, T. F.; Fang, Y.-Q.; Bio, M. M. *Org. Lett.* **2018**, *20* (5), 1338–1341.
- (79) Koyanagi, T.; Herath, A.; Chong, A.; Ratnikov, M.; Valiere, A.; Chang, J.; Molteni, V.; Loren, J. *Org. Lett.* **2019**, *21* (3), 816–820.

- (80) Perkins, R. J.; Hughes, A. J.; Weix, D. J.; Hansen, E. C. *Org. Process Res. Dev.* **2019**, *23* (8), 1746–1751.
- (81) Cherney, A. H.; Reisman, S. E. *J. Am. Chem. Soc.* **2014**, *136* (41), 14365–14368.
- (82) Everson, D. A.; Weix, D. J. *J. Org. Chem.* **2014**, *79* (11), 4793–4798.
- (83) Prinsell, M. R.; Everson, D. A.; Weix, D. J. *Chem. Commun.* **2010**, *46* (31), 5743–5745.
- (84) Colon, I.; Kelsey, D. R. *J. Org. Chem.* **1986**, *51* (14), 2627–2637.
- (85) Horn, E. J.; Rosen, B. R.; Chen, Y.; Tang, J.; Chen, K.; Eastgate, M. D.; Baran, P. S. *Nature* **2016**, *533* (7601), 77–81.
- (86) Blackmond, D. G. *Angew. Chem. Int. Ed.* **2005**, *44* (28), 4302–4320.
- (87) Nielsen, C. D.-T.; Burés, J. *Chem. Sci.* **2019**, *10* (2), 348–353.
- (88) Lei, C.; Liang, F.; Li, J.; Chen, W.; Huang, B. *Chem. Eng. J.* **2019**, *358*, 1054–1064.
- (89) Burés, J. *Angew. Chem. Int. Ed.* **2016**, *55* (6), 2028–2031.
- (90) Poremba, K. E.; Kadunce, N. T.; Suzuki, N.; Cherney, A. H.; Reisman, S. E. *J. Am. Chem. Soc.* **2017**, *139* (16), 5684–5687.
- (91) Kadunce, N. T.; Reisman, S. E. *J. Am. Chem. Soc.* **2015**, *137* (33), 10480–10483.
- (92) Hofstra, J. L.; DeLano, T. J.; Reisman, S. E. *Org. Synth.* **2020**, *97*, 172–188.
- (93) Still, C. W.; Kahn, M.; Mitra, A. *J. Org. Chem.* **1978**, *43*, 2923–2925.
- (94) Hofstra, J. L.; Cherney, A. H.; Ordner, C. M.; Reisman, S. E. *J. Am. Chem. Soc.* **2018**, *140* (1), 139–142.
- (95) Cherney, A. H.; Kadunce, N. T.; Reisman, S. E. *J. Am. Chem. Soc.* **2013**, *135* (20), 7442–7445.

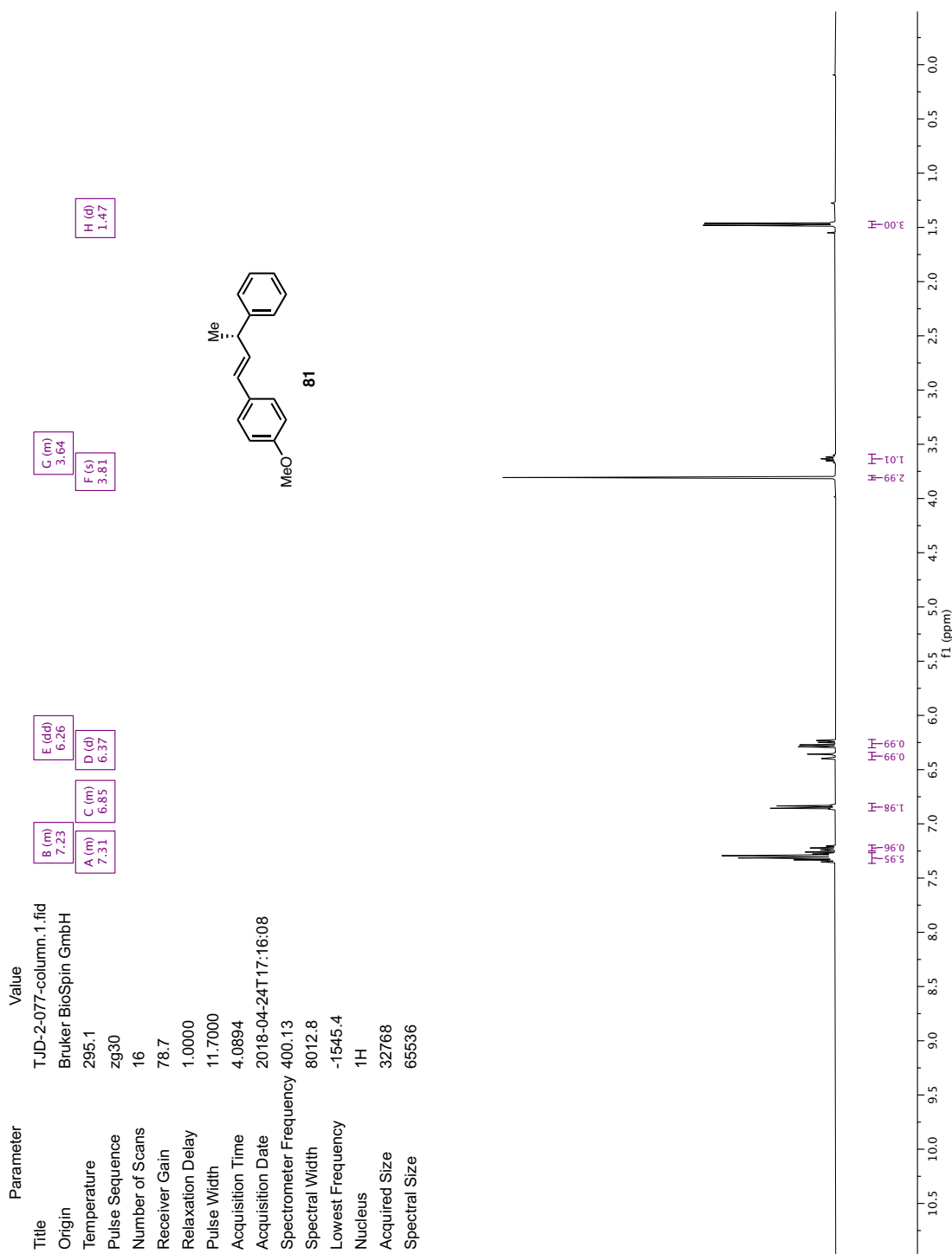
- (96) Mandal, S. K.; Jensen, D. R.; Pugsley, J. S.; Sigman, M. S. *J. Org. Chem.* **2003**, *68* (11), 4600–4603.
- (97) El Ahmad, Y.; Laurent, E.; Maillet, P.; Talab, A.; Teste, J. F.; Dokhan, R.; Tran, G.; Ollivier, R. *J. Med. Chem.* **1997**, *40* (6), 952–960.
- (98) Joncour, A.; Décor, A.; Liu, J.-M.; Tran Huu Dau, M.-E.; Baudoin, O. *Chem. – Eur. J.* **2007**, *13* (19), 5450–5465.
- (99) Yu, H.; Liu-Bujalski, L.; Johnson, T. L. WO2014159234 (A1), 2014.
- (100) Jiang, F.; Yuan, K.; Achard, M.; Bruneau, C. *Chem. – Eur. J.* **2013**, *19*, 20343–10352.
- (101) Liang, S.; Hammond, G. B.; Xu, B. *Green Chem.* **2018**, *20* (3), 680–684.

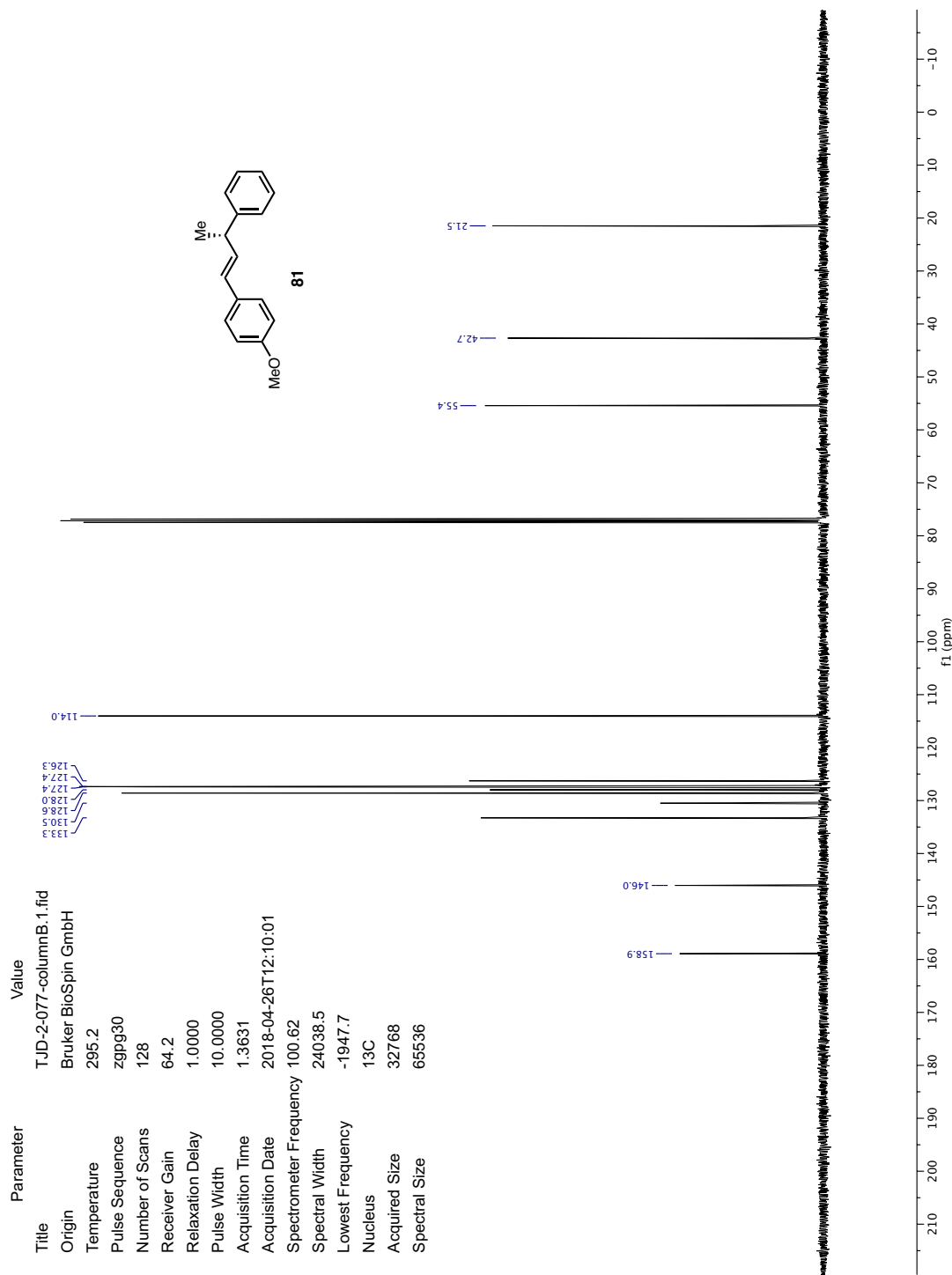
## ***Appendix 1***

*Spectra Relevant to Chapter 1:*

*Enantioselective Electroreductive Cross-Coupling of Alkenyl and Benzyl*

*Halides via Nickel Catalysis*

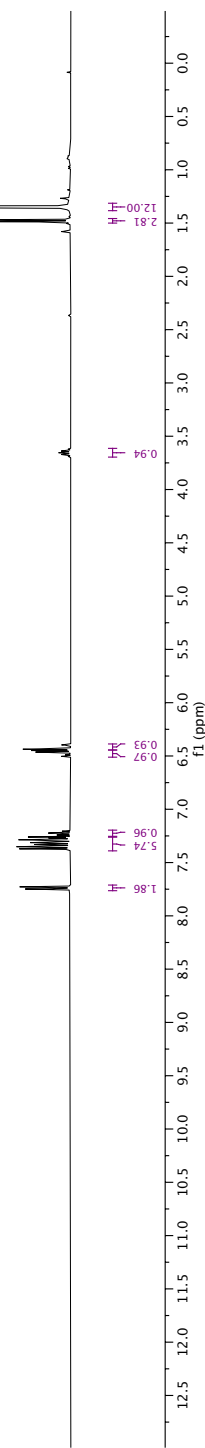
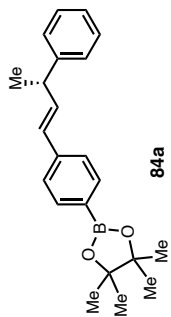


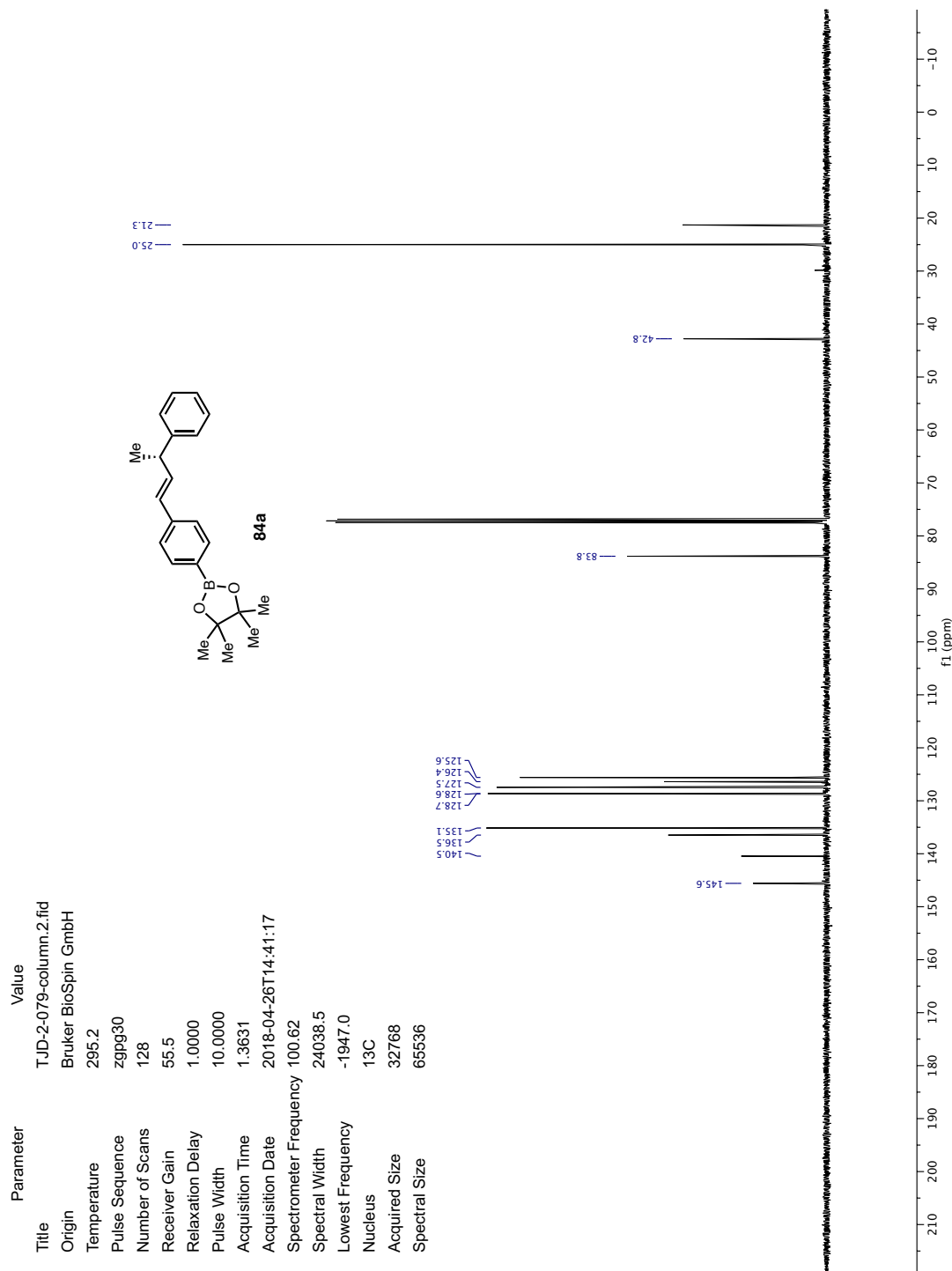


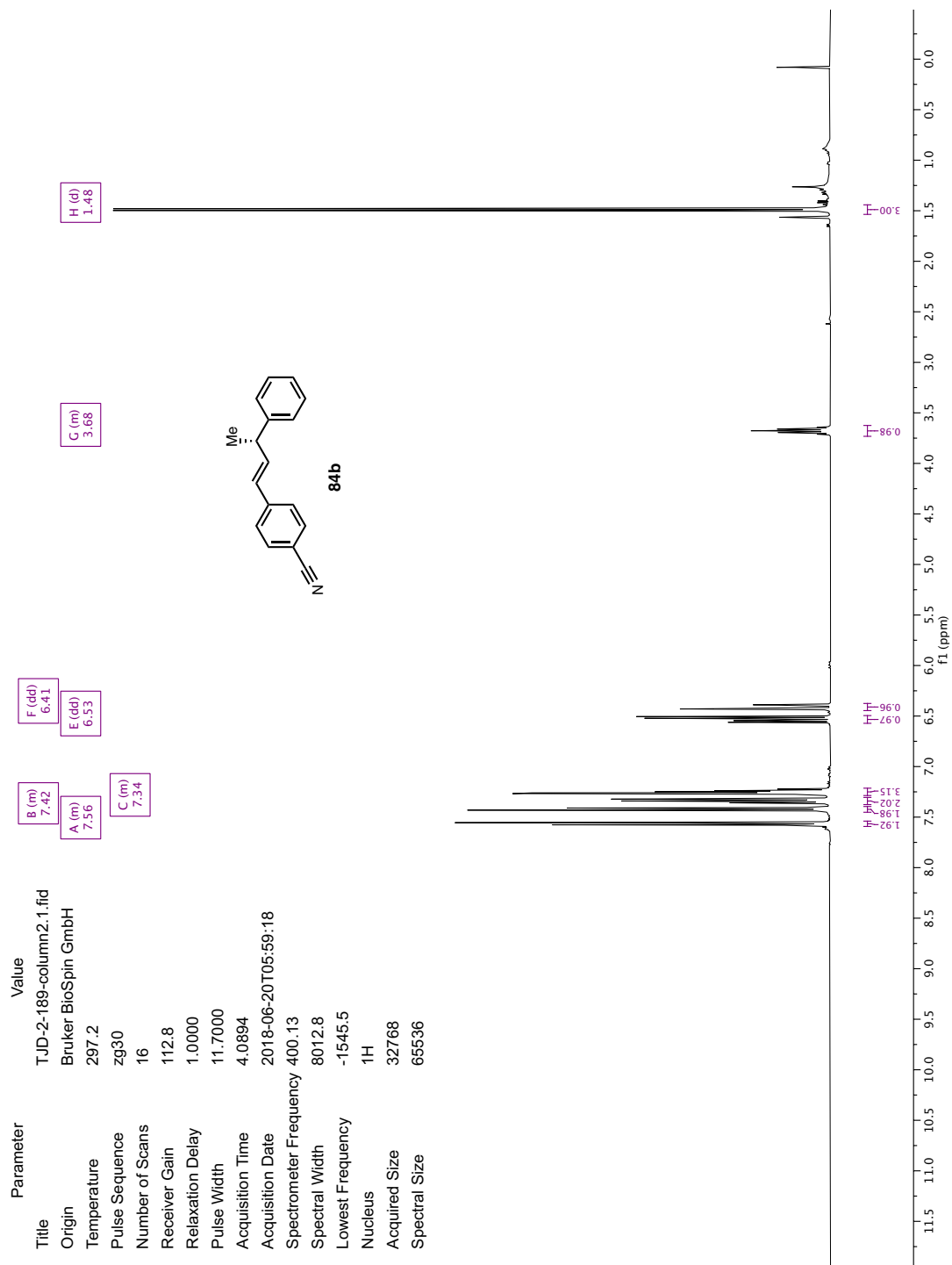


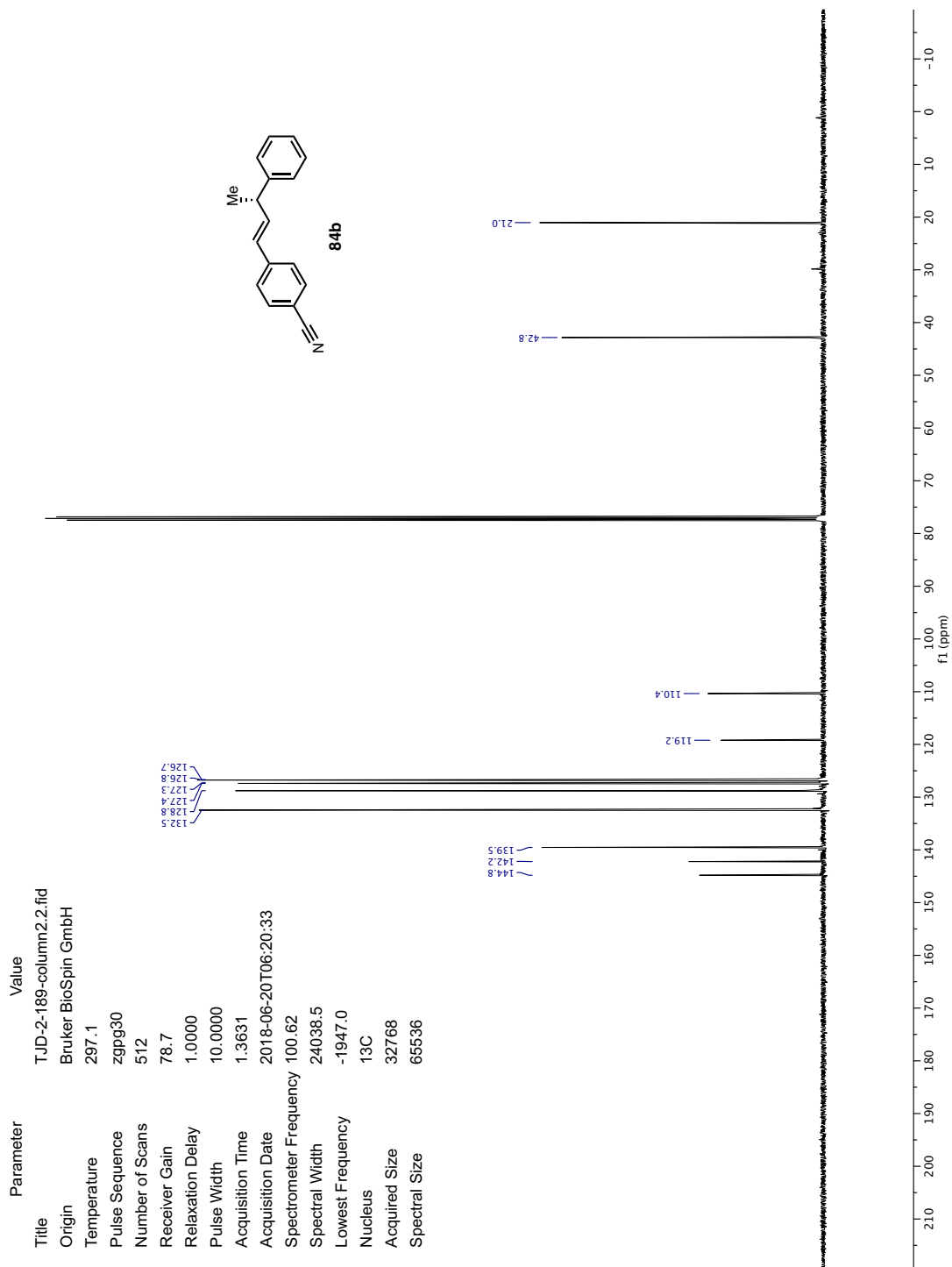
Parameter	Value
Title	TJD-2-079-column.1.fid
Origin	Bruker BioSpin GmbH
Temperature	295.2
Pulse Sequence	zg30
Number of Scans	16
Receiver Gain	72.0
Relaxation Delay	1.0000
Pulse Width	11.7000
Acquisition Time	4.0894
Acquisition Date	2018-04-26T14:34:22
Spectrometer Frequency	400.13
Spectral Width	8012.8
Lowest Frequency	-1545.3
Nucleus	<sup>1</sup> H
Acquired Size	32768
Spectral Size	65536

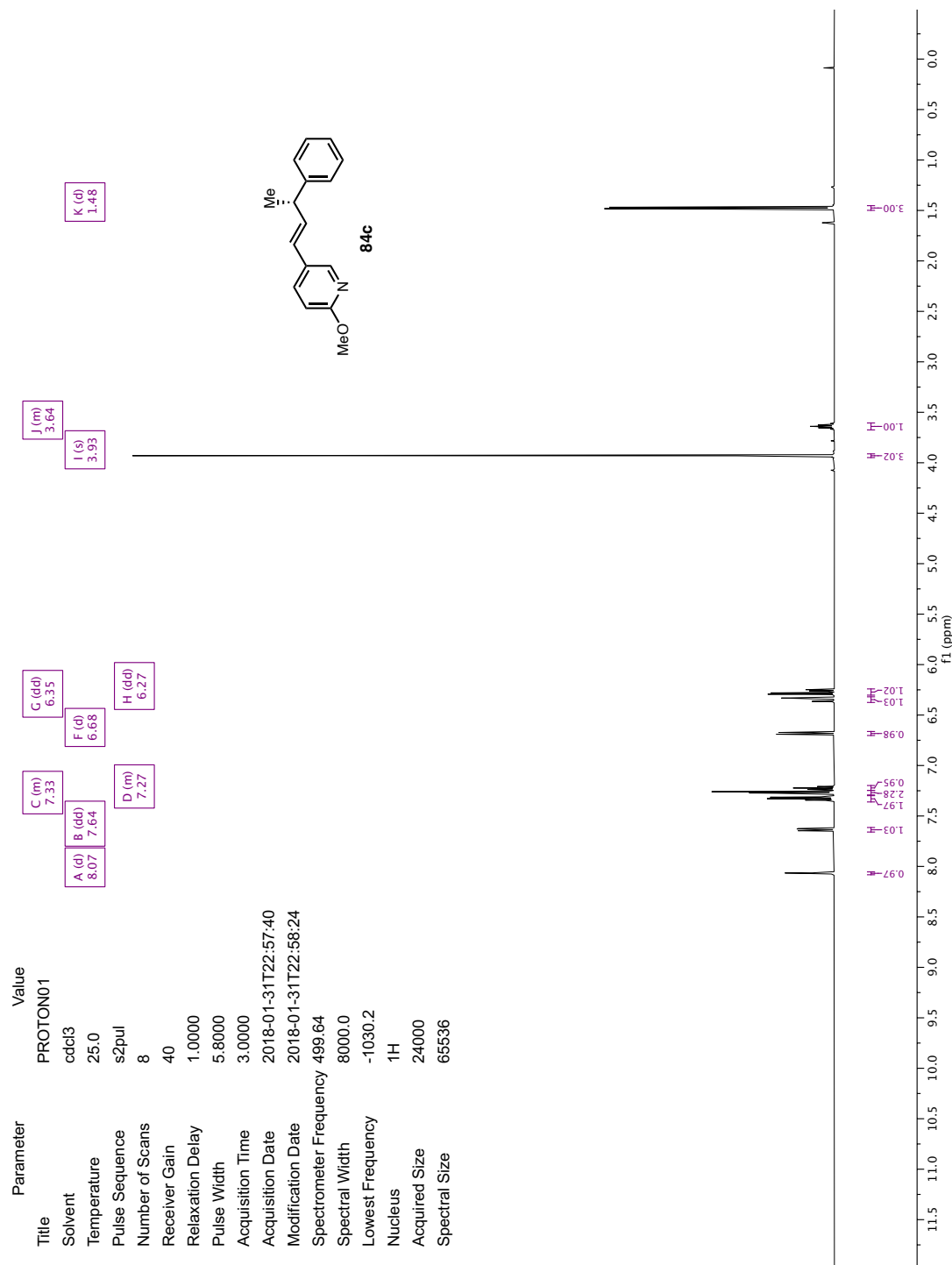
A (m)	7.74
B (m)	7.32
C (m)	7.23
D (dd)	6.48
E (d)	6.42
F (m)	3.65
C (d)	1.48
H (s)	1.35

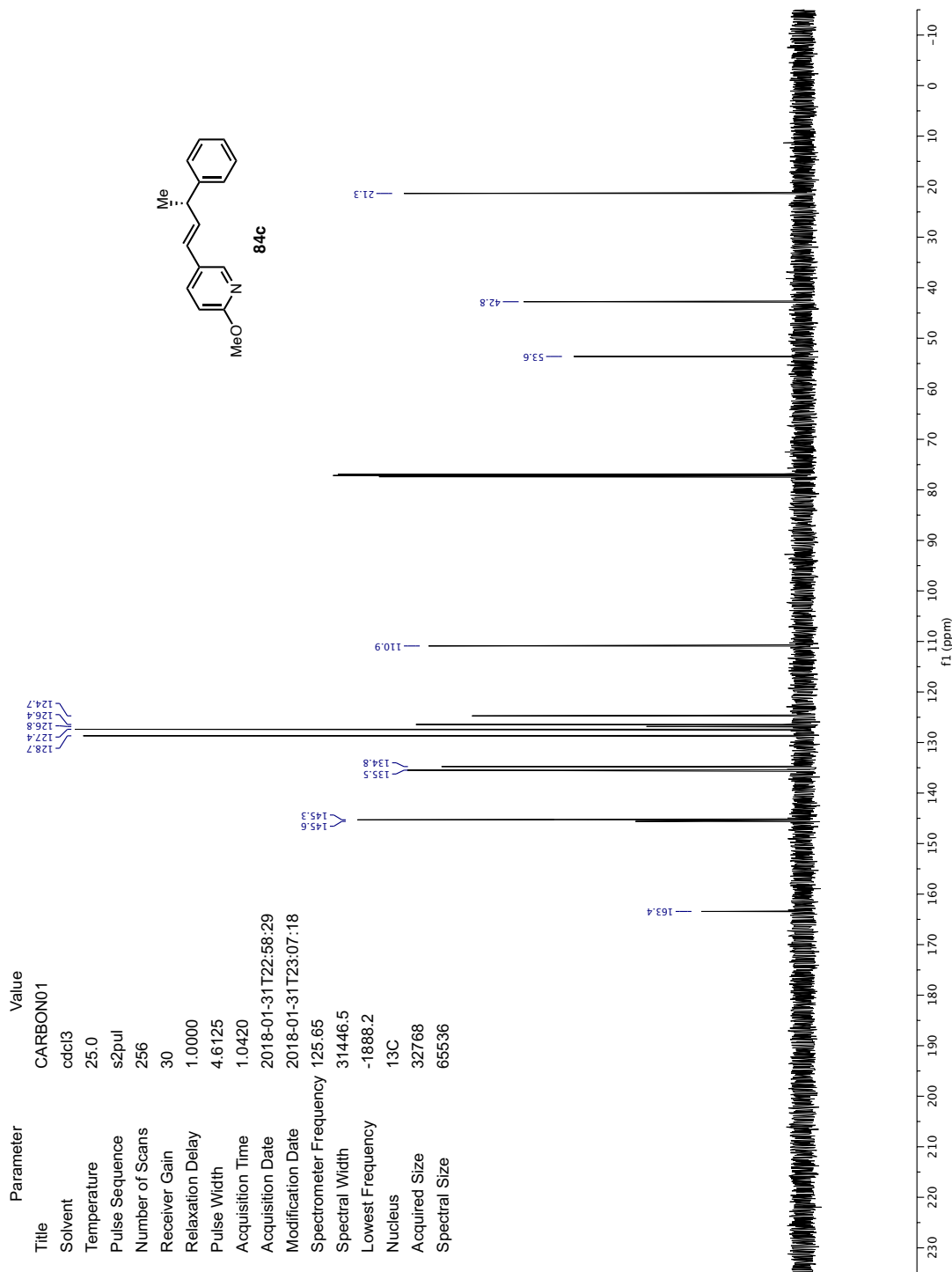


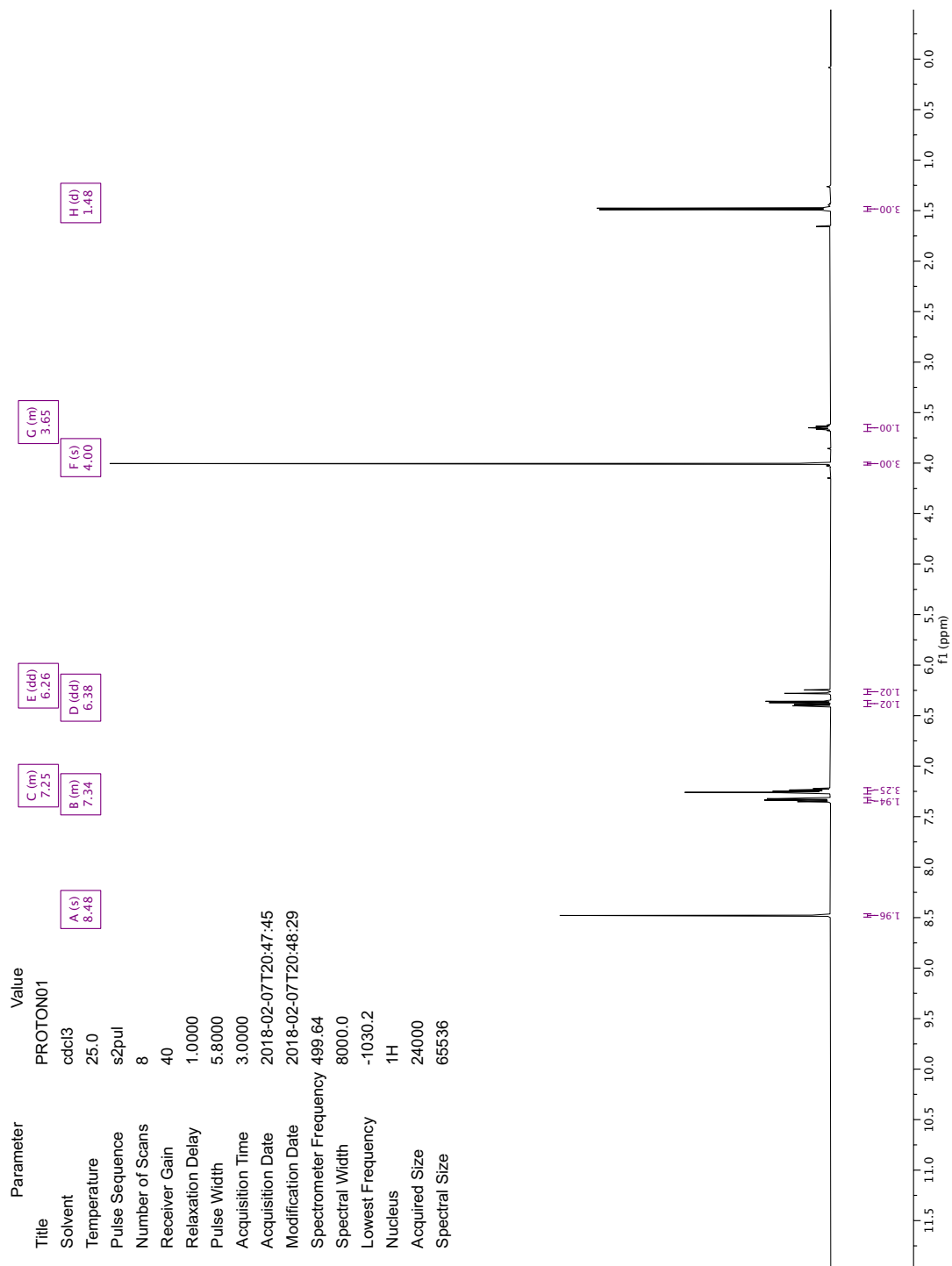


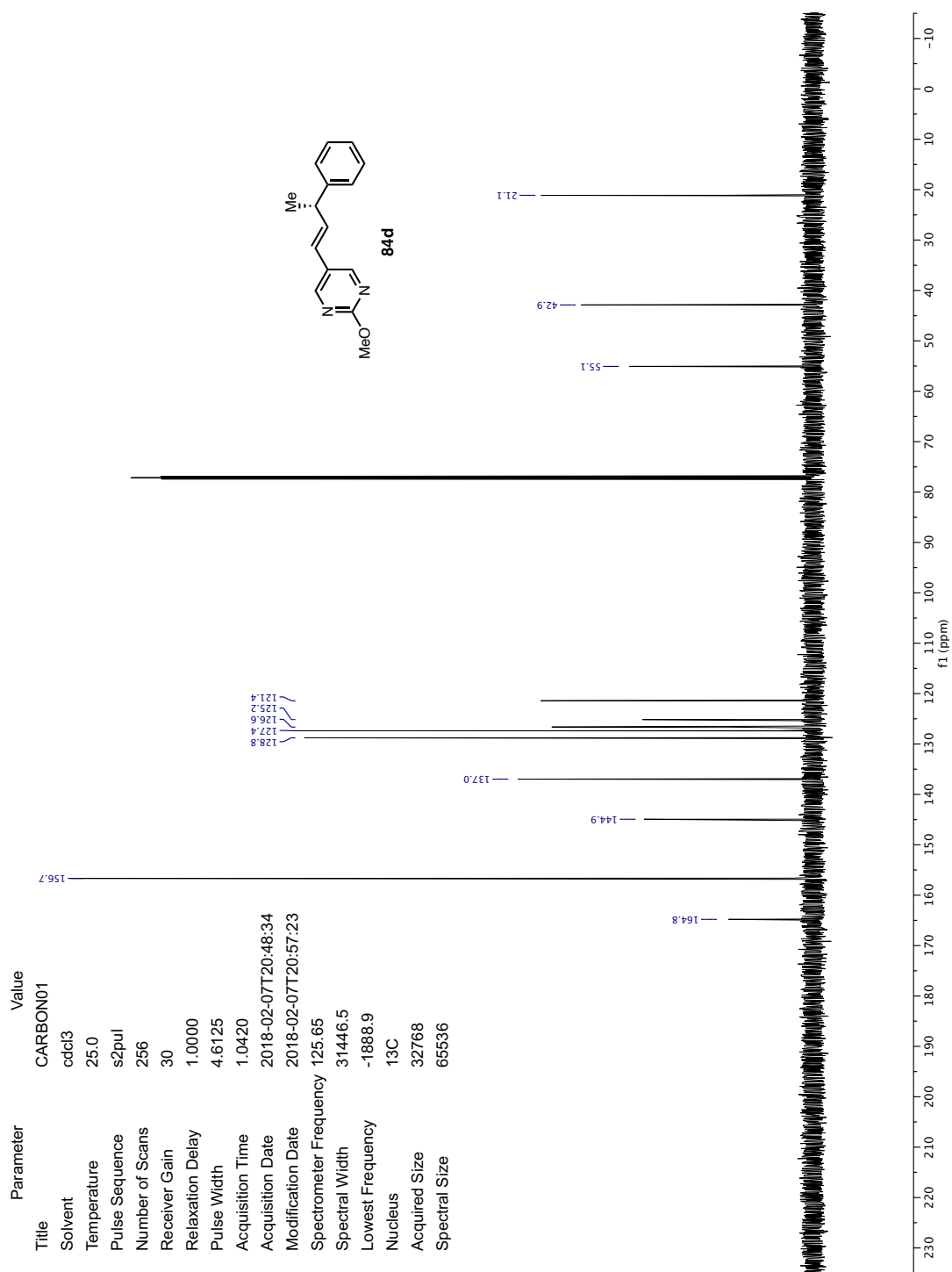




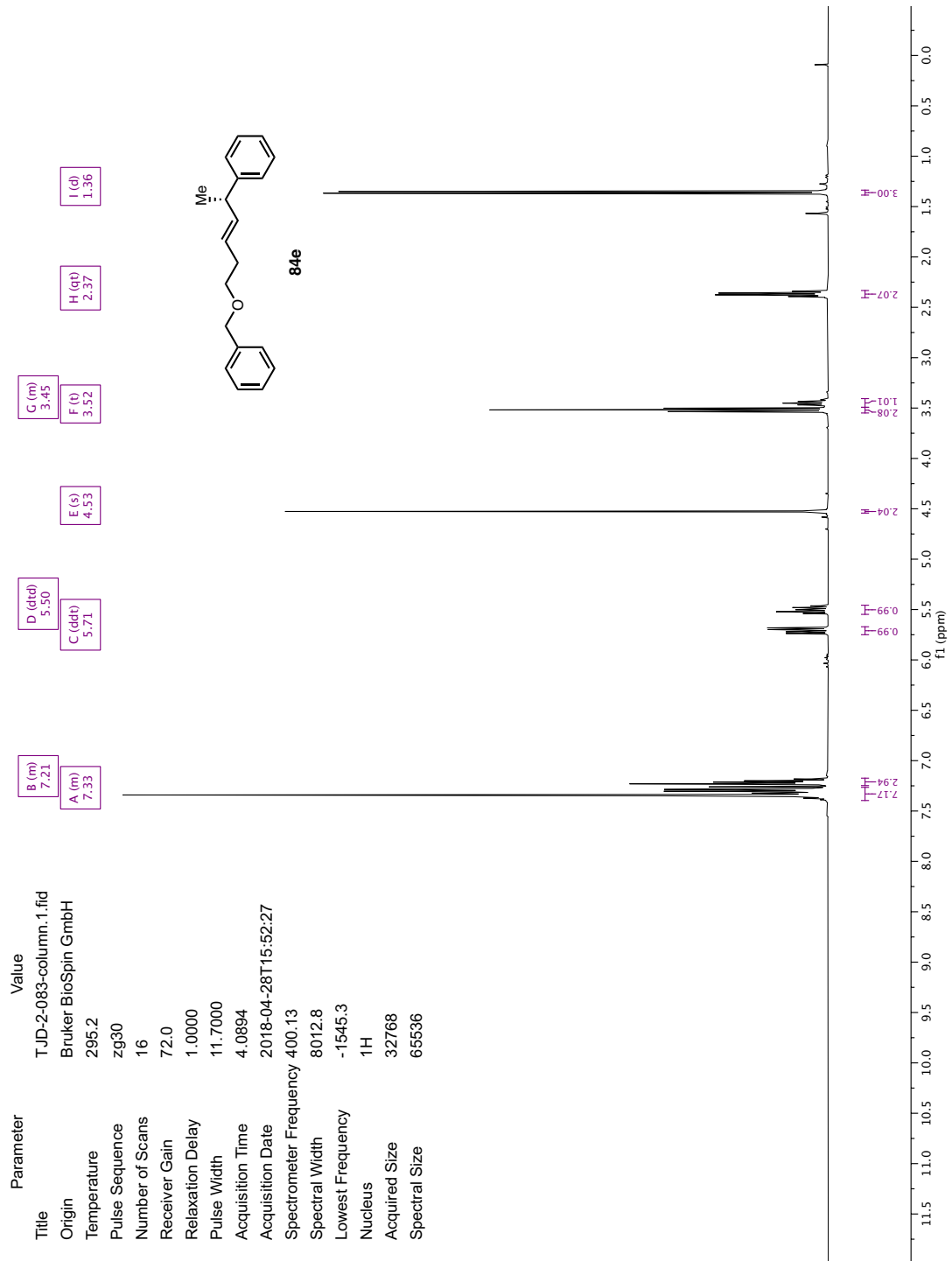


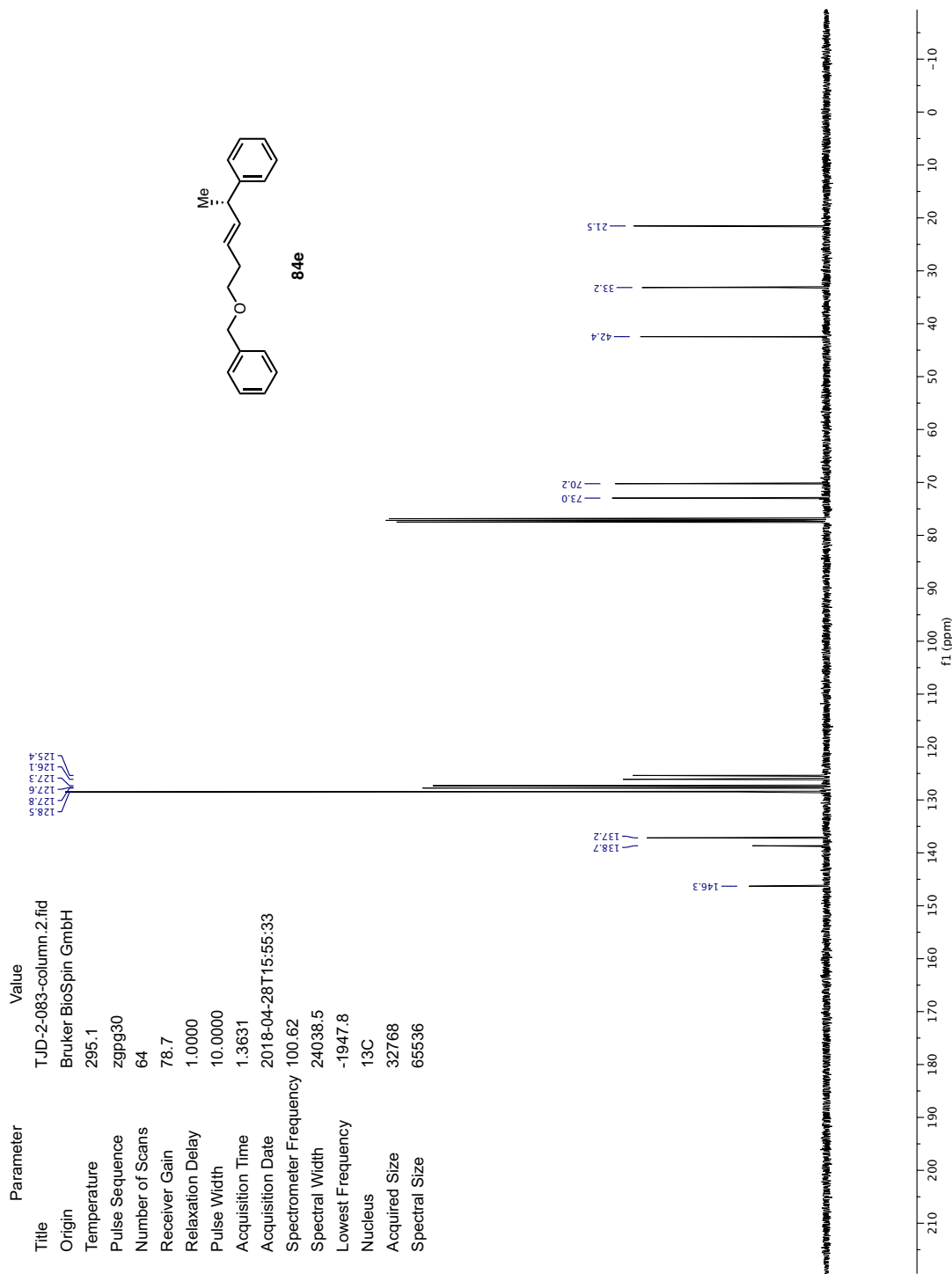


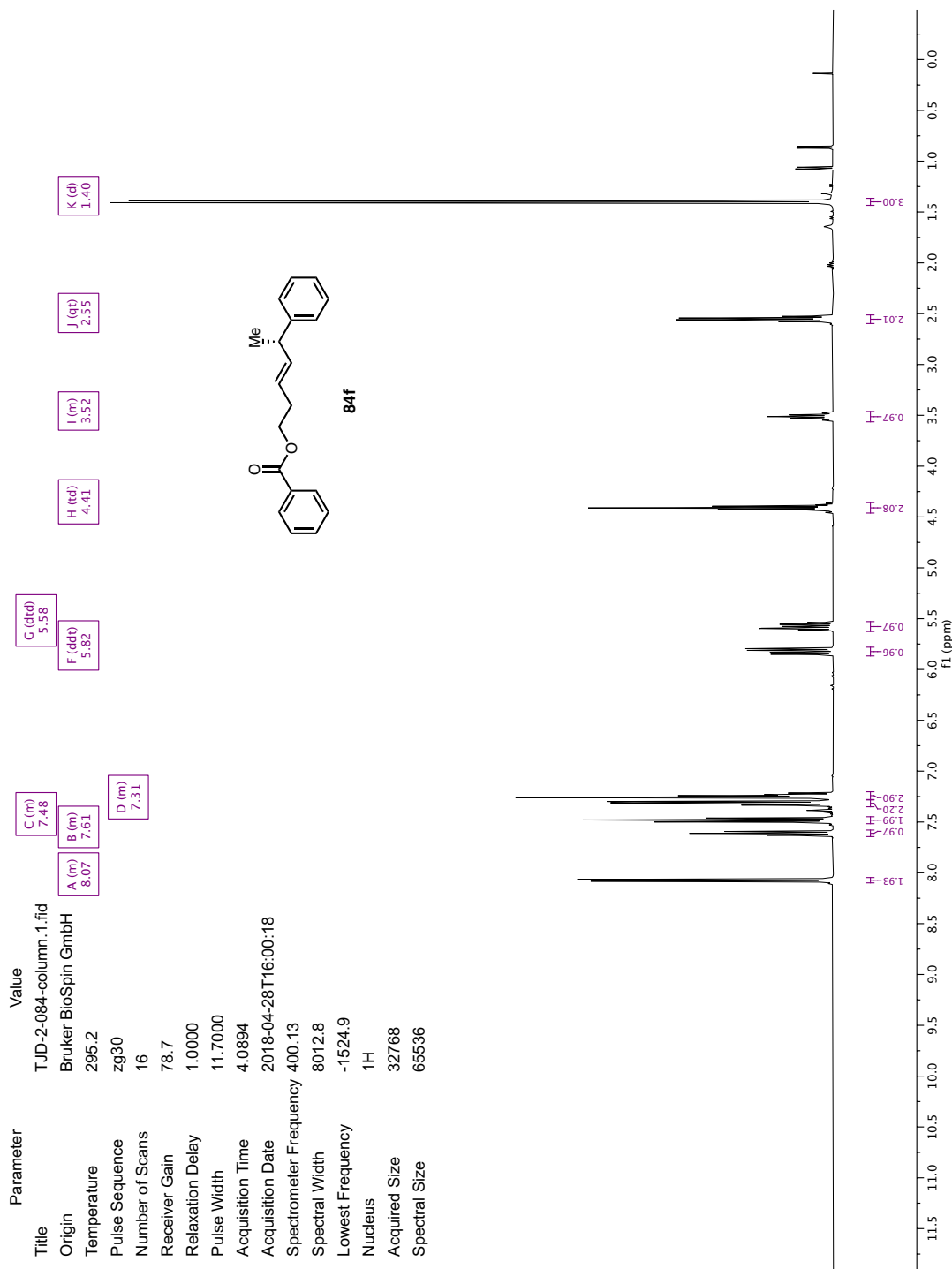


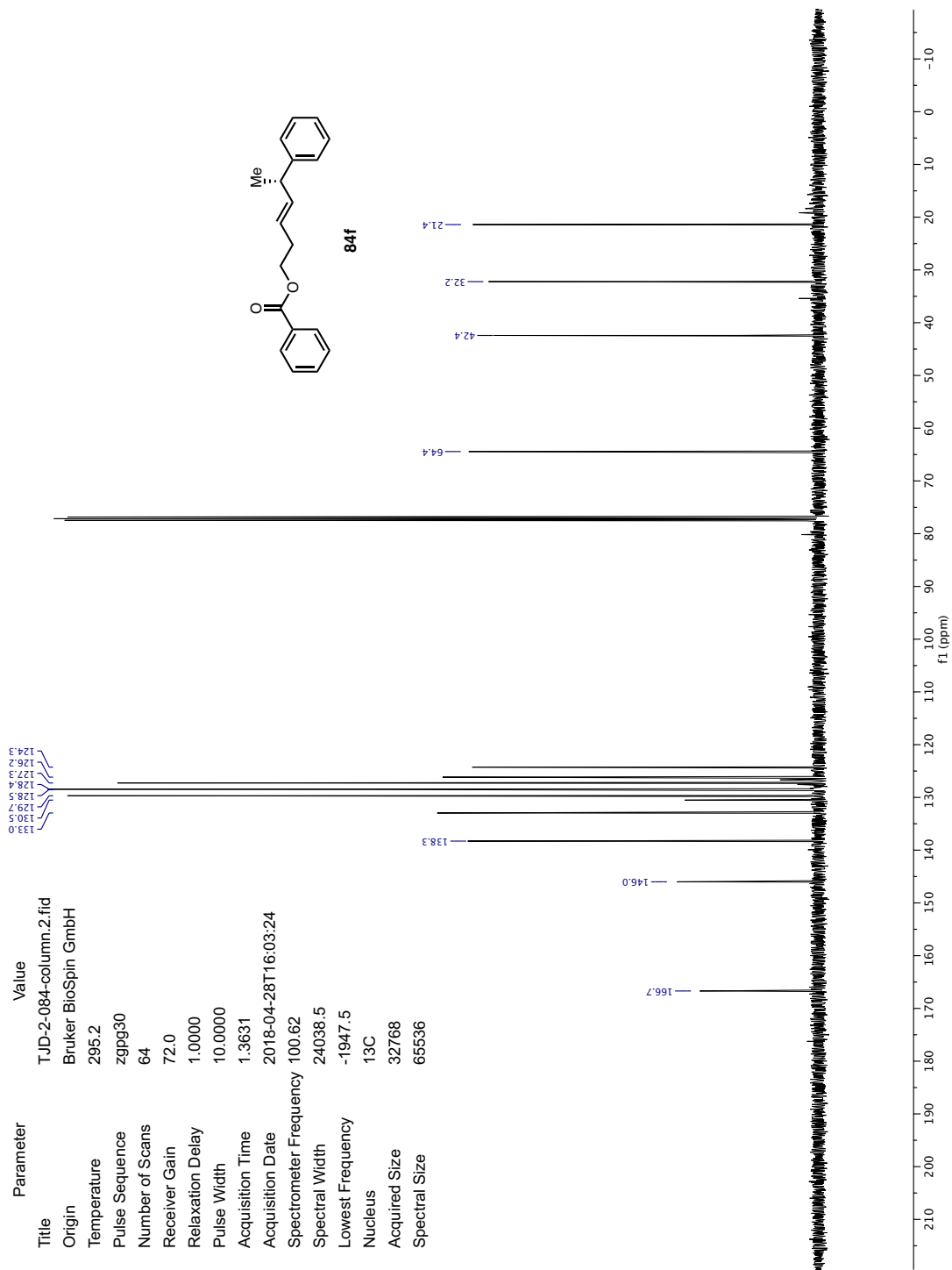


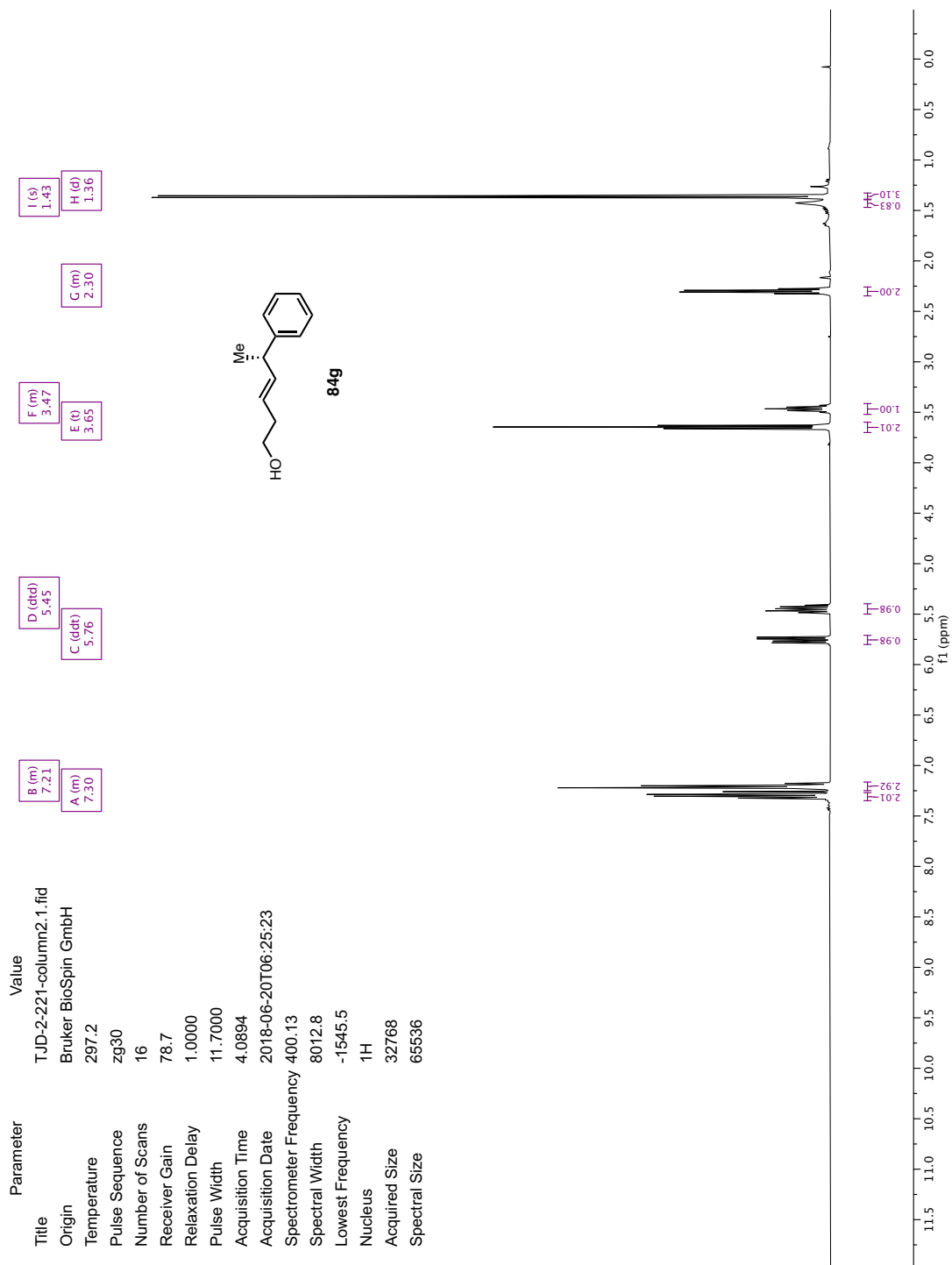


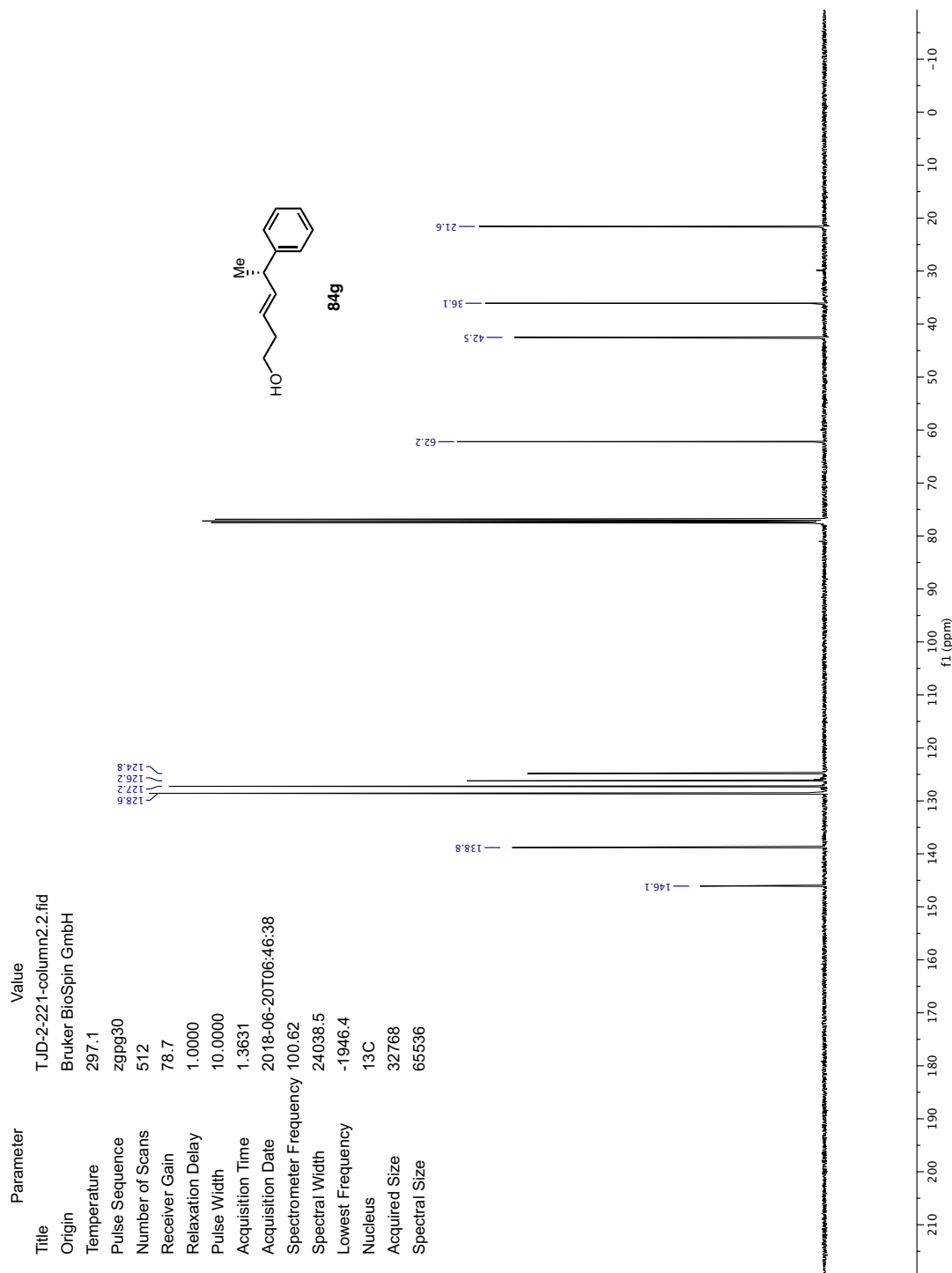


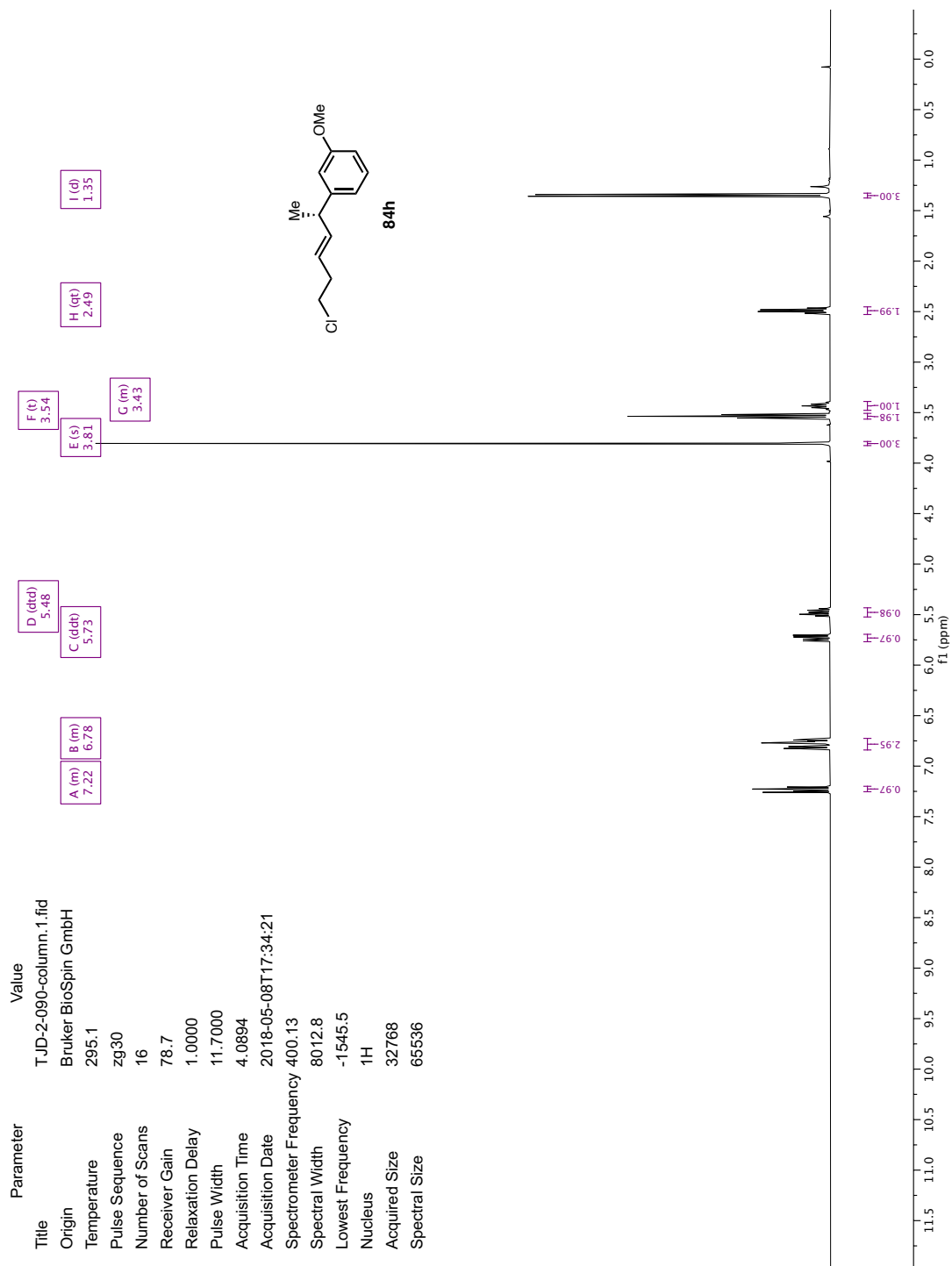


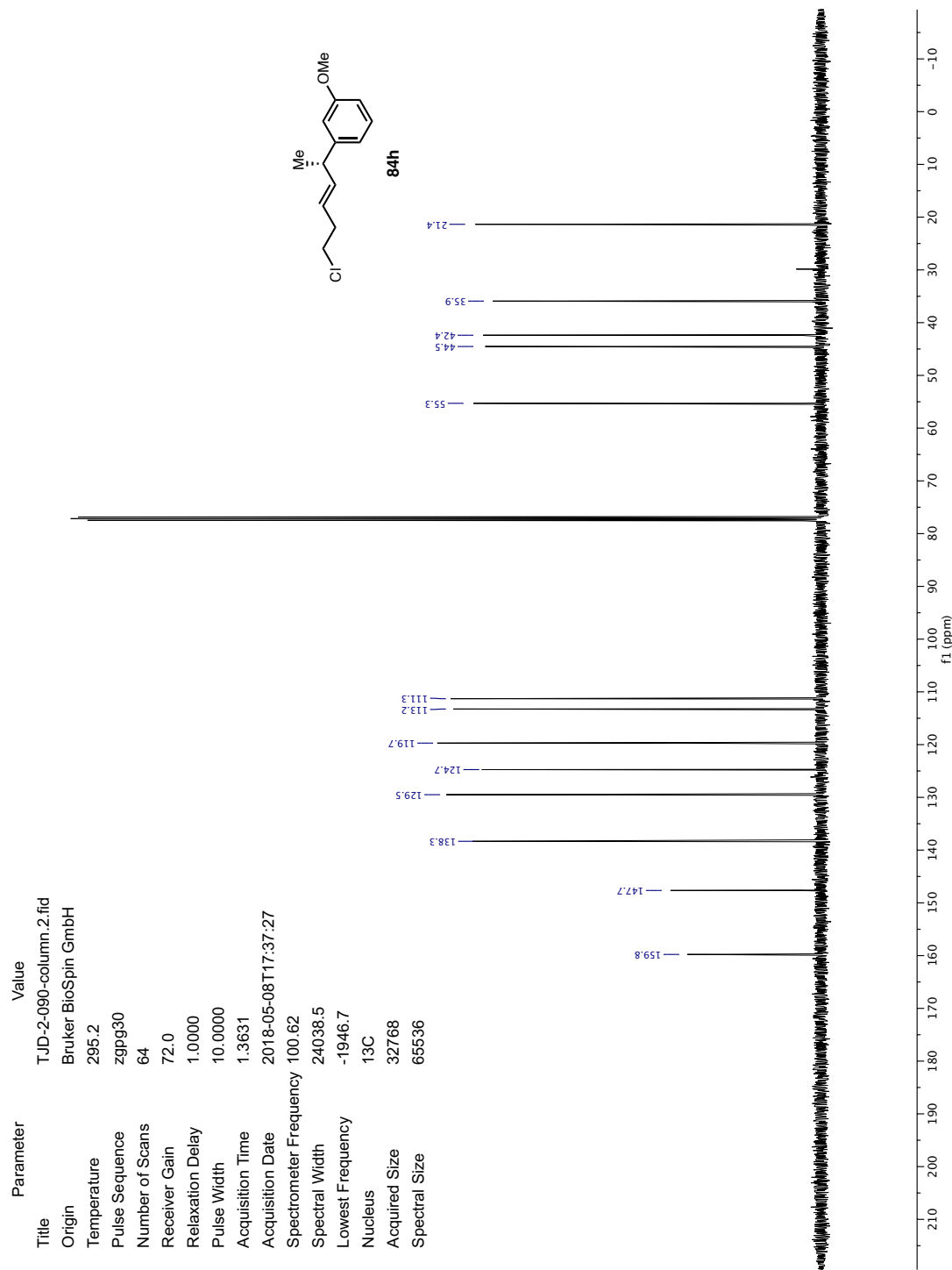




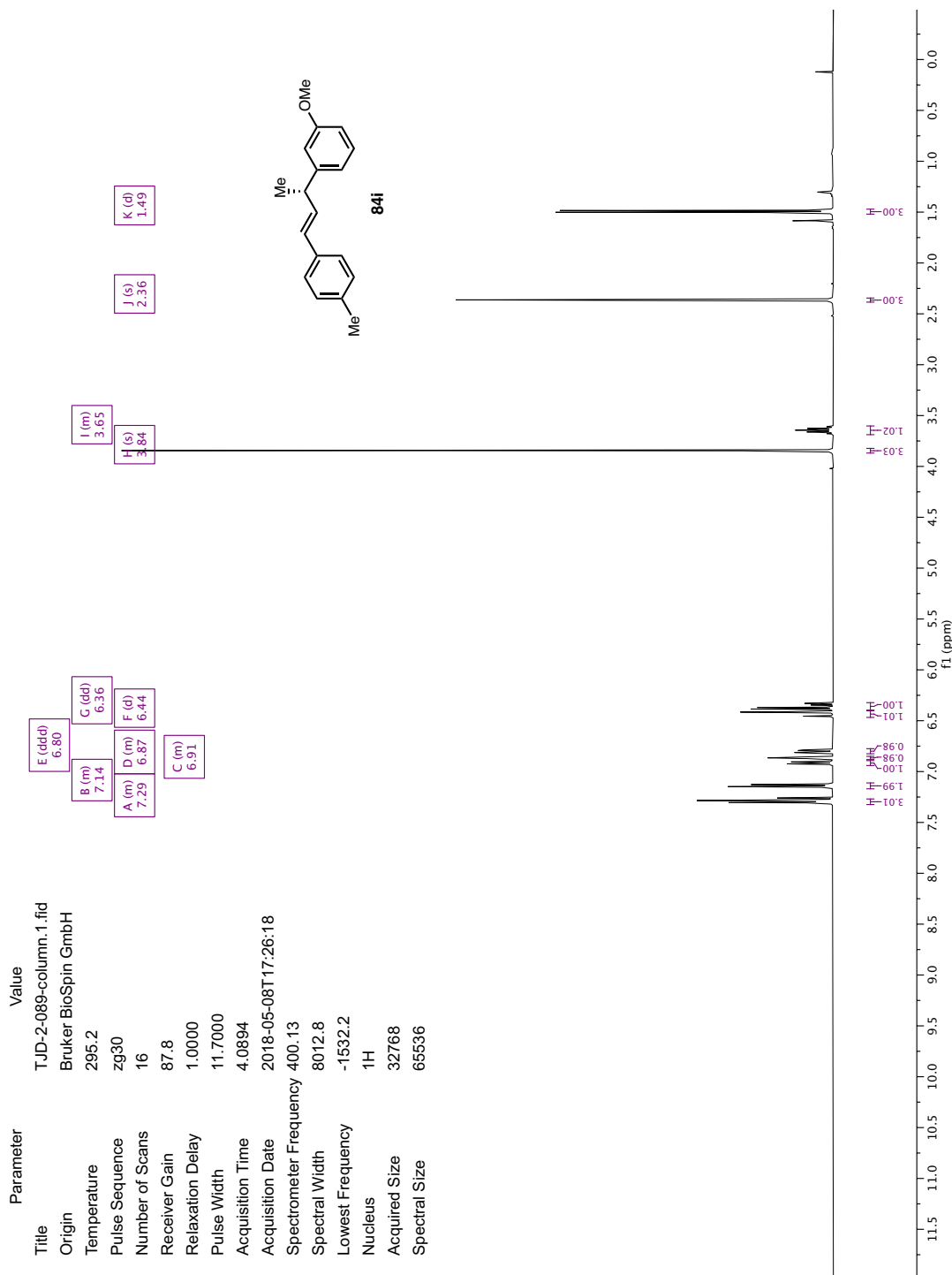


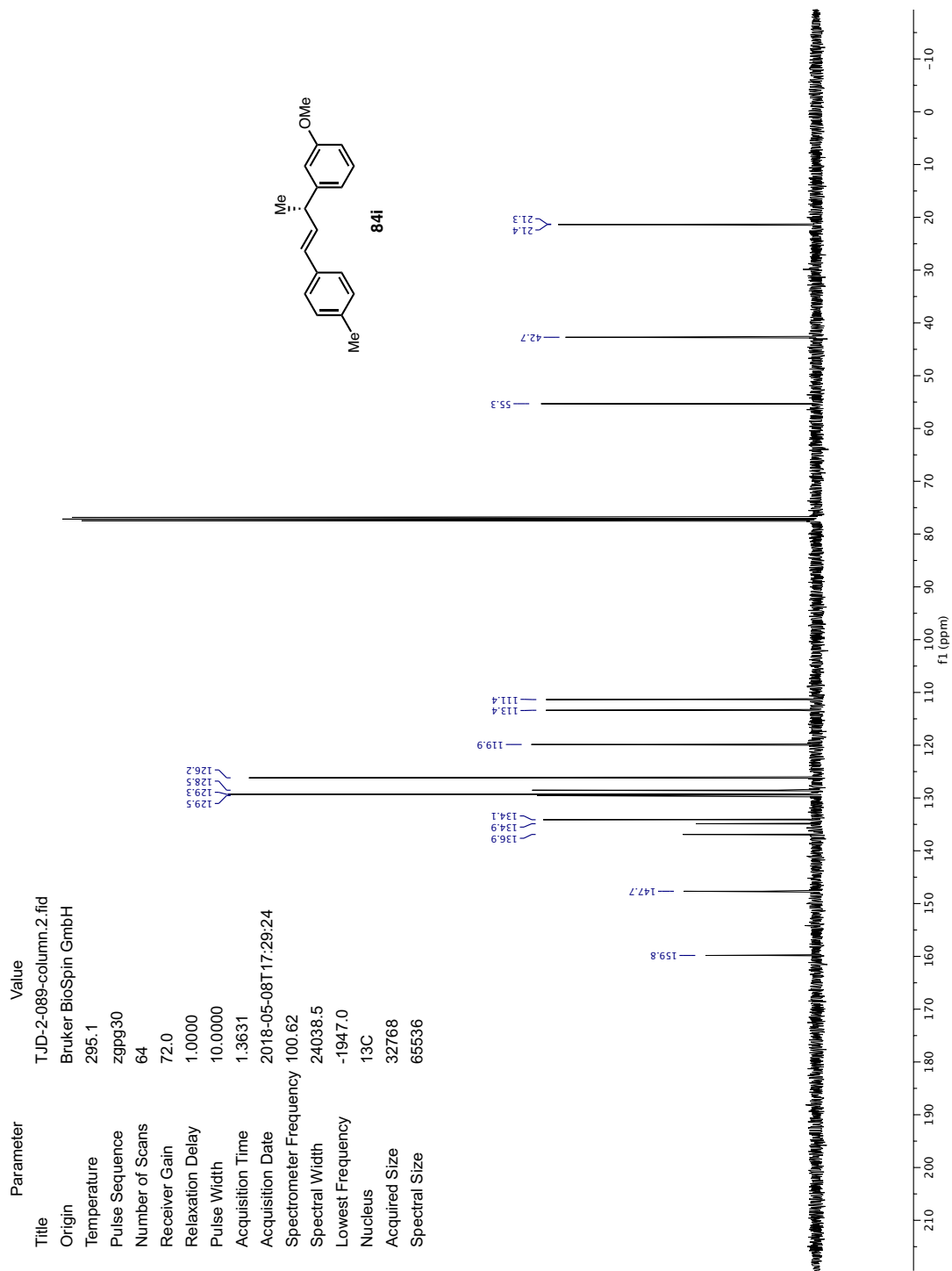


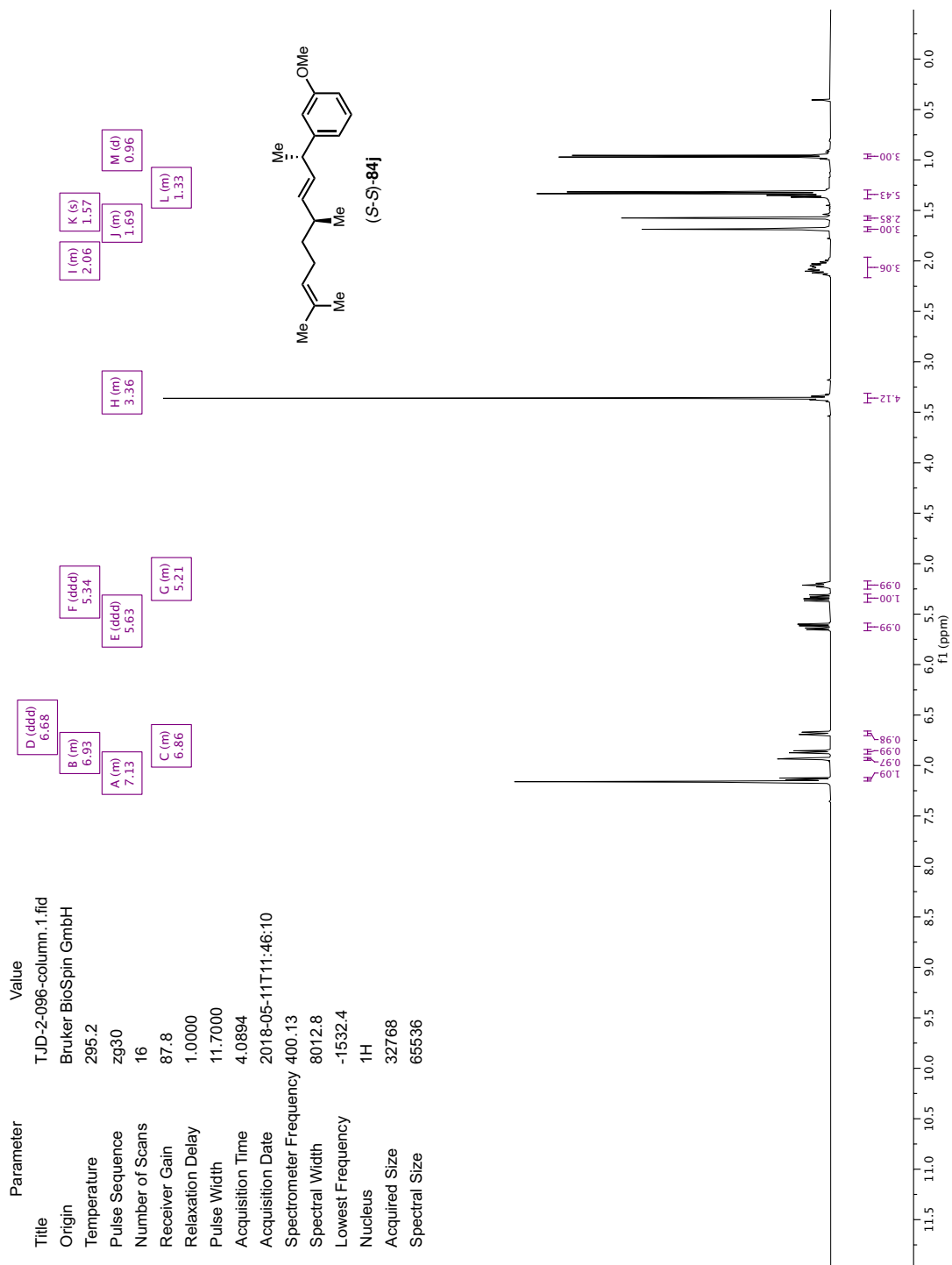


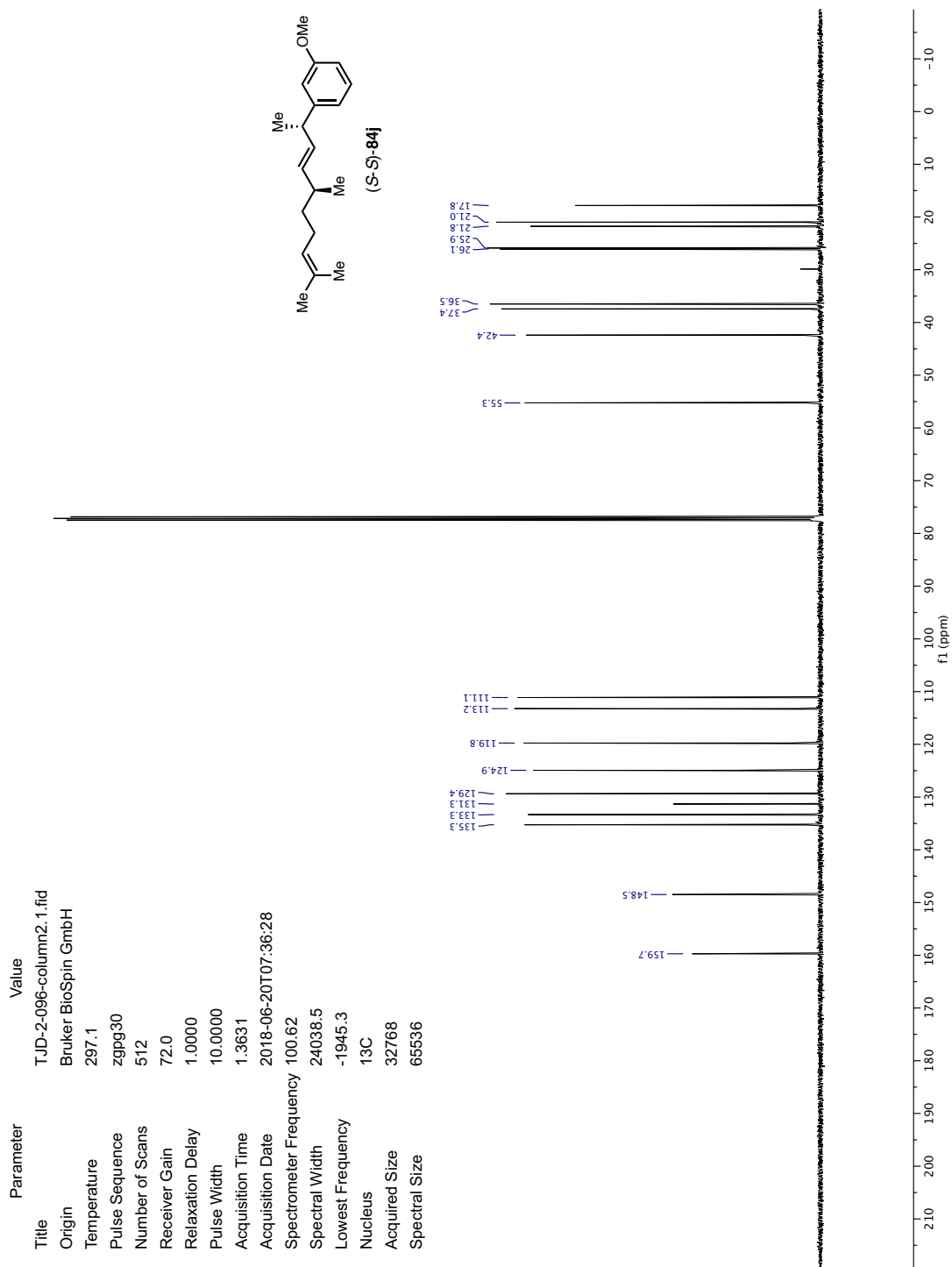




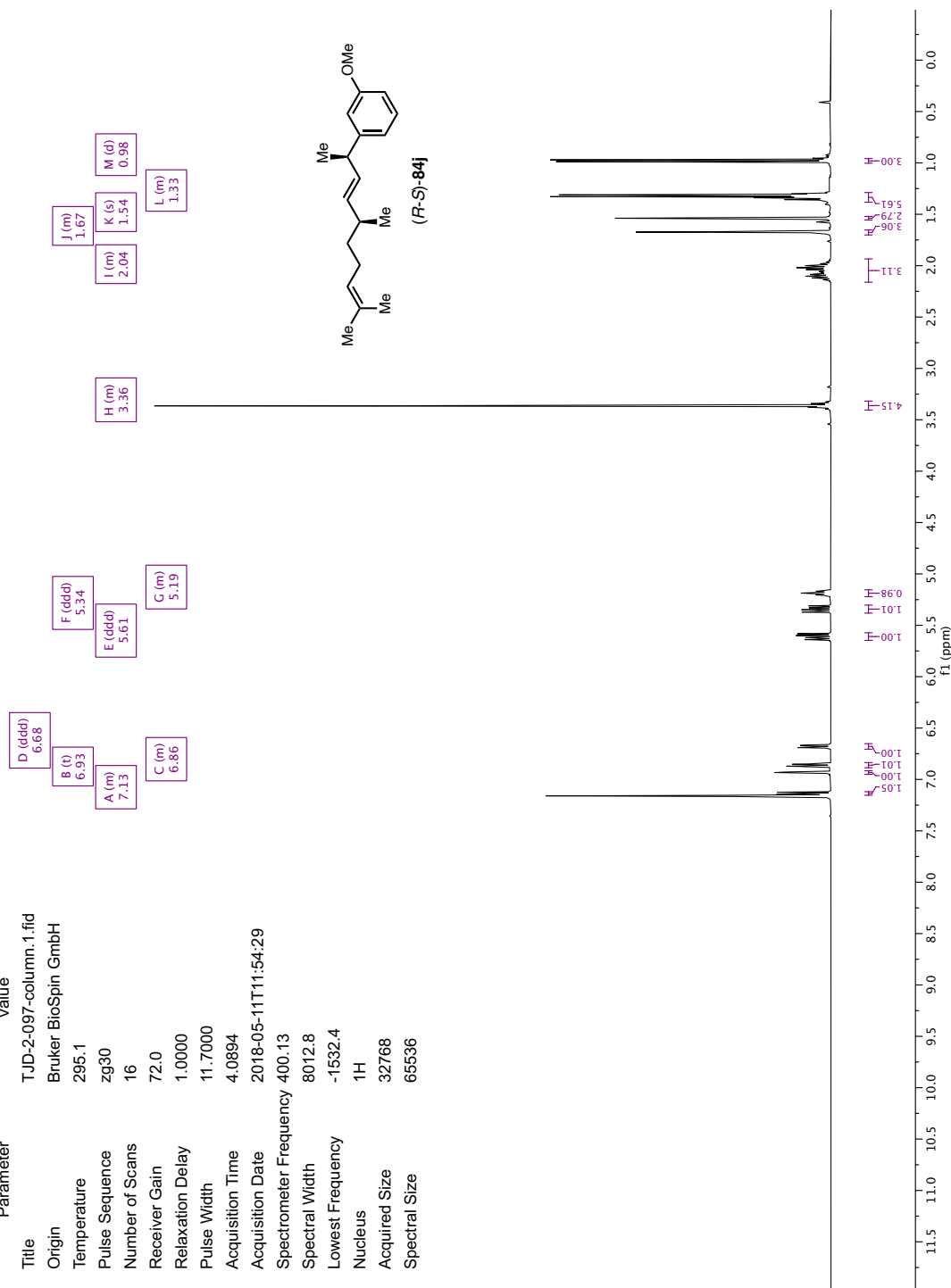


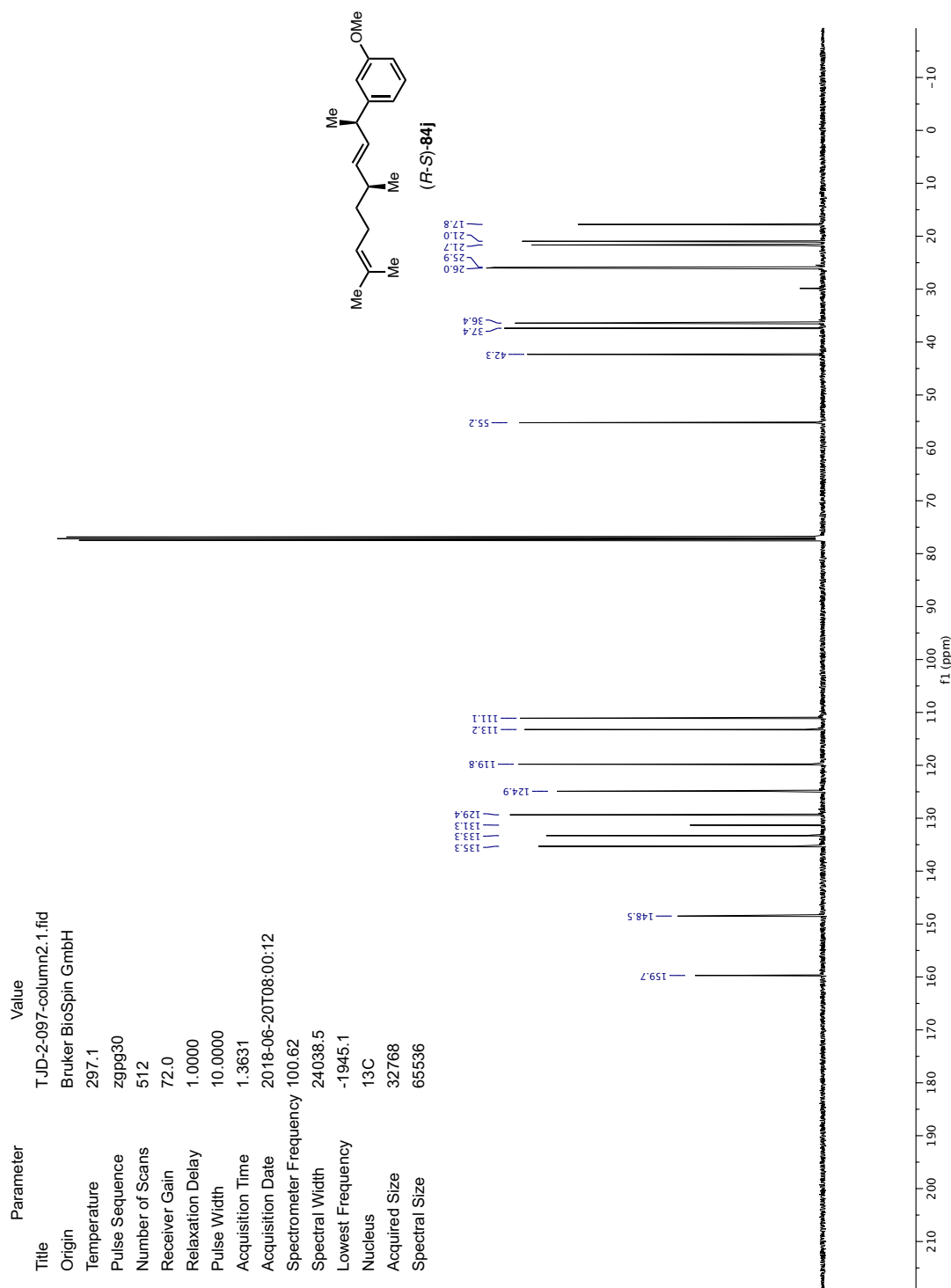




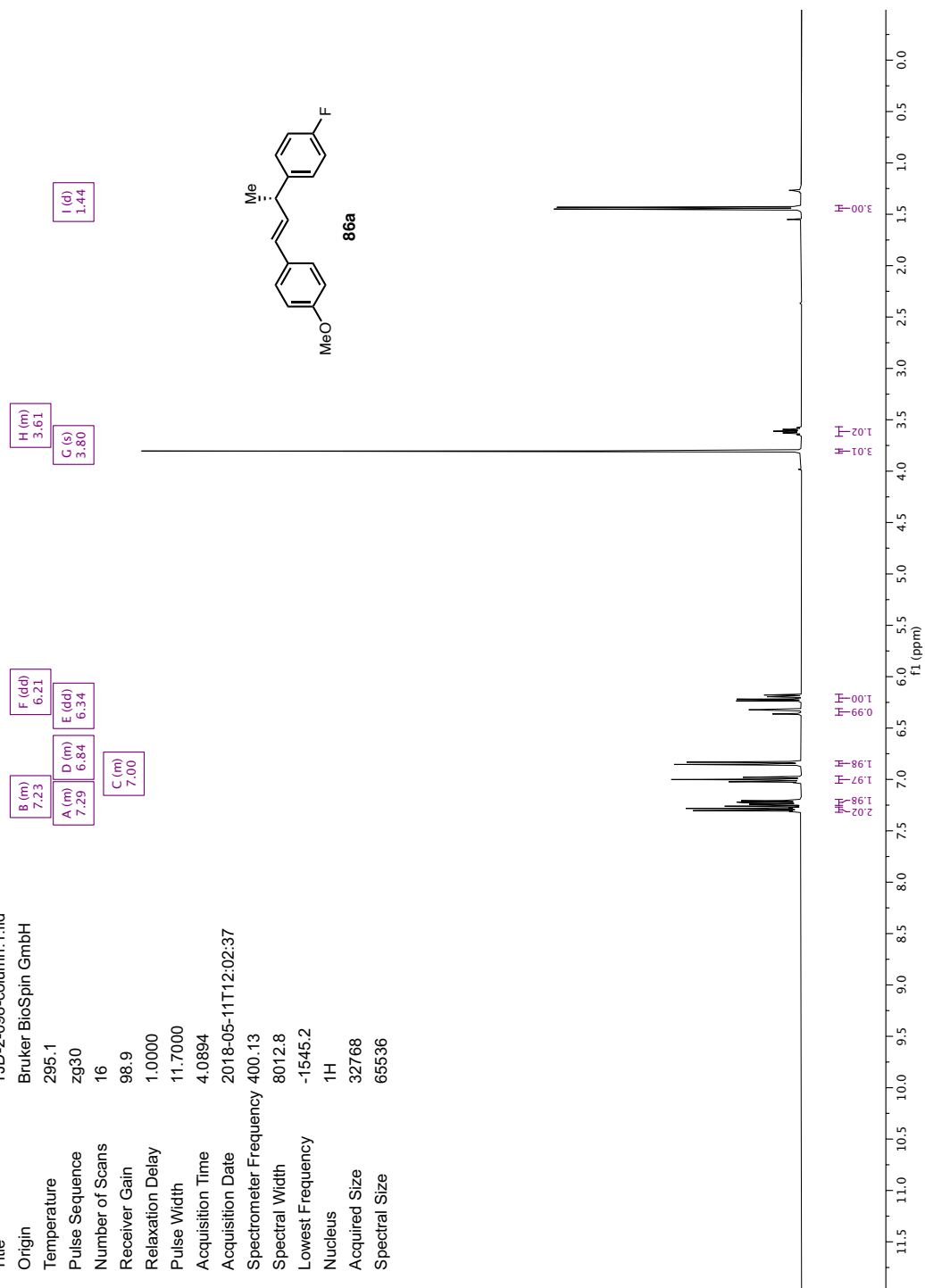


Parameter	Value
Title	T:JD-2-097-column.1.fid
Origin	Bruker BioSpin GmbH
Temperature	295.1
Pulse Sequence	zg30
Number of Scans	16
Receiver Gain	72.0
Relaxation Delay	1.0000
Pulse Width	11.7000
Acquisition Time	4.0894
Acquisition Date	2018-05-11T11:54:29
Spectrometer Frequency	400.13
Spectral Width	8012.8
Lowest Frequency	-1532.4
Nucleus	<sup>1</sup> H
Acquired Size	32768
Spectral Size	65536

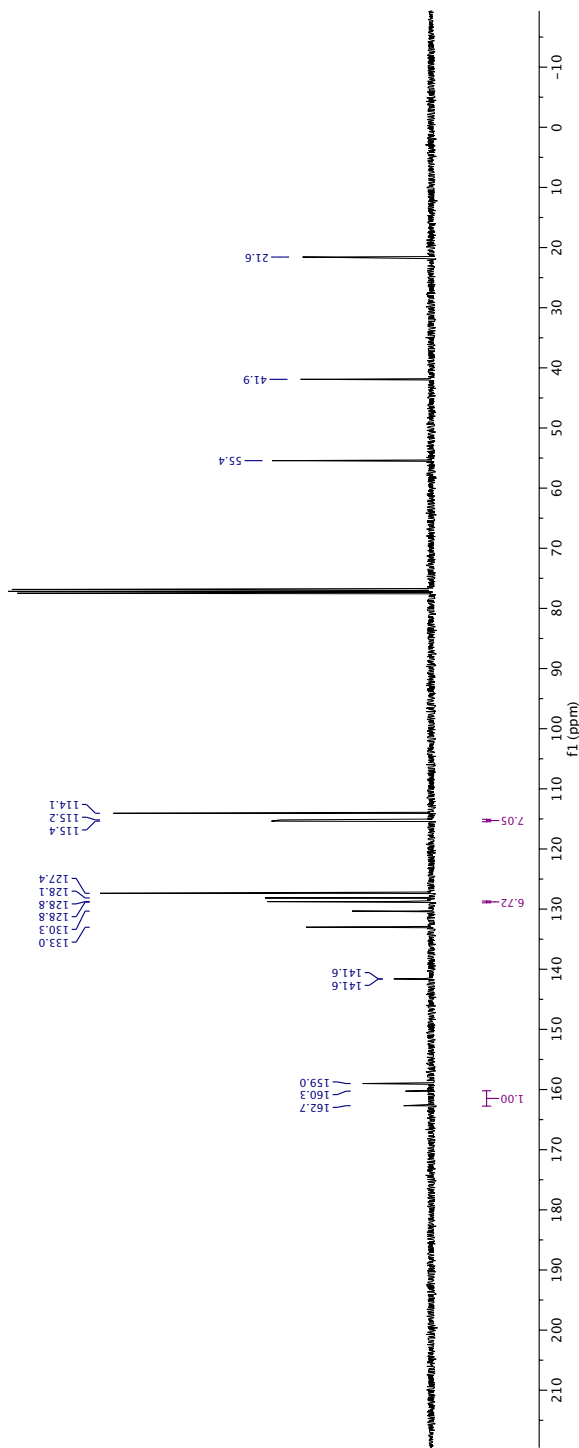
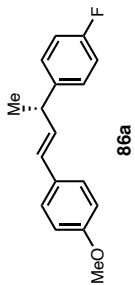




Parameter	Value
Title	T:JD-2-098-column.1.fid
Origin	Bruker BioSpin GmbH
Temperature	295.1
Pulse Sequence	zg30
Number of Scans	16
Receiver Gain	98.9
Relaxation Delay	1.0000
Pulse Width	11.7000
Acquisition Time	4.0894
Acquisition Date	2018-05-11T12:02:37
Spectrometer Frequency	400.13
Spectral Width	8012.8
Lowest Frequency	-1545.2
Nucleus	<sup>1</sup> H
Acquired Size	32768
Spectral Size	65536



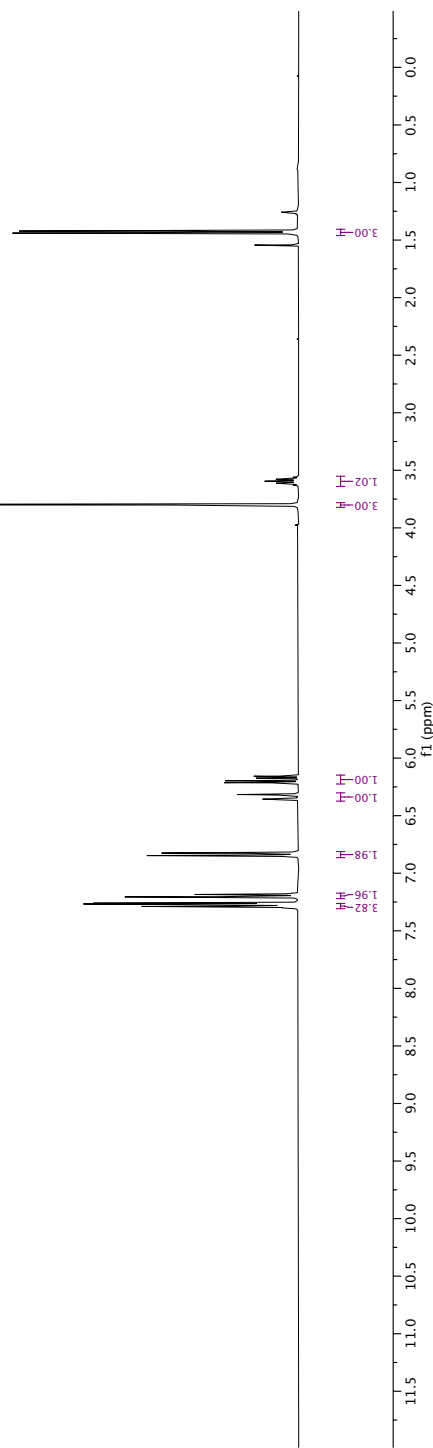
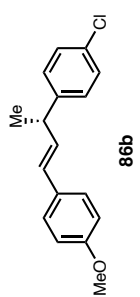
Parameter	Value
Title	T:JD-2-098-column.2.fid
Origin	Bruker BioSpin GmbH
Temperature	295.1
Pulse Sequence	zgpg30
Number of Scans	64
Receiver Gain	72.0
Relaxation Delay	1.0000
Pulse Width	10.0000
Acquisition Time	1.3631
Acquisition Date	2018-05-11T12:06:15
Spectrometer Frequency	100.62
Spectral Width	24038.5
Lowest Frequency	-1946.6
Nucleus	<sup>13</sup> C
Acquired Size	32768
Spectral Size	65536

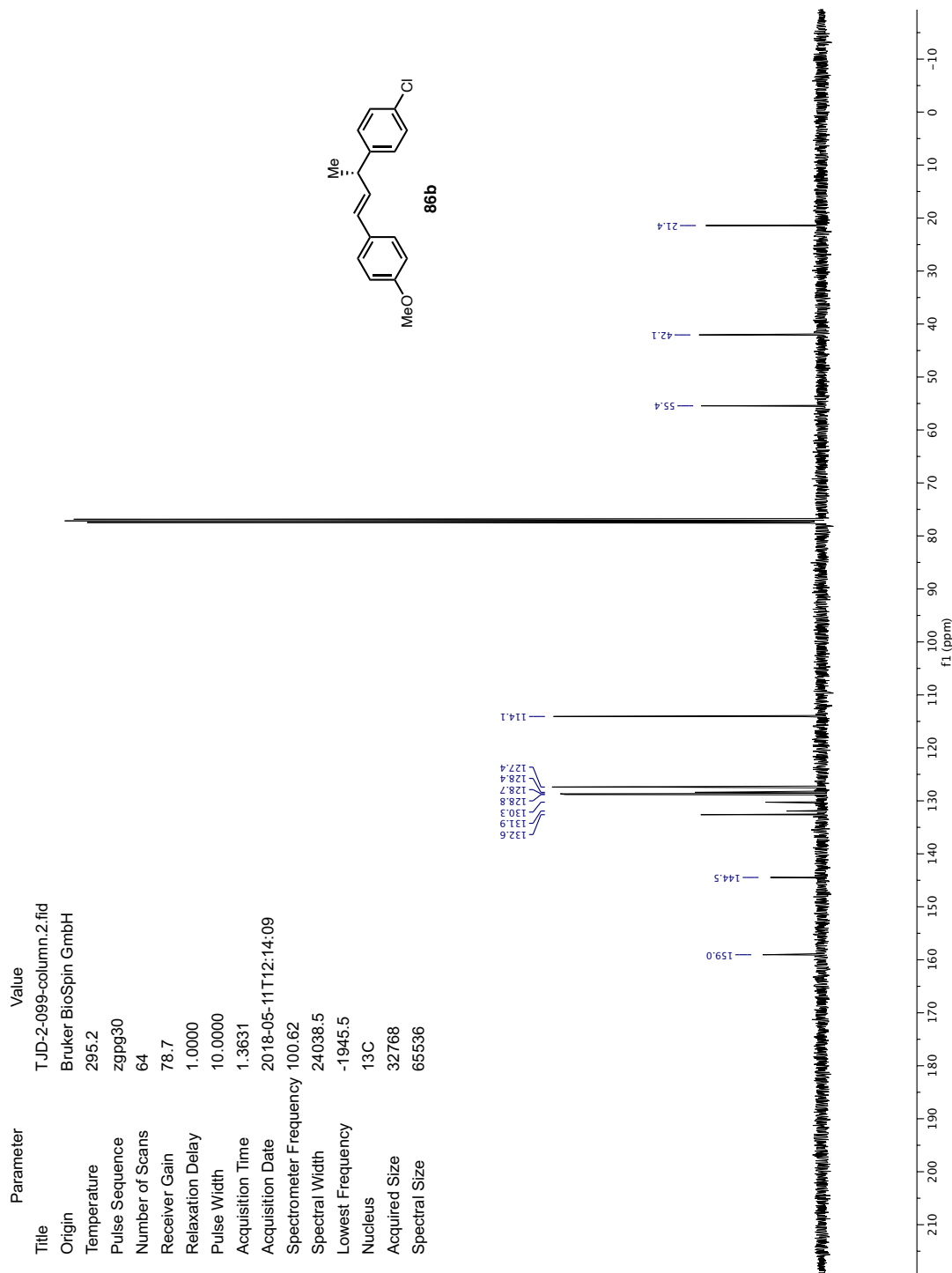




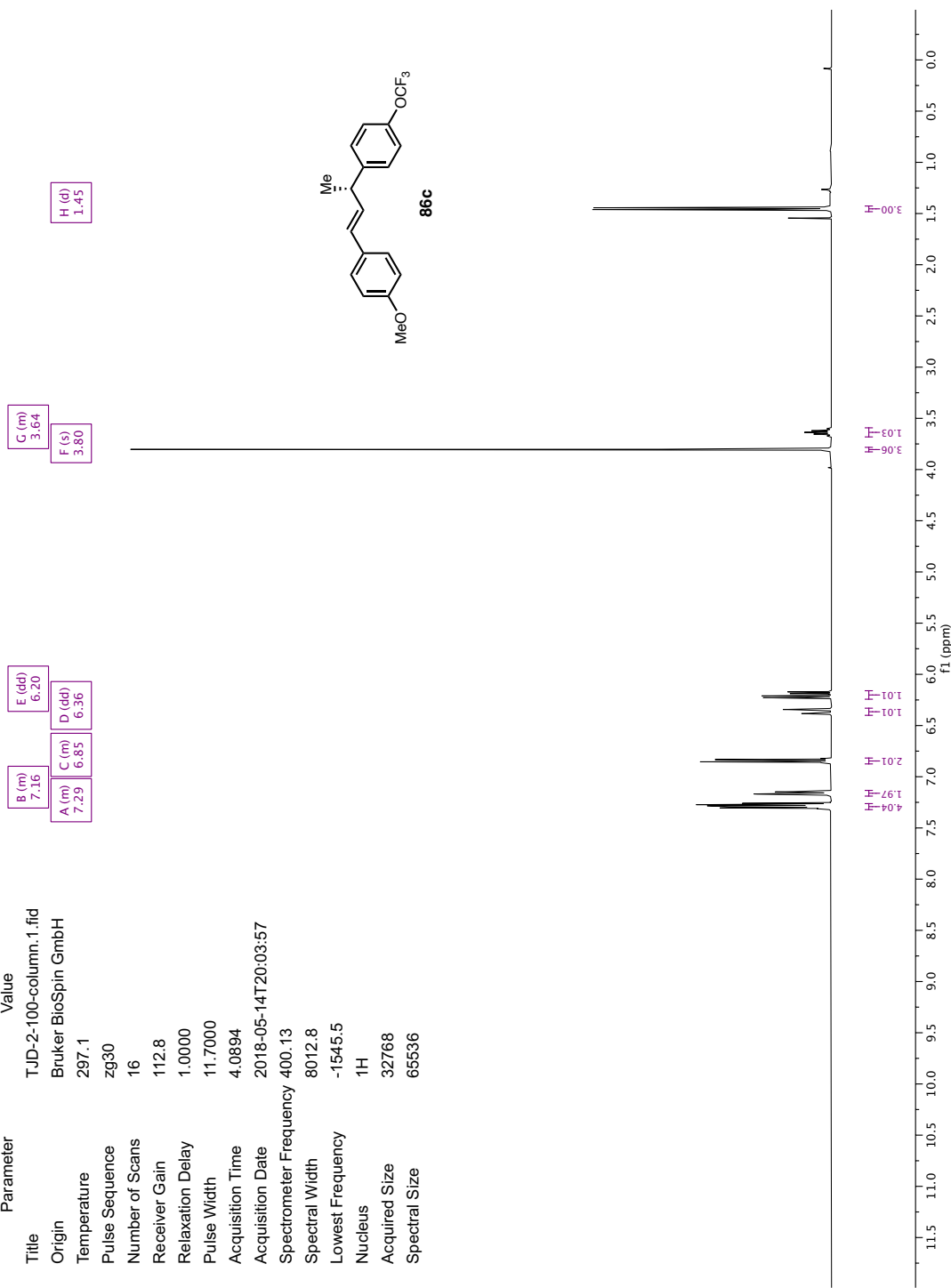
Parameter	Value
Title	T.JD-2-099-column.1.fid
Origin	Bruker BioSpin GmbH
Temperature	295.2
Pulse Sequence	zg30
Number of Scans	16
Receiver Gain	176.8
Relaxation Delay	1.0000
Pulse Width	11.7000
Acquisition Time	4.0894
Acquisition Date	2018-05-11T12:11:03
Spectrometer Frequency	400.13
Spectral Width	8012.8
Lowest Frequency	-1545.5
Nucleus	<sup>1</sup> H
Acquired Size	32768
Spectral Size	65536

B (m)	7.20
A (m)	7.28
C (m)	6.84
D (dd)	6.34
E (dd)	6.19
F (s)	3.80
G (m)	3.60
H (d)	1.43

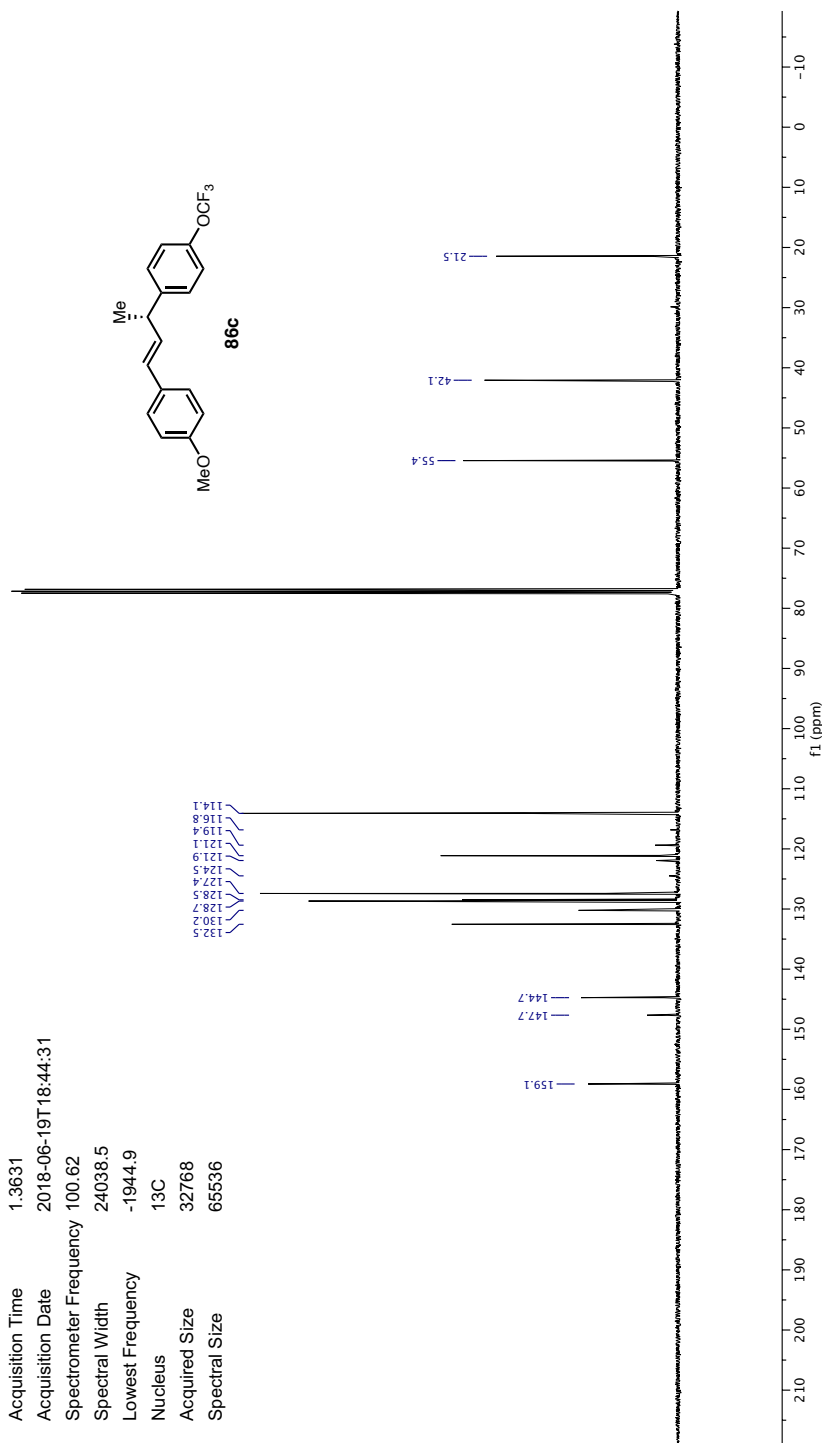




Parameter	Value
Title	T:JD-2-100-column.1.fid
Origin	Bruker BioSpin GmbH
Temperature	297.1
Pulse Sequence	zg30
Number of Scans	16
Receiver Gain	112.8
Relaxation Delay	1.0000
Pulse Width	11.7000
Acquisition Time	4.0894
Acquisition Date	2018-05-14T20:03:57
Spectrometer Frequency	400.13
Spectral Width	8012.8
Lowest Frequency	-1545.5
Nucleus	<sup>1</sup> H
Acquired Size	32768
Spectral Size	65536

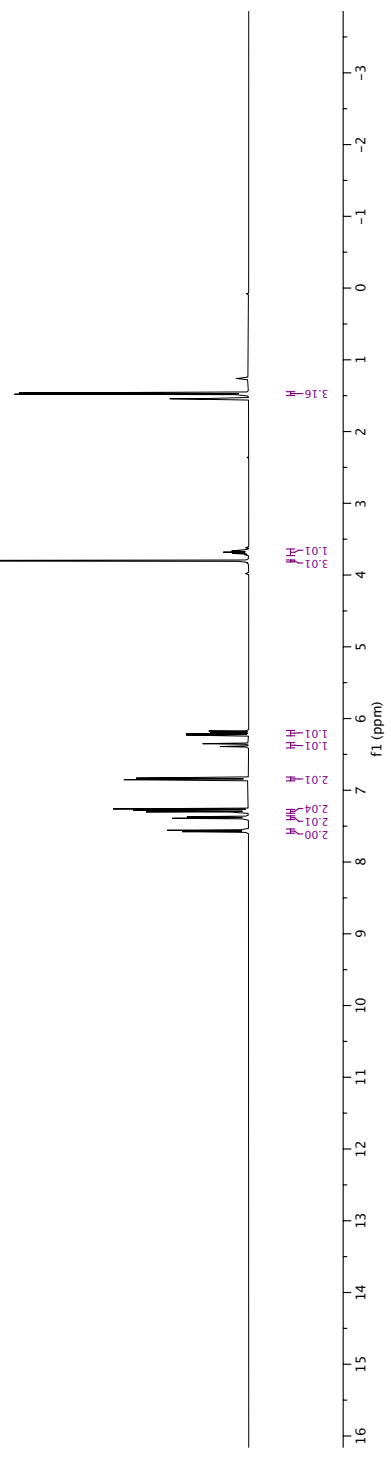
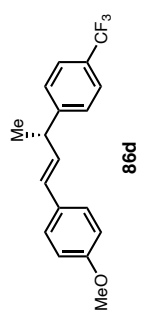


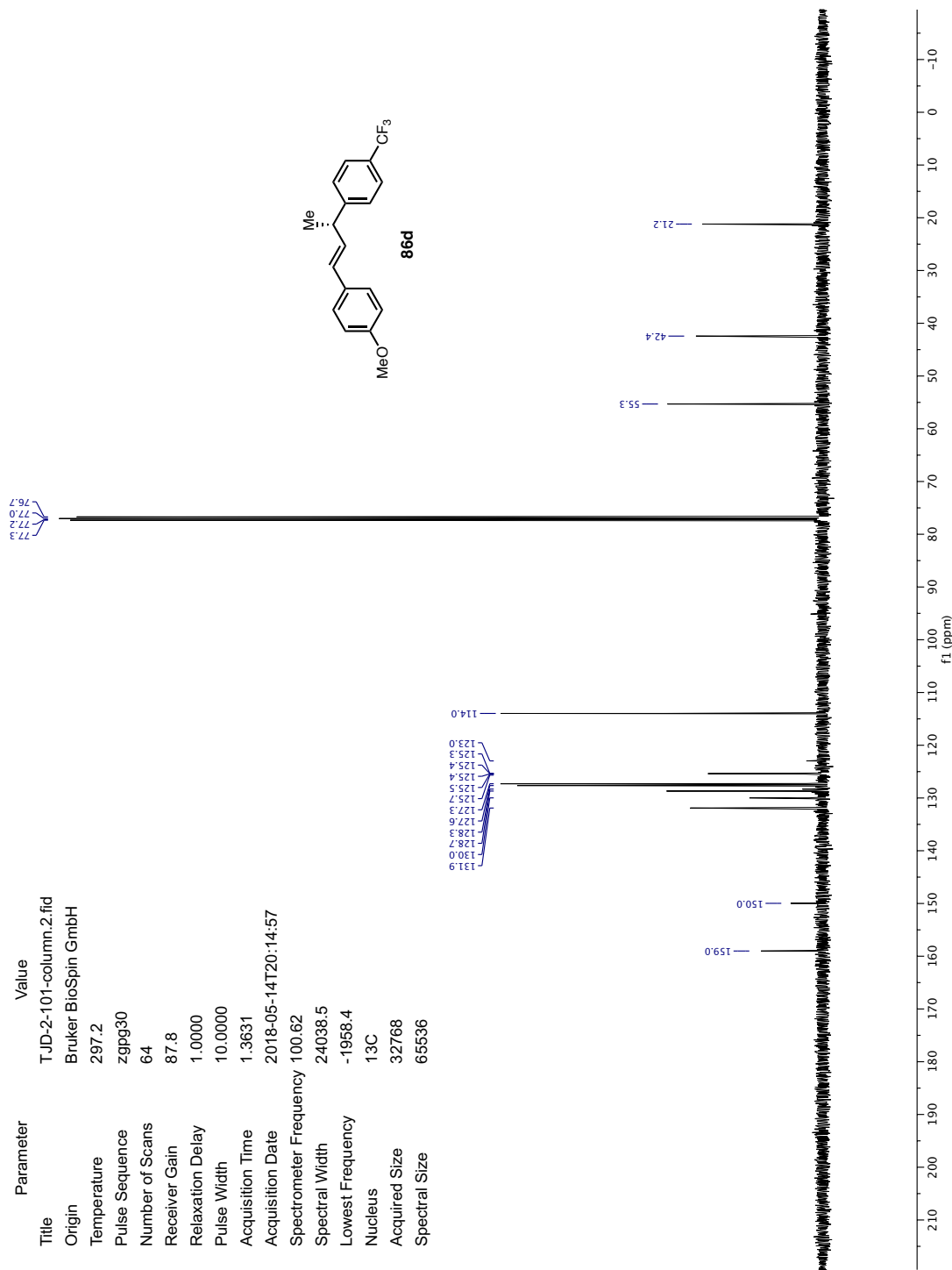
Parameter	Value
Title	T:JD-2-100-column2.1.fid
Origin	Bruker BioSpin GmbH
Temperature	297.1
Pulse Sequence	zgpg30
Number of Scans	512
Receiver Gain	64.2
Relaxation Delay	1.0000
Pulse Width	10.0000
Acquisition Time	1.3631
Acquisition Date	2018-06-19T18:44:31
Spectrometer Frequency	100.62
Spectral Width	24038.5
Lowest Frequency	-1944.9
Nucleus	<sup>13</sup> C
Acquired Size	32768
Spectral Size	65536

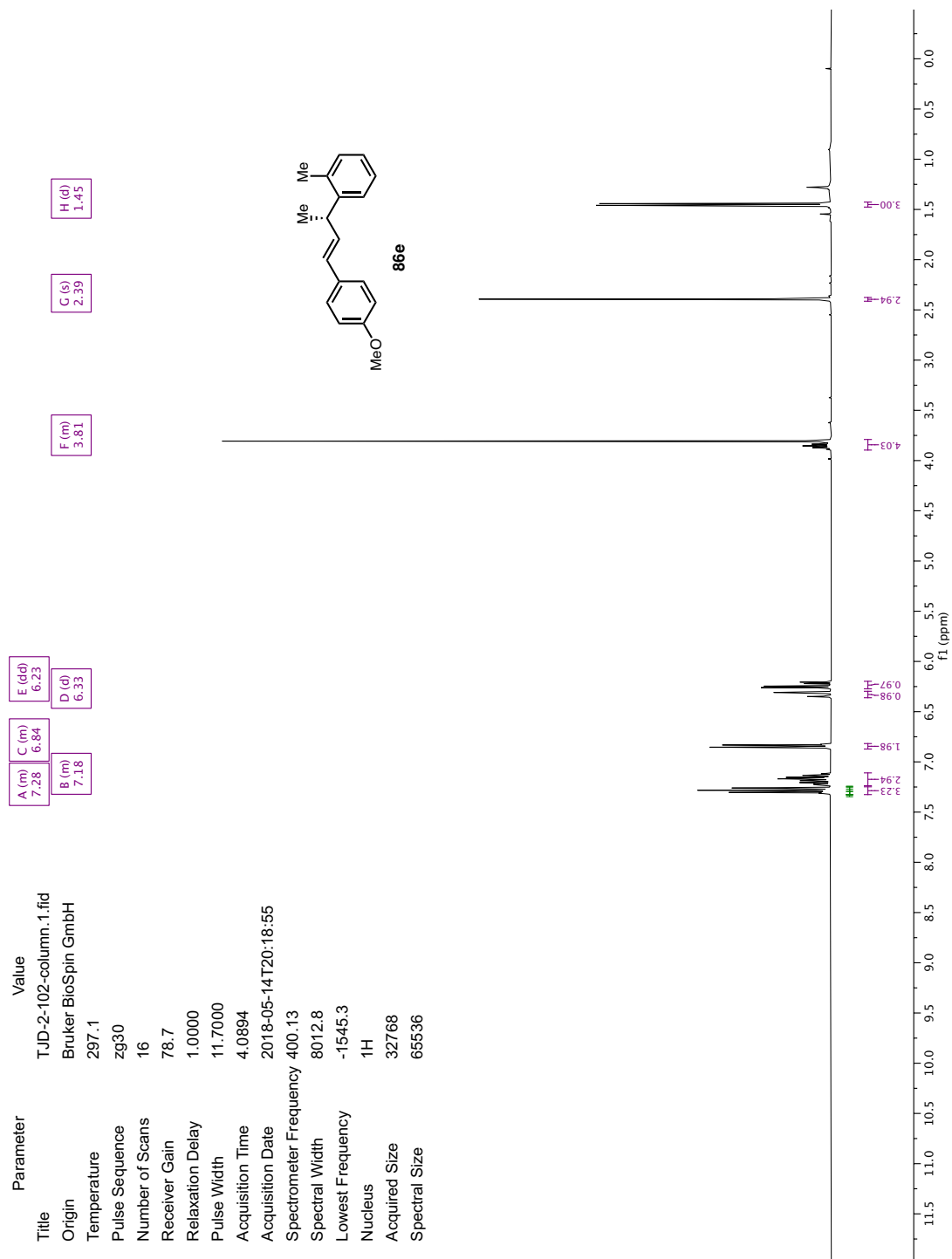


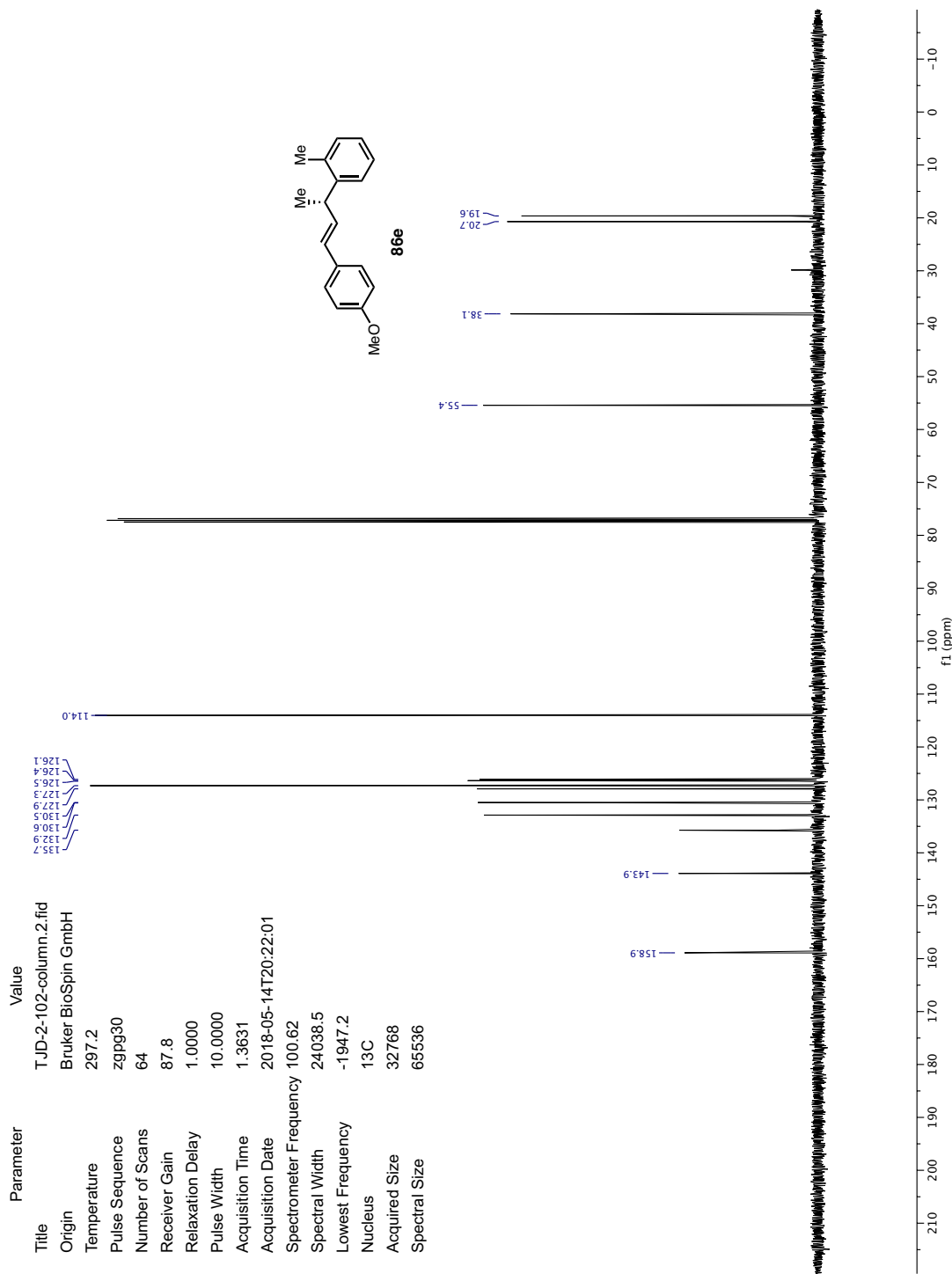
Parameter	Value
Title	T:JD-2-101-column.1.fid
Origin	Bruker BioSpin GmbH
Temperature	297.2
Pulse Sequence	zg30
Number of Scans	16
Receiver Gain	176.8
Relaxation Delay	1.0000
Pulse Width	11.7000
Acquisition Time	4.0894
Acquisition Date	2018-05-14T20:11:51
Spectrometer Frequency	400.13
Spectral Width	8012.8
Lowest Frequency	-1545.5
Nucleus	<sup>1</sup> H
Acquired Size	32768
Spectral Size	65536

B (m)	7.38	E (dd)	6.37
A (m)	7.57	D (m)	6.84
C (m)	7.29	F (dd)	6.20
H (m)	3.68	I (d)	1.47
G (s)	3.80		

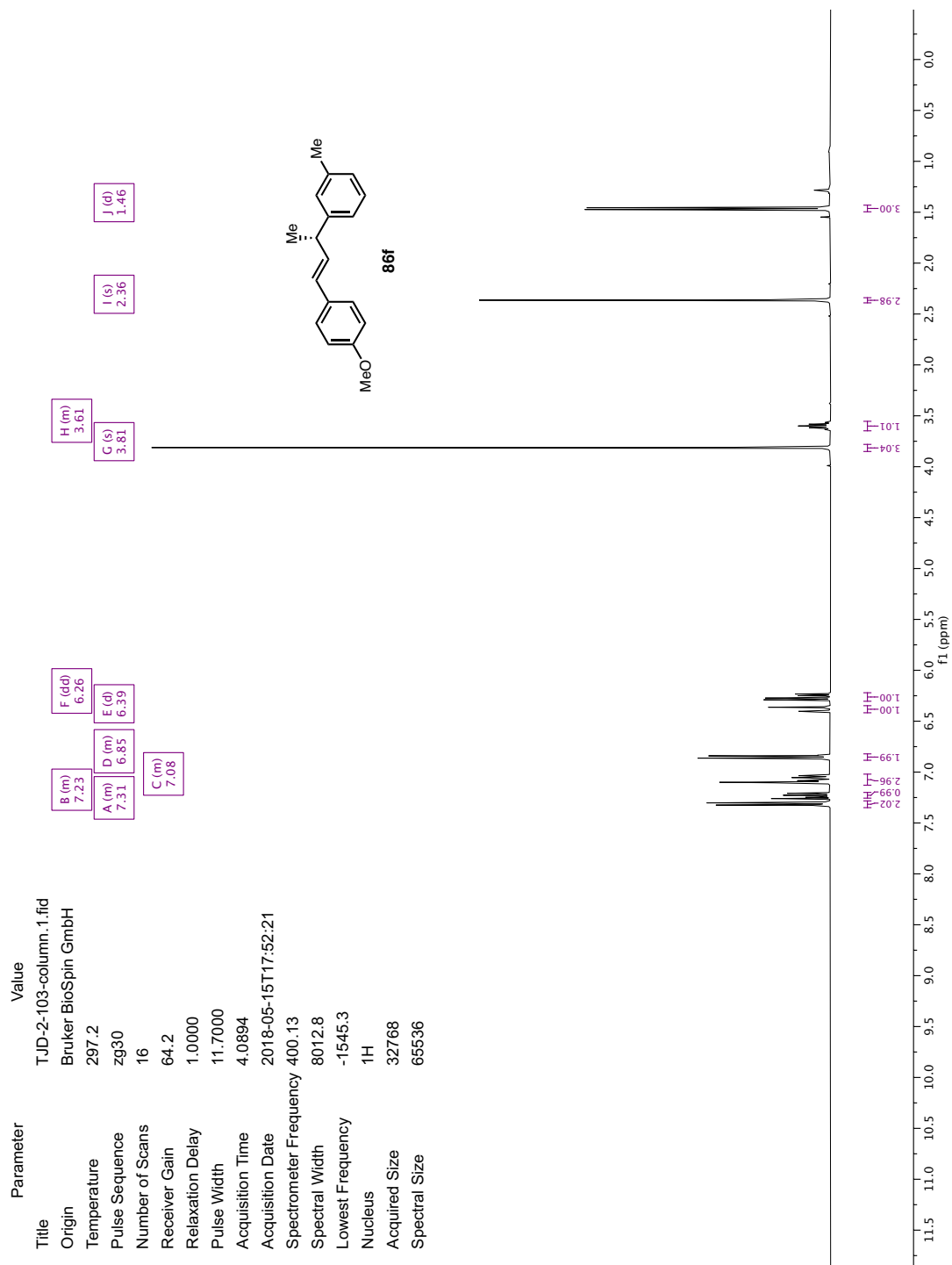


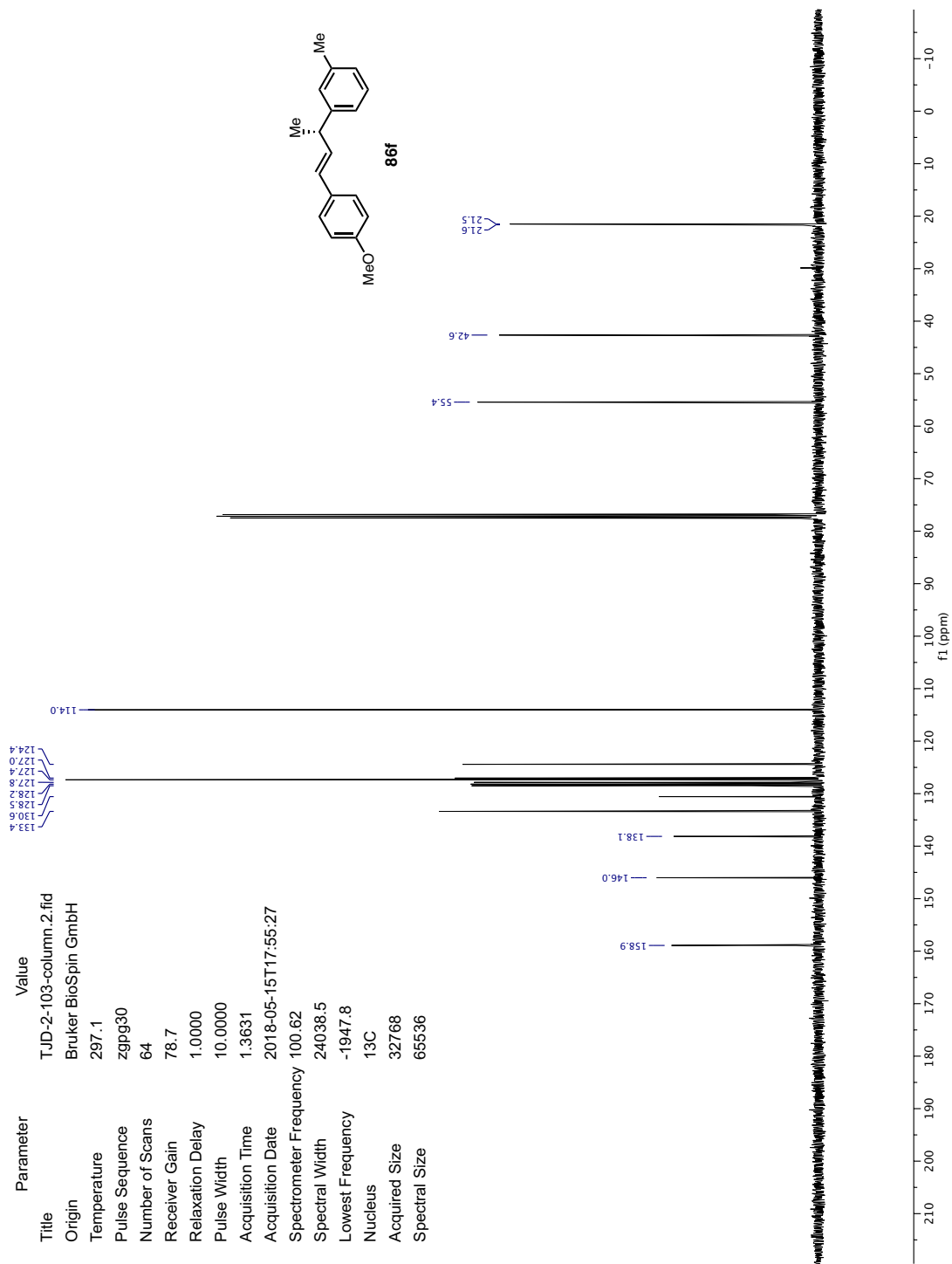


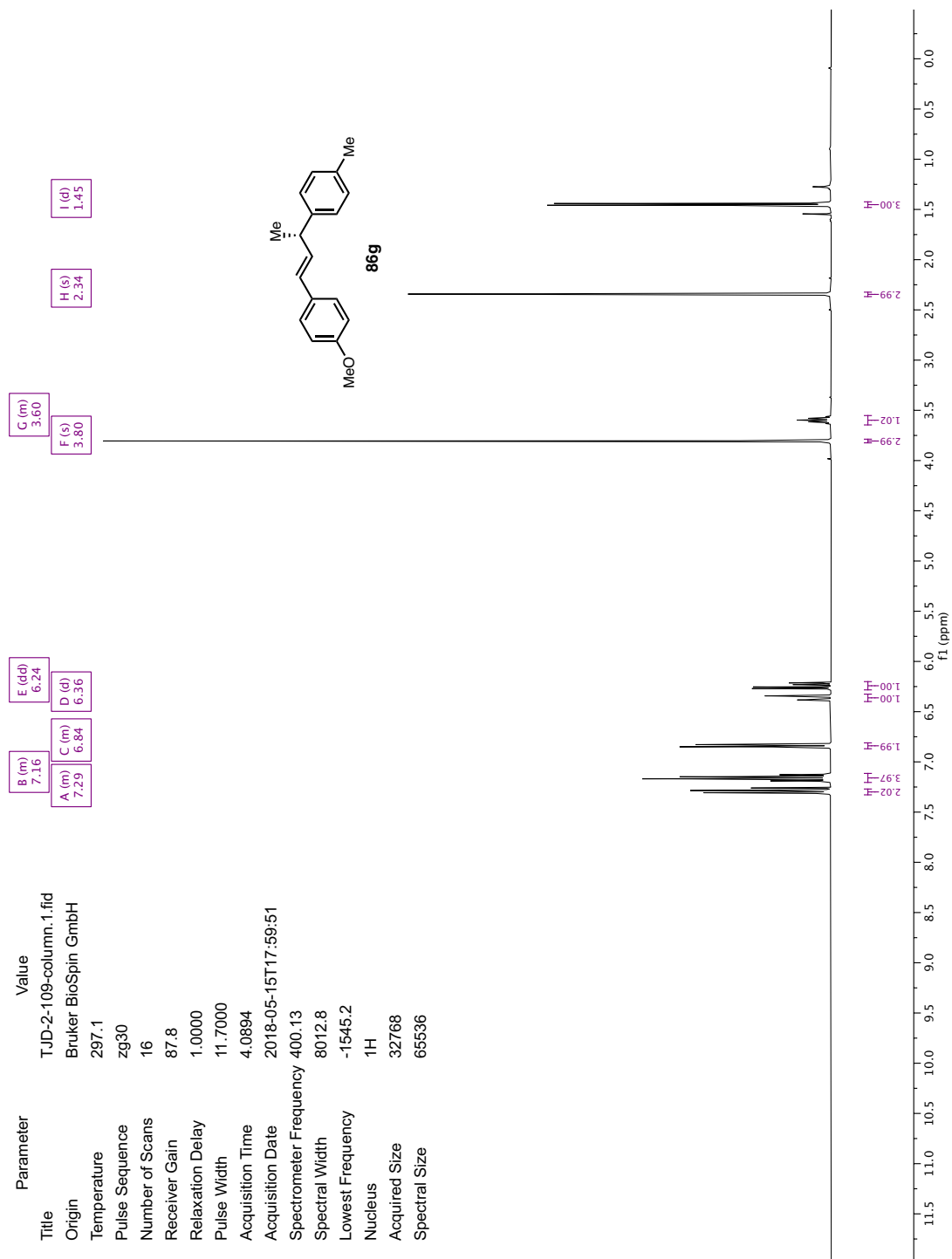


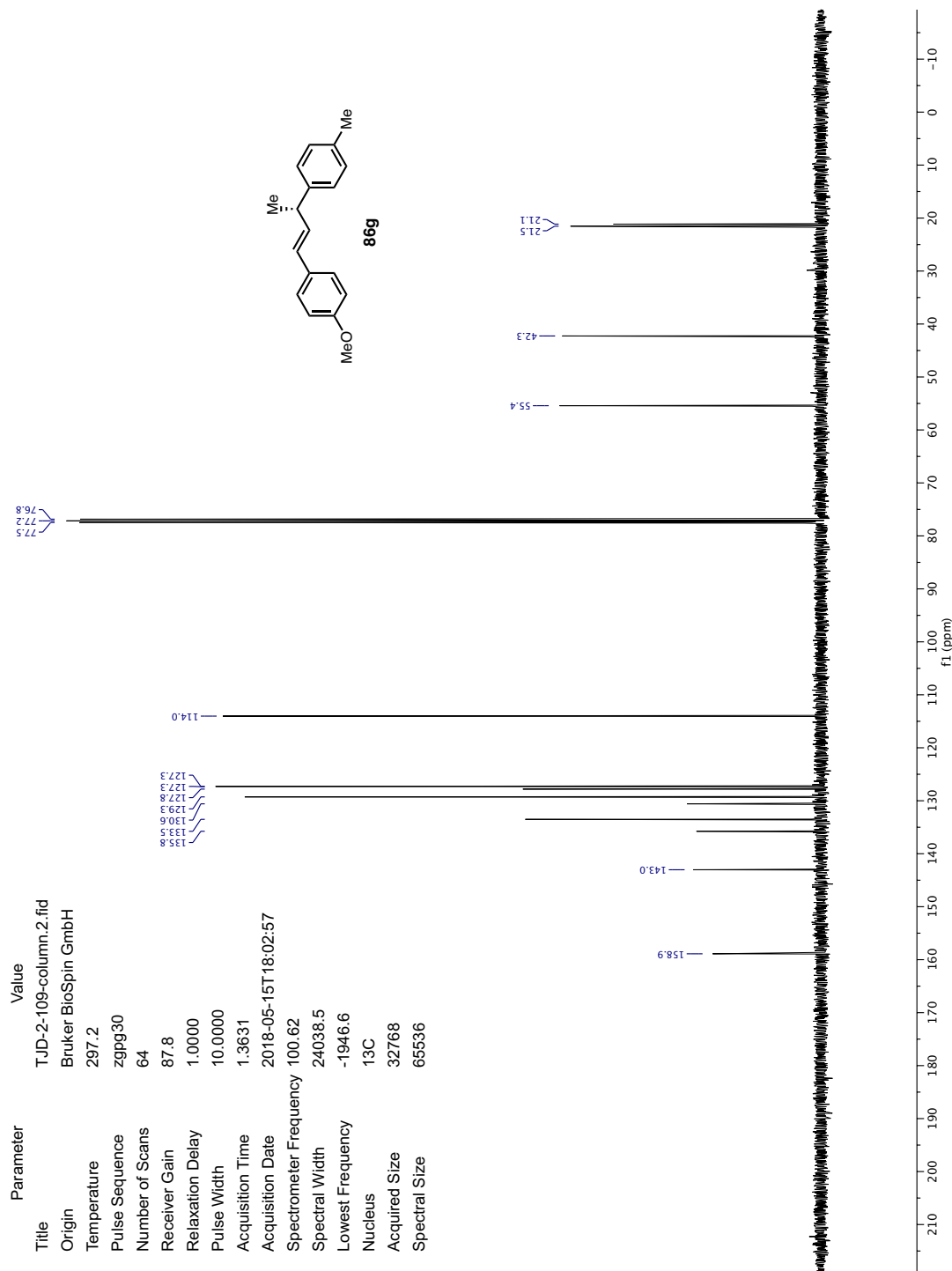










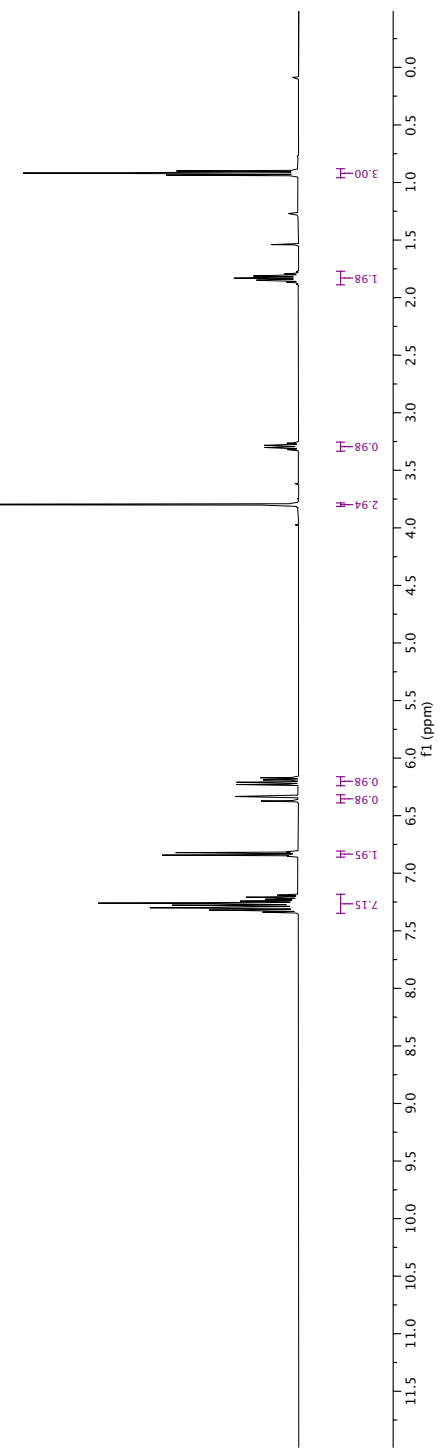
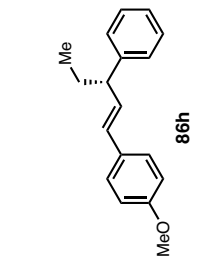


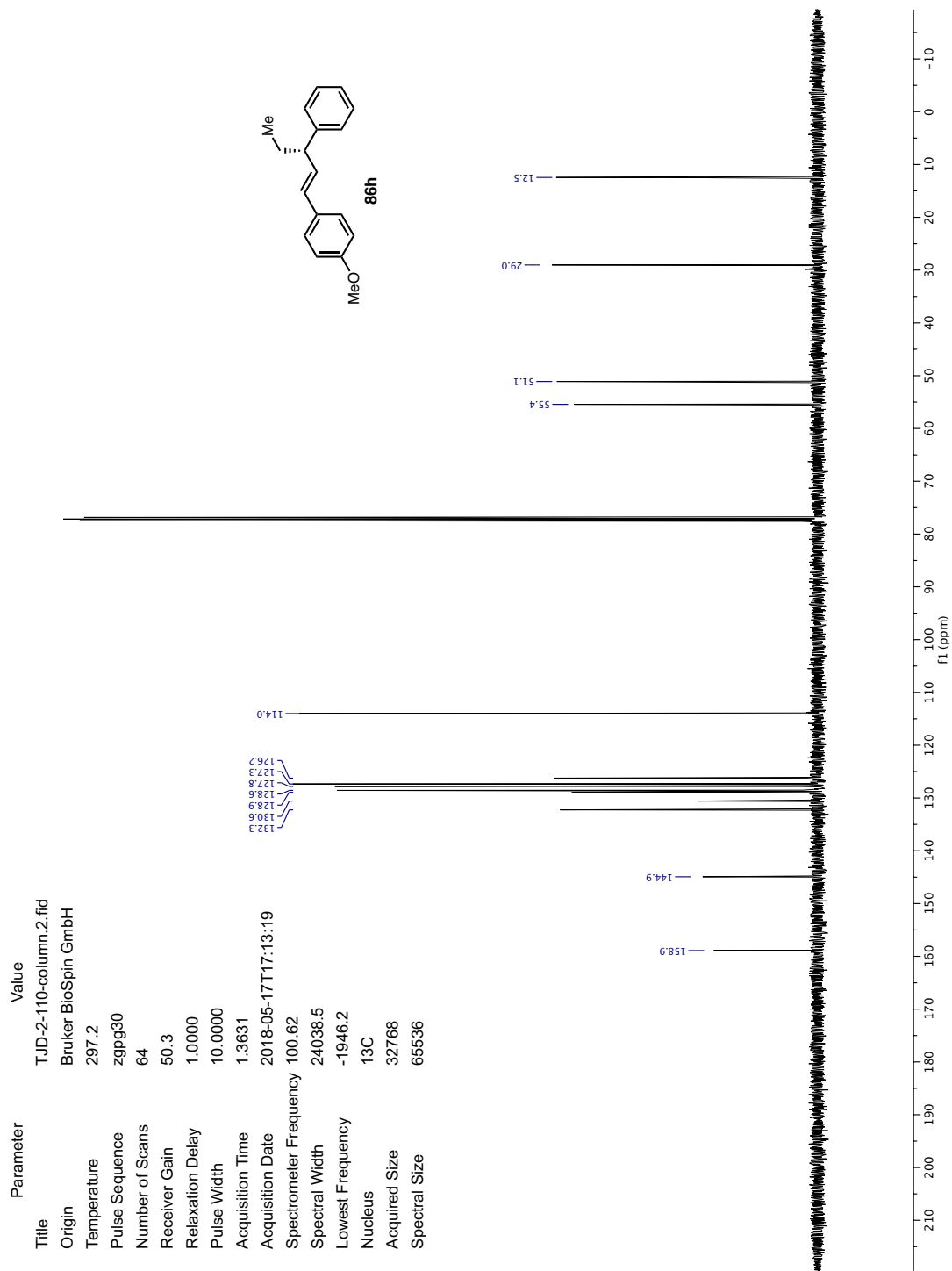
Parameter	Value
Title	T.JD-2-110-column.1.fid
Origin	Bruker BioSpin GmbH
Temperature	297.1
Pulse Sequence	zg30
Number of Scans	16
Receiver Gain	98.9
Relaxation Delay	1.0000
Pulse Width	11.7000
Acquisition Time	4.0894
Acquisition Date	2018-05-17T17:10:06
Spectrometer Frequency	400.13
Spectral Width	8012.8
Lowest Frequency	-1545.4
Nucleus	<sup>1</sup> H
Acquired Size	32768
Spectral Size	65536

A (m)	7.28
B (m)	6.83
C (d)	6.35
D (dd)	6.20

E (s)	3.80
F (m)	3.29

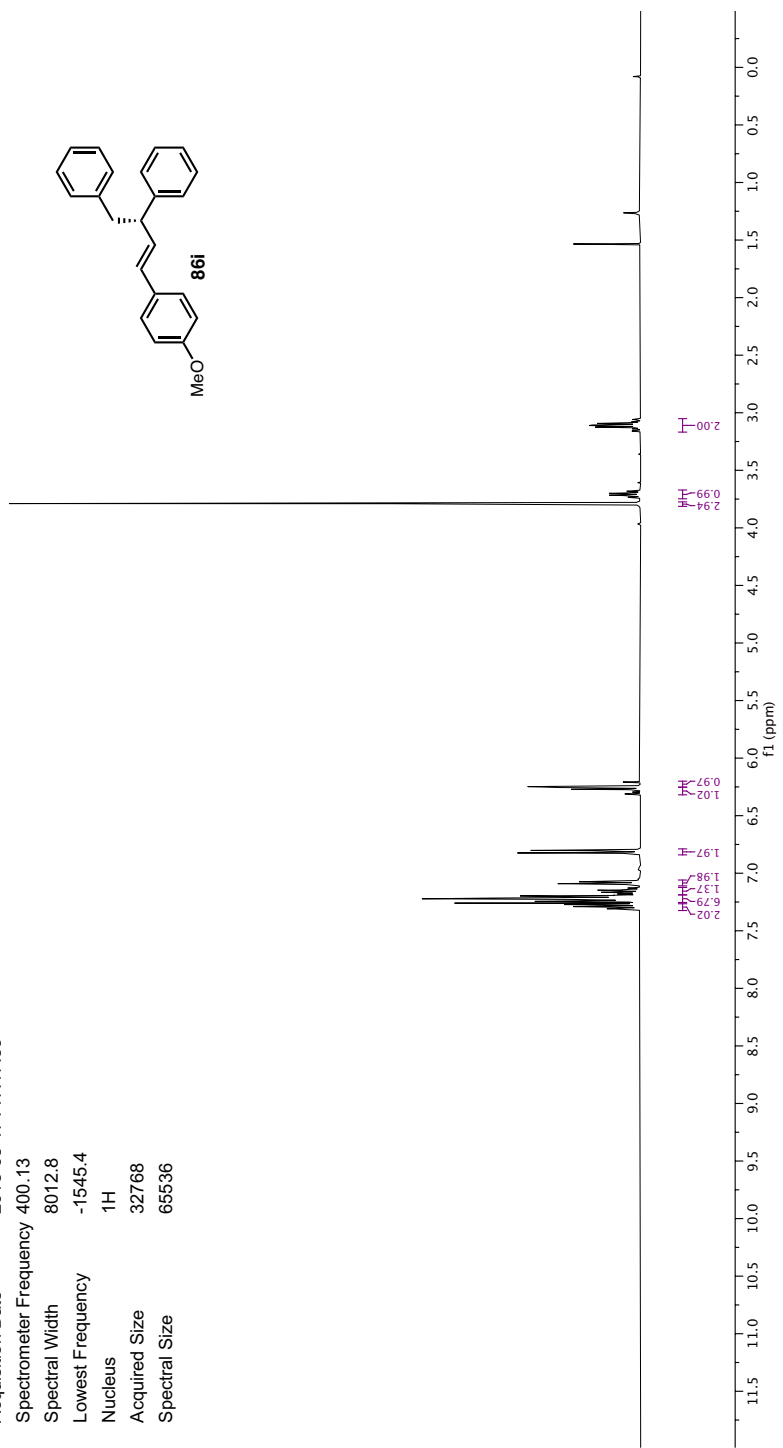
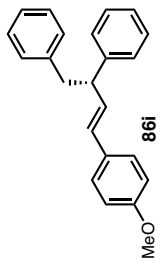
H (m)	1.83
I (t)	0.92



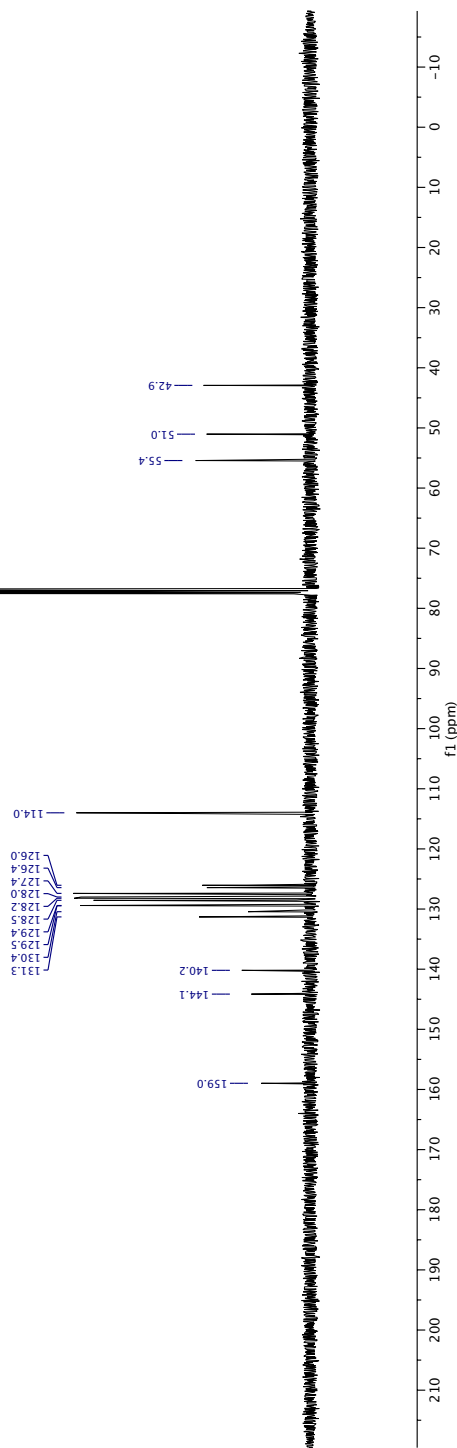
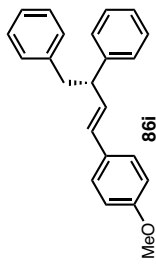


Parameter	Value
Title	T:JD-2-111-column.1.fid
Origin	Bruker BioSpin GmbH
Temperature	297.2
Pulse Sequence	zg30
Number of Scans	16
Receiver Gain	156.2
Relaxation Delay	1.0000
Pulse Width	11.7000
Acquisition Time	4.0894
Acquisition Date	2018-05-17T17:17:59
Spectrometer Frequency	400.13
Spectral Width	8012.8
Lowest Frequency	-1545.4
Nucleus	<sup>1</sup> H
Acquired Size	32768
Spectral Size	65536

D (m)	7.08
B (m)	7.21
A (m)	7.29
E (m)	6.81
C (m)	7.16
G (d)	6.23
F (dd)	6.26
I (m)	3.71
H (s)	3.79
J (m)	3.10



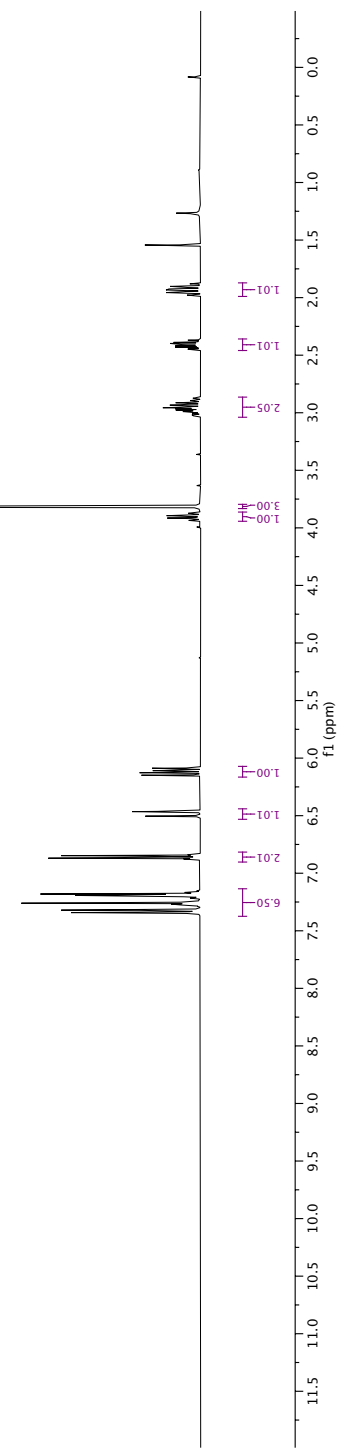
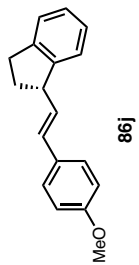
Parameter	Value
Title	T:JD-2-111-column.2.fid
Origin	Bruker BioSpin GmbH
Temperature	297.1
Pulse Sequence	zgpg30
Number of Scans	64
Receiver Gain	64.2
Relaxation Delay	1.0000
Pulse Width	10.0000
Acquisition Time	1.3631
Acquisition Date	2018-05-17T17:21:06
Spectrometer Frequency	100.62
Spectral Width	24038.5
Lowest Frequency	-1945.3
Nucleus	<sup>13</sup> C
Acquired Size	32768
Spectral Size	65536

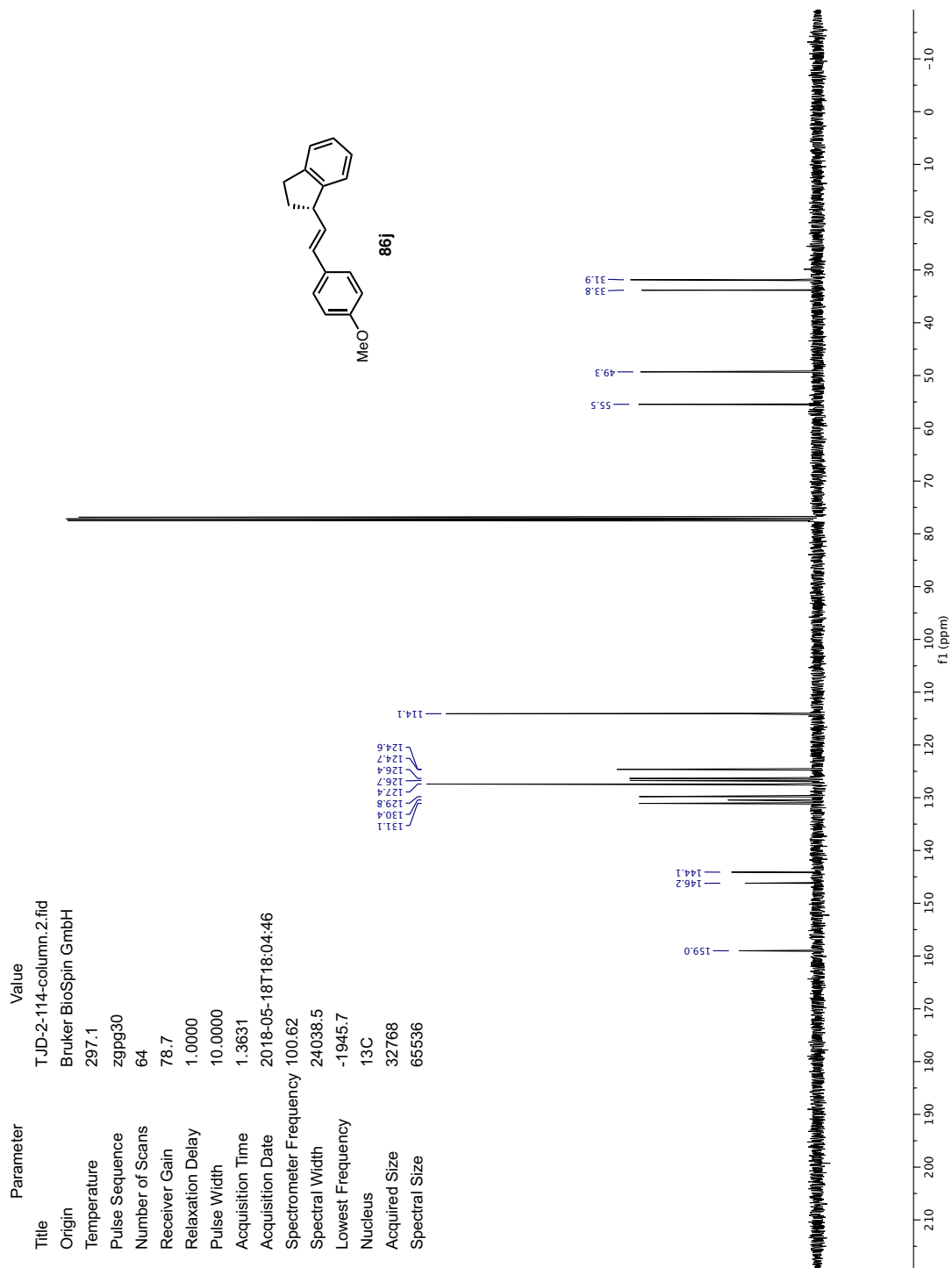


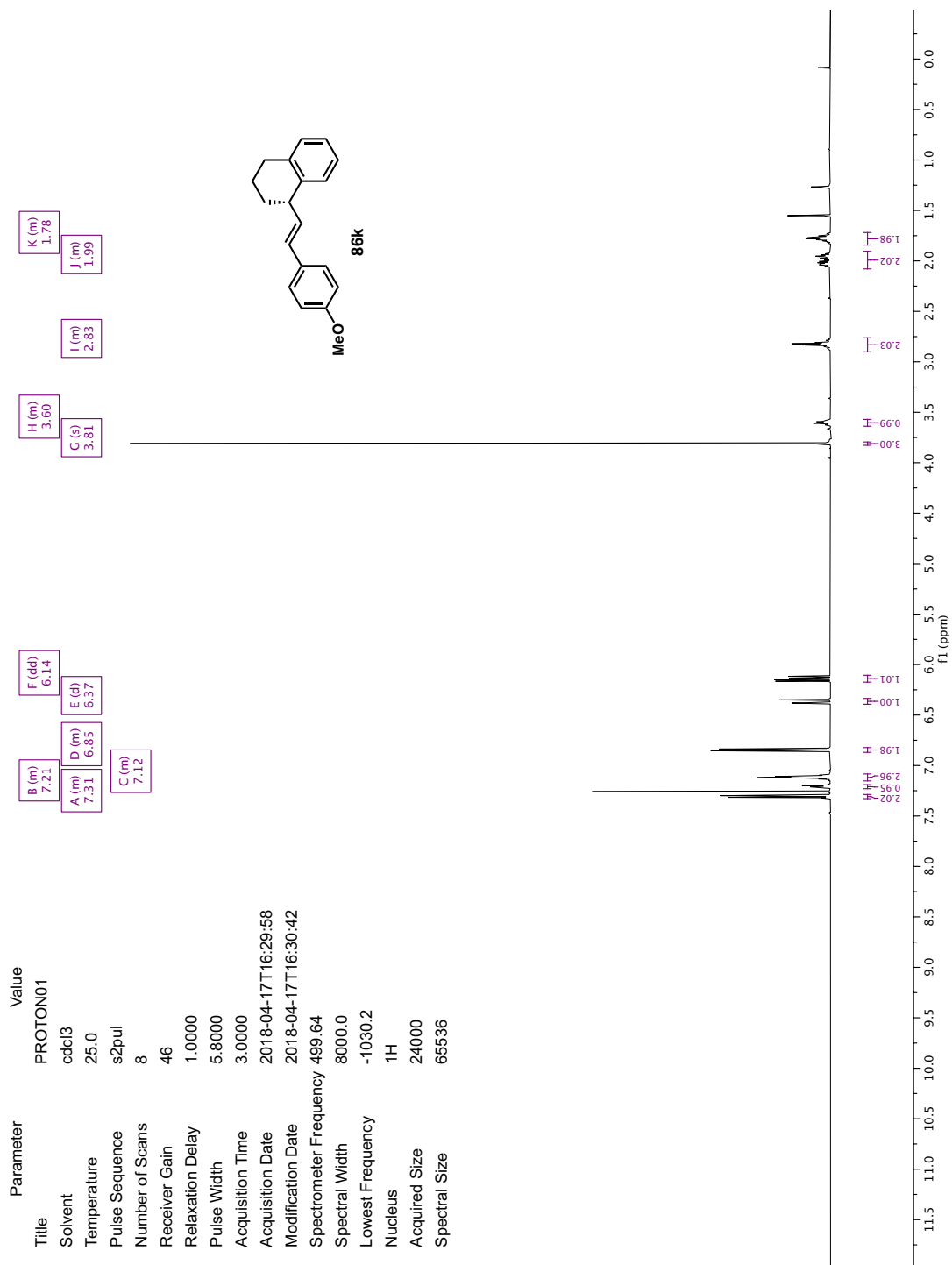


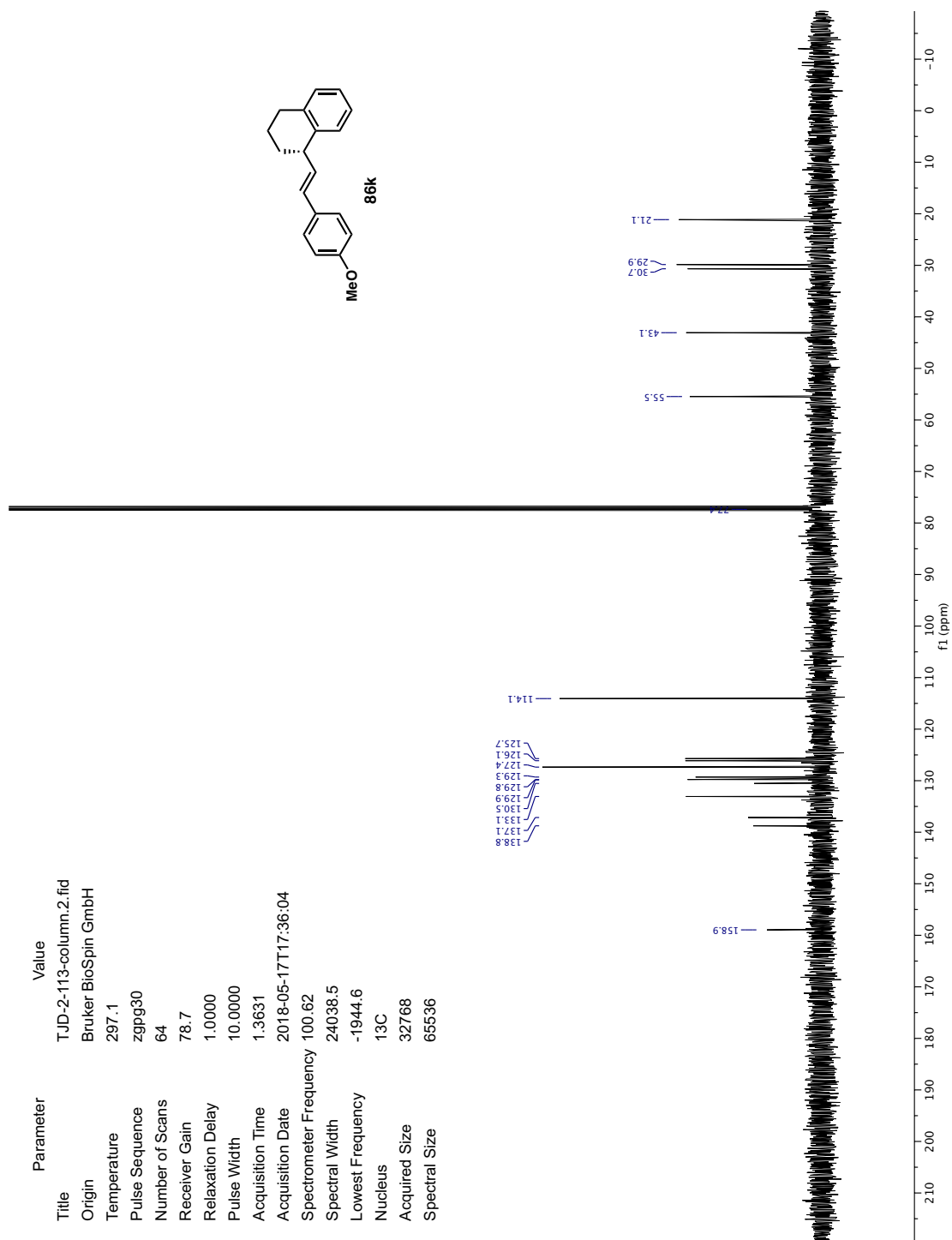
Parameter	Value
Title	T_JD-2-114-column.1.fid
Origin	Bruker BioSpin GmbH
Temperature	297.2
Pulse Sequence	zg30
Number of Scans	16
Receiver Gain	142.8
Relaxation Delay	1.0000
Pulse Width	11.7000
Acquisition Time	4.0894
Acquisition Date	2018-05-18T18:01:06
Spectrometer Frequency	400.13
Spectral Width	8012.8
Lowest Frequency	-1545.3
Nucleus	<sup>1</sup> H
Acquired Size	32768
Spectral Size	65536

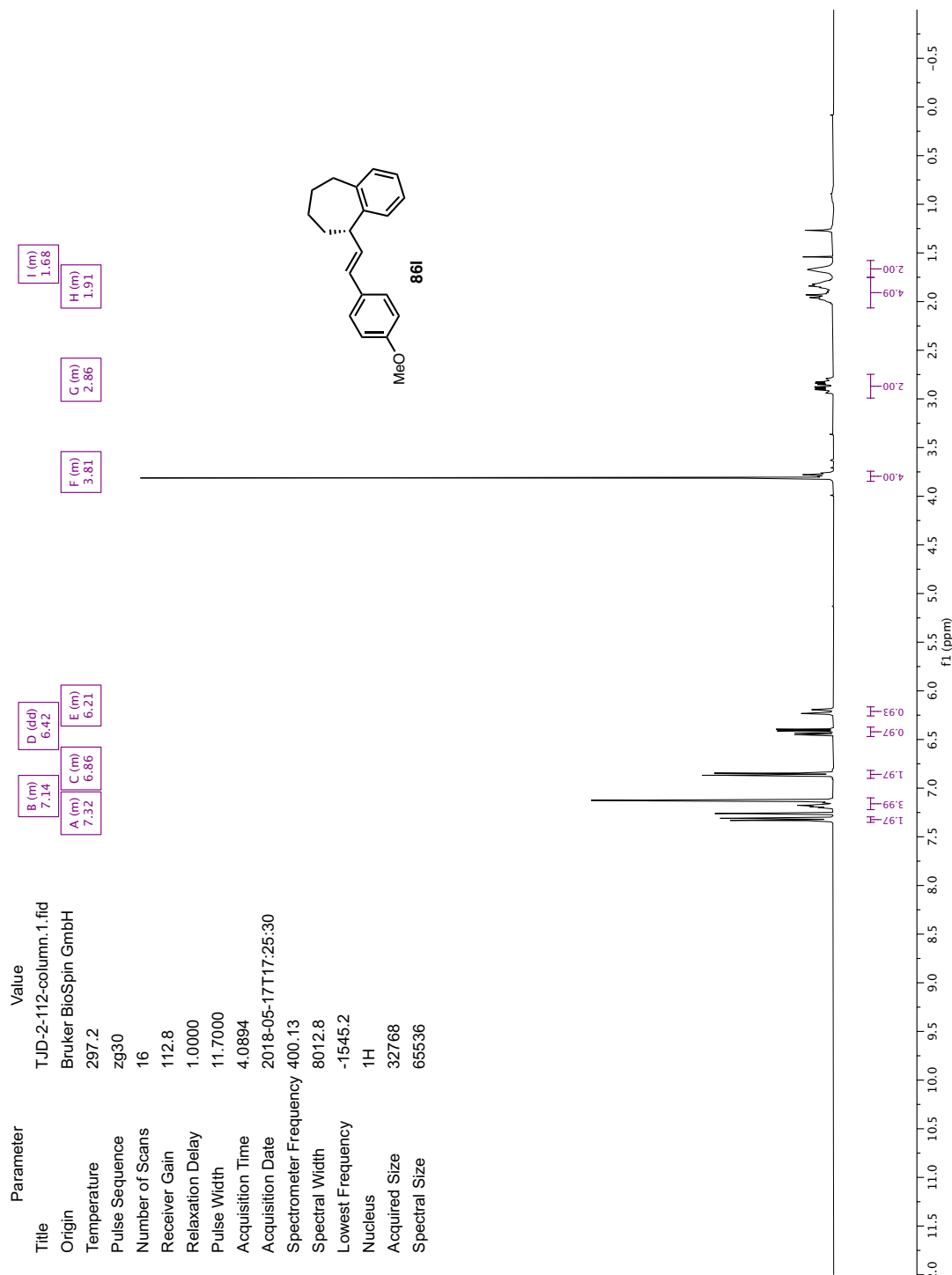
A (m)	7.27
B (m)	6.86
D (dd)	6.12
C (d)	6.48
E (m)	3.90
F (s)	3.81
G (m)	2.95
H (dtd)	2.41
I (dq)	1.93

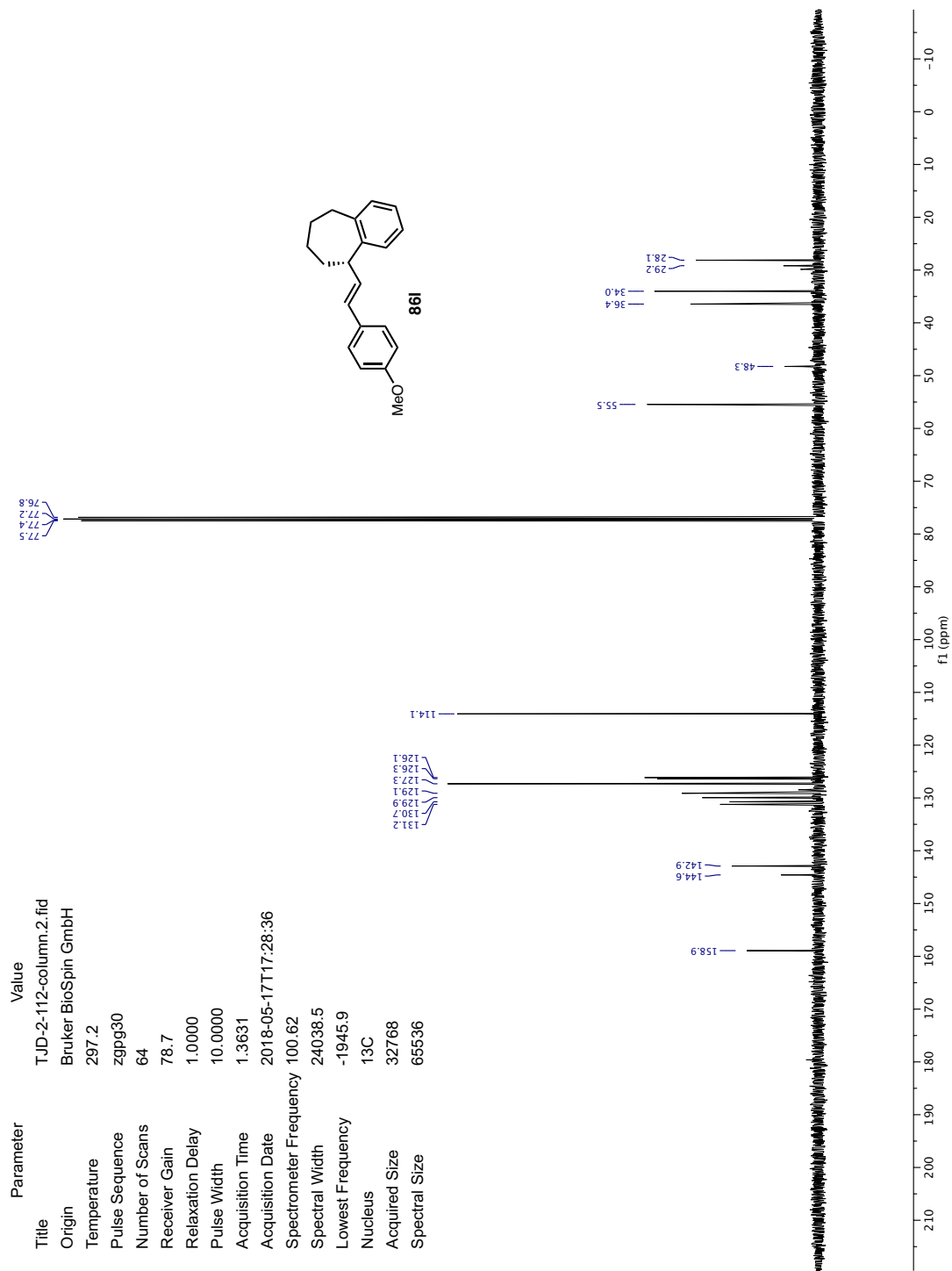






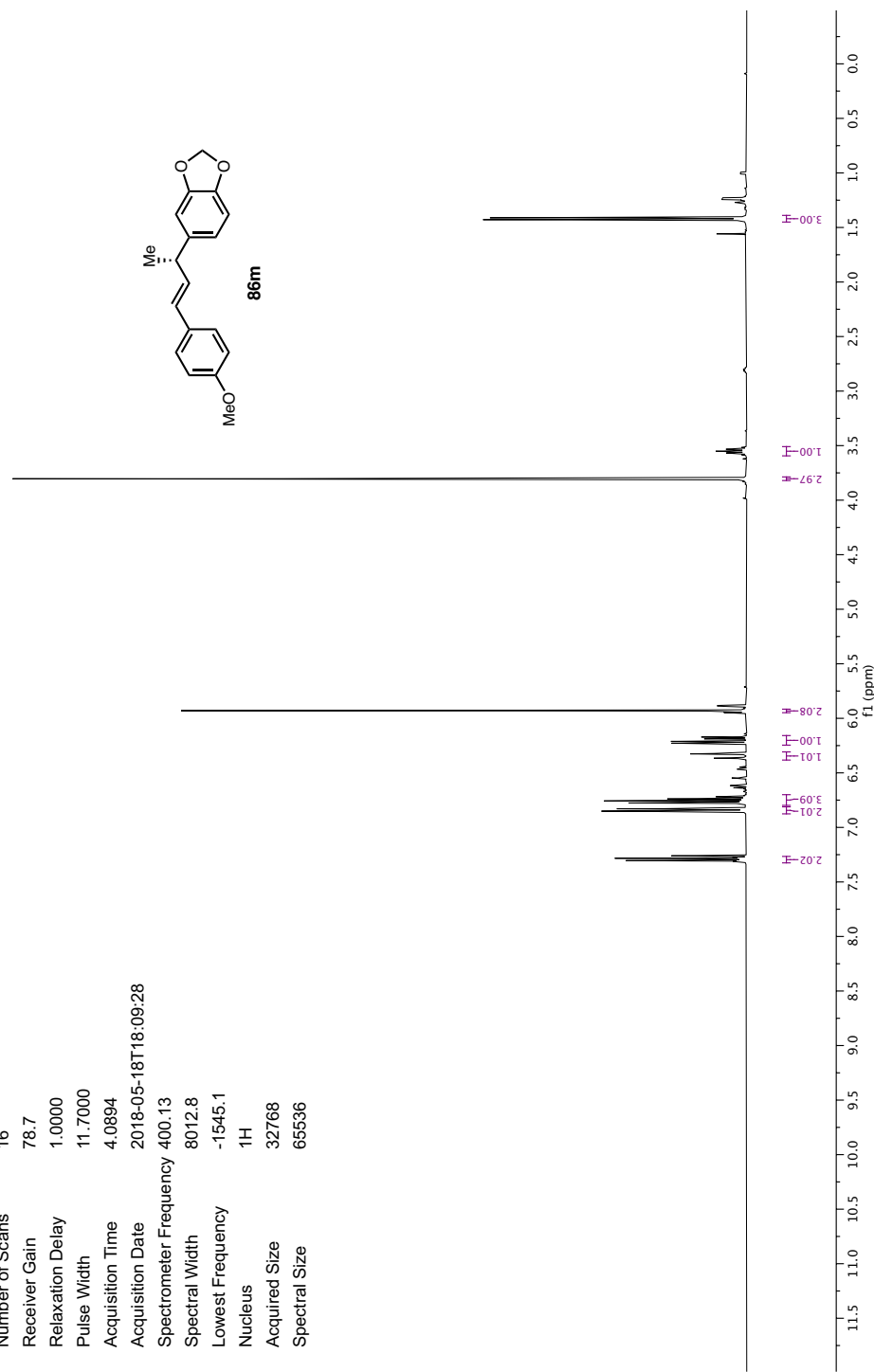


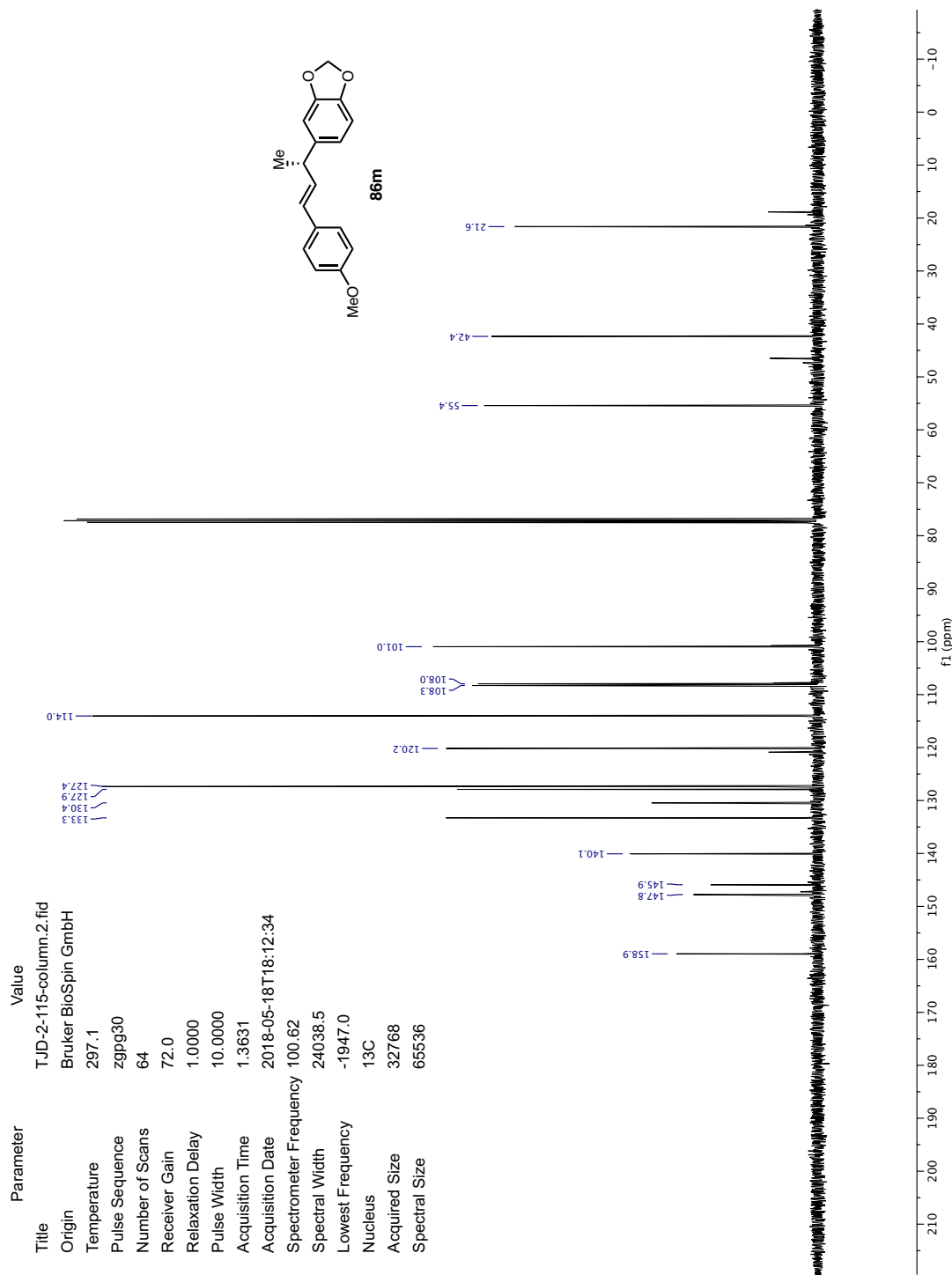




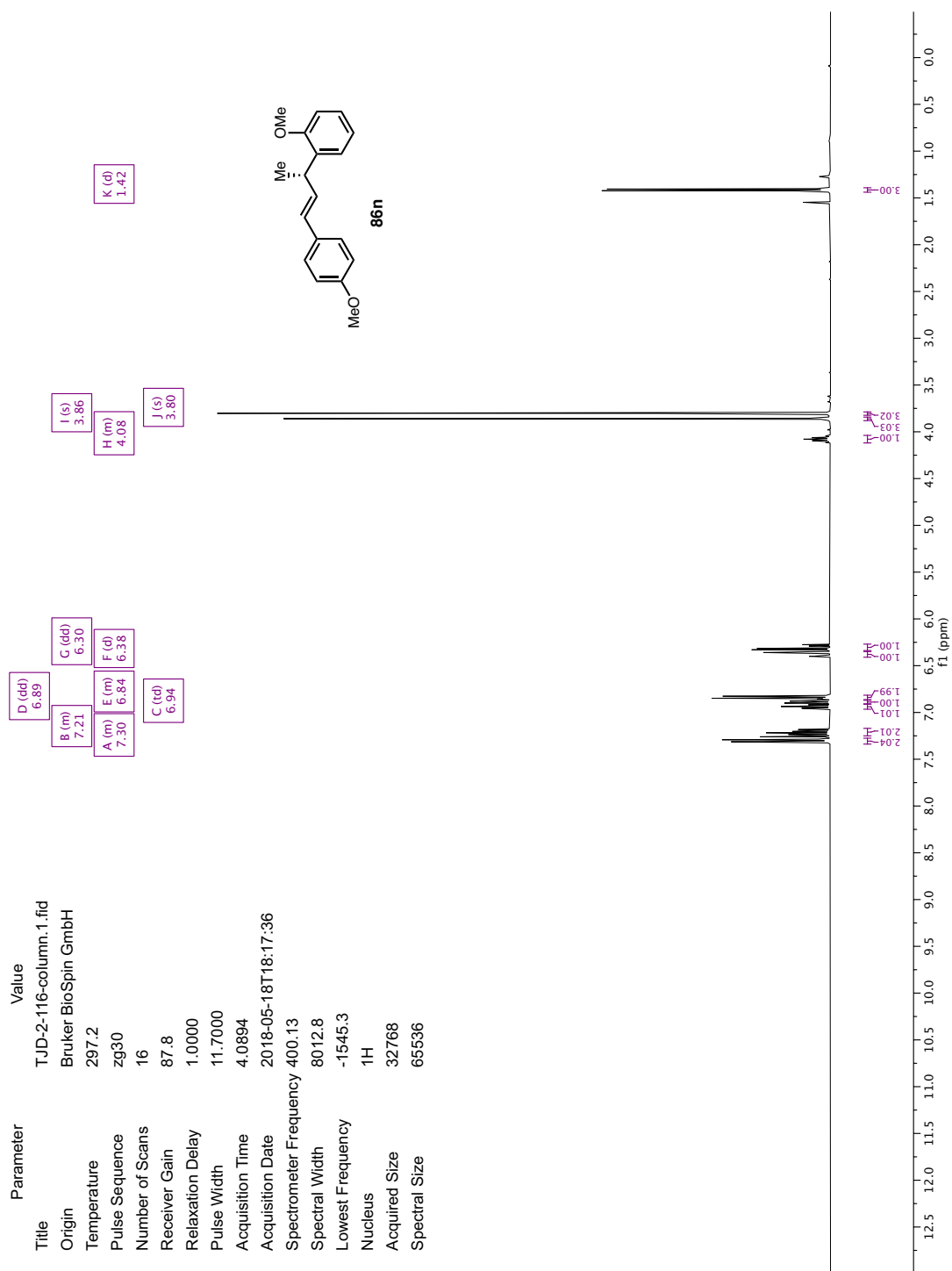
Parameter	Value
Title	T:JD-2-115-column.1.fid
Origin	Bruker BioSpin GmbH
Temperature	297.1
Pulse Sequence	zg30
Number of Scans	16
Receiver Gain	78.7
Relaxation Delay	1.0000
Pulse Width	11.7000
Acquisition Time	4.0894
Acquisition Date	2018-05-18T18:09:28
Spectrometer Frequency	400.13
Spectral Width	8012.8
Lowest Frequency	-1545.1
Nucleus	<sup>1</sup> H
Acquired Size	32768
Spectral Size	65536

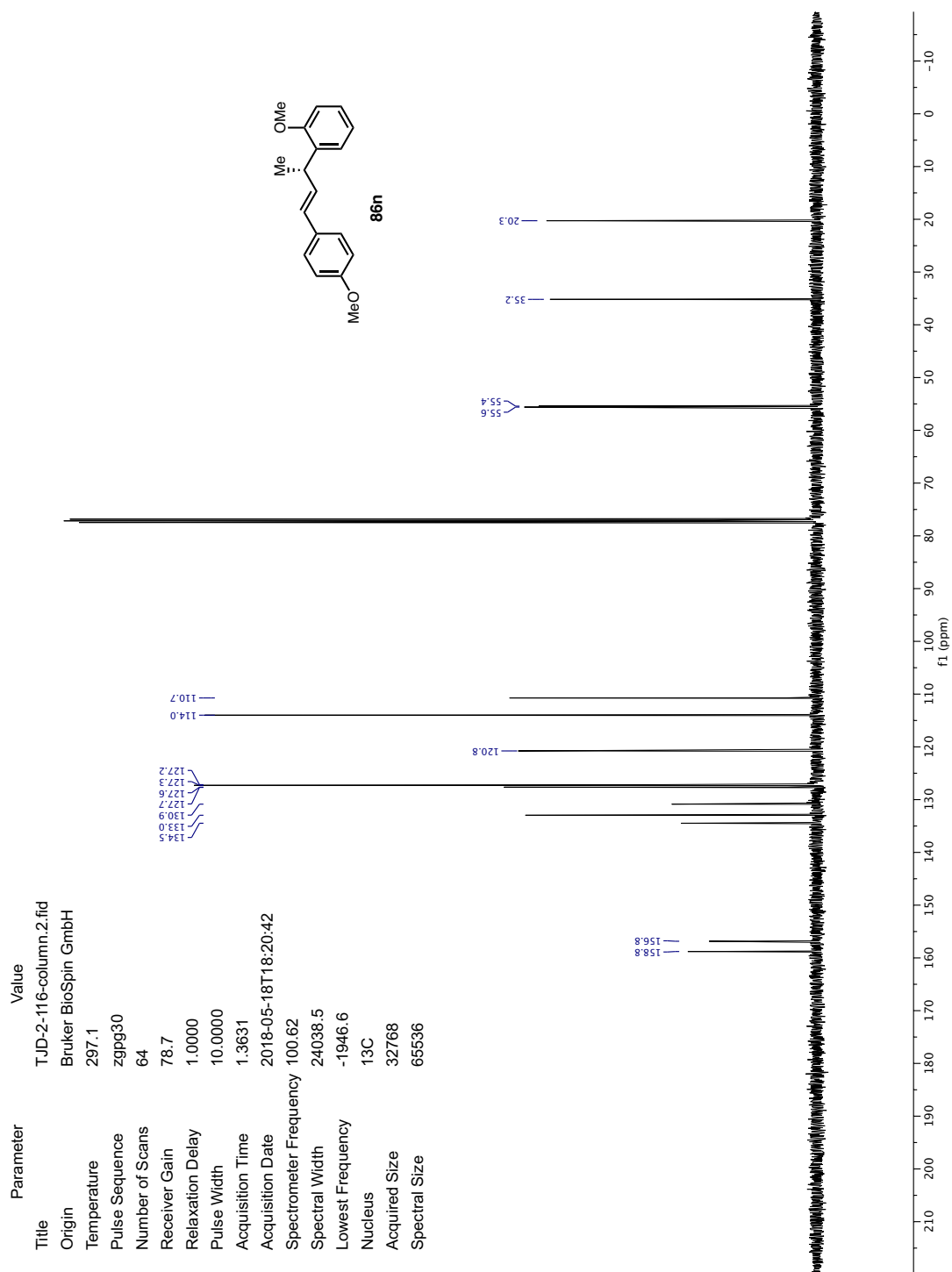
A (m)	7.29	D (m)	6.84	E (m)	6.76	C (dd)	6.20
B (d)	6.34	F (s)	5.93	H (m)	3.55	I (d)	1.42
G (s)	3.80						











## Chapter 2

### *Nickel-Catalyzed Asymmetric Reductive Cross-Coupling of $\alpha$ -Chloroesters with Aryl Iodides<sup>†</sup>*

#### 2.1 INTRODUCTION

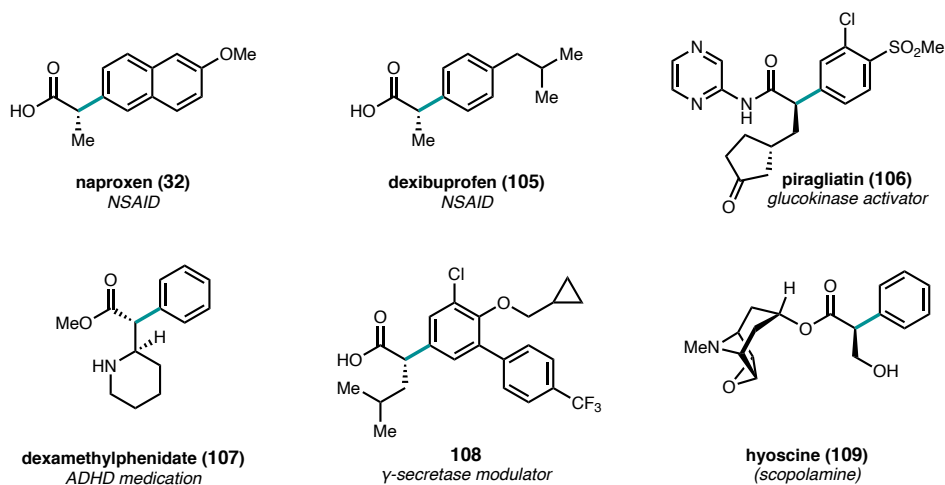
Carboxylic acid derivatives containing  $\alpha$ -aryl stereogenic centers are useful synthetic building blocks and are found in a variety of biologically active compounds (Figure 2.1).<sup>2-7</sup> Chiral  $\alpha$ -aryl carboxylic acid derivatives are especially prevalent in non-steroidal anti-inflammatory drugs (NSAIDs), including ibuprofen (**105**) and naproxen (**32**).

---

<sup>†</sup> Portions of this chapter have been reproduced from published studies.<sup>1</sup> This research was conducted in collaboration with 1) graduate students in the Reisman group: Sara E. Dibrell, Dr. Caitlin, R. Lacker, and Dr. Kelsey E. Poremba, 2) Dr. Leah Cleary, a postdoctoral scholar in the Reisman group, 3) Professor Matthew S. Sigman at the University of Utah, and 4) Adam R. Pancoast, a graduate student in the Sigman group. Fellowship support provided by the NSF (T.J.D, S.E.D, C.R.L., K.E.P, DGE-1144469). Financial support for this work provided by the NIH (S.E.R. R35GM118191, M.S.S. R35GM136271).

Classical methods for the synthesis of these compounds in enantioenriched form include chiral resolution or the use of chiral auxiliaries.<sup>8</sup>

**Figure 2.1** Bioactive chiral  $\alpha$ -aryl carboxylic acid derivatives.

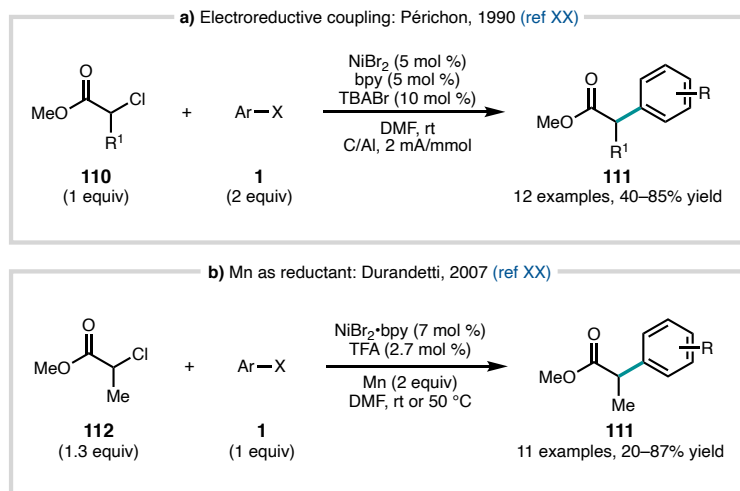


Given their prevalence in bioactive compounds, there has been significant interest in developing catalytic, enantioselective methods for the synthesis of  $\alpha,\alpha$ -disubstituted carbonyl motifs. A number of transition metal-catalyzed methods have been developed for the synthesis of these compounds; key to the development of these reactions is the identification of reaction conditions that are sufficiently mild to avoid racemization of the enantioenriched products.<sup>9</sup> Notably, Fu and coworkers have developed a variety of highly enantioselective nickel-catalyzed redox-neutral couplings of organometallic reagents with  $\alpha$ -halo carbonyl compounds.<sup>10–16</sup>

Reductive nickel catalysis has also been employed for the synthesis of  $\alpha,\alpha$ -disubstituted carbonyl compounds. In 1990, Périchon and coworkers reported the nickel-catalyzed electroreductive coupling of  $\alpha$ -chloroesters with aryl bromides and iodides to form racemic arylated products in moderate to good yields (Figure 2.2a).<sup>17</sup> This

electrochemical reactivity has subsequently been further developed.<sup>18–20</sup> Manganese powder has also been used to turn over nickel-catalyzed reductive cross-couplings between  $\alpha$ -chloroesters and aryl halides; acid additives were found to be important, presumably for activating the surface of the  $\text{Mn}^0$  powder (Figure 2.2b).<sup>21</sup> Inspired by these reductive coupling reactions, and hoping to expand on the couplings developed in our lab,<sup>22</sup> our group sought to develop an *enantioselective* nickel-catalyzed reductive cross-coupling to access enantioenriched  $\alpha,\alpha$ -disubstituted esters. We hoped that we could access a variety of arylated products highly selectively, and use a broader scope of  $\alpha$ -chloroesters than the methyl 2-chloropropanoate and methyl 2-chloroacetate employed by Durandetti and coworkers.<sup>17,21</sup> As we were completing our investigations, a related transformation was reported by Walsh, Mao, and coworkers (*vide infra*).<sup>23</sup>

**Figure 2.2** Early nickel-catalyzed reductive arylations of  $\alpha$ -chloroesters.

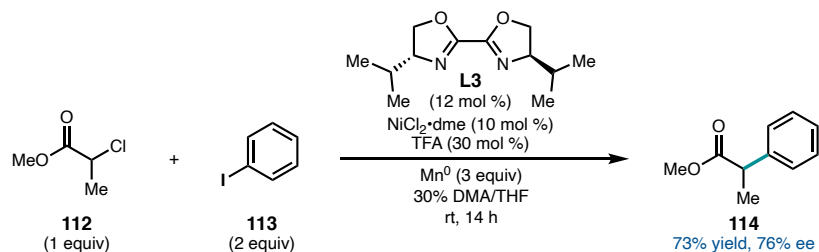


## 2.2 REACTION OPTIMIZATION

Reaction optimization began with conditions derived from prior asymmetric reductive couplings developed in our group.<sup>24,25</sup> Initial evaluation of the reaction

parameters identified BiOX ligands as giving the most promising combination of reactivity and enantioselectivity, with isopropyl BiOX (**L3**) giving cross-coupled product **114** in 73% yield and 76% ee (Figure 2.3).

**Figure 2.3** Initial hit conditions.

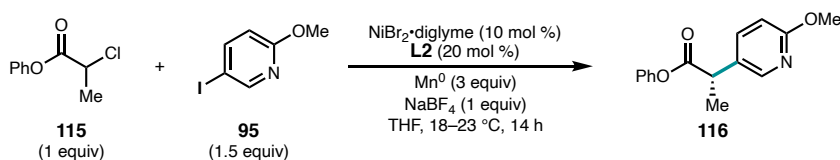


Extensive further optimization was required to improve the enantioselectivity and generality of the reaction and arrive at the finalized conditions. This work is thoroughly outlined in the thesis of Dr. Kelsey Poremba.<sup>26</sup> Through much experimentation, it was found that 4-heptyl BiOX (**L2**), a ligand previously developed in our lab,<sup>27</sup> was optimal in this reaction. When paired with  $\text{NiBr}_2 \cdot \text{diglyme}$  as nickel source, THF as solvent,  $\text{Mn}^0$  powder as reductant, and  $\text{NaBF}_4$  as an additive, cross-coupled product **116** could be obtained in 92% yield and 86% ee (Table 2.1, entry 1). Identification of two key considerations led to reproducible and broadly applicable conditions: 1) the use of phenyl ester **115** rather than methyl ester **112**, and 2) the need to briefly pre-complex nickel and **L2** before adding the electrophiles to the reaction.

The use of  $\text{NaBF}_4$  as an additive was found to be crucial for the formation of **116** (Table 2.1, entry 2).<sup>28</sup> BiOX ligands with branched alkyl sidechains performed best in the reaction; 4-heptyl BiOX (**L2**) gave the optimal combination of yield and enantioselectivity (entry 1), while isopropyl BiOX and cyclohexyl BiOX (**L3** and **L4**) gave somewhat lower

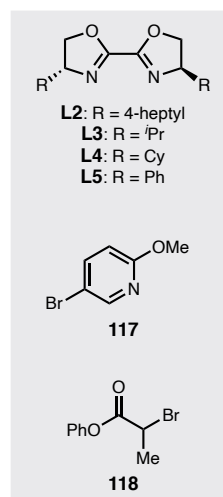
yield and ee (entries 3 and 4). Interestingly, replacement of the alkyl ligand sidechain with a phenyl group (**L5**) resulted in a complete loss of reactivity (entry 5).<sup>29</sup> Although 20 mol % **L2** gave optimal results, the ligand loading could be lowered with only minor reduction in reaction performance (entries 6 and 7).

**Table 2.1** Effects of reaction parameters.



Entry	Deviation from std. conditions	% Yield <sup>a</sup>	% ee <sup>b</sup>
1	None	92	86
2	No $\text{NaBF}_4$	0	–
3	<b>L3</b> instead of <b>L2</b>	62	76
4	<b>L4</b> instead of <b>L2</b>	89	70
5	<b>L5</b> instead of <b>L2</b>	0	–
6	10 mol % <b>L2</b>	81	83
7	12 mol % <b>L2</b>	83	85
8	Zn instead of Mn	29	81
9	TDAE instead of Mn	0	–
10	DMA instead of THF	67	84
11	1,4-dioxane instead of THF	0	–
12	Methyl ester	40	84
13	<i>t</i> -Butyl ester	20	89
14	1 equiv <b>95</b>	85	84
15	<b>117</b> instead of <b>95</b>	10	84
16	<b>118</b> instead of <b>115</b>	0	–
17	No $\text{NiBr}_2 \cdot \text{diglyme}$	0	–
18	No <b>L2</b>	0	–
19	No Mn	0	–

<sup>a</sup> Determined by  $^1\text{H}$  NMR, relative to 1,1,2,2-tetrachloroethane as an internal standard. <sup>b</sup> Determined by chiral SFC.



Alternate reductants were also tested in the reaction.  $\text{Zn}^0$  proved less effective than  $\text{Mn}^0$  (entry 8) and the use of tetrakis(dimethylamino)ethylene (TDAE) failed to afford any of the desired product (entry 9).<sup>30</sup> While the reaction performed reasonably well in DMA (entry 10), no reaction was observed in 1,4-dioxane, a solvent previously employed in other

[**L2**·Ni]-catalyzed reductive cross-couplings (entry 11).<sup>25,27</sup> Phenyl ester **115** was not unique in coupling with high enantioselectivity; the corresponding methyl and *tert*-butyl esters could be coupled in similar ee but significantly lower yields (entries 12 and 13).

Equimolar **115** and **95** could be used as coupling partners, giving **116** in slightly reduced yield and ee compared to the standard conditions employing 1.5 equiv **95** (entry 14). When pyridyl bromide **117** was used in place of **95**, **116** was formed in substantially lower yield (entry 15). Interestingly, when  $\alpha$ -bromoester **118** was employed in lieu of **115**, no product was formed, and **118** was recovered unreacted (entry 16). Finally, control experiments confirmed that NiBr<sub>2</sub>·diglyme, **L2**, and Mn<sup>0</sup> were all required in this reaction (entries 17–19). These optimized conditions offer several advantages over the related reductive cross-coupling reported by Walsh and Mao: 1) the use of only 1.5 equiv of aryl halide coupling partner (*vs.* 3.0 equiv); 2) the use of easy-to-functionalize esters derived from inexpensive phenol (*vs.* 2,2,3-trimethylbutan-2-ol); 3) the use of an inexpensive terminal reductant (Mn<sup>0</sup> *vs.* Hantzsch ester); and 4) shorter reaction time (14 *vs.* 48 h).<sup>23</sup>

## 2.3 REACTION SCOPE

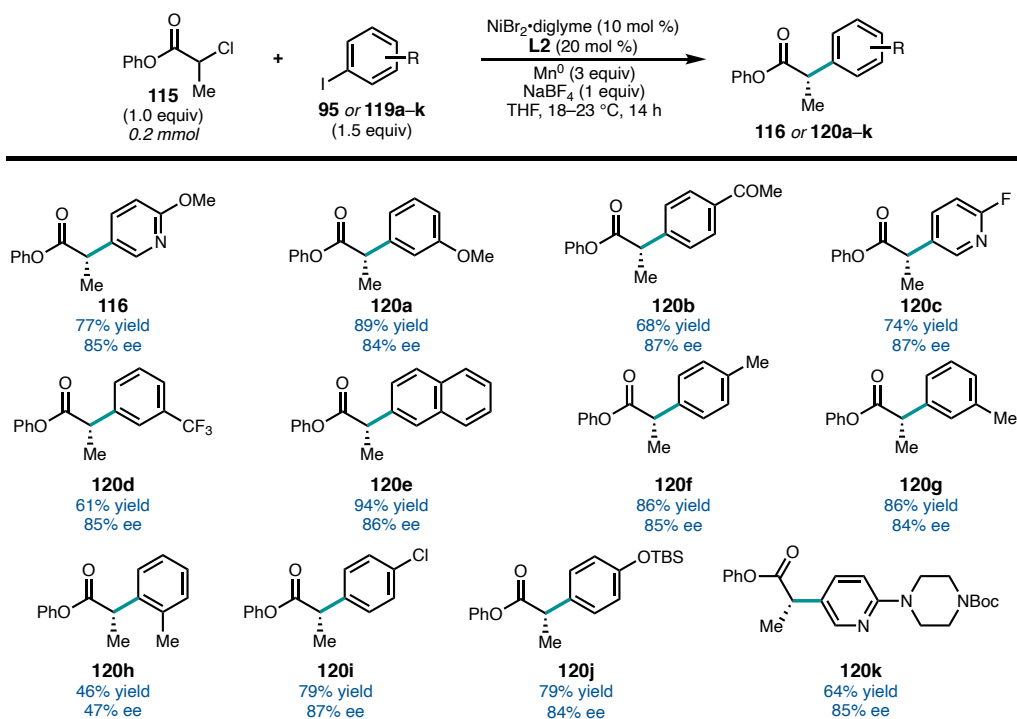
### 2.3.1 Scope of Aryl Iodides

With optimized reaction conditions in hand, the scope of aryl iodide coupling partners was explored (Figure 2.4). The reaction was found to tolerate both electron-rich (**120f** and **120j**) and electron-poor (**120b** and **120d**) aryl iodides. Several heteroaromatic iodides were also competent coupling partners (**116**, **120c**, and **120k**). Protected heteroatoms (**120j** and **120k**) and an aryl chloride (**120i**) were tolerated, giving enantioenriched products poised for further elaboration. Whereas *para*- and *meta*-tolyl



substrates **120f** and **120g** coupled efficiently, *ortho*-tolyl iodide gave the corresponding coupled product in significantly reduced yield and enantioselectivity (**120h**). Notably, this series of substrates reveals the relative insensitivity of this reaction to the electronic properties of the arene, especially with respect to enantioselectivity.

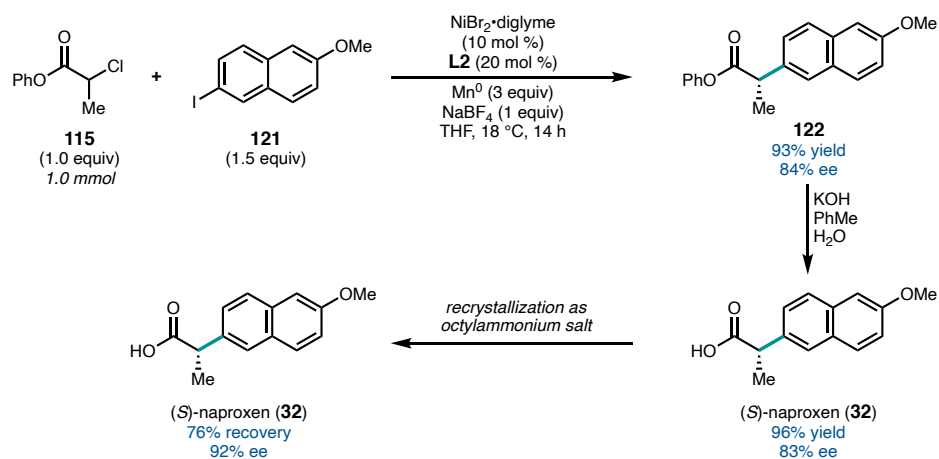
**Figure 2.4** Scope of (hetero)aryl iodides.



Having explored the scope of aryl iodide coupling partners in this reaction, we next sought to scale up this enantioselective reductive cross-coupling reaction and apply it towards the synthesis of the NSAID (*S*)-naproxen (**32**). With minor adjustments to the procedure (use of a round-bottomed flask in lieu of a vial, use of a larger stir bar, and addition of the electrophiles as a solution in THF), methoxy naphthyl iodide **121** could be coupled with **115** on 1.0 mmol scale to afford phenyl ester **122** in 93% yield and 84% ee (Scheme 2.1). Subsequent basic hydrolysis of **122** under biphasic conditions afforded (*S*)-

naproxen (**32**) with only minor erosion of enantioenrichment. The ee of this NSAID could be further upgraded by recrystallization as its *n*-octylammonium salt.<sup>31</sup> This synthesis both demonstrated our ability to conduct the optimized reaction on a larger scale and allowed for the unambiguous assignment of the configuration of **32** as (*S*). The absolute stereochemistries of the other products shown in Figures 2.4 and 2.5 were assigned by analogy to **32**.

**Scheme 2.1** Reaction scale up and synthesis of (*S*)-naproxen.

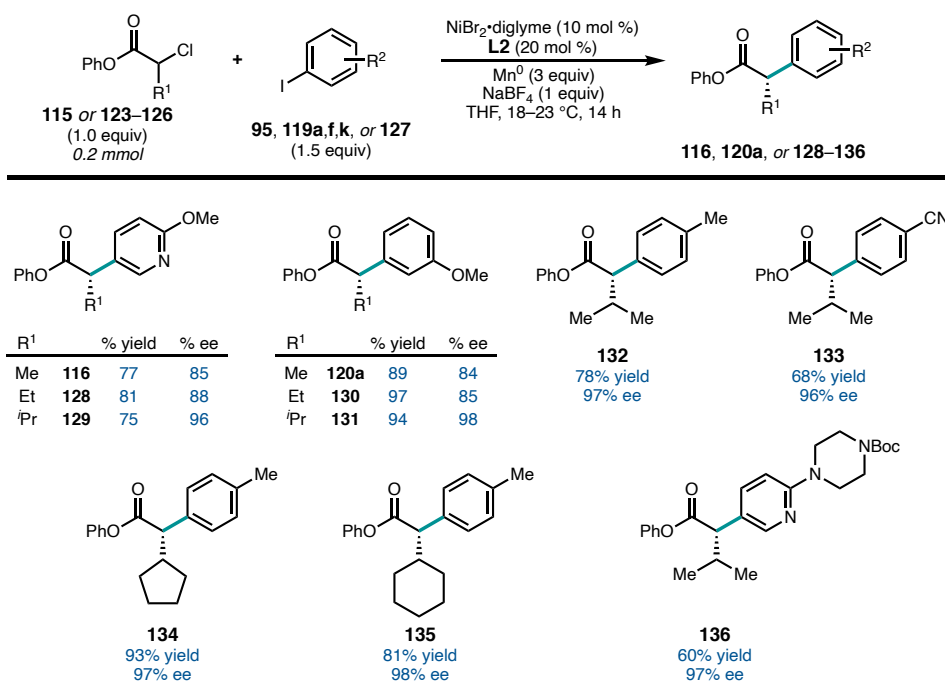


### 2.3.2 Scope of $\alpha$ -Chloroesters

The tolerance of the reaction to varied  $\alpha$ -sidechains on the chloroester coupling partner was next explored. In contrast to aryl iodides, the enantioselectivity of the reaction was found to be quite sensitive to the structure of the  $\alpha$ -chloroester (Figure 2.5). Increasing the steric bulk of the sidechain had a dramatic impact on the observed enantioselectivity. For a series of substrates where the  $\alpha$ -substituent was changed from methyl (**115**) to ethyl (**123**) to isopropyl (**124**), the ee of the product increased from 85% to 88% to 96%, respectively (**116**, **128**, and **129**). A similar trend was observed when 1-iodo-3-

methoxybenzene (**119a**) was employed as the coupling partner; increasing the steric bulk from methyl (**120a**) to ethyl (**130**) gave a small increase in ee, and introduction of  $\beta$ -branching to the sidechain to form isopropyl product **131** resulted in a large increase in ee to 98%. Energetically, the difference in enantioselectivities between these methyl (**120a**) and isopropyl (**131**) products is quite large, consistent with a 1.25 kcal/mol difference in their corresponding  $\Delta\Delta G^\ddagger$  values.

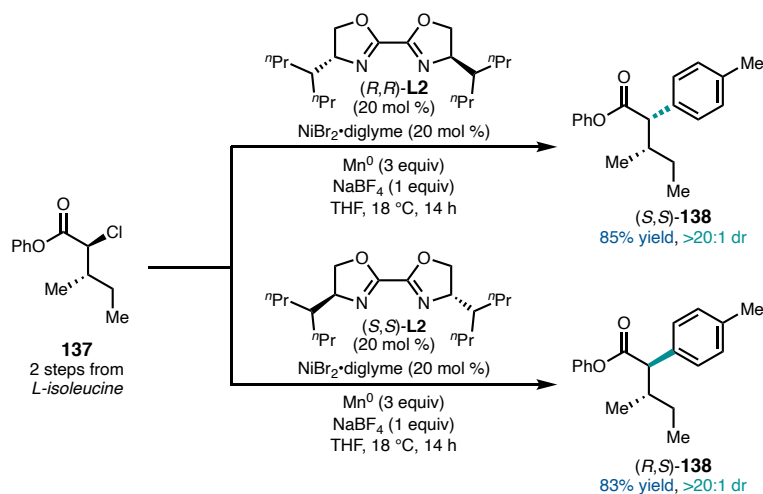
**Figure 2.5** Scope of  $\alpha$ -chloroesters.



The  $\alpha$ -isopropyl chloroester **124** could be coupled with several other aryl iodides in uniformly high ee (**132**, **133**, and **136**). Additional chloroesters with  $\beta$ -branched sidechains such as cyclopentyl and cyclohexyl could also be coupled to afford **134** and **135** in excellent yields and enantioselectivities. We next aimed to leverage the high enantioselectivity achieved with  $\beta$ -branched substrates to effect a diastereoselective reaction. Using an  $\alpha$ -chloroester derived from L-isoleucine (**137**), either the (*S,S*)- or (*R,S*)-

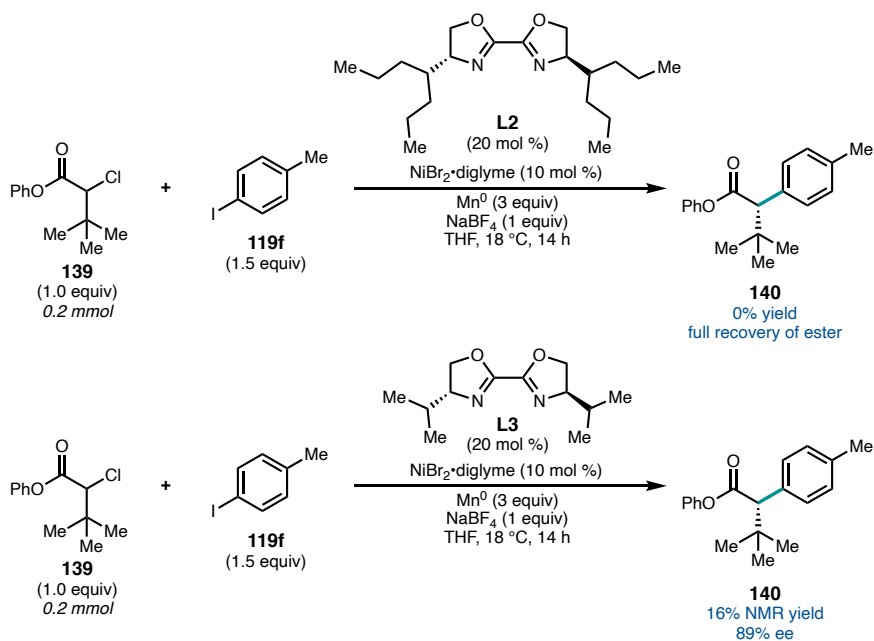
diastereomer of coupled product **138** could be obtained simply by changing the enantiomer of **L2** that was used, demonstrating that products containing vicinal stereogenic centers could be prepared with complete catalyst control over the configuration of the  $\alpha$ -carbon (Figure 2.6).

**Figure 2.6** Catalyst-controlled diastereoselectivity.

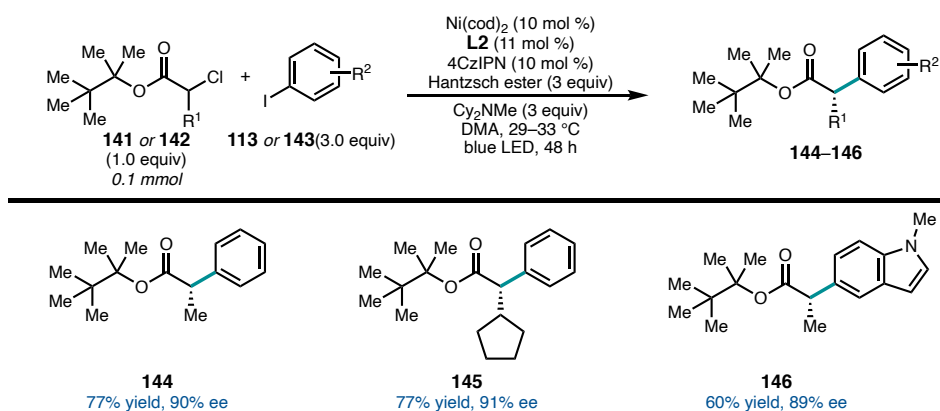


We note that, qualitatively, the increase in enantioselectivity moving from  $\alpha$ -methyl to  $\alpha$ -isopropyl did not come at the expense of yield, in contrast to related transformations.<sup>25,30</sup> However, this trend did not hold true when the steric bulk was further increased to  $\alpha$ -*tert*-butyl; in this case, the cross-coupled product (**140**) was not observed when **L2** was employed. By using **L3**, a ligand with a smaller steric profile, **140** could be formed in 16% yield and 89% ee (Figure 2.7).

During the completion of our study, a related report was published by the groups of Walsh and Mao.<sup>23</sup> Their coupling employs bulky  $\alpha$ -chloroesters and aryl iodides (3.0 equiv) in a Ni/photoredox reductive coupling with Hantzsch ester as a terminal reductant. Interestingly, even though the same ligand (**L2**), developed by our lab,<sup>27</sup> was employed in

**Figure 2.7** Ligand effects on the coupling of  $\alpha$ -tert-butyl chloroester **139**.

the Walsh and Mao coupling, an analogous enantioselectivity trend was not observed; the introduction of  $\beta$ -branching did not lead to a significant increase in enantioselectivity (**144** vs. **145**) (Figure 2.8).

**Figure 2.8** Photoredox reductive cross-coupling reported by Walsh and Mao.

To look at these differences more quantitatively and to compare our chloroester coupling to previous reactions developed in the Reisman group, we calculated the

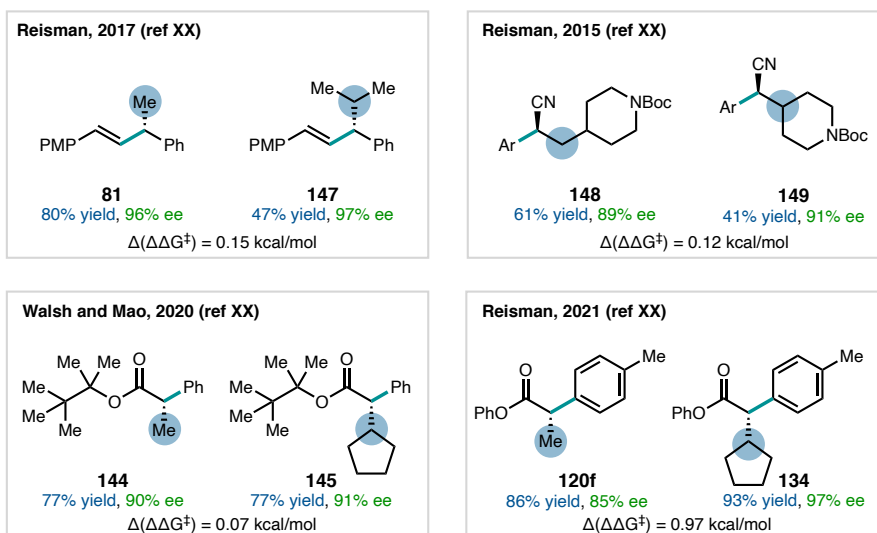
difference in transition state energies of enantiomers ( $\Delta\Delta G^\ddagger$ ) for pairs of coupling partners using Equation 2.1.

**Equation 2.1** Calculation of  $\Delta\Delta G^\ddagger$  from enantiomeric ratio at a given temperature.

$$\text{enantiomeric ratio} = e^{\frac{-\Delta\Delta G^\ddagger}{RT}}$$

In several previous enantioselective reductive cross-couplings developed in our group, the introduction of  $\beta$ -branching on the C(sp<sup>3</sup>) coupling partner results in a small increase in enantioselectivity and a moderate reduction in yield. When comparing pairs of substrates from our coupling of *N*-hydroxyphthalimide esters,<sup>30</sup> our coupling of  $\alpha$ -chloronitriles,<sup>25</sup> and the Walsh and Mao coupling of  $\alpha$ -chloroesters,<sup>23</sup> only minor increases in  $\Delta\Delta G^\ddagger$  values were observed with the introduction of  $\beta$  branching (Figure 2.9). These energetic differences, on the order of 0.1 kcal/mol, stand in stark contrast to the nearly 1.0 kcal/mol  $\Delta(\Delta\Delta G^\ddagger)$  observed for **120f** and **134**. Given that the enantioselectivity of our reductive arylation of chloroesters improves as a function of the size of the  $\alpha$ -substituent,

**Figure 2.9** Comparison of  $\Delta(\Delta\Delta G^\ddagger)$  values for several coupling pairs.



we hypothesized that a synergistic interaction between the substrate and ligand may be at play.

## 2.4 MULTIVARIATE LINEAR REGRESSION MODELLING

### 2.4.1 Introduction

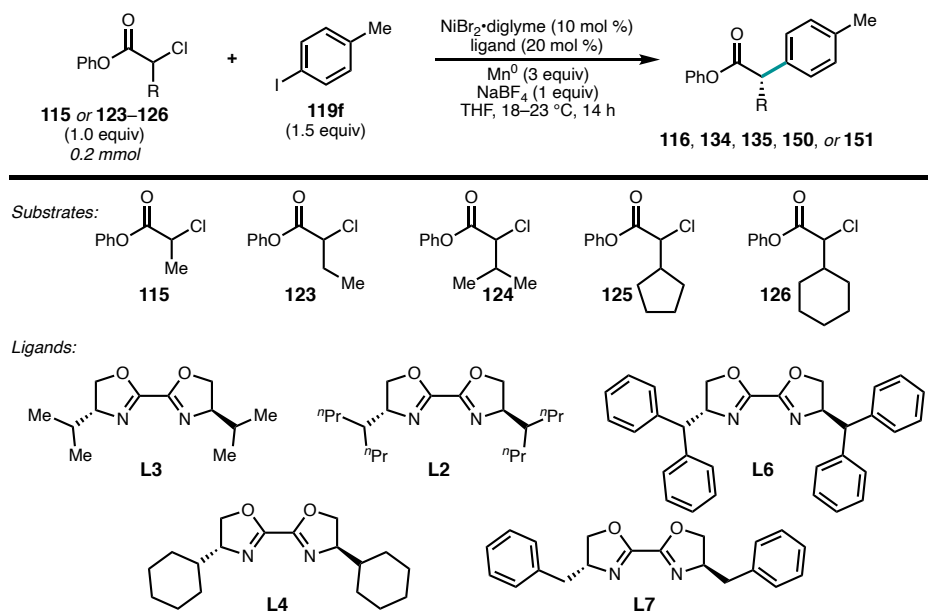
In order to quantify the hypothesized synergistic interaction between substrate and ligand in our reaction, we initiated a collaboration with Professor Matthew Sigman at the University of Utah, and a graduate student in his lab, Adam Pancoast. The Sigman group has significant experience using physical organic descriptors and multivariate linear regression (MLR) tools to probe organic reactions.<sup>32</sup> Through this collaboration, we hoped to use the following workflow to understand how ligand and substrate interact to give high enantioselectivity: 1) generate a dataset of coupling reactions, 2) identify relevant conformers of the substrates and ligands in that dataset, 3) optimize the conformers by DFT, 4) acquire steric and electronic physical organic descriptors, and 5) use multivariate linear regression to identify which of the descriptors best explain the observed trends in enantioselectivity.

### 2.4.2 Dataset Generation

Given the relatively flat enantioselectivity response upon variation of the aryl iodide, the dataset chosen for MLR studies varied the  $\alpha$ -chloroester and BiOX ligand while holding the aryl iodide constant. A five by five matrix of  $\alpha$ -chloroesters and BiOX ligands were exhaustively coupled in duplicate to generate the dataset for statistical modelling

(Figure 2.10).<sup>33</sup> Additionally, the coupling of  $\alpha$ -*tert*-butyl chloroester **139** using isopropyl BiOX (Figure 2.7) was included.

**Figure 2.10** Substrates and ligands used for MLR dataset generation.



### 2.4.3 Conformational Optimization and Parameter Acquisition

Low-energy conformers for each of the ligands and substrates were next identified. All conformational searches were performed using Macromodel with a dielectric constant of 7.58, corresponding to that of THF.<sup>33</sup> Several steps were taken to limit the number of conformers. For both ligands and  $\alpha$ -chloroesters, an energy window of 10 kJ/mol (2.4 kcal/mol) relative to the minimum energy was utilized, and mirror image conformations were not retained to avoid duplication of conformers. Ligand conformers were found using their  $\text{NiBr}_2$  complexes in order to restrict rotation around the central oxazoline–oxazoline bond. All conformers found under these conditions were submitted to DFT level



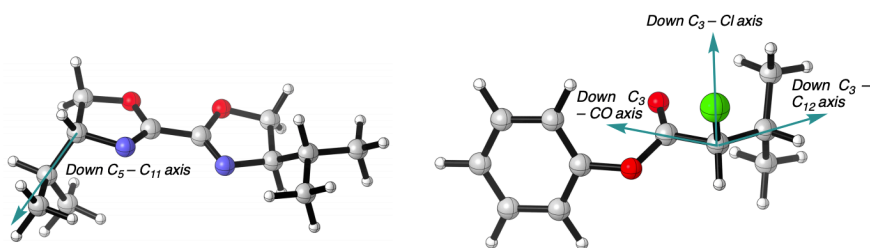
optimization; for the ligand complexes, NiBr<sub>2</sub> was removed before DFT optimization (Figure 2.11).<sup>33</sup>

**Figure 2.11** Ligand structures used for conformation search and DFT optimization.



A variety of steric and electronic parameters were collected for each DFT-optimized structure. A full listing of these parameters can be found in the Experimental Section.<sup>33</sup> For each ensemble of conformers representing a single ligand or substrate, Boltzmann weighting of conformer properties was used. Of particular interest to this study, Sterimol values were collected as parameters for substrates and ligands, with L, B<sub>1</sub>, and B<sub>5</sub> representing the length of a specified axis (bond) and the minimum and maximum widths, respectively, of a specified group along that axis. For the BiOX ligands, the C5–C11 axis (oxazoline–R group) was used. For the  $\alpha$ -chloroesters, three distinct axes were used to calculate Sterimol values (Figure 2.12).

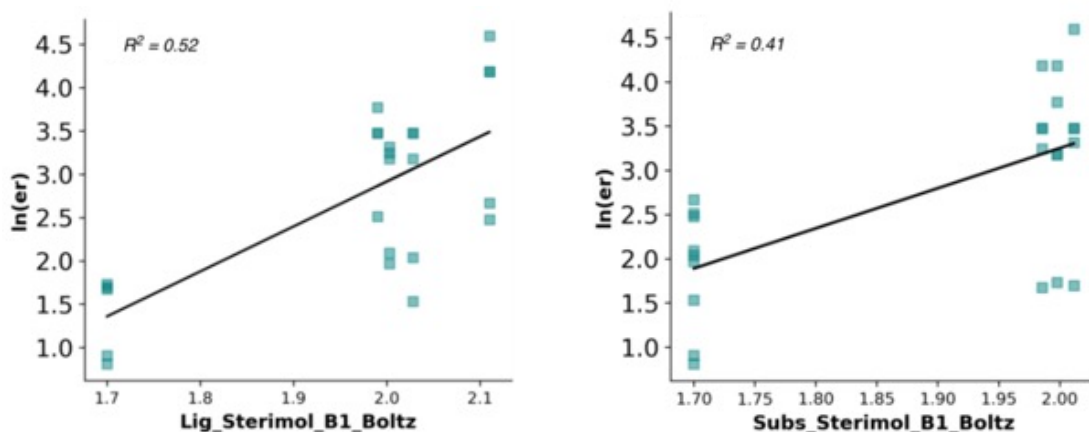
**Figure 2.12** Axes along which Sterimol values were calculated.



Somewhat surprisingly, poor correlations are observed between these Sterimol values and the observed enantioselectivities of the reactions (Figure 2.13). Although the

predictive power of single parameters seemed limited for this reaction, we were hopeful that multivariate models could still prove useful.

**Figure 2.13** Correlations between ligand ( $C_5$ – $C_{11}$ ) and substrate Sterimol  $B_1$  values and observed enantioselectivities.

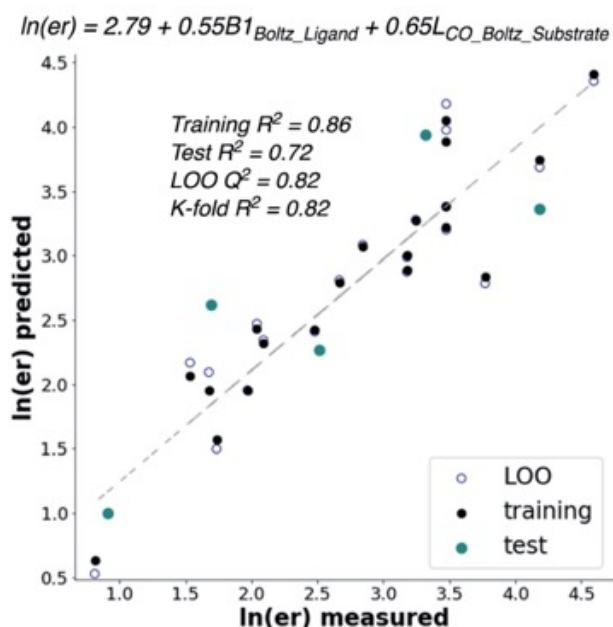


#### 2.4.4 Multivariate Correlation Analysis

Once parameters had been collected and Boltzmann weighted, multivariate correlation analysis was conducted using the experimental enantiomeric ratios determined for each substrate/ligand combination. Using methods similar to those previously reported by Sigman and coworkers, a forward stepwise linear regression algorithm produced models that were evaluated for robustness and overfitting with three distinct techniques: leave one out (LOO), K-fold, and test  $R^2$ .<sup>34</sup> Using this MLR process, two parameters stood out as most predictive when considered together: the Boltzmann-weighted minimum width of the ligand ( $B_1$ ), down the BiOX/R group axis, and the Boltzmann-weighted length ( $L$ ) down the  $C_3$ –CO axis of the  $\alpha$ -chloroester. In sharp contrast to the low predictive power of a single Sterimol parameter, models incorporating these steric parameters from *both* the

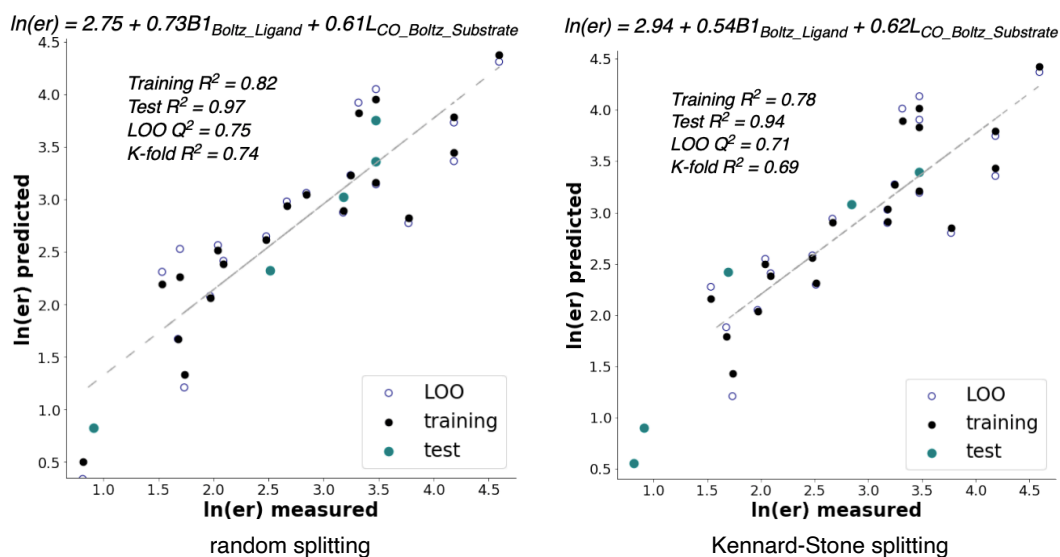
ligand and the substrate accurately described the observed enantioselectivities (Figure 2.14).

**Figure 2.14** Model for observed enantioselectivity (equidistant partition).



The robustness of these particular steric parameters (ligand  $B_1$ , substrate L) were further revealed by exploring different training/test splitting. For each model, 75% of the data points were used for building the model, and the remaining 25% were used for testing its predictive power. The 75:25 split was partitioned in several different manners: “equidistant,” “random,” or “Kennard-Stone.”<sup>33</sup> For each of the different train/test splits, the same two parameters proved most predictive of the observed enantioselectivities, with the resulting models only showing slight variation in statistics (Figure 2.15).

Taken together, these models reveal a clear correlation between the observed enantioselectivity and Boltzmann-weighted steric parameters of the ligand and substrate. The statistics of the models indicate high accuracy ( $R^2 = 0.86, 0.82, 0.78$ ), and the model

**Figure 2.15** Enantioselectivity models (random and Kennard-Stone splitting).

robustness is also high, as indicated by cross-validation (LOO,  $Q^2$ , and K-fold  $R^2$ ). The models indicate that steric matching between the catalyst and substrate is responsible for high selectivity, as evidenced by the fact that the ligand with the largest Boltzmann-weighted  $B_1$  value (**L2**) and the substrate with the largest Boltzmann-weighted L value (**126**) give the best selectivities, while those with smaller values give poorer selectivities. This simple model should be predictive if either a new substrate or ligand is considered for application of this reaction.

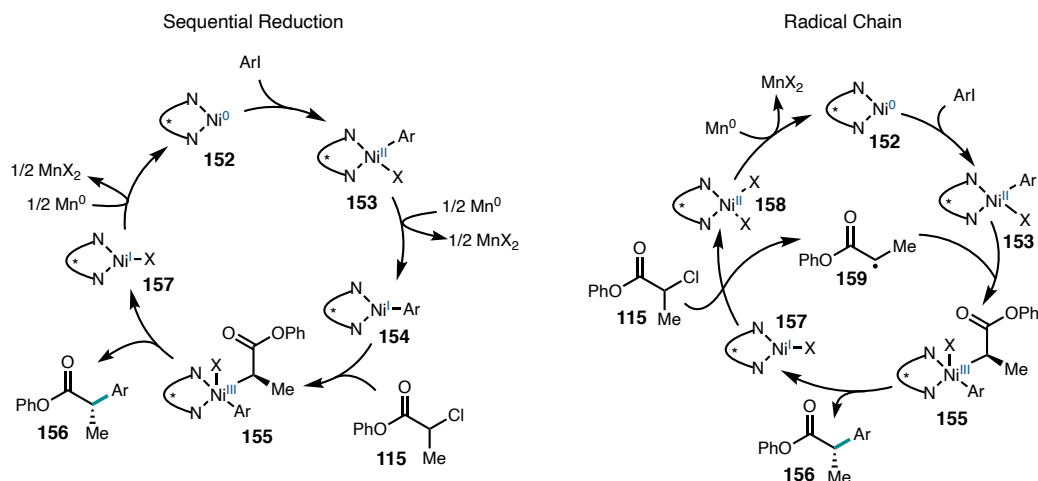
## 2.5 MECHANISTIC STUDIES

### 2.5.1 Introduction

Nickel-catalyzed reductive couplings between  $C(sp^3)$  and  $C(sp^2)$  electrophiles could proceed through several distinct mechanisms involving radical intermediates. Two

of the most commonly invoked mechanisms for these transformations are a “sequential reduction” mechanism and a “radical chain” mechanism (Figure 2.16).

**Figure 2.16** Sequential reduction and radical chain mechanisms.

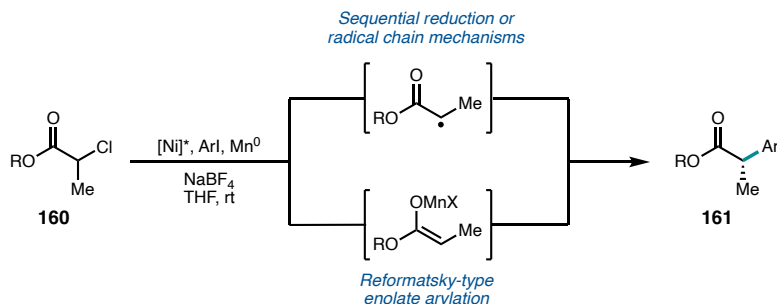


In the “sequential reduction” mechanism, a  $\text{BiOX}\cdot\text{Ni}^0$  complex (**152**), generated initially from reduction of the  $\text{Ni}^{\text{II}}$  precursor, undergoes oxidative addition of an aryl halide to give  $\text{Ni}^{\text{II}}\text{ArX}$  **153**. This  $\text{Ni}^{\text{II}}$  intermediate is then reduced by  $\text{Mn}^0$  to give  $\text{Ni}^{\text{I}}\text{Ar}$  **154**, which undergoes oxidative addition with the  $\text{C}(\text{sp}^3)$  electrophile **115** followed by reductive elimination from intermediate  $\text{Ni}^{\text{III}}$  species **155** to furnish **156**. Finally, a second reduction of **157** closes the catalytic cycle by regenerating **152**.

The “radical chain” mechanism begins in a similar manner, with reduction of **158** to **152**. After oxidative addition, rather than undergoing reduction, the  $\text{Ni}^{\text{II}}\text{ArX}$  species intercepts alkyl radical **159** to form the same  $\text{Ni}^{\text{III}}$  intermediate **155**. Following reductive elimination to form **156**,  $\text{Ni}^{\text{I}}$  **157** abstracts a chlorine atom from **115** to generate alkyl radical **159** and  $\text{Ni}^{\text{II}}$  **158**; **158** is then reduced by  $\text{Mn}^0$  to turn over the reaction. Importantly, the cage-escaped alkyl radical **159** is generated and captured at two different nickel centers.

In contrast to previous reductive cross-couplings developed in our group, the coupling of alpha-chloroesters may also proceed by a distinct mechanistic pathway involving a Reformatsky-type arylation of an in situ-generated manganese enolate (Figure 2.17).

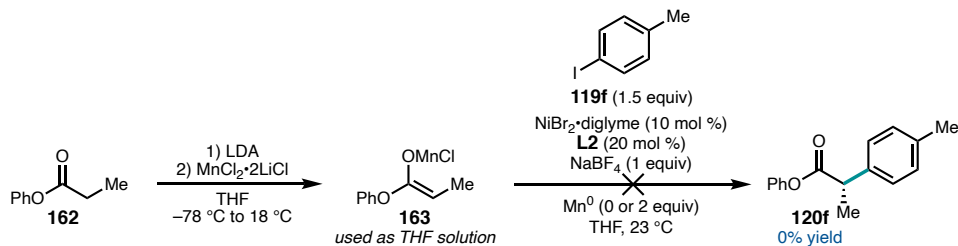
**Figure 2.17** Sequential reduction and radical chain mechanisms.



## 2.5.2 Manganese Enolate Studies

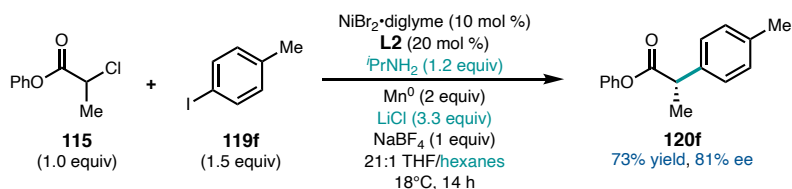
In order to probe the possibility of a manganese enolate intermediate in this reaction, we generated a solution of  $\text{MnCl}$  enolate **163** from **162** (Figure 2.18). Reaction of this manganese enolate with  $\text{MeI}$  gave a 45% yield of the methylated product, indicating that **163** was a competent nucleophile.<sup>33</sup> When a solution of **163** in THF was subjected to the remaining reaction components (with or without  $\text{Mn}^0$ ), no formation of the coupled product **120f** was observed.

**Figure 2.18** Generation and reaction of manganese enolate.



Because manganese enolate **163** was formed through deprotonation with lithium diisopropylamide followed by transmetalation with  $\text{MnCl}_2 \cdot 2\text{LiCl}$ , we wondered if residual reagents from this process could be shutting down reactivity in the coupling reaction. To probe this hypothesis, we conducted the reductive cross-coupling reaction with  $i\text{Pr}_2\text{NH}$ ,  $\text{LiCl}$ , and hexanes added to the otherwise standard conditions to mimic the residues of Mn enolate formation (Figure 2.19). Even with the inclusion of these reagents, **120f** was obtained in comparable yield and ee to the standard reaction conditions. Additionally, no consumption of **115** was observed in the absence of  $\text{NiBr}_2 \cdot \text{diglyme}$  and **L2**. Taken together, these experiments suggest that a manganese enolate is likely not an operative intermediate in this reaction.

**Figure 2.19** Reductive cross-coupling with added Mn enolate byproducts.

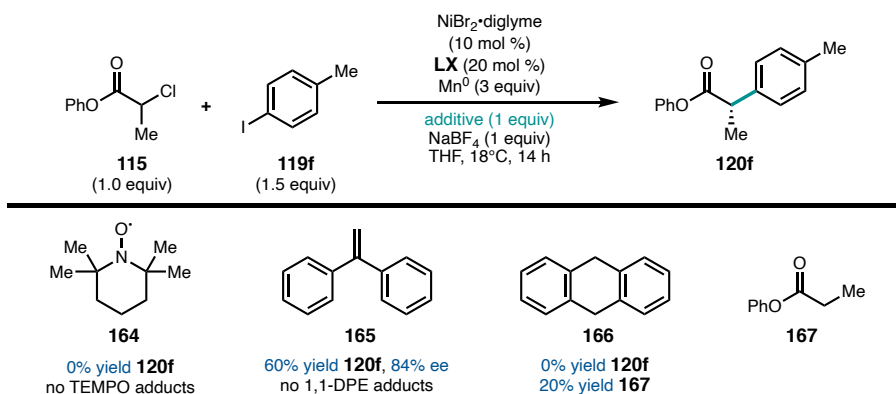


### 2.5.3 Radical Trapping Experiments

We next sought to probe our hypothesis that an  $\alpha$ -ester radical intermediate is present in the reaction by adding a series of radical trapping reagents (Figure 2.20). When TEMPO was added to the reaction, no productive reactivity was observed. The addition of 1,1-diphenylethylene (1,1-DPE, **165**) did not significantly disrupt productive reactivity, giving **120f** in 60% yield and 84% ee. No adducts of **164** or **165** were observed in the crude reaction mixtures. Although TEMPO and 1,1-DPE did not reveal the presence of a radical intermediate, when 9,10-dihydroanthracene was added to the reaction, no **120f** was formed,

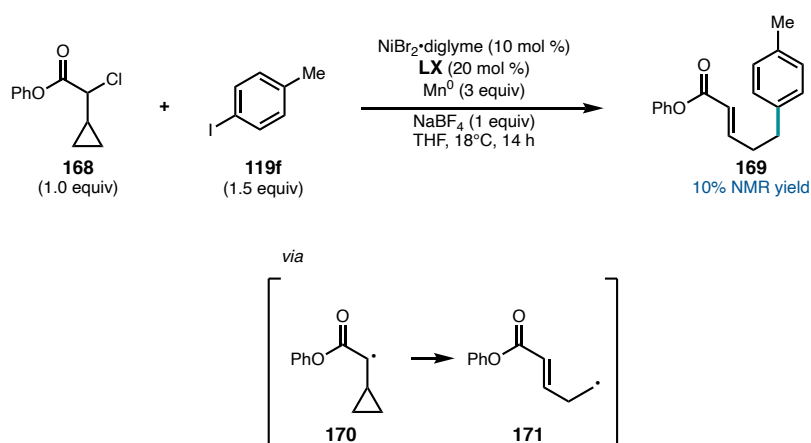
and the protodechlorinated ester **167** was observed in 20% yield, likely formed via the intermediacy of an  $\alpha$ -ester radical.

**Figure 2.20** Radical trapping experiments.



To further probe the presence of a radical intermediate in this cross-coupling reaction,  $\alpha$ -cyclopropyl ester **168** was synthesized and subjected to the standard reaction conditions. No direct cross-coupling was identified, but  $\alpha,\beta$ -unsaturated ester **169** was observed in 10% NMR yield, presumably forming via ring opening of the intermediate radical **170** (Figure 2.21).

**Figure 2.21** Cyclopropyl radical clock.

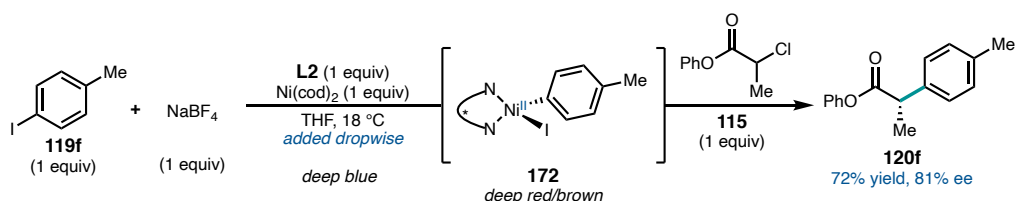




### 2.5.4 Stoichiometric Studies

Having identified  $\alpha$ -ester radical **159** (Figure 2.16) as a likely intermediate in this reaction, we considered that studies employing stoichiometric nickel could help differentiate between “radical chain” and “sequential reduction” mechanisms (Figure 2.22). When a solution of 1 equiv **L2** precomplexed with Ni(cod)<sub>2</sub> was added dropwise to a solution of **119f** and NaBF<sub>4</sub>, a deep red/brown solution formed, which we putatively assigned as the oxidative addition complex **172**. When this complex was treated with **115**, the cross-coupled product **120f** was obtained in comparable yield and ee to the catalytic reaction using Mn<sup>0</sup> as reductant. This result has two key mechanistic implications. First, it shows that reduction of **172** is not required for product formation. Similar studies have been used by Weix and coworkers to support a radical chain mechanism over a sequential reduction mechanism.<sup>35</sup> Second, the high yield obtained in the absence in any manganese source further suggest that a manganese enolate is not an operative intermediate in this reaction.

**Figure 2.22** Stoichiometric reaction.



## 2.6 CONCLUDING REMARKS

In conclusion, we have developed a nickel-catalyzed asymmetric reductive cross-coupling of  $\alpha$ -chloroesters and aryl iodides. The reaction, enabled by a chiral BiOX ligand, proceeds in good yields and enantioselectivities under mild conditions. The reaction proved

especially selective when  $\beta$ -branched substrates were employed, a trend not observed in the prior art.<sup>23</sup> Multivariate linear regression modelling was used to demonstrate the cooperative influence of the substrate and the ligand steric profiles on the enantioselectivity of the reaction. This model could prove useful in predicting the outcome when new ligands or substrates. Preliminary mechanistic studies implicate a radical intermediate and disfavor the intermediacy of a manganese enolate. The products of the reaction, enantioenriched  $\alpha,\alpha$ -disubstituted esters, are useful chiral building blocks and hold promise as intermediates in the synthesis of bioactive compounds, as demonstrated by the synthesis of the NSAID (*S*)-naproxen.

## 2.7 EXPERIMENTAL SECTION

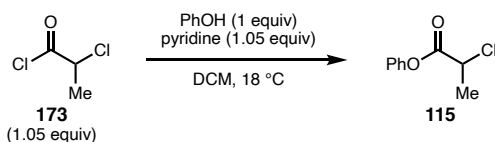
### 2.7.1 Materials and Methods

Unless otherwise stated, reactions were performed under a N<sub>2</sub> atmosphere using freshly dried solvents. Tetrahydrofuran (THF), diethyl ether (Et<sub>2</sub>O), methylene chloride (CH<sub>2</sub>Cl<sub>2</sub>), toluene (PhMe), hexanes, and benzene (C<sub>6</sub>H<sub>6</sub>) were dried by passing through activated alumina columns under a positive pressure of argon. Triethylamine (Et<sub>3</sub>N) and diisopropylamine (*i*Pr<sub>2</sub>NH) were distilled over calcium hydride prior to use. Anhydrous *N,N*-dimethylacetamide (DMA) was purchased from Aldrich and stored under N<sub>2</sub>. **L2** was synthesized using the procedure reported by Reisman and coworkers.<sup>27</sup> Unless otherwise stated, chemicals and reagents were used as received. All reactions were monitored by thin-layer chromatography using EMD/Merck silica gel 60 F254 pre-coated plates (0.25 mm) and were visualized by UV, CAM, *p*-anisaldehyde, or KMnO<sub>4</sub> staining. Flash column

chromatography was performed as described by Still et al. using silica gel (230-400 mesh, Silicycle).<sup>36</sup> Purified compounds were dried on a high vacuum line (0.2 torr) to remove trace solvent. Optical rotations were measured on a Jasco P-2000 polarimeter using a 100 mm path-length cell at 589 nm.  $^1\text{H}$  and  $^{13}\text{C}$  NMR spectra were recorded on a Bruker Avance III HD with Prodigy cyroprobe (at 400 MHz and 101 MHz, respectively), a Varian 400 MR (at 400 MHz and 101 MHz, respectively), or a Varian Inova 500 (at 500 MHz and 126 MHz, respectively).  $^1\text{H}$  NMR spectra were also recorded on a Varian Inova 300 (at 300 MHz). NMR data is reported relative to internal  $\text{CHCl}_3$  ( $^1\text{H}$ ,  $\delta = 7.26$ ) and  $\text{CDCl}_3$  ( $^{13}\text{C}$ ,  $\delta = 77.0$ ) Data for  $^1\text{H}$  NMR spectra are reported as follows: chemical shift ( $\delta$  ppm) (multiplicity, coupling constant (Hz), integration). Multiplicity and qualifier abbreviations are as follows: s = singlet, d = doublet, t = triplet, q = quartet, m = multiplet, br = broad. IR spectra were recorded on a Perkin Elmer Paragon 1000 spectrometer and are reported in frequency of absorption ( $\text{cm}^{-1}$ ). Analytical chiral SFC was performed with a Mettler SFC supercritical  $\text{CO}_2$  analytical chromatography system ( $\text{CO}_2 = 1450$  psi, column temperature =  $40$  °C) with Chiralcel AD-H, OD-H, AS-H, OB-H, and OJ-H columns (4.6 mm x 25 cm). HRMS were acquired from the Caltech Mass Spectral Facility using fast-atom bombardment (FAB), electrospray ionization (ESI-TOF), or electron impact (EI).

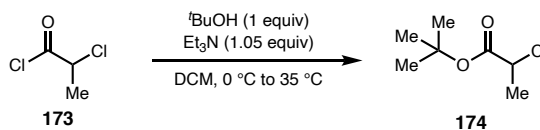
### 2.7.2 Substrate Preparation

#### phenyl 2-chloropropanoate (115)



To a 250-mL oven-dried round-bottomed flask equipped with a Teflon-coated stir bar were added phenol (1.88 g, 1 equiv, 20.0 mmol) and DCM (67 mL). The reaction was cooled to 0 °C under nitrogen, then 2-chloropropionyl chloride (**173**, 2.67 g, 1.05 equiv, 21.0 mmol) was added via syringe in a single portion. The reaction was allowed to slowly warm to 18 °C while stirring for 20 hours. The reaction solution was then transferred to a separatory funnel and diluted with water and DCM. The layers were separated, then the organic layer was washed thrice with water, dried with Na<sub>2</sub>SO<sub>4</sub>, filtered, and concentrated under reduced pressure. The crude material was purified by flash column chromatography over silica gel, eluting with 7% Et<sub>2</sub>O/hexanes to afford **115** as a colorless oil (3.69 g, 97% yield). Spectral data matched those reported in the literature.<sup>37</sup>

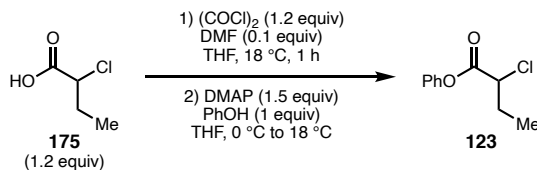
#### *tert*-butyl 2-chloropropanoate (**174**)



To a 25-mL oven-dried round-bottomed flask equipped with a Teflon-coated stir bar were added DCM (10 mL), 2-chloropropionyl chloride (**173**, 1.27 g, 1 equiv, 10.0 mmol), and *tert*-butanol (741 mg, 1.0 equiv, 10.0 mmol). The reaction was cooled to 0 °C, then triethylamine (1.01 g, 1 equiv, 10.0 mmol) was added dropwise to the reaction over 2 minutes. The reaction was warmed to 35 °C. After 24 hours of stirring, the reaction was cooled to room temperature, transferred to a separatory funnel, and diluted with water and DCM. The layers were separated, and the aqueous layer was extracted twice with DCM. Combined organics were dried with MgSO<sub>4</sub>, filtered, and concentrated. The crude material

was purified using a silica plug, eluting with 20% Et<sub>2</sub>O/pentane to afford **174** as a colorless oil (905 mg, 55% yield). Spectral data matched those reported in the literature.<sup>38</sup>

**phenyl 2-chlorobutanoate (123)**



To a 25-mL oven-dried round-bottomed flask equipped with a Teflon-coated stir bar were added THF (6.4 mL), DMF (60.9 mg, 0.1 equiv, 0.83 mmol), and 2-chlorobutyric acid (**175**, 1.23 g, 1.2 equiv, 10.0 mmol), under nitrogen. Oxalyl chloride (1.27 g, 1.2 equiv, 10.0 mmol) was added dropwise via syringe to the reaction, over the course of five minutes. The reaction was allowed to stir for 1 hour at 18 °C to form the acyl chloride. To a 50-mL oven-dried round-bottomed flask equipped with a Teflon-coated stir bar were added phenol (784 mg, 1 equiv, 8.33 mmol), 4-(dimethylamino)pyridine (1.53 g, 1.5 equiv, 12.5 mmol), and THF (6.4 mL), under nitrogen. This solution was cooled to 0 °C, then the acyl chloride solution was added dropwise over 2 minutes, resulting in a slurry that was slowly warmed to 18 °C. After 20 hours of stirring, the reaction was transferred to a separatory funnel and diluted with water and Et<sub>2</sub>O. The layers were separated, then the organic layer was washed sequentially with 1 M aqueous HCl, saturated aqueous NaHCO<sub>3</sub>, and brine. The organic layer was dried with Na<sub>2</sub>SO<sub>4</sub>, filtered, and concentrated. The crude material was purified by flash column chromatography over silica gel, eluting with 6% Et<sub>2</sub>O/hexanes to afford **123** as a colorless oil (1.01 g, 61% yield).

$R_f$  = 0.50 (silica, 8% Et<sub>2</sub>O/hexanes, UV)

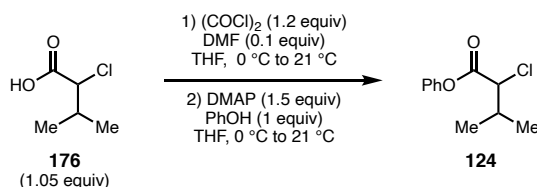
$^1\text{H}$  NMR (400 MHz,  $\text{CDCl}_3$ ):  $\delta$  7.45 – 7.36 (m, 2H), 7.30 – 7.23 (m, 1H), 7.16 – 7.10 (m, 2H), 4.46 (dd,  $J = 7.6, 6.0$  Hz, 1H), 2.29 – 2.04 (m, 2H), 1.15 (t,  $J = 7.4$  Hz, 3H).

$^{13}\text{C}$  NMR (101 MHz,  $\text{CDCl}_3$ ):  $\delta$  168.3, 150.5, 129.7, 126.4, 121.3, 58.8, 28.5, 10.7

FTIR (NaCl, thin film,  $\text{cm}^{-1}$ ): 3522, 3066, 2974, 2880, 1942, 1766, 1592, 1486, 1191

HRMS (FAB,  $m/z$ ): calc'd for  $\text{C}_{10}\text{H}_{12}\text{ClO}_2$   $[\text{M}+\text{H}]^+$ : 199.0526; found: 199.0508.

### phenyl 2-chloro-3-methylbutanoate (**124**)



To a flame-dried 100 mL round bottom flask equipped with a Teflon-coated stir bar were added 2-chloro-3-methylbutyric acid (**176**, 3.52 g, 1.00 equiv, 23.2 mmol) (synthesized according to reported procedure from *rac*-valine<sup>39</sup>) and THF (15.5 mL). The reaction mixture was cooled to  $0^\circ\text{C}$  in an ice bath. Once cool, oxalyl chloride (4.2 g, 1.4 equiv, 33.1 mmol) dropwise followed by DMF (0.18 mL, 0.1 equiv, 2.32 mmol). The reaction was allowed to stir at room temperature for 1 h. Once complete, the reaction was concentrated; the acid chloride was taken forward without further purification. To a flame-dried 200 mL round bottom flask were added phenol (2.1 g, 1.0 equiv, 22.1 mmol), 4-(dimethylamino)pyridine (4.1 g, 1.5 equiv, 33.1 mmol), and THF (20 mL). The reaction mixture was cooled to  $0^\circ\text{C}$  in an ice bath. Once cool, the acid chloride was added as a solution in 20 mL THF dropwise. Once the addition was complete, the ice bath was removed and the reaction was allowed to stir at  $21^\circ\text{C}$  overnight. After 22 h, the reaction

was stopped. The reaction was diluted with 40 mL *tert*-butyl methyl ether and washed with 40 mL 1.0 M aq HCl, 40 mL 5% aq NaHCO<sub>3</sub>, and 40 mL brine. The organic layer was dried over sodium sulfate, filtered, and concentrated. The crude material was purified by flash column chromatography over silica gel, eluting with a gradient of 20 to 50% toluene/hexanes to afford **124** as a colorless oil (891 mg g, 19% yield).

$R_f$  = 0.25 (silica, 30% toluene/hexanes, UV)

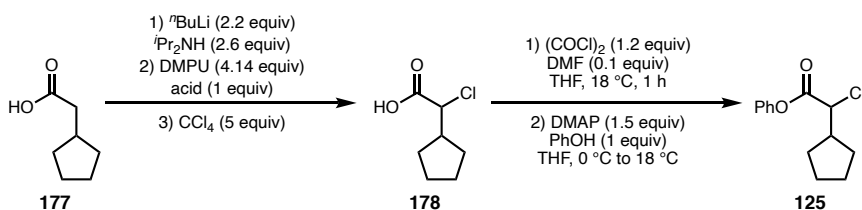
<sup>1</sup>H NMR (400 MHz, CDCl<sub>3</sub>):  $\delta$  7.39 – 7.27 (m, 2H), 7.23 – 7.14 (m, 1H), 7.08 – 7.00 (m, 2H), 4.26 (d,  $J$  = 6.7 Hz, 1H), 2.39 (dp,  $J$  = 13.3, 6.7 Hz, 1H), 1.09 (d,  $J$  = 6.7 Hz, 7H).

<sup>13</sup>C NMR (101 MHz, CDCl<sub>3</sub>):  $\delta$  168.1, 150.5, 129.7, 126.4, 121.3, 64.1, 33.0, 19.8, 18.4.

FTIR (NaCl, thin film, cm<sup>-1</sup>): 3064, 2967, 2936, 2876, 1770, 1593, 1494, 1297, 1232, 1194, 1138, 1079, 927, 726, 688.

HRMS (FAB,  $m/z$ ): calc'd for C<sub>11</sub>H<sub>13</sub>ClO<sub>2</sub> [M+H]<sup>+</sup>: 213.0682; found: 213.0692.

### phenyl 2-chloro-2-cyclopentylacetate (**125**)



To a 200-mL oven-dried round-bottomed flask equipped with a Teflon-coated stir bar were added diisopropylamine (2.63 g, 2.6 equiv, 26.0 mmol) and THF (20 mL). The reaction was cooled to -20 °C in a dry ice/acetone bath, then *n*-butyllithium (2.5 M in hexane, 8.80 mL, 2.2 equiv, 22.0 mmol) was added to the solution dropwise via syringe over 5 minutes. The reaction was stirred at -20 °C for 30 minutes. DMPU (5.31 g, 4.14

equiv, 41.4 mmol) was added to the reaction, followed by 2-cyclopentylacetic acid (**177**, 1.28 g, 1.0 equiv, 10.0 mmol). The resulting yellow solution was stirred at  $-20\text{ }^{\circ}\text{C}$  for 2 hours, then cooled to  $-78\text{ }^{\circ}\text{C}$ . Carbon tetrachloride (7.69 g, 5.0 equiv, 50.0 mmol) was dissolved in THF (20 mL) and the resulting solution was added to the reaction in a single portion via syringe, resulting in an immediate color change to black. The reaction was stirred for 1 hour at  $-78\text{ }^{\circ}\text{C}$ , then warmed to  $18\text{ }^{\circ}\text{C}$ .

A solution of sodium chloride (4.00 g, 6.84 equiv, 68.4 mmol) in HCl (2 M in water, 26.0 mL, 5.2 equiv, 52.0 mmol) was added to the reaction dropwise over 5 minutes via syringe. The reaction was transferred to a separatory funnel and diluted with water and Et<sub>2</sub>O. The layers were separated, and the aqueous layer extracted thrice with Et<sub>2</sub>O. The combined organics were dried with Na<sub>2</sub>SO<sub>4</sub>, filtered, and concentrated. The crude material was purified by flash column chromatography over silica gel, eluting with 50:50:0.1 hexanes/EtOAc/TFA. All fractions staining with bromocresol green were collected and concentrated, resulting in a brown oil. This oil was added to a separatory funnel and diluted with EtOAc and half-saturated aqueous Na<sub>2</sub>CO<sub>3</sub>. The layers were separated, then the aqueous layer was washed twice with EtOAc. The aqueous layer was acidified to pH=2 with 2 M HCl, then extracted thrice with EtOAc. These final three organic extractions were combined, dried with Na<sub>2</sub>SO<sub>4</sub>, filtered, and concentrated to afford 1.51 pale yellow oil, which was not fully pure by TLC or NMR, but was carried forward as-is without further purification (the impurities proved much easier to remove after esterification).

To a 10-mL oven-dried round-bottomed flask equipped with a Teflon-coated stir bar were added THF (2.0 mL), DMF (18.3 mg, 0.1 equiv, 0.25 mmol), and the impure 2-chloro-2-cyclopentylacetic acid (**178**, 488 mg, 3.00 mmol if pure), under nitrogen. Oxalyl



chloride (381 mg, 1.2 equiv, 3.00 mmol) was added dropwise via syringe to the reaction, over the course of five minutes. The reaction was allowed to stir for 1 hour at 18 °C to form the acyl chloride. To a 25-mL oven-dried round-bottomed flask equipped with a Teflon-coated stir bar were added phenol (235 mg, 1 equiv, 2.5 mmol), 4-(dimethylamino)pyridine (458 mg, 1.5 equiv, 3.75 mmol), and THF (2.0 mL), under nitrogen. This solution was cooled to 0 °C, then the acyl chloride solution was added dropwise over 2 minutes, resulting in a slurry that was slowly warmed to 18 °C. After 20 hours of stirring, the reaction was transferred to a separatory funnel and diluted with water and Et<sub>2</sub>O. The layers were separated, then the organic layer was washed sequentially with 1 M aqueous HCl, saturated aqueous NaHCO<sub>3</sub>, and brine. The organic layer was dried with Na<sub>2</sub>SO<sub>4</sub>, filtered, and concentrated. The crude material was purified by flash column chromatography over silica gel, eluting with 2.2% Et<sub>2</sub>O/hexanes to afford **125** as a colorless oil (106 mg, 18% yield).

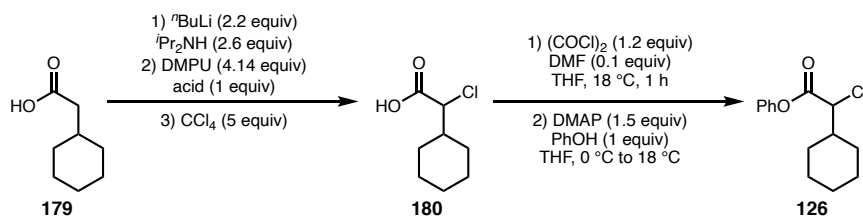
$R_f$  = 0.48 (silica, 8% Et<sub>2</sub>O/hexanes, UV)

**<sup>1</sup>H NMR (400 MHz, CDCl<sub>3</sub>):**  $\delta$  7.44 – 7.36 (m, 2H), 7.30 – 7.23 (m, 1H), 7.15 – 7.09 (m, 2H), 4.35 (d,  $J$  = 8.6 Hz, 1H), 2.72 – 2.58 (m, 1H), 2.08 – 1.83 (m, 2H), 1.82 – 1.40 (m, 6H).

**<sup>13</sup>C NMR (101 MHz, CDCl<sub>3</sub>):**  $\delta$  168.3, 150.5, 129.7, 126.4, 121.3, 61.8, 44.0, 30.1, 30.0, 26.0, 25.4.

**FTIR (NaCl, thin film, cm<sup>-1</sup>):** 3044, 2958, 2870, 1769, 1593, 1493, 1162, 1132

**HRMS (FAB,  $m/z$ ):** calc'd for C<sub>13</sub>H<sub>16</sub>ClO [M+H]<sup>+</sup>: 239.0839 ; found: 239.0832.

**phenyl 2-chloro-2-cyclohexylacetate (126)**

To a 200-mL oven-dried round-bottomed flask equipped with a Teflon-coated stir bar were added diisopropylamine (2.63 g, 2.6 equiv, 26.0 mmol) and THF (20 mL). The reaction was cooled to  $-20$  °C in a dry ice/acetone bath, then  $n$ -butyllithium (2.5 M in hexane, 8.80 mL, 2.2 equiv, 22.0 mmol) was added to the solution dropwise via syringe over 5 minutes. The reaction was stirred at  $-20$  °C for 30 minutes. DMPU (5.31 g, 4.14 equiv, 41.4 mmol) was added to the reaction, followed by 2-cyclohexylacetic acid (**179**, 1.42 g, 1.0 equiv, 10.0 mmol). The resulting yellow solution was stirred at  $-20$  °C for 2 hours, then cooled to  $-78$  °C. Carbon tetrachloride (7.69 g, 5.0 equiv, 50.0 mmol) was dissolved in THF (20 mL) and the resulting solution was added to the reaction in a single portion via syringe, resulting in an immediate color change to black. The reaction was stirred for 1 hour at  $-78$  °C, then warmed to room temperature.

A solution of sodium chloride (4.00 g, 6.84 equiv, 68.4 mmol) in HCl (2 M in water, 26.0 mL, 5.2 equiv, 52.0 mmol) was added to the reaction dropwise over 5 minutes via syringe. The reaction was transferred to a separatory funnel and diluted with water and Et<sub>2</sub>O. The layers were separated, and the aqueous layer extracted thrice with Et<sub>2</sub>O. The combined organics were dried with Na<sub>2</sub>SO<sub>4</sub>, filtered, and concentrated. The crude material was purified by flash column chromatography over silica gel, eluting with 50:50:0.1 hexanes/EtOAc/TFA. All fractions staining with bromocresol green were collected and

concentrated, resulting in a brown oil. This oil was added to a separatory funnel and diluted with EtOAc and half-saturated aqueous  $\text{Na}_2\text{CO}_3$ . The layers were separated; then the aqueous layer was washed twice with EtOAc. The aqueous layer was acidified to pH=2 with 2 M HCl, then extracted thrice with EtOAc. These final three organic extractions were combined, dried with  $\text{Na}_2\text{SO}_4$ , filtered, and concentrated to afford 1.42 g pale yellow amorphous solid, which was not fully pure by TLC or NMR, but was carried forward as-is without further purification (the impurities proved much easier to remove after esterification).

To a 10-mL oven-dried round-bottomed flask equipped with a Teflon-coated stir bar were added THF (3.2 mL), DMF (30.5 mg, 0.1 equiv, 0.42 mmol), and the impure 2-chloro-2-cyclohexylacetic acid (**180**, 883 mg, 5.00 mmol if pure), under nitrogen. Oxalyl chloride (635 mg, 1.2 equiv, 5.00 mmol) was added dropwise via syringe to the reaction, over the course of five minutes. The reaction was allowed to stir for 1 hour at 18 °C to form the acyl chloride. To a 25-mL oven-dried round-bottomed flask equipped with a Teflon-coated stir bar were added phenol (392 mg, 1 equiv, 4.17 mmol), 4-(dimethylamino)pyridine (764 mg, 1.5 equiv, 6.25 mmol), and THF (3.2 mL), under nitrogen. This solution was cooled to 0 °C, then the acyl chloride solution was added dropwise over 2 minutes, resulting in a slurry that was slowly warmed to 18 °C. After 20 hours of stirring, the reaction was transferred to a separatory funnel and diluted with water and  $\text{Et}_2\text{O}$ . The layers were separated, then the organic layer was washed sequentially with 1 M aqueous HCl, saturated aqueous  $\text{NaHCO}_3$ , and brine. The organic layer was dried with  $\text{Na}_2\text{SO}_4$ , filtered, and concentrated. The crude material was purified by flash column

chromatography over silica gel, eluting with 6% Et<sub>2</sub>O/hexanes to afford **126** as a colorless oil (488 mg, 46% yield).

$R_f$  = 0.52 (silica, 8% Et<sub>2</sub>O/hexanes, UV)

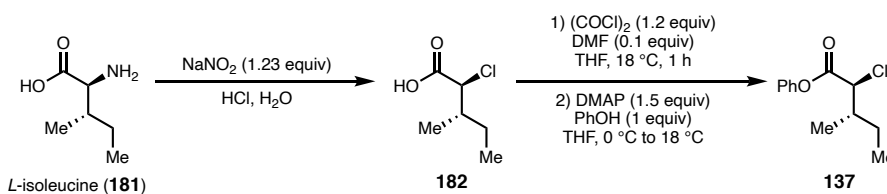
<sup>1</sup>H NMR (400 MHz, CDCl<sub>3</sub>):  $\delta$  7.44 – 7.37 (m, 2H), 7.30 – 7.23 (m, 1H), 7.15 – 7.09 (m, 2H), 4.29 (d,  $J$  = 7.4 Hz, 1H), 2.16 – 2.01 (m, 2H), 1.89 – 1.66 (m, 4H), 1.40 – 1.13 (m, 5H).

<sup>13</sup>C NMR (101 MHz, CDCl<sub>3</sub>):  $\delta$  168.1, 150.5, 129.7, 126.4, 121.4, 63.0, 42.0, 30.1, 28.9, 26.0, 25.9, 25.7.

FTIR (NaCl, thin film, cm<sup>-1</sup>): 2930, 2854, 1769, 1492, 1450, 1233, 1193, 1163, 1143

HRMS (FAB,  $m/z$ ): calc'd for C<sub>14</sub>H<sub>18</sub>ClO [M+H]<sup>+</sup>: 253.0995 ; found: 253.0988.

### phenyl (2*S*,3*S*)-2-chloro-3-methylpentanoate (**137**)



*L*-isoleucine (**181**) was converted to the corresponding  $\alpha$ -chloroacid **182** in 12:1 dr using the procedure reported by Bercaw and coworkers. Spectral data matched those reported.<sup>40</sup>

To a 25-mL oven-dried round-bottomed flask equipped with a Teflon-coated stir bar were added THF (4.3 mL), DMF (40.4 mg, 0.1 equiv, 0.55 mmol), and (2*S*,3*S*)-2-chloro-3-methylpentanoic acid (**182**, 1.00 g, 1.2 equiv, 6.64 mmol), under nitrogen. Oxalyl chloride (843 mg, 1.2 equiv, 6.64 mmol) was added dropwise via syringe to the reaction,

over the course of five minutes. The reaction was allowed to stir for 1 hour at 18 °C to form the acyl chloride. To a 50-mL oven-dried round-bottomed flask equipped with a Teflon-coated stir bar were added phenol (521 mg, 1 equiv, 5.53 mmol), 4-(dimethylamino)pyridine (1.01 g, 1.5 equiv, 8.30 mmol), and THF (4.3 mL), under nitrogen. This solution was cooled to 0 °C, then the acyl chloride solution was added dropwise over 2 minutes, resulting in a slurry that was slowly warmed to 18 °C. After 20 hours of stirring, the reaction was transferred to a separatory funnel and diluted with water and Et<sub>2</sub>O. The layers were separated, then the organic layer was washed sequentially with 1 M aqueous HCl, saturated aqueous NaHCO<sub>3</sub>, and brine. The organic layer was dried with Na<sub>2</sub>SO<sub>4</sub>, filtered, and concentrated. The crude material was purified by flash column chromatography over silica gel, eluting with 4% Et<sub>2</sub>O/hexanes to afford **137** as a colorless oil (679 mg, 54% yield, >20:1 dr).

$R_f$  = 0.54 (silica, 8% EtOAc/hexanes, UV)

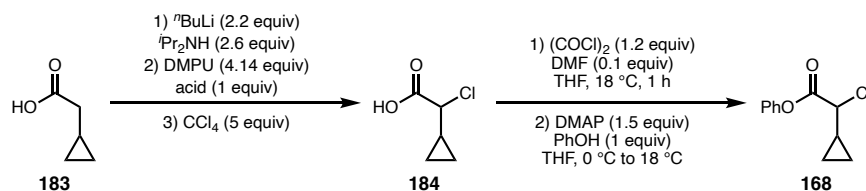
$[\alpha]_D^{21} = 2^\circ$  (c = 1.0, CHCl<sub>3</sub>).

**<sup>1</sup>H NMR (400 MHz, CDCl<sub>3</sub>):**  $\delta$  7.49 – 7.35 (m, 2H), 7.31 – 7.21 (m, 1H), 7.17 – 7.08 (m, 2H), 4.38 (d,  $J$  = 7.1 Hz, 1H), 2.32 – 2.14 (m, 1H), 1.84 – 1.70 (m, 1H), 1.50 – 1.35 (m, 1H), 1.14 (d,  $J$  = 6.8 Hz, 3H), 0.99 (t,  $J$  = 7.5 Hz, 3H).

**<sup>13</sup>C NMR (101 MHz, CDCl<sub>3</sub>):**  $\delta$  168.1, 150.6, 129.7, 126.4, 121.3, 62.8, 39.2, 25.3, 16.1, 11.0.

**FTIR (NaCl, thin film, cm<sup>-1</sup>):** 2926, 2852, 1755, 1492, 1196, 1140, 1107

**HRMS (FAB,  $m/z$ ):** calc'd for C<sub>21</sub>H<sub>25</sub>O<sub>2</sub> [M+H]<sup>+</sup>: 227.0839 ; found: 227.0848.

**phenyl 2-chloro-2-cyclopropylacetate (168)**

To a 200-mL oven-dried round-bottomed flask equipped with a Teflon-coated stir bar were added diisopropylamine (2.63 g, 2.6 equiv, 26.0 mmol) and THF (20 mL). The reaction was cooled to  $-20$  °C in a dry ice/acetone bath, then *n*-butyllithium (2.5 M in hexane, 8.80 mL, 2.2 equiv, 22.0 mmol) was added to the solution dropwise via syringe over 5 minutes. The reaction was stirred at  $-20$  °C for 30 minutes. DMPU (5.31 g, 4.14 equiv, 41.4 mmol) was added to the reaction, followed by 2-cyclopropylacetic acid (**183**, 1.00 g, 1.0 equiv, 10.0 mmol). The resulting yellow solution was stirred at  $-20$  °C for 2 hours, then cooled to  $-78$  °C. Carbon tetrachloride (7.69 g, 5.0 equiv, 50.0 mmol) was dissolved in THF (20 mL) and the resulting solution was added to the reaction in a single portion via syringe, resulting in an immediate color change to black. The reaction was stirred for 1 hour at  $-78$  °C, then warmed to room temperature.

A solution of sodium chloride (4.00 g, 6.84 equiv, 68.4 mmol) in HCl (2 M in water, 26.0 mL, 5.2 equiv, 52.0 mmol) was added to the reaction dropwise over 5 minutes via syringe. The reaction was transferred to a separatory funnel and diluted with water and Et<sub>2</sub>O. The layers were separated, and the aqueous layer extracted thrice with Et<sub>2</sub>O. The combined organics were dried with Na<sub>2</sub>SO<sub>4</sub>, filtered, and concentrated. The crude material was purified by flash column chromatography over silica gel, eluting with 50:50:0.1 hexanes/EtOAc/TFA. All fractions staining with bromocresol green were collected and

concentrated, resulting in a brown oil. This oil was added to a separatory funnel and diluted with EtOAc and half-saturated aqueous  $\text{Na}_2\text{CO}_3$ . The layers were separated; then the aqueous layer was washed twice with EtOAc. The aqueous layer was acidified to pH=2 with 2 M HCl, then extracted thrice with EtOAc. These final three organic extractions were combined, dried with  $\text{Na}_2\text{SO}_4$ , filtered, and concentrated to afford 1.97 g pale yellow oil, which was not fully pure by TLC or NMR (56 wt. % EtOAc, other small impurities), but was carried forward as-is without further purification (the impurities proved much easier to remove after esterification).

To a 10-mL oven-dried round-bottomed flask equipped with a Teflon-coated stir bar were added THF (2.6 mL), DMF (24.4 mg, 0.1 equiv, 0.33 mmol), and the impure 2-chloro-2-cyclopropylacetic acid (**184**, 1.22 g, 44% pure), under nitrogen. Oxalyl chloride (508 mg, 1.2 equiv, 4.00 mmol) was added dropwise via syringe to the reaction, over the course of five minutes. The reaction was allowed to stir for 1 hour at 18 °C to form the acyl chloride. To a 25-mL oven-dried round-bottomed flask equipped with a Teflon-coated stir bar were added phenol (314 mg, 1 equiv, 3.33 mmol), 4-(dimethylamino)pyridine (611 mg, 1.5 equiv, 5.00 mmol), and THF (2.6 mL), under nitrogen. This solution was cooled to 0 °C, then the acyl chloride solution was added dropwise over 2 minutes, resulting in a slurry that was slowly warmed to 18 °C. After 20 hours of stirring, the reaction was transferred to a separatory funnel and diluted with water and  $\text{Et}_2\text{O}$ . The layers were separated, then the organic layer was washed sequentially with 1 M aqueous HCl, saturated aqueous  $\text{NaHCO}_3$ , and brine. The organic layer was dried with  $\text{Na}_2\text{SO}_4$ , filtered, and concentrated. The crude material was purified by flash column chromatography over silica gel, eluting with 2.4%  $\text{Et}_2\text{O}$ /hexanes to afford **168** as a colorless oil (195.1 mg, 28% yield).

$R_f$  = 0.41 (silica, 8% Et<sub>2</sub>O/hexanes, UV)

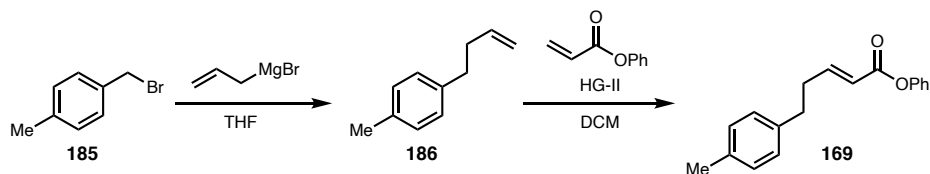
<sup>1</sup>H NMR (400 MHz, CDCl<sub>3</sub>):  $\delta$  7.45 – 7.37 (m, 2H), 7.30 – 7.24 (m, 1H), 7.18 – 7.12 (m, 2H), 3.86 (d,  $J$  = 9.7 Hz, 1H), 1.60 (dtt,  $J$  = 9.6, 8.1, 4.8 Hz, 1H), 0.92 – 0.80 (m, 2H), 0.71 – 0.64 (m, 1H), 0.62 – 0.55 (m, 1H).

<sup>13</sup>C NMR (101 MHz, CDCl<sub>3</sub>):  $\delta$  167.7, 150.6, 129.7, 126.5, 121.3, 62.4, 15.8, 6.2, 5.4.

FTIR (NaCl, thin film, cm<sup>-1</sup>): 2987, 1770, 1492, 1302, 1243, 1194, 1162, 1025, 680.

HRMS (FAB,  $m/z$ ): calc'd for C<sub>11</sub>H<sub>12</sub>ClO<sub>2</sub> [M+H]<sup>+</sup>: 211.0526; found: 211.0529.

#### phenyl (*E*)-5-(*p*-tolyl)pent-2-enoate (**169**)



1-(bromomethyl)-4-methylbenzene (**185**) was converted to 1-(but-3-en-1-yl)-4-methylbenzene (**186**) using the procedure reported by Wang and coworkers. Spectral data matched those reported.<sup>41</sup>

Olefin metathesis was carried out following the procedure of Matsubara.<sup>42</sup> In a nitrogen-filled glovebox, to a 2-dram oven-dried vial equipped with a Teflon-coated stir bar was added Hoveyda-Grubbs second generation catalyst (10.7 mg, 0.1 equiv, 0.0171 mmol), followed by anhydrous CH<sub>2</sub>Cl<sub>2</sub> (3.42 mL, 0.1 M). Phenyl acrylate (101 mg, 5.0 equiv, 0.684 mmol) was added to the vial, followed by 1-(but-3-en-1-yl)-4-methylbenzene (**186**, 50.0 mg, 1 equiv, 0.342 mmol). The reaction was sealed with a rubber septum, removed from the glovebox, and stirred under nitrogen at 18 °C for 18 hours. The reaction was filtered through a short plug of silica, eluting with CH<sub>2</sub>Cl<sub>2</sub>, then concentrated. NMR



analysis of the crude material showed a 4:1 ratio of phenyl acrylate to desired product. An aliquot (~5%) of the crude reaction was purified by preparative TLC (10% Et<sub>2</sub>O/hexanes) to afford **169** as a colorless oil (1.4 mg, 1.5% yield).

$R_f$  = 0.38 (silica, 10% Et<sub>2</sub>O/hexanes, UV)

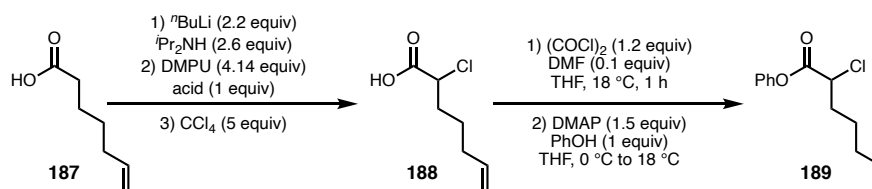
<sup>1</sup>H NMR (400 MHz, CDCl<sub>3</sub>):  $\delta$  7.43 – 7.35 (m, 1H), 7.25 – 7.16 (m, 1H), 7.16 – 7.07 (m, 3H), 6.05 (dt,  $J$  = 15.7, 1.6 Hz, 0H), 2.87 – 2.75 (m, 1H), 2.67 – 2.53 (m, 1H), 2.33 (s, 2H).

<sup>13</sup>C NMR (101 MHz, CDCl<sub>3</sub>):  $\delta$  165.05, 150.88, 150.75, 137.70, 135.91, 129.53, 129.37, 128.36, 125.84, 121.77, 121.20, 34.39, 33.96, 21.17.

FTIR (NaCl, thin film, cm<sup>-1</sup>): 2920, 1854, 1732, 1651, 1594, 1494, 1245, 1024, 810.

HRMS (FAB,  $m/z$ ): calc'd for C<sub>18</sub>H<sub>19</sub>O<sub>2</sub> [M+H]<sup>+</sup>: 267.1385 ; found: 267.1398.

### phenyl 2-chlorohept-6-enoate (**189**)



To a 500-mL oven-dried round-bottomed flask equipped with a Teflon-coated stir bar were added diisopropylamine (9.61 g, 2.6 equiv, 94.9 mmol) and THF (73 mL). The reaction was cooled to –20 °C in a dry ice/acetone bath, then *n*-butyllithium (2.5 M in hexane, 32.1 mL, 2.2 equiv, 80.3 mmol) was added to the solution dropwise via syringe over 5 minutes. The reaction was stirred at –20 °C for 30 minutes. DMPU (19.4 g, 4.14 equiv, 151 mmol) was added to the reaction, followed by hept-6-enoic acid (**187**, 4.68 g, 1.0 equiv, 36.5 mmol). The resulting yellow solution was stirred at –20 °C for 2 hours, then

cooled to  $-78\text{ }^{\circ}\text{C}$ . Carbon tetrachloride (28.1 g, 5.0 equiv, 183 mmol) was dissolved in THF (73 mL) and the resulting solution was added to the reaction in a single portion via syringe, resulting in an immediate color change to black. The reaction was stirred for 1 hour at  $-78\text{ }^{\circ}\text{C}$ , then warmed to room temperature.

A solution of sodium chloride (14.6 g, 6.84 equiv, 250 mmol) in HCl (2 M in water, 95 mL, 5.2 equiv, 190 mmol) was added to the reaction dropwise over 5 minutes via syringe. The reaction was transferred to a separatory funnel and diluted with water and Et<sub>2</sub>O. The layers were separated, and the aqueous layer extracted thrice with Et<sub>2</sub>O. The combined organics were dried with Na<sub>2</sub>SO<sub>4</sub>, filtered, and concentrated. The crude material was purified by flash column chromatography over silica gel, eluting with 50:50:0.1 hexanes/EtOAc/TFA. All fractions staining with bromocresol green were collected and concentrated, resulting in a brown oil. This oil was added to a separatory funnel and diluted with EtOAc and half-saturated aqueous Na<sub>2</sub>CO<sub>3</sub>. The layers were separated, then the aqueous layer was washed twice with EtOAc. The aqueous layer was acidified to pH=2 with 2 M HCl, then extracted thrice with EtOAc. These final three organic extractions were combined, dried with Na<sub>2</sub>SO<sub>4</sub>, filtered, and concentrated to afford 5.54 g pale yellow oil, which was not fully-pure by TLC or NMR (16 wt. % EtOAc, other small impurities), but was carried forward as-is without further purification (the impurities proved much easier to remove after esterification).

To a 25-mL oven-dried round-bottomed flask equipped with a Teflon-coated stir bar were added THF (7.9 mL), DMF (74.9 mg, 0.1 equiv, 1.02 mmol), and the impure 2-chlorohept-6-enoic acid (**188**, 2.38 g, 84% pure), under nitrogen. Oxalyl chloride (1.56 mg, 1.2 equiv, 12.3 mmol) was added dropwise via syringe to the reaction, over the course of

five minutes. The reaction was allowed to stir for 1 hour at 18 °C to form the acyl chloride. To a 50-mL oven-dried round-bottomed flask equipped with a Teflon-coated stir bar were added phenol (965 mg, 1 equiv, 10.2 mmol), 4-(dimethylamino)pyridine (1.88 g, 1.5 equiv, 15.4 mmol), and THF (7.9 mL), under nitrogen. This solution was cooled to 0 °C, then the acyl chloride solution was added dropwise over 2 minutes, resulting in a slurry that was slowly warmed to 18 °C. After 20 hours of stirring, the reaction was transferred to a separatory funnel and diluted with water and Et<sub>2</sub>O. The layers were separated, then the organic layer was washed sequentially with 1 M aqueous HCl, saturated aqueous NaHCO<sub>3</sub>, and brine. The organic layer was dried with Na<sub>2</sub>SO<sub>4</sub>, filtered, and concentrated. The crude material was purified by flash column chromatography over silica gel, eluting with 3% Et<sub>2</sub>O/hexanes to afford **189** as a colorless oil (1.03 g, 42% yield).

$R_f$  = 0.52 (silica, 8% Et<sub>2</sub>O/hexanes, UV)

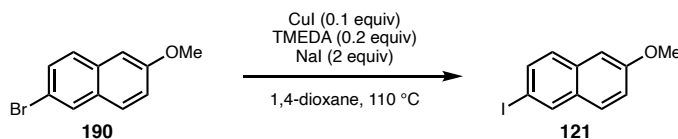
**<sup>1</sup>H NMR (400 MHz, CDCl<sub>3</sub>):**  $\delta$  7.46 – 7.36 (m, 2H), 7.30 – 7.23 (m, 1H), 7.16 – 7.09 (m, 2H), 5.90 – 5.74 (m, 1H), 5.13 – 4.98 (m, 2H), 4.51 (dd,  $J$  = 7.9, 6.2 Hz, 1H), 2.26 – 2.02 (m, 4H), 1.79 – 1.55 (m, 2H).

**<sup>13</sup>C NMR (101 MHz, CDCl<sub>3</sub>):**  $\delta$  168.3, 150.5, 137.7, 129.7, 126.5, 121.3, 115.6, 57.2, 34.3, 33.0, 25.3.

**FTIR (NaCl, thin film, cm<sup>-1</sup>):** 3076, 2931, 1768, 1593, 1494, 1243, 1192, 1164, 917, 688.

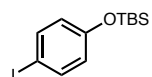
**HRMS (FAB,  $m/z$ ):** calc'd for C<sub>13</sub>H<sub>16</sub>ClO<sub>2</sub> [M+H]<sup>+</sup>: 239.0839; found: 239.0842.

### 2-iodo-6-methoxynaphthalene (**121**)



In a nitrogen-filled glovebox, to an oven-dried 150-mL pressure flask equipped with a Teflon-coated stir bar were added 2-bromo-6-methoxynaphthalene (**190**, 3.56 g, 1.0 equiv, 15.0 mmol), copper(I) iodide (286 mg, 0.10 equiv, 1.50 mmol), and sodium iodide (4.50 g, 2.0 equiv, 30.0 mmol). 1,4-dioxane (37.5 mL) was added to flask, followed by *N,N,N',N'*-tetramethylethylenediamine (264 mg, 0.20 equiv, 3.00 mmol). The pressure flask was sealed and removed from the glovebox, then heated to 110 °C for 17 hours. The reaction was cooled to room temperature, then filtered over a plug of Celite, eluting with DCM. The resulting filtrate was concentrated to afford **121** (4.12 g, 97% yield) as a colorless amorphous solid. Spectral data matched those reported.<sup>43</sup>

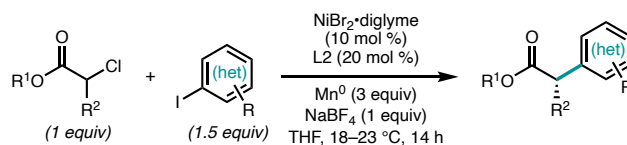
### *tert*-butyl(4-iodophenoxy)dimethylsilane (**119j**)



Prepared as previously described from 4-iodophenol (660 mg, 1.0 equiv, 3.0 mmol), *tert*-butyldimethylsilyl chloride (0.74 mL, 1.4 equiv, 4.3 mmol), triethylamine (0.5 mL, 1.2 equiv, 3.6 mmol), and DCM (6.8 mL, 0.44 M). The crude residue was purified by filtration over a silica plug with hexanes to yield **119j** (897 mg, 89% yield) as a colorless oil. Spectral data matched those reported in the literature.<sup>44</sup>

### 2.7.3 General Procedure for Reductive Cross-Coupling

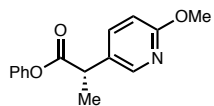
#### General Procedure 1: Reaction on 0.2 mmol scale.



On the benchtop, to a 1-dram vial were added a 12 mm Teflon-coated stir bar,  $\text{Mn}^0$  (3 equiv, 0.6 mmol, 33.0 mg), aryl iodide (if solid) (1.5 equiv, 0.3 mmol), and (*R,R*) 4-heptyl BiOX (**L2**, 20 mol %, 0.04 mmol, 13.5 mg). The vial was sealed under argon and transferred into a  $\text{N}_2$ -filled glovebox. Once in the glovebox, the vial was charged with  $\text{NiBr}_2 \cdot \text{diglyme}$  (10 mol %, 0.2 mmol, 7.05 mg), sodium tetrafluoroborate (1 equiv, 0.2 mmol, 22.0 mg), and anhydrous THF (0.1 M, 2.00 mL). The vial was briefly swirled to complex the nickel and ligand. Finally, the aryl iodide (if liquid) (1.5 equiv, 0.3 mmol) and the  $\alpha$ -chloroester (1 equiv, 0.2 mmol) were added. The vial was sealed with a Teflon-lined cap and electrical tape then removed from the glovebox. The mixture was stirred at 700 rpm for 14 hours. Due to fluctuation in ambient laboratory temperature, the reactions were run between 18 °C and 23 °C; results were consistent across this temperature range. The reaction was quenched by diluting with 1 mL of 20% EtOAc/hexanes then pushing through a ~8 mm by 6 cm plug of silica (in a monster pipette) into a scintillation vial. The reaction vial was rinsed twice with 1 mL of 20% EtOAc/hexanes, which were also pushed through the silica plug. The plug was eluted further with 20% EtOAc/hexanes (approximately 10 mL collected). The solution was concentrated *in vacuo*. The crude material was purified by column chromatography to afford the desired product.

## 2.7.4 Characterization of Reaction Products

### phenyl (*S*)-2-(6-methoxypyridin-3-yl)propanoate (**116**)



Prepared from phenyl 2-chloropropanoate (**115**, 36.9 mg, 0.2 mmol) and 5-iodo-2-methoxypyridine (**95**, 70.5 mg, 0.3 mmol) according to

General Procedure 1. The crude residue was purified by column chromatography (silica, 50:47:3 to 50:42.5:7.5 DCM/hexanes/EtOAc) to yield **116** (39.8 mg, 77% yield) in 85% ee as a colorless oil.

$R_f$  = 0.35 (silica, 20% EtOAc/hexanes, UV)

$[\alpha]_D^{22} = +73$  (c = 0.1.465, CH<sub>2</sub>Cl<sub>2</sub>).

**<sup>1</sup>H NMR (400 MHz, CDCl<sub>3</sub>):**  $\delta$  8.18 (dt,  $J$  = 2.6, 0.6 Hz, 1H), 7.65 (dd,  $J$  = 8.6, 2.5 Hz, 1H), 7.39 – 7.30 (m, 2H), 7.21 (ddt,  $J$  = 8.0, 6.9, 1.1 Hz, 1H), 7.04 – 6.94 (m, 2H), 6.77 (dd,  $J$  = 8.6, 0.7 Hz, 1H), 3.95 (s, 3H), 3.94 – 3.88 (m, 1H), 1.61 (d,  $J$  = 7.2 Hz, 3H).

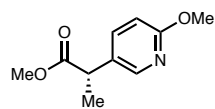
**<sup>13</sup>C NMR (101 MHz, CDCl<sub>3</sub>):**  $\delta$  172.9, 163.8, 150.8, 146.1, 137.8, 129.5, 128.5, 126.0, 121.4, 111.2, 53.6, 42.5, 18.6.

**FTIR (NaCl, thin film, cm<sup>-1</sup>):** 2980, 2945, 2848, 1755, 1608, 1494, 1395, 1296, 1280, 1194, 1141, 1072, 1026, 919, 834, 755, 689.

**HRMS (FAB,  $m/z$ ):** calc'd for C<sub>17</sub>H<sub>16</sub>O<sub>3</sub> [M+H]<sup>+</sup>: 258.1130 ; found: 258.1133.

**Chiral SFC:** (OJ-H, 2.5 mL/min, 10% IPA in CO<sub>2</sub>,  $\lambda$  = 210 nm:  $t_R$  (major) = 5.6 min,  $t_R$  (minor) = 6.1 min.

**methyl (*S*)-2-(6-methoxypyridin-3-yl)propanoate (**191**)**



Prepared from methyl 2-chloropropanoate (**112**, 24.5 mg, 0.2 mmol) and 5-iodo-2-methoxypyridine (**95**, 70.5 mg, 0.3 mmol) according to General Procedure 1. The crude residue was purified by column chromatography (silica, 70:15:15 hexanes/DCM/Et<sub>2</sub>O) to yield **191** (15.8 mg, 40% yield) in 84% ee as a colorless oil.

$R_f$  = 0.30 (70:15:15 hexanes/DCM/Et<sub>2</sub>O, UV)

$[\alpha]_D^{21} = +61$  (c = 1.0, CHCl<sub>3</sub>)

<sup>1</sup>H NMR (400 MHz, CDCl<sub>3</sub>):  $\delta$  8.10 – 8.02 (m, 1H), 7.59 – 7.50 (m, 1H), 6.75 – 6.68 (m, 1H), 3.92 (s, 3H), 3.73 – 3.62 (m, 4H), 1.48 (d,  $J$  = 7.2 Hz, 3H).

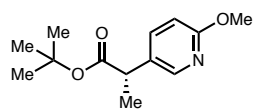
<sup>13</sup>C NMR (101 MHz, CDCl<sub>3</sub>):  $\delta$  174.8, 163.6, 145.9, 137.8, 128.9, 111.1, 53.6, 52.3, 42.3, 18.6.

FTIR (NaCl, thin film, cm<sup>-1</sup>): 2951, 1738, 1607, 1494, 1395, 1279, 1166, 1027.

HRMS (FAB,  $m/z$ ): calc'd for C<sub>10</sub>H<sub>14</sub>NO<sub>3</sub> [M+H]<sup>+</sup>: 196.0974; found: 196.0988.

Chiral SFC: (IC, 2.5 mL/min, 5% IPA in CO<sub>2</sub>,  $\lambda$  = 280 nm:  $t_R$  (major) = 3.5 min,  $t_R$  (minor) = 3.8 min.

***tert*-butyl (*S*)-2-(6-methoxypyridin-3-yl)propanoate (**192**)**



Prepared from *tert*-butyl 2-chloropropanoate (**174**, 32.9 mg, 0.2 mmol) and 5-iodo-2-methoxypyridine (**95**, 70.5 mg, 0.3 mmol) according to General Procedure 1. The crude residue was purified by column chromatography (silica, 80:10:10 hexanes/DCM/Et<sub>2</sub>O) to yield **192** (9.7 mg, 20% yield) in 89% ee as a colorless oil.

$R_f = 0.27$  (80:10:10 hexanes/DCM/Et<sub>2</sub>O, UV)

$[\alpha]_D^{21} = +31$  ( $c = 0.5$ , CHCl<sub>3</sub>)

<sup>1</sup>H NMR (400 MHz, CDCl<sub>3</sub>):  $\delta$  8.12 – 7.97 (m, 1H), 7.63 – 7.46 (m, 1H), 6.71 (d,  $J = 8.5$  Hz, 1H), 3.92 (s, 3H), 3.55 (q,  $J = 7.2$  Hz, 1H), 1.47 – 1.37 (m, 10H).

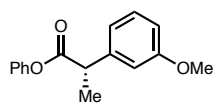
<sup>13</sup>C NMR (101 MHz, CDCl<sub>3</sub>):  $\delta$  173.6, 163.4, 145.8, 137.8, 129.5, 110.9, 81.0, 53.6, 43.4, 28.1, 18.6.

FTIR (NaCl, thin film, cm<sup>-1</sup>): 2978, 1728, 1607, 1493, 1394, 1278, 1151, 1029

HRMS (FAB,  $m/z$ ): calc'd for C<sub>13</sub>H<sub>20</sub>NO<sub>3</sub> [M+H]<sup>+</sup>: 238.1443; found: 238.1434.

Chiral SFC: (IC, 2.5 mL/min, 5% IPA in CO<sub>2</sub>,  $\lambda = 280$  nm:  $t_R$  (major) = 3.3 min,  $t_R$  (minor) = 3.7 min.

### phenyl (*S*)-2-(3-methoxyphenyl)propanoate (**120a**)



Prepared from phenyl 2-chloropropanoate (**115**, 36.9 mg, 0.2 mmol) and 1-iodo-3-methoxybenzene (**119a**, 70.2 mg, 0.3 mmol) according to

General Procedure 1. The crude residue was purified by column chromatography (silica, 2.4:3.6:10:84 Et<sub>2</sub>O/PhMe/DCM/hexanes) to yield **120a** (45.5 mg, 89% yield) in 84% ee as a colorless oil.

$R_f = 0.37$  (silica, 40% DCM/hexanes, UV)

$[\alpha]_D^{23} = +58$  ( $c = 1.0$ , CHCl<sub>3</sub>).

<sup>1</sup>H NMR (400 MHz, CDCl<sub>3</sub>):  $\delta$  7.37 – 7.26 (m, 3H), 7.24 – 7.16 (m, 1H), 7.04 – 6.93 (m, 4H), 6.84 (ddd,  $J = 8.2, 2.6, 0.9$  Hz, 1H), 3.94 (q,  $J = 7.1$  Hz, 1H), 3.83 (s, 3H), 1.61 (d,  $J = 7.1$  Hz, 3H).



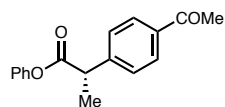
**$^{13}\text{C}$  NMR (101 MHz,  $\text{CDCl}_3$ ):**  $\delta$  173.0, 160.0, 151.0, 141.7, 129.9, 129.5, 125.9, 121.5, 120.0, 113.5, 112.9, 55.4, 45.8, 18.7.

**FTIR (NaCl, thin film,  $\text{cm}^{-1}$ ):** 2932, 1748, 1594, 1488, 1456, 1164, 1037.

**HRMS (FAB,  $m/z$ ):** calc'd for  $\text{C}_{16}\text{H}_{16}\text{O}_3$   $[\text{M}+\bullet]^+$ : 256.1100; found: 256.1104.

**Chiral SFC:** (AD-H, 2.5 mL/min, 5% IPA in  $\text{CO}_2$ ,  $\lambda = 210$  nm:  $t_R$  (major) = 9.6 min,  $t_R$  (minor) = 10.8 min.

**phenyl (*S*)-2-(4-acetylphenyl)propanoate (**120b**)**



Prepared from phenyl 2-chloropropanoate (**115**, 36.9 mg, 0.2 mmol) and 4-iodoacetophenone (**119b**, 73.8 mg, 0.3 mmol) according to

General Procedure 1 (run for 48 h). The crude residue was purified by column chromatography (silica, 20–50% EtOAc/hexanes) to yield **120b** (36.3 mg, 68% yield) in 87% ee as a colorless oil.

**$R_f$**  = 0.3 (silica, 20% EtOAc/hexanes, UV)

**$[\alpha]_D^{22}$**  = +79 ( $c = 1.39$ ,  $\text{CH}_2\text{Cl}_2$ ).

**$^1\text{H}$  NMR (400 MHz,  $\text{CDCl}_3$ ):**  $^1\text{H}$  NMR (400 MHz,  $\text{CDCl}_3$ )  $\delta$  8.01 – 7.94 (m, 2H), 7.55 – 7.47 (m, 2H), 7.39 – 7.29 (m, 2H), 7.25 – 7.16 (m, 1H), 7.02 – 6.95 (m, 2H), 4.04 (q,  $J = 7.2$  Hz, 1H), 2.61 (s, 3H), 1.64 (d,  $J = 7.2$  Hz, 3H).

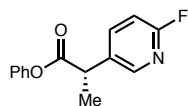
**$^{13}\text{C}$  NMR (101 MHz,  $\text{CDCl}_3$ ):**  $\delta$  197.8, 172.4, 150.8, 145.4, 136.4, 129.5, 129.0, 128.0, 126.1, 121.4, 45.8, 26.8, 18.5.

**FTIR (NaCl, thin film,  $\text{cm}^{-1}$ ):** 3058, 2983, 2834, 1752, 1684, 1607, 1492, 1414, 1359, 1268, 1195, 1163, 1144, 1073, 958, 845, 827, 750, 687.

**HRMS (FAB,  $m/z$ ):** calc'd for  $\text{C}_{17}\text{H}_{16}\text{O}_3$   $[\text{M}+\text{H}]^+$ : 269.1178; found: 269.1160

**Chiral SFC:** (AD-H, 2.5 mL/min, 10% IPA in CO<sub>2</sub>,  $\lambda$  = 254 nm:  $t_R$  (major) = 9.8 min,  $t_R$  (minor) = 11.2 min.

**phenyl (S)-2-(6-fluoropyridin-3-yl)propanoate (120c)**



Prepared from phenyl 2-chloropropanoate (**115**, 36.9 mg, 0.2 mmol) and 2-fluoro-5-iodopyridine (**119c**, 66.9 mg, 0.3 mmol) according to General

Procedure 1. The crude residue was purified by column chromatography (silica, 8:10:82 EtOAc/DCM/hexanes) to yield **120c** (36.1 mg, 74% yield) in 87% ee as a pale-yellow oil.

$R_f$  = 0.28 (silica, 8:10:82 EtOAc/DCM/hexanes, UV)

$[\alpha]_D^{23}$  = +45 (c = 0.5, CHCl<sub>3</sub>).

**<sup>1</sup>H NMR (400 MHz, CDCl<sub>3</sub>):**  $\delta$  8.29 – 8.22 (m, 0H), 7.87 (ddd,  $J$  = 8.5, 7.5, 2.7 Hz, 0H), 7.40 – 7.32 (m, 1H), 7.25 – 7.19 (m, 0H), 7.04 – 6.93 (m, 1H), 4.01 (q,  $J$  = 7.2 Hz, 0H), 1.66 (d,  $J$  = 7.2 Hz, 1H).

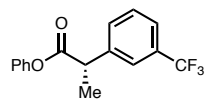
**<sup>13</sup>C NMR (101 MHz, CDCl<sub>3</sub>):**  $\delta$  172.3, 163.2 (d,  $J_{C-F}$  = 239.4 Hz), 150.6, 147.0 (d,  $J_{C-F}$  = 14.8 Hz), 140.3 (d,  $J_{C-F}$  = 8.0 Hz), 133.4 (d,  $J_{C-F}$  = 4.7 Hz), 129.6, 126.2, 121.3, 109.9 (d,  $J_{C-F}$  = 37.6 Hz), 42.5, 18.7.

**FTIR (NaCl, thin film, cm<sup>-1</sup>):** 2956, 2930, 1759, 1509, 1264, 1196, 916, 839.

**HRMS (FAB,  $m/z$ ):** calc'd for C<sub>14</sub>H<sub>13</sub>FNO<sub>2</sub> [M+H]<sup>+</sup>: 246.0930; found: 246.0925.

**Chiral SFC:** (AS-H, 2.5 mL/min, 7% IPA in CO<sub>2</sub>,  $\lambda$  = 210 nm:  $t_R$  (major) = 4.3 min,  $t_R$  (minor) = 4.6 min.

**phenyl (S)-2-(3-(trifluoromethyl)phenyl)propanoate (120d)**



Prepared from phenyl 2-chloropropanoate (**115**, 36.9 mg, 0.2 mmol) and 1-iodo-3-(trifluoromethyl)benzene (**119d**, 81.6 mg, 0.3 mmol) according

to General Procedure 1. The crude residue was purified by column chromatography (silica, 4% EtOAc/hexanes) to yield **120d** (36.2 mg, 61% yield) in 85% ee as a colorless oil.

$R_f$  = 0.55 (silica, 10% EtOAc/hexanes, UV).

$[\alpha]_D^{23}$  = +55 (c = 0.5, CHCl<sub>3</sub>).

<sup>1</sup>H NMR (400 MHz, CDCl<sub>3</sub>):  $\delta$  7.58 (d,  $J$  = 2.5 Hz, 1H), 7.55 – 7.46 (m, 2H), 7.41 (t,  $J$  = 7.7 Hz, 1H), 7.31 – 7.21 (m, 2H), 7.12 (td,  $J$  = 7.3, 1.2 Hz, 1H), 6.94 – 6.87 (m, 2H), 3.95 (q,  $J$  = 7.2 Hz, 1H), 1.57 (dd,  $J$  = 7.2, 0.9 Hz, 3H).

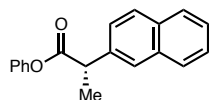
<sup>13</sup>C NMR (101 MHz, CDCl<sub>3</sub>):  $\delta$  172.5, 150.8, 141.1, 131.3 (q,  $^2J_{CF}$  = 32.3 Hz), 131.1, 129.6, 129.4, 126.1, 124.6 ( $^3J_{CF}$  = 3.9 Hz), 124.5 ( $^3J_{CF}$  = 3.8 Hz), 124.2 ( $^1J_{CF}$  = 272.4 Hz), 121.4, 45.6, 18.6.

FTIR (NaCl, thin film, cm<sup>-1</sup>): 1757, 1593, 1492, 1329, 1194, 1128, 1072, 807, 701.

HRMS (FAB, m/z): calc'd for C<sub>15</sub>H<sub>13</sub>F<sub>3</sub>O<sub>2</sub>: 295.0946 [M+H]<sup>+</sup>; found: 295.0920.

Chiral SFC: (OJ-H, 2.5 mL/min, 7% IPA in CO<sub>2</sub>,  $\lambda$  = 210 nm:  $t_R$  (minor) = 3.0 min,  $t_R$  (major) = 3.6 min.

**phenyl (S)-2-(naphthalen-2-yl)propanoate (120e)**



Prepared from phenyl 2-chloropropanoate (**115**, 36.9 mg, 0.2 mmol) and 2-iodonaphthalene (**119e**, 76.2 mg, 0.3 mmol) according to General

Procedure 1. The crude residue was purified by column chromatography (silica, 30% DCM/hexanes) to yield **120e** (51.8 mg, 94% yield) in 86% ee as a colorless oil.

$R_f$  = 0.37 (silica, 40% DCM/hexanes, UV)

$[\alpha]_D^{23} = +80$  (c = 1.0, CHCl<sub>3</sub>).

<sup>1</sup>H NMR (400 MHz, CDCl<sub>3</sub>):  $\delta$  7.92 – 7.80 (m, 4H), 7.59 – 7.44 (m, 3H), 7.37 – 7.28 (m, 2H), 7.23 – 7.14 (m, 1H), 7.03 – 6.94 (m, 2H), 4.14 (q,  $J$  = 7.1 Hz, 1H), 1.71 (d,  $J$  = 7.2 Hz, 3H).

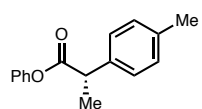
<sup>13</sup>C NMR (101 MHz, CDCl<sub>3</sub>):  $\delta$  173.2, 150.9, 137.6, 133.7, 132.8, 129.5, 128.7, 128.0, 127.8, 126.5, 126.4, 126.1, 125.9, 125.8, 121.5, 45.9, 18.7.

FTIR (NaCl, thin film, cm<sup>-1</sup>): 2918, 1750, 1328, 1193, 1160, 823, 746.

HRMS (FAB,  $m/z$ ): calc'd for C<sub>19</sub>H<sub>16</sub>O<sub>2</sub> [M+H]<sup>+</sup>: 276.1150; found: 276.1156.

Chiral SFC: (AD-H, 2.5 mL/min, 10% IPA in CO<sub>2</sub>,  $\lambda$  = 254 nm:  $t_R$  (major) = 13.4 min,  $t_R$  (minor) = 13.8 min.

### phenyl (*S*)-2-(*p*-tolyl)propanoate (**120f**)



Prepared from phenyl 2-chloropropanoate (**115**, 36.9 mg, 0.2 mmol) and 1-iodo-4-methylbenzene (**119f**, 65.4 mg, 0.3 mmol) according to General

Procedure 1. The crude residue was purified by column chromatography (silica, 20–50% DCM/hexanes) to yield **120f** (41.2 mg, 86% yield) in 85% ee as a colorless oil.

$R_f$  = 0.3 (silica, 30% DCM/hexanes, UV)

$[\alpha]_D^{22} = +73$  (c = 1.415, CH<sub>2</sub>Cl<sub>2</sub>).

**$^1\text{H}$  NMR (400 MHz,  $\text{CDCl}_3$ ):**  $\delta$  7.38 – 7.27 (m, 4H), 7.19 (ddd,  $J = 7.9, 5.9, 1.1$  Hz, 3H), 7.03 – 6.95 (m, 2H), 3.93 (q,  $J = 7.1$  Hz, 1H), 2.36 (s, 3H), 1.60 (d,  $J = 7.1$  Hz, 3H).

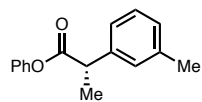
**$^{13}\text{C}$  NMR (101 MHz,  $\text{CDCl}_3$ ):**  $\delta$  173.3, 151.0, 137.2, 137.2, 129.6, 129.5, 127.5, 125.9, 121.5, 45.4, 21.2, 18.7.

**FTIR (NaCl, thin film,  $\text{cm}^{-1}$ ):** 2922, 2850, 1752, 1591, 1512, 1492, 1456, 1376, 1331, 1196, 1141, 1070, 917, 808, 755, 724.

**HRMS (FAB,  $m/z$ ):** calc'd for  $\text{C}_{16}\text{H}_{17}\text{O}_2$ : 241.1229  $[\text{M}+\text{H}]^+$ ; found 241.1234

**Chiral SFC:** (OB-H, 2.5 mL/min, 30% IPA in  $\text{CO}_2$ ,  $\lambda = 210$  nm:  $t_R$  (minor) = 3.6 min,  $t_R$  (major) = 4.2 min.

#### phenyl (*S*)-2-(*m*-tolyl)propanoate (**120g**)



Prepared from phenyl 2-chloropropanoate (**115**, 36.9 mg, 0.2 mmol) and 1-iodo-3-methylbenzene (**119g**, 65.4 mg, 0.3 mmol) according to General

Procedure 1. The crude residue was purified by column chromatography (silica, 10% DCM/hexanes) to yield **120g** (41.2 mg, 86% yield) in 84% ee as a colorless oil.

$R_f = 0.3$  (silica, 20% DCM/hexanes, UV)

$[\alpha]_D^{22} = +76$  ( $c = 1.215$ ,  $\text{CH}_2\text{Cl}_2$ )

**$^1\text{H}$  NMR (400 MHz,  $\text{CDCl}_3$ ):**  $\delta$  7.41 – 7.29 (m, 2H), 7.27 (td,  $J = 7.4, 1.0$  Hz, 1H), 7.23 – 7.16 (m, 4H), 7.16 – 7.08 (m, 1H), 7.04 – 6.96 (m, 2H), 3.93 (q,  $J = 7.2$  Hz, 1H), 2.38 (d,  $J = 0.7$  Hz, 3H), 1.61 (d,  $J = 7.2$  Hz, 3H).

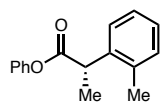
**$^{13}\text{C}$  NMR (101 MHz,  $\text{CDCl}_3$ ):**  $\delta$  173.3, 151.0, 140.2, 138.6, 129.5, 128.8, 128.4, 128.3, 125.9, 124.7, 121.5, 45.7, 21.6, 18.7.

**FTIR (NaCl, thin film,  $\text{cm}^{-1}$ ):** 3041, 2978, 2932, 2873, 1765, 1592, 1492, 1333, 1196, 1163, 1143, 1071, 920, 756, 720, 690.

**HRMS (FAB,  $m/z$ ):** calc'd for  $\text{C}_{16}\text{H}_{17}\text{O}_2$ : 241.1229  $[\text{M}+\text{H}]^+$ ; found 241.1223

**Chiral SFC:** (IC, 2.5 mL/min, 10% IPA in  $\text{CO}_2$ ,  $\lambda = 210$  nm:  $t_R$  (major) = 3.2 min,  $t_R$  (minor) = 3.5 min.

### phenyl (*S*)-2-(*o*-tolyl)propanoate (**120h**)



Prepared from phenyl 2-chloropropanoate (**115**, 36.9 mg, 0.2 mmol) and 1-iodo-2-methylbenzene (**119h**, 65.4 mg, 0.3 mmol) according to General Procedure 1. The crude residue was purified by column chromatography (silica, 80:17:3 hexanes/DCM/ $\text{Et}_2\text{O}$ ) to yield **120h** (41.3 mg, 46% yield) in 47% ee as a colorless oil.

$R_f = 0.30$  (silica, 80:17:3 hexanes/DCM/ $\text{Et}_2\text{O}$ , UV)

$[\alpha]_D^{20} = +50$  ( $c = 1.0$ ,  $\text{CHCl}_3$ )

$^1\text{H NMR}$  (400 MHz,  $\text{CDCl}_3$ ):  $\delta$  7.40 – 7.31 (m, 3H), 7.28 – 7.17 (m, 4H), 7.03 – 6.97 (m, 2H), 4.21 (q,  $J = 7.1$  Hz, 1H), 2.47 (s, 3H), 1.59 (d,  $J = 7.1$  Hz, 3H).

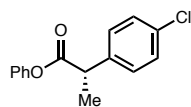
$^{13}\text{C NMR}$  (101 MHz,  $\text{CDCl}_3$ ):  $\delta$  173.5, 151.0, 138.8, 135.9, 130.8, 129.5, 127.3, 126.7, 126.6, 125.9, 121.5, 41.7, 19.8, 18.0.

**FTIR (NaCl, thin film,  $\text{cm}^{-1}$ ):** 2979, 1759, 1493, 1456, 1196, 1149, 1075, 728.

**HRMS (FAB,  $m/z$ ):** calc'd for  $\text{C}_{16}\text{H}_{17}\text{O}_2$ : 241.1229  $[\text{M}+\text{H}]^+$ ; found 241.1244.

**Chiral SFC:** (IC, 2.5 mL/min, 10% IPA in  $\text{CO}_2$ ,  $\lambda = 210$  nm:  $t_R$  (major) = 2.8 min,  $t_R$  (minor) = 3.4 min.

**phenyl (S)-2-(4-chlorophenyl)propanoate (120i)**



Prepared from phenyl 2-chloropropanoate (**115**, 36.9 mg, 0.2 mmol) and 1-chloro-4-iodobenzene (**119i**, 71.5 mg, 0.3 mmol) according to General Procedure 1. The crude residue was purified by column chromatography (silica, 4% EtOAc/hexanes) to yield **120i** (41.3 mg, 79% yield) in 87% ee as a colorless oil.

$R_f$  = 0.55 (silica, 10% EtOAc/hexanes, UV).

$[\alpha]_D^{23} = +37$  (c = 1.0, CHCl<sub>3</sub>).

<sup>1</sup>H NMR (400 MHz, CDCl<sub>3</sub>):  $\delta$  7.39 – 7.31 (m, 6H), 7.24 – 7.18 (m, 1H), 7.02 – 6.96 (m, 2H), 3.94 (q,  $J$  = 7.2 Hz, 1H), 1.61 (d,  $J$  = 7.1 Hz, 3H).

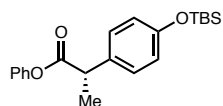
<sup>13</sup>C NMR (101 MHz, CDCl<sub>3</sub>):  $\delta$  172.8, 150.8, 138.6, 133.4, 129.5, 129.1, 126.0, 121.4, 45.2, 18.6.

FTIR (NaCl, thin film, cm<sup>-1</sup>): 2981, 1754, 1592, 1492, 1330, 1198, 1138, 1092, 828, 745, 691.

HRMS (FAB, m/z): calc'd for C<sub>15</sub>H<sub>13</sub>ClO<sub>2</sub>: 261.0682 [M+H]<sup>+</sup>; found: 261.0688.

Chiral SFC: (OJ-H, 2.5 mL/min, 20% IPA in CO<sub>2</sub>,  $\lambda$  = 280 nm:  $t_R$  (minor) = 4.9 min,  $t_R$  (major) = 5.1 min.

**phenyl (S)-2-(4-((tert-butyldimethylsilyl)oxy)phenyl)propanoate (120j)**



Prepared from phenyl 2-chloropropanoate (**115**, 36.9 mg, 0.2 mmol) and *tert*-butyl(4-iodophenoxy)dimethylsilane (**119j**, 100.0 mg, 0.3 mmol) according to General Procedure 1. The crude residue was purified by column

chromatography (silica, 30–35% DCM/hexanes) to yield **120j** (56.3 mg, 79% yield) in 84% ee as a colorless oil.

$R_f$  = 0.28 (silica, 35% DCM/hexanes, UV)

$[\alpha]_D^{23}$  = +45 (c = 1.0, CHCl<sub>3</sub>).

<sup>1</sup>H NMR (400 MHz, CDCl<sub>3</sub>):  $\delta$  7.36 – 7.30 (m, 2H), 7.28 – 7.23 (m, 2H), 7.23 – 7.15 (m, 1H), 7.02 – 6.94 (m, 2H), 6.88 – 6.79 (m, 2H), 3.90 (q,  $J$  = 7.2 Hz, 1H), 1.59 (d,  $J$  = 7.1 Hz, 3H), 0.99 (s, 9H), 0.21 (s, 6H).

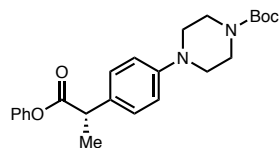
<sup>13</sup>C NMR (101 MHz, CDCl<sub>3</sub>):  $\delta$  173.5, 155.1, 151.0, 132.8, 129.5, 128.7, 125.9, 121.5, 120.4, 45.0, 25.8, 18.6, 18.3, –4.3.

FTIR (NaCl, thin film, cm<sup>-1</sup>): 2934, 1756, 1593, 1488, 1398, 1251, 1194, 1164, 1140, 1071, 1024.

HRMS (FAB,  $m/z$ ): calc'd for C<sub>21</sub>H<sub>28</sub>O<sub>3</sub>Si [M+•]<sup>+</sup>: 356.1808; found: 356.1802.

Chiral SFC: (AD-H, 2.5 mL/min, 3% IPA in CO<sub>2</sub>,  $\lambda$  = 254 nm:  $t_R$  (major) = 5.7 min,  $t_R$  (minor) = 6.7 min.

*tert*-butyl (S)-4-(4-(1-oxo-1-phenoxypropan-2-yl)phenyl)piperazine-1-carboxylate



(**120k**)

Prepared from phenyl 2-chloropropanoate (**115**, 36.9 mg, 0.2 mmol) and *tert*-butyl 4-(4-iodophenyl)piperazine-1-carboxylate (**119k**, 117.0 mg, 0.3 mmol) according to General Procedure 1. The crude residue was purified by column chromatography (silica, 35:10:55 Et<sub>2</sub>O/PhMe/hexanes) to yield **120k** (52.9 mg, 64% yield) in 85% ee as a colorless oil.

$R_f$  = 0.28 (silica, 40:10:50 Et<sub>2</sub>O/PhMe/hexanes, UV)



$[\alpha]_D^{23} = +41$  (c = 1.0, CHCl<sub>3</sub>).

**<sup>1</sup>H NMR (400 MHz, CDCl<sub>3</sub>):**  $\delta$  8.21 (d,  $J = 2.6, 0.6$  Hz, 1H), 7.57 (dd,  $J = 8.8, 2.6$  Hz, 1H), 7.39 – 7.30 (m, 2H), 7.20 (ddt,  $J = 8.0, 6.9, 1.2$  Hz, 1H), 7.04 – 6.95 (m, 2H), 6.67 (d,  $J = 8.8$  Hz, 1H), 3.87 (q,  $J = 7.2$  Hz, 1H), 3.62 – 3.47 (m, 8H), 1.59 (d,  $J = 7.2$  Hz, 3H), 1.49 (s, 9H).

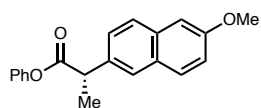
**<sup>13</sup>C NMR (101 MHz, CDCl<sub>3</sub>):**  $\delta$  173.1, 158.8, 155.0, 150.9, 147.3, 136.8, 129.5, 126.0, 125.1, 121.5, 107.4, 80.1, 45.3, 42.4, 28.6, 18.5.

**FTIR (NaCl, thin film, cm<sup>-1</sup>):** 2976, 2931, 1756, 1696, 1606, 1493, 1408, 1240, 1194, 1164, 1132.

**HRMS (FAB,  $m/z$ ):** calc'd for C<sub>23</sub>H<sub>30</sub>N<sub>3</sub>O<sub>4</sub> [M+H]<sup>+</sup>: 412.2236; found: 412.2230.

**Chiral SFC:** (IC, 2.5 mL/min, 35% IPA in CO<sub>2</sub>,  $\lambda = 280$  nm:  $t_R$  (major) = 3.5 min,  $t_R$  (minor) = 4.1 min.

### phenyl 2-(6-methoxynaphthalen-2-yl)propanoate (**122**)



Prepared from phenyl 2-chloropropanoate (**115**, 36.9 mg, 0.2 mmol) and 2-iodo-6-methoxynaphthalene (**121**, 85.2 mg, 0.3 mmol)

according to General Procedure 1. The crude residue was purified by column chromatography (silica, 5–20% EtOAc/hexanes) to yield **122** (59.3 mg, 97% yield) in 86% ee as a white powder.

$R_f = 0.55$  (silica, 20% EtOAc/hexanes, UV)

$[\alpha]_D^{21} = +83$  (c = 0.4, CH<sub>3</sub>CN).

**$^1\text{H}$  NMR (400 MHz,  $\text{CDCl}_3$ ):**  $\delta$  7.81 – 7.70 (m, 3H), 7.51 (dd,  $J$  = 8.5, 1.9 Hz, 1H), 7.37 – 7.29 (m, 2H), 7.23 – 7.12 (m, 3H), 7.03 – 6.95 (m, 2H), 4.11 (q,  $J$  = 7.1 Hz, 1H), 3.93 (s, 3H), 1.70 (d,  $J$  = 7.1 Hz, 3H).

**$^{13}\text{C}$  NMR (101 MHz,  $\text{CDCl}_3$ ):**  $\delta$  173.3, 157.9, 151.0, 135.3, 134.0, 129.5, 129.1, 127.5, 126.3, 125.9, 121.5, 119.2, 105.8, 55.5, 45.7, 18.7.

**FTIR (NaCl, thin film,  $\text{cm}^{-1}$ ):** 1755, 1744, 1604, 1484, 1264, 1134, 1025, 851.

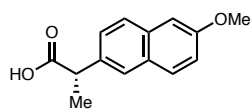
**HRMS (FAB,  $m/z$ ):** calc'd for  $\text{C}_{20}\text{H}_{18}\text{O}_3$ : 307.1334  $[\text{M}+\text{H}]^+$ ; found: 307.1316.

**Chiral SFC:** (IC, 2.5 mL/min, 20% IPA in  $\text{CO}_2$ ,  $\lambda$  = 210 nm:  $t_{\text{R}}$  (major) = 3.7 min,  $t_{\text{R}}$  (minor) = 4.0 min.

Compound **122** was also prepared on 1.0 mmol scale. On the benchtop, to a 50-mL round-bottomed flask were added a 12.5 cm football-shaped Teflon-coated stir bar,  $\text{Mn}^0$  (3 equiv, 3.0 mmol, 165mg) and (*R,R*) 4-heptyl BiOX (**L2**, 20 mol %, 0.2 mmol, 67.3 mg). The flask was sealed under argon and transferred into a  $\text{N}_2$ -filled glovebox. Once in the glovebox, the vial was charged with  $\text{NiBr}_2\cdot\text{diglyme}$  (10 mol %, 0.1 mmol, 35.3 mg), sodium tetrafluoroborate (1 equiv, 1.0 mmol, 110 mg), and anhydrous THF (5 mL). The reaction was stirred for one minute at 700 rpm. Finally, 2-iodo-6-methoxynaphthalene (**121**, 426 mg, 1.5 mmol) and phenyl 2-chloropropanoate (**115**, 185 mg, 1.0 mmol) were added as a single portion as a solution in anhydrous THF (5 mL). The flask was sealed with a rubber septum and electrical tape then removed from the glovebox. The mixture was stirred at 700 rpm for 14 hours. The reaction was quenched by diluting with 5 mL of 20% EtOAc/hexanes then eluting through 3.5 cm by 5.0 cm plug of silica. The reaction flask was rinsed twice with 5 mL of 20% EtOAc/hexanes, which were also eluted through the

silica plug. The plug was eluted further with 20% EtOAc/hexanes (approximately 50 mL collected). The solution was concentrated *in vacuo*. The crude material was purified by flash column chromatography over silica gel, eluting with 3:1:6 to 3.5:1:5.5 DCM/PhMe/hexanes to afford **122** (284 mg, 93% yield) as a white solid in 84% ee.

**(S)-2-(6-methoxynaphthalen-2-yl)propanoic acid (32)**



Following a procedure adapted from Shi et al,<sup>45</sup> to a 1-dram vial equipped with a Teflon-coated stir bar were added phenyl 2-(6-methoxynaphthalen-2-yl)propanoate (**122**, 277 mg, 0.905 mmol, 1 equiv), PhMe (181  $\mu$ L), KOH (79.8 mg, 1.57 equiv, 1.42 mmol), and water (181  $\mu$ L). The vial was sealed with a Teflon-lined cap and heated to 90 °C while stirring for 17 hours. The reaction was then cooled to 18 °C and transferred to a separatory funnel with water, then acidified to pH = 1 with 2 M HCl. The aqueous phase was extracted thrice with EtOAc. Combined organics were then extracted with saturated aqueous NaHCO<sub>3</sub>. The resulting aqueous solution was acidified to pH = 1 with 2 M HCl, then extracted thrice with EtOAc. Combined organics from these three extractions were dried with Na<sub>2</sub>SO<sub>4</sub>, filtered, and concentrated under reduced pressure. The crude material was purified by flash column chromatography over silica gel, eluting with 3:1 hexanes/EtOAc to give **32** as a white amorphous solid (201 mg, 96% yield). Spectral data matched those reported.<sup>45</sup>

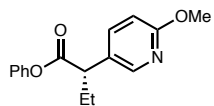
To determine the enantiomeric excess of **32**, an aliquot was converted to its methyl ester for SFC analysis.<sup>46</sup> To a 1-dram vial equipped with a Teflon-coated stir bar were added **32** (15 mg, 0.065 mmol), MeOH (2 mL), and HCl (12 M, 0.10 mL). The vial was

sealed with a Teflon-lined cap and heated to 70 °C while stirring for one hour. The reaction was then cooled to room temperature, concentrated under reduced pressure, diluted with water, and extracted thrice with Et<sub>2</sub>O. Combined organic extracts were dried with Na<sub>2</sub>SO<sub>4</sub>, filtered, and concentrated to give **32-OMe** as a white solid (15.2 mg, 96% yield) in 83% ee. The same procedure was followed for a commercial sample of (*S*)-naproxen and a commercial sample of racemic naproxen, showing no racemization under the acidic esterification conditions. Comparison on these traces was used to assign the product formed with (*R,R*)-**L2** as (*S*)-naproxen. All other coupled products were assigned in analogy to this compound.

The enantiopurity of **32** was further enriched by recrystallization.<sup>31</sup> To a 20-mL vial equipped with a 12-mm Teflon-coated stir bar were added **32** (185 mg, 1.0 equiv, 0.80 mmol), MeCN (5.9 mL), and *n*-octylamine (104 mg, 1.0 equiv, 0.80 mmol). The vial was sealed with a Teflon-lined cap and heated to 75 °C while stirring for one hour, resulting in a colorless solution. The reaction was cooled to room temperature (18 °C) while stirring; precipitating a white solid, which was collected by filtration, washing with 1 mL MeCN. This white solid was added to a 100-mL round-bottomed flask equipped with a Teflon-coated stir bar, followed by anhydrous MTBE (32 mL). The flask was equipped with a waterless condenser and heated to 60 °C while stirring until dissolved. After full dissolution, the reaction was allowed to cool to 18 °C while stirring for one hour. A white precipitate formed, which was then collected by filtration, washing with 5 mL MTBE. This material was resubjected to similar conditions. This white solid was added to a 100-mL round-bottomed flask equipped with a Teflon-coated stir bar, followed by anhydrous MTBE (25 mL). The flask was equipped with a waterless condenser and heated to 60 °C

while stirring until dissolved. After full dissolution, the reaction was allowed to cool to 18 °C *without* stirring and left for 16 hours. A white precipitate formed, which was then collected by filtration, washed with 5 mL MTBE. This solid was transferred to a separatory funnel with water, acidified to pH = 1 with 2 M HCl, then extracted twice with EtOAc. Combined organics were dried with Na<sub>2</sub>SO<sub>4</sub>, filtered, and concentrated under reduced pressure to give **32** (141 mg, 76% recovery). Methyl esterification of 15 mg of this material as above showed 92% ee.

**phenyl (S)-2-(6-methoxypyridin-3-yl)butanoate (128)**



Prepared from phenyl 2-chlorobutanoate (**123**, 39.7 mg, 0.2 mmol) and 5-iodo-2-methoxypyridine (**95**, 70.5 mg, 0.3 mmol) according to General Procedure 1. The crude residue was purified by column chromatography (silica, 4% EtOAc/hexanes) to yield **128** (44.1 mg, 81% yield) in 88% ee as a colorless oil.

$R_f$  = 0.6 (20% EtOAc/hexanes, UV)

$[\alpha]_D^{22} = +67$  (c = 1, CHCl<sub>3</sub>).

<sup>1</sup>H NMR (400 MHz, CDCl<sub>3</sub>):  $\delta$  8.16 (dt,  $J$  = 2.5, 0.6 Hz, 1H), 7.67 (dd,  $J$  = 8.6, 2.5 Hz, 1H), 7.39 – 7.30 (m, 2H), 7.26 – 7.16 (m, 1H), 7.04 – 6.96 (m, 2H), 6.77 (dd,  $J$  = 8.6, 0.8 Hz, 1H), 3.95 (s, 3H), 3.65 (t,  $J$  = 7.7 Hz, 1H), 2.22 (dp,  $J$  = 13.6, 7.4 Hz, 1H), 1.88 (dp,  $J$  = 13.6, 7.5 Hz, 1H), 1.00 (t,  $J$  = 7.4 Hz, 3H).

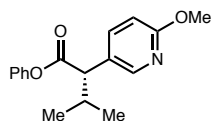
<sup>13</sup>C NMR (101 MHz, CDCl<sub>3</sub>):  $\delta$  172.5, 163.8, 150.8, 146.5, 138.1, 129.6, 127.0, 126.0, 121.5, 111.3, 53.7, 50.2, 26.8, 12.2.

FTIR (NaCl, thin film, cm<sup>-1</sup>): 2966, 1755, 1605, 1486, 1394, 1292, 1125, 1025, 829, 689.

HRMS (FAB,  $m/z$ ): calc'd for C<sub>16</sub>H<sub>17</sub>NO<sub>3</sub>: 272.1287 [M+H]<sup>+</sup>; found: 272.1308.

**Chiral SFC:** (AD-H, 2.5 mL/min, 10% IPA in CO<sub>2</sub>,  $\lambda$  = 230 nm:  $t_R$  (minor) = 3.6 min,  $t_R$  (major) = 3.8 min.

**phenyl (S)-2-(6-methoxypyridin-3-yl)-3-methylbutanoate (129)**



Prepared from phenyl 2-chloro-3-methylbutanoate (**124**, 42.5 mg, 0.2 mmol) and 5-iodo-2-methoxypyridine (**95**, 70.5 mg, 0.3 mmol) according to General Procedure 1. The crude residue was purified by column chromatography (silica, 2.5–10% EtOAc/hexanes) to yield **129** (42.7 mg, 75% yield) in 96% ee as a colorless oil.

$R_f$  = 0.53 (10% EtOAc/hex)

$[\alpha]_D^{23}$  = +56, (c = 1, CHCl<sub>3</sub>).

**<sup>1</sup>H NMR (400 MHz, CDCl<sub>3</sub>):**  $\delta$  8.15 (dd, J = 2.5, 0.7 Hz, 1H), 7.72 (dd, J = 8.6, 2.5 Hz, 1H), 7.41 – 7.30 (m, 2H), 7.25 – 7.16 (m, 1H), 7.05 – 6.94 (m, 2H), 6.80 – 6.71 (m, 1H), 3.95 (s, 3H), 3.36 (d, J = 10.3 Hz, 1H), 2.41 (dhept, J = 10.4, 6.6 Hz, 1H), 1.19 (d, J = 6.5 Hz, 3H), 0.81 (d, J = 6.7 Hz, 3H).

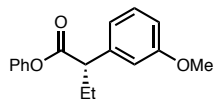
**<sup>13</sup>C NMR (101 MHz, CDCl<sub>3</sub>):**  $\delta$  172.3, 163.9, 150.7, 147.0, 138.4, 129.5, 126.3, 126.0, 121.5, 111.2, 56.5, 53.6, 32.1, 21.5, 20.2.

**FTIR (NaCl, thin film, cm<sup>-1</sup>):** 2963, 1754, 1605, 1492, 1397, 1286, 1193, 1140, 1105, 1026, 829, 728, 688.

**HRMS (FAB, m/z):** calc'd for C<sub>17</sub>H<sub>20</sub>O<sub>3</sub>N [M+H]<sup>+</sup>: 286.1443; found:286.1453.

**Chiral SFC:** (OJ-H, 2.5 mL/min, 5% IPA in CO<sub>2</sub>,  $\lambda$  = 280 nm:  $t_R$  (major) = 6.4 min,  $t_R$  (minor) = 6.9 min.

**phenyl (S)-2-(3-methoxyphenyl)butanoate (130)**



Prepared from phenyl 2-chloropropanoate (**123**, 39.7 mg, 0.2 mmol) and 1-iodo-3-methoxybenzene (**119a**, 70.2 mg, 0.3 mmol) according to General Procedure 1. The crude residue was purified by column chromatography (silica, 2% DCM/PhMe) to yield **130** (52.2 mg, 97% yield) in 85% ee as a colorless oil.

$R_f = 0.7$  (silica, 50% DCM/PhMe, UV)

$[\alpha]_D^{23} = +61$  ( $c = 1$ ,  $\text{CHCl}_3$ ).

$^1\text{H NMR}$  (400 MHz,  $\text{CDCl}_3$ ):  $\delta$  7.40 – 7.25 (m, 3H), 7.24 – 7.15 (m, 1H), 7.04 – 6.93 (m, 4H), 6.84 (ddd,  $J = 8.3, 2.6, 1.0$  Hz, 1H), 3.82 (s, 3H), 3.67 (t,  $J = 7.7$  Hz, 1H), 2.21 (ddq,  $J = 13.7, 8.1, 7.3$  Hz, 1H), 1.90 (dp,  $J = 13.6, 7.4$  Hz, 1H), 1.00 (t,  $J = 7.4$  Hz, 3H).

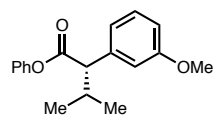
$^{13}\text{C NMR}$  (101 MHz,  $\text{CDCl}_3$ ):  $\delta$  172.6, 160.0, 150.9, 140.3, 129.8, 129.5, 125.9, 121.6, 120.6, 113.9, 112.9, 55.4, 53.7, 26.9, 12.3.

**FTIR** (NaCl, thin film,  $\text{cm}^{-1}$ ): 3478, 2965, 2935, 2836, 1754, 1609, 1483, 1273, 1069, 955, 774, 693.

**HRMS** (FAB,  $m/z$ ): calc'd for  $\text{C}_{17}\text{H}_{18}\text{O}_3$ : 270.1256  $[\text{M}+\bullet]^+$ ; found: 270.1251.

**Chiral SFC**: (OJ-H, 2.5 mL/min, 20% IPA in  $\text{CO}_2$ ,  $\lambda = 210$  nm:  $t_R$  (major) = 3.2 min,  $t_R$  (minor) = 3.9 min.

**phenyl 2-(3-methoxyphenyl)-3-methylbutanoate (131)**



Prepared from phenyl 2-chloro-3-methylbutanoate (**124**, 42.5 mg, 0.2 mmol) and 1-iodo-3-methoxybenzene (**119a**, 70.2 mg, 0.3 mmol) according to General Procedure 1. The crude residue was purified by column

chromatography (silica, 1:1.5:5:92.5 PhMe/Et<sub>2</sub>O/DCM/hexanes) to yield **131** (53.5 mg, 94% yield) in 98% ee as a colorless oil.

$R_f$  = 0.30 (5:5:10:80 PhMe/Et<sub>2</sub>O/DCM/hexanes, UV)

$[\alpha]_D^{22} = +49$  (c = 1, CHCl<sub>3</sub>).

<sup>1</sup>H NMR (400 MHz, CDCl<sub>3</sub>):  $\delta$  7.37 – 7.30 (m, 2H), 7.27 (ddd,  $J$  = 8.1, 7.4, 0.6 Hz, 1H), 7.19 (ddt,  $J$  = 8.0, 6.9, 1.2 Hz, 1H), 7.04 – 6.95 (m, 4H), 6.84 (ddd,  $J$  = 8.2, 2.5, 1.0 Hz, 1H), 3.82 (s, 3H), 3.36 (d,  $J$  = 10.5 Hz, 1H), 2.44 (dp,  $J$  = 10.6, 6.6 Hz, 1H), 1.18 (d,  $J$  = 6.5 Hz, 3H), 0.80 (d,  $J$  = 6.7 Hz, 3H).

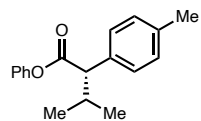
<sup>13</sup>C NMR (101 MHz, CDCl<sub>3</sub>):  $\delta$  172.5, 159.9, 150.9, 139.5, 129.7, 129.5, 125.9, 121.6, 121.2, 114.3, 113.0, 60.2, 55.4, 32.2, 21.6, 20.4.

FTIR (NaCl, thin film, cm<sup>-1</sup>): 2962, 2872, 1755, 1748, 1599, 1487, 1267, 1167, 1049, 976, 730, 694.

HRMS (FAB,  $m/z$ ): calc'd for C<sub>18</sub>H<sub>20</sub>O<sub>3</sub>: 285.1491 [M+H]<sup>+</sup>; found: 285.1498.

Chiral SFC: (AD-H, 2.5 mL/min, 20% IPA in CO<sub>2</sub>,  $\lambda$  = 254 nm:  $t_R$  (major) = 2.4 min,  $t_R$  (minor) = 2.5 min.

### phenyl (*S*)-3-methyl-2-(*p*-tolyl)butanoate (**132**)



Prepared from phenyl 2-chloro-3-methylbutanoate (**124**, 42.5 mg, 0.2 mmol) and 1-iodo-4-methylbenzene (**119f**, 65.4 mg, 0.3 mmol) according

to General Procedure 1. The crude residue was purified by column chromatography (silica, 10–40% DCM/hexanes) to yield **132** (42.0 mg, 78% yield) in 97% ee as a colorless oil.

$R_f$  = 0.5 (30% DCM, hexanes, UV)



$[\alpha]_D^{23} = +55$  ( $c = 1.37$ ,  $\text{CHCl}_3$ ).

$^1\text{H NMR}$  (400 MHz,  $\text{CDCl}_3$ ):  $\delta$  7.38 – 7.28 (m, 4H), 7.22 – 7.11 (m, 3H), 7.11 – 7.04 (m, 0H), 7.03 – 6.91 (m, 2H), 3.36 (d,  $J = 10.5$  Hz, 1H), 2.53 – 2.29 (m, 4H), 1.55 (s, 1H), 1.18 (d,  $J = 6.5$  Hz, 3H), 1.07 (d,  $J = 6.6$  Hz, 0H), 0.79 (d,  $J = 6.7$  Hz, 3H).

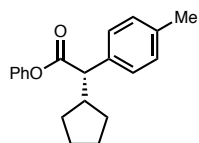
$^{13}\text{C NMR}$  (101 MHz,  $\text{CDCl}_3$ ):  $\delta$  172.7, 150.9, 137.2, 134.9, 129.4, 128.6, 125.9, 121.6, 59.8, 32.1, 21.6, 21.3, 20.4.

FTIR (NaCl, thin film,  $\text{cm}^{-1}$ ): 2961, 2926, 2871, 1756, 1593, 1492, 1197, 1112, 732, 688.

HRMS (FAB,  $m/z$ ): calc'd for  $\text{C}_{18}\text{H}_{21}\text{O}_2$ : 269.1542  $[\text{M}+\text{H}]^+$ ; found: 269.1534.

Chiral SFC: (OJ-H, 2.5 mL/min, 10% IPA in  $\text{CO}_2$ ,  $\lambda = 210$  nm:  $t_R$  (major) = 3.8 min,  $t_R$  (minor) = 4.4 min.

#### phenyl (*S*)-2-cyclopentyl-2-(*p*-tolyl)acetate (**134**)



Prepared from phenyl 2-chloro-2-cyclopentylacetate (**125**, 47.7 mg, 0.2 mmol) and 1-iodo-4-methylbenzene (**119f**, 65.4 mg, 0.3 mmol) according to General Procedure 1. The crude residue was purified by column chromatography (silica, 5%  $\text{Et}_2\text{O}$ /hexanes) to yield **134** (55.7 mg, 2.1 wt% ArAr homocoupling, 93% yield) in 97% ee as a colorless oil.

$R_f = 0.46$  (silica, 8%  $\text{Et}_2\text{O}$ /hexanes, UV)

$[\alpha]_D^{21} = +45$  ( $c = 1.0$ ,  $\text{CHCl}_3$ ).

$^1\text{H NMR}$  (400 MHz,  $\text{CDCl}_3$ ):  $\delta$  7.37 – 7.30 (m, 4H), 7.22 – 7.14 (m, 3H), 7.02 – 6.96 (m, 2H), 3.49 (d,  $J = 11.1$  Hz, 1H), 2.74 – 2.60 (m, 1H), 2.35 (s, 3H), 2.13 – 1.99 (m, 1H), 1.82 – 1.36 (m, 6H), 1.17 – 1.02 (m, 1H).

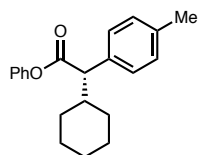
$^{13}\text{C}$  NMR (101 MHz,  $\text{CDCl}_3$ ):  $\delta$  172.8, 151.0, 137.1, 135.6, 129.5, 128.3, 125.8, 121.6, 57.7, 43.6, 31.7, 30.9, 25.4, 25.0, 21.2.

FTIR (NaCl, thin film,  $\text{cm}^{-1}$ ): 3027, 2951, 2869, 1756, 1494, 1196, 1118

HRMS (FAB,  $m/z$ ): calc'd for  $\text{C}_{20}\text{H}_{23}\text{O}_2$   $[\text{M}+\text{H}]^+$ : 295.1698; found: 295.1689.

Chiral SFC: (IC, 2.5 mL/min, 5% IPA in  $\text{CO}_2$ ,  $\lambda = 210$  nm:  $t_{\text{R}}$  (major) = 4.4 min,  $t_{\text{R}}$  (minor) = 4.8 min.

### phenyl (*S*)-2-cyclohexyl-2-(*p*-tolyl)acetate (**135**)



Prepared from phenyl 2-chloro-2-cyclohexylacetate (**126**, 50.5 mg, 0.2 mmol) and 1-iodo-4-methylbenzene (**119f**, 65.4 mg, 0.3 mmol) according to General Procedure 1. The crude residue was purified by column

chromatography (silica, 5%  $\text{Et}_2\text{O}$ /hexanes) to yield **135** (51.4 mg, 81% yield) in 98% ee as a colorless oil.

$R_f = 0.48$  (silica, 8%  $\text{Et}_2\text{O}$ /hexanes, UV)

$[\alpha]_D^{23} = +37$  ( $c = 1.0$ ,  $\text{CHCl}_3$ ).

$^1\text{H}$  NMR (400 MHz,  $\text{CDCl}_3$ ):  $\delta$  7.37 – 7.27 (m, 4H), 7.22 – 7.12 (m, 3H), 7.02 – 6.95 (m, 2H), 3.43 (d,  $J = 10.6$  Hz, 1H), 2.35 (s, 3H), 2.11 (qt,  $J = 11.0, 3.4$  Hz, 1H), 2.04 – 1.95 (m, 1H), 1.85 – 1.74 (m, 1H), 1.72 – 1.59 (m, 2H), 1.48 – 1.09 (m, 5H), 0.94 – 0.75 (m, 1H).

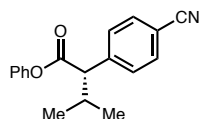
$^{13}\text{C}$  NMR (101 MHz,  $\text{CDCl}_3$ ):  $\delta$  172.7, 150.9, 137.2, 134.4, 129.4, 129.4, 128.7, 125.8, 121.7, 58.6, 41.3, 32.2, 30.6, 26.46, 26.2, 26.1, 21.2.

FTIR (NaCl, thin film,  $\text{cm}^{-1}$ ): 2926, 2852, 1755, 1593, 1492, 1196, 1165, 1140, 1107

HRMS (FAB,  $m/z$ ): calc'd for  $\text{C}_{21}\text{H}_{25}\text{ClO}_2$   $[\text{M}+\text{H}]^+$ : 309.1855; found: 309.1839.

**Chiral SFC:** (IC, 2.5 mL/min, 5% IPA in CO<sub>2</sub>,  $\lambda$  = 210 nm:  $t_R$  (major) = 4.1 min,  $t_R$  (minor) = 4.4 min.

**phenyl (S)-2-(4-cyanophenyl)-3-methylbutanoate (133)**



Prepared from phenyl 2-chloro-3-methylbutanoate (**124**, 42.5 mg, 0.2 mmol) and 4-iodobenzonitrile (**119f**, 68.7 mg, 0.3 mmol) according to General Procedure 1 for 48 hours. The crude residue was purified by column chromatography (silica, 4% EtOAc/hexanes) to yield **133** (37.8 mg, 68% yield) in 96% ee as a colorless oil.

$R_f$  = 0.3 (20% EtOAc/hexanes, UV)

$[\alpha]_D^{22} = +50$  (c = 1, CHCl<sub>3</sub>).

**<sup>1</sup>H NMR (400 MHz, CDCl<sub>3</sub>):**  $\delta$  7.70 – 7.63 (m, 2H), 7.59 – 7.53 (m, 2H), 7.39 – 7.31 (m, 2H), 7.25 – 7.18 (m, 1H), 7.01 – 6.94 (m, 2H), 3.47 (d,  $J$  = 10.4 Hz, 1H), 2.46 (dp,  $J$  = 10.4, 6.6 Hz, 1H), 1.20 (d,  $J$  = 6.5 Hz, 3H), 0.78 (d,  $J$  = 6.7 Hz, 3H).

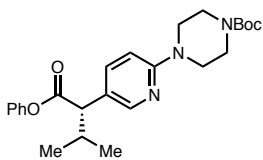
**<sup>13</sup>C NMR (101 MHz, CDCl<sub>3</sub>):**  $\delta$  171.6, 150.6, 143.3, 132.6, 129.6, 129.6, 126.2, 121.4, 118.8, 111.7, 60.1, 32.5, 21.5, 20.3.

**FTIR (NaCl, thin film, cm<sup>-1</sup>):** 2964, 2229, 1759, 1747, 1493, 1216, 1136, 828, 754, 688.

**HRMS (FAB,  $m/z$ ):** calc'd for C<sub>18</sub>H<sub>17</sub>NO<sub>2</sub>: 280.1338 [M+H]<sup>+</sup>; found: 280.1358.

**Chiral SFC:** (AD-H, 2.5 mL/min, 20% IPA in CO<sub>2</sub>,  $\lambda$  = 230 nm:  $t_R$  (major) = 2.5 min,  $t_R$  (minor) = 2.8 min.

***tert*-butyl (S)-4-(5-(3-methyl-1-oxo-1-phenoxybutan-2-yl)pyridin-2-yl)piperazine-1-carboxylate (136)**



Prepared from phenyl 2-chloro-3-methylbutanoate (**124**, 42.5 mg, 0.2 mmol) and *tert*-butyl 4-(5-iodopyridin-2-yl)piperazine-1-carboxylate (**119k**, 117 mg, 0.3 mmol) according to General

Procedure 1. The crude residue was purified by column chromatography (silica, 4–10% EtOAc/hexanes) to yield **136** (52.8 mg, 60% yield) in 97% ee as a colorless oil.

$R_f$  = 0.4 (silica, 20% EtOAc/hexanes, UV)

$[\alpha]_D^{23} = +35$  (c = 0.7, CHCl<sub>3</sub>).

**<sup>1</sup>H NMR (400 MHz, CDCl<sub>3</sub>):**  $\delta$  8.07 (d,  $J$  = 2.5 Hz, 1H), 7.53 (d,  $J$  = 8.7 Hz, 1H), 7.29 – 7.19 (m, 2H), 7.13 – 7.03 (m, 1H), 6.93 – 6.85 (m, 2H), 6.57 (d,  $J$  = 8.8 Hz, 1H), 3.45 (s, 8H), 3.20 (d,  $J$  = 10.4 Hz, 1H), 2.29 (dp,  $J$  = 10.3, 6.6 Hz, 1H), 1.39 (s, 9H), 1.07 (d,  $J$  = 6.5 Hz, 3H), 0.71 (d,  $J$  = 6.7 Hz, 3H).

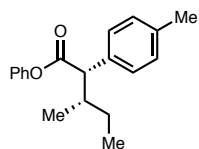
**<sup>13</sup>C NMR (101 MHz, CDCl<sub>3</sub>):**  $\delta$  172.5, 158.8, 154.9, 150.8, 148.2, 137.4, 129.5, 125.9, 122.9, 121.5, 107.3, 80.1, 56.5, 45.2, 43.5, 31.9, 28.5, 21.5, 20.2.

**FTIR (NaCl, thin film, cm<sup>-1</sup>):** 2965, 1754, 1697, 1494, 1415, 1239, 1167, 930, 754.

**HRMS (FAB,  $m/z$ ):** calc'd for C<sub>25</sub>H<sub>33</sub>NO<sub>4</sub>: 440.2549 [M+H]<sup>+</sup>; found: 440.2528.

**Chiral SFC:** (OD-H, 2.5 mL/min, 15% IPA in CO<sub>2</sub>,  $\lambda$  = 230 nm:  $t_R$  (major) = 4.4 min,  $t_R$  (minor) = 4.9 min.

**phenyl (2*S*,3*S*)-3-methyl-2-(*p*-tolyl)pentanoate (138)**



Prepared from phenyl (2*S*,3*S*)-2-chloro-3-methylpentanoate (**137**, 45.3 mg, 0.2 mmol) and 1-iodo-4-methylbenzene (**119f**, 65.4 mg, 0.3 mmol) according to General Procedure 1, using (*R,R*)-**L2**. The crude residue was purified by column chromatography (silica, 4% Et<sub>2</sub>O/hexanes) to yield **138** (47.9 mg, 85% yield) as a colorless oil in >20:1 dr.

$R_f$  = 0.46 (silica, 8% Et<sub>2</sub>O/hexanes, UV)

$[\alpha]_D^{21} = +50$  (c = 1.0, CHCl<sub>3</sub>).

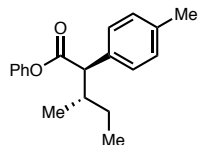
<sup>1</sup>H NMR (400 MHz, CDCl<sub>3</sub>):  $\delta$  7.37 – 7.27 (m, 4H), 7.22 – 7.13 (m, 3H), 7.01 – 6.94 (m, 2H), 3.47 (d,  $J$  = 10.5 Hz, 1H), 2.35 (s, 3H), 2.33 – 2.19 (m, 1H), 1.78 – 1.63 (m, 1H), 1.43 – 1.28 (m, 1H), 1.01 (t,  $J$  = 7.4 Hz, 3H), 0.74 (d,  $J$  = 6.8 Hz, 3H).

<sup>13</sup>C NMR (101 MHz, CDCl<sub>3</sub>):  $\delta$  172.8, 150.9, 137.2, 134.8, 129.5, 129.4, 128.7, 125.8, 121.6, 58.2, 38.0, 28.2, 21.3, 16.3, 11.4.

FTIR (NaCl, thin film, cm<sup>-1</sup>): 2964, 2926, 2876, 1755, 1593, 1514, 1493, 1281, 1197, 1113.

HRMS (FAB, m/z): calc'd for C<sub>19</sub>H<sub>23</sub>O<sub>2</sub> [M+H]<sup>+</sup>: 283.1698; found: 283.1718.

**phenyl (2*R*,3*S*)-3-methyl-2-(*p*-tolyl)pentanoate (138)**



Prepared from phenyl (2*S*,3*S*)-2-chloro-3-methylpentanoate (**137**, 45.3 mg, 0.2 mmol) and 1-iodo-4-methylbenzene (**119f**, 65.4 mg, 0.3 mmol) according to General Procedure 1, using (*S,S*)-**L2**. The crude residue was purified by

column chromatography (silica, 4% to 4.5% Et<sub>2</sub>O/hexanes) to yield **138** (46.6 mg, 83% yield) as a colorless oil in >20:1 dr.

$R_f$  = 0.46 (silica, 8% Et<sub>2</sub>O/hexanes, UV)

$[\alpha]_D^{21} = -44$  (c = 1.0, CHCl<sub>3</sub>).

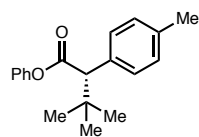
<sup>1</sup>H NMR (400 MHz, CDCl<sub>3</sub>):  $\delta$  7.37 – 7.28 (m, 4H), 7.22 – 7.13 (m, 3H), 7.01 – 6.95 (m, 2H), 3.47 (d,  $J$  = 10.7 Hz, 1H), 2.35 (s, 3H), 2.32 – 2.18 (m, 1H), 1.40 – 1.23 (m, 2H), 1.15 (d,  $J$  = 6.6 Hz, 3H), 1.03 – 0.93 (m, 1H), 0.83 (t,  $J$  = 7.4 Hz, 3H).

<sup>13</sup>C NMR (101 MHz, CDCl<sub>3</sub>):  $\delta$  172.8, 150.9, 137.2, 134.8, 129.5, 128.7, 125.9, 121.6, 58.3, 37.9, 26.2, 21.3, 17.5, 10.8.

FTIR (NaCl, thin film, cm<sup>-1</sup>): 2964, 2931, 2876, 1756, 1593, 1513, 1493, 1196, 1163, 1115.

HRMS (FAB, m/z): calc'd for C<sub>19</sub>H<sub>23</sub>O<sub>2</sub> [M+H]<sup>+</sup>: 283.1698; found: 283.1712.

### phenyl (*S*)-3,3-dimethyl-2-(*p*-tolyl)butanoate (**139**)



Prepared from phenyl 2-chloro-3,3-dimethylbutanoate (**193**, 45.3 mg, 0.2 mmol) and 1-iodo-4-methylbenzene (**119f**, 65.4 mg, 0.3 mmol) according to General Procedure 1. Addition of 1,1,2,2-tetrachloroethane as an internal standard showed 16% yield by NMR. The crude residue was purified by column chromatography (silica, 15–20% DCM/hexanes), followed by preparative TLC (50% DCM/hexanes) to yield **139** (5.2 mg, 9% yield) in 89% ee as a colorless oil.

$R_f$  = 0.17 (20% DCM, hexanes, UV)

$[\alpha]_D^{21} = -37$  (c = 0.3, CHCl<sub>3</sub>).

**$^1\text{H}$  NMR (400 MHz,  $\text{CDCl}_3$ ):**  $\delta$  7.38 – 7.31 (m, 4H), 7.23 – 7.12 (m, 3H), 7.04 – 6.98 (m, 2H), 3.65 (s, 1H), 2.36 (s, 3H), 1.08 (s, 9H).

**$^{13}\text{C}$  NMR (101 MHz,  $\text{CDCl}_3$ ):**  $\delta$  172.0, 150.8, 137.1, 132.8, 130.0, 129.7, 129.5, 128.8, 125.9, 121.8, 121.4, 61.2, 35.0, 27.9, 26.7, 21.2.

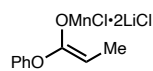
**FTIR (NaCl, thin film,  $\text{cm}^{-1}$ ):** 2958, 1756, 1593, 1492, 1365, 1197, 1162, 1112, 1024

**HRMS (FAB,  $m/z$ ):** calc'd for  $\text{C}_{19}\text{H}_{22}\text{O}_2$ : 283.1698  $[\text{M}+\text{H}]^+$ ; found: 283.1693.

**Chiral SFC:** (OJ-H, 2.5 mL/min, 10% IPA in  $\text{CO}_2$ ,  $\lambda = 210$  nm:  $t_R$  (minor) = 4.0 min,  $t_R$  (major) = 5.2 min.

### 2.7.5 Mechanistic Experiments

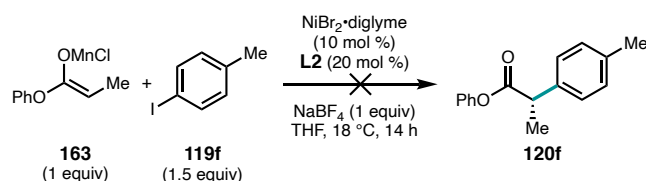
#### Manganese enolate of phenyl propionate (163)

 To a flame-dried 25-mL round-bottomed flask equipped with a Teflon-coated stir bar were added  $\text{MnCl}_2$  (629 mg, 1.0 equiv, 5.00 mmol) and  $\text{LiCl}$  (424 mg, 2.0 equiv, 10.0 mmol, freshly ground with mortar and pestle). The flask was sealed with a rubber septum and electrical tape, then evacuated under high vacuum at 100 °C for 22 hours. The flask was then cooled to 18 °C, and THF (8.0 mL) was added via syringe. The reaction turned light pink, then slowly became yellow as it was stirred for 24 hours at 18 °C. This  $\text{MnCl}_2 \cdot 2\text{LiCl}$  solution was used immediately.

A 50-mL flame-dried round-bottom flask equipped with a Teflon-coated stir bar was cooled to 0 °C under an atmosphere of nitrogen. THF (5.26 mL) was added to the flask, followed by diisopropylamine (336  $\mu\text{L}$ , 243 mg, 1.2 equiv, 2.20 mmol). *n*-butyllithium (880  $\mu\text{L}$ , 2.5 M in hexanes, 1.1 equiv, 2.20 mmol) was added dropwise to the

flask via syringe over one minute. The reaction was stirred for 15 minutes at 0 °C, then phenyl propionate (300 mg, 1.0 equiv, 2.00 mmol) was added dropwise via syringe over two minutes. The reaction was stirred for 30 minutes at 0 °C, then  $\text{MnCl}_2 \cdot 2\text{LiCl}$  (3.52 mL, 0.625 M in THF, 1.10 equiv) was added to the reaction in a single portion via syringe. The cooling bath was removed and the reaction was allowed to stir for 30 minutes. The resulting manganese enolate solution was used immediately.

### Coupling reaction with **119f**

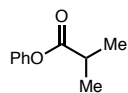


The reaction was conducted similarly to General Procedure 1. To a 1-dram vial was added a 12 mm Teflon-coated stir bar and 4-heptyl BiOX (**L2**, 13.5 mg, 0.20 equiv, 0.04 mmol). The vial was sealed under argon and transferred into a nitrogen-filled glovebox. Once in the glovebox, the vial was charged with  $\text{NiBr}_2 \cdot \text{diglyme}$  (7.05 mg, 0.10 equiv, 0.02 mmol), sodium tetrafluoroborate (22.0 mg, 1.0 equiv, 0.2 mmol), and THF (1 mL). The vial was briefly swirled to complex Ni and ligand. 1-iodo-4-methylbenzene (**119f**, 65.4 mg, 1.5 equiv, 0.30 mmol) was added to the vial, which was then sealed with a Teflon-lined septum cap and electrical tape. The vial was removed from the glovebox, then the manganese enolate solution (0.20 M, 1.0 mL, 1 equiv) was added dropwise over 30 seconds. The vial was sealed with vacuum grease and parafilm, then allowed to stir at 18 °C and 700 rpm. After 14 hours, the reaction was worked following General Procedure 1.



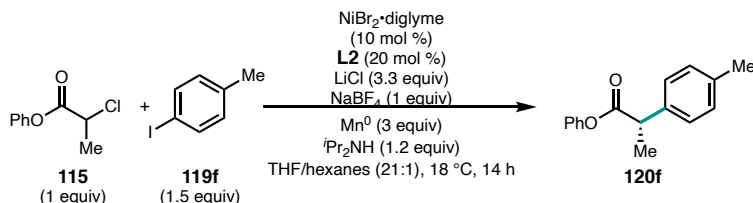
No product formation was observed. *Note: no product was observed when 2.0 equiv Mn<sup>0</sup> was included in the same reaction.*

### phenyl isobutyrate (**194**)



To test the viability of the manganese enolate **163** as a nucleophile, the same batch of enolate solution was treated with iodomethane.<sup>47</sup> To a 10-mL oven dried round-bottomed flask equipped with a Teflon-coated stir bar was added **163** solution (2.00 mL, 0.40 mmol). Iodomethane (68.1 mg, 1.20 equiv, 0.48 mmol) was added dropwise as a solution in DMSO (1.00 mL). The reaction was allowed to stir at 18 °C for 19 hours. The reaction was diluted with water and Et<sub>2</sub>O, then the layers were separated. The organic layer was washed thrice with water, then dried with Na<sub>2</sub>SO<sub>4</sub>, filtered, and concentrated. The crude material was filtered over a short silica plug, eluting with 15% EtOAc/hexanes to afford 31.6 mg phenyl isobutyrate (**194**, contaminated with 6% phenyl propionate, 45% yield) as a colorless oil. Spectral data match those reported.<sup>48</sup>

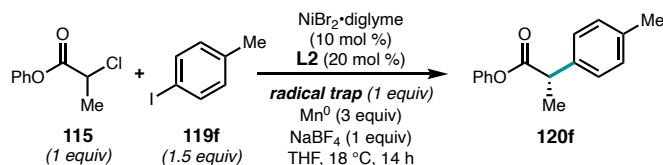
### Control with Mn enolate additives



A control reaction was conducted with the byproducts of Mn enolate formation (LiCl, hexanes, and diisopropylamine). The reaction was set up according to a modified General Procedure 1 using phenyl 2-chloropropionate (**115** 36.9 mg, 1.0 equiv, 0.20 mmol)

and 1-iodo-4-methylbenzene (**119f**, 65.4 mg, 1.5 equiv, 0.30 mmol). After the addition of NaBF<sub>4</sub>, LiCl (28.0 mg, 3.3 equiv, 0.66 mmol) was added to the vial. THF (1.88 mL) and hexanes (89.5  $\mu$ L) were added. After addition of the electrophiles, diisopropylamine was added (24.3 mg, 1.20 equiv, 0.24 mmol). Following the typical workup from General Procedure 1, 0.10 mmol 1,1,2,2-tetrachloroethane was added to the crude residue as a stock solution in CDCl<sub>3</sub>. <sup>1</sup>H-NMR analysis showed **120f** in 73% yield. An aliquot of the crude material was purified by preparative TLC (silica, 20:5:75 DCM/Et<sub>2</sub>O/hexanes) then analyzed by chiral SFC using the conditions reported above for **120f** to give 81% ee.

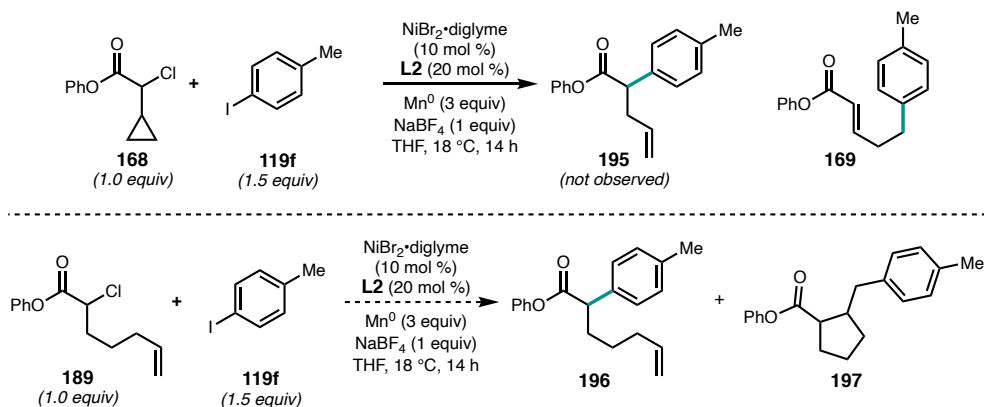
### Radical trapping experiments



Radical trapping experiments were conducted according to a modified General Procedure 1 using phenyl 2-chloropropionate (**115**, 36.9 mg, 1.0 equiv, 0.20 mmol) and 1-iodo-4-methylbenzene (**119f**, 65.4 mg, 1.5 equiv, 0.30 mmol). After the addition of solvent, 1.0 equiv radical trap was added (TEMPO, 31.3 mg, 0.2 mmol), (9,10-dihydroanthracene, 36.5 mg, 0.2 mmol), or (1,1-diphenylethylene, 36.0 mg, 0.2 mmol). The remainder of the procedure followed General Procedure 1. The addition of TEMPO resulted in 0% yield of **120f**, with both electrophiles remaining. The addition of 9,10-dihydroanthracene resulted in 0% yield of **120f**, but 20% phenyl propionate was formed, possibly through abstraction of a hydrogen atom by an intermediate  $\alpha$ -ester radical. The addition of 1,1-

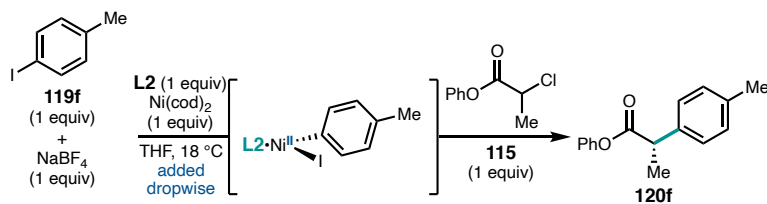
diphenylethylene resulted in a 60% yield of **120f** in 84% ee; none of the product from radical addition to 1,1-diphenylethylene was detected.

### Radical clock experiments



Radical clock substrates **168** and **189** were subjected to standard reaction conditions using General Procedure 1. Shown are the expected products. In both cases, no species could be cleanly isolated from the crude reaction mixture.  $^1\text{H-NMR}$  spectra of the crude reaction mixtures are included for reference. For the reaction of **168**, no direct coupling was observed. Comparison of the crude NMR to independently synthesized **169** shows a 10% yield of the ring-opened then coupled product.

### Stoichiometric Reaction

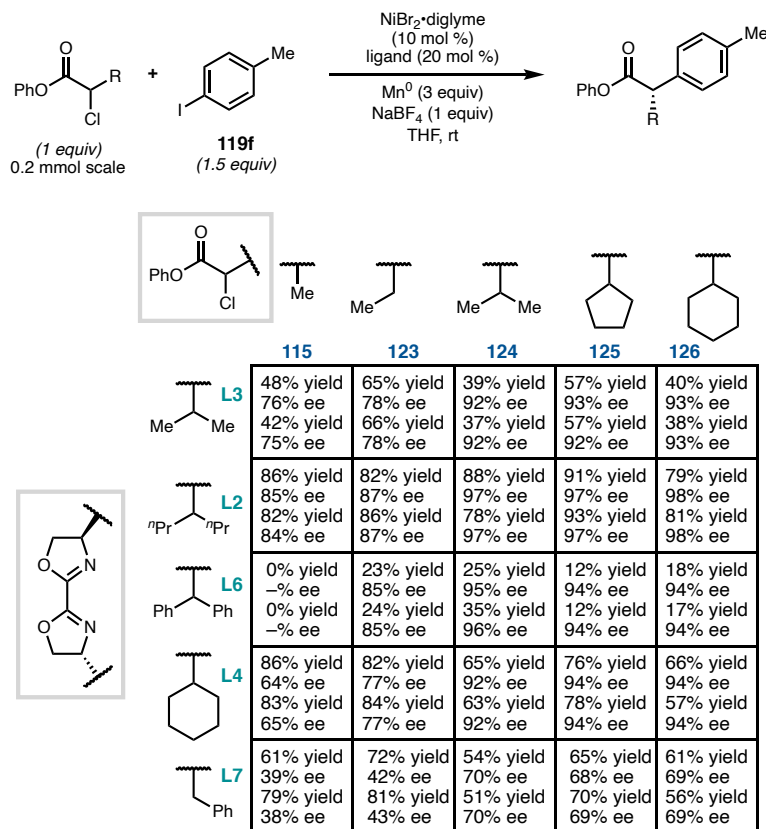


On the benchtop to a 1-dram vial equipped with a 12 mm Teflon-coated stir bar was added 4-heptyl BiOX **L2** (67.3 mg, 1.0 equiv, 0.2 mmol). The vial was sealed under argon and transferred to a nitrogen-filled glovebox. Ni(cod)<sub>2</sub> (55.0 mg, 1.0 equiv, 0.2 mmol) was added to the vial, followed by THF (1.0 mL). The vial was stirred at 50 °C for 5 minutes to fully dissolve; a deep blue solution formed. As the solution cooled to room temperature, a second 1-dram vial equipped with a 12-mm Teflon-coated stir bar was charged with 1-iodo-4-methylbenzene (**119f**, 43.6 mg, 1.0 equiv, 0.2 mmol), NaBF<sub>4</sub> (22.0 mg, 1.0 equiv, 0.2 mmol), and THF (1.0 mL). This vial was stirred at 700 rpm at room temperature. Once the solution became homogeneous (~2 minutes), the Ni(cod)<sub>2</sub>·**L2** solution was added dropwise over five minutes. Each drop of the deep blue solution quickly dissipated upon addition, resulting in the solution turning from colorless to deep red/brown. Phenyl 2-chloropropionate (**115**, 36.9 mg, 1.0 equiv, 0.2 mmol) was added via syringe. The reaction was sealed with a Teflon-lined cap and electrical tape, then removed from the glovebox and stirred at 18 °C for 14 hours. The reaction was worked up following General Procedure 1. To the crude residue was added 0.10 mmol 1,1,2,2-tetrachloroethane as an internal standard. <sup>1</sup>H-NMR analysis showed 72% yield of **120f**. An aliquot of the crude material was purified by preparative TLC (silica, 20:5:75 DCM/Et<sub>2</sub>O/hexanes) then analyzed by chiral SFC using the conditions reported above for **120f** to give 81% ee.

### 2.7.6 Dataset Generation for Statistical Modelling

A 5 by 5 matrix of  $\alpha$ -chloroesters and BiOX ligands were exhaustively explored to generate a dataset for statistical modelling. Each of the five phenyl chloroesters ( $\alpha$ -methyl

(**115**),  $\alpha$ -ethyl (**123**),  $\alpha$ -isopropyl (**124**),  $\alpha$ -cyclopentyl (**125**), and  $\alpha$ -cyclohexyl(**126**) were coupled with 1-iodo-4-methylbenzene (**119f**) using General Procedure 1 and each of five BiOX ligands (isopropyl (**L3**), 4-heptyl (**L2**), benzhydryl (**L6**), cyclohexyl (**L4**), and benzyl (**L7**)). All reactions were run in duplicate on 0.2 mmol scale. Yields were determined by  $^1\text{H-NMR}$  integration relative to 1,1,2,2-tetrachloroethane as an internal standard. Aliquots of the reactions were purified by preparative TLC to obtain clean material for chiral SFC analysis. The results of all runs are shown below, with the first yield and ee representing one trial and the second yield and ee representing the duplicate trial. For statistical modelling, the average ee of the two trials was used (yield was not used).



### 2.7.7 Computational Methods

Conformational searches were performed with Macromodel<sup>49</sup> version 11.7 with OPLS3e<sup>50</sup> (substrates) or OPLS\_2005<sup>51</sup> force field (complexes) and a constant dielectric of 7.58 corresponding to the dielectric constant of THF. To limit the number of conformers, an energy window of 10 kJ/mol relative to the minimum was utilized and mirror image conformations were not retained to avoid conformer duplication. Additionally, ligand conformers were found by performing the conformer searches with the full catalyst structure in order to restrict rotation about the central bond linking the two oxazoline rings. Subsequent DFT optimization of the ligand geometry was performed after removing the Ni and Br atoms. All conformers found under these conditions was submitted to DFT level optimization.

All structures were optimized in the gas phase with the B3LYP density functional,<sup>52,53</sup> the 6-31G\* basis set, and ultrafine integration grid as implemented in Gaussian16 (revision C.01).<sup>54</sup> Single point energy calculations were then performed on the optimized structures with the MO6-2X density functional<sup>55</sup> and the triple- $\zeta$  valence quality def2-TZVP basis set of Weigend and Ahlrichs.<sup>56</sup> Every geometry was confirmed to be optimized to a minimum as evidenced by the lack of imaginary frequencies. Gaussian input files were written using an in-house (Sigman lab) Python script and parameters were then collected from the optimized ground-states in a similar fashion to previous reports from the Sigman lab.<sup>34</sup> Optimized structures were visualized using CYLview.<sup>57</sup>

### Parameters Collected

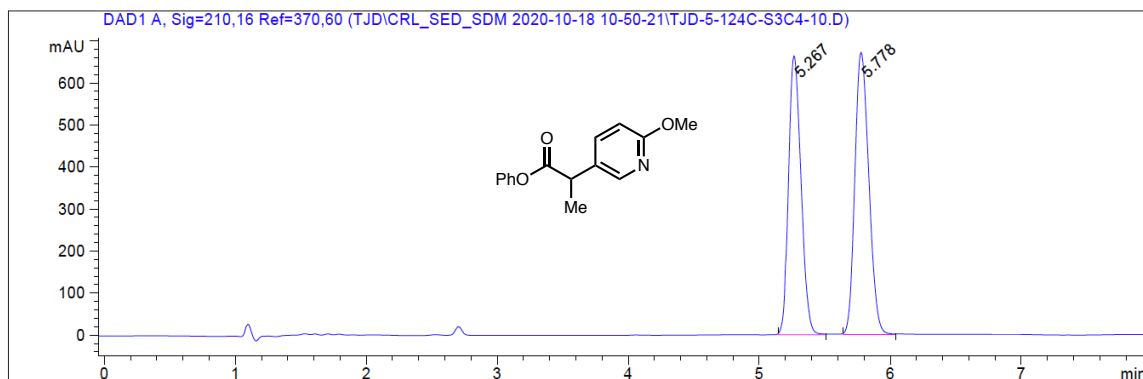
The full compilation of calculated parameters for each ligand and substrate are included in Appendix 2. Sterimol parameters  $L$ ,  $B_1$ , and  $B_5$  represent the length of a specified axis and the minimum and maximum widths, respectively, of a specified group along that axis. All Sterimol parameters were calculated with a modified version of Paton's Python script and CPK radii.<sup>58</sup> Sterimol values were collected along one distinct axis for the BiOX ligands and three distinct axes for the substrates as identified in Figure S3. Molecular surface area values were calculated in Macromodel.<sup>49</sup> All other parameters were collected using an in-house (Sigman lab) Python script. Boltzmann-weighting of conformer properties utilizing a 2.5 kcal/mol cutoff ( $T = 298$  K) was performed to obtain Boltzmann averaged properties.

### Multivariate Correlation Analysis

All model development was performed using an in-house (Sigman lab) Python script with a forward stepwise linear regression algorithm. In a similar manner to previous work in the Sigman group, the model was evaluated according to three different validation techniques (leave one out (LOO), K-fold, and test  $R^2$ ) to determine the robustness of the model as well as to check for model overfit.<sup>58</sup> The script normalized each molecular feature to allow the coefficients of the features to describe their relative importance and to allow for direct comparison. The ee data were split via a 75:25 ratio between the training set and test set. The split was partitioned based on the response values using either the "equidistant," "random," or "Kennard-Stone" functions written into the Python script.

### 2.7.8 SFC Traces of Racemic and Enantioenriched Products

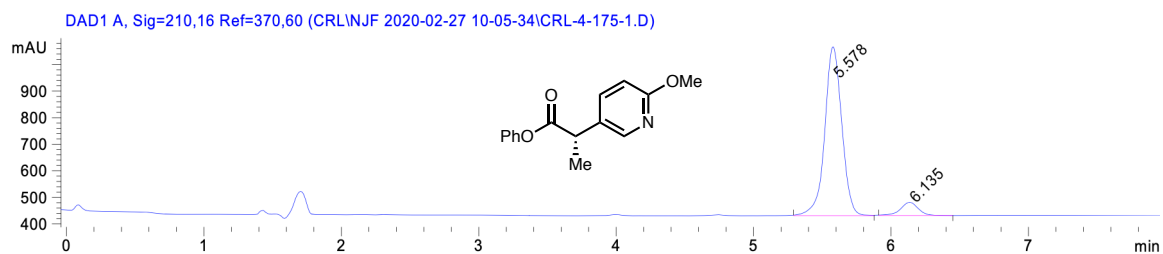
**116:** racemic



Signal 1: DAD1 A, Sig=210,16 Ref=370,60

Peak #	RetTime [min]	Type	Width [min]	Area [mAU*s]	Height [mAU]	Area %
1	5.267	BB	0.1056	4399.58740	661.64484	46.8769
2	5.778	BB	0.1187	4985.82080	670.74689	53.1231

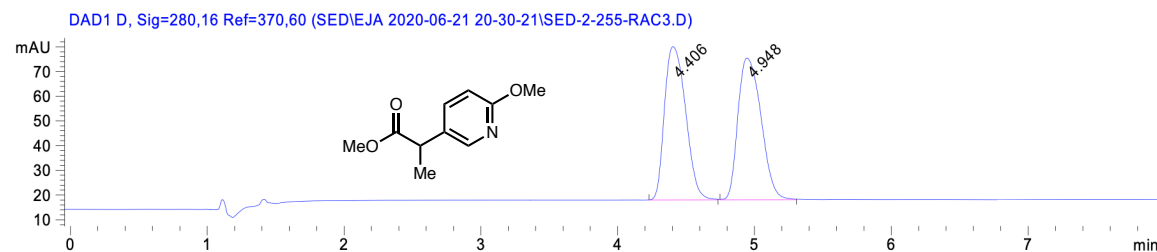
**116:** enantioenriched (85% ee)



Signal 1: DAD1 A, Sig=210,16 Ref=370,60

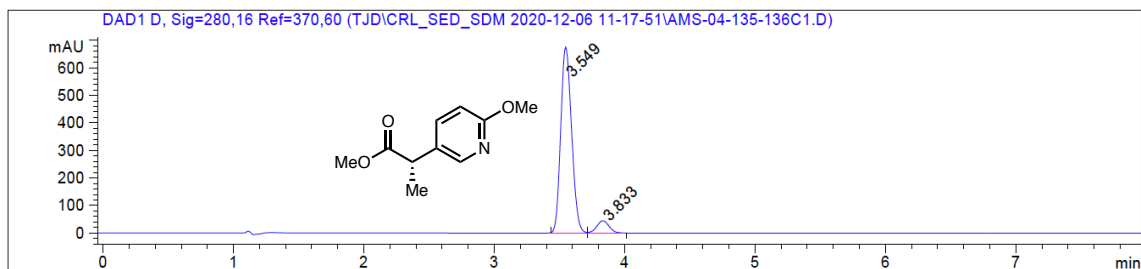
Peak #	RetTime [min]	Type	Width [min]	Area [mAU*s]	Height [mAU]	Area %
1	5.578	BB	0.1328	5477.42188	633.93433	92.4667
2	6.135	BB	0.1366	446.25061	49.78547	7.5333



**191: racemic**

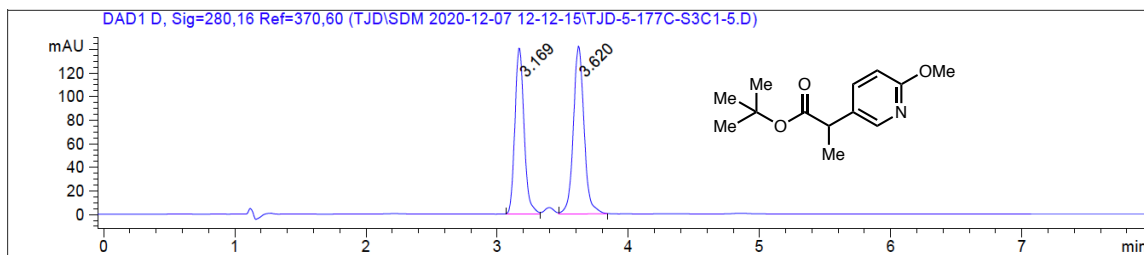
Signal 3: DAD1 D, Sig=280,16 Ref=370,60

Peak #	RetTime [min]	Type	Width [min]	Area [mAU*s]	Height [mAU]	Area %
1	4.406	BB	0.1733	666.45874	62.07742	49.7780
2	4.948	BB	0.1890	672.40375	57.26835	50.2220

**191: enantioenriched (84% ee)**

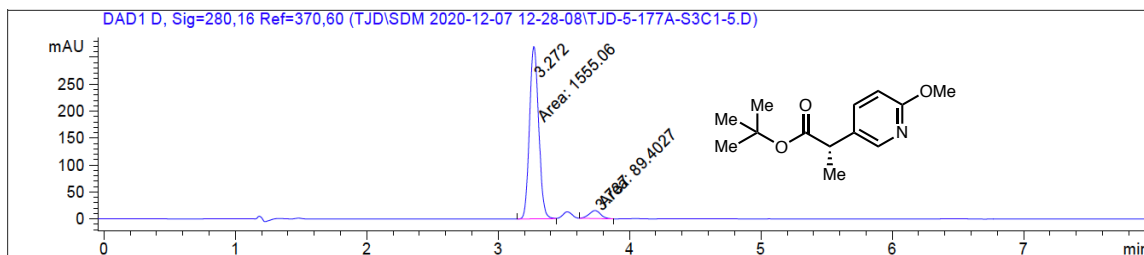
Signal 3: DAD1 D, Sig=280,16 Ref=370,60

Peak #	RetTime [min]	Type	Width [min]	Area [mAU*s]	Height [mAU]	Area %
1	3.549	BV	0.0917	3913.79761	674.04877	92.9594
2	3.833	VB	0.1011	296.42624	44.87164	7.0406

**192: racemic**

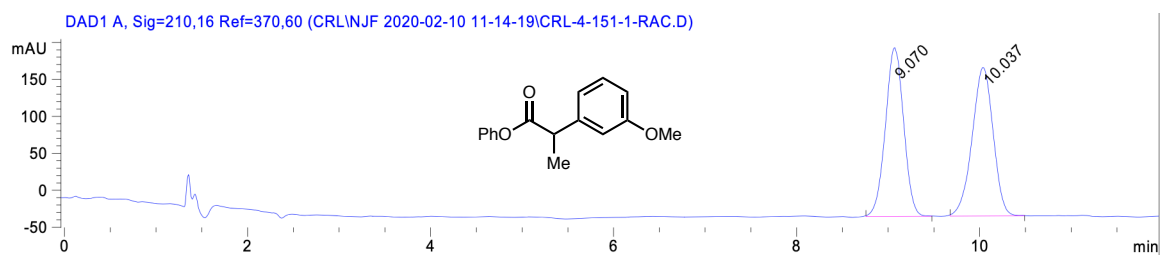
Signal 3: DAD1 D, Sig=280,16 Ref=370,60

Peak #	RetTime [min]	Type	Width [min]	Area [mAU*s]	Height [mAU]	Area %
1	3.169	BV	0.0770	684.62677	140.04613	45.8754
2	3.620	VB	0.0905	807.73425	141.75697	54.1246

**192: enantioenriched (89% ee)**

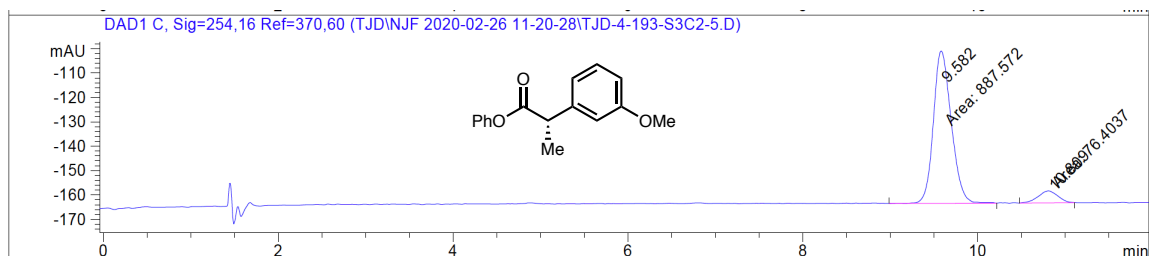
Signal 3: DAD1 D, Sig=280,16 Ref=370,60

Peak #	RetTime [min]	Type	Width [min]	Area [mAU*s]	Height [mAU]	Area %
1	3.272	MM	0.0803	1555.05725	322.73770	94.5634
2	3.737	MM	0.1000	89.40274	14.89493	5.4366

**120a: racemic**

Signal 1: DAD1 A, Sig=210,16 Ref=370,60

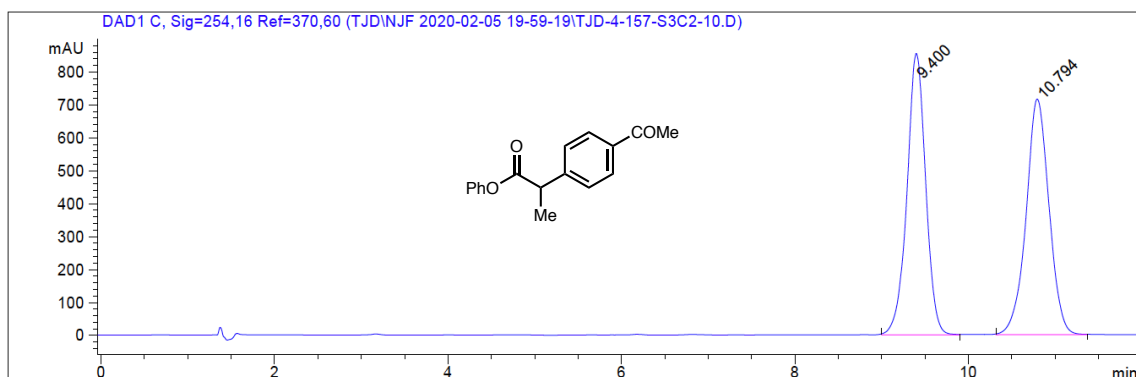
Peak #	RetTime [min]	Type	Width [min]	Area [mAU*s]	Height [mAU]	Area %
1	9.070	BB	0.2178	3161.34277	227.95787	49.6518
2	10.037	BB	0.2462	3205.68213	200.82071	50.3482

**120a: enantioenriched (84% ee)**

Signal 2: DAD1 C, Sig=254,16 Ref=370,60

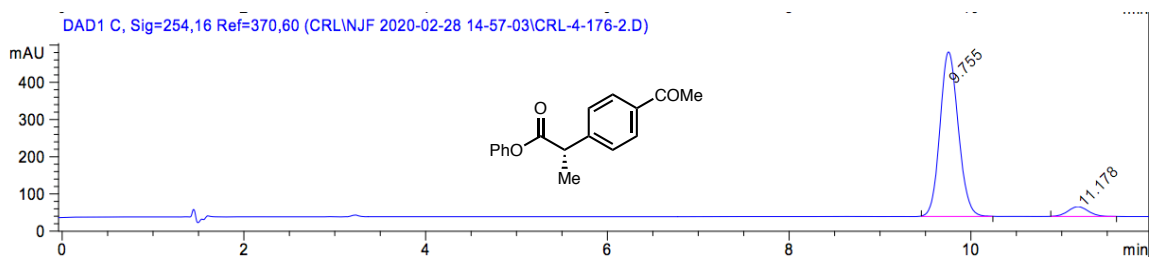
Peak #	RetTime [min]	Type	Width [min]	Area [mAU*s]	Height [mAU]	Area %
1	9.582	MM	0.2366	887.57214	62.52427	92.0741
2	10.809	MM	0.2580	76.40370	4.93502	7.9259

Totals : 963.97585 67.45928

**120b: racemic**

Signal 1: DAD1 C, Sig=254,16 Ref=370,60

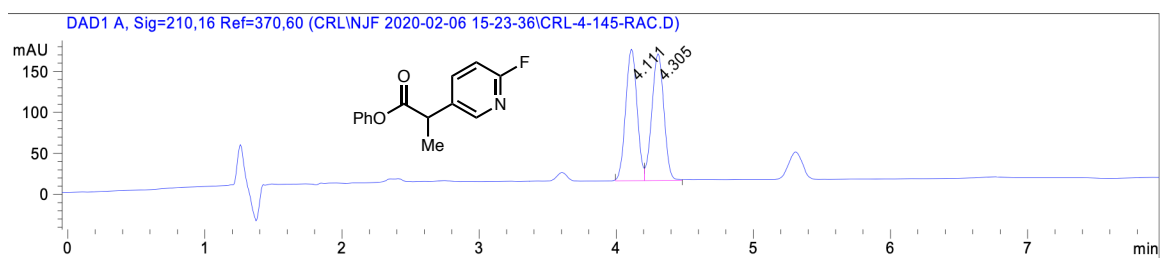
Peak #	RetTime [min]	Type	Width [min]	Area [mAU*s]	Height [mAU]	Area %
1	9.400	BB	0.2309	1.28069e4	854.31305	49.3412
2	10.794	BB	0.2785	1.31489e4	715.31354	50.6588

**120b: enantioenriched (87% ee)**

Signal 2: DAD1 C, Sig=254,16 Ref=370,60

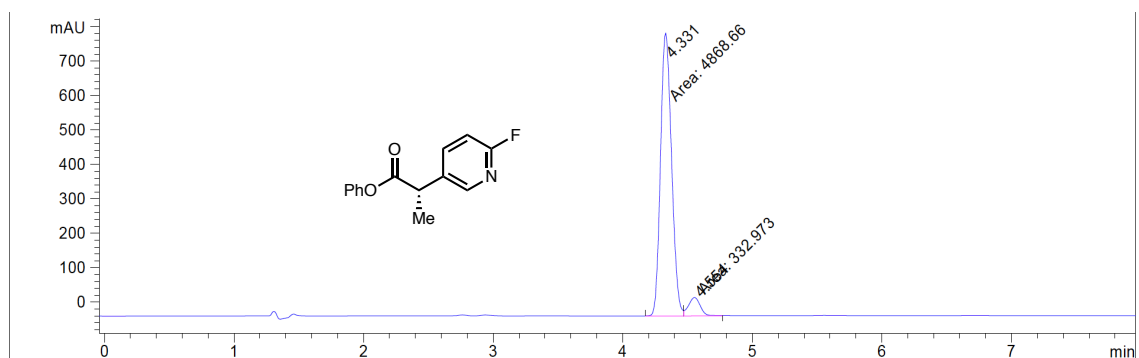
Peak #	RetTime [min]	Type	Width [min]	Area [mAU*s]	Height [mAU]	Area %
1	9.755	BB	0.2193	6186.69824	442.03229	93.7495
2	11.178	BB	0.2423	412.48062	26.39767	6.2505

Totals : 6599.17886 468.42995

**120c: racemic**

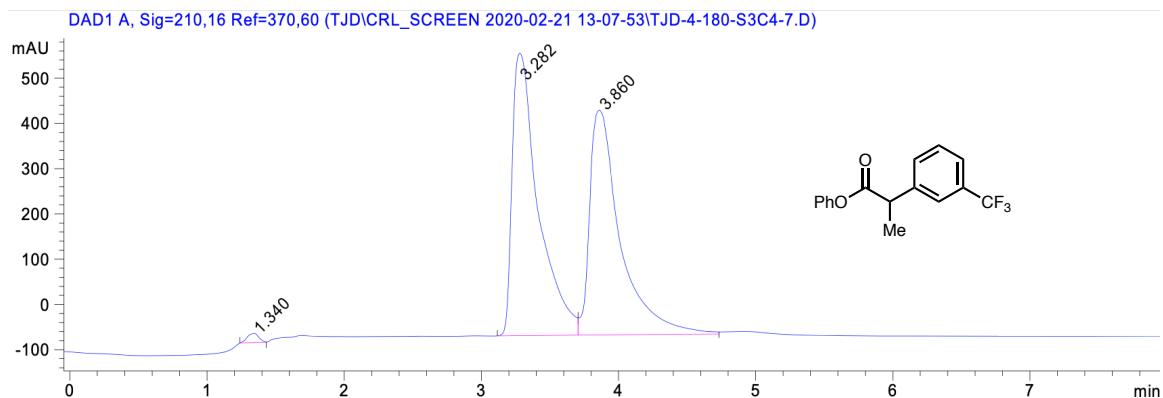
Signal 1: DAD1 A, Sig=210,16 Ref=370,60

Peak #	RetTime [min]	Type	Width [min]	Area [mAU*s]	Height [mAU]	Area %
1	4.111	BV	0.0917	926.81171	159.74318	49.6334
2	4.305	VB	0.0954	940.50269	153.77911	50.3666

**120c: enantioenriched (87% ee)**

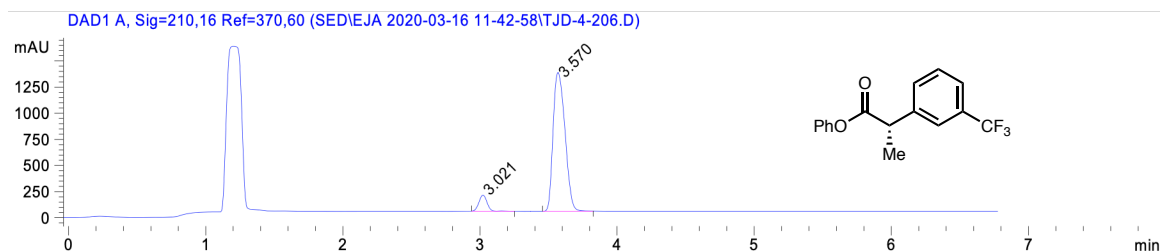
Signal 1: DAD1 C, Sig=254,16 Ref=370,60

Peak #	RetTime [min]	Type	Width [min]	Area [mAU*s]	Height [mAU]	Area %
1	4.331	MF	0.0982	4868.65674	826.07782	93.5987
2	4.554	FM	0.1038	332.97314	53.44642	6.4013

**120d: racemic**

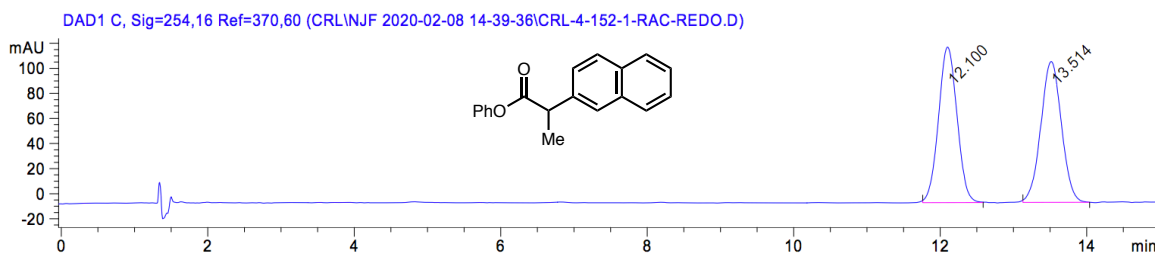
Signal 1: DAD1 A, Sig=210,16 Ref=370,60

Peak #	RetTime [min]	Type	Width [min]	Area [mAU*s]	Height [mAU]	Area %
1	1.340	BV	0.0950	117.00625	20.38576	0.7277
2	3.282	BV	0.1938	8219.68555	623.68298	51.1235
3	3.860	VB	0.2298	7741.40479	496.70050	48.1488

**120d: enantioenriched (85% ee)**

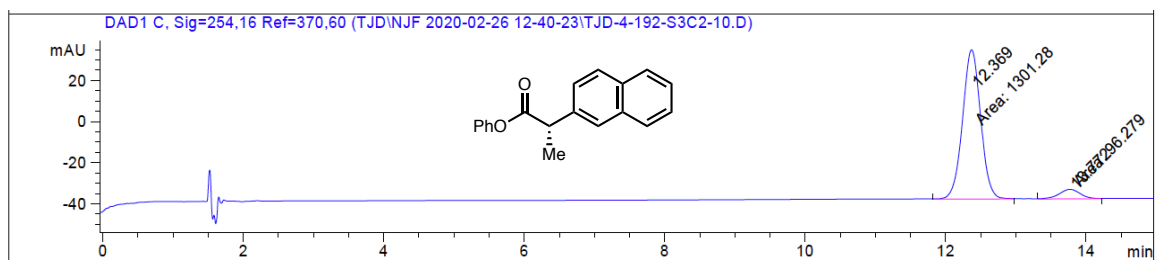
Signal 1: DAD1 A, Sig=210,16 Ref=370,60

Peak #	RetTime [min]	Type	Width [min]	Area [mAU*s]	Height [mAU]	Area %
1	3.021	BB	0.0654	648.23724	153.08775	7.4973
2	3.570	BB	0.0987	7997.99707	1320.49683	92.5027

**120e: racemic**

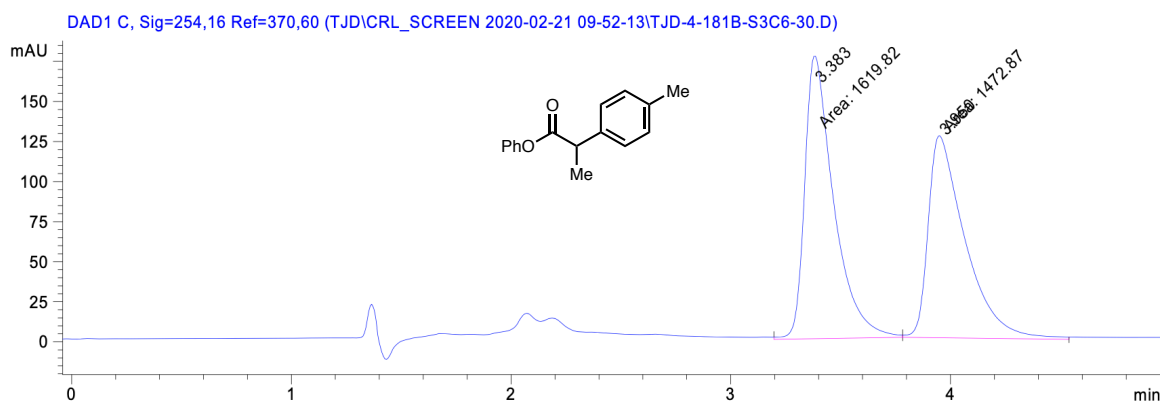
Signal 2: DAD1 C, Sig=254,16 Ref=370,60

Peak #	RetTime [min]	Type	Width [min]	Area [mAU*s]	Height [mAU]	Area %
1	12.100	BB	0.2733	2182.32544	124.00195	49.8075
2	13.514	BB	0.3042	2199.19604	112.41534	50.1925

**120e: enantioenriched (86% ee)**

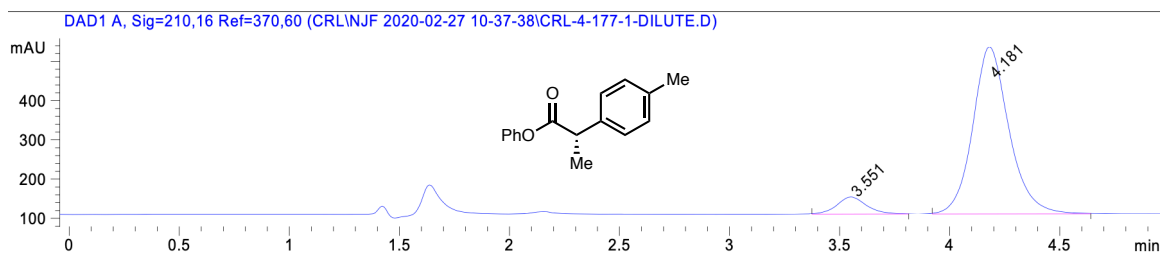
Signal 2: DAD1 C, Sig=254,16 Ref=370,60

Peak #	RetTime [min]	Type	Width [min]	Area [mAU*s]	Height [mAU]	Area %
1	12.369	MM	0.2984	1301.28259	72.68660	93.1109
2	13.772	MM	0.3490	96.27898	4.59845	6.8891

**120f: racemic**

Signal 1: DAD1 C, Sig=254,16 Ref=370,60

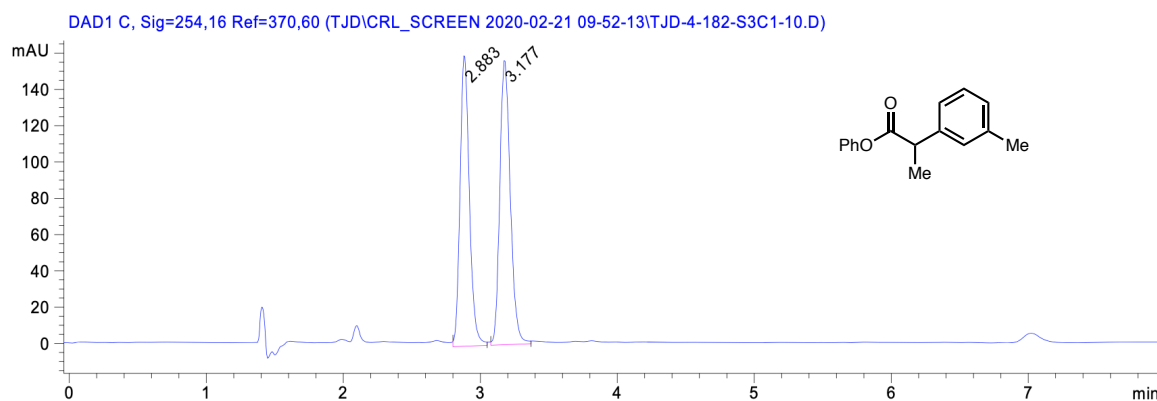
Peak #	RetTime [min]	Type	Width [min]	Area [mAU*s]	Height [mAU]	Area %
1	3.383	MM	0.1524	1619.82019	177.15884	52.3757
2	3.950	MM	0.1940	1472.87122	126.55457	47.6243

**120f: enantioenriched (85% ee)**

Signal 1: DAD1 A, Sig=210,16 Ref=370,60

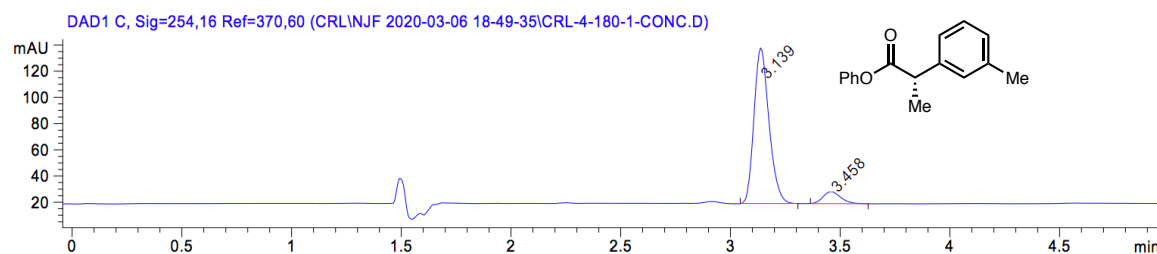
Peak #	RetTime [min]	Type	Width [min]	Area [mAU*s]	Height [mAU]	Area %
1	3.551	BB	0.1418	409.49893	43.51672	7.7344
2	4.181	BB	0.1741	4885.02783	425.09625	92.2656



**120g: racemic**

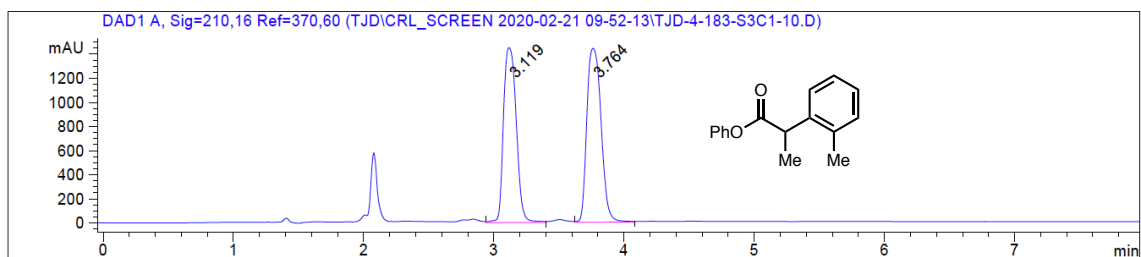
Signal 1: DAD1 C, Sig=254,16 Ref=370,60

Peak #	RetTime [min]	Type	Width [min]	Area [mAU*s]	Height [mAU]	Area %
1	2.883	BB	0.0716	760.25134	159.58742	47.6164
2	3.177	BB	0.0868	836.36414	155.34096	52.3836

**210g: enantioenriched (84% ee)**

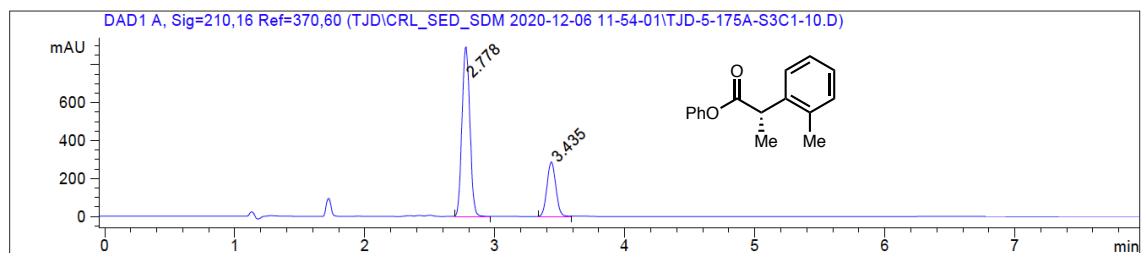
Signal 2: DAD1 C, Sig=254,16 Ref=370,60

Peak #	RetTime [min]	Type	Width [min]	Area [mAU*s]	Height [mAU]	Area %
1	3.139	BB	0.0756	562.89771	118.16418	91.8131
2	3.458	BB	0.0882	50.19327	9.11589	8.1869

**120h: racemic**

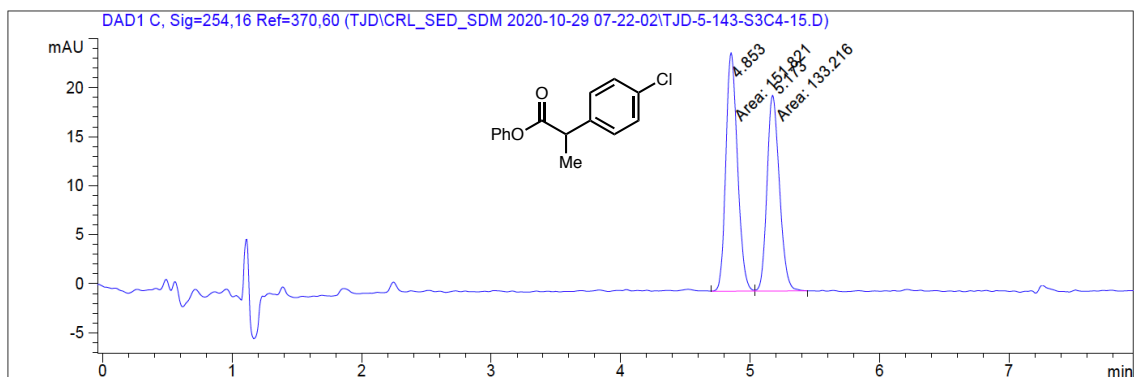
Signal 1: DAD1 A, Sig=210,16 Ref=370,60

Peak #	RetTime [min]	Type	Width [min]	Area [mAU*s]	Height [mAU]	Area %
1	3.119	VB	0.1078	9902.10938	1447.56604	47.4210
2	3.764	VB	0.1250	1.09792e4	1439.59082	52.5790

**120h: enantioenriched (47% ee)**

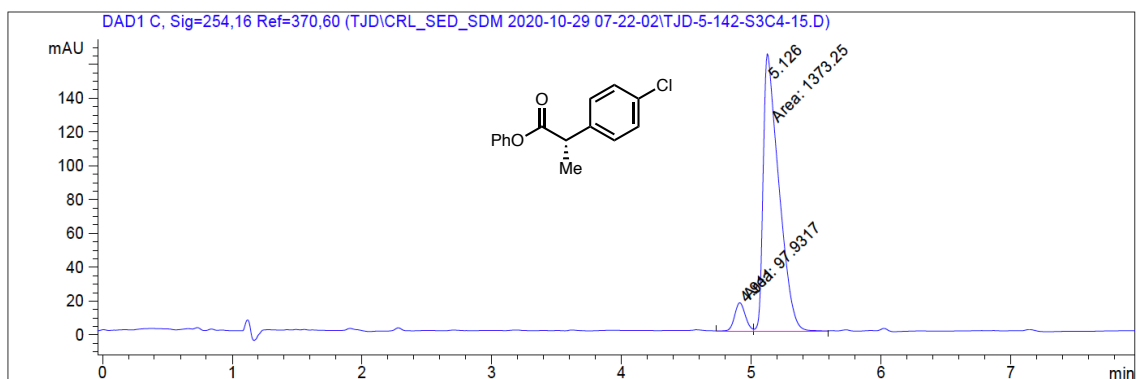
Peak #	RetTime [min]	Type	Width [min]	Area [mAU*s]	Height [mAU]	Area %
1	2.778	BB	0.0695	3782.13501	891.90027	73.4290
2	3.435	BB	0.0758	1368.59949	286.35406	26.5710

Totals : 5150.73450 1178.25433

**120i: racemic**

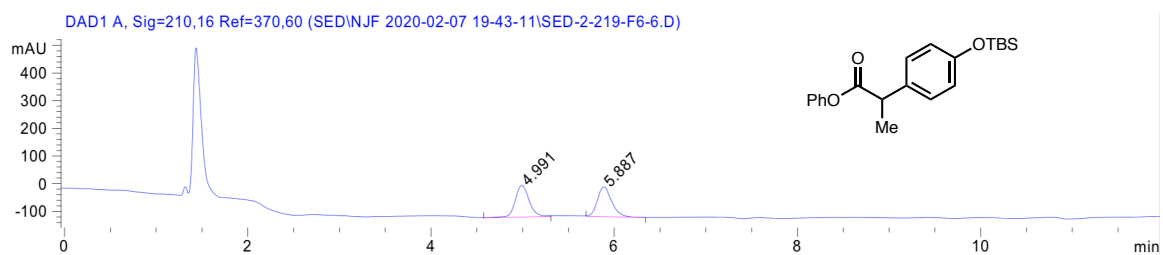
Signal 1: DAD1 C, Sig=254,16 Ref=370,60

Peak #	RetTime [min]	Type	Width [min]	Area [mAU*s]	Height [mAU]	Area %
1	4.853	MF	0.1035	151.82059	24.43783	53.2635
2	5.173	FM	0.1107	133.21631	20.05564	46.7365

**120i: enantioenriched (87% ee)**

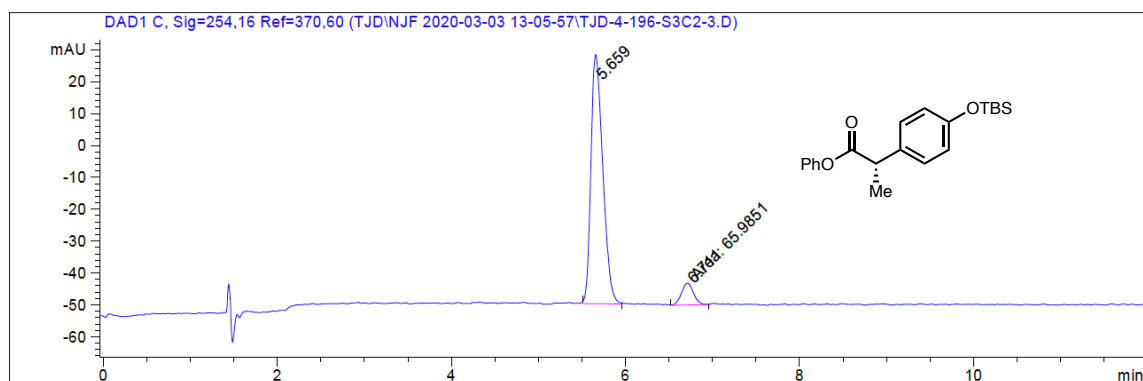
Signal 1: DAD1 C, Sig=254,16 Ref=370,60

Peak #	RetTime [min]	Type	Width [min]	Area [mAU*s]	Height [mAU]	Area %
1	4.911	MF	0.0966	97.93172	16.90302	6.6567
2	5.126	FM	0.1395	1373.25208	164.05779	93.3433

**120j: racemic**

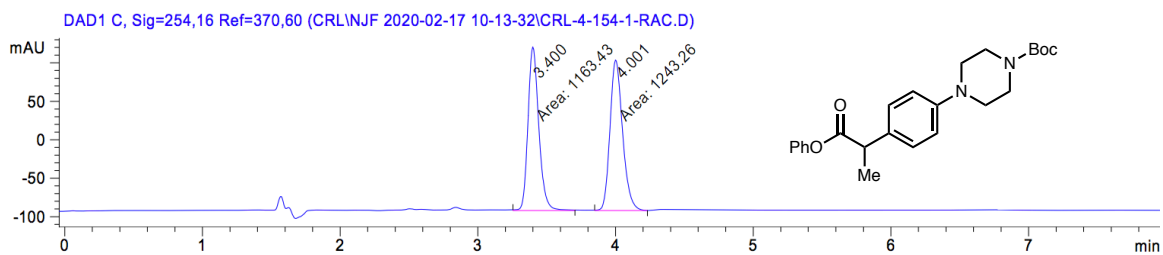
Signal 1: DAD1 A, Sig=210,16 Ref=370,60

Peak #	RetTime [min]	Type	Width [min]	Area [mAU*s]	Height [mAU]	Area %
1	4.991	VB	0.1636	1210.89258	114.33277	51.1595
2	5.887	BB	0.1674	1156.00208	107.50758	48.8405

**120j: enantioenriched (84% ee)**

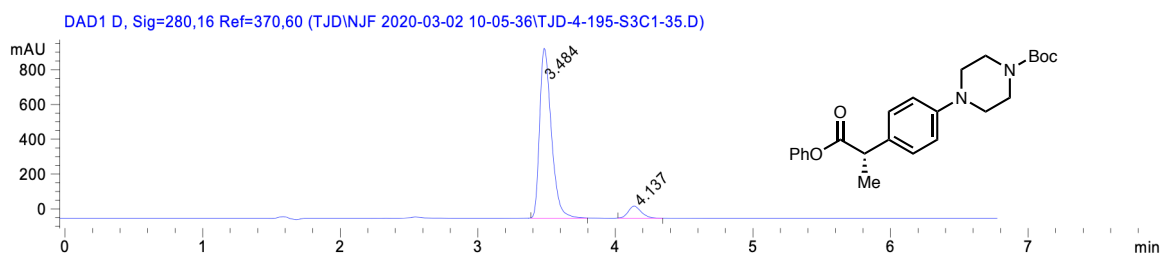
Signal 1: DAD1 C, Sig=254,16 Ref=370,60

Peak #	RetTime [min]	Type	Width [min]	Area [mAU*s]	Height [mAU]	Area %
1	5.659	BB	0.1465	741.06787	78.21878	91.8239
2	6.711	MM	0.1607	65.98505	6.84389	8.1761

**120k: racemic**

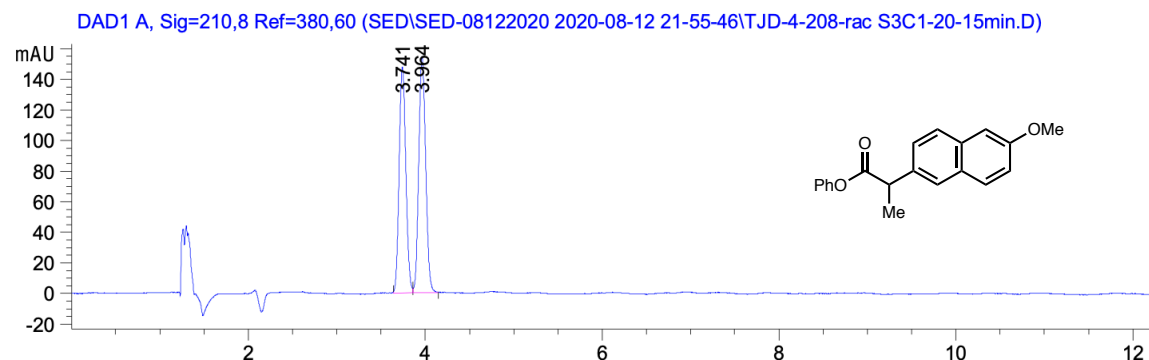
Signal 2: DAD1 C, Sig=254,16 Ref=370,60

Peak #	RetTime [min]	Type	Width [min]	Area [mAU*s]	Height [mAU]	Area %
1	3.400	MM	0.0908	1163.42700	213.53700	48.3415
2	4.001	MM	0.1052	1243.25525	196.90825	51.6585

**120k: enantioenriched (85% ee)**

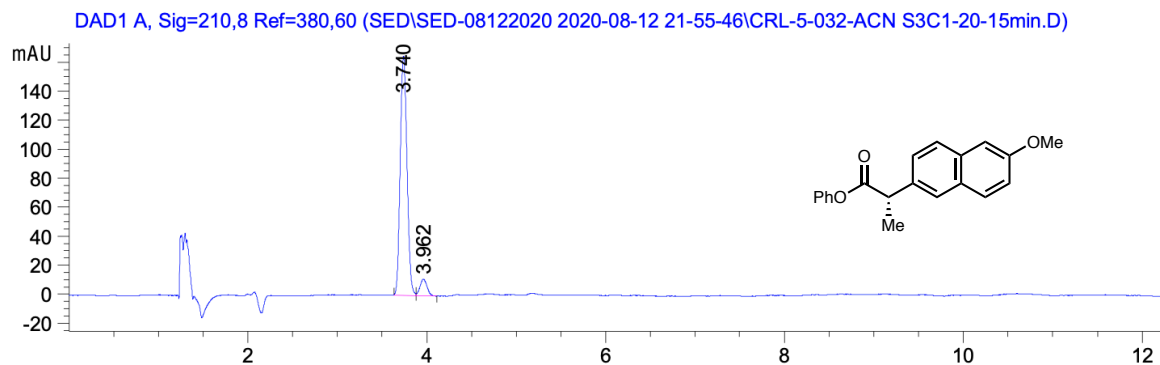
Signal 3: DAD1 D, Sig=280,16 Ref=370,60

Peak #	RetTime [min]	Type	Width [min]	Area [mAU*s]	Height [mAU]	Area %
1	3.484	BB	0.0929	5762.43311	976.36920	92.6488
2	4.137	BB	0.1010	457.21939	69.31146	7.3512

**122: racemic**

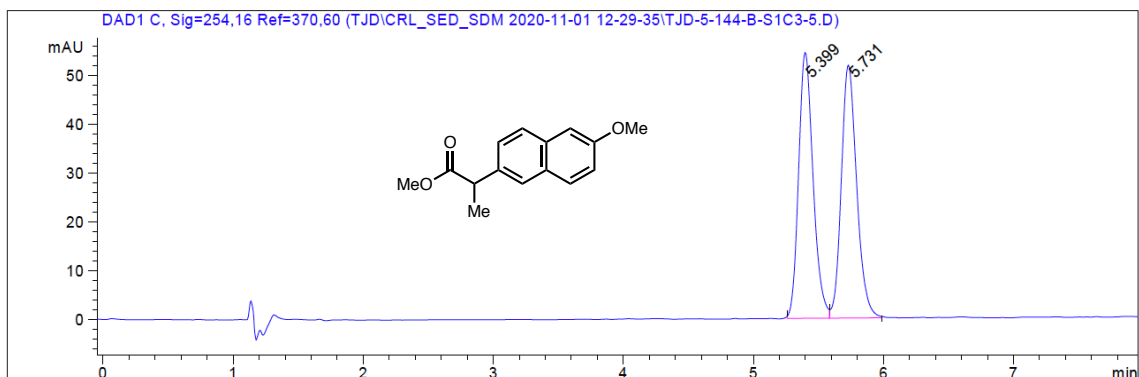
Signal 1: DAD1 A, Sig=210,8 Ref=380,60

Peak #	RetTime [min]	Type	Width [min]	Area [mAU*s]	Height [mAU]	Area %
1	3.741	BV	0.0827	781.13239	147.68906	48.0866
2	3.964	VB	0.0857	843.29541	154.40327	51.9134

**122: enantioenriched (86% ee)**

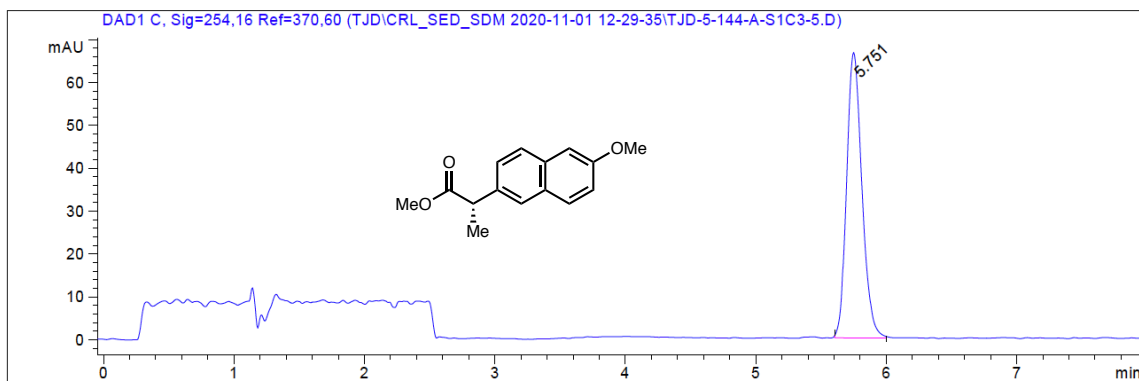
Signal 1: DAD1 A, Sig=210,8 Ref=380,60

Peak #	RetTime [min]	Type	Width [min]	Area [mAU*s]	Height [mAU]	Area %
1	3.740	BV	0.0836	871.17084	165.12762	93.2478
2	3.962	VB	0.0859	63.08263	11.51540	6.7522

**32-OMe: racemic**

Signal 1: DAD1 C, Sig=254,16 Ref=370,60

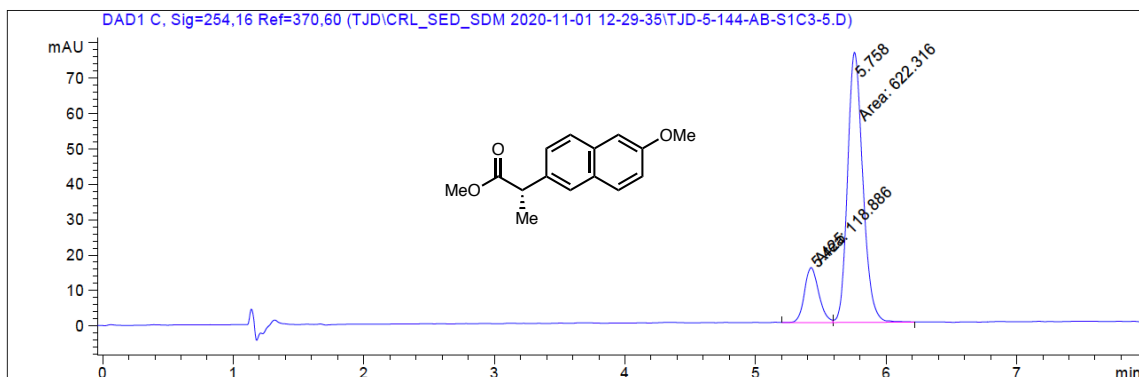
Peak #	RetTime [min]	Type	Width [min]	Area [mAU*s]	Height [mAU]	Area %
1	5.399	BV	0.1185	421.47626	54.33418	49.6834
2	5.731	VB	0.1283	426.84814	51.69842	50.3166

**32-OMe: from commercial (*S*)-naproxen**

Signal 1: DAD1 C, Sig=254,16 Ref=370,60

Peak #	RetTime [min]	Type	Width [min]	Area [mAU*s]	Height [mAU]	Area %
1	5.751	BB	0.1272	542.44702	66.49943	100.0000

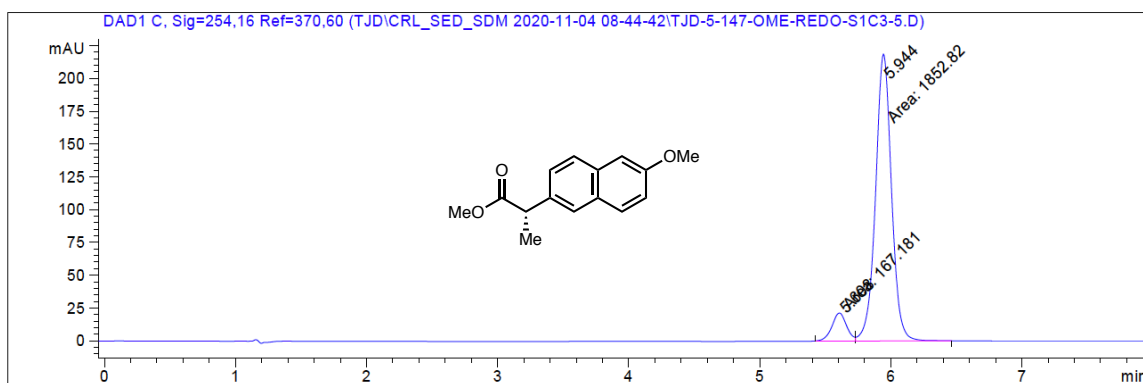
**32-OMe:** scalmic mixture of racemic **32-OMe** and **32-OMe** derived from (S)-naproxen



Signal 1: DAD1 C, Sig=254,16 Ref=370,60

Peak #	RetTime [min]	Type	Width [min]	Area [mAU*s]	Height [mAU]	Area %
1	5.425	MF	0.1271	118.88623	15.59370	16.0397
2	5.758	FM	0.1354	622.31573	76.57549	83.9603

**32-OMe:** enantioenriched (from coupling) (83% ee)

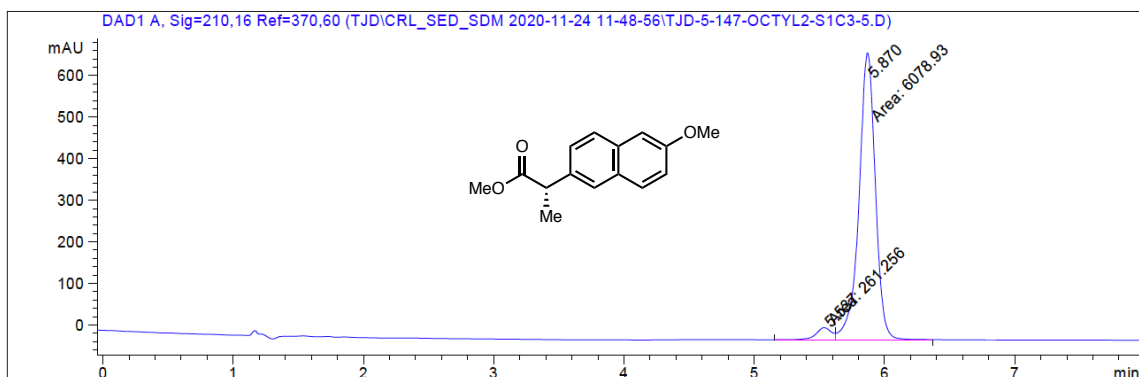


Signal 1: DAD1 C, Sig=254,16 Ref=370,60

Peak #	RetTime [min]	Type	Width [min]	Area [mAU*s]	Height [mAU]	Area %
1	5.608	MF	0.1294	167.18143	21.53582	8.2763
2	5.944	FM	0.1408	1852.82397	219.37854	91.7237

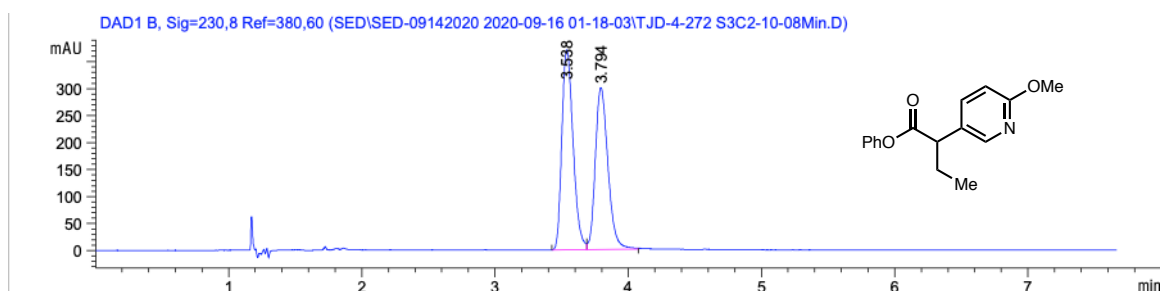


**32-OMe:** enantioenriched (after recrystallization) (92% ee)



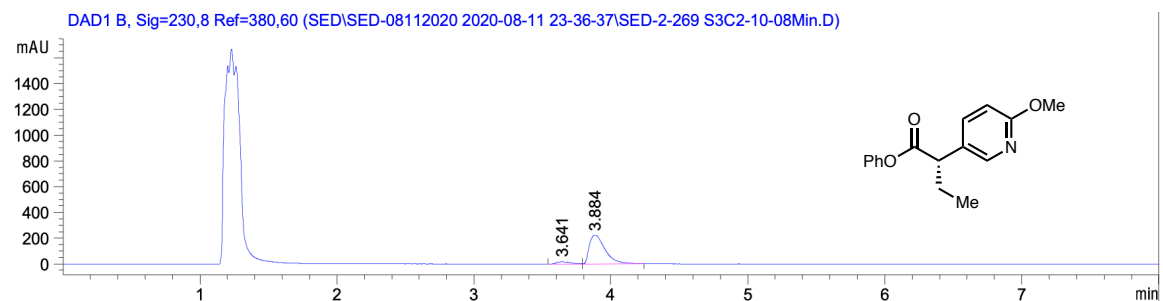
Signal 1: DAD1 A, Sig=210,16 Ref=370,60

Peak #	RetTime [min]	Type	Width [min]	Area [mAU*s]	Height [mAU]	Area %
1	5.537	MF	0.1456	261.25620	29.90784	4.1206
2	5.870	FM	0.1463	6078.92725	692.64124	95.8794

**128: racemic**

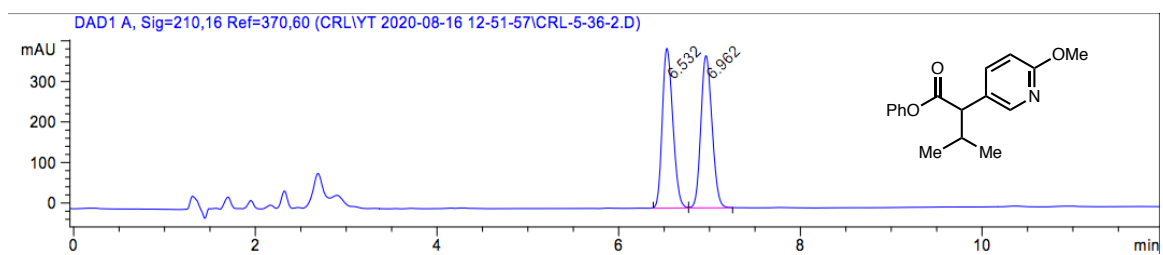
Signal 2: DAD1 B, Sig=230,8 Ref=380,60

Peak #	RetTime [min]	Type	Width [min]	Area [mAU*s]	Height [mAU]	Area %
1	3.538	BV	0.0914	2168.98657	370.22299	52.3424
2	3.794	VB	0.1029	1974.85364	299.69391	47.6576

**128: enantioenriched (88% ee)**

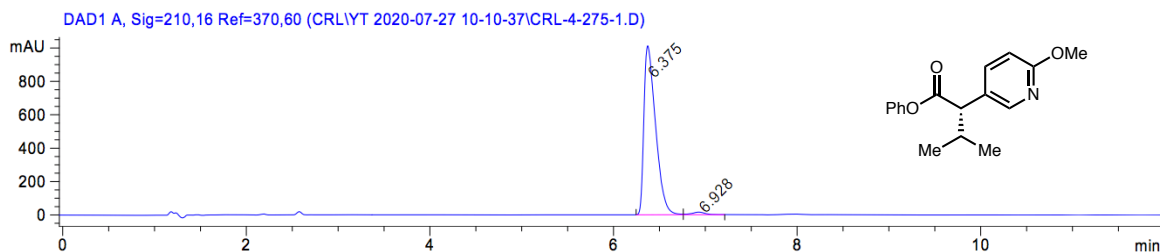
Signal 2: DAD1 B, Sig=230,8 Ref=380,60

Peak #	RetTime [min]	Type	Width [min]	Area [mAU*s]	Height [mAU]	Area %
1	3.641	BV	0.1008	117.22110	16.72034	6.0588
2	3.884	VB	0.1291	1817.48889	223.03073	93.9412

**129: racemic**

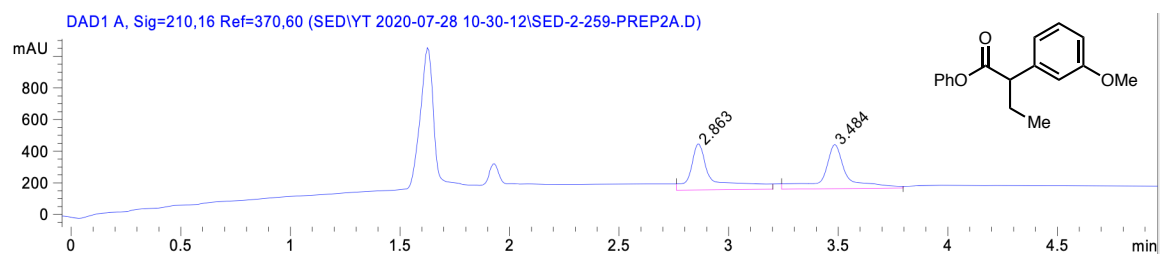
Signal 2: DAD1 C, Sig=254,16 Ref=370,60

Peak #	RetTime [min]	Type	Width [min]	Area [mAU*s]	Height [mAU]	Area %
1	6.532	BB	0.1258	477.47354	59.41205	50.2311
2	6.962	BB	0.1342	473.07962	56.19732	49.7689

**129: enantioenriched (96% ee)**

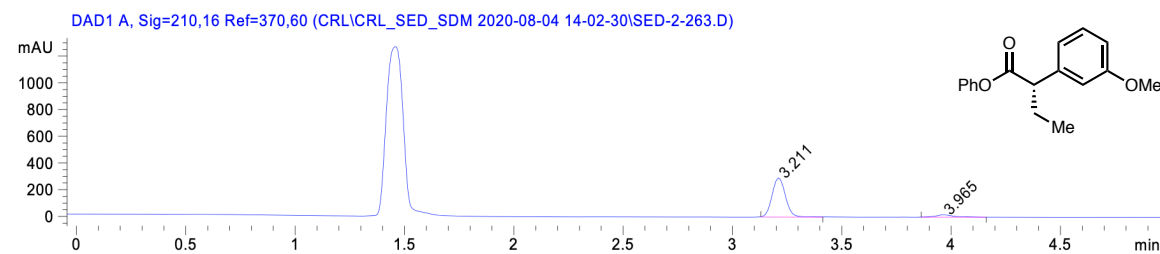
Peak #	RetTime [min]	Type	Width [min]	Area [mAU*s]	Height [mAU]	Area %
1	6.375	BV	0.1344	8893.69629	1013.02643	98.2261
2	6.928	VB	0.1465	160.61084	15.81807	1.7739

**130: racemic**



Peak #	RetTime [min]	Type	Width [min]	Area [mAU*s]	Height [mAU]	Area %
1	2.863	BB	0.0973	2002.59912	287.39008	49.3969
2	3.484	BV	0.1062	2051.50366	277.62616	50.6031

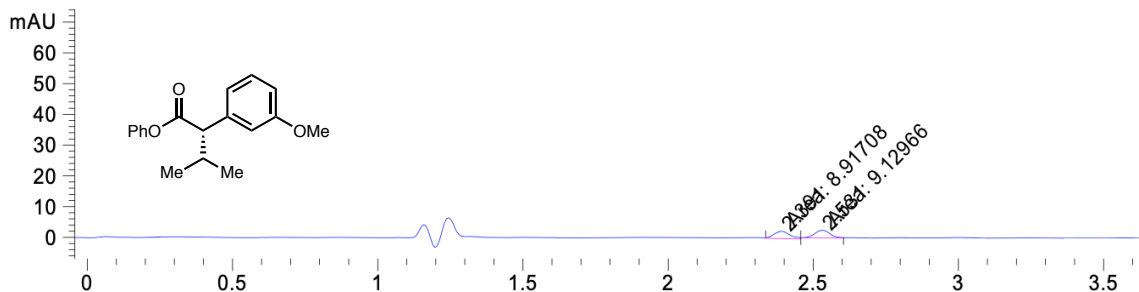
**130: enantioenriched (85% ee)**



Peak #	RetTime [min]	Type	Width [min]	Area [mAU*s]	Height [mAU]	Area %
1	3.211	BB	0.0700	1246.63501	291.08588	92.4092
2	3.965	BB	0.0851	102.40295	18.36087	7.5908

**131: racemic**

DAD1 C, Sig=254,16 Ref=370,60 (SED\YT 2020-07-26 18-06-08\SED-2-261-RAC.D)

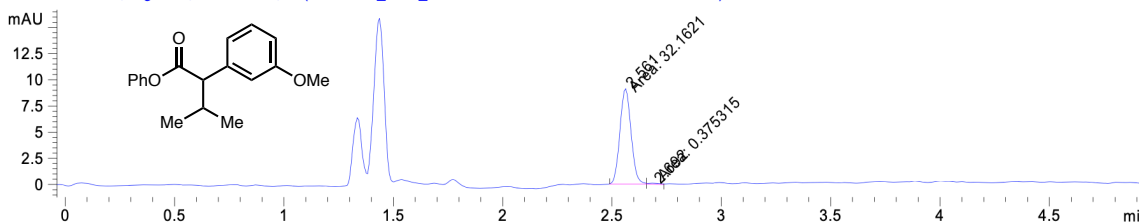


Signal 2: DAD1 C, Sig=254,16 Ref=370,60

Peak #	RetTime [min]	Type	Width [min]	Area [mAU*s]	Height [mAU]	Area %
1	2.391	MM	0.0622	8.91708	2.38762	49.4110
2	2.531	MM	0.0591	9.12966	2.57560	50.5890

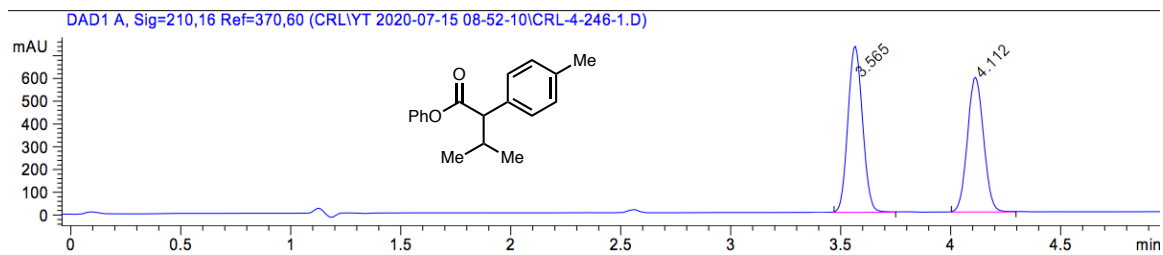
**131: enantioenriched (98% ee)**

DAD1 C, Sig=254,16 Ref=370,60 (CRL\CRL\_SED\_SDM 2020-08-04 14-02-30\SED-2-264.D)

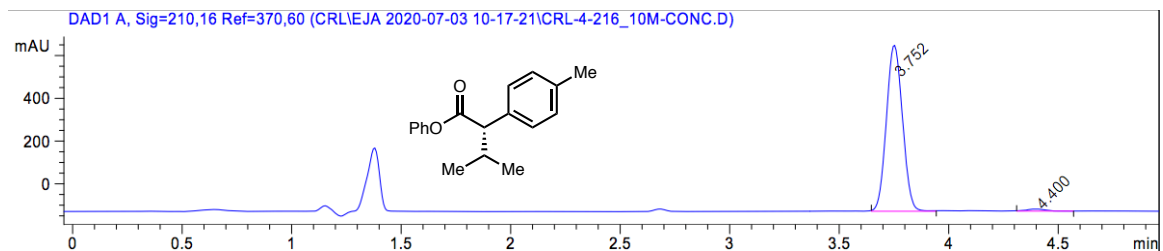


Signal 2: DAD1 C, Sig=254,16 Ref=370,60

Peak #	RetTime [min]	Type	Width [min]	Area [mAU*s]	Height [mAU]	Area %
1	2.561	MM	0.0584	32.16210	9.17854	98.8465
2	2.692	MM	0.0596	3.75315e-1	1.04957e-1	1.1535

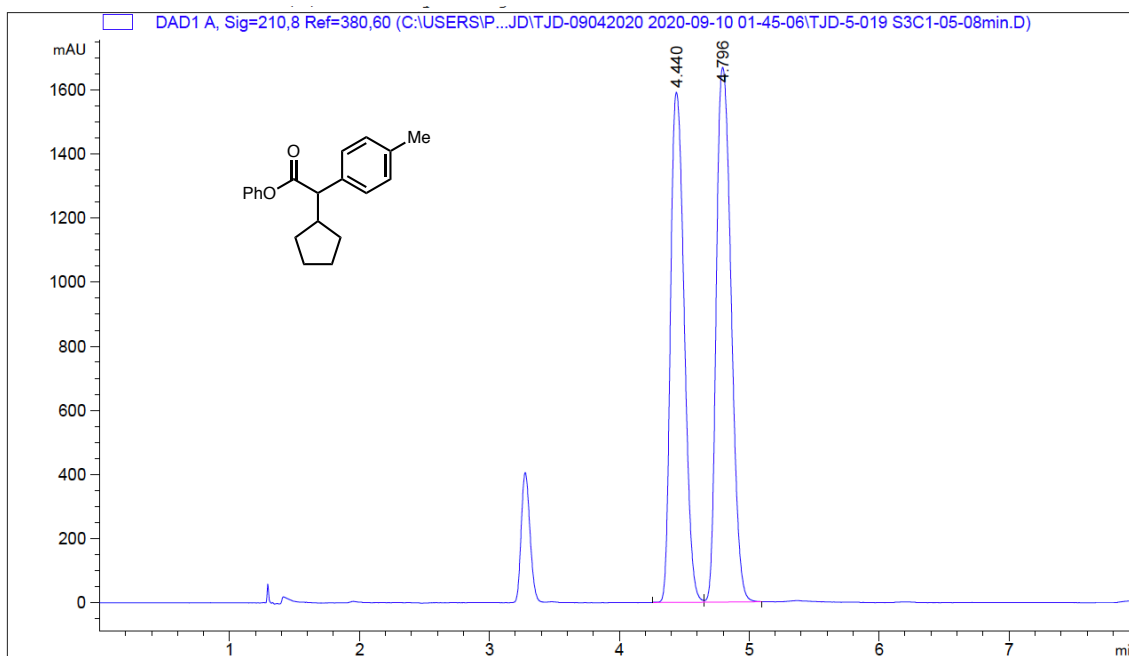
**132: racemic**

Peak #	RetTime [min]	Type	Width [min]	Area [mAU*s]	Height [mAU]	Area %
1	3.565	BB	0.0741	3370.06152	726.86560	52.6856
2	4.112	BB	0.0798	3026.49292	590.10248	47.3144

**132: enantioenriched (97% ee)**

Peak #	RetTime [min]	Type	Width [min]	Area [mAU*s]	Height [mAU]	Area %
1	3.752	BB	0.0840	3964.34082	771.31055	98.5706
2	4.400	BB	0.0911	57.48809	9.99575	1.4294

Totals : 4021.82891 781.30630

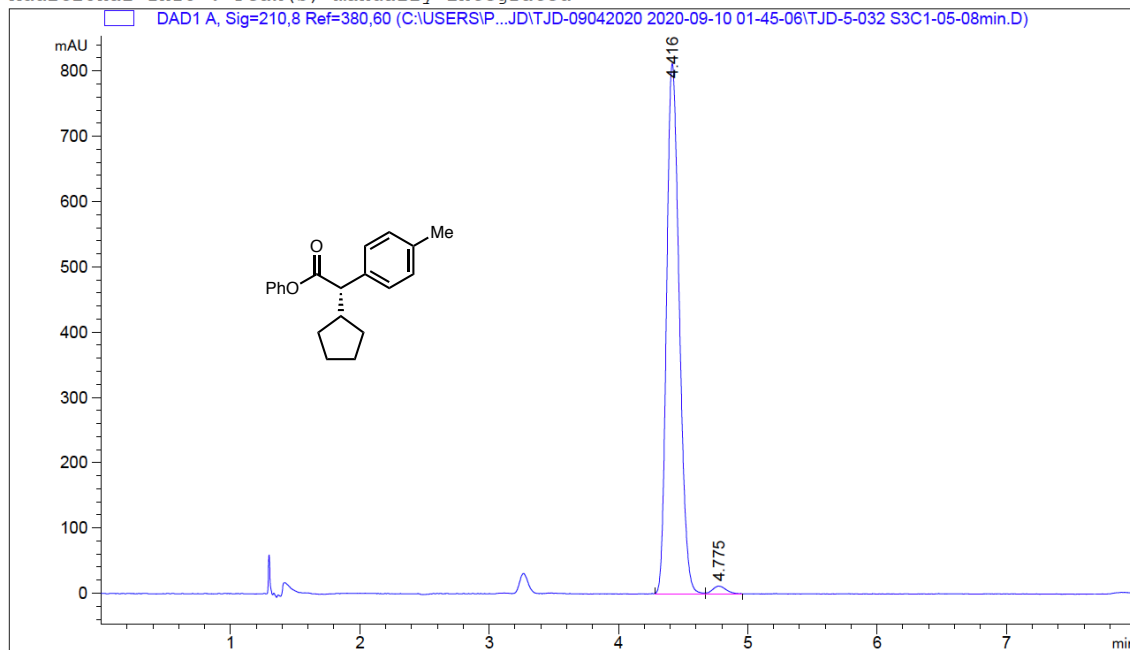
**134:** racemic

Signal 1: DAD1 A, Sig=210,8 Ref=380,60

Peak #	RetTime [min]	Type	Width [min]	Area [mAU*s]	Height [mAU]	Area %
1	4.440	BV	0.1160	1.16044e4	1592.55542	46.6413
2	4.796	VB	0.1278	1.32757e4	1669.30603	53.3587

**134: enantioenriched (97% ee)**

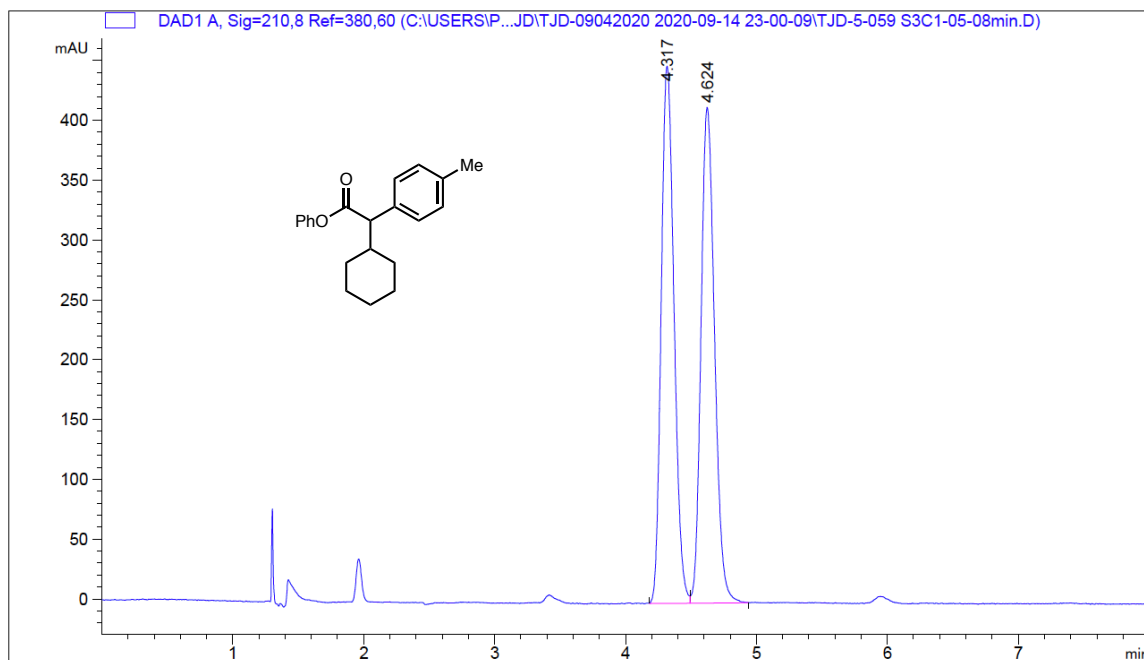
Additional Info : Peak(s) manually integrated



Signal 1: DAD1 A, Sig=210,8 Ref=380,60

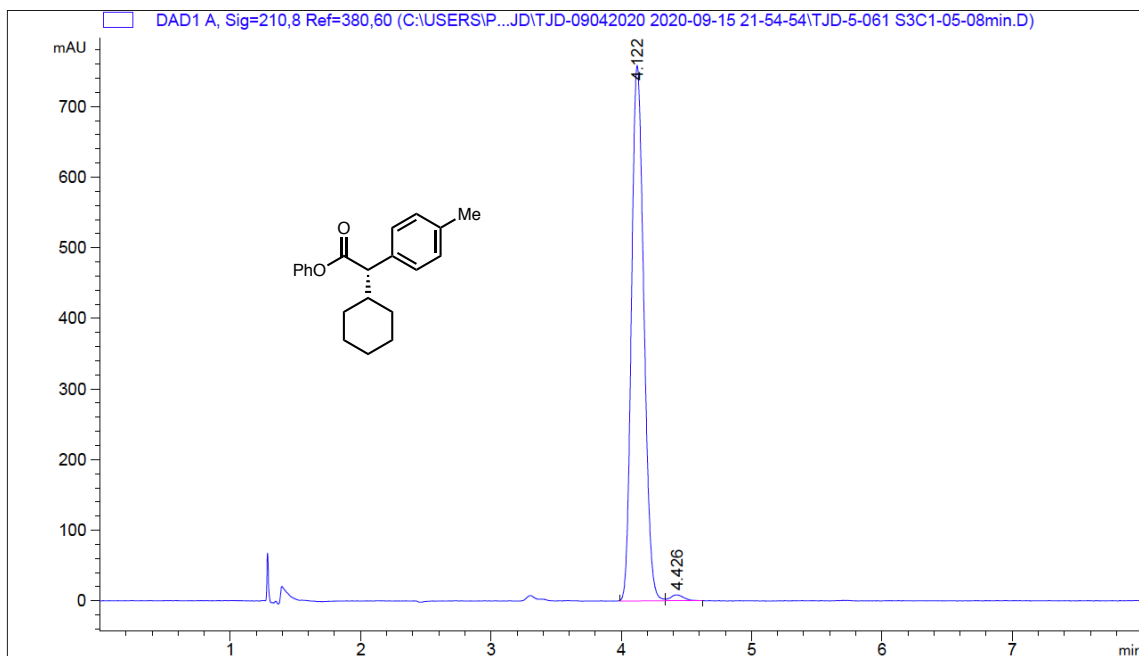
Peak #	RetTime [min]	Type	Width [min]	Area [mAU*s]	Height [mAU]	Area %
1	4.416	BB	0.1053	5520.55078	812.62140	98.4486
2	4.775	BB	0.1129	86.99767	11.95724	1.5514



**135:** racemic

Signal 1: DAD1 A, Sig=210,8 Ref=380,60

Peak #	RetTime [min]	Type	Width [min]	Area [mAU*s]	Height [mAU]	Area %
1	4.317	BV	0.1073	3052.68945	449.10693	50.5905
2	4.624	VB	0.1120	2981.42773	414.27054	49.4095

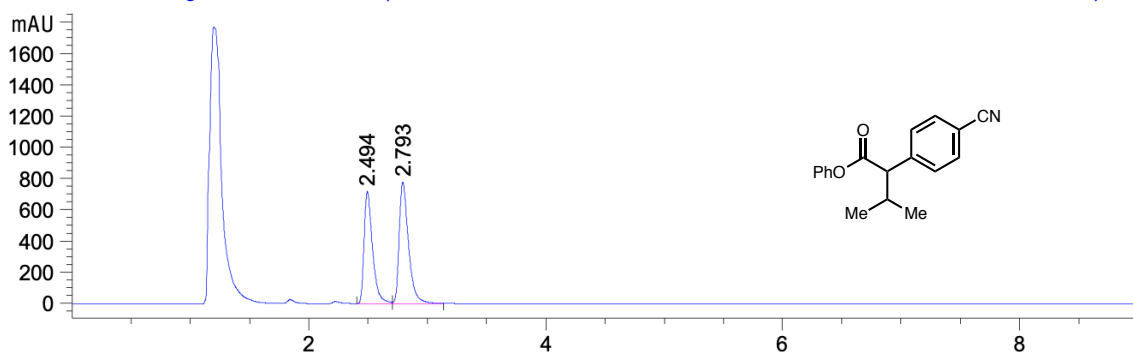
**135:** enantioenriched (98% ee)

Signal 1: DAD1 A, Sig=210,8 Ref=380,60

Peak #	RetTime [min]	Type	Width [min]	Area [mAU*s]	Height [mAU]	Area %
1	4.122	BV	0.1030	5002.38818	758.40417	98.7564
2	4.426	VB	0.1116	62.99316	8.48333	1.2436

**133: racemic**

DAD1 B, Sig=230,8 Ref=380,60 (SED\SED-08062020 2020-08-07 04-10-24\SED-2-273-B S3C2-20-12Min.D)

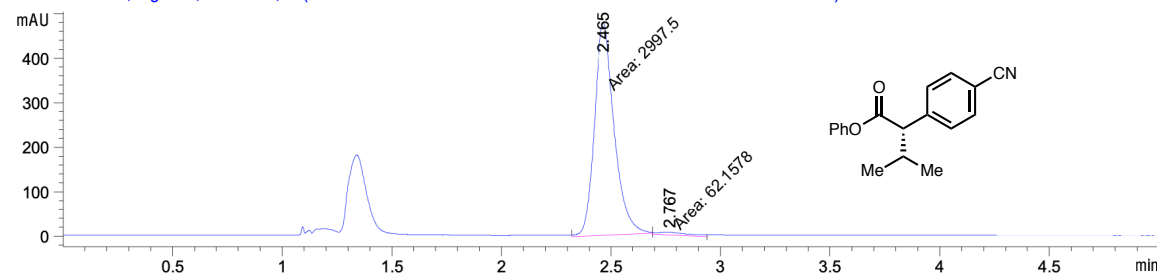


Signal 1: DAD1 A, Sig=210,8 Ref=380,60

Peak #	RetTime [min]	Type	Width [min]	Area [mAU*s]	Height [mAU]	Area %
1	2.494	BV	0.0749	1755.62146	354.03247	45.7863
2	2.793	VB	0.0824	2078.76001	382.38654	54.2137

**133: enantioenriched (96% ee)**

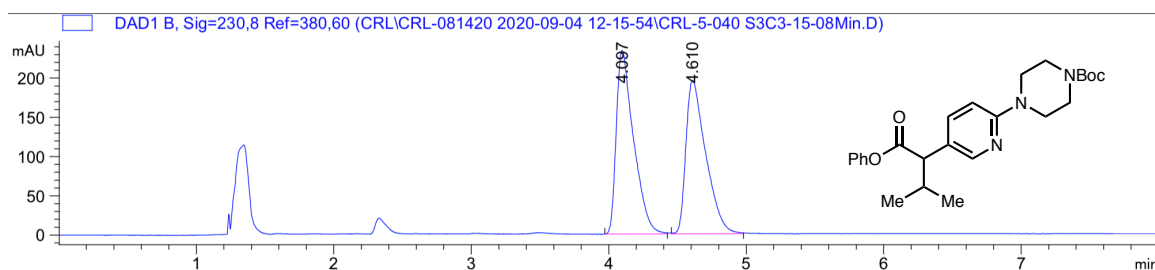
DAD1 B, Sig=230,8 Ref=380,60 (SED\SED-08112020 2020-08-11 23-36-37\SED-2-279 S3C2-20-05Min.D)



Signal 2: DAD1 B, Sig=230,8 Ref=380,60

Peak #	RetTime [min]	Type	Width [min]	Area [mAU*s]	Height [mAU]	Area %
1	2.465	MM	0.1044	2997.49683	478.73755	97.9685
2	2.767	MM	0.1767	62.15777	5.86131	2.0315

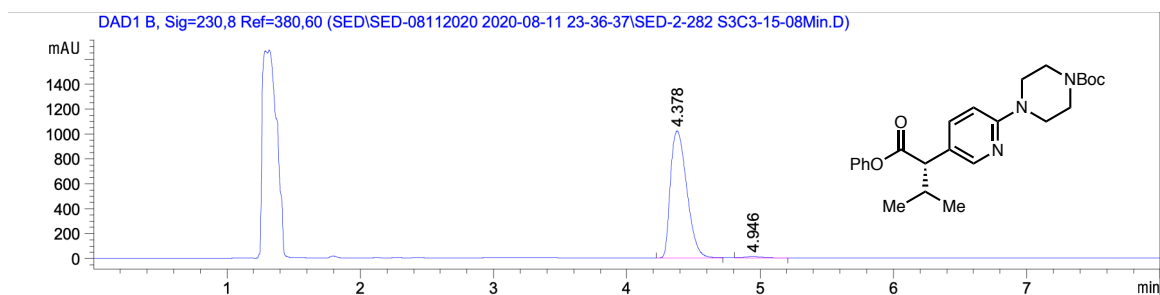
**136: racemic**



Signal 2: DAD1 B, Sig=230,8 Ref=380,60

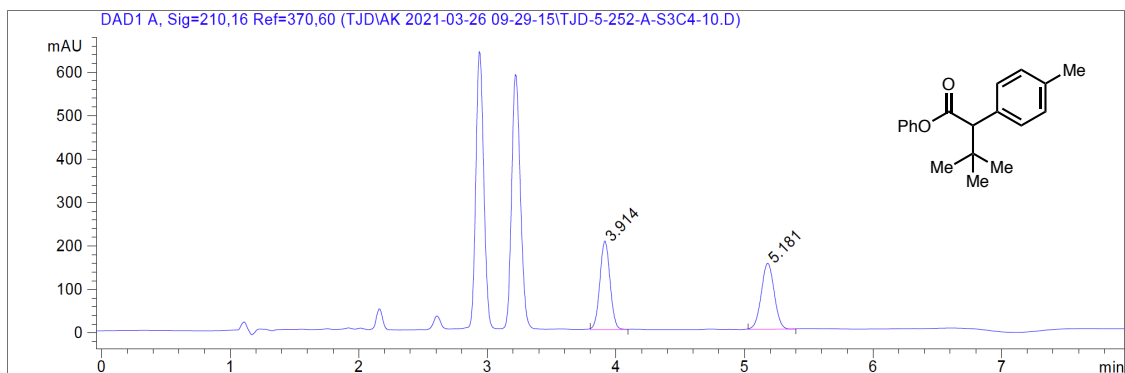
Peak #	RetTime [min]	Type	Width [min]	Area [mAU*s]	Height [mAU]	Area %
1	4.097	BB	0.1271	2048.80249	234.09145	51.1026
2	4.610	BB	0.1479	1960.39368	195.58250	48.8974

**136: enantioenriched (97% ee)**



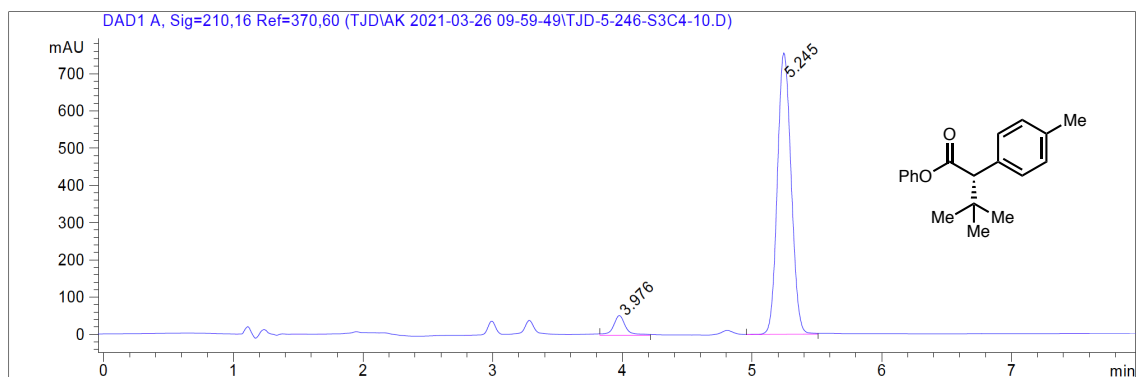
Signal 2: DAD1 B, Sig=230,8 Ref=380,60

Peak #	RetTime [min]	Type	Width [min]	Area [mAU*s]	Height [mAU]	Area %
1	4.378	BB	0.1357	8701.73438	1018.52362	98.6089
2	4.946	BB	0.1641	122.75417	11.09463	1.3911

**139: racemic**

Signal 1: DAD1 A, Sig=210,16 Ref=370,60

Peak #	RetTime [min]	Type	Width [min]	Area [mAU*s]	Height [mAU]	Area %
1	3.914	BB	0.0885	1121.01794	202.67258	51.2899
2	5.181	BB	0.1140	1064.63135	151.49474	48.7101

**139: enantioenriched (89% ee)**

Signal 1: DAD1 A, Sig=210,16 Ref=370,60

Peak #	RetTime [min]	Type	Width [min]	Area [mAU*s]	Height [mAU]	Area %
1	3.976	BB	0.0952	334.60458	51.92270	5.6587
2	5.245	VB	0.1182	5578.52588	754.67139	94.3413

## 2.8 NOTES AND REFERENCES

- (1) DeLano, T. J.; Dibrell, S. E.; Lacker, C. R.; Pancoast, A. R.; Poremba, K. E.; Cleary, L.; Sigman, M. S.; Reisman, S. E. *Chem. Sci.* **2021**, *12* (22), 7758–7762.
- (2) Putcha, L.; Cintrón, N. M.; Tsui, J.; Vanderploeg, J. M.; Kramer, W. G. *Pharm. Res.* **1989**, *6* (6), 481–485.
- (3) Hao, H.; Wang, G.; Sun, J. *EDrug Metab. Rev.* **2005**, *37* (1), 215–234.
- (4) Bonadonna, R. C.; Heise, T.; Arbet-Engels, C.; Kapitza, C.; Avogaro, A.; Grimsby, J.; Zhi, J.; Grippo, J. F.; Balena, R. *J. Clin. Endocrinol. Metab.* **2010**, *95* (11), 5028–5036.
- (5) Oehlrich, D.; Berthelot, D. J.-C.; Gijssen, H. J. M. *J. Med. Chem.* **2011**, *54* (3), 669–698.
- (6) Coghil, D.; Banaschewski, T.; Zuddas, A.; Pelaz, A.; Gagliano, A.; Doepfner, M. *BMC Psychiatry* **2013**, *13* (1), 237.
- (7) Angiolillo, D. J.; Weisman, S. M. *Am. J. Cardiovasc. Drugs* **2017**, *17* (2), 97–107.
- (8) Harrington, P. J.; Lodewijk, E. *Org. Process Res. Dev.* **1997**, *1* (1), 72–76.
- (9) Cherney, A. H.; Kadunce, N. T.; Reisman, S. E. *Chem. Rev.* **2015**, *115* (17), 9587–9652.
- (10) Dai, X.; Strotman, N. A.; Fu, G. C. *J. Am. Chem. Soc.* **2008**, *130* (11), 3302–3303.
- (11) Fischer, C.; Fu, G. C. *J. Am. Chem. Soc.* **2005**, *127* (13), 4594–4595.
- (12) Lou, S.; Fu, G. C. *J. Am. Chem. Soc.* **2010**, *132* (4), 1264–1266.
- (13) Lundin, P. M.; Fu, G. C. *J. Am. Chem. Soc.* **2010**, *132* (32), 11027–11029.
- (14) Wang, Z.; Yang, Z.-P.; Fu, G. C. *Nat. Chem.* **2021**, *13* (3), 236–242.

- (15) Yang, Z.-P.; Freas, D. J.; Fu, G. C. *J. Am. Chem. Soc.* **2021**, *143* (23), 8614–8618.
- (16) Yin, H.; Fu, G. C. *J. Am. Chem. Soc.* **2019**, *141* (38), 15433–15440.
- (17) Conan, A.; Sibille, S.; d’Incan, E.; Périchon, J. *J. Chem. Soc. Chem. Commun.* **1990**, *1*, 48–49.
- (18) Durandetti, M.; Sibille, S.; Nédélec, J.-Y.; Périchon, J. *Synth. Commun.* **1994**, *24* (2), 145–151.
- (19) Durandetti, M.; Nédélec, J.-Y.; Périchon, J. *J. Org. Chem.* **1996**, *61* (5), 1748–1755.
- (20) Durandetti, M.; Périchon, J. *Synthesis* **2004**, *2004* (18), 3079–3083.
- (21) Durandetti, M.; Gosmini, C.; Périchon, J. Ni-Catalyzed Activation of  $\alpha$ -Chloroesters: A Simple Method for the Synthesis of  $\alpha$ -Arylesters and  $\beta$ -Hydroxyesters. *Tetrahedron* **2007**, *63* (5), 1146–1153.  
<https://doi.org/10.1016/j.tet.2006.11.055>.
- (22) Poremba, K. E.; Dibrell, S. E.; Reisman, S. E. *ACS Catal.* **2020**, *10* (15), 8237–8246.
- (23) Guan, H.; Zhang, Q.; Walsh, P. J.; Mao, J. *Angew. Chem. Int. Ed.* **2020**, *59* (13), 5172–5177.
- (24) Cherney, A. H.; Kadunce, N. T.; Reisman, S. E. *J. Am. Chem. Soc.* **2013**, *135* (20), 7442–7445.
- (25) Kadunce, N. T.; Reisman, S. E. *J. Am. Chem. Soc.* **2015**, *137* (33), 10480–10483.
- (26) Poremba, K. E. Development of Nickel-Catalyzed Asymmetric Reductive Cross-Coupling Reactions. Ph.D., California Institute of Technology, 2019.
- (27) Poremba, K. E.; Kadunce, N. T.; Suzuki, N.; Cherney, A. H.; Reisman, S. E. *J. Am. Chem. Soc.* **2017**, *139* (16), 5684–5687.

- (28) Molander, G. A.; Traister, K. M.; O'Neill, B. T. *J. Org. Chem.* **2014**, *79* (12), 5771–5780.
- (29) This trend was not observed in our development of a related Ni/photoredox method (see Chapter 3).
- (30) Suzuki, N.; Hofstra, J. L.; Poremba, K. E.; Reisman, S. E. *Org. Lett.* **2017**, *19* (8), 2150–2153.
- (31) Jin, M.; Adak, L.; Nakamura, M. *J. Am. Chem. Soc.* **2015**, *137* (22), 7128–7134.
- (32) Santiago, C. B.; Guo, J.-Y.; Sigman, M. S. *Chem. Sci.* **2018**, *9* (9), 2398–2412.
- (33) See Experimental Section.
- (34) Zhao, S.; Gensch, T.; Murray, B.; Niemeyer, Z. L.; Sigman, M. S.; Biscoe, M. R. *Science* **2018**, *362* (6415), 670–674.
- (35) Biswas, S.; Weix, D. J. *J. Am. Chem. Soc.* **2013**, *135* (43), 16192–16197.
- (36) Still, W. C.; Kahn, M.; Mitra, A. *J. Org. Chem.* **1978**, *43* (14), 2923–2925.
- (37) Takeuchi, K.; Ishida, S.; Nishikata, T. *Chem. Lett.* **2017**, *46* (5), 644–646.
- (38) Mao, J.; Liu, F.; Wang, M.; Wu, L.; Zheng, B.; Liu, S.; Zhong, J.; Bian, Q.; Walsh, P. J. *J. Am. Chem. Soc.* **2014**, *136* (50), 17662–17668.
- (39) Hattori, H.; Roesslein, J.; Caspers, P.; Zerbe, K.; Miyatake-Onozabal, H.; Ritz, D.; Rueedi, G.; Gademann, K. *Angew. Chem. Int. Ed.* **2018**, *57* (34), 11020–11024.
- (40) Baar, C. R.; Levy, C. J.; Min, E. Y.-J.; Henling, L. M.; Day, M. W.; Bercaw, J. E. *J. Am. Chem. Soc.* **2004**, *126* (26), 8216–8231.
- (41) Wang, Y.-F.; Gao, Y.-R.; Mao, S.; Zhang, Y.-L.; Guo, D.-D.; Yan, Z.-L.; Guo, S.-H.; Wang, Y.-Q. *Org. Lett.* **2014**, *16* (6), 1610–1613.



- (42) Kurimoto, Y.; Nasu, T.; Fujii, Y.; Asano, K.; Matsubara, S. *Org. Lett.* **2019**, *21* (7), 2156–2160.
- (43) Smith, W. B. *J. Org. Chem.* **1985**, *50* (19), 3649–3651.
- (44) Ogawa, T.; Ohta, K.; Iijima, T.; Suzuki, T.; Ohta, S.; Endo, Y. *Bioorg. Med. Chem.* **2009**, *17* (3), 1109–1117.
- (45) Ren, W.; Chang, W.; Wang, Y.; Li, J.; Shi, Y. *Org. Lett.* **2015**, *17* (14), 3544–3547.
- (46) Hanna, G. M.; Lau-Cam, C. A. *J. AOAC Int.* **1992**, *75* (3), 417–422.
- (47) Cahiez, G.; Chau, K.; Cléry, P. *Tetrahedron Lett.* **1994**, *35* (19), 3069–3072.
- (48) Katayev, D.; Matoušek, V.; Koller, R.; Togni, A. *Org. Lett.* **2015**, *17* (23), 5898–5901.
- (49) MacroModel; Version 11.7 Ed.; Schrödinger, LLC: New York, NY, 2017.
- (50) Roos, K.; Wu, C.; Damm, W.; Reboul, M.; Stevenson, J. M.; Lu, C.; Dahlgren, M. K.; Mondal, S.; Chen, W.; Wang, L.; Abel, R.; Friesner, R. A.; Harder, E. D. *J. Chem. Theory Comput.* **2019**, *15* (3), 1863–1874.
- (51) Banks, J. L.; Beard, H. S.; Cao, Y.; Cho, A. E.; Damm, W.; Farid, R.; Felts, A. K.; Halgren, T. A.; Mainz, D. T.; Maple, J. R.; Murphy, R.; Philipp, D. M.; Repasky, M. P.; Zhang, L. Y.; Berne, B. J.; Friesner, R. A.; Gallicchio, E.; Levy, R. M. *J. Comput. Chem.* **2005**, *26* (16), 1752–1780.
- (52) Becke, A. D. *Phys. Rev. A* **1988**, *38* (6), 3098–3100.
- (53) Lee, C.; Yang, W.; Parr, R. G. *Phys. Rev. B* **1988**, *37* (2), 785–789.
- (54) Gaussian 16, Revision C.01, M. J. Frisch, G. W. Trucks, H. B. Schlegel, G. E. Scuseria, M. A. Robb, J. R. Cheeseman, G. Scalmani, V. Barone, G. A. Petersson, H. Nakatsuji, X. Li, M. Caricato, A. V. Marenich, J. Bloino, B. G. Janesko, R.

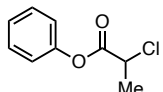
Gomperts, B. Mennucci, H. P. Hratchian, J. V. Ortiz, A. F. Izmaylov, J. L. Sonnenberg, D. Williams-Young, F. Ding, F. Lipparini, F. Egidi, J. Goings, B. Peng, A. Petrone, T. Henderson, D. Ranasinghe, V. G. Zakrzewski, J. Gao, N. Rega, G. Zheng, W. Liang, M. Hada, M. Ehara, K. Toyota, R. Fukuda, J. Hasegawa, M. Ishida, T. Nakajima, Y. Honda, O. Kitao, H. Nakai, T. Vreven, K. Throssell, J. A. Montgomery, Jr., J. E. Peralta, F. Ogliaro, M. J. Bearpark, J. J. Heyd, E. N. Brothers, K. N. Kudin, V. N. Staroverov, T. A. Keith, R. Kobayashi, J. Normand, K. Raghavachari, A. P. Rendell, J. C. Burant, S. S. Iyengar, J. Tomasi, M. Cossi, J. M. Millam, M. Klene, C. Adamo, R. Cammi, J. W. Ochterski, R. L. Martin, K. Morokuma, O. Farkas, J. B. Foresman, and D. J. Fox, Gaussian, Inc., Wallingford CT, 2016.

- (55) Zhao, Y.; Truhlar, D. G. *Theor. Chem. Acc.* **2008**, *120* (1), 215–241.
- (56) Weigend, F.; Ahlrichs, R. B. *Phys. Chem. Chem. Phys.* **2005**, *7* (18), 3297–3305.
- (57) Claude Legault. CYLview 1.0b; Université de Sherbrooke, 2009.
- (58) Werth, J.; Sigman, M. S. *J. Am. Chem. Soc.* **2020**, *142* (38), 16382–16391.

## ***Appendix 2***

*Cartesian Coordinates of Substrate and Ligand Conformers from*

*Chapter 2*

**Cartesian Coordinates of Substrate and Ligand Conformers****(B3LYP/6-31G\* Geometry)****115\_1 Ground State**

O	-0.07004	-0.36813	-0.59645
C	-0.99939	-0.39202	0.39348
C	-2.39074	-0.53421	-0.21291
O	-0.77011	-0.31675	1.57397
C	1.27561	-0.14518	-0.28117
C	2.19730	-1.02673	-0.83535
C	3.55782	-0.80996	-0.61691
C	3.98058	0.27633	0.15014
C	3.03841	1.15070	0.69558
C	1.67543	0.94870	0.48183
Cl	-2.89064	1.13596	-0.77212
C	-3.39549	-1.08679	0.77826
H	-2.33095	-1.12956	-1.12483
H	1.84260	-1.86232	-1.42960
H	4.28486	-1.49223	-1.04728
H	5.03986	0.44261	0.32121
H	3.36292	1.99864	1.29136
H	0.93692	1.62091	0.90126
H	-3.42293	-0.46880	1.67782
H	-4.39101	-1.12580	0.33016
H	-3.09737	-2.10078	1.06814

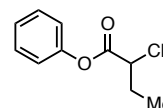
**115\_2 Ground State**

O	0.07003	0.36806	-0.59639
C	0.99948	0.39220	0.39338
C	2.39077	0.53404	-0.21324
O	0.77040	0.31734	1.57397
C	-1.27564	0.14521	-0.28101
C	-2.19727	1.02679	-0.83520
C	-3.55782	0.80998	-0.61691
C	-3.98062	-0.27633	0.15007
C	-3.03847	-1.15074	0.69551
C	-1.67547	-0.94874	0.48188
Cl	2.89043	-1.13635	-0.77168
C	3.39566	1.08707	0.77759
H	2.33091	1.12904	-1.12538

H	-1.84255	1.86240	-1.42939
H	-4.28482	1.49227	-1.04731
H	-5.03990	-0.44266	0.32108
H	-3.36304	-1.99873	1.29119
H	-0.93701	-1.62096	0.90138
H	3.42313	0.46949	1.67742
H	4.39115	1.12582	0.32940
H	3.09762	2.10122	1.06703

**115\_3 Ground State**

O	-0.21152	0.37875	-0.18310
C	-1.01539	-0.15561	0.77084
C	-2.47508	0.17101	0.48311
O	-0.64391	-0.78101	1.73187
C	1.17083	0.16820	-0.13198
C	1.97331	1.29485	-0.27556
C	3.35914	1.14015	-0.30749
C	3.92555	-0.13007	-0.19372
C	3.10142	-1.24828	-0.05275
C	1.71420	-1.10910	-0.02362
Cl	-2.99490	-0.77447	-0.98994
C	-2.73682	1.65600	0.27998
H	-3.05425	-0.23565	1.31135
H	1.50750	2.27075	-0.36414
H	3.99336	2.01432	-0.42111
H	5.00456	-0.24916	-0.21651
H	3.53771	-2.23895	0.03397
H	1.06726	-1.97052	0.08672
H	-2.17198	2.03281	-0.57493



H	-3.80240	1.83228	0.11319
H	-2.42807	2.20535	1.17747

**123\_1 Ground State**

O	0.23996	-0.37140	0.67727
C	-0.75687	-0.34364	-0.25847
C	-2.07782	-0.49598	0.49137
O	-0.59885	-0.18566	-1.43789
C	1.57012	-0.16809	0.29173
C	2.50065	-1.07372	0.79079

C	3.85272	-0.88405	0.50614				
C	4.26013	0.19974	-0.27278				
C	3.31058	1.09768	-0.76366				
C	1.95567	0.92318	-0.48288				
Cl	-3.40116	-0.92547	-0.65942				
C	-2.41061	0.78101	1.28105				
C	-2.48738	2.04760	0.42837				
H	-1.98832	-1.33798	1.18015				
H	2.15803	-1.90790	1.39399				
H	4.58520	-1.58606	0.89337				
H	5.31271	0.34475	-0.49639				
H	3.62243	1.94258	-1.37047				
H	1.21370	1.61241	-0.86610				
H	-3.35920	0.61168	1.80112				
H	-1.63432	0.88529	2.04853				
H	-3.24718	1.95113	-0.35234				
H	-2.74488	2.90848	1.05327				
H	-1.53052	2.26268	-0.05998				
<b>123_2 Ground State</b>							
O	-0.17726	-0.00130	-0.70598				
C	0.79138	0.14116	0.23548				
C	2.16270	-0.01875	-0.41073				
O	0.60381	0.35969	1.40594				
C	-1.52414	0.01333	-0.32402				
C	-2.36574	0.85034	-1.04847				
C	-3.73086	0.85106	-0.76172				
C	-4.23715	0.02326	0.24104				
C	-3.37474	-0.81119	0.95499				
C	-2.00862	-0.82538	0.67619				
Cl	2.49581	-1.81768	-0.45980				
C	3.25764	0.71138	0.35203				
C	3.06882	2.23164	0.29242				
H	2.11262	0.29104	-1.45576				
H	-1.94703	1.48265	-1.82437				
H	-4.39599	1.50010	-1.32356				
H	-5.29968	0.02638	0.46472				
H	-3.76476	-1.45860	1.73474				
H	-1.33130	-1.46824	1.22497				
H	4.22224	0.43005	-0.08218				
H	3.24567	0.36757	1.39038				
H	3.05820	2.59416	-0.74249				
H	2.13353	2.53259	0.77398				
H	3.88955	2.73468	0.81330				
				<b>123_3 Ground State</b>			
O	-0.17723	-0.00136	-0.70579				
C	0.79143	0.14107	0.23570				
C	2.16270	-0.01875	-0.41061				
O	0.60386	0.35961	1.40615				
C	-1.52408	0.01322	-0.32401				
C	-2.36553	0.85070	-1.04808				
C	-3.73068	0.85156	-0.76143				
C	-4.23721	0.02335	0.24085				
C	-3.37496	-0.81159	0.95447				
C	-2.00884	-0.82589	0.67579				
Cl	2.49589	-1.81763	-0.45992				
C	3.25759	0.71142	0.35217				
C	3.06869	2.23169	0.29227				
H	2.11252	0.29118	-1.45559				
H	-1.94667	1.48335	-1.82364				
H	-4.39559	1.50101	-1.32305				
H	-5.29975	0.02650	0.46448				
H	-3.76518	-1.45930	1.73388				
H	-1.33170	-1.46915	1.22429				
H	4.22222	0.43006	-0.08196				
H	3.24555	0.36777	1.39056				
H	2.13325	2.53267	0.77352				
H	3.88922	2.73486	0.81335				
H	3.05838	2.59403	-0.74270				
				<b>123_4 Ground State</b>			
O	0.29579	-0.27033	-0.61269				
C	-0.64054	-0.24725	0.37173				
C	-2.03316	-0.28197	-0.24496				
O	-0.41330	-0.20970	1.55455				
C	1.65104	-0.14673	-0.28510				
C	2.51372	-1.08101	-0.84794				
C	3.88436	-0.96249	-0.61771				
C	4.37560	0.07942	0.16985				
C	3.49218	1.00808	0.72378				
C	2.12009	0.90446	0.49829				
Cl	-2.41354	1.44054	-0.74280				
C	-3.07593	-0.82610	0.71976				
C	-4.47566	-0.93483	0.11698				
H	-2.00593	-0.84331	-1.18064				
H	2.10641	-1.88032	-1.45815				
H	4.56561	-1.68646	-1.05484				

H	5.44256	0.16919	0.35024	C	3.40035	-1.09458	0.35280
H	3.87023	1.82185	1.33545	C	2.00681	-1.10447	0.30145
H	1.42670	1.61935	0.92413	Cl	-2.69543	-1.54252	-0.79449
H	-3.07717	-0.20405	1.61971	C	-2.66630	1.18550	-0.37420
H	-2.72232	-1.81823	1.03184	C	-2.34889	2.38379	0.52774
H	-4.47636	-1.57089	-0.77626	H	-2.88695	-0.29663	1.20769
H	-5.16842	-1.37372	0.84187	H	1.49963	1.96281	-1.08288
H	-4.86123	0.04812	-0.16869	H	3.99807	1.97290	-0.99250

**123\_5 Ground State**

O	0.29578	0.27114	0.61284
C	-0.64052	0.24744	-0.37158
C	-2.03316	0.28205	0.24499
O	-0.41320	0.20947	-1.55435
C	1.65105	0.14708	0.28522
C	2.51401	1.08124	0.84775
C	3.88460	0.96231	0.61729
C	4.37546	-0.07991	-0.17005
C	3.49169	-1.00846	-0.72370
C	2.11969	-0.90439	-0.49804
Cl	-2.41334	-1.44044	0.74294
C	-3.07591	0.82596	-0.71987
C	-4.47575	0.93443	-0.11724
H	-2.00613	0.84347	1.18065
H	2.10701	1.88086	1.45775
H	4.56613	1.68618	1.05417
H	5.44238	-0.17001	-0.35053
H	3.86945	-1.82242	-1.33531
H	1.42603	-1.61913	-0.92371
H	-3.07693	0.20394	-1.61984
H	-2.72247	1.81817	-1.03187
H	-4.47664	1.57043	0.77605
H	-5.16850	1.37326	-0.84218
H	-4.86117	-0.04861	0.16831

**123\_6 Ground State**

O	-0.03892	0.04530	-0.36089
C	-0.83938	-0.23177	0.70086
C	-2.30520	-0.13592	0.29988
O	-0.45981	-0.48711	1.81572
C	1.35172	0.01051	-0.21419
C	2.05045	1.11847	-0.68152
C	3.44421	1.11283	-0.62803
C	4.12117	0.00846	-0.10899

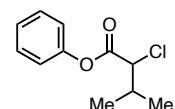
H	5.20612	0.00586	-0.06584
H	3.92319	-1.95687	0.75580
H	1.43888	-1.95449	0.65883
H	-3.73379	1.16173	-0.61675
H	-2.11689	1.25964	-1.31707
H	-1.27544	2.45666	0.73462
H	-2.65815	3.31506	0.04302
H	-2.87225	2.31388	1.48796

**123\_7 Ground State**

O	0.25493	0.69218	-0.30309
C	-0.72924	-0.23321	-0.43369
C	-2.08061	0.46501	-0.56400
O	-0.55716	-1.42573	-0.48512
C	1.57786	0.27818	-0.11265
C	2.53456	0.85288	-0.94219
C	3.87872	0.53451	-0.74817
C	4.25081	-0.35128	0.26376
C	3.27438	-0.91550	1.08711
C	1.92759	-0.60247	0.90747
Cl	-2.41784	1.36698	0.99094
C	-3.22713	-0.47402	-0.93017
C	-3.60959	-1.51235	0.12645
H	-1.97486	1.25196	-1.31459
H	2.21925	1.54052	-1.71990
H	4.63279	0.98034	-1.38999
H	5.29732	-0.59982	0.41225
H	3.55940	-1.60344	1.87756
H	1.16280	-1.03498	1.54103
H	-2.92533	-0.97962	-1.85657
H	-4.09432	0.14931	-1.17499
H	-3.94059	-1.02839	1.04987
H	-4.43350	-2.13068	-0.24460
H	-2.76590	-2.16603	0.35624

**123\_8 Ground State**

O	0.10239	0.20547	-0.21598	H	1.68093	-2.11245	0.16684
C	-0.64837	-0.36811	0.75878	H	-2.72429	0.19807	2.15245
C	-2.13072	-0.21331	0.45149	H	-3.96042	0.52492	0.93597
O	-0.21971	-0.89865	1.75270	H	-2.38018	2.19322	-0.17163
C	1.49865	0.15752	-0.14321				
C	2.16927	1.36026	-0.33745				
C	3.56400	1.36425	-0.35045				
C	4.27019	0.17467	-0.16770				
C	3.57726	-1.02234	0.02334	H	-2.78387	2.63474	1.49720
C	2.18296	-1.04197	0.03423	H	-1.21070	1.91491	1.12999
Cl	-2.52363	-1.23408	-1.01201	<b>124_1 Ground State</b>			
C	-2.54899	1.24141	0.24288	O	-0.40235	0.00308	-0.79087
C	-4.05995	1.42867	0.10998	C	0.59106	-0.44410	0.03294
H	-2.67258	-0.67019	1.27994	C	1.93046	-0.11335	-0.61249
H	1.59617	2.27057	-0.47924	O	0.42306	-0.95764	1.10771
H	4.09572	2.29872	-0.50334	C	-1.73596	-0.04639	-0.36739
H	5.35597	0.17921	-0.17581	C	-2.31743	-1.21823	0.10996
H	4.12259	-1.95088	0.16383	C	-3.67037	-1.20030	0.44892
H	1.63713	-1.96537	0.18303	C	-4.42452	-0.03403	0.30725
H	-2.02517	1.63439	-0.63360	C	-3.82284	1.12755	-0.17891
H	-2.17939	1.80174	1.11353	C	-2.47018	1.12586	-0.51832
H	-4.58508	1.05106	0.99504	Cl	3.02133	-1.55917	-0.50322
H	-4.30417	2.49013	0.00101	C	2.58172	1.13885	0.01604
H	-4.44663	0.89907	-0.76543	C	2.90403	0.98364	1.50519
<b>123_9 Ground State</b>				C	1.68953	2.36527	-0.23636
O	-0.02946	-0.09479	-0.39085	H	1.77236	0.05500	-1.67750
C	-0.79305	-0.74796	0.51088	H	-1.72423	-2.11677	0.22145
C	-2.28592	-0.61134	0.23912	H	-4.13498	-2.10662	0.82575
O	-0.38972	-1.32711	1.49098	H	-5.47722	-0.03146	0.57341
C	1.35790	-0.01919	-0.22112	H	-4.40364	2.03778	-0.29511
C	1.92031	1.24107	-0.39785	H	-1.97825	2.01398	-0.90115
C	3.30469	1.38380	-0.31103	H	3.52163	1.27855	-0.53280
C	4.10884	0.27339	-0.05003	H	3.55608	0.12508	1.68437
C	3.52428	-0.98290	0.11915	H	3.41363	1.88366	1.86565
C	2.14115	-1.14218	0.03230	H	1.99401	0.84453	2.09610
Cl	-2.68377	-0.36232	-1.51477	H	0.75461	2.30251	0.33181
C	-2.87971	0.50718	1.11125	H	2.21052	3.27351	0.08328
C	-2.27543	1.89176	0.87473	H	1.43409	2.47401	-1.29613
H	-2.73899	-1.56502	0.51118	<b>124_2 Ground State</b>			
H	1.27167	2.08544	-0.60601	O	0.48836	-0.16599	0.68807
H	3.75199	2.36371	-0.44887	C	-0.43287	-0.51087	-0.26268
H	5.18665	0.38556	0.01893	C	-1.80702	-0.44316	0.39602
H	4.14625	-1.85022	0.31982	O	-0.18271	-0.76847	-1.40856
				C	1.83816	-0.04406	0.33824

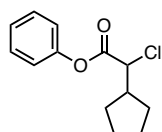


C	2.75096	-0.70564	1.15290	H	1.54785	1.51191	1.17008
C	4.11501	-0.56044	0.90054	H	-3.89216	-0.46926	-0.73797
C	4.55148	0.23596	-0.15894	H	-3.69458	0.80056	1.40319
C	3.61902	0.89192	-0.96481	H	-4.37886	-0.81483	1.64613
C	2.25240	0.75953	-0.72086	H	-2.68638	-0.49104	2.07935
Cl	-2.98914	-1.43029	-0.54936	H	-3.65507	-2.76480	0.15165
C	-2.26049	1.02580	0.56356	H	-2.48356	-2.50495	-1.14997
C	-3.54999	1.11829	1.38477	H	-1.95521	-2.47286	0.54721
C	-2.38473	1.76283	-0.77399				
H	-1.74127	-0.91100	1.38010	<b>124_4 Ground State</b>			
H	2.38572	-1.31895	1.96992	O	0.55839	0.70966	-0.11360
H	4.83421	-1.07249	1.53288	C	-0.41556	-0.20965	-0.33946
H	5.61355	0.34575	-0.35618	C	-1.78244	0.46410	-0.25364
H	3.95371	1.51259	-1.79069	O	-0.22261	-1.36971	-0.60622
H	1.52298	1.26123	-1.34471	C	1.89746	0.30595	-0.07479
H	-1.45076	1.48886	1.14425	C	2.78927	1.02912	-0.85917
H	-3.79747	2.16727	1.57895	C	4.14801	0.71861	-0.80146
H	-4.38913	0.66481	0.84842	C	4.59856	-0.30650	0.03111
H	-3.44741	0.60956	2.35011	C	3.68640	-1.01907	0.81217
H	-1.45826	1.71784	-1.35530	C	2.32620	-0.71607	0.76789
H	-3.18189	1.32787	-1.38452	Cl	-2.04087	0.98308	1.48332
H	-2.62551	2.81639	-0.59844	C	-2.93638	-0.39416	-0.78490
				C	-4.19048	0.46227	-0.99495
				C	-3.24167	-1.63081	0.06840
				H	-1.72291	1.40453	-0.80702
				H	2.41363	1.82283	-1.49637
				H	4.85193	1.27964	-1.40897
				H	5.65622	-0.54849	0.07334
				H	4.03272	-1.81610	1.46342
				H	1.61047	-1.26266	1.36998
				H	-2.58296	-0.73920	-1.76732
				H	-3.99162	1.31798	-1.65102
				H	-4.98526	-0.13622	-1.45198
				H	-4.56460	0.84653	-0.04013
				H	-3.62298	-1.33920	1.05199
				H	-4.01000	-2.23556	-0.42503
				H	-2.35227	-2.24860	0.20409
<b>124_3 Ground State</b>				<b>124_4 Ground State</b>			
O	0.48163	0.03168	-0.79256	O	-0.49262	0.03461	-0.69218
C	-0.53956	-0.11791	0.09485	C	0.46032	0.02988	0.27740
C	-1.86297	0.07782	-0.63725	C	1.83861	-0.08675	-0.36224
O	-0.40270	-0.36772	1.26622	O	0.25234	0.10041	1.46234
C	1.80331	-0.00580	-0.33327	C	-1.84570	0.04412	-0.33238
C	2.66893	-0.87481	-0.98804				
C	4.01419	-0.89585	-0.61925				
C	4.47641	-0.05681	0.39535				
C	3.59034	0.80947	1.03916				
C	2.24431	0.84404	0.67747				
Cl	-2.16214	1.88419	-0.68104				
C	-3.05863	-0.68858	-0.05787				
C	-3.47392	-0.26946	1.35666				
C	-2.76471	-2.19635	-0.13584				
H	-1.71580	-0.19650	-1.68272				
H	2.28453	-1.51573	-1.77457				
H	4.69834	-1.56965	-1.12644				
H	5.52334	-0.07592	0.68275				
H	3.94626	1.46549	1.82798				



C	-2.37472	-0.90104	0.54245	H	-3.79772	0.25544	-0.53129
C	-3.74491	-0.87843	0.79995	H	-2.01757	-0.36556	-2.20767
C	-4.56745	0.06963	0.18805	H	-2.74346	1.22158	-2.52551
C	-4.01686	1.00386	-0.69016	H	-1.13420	1.11290	-1.79812
C	-2.64711	0.99560	-0.95380	H	-1.89558	2.53587	0.25970
Cl	2.16769	-1.88790	-0.45130	H	-3.45630	2.71563	-0.55969
C	2.91727	0.66312	0.42069	H	-3.38719	2.09788	1.10124
C	2.55676	2.15856	0.45511				
C	4.31054	0.45739	-0.18093				
H	1.79377	0.24479	-1.40105	<b>124_7 Ground State</b>			
H	-1.72773	-1.63126	1.01296	O	0.25432	-0.04221	-0.33569
H	-4.16951	-1.60844	1.48267	C	-0.49676	-0.38695	0.74265
H	-5.63351	0.07857	0.39411	C	-1.97583	-0.37698	0.38515
H	-4.65092	1.74197	-1.17231	O	-0.06973	-0.63393	1.84218
H	-2.19420	1.70951	-1.63379	C	1.64668	0.02301	-0.22302
H	2.89830	0.27665	1.44584	C	2.25041	1.18656	-0.68782
H	1.59634	2.33484	0.94713	C	3.64172	1.28329	-0.66706
H	3.32236	2.71194	1.00848	C	4.41067	0.22435	-0.18268
H	2.51331	2.57652	-0.55863	C	3.78455	-0.93588	0.27713
H	4.34643	0.81628	-1.21737	C	2.39469	-1.04808	0.25816
H	5.05227	1.02229	0.39334	Cl	-2.27836	-1.75995	-0.76937
H	4.60409	-0.59512	-0.17541	C	-2.45497	0.96333	-0.19076
				C	-2.04789	2.09883	0.76329
				C	-3.96839	0.96414	-0.42502
<b>124_6 Ground State</b>				H	-2.52026	-0.62942	1.29608
O	0.20923	-0.44638	-0.09139	H	1.62918	1.99356	-1.06232
C	-0.62326	0.12268	0.80902	H	4.12167	2.18735	-1.02992
C	-2.07764	-0.26461	0.58306	H	5.49361	0.30140	-0.16498
O	-0.29751	0.90744	1.66788	H	4.37920	-1.76308	0.65321
C	1.58052	-0.16849	-0.06789	H	1.89965	-1.94298	0.61431
C	2.42440	-1.27023	-0.16350	H	-1.94006	1.10690	-1.14733
C	3.80221	-1.06483	-0.22426	H	-0.96185	2.16834	0.88256
C	4.32056	0.23065	-0.18878	H	-2.40271	3.05792	0.37233
C	3.45586	1.32254	-0.09619	H	-2.49002	1.95807	1.75682
C	2.07510	1.13298	-0.03717	H	-4.50865	0.81622	0.51842
Cl	-2.25796	-2.01328	0.11489	H	-4.28386	1.92567	-0.84360
C	-2.78250	0.66025	-0.43750	H	-4.26979	0.17474	-1.11830
C	-2.12727	0.65156	-1.82231				
C	-2.88411	2.08460	0.12838	<b>124_8 Ground State</b>			
H	-2.56811	-0.17113	1.55200	O	0.33753	-0.41446	-0.04860
H	1.99266	-2.26500	-0.19234	C	-0.47104	0.19250	0.84580
H	4.46842	-1.91910	-0.29941	C	-1.94152	-0.16011	0.66434
H	5.39379	0.38925	-0.23425	O	-0.12384	0.99410	1.68047
H	3.85462	2.33233	-0.06929	C	1.71280	-0.15384	-0.05734
H	1.39905	1.97456	0.04239	C	2.22602	1.14088	-0.05064

C	3.60772	1.30969	-0.14172	H	4.83810	0.95418	1.77763
C	4.45489	0.20478	-0.24210	H	6.11426	-0.72876	0.46859
C	3.91772	-1.08336	-0.25351	H	4.99023	-1.98332	-1.36142
C	2.53877	-1.26836	-0.16085	H	2.58072	-1.54764	-1.86487
Cl	-2.20109	-1.80058	-0.07271	H	-2.37247	0.28770	1.36050
C	-2.66332	0.95981	-0.11978	H	-4.11290	1.35885	0.03852
C	-4.18172	0.76167	-0.10219	H	-3.75331	0.34666	-1.36566
C	-2.12887	1.13002	-1.54585	H	-5.67335	-0.80170	-0.28959
H	-2.36480	-0.22115	1.66786	H	-4.92399	-0.61682	1.29996
H	1.56407	1.99280	0.03586	H	-3.99111	-2.39954	-0.99669
H	4.02119	2.31387	-0.13382	H	-4.16198	-2.85178	0.69584
H	5.52897	0.34774	-0.31246	H	-1.97340	-1.99010	1.18334
H	4.56982	-1.94786	-0.33508	H	-1.75221	-1.94359	-0.55632
H	2.09272	-2.25714	-0.17160				
H	-2.42800	1.86785	0.45310				
H	-4.55974	0.65526	0.92095				
H	-4.67797	1.62430	-0.55916				
H	-4.46736	-0.13223	-0.66509				
H	-2.30307	0.22557	-2.13694				

**125\_1 Ground State**

O	1.07413	0.17878	-0.70748
C	0.08948	0.16268	0.22935
C	-1.23361	0.56558	-0.40903
O	0.23345	-0.12820	1.39014
C	2.39745	-0.06982	-0.32512
C	3.00798	0.64929	0.69897
C	4.35120	0.40185	0.97939
C	5.06822	-0.54383	0.24356
C	4.43811	-1.24878	-0.78266
C	3.09360	-1.01451	-1.07120
Cl	-1.27015	2.39921	-0.37888
C	-2.42522	-0.03073	0.31443
C	-3.79507	0.35863	-0.26715
C	-4.71206	-0.76453	0.23299
C	-3.86583	-2.03552	0.02975
C	-2.39597	-1.58956	0.25895
H	-1.22901	0.30026	-1.46787
H	2.44252	1.37995	1.26437

**125\_2 Ground State**

O	1.07418	0.17868	-0.70760
C	0.08956	0.16253	0.22927
C	-1.23354	0.56552	-0.40906
O	0.23357	-0.12845	1.39003
C	2.39749	-0.06987	-0.32518
C	3.09358	-1.01492	-1.07086
C	4.43809	-1.24912	-0.78225
C	5.06823	-0.54376	0.24366
C	4.35127	0.40226	0.97911
C	3.00806	0.64963	0.69859
Cl	-1.26999	2.39915	-0.37875
C	-2.42519	-0.03078	0.31434
C	-3.79498	0.35883	-0.26718
C	-4.71228	-0.76415	0.23283
C	-3.86622	-2.03543	0.03042
C	-2.39617	-1.58957	0.25847
H	-1.22894	0.30030	-1.46792
H	2.58067	-1.54835	-1.86430
H	4.99017	-1.98394	-1.36069
H	6.11427	-0.72863	0.46875
H	4.83819	0.95491	1.77710
H	2.44263	1.38058	1.26368
H	-2.37241	0.28739	1.36050
H	-4.11265	1.35907	0.03855
H	-3.75319	0.34694	-1.36570
H	-5.67333	-0.80132	-0.29020
H	-4.92472	-0.61608	1.29964
H	-3.99203	-2.40057	-0.99556
H	-4.16213	-2.85090	0.69757

H	-1.97286	-1.99044	1.18239
H	-1.75318	-1.94334	-0.55752

**125\_3 Ground State**

O	-0.74913	0.25854	-0.33666
C	-0.07919	0.71738	0.75223
C	1.37199	1.00998	0.40064
O	-0.54245	0.83862	1.85852
C	-2.09982	-0.08711	-0.22991
C	-2.46025	-1.33339	-0.73110
C	-3.80409	-1.70667	-0.71823
C	-4.76796	-0.83754	-0.20550
C	-4.38505	0.41012	0.29076
C	-3.04563	0.79809	0.28015
Cl	1.41761	2.44953	-0.72371
C	2.08898	-0.19034	-0.20287
C	3.59618	0.00667	-0.43063
C	4.11261	-1.43381	-0.53841
C	3.35032	-2.18255	0.57456
C	1.99373	-1.43769	0.72453
H	1.85788	1.33853	1.32014
H	-1.69117	-1.98882	-1.12655
H	-4.09461	-2.67725	-1.10929
H	-5.81364	-1.12982	-0.19399
H	-5.13202	1.09038	0.68899
H	-2.73860	1.76292	0.66435
H	1.61118	-0.41839	-1.16151
H	3.81361	0.62154	-1.30790
H	4.04268	0.50303	0.44265
H	5.19980	-1.51029	-0.43626
H	3.84737	-1.84363	-1.52154
H	3.91208	-2.12564	1.51348
H	3.21813	-3.24484	0.34766
H	1.13887	-2.06074	0.44494
H	1.83089	-1.13511	1.76558

**125\_4 Ground State**

O	0.72187	-0.62782	0.76162
C	-0.25589	-0.76427	-0.18393
C	-1.58204	-1.03583	0.51790
O	-0.08472	-0.63999	-1.36801
C	2.00565	-0.24717	0.34612
C	3.05178	-1.11775	0.62631
C	4.35306	-0.73779	0.29538

C	4.59153	0.49633	-0.31048
C	3.52536	1.35602	-0.58361
C	2.22135	0.98972	-0.25409
Cl	-2.39947	-2.43337	-0.30696
C	-2.50075	0.19840	0.54135
C	-1.88784	1.34559	1.40484
C	-2.14205	2.63455	0.60300
C	-2.04226	2.17037	-0.85656
C	-2.78518	0.82399	-0.85532
H	-1.37950	-1.36912	1.53567
H	2.83932	-2.07195	1.09672
H	5.17847	-1.40964	0.51104
H	5.60481	0.78854	-0.56900
H	3.70690	2.31711	-1.05541
H	1.38445	1.64760	-0.45999
H	-3.43574	-0.14522	0.99339
H	-2.32049	1.37116	2.40969
H	-0.80964	1.19785	1.53132
H	-1.43983	3.43502	0.85908
H	-3.15434	3.00938	0.80275
H	-0.99152	2.01398	-1.13232
H	-2.46263	2.88679	-1.56971
H	-2.48013	0.17043	-1.67438
H	-3.86258	0.99489	-0.95493

**125\_5 Ground State**

O	-1.04296	0.38327	0.70463
C	-0.15172	0.75355	-0.26364
C	1.20878	0.91169	0.40519
O	-0.40466	0.86589	-1.43283
C	-2.34897	0.02801	0.34738
C	-3.37463	0.62427	1.07305
C	-4.69360	0.25148	0.81419
C	-4.97359	-0.70415	-0.16335
C	-3.92921	-1.29096	-0.88054
C	-2.60568	-0.93136	-0.62879
Cl	2.24019	2.03166	-0.57212
C	1.86017	-0.47047	0.59273
C	2.17878	-1.21417	-0.74053
C	3.70043	-1.45696	-0.72121
C	4.04072	-1.54758	0.77388
C	3.18917	-0.42613	1.38815
H	1.07275	1.39169	1.37580
H	-3.13018	1.36463	1.82749

H	-5.50042	0.71111	1.37728
H	-6.00101	-0.99109	-0.36593
H	-4.14217	-2.03479	-1.64258
H	-1.78984	-1.37726	-1.18444
H	1.12214	-1.04564	1.16473
H	1.64225	-2.16937	-0.76104
H	1.85710	-0.64513	-1.61647
H	4.21713	-0.59600	-1.16190
H	3.99467	-2.34607	-1.28816
H	5.10902	-1.43219	0.98443
H	3.72873	-2.52254	1.17199
H	3.02697	-0.53852	2.46513
H	3.68641	0.53644	1.22633

**125\_6 Ground State**

O	1.20394	0.79928	-0.08751
C	0.15715	-0.04095	-0.29861
C	-1.15314	0.72381	-0.15190
O	0.24875	-1.20958	-0.58033
C	2.50895	0.29459	-0.08499
C	3.43806	0.96763	-0.87082
C	4.77028	0.55467	-0.84838
C	5.15769	-0.52136	-0.04893
C	4.20912	-1.18222	0.73420
C	2.87501	-0.77717	0.72497
Cl	-1.38918	1.03836	1.64016
C	-2.34001	-0.00444	-0.76993
C	-2.75331	-1.33808	-0.07405
C	-4.24156	-1.16835	0.29387
C	-4.76946	-0.15252	-0.73022
C	-3.62156	0.86261	-0.82150
H	-1.02930	1.71837	-0.58596
H	3.11146	1.80250	-1.48193
H	5.50298	1.07582	-1.45739
H	6.19464	-0.84314	-0.03414
H	4.50641	-2.01871	1.35969
H	2.13159	-1.28352	1.32853
H	-2.02128	-0.22763	-1.79639
H	-2.61494	-2.16852	-0.77192
H	-2.13371	-1.55524	0.79820
H	-4.32934	-0.74510	1.30216
H	-4.78969	-2.11612	0.28598
H	-5.72077	0.30507	-0.43946
H	-4.92036	-0.64080	-1.70246

H	-3.66053	1.49140	-1.71748
H	-3.65582	1.52660	0.05045

**125\_7 Ground State**

O	0.63033	-0.51448	0.87717
C	-0.34896	-0.84210	-0.01876
C	-1.68736	-0.82814	0.70837
O	-0.16742	-1.04589	-1.19052
C	1.93320	-0.29604	0.41075
C	2.51030	0.93046	0.72307
C	3.82857	1.17549	0.33805
C	4.54965	0.20084	-0.35285
C	3.95100	-1.02363	-0.65619
C	2.63522	-1.28364	-0.27412
Cl	-2.70357	-2.21052	0.11798
C	-2.43617	0.50918	0.53440
C	-1.60326	1.70908	1.07614
C	-1.05989	2.41279	-0.17732
C	-2.22869	2.29483	-1.16574
C	-2.75812	0.86161	-0.94903
H	-1.51096	-1.01772	1.76704
H	1.92826	1.67123	1.26108
H	4.28886	2.12913	0.57886
H	5.57494	0.39378	-0.65380
H	4.50886	-1.78423	-1.19423
H	2.15843	-2.22747	-0.50842
H	-3.35646	0.40016	1.11567
H	-2.27608	2.38876	1.61171
H	-0.82365	1.40501	1.78052
H	-0.18258	1.88223	-0.56811
H	-0.75599	3.44693	0.01656
H	-1.93663	2.47926	-2.20431
H	-3.00114	3.03060	-0.90638
H	-2.24417	0.16714	-1.61821
H	-3.82742	0.77284	-1.15759

**125\_8 Ground State**

O	-1.02201	0.44431	0.68666
C	-0.12691	0.76704	-0.29586
C	1.23024	0.95700	0.37176
O	-0.37541	0.82423	-1.46948
C	-2.32718	0.07368	0.34294
C	-3.35403	0.69979	1.04131
C	-4.67260	0.31588	0.79701
C	-4.95117	-0.68049	-0.13936

C	-3.90570	-1.29689	-0.82967	H	5.60501	0.78818	-0.56891
C	-2.58260	-0.92648	-0.59187	H	3.70733	2.31692	-1.05563
Cl	2.30136	1.95530	-0.69050	H	1.38477	1.64779	-0.46034
C	1.84517	-0.41563	0.70174	H	-3.43576	-0.14533	0.99349
C	2.00314	-1.34164	-0.53390	H	-2.32074	1.37120	2.40967
C	3.32397	-2.09038	-0.29674	H	-0.80976	1.19780	1.53148
C	4.20947	-1.02856	0.37159	H	-1.43972	3.43493	0.85890
C	3.25570	-0.33047	1.35843	H	-3.15428	3.00949	0.80282
H	1.09740	1.53175	1.28978	H	-0.99172	2.01391	-1.13239
H	-3.11074	1.47164	1.76391	H	-2.46285	2.88667	-1.56973
H	-5.48021	0.79877	1.33913	H	-3.86273	0.99470	-0.95483
H	-5.97828	-0.97613	-0.33076	H	-2.48024	0.17030	-1.67430
H	-4.11752	-2.07250	-1.55967				
H	-1.76614	-1.39510	-1.12756				
H	1.14081	-0.86569	1.41078				
H	1.14433	-2.00904	-0.66008				
H	2.07988	-0.73664	-1.44342				
H	3.75233	-2.49462	-1.21961				
H	3.16621	-2.93250	0.39051				
H	4.55306	-0.31030	-0.38208				
H	5.09439	-1.44647	0.86262				
H	3.24143	-0.86864	2.31285				
H	3.55432	0.70007	1.57034				
<b>125_9 Ground State</b>				<b>125_10 Ground State</b>			
O	0.72183	-0.62751	0.76153	O	0.51740	-0.46899	0.89530
C	-0.25590	-0.76415	-0.18393	C	-0.41908	-0.93353	0.01188
C	-1.58201	-1.03581	0.51792	C	-1.79726	-0.77576	0.64296
O	-0.08482	-0.63999	-1.36806	O	-0.17575	-1.33629	-1.09404
C	2.00566	-0.24696	0.34607	C	1.83692	-0.31098	0.45080
C	3.05167	-1.11764	0.62646	C	2.59005	-1.40006	0.02358
C	4.35302	-0.73789	0.29557	C	3.91646	-1.18846	-0.35149
C	4.59168	0.49613	-0.31043	C	4.47386	0.09063	-0.29511
C	3.52564	1.35591	-0.58374	C	3.70086	1.16857	0.13825
C	2.22154	0.98982	-0.25427	C	2.37148	0.97164	0.51294
Cl	-2.39939	-2.43339	-0.30697	Cl	-2.87129	-2.11194	0.05386
C	-2.50081	0.19833	0.54141	C	-2.42920	0.60176	0.33413
C	-1.88795	1.34557	1.40489	C	-1.72202	1.75454	1.11765
C	-2.14207	2.63451	0.60297	C	-1.32974	2.80830	0.05877
C	-2.04244	2.17027	-0.85657	C	-1.18672	2.00480	-1.24186
C	-2.78531	0.82388	-0.85526	C	-2.34834	1.00144	-1.16286
H	-1.37946	-1.36913	1.53568	H	-1.71245	-0.91007	1.72195
H	2.83904	-2.07175	1.09697	H	2.14281	-2.38577	-0.02071
H	5.17833	-1.40983	0.51136	H	4.51485	-2.02900	-0.69001
				H	5.50772	0.24600	-0.58832
				H	4.12909	2.16541	0.18507
				H	1.74945	1.79313	0.85299
				H	-3.47159	0.51415	0.65146
				H	-2.37926	2.16642	1.88943
				H	-0.83063	1.37990	1.62770
				H	-0.42253	3.35893	0.33083
				H	-2.13436	3.54590	-0.05314
				H	-0.22578	1.47620	-1.26091
				H	-1.22751	2.62905	-2.14033
				H	-3.28216	1.49892	-1.44846

H	-2.22250	0.13869	-1.82123	C	3.96305	-0.09359	1.36245
				C	2.68086	0.31329	0.99616
				Cl	-1.31830	2.57339	0.00178
<b>125_11 Ground State</b>				C	-2.65662	0.19135	-0.48230
O	-0.63040	-0.51457	-0.87722	C	-2.68926	-1.21853	-1.13623
C	0.34888	-0.84208	0.01874	C	-3.65815	-2.01749	-0.25158
C	1.68729	-0.82818	-0.70837	C	-3.31105	-1.53290	1.16389
O	0.16734	-1.04571	1.19053	C	-3.09423	-0.01521	1.00114
C	-1.93326	-0.29605	-0.41078	H	-1.12494	1.02676	-1.76725
C	-2.51031	0.93047	-0.72312	H	2.71514	-0.66536	-2.26324
C	-3.82856	1.17556	-0.33807	H	5.01557	-1.38785	-1.60318
C	-4.54965	0.20096	0.35290	H	5.80339	-1.01899	0.72665
C	-3.95103	-1.02352	0.65626	H	4.30346	0.07214	2.38026
C	-2.63528	-1.28360	0.27416	H	2.01834	0.79017	1.70856
Cl	2.70344	-2.21063	-0.11795	H	-3.39570	0.82363	-0.98542
C	2.43616	0.50909	-0.53443	H	-2.98685	-1.17802	-2.18923
C	1.60328	1.70904	-1.07613	H	-1.69805	-1.68485	-1.09089
C	1.06012	2.41286	0.17736	H	-3.55377	-3.09996	-0.38013
C	2.22903	2.29483	1.16565	H	-4.69514	-1.75333	-0.49948
C	2.75819	0.86150	0.94899	H	-2.37585	-1.99981	1.49031
H	1.51090	-1.01780	-1.76703	H	-4.08324	-1.77299	1.90211
H	-1.92826	1.67118	-1.26120	H	-4.02781	0.52915	1.17733
H	-4.28883	2.12920	-0.57889	H	-2.35766	0.37099	1.70696
H	-5.57491	0.39397	0.65388				
H	-4.50891	-1.78407	1.19436				
H	-2.15851	-2.22743	0.50848	<b>125_13 Ground State</b>			
H	3.35642	0.40005	-1.11572	O	0.81241	-0.33214	-0.37211
H	2.27610	2.38863	-1.61181	C	0.13906	-0.98353	0.60415
H	0.82356	1.40501	-1.78039	C	-1.33332	-1.17783	0.26950
H	0.18283	1.88238	0.56829	O	0.59657	-1.31479	1.67098
H	0.75629	3.44702	-0.01651	C	2.15111	0.02646	-0.17816
H	1.93711	2.47937	2.20424	C	2.47749	1.35020	-0.45344
H	3.00156	3.03046	0.90615	C	3.80787	1.75538	-0.34887
H	3.82747	0.77251	1.15755	C	4.79186	0.84075	0.02910
H	2.24410	0.16717	1.61821	C	4.44268	-0.48388	0.29838
				C	3.11695	-0.90442	0.19411
<b>125_12 Ground State</b>				Cl	-1.59841	-1.56246	-1.48857
O	1.01132	0.53973	-0.76082	C	-2.14704	0.04179	0.73057
C	-0.11309	0.16678	-0.09342	C	-1.86291	1.36664	-0.04045
C	-1.31593	0.87926	-0.70302	C	-3.25119	1.94133	-0.40829
O	-0.14168	-0.60870	0.82955	C	-4.22716	1.26395	0.56778
C	2.25857	0.09049	-0.31156	C	-3.67559	-0.16425	0.66512
C	3.08195	-0.51666	-1.25305	H	-1.65776	-2.06396	0.81586
C	4.36426	-0.91474	-0.87428	H	1.69300	2.03963	-0.74733
C	4.80580	-0.70665	0.43291	H	4.07237	2.78654	-0.56358

H	5.82706	1.15782	0.11183	H	-2.35774	0.37073	1.70693
H	5.20534	-1.19939	0.59118				
H	2.83636	-1.92896	0.40367				
H	-1.86407	0.17203	1.78363	<b>125_15 Ground State</b>			
H	-1.30564	2.05714	0.60123	O	1.19933	0.76352	-0.25956
H	-1.25227	1.19139	-0.92879	C	0.15594	-0.10764	-0.29359
H	-3.50834	1.65284	-1.43451	C	-1.15397	0.67097	-0.32312
H	-3.28284	3.03438	-0.35916	O	0.25577	-1.30860	-0.31766
H	-5.26815	1.29844	0.23027	C	2.50498	0.27611	-0.13650
H	-4.18175	1.75243	1.55040	C	3.43962	0.76151	-1.04451
H	-4.05381	-0.72743	1.52484	C	4.77216	0.36772	-0.92104
H	-3.93720	-0.72130	-0.24188	C	5.15431	-0.50387	0.09938
				C	4.20015	-0.97819	1.00190
				C	2.86574	-0.58911	0.89307
<b>125_14 Ground State</b>				Cl	-1.41848	1.33603	1.36690
O	1.01136	0.53961	-0.76070	C	-2.34477	-0.14509	-0.81448
C	-0.11308	0.16675	-0.09331	C	-2.72483	-1.37434	0.05339
C	-1.31586	0.87933	-0.70291	C	-4.25862	-1.43726	-0.01327
O	-0.14176	-0.60877	0.82962	C	-4.67071	0.04108	-0.00493
C	2.25862	0.09041	-0.31149	C	-3.64581	0.70778	-0.94170
C	3.08225	-0.51606	-1.25320	H	-1.01319	1.56169	-0.93849
C	4.36459	-0.91409	-0.87452	H	3.11709	1.43966	-1.82760
C	4.80594	-0.70664	0.43284	H	5.50918	0.74363	-1.62450
C	3.96297	-0.09425	1.36261	H	6.19149	-0.81132	0.19295
C	2.68073	0.31257	0.99641	H	4.49338	-1.65489	1.79904
Cl	-1.31824	2.57339	0.00207	H	2.11782	-0.95144	1.58790
C	-2.65659	0.19143	-0.48236	H	-2.04236	-0.49331	-1.81095
C	-2.68921	-1.21841	-1.13638	H	-2.22920	-2.28360	-0.29012
C	-3.65830	-2.01738	-0.25197	H	-2.41096	-1.20676	1.08898
C	-3.31153	-1.53288	1.16361	H	-4.69459	-2.01368	0.80942
C	-3.09436	-0.01522	1.00101	H	-4.57965	-1.90979	-0.95168
H	-1.12479	1.02693	-1.76711	H	-4.56365	0.44569	1.00872
H	2.71558	-0.66427	-2.26352	H	-5.70509	0.20894	-0.32245
H	5.01608	-1.38666	-1.60360	H	-4.00326	0.67519	-1.97695
H	5.80356	-1.01894	0.72652	H	-3.47881	1.76004	-0.69122
H	4.30322	0.07099	2.38055				
H	2.01805	0.78891	1.70902	<b>125_16 Ground State</b>			
H	-3.39561	0.82375	-0.98550	O	1.00410	0.54228	-0.76889
H	-2.98660	-1.17782	-2.18943	C	-0.12183	0.16857	-0.10356
H	-1.69802	-1.68478	-1.09089	C	-1.32456	0.86418	-0.73400
H	-3.55388	-3.09985	-0.38055	O	-0.14725	-0.59416	0.83025
H	-4.69524	-1.75324	-0.50011	C	2.25180	0.11258	-0.30179
H	-2.37654	-2.00000	1.49034	C	2.66419	0.37239	1.00219
H	-4.08401	-1.77281	1.90158	C	3.94669	-0.01583	1.38704
H	-4.02782	0.52934	1.17722	C	4.79936	-0.64720	0.47899

C	4.36752	-0.89262	-0.82495	H	-5.51701	-0.68017	-0.31306
C	3.08493	-0.51350	-1.22194	H	-3.96514	-2.11209	0.99543
Cl	-1.38439	2.54843	-0.00952	H	-1.56276	-1.51906	1.17034
C	-2.65457	0.13930	-0.56540	H	3.65442	0.17025	0.06846
C	-2.57709	-1.32480	-1.11524	H	3.49188	-1.97657	0.90817
C	-2.93485	-2.23308	0.07696	H	2.09029	-1.41391	1.81733
C	-3.86182	-1.35931	0.93379	H	0.56183	-2.18538	0.04270
C	-3.18628	0.02029	0.88722	H	1.74735	-3.49144	0.12379
H	-1.10474	1.02955	-1.78955	H	1.37657	-2.35217	-2.28746
H	1.99367	0.86335	1.69747	H	3.04560	-2.48559	-1.72284
H	4.27957	0.17878	2.40222	H	1.24240	-0.02649	-1.65737
H	5.79717	-0.94482	0.78691	H	2.92772	-0.09636	-2.14414
H	5.02662	-1.38024	-1.53708				
H	2.72548	-0.69130	-2.23008				
H	-3.37662	0.70611	-1.16244	<b>125_18 Ground State</b>			
H	-3.30474	-1.44593	-1.92493	O	0.46475	-0.63757	-0.10908
H	-1.59536	-1.56750	-1.53807	C	-0.34782	-0.53750	0.96765
H	-2.02811	-2.46721	0.64411	C	-1.77111	-0.98089	0.65792
H	-3.39192	-3.17725	-0.23749	O	-0.02775	-0.09557	2.04578
H	-3.98600	-1.73437	1.95494	C	1.79792	-0.21785	-0.04877
H	-4.86001	-1.31046	0.47713	C	2.72262	-1.06729	-0.64791
H	-3.86202	0.84244	1.13811	C	4.06135	-0.68179	-0.70256
H	-2.35411	0.04475	1.59390	C	4.46176	0.54124	-0.16198
				C	3.51739	1.38020	0.43163
				C	2.17382	1.00940	0.49275
				Cl	-1.78555	-2.56407	-0.24447
<b>125_17 Ground State</b>				C	-2.60055	0.08220	-0.08800
O	-0.42776	0.60500	-0.09248	C	-2.73461	1.38742	0.76025
C	0.35454	0.53312	1.00859	C	-2.46944	2.54396	-0.22251
C	1.79731	0.92778	0.72232	C	-1.47300	1.94554	-1.22513
O	-0.00171	0.14747	2.09679	C	-2.02127	0.52911	-1.45990
C	-1.77751	0.23816	-0.05937	H	-2.23218	-1.19165	1.62283
C	-2.62964	1.05152	-0.80073	H	2.38148	-2.00971	-1.06296
C	-3.97974	0.71718	-0.89062	H	4.78942	-1.33903	-1.16858
C	-4.46482	-0.42101	-0.24411	H	5.50487	0.83988	-0.20368
C	-3.59297	-1.22532	0.49087	H	3.82389	2.33295	0.85317
C	-2.23825	-0.90533	0.59018	H	1.43948	1.65086	0.96185
Cl	1.88820	2.48280	-0.22256	H	-3.58421	-0.37438	-0.23099
C	2.61894	-0.18183	0.03796	H	-3.71403	1.45433	1.24338
C	2.49483	-1.53325	0.80809	H	-1.98592	1.40204	1.55917
C	1.62439	-2.42514	-0.09211	H	-2.09923	3.44419	0.27890
C	2.07117	-2.02876	-1.50547	H	-3.39591	2.81625	-0.74456
C	2.20253	-0.49499	-1.42987	H	-0.47163	1.89630	-0.77868
H	2.23235	1.15398	1.69539	H	-1.38653	2.52557	-2.14968
H	-2.22335	1.92737	-1.29538	H	-1.27550	-0.16622	-1.84920
H	-4.65046	1.34756	-1.46683				



H	-2.83810	0.57045	-2.18919	C	3.96213	-0.76844	0.44524
				C	2.61910	-1.14131	0.40074
<b>125_19 Ground State</b>				Cl	-2.10770	-2.19833	-0.96249
O	0.90390	-0.00612	-0.61056	C	-2.59144	0.28697	0.17999
C	0.02496	0.31780	0.37593	C	-2.33369	1.28674	1.34538
C	-1.36853	0.48177	-0.21708	C	-1.29506	2.27666	0.79539
O	0.30094	0.45438	1.54066	C	-1.72314	2.45033	-0.66900
C	2.26603	-0.12969	-0.31278	C	-2.16392	1.03839	-1.11690
C	2.96662	0.88103	0.34024	H	-2.28329	-1.54153	1.29549
C	4.33746	0.72130	0.53921	H	1.37994	1.51828	-1.32508
C	4.99245	-0.42621	0.08759	H	3.78980	2.17994	-1.24514
C	4.27186	-1.42396	-0.57002	H	5.43591	0.70540	-0.10442
C	2.89933	-1.27943	-0.77226	H	4.67787	-1.41606	0.94278
Cl	-1.50219	2.25059	-0.67680	H	2.27603	-2.06234	0.85591
C	-2.45944	0.06289	0.76493	H	-3.65190	0.02169	0.13697
C	-3.87772	0.20882	0.18762	H	-3.26674	1.81830	1.56518
C	-4.05372	-1.01137	-0.74209	H	-2.01256	0.79447	2.26804
C	-3.12853	-2.11902	-0.15891	H	-1.27491	3.21810	1.35396
C	-2.37365	-1.46052	1.02251	H	-0.28795	1.84680	0.85396
H	-1.42808	-0.05857	-1.16193	H	-0.93102	2.86217	-1.30397
H	2.44917	1.76648	0.68843	H	-2.57054	3.14566	-0.72064
H	4.89466	1.50109	1.04986	H	-2.98405	1.07285	-1.83905
H	6.06046	-0.54085	0.24647	H	-1.33939	0.51406	-1.60329
H	4.77500	-2.31765	-0.92712				
H	2.31621	-2.03918	-1.28215	<b>125_21 Ground State</b>			
H	-2.31529	0.63653	1.68404	O	0.78905	-0.36521	-0.37868
H	-4.58976	0.15499	1.01963	C	0.12482	-1.00886	0.60797
H	-4.04049	1.16390	-0.31833	C	-1.35510	-1.18514	0.29976
H	-3.74994	-0.75689	-1.76381	O	0.59403	-1.34545	1.66833
H	-5.09917	-1.32877	-0.79951	C	2.12930	-0.00401	-0.20230
H	-2.42651	-2.47751	-0.91966	C	2.45184	1.31301	-0.51305
H	-3.69508	-2.99340	0.17530	C	3.78189	1.72325	-0.42636
H	-2.88696	-1.67072	1.96724	C	4.76983	0.82012	-0.03135
H	-1.34831	-1.82600	1.13702	C	4.42469	-0.49796	0.27276
				C	3.09920	-0.92374	0.18716
<b>125_20 Ground State</b>				Cl	-1.67270	-1.49617	-1.46439
O	0.36435	-0.63722	-0.37383	C	-2.14724	0.02156	0.83069
C	-0.37686	-0.86895	0.73767	C	-1.77367	1.37749	0.17927
C	-1.85516	-1.04647	0.42437	C	-3.08943	2.16918	0.16503
O	0.04910	-0.86639	1.86728	C	-4.13228	1.09322	-0.17197
C	1.71534	-0.29761	-0.23772	C	-3.69128	-0.12271	0.66617
C	2.11767	0.89395	-0.83187	H	-1.67455	-2.09043	0.81641
C	3.46486	1.25268	-0.78268	H	1.66415	1.99259	-0.82081
C	4.38786	0.42418	-0.14325	H	4.04309	2.74914	-0.66857

H	5.80491	1.14094	0.03744
H	5.19047	-1.20461	0.57866
H	2.82237	-1.94306	0.42446
H	-1.89991	0.05327	1.89914
H	-0.96395	1.88394	0.71420
H	-1.43488	1.21264	-0.84884
H	-3.07728	2.99989	-0.54821
H	-3.29132	2.59020	1.15918
H	-4.07194	0.84848	-1.23920
H	-5.16085	1.40237	0.04027
H	-3.96954	-1.07065	0.19710
H	-4.16496	-0.09720	1.65358

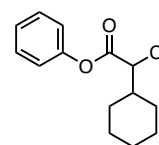
**125\_22 Ground State**

O	0.36432	-0.63746	-0.37375
C	-0.37700	-0.86895	0.73774
C	-1.85532	-1.04633	0.42433
O	0.04885	-0.86621	1.86739
C	1.71527	-0.29779	-0.23766
C	2.11758	0.89364	-0.83208
C	3.46476	1.25243	-0.78294
C	4.38778	0.42412	-0.14330
C	3.96208	-0.76840	0.44544
C	2.61907	-1.14132	0.40099
Cl	-2.10784	-2.19829	-0.96252
C	-2.59138	0.28715	0.17981
C	-2.33369	1.28688	1.34531
C	-1.29480	2.27661	0.79550
C	-1.72261	2.45039	-0.66893
C	-2.16357	1.03856	-1.11697
H	-2.28358	-1.54136	1.29539
H	1.37986	1.51782	-1.32546
H	3.78968	2.17959	-1.24561
H	5.43581	0.70538	-0.10450
H	4.67785	-1.41587	0.94313
H	2.27602	-2.06227	0.85634
H	-3.65187	0.02203	0.13666
H	-3.26672	1.81855	1.56494
H	-2.01281	0.79452	2.26801
H	-0.28779	1.84654	0.85425
H	-1.27449	3.21804	1.35408
H	-0.93036	2.86221	-1.30375
H	-2.56992	3.14584	-0.72067
H	-2.98360	1.07323	-1.83923

H	-1.33912	0.51408	-1.60335
---	----------	---------	----------

**125\_23 Ground State**

O	-0.78529	0.32143	-0.40497
C	0.03034	0.41547	0.67586
C	1.45862	0.70811	0.24673
O	-0.30375	0.23960	1.82125
C	-2.13991	0.02216	-0.22673
C	-2.64547	-1.03507	-0.97530
C	-4.00534	-1.33453	-0.89236
C	-4.83969	-0.58159	-0.06523
C	-4.31177	0.47691	0.67683
C	-2.95515	0.79021	0.59996
Cl	1.51513	2.36174	-0.52338
C	2.01966	-0.36510	-0.69560
C	3.53372	-0.20518	-0.92067
C	4.19182	-0.81506	0.33942
C	3.15627	-1.82680	0.91248
C	1.93879	-1.76201	-0.03807
H	2.04491	0.79231	1.16111
H	-1.97476	-1.60304	-1.61156
H	-4.40959	-2.15704	-1.47495
H	-5.89771	-0.81690	0.00014
H	-4.95797	1.06635	1.32048
H	-2.53492	1.60821	1.17211
H	1.44964	-0.31975	-1.62743
H	3.80996	-0.78386	-1.80983
H	3.82992	0.83121	-1.10390
H	4.41217	-0.03344	1.07468
H	5.14683	-1.29157	0.09896
H	2.86096	-1.54425	1.92843
H	3.55901	-2.84208	0.97501
H	2.03503	-2.51139	-0.83216



H	0.99032	-1.95783	0.47231
---	---------	----------	---------

**126\_1 Ground State**

O	-1.11863	0.56696	0.70775
C	-0.19514	0.98361	-0.20860
C	1.08822	1.33386	0.53438
O	-0.36500	1.01244	-1.39885

C	-2.34622	0.05062	0.27725	C	1.98818	-0.69990	-0.99607
C	-3.48057	0.54739	0.91038	C	2.72179	-2.04527	-0.91399
C	-4.72785	0.01622	0.58249	C	4.03473	-1.92174	-0.13057
C	-4.82992	-0.99805	-0.37046	C	3.79080	-1.33752	1.26669
C	-3.67890	-1.48381	-0.99371	C	3.06124	0.01015	1.18761
C	-2.42506	-0.96463	-0.67300	H	0.82324	1.55631	1.41576
Cl	1.76060	2.88124	-0.13373	H	-3.23626	0.82859	2.15401
C	2.12521	0.19489	0.47112	H	-5.57086	0.03509	1.74627
C	1.59972	-1.05346	1.20807	H	-6.08386	-1.29260	-0.29393
C	2.66609	-2.15630	1.24408	H	-4.27096	-1.82706	-1.90697
C	3.14414	-2.51560	-0.16839	H	-1.95445	-1.03446	-1.48949
C	3.64455	-1.27270	-0.91540	H	1.09482	-0.81275	0.95628
C	2.57957	-0.16840	-0.95068	H	1.03886	-0.81705	-1.53191
H	0.84322	1.54412	1.57545	H	2.58706	0.01160	-1.57773
H	-3.37366	1.33560	1.64815	H	2.91352	-2.42511	-1.92459
H	-5.61829	0.39817	1.07289	H	2.07354	-2.78306	-0.41879
H	-5.80178	-1.40884	-0.62677	H	4.72261	-1.26417	-0.68125
H	-3.75325	-2.27281	-1.73621	H	4.52599	-2.89933	-0.05387
H	-1.52890	-1.33074	-1.15838	H	4.73990	-1.21543	1.80227
H	2.99927	0.56660	1.02420	H	3.18663	-2.04417	1.85411
H	1.28438	-0.79008	2.22524	H	3.70413	0.74604	0.68924
H	0.70699	-1.43580	0.69493	H	2.85893	0.39553	2.19549
H	2.26628	-3.04228	1.75185				
H	3.52237	-1.81067	1.84085				
H	3.93207	-3.27702	-0.12048	<b>126_3 Ground State</b>			
H	2.30882	-2.96086	-0.72838	O	-1.51878	0.77523	0.19546
H	3.93978	-1.53520	-1.93823	C	-0.43102	-0.03751	0.20786
H	4.54727	-0.89018	-0.41717	C	0.84072	0.80653	0.17940
H	1.71506	-0.50924	-1.53352	O	-0.46826	-1.24104	0.27616
H	2.96622	0.72099	-1.45742	C	-2.80186	0.21921	0.15680
				C	-3.71463	0.69693	1.09085
<b>126_2 Ground State</b>				C	-5.02980	0.23374	1.05145
O	-1.18992	0.35044	0.69010	C	-5.41665	-0.69835	0.08780
C	-0.42196	1.00558	-0.23340	C	-4.48493	-1.16352	-0.84238
C	0.95570	1.20809	0.38940	C	-3.16827	-0.70544	-0.81760
O	-0.77750	1.31120	-1.33890	Cl	0.89421	1.69230	-1.42280
C	-2.48487	-0.06200	0.35694	C	2.11796	0.01093	0.45410
C	-3.48544	0.24739	1.27241	C	2.50142	-0.98924	-0.64979
C	-4.78460	-0.20122	1.03545	C	3.75390	-1.78440	-0.25778
C	-5.07141	-0.94676	-0.10875	C	4.93067	-0.85639	0.06802
C	-4.05279	-1.24737	-1.01494	C	4.55116	0.15203	1.15974
C	-2.74828	-0.80966	-0.78811	C	3.29539	0.94595	0.77700
Cl	1.82915	2.53255	-0.47713	H	0.72490	1.60332	0.91892
C	1.74541	-0.11719	0.40513	H	-3.38902	1.42318	1.82817
				H	-5.74970	0.60317	1.77574

H	-6.44019	-1.05972	0.05970
H	-4.78195	-1.88707	-1.59577
H	-2.43820	-1.06041	-1.53475
H	1.88666	-0.56890	1.36119
H	1.66499	-1.66481	-0.84441
H	2.69949	-0.43557	-1.57596
H	4.02354	-2.47224	-1.06826
H	3.52869	-2.40768	0.61980
H	5.22179	-0.31063	-0.84115
H	5.80537	-1.44084	0.37882
H	5.38280	0.84053	1.35261
H	4.36467	-0.38698	2.10007
H	3.50823	1.56797	-0.10232
H	3.01850	1.63133	1.58939

**126\_4 Ground State**

O	1.36984	0.24265	-0.72607
C	0.37866	0.28090	0.20409
C	-0.91412	0.75723	-0.44693
O	0.50047	-0.01056	1.36707
C	2.67339	-0.08500	-0.33460
C	3.31763	0.59314	0.69677
C	4.64165	0.26521	0.98591
C	5.30663	-0.71906	0.25179
C	4.64351	-1.38197	-0.78163
C	3.31756	-1.06703	-1.07917
Cl	-0.90495	2.57978	-0.23534
C	-2.15224	0.10693	0.16286
C	-3.45814	0.66522	-0.42373
C	-4.68545	-0.04169	0.16555
C	-4.61378	-1.55981	-0.03601
C	-3.30977	-2.12627	0.53673
C	-2.08058	-1.42055	-0.05176
H	-0.86551	0.59874	-1.52532
H	2.79215	1.35380	1.26106
H	5.15456	0.78477	1.78984
H	6.33808	-0.96664	0.48383
H	5.15530	-2.14619	-1.35903
H	2.77976	-1.56603	-1.87852
H	-2.12664	0.30295	1.24212
H	-3.52027	1.74251	-0.24373
H	-3.44636	0.52599	-1.51545
H	-5.59867	0.36293	-0.28707
H	-4.74407	0.17849	1.24114

H	-5.47828	-2.04881	0.42925
H	-4.66479	-1.78489	-1.11140
H	-3.24203	-3.20426	0.34690
H	-3.30550	-1.99809	1.62827
H	-2.02570	-1.62772	-1.13121
H	-1.17003	-1.82401	0.40287

**126\_5 Ground State**

O	-0.98585	0.66780	-0.14379
C	-0.19363	0.69370	0.95206
C	1.13651	1.38683	0.69576
O	-0.45067	0.17752	2.01358
C	-2.22020	0.00990	-0.10580
C	-2.34051	-1.30984	0.32188
C	-3.59215	-1.92144	0.25373
C	-4.69775	-1.22473	-0.23742
C	-4.55270	0.09555	-0.66610
C	-3.30789	0.72095	-0.60139
Cl	0.95484	2.84860	-0.37415
C	2.20660	0.42312	0.14160
C	2.57335	-0.64540	1.18948
C	3.71001	-1.54194	0.67910
C	3.35712	-2.18570	-0.66786
C	2.97051	-1.12346	-1.70487
C	1.82879	-0.23469	-1.19454
H	1.46521	1.77286	1.66090
H	-1.47944	-1.84070	0.70794
H	-3.70027	-2.94921	0.58754
H	-5.66801	-1.70974	-0.28668
H	-5.40765	0.64264	-1.05213
H	-3.16441	1.74465	-0.93039
H	3.09624	1.04602	-0.02538
H	2.86051	-0.16486	2.13292
H	1.69239	-1.26071	1.41146
H	3.93652	-2.31313	1.42508
H	4.62178	-0.93829	0.56389
H	2.51198	-2.87529	-0.52717
H	4.19764	-2.78858	-1.03249
H	2.67801	-1.59881	-2.64872
H	3.84617	-0.49660	-1.92730
H	0.92912	-0.84920	-1.05843
H	1.57565	0.53304	-1.93251

**126\_6 Ground State**

O	1.38508	0.35779	-0.80556
C	0.26056	0.21439	-0.05239
C	-0.91297	0.84699	-0.79310
O	0.21767	-0.32930	1.02287
C	2.61912	-0.05170	-0.28815
C	3.08424	0.41510	0.93838
C	4.35439	0.02694	1.36248
C	5.14378	-0.80800	0.56889
C	4.66045	-1.25904	-0.65992
C	3.38947	-0.88233	-1.09440
Cl	-0.84139	2.64126	-0.42059
C	-2.28959	0.25510	-0.48728
C	-2.31635	-1.23042	-0.90368
C	-3.72089	-1.82453	-0.72895
C	-4.22977	-1.64168	0.70636
C	-4.18776	-0.16597	1.12341
C	-2.78125	0.42511	0.95948
H	-0.70935	0.78663	-1.86324
H	2.46346	1.06246	1.54597
H	4.72744	0.38197	2.31858
H	6.13236	-1.10387	0.90682
H	5.27024	-1.90558	-1.28400
H	2.99093	-1.21761	-2.04619
H	-2.98834	0.79499	-1.14301
H	-1.98771	-1.33789	-1.94623
H	-1.60638	-1.78971	-0.28152
H	-3.71005	-2.88702	-1.00072
H	-4.41177	-1.32785	-1.42543
H	-5.24845	-2.03768	0.79978
H	-3.59810	-2.22724	1.38953
H	-4.51712	-0.05500	2.16347
H	-4.89829	0.40445	0.50693
H	-2.08484	-0.07709	1.63749
H	-2.78292	1.48687	1.22659

**126\_7 Ground State**

O	-0.97960	0.32279	-0.32324
C	-0.38336	0.86924	0.76890
C	1.05401	1.25445	0.45230
O	-0.89602	1.00209	1.85140
C	-2.30163	-0.12474	-0.24147
C	-2.54469	-1.42151	-0.68146
C	-3.85478	-1.90033	-0.68912

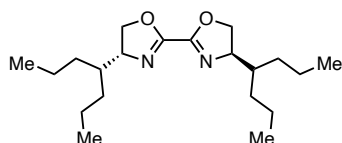
C	-4.90146	-1.08482	-0.25703
C	-4.63575	0.21480	0.17904
C	-3.33141	0.70793	0.18784
Cl	1.00917	2.65873	-0.71774
C	1.88825	0.08886	-0.08727
C	3.36041	0.48030	-0.28814
C	4.19325	-0.70677	-0.78849
C	4.08054	-1.91030	0.15484
C	2.61426	-2.30286	0.36971
C	1.77907	-1.11650	0.87010
H	1.48195	1.65379	1.37254
H	-1.71275	-2.03330	-1.01475
H	-4.05421	-2.91097	-1.03293
H	-5.92071	-1.45916	-0.26138
H	-5.44760	0.85325	0.51459
H	-3.11410	1.71365	0.52582
H	1.46070	-0.20082	-1.05542
H	3.43260	1.31755	-0.98905
H	3.76730	0.83206	0.67188
H	5.24115	-0.40383	-0.90038
H	3.84175	-0.99609	-1.78934
H	4.53159	-1.65361	1.12437
H	4.64786	-2.76139	-0.24089
H	2.53844	-3.13376	1.08123
H	2.19222	-2.66183	-0.58000
H	2.12992	-0.81638	1.86805
H	0.73272	-1.42318	0.98346

**126\_8 Ground State**

O	0.92560	0.18634	-0.63334
C	0.18507	0.97649	0.19897
C	-1.27327	0.89497	-0.22437
O	0.61062	1.57973	1.14835
C	2.27705	-0.04414	-0.35054
C	2.68238	-1.37502	-0.33293
C	4.02875	-1.67046	-0.12072
C	4.94989	-0.64012	0.07346
C	4.52205	0.68867	0.05098
C	3.17941	0.99957	-0.16397
Cl	-1.89571	2.58647	-0.47058
C	-2.09383	0.14626	0.84346
C	-3.56058	-0.05040	0.41867
C	-3.71238	-1.05308	-0.73455
C	-3.06078	-2.40235	-0.40057



H	2.19119	-1.41572	1.70997
H	1.92118	-2.19162	-1.24546
H	0.58960	-1.80797	-0.16868



**Cartesian Coordinates of Free Ligand Conformers**

**L2\_1 Ground State**

N	-1.26704	-0.75551	0.19939
C	-0.66791	-0.31659	1.23311
O	-1.27571	-0.40316	2.45033
C	-2.52203	-1.10077	2.20164
C	-2.59522	-1.20906	0.65495
C	0.66809	0.31390	1.23377
O	1.27596	0.39778	2.45113
C	2.52226	1.09596	2.20391
C	2.59537	1.20764	0.65746
N	1.26716	0.75510	0.20098
C	-3.71073	-0.35737	0.00727
C	-3.81706	-0.64311	-1.50168
C	-3.50127	1.14424	0.28252
C	3.71083	0.35736	0.00785
C	3.81699	0.64630	-1.50050
C	3.50144	-1.14484	0.27994
C	-4.38695	-2.02002	-1.86021
C	-4.51073	-2.22412	-3.37233
C	-4.76505	1.99322	0.10944
C	-4.51047	3.48054	0.36597
C	4.76522	-1.99345	0.10504
C	4.51068	-3.48127	0.35869
C	4.38617	2.02422	-1.85622
C	4.51013	2.23132	-3.36792
H	-3.33181	-0.51536	2.64452
H	-2.46680	-2.07400	2.69874
H	-2.72622	-2.25253	0.35225
H	3.33207	0.50960	2.64547
H	2.46704	2.06810	2.70314
H	2.72637	2.25177	0.35705
H	-4.65285	-0.66861	0.48779
H	-2.81973	-0.52714	-1.94420
H	-4.45378	0.12137	-1.96511

H	-2.70847	1.51571	-0.37909
H	-3.12859	1.29321	1.30524
H	4.65299	0.66762	0.48893
H	2.81971	0.53075	-1.94324
H	4.45409	-0.11691	-1.96551
H	2.70861	-1.51493	-0.38239
H	3.12882	-1.29595	1.30238
H	-3.75314	-2.81400	-1.44435
H	-5.37413	-2.13743	-1.39054
H	-4.92206	-3.21084	-3.61294
H	-5.16853	-1.46865	-3.81920
H	-3.53233	-2.14028	-3.86015
H	-5.54136	1.62811	0.79697
H	-5.17016	1.86446	-0.90238
H	-5.42566	4.07145	0.24792
H	-4.13309	3.64642	1.38246
H	-3.76288	3.87666	-0.33165
H	5.54160	-1.62969	0.79320
H	5.17021	-1.86271	-0.90657
H	5.42585	-4.07195	0.23935
H	4.13343	-3.64915	1.37489
H	3.76300	-3.87602	-0.33963
H	5.37320	2.14129	-1.38613
H	3.75183	2.81703	-1.43895
H	4.92090	3.21877	-3.60653
H	5.16849	1.47713	-3.81612
H	3.53188	2.14784	-3.85609

**L2\_2 Ground State**

N	1.35585	0.58746	-0.27296
C	0.70688	0.21448	0.75647
O	1.32911	0.17911	1.96728
C	2.67682	0.65172	1.71985
C	2.73146	0.86270	0.17992
C	-0.70689	-0.21455	0.75641
O	-1.32913	-0.17941	1.96723
C	-2.67685	-0.65194	1.71968
C	-2.73144	-0.86270	0.17972
N	-1.35583	-0.58735	-0.27309
C	3.74771	-0.02724	-0.57245
C	3.40229	-1.52021	-0.43439
C	5.19532	0.28192	-0.14929
C	-3.74771	0.02729	-0.57256
C	-3.40224	1.52024	-0.43442

C	-5.19532	-0.28186	-0.14935	H	-2.68665	3.97728	-1.58004
C	4.22403	-2.45320	-1.33120				
C	3.73350	-3.90177	-1.26286				
C	5.63144	1.74417	-0.30409	<b>L2_3 Ground State</b>			
C	7.12642	1.93681	-0.03664	N	1.12613	-0.14427	-0.09051
C	-5.63142	-1.74412	-0.30406	C	0.43438	-0.99151	-0.74123
C	-7.12640	-1.93675	-0.03661	O	1.01392	-2.15183	-1.15802
C	-4.22412	2.45333	-1.33100	C	2.41230	-2.02515	-0.80056
C	-3.73346	3.90187	-1.26269	C	2.47733	-0.72170	0.04112
H	3.36928	-0.10739	2.09116	C	-0.99273	-0.83185	-1.09009
H	2.82065	1.57494	2.28823	O	-1.58407	-1.92649	-1.64774
H	2.95300	1.90819	-0.05548	C	-2.93939	-1.51155	-1.95052
H	-3.36930	0.10716	2.09106	C	-3.05794	-0.10213	-1.31102
H	-2.82075	-1.57522	2.28793	N	-1.68018	0.22166	-0.89504
H	-2.95293	-1.90818	-0.05583	C	3.56881	0.26714	-0.40853
H	3.64028	0.23812	-1.63399	C	4.97275	-0.36984	-0.33315
H	2.34177	-1.64813	-0.68031	C	3.45001	1.58887	0.36865
H	3.51992	-1.83817	0.61246	C	-4.02103	-0.02885	-0.10421
H	5.87057	-0.34078	-0.74849	C	-4.20606	1.42485	0.36714
H	5.35119	-0.03438	0.89339	C	-3.54802	-0.93774	1.04672
H	-3.64033	-0.23801	-1.63411	C	5.49277	-0.68244	1.07547
H	-2.34175	1.64815	-0.68052	C	6.88151	-1.32607	1.04747
H	-3.51967	1.83811	0.61247	C	4.44836	2.66935	-0.05823
H	-5.87057	0.34080	-0.74859	C	4.19496	4.00458	0.64638
H	-5.35117	0.03451	0.89331	C	-4.64947	-1.30262	2.04749
H	5.28413	-2.41908	-1.05022	C	-4.13448	-2.18119	3.19011
H	4.16835	-2.09496	-2.36874	C	-5.01411	2.31476	-0.58377
H	4.32859	-4.55812	-1.90770	C	-5.20127	3.73260	-0.03768
H	3.79745	-4.29125	-0.23934	H	2.98791	-1.95779	-1.73043
H	2.68661	-3.97724	-1.57994	H	2.70791	-2.92643	-0.25948
H	5.06128	2.38673	0.37942	H	2.62783	-0.95122	1.10432
H	5.39074	2.08894	-1.31942	H	-3.62307	-2.25074	-1.52518
H	7.42112	2.98676	-0.14159	H	-3.05186	-1.50089	-3.03889
H	7.38945	1.61540	0.97859	H	-3.37383	0.63062	-2.06011
H	7.73079	1.34700	-0.73626	H	3.36860	0.48598	-1.46892
H	-5.06126	-2.38663	0.37951	H	5.68645	0.29896	-0.83010
H	-5.39071	-2.08897	-1.31936	H	4.98452	-1.29573	-0.92602
H	-7.42110	-2.98671	-0.14148	H	3.56292	1.39474	1.44487
H	-7.38945	-1.61526	0.97860	H	2.42916	1.96303	0.23875
H	-7.73077	-1.34700	-0.73628	H	-4.99301	-0.40460	-0.46392
H	-5.28416	2.41928	-1.04976	H	-3.21290	1.86174	0.53067
H	-4.16871	2.09514	-2.36857	H	-4.70910	1.42188	1.34266
H	-4.32868	4.55830	-1.90734	H	-2.71958	-0.44179	1.56824
H	-3.79713	4.29129	-0.23914	H	-3.12991	-1.87102	0.64515
				H	4.79490	-1.35096	1.59715



H	5.53160	0.23901	1.66928	C	-3.48814	1.22905	3.88472
H	7.24566	-1.53986	2.05838	H	2.95110	-2.53244	-0.81239
H	6.86862	-2.27033	0.48940	H	2.74843	-2.77064	0.94337
H	7.61046	-0.66618	0.56156	H	2.87845	-0.40603	1.34505
H	4.38666	2.81061	-1.14676	H	-3.60331	-2.07330	0.04068
H	5.47555	2.34191	0.14941	H	-3.24328	-2.27114	-1.69141
H	4.91640	4.76797	0.33395	H	-3.19989	0.08202	-1.98105
H	3.18912	4.38069	0.42527	H	3.47996	-0.24422	-1.62946
H	4.27378	3.89535	1.73499	H	5.83025	-0.33215	-1.09141
H	-5.45928	-1.82422	1.51762	H	5.04110	-1.75967	-0.47110
H	-5.09676	-0.39132	2.46463	H	3.95853	1.78164	0.61138
H	-4.93628	-2.44147	3.89015	H	2.76066	1.88299	-0.66068
H	-3.70732	-3.11602	2.80698	H	-3.66738	1.66494	-0.24561
H	-3.34834	-1.66749	3.75635	H	-2.30146	0.59501	1.52829
H	-5.99722	1.85596	-0.76242	H	-3.54678	-0.62021	1.78798
H	-4.52018	2.37229	-1.56242	H	-5.90321	0.91316	0.48074
H	-5.78275	4.35565	-0.72644	H	-5.51340	-0.75320	0.11897
H	-5.72621	3.71766	0.92532	H	5.05122	-0.74318	1.84671
H	-4.23301	4.22187	0.12147	H	5.87378	0.66669	1.20520
<b>L2_4 Ground State</b>				H	7.51780	-0.92103	2.21982
N	1.32763	-0.05546	0.00102	H	6.97847	-2.20555	1.12595
C	0.54197	-1.03845	-0.18902	H	7.80682	-0.78336	0.47787
O	1.02514	-2.30942	-0.10280	H	4.63779	1.91234	-2.37547
C	2.45326	-2.15795	0.08901	H	5.80500	1.93909	-1.06309
C	2.65369	-0.63189	0.29424	H	5.39014	4.25800	-1.89014
C	-0.89939	-0.92550	-0.49537	H	3.65877	4.08775	-1.55060
O	-1.59886	-2.09325	-0.45082	H	4.82261	4.10551	-0.21919
C	-2.96431	-1.73644	-0.77932	H	-5.36188	-0.21868	-2.31090
C	-2.92449	-0.19174	-0.95759	H	-5.56387	1.49199	-1.97005
N	-1.50512	0.15910	-0.77306	H	-7.72150	0.45523	-2.73448
C	3.75443	-0.01464	-0.58814	H	-7.66255	-0.68758	-1.38282
C	5.12501	-0.67336	-0.32342	H	-7.87721	1.04016	-1.06957
C	3.76805	1.51592	-0.43830	H	-5.15035	1.14511	2.51436
C	-3.82377	0.60782	0.01294	H	-3.97433	2.39241	2.12770
C	-3.38260	0.42190	1.47509	H	-3.99067	1.90041	4.59003
C	-5.31398	0.28247	-0.19588	H	-3.59308	0.20544	4.26491
C	5.73916	-0.41184	1.05739	H	-2.41958	1.47489	3.88918
C	7.08552	-1.11911	1.23281	<b>L2_5 Ground State</b>			
C	4.78252	2.23346	-1.33404	N	1.14056	-0.23114	0.09965
C	4.65870	3.75678	-1.24620	C	0.48812	-1.23355	-0.33515
C	-5.84197	0.48770	-1.62114	O	1.09748	-2.44849	-0.41435
C	-7.36049	0.31498	-1.70966	C	2.46332	-2.22026	0.01380
C	-4.07399	1.35476	2.47595	C	2.49867	-0.71522	0.40442

C	-0.92343	-1.19970	-0.77120	H	2.24150	3.93570	0.87461
O	-1.51232	-2.41724	-0.94250	H	-5.48661	-1.21865	1.86094
C	-2.85076	-2.12660	-1.41725	H	-5.12465	0.44847	2.27466
C	-2.96892	-0.58315	-1.30161	H	-5.04466	-0.99290	4.31817
N	-1.60027	-0.14085	-0.97340	H	-3.79810	-2.00681	3.57208
C	3.58052	0.09274	-0.33952	H	-3.43889	-0.32420	3.98216
C	4.97548	-0.37695	0.11298	H	-5.88987	1.45646	-1.56013
C	3.35899	1.61109	-0.20324	H	-4.37913	1.66498	-2.43337
C	-3.96809	-0.09820	-0.22655	H	-5.63794	3.81840	-2.36858
C	-4.14431	1.42995	-0.28636	H	-5.64661	3.78060	-0.59741
C	-3.54588	-0.56129	1.18120	H	-4.11972	3.97629	-1.46938
C	6.14511	0.29658	-0.61171				
C	7.49870	-0.30122	-0.22012				
C	3.47246	2.17322	1.21816	<b>L2_6 Ground State</b>			
C	3.23867	3.68565	1.25548	N	-1.44168	-0.35343	-0.72929
C	-4.68281	-0.55396	2.20841	C	-0.84381	-1.07381	0.13320
C	-4.21809	-0.99386	3.59883	O	-1.54085	-2.02597	0.81294
C	-4.90627	1.94551	-1.51225	C	-2.89253	-1.95567	0.29516
C	-5.08958	3.46515	-1.48811	C	-2.85318	-0.77738	-0.71944
H	3.12063	-2.45836	-0.82907	C	0.58478	-0.95605	0.49287
H	2.67662	-2.90262	0.83988	O	1.08274	-1.96965	1.25341
H	2.65806	-0.59889	1.48395	C	2.48689	-1.65898	1.43345
H	-3.55888	-2.67413	-0.78999	C	2.67404	-0.29080	0.71796
H	-2.92734	-2.48789	-2.44724	N	1.34589	0.00530	0.15212
H	-3.24995	-0.14961	-2.26637	C	-3.78492	0.41089	-0.38715
H	3.47375	-0.15095	-1.40827	C	-3.38955	1.08513	0.93801
H	5.05555	-1.46348	-0.03870	C	-5.26699	-0.00496	-0.41489
H	5.08214	-0.21954	1.19550	C	-5.26699	-0.00496	-0.41489
H	2.36133	1.84051	-0.59153	C	3.77339	-0.30242	-0.36266
H	4.07571	2.13102	-0.85200	C	5.14808	-0.49528	0.30405
H	-4.93428	-0.56986	-0.47018	C	3.69218	0.93356	-1.27843
H	-3.14994	1.89204	-0.24579	C	-4.11711	2.40287	1.22821
H	-4.67877	1.76245	0.61278	C	-3.57429	3.10076	2.47798
H	-2.72410	0.07718	1.52948	C	-5.74882	-0.64701	-1.72176
H	-3.13338	-1.57863	1.13736	C	-7.26367	-0.86736	-1.73800
H	6.14720	1.37136	-0.39323	C	3.94225	2.28292	-0.59577
H	6.00013	0.20480	-1.69726	C	3.84120	3.44996	-1.58130
H	8.32323	0.19771	-0.74123	C	6.32470	-0.59977	-0.67142
H	7.67592	-0.20155	0.85775	C	7.64345	-0.92405	0.03476
H	7.54547	-1.36940	-0.46492	H	-3.56501	-1.79316	1.14096
H	4.46227	1.94929	1.63846	H	-3.12764	-2.91813	-0.16766
H	2.73831	1.68051	1.86777	H	-3.09731	-1.13114	-1.72602
H	3.31759	4.08021	2.27479	H	3.06793	-2.46487	0.97285
H	3.97271	4.21372	0.63421	H	2.69258	-1.63544	2.50615
				H	2.90865	0.49750	1.44452
				H	-3.62290	1.14419	-1.19015

H	-3.55804	0.39336	1.77699	C	-3.84292	0.10926	-0.15095
H	-2.31160	1.28232	0.91035	C	-4.06574	0.99537	1.08796
H	-5.87895	0.88527	-0.22587	C	-3.49757	-1.33870	0.24745
H	-5.47477	-0.68812	0.42275	C	4.17943	2.59916	0.23912
H	3.58036	-1.18247	-0.99612	C	3.78799	3.90698	-0.45364
H	5.12561	-1.40884	0.91630	C	5.38469	-1.72095	1.07566
H	5.33366	0.32888	1.00713	C	5.12774	-1.69400	2.58532
H	2.69561	0.95013	-1.73153	C	-4.69736	-2.15456	0.74009
H	4.40903	0.81013	-2.10051	C	-4.30903	-3.57764	1.14852
H	-5.19285	2.22684	1.35354	C	-4.76108	2.33274	0.81015
H	-4.01284	3.06938	0.36055	C	-4.99669	3.14360	2.08705
H	-4.10255	4.04044	2.67460	H	3.40549	-0.92045	-1.98422
H	-3.68457	2.46352	3.36403	H	2.76451	-2.51654	-1.52408
H	-2.50793	3.33084	2.36752	H	2.71924	-1.85873	0.75162
H	-5.24661	-1.61011	-1.88114	H	-3.31344	-0.82926	-2.59270
H	-5.45979	-0.00818	-2.56795	H	-2.57249	0.63580	-3.28921
H	-7.59146	-1.33433	-2.67328	H	-2.99280	1.76627	-1.25199
H	-7.57596	-1.51792	-0.91190	H	3.39503	0.29853	1.56239
H	-7.80088	0.08265	-1.63086	H	2.29233	1.66140	-0.18025
H	4.93379	2.29278	-0.12326	H	3.55870	1.26157	-1.33473
H	3.21106	2.42859	0.20912	H	5.71482	0.37640	0.75185
H	4.01737	4.41152	-1.08605	H	5.29322	-0.49853	-0.70449
H	4.57722	3.34929	-2.38865	H	-4.77502	0.09287	-0.73943
H	2.84709	3.48637	-2.04208	H	-3.09234	1.17428	1.56167
H	6.43220	0.34100	-1.22486	H	-4.66984	0.44158	1.81803
H	6.10642	-1.37317	-1.42114	H	-2.71949	-1.31447	1.02089
H	8.47444	-0.98648	-0.67651	H	-3.05220	-1.86969	-0.60504
H	7.89385	-0.15337	0.77402	H	5.25013	2.41637	0.08406
H	7.58352	-1.88258	0.56463	H	4.03822	2.70138	1.32431
				H	4.38400	4.75001	-0.08647
				H	3.93847	3.83839	-1.53807
				H	2.73088	4.14162	-0.28132
				H	6.44423	-1.94377	0.89497
				H	4.82695	-2.55207	0.62339
				H	5.46640	-2.62136	3.06005
				H	5.66227	-0.86086	3.05802
				H	4.06341	-1.57450	2.81586
				H	-5.45726	-2.19317	-0.05347
				H	-5.17231	-1.65054	1.59147
				H	-5.17928	-4.15014	1.48854
				H	-3.85838	-4.11994	0.30828
				H	-3.57584	-3.56546	1.96384
				H	-5.72229	2.14507	0.31034
				H	-4.16447	2.93376	0.11170
<b>L2_7 Ground State</b>							
N	1.19662	-0.51909	0.27217				
C	0.64379	-0.58258	-0.87260				
O	1.34740	-1.06688	-1.93318				
C	2.64238	-1.43711	-1.39748				
C	2.57987	-0.99614	0.09234				
C	-0.73594	-0.14722	-1.17144				
O	-1.27113	-0.64588	-2.32183				
C	-2.58185	-0.03486	-2.42464				
C	-2.76040	0.71156	-1.07549				
N	-1.43145	0.62765	-0.43944				
C	3.59503	0.09481	0.50211				
C	3.35560	1.40792	-0.26315				
C	5.04699	-0.40182	0.36307				

H	-5.49659	4.09497	1.87321
H	-5.62227	2.58821	2.79650
H	-4.04801	3.36827	2.58884

**L2\_8 Ground State**

N	-1.26867	-0.59009	-0.28645
C	-0.65227	-0.31123	0.79162
O	-1.31136	-0.38340	1.98110
C	-2.65024	-0.82993	1.65117
C	-2.65719	-0.90291	0.09763
C	0.76015	0.11429	0.87354
O	1.34934	-0.04494	2.09084
C	2.70177	0.45125	1.93014
C	2.79889	0.81381	0.42118
N	1.43606	0.58964	-0.09456
C	-3.65120	0.05169	-0.60346
C	-3.30969	1.52597	-0.32578
C	-5.11059	-0.28934	-0.25074
C	3.83354	0.00027	-0.38889
C	3.48977	-1.49930	-0.40449
C	5.26999	0.26149	0.10358
C	-4.10823	2.53612	-1.15757
C	-3.61831	3.97173	-0.95097
C	-5.54024	-1.73302	-0.53941
C	-7.04235	-1.94546	-0.33402
C	5.70838	1.73313	0.16865
C	5.61840	2.46683	-1.17273
C	4.33656	-2.33824	-1.36846
C	3.85117	-3.78757	-1.45429
H	-3.35469	-0.10578	2.06712
H	-2.81047	-1.79985	2.13038
H	-2.86978	-1.92304	-0.23655
H	3.38636	-0.34012	2.24406
H	2.82598	1.31389	2.59087
H	3.02696	1.87726	0.29824
H	-3.51309	-0.12051	-1.68054
H	-2.24315	1.67264	-0.53199
H	-3.45430	1.75062	0.74167
H	-5.76818	0.38204	-0.81605
H	-5.29770	-0.06045	0.80949
H	3.74683	0.36158	-1.42212
H	2.43586	-1.60451	-0.68713
H	3.58454	-1.91798	0.60875
H	5.96255	-0.27149	-0.55908

H	5.39833	-0.19448	1.09621
H	-5.17494	2.48083	-0.90663
H	-4.02736	2.26965	-2.22078
H	-4.19690	4.68365	-1.55027
H	-3.70704	4.27047	0.10081
H	-2.56390	4.07153	-1.23463
H	-4.99009	-2.43087	0.10520
H	-5.26872	-1.99263	-1.57217
H	-7.33235	-2.98262	-0.53518
H	-7.33633	-1.70979	0.69615
H	-7.62617	-1.29855	-0.99979
H	6.74558	1.76375	0.52672
H	5.11977	2.27328	0.92242
H	6.02395	3.48156	-1.09573
H	6.18639	1.93670	-1.94712
H	4.58381	2.55027	-1.52339
H	5.38952	-2.32915	-1.06006
H	4.30384	-1.87990	-2.36688
H	4.46421	-4.37614	-2.14605
H	3.89284	-4.27552	-0.47269
H	2.81236	-3.83387	-1.80208

**L2\_9 Ground State**

N	-1.42745	-0.24287	-0.34548
C	-0.72071	-1.28576	-0.16469
O	-1.29595	-2.51452	-0.27894
C	-2.69773	-2.25748	-0.54248
C	-2.79276	-0.70873	-0.64560
C	0.72039	-1.28570	0.16423
O	1.29552	-2.51442	0.27942
C	2.69744	-2.25727	0.54215
C	2.79242	-0.70852	0.64502
N	1.42721	-0.24274	0.34428
C	-3.83777	-0.08800	0.30217
C	-5.24980	-0.51931	-0.13545
C	-3.66284	1.43705	0.43055
C	3.83785	-0.08796	-0.30237
C	5.24965	-0.51959	0.13568
C	3.66327	1.43714	-0.43071
C	-6.38087	-0.02740	0.77315
C	-7.74427	-0.59426	0.36971
C	-3.89269	2.24223	-0.85327
C	-3.69600	3.74380	-0.62950
C	3.89291	2.24221	0.85321

C	3.69654	3.74383	0.62946	C	2.52345	-1.99336	1.16766
C	6.38113	-0.02767	-0.77242	C	2.56724	-0.44265	1.11659
C	7.74430	-0.59479	-0.36859	C	-0.71276	-1.23305	-0.26897
H	-3.27465	-2.66510	0.29457	O	-1.28926	-2.46795	-0.23220
H	-2.97130	-2.78586	-1.45856	C	-2.55548	-2.31450	-0.92122
H	-3.02919	-0.40265	-1.67282	C	-2.67347	-0.78600	-1.16404
H	3.27391	-2.66487	-0.29523	N	-1.34882	-0.25833	-0.78442
H	2.97158	-2.78558	1.45808	C	3.65672	0.13225	0.18309
H	3.02836	-0.40226	1.67230	C	3.74308	1.66370	0.30717
H	-3.64933	-0.51609	1.29930	C	3.42097	-0.29658	-1.27950
H	-5.43631	-0.17605	-1.16276	C	-3.78774	-0.09381	-0.34635
H	-5.29335	-1.61767	-0.17648	C	-3.94108	1.38093	-0.76027
H	-2.64517	1.62873	0.78602	C	-3.53913	-0.23025	1.16831
H	-4.34238	1.80493	1.21016	C	4.31958	2.17364	1.63256
H	3.64965	-0.51595	-1.29958	C	4.42905	3.70005	1.67216
H	5.29301	-1.61796	0.17650	C	4.65138	-0.18582	-2.19226
H	5.43585	-0.17656	1.16312	C	5.76571	-1.18118	-1.85376
H	2.64574	1.62903	-0.78648	C	-4.78849	-0.01383	2.02863
H	4.34311	1.80492	-1.21011	C	-4.49554	-0.13343	3.52618
H	-6.42368	1.06831	0.75175	C	-4.54404	1.60304	-2.15175
H	-6.15755	-0.30516	1.81279	C	-4.71525	3.08791	-2.48251
H	-8.54155	-0.22537	1.02438	H	3.33136	-2.47809	0.61360
H	-7.99922	-0.31148	-0.65897	H	2.49613	-2.38973	2.18721
H	-7.74854	-1.68990	0.42153	H	2.71114	-0.03272	2.12102
H	-4.90541	2.06314	-1.23902	H	-3.34098	-2.72445	-0.28130
H	-3.19746	1.90120	-1.63048	H	-2.50573	-2.89443	-1.84783
H	-3.85859	4.31294	-1.55174	H	-2.83536	-0.58079	-2.22671
H	-4.39383	4.12471	0.12656	H	4.60775	-0.29729	0.53285
H	-2.67926	3.95600	-0.27860	H	2.73890	2.07890	0.15457
H	4.90550	2.06293	1.23922	H	4.36698	2.05192	-0.50839
H	3.19742	1.90127	1.63022	H	2.60345	0.31122	-1.68478
H	3.85898	4.31290	1.55177	H	3.06666	-1.33594	-1.31544
H	4.39465	4.12465	-0.12639	H	-4.72286	-0.62348	-0.59203
H	2.67993	3.95622	0.27829	H	-2.95465	1.85797	-0.70257
H	6.42408	1.06804	-0.75082	H	-4.57739	1.89237	-0.02669
H	6.15814	-0.30521	-1.81220	H	-2.75632	0.48070	1.46159
H	8.54186	-0.22590	-1.02291	H	-3.13651	-1.22643	1.39753
H	7.99892	-0.31222	0.66023	H	3.69606	1.83939	2.47190
H	7.74844	-1.69042	-0.42061	H	5.31259	1.72894	1.79148
				H	4.84460	4.04921	2.62407
				H	5.07695	4.06948	0.86787
				H	3.44506	4.16658	1.54424
				H	5.05183	0.83584	-2.16444
				H	4.32798	-0.35294	-3.22775
<b>L2_10 Ground State</b>							
N	1.22213	-0.05971	0.64658				
C	0.63551	-1.14357	0.32815				
O	1.26972	-2.33433	0.52444				

H	6.59365	-1.10669	-2.56752	H	2.71136	-0.03310	2.12105
H	6.17960	-1.00790	-0.85397	H	-4.72285	-0.62338	-0.59162
H	5.39152	-2.21239	-1.88334	H	-2.95412	1.85760	-0.70374
H	-5.55448	-0.74890	1.74302	H	-4.57663	1.89281	-0.02739
H	-5.22223	0.97298	1.82229	H	-2.75615	0.48158	1.46141
H	-5.40060	0.01392	4.12605	H	-3.13642	-1.22557	1.39821
H	-4.08860	-1.12227	3.77065	H	4.60774	-0.29749	0.53253
H	-3.75790	0.61375	3.84258	H	2.73879	2.07869	0.15466
H	-5.51896	1.09793	-2.20965	H	4.36688	2.05180	-0.50830
H	-3.91159	1.13794	-2.91902	H	2.60269	0.31082	-1.68453
H	-5.14957	3.23094	-3.47831	H	3.06681	-1.33617	-1.31557
H	-5.37333	3.57995	-1.75591	H	-3.91200	1.13646	-2.91950
H	-3.75026	3.60804	-2.45935	H	-5.51916	1.09756	-2.20958
<b>L2_11 Ground State</b>				H	-5.14933	3.22963	-3.47968
N	-1.34876	-0.25894	-0.78433	H	-5.37234	3.57980	-1.75742
C	-0.71282	-1.23352	-0.26849	H	-3.74950	3.60678	-2.46144
O	-1.28950	-2.46832	-0.23113	H	-5.55432	-0.74785	1.74351
C	-2.55579	-2.31496	-0.92005	H	-5.22215	0.97409	1.82166
C	-2.67352	-0.78657	-1.16362	H	-5.40053	0.01646	4.12605
C	0.63553	-1.14399	0.32845	H	-4.08841	-1.11982	3.77140
O	1.26984	-2.33472	0.52460	H	-3.75788	0.61627	3.84224
C	2.52364	-1.99370	1.16762	H	5.05038	0.83677	-2.16534
C	2.56732	-0.44299	1.11662	H	4.32698	-0.35273	-3.22814
N	1.22212	-0.06011	0.64684	H	6.59334	-1.10487	-2.56877
C	-3.78763	-0.09377	-0.34623	H	6.18012	-1.00578	-0.85504
C	-3.94069	1.38080	-0.76089	H	5.39232	-2.21115	-1.88358
C	-3.53899	-0.22948	1.16849	H	5.31245	1.72855	1.79158
C	3.65663	0.13205	0.18298	H	3.69590	1.83903	2.47196
C	3.74297	1.66348	0.30722	H	4.84453	4.04879	2.62431
C	3.42063	-0.29665	-1.27960	H	5.07695	4.06916	0.86812
C	-4.54401	1.60230	-2.15231	H	3.44504	4.16630	1.54443
C	-4.71471	3.08704	-2.48395	<b>L2_12 Ground State</b>			
C	-4.78836	-0.01256	2.02867	N	1.23743	-0.73173	0.17794
C	-4.49545	-0.13118	3.52630	C	0.58494	-0.82773	-0.91068
C	4.65065	-0.18519	-2.19281	O	1.17507	-1.39312	-2.00148
C	5.76582	-1.17967	-1.85455	C	2.48015	-1.82726	-1.54226
C	4.31946	2.17331	1.63266	C	2.59102	-1.24607	-0.10721
C	4.42900	3.69971	1.67237	C	-0.80080	-0.35718	-1.11001
H	-3.34129	-2.72442	-0.27979	O	-1.45467	-0.89812	-2.17817
H	-2.50630	-2.89539	-1.84636	C	-2.76248	-0.26964	-2.17995
H	-2.83542	-0.58184	-2.22639	C	-2.78374	0.57158	-0.87386
H	3.33151	-2.47836	0.61341	N	-1.40587	0.47148	-0.35764
H	2.49652	-2.39011	2.18716	C	3.64151	-0.12283	0.04774

C	3.79839	0.28635	1.52346	H	-5.78725	2.15412	0.33304
C	3.30076	1.09014	-0.83949	H	-4.30072	2.92852	-0.19105
C	-3.81098	0.14681	0.20668	H	-5.55959	4.43639	1.34728
C	-4.01425	1.29478	1.21686	H	-5.51927	3.20310	2.61835
C	-3.42791	-1.14291	0.95840	H	-4.01731	3.96953	2.08362
C	4.48135	-0.75653	2.41518				
C	4.65282	-0.26870	3.85608				
C	4.49043	2.01492	-1.11748	<b>L2_13 Ground State</b>			
C	4.10643	3.21821	-1.98202	N	1.19139	-0.26780	0.22944
C	-3.37101	-2.44279	0.14573	C	0.54151	-1.25660	-0.23918
C	-3.11051	-3.65921	1.03882	O	1.13186	-2.48210	-0.29600
C	-4.80325	2.49620	0.68432	C	2.48121	-2.27995	0.19343
C	-4.98683	3.58910	1.74062	C	2.52461	-0.77818	0.59533
H	3.22948	-1.44011	-2.23731	C	-0.84813	-1.19546	-0.73814
H	2.49707	-2.92109	-1.56575	O	-1.44555	-2.40138	-0.95557
H	2.81580	-2.04197	0.60935	C	-2.75677	-2.08373	-1.48581
H	-3.51763	-1.05629	-2.21961	C	-2.85910	-0.54091	-1.34894
H	-2.83295	0.34545	-3.08200	N	-1.50049	-0.12379	-0.95312
H	-2.97302	1.62045	-1.12215	C	3.65399	0.01328	-0.09269
H	4.59795	-0.54710	-0.29949	C	5.01639	-0.48366	0.42932
H	2.80359	0.52148	1.92224	C	3.45598	1.53448	0.04096
H	4.38166	1.21461	1.57538	C	-3.89809	-0.05977	-0.31048
H	2.49029	1.65706	-0.36410	C	-4.04980	1.47163	-0.35045
H	2.89992	0.75203	-1.80489	C	-3.54540	-0.55336	1.10603
H	-4.76651	-0.02392	-0.31525	C	6.24697	0.19709	-0.18672
H	-3.02936	1.62399	1.57386	C	6.34418	0.04537	-1.70744
H	-4.54354	0.90029	2.09468	C	3.49274	2.08652	1.47037
H	-4.16424	-1.28144	1.76221	C	3.29845	3.60462	1.50239
H	-2.46081	-0.98298	1.45083	C	-4.72644	-0.54613	2.08224
H	3.90253	-1.68924	2.42167	C	-4.33019	-1.01723	3.48359
H	5.46447	-1.00801	1.99191	C	-4.74904	2.01997	-1.59925
H	5.14421	-1.02317	4.48058	C	-4.91118	3.54160	-1.55572
H	5.25967	0.64424	3.89327	H	3.17102	-2.52367	-0.62142
H	3.68151	-0.03838	4.30971	H	2.64645	-2.97104	1.02323
H	5.28425	1.44085	-1.61643	H	2.63423	-0.67066	1.68200
H	4.92056	2.37066	-0.17257	H	-3.50028	-2.63151	-0.90117
H	4.96982	3.86336	-2.17956	H	-2.79084	-2.42655	-2.52438
H	3.70071	2.89574	-2.94876	H	-3.09140	-0.08739	-2.31747
H	3.33873	3.82653	-1.48901	H	3.58628	-0.22501	-1.16424
H	-2.58580	-2.39244	-0.61517	H	5.09489	-1.56577	0.24820
H	-4.32045	-2.58093	-0.39210	H	5.04872	-0.35892	1.52003
H	-3.07113	-4.58505	0.45408	H	2.48936	1.78794	-0.40650
H	-2.15559	-3.55605	1.56805	H	4.22238	2.04357	-0.55836
H	-3.89732	-3.77196	1.79470	H	-4.85907	-0.51276	-0.60486
				H	-3.05171	1.91790	-0.25759

H	-4.61891	1.79638	0.53006	C	-4.86614	-1.61458	2.88431
H	-2.73062	0.06639	1.50144	C	4.97415	-0.21067	-1.46035
H	-3.14628	-1.57603	1.06232	C	4.91664	0.06231	-2.96468
H	7.14454	-0.23271	0.27666	C	4.88676	1.92322	1.23208
H	6.25236	1.26209	0.07695	C	4.91944	3.16717	2.12411
H	7.27809	0.47368	-2.08758	H	-3.34124	-2.17559	-1.57459
H	6.31808	-1.01187	-2.00004	H	-2.35055	-1.63666	-2.95611
H	5.51758	0.55042	-2.21897	H	-2.62718	0.59905	-2.22794
H	4.44645	1.83316	1.95249	H	3.16568	-2.79184	-0.05682
H	2.70427	1.61112	2.06692	H	2.18821	-3.33765	1.33177
H	3.32020	3.99176	2.52735	H	2.46021	-1.19360	2.32027
H	4.08636	4.11525	0.93478	H	-4.67260	-0.10458	-0.97954
H	2.33597	3.88421	1.05805	H	-2.89044	2.04399	0.24675
H	-5.52378	-1.19216	1.68789	H	-4.57329	1.84269	0.71455
H	-5.15597	0.46174	2.14700	H	-2.92263	-0.19415	1.51687
H	-5.18768	-1.01595	4.16579	H	-3.29993	-1.65046	0.62244
H	-3.92440	-2.03596	3.45707	H	4.52055	-0.88832	0.99752
H	-3.55896	-0.36650	3.91284	H	3.69730	0.78107	2.61294
H	-5.73654	1.54693	-1.69927	H	2.75679	1.57394	1.36015
H	-4.18567	1.74749	-2.50113	H	3.17027	0.90346	-1.00637
H	-5.41486	3.91850	-2.45292	H	2.92789	-0.80365	-1.26273
H	-5.50245	3.84993	-0.68482	H	-3.62060	2.49508	-2.12185
H	-3.93579	4.03745	-1.48509	H	-5.29188	2.21150	-1.65838
<b>L2_14 Ground State</b>				H	-4.78521	4.66776	-1.73674
N	-1.29483	0.12959	-0.67941	H	-5.18158	4.18211	-0.07977
C	-0.71978	-1.00501	-0.63055	H	-3.49519	4.45131	-0.54195
O	-1.30407	-2.08115	-1.23017	H	-5.73904	-1.26677	0.93572
C	-2.49198	-1.55617	-1.87402	H	-5.41050	0.19731	1.84686
C	-2.57625	-0.08798	-1.37765	H	-5.82736	-1.71955	3.39979
C	0.56114	-1.27769	0.05336	H	-4.48970	-2.62197	2.66838
O	1.12757	-2.48642	-0.22510	H	-4.16226	-1.14192	3.57976
C	2.32311	-2.54182	0.59322	H	5.36190	-1.22449	-1.28441
C	2.41839	-1.12760	1.22666	H	5.69194	0.47155	-0.98990
N	1.14919	-0.47723	0.84943	H	5.89998	-0.05590	-3.43343
C	-3.76505	0.19864	-0.43206	H	4.22216	-0.62460	-3.46378
C	-3.86819	1.70141	-0.11462	H	4.57047	1.08352	-3.16516
C	-3.67356	-0.64380	0.85491	H	4.85827	2.23592	0.18078
C	3.62693	-0.29465	0.74547	H	5.81885	1.35442	1.35936
C	3.68769	1.02167	1.53948	H	5.77644	3.80814	1.88868
C	3.60280	-0.08099	-0.78642	H	4.00859	3.76451	1.99713
C	-4.32555	2.57954	-1.28463	H	4.98780	2.89150	3.18350
C	-4.45524	4.05337	-0.89154	<b>L2_15 Ground State</b>			
C	-5.00375	-0.79190	1.60094	N	1.11255	-0.11288	0.03156



C	0.45732	-0.81096	-0.80690	H	5.41202	2.29555	1.02420
O	1.07217	-1.84712	-1.44281	H	4.17650	3.37535	1.63648
C	2.45707	-1.77973	-1.02222	H	5.03046	4.26448	-0.50378
C	2.47164	-0.68525	0.07931	H	4.67370	2.74851	-1.33815
C	-0.96175	-0.59913	-1.16070	H	3.34944	3.75401	-0.73699
O	-1.52445	-1.57465	-1.92921	H	-5.49476	-2.07877	1.08397
C	-2.87611	-1.12010	-2.18824	H	-5.17200	-0.84577	2.29100
C	-3.02835	0.14600	-1.30309	H	-5.03575	-3.12428	3.31551
N	-1.66667	0.39513	-0.79337	H	-3.77055	-3.58282	2.16332
C	3.55181	0.39447	-0.11619	H	-3.45093	-2.33480	3.37520
C	4.96761	-0.21766	-0.14456	H	-6.00091	1.95562	-0.49091
C	3.38638	1.50762	0.93421	H	-4.50641	2.61809	-1.13580
C	-4.02647	-0.01006	-0.13324	H	-5.81299	4.40601	0.01464
C	-4.23928	1.33030	0.59332	H	-5.79782	3.47271	1.52038
C	-3.57836	-1.11454	0.84341	H	-4.28718	4.12430	0.86967
C	5.45409	-0.84842	1.16615				
C	6.86417	-1.43024	1.03672				
C	4.39434	2.66104	0.83195	<b>L2_16 Ground State</b>			
C	4.36151	3.39670	-0.51137	N	1.04511	-0.28374	0.43146
C	-4.70509	-1.66233	1.72555	C	0.45012	-1.11033	-0.33173
C	-4.21617	-2.73646	2.70022	O	1.08191	-2.25807	-0.70182
C	-5.02809	2.37767	-0.20034	C	2.37787	-2.20767	-0.05548
C	-5.24539	3.66860	0.59324	C	2.38686	-0.83820	0.68497
H	3.05683	-1.50740	-1.89775	C	-0.91423	-0.93367	-0.87149
H	2.75613	-2.77138	-0.67620	O	-1.46697	-2.04357	-1.43835
H	2.59821	-1.13388	1.07350	C	-2.75799	-1.61100	-1.93577
H	-3.56199	-1.92978	-1.92605	C	-2.91016	-0.16512	-1.39210
H	-2.95993	-0.90925	-3.25867	N	-1.58423	0.14764	-0.82560
H	-3.33067	1.00290	-1.91317	C	3.49575	0.11625	0.19971
H	3.36688	0.83057	-1.10848	C	4.89167	-0.48990	0.48813
H	5.67907	0.56286	-0.44282	C	3.31102	1.51218	0.81629
H	5.02099	-0.97495	-0.93987	C	-4.01098	0.00070	-0.31959
H	3.44838	1.06576	1.93808	C	-4.20464	1.48297	0.04797
H	2.36930	1.90299	0.84336	C	-3.71235	-0.85409	0.92722
H	-4.98394	-0.31673	-0.58554	C	5.89058	-0.34494	-0.66604
H	-3.25560	1.73344	0.86498	C	7.27635	-0.89473	-0.32282
H	-4.77040	1.14446	1.53570	C	4.29680	2.57481	0.32098
H	-2.76987	-0.72080	1.47238	C	4.00246	3.95682	0.91037
H	-3.14040	-1.95588	0.28899	C	-4.93838	-1.13027	1.80387
H	4.76365	-1.64152	1.48307	C	-4.59605	-1.95984	3.04377
H	5.44278	-0.09819	1.96612	C	-4.85790	2.33955	-1.04229
H	7.20323	-1.87540	1.97860	C	-5.06575	3.78971	-0.59806
H	6.90124	-2.20940	0.26549	H	3.14208	-2.28390	-0.83462
H	7.58514	-0.65324	0.75492	H	2.45533	-3.07160	0.60987
				H	2.50007	-0.97629	1.76831

H	-3.51450	-2.30691	-1.56421	N	-1.60814	0.19469	-0.78986
H	-2.72983	-1.65878	-3.02860	C	3.64697	0.18506	-0.39266
H	-3.10831	0.53134	-2.21266	C	5.04226	-0.46770	-0.29592
H	3.37179	0.20627	-0.89084	C	3.56295	1.56190	0.28724
H	4.80378	-1.55991	0.72519	C	-3.95137	0.03972	0.02661
H	5.30694	-0.02623	1.39383	C	-4.11268	1.52325	0.40256
H	3.39493	1.42604	1.91072	C	-3.48368	-0.79419	1.23674
H	2.28720	1.84447	0.61473	C	5.58397	-0.68670	1.12217
H	-4.94334	-0.36934	-0.77690	C	6.96156	-1.35444	1.11603
H	-3.22558	1.90180	0.31249	C	4.56924	2.59148	-0.23591
H	-4.82505	1.54796	0.95102	C	4.34958	3.97891	0.37262
H	-2.93568	-0.35331	1.51906	C	-4.57418	-1.08406	2.27899
H	-3.28217	-1.82021	0.62960	C	-5.66504	-2.03890	1.78361
H	5.97270	0.70972	-0.95429	C	-4.91193	2.36056	-0.60194
H	5.49269	-0.86808	-1.54709	C	-5.07706	3.81376	-0.14991
H	7.96764	-0.79708	-1.16715	H	3.01062	-2.12183	-1.53561
H	7.71178	-0.35926	0.52963	H	2.73734	-2.97463	0.00653
H	7.22505	-1.95700	-0.05359	H	2.71491	-0.90318	1.22172
H	4.25380	2.62717	-0.77607	H	-3.59777	-2.27826	-1.23579
H	5.32530	2.28662	0.57471	H	-3.03207	-1.64376	-2.80365
H	4.71239	4.70848	0.54726	H	-3.30122	0.55585	-1.96987
H	2.99265	4.29033	0.64358	H	3.43017	0.32917	-1.46256
H	4.06495	3.93861	2.00530	H	5.75650	0.15187	-0.85239
H	-5.69732	-1.65575	1.20677	H	5.02898	-1.43393	-0.82041
H	-5.39902	-0.18457	2.11682	H	3.69332	1.44537	1.37264
H	-5.48473	-2.15705	3.65371	H	2.54562	1.94233	0.14833
H	-4.16055	-2.92672	2.76330	H	-4.92761	-0.33897	-0.31228
H	-3.86497	-1.43972	3.67424	H	-3.11293	1.95575	0.53513
H	-5.82533	1.89711	-1.32025	H	-4.61211	1.59092	1.37791
H	-4.24377	2.33037	-1.95213	H	-2.64816	-0.26620	1.71126
H	-5.53578	4.38861	-1.38617	H	-3.07523	-1.75631	0.89828
H	-5.70739	3.84150	0.29006	H	4.88566	-1.30378	1.70325
H	-4.10965	4.26190	-0.34279	H	5.64885	0.27431	1.64702
				H	7.34166	-1.50064	2.13309
				H	6.92306	-2.33629	0.62847
				H	7.69138	-0.74410	0.57034
				H	4.48895	2.65338	-1.33062
				H	5.59514	2.26328	-0.02312
				H	4.44766	3.94881	1.46473
				H	5.07629	4.70529	-0.00834
				H	3.34545	4.35421	0.14253
				H	-5.03367	-0.14548	2.61528
				H	-4.09697	-1.51948	3.16635
				H	-6.38779	-2.26056	2.57670
<b>L2_17 Ground State</b>							
N	1.20482	-0.16078	-0.00457				
C	0.48902	-1.04049	-0.58205				
O	1.04286	-2.23776	-0.92234				
C	2.44853	-2.11034	-0.59521				
C	2.54881	-0.74995	0.14721				
C	-0.93999	-0.88062	-0.92312				
O	-1.55502	-1.99900	-1.40269				
C	-2.90677	-1.58220	-1.71841				
C	-2.99434	-0.13083	-1.17468				

H	-6.22426	-1.61899	0.93988
H	-5.23071	-2.99068	1.45242
H	-5.90216	1.90508	-0.74697
H	-4.42128	2.34628	-1.58386
H	-4.10143	4.29871	-0.02667
H	-5.59792	3.86967	0.81380
H	-5.65284	4.39827	-0.87622

**L2\_18 Ground State**

N	1.04914	-0.11317	-0.04164
C	0.34081	-0.93595	-0.70566
O	0.92378	-2.04603	-1.23793
C	2.33855	-1.89910	-0.96077
C	2.42194	-0.65395	-0.03644
C	-1.10987	-0.79946	-0.95030
O	-1.71821	-1.89883	-1.48203
C	-3.10665	-1.51705	-1.65697
C	-3.20089	-0.10963	-1.00557
N	-1.80396	0.23248	-0.68093
C	3.45263	0.39875	-0.48464
C	4.87596	-0.19508	-0.54623
C	3.34891	1.65898	0.39084
C	-4.10692	0.01404	0.24610
C	-4.43990	1.49727	0.50821
C	-3.50347	-0.61367	1.51762
C	5.49623	-0.59200	0.79912
C	6.89806	-1.18486	0.63471
C	4.28396	2.79932	-0.02344
C	4.04093	4.07355	0.78944
C	-3.27937	-2.13131	1.51780
C	-2.80703	-2.63498	2.88470
C	-5.42323	2.12733	-0.48462
C	-5.72607	3.59183	-0.15690
H	2.85053	-1.75086	-1.91799
H	2.69314	-2.82494	-0.50304
H	2.64828	-0.94957	0.99650
H	-3.73063	-2.27502	-1.18073
H	-3.31295	-1.50183	-2.73131
H	-3.55776	0.60984	-1.74909
H	3.17551	0.68374	-1.51147
H	5.53599	0.53148	-1.03620
H	4.87502	-1.07450	-1.20616
H	3.54103	1.39503	1.44068
H	2.31118	2.00665	0.35570

H	-5.04615	-0.51169	0.00939
H	-3.50233	2.06883	0.51801
H	-4.86648	1.58855	1.51622
H	-4.17911	-0.37387	2.35039
H	-2.55438	-0.10884	1.73629
H	4.85377	-1.32001	1.31231
H	5.54753	0.28431	1.45690
H	7.33379	-1.45999	1.60151
H	6.87566	-2.08547	0.00890
H	7.57427	-0.46699	0.15480
H	4.14377	3.01309	-1.09269
H	5.33199	2.49307	0.09187
H	4.71683	4.88049	0.48472
H	3.01182	4.42992	0.66287
H	4.19741	3.89239	1.85992
H	-2.53837	-2.41605	0.76412
H	-4.21549	-2.64019	1.24488
H	-2.64752	-3.71900	2.87952
H	-1.86135	-2.15848	3.16989
H	-3.54140	-2.40661	3.66680
H	-6.35781	1.54834	-0.48294
H	-5.02869	2.06605	-1.50750
H	-6.43648	4.02487	-0.86998
H	-6.15688	3.68986	0.84694
H	-4.81194	4.19675	-0.18432

**L2\_19 Ground State**

N	1.13861	-0.12363	-0.06797
C	0.41874	-0.90383	-0.76992
O	0.97167	-2.02959	-1.30179
C	2.38094	-1.94867	-0.97487
C	2.48589	-0.72359	-0.02633
C	-1.01499	-0.69905	-1.06327
O	-1.65635	-1.76708	-1.61769
C	-3.00712	-1.30672	-1.87040
C	-3.06772	0.08439	-1.18512
N	-1.66591	0.36824	-0.82305
C	3.57593	0.29018	-0.42073
C	4.97362	-0.36418	-0.44353
C	3.49580	1.53982	0.47218
C	-3.97305	0.14542	0.06539
C	-4.06301	1.57913	0.62192
C	-3.50091	-0.83993	1.15209
C	5.52937	-0.80748	0.91548

C	6.90896	-1.45894	0.78905	<b>L2_20 Ground State</b>			
C	4.49310	2.64473	0.11035	N	-1.42521	0.12569	-0.65453
C	4.27731	3.91485	0.93725	C	-0.82562	-0.89893	-0.19509
C	-4.54721	-1.14067	2.23091	O	-1.48712	-2.08690	-0.11954
C	-4.04448	-2.15219	3.26399	C	-2.80507	-1.82792	-0.66342
C	-4.59789	2.64983	-0.34137	C	-2.79931	-0.30326	-0.97093
C	-5.99209	2.35182	-0.90151	C	0.56725	-0.91636	0.29853
H	2.93142	-1.80705	-1.91156	O	1.09708	-2.15236	0.51056
H	2.67994	-2.89635	-0.52210	C	2.44420	-1.91510	0.98847
H	2.66375	-1.04557	1.00824	C	2.59731	-0.36612	0.95800
H	-3.70001	-2.04100	-1.45202	N	1.27303	0.11742	0.52867
H	-3.14692	-1.25633	-2.95465	C	-3.83437	0.53283	-0.18349
H	-3.40238	0.84234	-1.89961	C	-3.56909	0.48030	1.33118
H	3.34752	0.60306	-1.45142	C	-5.27733	0.13177	-0.54040
H	5.68104	0.33981	-0.89912	C	3.71284	0.12297	0.01307
H	4.95752	-1.23303	-1.11714	C	5.09132	-0.39239	0.49565
H	3.63909	1.25120	1.52333	C	3.66303	1.65264	-0.13058
H	2.47587	1.93291	0.40713	C	-4.40536	1.46027	2.16205
H	-4.97358	-0.17065	-0.26734	C	-3.99114	1.47004	3.63581
H	-3.06245	1.87297	0.96035	C	-5.63435	0.20629	-2.03012
H	-4.70689	1.56579	1.51048	C	-7.12524	-0.03090	-2.28413
H	-2.59140	-0.44115	1.61903	C	4.66094	2.24237	-1.13191
H	-3.20624	-1.79279	0.69146	C	4.49667	3.75643	-1.28904
H	4.83862	-1.51388	1.39499	C	5.99309	-0.92107	-0.62614
H	5.59603	0.05609	1.58853	C	7.36932	-1.36017	-0.12244
H	7.29900	-1.76656	1.76552	H	-3.54021	-2.12912	0.08670
H	6.86895	-2.34878	0.14888	H	-2.93043	-2.44847	-1.55517
H	7.63172	-0.76474	0.34335	H	-2.96098	-0.12801	-2.03909
H	4.39938	2.88198	-0.95903	H	3.13311	-2.43200	0.31385
H	5.52234	2.29109	0.25556	H	2.52728	-2.34875	1.98858
H	4.99753	4.69638	0.67010	H	2.79711	0.03032	1.96222
H	3.26953	4.31790	0.78232	H	-3.68034	1.57180	-0.50842
H	4.38872	3.70942	2.00899	H	-2.50843	0.70083	1.49850
H	-5.45958	-1.52498	1.75268	H	-3.73834	-0.53981	1.70739
H	-4.83799	-0.21560	2.74379	H	-5.96368	0.78784	0.00843
H	-4.80426	-2.36040	4.02560	H	-5.48099	-0.88408	-0.16878
H	-3.77774	-3.10344	2.78737	H	3.49946	-0.31905	-0.97277
H	-3.14990	-1.77817	3.77625	H	4.96303	-1.19843	1.23238
H	-3.89169	2.80043	-1.16760	H	5.60953	0.41273	1.03508
H	-4.62586	3.60505	0.19869	H	3.83722	2.10349	0.85869
H	-6.36639	3.19049	-1.49901	H	2.64624	1.93786	-0.42040
H	-5.99276	1.46499	-1.54586	H	-5.47140	1.21060	2.09010
H	-6.71070	2.17000	-0.09255	H	-4.29636	2.47042	1.74296
				H	-4.59666	2.17334	4.21842

H	-4.10899	0.47600	4.08454	H	2.70360	-2.70280	-0.91306
H	-2.93938	1.75955	3.74638	H	2.67492	-1.48772	1.12049
H	-5.05389	-0.53188	-2.59877	H	-3.40897	-1.47473	-2.30119
H	-5.34502	1.19084	-2.42338	H	-2.71628	-0.20336	-3.34255
H	-7.36303	0.01665	-3.35252	H	-3.15605	1.37650	-1.63502
H	-7.43566	-1.01643	-1.91593	H	3.30031	0.80404	1.35732
H	-7.73664	0.72069	-1.77042	H	2.13527	1.71488	-0.60044
H	4.52670	1.75571	-2.10827	H	3.30669	0.99488	-1.69700
H	5.68961	2.02228	-0.81779	H	5.59983	0.76720	0.47646
H	5.21429	4.16637	-2.00866	H	5.19674	-0.49110	-0.66900
H	3.48819	4.00753	-1.63831	H	-4.88524	-0.16935	-0.70847
H	4.65144	4.27005	-0.33228	H	-3.22075	1.48148	1.24121
H	6.11086	-0.15315	-1.39978	H	-4.77640	0.79305	1.68532
H	5.49078	-1.76747	-1.11557	H	-2.77820	-1.05216	1.31292
H	7.98944	-1.75049	-0.93695	H	-3.10594	-1.99395	-0.12521
H	7.90703	-0.52047	0.33448	H	3.72172	3.38121	-1.41469
H	7.28027	-2.14701	0.63684	H	5.09837	2.46945	-0.83392
<b>L2_21 Ground State</b>				H	4.49845	4.38384	0.69930
N	1.10823	-0.35430	0.34176	H	2.91058	3.64952	0.98446
C	0.54961	-0.71225	-0.74443	H	4.37728	2.83743	1.54512
O	1.25899	-1.42670	-1.66174	H	4.80260	-2.09898	1.19398
C	2.56381	-1.62854	-1.06383	H	5.01000	-0.81642	2.37516
C	2.50320	-0.82563	0.26631	H	7.09861	-2.19621	2.15381
C	-0.84361	-0.39877	-1.12264	H	7.19051	-1.79813	0.43058
O	-1.37121	-1.17584	-2.11077	H	7.40724	-0.52826	1.64287
C	-2.70003	-0.64383	-2.34101	H	-5.49735	-2.23610	0.52147
C	-2.89170	0.40289	-1.21101	H	-5.21548	-1.30464	1.98246
N	-1.55694	0.51165	-0.59126	H	-5.15190	-3.75428	2.48631
C	3.48906	0.36118	0.37059	H	-3.84153	-3.97623	1.31482
C	3.18998	1.43181	-0.69479	H	-3.56216	-3.03087	2.78330
C	4.95409	-0.10810	0.33386	H	-5.88183	2.05292	-0.17892
C	-3.95036	0.01440	-0.15380	H	-4.34703	2.80982	-0.57874
C	-4.19121	1.16847	0.83607	H	-5.70341	4.32822	0.86367
C	-3.56057	-1.28386	0.57915	H	-5.78407	3.08695	2.12514
C	4.04852	2.70358	-0.61530	H	-4.23262	3.83366	1.71853
C	3.95464	3.43308	0.72811	<b>L2_22 Ground State</b>			
C	5.33690	-1.15884	1.38333	N	1.17420	-0.11739	-0.13903
C	6.84195	-1.43767	1.40615	C	0.48433	-1.07484	-0.61548
C	-4.73285	-1.98710	1.27128	O	1.03659	-2.31668	-0.71040
C	-4.30097	-3.25870	2.00566	C	2.41748	-2.14757	-0.30554
C	-4.92413	2.38057	0.25052	C	2.48994	-0.68515	0.21154
C	-5.17678	3.47000	1.29592	C	-0.91271	-0.96206	-1.08424
H	3.31402	-1.26705	-1.77094	O	-1.50256	-2.13568	-1.45052

C	-2.82575	-1.76670	-1.91372	H	-5.66883	-0.35020	1.66547
C	-2.93129	-0.24954	-1.60086	H	-5.49276	-2.18768	3.36426
N	-1.57604	0.12214	-1.15344	H	-3.87366	-2.59475	2.77077
C	3.64599	0.13955	-0.38398	H	-4.15839	-1.04007	3.56462
C	5.01532	-0.50005	-0.07101	H	-4.93017	1.80402	1.58419
C	3.53838	1.60985	0.05420	H	-6.13191	1.71692	0.30474
C	-3.98201	0.10687	-0.52637	H	-5.51730	4.05471	-0.42891
C	-4.08848	1.63672	-0.40449	H	-4.29666	4.13106	0.84881
C	-3.68409	-0.59161	0.82136	H	-6.01431	4.03085	1.27144
C	5.43959	-0.48974	1.40281				
C	6.79901	-1.16073	1.61592				
C	4.60395	2.53185	-0.54649	<b>L2_23 Ground State</b>			
C	4.36756	4.00166	-0.18972	N	1.35657	-0.09127	0.06840
C	-4.92653	-1.14550	1.52920	C	0.58933	-1.09940	-0.05279
C	-4.59765	-1.77833	2.88276	O	1.09856	-2.35277	0.10812
C	-5.15561	2.14874	0.56723	C	2.52471	-2.16193	0.27805
C	-5.25391	3.67665	0.56642	C	2.69676	-0.62213	0.38266
H	3.04525	-2.31603	-1.18765	C	-0.85610	-1.03407	-0.35341
H	2.64594	-2.90417	0.44796	O	-1.53451	-2.20732	-0.21694
H	2.56983	-0.66214	1.30648	C	-2.90465	-1.90237	-0.57660
H	-3.55461	-2.37953	-1.37675	C	-2.89865	-0.37024	-0.84287
H	-2.88244	-1.99226	-2.98273	N	-1.48313	0.01663	-0.70427
H	-3.16264	0.31939	-2.50920	C	3.77514	-0.04152	-0.55085
H	3.51584	0.10829	-1.47691	C	5.16158	-0.65558	-0.26280
H	5.78386	0.01477	-0.66087	C	3.76000	1.49544	-0.49870
H	5.02257	-1.53865	-0.43186	C	-3.79326	0.46951	0.09810
H	3.58110	1.67149	1.15104	C	-3.31312	0.37369	1.55782
H	2.54328	1.97064	-0.22602	C	-5.28098	0.10723	-0.05466
H	-4.94325	-0.27405	-0.90774	C	5.78722	-0.29463	1.09020
H	-4.29551	2.05235	-1.40181	C	7.14964	-0.96311	1.29181
H	-3.10596	2.02676	-0.11079	C	4.74992	2.17355	-1.45088
H	-3.15944	0.10968	1.48286	C	4.59566	3.69658	-1.46024
H	-2.98478	-1.42464	0.67404	C	-5.83983	0.20357	-1.47956
H	4.68505	-0.99829	2.01773	C	-7.35769	0.00993	-1.52438
H	5.48340	0.54334	1.76885	C	-4.07595	1.24720	2.56565
H	7.09519	-1.14227	2.67053	C	-4.05726	2.74179	2.23151
H	6.77802	-2.20859	1.29222	H	3.02345	-2.58480	-0.60113
H	7.58203	-0.65350	1.03929	H	2.83776	-2.71204	1.16792
H	4.61004	2.41531	-1.63967	H	2.92823	-0.32483	1.41403
H	5.60305	2.23402	-0.20215	H	-3.54404	-2.20885	0.25470
H	4.38037	4.14895	0.89719	H	-3.16139	-2.49322	-1.46039
H	5.13687	4.65010	-0.62395	H	-3.19832	-0.16076	-1.87448
H	3.39244	4.34306	-0.55667	H	3.49326	-0.34206	-1.57194
H	-5.40210	-1.89352	0.87848	H	5.85054	-0.35080	-1.06034
				H	5.09768	-1.75051	-0.33984

H	3.95716	1.83095	0.52953	C	-3.47591	-0.45603	1.30069
H	2.74310	1.82831	-0.73127	C	6.22054	0.19138	-0.61428
H	-3.66233	1.50802	-0.23322	C	7.56547	-0.43456	-0.23706
H	-2.25377	0.65421	1.58174	C	3.62391	2.14232	1.23707
H	-3.36564	-0.67191	1.89377	C	3.42527	3.65994	1.26658
H	-5.86646	0.77702	0.58724	C	-4.59418	-0.43599	2.35353
H	-5.45944	-0.90533	0.33801	C	-5.68673	-1.48323	2.11557
H	5.11589	-0.58824	1.90826	C	-4.81987	2.06521	-1.38517
H	5.90189	0.79355	1.16733	C	-4.98222	3.58719	-1.36008
H	7.58995	-0.69434	2.25833	H	3.13404	-2.49655	-0.76538
H	7.06317	-2.05601	1.25541	H	2.70147	-2.91538	0.91307
H	7.85465	-0.66217	0.50738	H	2.74143	-0.60599	1.53550
H	4.60094	1.78276	-2.46761	H	-3.54270	-2.57131	-0.66407
H	5.78103	1.91775	-1.17353	H	-2.92410	-2.40083	-2.32820
H	5.31002	4.16944	-2.14359	H	-3.19600	-0.05560	-2.14876
H	3.58608	3.98714	-1.77389	H	3.52831	-0.20054	-1.37101
H	4.76278	4.11444	-0.45988	H	5.09912	-1.53976	-0.01537
H	-5.36513	-0.54562	-2.12655	H	5.17116	-0.28947	1.21052
H	-5.58011	1.18295	-1.90522	H	2.47351	1.82200	-0.55043
H	-7.74055	0.07301	-2.54893	H	4.18941	2.07038	-0.84278
H	-7.64189	-0.96962	-1.12079	H	-4.87484	-0.44650	-0.35328
H	-7.86977	0.77387	-0.92706	H	-3.05748	1.98749	-0.12779
H	-3.62310	1.09519	3.55400	H	-4.58327	1.87730	0.73867
H	-5.11453	0.90422	2.65801	H	-2.64472	0.17837	1.63034
H	-4.52306	3.33012	3.02990	H	-3.07254	-1.47700	1.25561
H	-3.02946	3.10206	2.10313	H	6.24995	1.26720	-0.40299
H	-4.59985	2.95831	1.30435	H	6.05871	0.09605	-1.69715
				H	8.39389	0.04214	-0.77260
				H	7.75961	-0.33209	0.83762
				H	7.58466	-1.50508	-0.47533
				H	4.61583	1.89897	1.64126
				H	2.89076	1.67141	1.90378
				H	3.53139	4.06025	2.28116
				H	4.15991	4.16636	0.62821
				H	2.42741	3.92989	0.90146
				H	-5.04798	0.56237	2.40318
				H	-4.14360	-0.61015	3.33911
				H	-6.43013	-1.47032	2.92037
				H	-6.22101	-1.31083	1.17442
				H	-5.25830	-2.49263	2.07326
				H	-5.81039	1.58970	-1.42751
				H	-4.30194	1.77729	-2.30926
				H	-5.53081	3.94797	-2.23734
				H	-5.52964	3.91021	-0.46613
<b>L2_24 Ground State</b>							
N	1.21528	-0.21755	0.16620				
C	0.53560	-1.20931	-0.25109				
O	1.11707	-2.43811	-0.32586				
C	2.49280	-2.23614	0.08324				
C	2.56607	-0.72872	0.45914				
C	-0.87974	-1.14852	-0.67180				
O	-1.49292	-2.35474	-0.83784				
C	-2.83026	-2.03922	-1.29977				
C	-2.91748	-0.49361	-1.18521				
N	-1.53862	-0.07704	-0.86689				
C	3.65602	0.04820	-0.30573				
C	5.04595	-0.45082	0.13057				
C	3.47220	1.57229	-0.17762				
C	-3.90357	0.00849	-0.10642				
C	-4.05811	1.53856	-0.16396				

H	-4.00535	4.08497	-1.34702	H	-4.12465	1.96661	-2.47821
				H	-4.26201	4.44981	-2.13185
				H	-3.76650	4.25248	-0.44298
<b>L2_25 Ground State</b>				H	-2.63419	3.86487	-1.74583
N	-1.38735	-0.65181	-0.21013	H	-5.12745	-2.37366	0.45468
C	-0.75324	-0.23871	0.81325	H	-5.42064	-2.15136	-1.26228
O	-1.39753	-0.14063	2.00905	H	-7.48452	-2.96894	-0.08438
C	-2.74559	-0.61018	1.75799	H	-7.45650	-1.54753	0.97167
C	-2.77453	-0.88984	0.22839	H	-7.76158	-1.35495	-0.76012
C	0.66500	0.17490	0.82057	H	5.06850	2.23865	0.45734
O	1.26403	0.18997	2.04374	H	5.41909	1.86818	-1.22284
C	2.61735	0.64880	1.80132	H	7.44920	2.76859	-0.04629
C	2.70862	0.76921	0.25384	H	7.36984	1.44272	1.12517
N	1.33745	0.49241	-0.21233	H	7.73282	1.10079	-0.57203
C	-3.76509	-0.02252	-0.58249	H	3.82410	-3.68534	-0.70508
C	-3.40291	1.47088	-0.50533	H	5.23574	-2.66820	-0.51391
C	-5.22419	-0.29431	-0.17343	H	4.84115	-3.31767	-2.92112
C	3.72070	-0.18170	-0.42656	H	3.27637	-2.48587	-2.88318
C	3.33230	-1.65631	-0.21288	H	4.77578	-1.56308	-2.72410
C	5.16574	0.11276	0.01258				
C	-4.19547	2.37207	-1.45913	<b>L2_26 Ground State</b>			
C	-3.68786	3.81631	-1.44644	N	1.16319	-0.16426	0.12151
C	-5.67618	-1.75684	-0.26892	C	0.46941	-1.16375	-0.25186
C	-7.17834	-1.91887	-0.02227	O	1.03163	-2.40357	-0.26680
C	5.63596	1.55828	-0.19096	C	2.40718	-2.20540	0.14487
C	7.13019	1.72993	0.09403	C	2.50540	-0.68166	0.44145
C	4.21971	-2.68614	-0.92889	C	-0.94373	-1.10027	-0.67918
C	4.28288	-2.50213	-2.44808	O	-1.57746	-2.30280	-0.78630
H	-3.43631	0.17181	2.08202	C	-2.90437	-1.98750	-1.27678
H	-2.90988	-1.50540	2.36438	C	-2.97249	-0.43837	-1.21558
H	-3.00530	-1.94213	0.03602	N	-1.58471	-0.02876	-0.92728
H	3.30088	-0.08517	2.23434	C	3.60771	0.03580	-0.36315
H	2.74703	1.60495	2.31644	C	4.98952	-0.45627	0.10559
H	2.95589	1.79503	-0.03589	C	3.44438	1.56695	-0.32315
H	-3.64162	-0.33705	-1.62873	C	-3.93568	0.12018	-0.14446
H	-2.33639	1.57470	-0.73616	C	-4.02558	1.65633	-0.21895
H	-3.53613	1.83744	0.52361	C	-3.53545	-0.34148	1.27033
H	-5.88001	0.30800	-0.81364	C	6.17471	0.12523	-0.67161
H	-5.39534	0.07194	0.85032	C	7.50974	-0.49704	-0.25517
H	3.64210	0.03657	-1.49967	C	3.59536	2.21468	1.05777
H	2.29934	-1.78520	-0.55604	C	3.41550	3.73380	0.99958
H	3.33367	-1.88391	0.86284	C	-4.63916	-0.18477	2.32213
H	5.83783	-0.54675	-0.55024	C	-4.20596	-0.68940	3.70083
H	5.29769	-0.16677	1.06887	C	-4.49650	2.24530	-1.55755
H	-5.26108	2.36333	-1.19770				



C	-5.86911	1.74395	-2.01678	C	-0.83978	-0.90297	-0.41082
H	3.05107	-2.52266	-0.68201	O	-1.52777	-2.07050	-0.54662
H	2.59523	-2.84312	1.01184	C	-2.85950	-1.68546	-0.96743
H	2.68348	-0.50543	1.50985	C	-2.82094	-0.13030	-0.98605
H	-3.63189	-2.49205	-0.63617	N	-1.42898	0.20278	-0.63565
H	-2.98749	-2.37978	-2.29507	C	3.79788	-0.00591	-0.03647
H	-3.25842	-0.03455	-2.19135	C	5.12490	-0.67662	0.36206
H	3.47940	-0.27165	-1.41294	C	3.80356	1.52128	0.20876
H	5.02759	-1.55252	0.02338	C	-3.81574	0.56576	-0.02891
H	5.11450	-0.23412	1.17471	C	-3.50854	0.23658	1.44220
H	2.45134	1.80847	-0.71593	C	-5.27635	0.25851	-0.40665
H	4.17211	2.01666	-1.01096	C	6.35848	-0.16875	-0.39127
H	-4.92468	-0.30575	-0.37274	C	7.63410	-0.91630	0.00516
H	-3.03667	2.06423	0.02125	C	4.04739	2.35032	-1.05780
H	-4.70995	2.00155	0.56638	C	4.09382	3.85332	-0.77609
H	-2.64306	0.21487	1.58404	C	-5.67196	0.59867	-1.84886
H	-3.23574	-1.39820	1.24915	C	-7.17417	0.43525	-2.09420
H	6.21909	1.21088	-0.52235	C	-4.30501	1.05808	2.46237
H	6.01379	-0.02988	-1.74768	C	-3.84678	0.79787	3.89972
H	8.34603	-0.06368	-0.81476	H	3.02836	-2.50119	-0.49456
H	7.70309	-0.33581	0.81243	H	2.66694	-2.85853	1.21518
H	7.51404	-1.57963	-0.43158	H	2.77460	-0.52387	1.78525
H	4.58183	1.98278	1.48161	H	-3.57000	-2.10442	-0.25066
H	2.85245	1.79143	1.74527	H	-3.04393	-2.12598	-1.95113
H	3.52104	4.18995	1.99039	H	-3.00320	0.24450	-1.99819
H	4.15988	4.19411	0.33800	H	3.62769	-0.18611	-1.10918
H	2.42308	3.99454	0.61354	H	5.05363	-1.76305	0.20692
H	-5.53296	-0.73390	1.99289	H	5.27970	-0.53443	1.44251
H	-4.93938	0.86737	2.40103	H	4.56353	1.76944	0.96387
H	-5.00630	-0.57522	4.44048	H	2.83687	1.82073	0.62612
H	-3.93194	-1.75090	3.66428	H	-3.64930	1.64392	-0.16583
H	-3.33190	-0.13588	4.06444	H	-2.43994	0.41163	1.61287
H	-3.75100	2.05014	-2.33873	H	-3.68281	-0.83305	1.63283
H	-4.53149	3.33726	-1.45137	H	-5.93294	0.82008	0.26882
H	-6.20073	2.26887	-2.91953	H	-5.49282	-0.80302	-0.21211
H	-5.85682	0.67234	-2.24729	H	6.49266	0.90320	-0.20266
H	-6.62672	1.90354	-1.23931	H	6.19042	-0.27197	-1.47212
				H	8.50565	-0.53883	-0.54093
				H	7.83815	-0.80630	1.07723
				H	7.54599	-1.98912	-0.20578
				H	3.24310	2.13399	-1.77367
				H	4.98146	2.03751	-1.54190
				H	4.24615	4.43036	-1.69516
				H	3.15857	4.19487	-0.31664
<b>L2_27 Ground State</b>							
N	1.33259	-0.08001	0.34237				
C	0.56871	-1.04357	0.01434				
O	1.04521	-2.31918	0.05175				
C	2.44996	-2.18739	0.38183				
C	2.62996	-0.67924	0.70611				

H	4.91079	4.10075	-0.08675	H	5.97554	-0.29875	-0.82271
H	-5.12399	-0.03877	-2.55498	H	5.21071	-1.74993	-0.22768
H	-5.37162	1.63163	-2.07353	H	3.96595	1.75890	0.78300
H	-7.43997	0.67291	-3.13010	H	2.81626	1.81044	-0.53581
H	-7.49631	-0.59397	-1.89388	H	-3.54508	-0.23988	0.94268
H	-7.75436	1.09589	-1.43881	H	-5.21200	-1.16650	-1.09176
H	-5.37622	0.83509	2.38082	H	-5.74000	0.49462	-0.97136
H	-4.19390	2.12631	2.22888	H	-3.85667	2.06977	-1.03370
H	-4.42413	1.38985	4.61869	H	-2.59170	1.91113	0.17304
H	-3.96572	-0.25974	4.16554	H	5.88766	0.71097	1.46839
H	-2.78801	1.05306	4.02683	H	5.08842	-0.72433	2.08255

**L2\_28 Ground State**

N	1.42379	-0.17561	0.07112
C	0.68257	-1.18916	-0.13616
O	1.20688	-2.44029	-0.00905
C	2.61957	-2.23381	0.23697
C	2.75519	-0.69933	0.43134
C	-0.74676	-1.13366	-0.50914
O	-1.36863	-2.33990	-0.62036
C	-2.74025	-2.03336	-0.97159
C	-2.78505	-0.47832	-1.03406
N	-1.40466	-0.06586	-0.72510
C	3.87083	-0.05121	-0.40907
C	5.25072	-0.66073	-0.08295
C	3.82607	1.47989	-0.27119
C	-3.79845	0.14767	-0.05647
C	-5.23724	-0.30484	-0.40935
C	-3.64237	1.67661	-0.02786
C	5.79695	-0.37221	1.32090
C	7.15852	-1.03131	1.55612
C	4.84989	2.22610	-1.13219
C	4.66927	3.74471	-1.06321
C	-4.52829	2.39990	0.99107
C	-4.25933	3.90672	1.02514
C	-6.09004	-0.69232	0.80464
C	-7.52312	-1.07030	0.42544
H	3.16647	-2.59906	-0.63951
H	2.90292	-2.82582	1.10967
H	2.92383	-0.45363	1.48826
H	-3.38605	-2.45203	-0.19351
H	-2.96082	-2.52320	-1.92337
H	-3.02488	-0.13125	-2.04808
H	3.64784	-0.29705	-1.45894

H	7.54186	-0.81460	2.55929
H	7.09379	-2.12121	1.45044
H	7.89871	-0.67337	0.83023
H	4.75862	1.89212	-2.17563
H	5.87028	1.97022	-0.81785
H	5.40816	4.26657	-1.68175
H	3.67150	4.03774	-1.41058
H	4.77909	4.10693	-0.03367
H	-4.35629	1.97385	1.98959
H	-5.58823	2.22838	0.76233
H	-4.89718	4.41278	1.75857
H	-3.21494	4.11318	1.28736
H	-4.44923	4.36210	0.04550
H	-6.10445	0.13340	1.52581
H	-5.60929	-1.53520	1.32100
H	-8.10810	-1.36065	1.30511
H	-8.03742	-0.22940	-0.05559
H	-7.53736	-1.91171	-0.27839

**L2\_29 Ground State**

N	1.30317	-0.71700	0.77797
C	0.74942	-1.41587	-0.13052
O	1.36133	-2.55038	-0.57030
C	2.54508	-2.68422	0.25543
C	2.60157	-1.35698	1.06172
C	-0.53339	-1.08616	-0.78391
O	-1.13877	-2.11420	-1.44282
C	-2.32475	-1.53260	-2.04113
C	-2.38193	-0.09694	-1.45375
N	-1.09005	0.05823	-0.75758
C	3.79306	-0.44427	0.68143
C	4.00338	0.69531	1.70035
C	3.68988	0.04179	-0.77421

C	-3.55564	0.14832	-0.47828	H	-4.50514	4.70954	-1.48474
C	-3.62928	1.62939	-0.06496	H	-4.89861	4.12447	0.14050
C	-3.46498	-0.77516	0.75204	H	-3.21095	4.39401	-0.31682
C	2.99638	1.85179	1.65091				
C	3.25201	2.87759	2.75789				
C	4.92440	0.79958	-1.27212	<b>L2_30 Ground State</b>			
C	4.81396	1.18640	-2.74890	N	1.10554	0.24413	0.71464
C	-4.78906	-0.94606	1.50396	C	0.52230	-0.78207	1.19144
C	-4.65225	-1.84984	2.73167	O	1.20131	-1.61538	2.02687
C	-4.07939	2.58882	-1.17224	C	2.50329	-0.99802	2.19990
C	-4.18028	4.03613	-0.68370	C	2.49967	0.18655	1.19641
H	3.40214	-2.83756	-0.40496	C	-0.88118	-1.14430	0.91375
H	2.41436	-3.56702	0.88872	O	-1.52910	-1.80420	1.91461
H	2.65969	-1.56081	2.13710	C	-2.86714	-2.03534	1.40371
H	-3.18038	-2.15708	-1.77207	C	-2.91703	-1.21621	0.08555
H	-2.19411	-1.54780	-3.12741	N	-1.51260	-0.83084	-0.14563
H	-2.43109	0.64215	-2.25924	C	3.47545	0.02431	0.00899
H	4.68051	-1.09394	0.75404	C	3.51663	1.30280	-0.84762
H	5.01504	1.10163	1.56613	C	3.12324	-1.21168	-0.84125
H	3.99340	0.25790	2.70958	C	-3.83264	0.03053	0.15561
H	2.80192	0.67489	-0.88163	C	-4.03858	0.67710	-1.22487
H	3.52272	-0.82099	-1.43460	C	-3.36504	1.05637	1.21703
H	-4.47401	-0.10454	-1.03324	C	4.19102	2.50744	-0.18188
H	-2.64278	1.93092	0.30900	C	4.24559	3.72780	-1.10453
H	-4.32533	1.72964	0.77767	C	4.27232	-1.71250	-1.72251
H	-2.69804	-0.38179	1.43126	C	3.87644	-2.92764	-2.56483
H	-3.11311	-1.77180	0.45225	C	-2.28308	2.05990	0.78181
H	3.05928	2.35206	0.67576	C	-1.74941	2.86475	1.96893
H	1.97865	1.45708	1.72351	C	-4.84201	-0.16814	-2.21977
H	2.53930	3.70820	2.70485	C	-5.08725	0.56510	-3.54114
H	3.15642	2.41996	3.75050	H	3.26560	-1.75304	1.99239
H	4.26276	3.29946	2.68618	H	2.58559	-0.67812	3.24288
H	5.82022	0.18103	-1.11787	H	2.72372	1.12398	1.71418
H	5.07167	1.70555	-0.67110	H	-3.57937	-1.70050	2.16166
H	5.70085	1.73259	-3.08914	H	-2.98474	-3.11184	1.24564
H	4.70337	0.29811	-3.38281	H	-3.24793	-1.84936	-0.74285
H	3.93981	1.82565	-2.92192	H	4.47366	-0.13192	0.45003
H	-5.54059	-1.36505	0.81964	H	2.48776	1.56167	-1.12756
H	-5.17451	0.03286	1.81628	H	4.04864	1.08733	-1.78301
H	-5.60929	-1.96921	3.25176	H	2.25129	-0.97392	-1.46359
H	-4.29765	-2.84853	2.44871	H	2.80714	-2.03981	-0.19208
H	-3.93150	-1.43457	3.44619	H	-4.80994	-0.35569	0.48709
H	-5.05466	2.26235	-1.56107	H	-3.06112	0.92089	-1.65752
H	-3.38191	2.54662	-2.01885	H	-4.56190	1.63313	-1.08316
				H	-3.00739	0.52028	2.10747

H	-4.24457	1.62402	1.55150	C	-4.66721	-1.00784	3.12537
H	3.65900	2.78093	0.73852	C	-5.14110	2.13056	-0.19391
H	5.21034	2.23021	0.12316	C	-5.24062	3.59902	-0.61571
H	4.73203	4.57978	-0.61650	H	3.16353	-2.55990	-0.27335
H	4.80346	3.50351	-2.02190	H	2.59499	-2.64310	1.41475
H	3.23703	4.04101	-1.39948	H	2.59404	-0.25568	1.56910
H	5.13015	-1.96958	-1.08476	H	-3.46168	-2.73820	-0.76937
H	4.61671	-0.90902	-2.38596	H	-2.72392	-2.79527	-2.39221
H	4.71130	-3.27830	-3.18185	H	-3.03015	-0.44614	-2.57905
H	3.55666	-3.76162	-1.92815	H	3.62714	-0.42712	-1.28295
H	3.04240	-2.68596	-3.23444	H	5.06783	-1.45328	0.44014
H	-2.70276	2.74641	0.03575	H	5.04356	0.01653	1.39430
H	-1.45258	1.54109	0.29647	H	2.51966	1.70659	-0.97491
H	-1.01223	3.60775	1.64510	H	4.25584	1.91046	-1.16319
H	-2.55482	3.39553	2.49288	H	-4.86980	-0.60071	-0.94237
H	-1.25795	2.20601	2.69566	H	-4.20692	1.50996	-2.02921
H	-5.80541	-0.44498	-1.76774	H	-3.06715	1.85153	-0.73820
H	-4.31872	-1.11022	-2.42810	H	-3.17848	0.44156	1.31566
H	-5.66190	-0.05050	-4.24221	H	-2.97238	-1.25332	0.96388
H	-5.64398	1.49589	-3.37779	H	6.26626	1.23252	-0.39878
H	-4.13906	0.82803	-4.02508	H	6.17781	-0.17403	-1.44612
<b>L2_31 Ground State</b>				H	8.42552	-0.01940	-0.33496
N	1.19143	-0.16148	0.02719	H	7.65412	-0.07325	1.25791
C	0.54088	-1.22298	-0.23666	H	7.58348	-1.48514	0.19396
O	1.11802	-2.43636	-0.01647	H	4.46630	2.24306	1.33188
C	2.45761	-2.14350	0.45299	H	2.72387	2.05139	1.48681
C	2.50928	-0.59086	0.52750	H	3.34224	4.47511	1.43336
C	-0.83553	-1.26131	-0.77355	H	4.11018	4.25759	-0.14824
O	-1.40873	-2.49742	-0.82556	H	2.35949	4.05922	0.01891
C	-2.71213	-2.28585	-1.42408	H	-5.39495	-1.67551	1.20129
C	-2.83277	-0.74242	-1.54201	H	-5.69286	0.02099	1.52594
N	-1.49634	-0.24592	-1.16410	H	-5.57952	-1.28023	3.66770
C	3.66526	0.02995	-0.28163	H	-3.93862	-1.81547	3.26729
C	5.00969	-0.35767	0.36143	H	-4.25496	-0.10638	3.59477
C	3.48101	1.54694	-0.47587	H	-4.95406	2.07907	0.88600
C	-3.92444	-0.11886	-0.64470	H	-6.10636	1.63261	-0.36370
C	-4.03737	1.38484	-0.94945	H	-6.02759	4.12366	-0.06239
C	-3.67727	-0.41944	0.85248	H	-4.29519	4.12397	-0.43363
C	6.24764	0.13593	-0.39401	H	-5.46633	3.68801	-1.68535
C	7.55136	-0.38888	0.21246	<b>L2_32 Ground State</b>			
C	3.51391	2.38898	0.80445	N	-1.34484	-0.20084	-0.93291
C	3.32115	3.87954	0.51371	C	-0.79043	-1.01302	-0.12447
C	-4.94515	-0.77279	1.63934	O	-1.51513	-2.03739	0.40097

C	-2.84172	-1.90176	-0.16867	H	-7.94457	-1.66854	-0.52246
C	-2.75165	-0.62849	-1.06115	H	-7.90695	0.07665	-0.82440
C	0.61713	-0.93747	0.32074	H	-7.41623	-1.05052	-2.09627
O	1.06021	-2.00344	1.04290	H	5.03682	2.28207	0.17361
C	2.45704	-1.72822	1.31370	H	3.30020	2.42313	0.41979
C	2.69746	-0.31802	0.70369	H	4.20268	4.47673	-0.68851
N	1.40750	0.03118	0.08270	H	4.82058	3.49721	-2.02915
C	-3.69511	0.54526	-0.71231	H	3.07572	3.63895	-1.76904
C	-3.58755	0.95729	0.76523	H	6.57006	0.39386	-0.96664
C	-5.13638	0.30631	-1.20581	H	6.23907	-1.29736	-1.30305
C	3.85860	-0.27116	-0.30898	H	8.56267	-0.99843	-0.39631
C	5.18940	-0.52955	0.42148	H	7.90621	-0.26095	1.07350
C	3.84475	1.02602	-1.13967	H	7.59082	-1.96649	0.72420
C	-4.34501	2.24227	1.11661				
C	-4.08999	2.69375	2.55673				
C	-5.93783	-0.80273	-0.51291	<b>L2_33 Ground State</b>			
C	-7.38275	-0.86749	-1.01541	N	1.35587	0.50946	-0.28882
C	4.07318	2.32102	-0.35211	C	0.76038	0.15986	0.78030
C	4.04207	3.55449	-1.25823	O	1.41703	0.23371	1.97100
C	6.42051	-0.58192	-0.48874	C	2.72564	0.77068	1.65441
C	7.69185	-0.97406	0.26810	C	2.72481	0.89104	0.10383
H	-3.54701	-1.82142	0.65939	C	-0.62342	-0.35276	0.84935
H	-3.05883	-2.81036	-0.73681	O	-1.22935	-0.23856	2.06394
H	-2.92550	-0.88889	-2.11291	C	-2.53030	-0.85631	1.89839
H	3.05085	-2.50996	0.82821	C	-2.62033	-1.14529	0.37307
H	2.60826	-1.78106	2.39432	N	-1.26384	-0.85968	-0.12720
H	2.89502	0.41729	1.49419	C	3.77080	0.01712	-0.62640
H	-3.30364	1.38610	-1.30113	C	3.51430	-1.48222	-0.39500
H	-3.94081	0.15176	1.42304	C	5.20886	0.42942	-0.26263
H	-2.52468	1.09907	0.99834	C	-3.68005	-0.31488	-0.38606
H	-5.10143	0.09273	-2.28390	C	-3.36761	1.18962	-0.31922
H	-5.69402	1.24661	-1.11009	C	-5.09740	-0.67627	0.12001
H	3.69404	-1.10255	-1.01234	C	4.37162	-2.41871	-1.25403
H	5.12174	-1.48335	0.96517	C	3.96532	-3.88586	-1.09265
H	5.34118	0.24069	1.19070	C	5.55402	1.90453	-0.50168
H	2.87557	1.08995	-1.64496	C	7.04201	2.19584	-0.29054
H	4.60520	0.94761	-1.92741	C	-6.14624	-0.81924	-0.99013
H	-5.42294	2.09543	0.96981	C	-7.54124	-1.13566	-0.44718
H	-4.04607	3.03933	0.42173	C	-4.31665	2.08934	-1.11709
H	-4.64115	3.61059	2.79386	C	-3.87981	3.55639	-1.09077
H	-4.40071	1.92247	3.27226	H	3.47359	0.07840	2.04798
H	-3.02419	2.88939	2.72437	H	2.82761	1.73362	2.16278
H	-5.93937	-0.64225	0.57302	H	2.87708	1.93141	-0.19937
H	-5.45916	-1.77639	-0.68046	H	-3.28359	-0.15732	2.26787
				H	-2.55097	-1.76350	2.50940

H	-2.83879	-2.20448	0.19486	C	-4.42722	1.39647	0.55873
H	3.62175	0.21475	-1.69764	C	-3.76473	-1.06559	0.17337
H	2.45842	-1.68375	-0.60944	C	3.35945	0.13902	0.59081
H	3.66956	-1.73063	0.66571	C	3.19819	1.36097	-0.33007
H	5.90251	-0.18334	-0.85091	C	4.79817	-0.40907	0.59246
H	5.41134	0.17545	0.78902	C	-3.46490	1.60022	1.73612
H	-3.59679	-0.62325	-1.43750	C	-3.90330	2.75795	2.63640
H	-2.34639	1.34297	-0.68740	C	-4.94797	-1.64712	0.95308
H	-3.37151	1.52084	0.73019	C	-4.65721	-3.04977	1.49228
H	-5.43520	0.07701	0.84604	C	5.04813	-1.60691	1.51712
H	-5.06457	-1.62684	0.67261	C	6.53101	-1.97783	1.60107
H	5.43289	-2.30940	-0.99765	C	4.03266	2.58183	0.07377
H	4.27748	-2.12518	-2.30899	C	3.71398	3.80971	-0.78322
H	4.58538	-4.54461	-1.71097	H	-3.42542	-0.95157	-2.72107
H	4.06919	-4.21068	-0.05002	H	-2.59480	0.38525	-3.56027
H	2.91902	-4.03788	-1.38304	H	-3.07330	1.78329	-1.70028
H	4.96649	2.54681	0.16726	H	3.26386	-1.15592	-1.76718
H	5.26499	2.18359	-1.52458	H	2.54577	-2.66862	-1.16186
H	7.27136	3.25426	-0.45614	H	2.40498	-1.74564	1.01785
H	7.35208	1.94222	0.73060	H	-4.90832	0.19256	-1.13662
H	7.66003	1.60681	-0.97878	H	-5.42608	1.16757	0.95429
H	-5.82659	-1.61570	-1.67609	H	-4.53558	2.34877	0.01894
H	-6.18369	0.09829	-1.58847	H	-2.89264	-0.98789	0.83233
H	-8.26993	-1.25239	-1.25697	H	-3.48206	-1.78052	-0.61242
H	-7.53758	-2.06484	0.13597	H	3.11886	0.46384	1.61327
H	-7.89883	-0.33442	0.21116	H	2.14046	1.64866	-0.33139
H	-5.33664	2.00952	-0.71973	H	3.44742	1.08634	-1.36608
H	-4.36187	1.73799	-2.15715	H	5.47518	0.40025	0.89140
H	-4.56612	4.19025	-1.66338	H	5.09333	-0.67546	-0.43388
H	-3.84894	3.93943	-0.06332	H	-2.45251	1.77195	1.35879
H	-2.87674	3.67500	-1.51737	H	-3.41445	0.68010	2.33271
				H	-3.22016	2.88569	3.48355
				H	-3.92537	3.70400	2.08109
				H	-4.90979	2.59055	3.04099
				H	-5.83477	-1.67702	0.30378
				H	-5.20376	-0.98421	1.78905
				H	-5.50959	-3.45017	2.05247
				H	-4.43402	-3.74821	0.67648
				H	-3.79006	-3.03922	2.16357
				H	4.48106	-2.48081	1.17079
				H	4.66833	-1.37508	2.52197
				H	6.69264	-2.84003	2.25736
				H	6.93028	-2.23130	0.61137
				H	7.12430	-1.14252	1.99204
<b>L2_34 Ground State</b>							
N	-1.57938	0.71193	-0.69021				
C	-0.88504	-0.17736	-1.27948				
O	-1.39211	-0.80692	-2.37559				
C	-2.67027	-0.16825	-2.61930				
C	-2.88044	0.75155	-1.38453				
C	0.46182	-0.61312	-0.85805				
O	1.20211	-1.23846	-1.81436				
C	2.45423	-1.57885	-1.16787				
C	2.32927	-0.96430	0.25547				
N	0.95561	-0.43090	0.30082				
C	-4.04284	0.30648	-0.46363				

H	5.10365	2.35673	-0.00491
H	3.84300	2.81263	1.13147
H	4.31685	4.67482	-0.48518
H	3.91382	3.61233	-1.84361
H	2.65738	4.08833	-0.69274

**L2\_35 Ground State**

N	-1.48024	-0.25914	-0.48312
C	-0.77174	-1.29941	-0.29421
O	-1.33465	-2.53052	-0.44015
C	-2.73066	-2.27961	-0.73819
C	-2.83267	-0.73069	-0.82968
C	0.65899	-1.29386	0.07719
O	1.24043	-2.51999	0.18880
C	2.63218	-2.25660	0.49551
C	2.71086	-0.70943	0.63019
N	1.35170	-0.24880	0.29581
C	-3.90865	-0.12685	0.09330
C	-5.30382	-0.56459	-0.39391
C	-3.75261	1.39809	0.23954
C	3.78008	-0.06269	-0.27192
C	5.18102	-0.49289	0.20106
C	3.59760	1.46338	-0.37553
C	-6.48486	-0.05603	0.44504
C	-6.43854	-0.49399	1.91171
C	-3.93516	2.21190	-1.04651
C	-3.77265	3.71405	-0.80054
C	3.78083	2.24428	0.93058
C	3.58066	3.74872	0.73034
C	6.33617	0.02554	-0.66133
C	7.69052	-0.54024	-0.22707
H	-3.32674	-2.69788	0.08000
H	-2.97696	-2.80143	-1.66566
H	-3.03955	-0.41591	-1.86068
H	3.23529	-2.64326	-0.33304
H	2.88531	-2.80018	1.40852
H	2.91197	-0.42096	1.66997
H	-3.73754	-0.56258	1.08854
H	-5.43856	-0.23828	-1.43390
H	-5.34548	-1.66352	-0.41607
H	-2.75274	1.59636	0.63930
H	-4.46799	1.75495	0.99227
H	3.62603	-0.47208	-1.28270
H	5.23169	-1.59153	0.22105

H	5.33269	-0.16957	1.24051
H	2.59017	1.65498	-0.75913
H	4.29849	1.85155	-1.12586
H	-7.41318	-0.42299	-0.01173
H	-6.53438	1.03864	0.39028
H	-7.34097	-0.17789	2.44634
H	-6.36640	-1.58578	1.99451
H	-5.57751	-0.06512	2.43584
H	-4.92560	2.02095	-1.48096
H	-3.19857	1.88865	-1.79252
H	-3.89919	4.28933	-1.72461
H	-4.51201	4.07740	-0.07594
H	-2.77743	3.93822	-0.39899
H	4.78202	2.06410	1.34484
H	3.06369	1.88331	1.67831
H	3.70971	4.30038	1.66836
H	4.29949	4.14919	0.00467
H	2.57413	3.96127	0.35132
H	6.37009	1.12085	-0.61608
H	6.14747	-0.23207	-1.71295
H	8.50505	-0.15247	-0.84876
H	7.91117	-0.27707	0.81466
H	7.70455	-1.63452	-0.30115

**L2\_36 Ground State**

N	1.08583	-0.23966	-0.08656
C	0.38271	-1.28173	-0.28508
O	0.94601	-2.51131	-0.13551
C	2.34971	-2.25373	0.12412
C	2.43533	-0.71086	0.28191
C	-1.05032	-1.26425	-0.63986
O	-1.77408	-2.33762	-0.21473
C	-3.12539	-2.08396	-0.67971
C	-3.07672	-0.62297	-1.20625
N	-1.63672	-0.30987	-1.24321
C	3.52580	-0.04516	-0.57763
C	4.92761	-0.59219	-0.23448
C	3.42217	1.48643	-0.48293
C	-3.82701	0.40962	-0.33203
C	-3.23598	0.50998	1.09332
C	-5.33685	0.10551	-0.32909
C	5.46320	-0.23860	1.15852
C	6.84848	-0.83862	1.41250
C	4.42007	2.24670	-1.36177

C	4.17993	3.75841	-1.33751	C	0.29285	-1.18925	-0.22502
C	-6.20360	1.29483	0.09907	O	0.79755	-2.45224	-0.18193
C	-7.69606	0.95778	0.13326	C	2.22853	-2.28051	-0.01761
C	-2.13452	1.56855	1.24450	C	2.40859	-0.75601	0.21802
C	-1.46428	1.52341	2.61840	C	-1.15911	-1.07879	-0.46810
H	2.91873	-2.62396	-0.73555	O	-1.90810	-2.13640	-0.04705
H	2.63817	-2.81463	1.01549	C	-3.27490	-1.78490	-0.38456
H	2.59708	-0.43464	1.33191	C	-3.18337	-0.30484	-0.84856
H	-3.80067	-2.23560	0.16449	N	-1.73452	-0.06228	-0.97171
H	-3.35433	-2.81363	-1.46227	C	3.47306	-0.09735	-0.67843
H	-3.47950	-0.56389	-2.22357	C	4.86320	-0.73248	-0.46306
H	3.31283	-0.32879	-1.61996	C	3.45829	1.42960	-0.49462
H	5.63801	-0.22712	-0.98659	C	-3.81625	0.72125	0.12368
H	4.92813	-1.68621	-0.34442	C	-3.10459	0.74433	1.49628
H	3.54698	1.80005	0.56342	C	-5.33097	0.49260	0.28503
H	2.40169	1.77072	-0.75996	C	5.50824	-0.48611	0.90639
H	-3.68427	1.37898	-0.82947	C	6.87328	-1.16782	1.03145
H	-4.03797	0.73446	1.80850	C	4.43510	2.18827	-1.39817
H	-2.83939	-0.46818	1.40030	C	4.28011	3.70620	-1.27417
H	-5.54350	-0.74692	0.33476	C	-6.14429	0.47998	-1.01421
H	-5.65045	-0.20871	-1.33569	C	-7.65284	0.43154	-0.75805
H	5.51338	0.85141	1.27060	C	-1.92841	1.72748	1.58549
H	4.76867	-0.59201	1.93237	C	-1.16209	1.60256	2.90324
H	7.22392	-0.57554	2.40752	H	2.71147	-2.62638	-0.93803
H	6.82436	-1.93300	1.34208	H	2.55171	-2.90708	0.81620
H	7.57445	-0.47693	0.67423	H	2.65612	-0.55029	1.26751
H	4.34643	1.87939	-2.39531	H	-3.88581	-1.93998	0.50687
H	5.44819	2.04011	-1.03660	H	-3.61210	-2.46189	-1.17540
H	4.90082	4.29068	-1.96824	H	-3.63900	-0.17889	-1.83481
H	3.17319	4.00190	-1.69702	H	3.17630	-0.30988	-1.71719
H	4.27063	4.15426	-0.31853	H	5.54073	-0.36116	-1.24195
H	-6.02815	2.12956	-0.59329	H	4.79757	-1.81713	-0.63109
H	-5.88711	1.64887	1.08863	H	3.66860	1.67624	0.55593
H	-8.29609	1.82548	0.42897	H	2.43840	1.77983	-0.68471
H	-8.04931	0.62675	-0.85099	H	-3.67847	1.70430	-0.34765
H	-7.90172	0.15043	0.84668	H	-2.75156	-0.26507	1.75186
H	-2.57640	2.56115	1.07659	H	-3.83645	1.00198	2.27436
H	-1.37878	1.42624	0.46636	H	-5.71772	1.29043	0.93369
H	-0.70905	2.31076	2.71885	H	-5.51146	-0.44310	0.83499
H	-2.19357	1.65087	3.42884	H	4.84879	-0.84811	1.70650
H	-0.96047	0.56105	2.77154	H	5.62420	0.59183	1.07308
				H	7.32746	-0.98073	2.01072
				H	6.78613	-2.25389	0.90464
				H	7.56698	-0.80128	0.26508
<b>L2_37 Ground State</b>							
N	1.06452	-0.19688	-0.02616				



H	4.27234	1.88625	-2.44260	H	-3.54566	-2.22665	-0.51263
H	5.46989	1.91105	-1.15768	H	-2.97559	-2.28568	-2.19945
H	4.98493	4.23724	-1.92381	H	-3.11229	0.08146	-2.29834
H	3.26626	4.02109	-1.54809	H	3.59201	-0.09425	-1.58367
H	4.46066	4.03656	-0.24387	H	5.91103	-0.15027	-0.92293
H	-5.85916	-0.38159	-1.63225	H	5.13638	-1.63673	-0.43783
H	-5.89835	1.37370	-1.60472	H	3.88307	1.79390	0.80454
H	-8.21902	0.41412	-1.69581	H	2.75358	1.94382	-0.52414
H	-7.92653	-0.46301	-0.18530	H	-3.62508	1.51943	-0.45352
H	-7.98270	1.30503	-0.18299	H	-2.28553	0.42658	1.27849
H	-2.31682	2.75012	1.47527	H	-3.39402	-0.93628	1.35286
H	-1.24333	1.56081	0.74952	H	-5.56613	-0.72230	0.08861
H	-0.35311	2.33894	2.96410	H	-5.31639	-0.33264	-1.60150
H	-1.81923	1.75148	3.76978	H	4.99109	-0.77240	1.93633
H	-0.70996	0.60724	2.99469	H	5.80057	0.69918	1.43109
<b>L2_38 Ground State</b>				H	7.43902	-0.90278	2.43191
N	1.35027	-0.07248	-0.06892	H	6.99986	-2.12892	1.23142
C	0.60967	-1.06149	-0.37374	H	7.81491	-0.64453	0.72050
O	1.12708	-2.32136	-0.34403	H	4.72037	2.13691	-2.12480
C	2.53508	-2.14457	-0.05105	H	5.81180	2.11419	-0.74865
C	2.67565	-0.62995	0.26207	H	4.71303	4.19241	0.17056
C	-0.81311	-0.96720	-0.76181	H	5.36718	4.46783	-1.45228
O	-1.49673	-2.14551	-0.76330	H	3.62618	4.22544	-1.22414
C	-2.82931	-1.81127	-1.22467	H	-5.90182	2.03323	-1.20529
C	-2.82698	-0.25763	-1.29572	H	-6.13136	1.72608	0.50523
N	-1.41953	0.11085	-1.06382	H	-8.33405	1.71779	-0.69233
C	3.80242	0.07467	-0.51616	H	-7.76991	0.41170	-1.74713
C	5.17724	-0.56024	-0.21787	H	-8.00116	0.11444	-0.01835
C	3.75859	1.59198	-0.26896	H	-5.20458	0.54816	2.20106
C	-3.76124	0.44245	-0.28285	H	-4.15289	1.94749	2.04049
C	-3.33968	0.14688	1.16638	H	-2.57136	0.95524	3.73777
C	-5.23539	0.08083	-0.58538	H	-3.62173	-0.46020	3.88839
C	5.70869	-0.37095	1.20833	H	-4.20054	1.12954	4.41297
C	7.06602	-1.04903	1.41223	<b>L2_39 Ground State</b>			
C	4.79669	2.39496	-1.05886	N	-1.47501	-0.07207	-0.84356
C	4.61801	3.90524	-0.88384	C	-0.92281	-1.17345	-0.52533
C	-6.20837	1.26243	-0.48488	O	-1.59464	-2.34312	-0.72262
C	-7.65944	0.85645	-0.75042	C	-2.84127	-1.95934	-1.35747
C	-4.15550	0.86779	2.24409	C	-2.83247	-0.40492	-1.31440
C	-3.60862	0.61062	3.65071	C	0.41507	-1.30253	0.08629
H	3.09950	-2.44743	-0.93990	O	0.99465	-2.53115	-0.02206
H	2.79454	-2.80273	0.78085	C	2.24707	-2.42245	0.70115
H	2.83546	-0.46680	1.33603	C	2.35663	-0.91320	1.04686



H	3.70843	0.16567	-1.69449	C	-5.71484	2.66597	1.68794
H	2.82844	-1.85738	0.37392	C	-2.47182	-1.61021	1.67858
H	4.08269	-2.35275	-0.73830	C	-1.83756	-2.95649	2.03527
H	5.82509	-0.83101	-0.98746	C	5.21035	-1.13860	1.21860
H	5.44263	-0.61263	0.70474	C	6.73450	-1.28149	1.22797
H	-5.00520	2.57084	-0.98812	C	3.50346	2.97195	0.29074
H	-3.89225	2.21305	-2.30036	C	2.97316	4.22163	-0.41685
H	-3.99858	4.68205	-1.85661	H	-3.50164	-1.62880	-2.39362
H	-3.48012	4.41488	-0.18433	H	-2.99277	-0.20241	-3.33731
H	-2.37131	4.06673	-1.51810	H	-3.51970	1.14663	-1.46260
H	-4.89358	-2.22792	0.47896	H	3.24238	-0.60685	-1.96472
H	-5.21281	-1.93654	-1.22294	H	2.80782	-2.27555	-1.51994
H	-7.26481	-2.78014	-0.04276	H	2.60181	-1.63560	0.75440
H	-7.20544	-1.40104	1.06672	H	-4.95965	-0.69065	-0.61770
H	-7.53723	-1.13873	-0.65095	H	-3.49662	0.98797	1.46304
H	5.52606	1.86454	0.44233	H	-4.94148	0.05119	1.81638
H	5.73787	1.69524	-1.29260	H	-3.00762	-2.33746	-0.27961
H	7.93117	2.13490	-0.14781	H	-4.32421	-2.34868	0.87135
H	7.71968	0.67922	0.83854	H	2.99251	0.57897	1.58521
H	7.94682	0.53577	-0.90988	H	1.77095	1.79993	-0.19899
H	2.66273	-1.88097	-2.68045	H	3.11909	1.57492	-1.30686
H	1.40378	-1.19713	-1.66039	H	5.30228	0.96505	0.80727
H	0.84969	-3.55921	-2.30919	H	5.03703	-0.01206	-0.61907
H	2.33331	-4.13131	-1.52491	H	-6.19769	1.33540	0.05168
H	1.03683	-3.40783	-0.55729	H	-4.77755	2.33416	-0.22187
				H	-6.34765	3.48768	1.33432
				H	-6.27573	2.11614	2.45352
				H	-4.83570	3.10517	2.17437
				H	-2.98574	-1.20551	2.55952
				H	-1.68448	-0.89682	1.42212
				H	-1.15657	-2.86082	2.88815
				H	-2.59732	-3.70556	2.29336
				H	-1.25771	-3.34947	1.19085
				H	4.76957	-2.04883	0.79148
				H	4.83932	-1.07513	2.25108
				H	7.05079	-2.17218	1.78190
				H	7.12862	-1.36461	0.20771
				H	7.20877	-0.40987	1.69478
				H	4.59408	2.93018	0.17769
				H	3.30807	3.04969	1.36950
				H	3.43978	5.13275	-0.02592
				H	3.17401	4.17907	-1.49442
				H	1.88858	4.31612	-0.28674
<b>L2_41 Ground State</b>							
N	-1.74851	0.40266	-0.61828				
C	-0.98648	-0.39416	-1.25357				
O	-1.49472	-1.14665	-2.26966				
C	-2.87961	-0.73055	-2.38549				
C	-3.10613	0.18313	-1.15069				
C	0.43505	-0.62990	-0.93400				
O	1.22118	-1.02767	-1.97018				
C	2.53999	-1.22245	-1.39800				
C	2.37927	-0.79575	0.08926				
N	0.94256	-0.49248	0.22540				
C	-4.03572	-0.43158	-0.07598				
C	-4.41258	0.58558	1.01470				
C	-3.47501	-1.74589	0.52023				
C	3.24091	0.41064	0.52747				
C	2.86039	1.68686	-0.24318				
C	4.74522	0.09613	0.43670				
C	-5.30016	1.74171	0.54005				

**L2\_42 Ground State**

N	1.08585	-0.23969	-0.08650
C	0.38272	-1.28175	-0.28506
O	0.94602	-2.51134	-0.13555
C	2.34972	-2.25377	0.12407
C	2.43534	-0.71089	0.28191
C	-1.05031	-1.26425	-0.63982
O	-1.77408	-2.33764	-0.21472
C	-3.12539	-2.08395	-0.67971
C	-3.07671	-0.62295	-1.20621
N	-1.63671	-0.30985	-1.24315
C	3.52580	-0.04517	-0.57763
C	4.92763	-0.59217	-0.23449
C	3.42213	1.48642	-0.48296
C	-3.82701	0.40964	-0.33198
C	-3.23597	0.50998	1.09336
C	-5.33685	0.10557	-0.32910
C	5.46323	-0.23853	1.15849
C	6.84851	-0.83855	1.41247
C	4.42005	2.24671	-1.36176
C	4.17985	3.75840	-1.33755
C	-6.20363	1.29481	0.09920
C	-7.69611	0.95777	0.13306
C	-2.13450	1.56854	1.24455
C	-1.46423	1.52336	2.61842
H	2.91872	-2.62398	-0.73563
H	2.63820	-2.81470	1.01541
H	2.59713	-0.43471	1.33191
H	-3.80067	-2.23559	0.16450
H	-3.35433	-2.81360	-1.46227
H	-3.47947	-0.56384	-2.22354
H	3.31282	-0.32881	-1.61996
H	5.63801	-0.22712	-0.98663
H	4.92817	-1.68619	-0.34440
H	3.54688	1.80005	0.56340
H	2.40165	1.77069	-0.76002
H	-3.68424	1.37900	-0.82942
H	-4.03796	0.73444	1.80856
H	-2.83937	-0.46818	1.40033
H	-5.54354	-0.74696	0.33463
H	-5.65042	-0.20852	-1.33576
H	5.51342	0.85148	1.27052
H	4.76870	-0.59190	1.93236
H	7.22396	-0.57546	2.40749

H	6.82438	-1.93294	1.34208
H	7.57448	-0.47689	0.67419
H	4.34650	1.87936	-2.39529
H	5.44816	2.04017	-1.03651
H	4.90077	4.29068	-1.96825
H	3.17313	4.00184	-1.69714
H	4.27046	4.15429	-0.31858
H	-6.02807	2.12970	-0.59293
H	-5.88731	1.64861	1.08889
H	-8.29617	1.82539	0.42893
H	-8.04921	0.62703	-0.85134
H	-7.90189	0.15021	0.84622
H	-2.57637	2.56114	1.07666
H	-1.37879	1.42623	0.46638
H	-0.70898	2.31069	2.71886
H	-2.19349	1.65082	3.42889
H	-0.96043	0.56099	2.77152

**L2\_43 Ground State**

N	1.11136	-0.24916	0.54681
C	0.53656	-1.11021	-0.19347
O	1.17472	-2.27538	-0.48871
C	2.45081	-2.19718	0.19443
C	2.44367	-0.79288	0.86656
C	-0.80997	-0.95559	-0.78259
O	-1.34500	-2.08678	-1.32388
C	-2.61878	-1.67431	-1.87932
C	-2.78730	-0.20859	-1.39721
N	-1.48041	0.12632	-0.80012
C	3.56829	0.14012	0.37241
C	4.95469	-0.44128	0.74745
C	3.35425	1.56311	0.91497
C	-3.92279	-0.00194	-0.36899
C	-4.12623	1.49316	-0.06400
C	-3.66768	-0.80911	0.91868
C	6.03226	-0.31012	-0.34177
C	5.79971	-1.22511	-1.54787
C	4.34716	2.61264	0.40608
C	4.00718	4.01919	0.90635
C	-4.92367	-1.05311	1.76178
C	-4.62519	-1.83274	3.04466
C	-4.74175	2.30835	-1.20667
C	-4.96182	3.77424	-0.82425
H	3.23700	-2.31648	-0.55550

H	2.50226	-3.02644	0.90500	C	-2.67665	-0.56951	-2.36460
H	2.52358	-0.87844	1.95829	C	-2.81909	0.46630	-1.21742
H	-3.38760	-2.35556	-1.50587	N	-1.47117	0.52925	-0.62027
H	-2.55524	-1.76438	-2.96800	C	3.58665	0.22898	0.23313
H	-2.95776	0.45564	-2.25014	C	3.30988	1.30715	-0.83037
H	3.47915	0.17924	-0.72345	C	5.03645	-0.28646	0.17265
H	4.86497	-1.50736	1.00118	C	-3.86954	0.09272	-0.14672
H	5.30163	0.04852	1.66686	C	-4.05988	1.23890	0.86314
H	3.39907	1.52944	2.01462	C	-3.50401	-1.22633	0.56117
H	2.33583	1.87604	0.66201	C	4.20202	2.55583	-0.75073
H	-4.84004	-0.38855	-0.84285	C	4.13769	3.27964	0.59756
H	-3.15580	1.92134	0.21684	C	5.41207	-1.37202	1.19352
H	-4.77606	1.59220	0.81497	C	5.20840	-0.94720	2.65089
H	-2.91199	-0.28553	1.51791	C	-4.68376	-1.90647	1.26362
H	-3.22768	-1.78537	0.67299	C	-4.27538	-3.19962	1.97340
H	7.00927	-0.54646	0.09980	C	-4.76930	2.47886	0.30776
H	6.09280	0.73046	-0.68047	C	-4.97168	3.56045	1.37206
H	6.59569	-1.10962	-2.29172	H	3.32365	-1.38754	-1.90881
H	5.77922	-2.27926	-1.24369	H	2.68327	-2.80611	-1.04416
H	4.84979	-1.00547	-2.04879	H	2.73459	-1.59894	0.99233
H	4.35232	2.60592	-0.69315	H	-3.40807	-1.38063	-2.32353
H	5.36710	2.35599	0.71985	H	-2.69761	-0.11479	-3.35967
H	4.72276	4.76185	0.53584	H	-3.06343	1.45270	-1.62349
H	3.00617	4.32170	0.57684	H	3.41865	0.68385	1.21643
H	4.01959	4.06005	2.00239	H	2.26349	1.61814	-0.73054
H	-5.66077	-1.60298	1.15931	H	3.41135	0.86968	-1.83403
H	-5.39552	-0.09667	2.02076	H	5.71062	0.56632	0.32005
H	-5.53489	-2.00746	3.62999	H	5.24635	-0.65797	-0.84097
H	-4.17963	-2.80913	2.81810	H	-4.81893	-0.05658	-0.68690
H	-3.91718	-1.28695	3.67975	H	-3.07378	1.51919	1.25425
H	-5.70019	1.85614	-1.49965	H	-4.63969	0.86789	1.71800
H	-4.09788	2.26467	-2.09467	H	-2.70319	-1.02708	1.28449
H	-5.40471	4.34333	-1.64931	H	-3.08147	-1.93863	-0.16073
H	-5.63226	3.85949	0.03968	H	3.88728	3.24633	-1.54391
H	-4.01391	4.25534	-0.55545	H	5.24368	2.29534	-0.97845
				H	4.70346	4.21751	0.56875
				H	3.10146	3.51916	0.86501
				H	4.55382	2.66956	1.40722
				H	6.46662	-1.63476	1.03925
				H	4.84637	-2.29280	0.99739
				H	5.57614	-1.71420	3.34118
				H	5.74841	-0.01667	2.86575
				H	4.15145	-0.77470	2.88166
				H	-5.46724	-2.12378	0.52361
<b>L2_44 Ground State</b>							
N	1.18701	-0.41599	0.25002				
C	0.59705	-0.75078	-0.82701				
O	1.26678	-1.48107	-1.76141				
C	2.57547	-1.72734	-1.18897				
C	2.56562	-0.92787	0.14427				
C	-0.79315	-0.39339	-1.17629				
O	-1.35969	-1.14182	-2.16496				

H	-5.13530	-1.22086	1.99198	H	3.34428	1.44643	1.27661
H	-5.13171	-3.67814	2.46168	H	2.17009	1.92252	0.06922
H	-3.84762	-3.91989	1.26530	H	-5.15641	-0.54202	-0.19416
H	-3.51775	-3.00316	2.74144	H	-5.53226	1.67719	0.63949
H	-5.74366	2.18385	-0.10761	H	-5.18587	1.72598	-1.08083
H	-4.19599	2.90320	-0.52665	H	-4.34015	0.16205	2.10212
H	-5.48207	4.43881	0.96131	H	-2.70628	0.22563	1.45798
H	-5.57382	3.18309	2.20762	H	4.62022	-1.26999	1.56652
H	-4.00995	3.89192	1.78127	H	5.33650	0.33017	1.51738

**L2\_45 Ground State**

N	0.88892	-0.21601	-0.08597
C	0.19212	-1.10765	-0.66806
O	0.77377	-2.28468	-1.02976
C	2.17920	-2.12384	-0.71373
C	2.25097	-0.76892	0.04222
C	-1.24510	-0.98251	-0.98584
O	-1.87361	-2.14355	-1.32581
C	-3.24037	-1.75986	-1.62298
C	-3.31341	-0.25791	-1.22661
N	-1.91275	0.09971	-0.93597
C	3.31526	0.20272	-0.50083
C	4.72967	-0.41055	-0.42598
C	3.19922	1.56987	0.19385
C	-4.25765	0.07594	-0.03963
C	-4.72692	1.54496	-0.09731
C	-3.67480	-0.27294	1.34270
C	5.29358	-0.62724	0.98379
C	6.68982	-1.25448	0.95571
C	4.17006	2.63304	-0.32910
C	3.91694	4.00741	0.29584
C	-3.50660	-1.76563	1.65425
C	-3.02676	-1.99924	3.08933
C	-3.64981	2.60921	0.14959
C	-4.20481	4.02858	0.00675
H	2.73217	-2.11119	-1.65936
H	2.49555	-2.98652	-0.12370
H	2.43484	-0.92872	1.11276
H	-3.90635	-2.40575	-1.04817
H	-3.40638	-1.92690	-2.69153
H	-3.64485	0.33558	-2.08668
H	3.08213	0.35085	-1.56672
H	5.41934	0.23456	-0.98435
H	4.73813	-1.37177	-0.95972

**L2\_46 Ground State**

H	3.34428	1.44643	1.27661
H	2.17009	1.92252	0.06922
H	-5.15641	-0.54202	-0.19416
H	-5.53226	1.67719	0.63949
H	-5.18587	1.72598	-1.08083
H	-4.34015	0.16205	2.10212
H	-2.70628	0.22563	1.45798
H	4.62022	-1.26999	1.56652
H	5.33650	0.33017	1.51738
H	7.08549	-1.39928	1.96700
H	6.67428	-2.23232	0.45892
H	7.39534	-0.61792	0.40806
H	4.07648	2.70343	-1.42222
H	5.20711	2.33240	-0.13012
H	4.02727	3.96930	1.38652
H	4.61846	4.75817	-0.08503
H	2.90011	4.35588	0.07976
H	-2.79004	-2.22466	0.96486
H	-4.46481	-2.28278	1.49906
H	-2.90890	-3.06715	3.30452
H	-2.05819	-1.51404	3.25997
H	-3.73643	-1.58588	3.81640
H	-2.81358	2.45875	-0.54093
H	-3.23208	2.48189	1.15584
H	-5.02609	4.20826	0.71210
H	-4.59613	4.20089	-1.00385
H	-3.43122	4.78099	0.19673
H	-6.76647	0.19276	-2.13389
H	-5.13269	-0.11142	-2.67942
H	-5.90385	2.21706	-3.25721
H	-6.11157	2.57505	-1.53486
H	-4.49692	2.27613	-2.18899
H	4.38497	2.35568	-1.42609
H	5.53569	2.25156	-0.10180
H	4.99163	4.64094	-0.58708
H	3.27107	4.32305	-0.30356
H	4.42248	4.20981	1.03405
H	6.02978	0.37425	-1.31413
H	5.46433	-1.26835	-1.54516
H	7.96057	-1.22795	-1.34017
H	7.83476	-0.44942	0.24548
H	7.26272	-2.10939	0.02840



H	-3.29807	1.51760	-1.77954	C	-2.70975	0.72963	-1.17834
H	3.35225	-0.69987	-1.87397	N	-1.38160	0.62897	-0.54323
H	2.77304	-2.33381	-1.46661	C	3.61785	0.01431	0.24953
H	2.47585	-1.68183	0.79416	C	3.63553	0.54729	1.69417
H	-4.90761	-0.22211	-1.05936	C	3.39419	1.15734	-0.75956
H	-4.63231	1.97938	0.04675	C	-3.81185	0.24219	-0.21023
H	-3.51968	1.27856	1.20599	C	-3.98567	1.22047	0.96558
H	-3.10538	-1.99113	-0.58704	C	-3.52990	-1.18948	0.28515
H	-4.48720	-1.91928	0.47666	C	3.87295	-0.49412	2.79824
H	2.95490	0.50382	1.65664	C	5.17577	-1.28463	2.64237
H	1.92863	1.80112	-0.19476	C	4.49518	2.22847	-0.79906
H	3.32448	1.48757	-1.21878	C	5.88846	1.68215	-1.12458
H	5.32874	0.74037	1.02516	C	-4.76164	-1.91332	0.83903
H	5.09082	-0.21880	-0.41801	C	-4.43579	-3.32228	1.34047
H	-5.36383	-0.24762	2.02039	C	-4.61842	2.56725	0.59819
H	-6.44829	0.43978	0.82352	C	-4.81008	3.47323	1.81722
H	-6.81655	1.49708	3.06894	H	3.36073	-1.43540	-1.99084
H	-5.12111	2.00779	3.11997	H	2.53466	-2.85435	-1.29557
H	-6.21829	2.70726	1.92173	H	2.73419	-1.86628	0.83832
H	-3.18355	-0.86617	2.25402	H	-3.34356	-0.88383	-2.58448
H	-1.80385	-0.62941	1.19581	H	-2.53910	0.49358	-3.38209
H	-1.47854	-2.62574	2.67722	H	-2.89557	1.77921	-1.42610
H	-2.92708	-3.38365	1.99120	H	4.58809	-0.45518	0.03472
H	-1.50519	-3.10083	0.97344	H	2.68263	1.05611	1.88214
H	4.60539	-2.23307	0.96742	H	4.42163	1.30924	1.77107
H	4.64767	-1.26417	2.43124	H	2.43427	1.63582	-0.53153
H	6.80860	-2.50195	2.09617	H	3.29397	0.73888	-1.77049
H	7.03513	-1.70308	0.53193	H	-4.74779	0.22809	-0.79265
H	7.08480	-0.75360	2.02370	H	-3.00233	1.38494	1.42376
H	4.79085	2.74573	0.35668	H	-4.61131	0.74722	1.73317
H	3.44522	2.94933	1.46860	H	-2.74514	-1.14846	1.05112
H	3.79629	5.01821	0.08980	H	-3.11653	-1.79762	-0.53114
H	3.55875	4.08223	-1.39484	H	3.88709	0.03230	3.76130
H	2.21405	4.30371	-0.26687	H	3.02307	-1.18577	2.85348
				H	5.34807	-1.93944	3.50373
<b>L2_48 Ground State</b>				H	5.16579	-1.91729	1.74716
N	1.20080	-0.57079	0.23469	H	6.03712	-0.61003	2.55744
C	0.63102	-0.70606	-0.89568	H	4.52851	2.77052	0.15396
O	1.29650	-1.32020	-1.91468	H	4.21523	2.97274	-1.55579
C	2.54976	-1.76072	-1.33488	H	6.61314	2.49489	-1.24574
C	2.56661	-1.10461	0.07135	H	6.26285	1.02444	-0.33202
C	-0.72779	-0.22696	-1.22161	H	5.87696	1.10356	-2.05710
O	-1.29336	-0.77876	-2.33252	H	-5.52970	-1.96972	0.05445
C	-2.57461	-0.11509	-2.47344	H	-5.20493	-1.33147	1.65716



H	-5.32838	-3.82916	1.72393
H	-4.01873	-3.94049	0.53606
H	-3.69517	-3.28961	2.14849
H	-5.58956	2.39172	0.11341
H	-3.99718	3.09056	-0.14021
H	-5.26525	4.43054	1.53958
H	-5.45833	2.99768	2.56338
H	-3.84977	3.68617	2.30172

**L2\_49 Ground State**

N	-1.30462	-0.63788	-0.26484
C	-0.70450	-0.37528	0.82647
O	-1.38700	-0.44567	2.00287
C	-2.72578	-0.86996	1.64485
C	-2.70435	-0.93330	0.09102
C	0.71215	0.02878	0.93794
O	1.27062	-0.13000	2.16997
C	2.63060	0.35386	2.03901
C	2.77258	0.68931	0.52769
N	1.41778	0.48604	-0.01757
C	-3.67178	0.03918	-0.62251
C	-3.31582	1.50693	-0.32887
C	-5.14207	-0.28407	-0.29955
C	3.80637	-0.15951	-0.24671
C	3.42270	-1.65046	-0.24696
C	5.23673	0.07133	0.27487
C	-4.08389	2.53286	-1.17001
C	-3.57948	3.96051	-0.94403
C	-5.58602	-1.71961	-0.60662
C	-7.09441	-1.91273	-0.43036
C	5.71313	1.53175	0.31963
C	5.67309	2.23679	-1.03948
C	4.33037	-2.56498	-1.08430
C	4.42543	-2.16332	-2.55931
H	-3.42717	-0.13787	2.05203
H	-2.90964	-1.84026	2.11472
H	-2.92479	-1.94830	-0.25360
H	3.30048	-0.43576	2.38700
H	2.74205	1.22798	2.68701
H	3.02769	1.74529	0.39399
H	-3.51566	-0.12816	-1.69789
H	-2.24349	1.64024	-0.51304
H	-3.47856	1.72714	0.73689
H	-5.77964	0.40033	-0.87212

H	-5.34585	-0.06001	0.75864
H	3.75106	0.19639	-1.28222
H	2.39722	-1.73441	-0.62501
H	3.40658	-2.02692	0.78600
H	5.92967	-0.49255	-0.36178
H	5.33181	-0.36884	1.27822
H	-5.15616	2.49013	-0.94121
H	-3.98483	2.27207	-2.23308
H	-4.13616	4.68380	-1.55042
H	-3.68591	4.25383	0.10763
H	-2.51823	4.04805	-1.20535
H	-5.05738	-2.42948	0.04284
H	-5.29908	-1.97561	-1.63610
H	-7.39487	-2.94428	-0.64459
H	-7.40405	-1.68049	0.59599
H	-7.65695	-1.25298	-1.10183
H	6.74243	1.54317	0.70084
H	5.12203	2.10397	1.04729
H	6.10727	3.24059	-0.97696
H	6.24123	1.67234	-1.78933
H	4.64908	2.34267	-1.41421
H	3.93514	-3.58677	-1.01559
H	5.33716	-2.60498	-0.64893
H	4.99450	-2.90307	-3.13331
H	3.42839	-2.08232	-3.00875
H	4.92311	-1.19524	-2.68616

**L2\_50 Ground State**

N	-1.60517	-0.99964	-1.14354
C	-1.01468	-1.62883	-0.21006
O	-1.73964	-2.39093	0.65575
C	-3.10933	-2.28895	0.18280
C	-3.04975	-1.19494	-0.91915
C	0.42529	-1.51513	0.10002
O	1.06606	-2.65515	0.47116
C	2.45086	-2.26117	0.67087
C	2.43314	-0.71441	0.52706
N	1.05850	-0.41227	0.08808
C	-3.70842	0.15311	-0.53803
C	-2.99800	0.83465	0.65569
C	-5.21859	-0.03755	-0.30537
C	3.48720	-0.15337	-0.44405
C	4.89292	-0.36225	0.14813
C	3.17598	1.30538	-0.83133

C	-1.88569	1.81053	0.24392				
C	-1.06309	2.30762	1.43315				
C	-6.02195	1.26501	-0.38930	N	-1.34775	-0.47362	-0.98399
C	-7.51322	1.06013	-0.11321	C	-0.75013	-1.25307	-0.17389
C	3.16289	2.31120	0.32538	O	-1.43078	-2.29269	0.38415
C	2.80266	3.72165	-0.14782	C	-2.74745	-2.25276	-0.22066
C	6.04469	0.08144	-0.75912	C	-2.74670	-0.93223	-1.04209
C	7.41636	-0.27331	-0.17978	C	0.65797	-1.11553	0.25283
H	-3.73566	-2.03113	1.03883	O	1.19659	-2.20938	0.85851
H	-3.40596	-3.26912	-0.20219	C	2.57350	-1.85291	1.13808
H	-3.51283	-1.55241	-1.84545	C	2.69596	-0.37927	0.65592
H	3.05216	-2.75114	-0.10301	N	1.36685	-0.06992	0.09915
H	2.76295	-2.62011	1.65343	C	-3.71207	0.15812	-0.52419
H	2.57324	-0.23691	1.50540	C	-3.33314	0.61457	0.89482
H	-3.58816	0.79965	-1.41838	C	-5.17596	-0.32872	-0.64830
H	-3.73510	1.37531	1.26350	C	3.82001	-0.15600	-0.37530
H	-2.57712	0.06947	1.32314	C	5.18729	-0.37746	0.29762
H	-5.38863	-0.50116	0.67748	C	3.68689	1.20501	-1.08442
H	-5.61963	-0.74245	-1.04890	C	-4.18240	1.75601	1.46284
H	3.41840	-0.75045	-1.36672	C	-3.67764	2.22590	2.82966
H	5.02727	-1.42932	0.38090	C	-6.15312	0.73567	-1.16328
H	4.96743	0.16385	1.11037	C	-7.59515	0.22904	-1.23258
H	2.19347	1.31926	-1.31412	C	3.84061	2.43849	-0.18760
H	3.90117	1.63423	-1.58663	C	3.69292	3.74164	-0.97719
H	-2.34360	2.66221	-0.27962	C	6.39102	-0.25919	-0.64256
H	-1.21904	1.31983	-0.47049	C	7.70946	-0.62007	0.04620
H	-0.30606	3.03364	1.11496	H	-3.48707	-2.28124	0.58233
H	-1.69365	2.78862	2.19226	H	-2.85796	-3.14566	-0.84293
H	-0.53621	1.47198	1.90823	H	-3.00243	-1.13094	-2.08929
H	-5.88671	1.70194	-1.38816	H	3.21565	-2.54055	0.57782
H	-5.61679	1.99769	0.32047	H	2.74712	-1.99005	2.20795
H	-8.06823	2.00152	-0.19145	H	2.86461	0.29375	1.50613
H	-7.95370	0.35208	-0.82582	H	-3.57280	1.01667	-1.19577
H	-7.67616	0.65891	0.89453	H	-3.39044	-0.24066	1.58493
H	4.14160	2.33191	0.82392	H	-2.28354	0.93110	0.88241
H	2.43250	1.99419	1.07965	H	-5.52551	-0.70485	0.32382
H	2.79753	4.43573	0.68341	H	-5.22609	-1.18744	-1.33393
H	3.51776	4.08402	-0.89678	H	3.69522	-0.93173	-1.14709
H	1.80701	3.73394	-0.60723	H	5.20458	-1.37725	0.75595
H	5.99042	1.16441	-0.92376	H	5.30652	0.33215	1.12839
H	5.92834	-0.38516	-1.74734	H	2.70193	1.23958	-1.56124
H	8.22729	0.05907	-0.83718	H	4.42867	1.25520	-1.89198
H	7.56461	0.19959	0.79874	H	-5.22914	1.43896	1.55448
H	7.51975	-1.35657	-0.04198	H	-4.17549	2.59947	0.75876

H	-4.29304	3.04094	3.22671	H	3.34656	-2.56259	0.38057
H	-3.69616	1.40669	3.55895	H	2.54771	-2.60703	1.97474
H	-2.64402	2.58585	2.76399	H	2.81957	-0.25986	2.12983
H	-5.82647	1.06037	-2.16076	H	-3.34664	-2.56248	-0.38080
H	-6.10598	1.62543	-0.52507	H	-2.54779	-2.60678	-1.97497
H	-8.27232	0.99802	-1.62050	H	-2.81959	-0.25957	-2.12982
H	-7.67545	-0.64809	-1.88652	H	4.67711	-0.41663	0.48173
H	-7.95743	-0.06527	-0.23991	H	2.86391	2.02913	0.38215
H	4.81870	2.42668	0.31211	H	4.47327	2.02883	-0.32552
H	3.08383	2.41228	0.60637	H	2.65142	0.45839	-1.62368
H	3.80032	4.61915	-0.32961	H	3.06614	-1.23032	-1.42348
H	4.45184	3.81287	-1.76626	H	-4.67713	-0.41649	-0.48175
H	2.70921	3.79705	-1.45796	H	-2.86388	2.02922	-0.38191
H	6.45564	0.76280	-1.03528	H	-4.47326	2.02891	0.32570
H	6.23697	-0.91269	-1.51266	H	-2.65149	0.45832	1.62378
H	8.55943	-0.52148	-0.63803	H	-3.06614	-1.23039	1.42336
H	7.89586	0.03410	0.90670	H	5.46950	1.46148	1.90356
H	7.69403	-1.65324	0.41426	H	3.87470	1.53885	2.63760

**L2\_52 Ground State**

N	1.30181	-0.10983	0.69265
C	0.68088	-1.14404	0.28628
O	1.28787	-2.36296	0.35445
C	2.56323	-2.11488	0.99756
C	2.64557	-0.56791	1.09419
C	-0.68093	-1.14400	-0.28636
O	-1.28794	-2.36290	-0.35465
C	-2.56330	-2.11472	-0.99774
C	-2.64560	-0.56774	-1.09422
N	-1.30184	-0.10973	-0.69262
C	3.73100	0.06787	0.19630
C	3.86047	1.57751	0.46568
C	3.45529	-0.21091	-1.29530
C	-3.73102	0.06797	-0.19627
C	-3.86045	1.57763	-0.46551
C	-3.45532	-0.21097	1.29531
C	4.48384	1.94124	1.81777
C	4.63154	3.45345	2.00438
C	4.67326	-0.05118	-2.21749
C	5.75576	-1.11381	-2.00297
C	-4.67331	-0.05142	2.21750
C	-5.75578	-1.11405	2.00280
C	-4.48375	1.94148	-1.81760
C	-4.63133	3.45371	-2.00414

**L2\_53 Ground State**

N	-1.25206	0.48384	-0.42410
C	-0.61819	-0.43959	-1.02896
O	-1.20457	-1.08098	-2.07945
C	-2.47711	-0.41247	-2.26788
C	-2.58478	0.54853	-1.05379
C	0.73764	-0.90767	-0.67570

O	1.36504	-1.65791	-1.62584	H	5.60456	1.15261	-1.37046
C	2.62340	-2.05239	-1.02425	H	5.02520	2.36135	-0.23627
C	2.68693	-1.23274	0.29184	H	5.35320	3.38224	-2.49292
N	1.33701	-0.65032	0.41753	H	4.22571	2.21489	-3.20355
C	-3.68754	0.16952	-0.03933	H	3.63749	3.42357	-2.05397
C	-3.84001	1.25054	1.04526	H	3.28766	-1.01891	3.05366
C	-3.41836	-1.21419	0.58647	H	4.15878	0.31006	3.78046
C	3.76028	-0.12168	0.30654	H	5.64501	-1.65692	3.70363
C	3.82477	0.57606	1.67865	H	5.40290	-1.84546	1.96439
C	3.53010	0.90140	-0.82275	H	6.27827	-0.43991	2.58297
C	-4.45712	2.56787	0.56273				
C	-4.62820	3.58175	1.69684				
C	-4.64423	-1.88350	1.22568	<b>L2_54 Ground State</b>			
C	-5.71205	-2.31429	0.21516	N	-1.91703	-0.86073	-0.77437
C	4.74151	1.78921	-1.12813	C	-1.19289	-1.68233	-0.12840
C	4.47763	2.75739	-2.28407	O	-1.77878	-2.67928	0.59246
C	4.12172	-0.32578	2.88647	C	-3.20211	-2.52315	0.35385
C	5.43240	-1.11107	2.77772	C	-3.31301	-1.18420	-0.42494
H	-3.25918	-1.17534	-2.29993	C	0.27461	-1.58381	0.00580
H	-2.44259	0.11013	-3.22864	O	0.96750	-2.75301	0.04044
H	-2.75596	1.57445	-1.39419	C	2.36385	-2.36076	0.13248
H	3.42425	-1.82427	-1.73188	C	2.31581	-0.82126	0.33257
H	2.58948	-3.13296	-0.85405	N	0.89366	-0.48131	0.14478
H	2.85825	-1.89872	1.14268	C	-3.95378	-0.03506	0.39377
H	-4.62325	0.12480	-0.61707	C	-4.30344	1.17771	-0.48549
H	-2.85198	1.44124	1.48288	C	-3.10281	0.36161	1.62640
H	-4.46741	0.85595	1.85509	C	3.23258	-0.02672	-0.61401
H	-2.62571	-1.10055	1.33532	C	4.70415	-0.31349	-0.26315
H	-3.01649	-1.89987	-0.17209	C	2.86705	1.47029	-0.62546
H	4.72111	-0.62452	0.11766	C	-5.44017	0.94143	-1.48636
H	2.86872	1.08699	1.84278	C	-5.79055	2.20390	-2.27828
H	4.59677	1.35470	1.63504	C	-1.97188	1.37755	1.38403
H	2.66798	1.52805	-0.56127	C	-1.03842	1.49330	2.59068
H	3.25046	0.38062	-1.74878	C	2.99493	2.19488	0.71937
H	-3.83397	3.01409	-0.22315	C	2.58263	3.66558	0.61823
H	-5.43387	2.36336	0.10100	C	5.72709	0.35862	-1.18426
H	-5.07264	4.51663	1.33741	C	7.16375	-0.06919	-0.87453
H	-5.27734	3.18370	2.48635	H	-3.70552	-2.51397	1.32369
H	-3.66175	3.82380	2.15470	H	-3.54241	-3.38755	-0.22446
H	-5.09383	-1.21488	1.97121	H	-3.88546	-1.32586	-1.34614
H	-4.30396	-2.76672	1.78145	H	2.85458	-2.65016	-0.80360
H	-6.53697	-2.83895	0.70985	H	2.81257	-2.91078	0.96173
H	-6.14165	-1.45778	-0.31655	H	2.57621	-0.56131	1.36680
H	-5.28844	-2.99239	-0.53651	H	-4.90153	-0.45065	0.77206
				H	-4.59121	2.00995	0.17191

H	-3.40455	1.50502	-1.02143	C	3.78093	1.37773	0.65204
H	-2.67102	-0.54438	2.07480	C	3.51819	-0.24256	-1.30790
H	-3.77833	0.77206	2.38974	C	-4.50224	2.19495	-1.66894
H	3.04805	-0.40882	-1.63011	C	-4.64079	3.71749	-1.59031
H	4.87301	-1.40040	-0.29351	C	-4.84954	-0.48653	1.91334
H	4.89927	-0.01089	0.77538	C	-4.58699	-1.00837	3.32807
H	1.83135	1.55777	-0.96948	C	4.83260	-0.50803	-2.05789
H	3.48939	1.98160	-1.37093	C	5.89813	0.58337	-1.92146
H	-6.33033	0.58538	-0.94796	C	4.33111	1.60209	2.06428
H	-5.16875	0.14409	-2.19033	C	4.44914	3.08761	2.41466
H	-6.60510	2.02067	-2.98794	H	-3.40359	-2.50017	-1.01907
H	-6.10459	3.01415	-1.60906	H	-2.54500	-2.25988	-2.56355
H	-4.92445	2.56260	-2.84716	H	-2.82672	0.07699	-2.30886
H	-2.40781	2.36030	1.16362	H	3.21388	-2.71644	0.05203
H	-1.38375	1.08839	0.51035	H	2.36201	-2.93775	1.60324
H	-0.26534	2.25113	2.41926	H	2.66161	-0.63158	2.05859
H	-1.58365	1.76728	3.50332	H	-4.74394	-0.36449	-0.77126
H	-0.52862	0.54036	2.77592	H	-2.93209	2.01709	-0.18765
H	4.02662	2.12984	1.09105	H	-4.56462	1.90265	0.45513
H	2.36065	1.69965	1.46474	H	-2.80062	0.10640	1.53160
H	2.67784	4.17714	1.58266	H	-3.20160	-1.51325	1.00318
H	3.20417	4.20277	-0.10889	H	4.60144	-0.61378	0.52718
H	1.53944	3.75469	0.29240	H	2.78549	1.83035	0.56346
H	5.64666	1.44871	-1.09420	H	4.42565	1.90802	-0.05841
H	5.48671	0.11872	-2.22950	H	3.03779	0.66127	-1.70349
H	7.88146	0.42761	-1.53661	H	2.83235	-1.06448	-1.54547
H	7.43464	0.18006	0.15873	H	-3.86632	1.93903	-2.52633
H	7.28941	-1.15197	-0.99674	H	-5.48522	1.74547	-1.87054
				H	-5.05660	4.13208	-2.51548
				H	-5.30112	4.01082	-0.76504
				H	-3.66686	4.19092	-1.41834
				H	-5.61874	-1.10503	1.42916
				H	-5.26722	0.52664	1.97279
				H	-5.50166	-1.01250	3.93142
				H	-4.19646	-2.03311	3.30423
				H	-3.84691	-0.38572	3.84490
				H	4.60230	-0.65041	-3.12204
				H	5.25157	-1.46301	-1.70833
				H	6.78081	0.34461	-2.52545
				H	5.51564	1.55449	-2.25811
				H	6.23128	0.69908	-0.88417
				H	5.31818	1.12441	2.14877
				H	3.68845	1.11023	2.80600
				H	4.84795	3.23274	3.42491
<b>L2_55 Ground State</b>							
N	-1.36122	-0.03277	-0.81444				
C	-0.75030	-1.12350	-0.57456				
O	-1.34889	-2.31013	-0.87883				
C	-2.60028	-1.94991	-1.51558				
C	-2.68756	-0.41030	-1.33886				
C	0.58964	-1.22774	0.03905				
O	1.16240	-2.46427	-0.01219				
C	2.42038	-2.32871	0.69614				
C	2.53249	-0.80758	0.98592				
N	1.22088	-0.26592	0.58360				
C	-3.80473	0.05947	-0.37945				
C	-3.92565	1.59410	-0.38223				
C	-3.58674	-0.48520	1.04548				
C	3.67511	-0.09858	0.22480				

H	5.11505	3.60555	1.71364
H	3.47073	3.58008	2.36592

**L2\_56 Ground State**

N	-1.56309	-0.00375	-0.67270
C	-0.90363	-1.07543	-0.48035
O	-1.54604	-2.27580	-0.51982
C	-2.92606	-1.96254	-0.83185
C	-2.96683	-0.40867	-0.86791
C	0.54411	-1.14045	-0.19104
O	1.09006	-2.38859	-0.20728
C	2.51065	-2.18183	-0.01112
C	2.63803	-0.66781	0.30966
N	1.28223	-0.13734	0.07100
C	-3.88146	0.25646	0.18539
C	-3.40369	-0.04697	1.61704
C	-5.35936	-0.12121	-0.02496
C	3.69718	0.06942	-0.53059
C	5.10188	-0.53654	-0.32571
C	3.63504	1.58311	-0.26569
C	-4.18370	0.66007	2.73639
C	-4.19173	2.18720	2.61875
C	-5.93059	0.13586	-1.42826
C	-5.83381	1.59708	-1.87698
C	4.60306	2.41666	-1.11094
C	4.40189	3.92084	-0.90977
C	5.71735	-0.34795	1.06634
C	7.09957	-0.99653	1.17809
H	-3.55311	-2.40788	-0.05582
H	-3.16802	-2.42336	-1.79372
H	-3.27588	-0.05888	-1.85824
H	3.01851	-2.46155	-0.94085
H	2.84262	-2.84253	0.79246
H	2.86289	-0.51209	1.37309
H	-3.76990	1.33476	0.02160
H	-2.34890	0.24286	1.68809
H	-3.44225	-1.13106	1.79677
H	-5.96414	0.44221	0.69635
H	-5.50221	-1.18077	0.23277
H	3.42372	-0.09485	-1.58446
H	5.78071	-0.10362	-1.07099
H	5.07101	-1.61168	-0.55391
H	3.82218	1.77867	0.79988
H	2.60827	1.91383	-0.45361

H	-3.72994	0.37650	3.69489
H	-5.21608	0.28926	2.77423
H	-4.66662	2.64728	3.49243
H	-3.17064	2.58027	2.54410
H	-4.73951	2.52405	1.73139
H	-6.98424	-0.17189	-1.42912
H	-5.43388	-0.50824	-2.16632
H	-6.33529	1.74917	-2.83897
H	-6.30623	2.26296	-1.14413
H	-4.79346	1.92035	-1.99220
H	4.46573	2.16619	-2.17258
H	5.64170	2.15668	-0.86780
H	5.10087	4.50549	-1.51845
H	3.38361	4.22105	-1.18373
H	4.55677	4.20095	0.13942
H	5.05591	-0.77215	1.83356
H	5.79900	0.72198	1.29388
H	7.53238	-0.85087	2.17395
H	7.04629	-2.07601	0.99068
H	7.79448	-0.56889	0.44517

**L2\_57 Ground State**

N	-1.71038	-0.69239	-0.96414
C	-1.13985	-1.36671	-0.05033
O	-1.89314	-2.05945	0.84896
C	-3.26687	-1.83680	0.43392
C	-3.15726	-0.76717	-0.68798
C	0.31598	-1.37843	0.19975
O	0.86766	-2.56666	0.56305
C	2.28922	-2.29623	0.69940
C	2.40360	-0.75613	0.53094
N	1.04420	-0.33729	0.14359
C	-3.69101	0.63673	-0.30566
C	-2.86616	1.28757	0.83027
C	-5.19158	0.60294	0.03890
C	3.46204	-0.30439	-0.49109
C	4.86704	-0.62827	0.04889
C	3.26441	1.17052	-0.89168
C	-1.68535	2.13991	0.34090
C	-0.77665	2.60118	1.48113
C	-6.10543	-0.00400	-1.03165
C	-7.58962	0.16045	-0.69438
C	3.37978	2.18927	0.24788
C	3.12885	3.61950	-0.23637

C	6.01509	-0.30512	-0.91242	C	-2.63756	-0.82367	0.13864
C	7.37238	-0.77361	-0.38209	C	0.80704	0.08364	0.92917
H	-3.82719	-1.51128	1.31247	O	1.41847	-0.18594	2.11581
H	-3.67106	-2.78985	0.07963	C	2.77231	0.31111	1.97139
H	-3.66895	-1.10263	-1.59438	C	2.84305	0.80469	0.49853
H	2.81124	-2.84807	-0.09025	N	1.46856	0.63648	-0.00724
H	2.60928	-2.66922	1.67414	C	-3.63061	0.21556	-0.43176
H	2.62689	-0.28078	1.49479	C	-3.24753	1.64520	-0.00714
H	-3.57359	1.25498	-1.20652	C	-5.08713	-0.13111	-0.07625
H	-3.52856	1.91826	1.43914	C	3.85485	0.05898	-0.40073
H	-2.49333	0.51174	1.51421	C	3.49634	-1.43039	-0.54331
H	-5.51001	1.63720	0.22805	C	5.30260	0.26367	0.08555
H	-5.34560	0.07243	0.99034	C	-4.11690	2.76713	-0.59543
H	3.30355	-0.90620	-1.39953	C	-4.14340	2.79427	-2.12655
H	4.91554	-1.69901	0.29800	C	-5.55030	-1.53378	-0.48850
H	5.02765	-0.09467	0.99633	C	-7.05178	-1.73873	-0.27181
H	2.26993	1.26336	-1.34004	C	5.75477	1.71973	0.27879
H	3.98749	1.42472	-1.67722	C	5.64671	2.57604	-0.98646
H	-2.08303	3.01166	-0.19865	C	4.32067	-2.18823	-1.59032
H	-1.09387	1.56536	-0.37655	C	3.81885	-3.61965	-1.79703
H	0.02986	3.24352	1.10915	H	-3.28512	-0.24764	2.20056
H	-1.33190	3.16387	2.24288	H	-2.73576	-1.93571	2.06437
H	-0.30907	1.73818	1.96927	H	-2.87607	-1.79881	-0.29679
H	-5.88392	-1.07203	-1.15824	H	3.45498	-0.51060	2.20008
H	-5.89228	0.46851	-2.00081	H	2.91857	1.11097	2.70282
H	-8.22839	-0.28578	-1.46451	H	3.07774	1.87328	0.46522
H	-7.83193	-0.32041	0.26125	H	-3.52311	0.14638	-1.52220
H	-7.85842	1.22004	-0.60786	H	-2.20634	1.81645	-0.30384
H	4.37311	2.13031	0.71331	H	-3.27527	1.72195	1.08936
H	2.65066	1.94816	1.03083	H	-5.74386	0.60133	-0.56169
H	3.21455	4.34228	0.58284	H	-5.24808	0.00171	1.00436
H	3.84716	3.90736	-1.01406	H	3.75271	0.51195	-1.39575
H	2.12309	3.71348	-0.66316	H	2.43735	-1.50111	-0.81757
H	6.05161	0.77556	-1.09583	H	3.60174	-1.93752	0.42758
H	5.81604	-0.77479	-1.88588	H	5.97793	-0.20993	-0.63723
H	8.18165	-0.52633	-1.07795	H	5.44583	-0.28359	1.02878
H	7.60348	-0.30098	0.58038	H	-3.72639	3.72450	-0.22672
H	7.38364	-1.85952	-0.22777	H	-5.14268	2.69603	-0.21128
<b>L2_58 Ground State</b>				H	-4.68938	3.66947	-2.49599
N	-1.25385	-0.49005	-0.24612	H	-3.12667	2.83387	-2.53561
C	-0.61076	-0.32172	0.83922	H	-4.63025	1.90421	-2.54092
O	-1.24399	-0.50411	2.03127	H	-5.00055	-2.29793	0.07636
C	-2.59029	-0.91836	1.68990	H	-5.30411	-1.70034	-1.54657
				H	-7.36556	-2.74732	-0.56259

H	-7.32088	-1.59547	0.78188	H	4.54050	-0.43206	0.00278
H	-7.63605	-1.02228	-0.86170	H	2.70812	1.60796	1.33017
H	6.79859	1.70965	0.61830	H	4.27864	2.04754	0.67385
H	5.18484	2.19137	1.09066	H	2.39187	1.37089	-1.19640
H	6.06284	3.57614	-0.82306	H	2.84059	-0.13407	-1.96963
H	6.19547	2.11635	-1.81764	H	-4.83544	-0.24901	-0.32111
H	4.60665	2.69948	-1.30784	H	-3.17630	2.17405	0.50269
H	5.37784	-2.21635	-1.29792	H	-4.68634	1.76341	1.30209
H	4.27895	-1.64277	-2.54359	H	-4.24981	-0.27753	2.11133
H	4.41615	-4.15029	-2.54698	H	-2.54717	-0.12582	1.70470
H	3.86876	-4.19303	-0.86316	H	3.83692	0.00221	2.90981
H	2.77496	-3.62530	-2.13241	H	5.39217	0.39004	2.18944

**L2\_59 Ground State**

N	1.17951	-0.40993	0.48783
C	0.54564	-1.07541	-0.39281
O	1.16368	-2.11136	-1.02751
C	2.46944	-2.21088	-0.40499
C	2.54645	-0.96500	0.51755
C	-0.84618	-0.81284	-0.81152
O	-1.46386	-1.83792	-1.46641
C	-2.78518	-1.33640	-1.79474
C	-2.85529	0.04577	-1.08870
N	-1.48699	0.26239	-0.58301
C	3.57698	0.09576	0.06859
C	3.71049	1.21753	1.11359
C	3.22210	0.66558	-1.31991
C	-3.89532	0.18867	0.05199
C	-4.14568	1.68145	0.34956
C	-3.50006	-0.53912	1.35177
C	4.40056	0.80613	2.41881
C	4.54872	1.97645	3.39445
C	4.38348	1.35451	-2.05197
C	5.49522	0.39599	-2.49054
C	-3.39836	-2.06895	1.30119
C	-3.13360	-2.66596	2.68635
C	-4.94755	2.43165	-0.71992
C	-5.17923	3.89988	-0.35311
H	3.22236	-2.22297	-1.19715
H	2.50771	-3.15637	0.14446
H	2.77399	-1.26553	1.54493
H	-3.52113	-2.05978	-1.44013
H	-2.84893	-1.25988	-2.88429
H	-3.06467	0.82140	-1.83178

**L2\_60 Ground State**

N	1.14794	-0.38953	0.36253
C	0.49693	-1.19449	-0.37766
O	1.05390	-2.38854	-0.72177
C	2.39470	-2.35275	-0.17242
C	2.43581	-1.04238	0.66119
C	-0.85913	-0.94697	-0.91037
O	-1.44652	-2.00939	-1.53073
C	-2.72038	-1.51085	-2.01001
C	-2.82460	-0.08616	-1.40248
N	-1.49282	0.15290	-0.81472
C	3.62866	-0.12455	0.33598
C	4.94479	-0.85461	0.66688



C	3.50152	1.23069	1.07084	H	-4.06874	2.47634	-1.85931
C	-3.92714	0.07095	-0.33049	H	-5.28970	4.55290	-1.20866
C	-4.07123	1.54135	0.10175	H	-5.48987	3.93954	0.44126
C	-3.66853	-0.84850	0.87863	H	-3.87470	4.32956	-0.16636
C	6.23175	-0.11933	0.26685				
C	6.40658	0.04295	-1.24596				
C	3.82643	2.44951	0.19904	<b>L2_61 Ground State</b>			
C	3.69219	3.76824	0.96308	N	1.15770	-0.10887	-0.06660
C	-4.91064	-1.12113	1.73350	C	0.43548	-0.88123	-0.77480
C	-4.60733	-2.01620	2.93746	O	0.98659	-2.00169	-1.31980
C	-4.68729	2.46776	-0.95246	C	2.39681	-1.92422	-0.99655
C	-4.84566	3.90363	-0.44578	C	2.50422	-0.71096	-0.03335
H	3.09774	-2.34055	-1.01272	C	-0.99894	-0.67307	-1.06289
H	2.54634	-3.26363	0.41029	O	-1.62980	-1.71685	-1.67241
H	2.45401	-1.26144	1.73866	C	-2.98713	-1.26012	-1.89565
H	-3.50155	-2.19616	-1.67113	C	-3.05503	0.10773	-1.16494
H	-2.69064	-1.51082	-3.10382	N	-1.65852	0.37637	-0.77354
H	-2.99149	0.65316	-2.19198	C	3.59533	0.30596	-0.41627
H	3.58299	0.05887	-0.74717	C	4.99191	-0.35030	-0.44980
H	4.95474	-1.84207	0.18284	C	3.51862	1.54409	0.49282
H	4.96311	-1.04579	1.74960	C	-3.97898	0.12488	0.07487
H	4.15186	1.23049	1.95754	C	-4.14502	1.56247	0.62269
H	2.47514	1.34379	1.43440	C	-3.47691	-0.84667	1.15869
H	-4.86840	-0.24494	-0.80963	C	5.54911	-0.81213	0.90243
H	-3.07979	1.91339	0.38917	C	6.92703	-1.46495	0.76520
H	-4.69464	1.58813	1.00389	C	4.51683	2.65215	0.14335
H	-2.88040	-0.40157	1.49781	C	4.30468	3.91174	0.98712
H	-3.26890	-1.81458	0.54096	C	-4.54444	-1.21208	2.19457
H	7.08633	-0.68091	0.66623	C	-4.00760	-2.13182	3.29377
H	6.26420	0.86380	0.75260	C	-5.41457	2.29013	0.15703
H	7.36473	0.51817	-1.48343	C	-5.51559	2.51778	-1.35435
H	6.38348	-0.93163	-1.74951	H	2.94427	-1.77063	-1.93316
H	5.61504	0.65990	-1.68406	H	2.69770	-2.87729	-0.55658
H	3.14576	2.45252	-0.66296	H	2.68244	-1.04580	0.99712
H	4.84104	2.36606	-0.21061	H	-3.66854	-2.01295	-1.49087
H	3.90975	4.62909	0.32085	H	-3.14082	-1.17901	-2.97596
H	2.67603	3.89097	1.35640	H	-3.37557	0.89650	-1.85162
H	4.38326	3.80321	1.81449	H	3.36584	0.63248	-1.44249
H	-5.68180	-1.59329	1.10821	H	5.69979	0.35837	-0.89735
H	-5.34159	-0.17497	2.08503	H	4.97327	-1.21029	-1.13459
H	-5.50742	-2.20981	3.53162	H	3.66348	1.24171	1.53987
H	-4.20240	-2.98398	2.61716	H	2.49912	1.93938	0.43479
H	-3.86457	-1.54997	3.59585	H	-4.96167	-0.23527	-0.27064
H	-5.66831	2.07296	-1.25354	H	-3.25524	2.14574	0.35537
				H	-4.15997	1.53014	1.71846

H	-2.60831	-0.39801	1.65698	C	3.42805	2.57840	-0.72942
H	-3.11146	-1.77531	0.69865	C	3.07151	3.77858	-1.61035
H	4.85763	-1.52308	1.37414	C	5.83964	-1.21550	0.43323
H	5.61890	0.04261	1.58635	C	7.32006	-1.08834	0.80292
H	7.31820	-1.78572	1.73698	H	-3.34522	-2.02941	0.91052
H	6.88388	-2.34655	0.11393	H	-2.96638	-2.90458	-0.59288
H	7.65048	-0.76676	0.32695	H	-3.08048	-0.88099	-1.82340
H	4.42131	2.90342	-0.92266	H	3.29235	-2.43863	0.18511
H	5.54583	2.29512	0.28184	H	2.98846	-1.94053	1.86934
H	5.02552	4.69561	0.72864	H	3.07359	0.36660	1.24621
H	3.29718	4.31827	0.83957	H	-3.60335	1.25768	-0.87740
H	4.41798	3.69224	2.05586	H	-3.32474	0.02117	1.90921
H	-5.38814	-1.69892	1.68483	H	-2.15426	1.07649	1.12729
H	-4.95156	-0.29981	2.65036	H	-5.78393	0.78048	0.17273
H	-4.78802	-2.39176	4.01770	H	-5.31250	-0.86809	0.51843
H	-3.61815	-3.06596	2.87088	H	3.78053	-0.83854	-1.44195
H	-3.18813	-1.65136	3.84160	H	5.37096	0.88314	0.52636
H	-5.46512	3.26179	0.66592	H	5.94409	0.34411	-1.04066
H	-6.29365	1.72299	0.49538	H	2.52194	1.12369	-2.01868
H	-6.41089	3.09762	-1.60547	H	4.23541	1.38796	-2.34091
H	-4.64454	3.06811	-1.73059	H	-3.91713	2.88373	0.99877
H	-5.57644	1.57199	-1.90521	H	-5.01277	1.85507	1.90974
<b>L2_62 Ground State</b>				H	-3.86237	3.45052	3.44435
N	-1.37298	-0.23559	-0.81870	H	-3.37378	1.79216	3.82879
C	-0.70740	-1.06939	-0.12450	H	-2.28190	2.84526	2.91853
O	-1.34095	-2.13921	0.43076	H	-5.22769	-1.38451	-1.91782
C	-2.72381	-2.02629	0.01181	H	-5.51157	0.30362	-2.30894
C	-2.77346	-0.69423	-0.78965	H	-7.62484	-1.04246	-2.49907
C	0.73900	-0.97006	0.16158	H	-7.48683	-1.51780	-0.79867
O	1.31687	-2.09330	0.66547	H	-7.78467	0.17398	-1.22120
C	2.71960	-1.76266	0.82534	H	4.38782	2.76792	-0.23085
C	2.82215	-0.27099	0.38868	H	2.67305	2.47456	0.05832
N	1.44661	0.07103	-0.02298	H	3.02359	4.70498	-1.02677
C	-3.69883	0.39590	-0.20137	H	3.81415	3.92179	-2.40529
C	-3.22458	0.84837	1.19052	H	2.09602	3.63321	-2.08919
C	-5.17274	-0.04887	-0.20327	H	5.70669	-2.05762	-0.26021
C	3.84556	0.00545	-0.73761	H	5.27020	-1.46624	1.33757
C	5.28896	0.06595	-0.20336	H	7.69952	-2.00705	1.26365
C	3.49319	1.27700	-1.53731	H	7.93017	-0.88062	-0.08424
C	-3.95107	2.07862	1.74616	H	7.47893	-0.26730	1.51250
C	-3.33448	2.57152	3.05783	<b>L2_63 Ground State</b>			
C	-5.73255	-0.47538	-1.56597	N	1.16730	-0.48244	0.57056
C	-7.24144	-0.73007	-1.52149	C	0.69680	-0.40868	-0.60937

O	1.49409	-0.72269	-1.67097	H	5.18428	-1.49788	2.41122
C	2.74612	-1.16324	-1.08658	H	7.32262	-2.55236	1.62112
C	2.58510	-0.86179	0.43043	H	7.30960	-1.52475	0.17879
C	-0.67110	0.03031	-0.95127	H	7.52696	-0.79966	1.77759
O	-1.08763	-0.27659	-2.21253	H	-5.37517	-2.31104	-0.63903
C	-2.40784	0.31157	-2.32752	H	-5.24829	-2.06731	1.09479
C	-2.73145	0.80263	-0.89120	H	-5.14052	-4.50632	0.54849
N	-1.45707	0.64818	-0.16331	H	-3.73067	-4.22714	-0.48734
C	3.50105	0.23327	1.03445	H	-3.60730	-3.97403	1.25880
C	3.11826	1.67361	0.63510	H	-5.84583	1.88940	0.45723
C	4.99235	-0.06659	0.80266	H	-4.30940	2.73755	0.55032
C	-3.85809	0.01394	-0.18545	H	-5.83565	3.52509	2.36016
C	-4.21886	0.65611	1.16629	H	-5.98177	1.87216	2.98072
C	-3.48463	-1.47202	-0.02032	H	-4.42763	2.71330	3.06513
C	3.28110	2.07945	-0.83668				
C	2.93481	3.55527	-1.05448				
C	5.47817	-1.41177	1.35579	<b>L2_64 Ground State</b>			
C	6.99373	-1.58428	1.22753	N	1.25912	-0.07198	-0.05240
C	-4.68471	-2.39593	0.21228	C	0.52223	-0.98951	-0.53678
C	-4.27065	-3.85830	0.39332	O	1.06238	-2.20973	-0.81057
C	-4.94033	2.00497	1.07014	C	2.48009	-2.06222	-0.54890
C	-5.31900	2.56247	2.44468	C	2.60889	-0.65172	0.08802
H	3.55377	-0.61955	-1.57725	C	-0.91989	-0.85245	-0.82359
H	2.85331	-2.23207	-1.29503	O	-1.60026	-2.02548	-0.96350
H	2.74588	-1.77762	1.00766	C	-2.97691	-1.64266	-1.21793
H	-3.08998	-0.45754	-2.69844	C	-2.96336	-0.09018	-1.13655
H	-2.35008	1.12519	-3.05700	N	-1.54829	0.25042	-0.89917
H	-2.99646	1.86428	-0.90251	C	3.68367	0.24005	-0.56094
H	3.32514	0.17316	2.11780	C	5.08206	-0.40759	-0.47553
H	3.72822	2.35281	1.24801	C	3.62672	1.66126	0.02392
H	2.07700	1.84253	0.93229	C	-3.90687	0.55162	-0.09338
H	5.57367	0.73882	1.27306	C	-3.88503	-0.07596	1.31521
H	5.23319	-0.01496	-0.26775	C	-5.33958	0.57447	-0.66397
H	-4.73773	0.07762	-0.84691	C	5.67943	-0.53171	0.93162
H	-3.29658	0.76930	1.74980	C	7.05638	-1.20064	0.91608
H	-4.86003	-0.03482	1.72854	C	4.61003	2.64979	-0.61028
H	-2.77474	-1.56597	0.81124	C	4.41424	4.07661	-0.09126
H	-2.94839	-1.82876	-0.91035	C	-6.36797	1.34069	0.17508
H	4.31191	1.89795	-1.16893	C	-7.72215	1.45951	-0.52908
H	2.63345	1.46887	-1.47495	C	-2.51704	-0.28251	1.98060
H	3.04514	3.84264	-2.10611	C	-2.65520	-0.58681	3.47472
H	1.89946	3.76078	-0.75706	H	3.00467	-2.14372	-1.50729
H	3.58547	4.20650	-0.45801	H	2.79250	-2.88108	0.10254
H	4.97874	-2.23805	0.83235	H	2.81753	-0.72707	1.16331
				H	-3.60209	-2.12238	-0.46132

H	-3.25315	-2.02267	-2.20484	C	3.78831	-0.02932	-0.40325
H	-3.23465	0.33845	-2.10951	C	5.15947	-0.66366	-0.08760
H	3.42316	0.30942	-1.62849	C	3.75066	1.49326	-0.18992
H	5.77337	0.17158	-1.10027	C	-3.88118	0.22890	-0.15620
H	5.04871	-1.40695	-0.93272	C	-5.32283	-0.18348	-0.54700
H	3.80149	1.62046	1.10858	C	-3.69873	1.75409	-0.08246
H	2.60431	2.03325	-0.09976	C	5.68699	-0.44776	1.33630
H	-3.56073	1.59039	-0.00082	C	7.04074	-1.12723	1.55852
H	-4.48106	0.57641	1.96564	C	4.79219	2.27439	-0.99701
H	-4.42429	-1.03549	1.29992	C	4.62014	3.78889	-0.85475
H	-5.69243	-0.45948	-0.80499	C	-4.57939	2.46871	0.94715
H	-5.30852	1.02275	-1.66743	C	-4.26760	3.96521	1.03391
H	5.76396	0.46224	1.38791	C	-6.23870	-0.54731	0.63358
H	5.00521	-1.10733	1.57986	C	-5.87286	-1.87305	1.30773
H	7.47631	-1.27913	1.92493	H	3.07000	-2.55681	-0.77255
H	6.99966	-2.21284	0.49718	H	2.78396	-2.86971	0.95977
H	7.76359	-0.62939	0.30252	H	2.81107	-0.51942	1.45769
H	4.48497	2.63559	-1.70242	H	-3.48641	-2.37785	-0.37286
H	5.64404	2.33510	-0.41717	H	-3.05202	-2.39065	-2.10135
H	5.12426	4.77328	-0.55103	H	-3.08371	0.00288	-2.14466
H	3.40126	4.43699	-0.30593	H	3.57967	-0.22116	-1.46722
H	4.55673	4.12228	0.99541	H	5.89733	-0.27116	-0.79834
H	-5.97658	2.34398	0.39485	H	5.11468	-1.74420	-0.28589
H	-6.50826	0.84636	1.14365	H	3.87575	1.71848	0.87887
H	-8.44701	2.00390	0.08620	H	2.74708	1.84340	-0.45311
H	-7.62634	1.99120	-1.48352	H	-3.64375	-0.18835	0.83362
H	-8.14302	0.46943	-0.74336	H	-5.30128	-1.04485	-1.22998
H	-1.89138	0.60526	1.83374	H	-5.77590	0.63378	-1.12355
H	-1.98718	-1.11123	1.49971	H	-3.89445	2.17910	-1.07918
H	-1.67786	-0.76211	3.93786	H	-2.64591	1.96225	0.13525
H	-3.13315	0.24572	4.00572	H	5.78264	0.62627	1.53771
H	-3.26924	-1.48073	3.64257	H	4.96523	-0.83142	2.06975
				H	7.41089	-0.96203	2.57634
				H	6.97058	-2.21026	1.39926
				H	7.79367	-0.73989	0.86140
				H	4.71478	1.99362	-2.05712
				H	5.80604	1.99593	-0.68069
				H	5.37175	4.33577	-1.43517
				H	3.62972	4.10602	-1.20196
				H	4.71642	4.09836	0.19319
				H	-4.43428	2.00627	1.93381
				H	-5.64013	2.33606	0.69851
				H	-4.90224	4.46618	1.77361
				H	-3.22197	4.13249	1.31814
<b>L2_65 Ground State</b>							
N	1.33349	-0.16113	0.03526				
C	0.58882	-1.15836	-0.23077				
O	1.10384	-2.41769	-0.15806				
C	2.51461	-2.23275	0.11474				
C	2.65651	-0.71096	0.38747				
C	-0.83541	-1.07555	-0.61799				
O	-1.46615	-2.27032	-0.78323				
C	-2.83306	-1.93755	-1.13120				
C	-2.86219	-0.38094	-1.13962				
N	-1.48150	0.00594	-0.79894				

H	-4.42875	4.45683	0.06672
H	-7.27309	-0.60743	0.27052
H	-6.22160	0.25682	1.37809
H	-6.55809	-2.10050	2.13173
H	-5.92373	-2.70458	0.59354
H	-4.85835	-1.85300	1.72231

**L2\_66 Ground State**

N	-1.50972	0.39800	-0.48703
C	-0.88941	-0.66949	-0.79772
O	-1.53474	-1.64094	-1.50076
C	-2.86536	-1.11997	-1.74367
C	-2.88192	0.24701	-1.00327
C	0.51299	-0.96990	-0.44112
O	1.00836	-2.13596	-0.94096
C	2.40339	-2.15315	-0.54736
C	2.55558	-0.92235	0.38738
N	1.25556	-0.23408	0.28484
C	-3.91846	0.36818	0.13668
C	-3.64108	-0.63953	1.26531
C	-5.36003	0.26065	-0.39698
C	3.72530	0.00923	0.02144
C	5.05542	-0.75810	0.13079
C	3.70417	1.29261	0.88403
C	-4.48929	-0.43603	2.52596
C	-4.06352	-1.36384	3.66680
C	-5.73486	1.21964	-1.53802
C	-5.56114	2.70015	-1.18646
C	3.95891	2.57715	0.08637
C	3.97932	3.82451	0.97185
C	6.29428	0.02552	-0.31429
C	7.57292	-0.81301	-0.24115
H	-3.58360	-1.84616	-1.35570
H	-2.99970	-1.02818	-2.82507
H	-3.05744	1.06247	-1.71225
H	3.00649	-2.06807	-1.45827
H	2.60830	-3.11280	-0.06866
H	2.68195	-1.23608	1.43375
H	-3.77548	1.37179	0.55853
H	-2.58335	-0.55791	1.54167
H	-3.78904	-1.66642	0.89883
H	-6.04959	0.43780	0.43721
H	-5.54652	-0.77328	-0.72241
H	3.57568	0.29433	-1.03137

H	5.00279	-1.68041	-0.46592
H	5.18976	-1.08006	1.17473
H	4.44681	1.20605	1.69042
H	2.72587	1.38426	1.36660
H	-5.55069	-0.60302	2.30396
H	-4.40340	0.61026	2.85132
H	-4.67682	-1.20793	4.56139
H	-4.15979	-2.41682	3.37481
H	-3.01628	-1.19226	3.94282
H	-6.78271	1.03437	-1.80755
H	-5.15254	0.98608	-2.43952
H	-5.92515	3.34316	-1.99524
H	-6.12115	2.95456	-0.27819
H	-4.51112	2.95666	-1.00785
H	3.17072	2.67593	-0.67204
H	4.90572	2.50037	-0.46347
H	4.13861	4.73416	0.38188
H	3.03185	3.93689	1.51236
H	4.78117	3.76553	1.71842
H	6.41127	0.92021	0.30900
H	6.14588	0.38412	-1.34215
H	8.44831	-0.23730	-0.56140
H	7.75787	-1.16078	0.78252
H	7.50223	-1.69946	-0.88334

**L2\_67 Ground State**

N	1.26510	-0.25674	0.29667
C	0.58683	-1.23973	-0.14310
O	1.15043	-2.47829	-0.18735
C	2.51180	-2.29611	0.27575
C	2.59342	-0.78868	0.64952
C	-0.80925	-1.15828	-0.62087
O	-1.43251	-2.35536	-0.81339
C	-2.74552	-2.02004	-1.32815
C	-2.81570	-0.47366	-1.21273
N	-1.44453	-0.07724	-0.84005
C	3.72709	-0.03377	-0.07171
C	5.08765	-0.55159	0.43452
C	3.56448	1.49345	0.03939
C	-3.83546	0.03974	-0.17106
C	-3.96582	1.57200	-0.22980
C	-3.46877	-0.43455	1.24992
C	6.32138	0.09157	-0.21474
C	6.38809	-0.08785	-1.73409

C	3.64016	2.06861	1.45811	N	-1.23275	-0.41527	-0.94905
C	3.47964	3.59096	1.46734	C	-0.61311	-1.28136	-0.25185
C	-4.62455	-0.39649	2.26090	O	-1.16509	-2.51411	-0.06457
C	-5.72784	-1.42125	1.97859	C	-2.39060	-2.50187	-0.83924
C	-4.67261	2.11266	-1.47763	C	-2.51318	-1.03653	-1.33736
C	-4.81320	3.63683	-1.45443	C	0.69164	-1.06407	0.40640
H	3.18235	-2.56894	-0.54592	O	1.31600	-2.19036	0.85424
H	2.67674	-2.97563	1.11511	C	2.52389	-1.72041	1.50365
H	2.72395	-0.66411	1.73207	C	2.56384	-0.20293	1.17967
H	-3.49047	-2.54359	-0.72340	N	1.25198	0.06825	0.56158
H	-2.80263	-2.37781	-2.36063	C	-3.70541	-0.25787	-0.73903
H	-3.05081	-0.02950	-2.18500	C	-3.79795	1.12460	-1.40762
H	3.63487	-0.28839	-1.13766	C	-3.62622	-0.18368	0.80405
H	5.13956	-1.63803	0.27064	C	3.71153	0.21440	0.23236
H	5.14234	-0.40938	1.52219	C	3.78484	1.74487	0.08918
H	2.59530	1.76040	-0.39446	C	3.57564	-0.46894	-1.14353
H	4.33028	1.97546	-0.58268	C	-4.98718	1.98830	-0.97754
H	-4.80284	-0.40081	-0.45640	C	-5.05390	3.30767	-1.75147
H	-2.96097	2.00633	-0.15399	C	-4.97200	-0.38243	1.51181
H	-4.52028	1.91610	0.65303	C	-4.86138	-0.24627	3.03170
H	-2.63936	0.18450	1.61172	C	4.86545	-0.50514	-1.97687
H	-3.08212	-1.46244	1.21736	C	5.95357	-1.41327	-1.39520
H	7.21761	-0.34997	0.24014	C	4.27640	2.48750	1.33652
H	6.35461	1.16048	0.03038	C	4.37413	3.99906	1.11507
H	7.32419	0.31324	-2.13779	H	-3.20742	-2.81491	-0.18363
H	6.33374	-1.14903	-2.00798	H	-2.28174	-3.22647	-1.65170
H	5.56374	0.42668	-2.23975	H	-2.59496	-1.00323	-2.43019
H	4.59704	1.80241	1.92687	H	3.36819	-2.28272	1.09659
H	2.85293	1.62093	2.07733	H	2.43287	-1.92992	2.57377
H	3.52919	3.99490	2.48482	H	2.63761	0.38156	2.10201
H	4.26764	4.07430	0.87642	H	-4.60617	-0.83131	-1.01161
H	2.51526	3.88418	1.03609	H	-3.84558	0.98213	-2.49746
H	-5.06042	0.61034	2.29832	H	-2.86247	1.66350	-1.21219
H	-4.21387	-0.58302	3.26154	H	-3.18905	0.77952	1.09684
H	-6.49905	-1.39765	2.75652	H	-2.93225	-0.94220	1.18833
H	-6.22482	-1.23412	1.01999	H	4.63831	-0.13268	0.71393
H	-5.31769	-2.43858	1.94612	H	2.79064	2.11237	-0.19469
H	-5.66777	1.65210	-1.55890	H	4.45677	1.99261	-0.74286
H	-4.12423	1.81906	-2.38215	H	2.78724	0.04755	-1.70361
H	-5.32278	4.00775	-2.35078	H	3.22513	-1.50271	-1.01872
H	-5.38919	3.96598	-0.58091	H	-4.92196	2.20476	0.09611
H	-3.83024	4.11994	-1.40304	H	-5.92213	1.42862	-1.12300
				H	-5.90336	3.92020	-1.42908
				H	-4.14037	3.89585	-1.60287

**L2\_68 Ground State**

H	-5.15909	3.12861	-2.82844	H	2.64041	-0.63663	1.35545
H	-5.36280	-1.37855	1.25854	H	-3.59509	-2.38686	-0.99545
H	-5.70819	0.33509	1.13082	H	-2.96607	-2.14470	-2.64698
H	-5.82692	-0.41243	3.52239	H	-3.19744	0.19955	-2.35608
H	-4.14744	-0.97120	3.44159	H	3.50680	0.02098	-1.48220
H	-4.51121	0.75473	3.31143	H	5.79796	-0.05785	-0.73095
H	5.26351	0.51031	-2.10104	H	5.03454	-1.59646	-0.42273
H	4.61357	-0.85403	-2.98660	H	3.66070	1.68093	1.08196
H	6.82879	-1.45428	-2.05307	H	2.58408	1.93582	-0.27407
H	6.29755	-1.06393	-0.41512	H	-4.91965	-0.21053	-0.64292
H	5.58207	-2.43825	-1.26996	H	-4.23908	2.04420	-1.36516
H	5.26052	2.09368	1.62890	H	-3.00944	2.10541	-0.11354
H	3.60502	2.29406	2.18321	H	-3.02310	0.34965	1.62179
H	4.72931	4.51544	2.01391	H	-2.91550	-1.26058	0.96242
H	5.06722	4.23337	0.29784	H	4.77438	-0.96624	2.01414
H	3.39691	4.41995	0.85023	H	5.57204	0.56092	1.68613

**L2\_69 Ground State**

N	1.20504	-0.13829	-0.06744
C	0.49494	-1.10926	-0.48293
O	1.03676	-2.35789	-0.54445
C	2.43119	-2.18167	-0.19253
C	2.52767	-0.70107	0.26507
C	-0.91572	-1.00586	-0.91127
O	-1.54242	-2.19314	-1.14907
C	-2.87278	-1.83513	-1.60171
C	-2.93887	-0.29572	-1.41269
N	-1.55935	0.08318	-1.05280
C	3.67013	0.09213	-0.39563
C	5.04433	-0.54538	-0.10010
C	3.58490	1.57854	-0.01005
C	-3.93678	0.17580	-0.33185
C	-4.00823	1.71283	-0.34181
C	-3.59210	-0.40215	1.06235
C	5.51253	-0.48441	1.35911
C	6.87459	-1.15505	1.55589
C	4.63767	2.46978	-0.67614
C	4.42100	3.95350	-0.36763
C	-4.80556	-0.86019	1.88817
C	-5.45962	-2.13761	1.35227
C	-5.03442	2.33153	0.61183
C	-5.10531	3.85498	0.47653
H	3.02833	-2.38724	-1.08798
H	2.68130	-2.91031	0.58137

**L2\_70 Ground State**

N	-1.60508	-0.99995	-1.14348
C	-1.01463	-1.62894	-0.20985
O	-1.73963	-2.39079	0.65616
C	-3.10929	-2.28889	0.18312
C	-3.04969	-1.19509	-0.91899
C	0.42535	-1.51526	0.10018
O	1.06624	-2.65538	0.47078
C	2.45097	-2.26134	0.67085

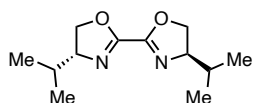
C	2.43316	-0.71453	0.52729	H	2.79713	4.43552	0.68396
N	1.05846	-0.41235	0.08864	H	3.51672	4.08399	-0.89656
C	-3.70822	0.15311	-0.53812	H	1.80614	3.73367	-0.60629
C	-2.99778	0.83476	0.65551	H	5.98994	1.16466	-0.92417
C	-5.21841	-0.03741	-0.30552	H	5.92799	-0.38494	-1.74769
C	3.48700	-0.15337	-0.44402	H	8.22700	0.05962	-0.83791
C	4.89284	-0.36213	0.14793	H	7.56456	0.20019	0.79810
C	3.17559	1.30536	-0.83115	H	7.51977	-1.35605	-0.04248
C	-1.88531	1.81044	0.24366				
C	-1.06282	2.30768	1.43291				
C	-6.02174	1.26518	-0.38918	<b>L2_71 Ground State</b>			
C	-7.51310	1.06012	-0.11367	N	1.22248	-0.16067	0.01296
C	3.16260	2.31106	0.32567	C	0.49750	-1.01732	-0.58725
C	2.80200	3.72149	-0.14731	O	1.04511	-2.20044	-0.98228
C	6.04441	0.08171	-0.75950	C	2.45547	-2.08710	-0.66985
C	7.41622	-0.27282	-0.18035	C	2.56877	-0.75440	0.11968
H	-3.73565	-2.03099	1.03910	C	-0.93673	-0.84403	-0.89821
H	-3.40589	-3.26912	-0.20175	O	-1.57950	-1.96349	-1.33671
H	-3.51282	-1.55268	-1.84522	C	-2.92838	-1.52976	-1.64057
H	3.05248	-2.75117	-0.10296	C	-2.98844	-0.07555	-1.10176
H	2.76286	-2.62039	1.65343	N	-1.58687	0.24305	-0.76999
H	2.57353	-0.23715	1.50565	C	3.65776	0.20006	-0.40467
H	-3.58785	0.79948	-1.41858	C	5.05492	-0.45375	-0.35052
H	-3.73485	1.37562	1.26318	C	3.58269	1.55292	0.32285
H	-2.57703	0.06964	1.32311	C	-3.90229	0.11860	0.12946
H	-5.38854	-0.50122	0.67723	C	-3.98764	1.59995	0.54126
H	-5.61948	-0.74213	-1.04920	C	-3.44319	-0.75875	1.31028
H	3.41808	-0.75041	-1.36670	C	5.61816	-0.71791	1.05137
H	5.02733	-1.42919	0.38064	C	6.99702	-1.38126	1.00289
H	4.96744	0.16395	1.11017	C	4.58115	2.60069	-0.17873
H	2.19299	1.31917	-1.31376	C	4.36982	3.96600	0.48067
H	3.90063	1.63434	-1.58654	C	-4.39440	-0.79390	2.51649
H	-2.34307	2.66207	-0.28009	C	-5.80584	-1.28838	2.18634
H	-1.21863	1.31955	-0.47057	C	-4.46390	2.57866	-0.54283
H	-0.30565	3.03354	1.11466	C	-5.83822	2.24145	-1.12943
H	-1.69342	2.78892	2.19183	H	3.00467	-2.06600	-1.61762
H	-0.53609	1.47208	1.90824	H	2.75044	-2.97291	-0.10338
H	-5.88619	1.70253	-1.38780	H	2.75348	-0.94648	1.18482
H	-5.61687	1.99756	0.32105	H	-3.62450	-2.21676	-1.15335
H	-8.06812	2.00154	-0.19157	H	-3.06332	-1.58940	-2.72500
H	-7.95334	0.35246	-0.82681	H	-3.31984	0.60389	-1.89247
H	-7.67636	0.65834	0.89380	H	3.42496	0.38012	-1.46571
H	4.14144	2.33188	0.82396	H	5.76010	0.18461	-0.89721
H	2.43247	1.99384	1.08010	H	5.03453	-1.40242	-0.90596
				H	3.72821	1.39953	1.40173



H	2.56338	1.93697	0.21121	C	-4.46423	2.78263	-0.46658
H	-4.89958	-0.21765	-0.18707	C	-4.62528	4.08022	0.32956
H	-2.99859	1.91329	0.89607	C	-5.01634	-1.28654	1.34390
H	-4.67095	1.68165	1.39617	C	-4.84173	-2.43452	2.34110
H	-2.45804	-0.40646	1.63855	C	4.89058	0.51934	-1.38064
H	-3.29806	-1.79156	0.96469	C	4.78744	1.19227	-2.75101
H	4.93000	-1.35569	1.62210	C	4.74593	1.67943	1.89609
H	5.68852	0.22555	1.60644	C	6.10705	1.01796	2.13276
H	7.39243	-1.56003	2.00885	H	-3.35585	-1.66387	-2.10080
H	6.95354	-2.34652	0.48365	H	-2.39654	-0.72662	-3.27633
H	7.71731	-0.75117	0.46707	H	-2.72355	1.20160	-1.94179
H	4.48518	2.70041	-1.26937	H	3.20051	-2.45581	-0.85263
H	5.61010	2.26615	0.00790	H	2.25421	-3.44269	0.29274
H	5.09077	4.70575	0.11478	H	2.44380	-1.70112	1.89736
H	3.36237	4.34826	0.27819	H	-4.73468	0.11419	-0.93632
H	4.48361	3.89806	1.56955	H	-2.99348	1.87688	0.84030
H	-4.45382	0.19882	2.97927	H	-4.66348	1.50194	1.24246
H	-3.95209	-1.45115	3.27633	H	-2.95270	-0.63028	1.42441
H	-6.40945	-1.39548	3.09441	H	-3.30255	-1.78313	0.15491
H	-6.33413	-0.59604	1.52118	H	4.48124	-0.92707	0.74912
H	-5.77462	-2.26631	1.68917	H	3.55440	0.13355	2.80007
H	-3.72147	2.64052	-1.34826	H	2.62696	1.25020	1.81243
H	-4.50084	3.58189	-0.09901	H	3.04316	1.34595	-0.60689
H	-6.17672	3.02120	-1.82068	H	2.88061	-0.20713	-1.38120
H	-5.82557	1.29576	-1.68373	H	-3.77021	2.95912	-1.29860
H	-6.59149	2.14697	-0.33702	H	-5.42649	2.50811	-0.92225
				H	-4.98389	4.89924	-0.30394
				H	-5.34196	3.95251	1.15004
				H	-3.67037	4.39020	0.77038
				H	-5.74664	-1.57464	0.57427
				H	-5.44629	-0.41958	1.86159
				H	-5.79364	-2.70863	2.80952
				H	-4.44144	-3.32842	1.84723
				H	-4.14234	-2.15802	3.13915
				H	5.34890	-0.47402	-1.49201
				H	5.57023	1.09498	-0.74202
				H	5.76855	1.28137	-3.23069
				H	4.13573	0.62035	-3.42284
				H	4.36517	2.20051	-2.66208
				H	4.55703	2.39963	2.70285
				H	4.77362	2.27016	0.97151
				H	6.90399	1.76621	2.20879
				H	6.10225	0.43926	3.06482
				H	6.37581	0.33259	1.32155
<b>L2_72 Ground State</b>							
N	-1.36103	0.35021	-0.59538				
C	-0.75575	-0.73460	-0.87289				
O	-1.31789	-1.61231	-1.75186				
C	-2.52701	-0.96070	-2.21539				
C	-2.64432	0.30314	-1.32201				
C	0.53890	-1.15429	-0.29792				
O	1.15076	-2.19514	-0.93168				
C	2.35255	-2.45279	-0.16269				
C	2.39492	-1.30110	0.87778				
N	1.09921	-0.61608	0.71028				
C	-3.82877	0.27526	-0.32907				
C	-3.96702	1.62244	0.40280				
C	-3.69958	-0.89489	0.66521				
C	3.56882	-0.31437	0.68919				
C	3.57060	0.69405	1.85355				
C	3.52487	0.36424	-0.70056				

				H	7.94022	-0.83653	-1.34555
				H	7.73111	-0.50451	0.38138
<b>L2_73 Ground State</b>				H	7.19480	-2.04988	-0.29244
N	1.06796	-0.27520	0.45096	H	4.31904	2.63054	-0.65758
C	0.43543	-1.03577	-0.34978	H	5.40898	2.18691	0.64781
O	1.02997	-2.17105	-0.80917	H	4.84982	4.61818	0.77829
C	2.34061	-2.19414	-0.19135	H	3.12331	4.23142	0.88448
C	2.40167	-0.87520	0.63347	H	4.21330	3.77567	2.20056
C	-0.93560	-0.79141	-0.84407	H	-5.75133	-1.33560	1.37426
O	-1.53975	-1.85657	-1.44376	H	-5.19939	-0.01964	2.39742
C	-2.82297	-1.35689	-1.89601	H	-5.43591	-2.11464	3.73820
C	-2.91904	0.06022	-1.27094	H	-4.29662	-2.94835	2.66768
N	-1.56785	0.30780	-0.73241	H	-3.73655	-1.61682	3.68837
C	3.52101	0.08280	0.17982	H	-3.60996	2.80492	-1.44670
C	4.90850	-0.57059	0.39615	H	-4.49552	3.68559	-0.22465
C	3.38296	1.44186	0.88478	H	-5.99402	3.27550	-2.14043
C	-3.98052	0.20089	-0.15714	H	-5.69132	1.53654	-2.08040
C	-4.08480	1.65660	0.33635	H	-6.57710	2.32068	-0.76697
C	-3.70032	-0.76078	1.01386				
C	5.88551	-0.37250	-0.76882	<b>L2_74 Ground State</b>			
C	7.26511	-0.97372	-0.49366	N	1.21652	-0.17848	-0.01173
C	4.38235	2.51128	0.43323	C	0.52587	-1.10076	-0.55227
C	4.13032	3.86118	1.11018	O	1.10827	-2.30147	-0.82623
C	-4.89053	-0.97491	1.95544	C	2.50785	-2.12633	-0.49456
C	-4.57520	-1.96908	3.07587	C	2.56961	-0.73221	0.18634
C	-4.43186	2.71107	-0.72579	C	-0.90187	-0.98854	-0.91722
C	-5.74410	2.44564	-1.47010	O	-1.47903	-2.13532	-1.37684
H	3.08533	-2.23977	-0.99142	C	-2.83901	-1.76571	-1.71752
H	2.40970	-3.10026	0.41637	C	-2.96929	-0.29776	-1.22860
H	2.53876	-1.08439	1.70252	N	-1.60045	0.07130	-0.82294
H	-3.59642	-2.04913	-1.55423	C	3.65710	0.20039	-0.37842
H	-2.81038	-1.34215	-2.99024	C	5.06284	-0.42146	-0.23966
H	-3.12424	0.80192	-2.04850	C	3.53955	1.60134	0.24507
H	3.37373	0.24238	-0.89982	C	-3.95946	-0.10410	-0.05845
H	4.80112	-1.65167	0.56531	C	-4.10994	1.38974	0.28657
H	5.35348	-0.17601	1.32028	C	-3.55473	-0.94112	1.17847
H	3.48831	1.28646	1.96967	C	5.58958	-0.57719	1.19232
H	2.36313	1.80854	0.72760	C	6.97906	-1.21885	1.22840
H	-4.93961	-0.08976	-0.61255	C	4.53116	2.62908	-0.30889
H	-3.12992	1.92382	0.80412	C	4.27935	4.03457	0.24311
H	-4.84714	1.70102	1.12443	C	-4.73171	-1.61221	1.90301
H	-2.84120	-0.38339	1.58289	C	-5.78740	-0.65567	2.46483
H	-3.39390	-1.74236	0.62708	C	-4.88420	2.21478	-0.74656
H	5.98609	0.69659	-0.99017	C	-5.03366	3.67997	-0.32909
H	5.45670	-0.82837	-1.67246				

H	3.07806	-2.16646	-1.42932	C	-0.85898	-0.58220	-0.31497
H	2.81151	-2.95573	0.14751	O	-1.46292	-1.80130	-0.24049
H	2.72166	-0.83364	1.26912	C	-2.82632	-1.57619	-0.67662
H	-3.51459	-2.46158	-1.21315	C	-2.92777	-0.03448	-0.83022
H	-2.95432	-1.87222	-2.80027	N	-1.54109	0.43691	-0.65685
H	-3.26937	0.35466	-2.05491	C	3.69196	0.67236	-0.37456
H	3.45059	0.29749	-1.45560	C	5.09815	0.19951	0.01551
H	5.77274	0.19038	-0.81004	C	3.59563	2.20055	-0.34727
H	5.07454	-1.40665	-0.72762	C	-3.87123	0.64957	0.18432
H	3.66124	1.53044	1.33541	C	-4.01419	2.14082	-0.13866
H	2.51654	1.95585	0.08137	C	-3.40782	0.44303	1.63157
H	-4.93128	-0.47456	-0.42350	H	3.13622	-1.91416	-0.39434
H	-3.10614	1.81077	0.42352	H	2.84081	-2.03714	1.35995
H	-4.61799	1.48200	1.25351	H	2.84744	0.35396	1.57586
H	-3.00191	-0.30035	1.87706	H	-3.49672	-1.99123	0.08036
H	-2.85170	-1.73185	0.89028	H	-2.97090	-2.11340	-1.61872
H	5.62993	0.40374	1.68168	H	-3.26126	0.23369	-1.83972
H	4.89500	-1.18526	1.78725	H	3.47489	0.32766	-1.39664
H	7.34816	-1.32043	2.25491	H	5.34053	0.51041	1.03983
H	6.96484	-2.21850	0.77705	H	5.20185	-0.89076	-0.03711
H	7.70487	-0.61551	0.66975	H	5.85104	0.63488	-0.65030
H	4.46034	2.64683	-1.40585	H	2.59261	2.53213	-0.62550
H	5.56097	2.32924	-0.07421	H	3.81102	2.58345	0.65877
H	4.99574	4.75955	-0.15946	H	4.32200	2.64611	-1.03638
H	3.27051	4.38115	-0.01028	H	-4.85372	0.16894	0.05900
H	4.36754	4.04879	1.33638	H	-4.40679	2.29317	-1.15108
H	-4.33177	-2.22338	2.72291	H	-4.69686	2.62946	0.56550
H	-5.21776	-2.31507	1.21057	H	-3.04039	2.63665	-0.07699
H	-6.56305	-1.20638	3.00892	H	-3.28542	-0.61701	1.88247
H	-5.33919	0.06465	3.15979	H	-2.44700	0.94034	1.79851
H	-6.28379	-0.08657	1.67108	H	-4.13670	0.86690	2.33061
H	-5.87955	1.77033	-0.89277				
H	-4.38296	2.17079	-1.72224				
H	-5.59319	4.25613	-1.07455				



H	-5.56409	3.76450	0.62728
H	-4.05261	4.15378	-0.20570

**L3\_1 Ground State**

N	1.27256	0.48766	0.20938
C	0.57658	-0.56390	0.03691
O	1.15847	-1.78626	0.18494
C	2.55739	-1.51296	0.44468
C	2.63536	0.03630	0.54474

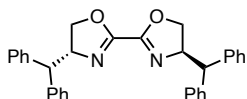
**L2\_2 Ground State**

N	-1.44525	0.50121	-0.27118
C	-0.72638	-0.54057	-0.13663
O	-1.29941	-1.77082	-0.25194
C	-2.71551	-1.51556	-0.42103
C	-2.81564	0.03024	-0.54218
C	0.72640	-0.54055	0.13674
O	1.29949	-1.77078	0.25190
C	2.71556	-1.51548	0.42120
C	2.81564	0.03034	0.54226
N	1.44521	0.50125	0.27139
C	-3.84118	0.66953	0.40880

C	-5.25537	0.16751	0.09054	H	2.71127	-2.05310	1.73928
C	-3.76992	2.19799	0.34586	H	2.99012	0.30138	1.89192
C	3.84106	0.66960	-0.40888	H	-3.36926	-1.99143	-0.08324
C	5.25523	0.16732	-0.09100	H	-2.71126	-2.05309	-1.73929
C	3.77005	2.19806	-0.34576	H	-2.99017	0.30138	-1.89193
H	-3.23238	-1.90549	0.46292	H	4.70695	0.18027	0.10909
H	-3.05459	-2.05961	-1.30500	H	4.16511	2.34528	1.20344
H	-3.07319	0.32840	-1.56904	H	4.57159	2.61796	-0.50075
H	3.23259	-1.90547	-0.46262	H	2.87458	2.63630	0.02498
H	3.05450	-2.05944	1.30529	H	2.41878	0.86233	-1.81812
H	3.07332	0.32855	1.56908	H	4.14131	0.78703	-2.23120
H	-3.57454	0.34975	1.42723	H	3.27369	-0.68802	-1.78546
H	-5.54622	0.45066	-0.92922	H	-4.70694	0.18030	-0.10905
H	-5.33975	-0.92260	0.17264	H	-4.57155	2.61798	0.50079
H	-5.98571	0.60751	0.77807	H	-2.87455	2.63631	-0.02499
H	-2.76040	2.54984	0.57070	H	-4.16511	2.34529	-1.20341
H	-4.03697	2.55645	-0.65680	H	-2.41871	0.86234	1.81810
H	-4.47067	2.64762	1.05848	H	-4.14124	0.78704	2.23123
H	3.57414	0.34996	-1.42729	H	-3.27364	-0.68801	1.78546
H	5.33941	-0.92281	-0.17320				
H	5.98548	0.60724	-0.77868				
H	5.54638	0.45034	0.92871				
H	2.76054	2.55011	-0.57035				
H	4.03737	2.55637	0.65688				
H	4.47073	2.64765	-1.05847				
<b>L2_3 Ground State</b>				<b>L2_4 Ground State</b>			
N	1.35223	0.45070	0.58940	N	1.41410	0.55096	0.19668
C	0.70272	-0.58289	0.22813	C	0.65669	-0.46167	0.05246
O	1.31601	-1.79945	0.23567	O	1.16596	-1.71207	0.23165
C	2.64070	-1.55191	0.76923	C	2.57939	-1.51521	0.48142
C	2.72626	-0.00534	0.87297	C	2.74845	0.02871	0.54313
C	-0.70274	-0.58289	-0.22814	C	-0.77822	-0.40536	-0.29830
O	-1.31605	-1.79944	-0.23564	O	-1.44495	-1.59011	-0.21963
C	-2.64073	-1.55191	-0.76924	C	-2.79957	-1.29517	-0.64112
C	-2.72628	-0.00533	-0.87298	C	-2.81220	0.24771	-0.83284
N	-1.35224	0.45069	-0.58946	N	-1.40613	0.64682	-0.64444
C	3.73250	0.64748	-0.10115	C	3.83928	0.57871	-0.39156
C	3.84443	2.15112	0.17299	C	5.21578	0.03305	0.00924
C	3.36998	0.38194	-1.56746	C	3.83350	2.11013	-0.40121
C	-3.73249	0.64750	0.10116	C	-3.73203	1.02565	0.13305
C	-3.84441	2.15114	-0.17297	C	-3.36032	0.80408	1.60296
C	-3.36992	0.38195	1.56747	C	-5.20490	0.69654	-0.13787
H	3.36922	-1.99143	0.08321	H	3.13065	-1.96999	-0.34884
				H	2.83500	-2.03269	1.40861
				H	2.98036	0.35869	1.56612
				H	-3.47709	-1.65537	0.13666
				H	-2.99221	-1.84650	-1.56573
				H	-3.10900	0.50613	-1.85656
				H	3.60043	0.22293	-1.40495

H	5.47785	0.35324	1.02583	H	4.82097	0.02455	0.06761
H	5.25492	-1.06239	-0.01755	H	4.42105	2.23791	1.12574
H	5.99193	0.40732	-0.66693	H	4.82116	2.45410	-0.58804
H	4.07341	2.50377	0.59508	H	3.13495	2.58225	-0.04316
H	4.58340	2.49519	-1.10151	H	2.55225	0.80365	-1.84579
H	2.85119	2.49361	-0.68652	H	4.26212	0.61999	-2.27740
H	-3.56716	2.08618	-0.09708	H	3.31575	-0.79319	-1.79311
H	-3.49914	-0.24148	1.90543				
H	-2.31710	1.07692	1.78655				
H	-3.99345	1.41745	2.25335	<b>L2_6 Ground State</b>			
H	-5.47133	0.87986	-1.18570	N	1.36087	-0.69702	-0.57722
H	-5.43084	-0.35363	0.08708	C	0.70772	0.33311	-0.21254
H	-5.86081	1.31074	0.48854	O	1.32619	1.54599	-0.18435
				C	2.66698	1.30172	-0.67771
				C	2.73978	-0.24312	-0.83411
<b>L2_5 Ground State</b>				C	-0.70765	0.33316	0.21238
N	-1.21558	0.63140	-0.58761	O	-1.32603	1.54608	0.18418
C	-0.62822	-0.42672	-0.19221	C	-2.66691	1.30189	0.67734
O	-1.31755	-1.60001	-0.14388	C	-2.73971	-0.24293	0.83407
C	-2.63575	-1.28907	-0.65988	N	-1.36084	-0.69692	0.57713
C	-2.61634	0.25368	-0.84950	C	3.72942	-0.95674	0.11246
C	0.78048	-0.49951	0.24829	C	3.40656	-0.71183	1.59026
O	1.32138	-1.74978	0.27360	C	5.17524	-0.57460	-0.22612
C	2.66542	-1.57024	0.78540	C	-3.72951	-0.95674	-0.11219
C	2.84253	-0.02961	0.85762	C	-3.40677	-0.71232	-1.59009
N	1.49414	0.50087	0.58061	C	-5.17526	-0.57439	0.22642
C	-3.57104	1.04423	0.07155	H	3.37020	1.71236	0.05051
C	-3.27763	0.81179	1.55751	H	2.77995	1.83670	-1.62493
C	-5.03362	0.74135	-0.27494	H	3.00630	-0.51430	-1.86265
C	3.87304	0.54434	-0.14043	H	-3.37001	1.71233	-0.05112
C	4.07647	2.04366	0.10305	H	-2.78009	1.83709	1.62441
C	3.47697	0.27320	-1.59703	H	-3.00608	-0.51388	1.86271
H	-3.37041	-1.64245	0.06730	H	3.60055	-2.02887	-0.08452
H	-2.76832	-1.83678	-1.59726	H	3.50894	0.34693	1.85957
H	-2.85693	0.51774	-1.88624	H	2.38522	-1.02623	1.82357
H	3.35757	-2.06449	0.09896	H	4.09274	-1.27788	2.22966
H	2.72002	-2.05630	1.76413	H	5.36576	0.48945	-0.03645
H	3.13651	0.28035	1.86731	H	5.88055	-1.14480	0.38809
H	-3.37689	2.10251	-0.14578	H	5.40750	-0.77431	-1.27907
H	-3.44613	-0.23293	1.84762	H	-3.60071	-2.02883	0.08510
H	-2.24150	1.06929	1.79538	H	-3.50912	0.34636	-1.85974
H	-3.93452	1.43149	2.17762	H	-2.38547	-1.02685	-1.82340
H	-5.28870	-0.30553	-0.06656	H	-4.09305	-1.27853	-2.22926
H	-5.70972	1.36452	0.32036	H	-5.36573	0.48962	0.03644
H	-5.24355	0.93314	-1.33404	H	-5.88068	-1.14473	-0.38753

H -5.40742 -0.77375 1.27947



**L6\_1 Ground State**

N -1.45309 -0.22565 -0.20304  
 C -0.72462 -1.26877 -0.14542  
 O -1.28123 -2.48785 -0.36958  
 C -2.70242 -2.23436 -0.51280  
 C -2.80790 -0.68519 -0.55568  
 C 0.72458 -1.26880 0.14511  
 O 1.28113 -2.48791 0.36928  
 C 2.70235 -2.23448 0.51236  
 C 2.80787 -0.68533 0.55543  
 N 1.45309 -0.22571 0.20274  
 C -3.89183 -0.12113 0.38854  
 C -5.20734 -0.83487 0.10834  
 C -4.06566 1.39620 0.32699  
 C 3.89189 -0.12120 -0.38861  
 C 5.20740 -0.83487 -0.10822  
 C 4.06564 1.39613 -0.32704  
 C -5.74132 -1.74936 1.02117  
 C -6.92868 -2.43003 0.74173  
 C -7.59591 -2.20371 -0.46087  
 C -7.07340 -1.28824 -1.37834  
 C -5.89182 -0.60821 -1.09370  
 C -5.13883 1.96816 1.02714  
 C -5.35737 3.34271 1.01148  
 C -4.50648 4.17783 0.28402  
 C -3.43657 3.62147 -0.41306  
 C -3.21308 2.24221 -0.39031  
 C 5.13866 1.96814 -1.02738  
 C 5.35720 3.34269 -1.01168  
 C 4.50645 4.17775 -0.28399  
 C 3.43669 3.62135 0.41328  
 C 3.21321 2.24209 0.39050  
 C 5.89177 -0.60803 1.09385  
 C 7.07334 -1.28799 1.37868  
 C 7.59596 -2.20356 0.46136  
 C 6.92884 -2.43006 -0.74126  
 C 5.74149 -1.74944 -1.02090  
 H -3.21078 -2.67269 0.35090  
 H -3.04918 -2.73025 -1.42035  
 H -3.02658 -0.33881 -1.57395

H 3.21059 -2.67268 -0.35148

H 3.04922 -2.73052 1.41979

H 3.02646 -0.33908 1.57377

H -3.57648 -0.38593 1.40747

H 3.57672 -0.38601 -1.40760

H -5.22545 -1.92551 1.96219

H -7.33018 -3.13392 1.46543

H -8.51961 -2.73105 -0.68141

H -7.59197 -1.09993 -2.31436

H -5.50239 0.12183 -1.79814

H -5.81640 1.32298 1.57980

H -6.19525 3.76153 1.56238

H -4.67600 5.25088 0.26528

H -2.76139 4.26027 -0.97599

H -2.34944 1.83637 -0.90163

H 5.81612 1.32299 -1.58022

H 6.19496 3.76156 -1.56273

H 4.67596 5.25081 -0.26522

H 2.76162 4.26011 0.97638

H 2.34968 1.83621 0.90197

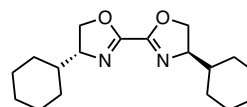
H 5.50226 0.12209 1.79816

H 7.59183 -1.09955 2.31471

H 8.51965 -2.73085 0.68205

H 7.33042 -3.13402 -1.46485

H 5.22570 -1.92572 -1.96194



**L4\_1 Ground State**

N 1.18470 -0.15939 0.87980  
 C 0.63706 -1.19140 0.37411  
 O 1.24573 -2.40399 0.49592  
 C 2.42247 -2.15693 1.30545  
 C 2.47156 -0.61123 1.44358  
 C -0.63692 -1.19138 -0.37413  
 O -1.24548 -2.40399 -0.49621  
 C -2.42238 -2.15683 -1.30549  
 C -2.47146 -0.61112 -1.44350  
 N -1.18467 -0.15930 -0.87957  
 C 3.65521 0.05839 0.71671  
 C -3.65521 0.05839 -0.71671  
 C -3.63211 -0.18345 0.80188  
 C -4.82580 0.48514 1.49619  
 C -4.87485 1.98778 1.19204

C	-4.89302	2.24382	-0.32040	C	-2.80090	-2.27880	-1.00849
C	-3.70709	1.56476	-1.01730	C	-2.87691	-0.76298	-1.33746
C	3.63203	-0.18334	-0.80190	N	-1.53312	-0.25418	-1.00309
C	4.82566	0.48531	-1.49624	C	3.58299	0.09913	0.04635
C	4.87466	1.98794	-1.19202	C	-3.96622	0.00570	-0.56288
C	4.89290	2.24390	0.32043	C	-3.75054	-0.03279	0.95924
C	3.70706	1.56474	1.01738	C	-4.85314	0.73157	1.70355
H	3.28492	-2.58319	0.78706	C	-4.95340	2.18091	1.21141
H	2.28612	-2.67050	2.26193	C	-5.16402	2.23408	-0.30718
H	2.50948	-0.31645	2.49903	C	-4.06921	1.45921	-1.05162
H	-2.28625	-2.67036	-2.26202	C	3.48722	1.62438	-0.11011
H	-3.28474	-2.58308	-0.78694	C	4.66846	2.18606	-0.91099
H	-2.50926	-0.31625	-2.49894	C	6.01175	1.78866	-0.28561
H	4.57049	-0.40247	1.12415	C	6.11552	0.26695	-0.12174
H	-4.57043	-0.40249	-1.12424	C	4.93042	-0.29254	0.67680
H	-3.62345	-1.25838	1.02414	H	3.05691	-2.48486	0.21197
H	-2.69858	0.22861	1.20550	H	2.48436	-2.44007	1.90007
H	-4.77193	0.31608	2.57874	H	2.46420	-0.04074	1.87432
H	-5.75873	0.01530	1.15094	H	-2.80047	-2.91353	-1.89963
H	-3.98910	2.47118	1.62857	H	-3.57901	-2.62233	-0.32216
H	-5.75145	2.44526	1.66741	H	-3.04827	-0.60666	-2.40931
H	-4.88236	3.32145	-0.52542	H	3.52679	-0.35189	-0.95750
H	-5.83239	1.85400	-0.74010	H	-4.92115	-0.49810	-0.78748
H	-2.76596	2.01774	-0.68123	H	-3.70462	-1.06874	1.31936
H	-3.76323	1.72451	-2.10244	H	-2.77718	0.42155	1.18365
H	3.62338	-1.25826	-1.02425	H	-4.66206	0.70712	2.78351
H	2.69847	0.22872	-1.20545	H	-5.81790	0.22759	1.54380
H	4.77174	0.31630	-2.57878	H	-4.02411	2.71098	1.46494
H	5.75862	0.01549	-1.15104	H	-5.76723	2.70440	1.72847
H	3.98887	2.47131	-1.62848	H	-5.18900	3.27485	-0.65302
H	5.75121	2.44546	-1.66742	H	-6.14521	1.79936	-0.54974
H	4.88221	3.32152	0.52550	H	-3.09733	1.94541	-0.90012
H	5.83233	1.85411	0.74006	H	-4.26304	1.47386	-2.13254
H	2.76589	2.01771	0.68141	H	2.53418	1.88286	-0.58009
H	3.76327	1.72443	2.10252	H	3.47769	2.08092	0.89163
				H	4.58871	3.27776	-0.98178
				H	4.62182	1.80186	-1.94050
				H	6.10440	2.26387	0.70202
				H	6.84469	2.16274	-0.89376
				H	7.05923	-0.00297	0.36820
				H	6.13185	-0.20322	-1.11567
				H	4.96616	0.10145	1.70398
				H	5.01918	-1.38403	0.75801
<b>L4_2 Ground State</b>							
N	1.10770	-0.06771	0.28520				
C	0.45244	-1.14405	0.10650				
O	1.01141	-2.33652	0.45302				
C	2.35023	-2.01371	0.90347				
C	2.40765	-0.46065	0.86006				
C	-0.91167	-1.22194	-0.45721				
O	-1.52011	-2.43614	-0.34926				

**L4\_3 Ground State**

N	1.40962	-0.02397	0.42069
C	0.70517	-1.06523	0.22206
O	1.25229	-2.29549	0.42874
C	2.63817	-2.04358	0.76733
C	2.73621	-0.49532	0.85972
C	-0.70491	-1.06516	-0.22181
O	-1.25188	-2.29534	-0.42941
C	-2.63791	-2.04333	-0.76729
C	-2.73595	-0.49506	-0.85930
N	-1.40949	-0.02385	-0.41971
C	3.86632	0.11106	0.01680
C	-3.86637	0.11106	-0.01665
C	-3.80891	1.64614	-0.01363
C	-4.94700	2.25321	0.81610
C	-6.31825	1.76325	0.33327
C	-6.38461	0.23072	0.32356
C	-5.24248	-0.37421	-0.50394
C	3.80867	1.64613	0.01396
C	4.94644	2.25342	-0.81605
C	6.31790	1.76359	-0.33370
C	6.38444	0.23106	-0.32416
C	5.24263	-0.37409	0.50364
H	3.25870	-2.46051	-0.03353
H	2.85885	-2.56489	1.70119
H	2.87604	-0.17181	1.90118
H	-2.85907	-2.56448	-1.70111
H	-3.25808	-2.46034	0.03383
H	-2.87538	-0.17129	-1.90073
H	3.72283	-0.23883	-1.01823
H	-3.72315	-0.23891	1.01838
H	-2.83326	1.97308	0.35690
H	-3.88618	2.00324	-1.05212
H	-4.89760	3.34828	0.77658
H	-4.81435	1.97220	1.87115
H	-6.49670	2.13748	-0.68552
H	-7.11698	2.17392	0.96332
H	-7.35188	-0.10923	-0.06670
H	-6.31455	-0.14051	1.35630
H	-5.36488	-0.08402	-1.55865
H	-5.30130	-1.47030	-0.47297
H	2.83288	1.97299	-0.35623
H	3.88621	2.00312	1.05247
H	4.89691	3.34848	-0.77639

H	4.81350	1.97251	-1.87109
H	6.49662	2.13773	0.68508
H	7.11637	2.17441	-0.96395
H	7.35187	-0.10882	0.06577
H	6.31411	-0.14008	-1.35691
H	5.36531	-0.08397	1.55833
H	5.30159	-1.47017	0.47257

**L4\_4 Ground State**

N	-1.30701	-0.08605	0.28971
C	-0.57342	0.94212	0.13384
O	-1.04470	2.16591	0.50166
C	-2.40603	1.93420	0.94058
C	-2.57704	0.39067	0.86808
C	0.79494	0.93078	-0.42487
O	1.50201	2.08332	-0.26110
C	2.76799	1.85123	-0.92692
C	2.71779	0.35023	-1.32755
N	1.33622	-0.05948	-1.01424
C	-3.78670	-0.06668	0.04078
C	3.72610	-0.56270	-0.60324
C	5.17229	-0.23460	-1.00873
C	6.17715	-1.17363	-0.32784
C	6.01308	-1.15433	1.19742
C	4.57143	-1.48789	1.60204
C	3.56532	-0.54755	0.92501
C	-3.80200	-1.59181	-0.14279
C	-5.01757	-2.05148	-0.95722
C	-6.33101	-1.56821	-0.32895
C	-6.32406	-0.04614	-0.13806
C	-5.10472	0.41116	0.67398
H	-3.07255	2.46846	0.25508
H	-2.51396	2.35108	1.94434
H	-2.66843	-0.04246	1.87420
H	2.82393	2.52384	-1.78775
H	3.56583	2.10239	-0.22465
H	2.87700	0.23445	-2.40645
H	-3.69323	0.39679	-0.95457
H	3.50207	-1.58304	-0.94609
H	5.27696	-0.29122	-2.10053
H	5.40784	0.80226	-0.72489
H	7.20114	-0.89648	-0.60726
H	6.01658	-2.19749	-0.69493
H	6.27207	-0.15413	1.57533



H	6.71408	-1.85732	1.66408	H	-2.75492	0.43907	2.46212
H	4.45880	-1.43669	2.69192	H	3.15922	-1.72173	-0.68421
H	4.34590	-2.52409	1.31159	H	-4.76031	0.60924	1.01160
H	3.72126	0.47255	1.30617	H	-3.67959	1.25497	-1.14708
H	2.54066	-0.83150	1.18694	H	-2.87290	-0.30868	-1.20752
H	-2.86835	-1.91095	-0.61439	H	-4.90142	-0.31570	-2.64877
H	-3.83017	-2.06547	0.85062	H	-5.90596	0.14905	-1.27845
H	-5.01734	-3.14467	-1.04734	H	-4.32750	-2.46401	-1.54632
H	-4.93856	-1.65360	-1.97952	H	-6.07976	-2.30086	-1.65157
H	-6.46245	-2.05282	0.64968	H	-5.35625	-3.10733	0.61932
H	-7.18638	-1.86956	-0.94629	H	-6.18918	-1.55820	0.71254
H	-7.24765	0.28336	0.35380	H	-3.14615	-1.96939	0.77633
H	-6.30176	0.44150	-1.12343	H	-4.16106	-1.51143	2.14039
H	-5.17361	0.00282	1.69384	H	4.80076	-0.70790	-2.24230
H	-5.11398	1.50463	0.77438	H	5.08493	0.61812	-1.11717

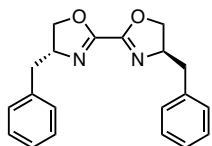
**L4\_5 Ground State**

N	1.00394	-0.18812	-0.80045
C	0.53969	0.90323	-0.33766
O	1.26422	2.04938	-0.46432
C	2.44063	1.67315	-1.22303
C	2.34375	0.12589	-1.33203
C	-0.75346	1.04330	0.36323
O	-1.26532	2.30537	0.40042
C	-2.48640	2.19605	1.17367
C	-2.66226	0.66913	1.39401
N	-1.39912	0.08690	0.90055
C	3.42276	-0.66119	-0.56311
C	-3.87328	0.05320	0.66495
C	-3.78244	0.19955	-0.86322
C	-5.00367	-0.41347	-1.56094
C	-5.18452	-1.88615	-1.17169
C	-5.27197	-2.04688	0.35136
C	-4.05738	-1.42319	1.05059
C	4.81664	-0.44758	-1.17545
C	5.88754	-1.26727	-0.44301
C	5.89170	-0.96216	1.06050
C	4.50232	-1.18190	1.67248
C	3.43023	-0.36042	0.94402
H	3.31723	2.03159	-0.67924
H	2.39030	2.17582	-2.19330
H	2.38293	-0.18933	-2.38158
H	-3.29334	2.65610	0.59785
H	-2.34521	2.75229	2.10522

**L4\_6 Ground State**

N	1.22332	-0.83137	0.34286
C	0.65477	-0.34455	-0.68694
O	1.27325	-0.42622	-1.89774
C	2.48750	-1.17910	-1.65383
C	2.53595	-1.33136	-0.10806
C	-0.65445	0.34038	-0.68855
O	-1.27275	0.41672	-1.89978
C	-2.48702	1.17070	-1.65939
C	-2.53547	1.33022	-0.11434
N	-1.22306	0.83188	0.33899
C	3.67158	-0.56480	0.59758
C	-3.67149	0.56755	0.59486
C	-5.04836	1.14945	0.23564
C	-6.17944	0.42446	0.97746
C	-6.13467	-1.08753	0.72132
C	-4.76274	-1.66900	1.08584
C	-3.63050	-0.94787	0.34232
C	5.04876	-1.14774	0.24125
C	6.17942	-0.41866	0.97970

C	6.13395	1.09207	0.71634
C	4.76171	1.67461	1.07796
C	3.62989	0.94939	0.33780
H	3.32113	-0.61436	-2.07657
H	2.40101	-2.13612	-2.17672
H	2.61977	-2.38809	0.17250
H	-3.32065	0.60395	-2.07945
H	-2.40058	2.12524	-2.18679
H	-2.61884	2.38831	0.16123
H	3.50816	-0.71720	1.67410
H	-3.50808	0.72502	1.67066
H	-5.07137	2.22389	0.46201
H	-5.21703	1.05401	-0.84768
H	-7.15116	0.83599	0.67773
H	-6.07763	0.61065	2.05626
H	-6.33703	-1.27910	-0.34294
H	-6.92719	-1.59251	1.28728
H	-4.73213	-2.74311	0.86573
H	-4.60352	-1.56602	2.16888
H	-3.72906	-1.14883	-0.73476
H	-2.65750	-1.34352	0.65189
H	5.07228	-2.22108	0.47276
H	5.21749	-1.05740	-0.84249
H	7.15137	-0.83115	0.68204
H	6.07761	-0.59974	2.05937
H	6.33631	1.27865	-0.34881
H	6.92618	1.60013	1.27994
H	4.73060	2.74764	0.85271
H	4.60245	1.57673	2.16146
H	3.72845	1.14522	-0.74024
H	2.65668	1.34605	0.64538

**L7\_1 Ground State**

N	-1.31984	-1.23190	-0.62715
C	-0.71896	-2.24630	-0.14872
O	-1.42758	-3.36644	0.15732
C	-2.78362	-3.07291	-0.28292
C	-2.75681	-1.55031	-0.57268
C	0.72639	-2.24484	0.14980
O	1.43770	-3.36259	-0.15896

C	2.79290	-3.06684	0.28248
C	2.76280	-1.54462	0.57321
N	1.32504	-1.22993	0.62995
C	-3.41269	-0.71280	0.54835
C	3.41450	-0.70497	-0.54873
C	3.22245	0.78431	-0.38081
C	-3.22523	0.77708	0.38053
C	2.00768	1.39282	-0.72852
C	1.82872	2.76389	-0.55655
C	2.85723	3.54889	-0.02965
C	4.06728	2.95254	0.32321
C	4.24556	1.57926	0.14575
C	-2.01261	1.38942	0.72900
C	-1.83785	2.76105	0.55710
C	-2.86848	3.54278	0.02949
C	-4.07641	2.94260	-0.32414
C	-4.25049	1.56879	-0.14675
H	-3.46520	-3.36187	0.52052
H	-2.98606	-3.67718	-1.17292
H	-3.22370	-1.30490	-1.53150
H	2.99568	-3.67114	1.17241
H	3.47562	-3.35415	-0.52054
H	3.23068	-1.29848	1.53134
H	-2.98014	-1.04180	1.50222
H	-4.48157	-0.95951	0.57771
H	4.48412	-0.94826	-0.57947
H	2.98173	-1.03544	-1.50199
H	1.19359	0.78678	-1.11278
H	0.88162	3.21672	-0.83548
H	2.71658	4.61835	0.10182
H	4.87500	3.55416	0.73132
H	5.19402	1.11953	0.41601
H	-1.19690	0.78590	1.11379
H	-0.89239	3.21688	0.83666
H	-2.73112	4.61267	-0.10193
H	-4.88574	3.54168	-0.73283
H	-5.19731	1.10605	-0.41762

**L7\_2 Ground State**

N	1.88389	-0.64863	0.31201
C	0.93809	-1.44732	0.01601
O	1.18905	-2.78230	-0.07600
C	2.60560	-2.92418	0.19523
C	3.09876	-1.47058	0.44384

C	-0.45656	-1.04056	-0.25654	C	1.26906	2.60620	-1.60420
O	-1.36797	-2.05054	-0.27507	C	1.88821	1.27173	-1.10062
C	-2.62869	-1.42105	-0.62104	C	-1.32700	1.38119	0.61094
C	-2.30221	0.09645	-0.62165	O	-2.44879	1.93798	0.08562
N	-0.83867	0.15707	-0.46373	C	-3.50090	1.63078	1.03720
C	4.18211	-1.02173	-0.55617	C	-2.83611	0.62652	2.01272
C	-2.98498	0.88301	0.51563	N	-1.40043	0.71447	1.69376
C	-4.48805	0.90018	0.37435	C	3.20792	1.46745	-0.32883
C	4.77320	0.33553	-0.25320	C	-3.30870	-0.83911	1.83811
C	-5.09934	1.68560	-0.61277	C	-3.19140	-1.34497	0.41959
C	-6.48235	1.67170	-0.78319	C	3.86144	0.17155	0.09014
C	-7.28128	0.86846	0.03368	C	-4.32554	-1.45274	-0.39474
C	-6.68633	0.08464	1.02160	C	-4.21997	-1.86712	-1.72314
C	-5.30041	0.10219	1.18827	C	-2.97045	-2.17970	-2.25779
C	4.01640	1.50547	-0.41023	C	-1.83270	-2.08160	-1.45440
C	4.56960	2.74983	-0.11406	C	-1.94096	-1.67295	-0.12632
C	5.88569	2.84769	0.34306	C	3.32767	-0.60112	1.13111
C	6.64576	1.69006	0.50467	C	3.92572	-1.80587	1.49564
C	6.08975	0.44475	0.20800	C	5.06534	-2.25923	0.82744
H	3.06992	-3.39196	-0.67885	C	5.60280	-1.49904	-0.21054
H	2.72062	-3.58195	1.06068	C	5.00216	-0.29270	-0.57381
H	3.49085	-1.34801	1.46009	H	1.85872	3.48641	-1.33026
H	-2.93712	-1.79901	-1.59980	H	1.07395	2.62087	-2.67974
H	-3.37121	-1.71181	0.12546	H	2.06721	0.57504	-1.92735
H	-2.57499	0.55873	-1.57641	H	-3.79935	2.56539	1.52221
H	3.73639	-1.03688	-1.55946	H	-4.34160	1.21779	0.47680
H	4.97888	-1.77644	-0.55058	H	-2.99469	0.91544	3.05681
H	-2.69550	0.43109	1.47159	H	2.99380	2.09496	0.54605
H	-2.57788	1.89994	0.50645	H	3.89372	2.03559	-0.97016
H	-4.48340	2.31809	-1.24821	H	-2.70837	-1.45451	2.51694
H	-6.93824	2.29087	-1.55091	H	-4.35087	-0.90375	2.17466
H	-8.35959	0.85822	-0.09713	H	-5.30360	-1.21619	0.01913
H	-7.29952	-0.53902	1.66624	H	-5.11288	-1.94613	-2.33732
H	-4.84247	-0.50362	1.96672	H	-2.88390	-2.50054	-3.29226
H	2.98636	1.42962	-0.74162	H	-0.85408	-2.32217	-1.86026
H	3.96955	3.64706	-0.23923	H	-1.04837	-1.58333	0.48344
H	6.31453	3.81960	0.57136	H	2.42913	-0.26216	1.63572
H	7.67112	1.75378	0.85896	H	3.49966	-2.39376	2.30411
H	6.68810	-0.45536	0.33222	H	5.53071	-3.19795	1.11520
				H	6.49025	-1.84108	-0.73621
				H	5.42751	0.29914	-1.38157
<b>L7_3 Ground State</b>							
N	0.85067	0.69961	-0.22517				
C	-0.09395	1.55164	-0.18294	<b>L7_4 Ground State</b>			
O	-0.00553	2.69289	-0.91680	N	1.42175	-0.86883	-0.38294

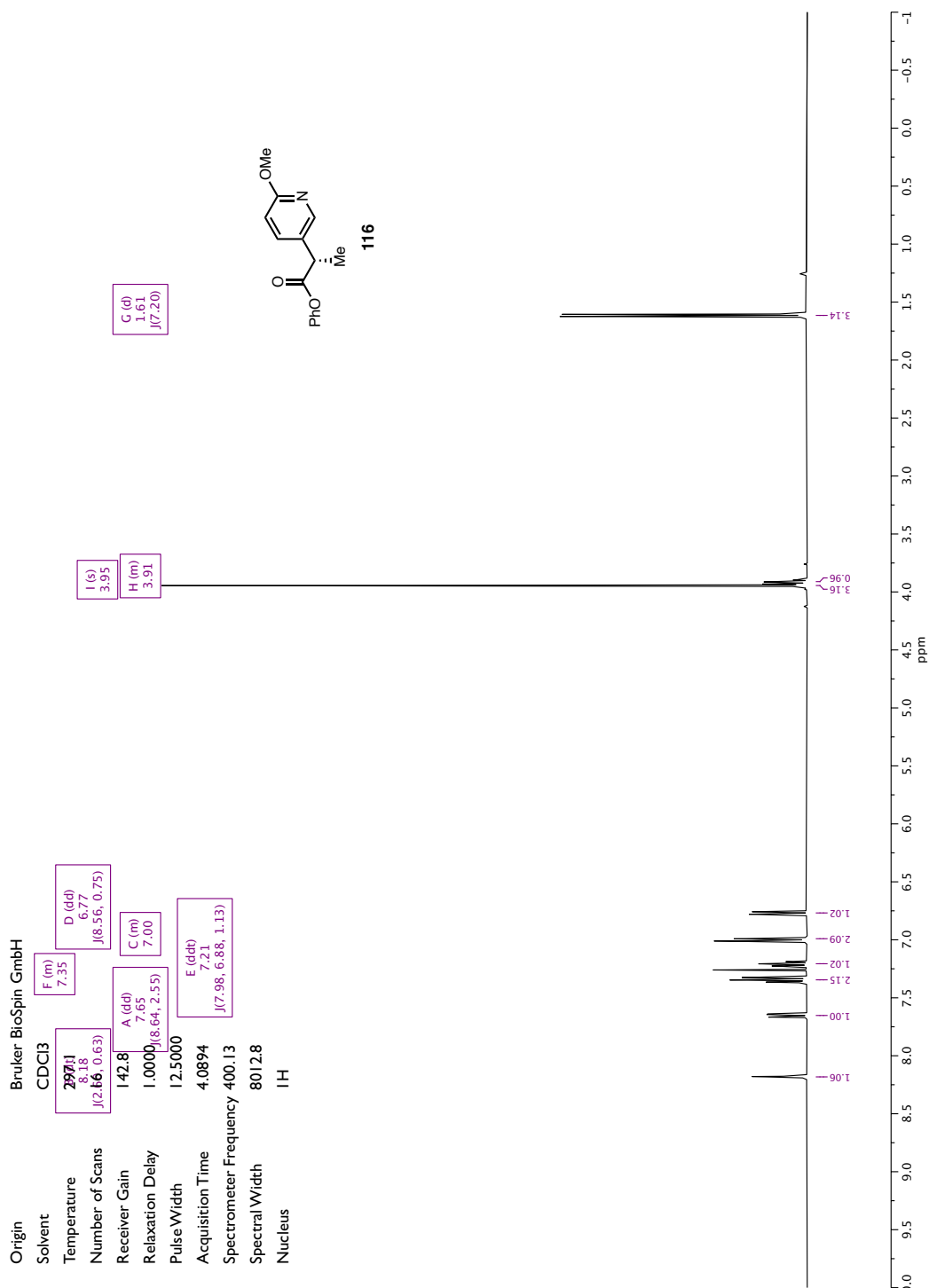
C	0.72154	0.17223	-0.16081
O	1.30912	1.39939	-0.20641
C	2.68371	1.15096	-0.59667
C	2.80138	-0.39670	-0.58998
C	-0.72153	0.17223	0.16075
O	-1.30910	1.39938	0.20639
C	-2.68370	1.15095	0.59660
C	-2.80136	-0.39671	0.58993
N	-1.42174	-0.86883	0.38286
C	3.71696	-0.94902	0.52135
C	-3.71698	-0.94904	-0.52137
C	-5.15807	-0.54252	-0.32802
C	5.15806	-0.54251	0.32804
C	-5.73917	0.45910	-1.11431
C	-7.05744	0.86538	-0.89984
C	-7.81589	0.27274	0.10905
C	-7.24906	-0.73012	0.89882
C	-5.93269	-1.13203	0.68067
C	5.73914	0.45913	1.11432
C	7.05741	0.86540	0.89988
C	7.81590	0.27273	-0.10896
C	7.24909	-0.73015	-0.89873
C	5.93271	-1.13205	-0.68061
H	3.33806	1.64597	0.12450
H	2.83972	1.59342	-1.58460
H	3.16238	-0.76962	-1.55458
H	-3.33804	1.64595	-0.12461
H	-2.83976	1.59343	1.58452
H	-3.16234	-0.76962	1.55454
H	3.61355	-2.03955	0.52454
H	3.34435	-0.58925	1.48763
H	-3.61358	-2.03958	-0.52455
H	-3.34440	-0.58929	-1.48767
H	-5.15524	0.91791	-1.90880
H	-7.49099	1.64220	-1.52362
H	-8.84249	0.58555	0.27708
H	-7.83507	-1.20209	1.68270
H	-5.49915	-1.91784	1.29527
H	5.15519	0.91795	1.90879
H	7.49095	1.64223	1.52367
H	8.84250	0.58553	-0.27697
H	7.83512	-1.20213	-1.68258
H	5.49918	-1.91787	-1.29521

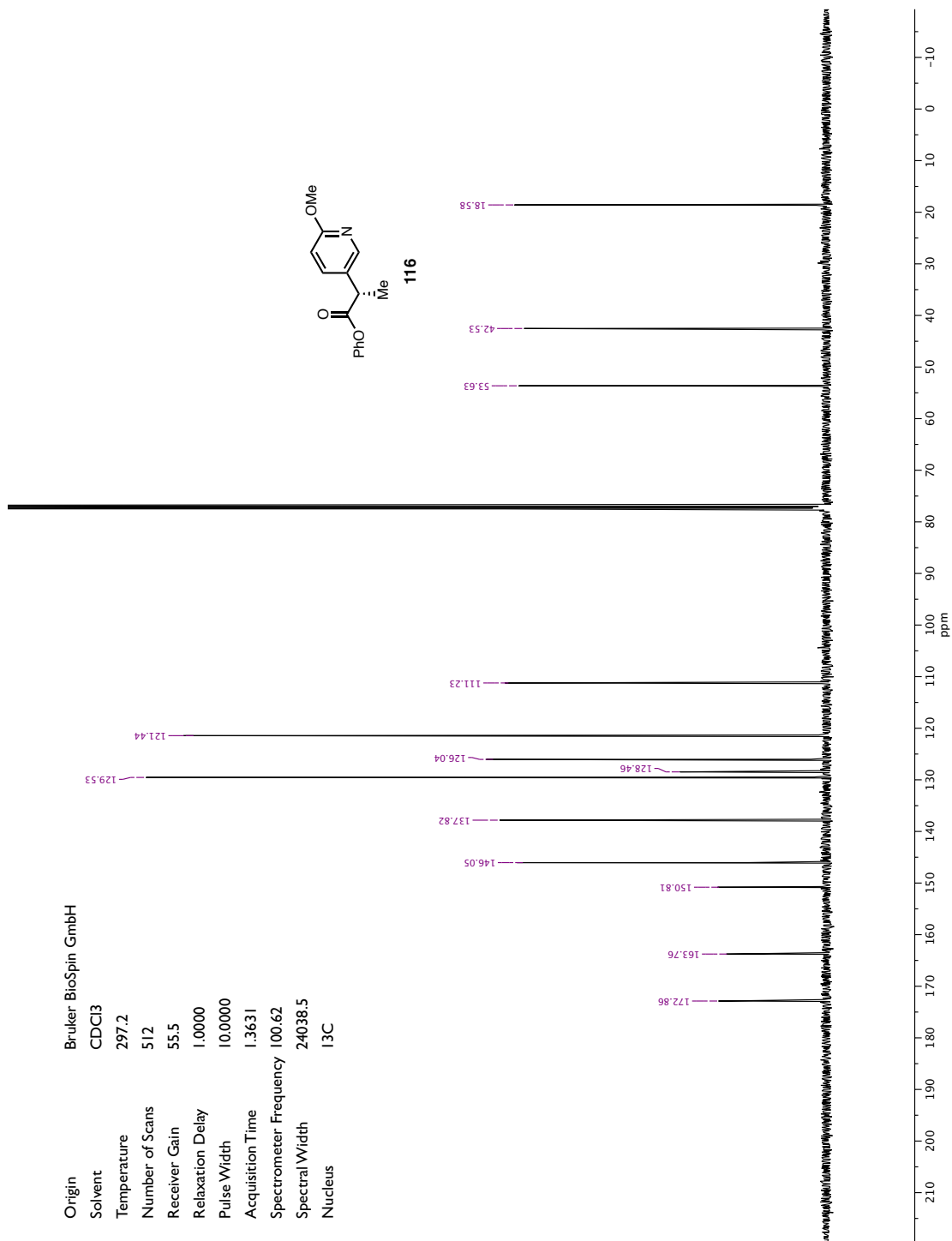
## ***Appendix 3***

*Spectra Relevant to Chapter 2:*

*Nickel-Catalyzed Asymmetric Reductive Cross-Coupling of  $\alpha$ -*

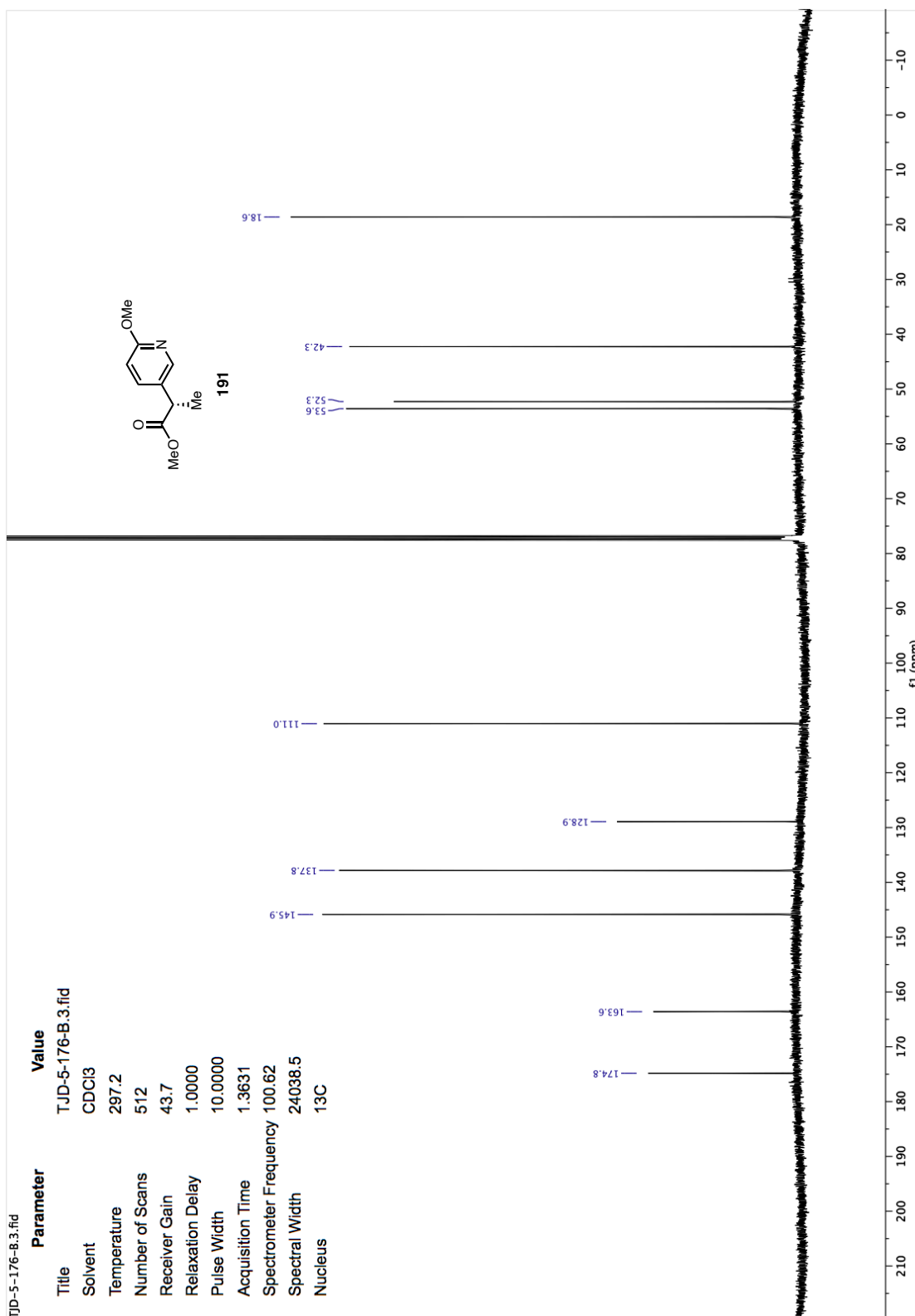
*Chloroesters with Aryl Iodides*

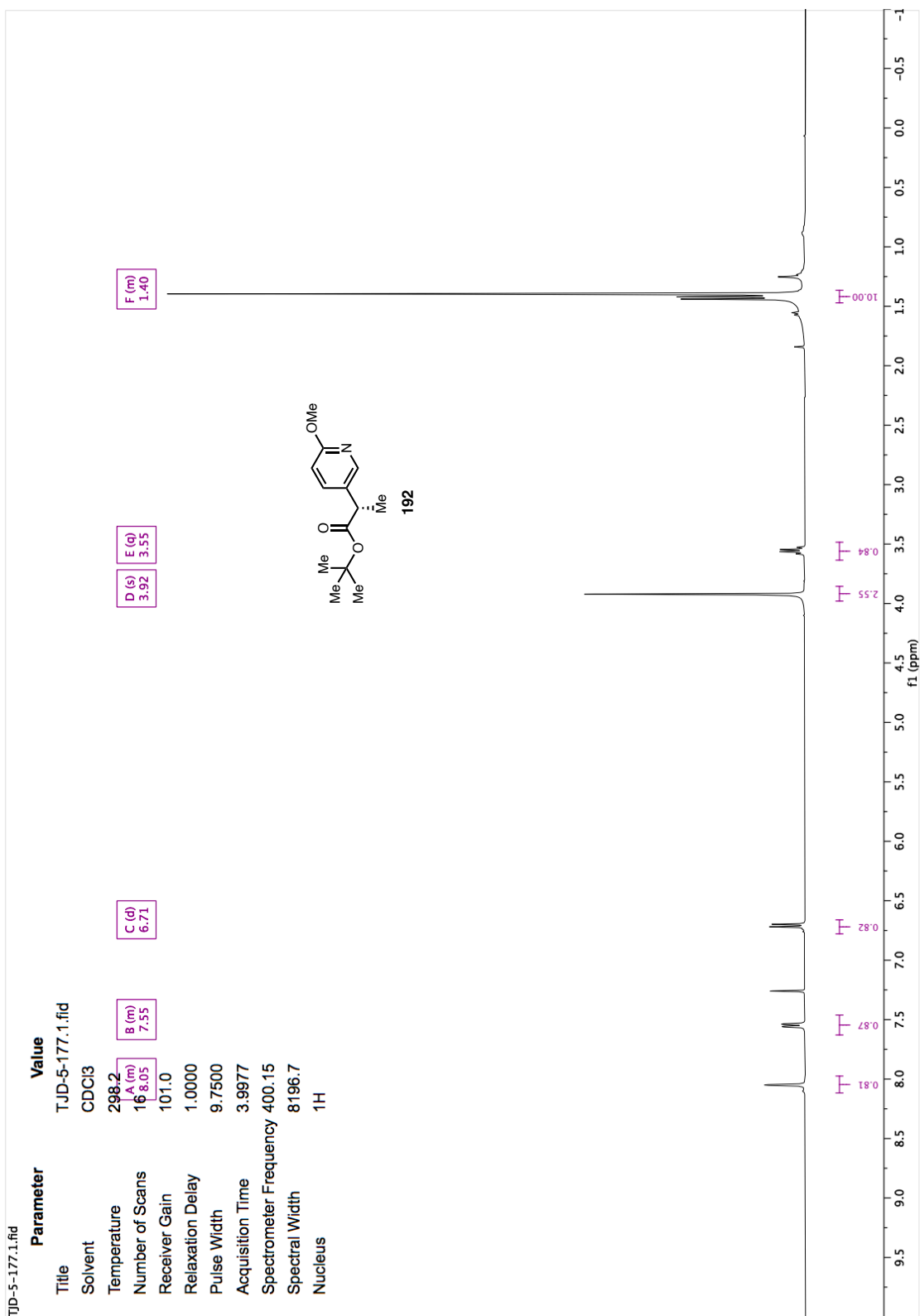


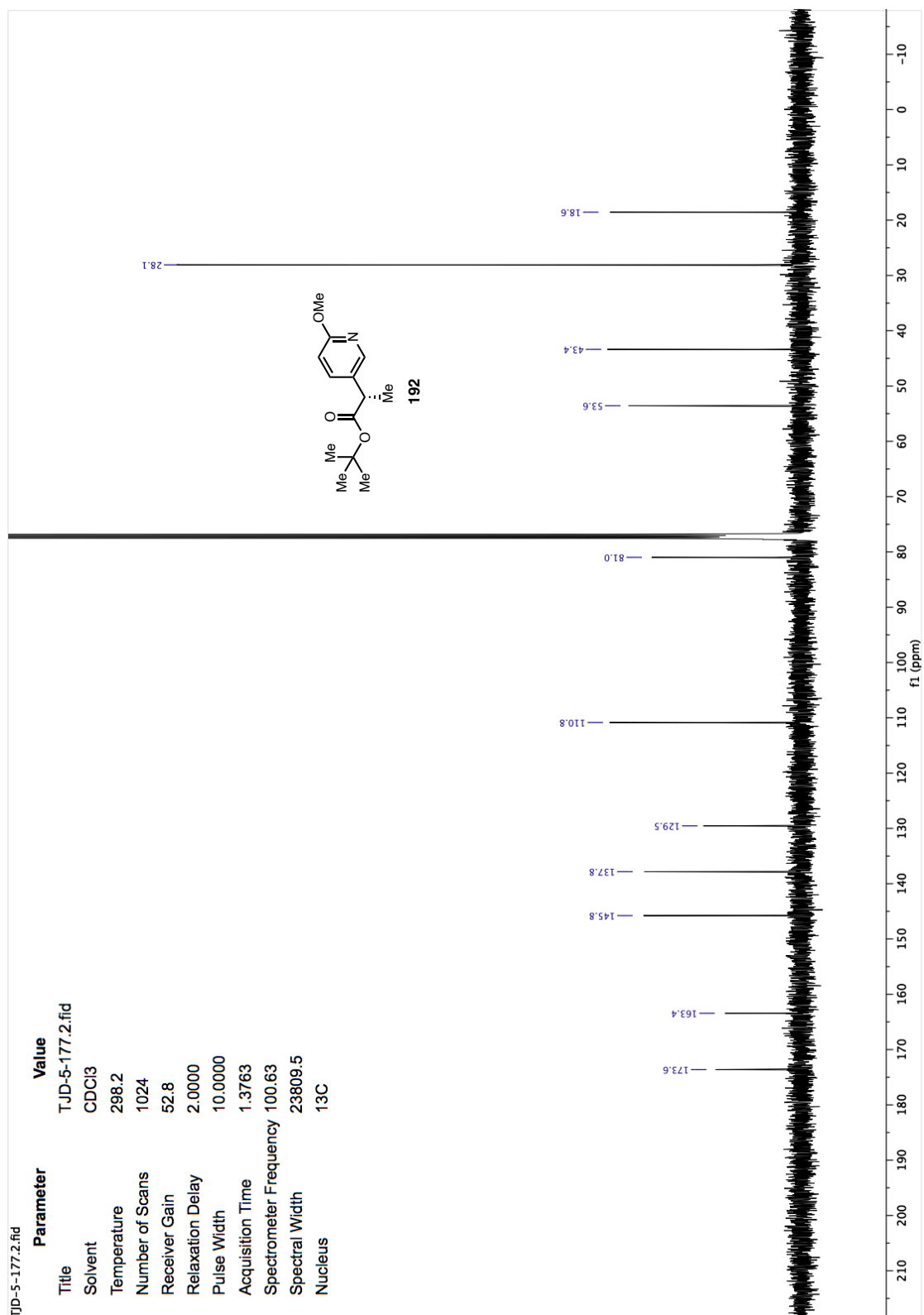


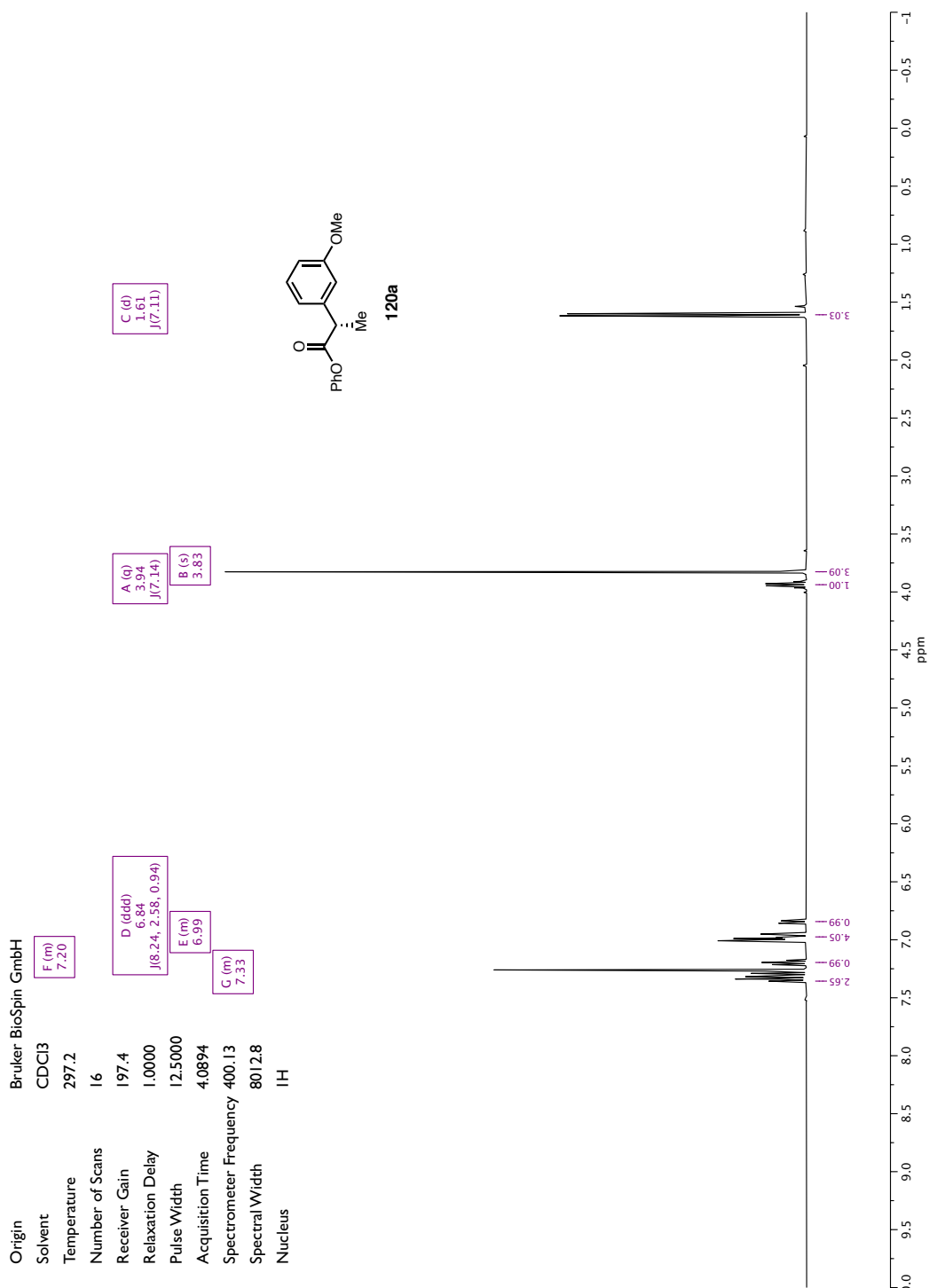


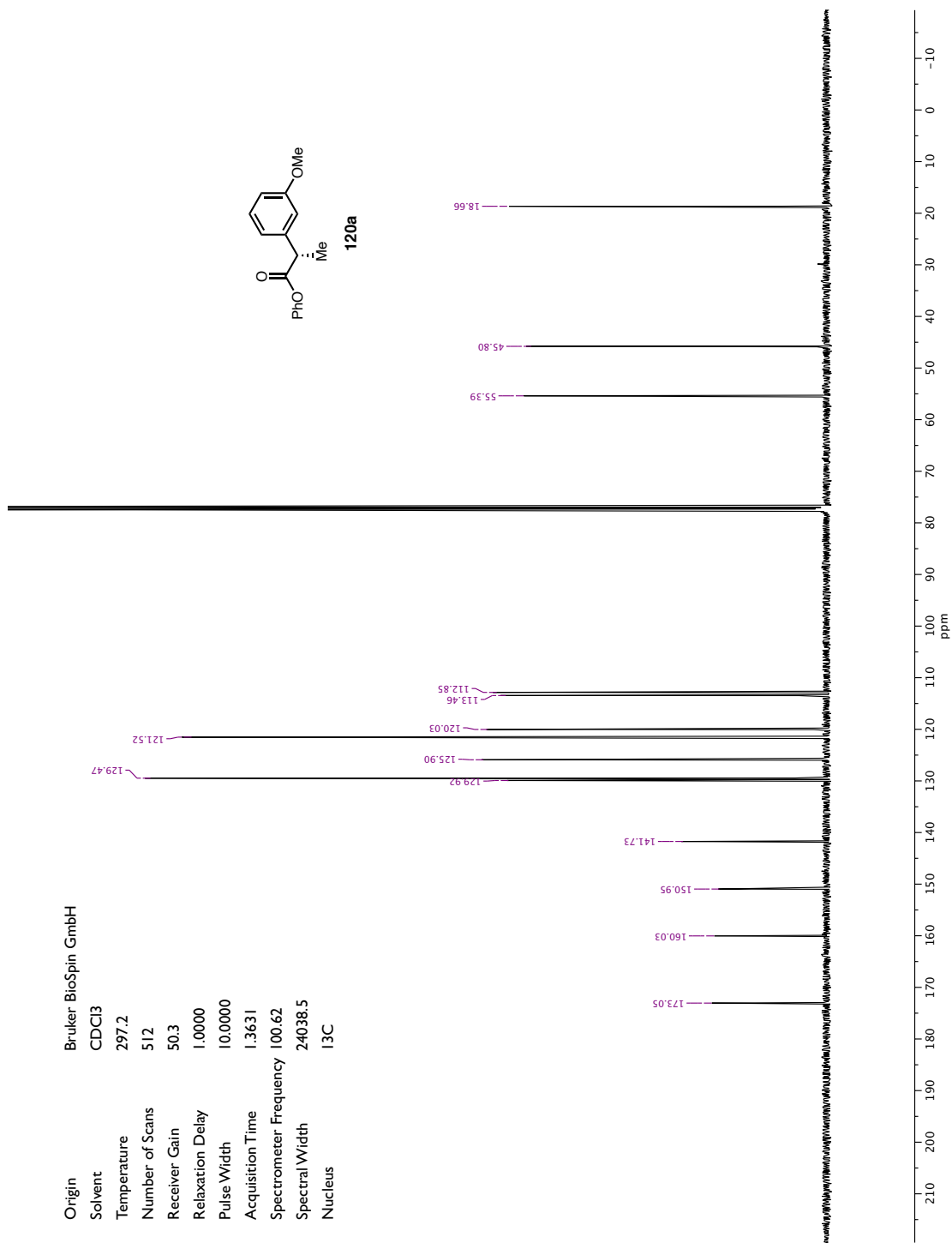


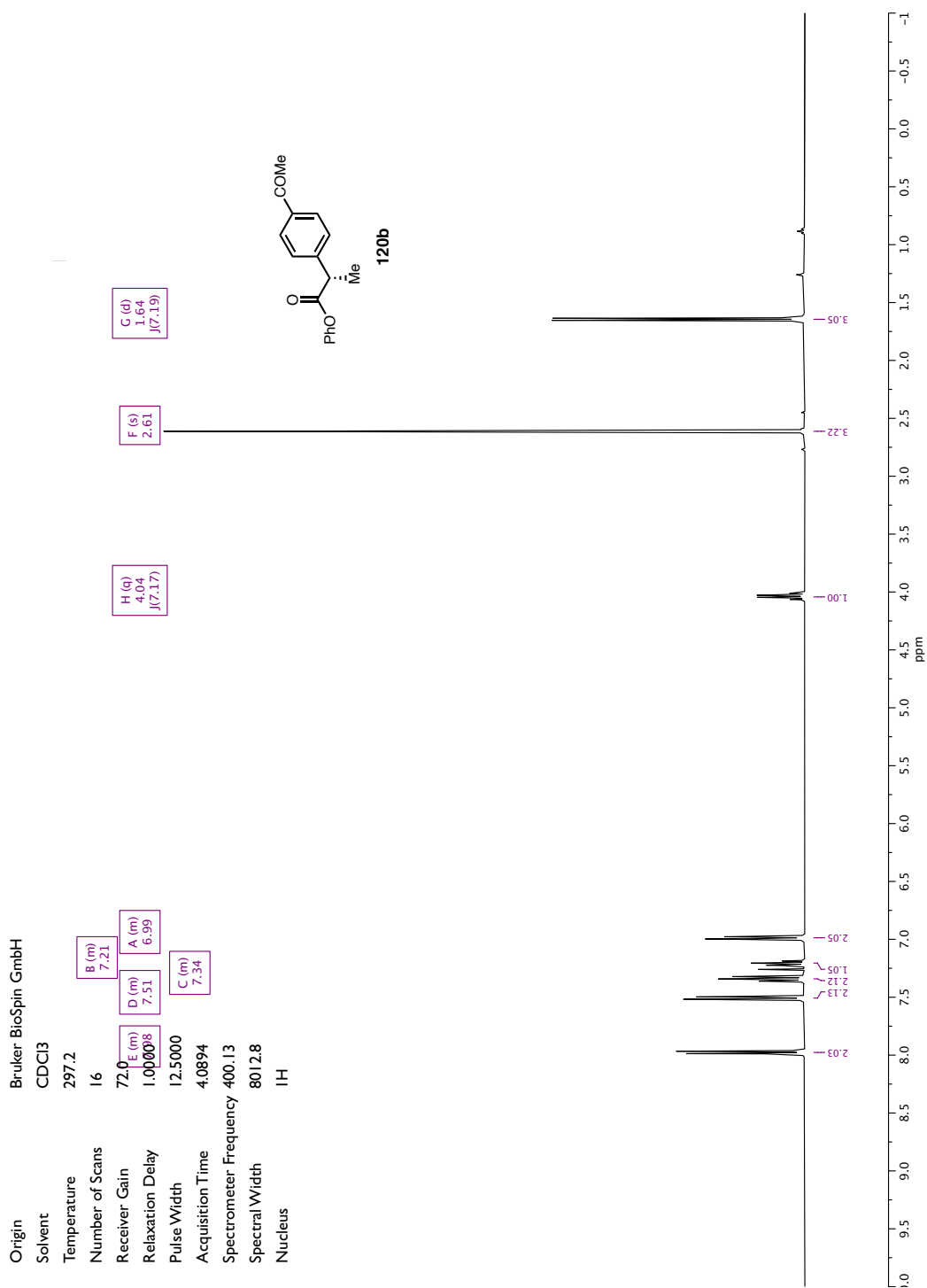


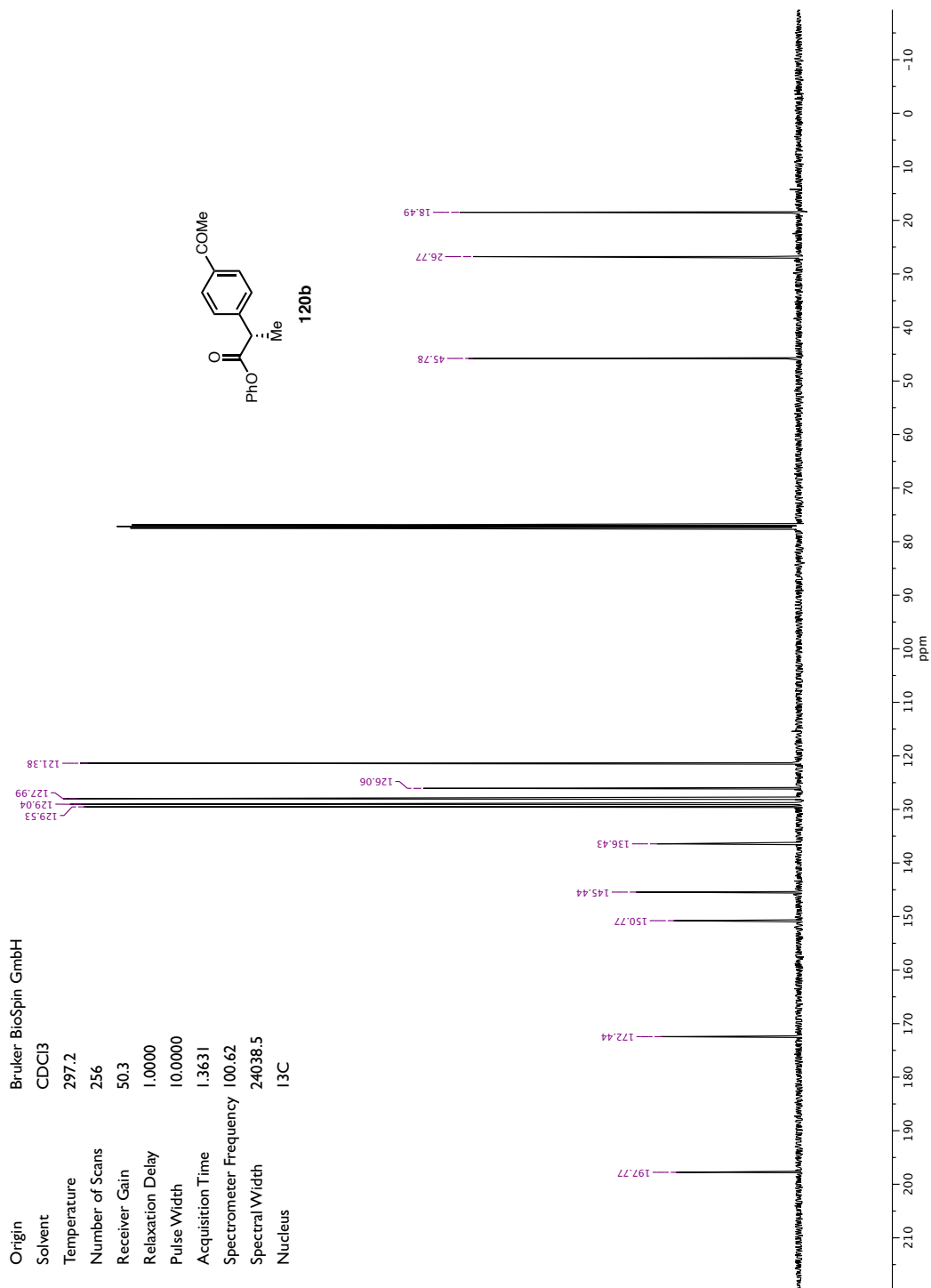


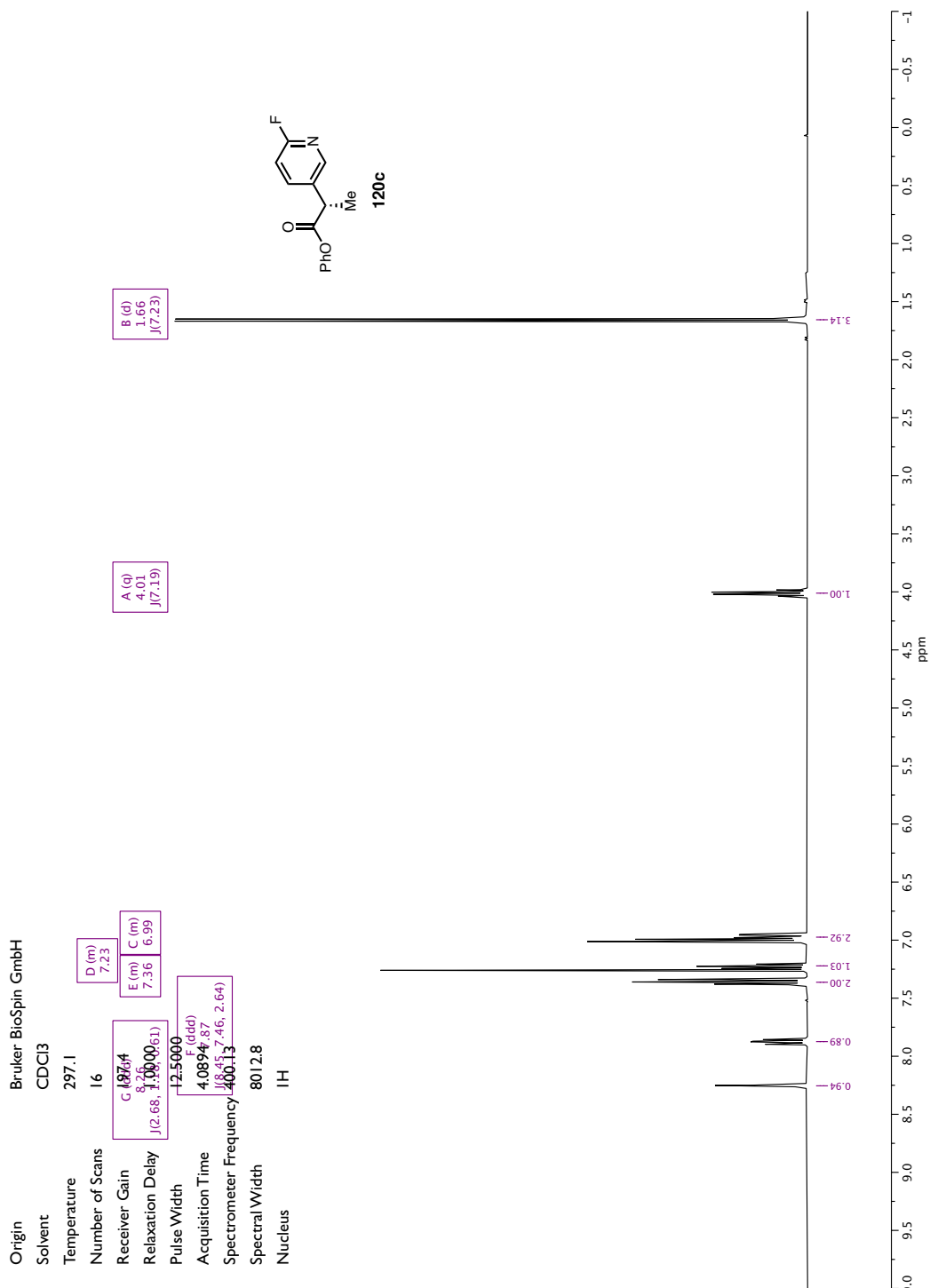




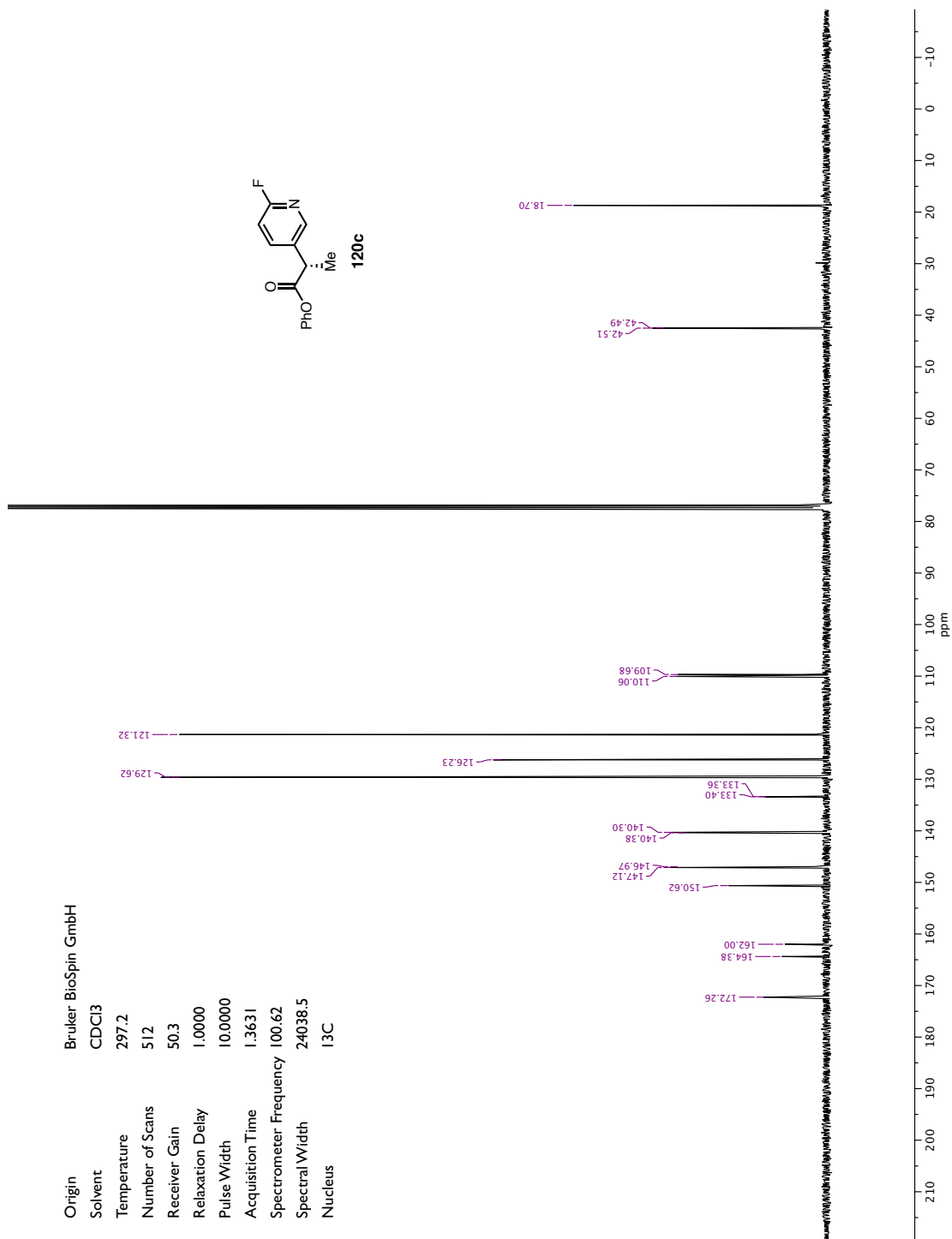


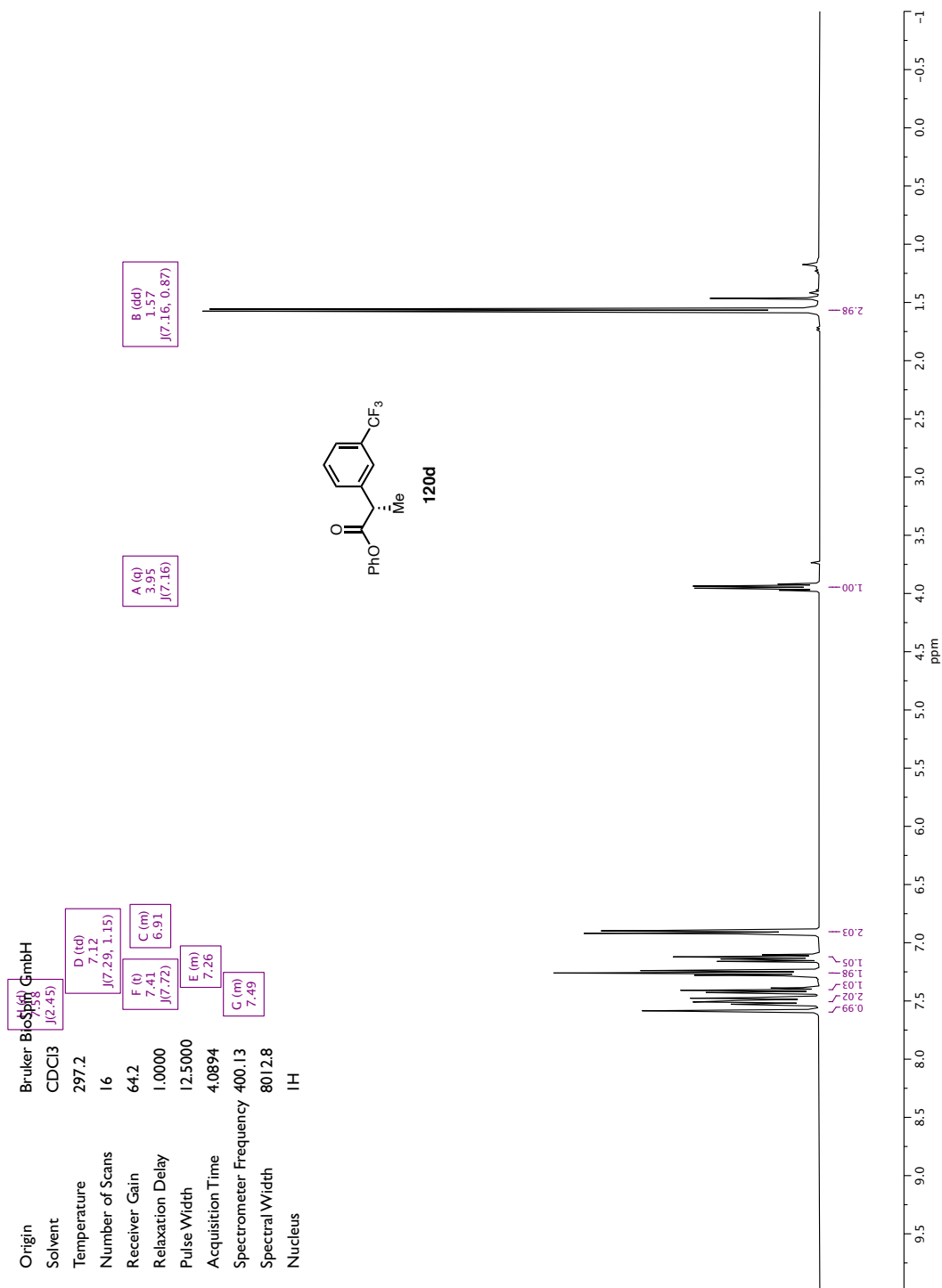


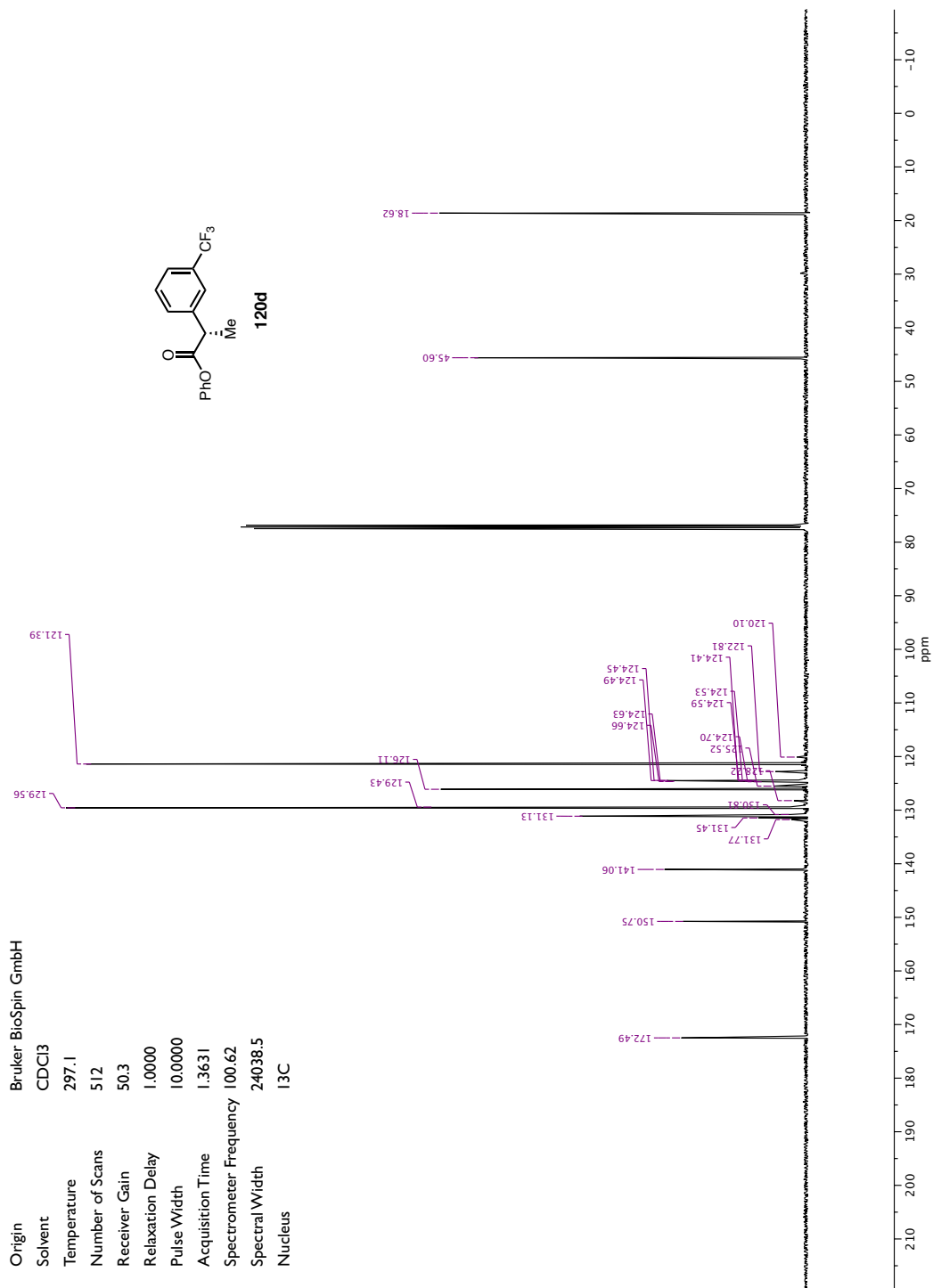


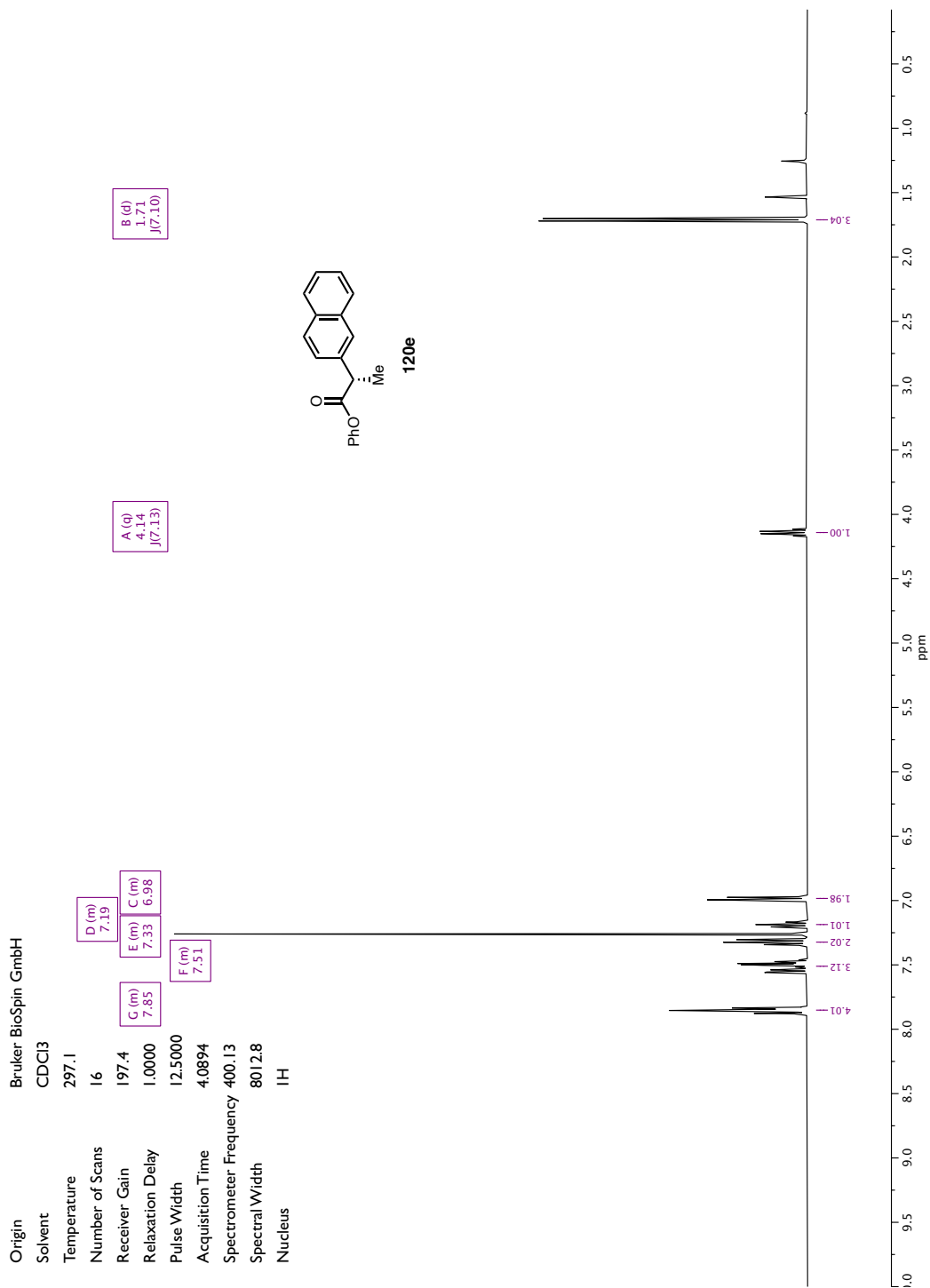


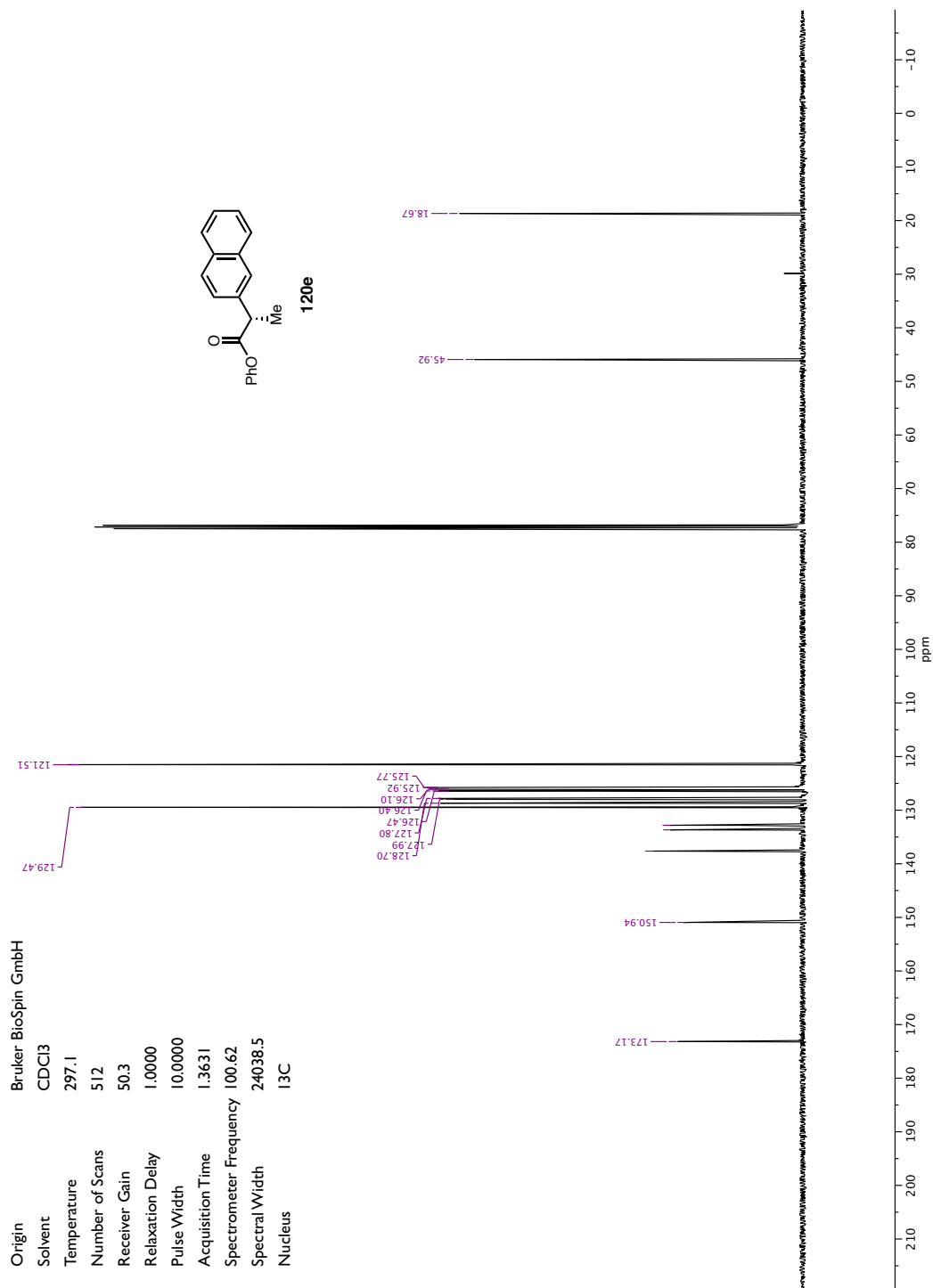


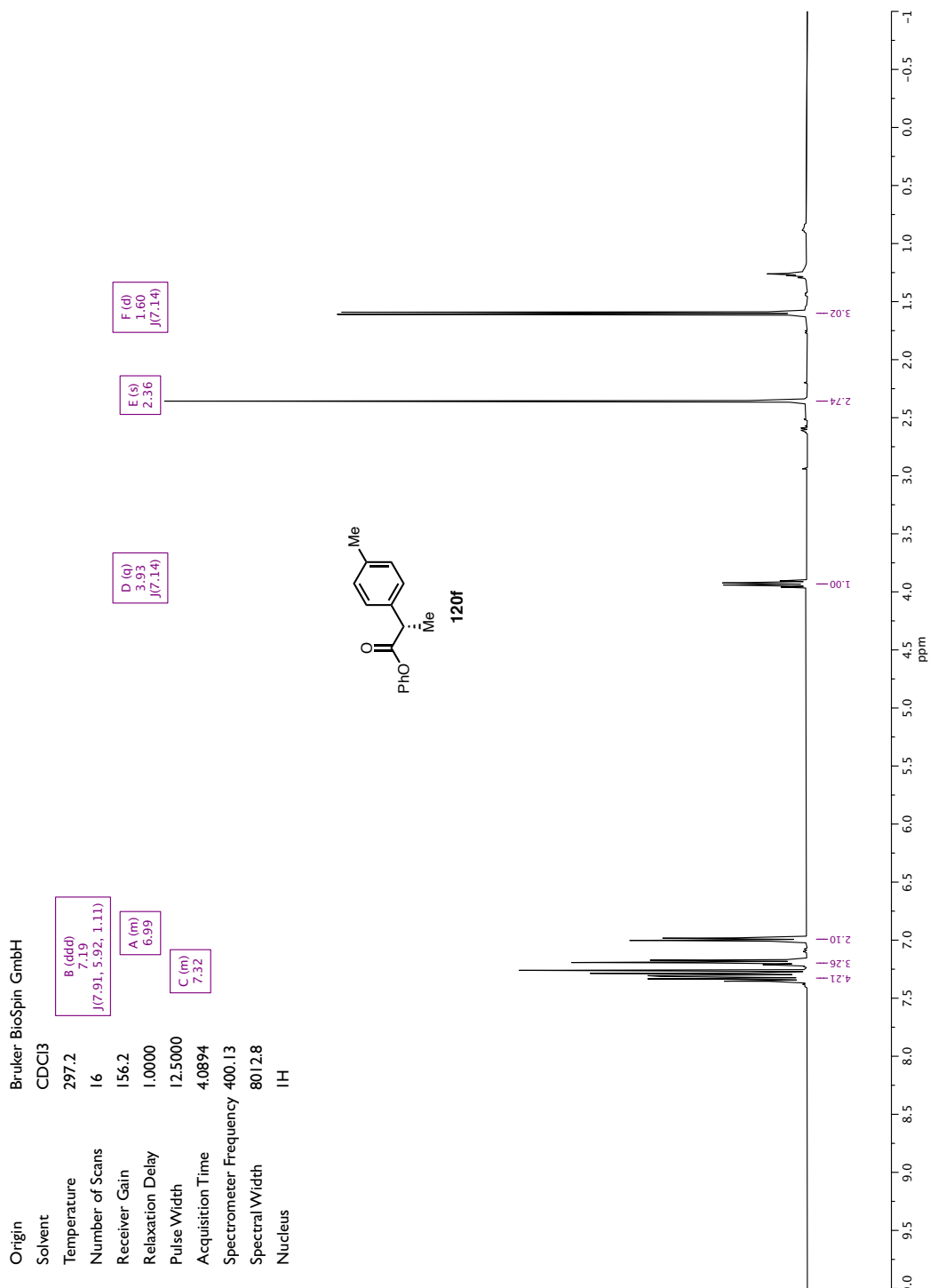


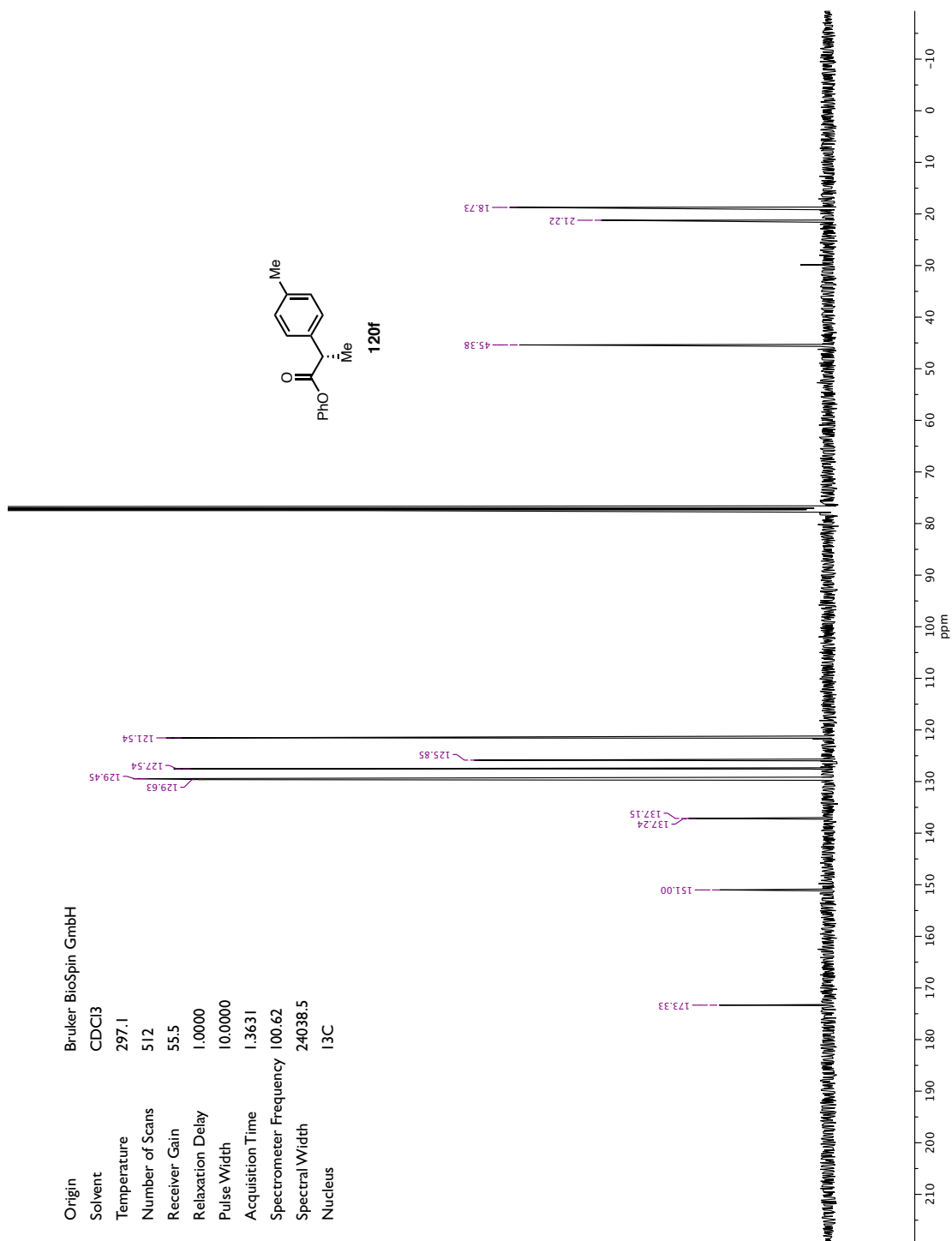


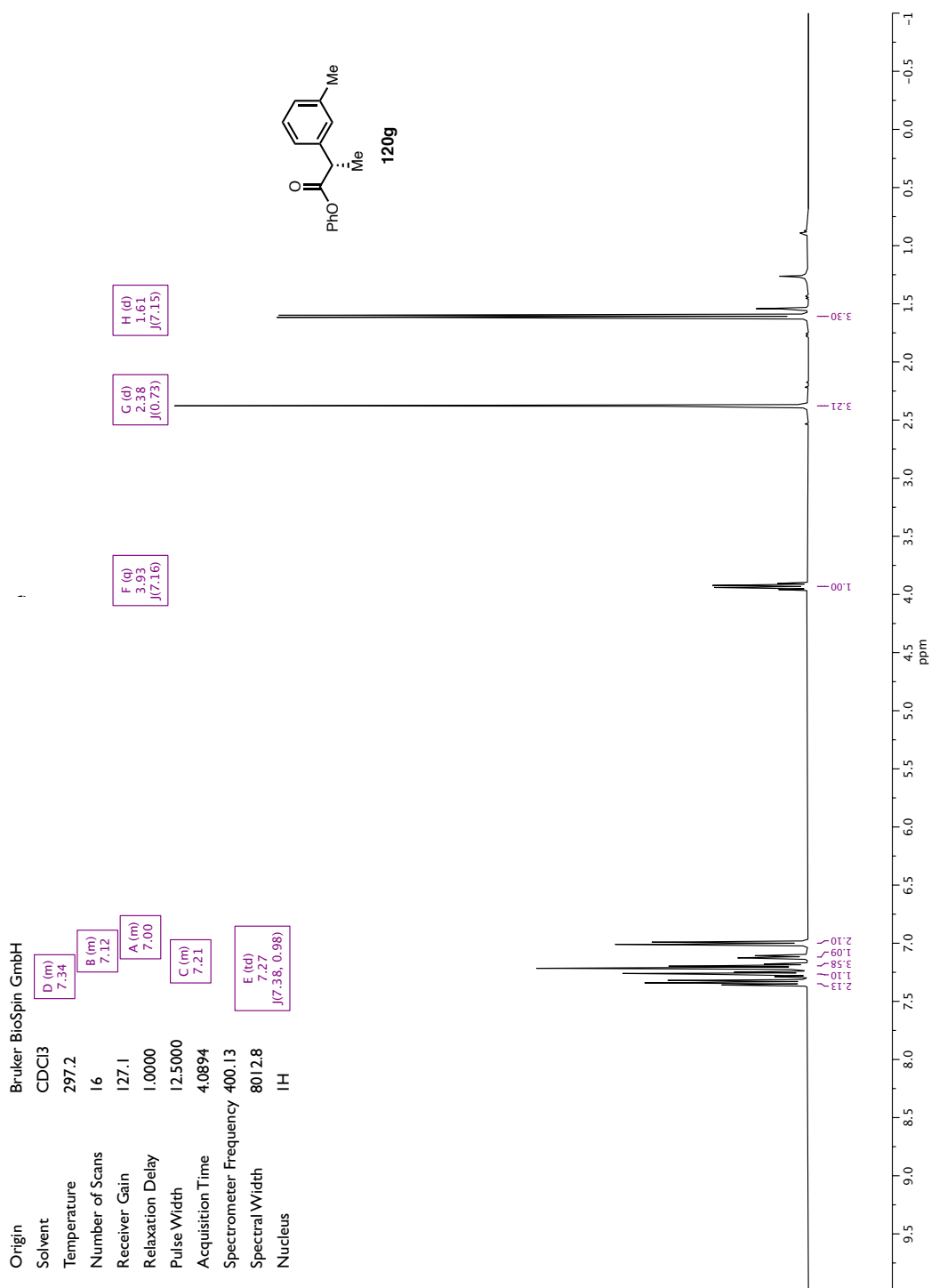




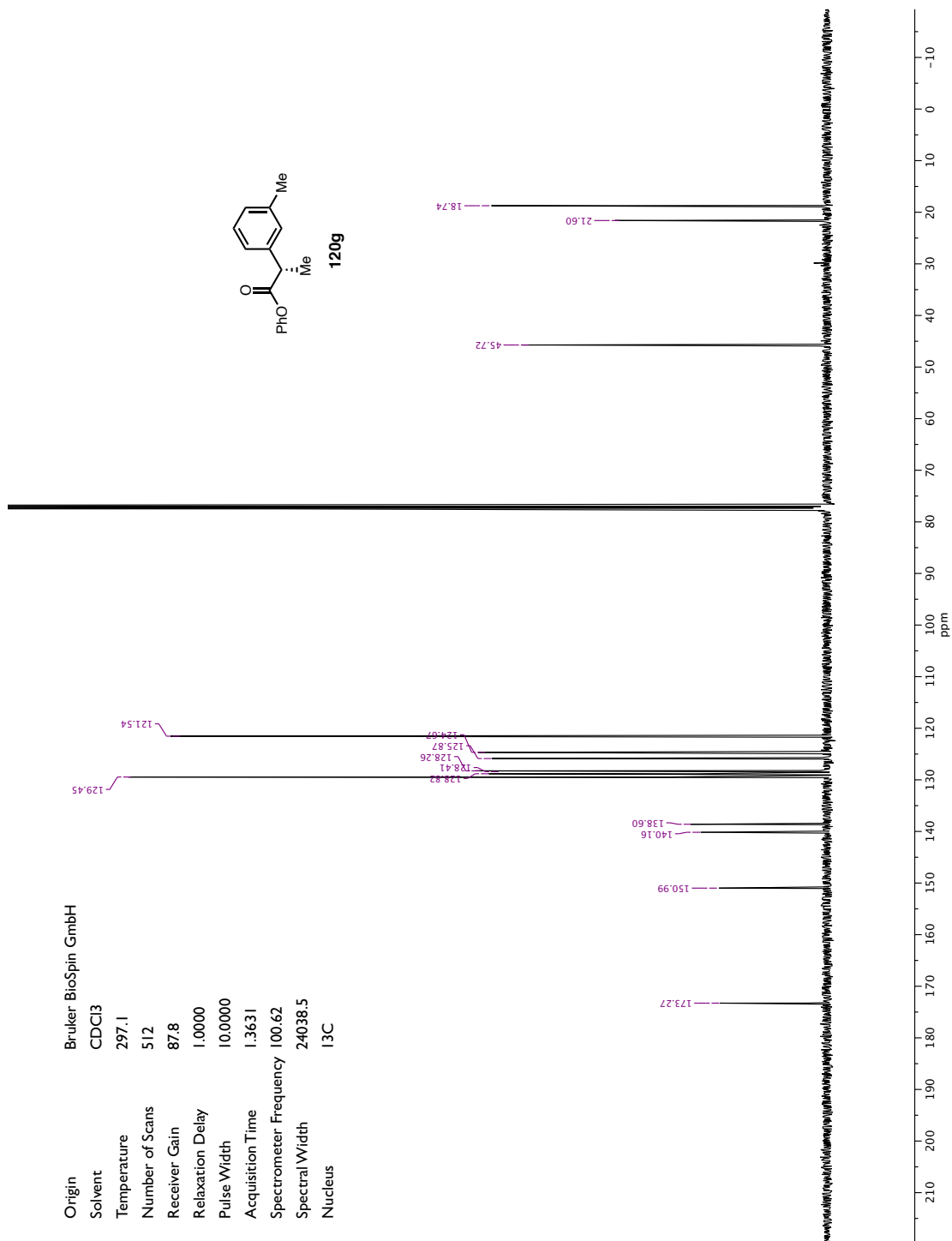


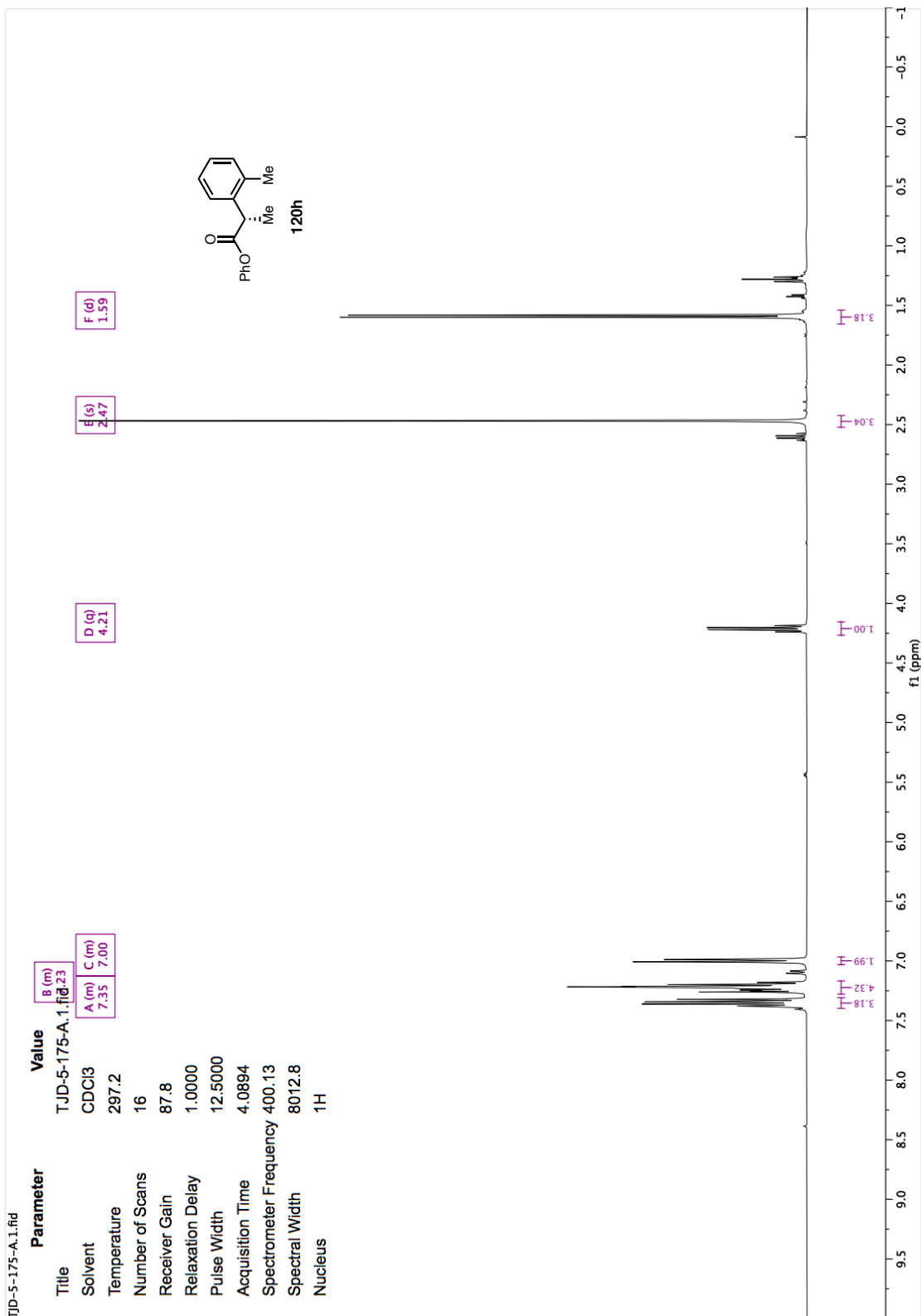


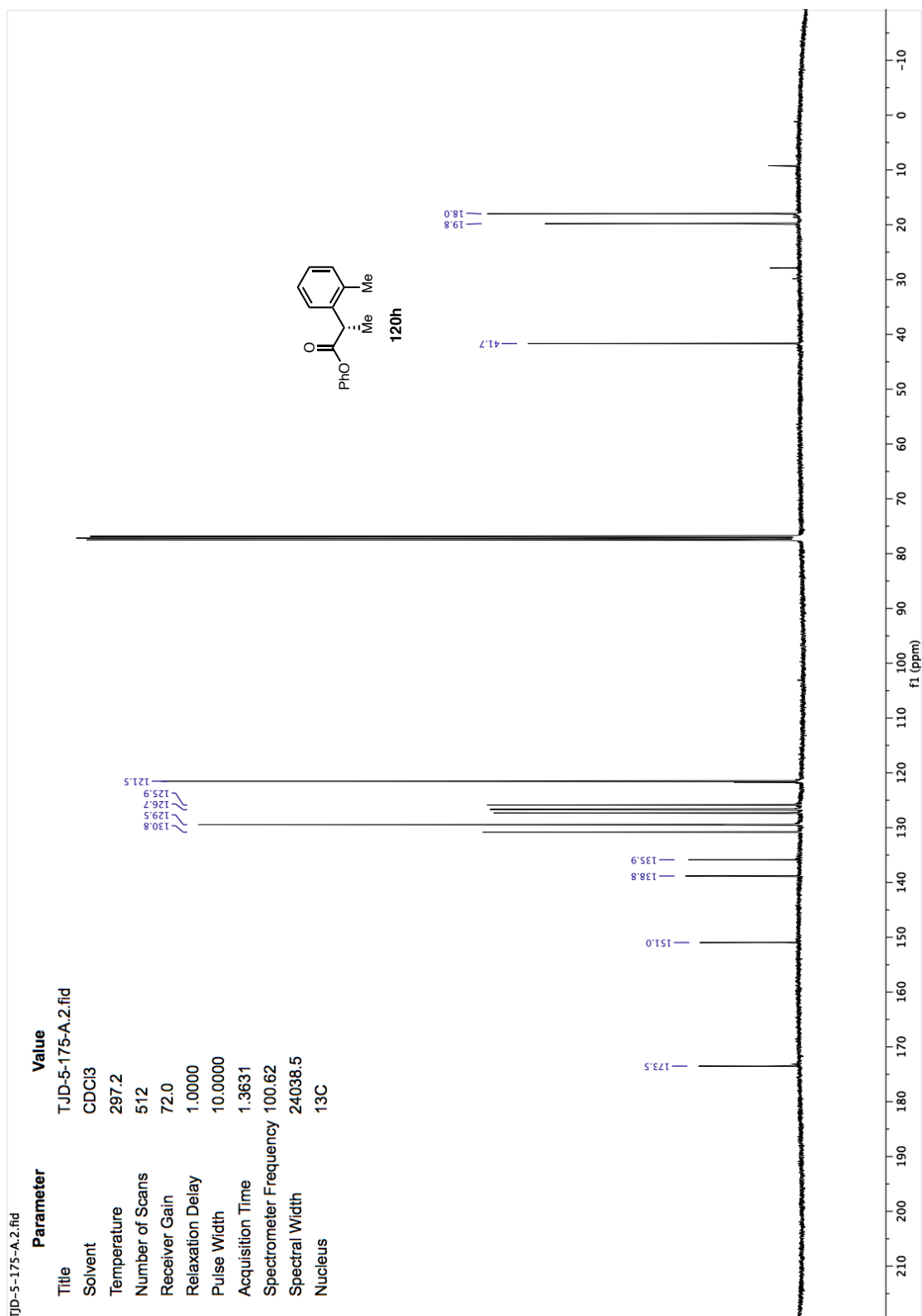


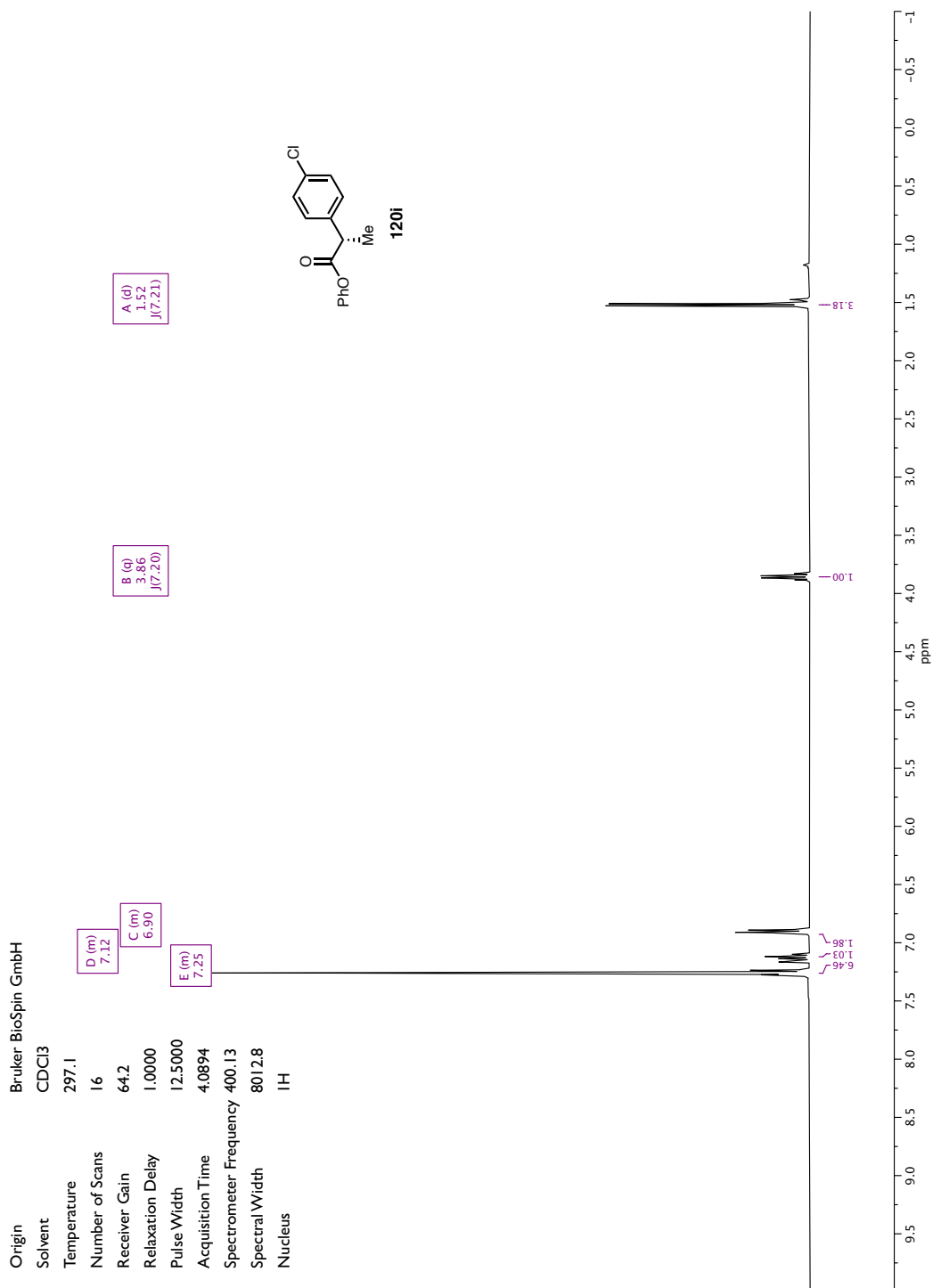


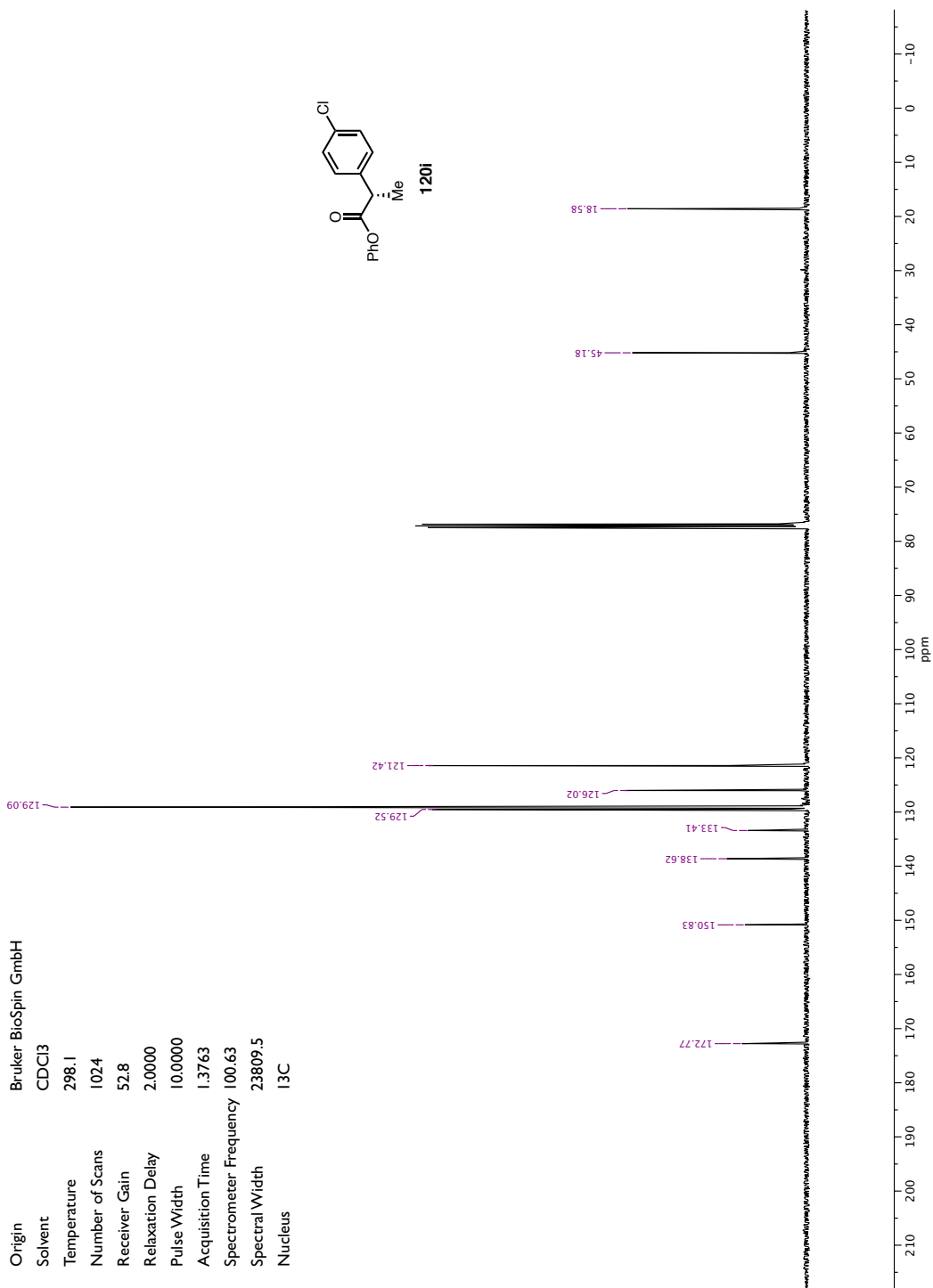


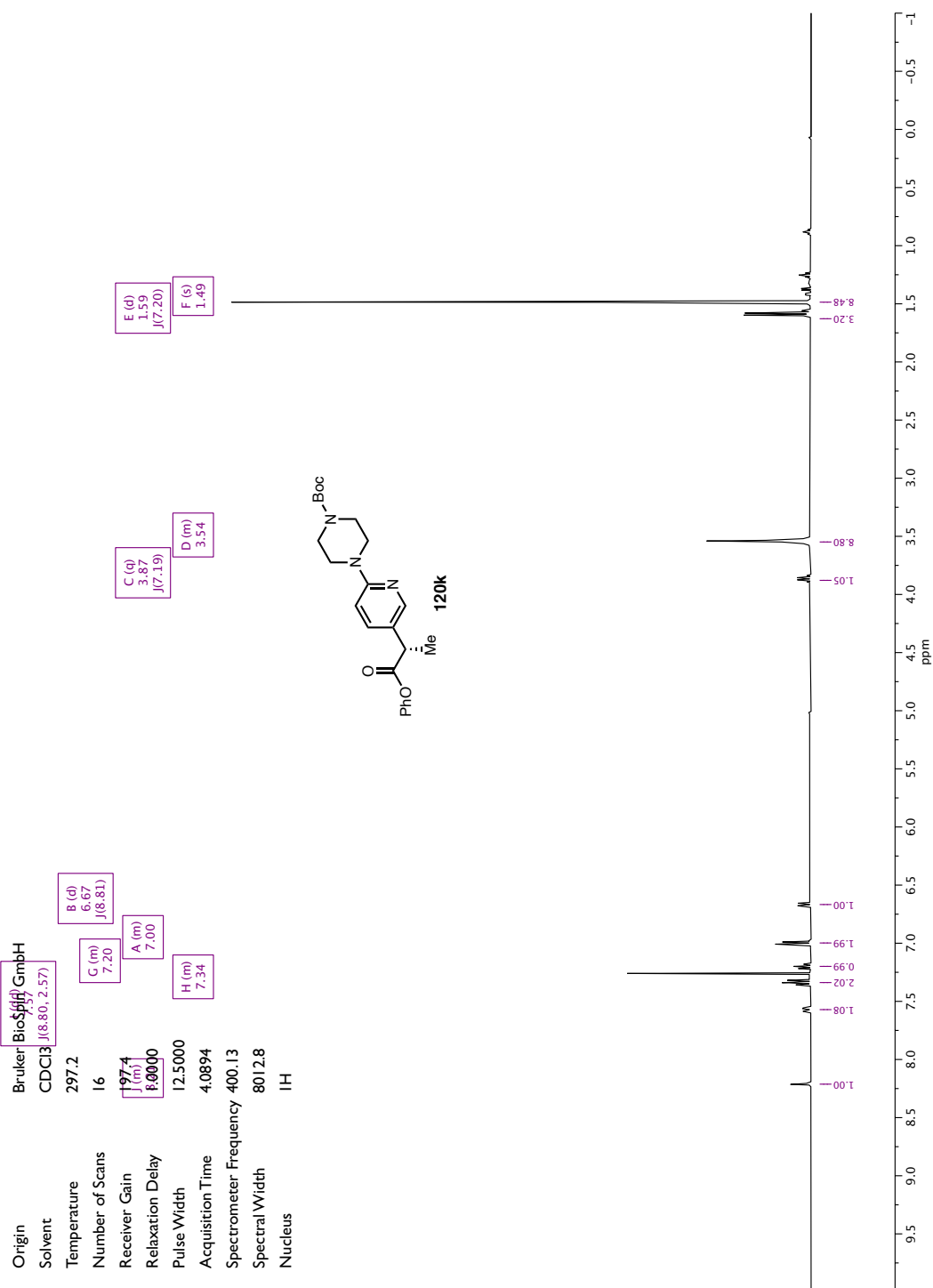


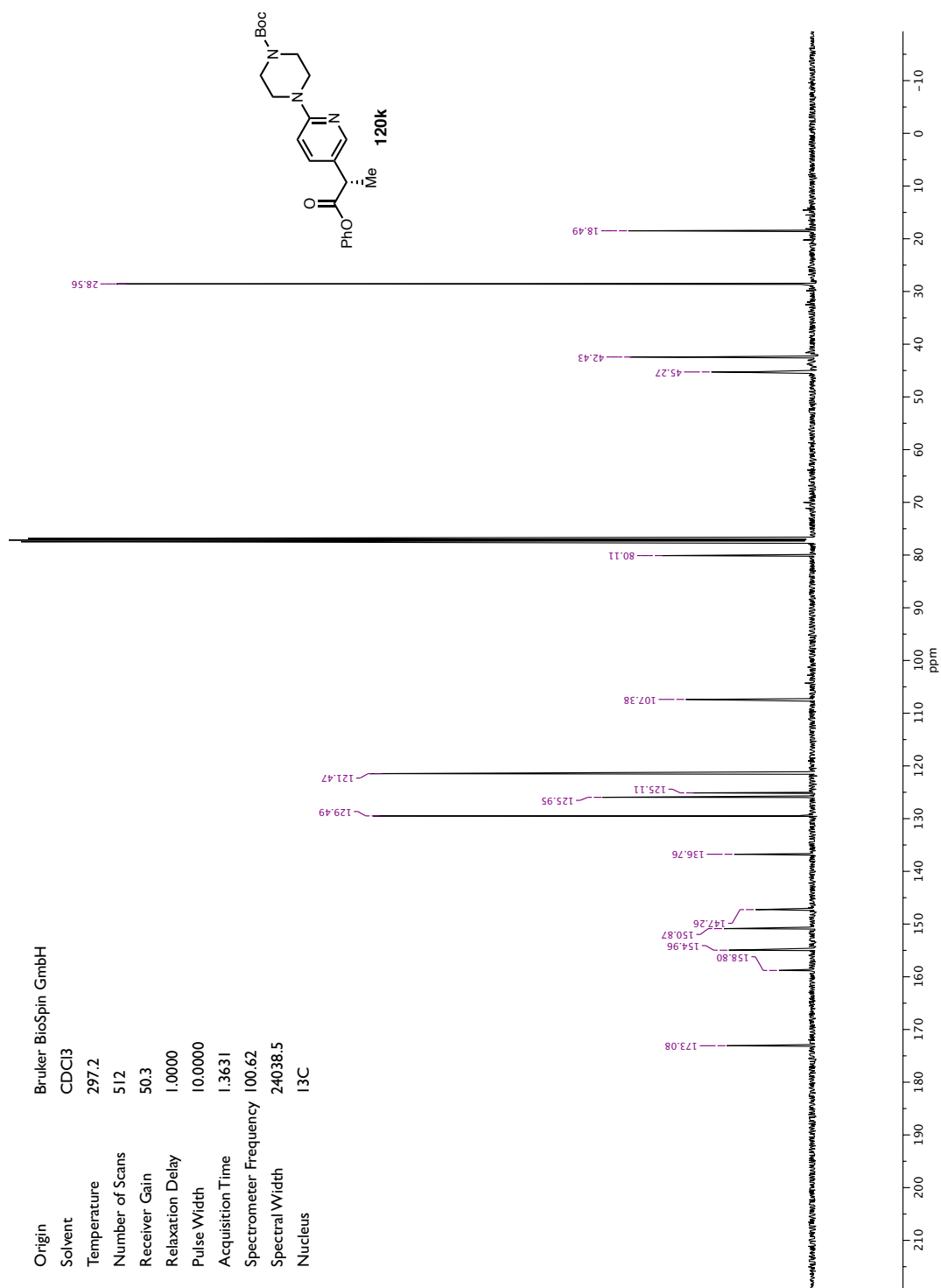


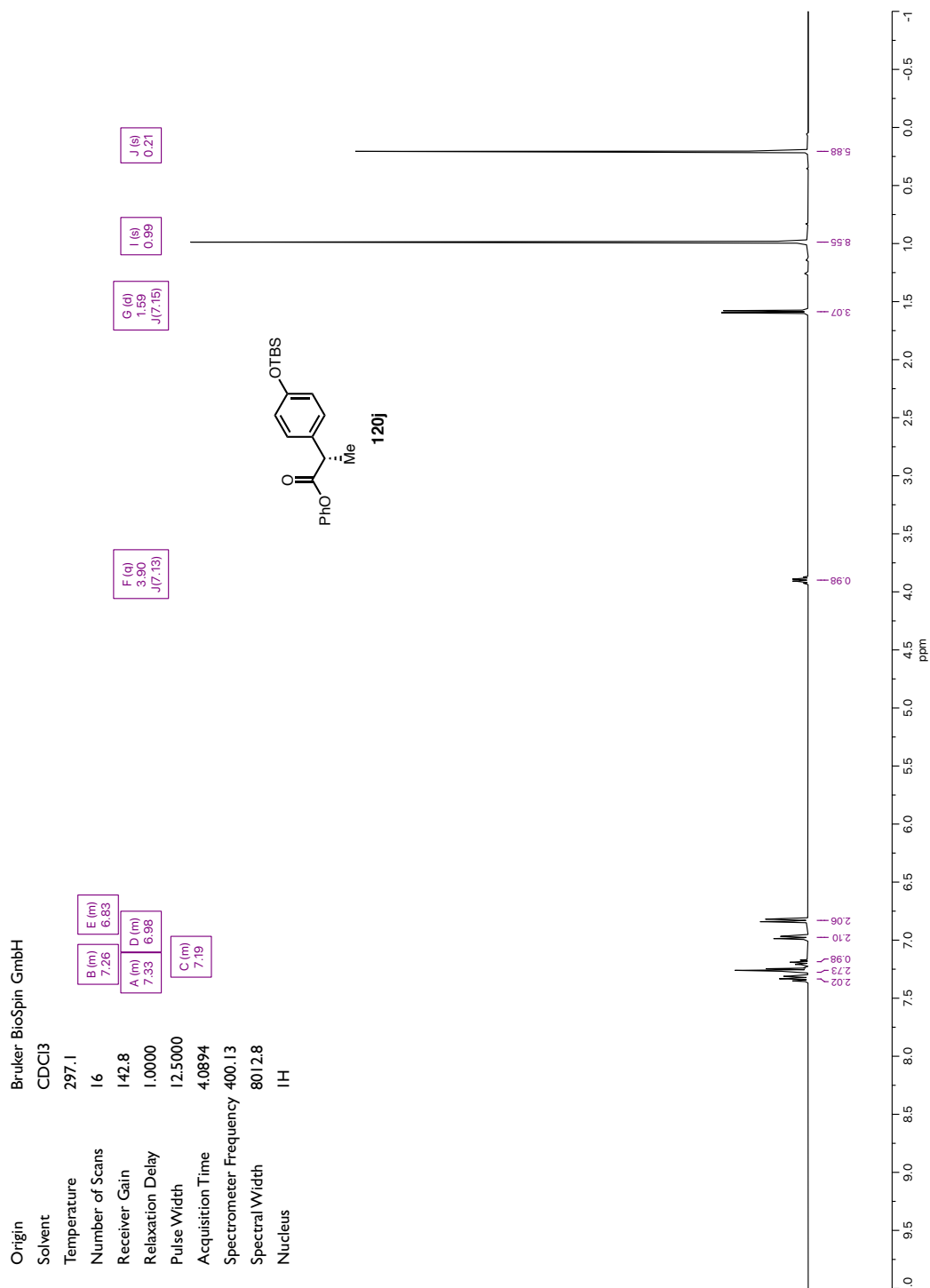




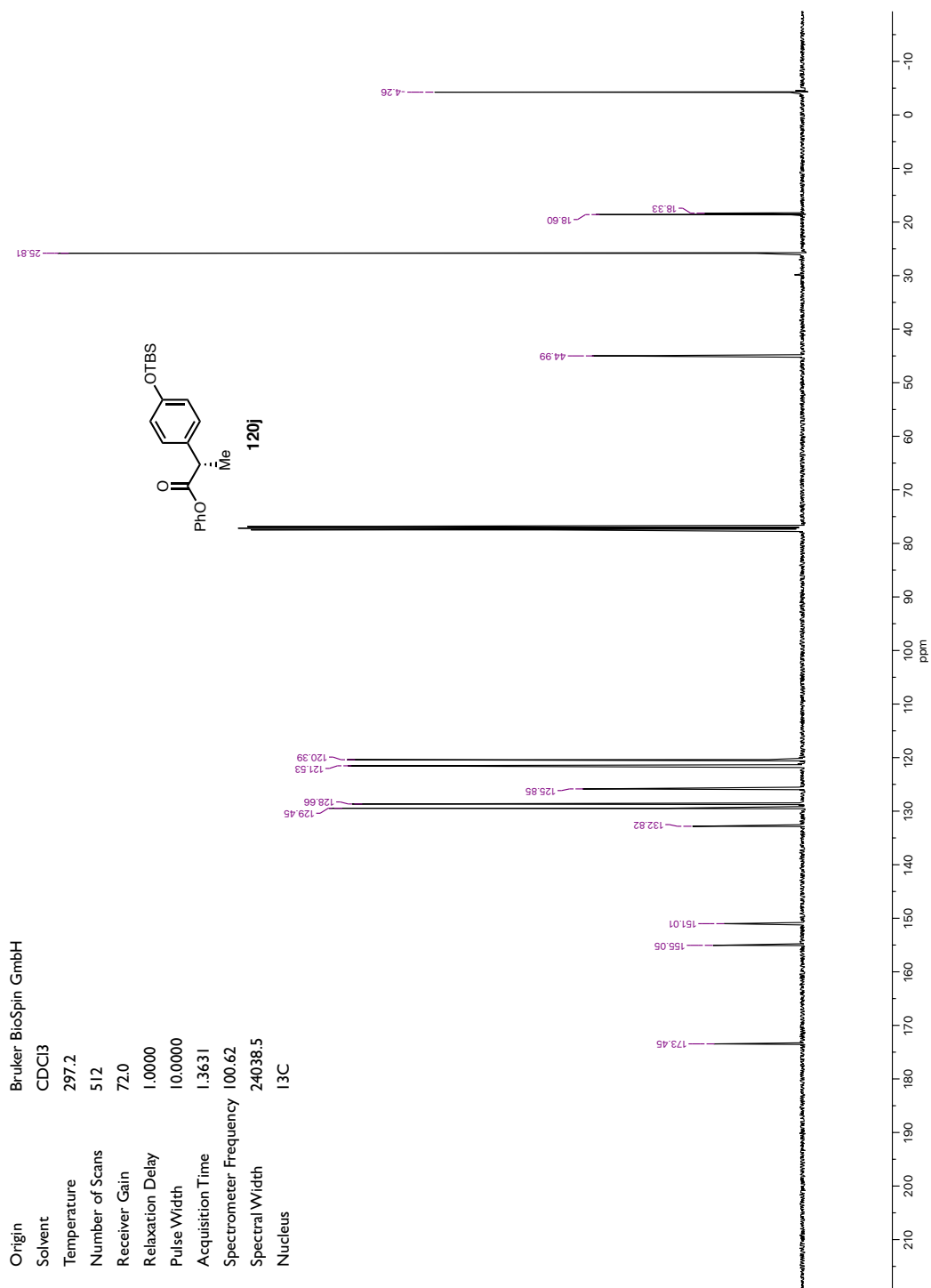


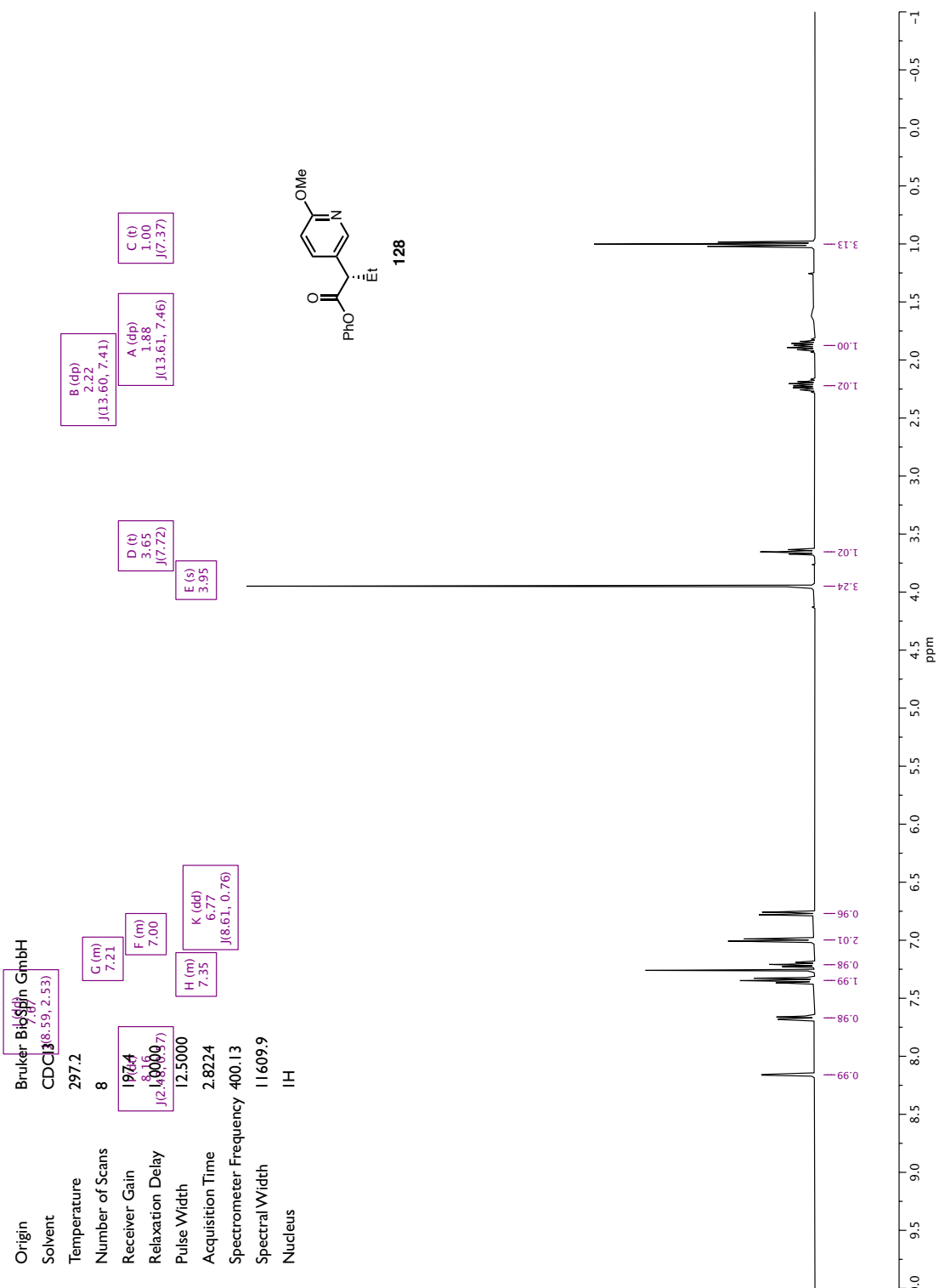


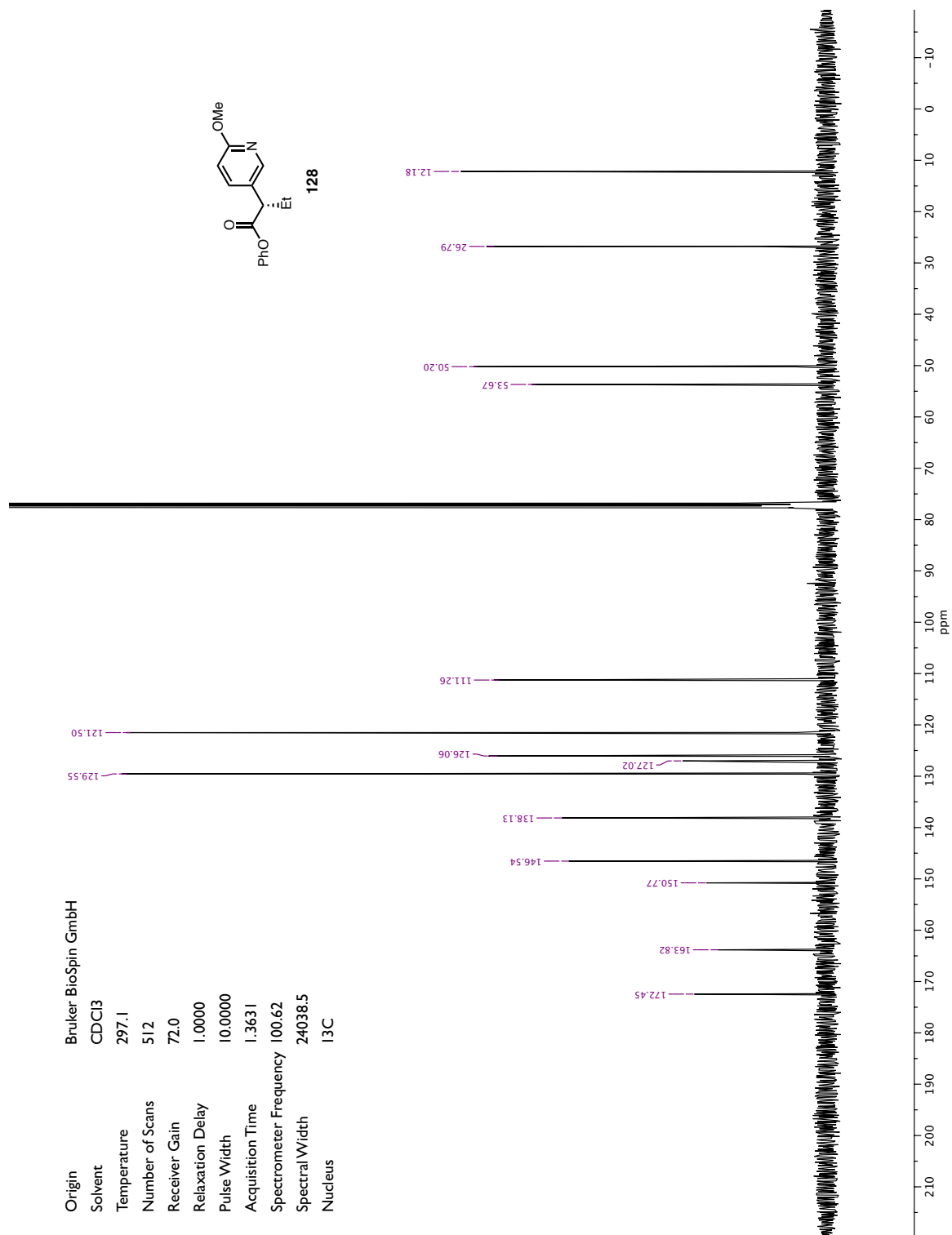


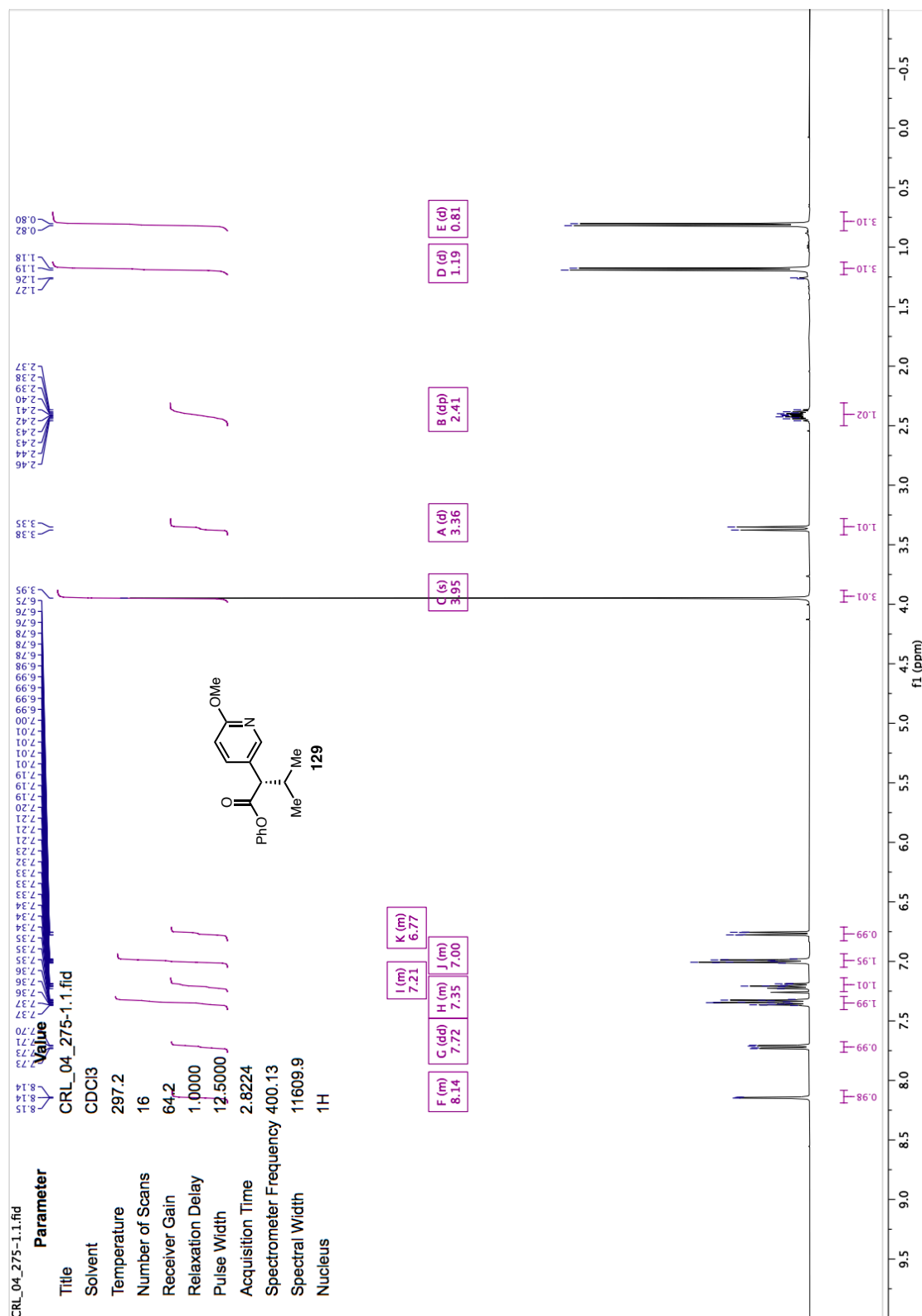


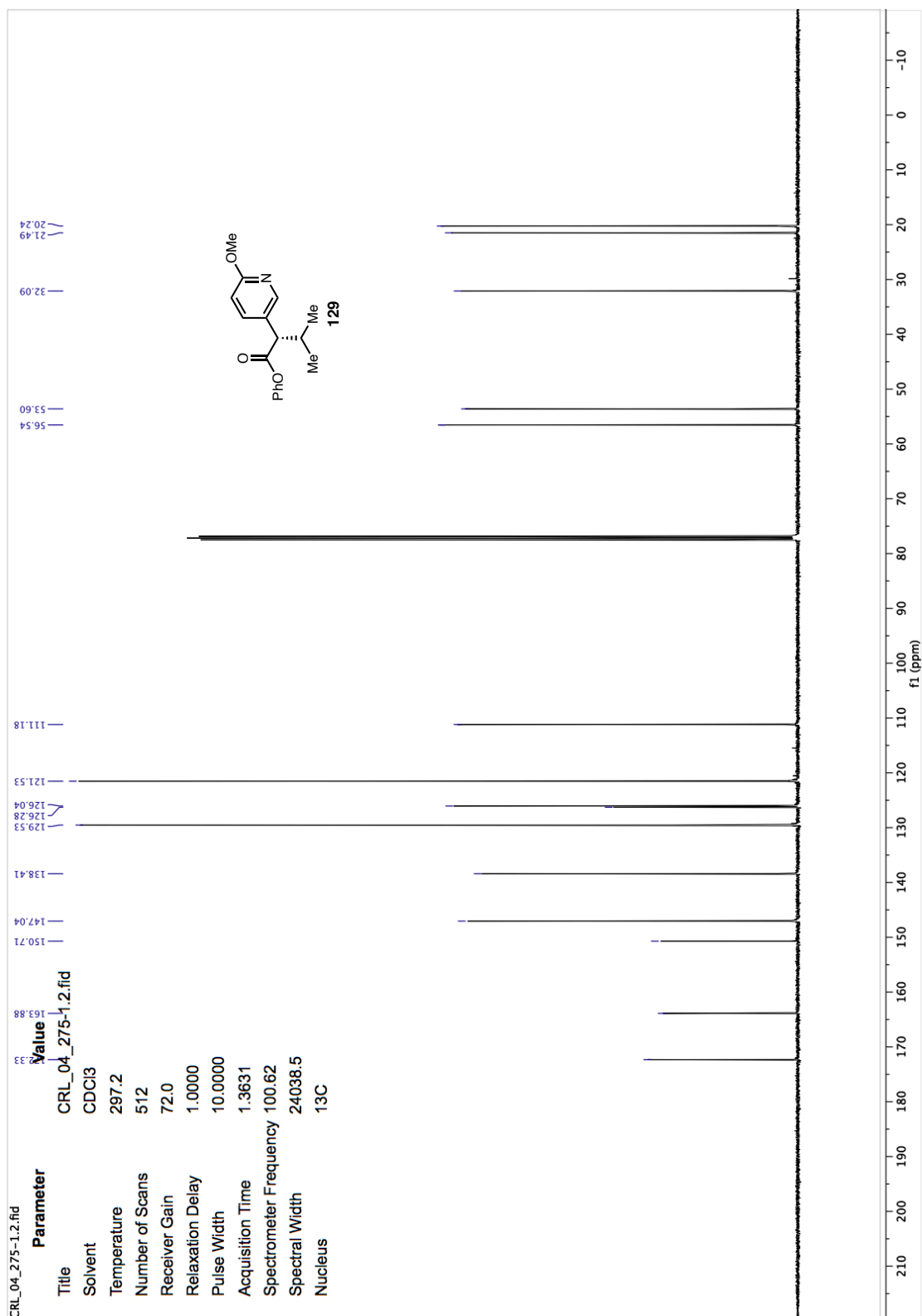


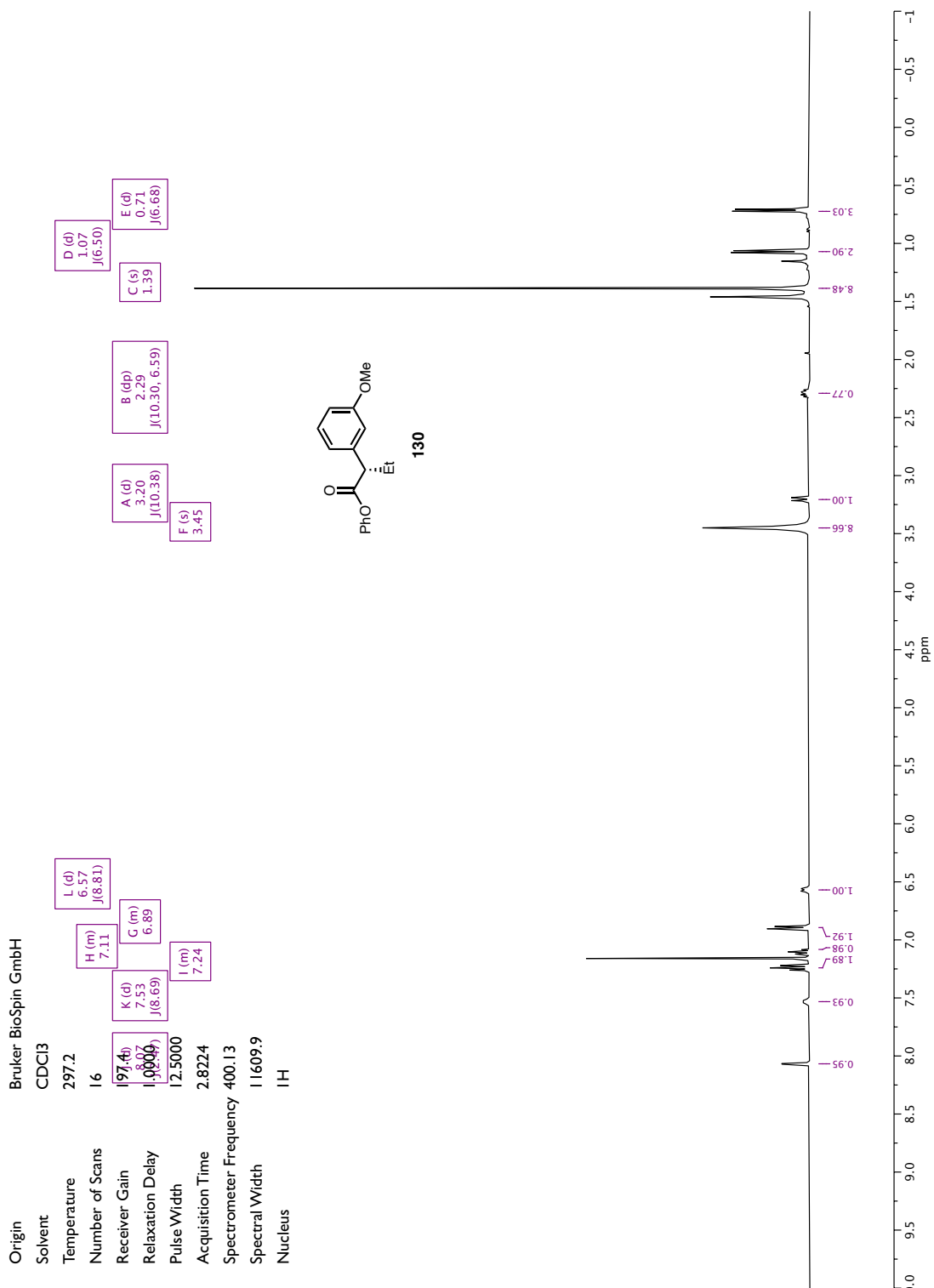


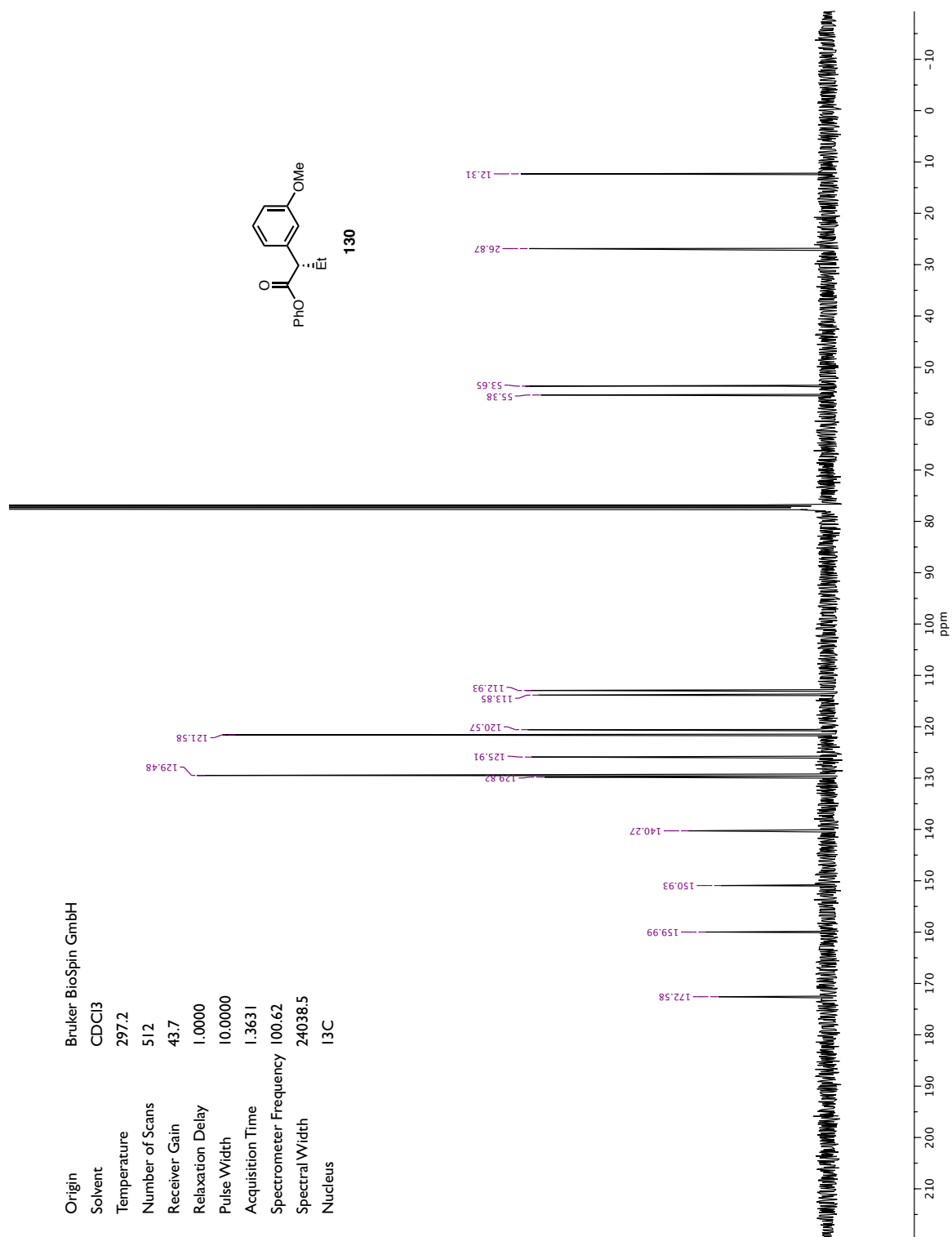


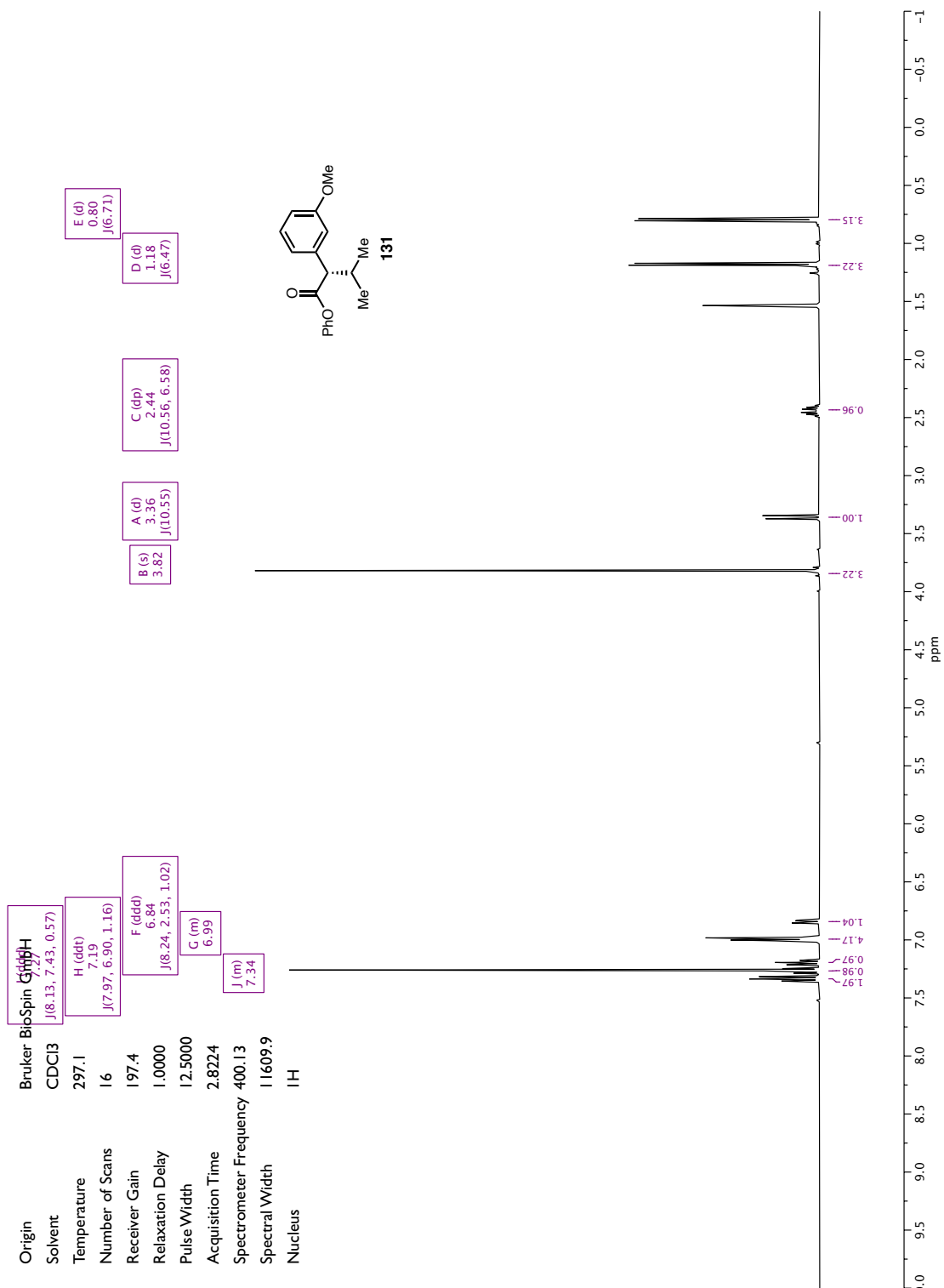




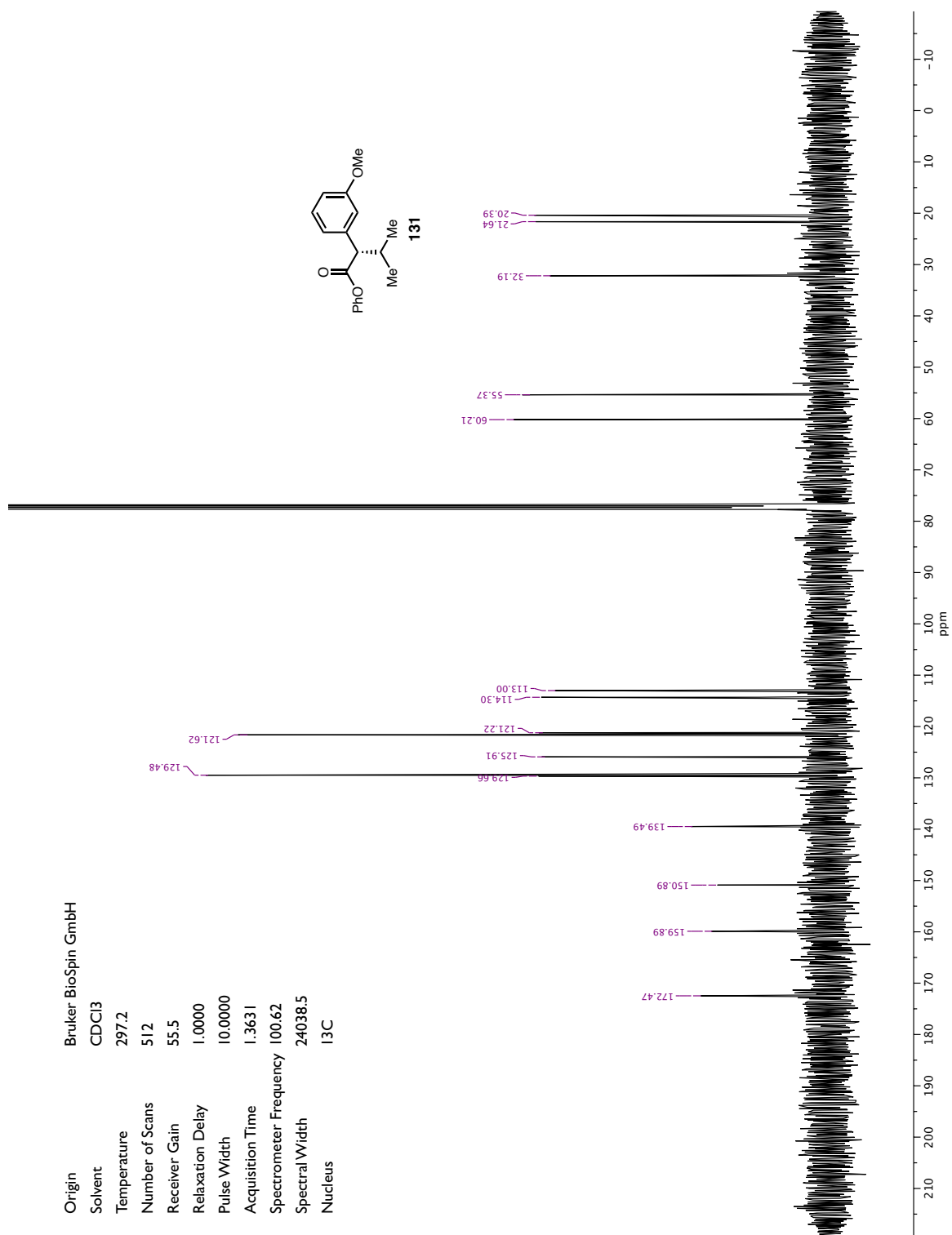


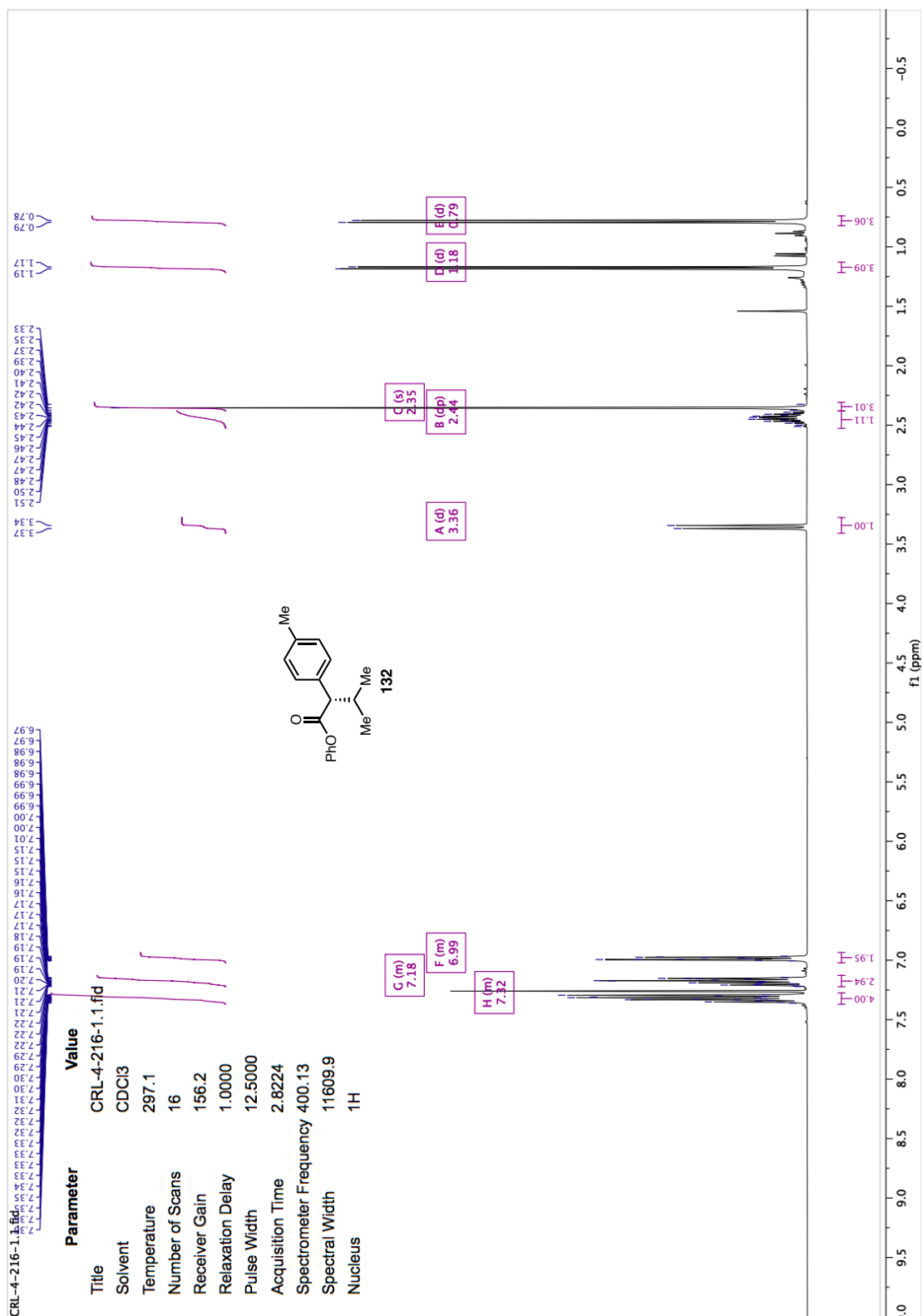


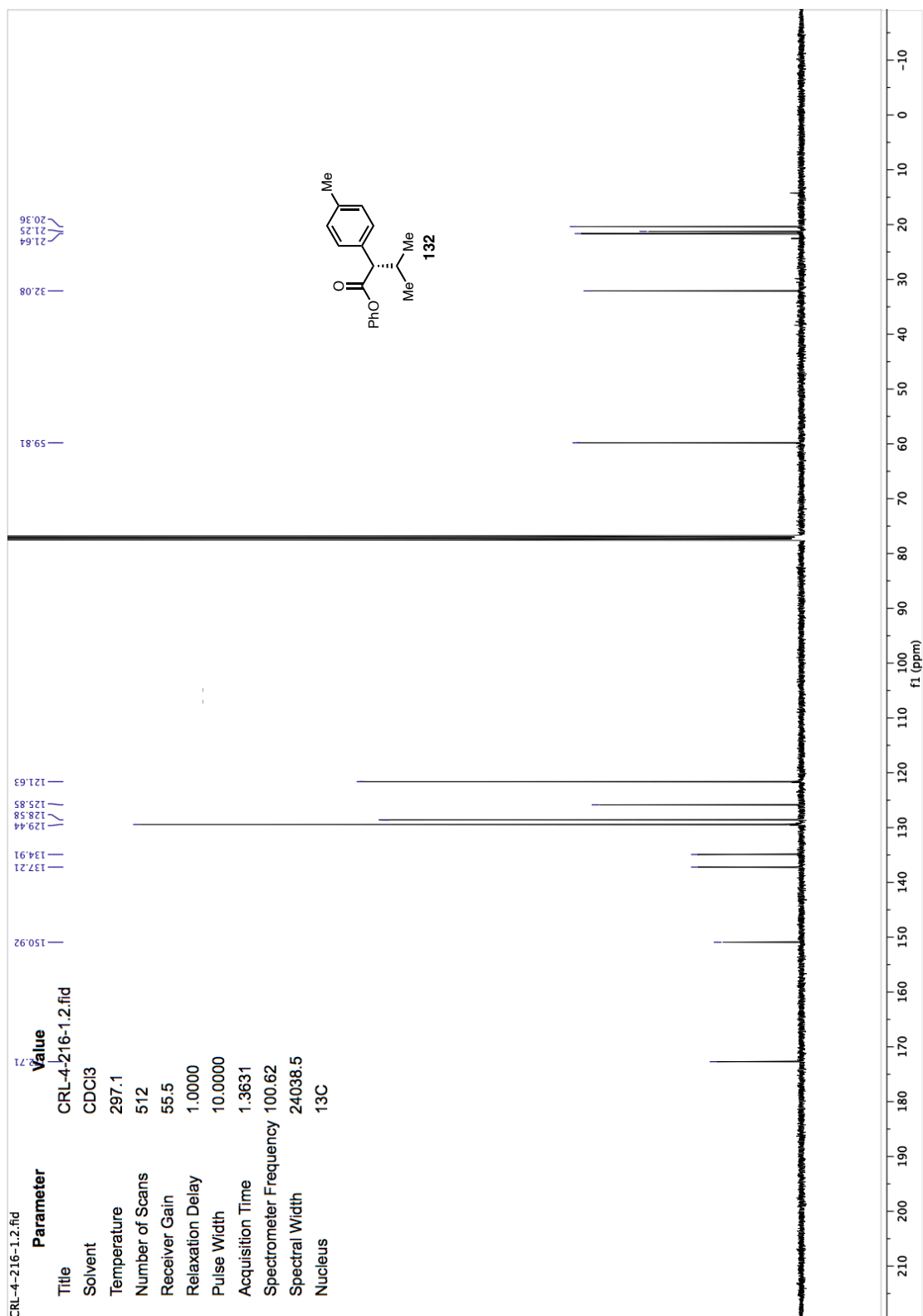


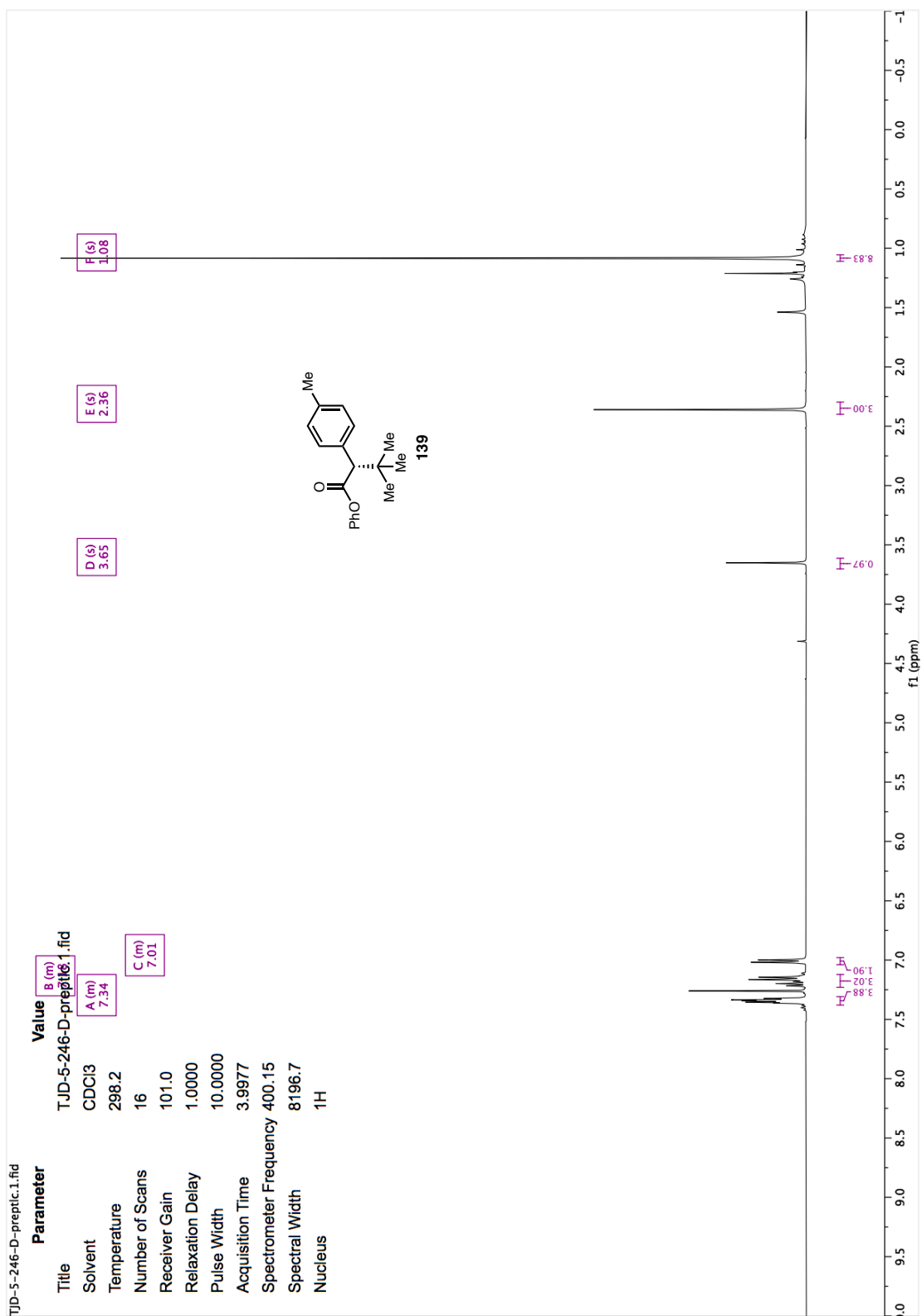


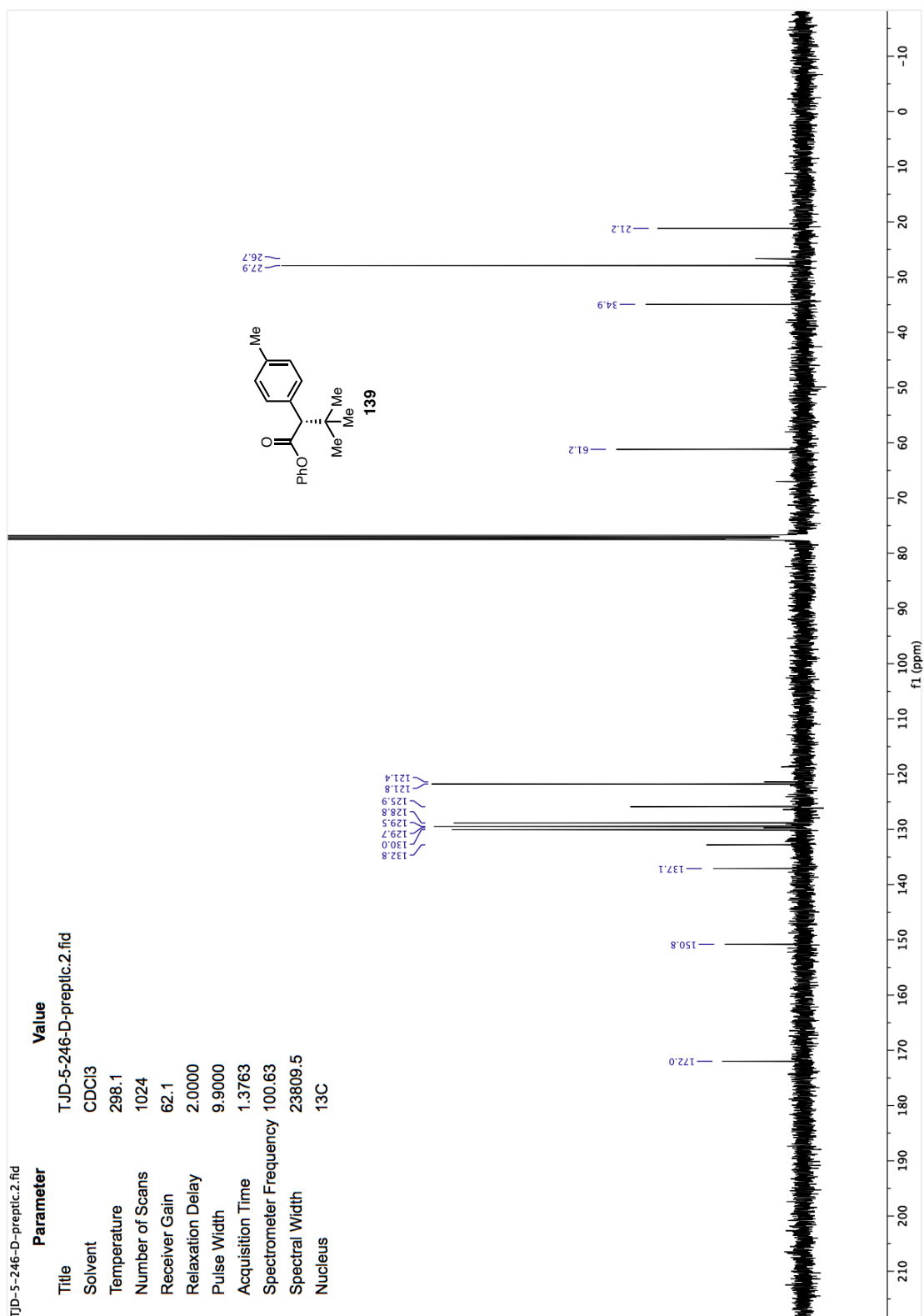


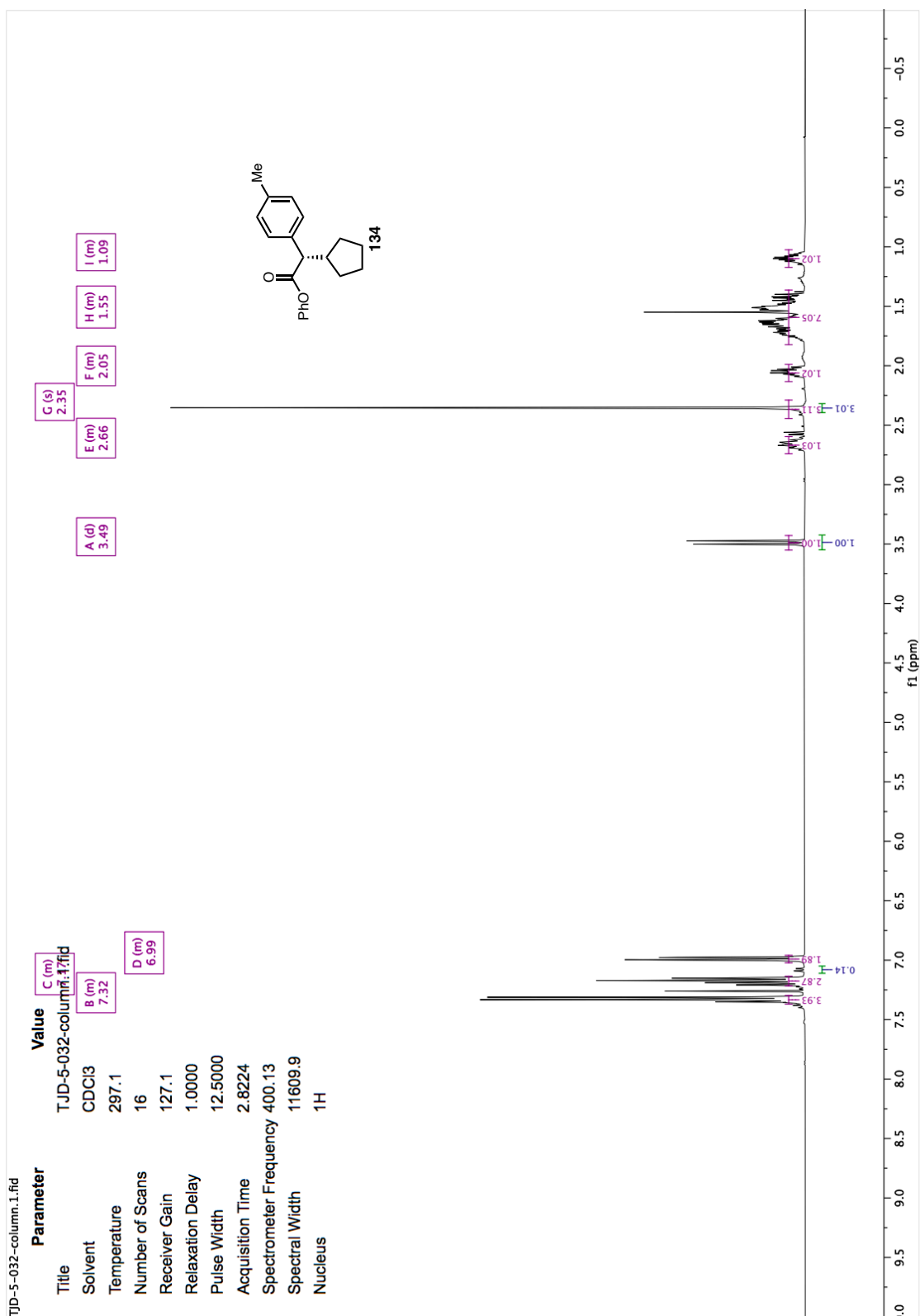


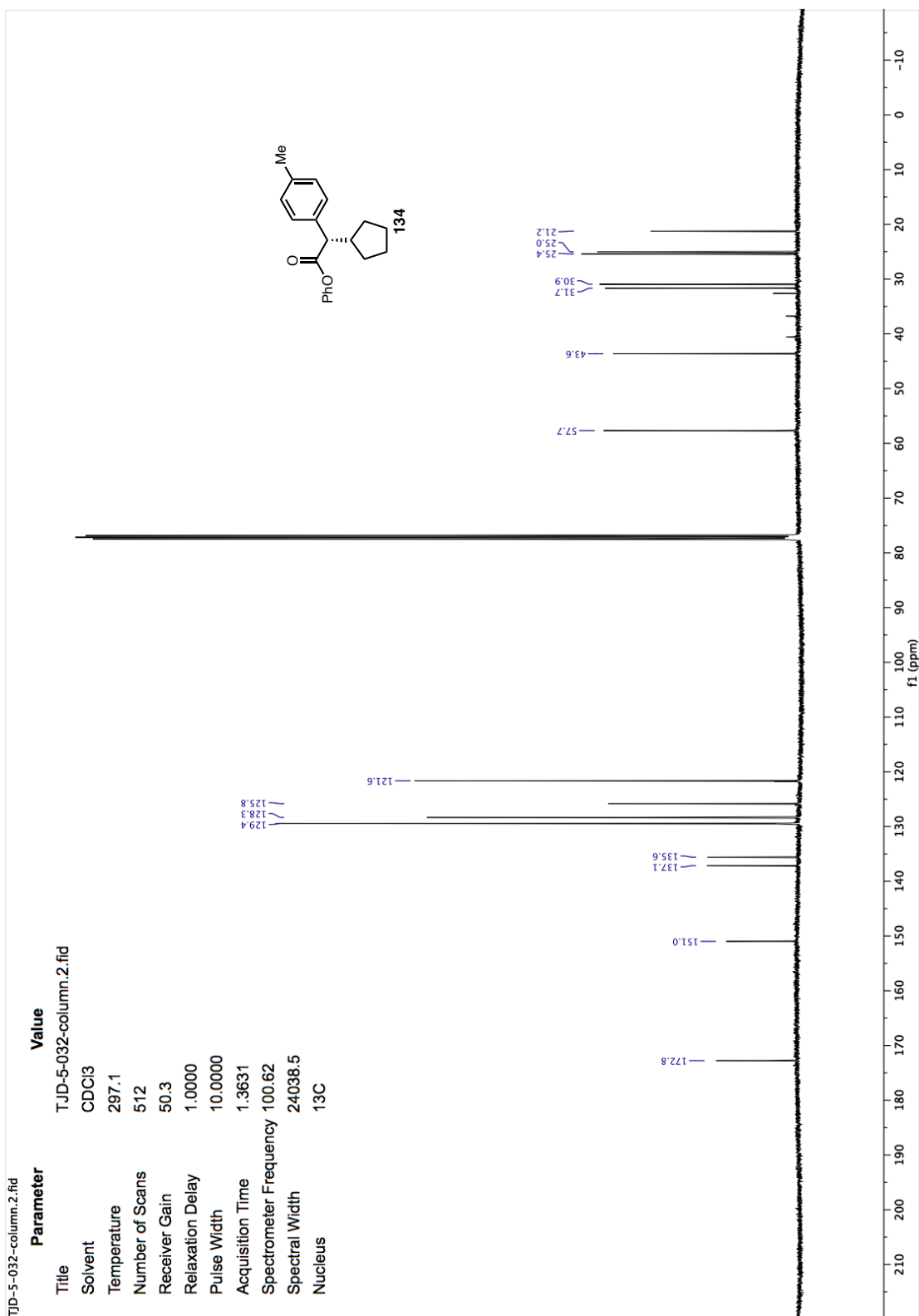


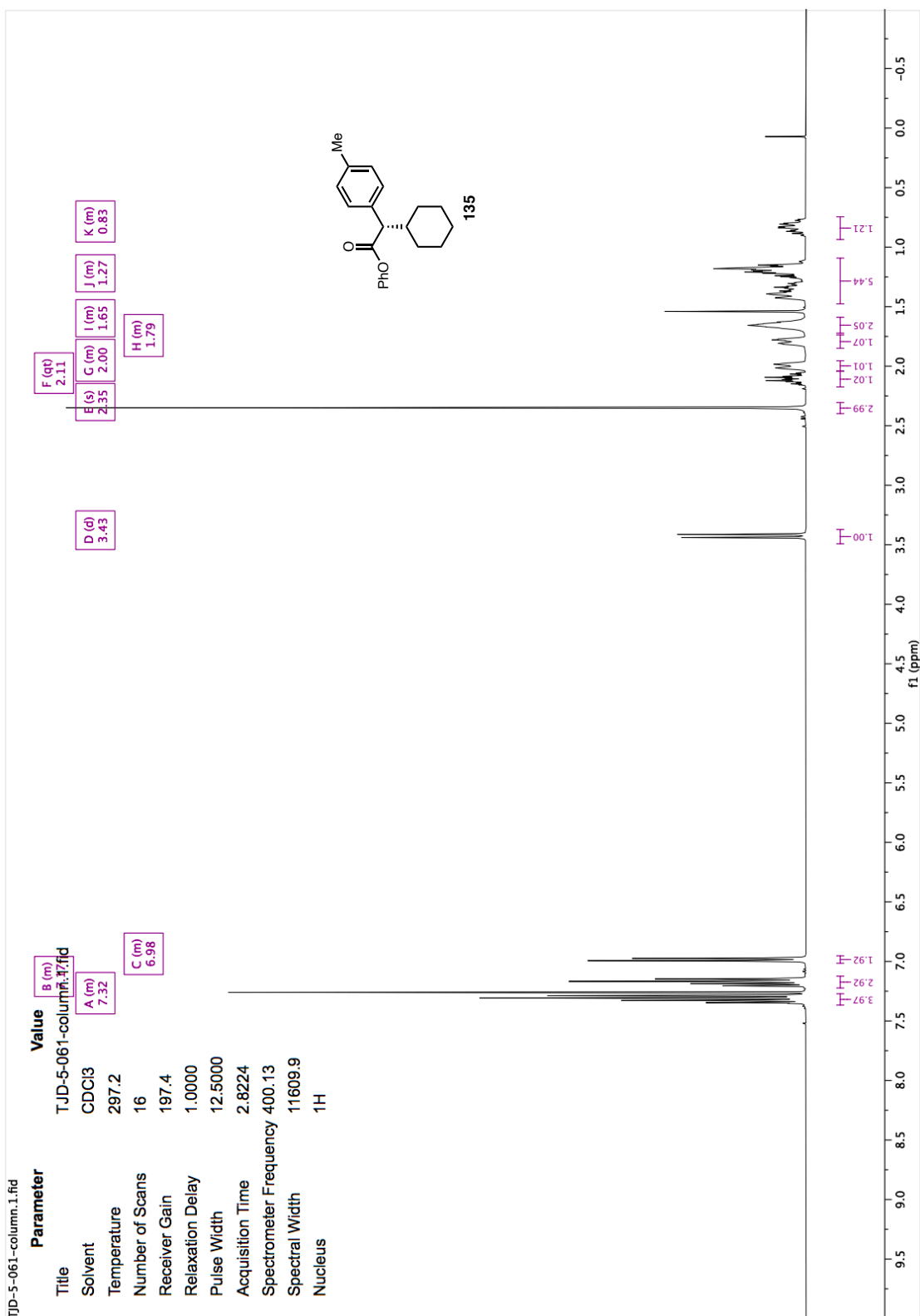




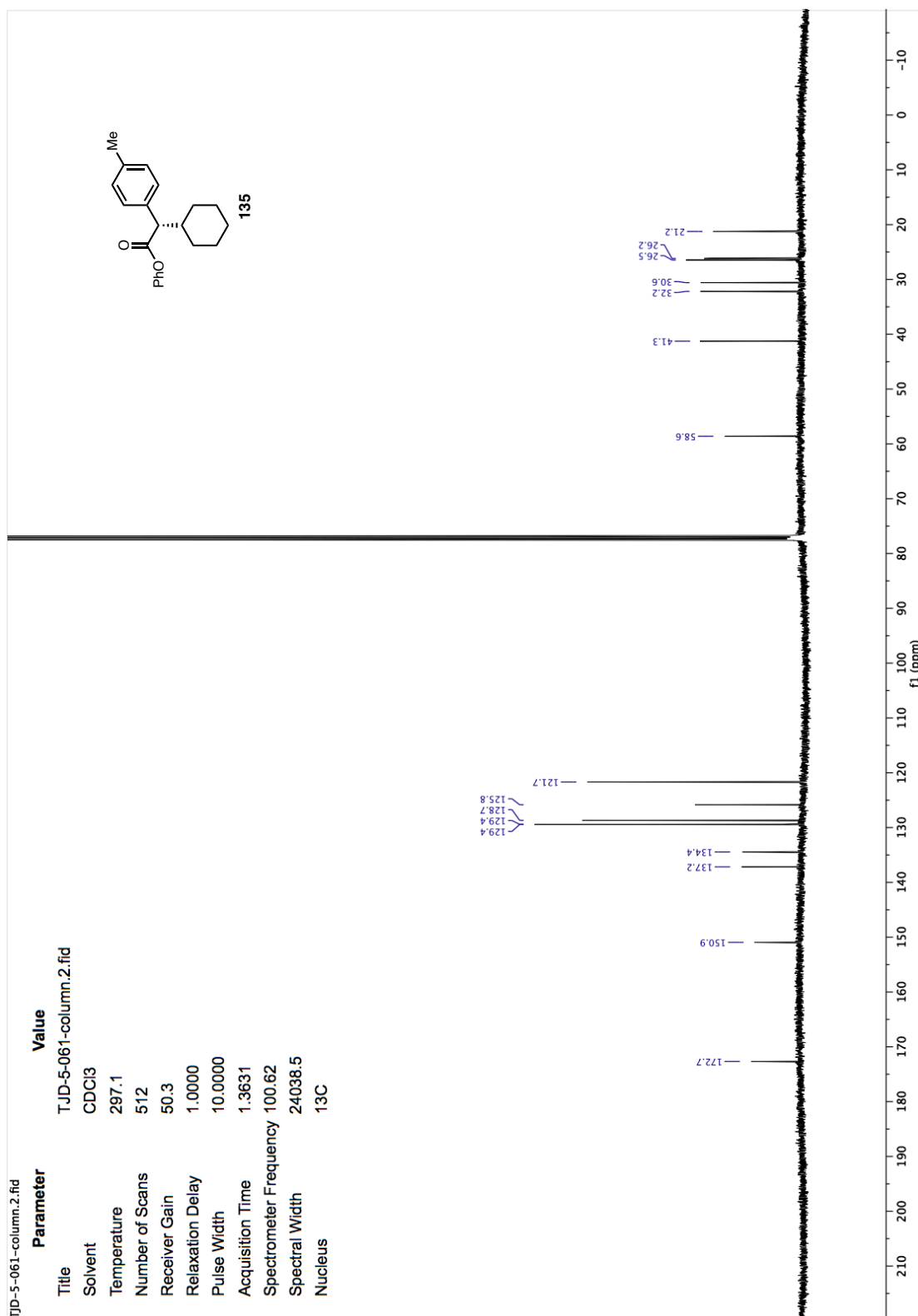


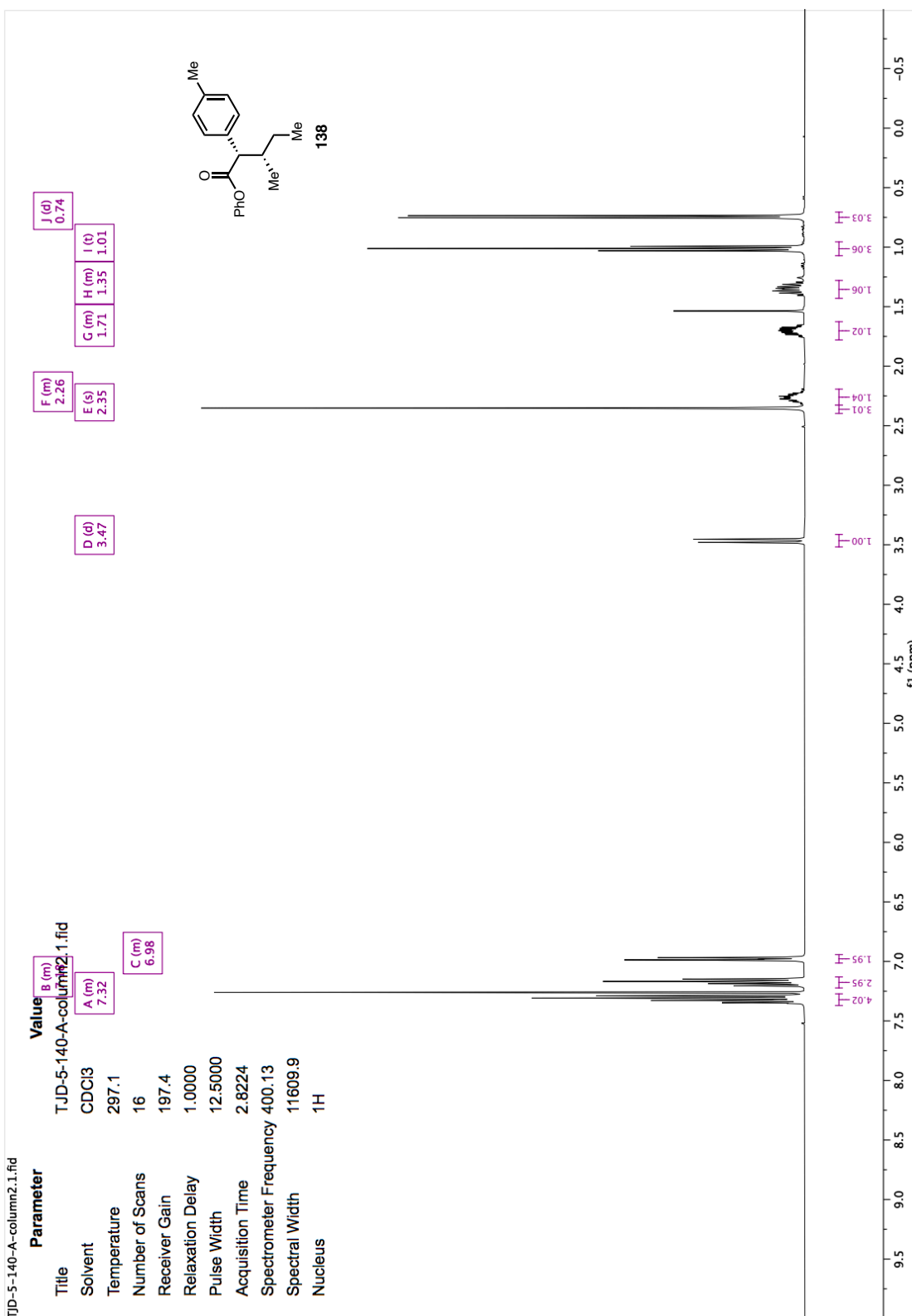


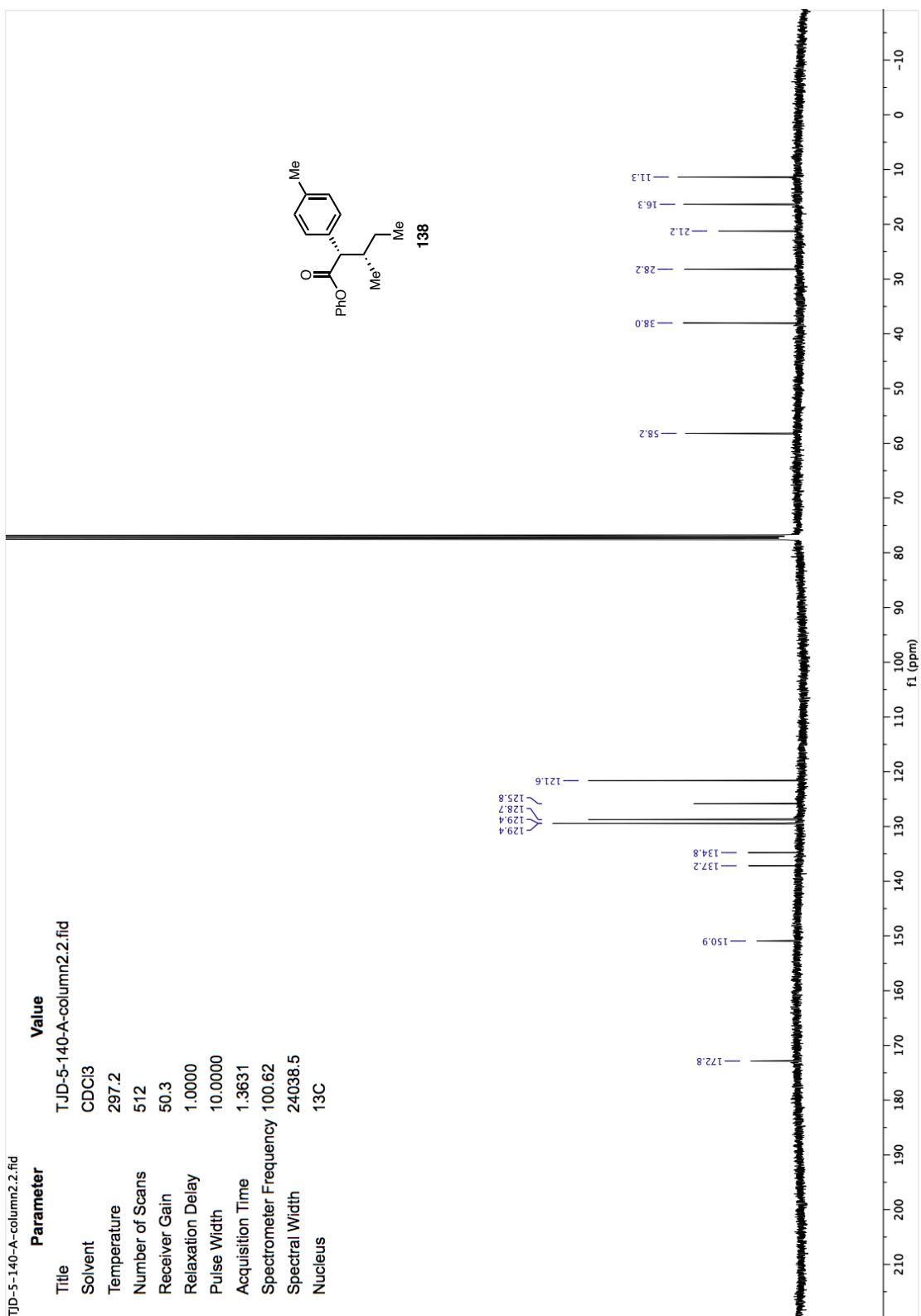


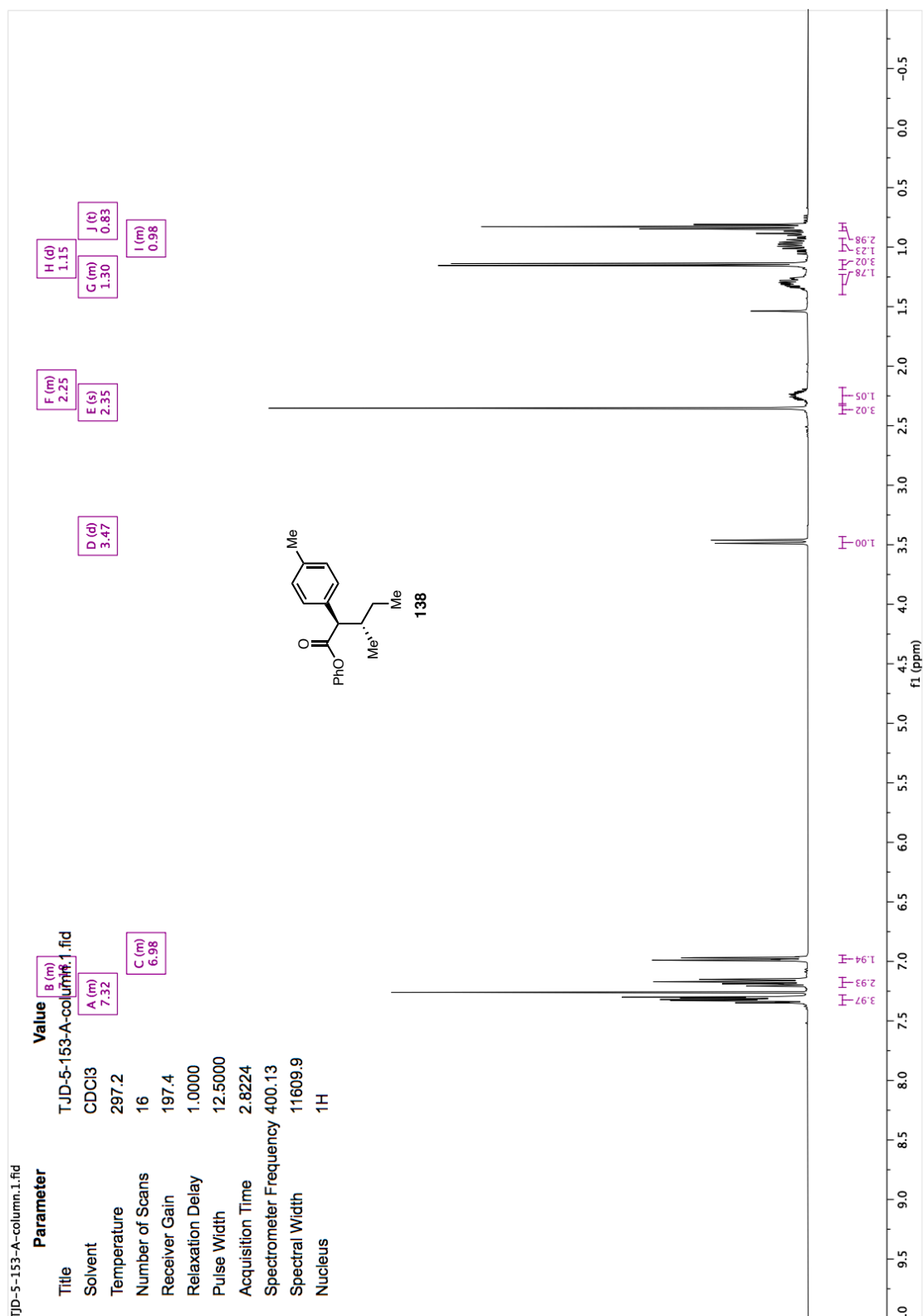


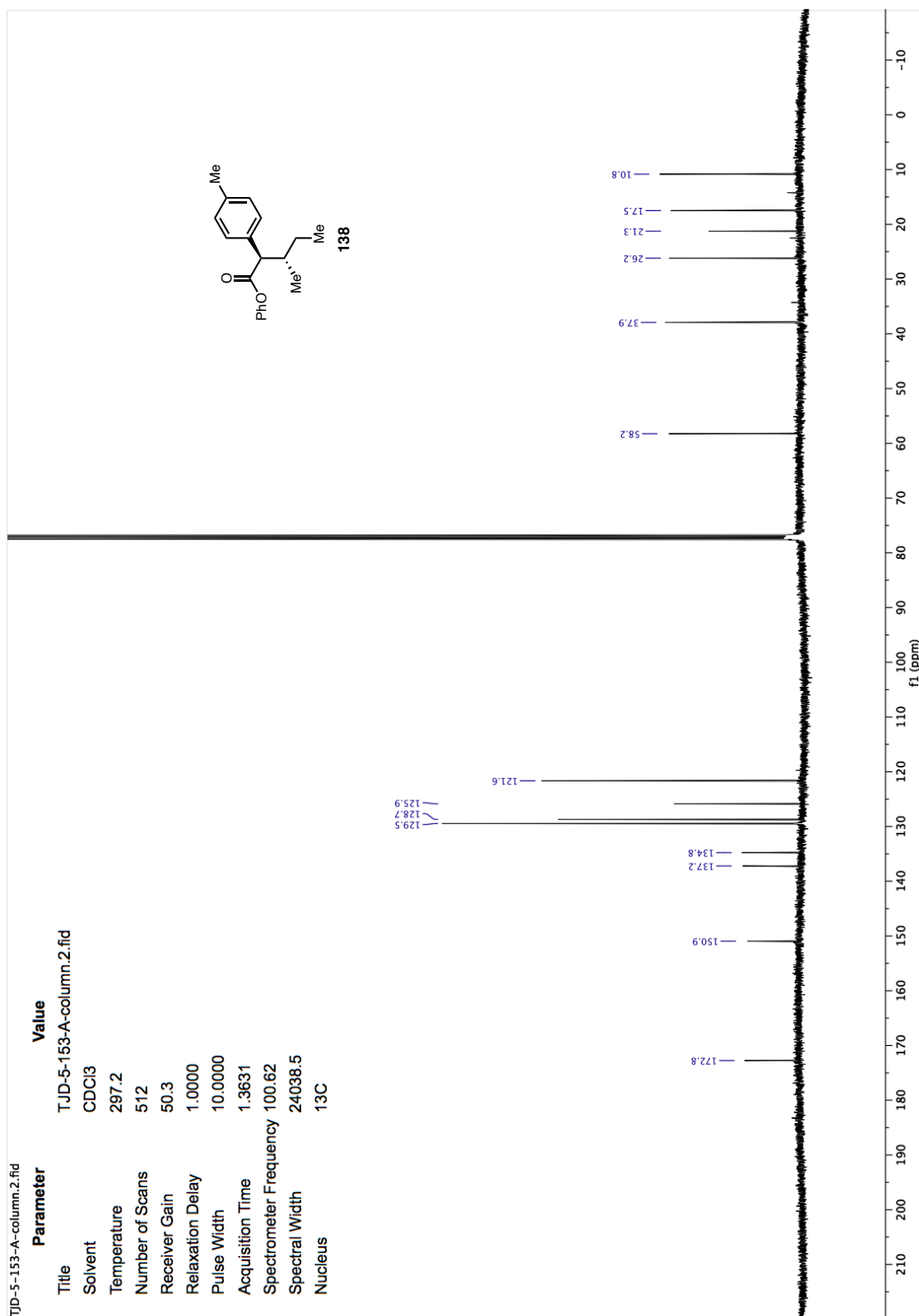


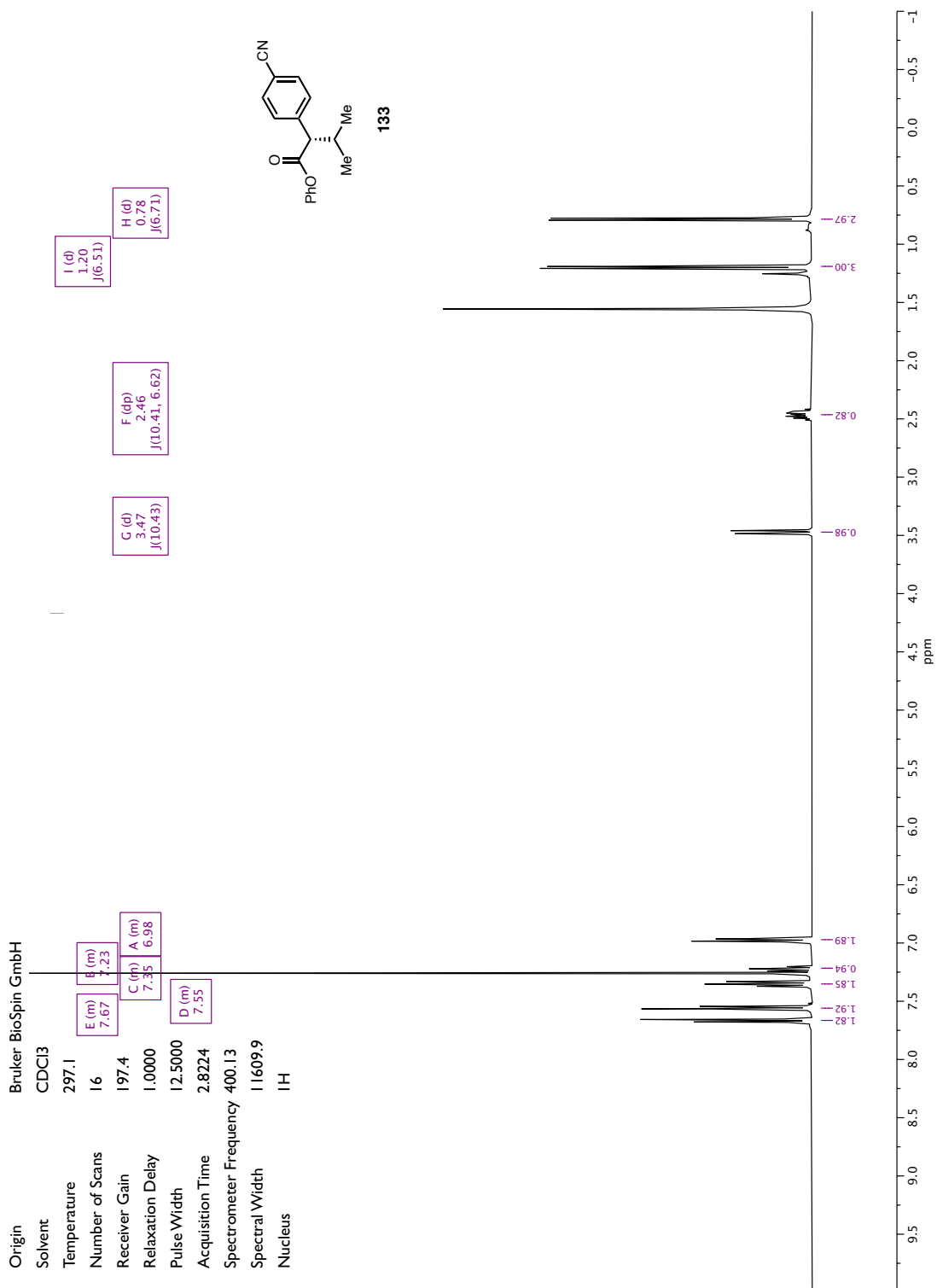


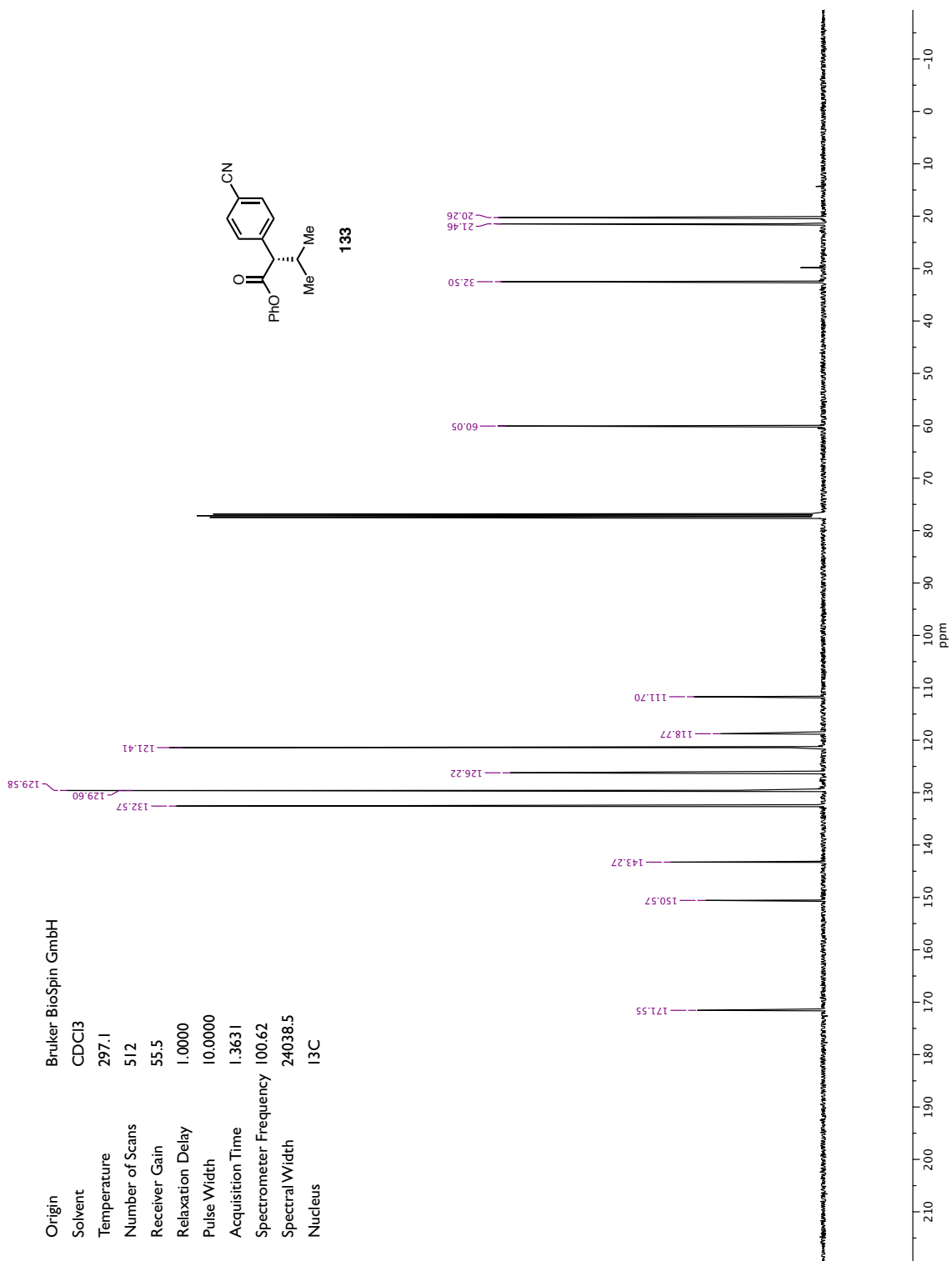






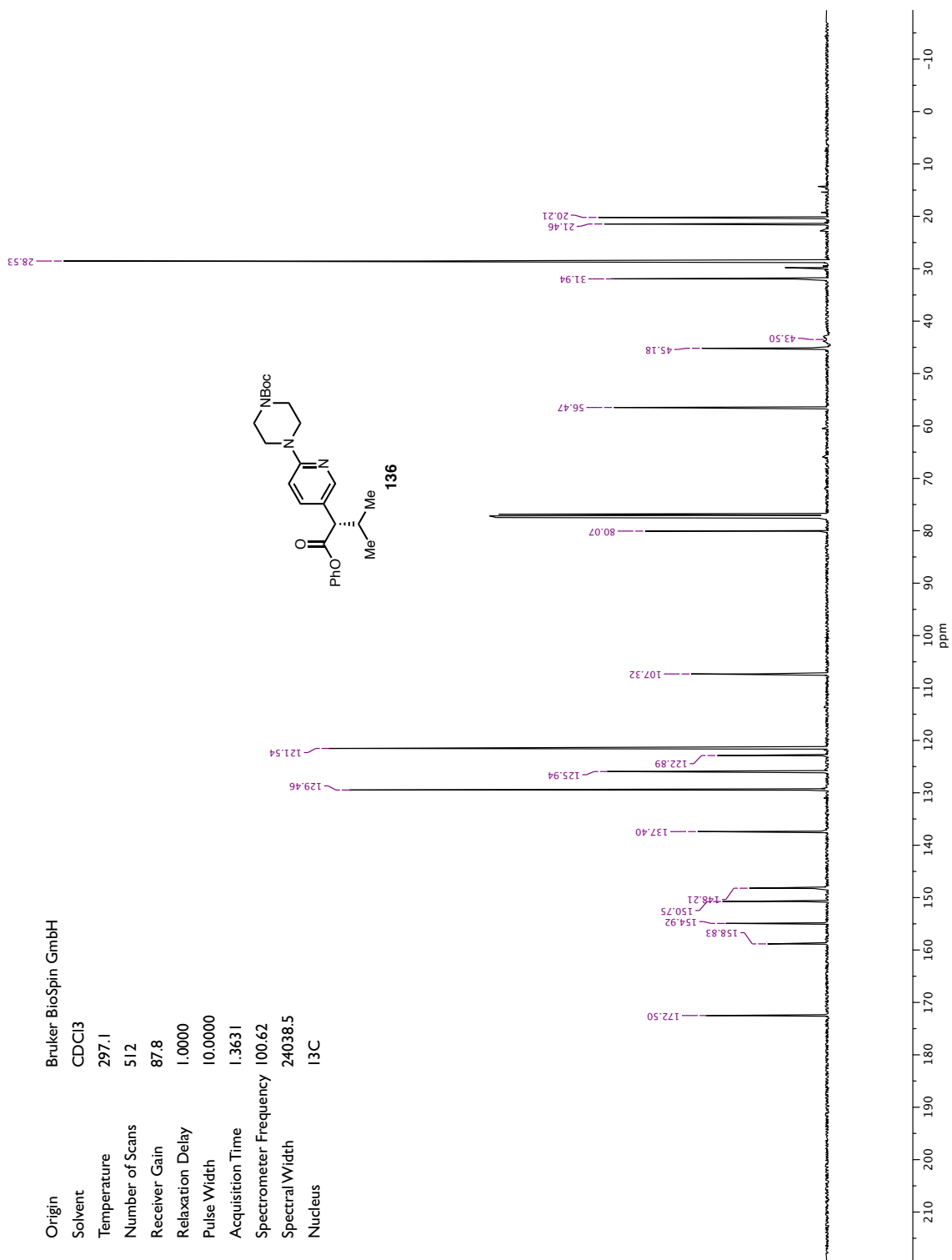


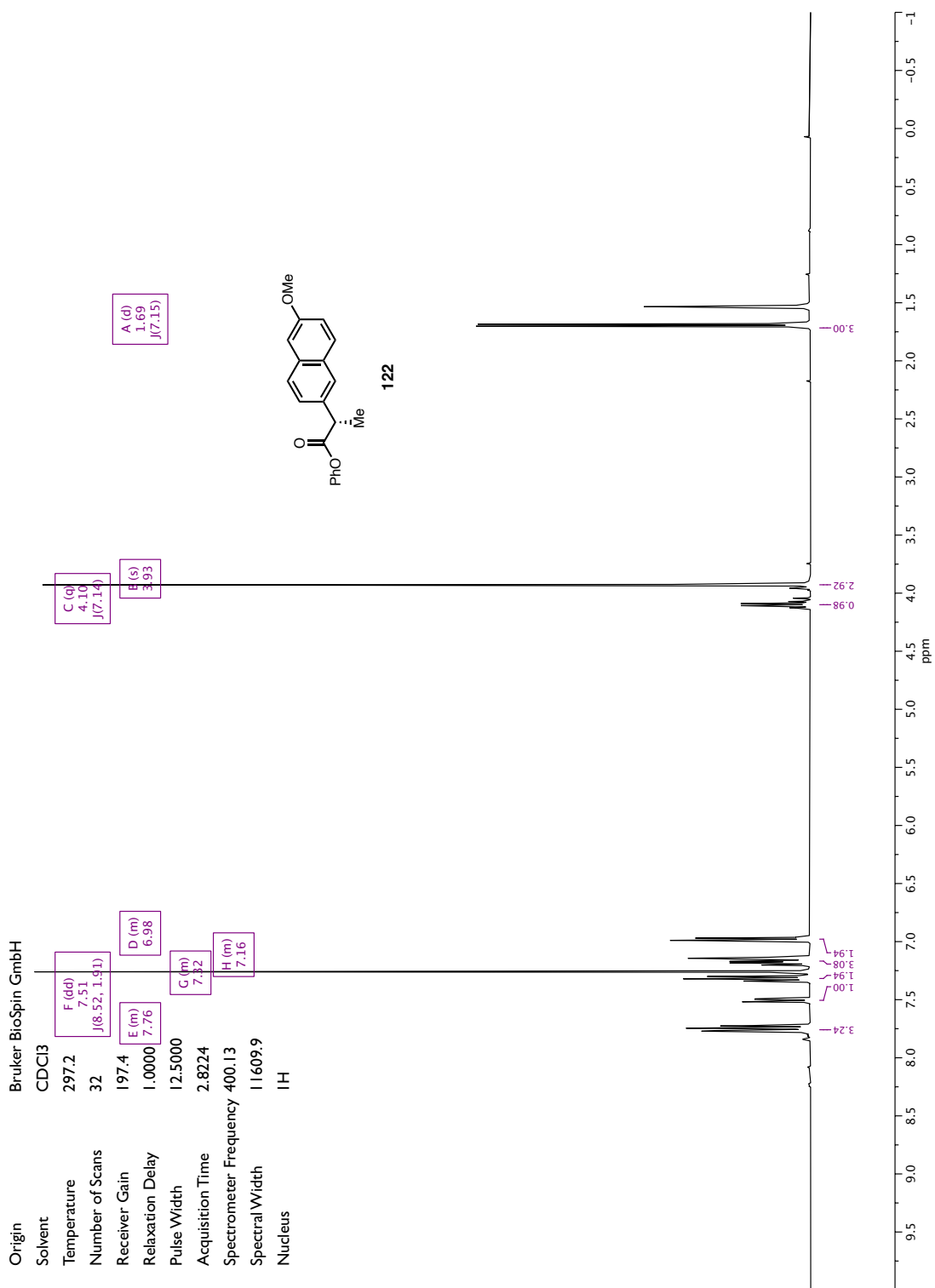


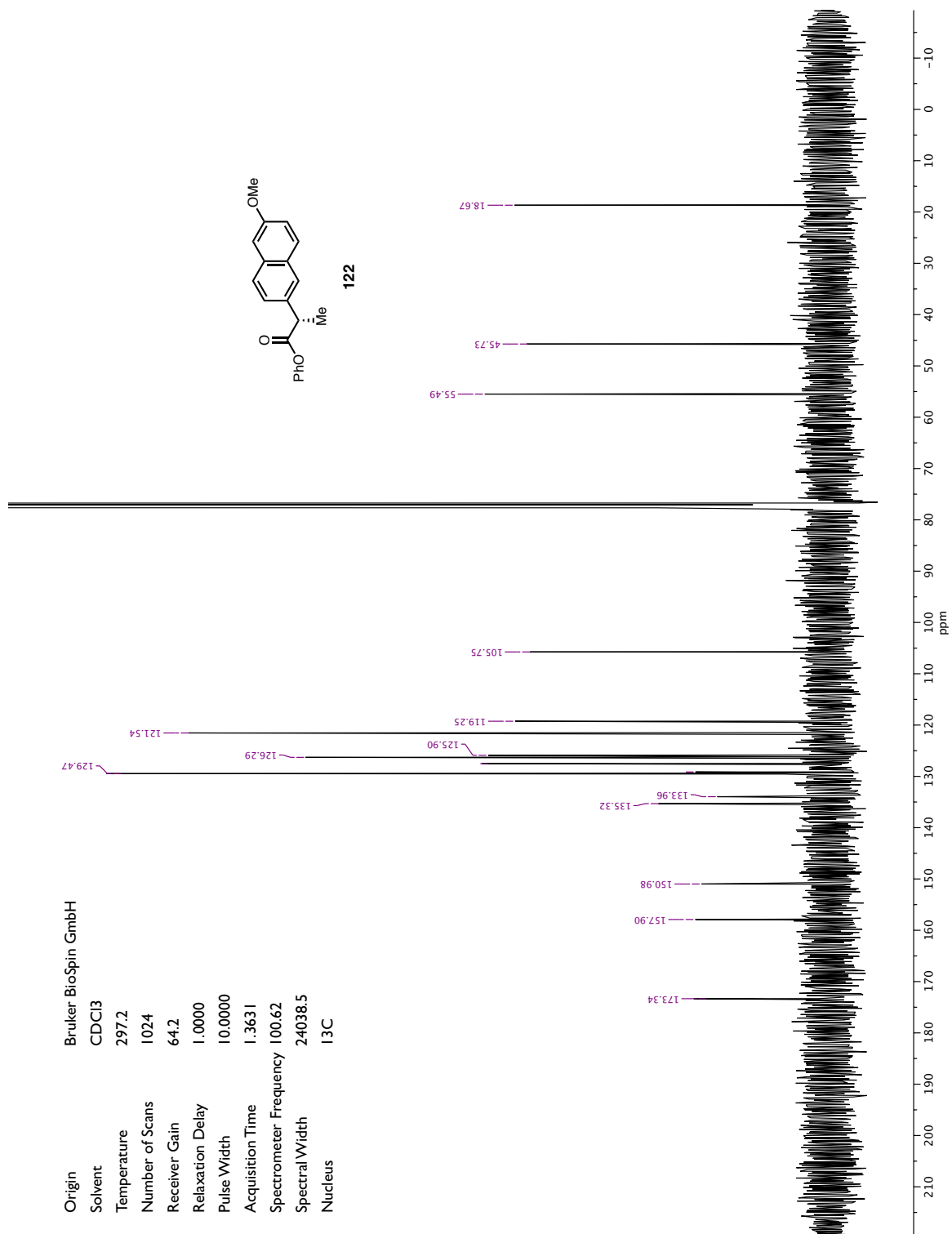


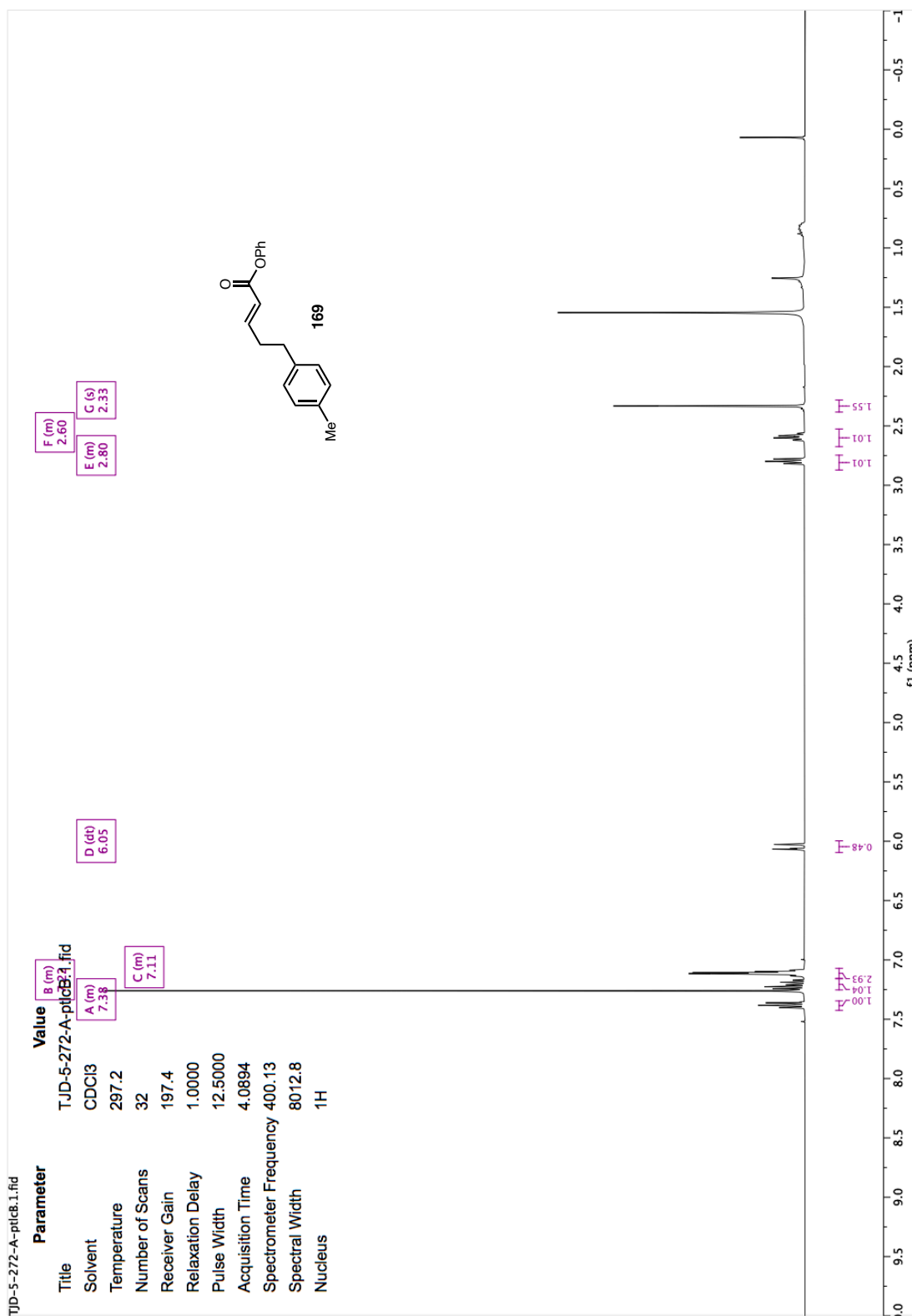


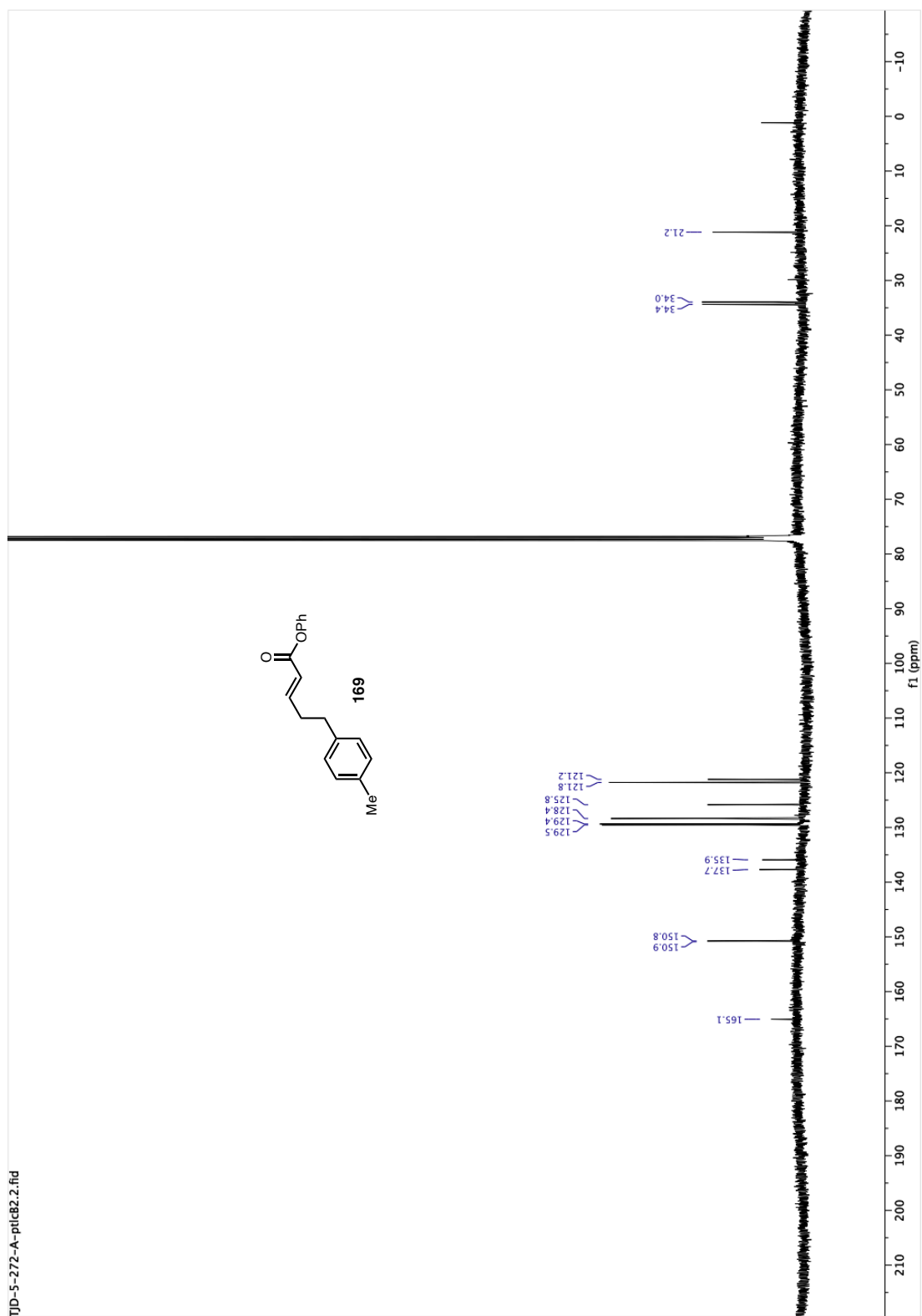


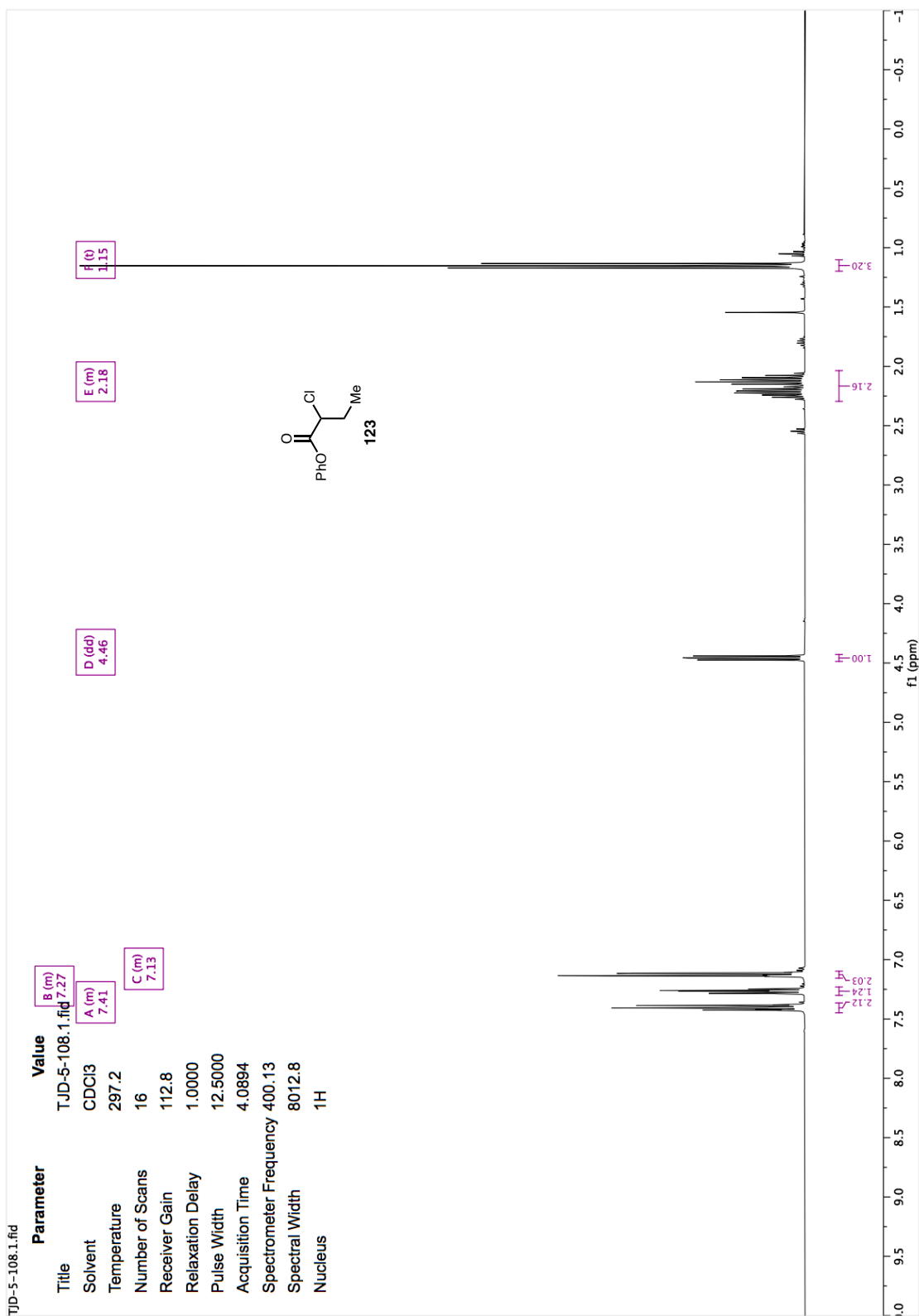


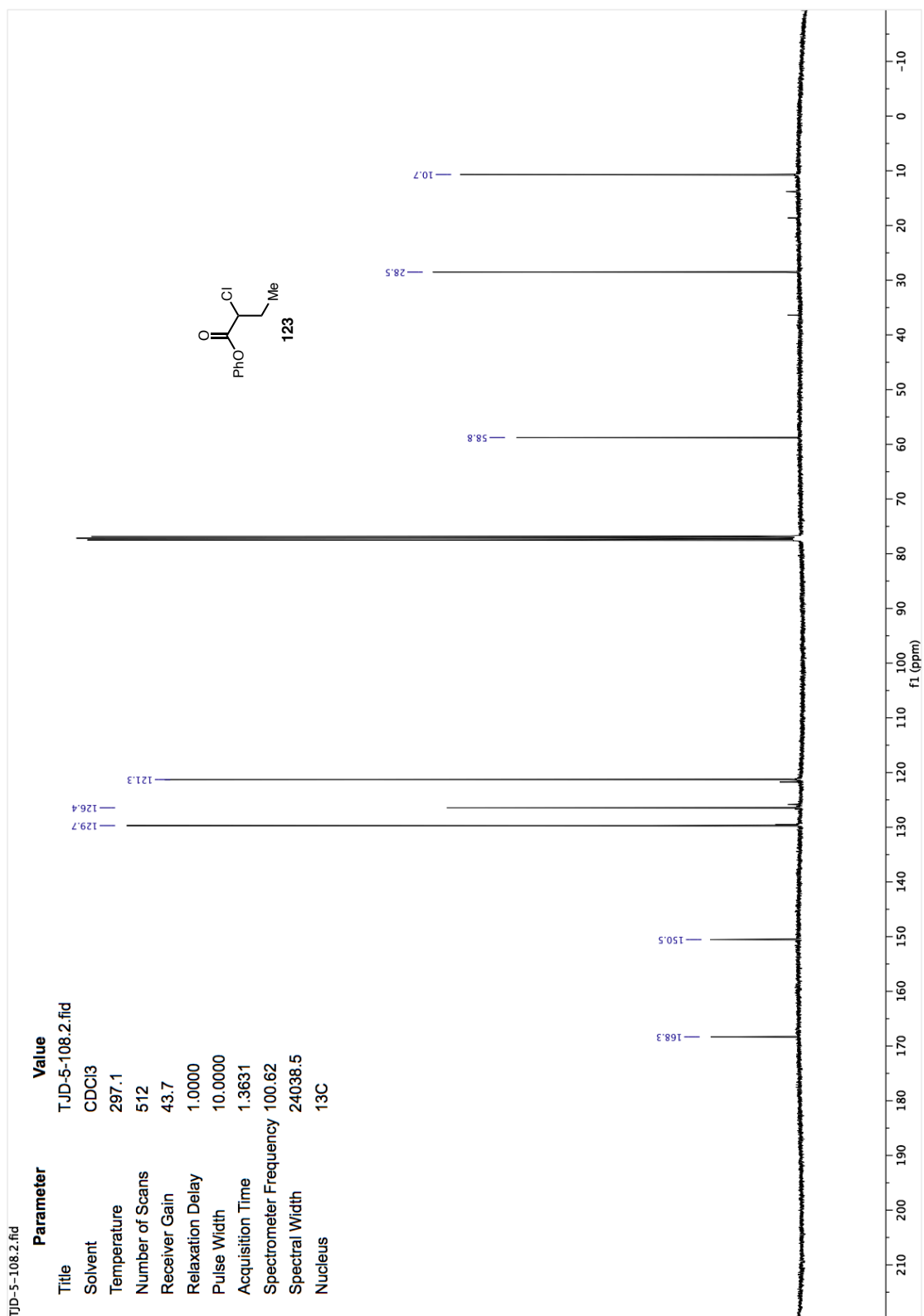


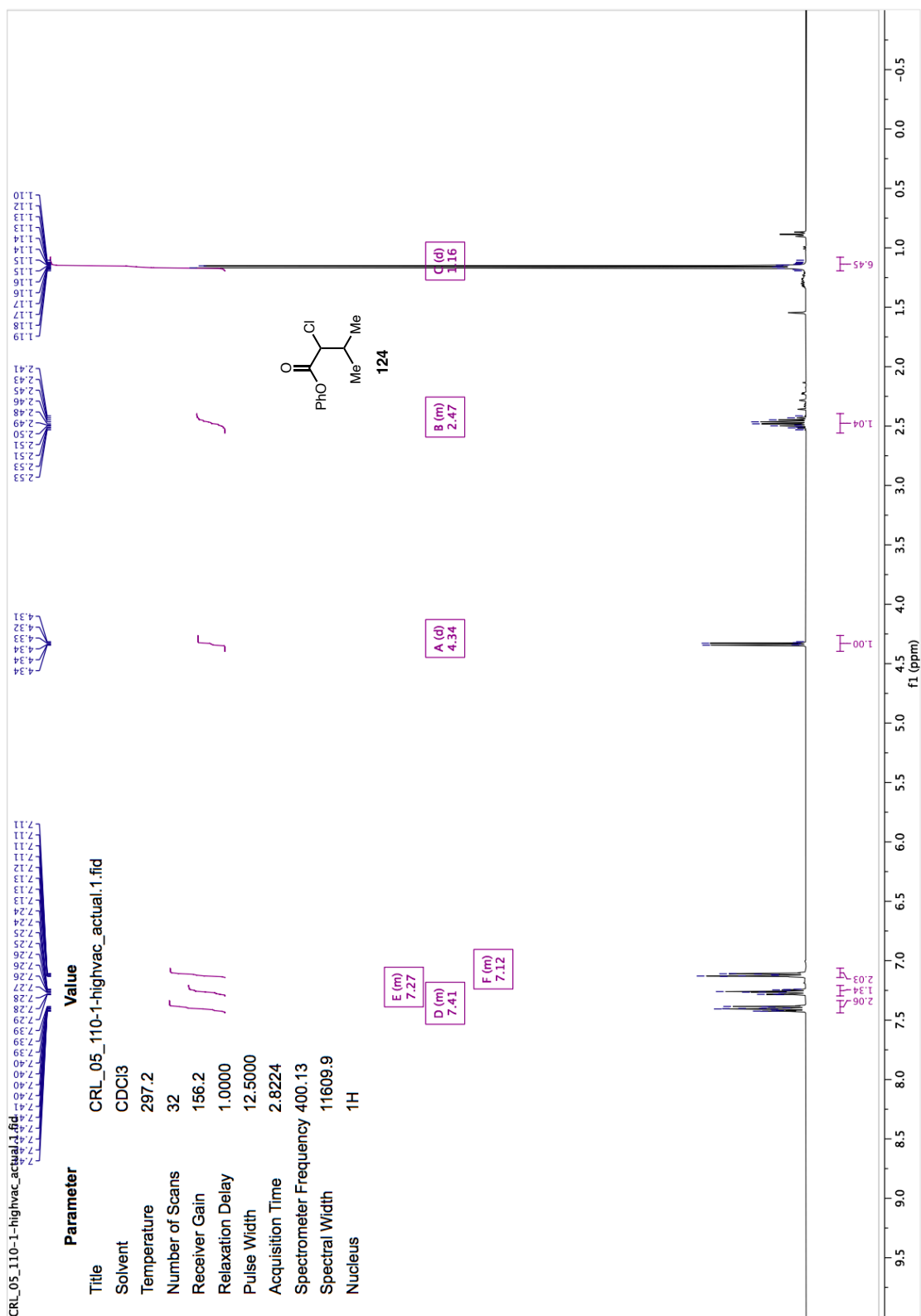




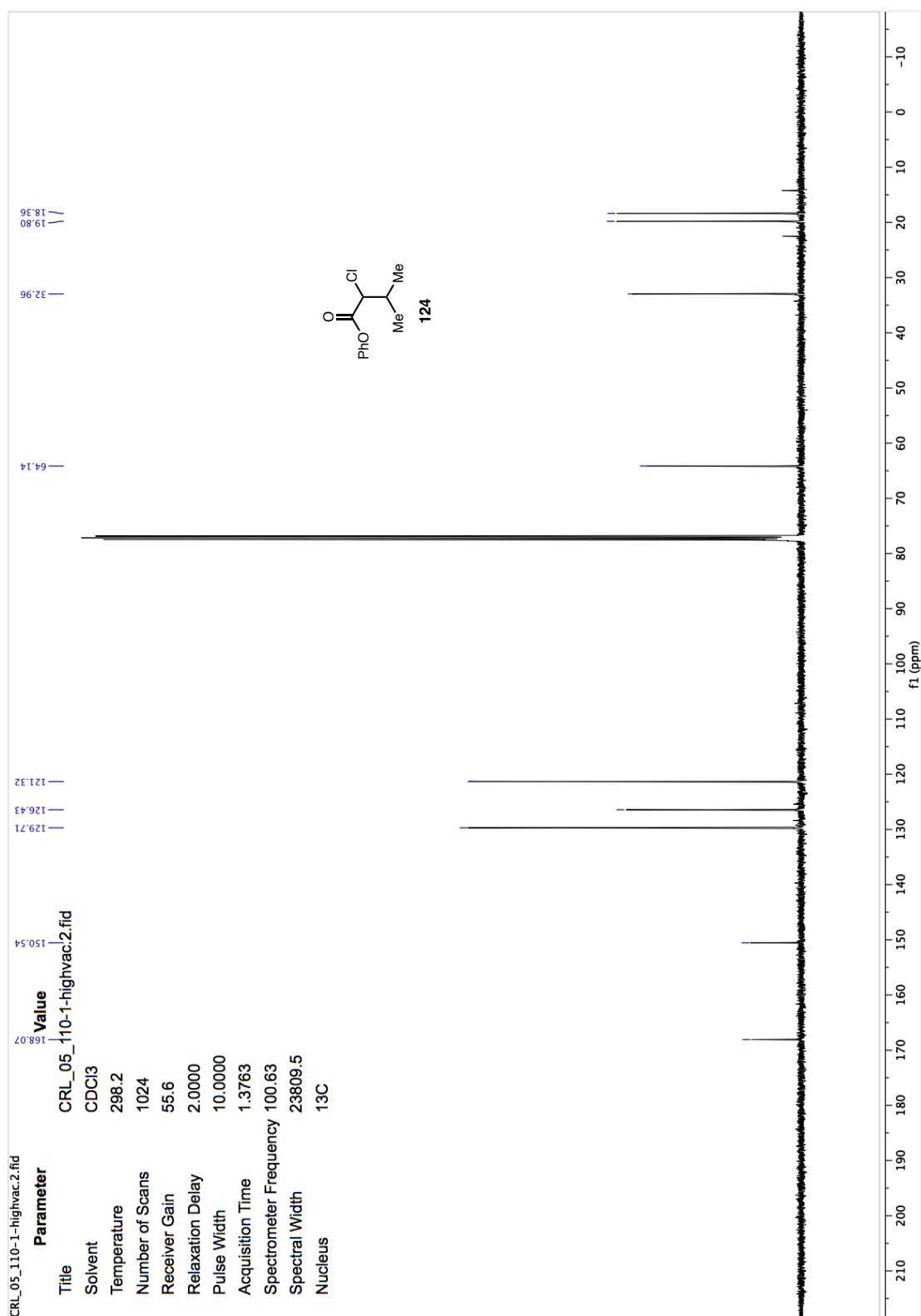


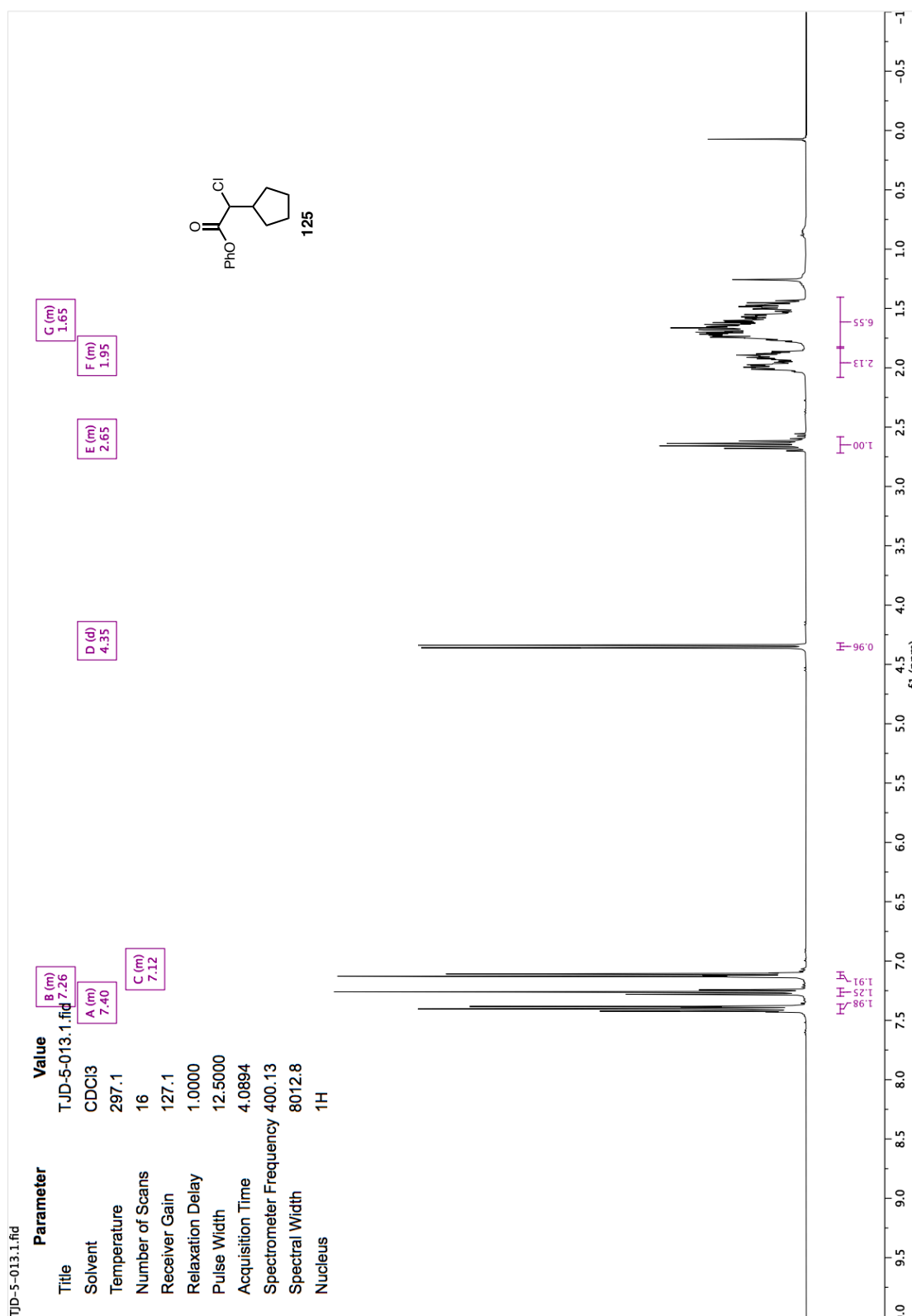


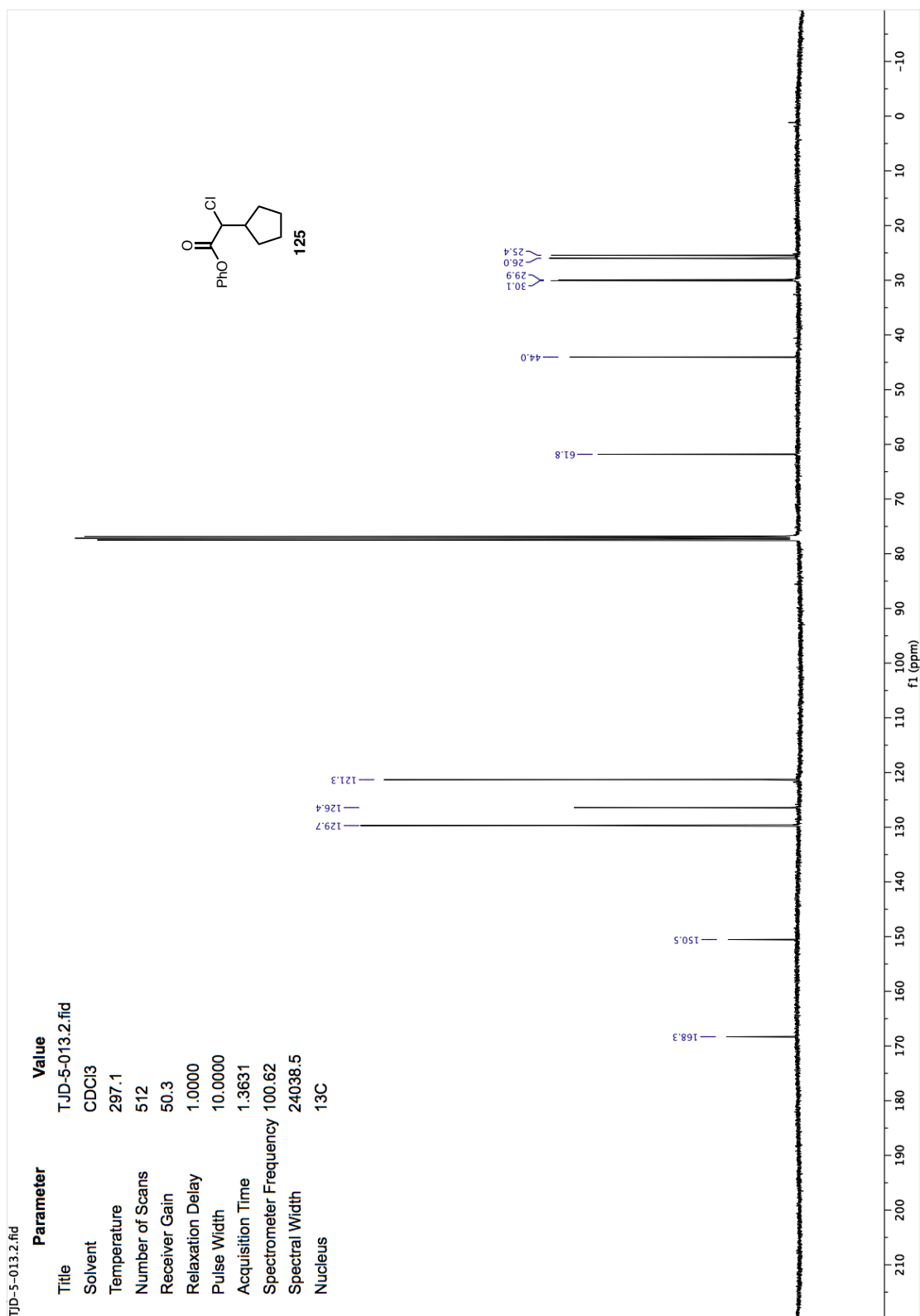


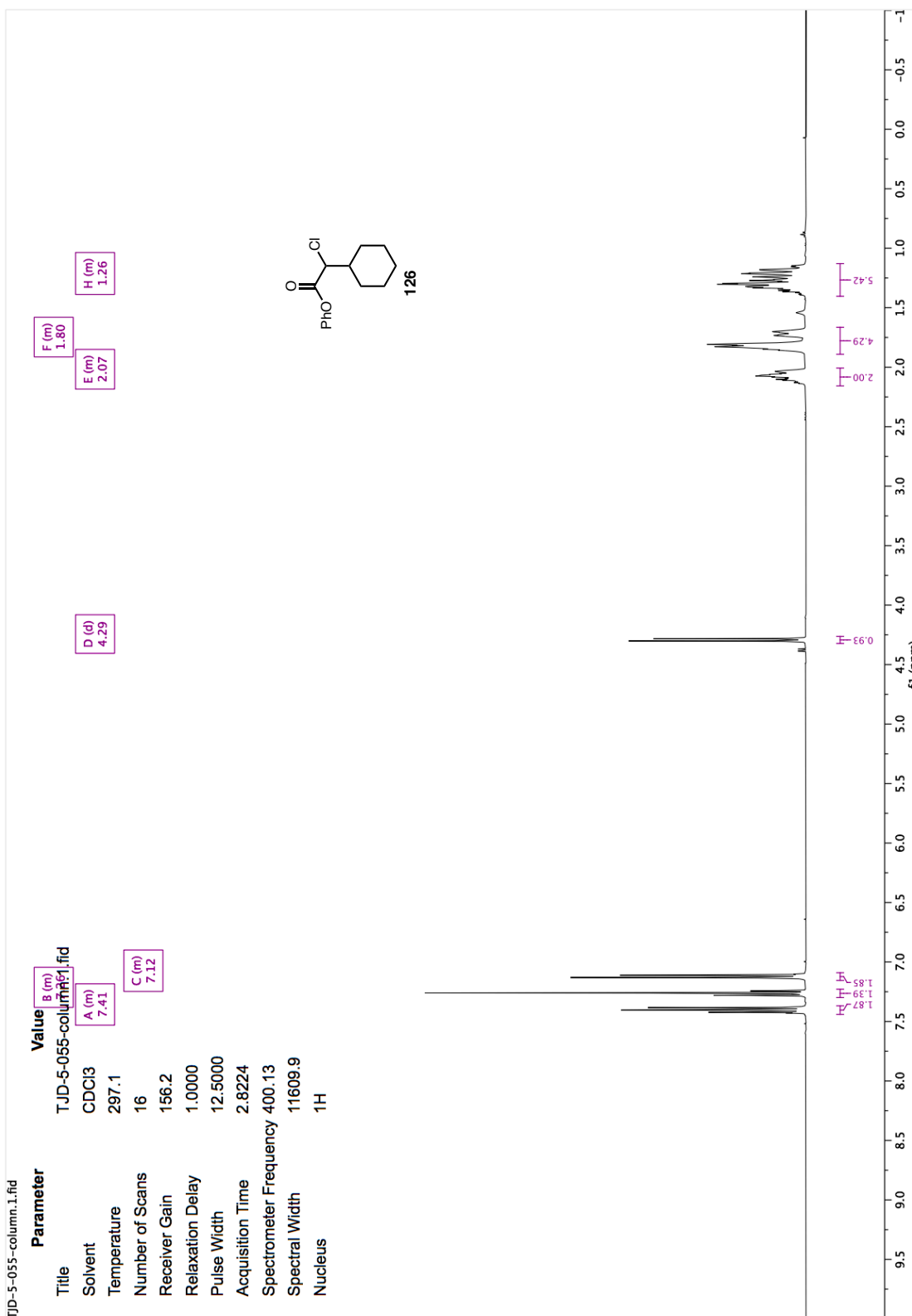


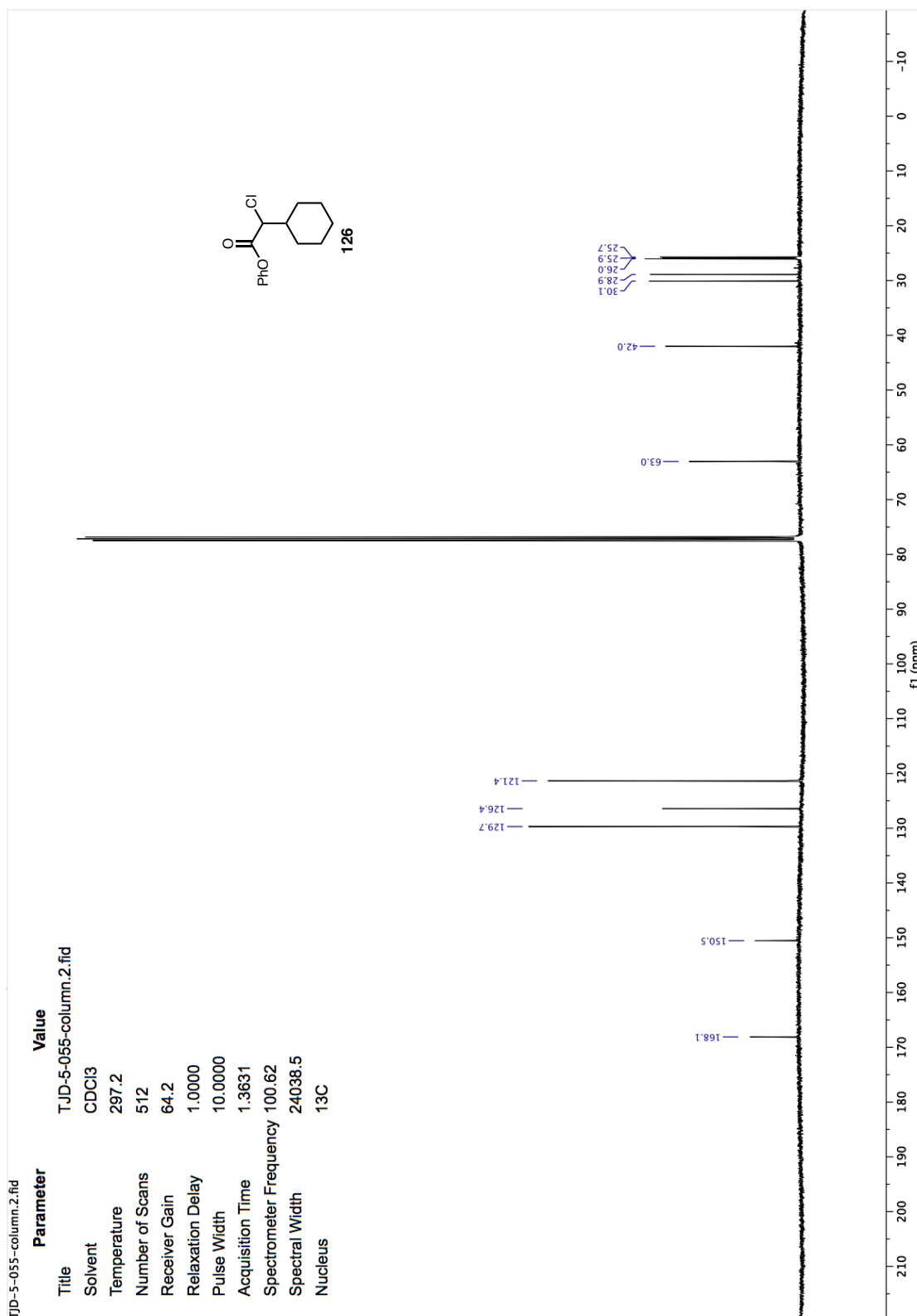


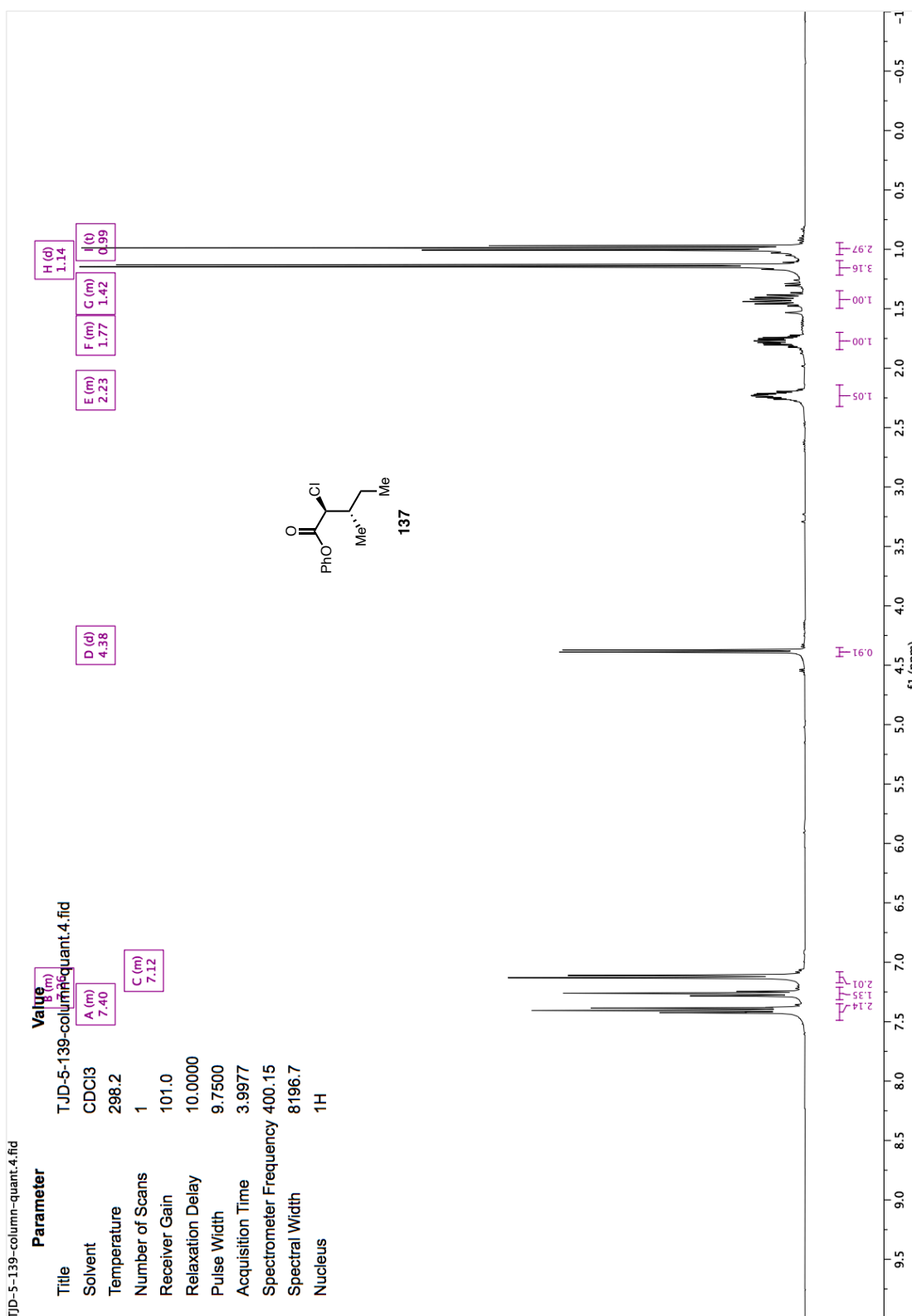


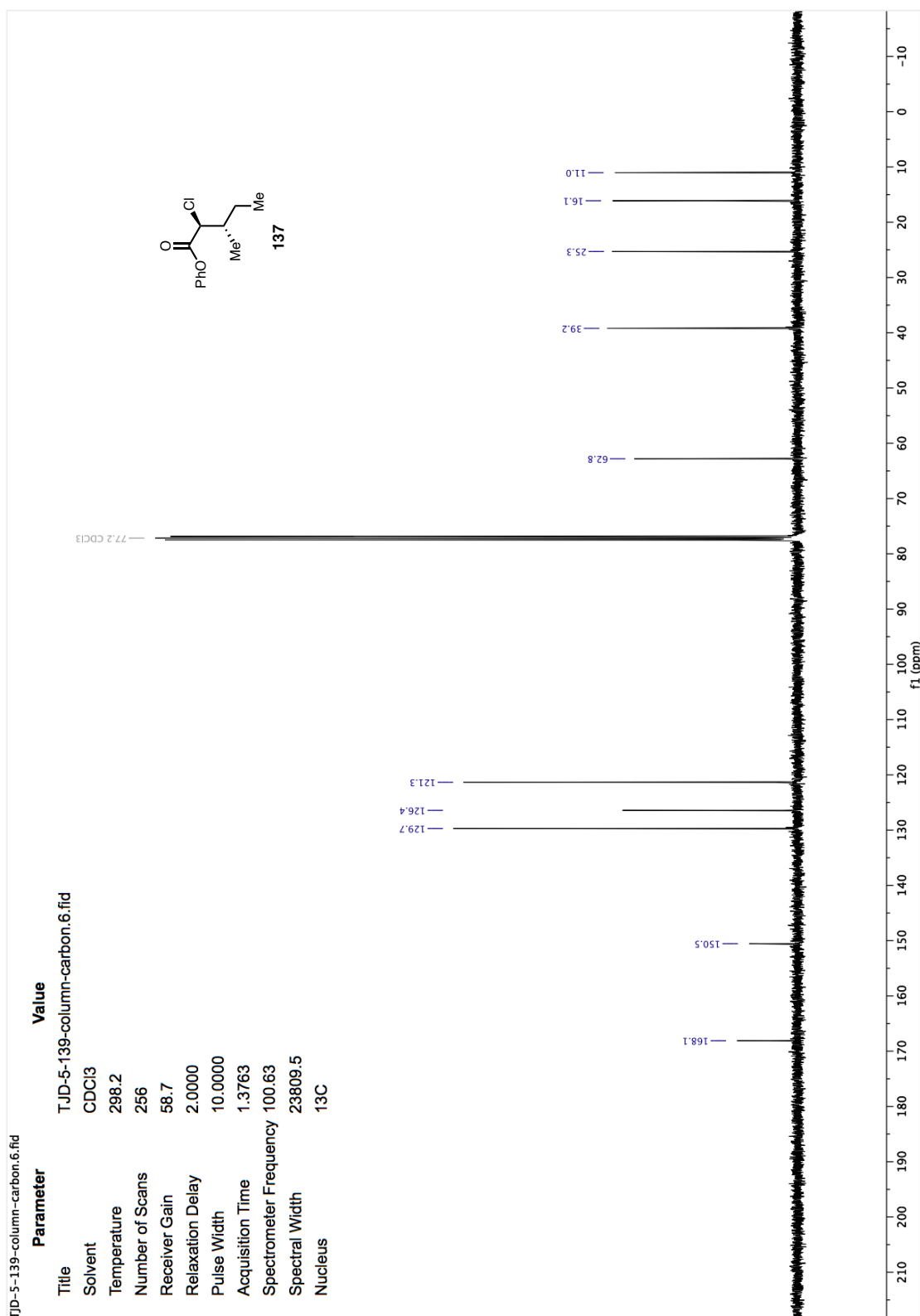


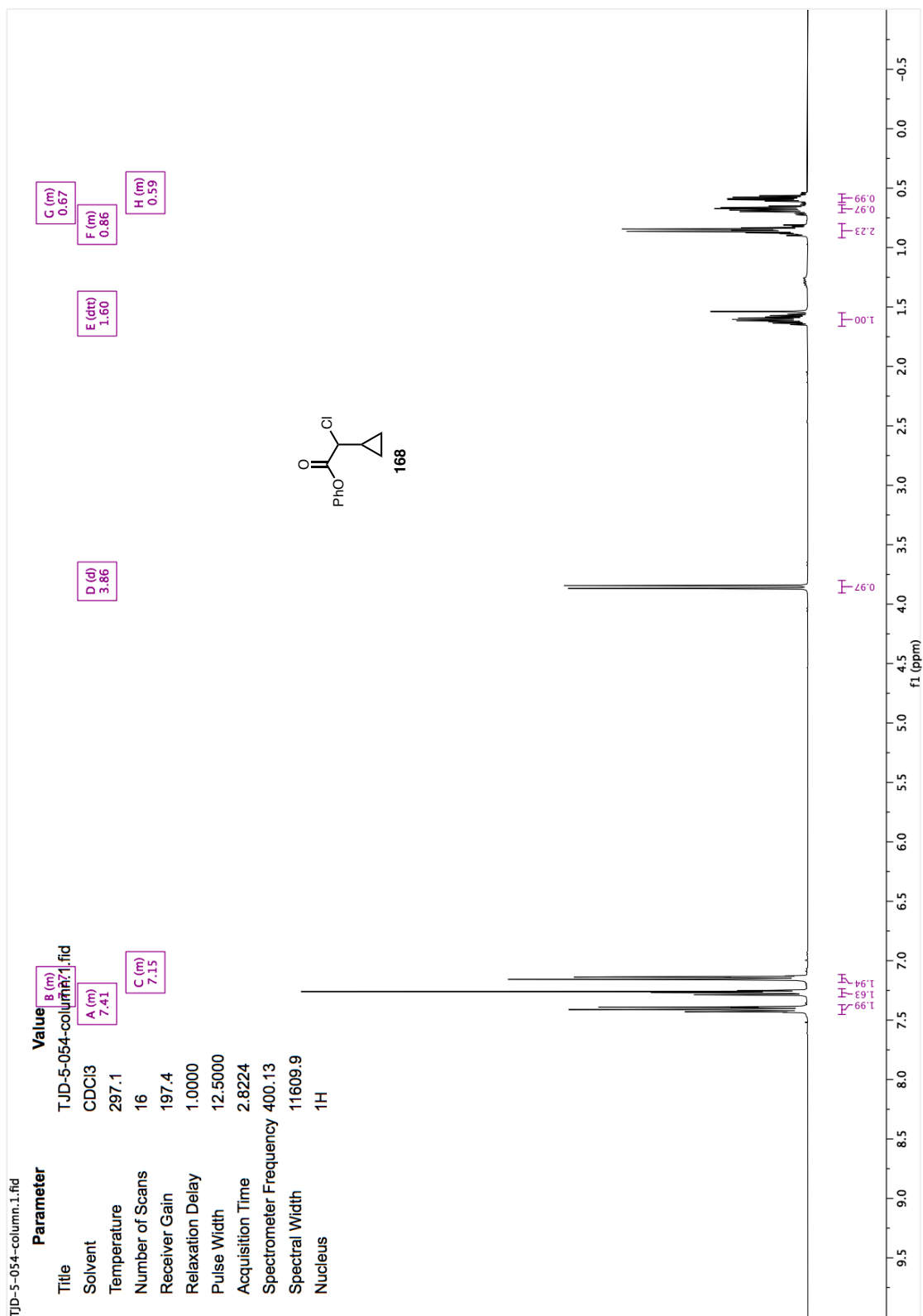




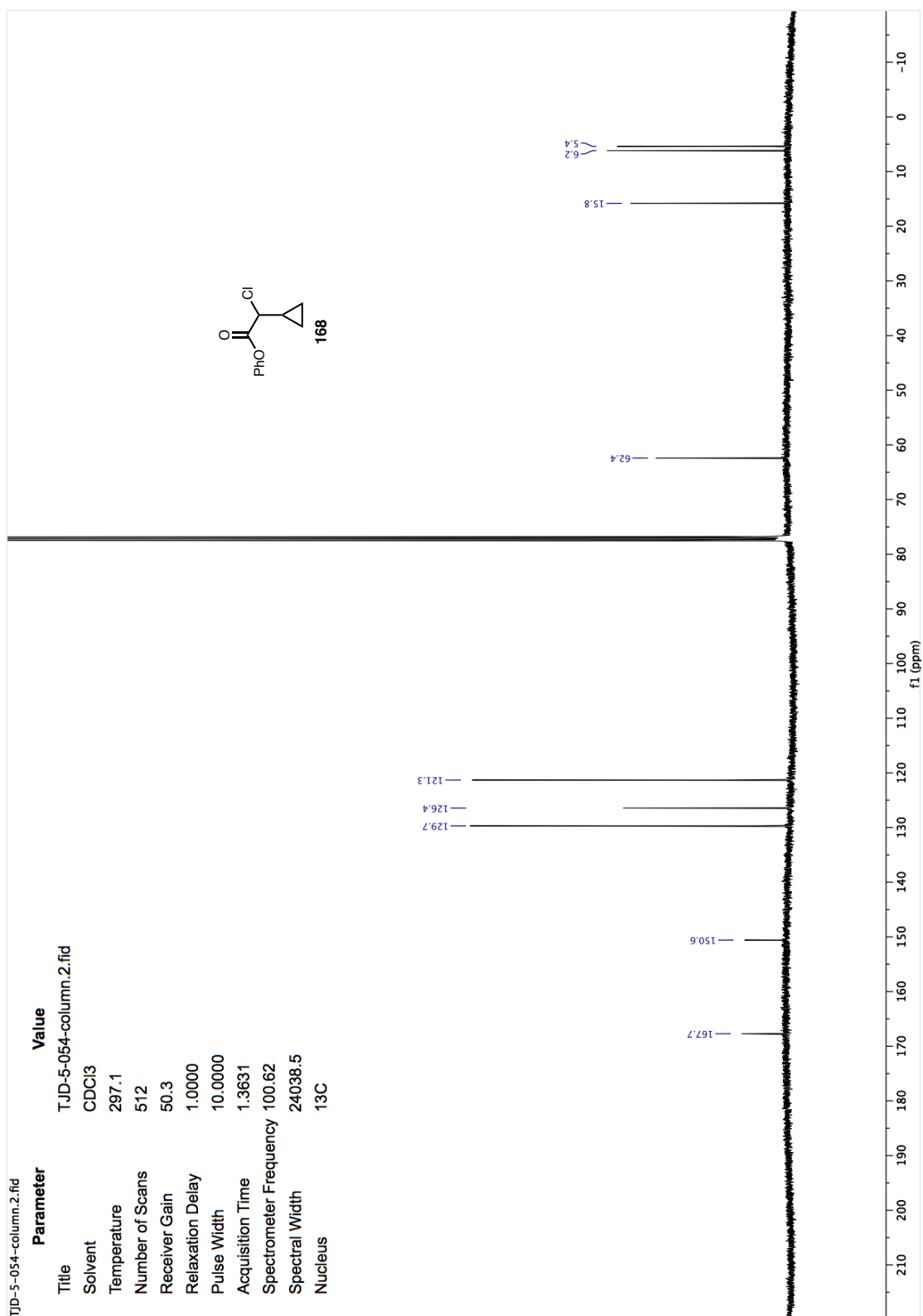


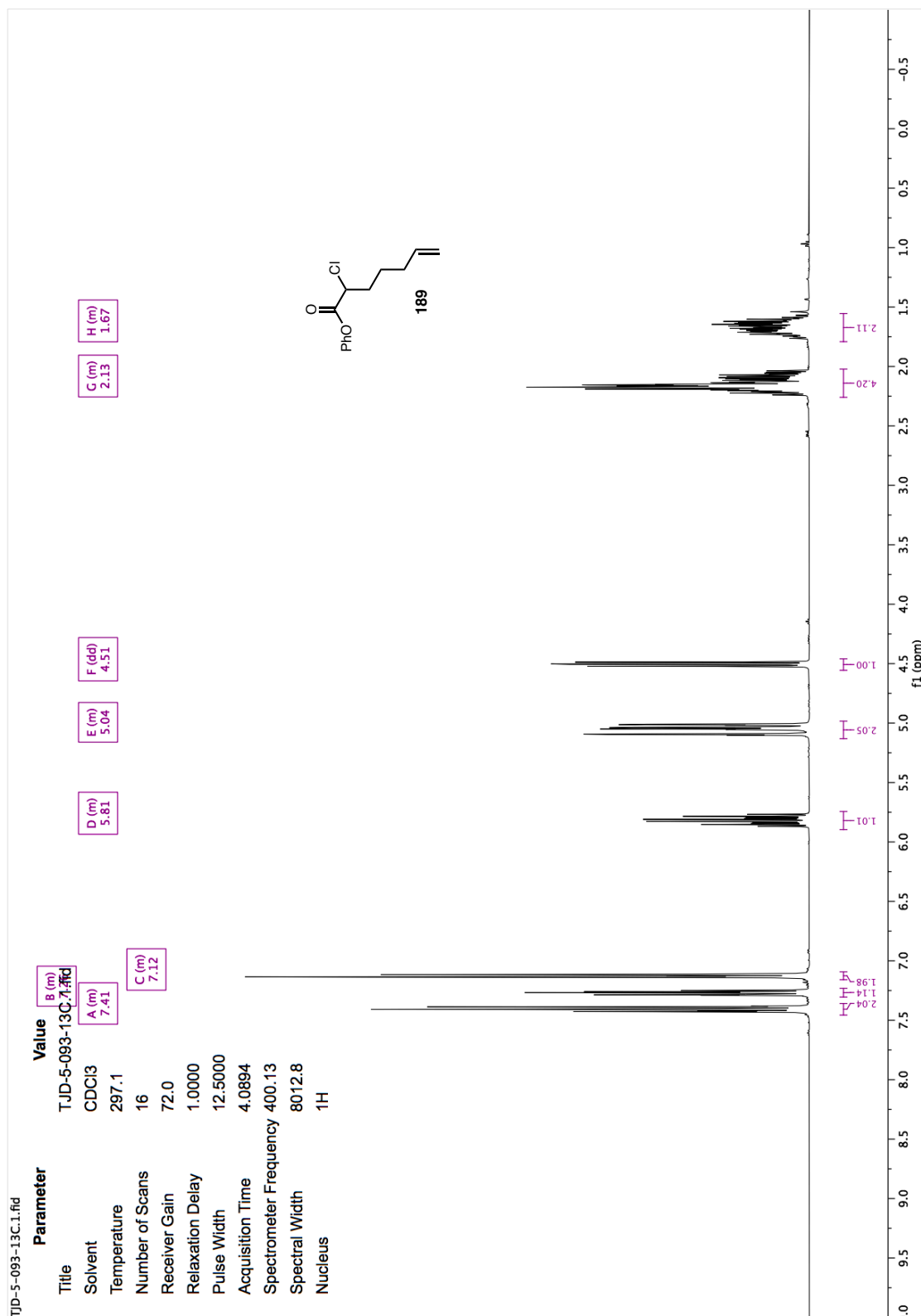


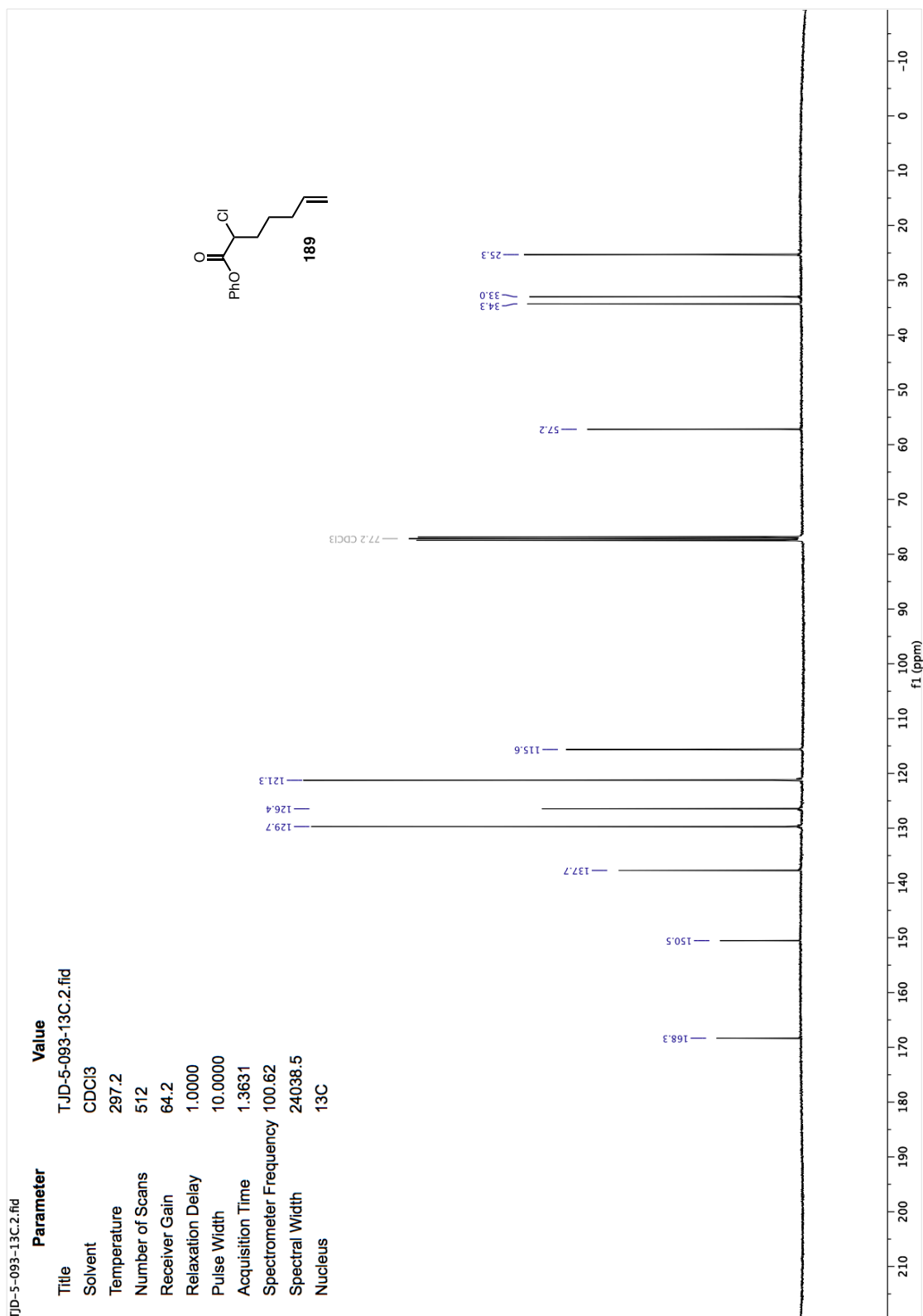


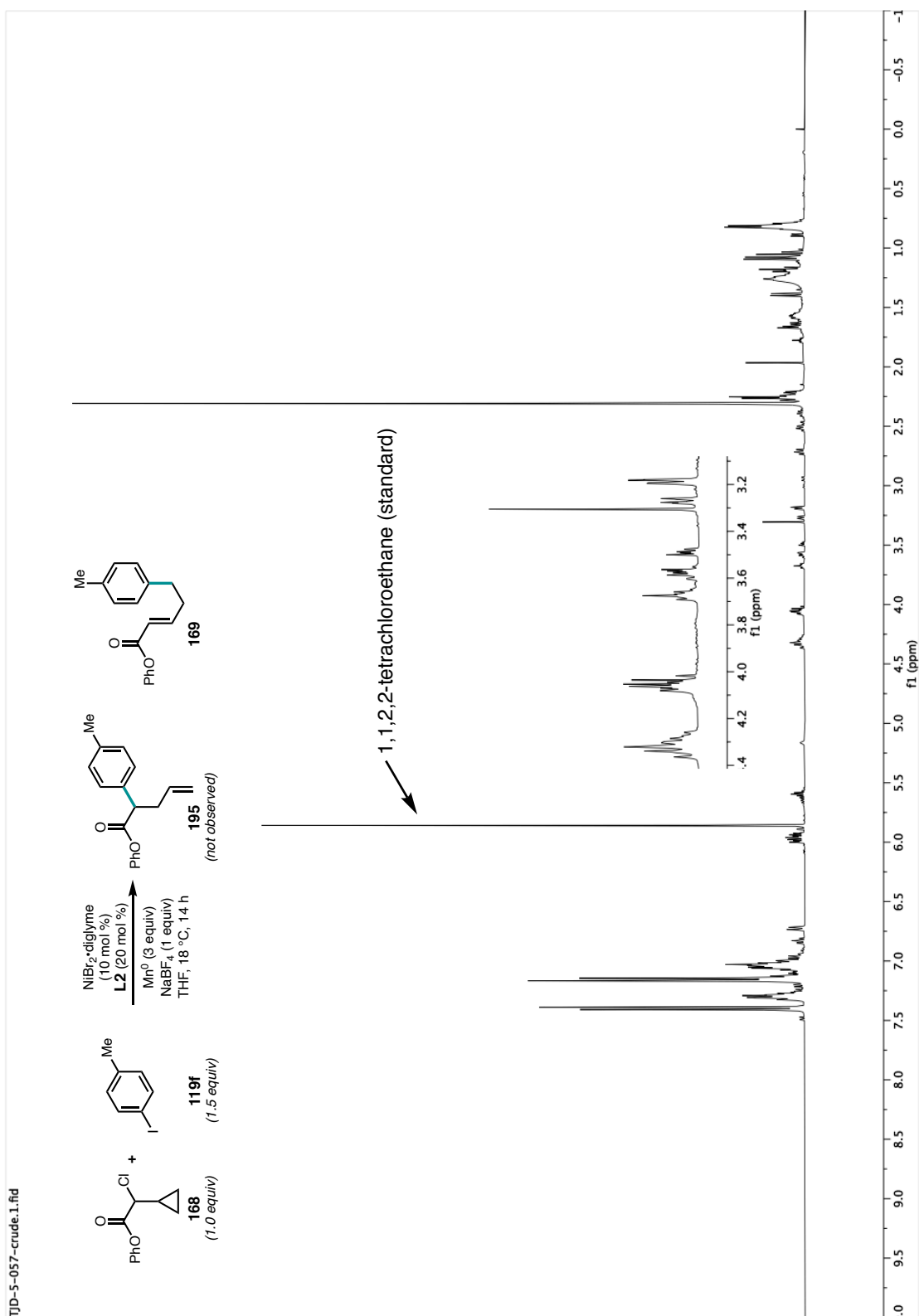


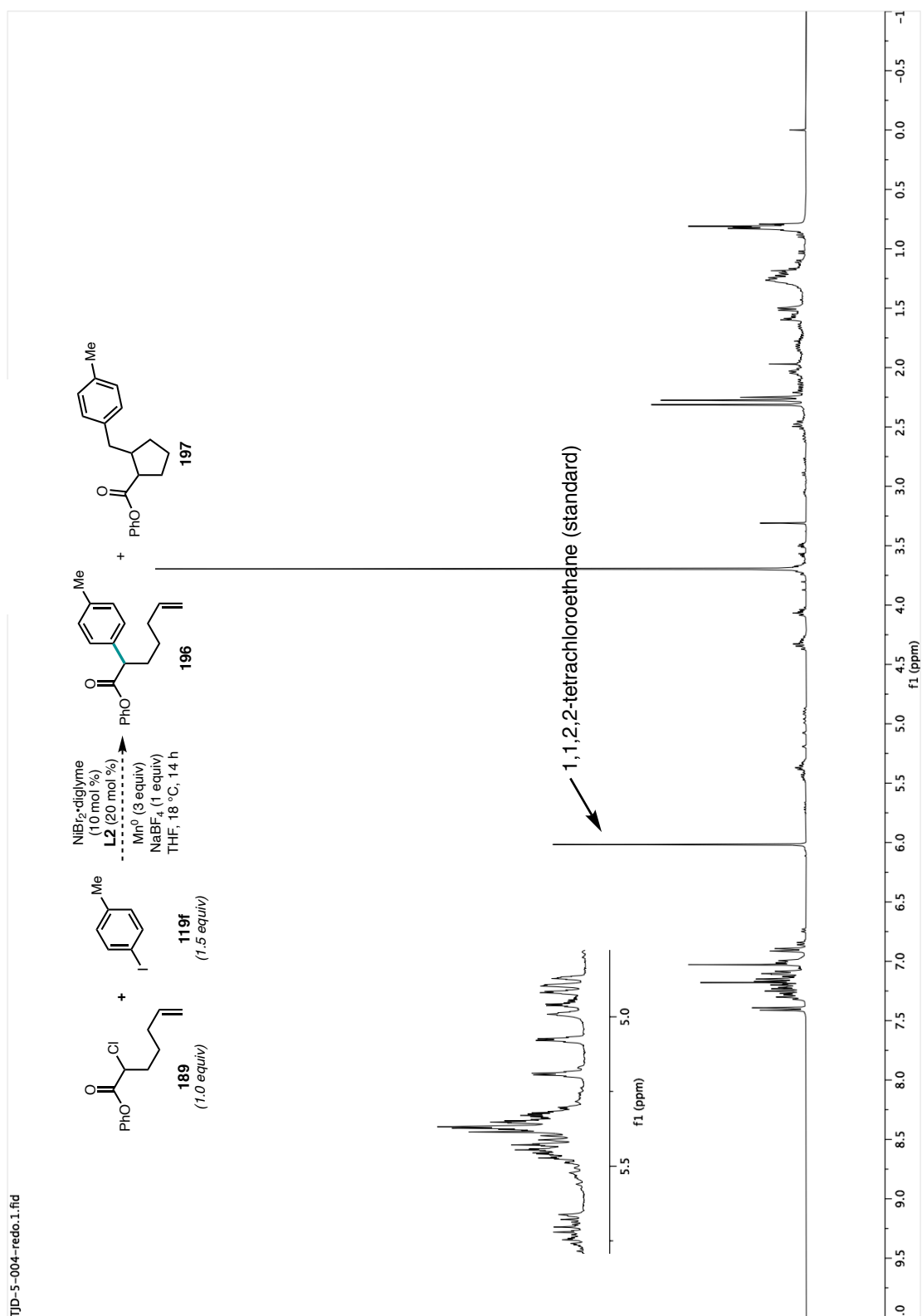












## Chapter 3

### *Enantioselective Synthesis of N-Benzylic Heterocycles by*

### *Nickel/Photoredox Dual Catalysis* †

#### 3.1 INTRODUCTION

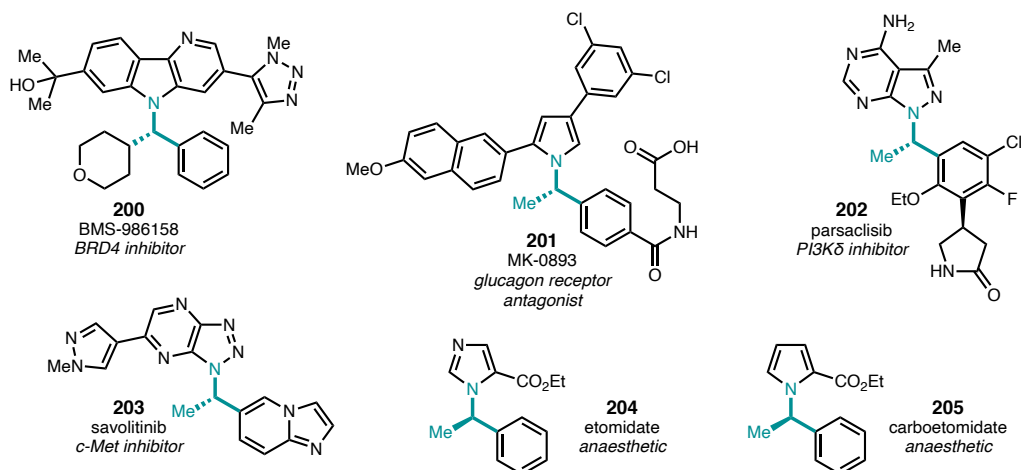
Nitrogen-containing heterocycles are among the most common structural elements present in small molecule pharmaceuticals.<sup>1</sup> The inclusion of a stereocenter and a high fraction of sp<sup>3</sup>-hybridized carbon atoms have both been correlated with small molecule success in medicinal chemistry, as compounds transition from discovery to clinical trials, to eventual approval as drugs. Chiral  $\alpha,\alpha$ -disubstituted *N*-benzylic heterocycles, comprised of both a nitrogen-containing heterocycle and a stereogenic center, are common

---

† Portions of this chapter have been reproduced from a manuscript in preparation and the supporting information found therein. This research was conducted in collaboration with 1) Dr. Caitlin R. Lacker, a graduate student in the Reisman group, and 2) Kevin Belyk, Dr. Jongrock Kong, and Dr. Tiffany Piou, researchers employed by Merck & Co., Inc. Fellowship support was provided by the NSF (T.J.D, C.R.L. DGE-1144469). Financial support was provided by the NIH (S.E.R. R35GM118191) and Merck Sharp and Dohme, a subsidiary of Merck & Co., Inc.

substructures in bioactive compounds; a number of marketed drugs and clinical candidates possess this conserved structural motif (Figure 3.1).<sup>1–6</sup>

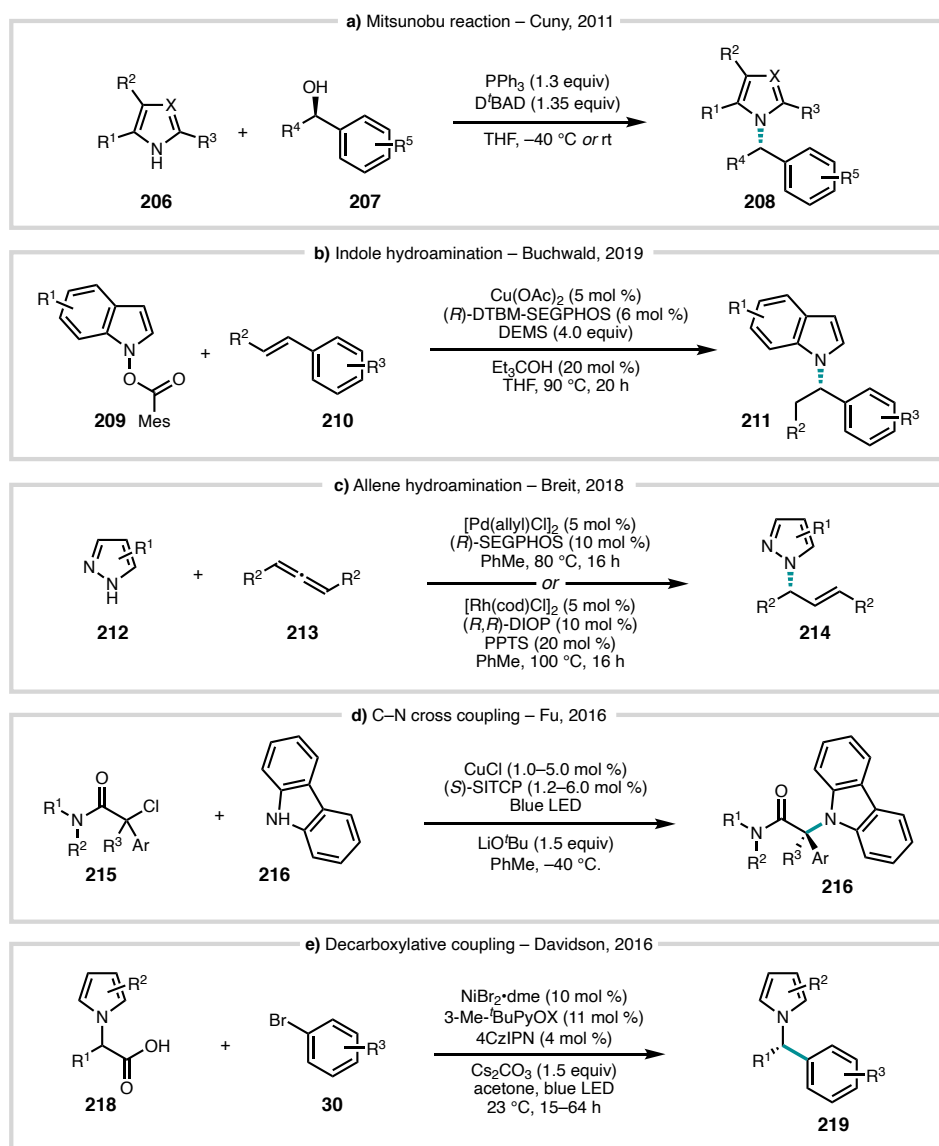
**Figure 3.1** Bioactive chiral  $\alpha$ -substituted *N*-benzylic heterocycles.



In early-stage discovery chemistry, small molecules are often synthesized as racemates or mixture of diastereomers, which can be separated by chiral chromatography and individually tested in assays of interest. This approach can prove quite successful, but as a lead compound progresses through development, synthesis of the compound as a single stereoisomer is typically desired.<sup>7</sup> A number of strategies have been developed for the synthesis of enantioenriched *N*-benzylic heterocycles (Figure 3.2). A common approach, as exemplified by Cuny and coworkers, is the Mitsunobu displacement of an enantioenriched alcohol by an N–H heterocycle (Figure 3.2a).<sup>8,9</sup> Though powerful, this approach requires the enantioselective synthesis of an alcohol precursor, is sensitive to the acidity and nucleophilicity of the N–H heterocycle, and can suffer from erosion of enantiopurity depending on the coupling partners and conditions employed. Hydroamination has also been leveraged for the formation of enantioenriched *N*-benzylic

and allylic heterocycles.<sup>10–12</sup> In 2019, Buchwald and coworkers reported an elegant highly enantioselective CuH-catalyzed alkylation of indole derivatives (Figure 3.2b).<sup>11</sup> Breit and coworkers reported two systems for asymmetric hydroamination of allenes with pyrazoles, using either Pd or Rh catalysts (Figure 3.2c).<sup>10</sup> In a related report, Dong and coworkers reported the enantioselective addition of pyrazoles to 1,3-dienes.<sup>12</sup> In general, these

**Figure 3.2** Enantioselective synthesis of N-benzylic and N-allylic heterocycles.





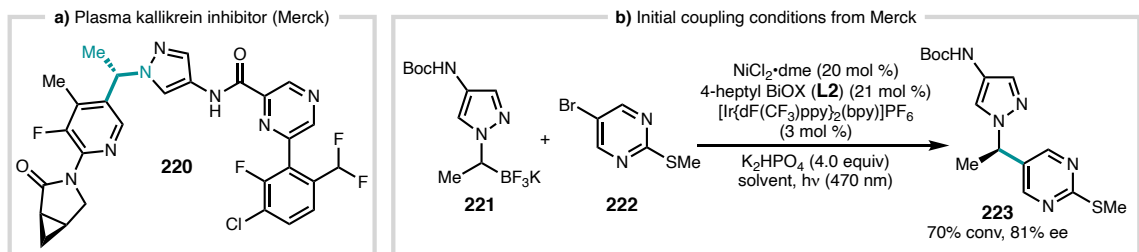
enantioselective hydroamination reactions tend to require substantially different conditions for different classes of heterocycles, limiting their generality and applicability to analog synthesis.

Several photochemical methods have also been reported for the synthesis of enantioenriched *N*-benzylic heterocycles. Fu and coworkers reported an elegant C–N cross-coupling promoted by a single copper complex as both the photocatalyst and source of enantioselectivity (Figure 3.2d).<sup>13</sup> This reaction forms  $\alpha$ -tertiary carbazoles and indoles in excellent yields and enantioselectivities, though an amide radical-stabilizing group is required on the alkyl chloride. Especially interesting to us was a report from Bonifazi and Davidson detailing the decarboxylative coupling of  $\alpha$ -*N*-heterocyclic carboxylic acids with aryl bromides under Ni/photoredox catalysis (Figure 3.2e).<sup>14</sup> This reaction provides rapid access to *N*-benzylic heterocycles from easily-synthesizable precursors. Although powerful, this reaction typically proceeded in 40–80% ee, with the most selective examples being formed in low yields.

Nickel/photoredox dual catalysis has emerged in recent decades as a powerful strategy for forming carbon–carbon and carbon–heteroatom bonds due to its mild reaction conditions and often broad substrate scopes.<sup>15,16</sup> Despite the widespread adoption of Ni/photoredox catalysis, there have been relatively few reports of enantioselective methods.<sup>17</sup> Inspired by seminal reports from Molander<sup>18</sup> and Fu/MacMillan<sup>19</sup> as well as the work of Bonifazi and Davidson,<sup>14</sup> we sought to leverage this reaction manifold for the highly enantioselective synthesis of *N*-benzylic heterocycles. We hoped that we could use potassium alkyl trifluoroborates as radical precursors,<sup>20,21</sup> and find a chiral catalyst system that would enable high enantioselectivities across a broad range of substrates.

This transformation was of particular interest to researchers at Merck, who have recently disclosed a series of plasma kallikrein inhibitors containing this motif (Figure 3.3a).<sup>22</sup> Using high-throughput screening,<sup>23</sup> chemists at Merck identified preliminary conditions for the coupling of potassium trifluoroborate **221** with aryl bromides to form enantioenriched *N*-benzylic heterocycles such as **223**, using a ligand, 4-heptyl BiOX (**L2**), developed in our lab (Figure 3.3b).<sup>24</sup> Promisingly, their initial results using **L2** were higher yielding and more selective than Bonifazi and Davidson's reaction for similar substrates.<sup>14</sup> Unfortunately, issues were encountered with reproducibility and increasing the enantioselectivity above ~80% ee. At this point, Merck initiated a collaboration with our lab to further optimize and explore this reaction.

**Figure 3.3** Initial conditions from Merck.

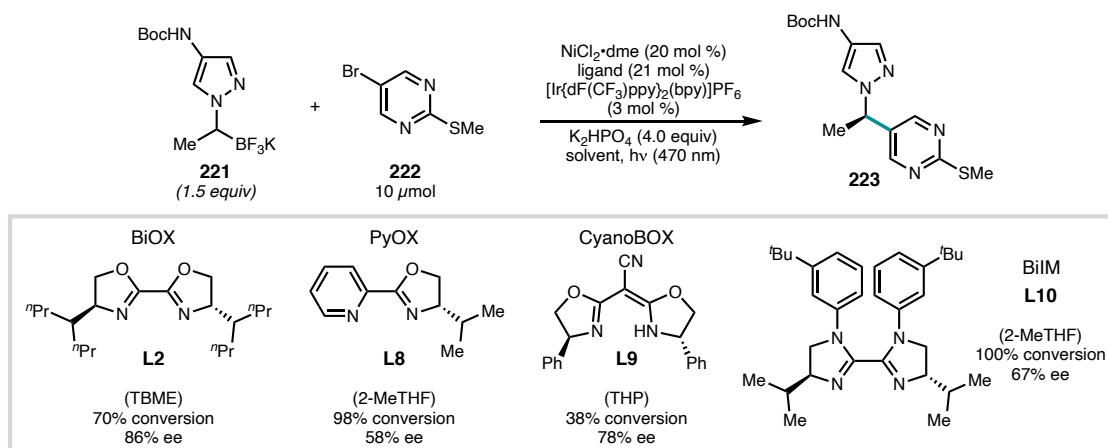


### 3.2 REACTION OPTIMIZATION

The initial conditions provided to us by Merck were discovered through several rounds of high-throughput screening, with an emphasis on coverage of a broad range of ligands. Productive reactivity was observed with a variety of ligand scaffolds. The best performing BiOX, pyridine-oxazoline (PyOX), cyanobis(oxazoline) (CyanoBOX), and biimidazole (BiIM) ligands are shown in Figure 3.4. Of the ligands screened, 4-heptyl

BiOX **L2** gave the highest enantioselectivity (86% ee) on HTE scale, using 20 mol %  $\text{NiCl}_2 \cdot \text{dme}$ , 21 mol % ligand, and 3 mol %  $[\text{Ir}\{\text{dF}(\text{CF}_3)\text{ppy}\}_2(\text{bpy})]\text{PF}_6$  as the photocatalyst in TBME as the solvent. Several other ligand classes gave less promising results. PyOX and BiIM ligands generally gave good conversion but formed **223** with diminished enantioselectivity. In contrast, CyanoBOX ligands such as **L9** formed **223** in relatively high ee, but with reduced conversion compared to **L2** and other related BiOX ligands.

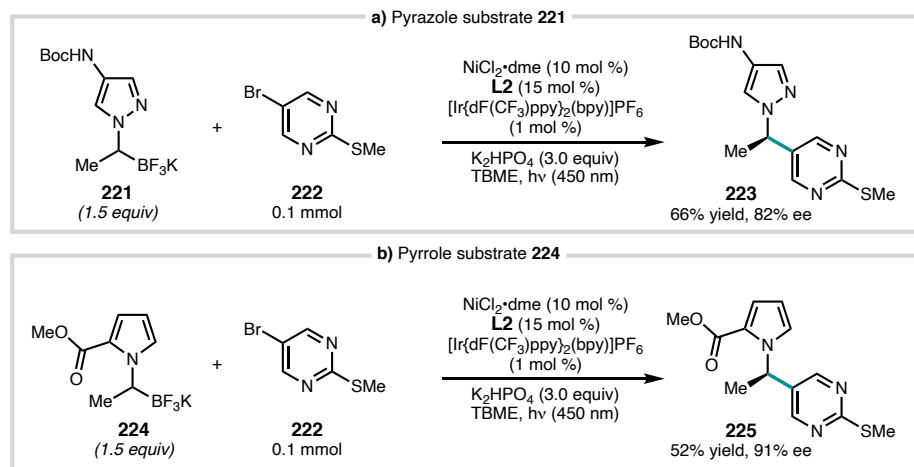
**Figure 3.4** HTE ligand/solvent screening best results.



With promising initial conditions in hand, we next sought to run the reaction on larger scale. Increasing the scale 10-fold while lowering the **L2**,  $\text{NiCl}_2 \cdot \text{dme}$ , and  $[\text{Ir}\{\text{dF}(\text{CF}_3)\text{ppy}\}_2(\text{bpy})]\text{PF}_6$  loading gave comparable results to the 10  $\mu\text{mol}$  HTE hit (Figure 3.5a). Interestingly, a significant increase in ee (to 91%) was observed when ester-containing pyrrole  $\text{BF}_3\text{K}$  **224** was used in place of **221** under identical conditions (Figure 3.5b). As hypothesized by Bonifazi and coworkers, we envisioned that the methyl ester at the 2-position may coordinate to nickel, leading to higher enantioselectivity.<sup>14</sup> In increasing the scale of these reactions, we made two key changes to the setup procedure that improved the reproducibility of the reaction: 1) reaction components were generally added as stock

solutions or weighed out as solids, rather than added as slurries, and 2) 4-heptylBiOX **L2** was repurified to remove ~5% of a hydrolysis impurity likely left over from separation of the enantiomers of the ligand.

**Figure 3.5** Scaleup under initial conditions.

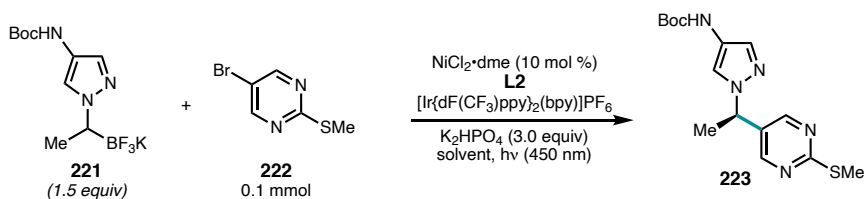


Further optimization of these reaction conditions was somewhat hindered by the limited solubility of several of the reaction components in TBME. In particular, the complex of  $\text{NiCl}_2 \cdot \text{dme}$  with **L2** required extended stirring at 60 °C to form, and the iridium photocatalyst was only sparingly soluble. We hypothesized that finding a better solvent could allow us to more precisely explore the effects of ligand and photocatalyst loading – two key factors in this reaction – and perhaps lead to more robust and reproducible conditions. To this end, 2-MeTHF was identified as a more polar alternative to TBME that exhibited both promising reactivity on HTE scale and better solubility of both  $[\text{Ni}] \cdot \text{L2}$  and  $[\text{Ir}\{\text{dF}(\text{CF}_3)\text{ppy}\}_2(\text{bpy})]\text{PF}_6$ . TBME had initially been selected over 2-MeTHF due to slightly higher enantioselectivities, but we hypothesized that with better control over

photocatalyst loading in a more solubilizing solvent, we may be able to improve the ee with 2-MeTHF.

Similar to our initial HTE results, we did observe a decrease in ee when switching from TBME to 2-MeTHF, even with increased ligand loading (Table 3.1, entries 1 and 2). Reducing the loading of the iridium photocatalyst to 0.25 or 0.125 mol % retained reactivity and resulted in higher enantioselectivity than had been observed in TBME (entries 3 and 4). Decreasing the ligand loading to 20 or 15 mol % gave reduced yield and enantioselectivity (entries 5 and 6). Directly translating the best conditions to date (30 mol % **L2**, 0.125 mol % iridium photocatalyst, entry 4), to the original solvent, TBME, gave substantially lower yield (entry 7).

**Table 3.1** Optimization of ligand and photocatalyst loading, solvent.



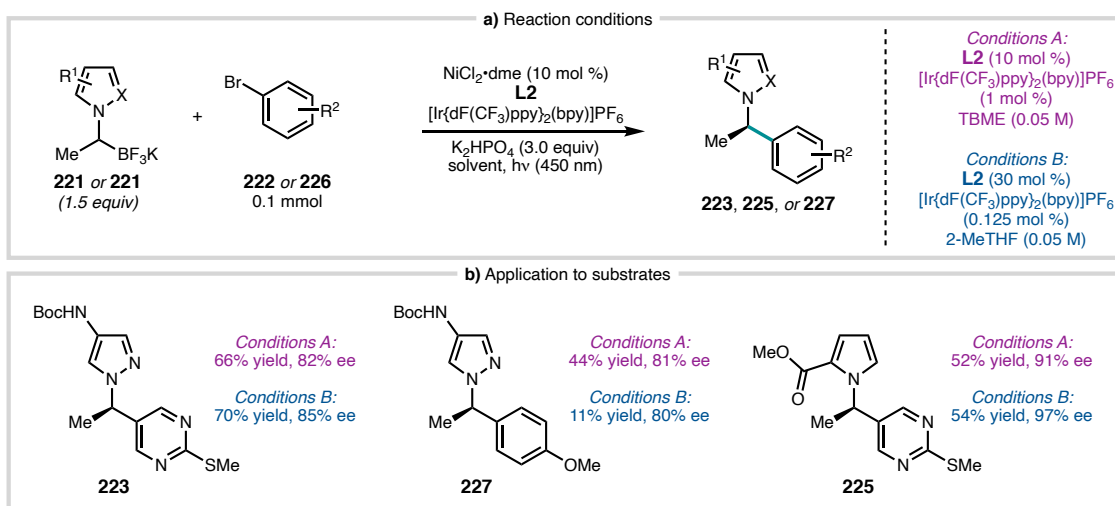
Entry	Solvent	mol % [Ir]	mol % <b>L2</b>	% Yield <b>223</b> <sup>a</sup>	% ee <b>223</b> <sup>b</sup>
1	TBME	1.0	15	66	82
2	2-MeTHF	1.0	30	73	74
3	2-MeTHF	0.25	30	72	84
4	2-MeTHF	0.125	30	70	85
5	2-MeTHF	0.125	20	72	83
6	2-MeTHF	0.125	15	65	81
7	TBME	0.125	30	51	85

<sup>a</sup> Determined by <sup>1</sup>H NMR. <sup>b</sup> Determined by chiral SFC.

We next sought to compare our new 2-MeTHF conditions (Conditions B) to the original TBME conditions (Conditions A) on a small selection of substrates in order to understand their generality (Figure 3.6a). For the coupling of Boc-protected aminopyrazole **221** with (methylthio)pyrimidine **222**, switching to the 2-MeTHF conditions resulted in a

small but notable increase in both yield and enantioselectivity (Figure 3.6b). Interestingly, when an electron-rich aryl bromide (**226**) was coupled with the same trifluoroborate salt, the product (**227**) was formed in substantially lower yield under Conditions B. We were excited to see that under Conditions B, we achieved our highest enantioselectivity to date; when pyrrole-2-ester BF<sub>3</sub>K **224** was coupled, product **225** was formed in 97% ee, possibly due to coordination of the ester functionality.

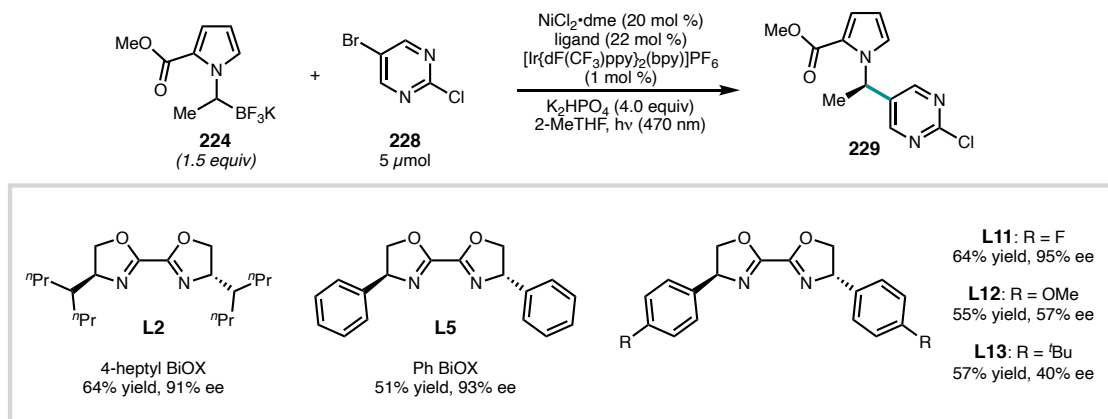
**Figure 3.6** Comparison of reaction conditions.



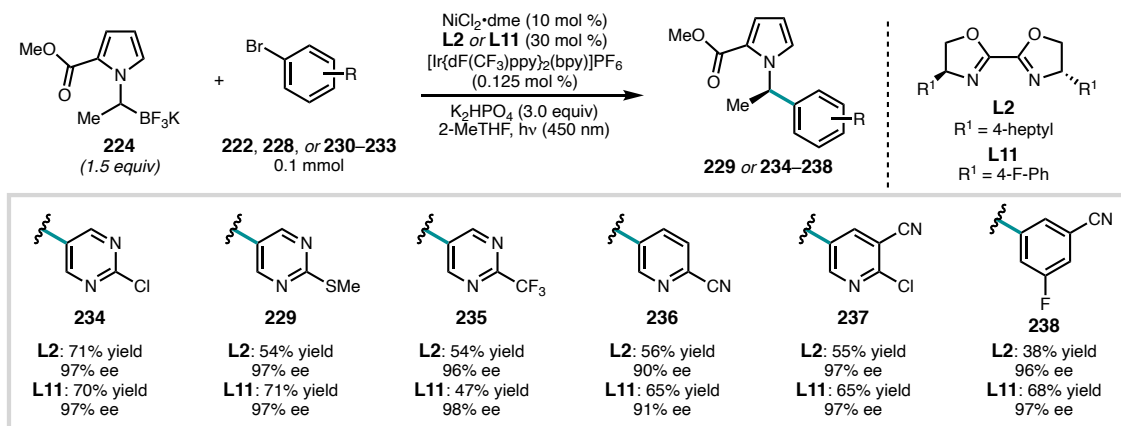
With our now most promising trifluoroborate (**224**), our collaborators at Merck further explored ligand space. Interestingly, a high-throughput screen of 48 ligands using chloropyrimidyl bromide **228** in 2-MeTHF under slightly modified conditions identified several new promising ligands for this transformation, namely 4-F-Ph BiOX (**L11**) and 4-Ph BiOX (**L5**), with the former giving 95% ee under conditions that gave only 91% ee for our previous best ligand (**L2**) (Figure 3.7). Notably, related ligands bearing electron-rich aryl substituents resulted in significantly lower enantioselectivities (**L12** and **L13**). Some of these aryl BiOX ligands had been previously screened using TBME as the solvent, but

poor solubility of the nickel-ligand complexes resulted in only trace reactivity. Future research on this reaction could involve the synthesis of more electron-deficient analogs and ligand parameterization studies.<sup>25</sup>

**Figure 3.7** HTE results: BiOX ligands.



Excited by the identification of a ligand giving superior ee to **L2** on 5  $\mu\text{mol}$  scale, we evaluated several aryl bromide coupling partners using both **L2** and **L11** to compare ligand performance on a 0.1 mmol scale (Figure 3.8). Surprisingly, upon scaling, **L2** and **L11** gave nearly identical ee across a range of substrates. Although enantioselectivity was not generally improved by using **L11**, yields went up substantially for a number of aryl bromides, with an average increase of nearly 10% across six substrates. Given these increased yields, we sought to further explore the scope of our cross-coupling reaction using **L11**.

**Figure 3.8** Comparison of **L2** and **L11**.

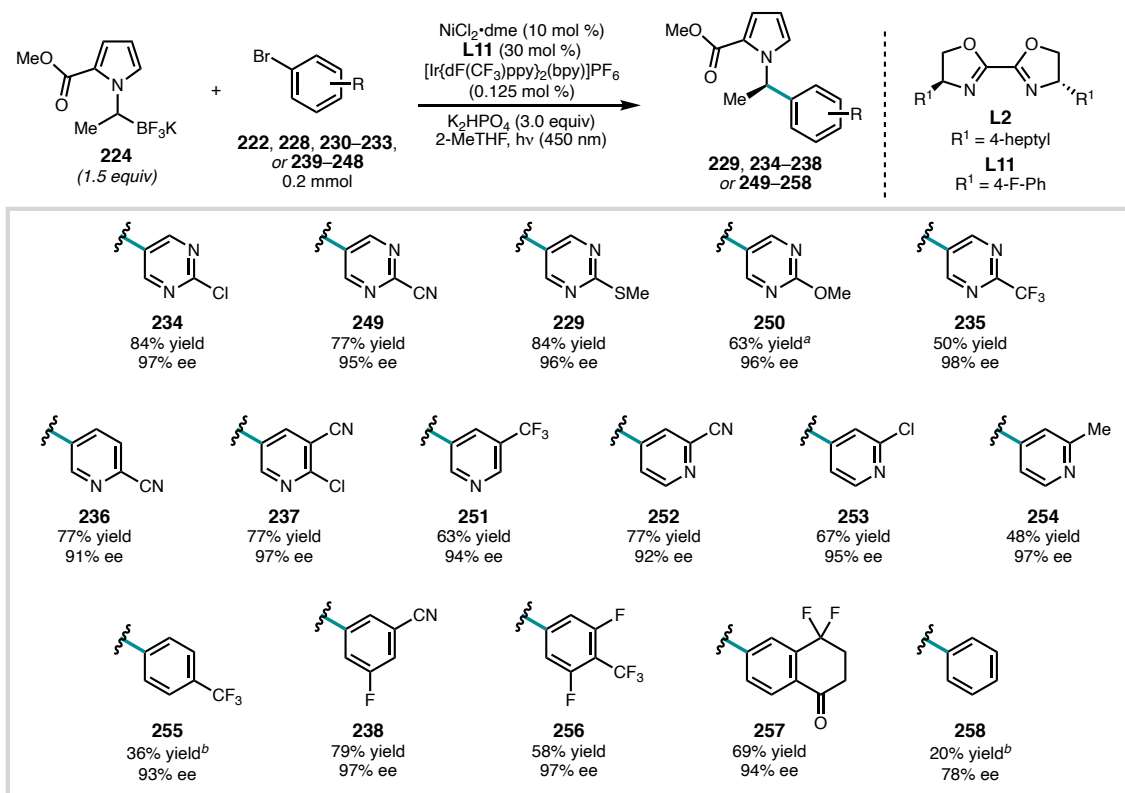
### 3.3 REACTION SCOPE

Having identified optimal conditions, we next explored the scope of the transformation. Surprisingly, under our optimized conditions using **L11**, we observed a moderate increase in yield for many substrates upon scaling the reaction from 0.1 mmol to 0.2 mmol. This same trend was not generally observed when **L2** was employed, leading to **L11** being the optimal ligand for most substrates explored (Figure 3.9). A variety of aryl bromides, generally electron-poor, coupled in good yields and excellent enantioselectivities. Both electron-donating and electron-withdrawing substituents were well tolerated at the 2-position of pyrimidyl bromides, giving coupled products **229**, **234**, **235**, **249**, and **250**. Several 3-pyridyl bromides coupled well, including **241**, which lacks a substituent *ortho* to the Lewis basic nitrogen, forming **251** in good yield and enantioselectivity. We were pleased to see that 4-bromopyridine derivatives, often a challenging substrate class, coupled in good yields and enantioselectivities, with both electron-donating and electron-withdrawing substituents *ortho* to the nitrogen well-



tolerated (**242–244**). Unfortunately, no productive reactivity was observed when unsubstituted 4-bromopyridine was used, possibly due to its instability.<sup>26</sup>

**Figure 3.9** Scope of aryl bromides.

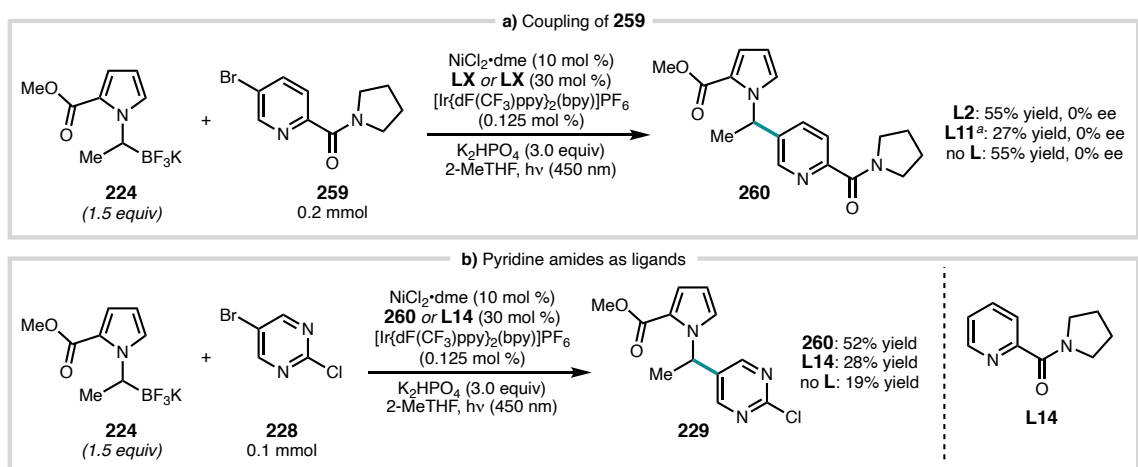


Several electron-deficient benzene derivatives also coupled to form products in high enantioselectivities and modest to good yields (**238**, **255–257**). Simple bromobenzene coupled in significantly lower yield and enantioselectivity (**258**). In general, we found that **L2** performed better than **L11** for less electron-deficient aryl bromides (products **255** and **258**), similar to trends we saw early in optimization (Figure 3.6b). Overall, we found our conditions to be applicable to a wide variety of electron-deficient aryl and heteroaryl bromides, giving products in moderate to high yields and excellent enantioselectivities.

Further optimization of separate conditions for electron-rich substrates could likely improve the generality of this transformation.

In exploring the substrate scope of this transformation, we found one surprising example of an electron-deficient aryl bromide that coupled with no enantioselectivity (Figure 3.10a). Using either **L2** or **L11**, **224** and **259** coupled to form racemic **260**. Interestingly, we found that in the absence of ligand, the reaction still gave **260** in 55% yield, suggesting that the amide-containing pyridine may be serving as a ligand in the reaction. To probe this hypothesis, we conducted the coupling of model  $\text{BF}_3\text{K}$  **224** and aryl bromide **228** in the presence of **260** as ligand (Figure 3.10b). Under these conditions, coupled product **229** was formed in 52% yield. When the parent pyridyl amide **L14** was employed, **229** was formed in significantly lower yield, comparable to the reaction with no ligand present, indicating that substitution at the 5-position of the pyridine amide is key to its ability to serve as a competent ligand in this reaction. Although no pyridine-2-amides

**Figure 3.10** Pyridine-2-amides as coupling partners and ligands.

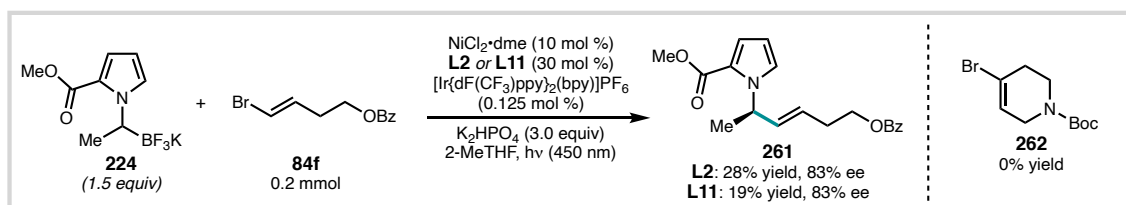


<sup>a</sup> Yield determined by  $^1\text{H NMR}$ .

were screened in their report, related pyridine-amidine ligands were discovered by Weix and coworkers for Ni-catalyzed couplings.<sup>27</sup>

We sought to further expand the scope of products accessible by this methodology by testing additional C(sp<sup>2</sup>) electrophiles, namely alkenyl bromides **84f** and **262** (Figure 3.11). Although trisubstituted alkenyl bromide **262** did not couple productively, we found that disubstituted alkenyl bromide was a competent electrophile in this reaction, giving **261** in 28% yield and 83% ee when **L2** was used as ligand. Although the yield of this reaction was modest, we were encouraged that this substrate was compatible with our standard reaction conditions without any further optimization.

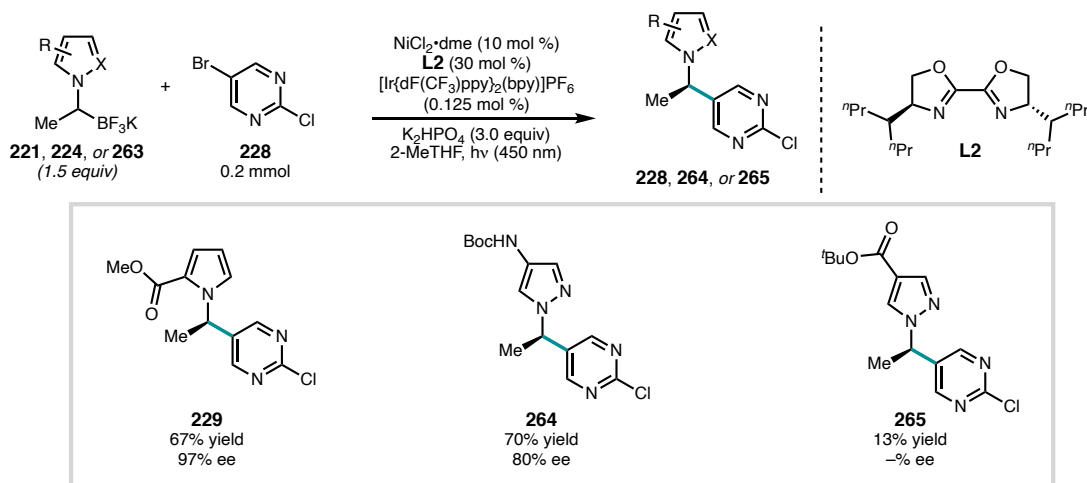
**Figure 3.11** Cross-coupling of alkenyl bromides.



We next set out to explore the scope of  $\alpha$ -*N*-heterocyclic potassium alkyl trifluoroborates tolerated in this reaction. Unfortunately, application of our optimal reaction conditions with **L2** to additional substrates **221** and **263** showed the lack of generality of these conditions (Figure 3.12). Although pyrazole **221** coupled to give **264** in good yield and moderate ee, structurally similar **265** was formed in very low yield. Qualitatively, we noticed that while both **221** and **263** were relatively insoluble in 2-MeTHF, ester-containing pyrazole trifluoroborate **263** was highly soluble in 2-MeTHF. Given this observation, we wondered if low solubility of trifluoroborate substrate was

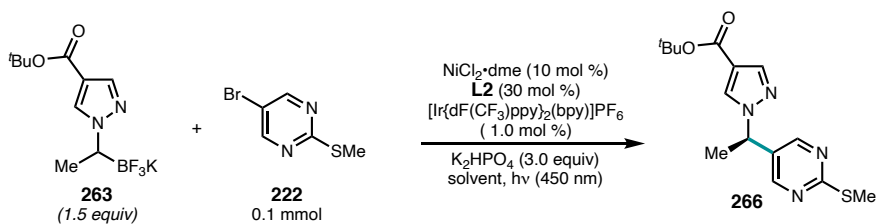
beneficial for the reaction, perhaps by slowly releasing substrate into solution leading to gradual radical generation.

**Figure 3.12** Initial  $BF_3K$  scope exploration.



To probe this solubility-based hypothesis, we tested several solvents in which **263** was relatively insoluble (Table 3.2). We found that the yield of **266** could be substantially improved using cyclopentyl methyl ether (CPME) as solvent with 1 mol %  $[Ir\{dF(CF_3)ppy\}_2(bpy)]PF_6$  (entry 4). One downside about the use of CPME as solvent is that the  $NiCl_2 \cdot L11$  complex is insoluble in CPME, precluding its use as an effective catalyst.

After our discovery that using a solvent in which the  $BF_3K$  salt is relatively insoluble can improve our reaction, our collaborators at Merck applied this idea to additional substrates using HTE. Several solvents were identified that perform reasonably well across a variety of substrates: 2-MeTHF,  $iPrOAc$ , CPME, and DME. For further optimization of this reaction on untested substrates, we recommend screening these solvents. Qualitatively, solvents in which the  $BF_3K$  was not fully soluble performed well;

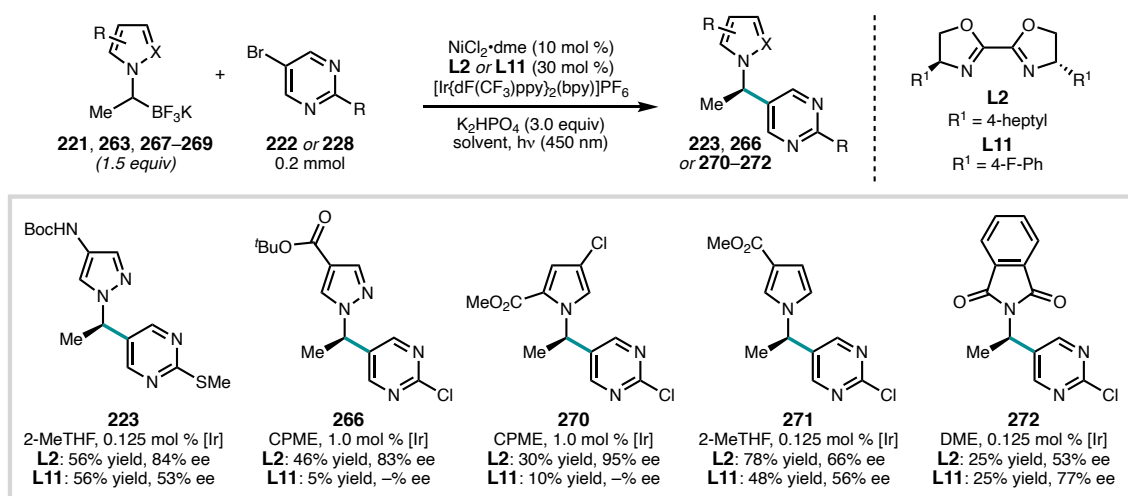
**Table 3.2** Solvent optimization for  $\text{BF}_3\text{K}$  **263**.

Entry	Solvent	<b>263</b> fully soluble?	% Yield <b>266</b> <sup>a</sup>	% ee <b>266</b> <sup>b</sup>
1	2-MeTHF <sup>c</sup>	yes	13	–
2	TBME	no	22	82
3	CPME	no	47	86
4	PhCl	no	37	83
5	1,4-dioxane	no	5	–

<sup>a</sup> Determined by  $^1\text{H}$  NMR. <sup>b</sup> Determined by chiral SFC. <sup>c</sup> 0.2 mmol scale, 0.125 mol %  $[\text{Ir}]$

in cases where the photocatalyst was also not fully soluble, increased loading was beneficial.

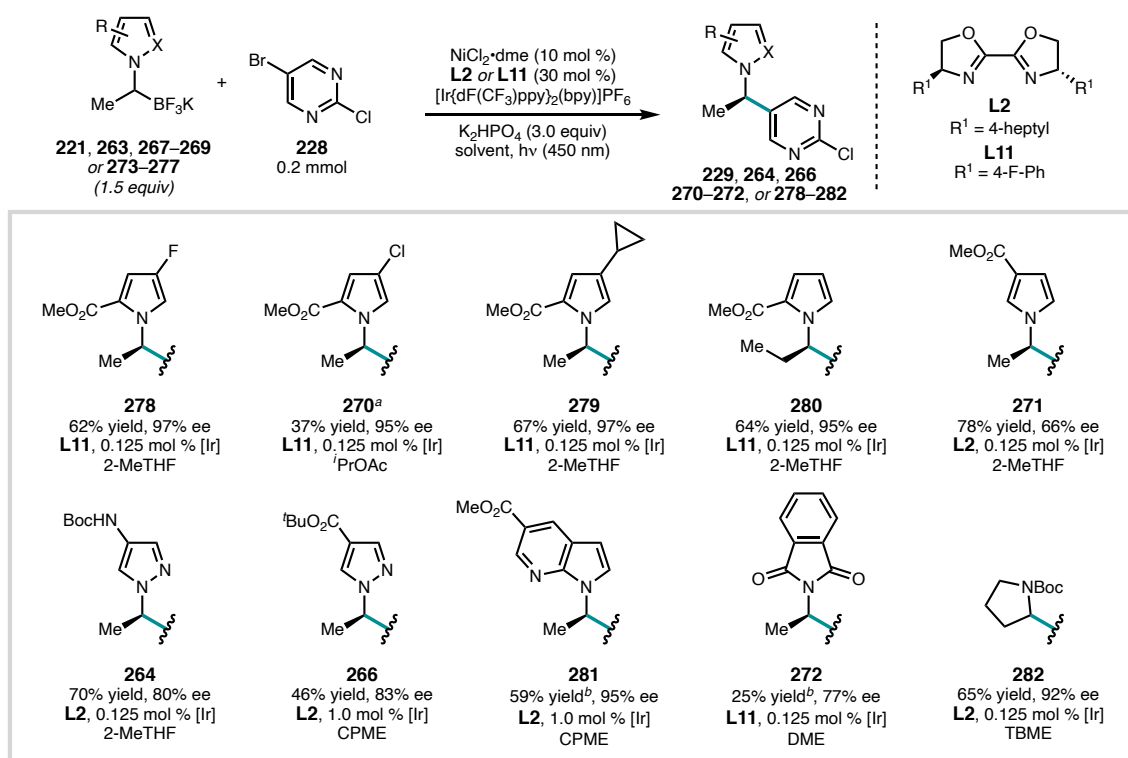
Scaling up the optimal (as identified by HTE) solvents for several additional  $\alpha$ -*N*-heterocyclic potassium alkyl trifluoroborates showed ligand trends differing from our aryl bromide scope (Figure 3.13). In general, we found 4-heptyl BiOX **L2** gave higher enantioselectivities than 4-F-Ph BiOX **L11**. For example, **L2** formed **223** and **271** in 84% ee and 66% ee, respectively, compared to 53% ee and 56% ee for **L11**. The very low yields of **266** and **270** obtained when **L11** was used as ligand was likely due to insolubility of the  $\text{NiCl}_2 \cdot \text{L11}$  complex in CPME. Phthalimide-containing trifluoroborate **269** was an exception to this ligand trend: **L11** gave a notably higher ee than **L2**, although the yield was low for both ligands.

**Figure 3.13** Ligand comparison for  $\text{BF}_3\text{K}$  salts.

Having learned these trends, we sought to further explore the scope of  $\text{BF}_3\text{K}$  salts that could be employed in this cross-coupling reaction (Figure 3.14). Substitution at the 4-position of parent  $\text{BF}_3\text{K}$  was generally well tolerated, giving coupled products **278**, **270**, and **279** in excellent enantioselectivities, although chloro pyrrole **270** was formed in somewhat reduced yield. The alkyl chain at the newly formed stereocenter could be extended from methyl to ethyl with a moderate drop in yield and a small reduction in ee (**280**). Interestingly, shifting the methyl ester from the 2-position of the pyrrole to the 3-position resulted in similar yield but a dramatic decrease in ee, from 97% ee to 66% ee (**234**, **271**). This large decrease in ee may suggest that a proximal coordinating group on the trifluoroborate coupling partner can play a role in the selectivity-determining step of the reaction.<sup>14</sup> Consistent with this hypothesis, 7-azaindole **276** also coupled with excellent enantioselectivity to give **281**. Pyrazole products **264** and **266**, and phthalimide **282** can also be formed, albeit with lower enantioselectivities. We were pleased to see that an arene  $\alpha$  to the trifluoroborate was not required for good reactivity or selectivity in this reaction:

subjection of commercially available *N*-Boc-pyrrolidine-containing  $\text{BF}_3\text{K}$  to the cross-coupling conditions gave arylated product **282** in 65% yield and 92% ee, with **L2** as ligand. Notably, in the decarboxylative asymmetric Ni/photoredox arylation developed by Fu, MacMillan, and coworkers, *N*-Boc-proline was not a suitable coupling partner, demonstrating the orthogonality of our approach.<sup>19</sup>

**Figure 3.14** Scope of  $\text{BF}_3\text{K}$  salts.



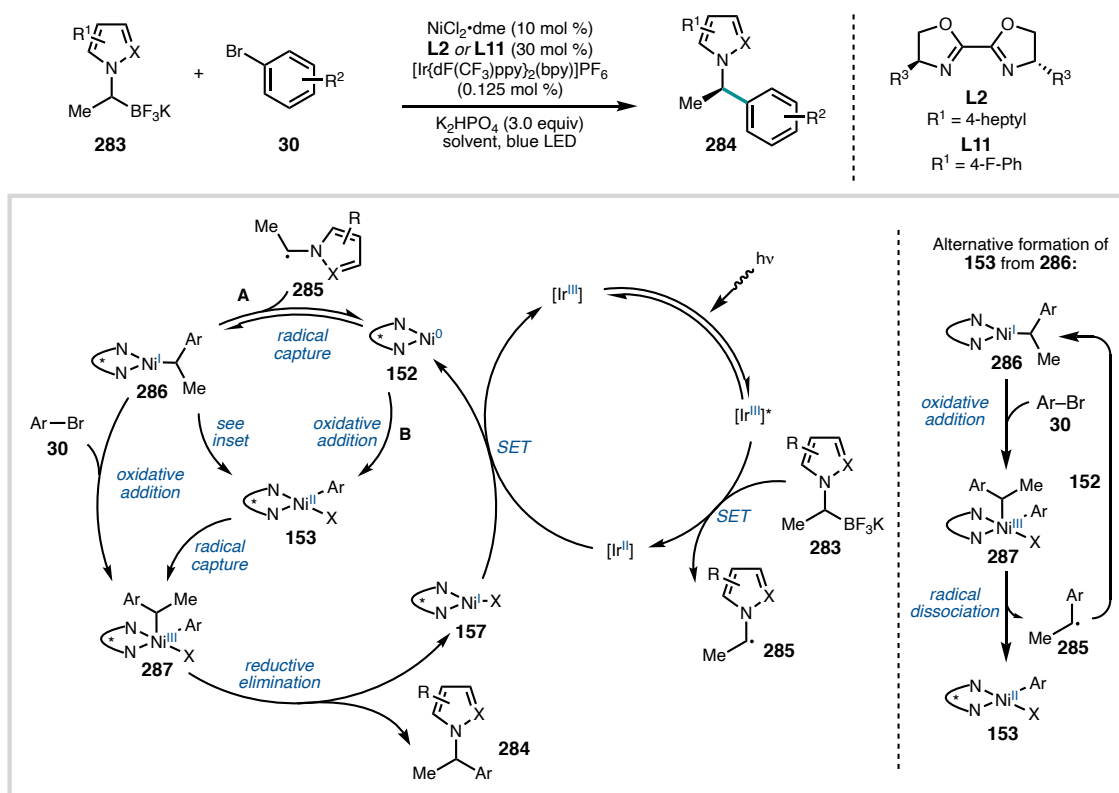
<sup>a</sup> Reaction run on 0.1 mmol scale; <sup>b</sup> yield determined by <sup>1</sup>H NMR.

### 3.4 PRELIMINARY MECHANISTIC EXPERIMENTS

Having established the scope of our Ni/photoredox catalyzed arylation of *N*-heterobenzylic potassium trifluoroborate salts, we conducted some initial investigations to probe possible mechanisms of this transformation. Three mechanistic possibilities, based on computational studies from Molander, Kozłowski, and Gutierrez are shown in Figure

3.15.<sup>28,29</sup> Each cycle would begin with photoexcitation of the Ir<sup>III</sup> photocatalyst, which oxidizes the potassium trifluoroborate salt to generate stabilized alkyl radical **285** and the reduced Ir<sup>I</sup> complex. This reduced photocatalyst would then undergo single electron transfer (SET) with in situ-generated Ni<sup>I</sup> complex **157**, regenerating the Ir<sup>III</sup> photocatalyst and forming Ni<sup>0</sup> complex **152**. Two possible next steps could be envisioned from this Ni<sup>0</sup> complex. The first (pathway A), calculated as favored by Kozłowski and Molander for a related transformation, albeit with a different ligand and substrate and water as solvent, would start with radical capture of **285** to generate Ni<sup>I</sup> intermediate **286**. Oxidative addition of an aryl bromide to this Ni<sup>I</sup> intermediate would give Ni<sup>III</sup> **287**, poised for reductive elimination to form cross-coupled product **284** and Ni<sup>I</sup>X, completing the catalytic cycle.

**Figure 3.15** Possible reaction mechanisms.





Alternatively, the aryl bromide could oxidatively add to Ni<sup>0</sup> complex **152** (pathway B), giving Ni<sup>II</sup> complex **153**. This species could then intercept the radical generated by BF<sub>3</sub>K oxidation to form the same Ni<sup>III</sup> intermediate **287** encountered on the first mechanistic pathway. More recent computational work from Gutierrez and Chu on a related transformation (calculated in THF) favors the second of these pathways, also finding plausible an alternative mechanism for the formation of **153** from **286**. Ni<sup>0</sup> complex **152** could capture alkyl radical **285**, as in pathway A, followed by oxidative addition of aryl bromide **30**. This Ni<sup>III</sup> intermediate **287** could then undergo reversible radical dissociation to form **153**. Thus, the Ni<sup>II</sup>ArX species **153** could plausibly derive from either initial radical trapping by Ni<sup>0</sup>, or initial oxidative addition of the aryl bromide.

We first sought to determine if we could trap an intermediate on these catalytic cycles – namely alkyl radical **285**. We conducted our reaction of model substrates **224** and **228** with the addition of 1.5 equivalents of several radical trapping agents (Table 3.3, entries 1–4). A control reaction without additive confirmed that product **229** was formed in high yield and enantioselectivity (entry 1). When TEMPO was added to the reaction, product **229** was formed in significantly diminished yield (19%), but still in high enantioselectivity (96% ee). Analysis of the reaction mixture revealed that TEMPO-trapped adduct **288**, presumably arising from capture of alkyl radical **285**, was formed in 69% yield (relative to the 1.5 equivalents of TEMPO employed in the reaction). Bimolecular combination of carbon-centered radicals with nitroxyl radicals such as TEMPO is very rapid.<sup>30,31</sup> Given this, it is somewhat surprising that coupled product **229** is still observed when TEMPO is added to the reaction, indicating that capture of **285** by nickel is likely quite rapid. In a related report from Chu and coworkers, addition of TEMPO

resulted in formation of a TEMPO adduct and complete shutdown of cross-coupling.<sup>29</sup> Interestingly, the other radical traps employed did not result in the detection of trapped **285**: 1,1-diphenylethylene had almost no effect on the reaction, and 9,10-dihydroanthracene inhibited product formation but did not form detectable amounts of protodeborylation.<sup>32</sup> The same set of experiments conducted in THF, in which **224** is fully soluble, gave similar results to 2-MeTHF, where **224** has limited solubility (entries 5–8). This result is somewhat surprising given the dependence on  $\text{BF}_3\text{K}$  solubility observed when exploring the scope of this reaction. It is possible that the optimized reaction conditions are particularly well-matched to these coupling partners and are robust enough that solubility is less important, but for other substrates, the conditions are more sensitive.

**Table 3.3** Radical trapping experiments.

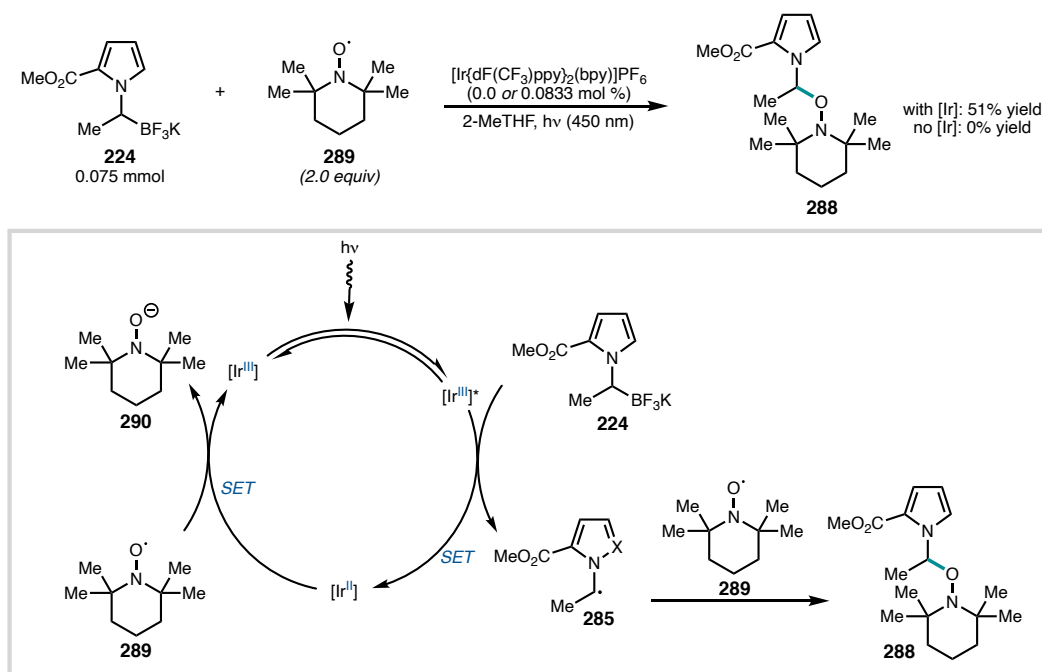
Entry	Solvent	additive	% Yield <b>229</b> <sup>a</sup>	% ee <b>229</b> <sup>b</sup>	% yield trapping <sup>a</sup>
1	2-MeTHF	none	74	98	–
2	2-MeTHF	TEMPO	19	96	69% <b>288</b>
3	2-MeTHF	1,1-DPE	70	97	n.d.
4	2-MeTHF	9,10-DHA	19	98	n.d.
5	THF	none	77	96	–
6	THF	TEMPO	11	91	65% <b>288</b>
7	THF	1,1-DPE	68	96	n.d.
8	THF	9,10-DHA	41	97	n.d.

<sup>a</sup> Determined by <sup>1</sup>H NMR. <sup>b</sup> Determined by chiral SFC. <sup>c</sup> n.d. = not detected.

We next sought to probe the feasibility of the iridium photocatalyst cycle shown in Figure 3.15. Prior to Molander's seminal report of the Ni/photoredox cross-coupling of aryl bromides with alkyl potassium trifluoroborate salts, there were already reports that

single-electron oxidation of alkyl  $\text{BF}_3\text{K}$  salts could result in radical formation using both chemical oxidants<sup>33,34</sup> and iridium photocatalysts.<sup>20,35</sup> In the latter case, these radicals, typically benzylic or allylic, were trapped with either TEMPO or Giese acceptors. Though the oxidation of various alkyl  $\text{BF}_3\text{K}$  salts by excited state iridium photocatalysts to generate radicals is commonly invoked in Ni/photoredox coupling mechanisms, we wanted to verify that our specific  $\alpha$ -*N*-heterocyclic radicals could be generated in this manner. To this end, we subjected model trifluoroborate **224** to irradiation with blue light (450 nm) in the presence of catalytic  $[\text{Ir}\{\text{dF}(\text{CF}_3)\text{ppy}\}_2(\text{bpy})]\text{PF}_6$  and 2.0 equivalents of TEMPO (Figure 3.16). The concentrations of **224** and the photocatalyst were held constant relative to the standard catalytic reaction conditions. Gratifyingly, when the iridium photocatalyst was included, the TEMPO adduct **288**, presumably resulting from radical combination with

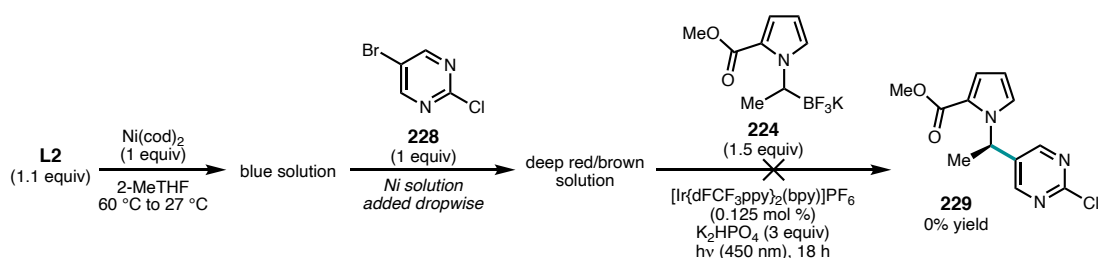
**Figure 3.16** Radical generation by  $[\text{Ir}\{\text{dF}(\text{CF}_3)\text{ppy}\}_2(\text{bpy})]\text{PF}_6$ .



**285**, was formed in 51% yield. A control experiment in the absence of photocatalyst revealed that 450 nm irradiation alone was insufficient for generation of this radical.

Having established the feasibility of radical generation from BF<sub>3</sub>K salt **224** catalyzed by our iridium photocatalyst, we tried to probe the feasibility of one of the reaction mechanisms outlined in Figure 3.15 (pathway B). Analogous to studies conducted in our asymmetric nickel-catalyzed reductive cross-coupling of  $\alpha$ -chloroesters with aryl iodides,<sup>25</sup> we sought to conduct a stoichiometric experiment in which we pre-generated a L2·Ni<sup>II</sup>ArBr oxidative addition complex, then exposed it to the remaining components of the reaction (Figure 3.17). Although the complexation and oxidative addition steps proceeded with the expected color changes, irradiation of this solution in the presence of **224**, K<sub>2</sub>HPO<sub>4</sub>, and iridium photocatalyst did not result in the formation of any **229**. The only identified side products were small amounts of aryl bromide homocoupling and defluorination of the trifluoroborate salt.

**Figure 3.17** Stoichiometric study.



Lack of formation of **229** in this reaction does not necessarily signify that **153** is not an intermediate in the reaction. There are several differences between this stoichiometric study and the catalytic reaction that could be confounding: 1) the concentration of the stoichiometric reaction is lower due to solubility constraints, 2) two

equivalents of 1,5-cyclooctadiene are present in the reaction due to the Ni(cod)<sub>2</sub> precatalyst, and 3) successful coupling under these conditions would likely require the **L2**·Ni<sup>II</sup>ArBr oxidative addition complex to be stable for extended periods of time in order to capture slowly-generated alkyl radicals. Given these challenges, significant further experimentation would be required to fully understand the mechanism of this reaction.

### 3.5 CONCLUDING REMARKS

In conclusion, we have developed the first enantioselective cross-coupling of  $\alpha$ -*N*-heterocyclic potassium trifluoroborate salts with aryl bromides. The reaction, co-catalyzed by chiral nickel complexes and an iridium photocatalyst, proceeds in good yield, forming chiral *N*-benzylic heterocycles with enantioselectivities up to 98% ee. Electron-deficient (hetero)aryl bromides and trifluoroborate salts containing coordinating groups are especially good substrates for this reaction. A key observation made during the optimization of the reaction—solvents that do not fully solubilize the trifluoroborate salt often prove more effective—prompted us to develop a simple workflow for optimizing new reactions using HTE.

### 3.6 EXPERIMENTAL SECTION

#### 3.6.1 *Materials and Methods*

Unless otherwise stated, reactions were performed under a nitrogen atmosphere using dried solvents. Anhydrous 2-Methyltetrahydrofuran (2-MeTHF), anhydrous *tert*-butyl methyl ether (TBME), anhydrous cyclopentyl methyl ether (CPME), anhydrous tetrahydrofuran (THF), and anhydrous potassium phosphate monobasic (K<sub>2</sub>HPO<sub>4</sub>) were

purchased from Millipore Sigma and stored in the glovebox. Nickel(II) chloride dimethoxyethane adduct ( $\text{NiCl}_2 \cdot \text{dme}$ ) was purchased from Strem or Aldrich. Potassium (1-(tert-butoxycarbonyl)pyrrolidin-2-yl)trifluoroborate (**277**) was purchased from Combi-Blocks. Unless otherwise stated, chemicals were used as received. All reactions were monitored by thin-layer chromatography (TLC) using EMD/Merck silica gel 60 F254 pre-coated plates (0.25 mm) and were visualized by ultraviolet (UV) light or with *p*-anisaldehyde or potassium permanganate staining. Flash column chromatography was performed as described by Still et al.<sup>1</sup> using silica gel (230-400 mesh) purchased from Silicycle. Optical rotations were measured on a Jasco P-2000 polarimeter using a 100 mm path-length cell at 589 nm or on a Rudolph Automatic Polarimeter (part # A22502; model APV-Plus 6W) using a 100 mm path-length cell at 589 nm. Melting points were measured on a Buchi melting point B-545 apparatus.  $^1\text{H}$  and  $^{13}\text{C}$  NMR spectra were recorded on a Bruker Avance III HD with Prodigy cryoprobe (at 400 MHz and 101 MHz, respectively), a Varian 400 MR (at 400 MHz and 101 MHz, respectively), or a Varian Inova 500 (at 500 MHz and 126 MHz, respectively).  $^1\text{H}$  and  $^{19}\text{F}$  NMR spectra were also recorded on a Varian Inova 300 (at 300 MHz and 282 MHz, respectively). Proton nuclear magnetic resonance for compound **282** ( $^1\text{H}$  NMR) spectra, proton decoupled carbon nuclear magnetic resonance ( $^{13}\text{C}\{^1\text{H}\}$  NMR) spectra were recorded at 25 °C on a Bruker DRX-500 spectrometer using  $\text{CDCl}_3$ . NMR chemical shifts are reported relative to internal  $\text{CHCl}_3$  ( $^1\text{H}$ ,  $\delta = 7.26$ ),  $\text{CDCl}_3$  ( $^{13}\text{C}$ ,  $\delta = 77.1$ ),  $\text{C}_6\text{F}_6$  ( $^{19}\text{F}$ ,  $\delta = -164.9$ ). Data for  $^1\text{H}$  NMR spectra are reported as follows: chemical shift ( $\delta$  ppm) (multiplicity, coupling constant (Hz), integration). Multiplicity and qualifier abbreviations are as follows: s = singlet, d = doublet, t = triplet, q = quartet, m = multiplet. IR spectra were recorded on a Perkin Elmer Paragon

1000 spectrometer or a Thermo Fischer Scientific Nicolet 6700 FT-IR (compound 5g) and are reported in frequency of absorption ( $\text{cm}^{-1}$ ). Analytical chiral SFC was performed with a Mettler SFC supercritical  $\text{CO}_2$  chromatography system with Chiralcel AD-H, OD-H, AS-H, OB-H, and OJ-H columns (4.6 mm x 25 cm) or a Waters Acquity UPC<sup>2</sup> with Chiralpak IC-3 (4.6 mm x 15 cm). LRMS were obtained using an Agilent 1290 Infinity/6140 Quadrupole system (LC-MS) or an Agilent 7890A GC/5975C VL MSD system (GC-MS). HRMS were acquired from the Caltech Mass Spectral Facility using fast-atom bombardment (FAB), electrospray ionization (ESI-TOF), electron impact (EI), or field ionization (FI). X-ray diffraction was performed at the Caltech X-ray Crystal Facility.

### 3.6.2 Ligand Preparation

4-Heptyl BiOX (**L2**) was prepared as previously described.<sup>24</sup> 4-F-Ph BiOX (**L11**) was prepared as described by Hu and coworkers.<sup>36</sup>

### 3.6.3 Optimization of Reaction Parameters

#### High Throughput Experimentation Methods

All reactions were performed inside a positive-pressure glovebox under a nitrogen atmosphere using standard high-throughput experimentation techniques unless stated otherwise.<sup>37</sup> All reactions were carried out in 8x30 shell vials (Analytical Sales & Services, Inc.; Part No. 884001) using parylene coated stir dowels (V&P Scientific, Inc.; Part No. VP711D-1) as stir bars. The 8x30 shell vials were sealed in a Para-dox 96-well photoredox block assembly (Analytical Sales & Services, Inc.; Part No. 96973). Irradiation of all parallel reactions were carried out in 96-well plate format using a Lumidox™ Gen 1 Blue LED array (Analytical Sales & Services; catalog number LUM96B;  $\lambda = 470$  nm, 30 mW intensity). The stirring mechanism used for all parallel experimentation was a

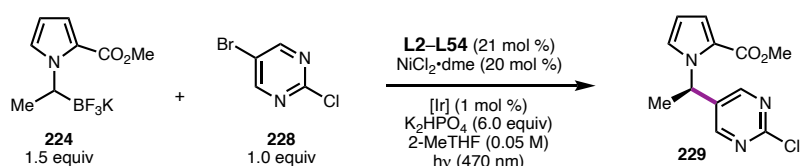
heated/cooled tumble stirring module obtained from Symyx Technologies (Unchained Labs). All *in vacuo* solvent removal from 96-well reaction blocks were performed inside a glovebox under a nitrogen atmosphere using a Genevac™ centrifugal evaporator. Analytical chiral RPLC-MS analysis was performed on a Waters Acquity UPLC interfaced with a Waters Xevo G2 QToF ESI. Chiral UPLC Column: Regis (S,S)-Whelk-O1 (4.6 mm x 10 cm; Part 1-780161-300), Binary eluent system: eluent A = aqueous mobile phase (3960 mL H<sub>2</sub>O, 40 mL pH 3.5 buffer, details below), eluent B = (3600 mL MeCN, 360 mL H<sub>2</sub>O, 40 mL pH 3.5 buffer. The pH 3.5 buffer is prepared by dissolving ammonium formate (12.6 g, 0.200 mol) and formic acid (7.9 mL, 9.6 g, 0.21 mol) in 1000 mL water. Isocratic conditions: 20% A until *t* = 3.0 min. Flow rate: 0.8 mL/min; Column temperature: 40 °C; UV detection: 210 nm (primary); 254 nm (secondary).

### Chiral Ligand Evaluation Procedure and Results

*Note: conducted by Kevin Belyk at Merck.* A solution of NiCl<sub>2</sub>·dme (0.20 equiv, 1.0 μmol, 0.22 mg) in a 27:1 (v:v) mixture of THF:MeOH (58.3 μL) was added to each ligand (0.21 equiv, 1.05 μmol) in a 8x30 shell vial containing a dowel, the vial sealed, and the mixture agitated at 45 °C for 1 h. The solvent was removed *in vacuo* and K<sub>2</sub>HPO<sub>4</sub> (6 equiv, 30 μmol, 5.2 mg) was added. Next, a well-stirred suspension of methyl 1-(1-(trifluoroborate)ethyl)-1*H*-pyrrole-2-carboxylate, potassium salt (**224**, 1.5 equiv, 7.5 μmol, 1.94 mg), 5-bromo-2-chloropyrimidine (**228**, 1.0 equiv, 5 μmol, 0.97 mg), and Ir[dF(CF<sub>3</sub>)ppy]<sub>2</sub>(bpy)PF<sub>6</sub> (0.01 equiv, 0.05 μmol, 50.5 μg) in 2-MeTHF (100 μL; 0.05 M in **228**) was added. The sealed reaction was agitated at 350 RPM while being irradiated for 20 h, maintaining a measured external reaction block temperature of about 35 °C.

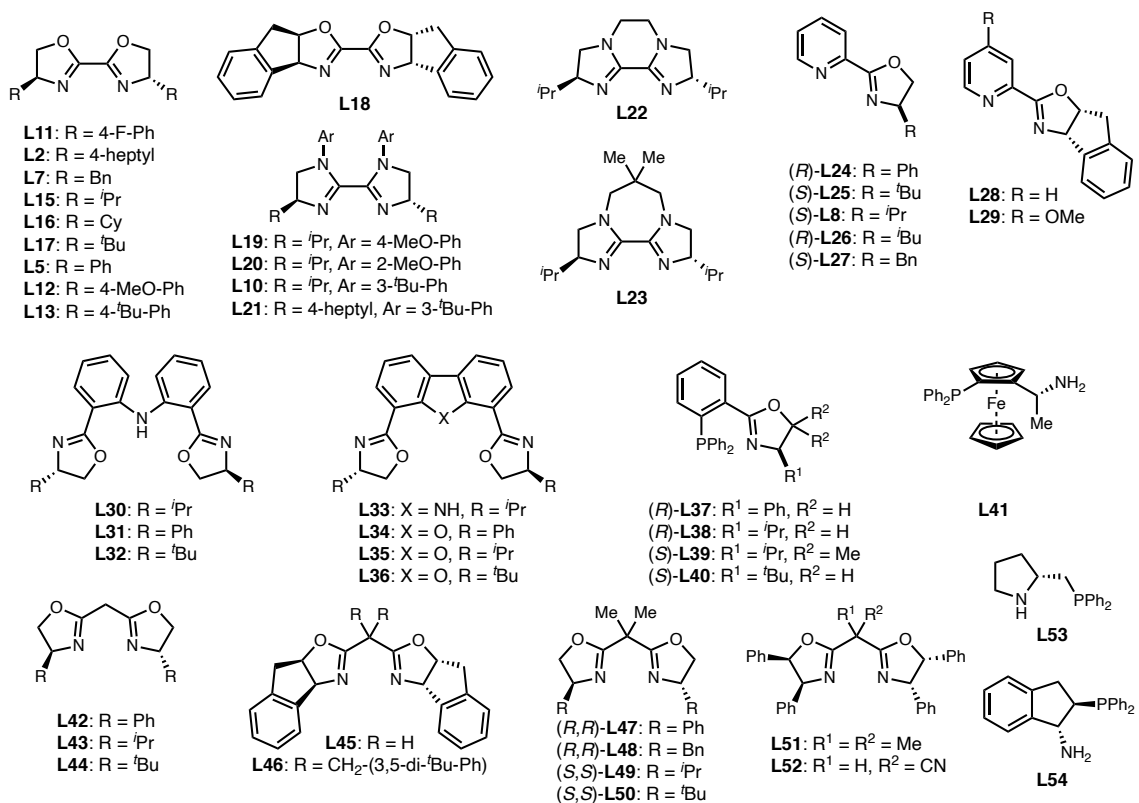


Following reaction completion, a solution of biphenyl (0.20 equiv, 1.0  $\mu$ mol, 0.15 mg) in MeCN (400  $\mu$ L) was added and the resulting mixture analyzed by chiral stationary RPLC for the yield determination (vs. biphenyl as a standard) and enantiomeric excess of **229**. Chiral RPLC:  $t_R$  (**228**) = 2.0 min,  $t_R$  (**229**, major) = 2.2 min,  $t_R$  (**229**, minor) = 2.3 min,  $t_R$  (biphenyl) = 2.8 min.



Ligand	Yield <sup>b</sup> (%) / ee <sup>c</sup> (%)	Ligand	Yield <sup>b</sup> (%) / ee <sup>c</sup> (%)	Ligand	Yield <sup>b</sup> (%) / ee <sup>c</sup> (%)
L11	64 / 95	L24	28 / 0	L39	6 / 5
L2	64 / 91	L25	33 / 1	L40	2 / -
L7	65 / 73	L8	34 / 0	L41	2 / -
L15	53 / 87	L26	42 / -36	L42	35 / 41
L16	55 / 75	L27	46 / 38	L43	29 / 3
L17	63 / 73	L28	43 / 56	L44	31 / -2
L5	51 / 93	L29	43 / 56	L45	29 / -7
L12	55 / 57	L30	8 / 6	L46	31 / -27
L13	57 / 40	L31	1 / -	L47	27 / 11
L18	55 / 59	L32	1 / -	L48	29 / 1
L19	46 / 52	L33	9 / -15	L49	31 / 0
L20	31 / 49	L34	6 / -2	L50	29 / 0
L10	46 / 58	L35	4 / -17	L51	35 / 10
L21	58 / 75	L36	6 / -8	L52	54 / -32
L22	19 / 66	L37	2 / -	L53	2 / -
L23	26 / 71	L38	2 / -	L54	2 / -

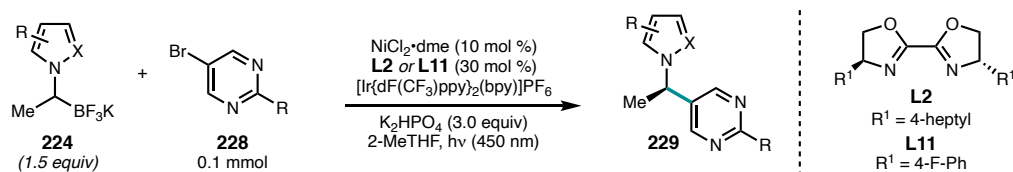
<sup>a</sup>Reaction conditions: **224** (7.5  $\mu$ mol, 150 mol %), **228** (5  $\mu$ mol), NiCl<sub>2</sub>·dme (1  $\mu$ mol, 20 mol %), **L2-L54** (1.05  $\mu$ mol, 21 mol %), K<sub>2</sub>HPO<sub>4</sub> (30  $\mu$ mol, 600 mol %), [Ir] = Ir[dF(CF<sub>3</sub>)ppy]<sub>2</sub>(bpy)PF<sub>6</sub> (0.05  $\mu$ mol, 1.0 mol %), 2-MeTHF (100  $\mu$ L, 0.05 M in **228**), irradiation at 470 nm, 35 °C (20 h). <sup>b</sup>Determined by stationary RPLC vs. biphenyl as an internal standard. <sup>c</sup>Enantiomeric excess determined by chiral stationary RPLC.



### Standard Procedure for Optimization of Reaction Conditions using L11

*Note:* conducted by Kevin Belyk at Merck. 2-MeTHF (1.0 mL) was added to NiCl<sub>2</sub>·dme (0.10 equiv, 0.01 mmol, 2.2 mg) and ligand **L11** (0.30 equiv, 0.03 mmol, 9.8 mg) in a sealed vial containing a Teflon-coated stir bar and the mixture agitated at approximately 55 °C for 1 h then cooled to ambient temperature. Separately, K<sub>2</sub>HPO<sub>4</sub> (3 equiv, 0.30 mmol, 52.3 mg), methyl 1-(1-(trifluoroborate)ethyl)-1*H*-pyrrole-2-carboxylate, potassium salt (**224**, 1.5 equiv, 0.15 mmol, 38.9 mg), and 5-bromo-2-chloropyrimidine (**228**, 1.0 equiv, 0.10 mol, 19.3 mg) were added to a 1-dram vial containing a Teflon-coated stir bar. Next, the NiCl<sub>2</sub>·dme/**L11** mixture in 2-MeTHF was added to the 1-dram vial containing the substrates and base. A solution of Ir[dF(CF<sub>3</sub>)ppy]<sub>2</sub>(bpy)PF<sub>6</sub> (0.00125 equiv, 125 μmol, 0.126 mg) in 2-MeTHF (1.0 mL) was

added to the 1 dram reaction vial, the vial sealed with Teflon-lined cap and parafilm, then removed from the glovebox. The vial was mounted in a PennOC 8 mL cone reflector (Part No. PR-R08001-2) inside a PennOC M1 Photoreactor Base Unit (Model No. PR001) with the bottom of the vial 2.1 cm from the LED. The vial was irradiated with a PennOC 450 nm Light source (part no. PR1M-102AD-01) for 18 h at 100% LED intensity with an agitation setpoint of 500 RPM and a fan speed of 5200 RPM. After 18 hours, the reaction was diluted with EtOAc (1.5 mL) and washed with saturated aqueous NH<sub>4</sub>Cl (0.5 mL). The aqueous layer was extracted 3 times with EtOAc (3 mL), and the combined organic layers were dried over Na<sub>2</sub>SO<sub>4</sub>. The dried organic layer was concentrated *in vacuo* and the resulting residue dissolved in a solution of ethylene carbonate (1.0 equiv, 0.10 mmol, 8.8 mg) in CDCl<sub>3</sub> (1.0 mL). The resulting mixture analyzed by quantitative <sup>1</sup>H NMR (CDCl<sub>3</sub>) for yield determination of **229** vs. ethylene carbonate as internal standard. The enantiomeric excess of **229** was determined by chiral stationary RPLC.



entry	deviation from Standard conditions <sup>a</sup>	<b>L2</b> : yield <sup>b</sup> (%) / ee <sup>c</sup> (%)	<b>L11</b> : yield <sup>b</sup> (%) / ee <sup>c</sup> (%)
1	none	81 / 97	80 / 97
2	10% [Ni], 10% <b>L</b>	53 / 94	48 / 97
3	10% [Ni], 15% <b>L</b>	81 / 96	62 / 97
4	10% [Ni], 20% <b>L</b>	81 / 97	78 / 97
5	5% [Ni], 15% <b>L</b>	73 / 97	74 / 96
6	1.0% [Ir]	74 / 93	73 / 96
7	0.5% [Ir]	71 / 95	73 / 96
8	0.25% [Ir]	81 / 97	72 / 96
9	1.0% 4 CziPN	69 / 94	76 / 97
10	no base	32 / 97	33 / 97
11	no light	N.D. / -	<1 / -
12	no [Ir]	N.D. / -	N.D. / -
13	no [Ni] and <b>L</b>	N.D. / -	N.D. / -
14	no <b>L</b>	19 / 0	19 / 0

<sup>a</sup>Reaction conditions: **228** (0.1 mmol), **224** (0.15 mmol),  $\text{NiCl}_2 \cdot \text{dme}$  (10  $\mu\text{mol}$ , 10 mol%), **L2** or **L11** (30  $\mu\text{mol}$ , 30 mol%),  $[\text{Ir}(\text{dF}(\text{CF}_3)\text{ppy})_2(\text{bpy})]\text{PF}_6$  (0.125  $\mu\text{mol}$ , 0.125 mol%),  $\text{K}_2\text{HPO}_4$  (0.3 mmol, 3 equiv), 2-MeTHF (2 mL, 0.05 molar in **228**), Pennoc M1 photoreactor, hv (450 nm), 7 cm sample holder, 500 RPM stir rate, 5200 RPM fan speed (18 h).  
<sup>b</sup>Determined by  $^1\text{H}$  NMR analysis vs ethylene carbonate as an internal standard. <sup>c</sup>Enantiomeric excess determined by chiral RP-HPLC.

### Potassium Alkyl Trifluoroborate Solvent Screening

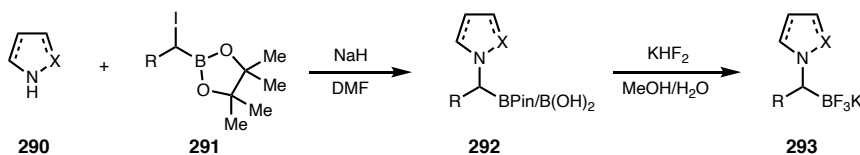
A solution of  $\text{NiCl}_2 \cdot \text{dme}$  (0.20 equiv, 1.0  $\mu\text{mol}$ , 0.22 mg) in a 27:1 (v:v) mixture of THF:MeOH (58.3  $\mu\text{L}$ ) was added to each ligand (**L2** and **L11**) (0.21 equiv, 1.05  $\mu\text{mol}$ ) in a 8x30 shell vial containing a dowel, the vial sealed, and the mixture agitated at 45 °C for 1 h. The solvent was removed *in vacuo* and a well-stirred suspension of the aryl bromide (**228**, 1.0 equiv, 5  $\mu\text{mol}$ ) and  $\text{K}_2\text{HPO}_4$  (6 equiv, 30  $\mu\text{mol}$ , 5.2 mg) in TBME (100  $\mu\text{L}$ ) was added. The solvent was removed *in vacuo* and a well-stirred suspension of the  $\text{BF}_3\text{K}$  salt (**221**, **264**, **267–269**, or **273–277**, 1.5 equiv, 7.5  $\mu\text{mol}$ ) in TBME (100  $\mu\text{L}$ ) was added. The solvent was removed *in vacuo* and a solution (or well-stirred suspension) of  $[\text{Ir}(\text{dF}(\text{CF}_3)\text{ppy})_2(\text{bpy})]\text{PF}_6$  (0.01 equiv, 5  $\mu\text{L}$ , 0.05  $\mu\text{mol}$ , 50.5  $\mu\text{g}$ ) in the desired reaction solvent (100  $\mu\text{L}$ ; 0.5 mM in [Ir]) was added. The sealed reaction was agitated at 350 RPM while being irradiated for 20 h, maintaining a measured external reaction block temperature

of about 36–42 °C. Following reaction completion, a solution of biphenyl (0.20 equiv, 1.0  $\mu$ mole, 0.15 mg) in acetonitrile (400  $\mu$ L) was added and the resulting mixture analyzed by chiral stationary RPLC for the determination of the ratio of product **229**, **264**, **266**, **270**–**272**, **278**–**282** and biphenyl.

Substrate	Ligand	Ratio of product integral to biphenyl integral											
		THF	2-MeTHF	CPME	DME	TBME	95:5 TBME/2Me- THF	80:20 TBME/2- MeTHF	Acetone	<sup>i</sup> PrOAc	Toluene	PhCF <sub>3</sub>	90:10 2- MeTHF/Me OH
224	L11	0.75	1.46	1.5	1.36	1.51	1.56	1.63	1.22	1.48	ND	0.92	1.43
	L2	0.97	1.35	1.27	1.36	1.26	1.34	1.38	1.13	1.38	ND	1.03	1.31
267	L11	1.44	1.44	0.63	1.37	0.53	0.63	0.92	1.19	1.57	0.34	0.42	1.09
	L2	1.36	1.25	1.03	1.23	0.73	0.95	1.06	1.05	1.24	0.74	1.12	1.09
274	L11	1.17	1.91	1.86	1.65	1.86	1.84	1.94	1.44	1.87	1.89	1.45	1.27
	L2	1.17	1.53	1.44	1.28	1.37	1.35	1.41	1.01	1.45	1.51	1.36	0.95
275	L11	0.86	1.47	1.63	1.51	1.65	1.64	1.63	1.17	1.67	ND	ND	1.24
	L2	0.85	1.25	1.28	1.23	1.17	1.21	1.3	1.03	1.4	ND	ND	1.28
268	L11	0.58	0.33	0.83	0.18	1.12	0.98	0.97	0.13	0.45	0.73	ND	0.33
	L2	0.31	0.19	0.8	0.14	0.99	0.98	0.95	0.08	0.26	0.71	ND	0.28
276	L11	1.29	1.42	1.99	1.34	1.86	1.89	1.74	0.95	1.41	1.95	1.8	1.32
	L2	1.56	1.46	1.67	1.18	1.8	1.76	1.64	0.85	1.12	1.36	1.45	1.02
263	L11	0.37	0.44	0.28	1.09	0.27	0.28	0.29	0.42	0.45	ND	0.32	0.36
	L2	1.07	1.21	1.41	1.48	1.17	0.88	1.47	0.25	0.45	ND	1.61	0.34
269	L11	1.06	0.82	0.62	1.7	0.64	0.74	0.91	1.33	1.37	0.33	0.41	0.7
	L2	1.55	0.87	0.64	1.62	0.56	0.71	0.8	1.68	1.65	0.3	0.3	0.75
277	L11	0.2	0.24	0.32	0.06	0.48	0.49	0.41	0.56	0.34	ND	ND	0.69
	L2	0.06	0.17	0.22	0.08	0.31	0.35	0.2	0.54	0.12	ND	ND	1.13

### 3.6.4 Substrate Preparation

#### General Procedure 1

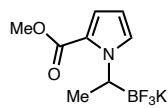


A round bottom flask was charged with the corresponding N-heterocycle (**290**, 1.0 equiv, 6.98 mmol) and anhydrous DMF (0.3 M) was added under N<sub>2</sub> atmosphere. The resulting solution was cooled at 0 °C, then NaH (1.2 equiv, 60 wt. %, 8.38 mmol) was added portionwise. The reaction mixture was stirred at 0 °C for 30–60 min. The iodoalkyl borane (**291**, 2.0 equiv, 13.97 mmol) was added dropwise at 0 °C over 2 h. The allowed to room to ambient temperature and stirred overnight. Approximately 30% of the DMF was

removed *in vacuo* and the resulting crude material was directly charged in a ISCO C18 column and purified by reverse phase chromatography (water/MeCN). The corresponding product **292** was obtained in the form of a mixture of boronic acid and pinacol borane. The material was used in the next step without further purification.

The residue was charged in a round bottom flask and dissolved in a mixture of MeOH/H<sub>2</sub>O (2/1, 0.2 M). Potassium bifluoride (4.0 equiv, 14.54 mmol) was introduced in one portion in the reaction mixture. The reaction was stirred at ambient temperature overnight. The mixture was then concentrated *in vacuo* and the resulting residue was redissolved in anhydrous acetone (10 ml/g) then filtered. The filtrate was concentrated *in vacuo* and recrystallized in a mixture of acetone/MTBE (1/10, 100 mL/g). The solid was filtrated, washed with a mixture of acetone/MTBE (1/10), and dried under vacuum to give the desired potassium alkyl trifluoroborate starting material. *Note: Potassium alkyl trifluoroborates were synthesized and largely characterized by our collaborators at Merck.*

**Potassium trifluoro(1-(2-(methoxycarbonyl)-1H-pyrrol-1-yl)ethyl)borate (224)**



Prepared from commercially available methyl 1H-pyrrole-2-carboxylate and 2-(1-iodoethyl)-4,4,5,5-tetramethyl-1,3,2-dioxaborolane.<sup>38</sup> following

General Procedure 1. The crude residue was purified by recrystallization in acetone/MTBE (1/10) to yield **224** (2.6 g, 65% yield over two steps).

**<sup>1</sup>H NMR (400 MHz, DMSO-*d*<sub>6</sub>):** δ 7.28 – 7.10 (m, 1H), 6.79 – 6.61 (m, 1H), 6.01 – 5.85 (m, 1H), 4.08 (m, 1H), 3.66 (s, 3H), 1.17 – 0.86 (m, 4H).

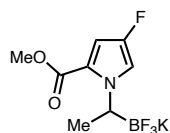
**<sup>13</sup>C NMR (101 MHz, DMSO-*d*<sub>6</sub>)** δ 160.8, 128.5, 120.7, 116.4, 106.0, 50.3, 25.0, 20.1.

**<sup>19</sup>F NMR (471 MHz, DMSO-*d*<sub>6</sub>):** δ -144.47.

**$^{11}\text{B}$  NMR (161 MHz, DMSO- $d_6$ ):**  $\delta$  3.58.

**HRMS (FAB, m/z):** calc'd for  $\text{C}_8\text{H}_{10}\text{BF}_3\text{NO}_2$   $[\text{M}+\text{H}]^+$  : 219.0793 ; found: 219.0798.

**Potassium trifluoro(1-(4-fluoro-2-(methoxycarbonyl)-1H-pyrrol-1-yl)ethyl)borate (273)**



Prepared from commercially available methyl 4-fluoro-1H-pyrrole-2-carboxylate and 2-(1-iodoethyl)-4,4,5,5-tetramethyl-1,3,2-dioxaborolane following General Procedure 1. The crude residue was purified by recrystallization in acetone/MTBE (1/10) to yield **273** (654 mg, 56% yield over two steps).

**$^1\text{H}$  NMR (500 MHz, DMSO- $d_6$ ):**  $\delta$  6.99 (s, 1H), 6.43 (d,  $J$  = 2.0 Hz, 1H), 4.12 (s, 1H), 3.68 (s, 3H), 3.32 (s, 1H), 1.06 (d,  $J$  = 7.2 Hz, 3H).

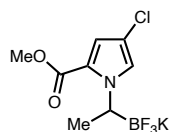
**$^{13}\text{C}$  NMR (126 MHz, DMSO- $d_6$ ):**  $\delta$  160.92, 149.93, 148.07, 117.33, 113.24 (dd,  $J$  = 27.2, 2.2 Hz), 101.77 (d,  $J$  = 14.4 Hz), 51.08, 31.72, 22.56, 20.11, 14.41.

**$^{19}\text{F}$  NMR (471 MHz, DMSO):**  $\delta$  -145.04, -167.21.

**$^{11}\text{B}$  NMR (161 MHz, DMSO- $d_6$ ):**  $\delta$  3.31.

**HRMS (FAB, m/z):** calc'd for  $\text{C}_8\text{H}_9\text{BF}_4\text{NO}_2$   $[\text{M}+\text{H}]^+$  : 237.0699 ; found: 237.0704.

**Potassium (1-(4-chloro-2-(methoxycarbonyl)-1H-pyrrol-1-yl)ethyl)trifluoroborate (267)**



Prepared from commercially available methyl 4-chloro-1H-pyrrole-2-carboxylate and 2-(1-iodoethyl)-4,4,5,5-tetramethyl-1,3,2-dioxaborolane following General Procedure 1. The crude residue was purified by recrystallization in acetone/MTBE (1/10) to yield **267** (390 mg, 74% yield over two steps).

**<sup>1</sup>H NMR (400 MHz, DMSO-*d*<sub>6</sub>):** δ 7.12 (d, *J* = 2.1 Hz, 1H), 6.64 (d, *J* = 2.1 Hz, 1H), 4.17 – 4.00 (m, 1H), 3.68 (s, 3H), 1.06 (d, *J* = 7.1 Hz, 3H).

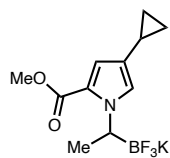
**<sup>13</sup>C NMR (101 MHz, DMSO-*d*<sub>6</sub>):** δ 160.1, 125.4, 120.8, 114.5, 107.9, 50.8, 19.7.

**<sup>19</sup>F NMR (471 MHz, DMSO-*d*<sub>6</sub>):** δ -145.15.

**<sup>11</sup>B NMR (161 MHz, DMSO-*d*<sub>6</sub>):** δ 2.20.

**HRMS (FAB, *m/z*):** calc'd for C<sub>8</sub>H<sub>9</sub>BClF<sub>3</sub>NO<sub>2</sub> [M+H]<sup>+</sup> : 253.0403 ; found: 253.0409

**Potassium (1-(4-cyclopropyl-2-(methoxycarbonyl)-1H-pyrrol-1-yl)ethyl)trifluoroborate (274)**



Prepared from commercially available methyl 4-cyclopropyl-1H-pyrrole-2-carboxylate and 2-(1-iodoethyl)-4,4,5,5-tetramethyl-1,3,2-dioxaborolane following General Procedure 1. The crude residue was purified by

recrystallization in acetone/MTBE (1/10) to yield **274** (780 mg, 68% yield over two steps).

**<sup>1</sup>H NMR (500 MHz, DMSO-*d*<sub>6</sub>):** δ 7.01 (d, *J* = 2.0 Hz, 1H), 6.40 (d, *J* = 2.0 Hz, 1H), 4.13 – 3.91 (m, 1H), 3.64 (s, 3H), 1.70 – 1.43 (m, 1H), 1.03 (d, *J* = 7.2 Hz, 3H), 0.72 (dd, *J* = 8.3, 2.2 Hz, 2H), 0.37 (td, *J* = 4.9, 1.9 Hz, 2H).

**<sup>13</sup>C NMR (126 MHz, DMSO-*d*<sub>6</sub>):** δ 161.13, 126.54, 123.82, 120.58, 113.65, 50.63, 20.47, 8.36, 8.24, 8.16.

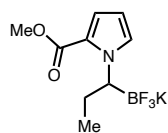
**<sup>19</sup>F NMR (471 MHz, DMSO-*d*<sub>6</sub>):** δ -144.37.

**<sup>11</sup>B NMR (161 MHz, DMSO-*d*<sub>6</sub>):** δ 3.35.

**HRMS (FAB, *m/z*):** calc'd for C<sub>11</sub>H<sub>14</sub>BF<sub>3</sub>NO<sub>2</sub> [M+H]<sup>+</sup> : 259.1106 ; found: 259.1114.



**Potassium trifluoro(1-(2-(methoxycarbonyl)-1H-pyrrol-1-yl)propyl)borate (275)**



Prepared from commercially available methyl 1H-pyrrole-2-carboxylate and 2-(1-iodoethyl)-4,4,5,5-tetramethyl-1,3,2-dioxaborolane.<sup>39</sup> The crude residue was purified by recrystallization in acetone/MTBE (1/10) to yield **275** (480 mg, 84% yield over two steps).

**<sup>1</sup>H NMR (500 MHz, DMSO-*d*<sub>6</sub>):**  $\delta$  7.72 (s, 1H), 7.40 – 7.25 (m, 1H), 6.58 (s, 1H), 4.83 (s, 1H), 4.29 (s, 3H), 2.30 (dp,  $J = 13.7, 7.2$  Hz, 1H), 2.17 (dp,  $J = 14.9, 7.5$  Hz, 1H), 1.24 (t,  $J = 7.4$  Hz, 3H).

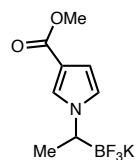
**<sup>13</sup>C NMR (126 MHz, DMSO-*d*<sub>6</sub>):**  $\delta$  162.57, 128.59, 123.04, 117.88, 116.58, 106.87, 50.57, 27.00, 11.76, 0.88 (dp,  $J = 41.5, 20.8$  Hz).

**<sup>19</sup>F NMR (471 MHz, DMSO-*d*<sub>6</sub>):**  $\delta$  -145.94.

**<sup>11</sup>B NMR (161 MHz, DMSO-*d*<sub>6</sub>):**  $\delta$  5.60 – 2.44 (m).

**HRMS (FAB, m/z):** calc'd for C<sub>9</sub>H<sub>12</sub>BF<sub>3</sub>NO<sub>2</sub> [M+H]<sup>+</sup> : 233.0950 ; found: 233.0955.

**Potassium trifluoro(1-(3-(methoxycarbonyl)-1H-pyrrol-1-yl)ethyl)borate (268)**



Prepared from commercially available methyl 1H-pyrrole-3-carboxylate and 2-(1-iodoethyl)-4,4,5,5-tetramethyl-1,3,2-dioxaborolane following General Procedure 1. The crude residue was purified by recrystallization in acetone/MTBE (1/10) to yield **268** (270 mg, 45% yield over two steps).

**<sup>1</sup>H NMR (400 MHz, DMSO-*d*<sub>6</sub>):**  $\delta$  7.30 (t,  $J = 2.0$  Hz, 1H), 6.65 (t,  $J = 2.4$  Hz, 1H), 6.29 – 6.09 (m, 1H), 3.64 (s, 3H), 3.06 – 2.82 (m, 1H), 1.13 (d,  $J = 7.3$  Hz, 3H).

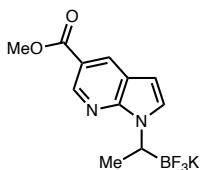
**<sup>13</sup>C NMR (101 MHz, DMSO-*d*<sub>6</sub>):**  $\delta$  164.7, 126.1, 122.4, 112.2, 107.4, 50.2, 19.2.

**<sup>19</sup>F NMR (471 MHz, DMSO-*d*<sub>6</sub>):**  $\delta$  -145.86.

**$^{11}\text{B}$  NMR (161 MHz, DMSO- $d_6$ ):**  $\delta$  3.25.

**HRMS (FAB,  $m/z$ ):** calc'd for  $\text{C}_{10}\text{H}_{15}\text{BF}_3\text{N}_2\text{O}_2$   $[\text{M}+\text{H}]^+$  : 262.1215 ; found: 262.1220.

**Potassium trifluoro(1-(5-(methoxycarbonyl)-1H-pyrrolo[2,3-b]pyridin-1-yl)ethyl)borate (276)**



Prepared from commercially available methyl 1H-pyrrolo[2,3-b]pyridine-5-carboxylate and 2-(1-iodoethyl)-4,4,5,5-tetramethyl-1,3,2-dioxaborolane following General Procedure 1. The crude residue was purified by recrystallization in acetone/MTBE (1/10) to yield **276** (841 mg, 68% yield over two steps).

**$^1\text{H}$  NMR (500 MHz, DMSO- $d_6$ ):**  $\delta$  8.77 (d,  $J$  = 2.0 Hz, 1H), 8.44 (d,  $J$  = 2.0 Hz, 1H), 7.67 (d,  $J$  = 3.4 Hz, 1H), 6.46 (d,  $J$  = 3.5 Hz, 1H), 3.95 (dd,  $J$  = 7.1, 3.7 Hz, 1H), 3.87 (s, 4H), 1.16 (d,  $J$  = 7.3 Hz, 3H).

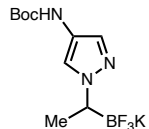
**$^{13}\text{C}$  NMR (126 MHz, DMSO- $d_6$ ):**  $\delta$  167.26, 149.71, 143.21, 131.77, 129.61, 119.57, 116.69, 98.99, 52.19, 18.73.

**$^{19}\text{F}$  NMR (471 MHz, DMSO- $d_6$ ):**  $\delta$  -144.86.

**$^{11}\text{B}$  NMR (161 MHz, DMSO- $d_6$ ):**  $\delta$  2.70.

**HRMS (FAB,  $m/z$ ):** calc'd for  $\text{C}_{11}\text{H}_{11}\text{BF}_3\text{N}_2\text{O}_2$   $[\text{M}+\text{H}]^+$  : 270.0902 ; found: 278.0913.

**Potassium (1-(4-((tert-butoxycarbonyl)amino)-1H-pyrazol-1-yl)ethyl)trifluoroborate (221)**



Prepared from commercially available tert-butyl (1H-pyrazol-4-yl)carbamate and 2-(1-iodoethyl)-4,4,5,5-tetramethyl-1,3,2-dioxaborolane following

General Procedure 1. The crude residue was purified by recrystallization in acetone/MTBE (1/10) to yield **221** (4.5 g, 76% yield over two steps).

**<sup>1</sup>H NMR (400 MHz, DMSO-*d*<sub>6</sub>):** δ 8.82 (s, 1H), 7.54 (s, 1H), 7.07 (s, 1H), 3.18 – 3.02 (m, 1H), 1.43 (s, 9H), 1.08 (d, *J* = 7.3 Hz, 3H).

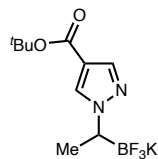
**<sup>13</sup>C NMR (101 MHz, DMSO-*d*<sub>6</sub>):** δ 152.7, 126.8, 120.3, 118.6, 78.0, 28.2, 18.9.

**<sup>19</sup>F NMR (471 MHz, DMSO-*d*<sub>6</sub>):** δ -145.35.

**<sup>11</sup>B NMR (161 MHz, DMSO-*d*<sub>6</sub>):** δ 3.26.

**HRMS (FAB, *m/z*):** calc'd for C<sub>10</sub>H<sub>16</sub>BF<sub>3</sub>N<sub>3</sub>O<sub>2</sub> [M+H]<sup>+</sup> : 277.1324 ; found: 277.1316.

**Potassium (1-(4-(tert-butoxycarbonyl)-1H-pyrazol-1-yl)ethyl)trifluoroborate (263)**



Prepared from commercially available *tert*-butyl 1H-pyrazole-4-carboxylate compound with carbon dioxide and 2-(1-iodoethyl)-4,4,5,5-tetramethyl-

1,3,2-dioxaborolane following General Procedure 1. The crude residue was

purified by recrystallization in acetone/MTBE (1/10) to yield **263** (2.8 g, 82% yield over two steps).

**<sup>1</sup>H NMR (400 MHz, DMSO-*d*<sub>6</sub>):** δ 7.88 (s, 1H), 7.58 (s, 1H), 3.28 – 3.15 (m, 1H), 1.47 (s, 9H), 1.14 (d, *J* = 7.3 Hz, 3H).

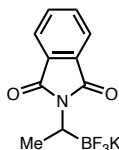
**<sup>13</sup>C NMR (101 MHz, DMSO-*d*<sub>6</sub>):** δ 162.4, 138.4, 131.4, 113.7, 79.0, 28.1, 18.5.

**<sup>19</sup>F NMR (471 MHz, DMSO-*d*<sub>6</sub>):** δ -144.86.

$^{11}\text{B}$  NMR (161 MHz, DMSO- $d_6$ ):  $\delta$  3.26.

HRMS (FAB, m/z): calc'd for  $\text{C}_{10}\text{H}_{15}\text{BF}_3\text{N}_2\text{O}_2$   $[\text{M}+\text{H}]^+$  : 262.1215 ; found: 262.1220.

### Potassium (1-(1,3-dioxoisindolin-2-yl)ethyl)trifluoroborate (269)



Prepared from commercially available isoindoline-1,3-dione and 2-(1-iodoethyl)-4,4,5,5-tetramethyl-1,3,2-dioxaborolane following General Procedure 1. The crude residue was purified by recrystallization in acetone/MTBE (1/10) to yield **269** (1.1 g, 35% yield over two steps).

$^1\text{H}$  NMR (400 MHz, DMSO- $d_6$ ):  $\delta$  7.80 – 7.68 (m, 4H), 3.29 – 3.21 (m, 1H), 1.18 (d,  $J$  = 7.7 Hz, 3H).

$^{13}\text{C}$  NMR (101 MHz, DMSO- $d_6$ ):  $\delta$  168.6, 133.5, 132.2, 121.9, 14.5.

$^{19}\text{F}$  NMR (471 MHz, DMSO- $d_6$ ):  $\delta$  -143.38.

$^{11}\text{B}$  NMR (161 MHz, DMSO- $d_6$ ):  $\delta$  2.82.

HRMS (FAB, m/z): calc'd for  $\text{C}_{10}\text{H}_8\text{BF}_3\text{NO}_2$   $[\text{M}+\text{H}]^+$  : 241.0637 ; found: 241.0636.

## 3.6.5 Enantioselective Cross-Coupling

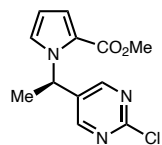
### General Procedure 2: Cross-Coupling on 0.2 mmol Scale

On the benchtop, to a 2-dram vial containing a 12 mm Teflon-coated stir bar were added aryl bromide (if solid) (1.0 equiv, 0.2 mmol) and potassium alkyl trifluoroborate salt (1.5 equiv, 0.3 mmol). The reaction vial was then brought into a  $\text{N}_2$ -filled glovebox and  $\text{K}_2\text{HPO}_4$  (3 equiv, 0.6 mmol, 105 mg) was added.  $\text{Ir}[\text{dF}(\text{CF}_3)\text{ppy}]_2(\text{bpy})\text{PF}_6$  (0.125 mol%, 0.25  $\mu\text{mol}$ , 0.25 mg) was added as a stock solution in 2.0 mL solvent followed by aryl bromide (if liquid) (1.0 equiv, 0.2 mmol). Meanwhile,  $\text{NiCl}_2\cdot\text{dme}$  (0.1 equiv, 0.02 mmol,

4.4 mg), ligand (**L2** or **L11**) (0.30 equiv, 0.06 mmol) and the remaining solvent (2.0 mL) (4.0 mL total in final reaction, 0.05 M in aryl bromide) were added to a 1-dram vial with a stir bar, sealed with a Teflon-lined cap, heated to 55–60 °C in a heating block, and stirred until complexation was complete, everything was dissolved, and a color change occurred (4-heptyl BiOX **L2**: clear peachy orange solution; 4-F-Ph BiOX **L11**: clear yellow solution). Once complexation was complete, the complexed catalyst solution was cooled to ambient temperature then added to the 2-dram reaction vial. The vial was sealed with a Teflon-lined cap and electrical tape, then removed from the glovebox. The reaction vial was then placed in a vial holder in a 7 cm tall cone in a Penn PhD m2 photoreactor with a 450 nm light module. Stirring was set to 500 rpm, the fan speed was set to 5200 rpm, the LED intensity was set to 100%, and the reaction time was set to 18 hours. After 18 hours, the reaction was diluted with EtOAc and sat. aq. NH<sub>4</sub>Cl. The aqueous layer was extracted 3 times with EtOAc, and the combined organic layers were pushed through a ~8 mm by 6 cm plug of MgSO<sub>4</sub> with a layer of celite on top. The solution was concentrated *in vacuo*, and the crude material was purified by flash column chromatography over silica gel to afford the desired product.

### 3.6.6 Characterization of Reaction Products

**methyl (R)-1-(1-(2-chloropyrimidin-5-yl)ethyl)-1H-pyrrole-2-carboxylate (234)**



Prepared from 5-bromo-2-chloropyrimidine (**228**, 38.7 mg, 0.2 mmol) and

**methyl 1-(1-(trifluoro- $\lambda^4$ -boraneyl)ethyl)-1H-pyrrole-2-carboxylate, potassium salt (**224**, 77.7 mg, 0.3 mmol) according to General Procedure 2 in 2-MeTHF with 4-F-Ph BiOX (**L11**). The crude residue was purified by column chromatography**

(silica gel, 8.5–9% EtOAc/hexane) to yield **234** (44.5 mg, 84% yield) in 97% ee as a colorless oil.

$R_f$  = 0.36 (silica gel, 20% EtOAc/hexanes, UV).

$[\alpha]_D^{21} = 79^\circ$  ( $c = 1.1$ ,  $\text{CHCl}_3$ ).

$^1\text{H NMR}$  (400 MHz,  $\text{CDCl}_3$ ):  $\delta$  8.33 (d,  $J = 0.6$  Hz, 2H), 7.10 (dd,  $J = 2.8, 1.7$  Hz, 1H), 7.03 (dd,  $J = 4.0, 1.7$  Hz, 1H), 6.59 (q,  $J = 7.3$  Hz, 1H), 6.28 (dd,  $J = 4.0, 2.8$  Hz, 1H), 3.75 (s, 3H), 1.86 (d,  $J = 7.3$  Hz, 3H)

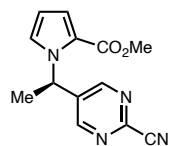
$^{13}\text{C NMR}$  (101 MHz,  $\text{CDCl}_3$ ):  $\delta$  161.6, 160.5, 157.7, 135.5, 124.6, 122.2, 119.5, 109.8, 51.4, 51.3, 21.7.

**FTIR** (NaCl, thin film,  $\text{cm}^{-1}$ ): 3126, 2984, 2949, 1698, 1549, 1439, 1398, 1338, 1226, 1113, 1059, 940, 829, 740

**HRMS** (ESI-TOF,  $m/z$ ): calc'd for  $\text{C}_{12}\text{H}_{13}\text{ClN}_3\text{O}_2$   $[\text{M}+\text{H}]^+$  : 266.0696 ; found: 266.0702.

**Chiral SFC**: (IC, 2.5 mL/min, 30% IPA in  $\text{CO}_2$ ,  $\lambda = 254$  nm):  $t_R$  (minor) = 3.3 min,  $t_R$  (major) = 3.9 min.

**methyl (R)-1-(1-(2-cyanopyrimidin-5-yl)ethyl)-1H-pyrrole-2-carboxylate (249)**



Prepared from 5-bromopyrimidine-2-carbonitrile (**239**, 36.8 mg, 0.2 mmol) and methyl 1-(1-(trifluoro- $\lambda^4$ -boraneyl)ethyl)-1H-pyrrole-2-carboxylate, potassium salt (**224**, 77.7mg, 0.3 mmol) according to General Procedure 2 in 2-MeTHF with 4-F-Ph BiOX (**L11**). The crude residue was purified by column chromatography (silica gel, 10 to 40% EtOAc/hexanes) to yield **249** (39 mg, 77% yield) in 95% ee as a colorless oil.

$R_f$  = 0.43 (silica gel, 30% EtOAc/hexanes, UV).

$[\alpha]_D^{22} = 60^\circ$  (c = 1.1, CHCl<sub>3</sub>).

**<sup>1</sup>H NMR (400 MHz, CDCl<sub>3</sub>):** δ 8.48 (d, *J* = 0.6 Hz, 2H), 7.15 (dd, *J* = 2.8, 1.7 Hz, 1H), 7.06 (dd, *J* = 4.0, 1.7 Hz, 1H), 6.61 (q, *J* = 7.3 Hz, 1H), 6.32 (dd, *J* = 4.0, 2.8 Hz, 1H), 3.74 (s, 3H), 1.90 (d, *J* = 7.3 Hz, 3H).

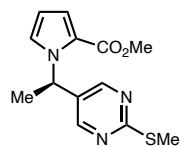
**<sup>13</sup>C NMR (101 MHz, CDCl<sub>3</sub>):** δ 161.53, 155.84, 144.01, 139.70, 124.57, 122.25, 119.79, 115.68, 110.07, 51.97, 51.46, 21.60.

**FTIR (NaCl, thin film, cm<sup>-1</sup>):** 2950, 1699, 1555, 1438, 1416, 1339, 1242, 1214, 1114, 942, 793, 761, 743

**HRMS (ESI-TOF, m/z):** calc'd for C<sub>13</sub>H<sub>13</sub>N<sub>4</sub>O<sub>2</sub> [M+H]<sup>+</sup> : 257.1039 ; found: 257.1023.

**Chiral SFC:** (AD-H, 2.5 mL/min, 10% IPA in CO<sub>2</sub>, λ = 280 nm): *t*<sub>R</sub> (minor) = 4.5 min, *t*<sub>R</sub> (major) = 4.2 min.

**methyl (R)-1-(1-(2-(methylthio)pyrimidin-5-yl)ethyl)-1H-pyrrole-2-carboxylate (229)**



Prepared from 5-bromo-2-(methylthio)pyrimidine (**222**, 41.0 mg, 0.2 mmol) and methyl 1-(1-(trifluoro-λ<sup>4</sup>-boraneyl)ethyl)-1H-pyrrole-2-carboxylate, potassium salt (**224**, 77.7 mg, 0.3 mmol) according to General Procedure 2 in 2-MeTHF with 4-F-Ph BiOX (**L11**). The crude residue was purified by column chromatography (silica gel, 15% EtOAc/hexanes) to yield **229** (46.5 mg, 84% yield) in 96% ee as a colorless oil.

**R<sub>f</sub>** = 0.39 (silica gel, 20% EtOAc/hexanes, UV).

$[\alpha]_D^{22} = 127^\circ$  (c = 1.0, CHCl<sub>3</sub>).

**<sup>1</sup>H NMR (400 MHz, CDCl<sub>3</sub>):** δ 8.27 (s, 2H), 7.06 (dd, *J* = 2.8, 1.7 Hz, 1H), 7.01 (dd, *J* = 3.9, 1.7 Hz, 1H), 6.55 (q, *J* = 7.2 Hz, 1H), 6.23 (dd, *J* = 3.9, 2.7 Hz, 1H), 3.76 (s, 3H), 2.53 (s, 3H), 1.83 (d, *J* = 7.2 Hz, 3H).

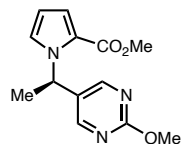
**<sup>13</sup>C NMR (101 MHz, CDCl<sub>3</sub>):** δ 171.87, 161.63, 155.41, 131.33, 124.70, 122.15, 119.25, 109.46, 51.46, 51.31, 21.65, 14.25

**FTIR (NaCl, thin film, cm<sup>-1</sup>):** 2948, 1699, 1584, 1537, 1438, 1400, 1338, 1227, 1111, 942, 738

**HRMS (ESI-TOF, *m/z*):** calc'd for C<sub>13</sub>H<sub>16</sub>N<sub>3</sub>O<sub>2</sub>S [M+H]<sup>+</sup> : 278.0963 ; found: 278.0970.

**Chiral SFC:** (IC, 2.5 mL/min, 25% IPA in CO<sub>2</sub>, λ = 280 nm): *t*<sub>R</sub> (minor) = 3.7 min, *t*<sub>R</sub> (major) = 4.3 min.

**methyl (R)-1-(1-(2-methoxypyrimidin-5-yl)ethyl)-1H-pyrrole-2-carboxylate (250)**



Prepared from 5-bromo-2-methoxypyrimidine (**240**, 37.8 mg, 0.2 mmol) and methyl 1-(1-(trifluoro-λ<sup>4</sup>-boraneyl)ethyl)-1H-pyrrole-2-carboxylate, potassium salt (**224**, 77.7 mg, 0.3 mmol) according to General Procedure 2 in 2-MeTHF with 4-F-Ph BiOX (**L11**). The crude residue was purified by column chromatography (silica gel, 30 to 40% EtOAc/hexanes) to yield **250** (33 mg, 63% yield) in 96% ee as a colorless oil.

**R<sub>f</sub>** = 0.30 (silica gel, 30% EtOAc/hexanes, UV).

**[α]<sub>D</sub><sup>21</sup>** = 99° (c = 1.51, CHCl<sub>3</sub>).

**<sup>1</sup>H NMR (400 MHz, CDCl<sub>3</sub>):** δ 8.28 (d, *J* = 0.6 Hz, 2H), 7.04 (dd, *J* = 2.8, 1.7 Hz, 1H), 6.99 (dd, *J* = 4.0, 1.8 Hz, 1H), 6.57 (q, *J* = 7.2 Hz, 1H), 6.22 (dd, *J* = 4.0, 2.8 Hz, 1H), 3.97 (s, 3H), 3.76 (s, 3H), 1.82 (d, *J* = 7.2 Hz, 3H).



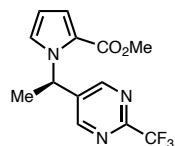
**$^{13}\text{C}$  NMR (101 MHz,  $\text{CDCl}_3$ ):**  $\delta$  165.15, 161.63, 157.55, 129.74, 124.67, 122.06, 119.13, 109.38, 55.07, 51.28, 51.17, 21.74.

**FTIR (NaCl, thin film,  $\text{cm}^{-1}$ ):** 2952, 1702, 1598, 1560, 1474, 1411, 1338, 1228, 1112, 1039, 943, 805, 738

**HRMS (ESI-TOF, m/z):** calc'd for  $\text{C}_{13}\text{H}_{16}\text{N}_3\text{O}_3$   $[\text{M}+\text{H}]^+$  : 262.1192 ; found: 262.1183.

**Chiral SFC:** (IC, 2.5 mL/min, 25% IPA in  $\text{CO}_2$ ,  $\lambda = 254$  nm):  $t_R$  (minor) = 4.1 min,  $t_R$  (major) = 4.4 min.

**methyl (R)-1-(1-(2-(trifluoromethyl)pyrimidin-5-yl)ethyl)-1H-pyrrole-2-carboxylate**



**(235)** Prepared from 5-bromo-2-(trifluoromethyl)pyrimidine (**230**, 45.4 mg, 0.3 mmol) and methyl 1-(1-(trifluoro- $\lambda^4$ -boraneyl)ethyl)-1H-pyrrole-2-carboxylate, potassium salt (**224**, 77.7 mg, 0.2 mmol) according to General

Procedure 2 in 2-MeTHF with 4-F-Ph BiOX (**L11**). The crude residue was purified by column chromatography (silica gel, 2.5% EtOAc/PhMe) to yield **235** (30 mg, 50% yield) in 98% ee as a colorless oil.

$R_f = 0.54$  (silica gel, 30% EtOAc/hexanes, UV).

$[\alpha]_D^{21} = 46^\circ$  ( $c = 1.5$ ,  $\text{CHCl}_3$ ).

**$^1\text{H}$  NMR (400 MHz,  $\text{CDCl}_3$ ):**  $\delta$  8.55 (s, 2H), 7.15 (dd,  $J = 2.8, 1.7$  Hz, 1H), 7.05 (dd,  $J = 4.0, 1.7$  Hz, 1H), 6.67 (q,  $J = 7.3$  Hz, 1H), 6.31 (dd,  $J = 4.0, 2.7$  Hz, 1H), 3.74 (s, 3H), 1.91 (d,  $J = 7.2$  Hz, 3H).

**$^{13}\text{C}$  NMR (101 MHz,  $\text{CDCl}_3$ ):**  $\delta$  161.6, 155.8 (q,  $J = 36.9$  Hz), 155.8, 139.1, 124.6, 122.3, 119.6 (q,  $J = 275.3$  Hz), 119.7, 110.0, 51.8, 51.4, 21.7.

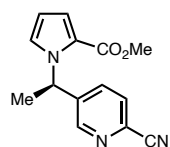
**$^{19}\text{F}$  NMR (282 MHz,  $\text{CDCl}_3$ )  $\delta$  -73.42.**

**FTIR (NaCl, thin film,  $\text{cm}^{-1}$ ):** 3124, 2991, 1956, 1704, 1698, 1714, 1568, 1441, 1353, 1118, 941

**HRMS (ESI-TOF, m/z):** calc'd for  $\text{C}_{13}\text{H}_{13}\text{F}_3\text{O}_2\text{N}_3$   $[\text{M}+\text{H}]^+$  : 300.0960 ; found: 300.0973.

**Chiral SFC:** (IC, 2.5 mL/min, 5% IPA in  $\text{CO}_2$ ,  $\lambda = 254$  nm):  $t_R$  (minor) = 3.0 min,  $t_R$  (major) = 3.7 min.

**methyl (R)-1-(1-(6-cyanopyridin-3-yl)ethyl)-1H-pyrrole-2-carboxylate (236)**



Prepared from 5-bromo-2-pyridinecarbonitrile (**231**, 36.6 mg, 0.2 mmol) and methyl 1-(1-(trifluoro- $\lambda^4$ -boraneyl)ethyl)-1H-pyrrole-2-carboxylate, potassium salt (**224**, 77.7 mg, 0.3 mmol) according to General Procedure 2 in 2-MeTHF with 4-F-Ph BiOX (**L11**). The crude residue was purified by column chromatography (silica gel, 10-30% EtOAc/hex) to yield **236** (39 mg, 77% yield) in 91% ee as a colorless oil.

$R_f = 0.39$  (silica gel, 30% EtOAc/hex, UV).

$[\alpha]_D^{25} = 71^\circ$  ( $c = 0.7784$ ,  $\text{CHCl}_3$ ).

**$^1\text{H}$  NMR (400 MHz,  $\text{CDCl}_3$ ):**  $\delta$  8.46 (d,  $J = 2.3$  Hz, 1H), 7.61 (dd,  $J = 8.1, 0.8$  Hz, 1H), 7.39 (ddd,  $J = 8.1, 2.3, 0.7$  Hz, 1H), 7.12 (dd,  $J = 2.8, 1.7$  Hz, 1H), 7.04 (dd,  $J = 4.0, 1.8$  Hz, 1H), 6.63 (q,  $J = 7.2$  Hz, 1H), 6.29 (dd,  $J = 4.0, 2.7$  Hz, 1H), 3.73 (d,  $J = 0.5$  Hz, 3H), 1.86 (d,  $J = 7.3$  Hz, 3H).

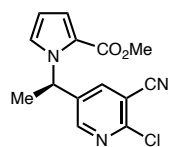
**$^{13}\text{C}$  NMR (101 MHz,  $\text{CDCl}_3$ ):**  $\delta$  161.51, 149.29, 143.21, 134.26, 132.70, 128.49, 124.82, 122.29, 119.46, 117.24, 109.59, 53.63, 51.35, 21.92.

**FTIR (NaCl, thin film,  $\text{cm}^{-1}$ ):** 2987, 2950, 2236, 1702, 1438, 1414, 1339, 1240, 1213, 1112, 1054, 1022, 946, 848, 760, 741

**HRMS (ESI-TOF, m/z):** calc'd for C<sub>14</sub>H<sub>14</sub>N<sub>3</sub>O<sub>2</sub> [M+H]<sup>+</sup> : 256.1086 ; found: 256.1074.

**Chiral SFC:** (AD-H, 2.5 mL/min, 15% IPA in CO<sub>2</sub>, λ = 254 nm): t<sub>R</sub> (minor) = 3.3 min, t<sub>R</sub> (major) = 3.1 min.

**methyl (R)-1-(1-(6-chloro-5-cyanopyridin-3-yl)ethyl)-1H-pyrrole-2-carboxylate (237)**



Prepared from 5-bromo-2-chloronicotinonitrile (**232**, 43.5 mg, 0.2 mmol) and methyl 1-(1-(trifluoro-λ<sup>4</sup>-boraneyl)ethyl)-1H-pyrrole-2-carboxylate, potassium salt (**224**, 77.7 mg, 0.3 mmol) according to General Procedure 2 in 2-MeTHF with 4-F-Ph BiOX (**L11**). The crude residue was purified by column chromatography (silica gel, 15% EtOAc/hexanes) to yield **237** (44.6 mg, 77% yield) in 97% ee as a colorless oil.

**R<sub>f</sub>** = 0.39 (silica gel, 20% EtOAc/hexanes, UV).

[α]<sub>D</sub><sup>22</sup> = 87° (c = 1.0, CHCl<sub>3</sub>).

**<sup>1</sup>H NMR (400 MHz, CDCl<sub>3</sub>):** δ 8.35 (dd, J = 2.5, 0.6 Hz, 1H), 7.55 (dd, J = 2.5, 0.7 Hz, 1H), 7.12 (dd, J = 2.8, 1.7 Hz, 1H), 7.04 (dd, J = 4.0, 1.7 Hz, 1H), 6.58 (q, J = 7.2 Hz, 1H), 6.30 (dd, J = 4.0, 2.8 Hz, 1H), 3.75 (s, 3H), 1.85 (d, J = 7.3 Hz, 3H)

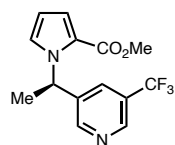
**<sup>13</sup>C NMR (101 MHz, CDCl<sub>3</sub>):** δ 161.5, 151.5, 150.9, 140.0, 138.9, 124.5, 122.2, 119.7, 114.7, 110.8, 109.9, 52.7, 51.4, 21.9

**FTIR (NaCl, thin film, cm<sup>-1</sup>):** 2949, 1698, 1558, 1532, 1414, 1341, 1238, 1115, 913, 739

**HMRS (ESI-TOF, m/z):** C<sub>14</sub>H<sub>13</sub>N<sub>3</sub>O<sub>2</sub>Cl; calc'd for [M+H]<sup>+</sup>: 290.0696, found: 290.0682

**Chiral SFC:** (IC, 2.5 mL/min, 15% MeOH in CO<sub>2</sub>, λ = 254 nm): t<sub>R</sub> (minor) = 3.8 min, t<sub>R</sub> (major) = 4.0 min.

**methyl (R)-1-(1-(5-(trifluoromethyl)pyridin-3-yl)ethyl)-1*H*-pyrrole-2-carboxylate**



**(251)**: Prepared from 3-bromo-5-(trifluoromethyl)pyridine (**241**, 45.2 mg, 0.2 mmol) and methyl 1-(1-(trifluoro- $\lambda^4$ -boraneyl)ethyl)-1*H*-pyrrole-2-carboxylate, potassium salt (**224**, 77.7 mg, 0.3 mmol) according to General Procedure 2 in 2-MeTHF with 4-F-Ph BiOX (**L11**). The crude residue was purified by column chromatography (silica gel, 12.5% EtOAc/hexanes). The resulting colorless oil was purified again by column chromatography (silica gel, 0–1.5% Et<sub>2</sub>O/DCM) to yield **251** (37.6 mg, 63% yield) in 94% ee as a colorless oil.

$R_f$  = 0.42 (silica gel, 20% EtOAc/hexanes, UV).

$[\alpha]_D^{22} = 40^\circ$  (c = 1.0, CHCl<sub>3</sub>).

**<sup>1</sup>H NMR (400 MHz, CDCl<sub>3</sub>)**:  $\delta$  8.76 (s, 1H), 8.56 (s, 1H), 7.63 – 7.51 (m, 1H), 7.10 (dd, J = 2.8, 1.8 Hz, 1H), 7.03 (dd, J = 3.9, 1.8 Hz, 1H), 6.69 (q, J = 7.2 Hz, 1H), 6.27 (dd, J = 3.9, 2.8 Hz, 1H), 3.75 (s, 3H), 1.87 (d, J = 7.3 Hz, 3H).

**<sup>13</sup>C NMR (101 MHz, CDCl<sub>3</sub>)**:  $\delta$  161.9, 151.2, 145.6 (q, J = 4.6 Hz), 139.4, 130.6 (q, J = 3.8 Hz), 126.8 (q, J = 32.9), 124.8, 123.5 (q, J = 272.8 Hz), 122.2, 119.3, 109.6, 53.2, 51.3, 22.0.

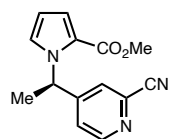
**<sup>19</sup>F NMR (282 MHz, CDCl<sub>3</sub>)**:  $\delta$  -65.6.

**FTIR (NaCl, thin film, cm<sup>-1</sup>)**: 2952, 1703, 1531, 1440, 1339, 11240, 1132, 1026, 735.

**HRMS (FI, m/z)**: calc'd for C<sub>14</sub>H<sub>13</sub>N<sub>2</sub>O<sub>2</sub>F<sub>3</sub> [M+•]<sup>+</sup> : 298.0924 ; found: 298.0936.

**Chiral SFC**: (AD-H, 2.5 mL/min, 3% IPA in CO<sub>2</sub>, ( $\lambda$  = 280 nm):  $t_R$  (major) = 3.8 min,  $t_R$  (minor) = 4.3 min.

**methyl (R)-1-(1-(2-cyanopyridin-4-yl)ethyl)-1H-pyrrole-2-carboxylate (252)**



Prepared from 4-bromopicolinonitrile (**242**, 36.6 mg, 0.2 mmol) and methyl 1-(1-(trifluoro- $\lambda^4$ -boraneyl)ethyl)-1H-pyrrole-2-carboxylate, potassium salt (**224**, 77.7 mg, 0.3 mmol) according to General Procedure 2 in 2-MeTHF with 4-F-Ph BiOX (**L11**). The crude residue was purified by column chromatography (silica gel, 20% EtOAc/hexanes) to yield **252** (39.2 mg, 77% yield) in 92% ee as a colorless oil.

$R_f$  = 0.25 (silica gel, 20% EtOAc/hexanes, UV).

$[\alpha]_D^{22} = 38^\circ$  (c = 1.0, CHCl<sub>3</sub>).

**<sup>1</sup>H NMR (400 MHz, CDCl<sub>3</sub>):**  $\delta$  8.60 (d, J = 5.1 Hz, 1H), 7.26 – 7.23 (m, 1H), 7.15 – 7.08 (m, 2H), 7.08 – 7.03 (m, 1H), 6.55 (q, J = 7.3 Hz, 1H), 6.34 – 6.27 (m, 1H), 3.73 (s, 3H), 1.83 (d, J = 7.3 Hz, 3H).

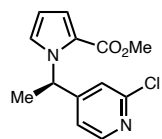
**<sup>13</sup>C NMR (101 MHz, CDCl<sub>3</sub>):**  $\delta$  161.5, 154.7, 151.5, 134.5, 125.7, 124.9, 124.0, 122.3, 119.5, 117.3, 109.7, 54.6, 51.4, 21.6.

**FTIR (NaCl, thin film, cm<sup>-1</sup>):** 2949, 2237, 1703, 1596, 1438, 1342, 1240, 1213, 1114, 948, 743.

**HRMS (FI, m/z):** calc'd for C<sub>14</sub>H<sub>13</sub>N<sub>3</sub>O<sub>2</sub> [M+•]<sup>+</sup>: 255.1002; found: 255.1006.

**Chiral SFC:** (OJ-H, 2.5 mL/min, 10% IPA in CO<sub>2</sub>, ( $\lambda$  = 254 nm):  $t_R$  (minor) = 3.9 min,  $t_R$  (major) = 4.6 min.

**methyl (R)-1-(1-(2-chloropyridin-4-yl)ethyl)-1H-pyrrole-2-carboxylate (253)**



Prepared from 4-bromo-2-chloropyridine (**243**, 38.5 mg, 0.2 mmol) and methyl 1-(1-(trifluoro- $\lambda^4$ -boraneyl)ethyl)-1H-pyrrole-2-carboxylate, potassium salt (**224**, 77.7 mg, 0.3 mmol) according to General Procedure 2 in 2-MeTHF

with 4-F-Ph BiOX (**L11**). The crude residue was purified by column chromatography (silica gel, 15% EtOAc/hexanes). The resulting sticky white solid was dissolved in CDCl<sub>3</sub>, then pentane was added to precipitate a white solid. The solid was filtered off, then the filtrate was concentrated to yield **253** (35.6 mg, 67% yield) in 95% ee as a colorless oil.

$R_f = 0.40$  (silica gel, 20% EtOAc/hexanes, UV).

$[\alpha]_D^{22} = 47^\circ$  (c = 1.0, CHCl<sub>3</sub>).

**<sup>1</sup>H NMR (400 MHz, CDCl<sub>3</sub>):** δ 8.28 (d, J = 5.2 Hz, 1H), 7.09 – 7.06 (m, 1H), 7.06 – 7.02 (m, 1H), 6.94 – 6.90 (m, 1H), 6.87 – 6.82 (m, 1H), 6.53 (q, J = 7.2 Hz, 1H), 6.30 – 6.24 (m, 1H), 3.74 (s, 3H), 1.80 (d, J = 7.2 Hz, 3H).

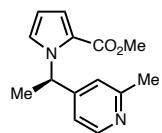
**<sup>13</sup>C NMR (101 MHz, CDCl<sub>3</sub>):** δ 161.5, 156.1, 152.2, 150.08, 125.0, 122.3, 121.3, 119.8, 119.2, 109.4, 54.5, 51.3, 21.6.

**FTIR (NaCl, thin film, cm<sup>-1</sup>):** 3124, 2986, 1949, 1698, 1593, 1549, 1415, 1342, 1240, 1110, 948, 839.

**HRMS (FI, m/z):** calc'd for C<sub>13</sub>H<sub>13</sub>N<sub>2</sub>O<sub>2</sub>Cl [M+•]<sup>+</sup>: 264.0660; found: 264.0665.

**Chiral SFC:** (AD-H, 2.5 mL/min, 10% IPA in CO<sub>2</sub>, (λ = 254 nm):  $t_R$  (minor) = 4.0 min,  $t_R$  (major) = 4.4 min.

**methyl (*R*)-1-(1-(2-methylpyridin-4-yl)ethyl)-1*H*-pyrrole-2-carboxylate (**254**)**



Prepared from 4-bromo-2-methylpyridine (**244**, 34.4 mg, 0.2 mmol) and methyl 1-(1-(trifluoro-λ<sup>4</sup>-boraneyl)ethyl)-1*H*-pyrrole-2-carboxylate, potassium salt (**224**, 77.7 mg, 0.3 mmol) according to General Procedure 2 in 2-MeTHF with 4-heptyl BiOX (**L2**). The crude residue was purified by column chromatography

(silica gel, 70% EtOAc/hexanes). to yield **254** (23.4 mg, 48% yield) in 97% ee as a colorless oil.

$R_f = 0.44$  (silica gel, 80% EtOAc/hexanes, UV).

$[\alpha]_D^{21} = 27^\circ$  (c = 1.0, CHCl<sub>3</sub>).

**<sup>1</sup>H NMR (400 MHz, CDCl<sub>3</sub>):** δ 8.39 (d, J = 5.2 Hz, 1H), 7.09 – 6.99 (m, 2H), 6.82 – 6.77 (m, 1H), 6.73 (ddd, J = 5.2, 1.5, 0.8 Hz, 1H), 6.52 (q, J = 7.2 Hz, 1H), 6.24 (dd, J = 3.9, 2.7 Hz, 1H), 3.74 (s, 3H), 2.50 (s, 3H), 1.78 (d, J = 7.2 Hz, 3H).

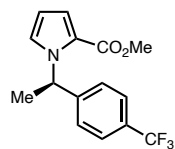
**<sup>13</sup>C NMR (101 MHz, CDCl<sub>3</sub>):** δ 161.6, 158.9, 152.8, 149.6, 125.3, 122.3, 120.4, 118.9, 118.1, 109.0, 54.8, 51.2, 24.7, 21.8.

**FTIR (NaCl, thin film, cm<sup>-1</sup>):** 2930, 1702, 1602, 1438, 1414, 1340, 1236, 1210, 1110.

**HRMS (FD+, m/z):** calc'd for C<sub>14</sub>H<sub>16</sub>N<sub>2</sub>O<sub>2</sub> [M+•]<sup>+</sup> : 244.1206; found: 244.1215.

**Chiral SFC:** (OB-H, 2.5 mL/min, 15% IPA in CO<sub>2</sub>, (λ = 254 nm):  $t_R$  (major) = 2.1 min,  $t_R$  (minor) = 3.7 min.

**methyl (R)-1-(1-(4-(trifluoromethyl)phenyl)ethyl)-1H-pyrrole-2-carboxylate (255)**



Prepared from 1-bromo-4-(trifluoromethyl)benzene (**245**, 45.0 mg, 0.2 mmol) and methyl 1-(1-(trifluoro-λ<sup>4</sup>-boraneyl)ethyl)-1H-pyrrole-2-carboxylate, potassium salt (**224**, 77.7 mg, 0.3 mmol) according to General Procedure 2 in 2-MeTHF with 4-heptyl BiOX (**L2**). The crude residue was purified by column chromatography (silica gel, 3% EtOAc/hexanes) to yield **255** (21.4 mg, 36% yield) in 93% ee as a colorless oil.

$R_f = 0.32$  (silica gel, 3.5% EtOAc/hexanes, UV).

$[\alpha]_D^{22} = 44^\circ$  (c = 1.0, CHCl<sub>3</sub>).

**<sup>1</sup>H NMR (400 MHz, CDCl<sub>3</sub>):** δ 7.59 – 7.49 (m, 2H), 7.23 – 7.14 (m, 2H), 7.07 (dd, *J* = 2.8, 1.7 Hz, 1H), 7.02 (dd, *J* = 3.9, 1.8 Hz, 1H), 6.62 (q, *J* = 7.2 Hz, 1H), 6.24 (dd, *J* = 3.9, 2.7 Hz, 1H), 3.75 (s, 3H), 1.82 (d, *J* = 7.2 Hz, 3H).

**<sup>13</sup>C NMR (101 MHz, CDCl<sub>3</sub>):** δ 161.6, 147.5 (q, *J* = 1.4 Hz), 129.6 (q, *J* = 23.3 Hz), 126.4, 125.7 (q, *J* = 3.8 Hz), 125.3, 124.9 (q, *J* = 272.3 Hz), 122.3, 118.9, 108.9, 55.3, 51.2, 22.2.

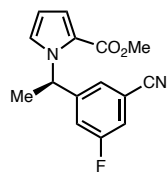
**<sup>19</sup>F NMR (282 MHz, CDCl<sub>3</sub>):** δ -65.7.

**FTIR (NaCl, thin film, cm<sup>-1</sup>):** 2988, 2951, 1704, 1621, 1530, 1440, 1324, 1240, 1108, 1017, 948, 739.

**HRMS (FI, *m/z*):** calc'd for C<sub>15</sub>H<sub>14</sub>NO<sub>2</sub>F<sub>3</sub> [*M*+•]<sup>+</sup>: 297.0971; found: 297.0976.

**Chiral SFC:** (OD-H, 2.5 mL/min, 5% IPA in CO<sub>2</sub>, (λ = 254 nm): *t<sub>R</sub>* (major) = 2.5 min, *t<sub>R</sub>* (minor) = 3.5 min.

**methyl (R)-1-(1-(3-cyano-5-fluorophenyl)ethyl)-1*H*-pyrrole-2-carboxylate (238)**



Prepared from 3-bromo-5-fluorobenzonitrile (**233**, 40.0 mg, 0.2 mmol) and methyl 1-(1-(trifluoro-λ<sup>4</sup>-boraneyl)ethyl)-1*H*-pyrrole-2-carboxylate, potassium salt (**224**, 77.7 mg, 0.3 mmol) according to General Procedure 2

in 2-MeTHF with 4-F-Ph BiOX (**L11**). The crude residue was purified by column chromatography (silica gel, 8.5% EtOAc/hexanes) to yield **238** (43 mg, 79% yield) in 97% ee as a colorless oil.

**R<sub>f</sub>** = 0.55 (silica gel, 20% EtOAc/hexanes, UV).

**[α]<sub>D</sub><sup>21</sup>** = 56° (c = 1.0, CHCl<sub>3</sub>).



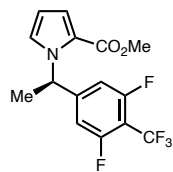
**<sup>1</sup>H NMR (400 MHz, CDCl<sub>3</sub>):** δ 7.24 – 7.17 (m, 1H), 7.15 – 6.94 (m, 4H), 6.58 (q, *J* = 7.2 Hz, 1H), 6.33 – 6.22 (m, 1H), 3.75 (d, *J* = 1.6 Hz, 3H), 1.87 – 1.76 (m, 3H)

**<sup>13</sup>C NMR (101 MHz, CDCl<sub>3</sub>):** δ 162.5 (d, *J* = 250.9 Hz), 161.6, 148.4 (d, *J* = 7.3 Hz), 125.6 (d, *J* = 3.3 Hz), 124.9, 122.2, 119.3, 118.3 (d, *J* = 20.2 Hz), 118.2 (d, *J* = 22.9 Hz), 114.1 (d, *J* = 9.6 Hz), 109.5, 54.7, 51.3, 2.0

**<sup>19</sup>F NMR (282 MHz, CDCl<sub>3</sub>)** δ -112.41 (dd, *J* = 9.3, 7.9 Hz).

**FTIR (NaCl, thin film, cm<sup>-1</sup>):** 2950, 2233, 1699, 1596, 1531, 1437, 1343, 1236, 1115, 964, 874, 743.

**methyl (R)-1-(1-(3,5-difluoro-4-(trifluoromethyl)phenyl)ethyl)-1*H*-pyrrole-2-**



**carboxylate (256):** Prepared from 5-bromo-1,3-difluoro-2-(trifluoromethyl)benzene (**246**, 52.2 mg, 0.2 mmol) and methyl 1-(1-(trifluoro-λ<sup>4</sup>-boraneyl)ethyl)-1*H*-pyrrole-2-carboxylate, potassium salt

(**224**, 77.7 mg, 0.3 mmol) according to General Procedure 2 in 2-MeTHF with 4-F-Ph BiOX (**L11**). The crude residue was purified by column chromatography (silica gel, 2–20% EtOAc/hexanes) to yield **256** (38.7 mg, 58% yield) in 97% ee as a colorless oil.

**R<sub>f</sub>** = 0.68 (silica gel, 30% EtOAc/hexanes, UV).

**[α]<sub>D</sub><sup>25</sup>** = 38° (c = 0.97, CHCl<sub>3</sub>).

**<sup>1</sup>H NMR (400 MHz, CDCl<sub>3</sub>):** δ 7.09 (dd, *J* = 2.8, 1.8 Hz, 1H), 7.05 (dd, *J* = 3.9, 1.7 Hz, 1H), 6.70 – 6.61 (m, 2H), 6.55 (q, *J* = 7.2 Hz, 1H), 6.28 (dd, *J* = 4.0, 2.7 Hz, 1H), 3.76 (s, 3H), 1.81 (d, *J* = 7.2 Hz, 3H).

<sup>13</sup>C NMR (101 MHz, CDCl<sub>3</sub>): δ 161.7 – 158.8 (m) 161.6, 151.6 (t, *J* = 9.3 Hz), 124.9, 122.3, 122.1 (qt, *J* = 274.8, 1.5 Hz), 119.3, 110.3 – 110.0 (m), 109.5, 107.0 – 106.1 (m), 54.9, 51.3, 21.8.

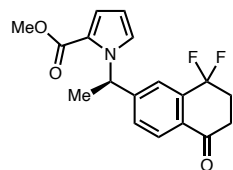
<sup>19</sup>F NMR (282 MHz, CDCl<sub>3</sub>) δ -59.59 (t, *J* = 21.6 Hz), -111.09 – -114.78 (m).

FTIR (NaCl, thin film, cm<sup>-1</sup>): 2952, 1704, 1644, 1584, 1532, 1440, 1340, 1240, 1214, 1139, 1115, 1046, 859, 762, 737, 573.

HRMS (ESI-TOF, *m/z*): calc'd for C<sub>15</sub>H<sub>13</sub>NO<sub>2</sub>F<sub>5</sub> [M+H]<sup>+</sup> : 334.0866 ; found: 334.0862.

Chiral SFC: (OJ-H, 2.5 mL/min, 7% IPA in CO<sub>2</sub>, λ = 254 nm): *t*<sub>R</sub> (minor) = 2.9 min, *t*<sub>R</sub> (major) = 2.3 min.

**methyl (R)-1-(1-(8,8-difluoro-5-oxo-5,6,7,8-tetrahydronaphthalen-2-yl)ethyl)-1*H*-**



**pyrrole-2-carboxylate (257):** Prepared from 6-bromo-4,4-difluoro-3,4-dihydronaphthalen-1(2*H*)-one (**247**, 52.2 mg, 0.2 mmol) and methyl 1-(1-(trifluoro-λ<sup>4</sup>-boraneyl)ethyl)-1*H*-pyrrole-2-carboxylate,

potassium salt (**224**, 77.7 mg, 0.3 mmol) according to General Procedure 2 in 2-MeTHF with 4-F-Ph BiOX (**L11**). The crude residue was purified by column chromatography (silica gel, 15% EtOAc/hexanes) to yield **257** (45.9 mg, 69% yield) in 94% ee as a colorless oil.

*R*<sub>f</sub> = 0.43 (silica gel, 20% EtOAc/hexanes, UV).

[α]<sub>D</sub><sup>22</sup> = 73° (c = 1.0, CHCl<sub>3</sub>).

<sup>1</sup>H NMR (400 MHz, CDCl<sub>3</sub>): δ 7.97 (dt, *J* = 8.2, 1.3 Hz, 1H), 7.52 – 7.46 (m, 1H), 7.29 – 7.23 (m, 1H), 7.08 (dd, *J* = 2.8, 1.8 Hz, 1H), 7.03 (dd, *J* = 3.9, 1.7 Hz, 1H), 6.66 (q, *J* = 7.2

Hz, 1H), 6.26 (dd,  $J = 3.9, 2.7$  Hz, 1H), 3.75 (s, 3H), 2.94 – 2.82 (m, 2H), 2.70 – 2.55 (m, 2H), 1.85 (d,  $J = 7.2$  Hz, 3H).

**$^{13}\text{C}$  NMR (101 MHz,  $\text{CDCl}_3$ ):**  $\delta$  194.4 (t,  $J = 1.4$  Hz), 161.6, 150.6 (t,  $J = 1.1$  Hz), 137.3 (t,  $J = 25.9$  Hz), 130.5 (t,  $J = 5.5$  Hz), 128.9 (t,  $J = 1.4$  Hz), 127.8, 125.2, 122.3, 122.0 (t,  $J = 4.1$  Hz), 119.1, 119.09 (t,  $J = 238.7$  Hz), 109.2, 55.4, 51.2, 34.6 (t,  $J = 5.3$  Hz), 32.4 (t,  $J = 25.7$  Hz), 22.0.

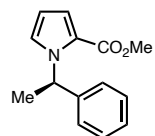
**$^{19}\text{F}$  NMR (282 MHz,  $\text{CDCl}_3$ )**  $\delta$  -95.60 (t,  $J = 13.0$  Hz)

**FTIR (NaCl, thin film,  $\text{cm}^{-1}$ ):** 3378, 2950, 1694, 1611, 1530, 1448, 1238, 975, 849, 746

**HRMS (ESI-TOF,  $m/z$ ):**  $\text{C}_{18}\text{H}_{18}\text{NO}_3\text{F}_2$ ; calc'd for  $[\text{M}+\text{H}]^+$ : 334.1255, found: 334.1259

**Chiral SFC:** (OD-H, 2.5 mL/min, 20% IPA in  $\text{CO}_2$ , ( $\lambda = 254$  nm):  $t_{\text{R}}$  (minor) = 2.6 min,  $t_{\text{R}}$  (major) = 3.2 min.

**methyl (*R*)-1-(1-phenylethyl)-1*H*-pyrrole-2-carboxylate (258)**



Prepared from bromobenzene (**248**, 31.4 mg, 0.2 mmol) and methyl 1-(1-(trifluoro- $\lambda^4$ -boraneyl)ethyl)-1*H*-pyrrole-2-carboxylate, potassium salt (**224**, 77.7 mg, 0.3 mmol) according to General Procedure 2 in 2-MeTHF with 4-heptyl BiOX (**L2**). The crude residue was purified by column chromatography (silica gel, 2.5% EtOAc/hexanes) to yield **258** (9.1 mg, 20% yield) in 78% ee as a colorless oil.

$R_f = 0.33$  (silica gel, 3% EtOAc/hexanes, UV).

$[\alpha]_D^{21} = 62^\circ$  ( $c = 0.51$ ,  $\text{CHCl}_3$ ).

**$^1\text{H}$  NMR (400 MHz,  $\text{CDCl}_3$ ):**  $\delta$  7.34 – 7.27 (m, 2H), 7.25 – 7.20 (m, 1H), 7.17 – 7.10 (m, 2H), 7.03 – 6.98 (m, 2H), 6.59 (q,  $J = 7.1$  Hz, 1H), 6.18 (dd,  $J = 3.9, 2.7$  Hz, 1H), 3.77 (s, 3H), 1.80 (d,  $J = 7.1$  Hz, 3H).

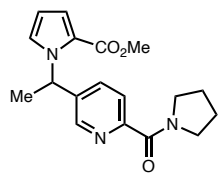
$^{13}\text{C}$  NMR (101 MHz,  $\text{CDCl}_3$ ):  $\delta$  161.7, 143.1, 128.7, 127.4, 126.3, 125.6, 122.2, 118.6, 108.5, 55.5, 51.2, 22.3.

FTIR (NaCl, thin film,  $\text{cm}^{-1}$ ): 2947, 2478, 1699, 1462, 1436, 1340, 1231, 1110, 1024, 946.

HRMS (FI, m/z): calc'd for  $\text{C}_{14}\text{H}_{15}\text{NO}_2$   $[\text{M}+\bullet]^+$ : 229.1097; found: 229.1105.

Chiral SFC: (OD-H, 2.5 mL/min, 5% IPA in  $\text{CO}_2$ , ( $\lambda = 254$  nm):  $t_R$  (major) = 5.1 min,  $t_R$  (minor) = 5.8 min.

**methyl 1-(1-(6-(pyrrolidine-1-carbonyl)pyridin-3-yl)ethyl)-1H-pyrrole-2-carboxylate**



**(260)**: Prepared from (5-bromopyridin-2-yl)(pyrrolidin-1-yl)methanone

**(259**, 51 mg, 0.2 mmol) and methyl 1-(1-(trifluoro- $\lambda^4$ -boraneyl)ethyl)-1H-pyrrole-2-carboxylate, potassium salt **(224**, 77.7 mg, 0.3 mmol)

according to General Procedure 2 in 2-MeTHF with 4-heptyl BiOX (**L2**). The crude residue was purified by column chromatography (silica gel, 60–100% EtOAc/hexanes) to yield **260** (35.8 mg, 55% yield) in 0% ee as a colorless oil.

$R_f = 0.3$  (silica gel, 80% EtOAc/DCM, UV).

$[\alpha]_D^{25} = -1.5^\circ$  ( $c = 1.89$ ,  $\text{CHCl}_3$ ).

$^1\text{H}$  NMR (400 MHz,  $\text{CDCl}_3$ ):  $\delta$  8.35 (d,  $J = 2.3$  Hz, 1H), 7.77 (dd,  $J = 8.1, 0.8$  Hz, 1H), 7.43 (ddd,  $J = 8.2, 2.3, 0.7$  Hz, 1H), 7.07 (dd,  $J = 2.8, 1.7$  Hz, 1H), 7.02 (dd,  $J = 3.9, 1.7$  Hz, 1H), 6.65 (q,  $J = 7.2$  Hz, 1H), 6.24 (dd,  $J = 3.9, 2.7$  Hz, 1H), 3.78 – 3.70 (m, 5H), 3.70 – 3.62 (m, 2H), 1.95 – 1.87 (m, 4H), 1.84 (d,  $J = 7.2$  Hz, 3H).

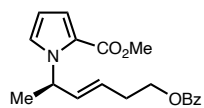
$^{13}\text{C}$  NMR (101 MHz,  $\text{CDCl}_3$ ):  $\delta$  166.2, 161.6, 153.5, 146.1, 140.0, 134.4, 125.1, 124.0, 122.2, 119.1, 109.2, 53.5, 51.2, 49.3, 47.0, 26.8, 24.1, 22.0.

**FTIR (NaCl, thin film, cm<sup>-1</sup>):** 2967, 2876, 1702, 1625, 1436, 1339, 1237, 1212, 1111, 1022, 736.

**HRMS (FAB, m/z):** calc'd for C<sub>18</sub>H<sub>22</sub>N<sub>3</sub>O<sub>3</sub> [M+H]<sup>+</sup> : 328.1661 ; found: 328.1657.

**Chiral SFC:** (OD-H, 2.5 mL/min, 30% IPA in CO<sub>2</sub>, (λ = 254 nm): *t*<sub>R</sub> (major) = 3.3 min, *t*<sub>R</sub> (major) = 3.7 min.

**methyl (R,E)-1-(6-(benzoyloxy)hex-3-en-2-yl)-1*H*-pyrrole-2-carboxylate (261):**



Prepared from (*E*)-4-bromobut-3-en-1-yl benzoate (**84f**, 51.0 mg, 0.2 mmol) and methyl 1-(1-(trifluoro-λ<sup>4</sup>-boraneyl)ethyl)-1*H*-pyrrole-2-carboxylate, potassium salt (**224**, 77.7 mg, 0.3 mmol) according to General Procedure 2 in 2-MeTHF with 4-heptyl BiOX (**L2**). The crude residue was purified by column chromatography (silica gel, 10% EtOAc/hexanes) to yield **261** (18.2 mg, 28% yield) in 83% ee as a colorless oil.

**R<sub>f</sub>** = 0.29 (silica gel, 10% EtOAc/DCM, UV).

**[α]<sub>D</sub><sup>21</sup>** = 21° (c = 1.0, CHCl<sub>3</sub>).

**<sup>1</sup>H NMR (500 MHz, CDCl<sub>3</sub>):** δ 8.06 – 7.96 (m, 2H), 7.60 – 7.52 (m, 1H), 7.43 (t, J = 7.7 Hz, 2H), 6.98 – 6.92 (m, 2H), 6.14 – 6.07 (m, 1H), 6.01 – 5.93 (m, 1H), 5.80 (ddt, J = 15.5, 5.6, 1.4 Hz, 1H), 5.58 (dtd, J = 15.3, 6.9, 1.5 Hz, 1H), 4.35 (td, J = 6.6, 1.2 Hz, 2H), 3.79 (s, 3H), 2.51 (q, J = 6.7 Hz, 2H), 1.51 (d, J = 6.9 Hz, 3H).

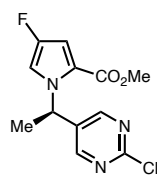
**<sup>13</sup>C NMR (101 MHz, CDCl<sub>3</sub>):** δ 166.6, 161.8, 134.4, 133.1, 130.4, 129.7, 128.5, 127.0, 125.1, 121.5, 118.3, 108.4, 64.0, 53.3, 51.1, 31.9, 21.3.

**FTIR (NaCl, thin film, cm<sup>-1</sup>):** 2953, 1715, 1437, 1411, 1378, 1338, 1274, 1227, 1107, 1026, 970, 713.

**HRMS (FD+, m/z):** calc'd for C<sub>19</sub>H<sub>21</sub>NO<sub>4</sub> [M+•]<sup>+</sup> : 327.1465; found: 327.1479.

**Chiral SFC:** (OJ-H, 2.5 mL/min, 15% IPA in CO<sub>2</sub>, (λ = 254 nm): t<sub>R</sub> (minor) = 2.8 min, t<sub>R</sub> (major) = 3.2 min.

**methyl (R)-1-(1-(2-chloropyrimidin-5-yl)ethyl)-4-fluoro-1H-pyrrole-2-carboxylate**



**(278):** Prepared from 5-bromo-2-chloropyrimidine (**228**, 38.7 mg, 0.2 mmol) and methyl 4-fluoro-1-(1-(trifluoro-λ<sup>4</sup>-boraneyl)ethyl)-1H-pyrrole-2-carboxylate, potassium salt (**273**, 83.1 mg, 0.3 mmol) according to General

Procedure 2 in 2-MeTHF with 4-F-Ph BiOX (**L11**). The crude residue was purified by column chromatography (silica gel, 5–30% EtOAc/hexanes) to yield **278** (35.4 mg, 62% yield) in 97% ee as a colorless oil.

**R<sub>f</sub>** = 0.47 (silica gel, 30% EtOAc/hexanes, UV).

**[α]<sub>D</sub><sup>21</sup>** = 84° (c = 1.8, CHCl<sub>3</sub>).

**<sup>1</sup>H NMR (400 MHz, CDCl<sub>3</sub>):** δ 8.36 (d, J = 0.6 Hz, 2H), 6.87 (dd, J = 3.3, 2.1 Hz, 1H), 6.69 (d, J = 2.1 Hz, 1H), 6.64 – 6.52 (m, 1H), 3.75 (s, 3H), 1.82 (d, J = 7.2 Hz, 3H).

**<sup>13</sup>C NMR (101 MHz, CDCl<sub>3</sub>):** δ 161.06 (d, J = 2.9 Hz), 160.7, 157.6, 151.01 (d, J = 243.5 Hz), 134.9, 118.74 (d, J = 5.8 Hz), 109.16 (d, J = 28.0 Hz), 105.73 (d, J = 15.3 Hz), 51.7, 51.3, 21.4.

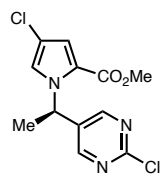
**<sup>19</sup>F NMR (282 MHz, CDCl<sub>3</sub>):** δ -165.22 (dd, J = 3.3, 1.6 Hz).

**FTIR (NaCl, thin film, cm<sup>-1</sup>):** 3139, 2954, 1708, 1574, 1549, 1474, 1440, 1399, 1295, 1242, 1174, 1160, 1095, 1008, 773.

**HRMS (FAB, m/z):** calc'd for C<sub>12</sub>H<sub>12</sub>ClN<sub>3</sub>O<sub>2</sub>F [M+H]<sup>+</sup> : 284.0602 ; found: 284.0601.

**Chiral SFC:** (IC, 2.5 mL/min, 15% IPA in CO<sub>2</sub>,  $\lambda$  = 254 nm):  $t_R$  (minor) = 7.8 min,  $t_R$  (major) = 8.6 min.

**methyl (R)-4-chloro-1-(1-(2-chloropyrimidin-5-yl)ethyl)-1H-pyrrole-2-carboxylate**



**(270):** Prepared from 5-bromo-2-chloropyrimidine (**228**, 38.7 mg, 0.1 mmol) and methyl 4-chloro-1-(1-(trifluoro- $\lambda^4$ -boraneyl)ethyl)-1H-pyrrole-2-carboxylate, potassium salt (**267**, 44 mg, 0.15 mmol) according to General

Procedure 2 (on 0.1 mmol scale) in *i*-PrOAc with 4-F-Ph BiOX (**L11**). The crude residue was purified by column chromatography (silica gel, 5–30% EtOAc/hexanes) to yield **270** (11.1 mg, 37% yield) in 95% ee as white solid.

$R_f$  = 0.52 (silica gel, 30% EtOAc/hexanes, UV).

$[\alpha]_D^{21} = 2.3^\circ$  (c = 0.54, CHCl<sub>3</sub>).

**<sup>1</sup>H NMR (400 MHz, CDCl<sub>3</sub>):**  $\delta$  8.38 (d, J = 0.6 Hz, 2H), 7.03 (d, J = 2.0 Hz, 1H), 6.92 (d, J = 1.9 Hz, 1H), 6.57 (q, J = 7.2 Hz, 1H), 3.76 (s, 3H), 1.84 (d, J = 7.3 Hz, 3H).

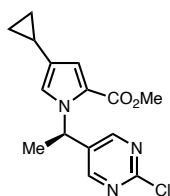
**<sup>13</sup>C NMR (101 MHz, CDCl<sub>3</sub>):**  $\delta$  160.82, 160.79, 157.67, 134.64, 121.86, 121.75, 118.41, 113.69, 51.73, 51.67, 21.56.

**FTIR (NaCl, thin film, cm<sup>-1</sup>):** 2924, 2357, 1706, 1550, 1456, 1436, 1399, 1347, 1233, 1181, 1085, 944, 775.

**HRMS (ESI-TOF, m/z):** calc'd for C<sub>12</sub>H<sub>12</sub>Cl<sub>2</sub>N<sub>3</sub>O<sub>2</sub> [M+H]<sup>+</sup> : 300.0307 ; found: 300.0293.

**Chiral SFC:** (AD-H, 2.5 mL/min, 15% IPA in CO<sub>2</sub>, ( $\lambda$  = 210 nm):  $t_R$  (minor) = 3.0 min,  $t_R$  (major) = 3.3 min.

**methyl (R)-1-(1-(2-chloropyrimidin-5-yl)ethyl)-4-cyclopropyl-1*H*-pyrrole-2-**



**carboxylate (279):** Prepared from 5-bromo-2-chloropyrimidine (**228**, 38.7

mg, 0.2 mmol) and methyl 4-cyclopropyl-1-(1-(trifluoro- $\lambda^4$ -boraneyl)ethyl)-1*H*-pyrrole-2-carboxylate, potassium salt (**274**, 89.7 mg,

0.3 mmol) according to General Procedure 2 in 2-MeTHF with 4-F-Ph BiOX (**L11**). The crude residue was purified by column chromatography (silica gel, 10% EtOAc/PhMe) to yield **228** (41.2 mg, 67% yield) in 97% ee as a colorless oil.

$R_f$  = 0.49 (silica gel, 20% EtOAc/hexanes, UV).

$[\alpha]_D^{22}$  = 24° (c = 1.0, CHCl<sub>3</sub>).

**<sup>1</sup>H NMR (400 MHz, CDCl<sub>3</sub>):**  $\delta$  8.32 (s, 2H), 6.89 (d, J = 2.0 Hz, 1H), 6.72 (d, J = 1.9 Hz, 1H), 6.53 (q, J = 7.2 Hz, 1H), 3.73 (s, 3H), 1.83 (d, J = 7.3 Hz, 3H), 1.76 – 1.62 (m, 1H), 0.91 – 0.76 (m, 2H), 0.56 – 0.44 (m, 2H).

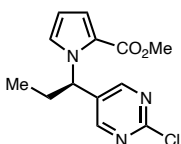
**<sup>13</sup>C NMR (101 MHz, CDCl<sub>3</sub>):** 161.5, 160.4, 157.7, 135.5, 128.2, 121.7, 121.7, 116.7, 51.3, 51.0, 21.5, 8.2, 8.1, 7.8.

**FTIR (NaCl, thin film, cm<sup>-1</sup>):** 2950, 1699, 1549, 1439, 1401, 1340, 1238, 1105, 980, 830, 677

**HRMS (ESI-TOF, m/z):** C<sub>15</sub>H<sub>17</sub>N<sub>3</sub>O<sub>2</sub>Cl; calc'd for [M+H]<sup>+</sup>: 306.1009, found: 306.0992

**Chiral SFC:** (IC, 2.5 mL/min, 30% IPA in CO<sub>2</sub>,  $\lambda$  = 254 nm):  $t_R$  (minor) = 3.3 min,  $t_R$  (major) = 5.8 min.

**methyl (R)-1-(1-(2-chloropyrimidin-5-yl)propyl)-1*H*-pyrrole-2-carboxylate (280):**



Prepared from 5-bromo-2-chloropyrimidine (**228**, 38.7 mg, 0.2 mmol) and

methyl 1-(1-(trifluoro- $\lambda^4$ -boraneyl)propyl)-1*H*-pyrrole-2-carboxylate,



potassium salt (**280**, 81.9 mg, 0.3 mmol) according to General Procedure 2 in 2-MeTHF with 4-F-Ph BiOX (**L11**). The crude residue was purified by column chromatography (silica gel, 9% EtOAc/hexanes) to yield **280** (35.6 mg, 64% yield) in 95% ee as a colorless oil.

$R_f = 0.56$  (silica gel, 20% EtOAc/hexanes, UV).

$[\alpha]_D^{22} = 71^\circ$  ( $c = 1.0$ ,  $\text{CHCl}_3$ ).

$^1\text{H NMR}$  (400 MHz,  $\text{CDCl}_3$ ):  $\delta$  8.41 (s, 2H), 7.10 (dd,  $J = 2.8, 1.7$  Hz, 1H), 7.00 (dd,  $J = 4.0, 1.7$  Hz, 1H), 6.36 (dd,  $J = 9.0, 6.9$  Hz, 1H), 6.27 (dd,  $J = 4.0, 2.8$  Hz, 1H), 3.76 (s, 3H), 2.37 – 2.08 (m, 2H), 0.98 (t,  $J = 7.3$  Hz, 3H).

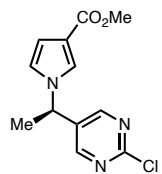
$^{13}\text{C NMR}$  (101 MHz,  $\text{CDCl}_3$ ):  $\delta$  161.7, 160.6, 158.2, 134.2, 124.4, 122.5, 119.2, 110.0, 57.1, 51.4, 28.5, 11.0.

FTIR (NaCl, thin film,  $\text{cm}^{-1}$ ): 2972, 1698, 1579, 1549, 1439, 1400, 1338, 1227, 1155, 1109, 1070, 851, 744

HRMS (ESI-TOF,  $m/z$ ):  $\text{C}_{13}\text{H}_{15}\text{N}_3\text{O}_2\text{Cl}$ ; calc'd for  $[\text{M}+\text{H}]^+$ : 280.0853, found: 280.0842

Chiral SFC: (IC, 2.5 mL/min, 20% IPA in  $\text{CO}_2$ ,  $\lambda = 254$  nm):  $t_R$  (minor) = 4.0 min,  $t_R$  (major) = 4.4 min.

**methyl (R)-1-(1-(2-chloropyrimidin-5-yl)ethyl)-1H-pyrrole-3-carboxylate (271)**



Prepared from 5-bromo-2-chloropyrimidine (**228**, 38.7 mg, 0.2 mmol) and methyl 1-(1-(trifluoro- $\lambda^4$ -boraneyl)ethyl)-1H-pyrrole-3-carboxylate, potassium salt (**268**, 77.7 mg, 0.3 mmol) according to General Procedure 2

in 2-MeTHF with 4-heptyl BiOX (**L2**). The crude residue was purified by column

chromatography (silica gel, 30% EtOAc/hexanes) to yield **271** (41.2 mg, 78% yield) in 66% ee as a colorless oil.

$R_f = 0.50$  (silica gel, 50% EtOAc/hexanes, UV).

$[\alpha]_D^{22} = -13^\circ$  (c = 1.0, CHCl<sub>3</sub>).

<sup>1</sup>H NMR (400 MHz, CDCl<sub>3</sub>): δ 8.34 (d, J = 0.6 Hz, 2H), 7.39 (t, J = 1.9 Hz, 1H), 6.70 – 6.63 (m, 2H), 5.33 (q, J = 7.1 Hz, 1H), 3.81 (s, 3H), 1.91 (d, J = 7.1 Hz, 3H).

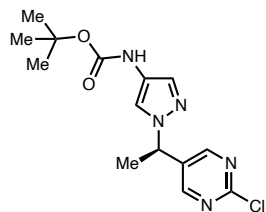
<sup>13</sup>C NMR (101 MHz, CDCl<sub>3</sub>): δ 164.9, 161.3, 157.5, 134.2, 124.2, 120.4, 117.3, 111.5, 54.3, 51.4, 21.4.

FTIR (NaCl, thin film, cm<sup>-1</sup>): 2950, 1698, 1538, 1398, 1158, 994, 826, 762, 67

HRMS (ESI-TOF, m/z): C<sub>12</sub>H<sub>13</sub>N<sub>3</sub>O<sub>2</sub>Cl; calc'd for [M+H]<sup>+</sup>: 266.0696, found: 266.0703

Chiral SFC: (AD-H, 2.5 mL/min, 25% IPA in CO<sub>2</sub>, (λ = 280 nm):  $t_R$  (minor) = 3.0 min,  $t_R$  (major) = 3.2 min.

***tert*-butyl (*R*)-(1-(1-(2-chloropyrimidin-5-yl)ethyl)-1*H*-pyrazol-4-yl)carbamate (**264**)**



Prepared from 5-bromo-2-chloropyrimidine (**228**, 38.7 mg, 0.2 mmol) and *tert*-butyl (1-(1-(trifluoro-λ<sup>4</sup>-boraneyl)ethyl)-1*H*-pyrrol-3-yl)carbamate, potassium salt (**221**, 95.1 mg, 0.3 mmol) according to General Procedure 2 in 2-MeTHF with 4-heptyl BiOX (**L2**). The crude residue was purified by column chromatography (silica gel, 30/20/50 EtOAc/DCM/hexanes) to yield **264** (45.6 mg, 70% yield) in 80% ee as a white solid. The white solid was dissolved in minimal CHCl<sub>3</sub> and filtered through a cotton-plugged pipette into a 1-dram vial. The vial was equipped with a septum cap that was punctured with a 21G needle. This vial was then placed in a sealed jar with pentane and allowed to crystallize over 4 days. A single crystal

was analyzed by X-ray diffraction to confirm the structure and assign absolute stereochemistry.

$R_f$  = 0.4.6 (silica gel, 50% EtOAc/hexanes, UV).

**Melting point** = 149–150 °C

$[\alpha]_D^{22} = -7^\circ$  (c = 1.0, CHCl<sub>3</sub>).

**<sup>1</sup>H NMR (400 MHz, CDCl<sub>3</sub>):** δ 8.46 (s, 2H), 7.82 (s, 1H), 7.35 (s, 1H), 6.29 (s, 1H), 5.44 (q, J = 7.1 Hz, 1H), 1.92 (d, J = 7.1 Hz, 3H), 1.49 (s, 9H)

**<sup>13</sup>C NMR (101 MHz, CDCl<sub>3</sub>):** δ 161.0, 157.9, 153.0, 134.0, 130.8, 122.5, 118.7, 80.9, 56.7, 28.4, 20.8.

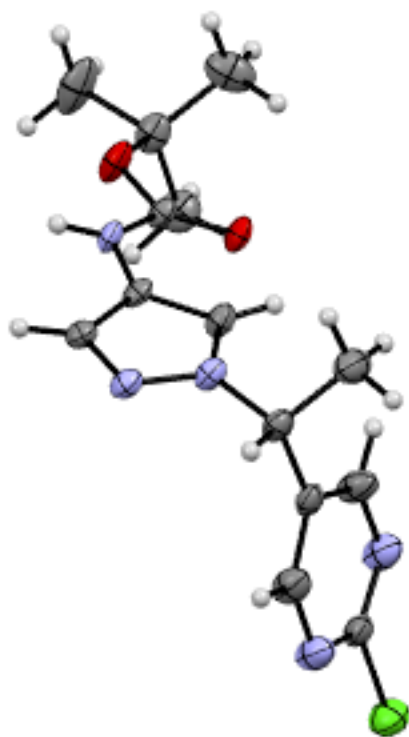
**FTIR (NaCl, thin film, cm<sup>-1</sup>):** 2954, 1700, 1598, 1550, 1399, 1249, 1164, 772, 676

**HRMS (ESI-TOF, m/z):** C<sub>14</sub>H<sub>19</sub>N<sub>5</sub>O<sub>2</sub>Cl; calc'd for [M+H]<sup>+</sup>: 324.1227, found: 324.1240

**Chiral SFC:** (AD-H, 2.5 mL/min, 35% IPA in CO<sub>2</sub>, λ = 254 nm):  $t_R$  (major) = 1.9 min,  $t_R$  (minor) = 2.3 min.

Low-temperature diffraction data ( $\phi$ - and  $\omega$ -scans) were collected on a Bruker AXS D8 VENTURE KAPPA diffractometer coupled to a PHOTON II CPAD detector with Cu  $K_\alpha$  radiation ( $\lambda = 1.54178 \text{ \AA}$ ) from an I $\mu$ S micro-source for the structure of compound **264**. The structure was solved by direct methods using SHELXS<sup>6</sup> and refined against  $F^2$  on all data by full-matrix least squares with SHELXL-2017<sup>7</sup> using established refinement techniques.<sup>8</sup> All non-hydrogen atoms were refined anisotropically. All hydrogen atoms were included into the model at geometrically calculated positions and refined using a riding model. The isotropic displacement parameters of all hydrogen atoms were fixed to 1.2 times the  $U$  value of the atoms they are linked to (1.5 times for methyl groups).

Compound **264** crystallizes in the monoclinic space group  $P2_1$  with one molecule in the asymmetric unit. The coordinates for the hydrogen atoms bound to N5 and N25 were located in the difference Fourier synthesis and refined semi-freely with the help of a restraint on the N-H distance (0.88(4) Å).



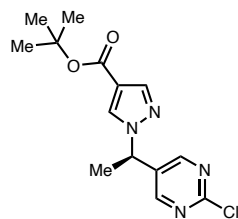
**Crystal data and structure refinement for 264.**

Identification code	V21273
CCDC deposition number	2121889
Empirical formula	C <sub>28</sub> H <sub>36</sub> N <sub>10</sub> O <sub>4</sub> Cl <sub>2</sub>
Formula weight	647.57

Temperature/K	100(2)
Crystal system	monoclinic
Space group	P2 <sub>1</sub>
a/Å	9.4715(9)
b/Å	13.2722(10)
c/Å	13.5160(13)
α/°	90
β/°	105.965(6)
γ/°	90
Volume/Å <sup>3</sup>	1633.5(3)
Z	2
ρ <sub>calc</sub> /cm <sup>3</sup>	1.317
μ/mm <sup>-1</sup>	2.200
F(000)	680.0
Crystal size/mm <sup>3</sup>	0.15 × 0.1 × 0.05
Radiation	CuKα (λ = 1.54178)
2θ range for data collection/°	6.802 to 148.614
Index ranges	-11 ≤ h ≤ 11, -16 ≤ k ≤ 16, -16 ≤ l ≤ 16
Reflections collected	41899
Independent reflections	6561 [R <sub>int</sub> = 0.0397, R <sub>sigma</sub> = 0.0243]
Data/restraints/parameters	6561/3/411
Goodness-of-fit on F <sup>2</sup>	1.040

Final R indexes [ $I \geq 2\sigma$ (I)]	$R_1 = 0.0380$ , $wR_2 = 0.1007$
Final R indexes [all data]	$R_1 = 0.0395$ , $wR_2 = 0.1025$
Largest diff. peak/hole / $e \text{ \AA}^{-3}$	0.80/-0.41
Flack parameter	-0.007(4)

***tert*-butyl (R)-1-(1-(2-chloropyrimidin-5-yl)ethyl)-1*H*-pyrazole-4-carboxylate (266)**



Prepared from 5-bromo-2-chloropyrimidine (**228**, 38.7 mg, 0.2 mmol) and *tert*-butyl 1-(1-(trifluoro- $\lambda^4$ -boraneyl)ethyl)-1*H*-pyrazole-4-carboxylate, potassium salt (**263**, 90.6 mg, 0.3 mmol) according to General Procedure 2 in CPME with 4-heptyl BiOX (**L2**) and 1.0 mol % [Ir]. The crude residue was purified by column chromatography (silica gel, 5–25% EtOAc/DCM) to yield **266** (28.3 mg, 46% yield) in 83% ee as a yellow oil.

$R_f = 0.43$  (silica gel, 20% EtOAc/DCM, UV).

$[\alpha]_D^{21} = -2^\circ$  ( $c = 1.0$ ,  $\text{CHCl}_3$ ).

$^1\text{H NMR}$  (400 MHz,  $\text{CDCl}_3$ ):  $\delta$  8.52 (s, 2H), 7.93 (d,  $J = 0.6$  Hz, 1H), 7.91 – 7.86 (m, 1H), 5.52 (q,  $J = 7.1$  Hz, 1H), 1.96 (d,  $J = 7.1$  Hz, 3H), 1.54 (s, 9H).

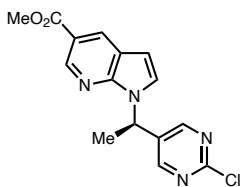
$^{13}\text{C NMR}$  (101 MHz,  $\text{CDCl}_3$ ):  $\delta$  162.11, 161.35, 157.99, 141.98, 133.15, 131.19, 117.65, 81.15, 56.99, 29.85, 28.42, 21.04.

FTIR (NaCl, thin film,  $\text{cm}^{-1}$ ): 2979, 2927, 1710, 1552, 1401, 1253, 1164, 1001, 832, 770.

HRMS (ESI-TOF,  $m/z$ ): calc'd for  $\text{C}_{14}\text{H}_{18}\text{ClN}_4\text{O}_2$   $[\text{M}+\text{H}]^+$  : 309.1118 ; found: 309.1122.

Chiral SFC: (IC, 2.5 mL/min, 30% IPA in  $\text{CO}_2$ ,  $\lambda = 210$  nm):  $t_R$  (minor) = 3.0 min,  $t_R$  (major) = 4.0 min.

**methyl (R)-1-(1-(2-chloropyrimidin-5-yl)ethyl)-1H-pyrrolo[2,3-b]pyridine-5-**



**carboxylate (281):** Prepared from 5-bromo-2-chloropyrimidine (**228**, 38.7 mg, 0.2 mmol) and methyl 1-(1-(trifluoro- $\lambda$ 4-borane)ethyl)-1H-pyrrolo[2,3-b]pyridine-5-carboxylate, potassium salt (**276**, 93.0

mg, 0.3 mmol) according to General Procedure 2 in CPME with 4-heptyl BiOX (**L2**) and 1.0 mol % [Ir]. Added 21.0 mg 1,1,2,2-tetrachloroethane, and the yield was calculated by  $^1\text{H}$  NMR (59% yield **281**). The crude material was purified by column chromatography (silica, 1.1% MeOH/DCM). The resulting colorless oil was purified by prep TLC (1.5% MeOH/DCM). The middle of the band containing product was collected and purified again by prep TLC (40% Et<sub>2</sub>O/PhMe) to afford 0.9 mg **281** (95% ee).

$R_f$  = 0.28 (silica gel, 1.5% MeOH/DCM, UV).

$[\alpha]_D^{21} = 190^\circ$  (c = 0.3, CHCl<sub>3</sub>).

$^1\text{H}$  NMR (500 MHz, CDCl<sub>3</sub>):  $\delta$  8.96 (s, 1H), 8.60 (s, 1H), 8.53 (s, 2H), 7.35 (d, J = 3.5 Hz, 1H), 6.67 (d, J = 3.5 Hz, 1H), 6.38 – 6.26 (m, 1H), 3.97 (s, 3H), 2.09 – 1.96 (m, 3H).

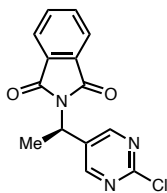
$^{13}\text{C}$  NMR (101 MHz, CDCl<sub>3</sub>):  $\delta$  167.0, 160.9, 158.1, 149.0, 145.5, 134.0, 131.6, 125.6, 120.1, 119.6, 103.1, 52.3, 48.6, 20.0.

FTIR (NaCl, thin film, cm<sup>-1</sup>): 2922, 1716, 1602, 1576, 1549, 1404, 1315, 1210, 1162, 937, 730

HRMS (ESI-TOF, m/z): C<sub>15</sub>H<sub>14</sub>N<sub>4</sub>O<sub>2</sub>Cl; calc'd for [M+H]<sup>+</sup>: 317.0805, found: 317.0805

Chiral SFC: (OJ-H, 2.5 mL/min, 30% IPA in CO<sub>2</sub>,  $\lambda$  = 280 nm):  $t_R$  (major) = 3.6 min,  $t_R$  (minor) = 4.0 min.

**(R)-2-(1-(2-chloropyrimidin-5-yl)ethyl)isoindoline-1,3-dione (272)**



Prepared from 5-bromo-2-chloropyrimidine (**228**, 38.7 mg, 0.2 mmol) and 2-(1-(trifluoro- $\lambda^4$ -boraneyl)ethyl)isoindoline-1,3-dione, potassium salt (**269**, 84.3 mg, 0.3 mmol) according to General Procedure 2 in 1,2-DME with 4-F-Ph BiOX (**L11**). 2.0 mg ethylene carbonate added, and the  $^1\text{H}$  NMR yield was calculated (25% yield **272**). The crude residue was purified by column chromatography (silica gel, 20–40% EtOAc/hexanes). The material was then repurified by prep TLC (5% EtOAc/DCM) to afford **272** as a white solid (77% ee).

$R_f$  = 0.4 (silica gel, 30% EtOAc/hexanes, UV).

$[\alpha]_D^{21} = 65^\circ$  (c = 0.37,  $\text{CHCl}_3$ ).

$^1\text{H}$  NMR (400 MHz,  $\text{CDCl}_3$ ):  $\delta$  8.78 (d,  $J = 0.5$  Hz, 2H), 7.91 – 7.79 (m, 2H), 7.79 – 7.69 (m, 2H), 5.67 – 5.49 (m, 1H), 1.94 (d,  $J = 7.4$  Hz, 3H).

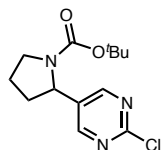
$^{13}\text{C}$  NMR (101 MHz,  $\text{CDCl}_3$ ):  $\delta$  167.71, 160.96, 159.27, 134.60, 132.16, 131.67, 123.74, 44.90, 17.13.

FTIR (NaCl, thin film,  $\text{cm}^{-1}$ ): 2924, 1774, 1712, 1550, 1400, 1382, 1160, 1030, 878, 771, 723.

HRMS (ESI-TOF, m/z): calc'd for  $\text{C}_{14}\text{H}_{11}\text{ClN}_3\text{O}_2$   $[\text{M}+\text{H}]^+$  : 288.0540 ; found: 288.0543.

Chiral SFC: IC, 2.5 mL/min, 35% MeCN in  $\text{CO}_2$ ,  $\lambda = 254$  nm):  $t_R$  (minor) = 3.3 min,  $t_R$  (major) = 4.0 min.

**tert-butyl 2-(2-chloropyrimidin-5-yl)pyrrolidine-1-carboxylate (282)**



Prepared from 5-bromo-2-chloropyrimidine (**228**, 38.7 mg, 0.2 mmol) and potassium (1-(tert-butoxycarbonyl)pyrrolidin-2-yl)trifluoroborate (**277**, 83



mg, 0.3 mmol) according to General Procedure 2 in *tert*-butyl methyl ether with heptyl BiOX (**L2**) with modifications to the work-up. A 50% (v:v) aqueous solution of trifluoroacetic acid (6 equiv, 92 mL, 137 mg, 1.2 mmol) was added to the reaction with vigorous agitation upon reaction completion. The resulting biphasic mixture was diluted with water (1 mL) after 0.5 h following hydrolysis of the ligand (as determined by SFC analysis). The layers were separated, the organic phase washed with brine (1 mL), the layers separated, the organic phase dried over anhydrous sodium sulfate, and the solvent removed *in vacuo*. The crude residue was purified by column chromatography (silica gel, 0 to 30% EtOAc/hexanes) to yield **282** (37 mg, 65% yield, mixture of rotamers 1.1:1 A:B) in 92% *ee* as a white solid.

$R_f = 0.21$  (silica gel, 30% EtOAc/hexanes, UV).

$[\alpha]_{589}^{25} = 90^\circ$  (c = 1.0, CHCl<sub>3</sub>).

**m.p.:** 101-102 °C.

**<sup>1</sup>H NMR (500 MHz, CDCl<sub>3</sub>):** δ 8.47 (br. s, 4H, A+B), 4.91 (br. m, 1H, B), 4.77 (br. m, 1H, A), 3.75-3.45 (br. m, 4H, A+B), 2.41 (br. m, 2H, A+B), 2.02-1.88 (br. m, 4H, A+B), 1.84 (br. m, 2H, A+B), 1.44 (br. s, 9H, B), 1.26 (br. s, 9H, A).

**<sup>13</sup>C{<sup>1</sup>H} NMR (126 MHz, CDCl<sub>3</sub>):** δ 160.04 (A+B), 157.58 (A+B), 154.59 (B), 154.00 (A), 136.62 (A), 135.74 (B), 80.63 (A), 80.55 (B), 56.85 (A), 56.52 (B), 47.38 (B), 47.25 (A), 35.71 (A), 34.37 (B), 28.50 (B), 28.41 (A), 24.03 (B), 23.54 (A).

**FT-IR (KBr, thin film, cm<sup>-1</sup>):** 2970, 1688, 1681, 1580, 1551, 1390, 1365, 1149, 1114, 899, 873, 773.

**HRMS (ESI-TOF, m/z):** calc'd for C<sub>13</sub>H<sub>19</sub>ClN<sub>3</sub>O<sub>2</sub> [M+H]<sup>+</sup> : 284.1166; found: 284.1169.

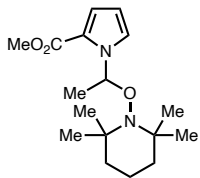
**Chiral SFC:** (Chiralpak IC-3, 3.0 mL/min, 1 to 40% IPA over 5 min. in CO<sub>2</sub> (2900 psi; 45 °C column temp.;  $\lambda$  = 210 nm):  $t_R$  (ligand **L2**) = 3.2 min;  $t_R$  (minor) = 3.6 min,  $t_R$  (major) = 3.8 min.

**Mechanistic Experiments: Radical Trapping** (Shown in Table 3.3)

The reactions were conducted according to General Procedure 2 on 0.5 mmol scale using 5-bromo-2-chloropyrimidine (**228**, 9.7 mg, 0.05 mmol) and methyl 1-(1-(trifluoro- $\lambda^4$ -boraneyl)ethyl)-1*H*-pyrrole-2-carboxylate, potassium salt (**224**, 19.4 mg, 0.075 mmol) in both 2-MeTHF and THF (separately) with 4-F-Ph BiOX (**L11**). Solid radical traps were added outside of the glovebox (TEMPO, 11.7 mg, 0.075 mmol, 1.5 equiv; 9,10-dihydroanthracene, 13.5 mg, 0.075 mmol, 1.5 equiv). Liquid radical trap 1,1-diphenylethylene (13.5 mg, 0.075 mmol, 1.5 equiv) was added via syringe in the glovebox after addition of all other reaction components. After workup as described in General Procedure 2, 0.025 mmol 1,1,2,2-tetrachloroethane was added each reaction as an internal standard. <sup>1</sup>H-NMR yields of **234** were determined relative to this internal standard. An aliquot of each reaction was purified by preparative TLC (10% EtOAc/PhMe) and analyzed by SFC to determine ee, using the method described above for **234**. An additional aliquot of the reaction containing TEMPO was purified by preparative TLC (10% EtOAc/hexanes) to isolate TEMPO adduct **288**.

**methyl 1-(1-((2,2,6,6-tetramethylpiperidin-1-yl)oxy)ethyl)-1H-pyrrole-2-carboxylate**

**(288)** Prepared as described above.



$R_f = 0.46$  (silica gel, 10% EtOAc/hexanes, UV).

$^1\text{H NMR}$  (500 MHz,  $\text{CDCl}_3$ ):  $\delta$  7.18 (t,  $J = 2.3$  Hz, 1H), 6.92 – 6.79 (m, 2H), 6.18 (dd,  $J = 3.8, 2.7$  Hz, 1H), 3.82 (s, 3H), 1.64 (d,  $J = 6.2$  Hz, 3H),

1.56 – 1.21 (m, 9H), 1.15 (s, 3H), 0.98 (s, 3H), 0.35 (s, 3H).

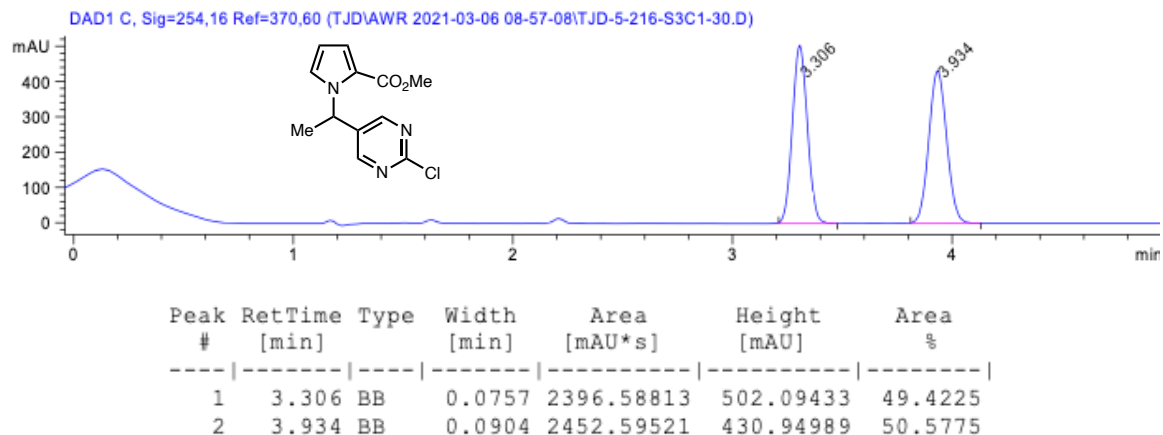
$^{13}\text{C NMR}$  (101 MHz,  $\text{CDCl}_3$ ):  $\delta$  161.9, 124.7, 122.1, 117.5, 109.1, 88.0, 60.7, 59.2, 51.2, 40.6, 40.2, 33.6, 31.1, 29.9, 22.6, 20.2, 17.2.

**FTIR** (NaCl, thin film,  $\text{cm}^{-1}$ ): 2934, 1698, 1435, 1410, 1346, 1278, 1231, 1210, 1134, 1108, 1067, 930

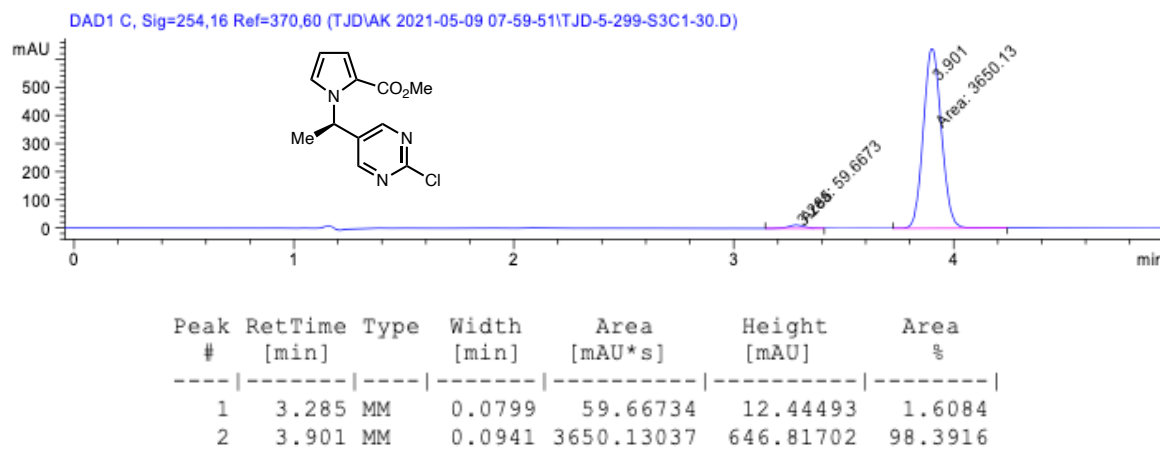
**HRMS** (FD+, m/z): calc'd for  $\text{C}_{17}\text{H}_{28}\text{N}_2\text{O}_3$   $[\text{M}+\cdot]^+$  : 308.2094 ; found: 308.2109.

### 3.6.7 SFC Traces of Racemic and Enantioenriched Products

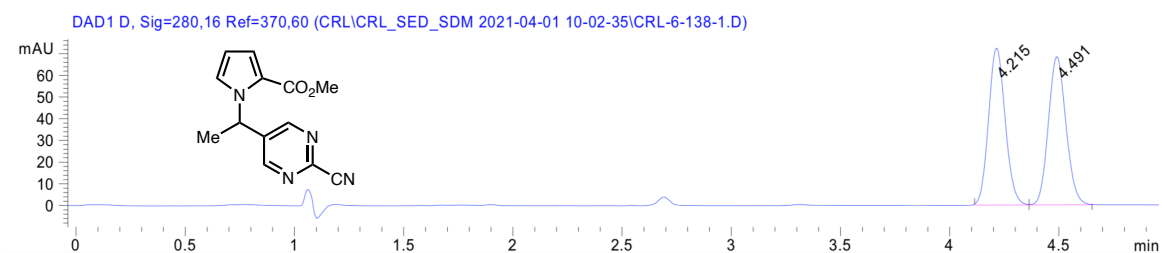
234: racemic



234: enantioenriched (97% ee)

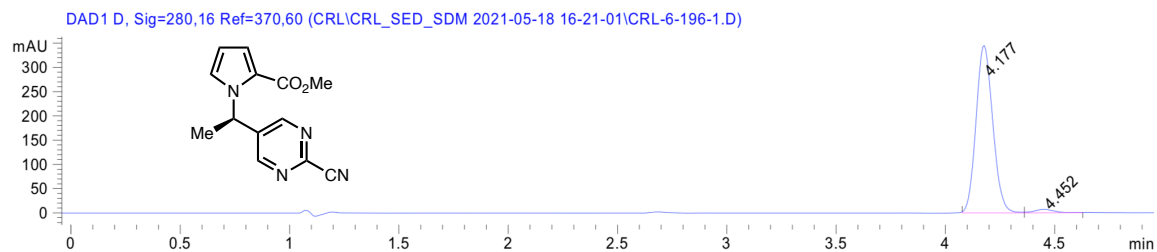


**249: racemic**



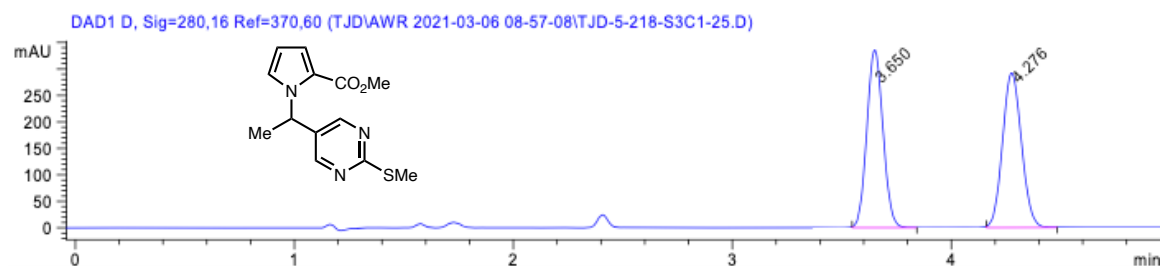
Peak #	RetTime [min]	Type	Width [min]	Area [mAU*s]	Height [mAU]	Area %
1	4.215	BV	0.0820	383.80136	72.16452	49.9491
2	4.491	VB	0.0858	384.58405	68.16901	50.0509

**249: enantioenriched (95% ee)**



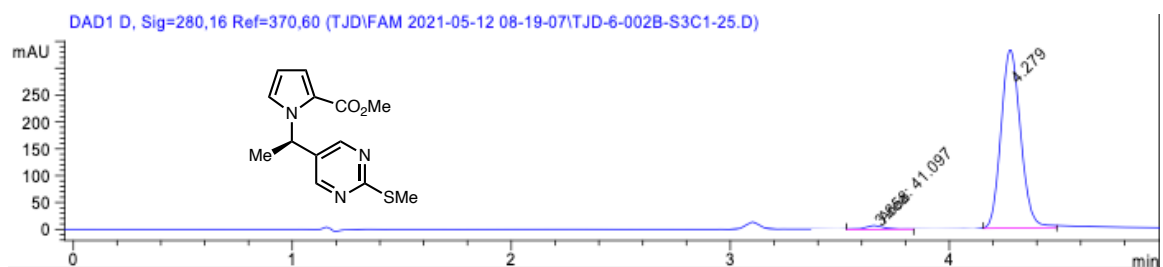
Peak #	RetTime [min]	Type	Width [min]	Area [mAU*s]	Height [mAU]	Area %
1	4.177	BB	0.0822	1836.40137	344.35587	97.6094
2	4.452	BB	0.0936	44.97677	7.12691	2.3906

**229: racemic**



Peak #	RetTime [min]	Type	Width [min]	Area [mAU*s]	Height [mAU]	Area %
1	3.650	BB	0.0842	1720.55884	333.28915	49.4602
2	4.276	BB	0.0944	1758.11243	291.36157	50.5398

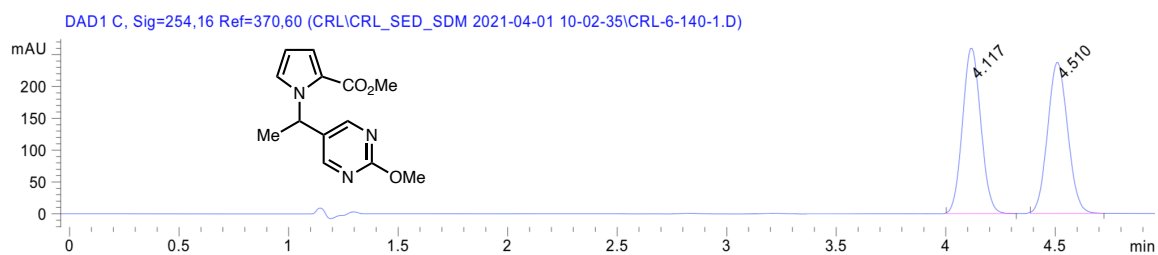
**229: enantioenriched (96% ee)**



Signal 3: DAD1 D, Sig=280,16 Ref=370,60

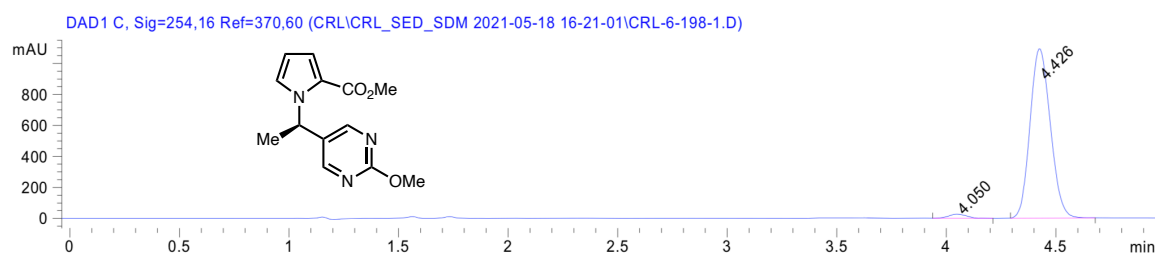
Peak #	RetTime [min]	Type	Width [min]	Area [mAU*s]	Height [mAU]	Area %
1	3.658	MM	0.0949	41.09700	7.22124	1.9534
2	4.279	BB	0.1006	2062.78174	331.37088	98.0466

**250: racemic**



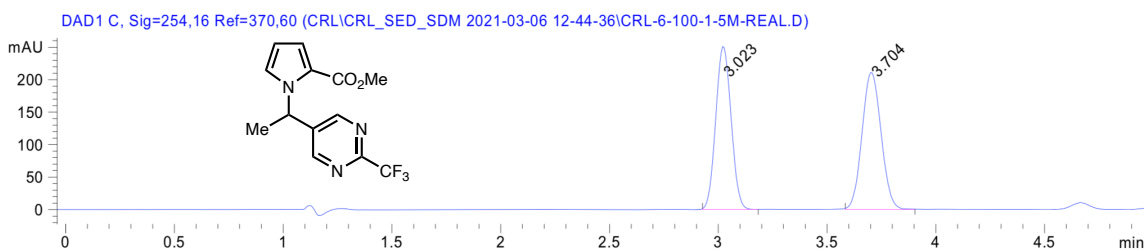
Peak #	RetTime [min]	Type	Width [min]	Area [mAU*s]	Height [mAU]	Area %
1	4.117	BB	0.0919	1510.22778	259.38214	49.8532
2	4.510	BB	0.1027	1519.12488	237.14029	50.1468

**250: enantioenriched (96% ee)**



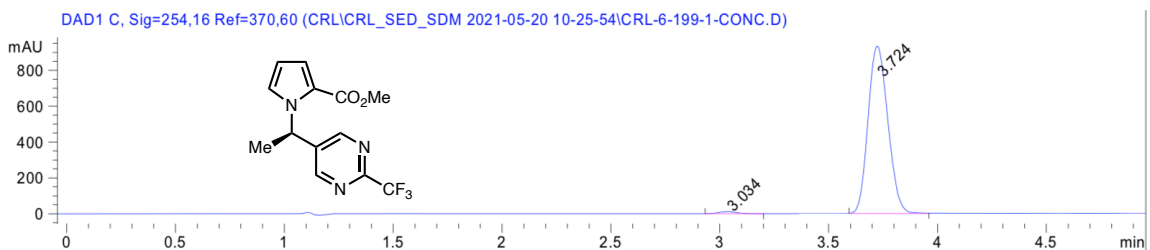
Peak #	RetTime [min]	Type	Width [min]	Area [mAU*s]	Height [mAU]	Area %
1	4.050	BB	0.0916	156.39600	26.99751	2.1664
2	4.426	BB	0.1035	7062.76270	1091.91553	97.8336

**235: racemic**



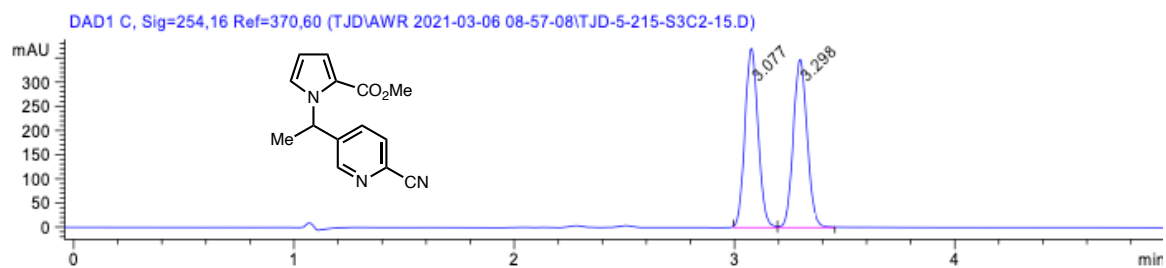
Peak #	RetTime [min]	Type	Width [min]	Area [mAU*s]	Height [mAU]	Area %
1	3.023	BB	0.0775	1233.25696	250.06862	48.8945
2	3.704	BB	0.0994	1289.02258	210.48514	51.1055

**235: enantioenriched (98% ee)**

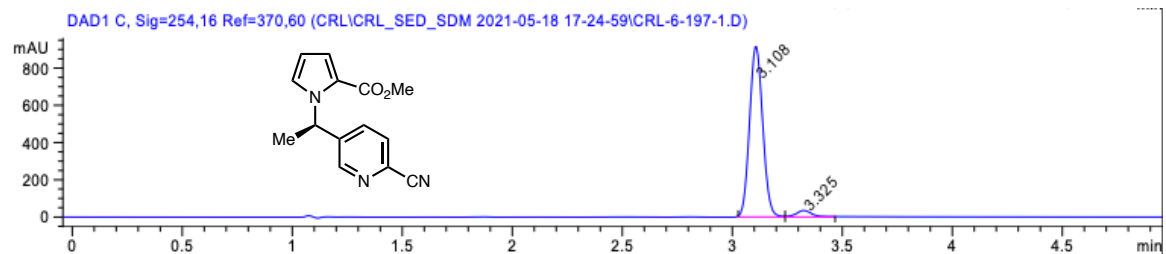


Peak #	RetTime [min]	Type	Width [min]	Area [mAU*s]	Height [mAU]	Area %
1	3.034	BB	0.0840	62.00253	12.06090	1.0375
2	3.724	BB	0.1019	5913.95166	933.12457	98.9625

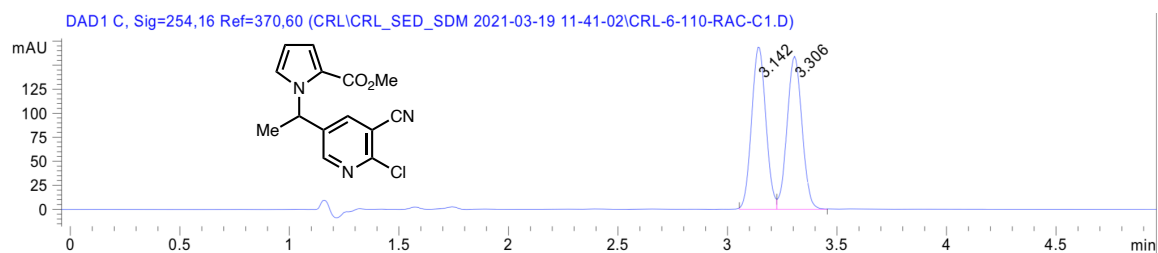


**236:** racemic

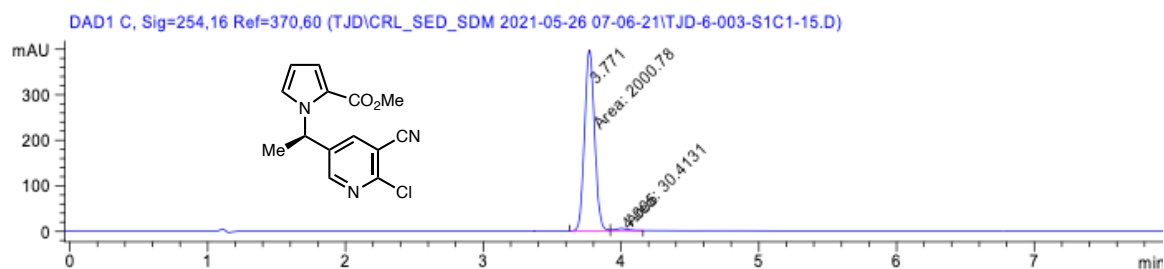
Peak #	RetTime [min]	Type	Width [min]	Area [mAU*s]	Height [mAU]	Area %
1	3.077	BV	0.0651	1543.68237	366.68329	50.3084
2	3.298	VB	0.0714	1524.75342	345.91885	49.6916

**236:** enantioenriched (91% ee)

Peak #	RetTime [min]	Type	Width [min]	Area [mAU*s]	Height [mAU]	Area %
1	3.108	BV	0.0686	3808.04321	913.25690	95.7035
2	3.325	VB	0.0737	170.95973	34.54604	4.2965

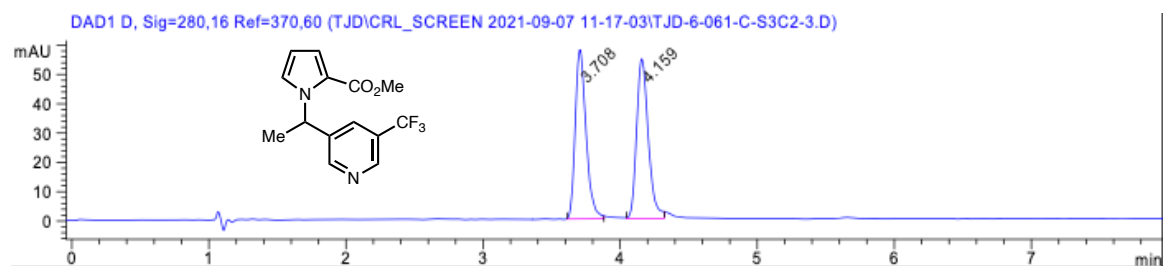
**237: racemic**

Peak #	RetTime [min]	Type	Width [min]	Area [mAU*s]	Height [mAU]	Area %
1	3.142	BV	0.0690	761.36145	167.68916	50.2497
2	3.306	VB	0.0757	753.79431	157.81111	49.7503

**237: enantioenriched (97% ee)**

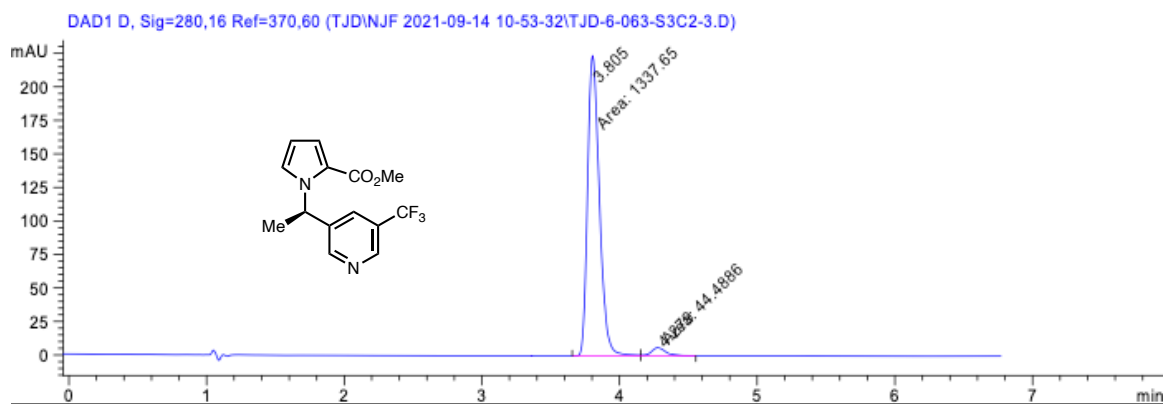
Peak #	RetTime [min]	Type	Width [min]	Area [mAU*s]	Height [mAU]	Area %
1	3.771	MF	0.0835	2000.78320	399.36548	98.5027
2	4.005	FM	0.1005	30.41313	5.04541	1.4973

**251: racemic**



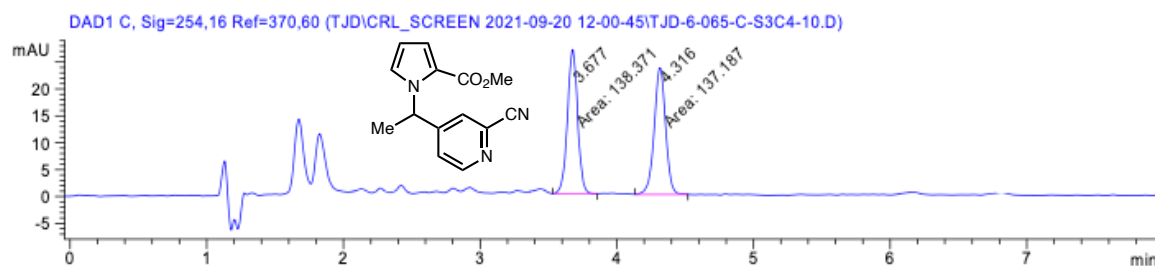
Peak #	RetTime [min]	Type	Width [min]	Area [mAU*s]	Height [mAU]	Area %
1	3.708	BB	0.0844	316.93723	57.42631	49.5084
2	4.159	BB	0.0936	323.23148	54.17910	50.4916

**251: enantioenriched (94% ee)**



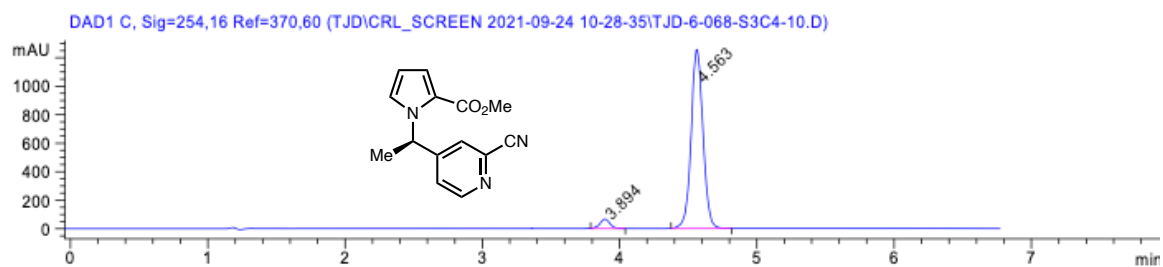
Peak #	RetTime [min]	Type	Width [min]	Area [mAU*s]	Height [mAU]	Area %
1	3.805	MF	0.0990	1337.65198	225.15393	96.7812
2	4.279	FM	0.1193	44.48857	6.21610	3.2188

252: racemic



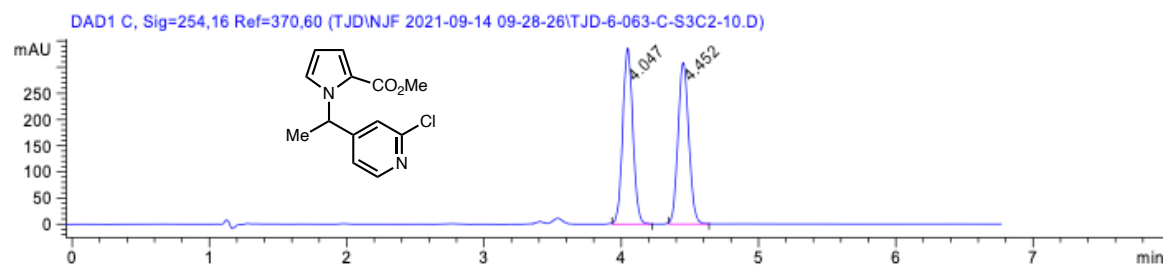
Peak #	RetTime [min]	Type	Width [min]	Area [mAU*s]	Height [mAU]	Area %
1	3.677	MM	0.0853	138.37132	27.03662	50.2149
2	4.316	MM	0.0964	137.18721	23.72045	49.7851

252: enantioenriched (92% ee)



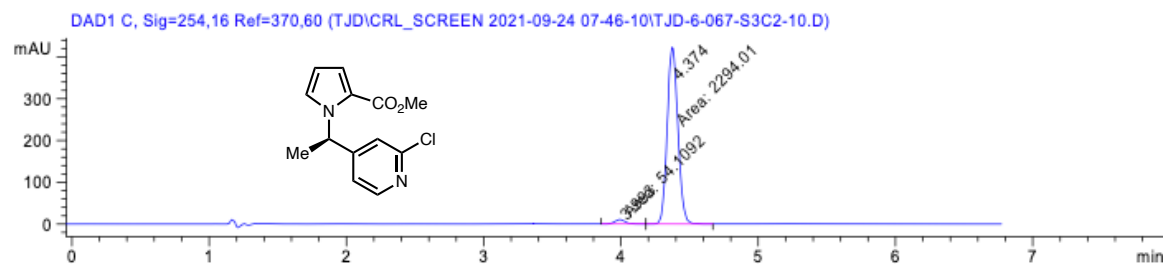
Peak #	RetTime [min]	Type	Width [min]	Area [mAU*s]	Height [mAU]	Area %
1	3.894	BB	0.0790	335.42270	66.35056	4.2426
2	4.563	BB	0.0943	7570.69482	1255.95886	95.7574

**253: racemic**



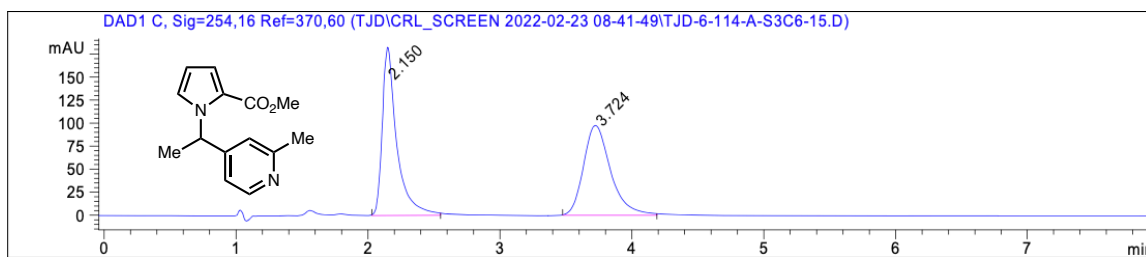
Peak #	RetTime [min]	Type	Width [min]	Area [mAU*s]	Height [mAU]	Area %
1	4.047	BB	0.0840	1717.59399	334.03677	50.6055
2	4.452	BB	0.0837	1676.48828	306.96725	49.3945

**253: enantioenriched (95% ee)**



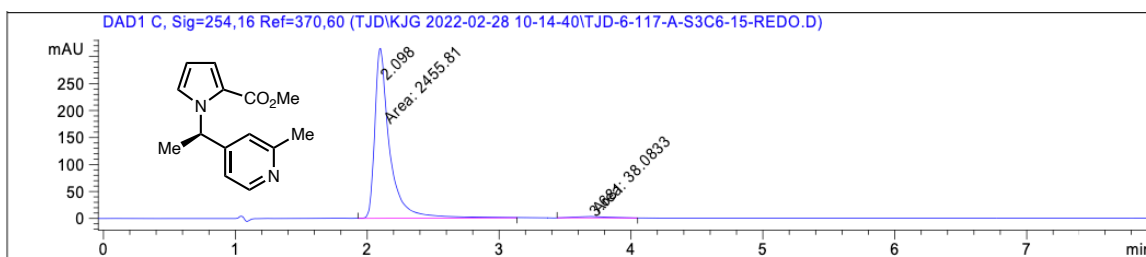
Peak #	RetTime [min]	Type	Width [min]	Area [mAU*s]	Height [mAU]	Area %
1	3.993	MF	0.0825	54.10918	10.93003	2.3044
2	4.374	FM	0.0899	2294.01367	425.30963	97.6956

**254: racemic**



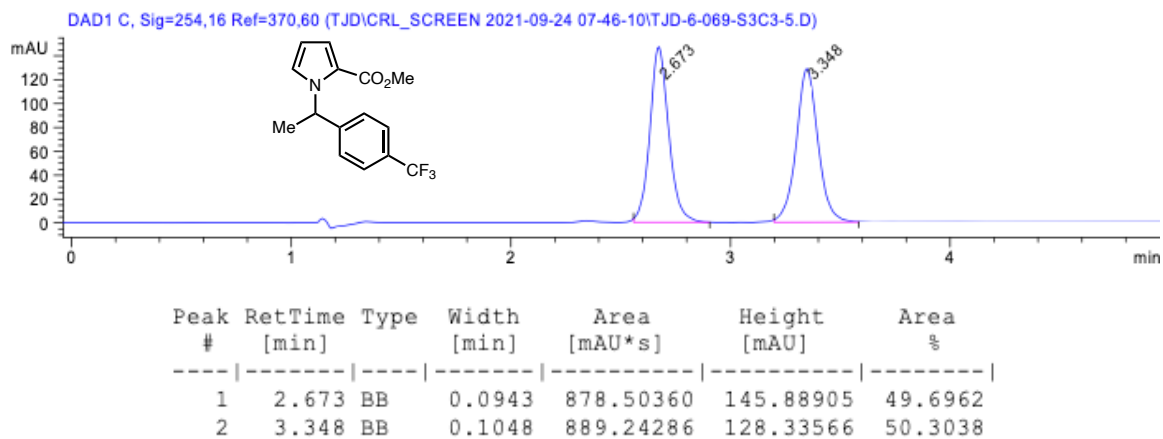
Peak #	RetTime [min]	Type	Width [min]	Area [mAU*s]	Height [mAU]	Area %
1	2.150	BB	0.1136	1400.61621	182.32489	50.0904
2	3.724	BB	0.2189	1395.56311	97.53919	49.9096

**254: enantioenriched (97% ee)**

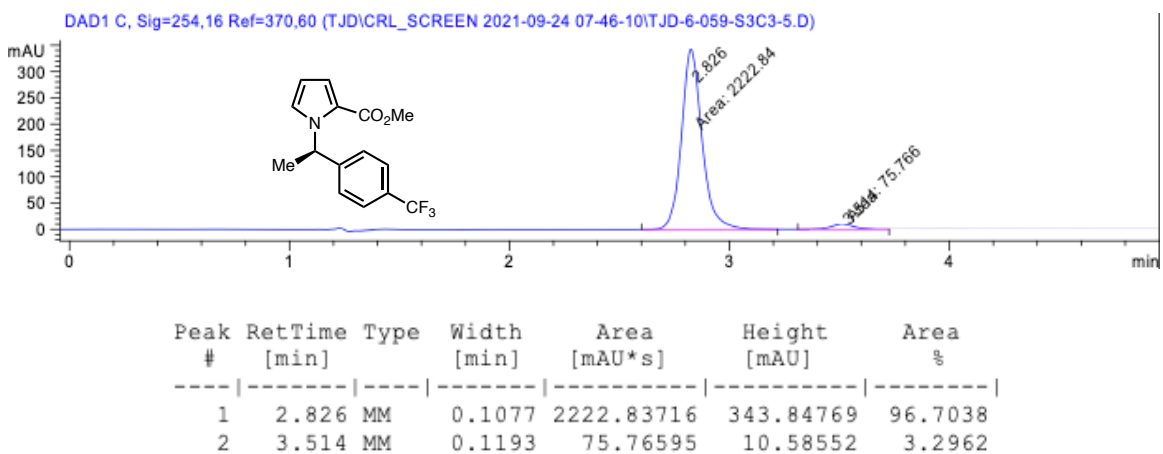


Peak #	RetTime [min]	Type	Width [min]	Area [mAU*s]	Height [mAU]	Area %
3	1.637	BB	0.1371	28.06691	2.53632	2.0115
4	2.098	BB	0.1096	1303.62463	173.60469	93.4281

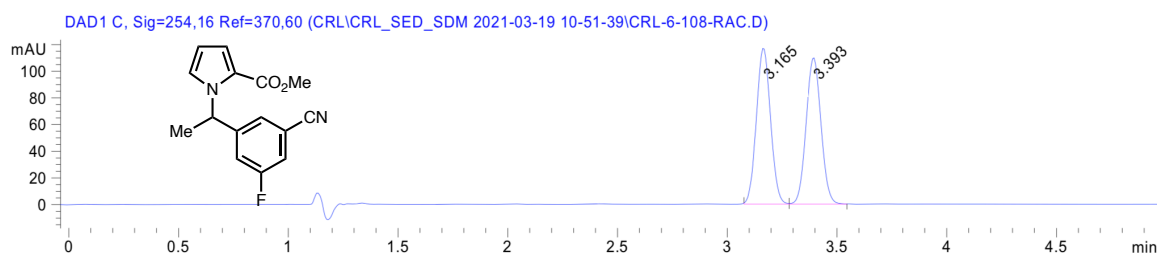
255: racemic



255: enantioenriched (93% ee)

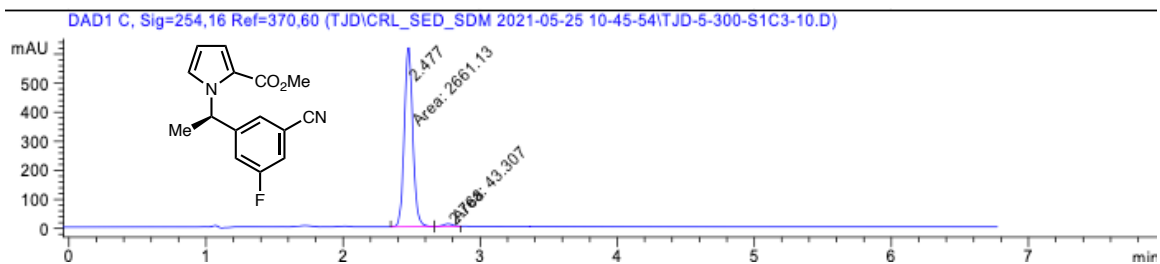


**238:** racemic



Peak #	RetTime [min]	Type	Width [min]	Area [mAU*s]	Height [mAU]	Area %
1	3.165	BV	0.0687	524.86218	116.11243	50.4006
2	3.393	VB	0.0753	516.51965	108.89555	49.5994

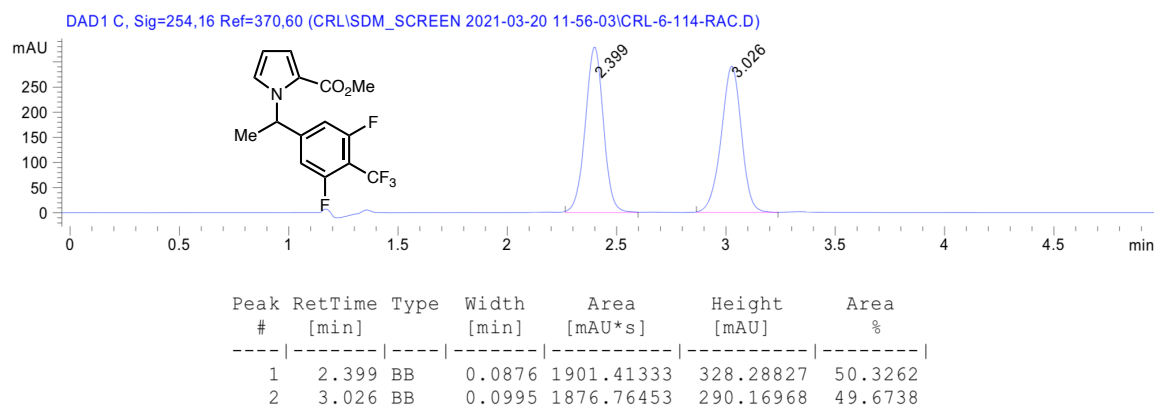
**238:** enantioenriched (97% ee)



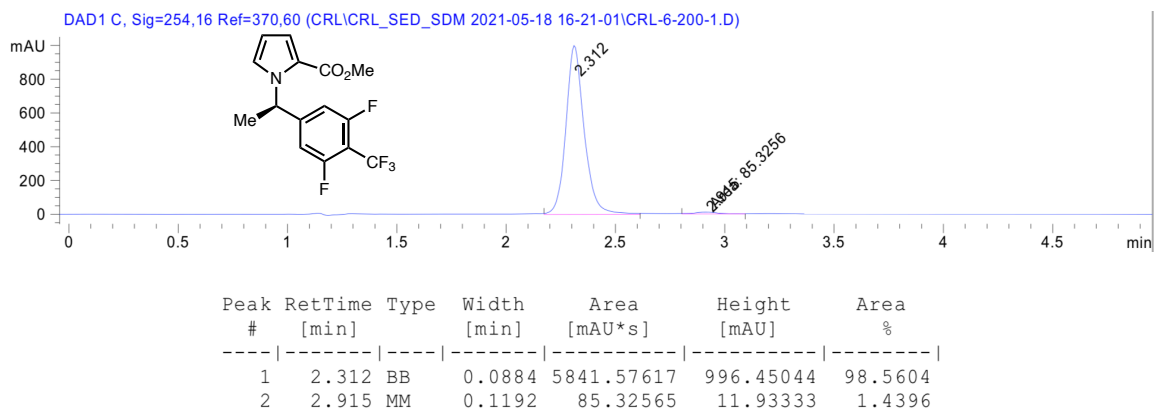
Peak #	RetTime [min]	Type	Width [min]	Area [mAU*s]	Height [mAU]	Area %
1	2.477	MF	0.0711	2661.13379	624.01465	98.3987
2	2.768	FM	0.0760	43.30695	9.49704	1.6013



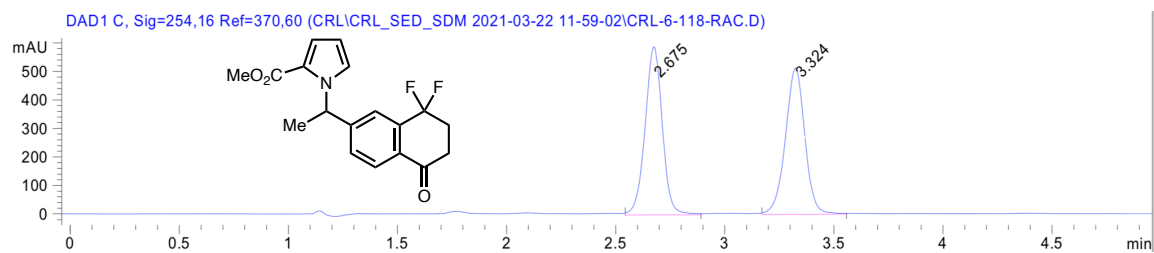
**256: racemic**



**256: enantioenriched (97% ee)**

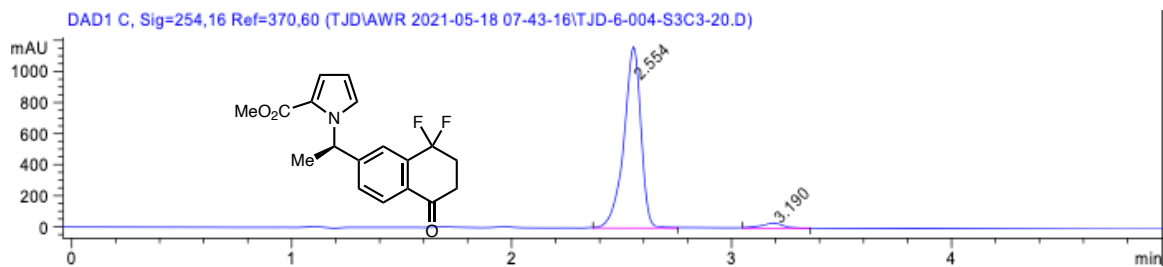


**257: racemic**



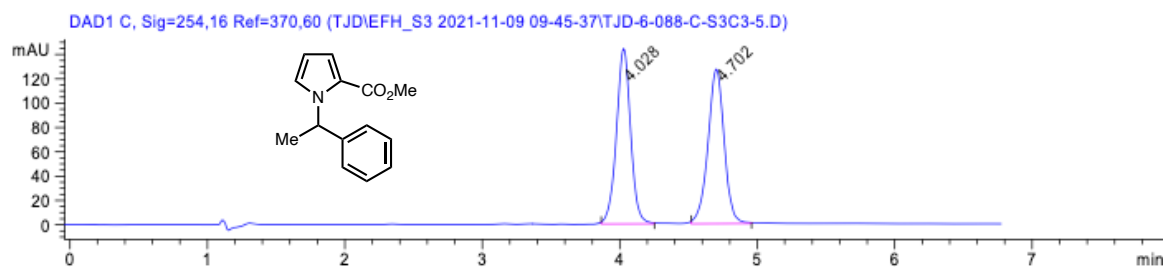
Peak #	RetTime [min]	Type	Width [min]	Area [mAU*s]	Height [mAU]	Area %
1	2.675	BB	0.0845	3254.42847	588.33789	50.4921
2	3.324	BB	0.0970	3190.99146	510.11090	49.5079

**257: enantioenriched (94% ee)**



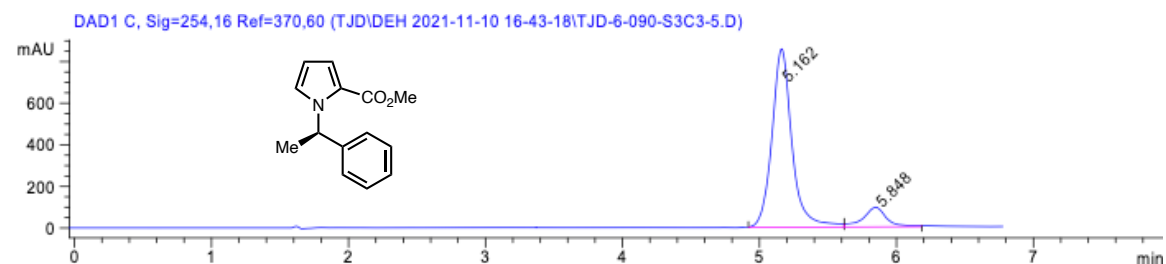
Peak #	RetTime [min]	Type	Width [min]	Area [mAU*s]	Height [mAU]	Area %
1	2.554	BB	0.0832	6293.52490	1162.08484	96.3923
2	3.190	BB	0.1062	235.55145	33.43969	3.6077

258: racemic



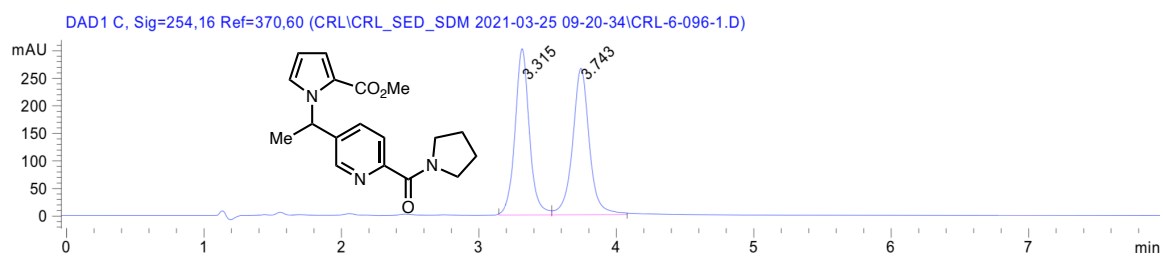
Peak #	RetTime [min]	Type	Width [min]	Area [mAU*s]	Height [mAU]	Area %
1	4.028	BB	0.1120	1034.42847	143.61986	49.8256
2	4.702	BB	0.1239	1041.66968	126.78773	50.1744

258: enantioenriched (78% ee)



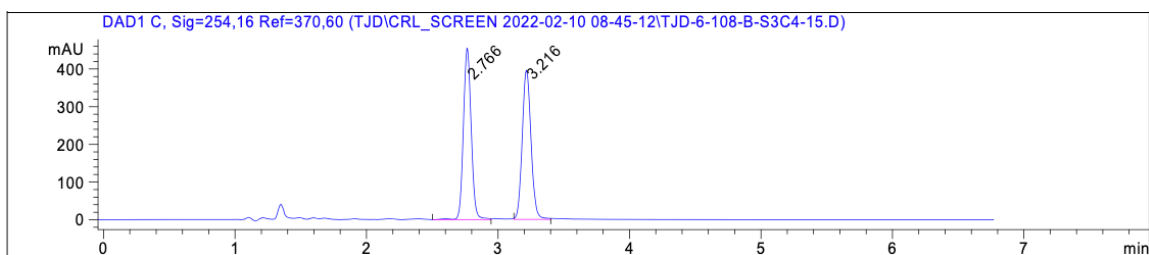
Peak #	RetTime [min]	Type	Width [min]	Area [mAU*s]	Height [mAU]	Area %
1	5.162	BV	0.1546	8711.05469	856.59308	88.7565
2	5.848	VB	0.1684	1103.49768	94.36774	11.2435

**260:** racemic



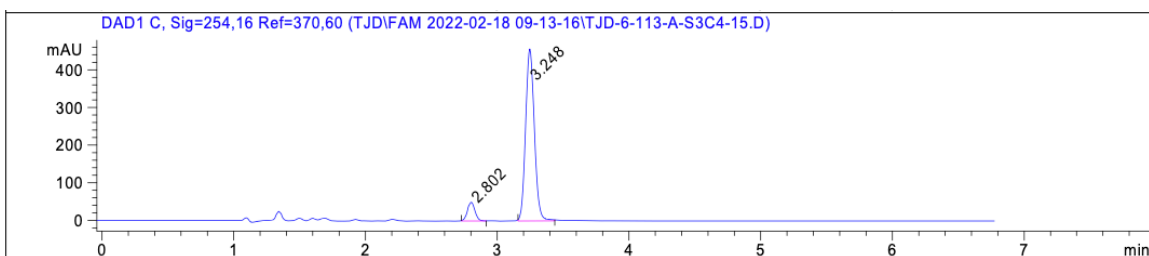
Peak #	RetTime [min]	Type	Width [min]	Area [mAU*s]	Height [mAU]	Area %
1	3.315	BV	0.1088	2184.90063	300.76508	49.1868
2	3.743	VB	0.1272	2257.14722	265.48404	50.8132

**261: racemic**



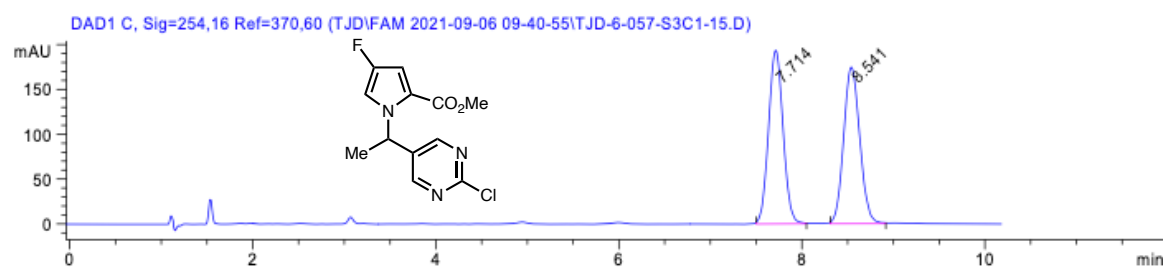
Peak #	RetTime [min]	Type	Width [min]	Area [mAU*s]	Height [mAU]	Area %
1	2.766	VB	0.0645	1871.41614	450.40173	50.3413
2	3.216	BB	0.0746	1846.04333	394.16595	49.6587

**261: enantioenriched (83% ee)**



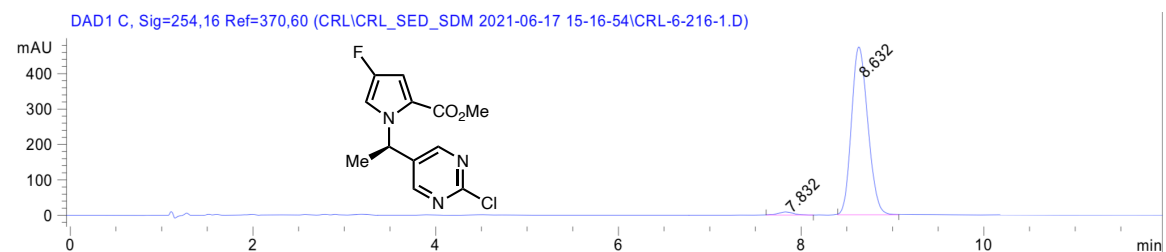
Peak #	RetTime [min]	Type	Width [min]	Area [mAU*s]	Height [mAU]	Area %
1	2.802	BB	0.0629	198.14445	49.28078	8.5774
2	3.248	BB	0.0744	2111.92212	452.89645	91.4226

**278:** racemic



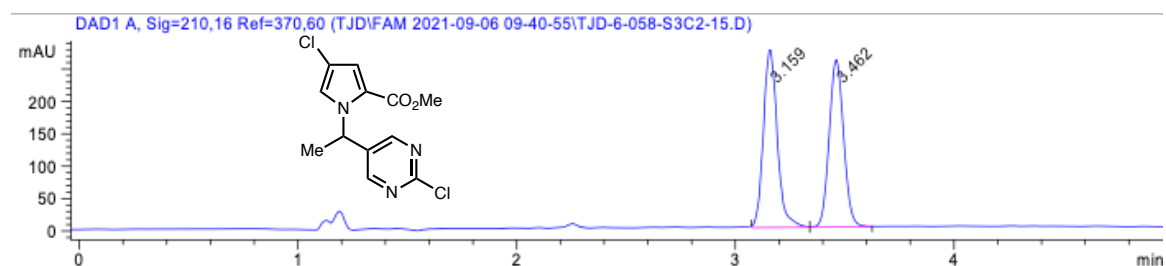
Peak #	RetTime [min]	Type	Width [min]	Area [mAU*s]	Height [mAU]	Area %
1	7.714	BB	0.1728	2134.23486	193.37785	49.9726
2	8.541	BB	0.1909	2136.57275	174.41992	50.0274

**278:** enantioenriched (97% ee)



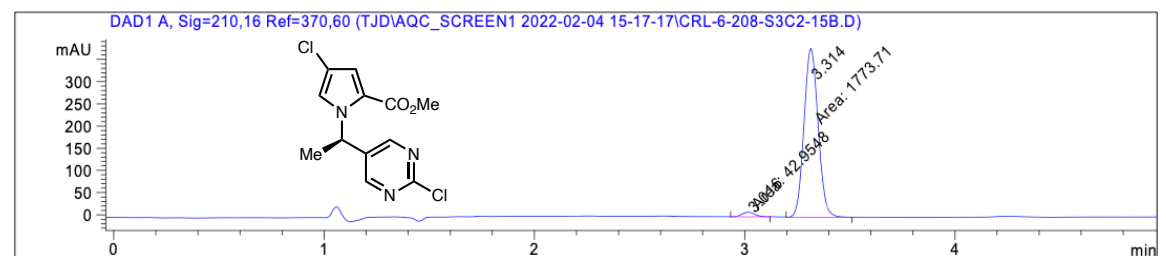
Peak #	RetTime [min]	Type	Width [min]	Area [mAU*s]	Height [mAU]	Area %
1	7.832	BB	0.1709	92.79287	8.53381	1.5434
2	8.632	BB	0.1937	5919.38672	474.11859	98.4566

**270: racemic**



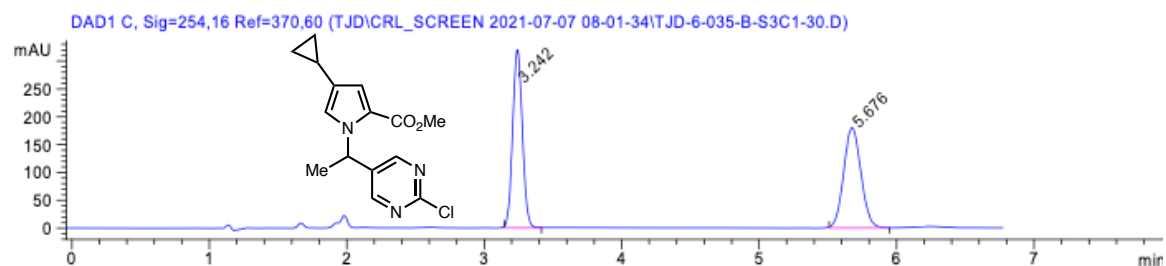
Peak #	RetTime [min]	Type	Width [min]	Area [mAU*s]	Height [mAU]	Area %
1	3.159	BV	0.0717	1213.64319	273.67831	50.6024
2	3.462	VB	0.0740	1184.74756	256.19836	49.3976

**270: enantioenriched (95% ee)**



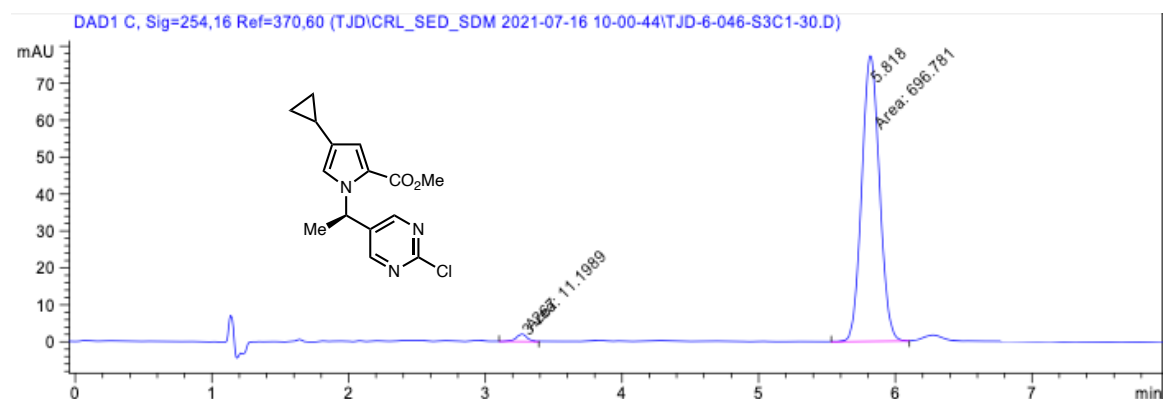
Peak #	RetTime [min]	Type	Width [min]	Area [mAU*s]	Height [mAU]	Area %
1	3.016	MM	0.0677	42.95485	10.57910	2.3645
2	3.314	MM	0.0773	1773.71338	382.33533	97.6355

**279:** racemic



Peak #	RetTime [min]	Type	Width [min]	Area [mAU*s]	Height [mAU]	Area %
1	3.242	BB	0.0775	1568.50537	318.35016	49.9702
2	5.676	BB	0.1339	1570.37366	179.87247	50.0298

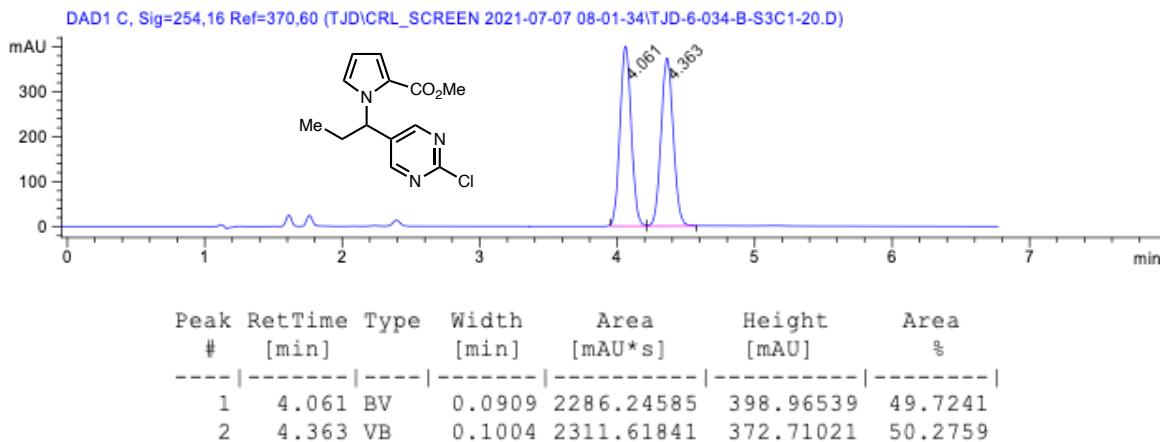
**279:** enantioenriched (97% ee)



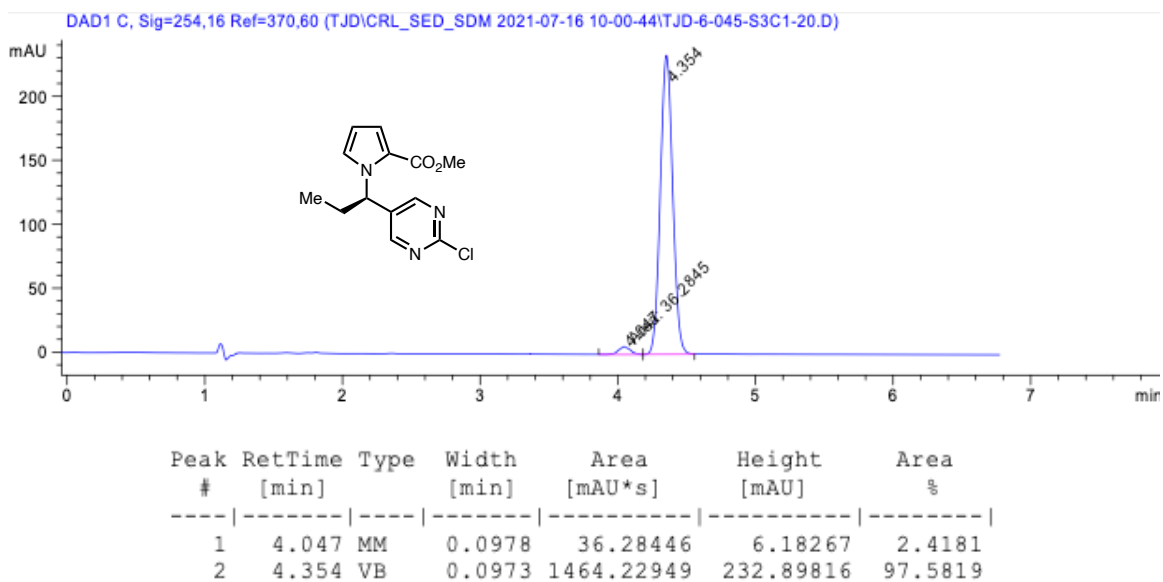
Peak #	RetTime [min]	Type	Width [min]	Area [mAU*s]	Height [mAU]	Area %
1	3.267	MM	0.0909	11.19889	2.05334	1.5818
2	5.818	MM	0.1499	696.78052	77.48254	98.4182



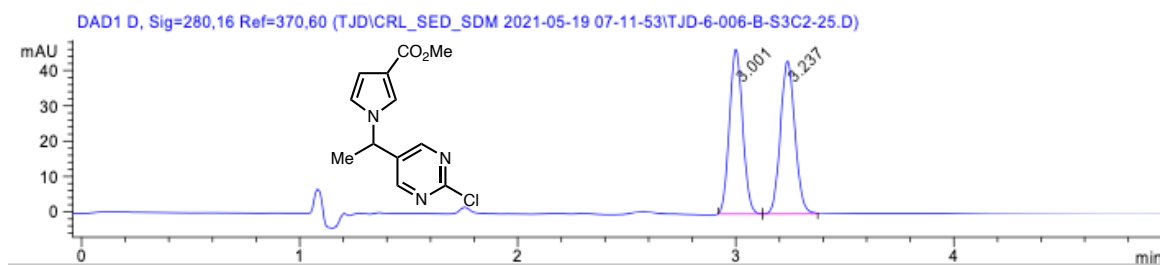
**280: racemic**



**280: enantioenriched (95% ee)**

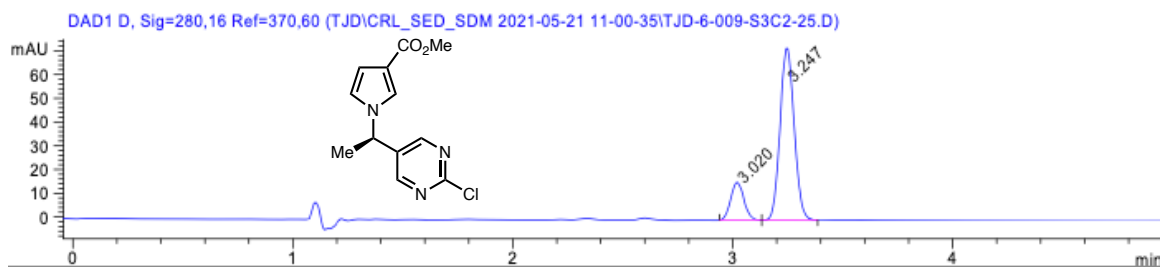


**271:** racemic



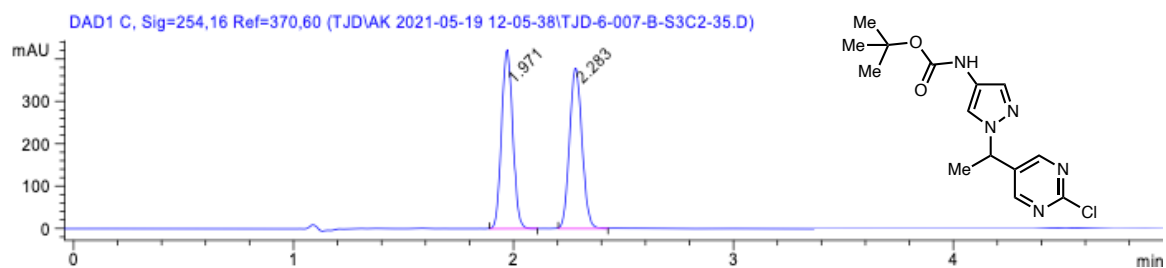
Peak #	RetTime [min]	Type	Width [min]	Area [mAU*s]	Height [mAU]	Area %
1	3.001	BV	0.0695	196.21571	46.26278	49.4233
2	3.237	VB	0.0746	200.79509	42.87277	50.5767

**271:** enantioenriched (66% ee)



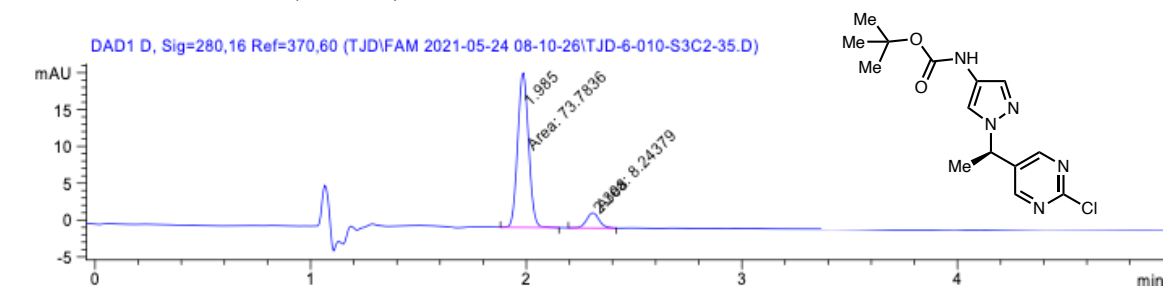
Peak #	RetTime [min]	Type	Width [min]	Area [mAU*s]	Height [mAU]	Area %
1	3.020	BV	0.0653	66.32412	15.70622	16.9718
2	3.247	VB	0.0687	324.46671	71.82458	83.0282

264: racemic



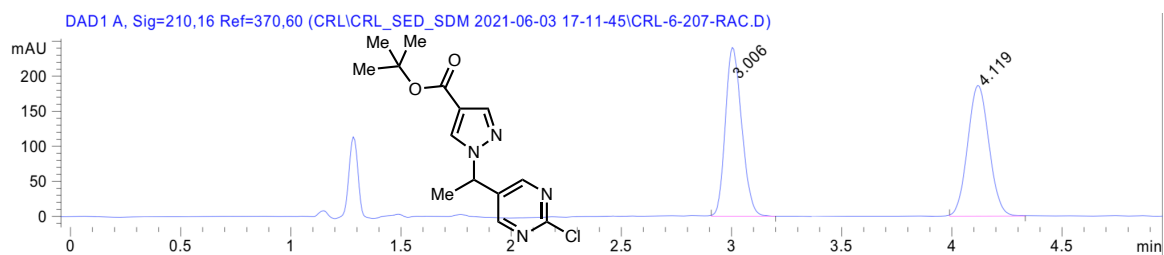
Peak #	RetTime [min]	Type	Width [min]	Area [mAU*s]	Height [mAU]	Area %
1	1.971	BB	0.0605	3619.66187	948.77588	48.6515
2	2.282	BB	0.0658	3820.31689	894.14740	51.3485

264: enantioenriched (80% ee)



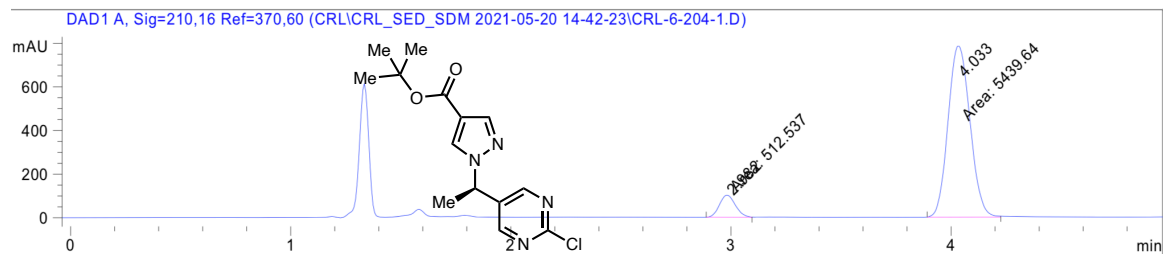
Peak #	RetTime [min]	Type	Width [min]	Area [mAU*s]	Height [mAU]	Area %
1	1.985	MM	0.0581	73.78355	21.17700	89.9500
2	2.308	MM	0.0660	8.24379	2.08046	10.0500

**266: racemic**



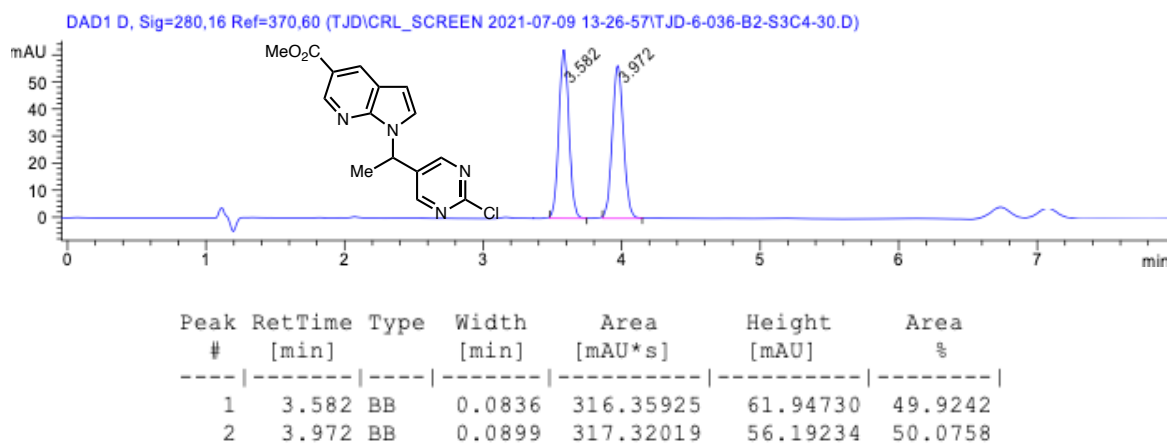
Peak #	RetTime [min]	Type	Width [min]	Area [mAU*s]	Height [mAU]	Area %
1	3.006	BB	0.0845	1247.60950	240.49585	49.8341
2	4.119	BB	0.1068	1255.91431	185.95889	50.1659

**266: enantioenriched (83% ee)**

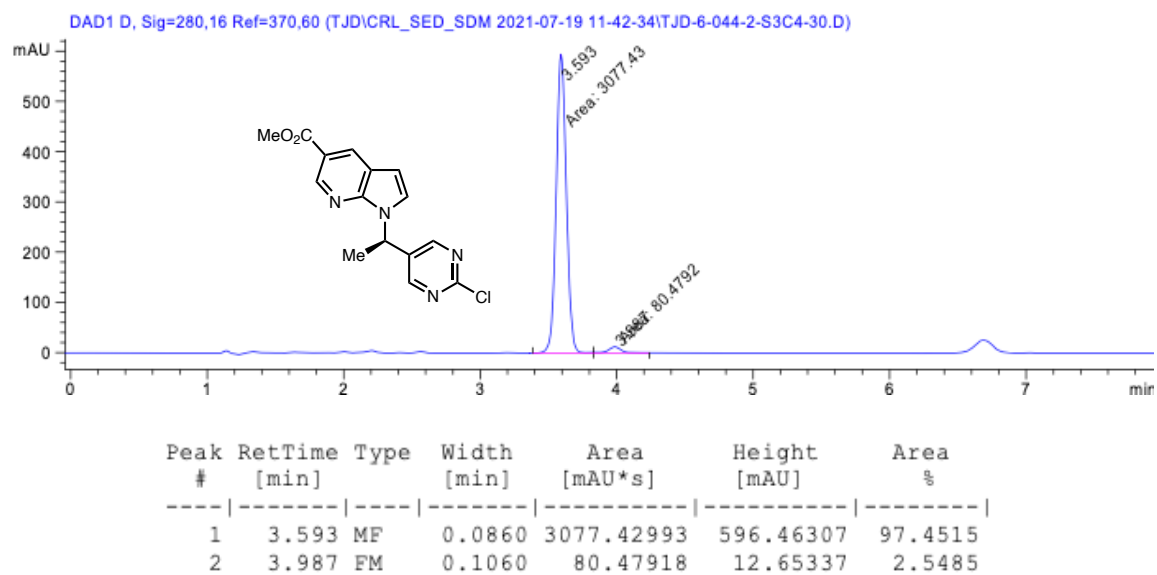


Peak #	RetTime [min]	Type	Width [min]	Area [mAU*s]	Height [mAU]	Area %
1	2.982	MF	0.0832	512.53680	102.70668	8.6109
2	4.033	MF	0.1149	5439.63916	789.00952	91.3891

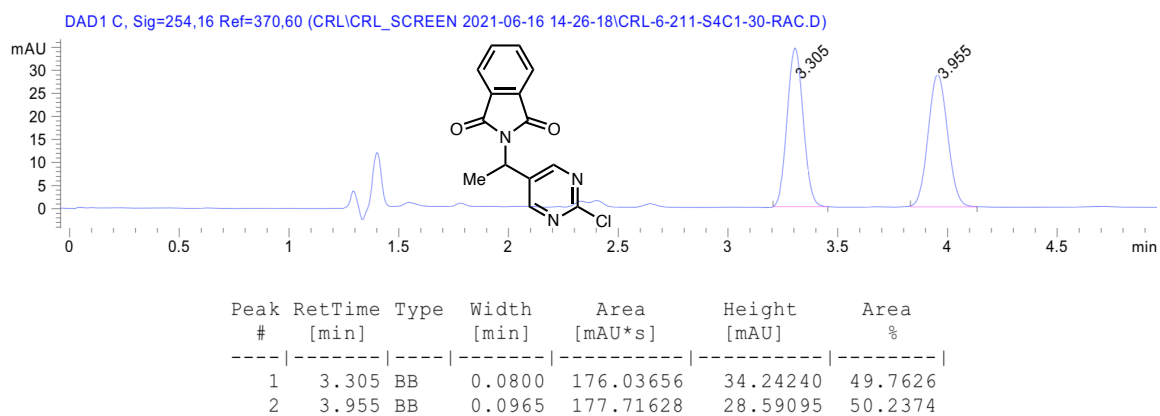
**281: racemic**



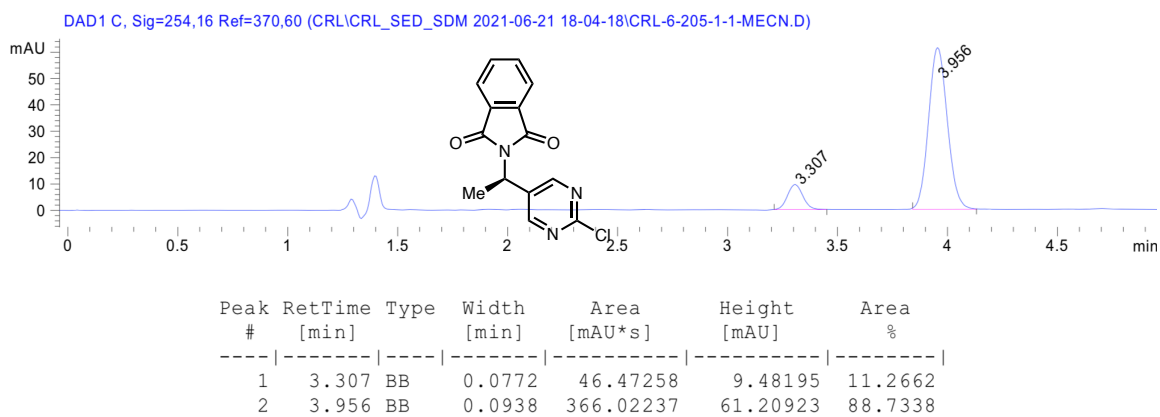
**281: enantioenriched (95% ee)**



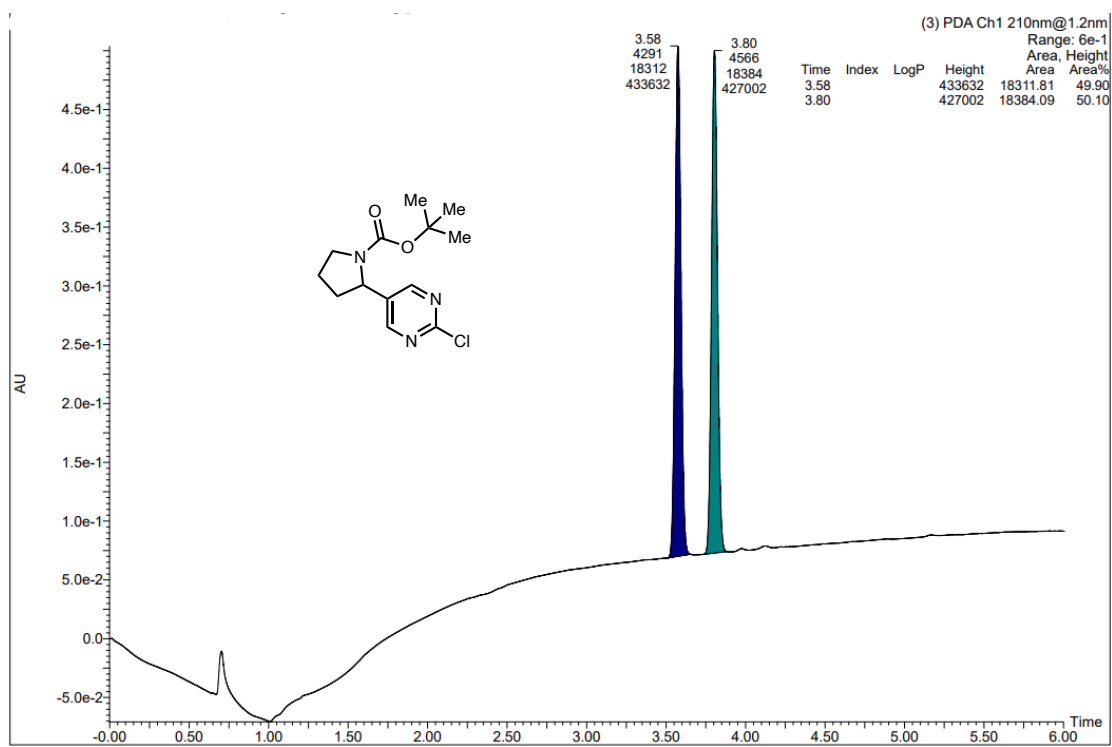
**272: racemic**



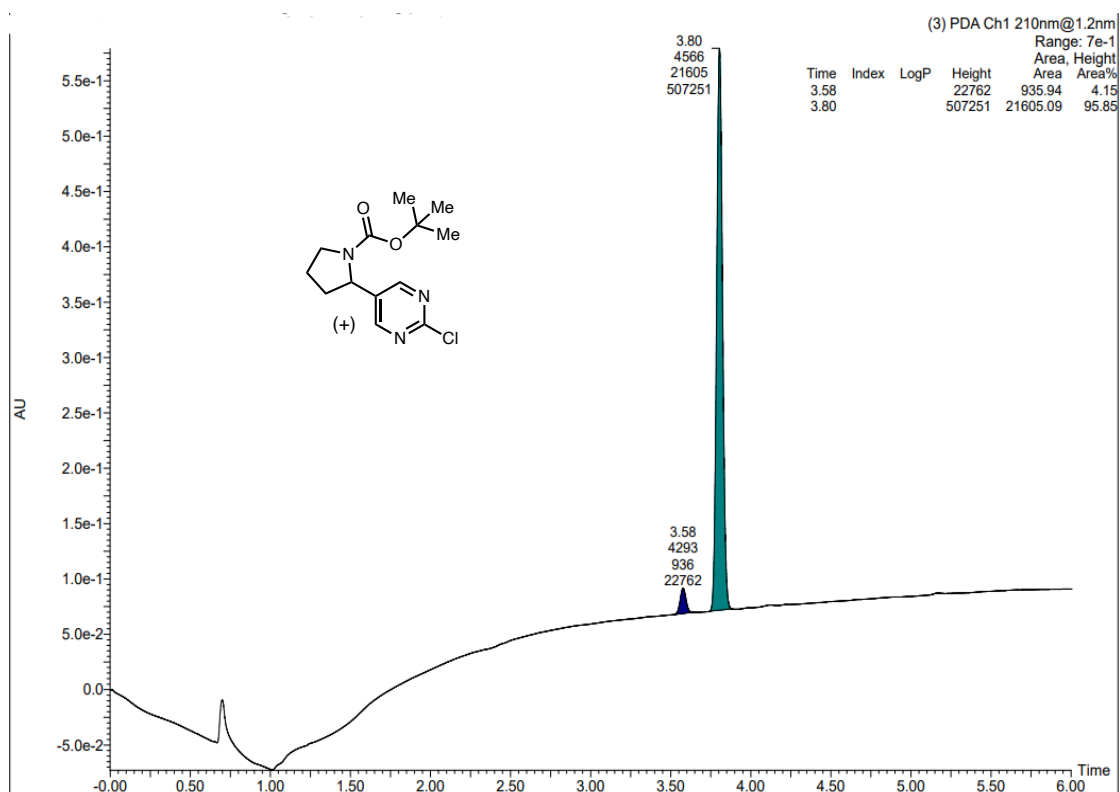
**272: enantioenriched (77% ee)**



282: racemic



**282:** enantioenriched (92% ee)





### 3.7 NOTES AND REFERENCES

- (1) Vitaku, E.; Smith, D. T.; Njardarson, J. T. *J. Med. Chem.* **2014**, *57* (24), 10257–10274.
- (2) Yin, M.; Guo, Y.; Hu, R.; Cai, W. L.; Li, Y.; Pei, S.; Sun, H.; Peng, C.; Li, J.; Ye, R.; Yang, Q.; Wang, N.; Tao, Y.; Chen, X.; Yan, Q. *Nat. Commun.* **2020**, *11* (1), 1833.
- (3) Ren, S.; Vishwanathan, K.; Cantarini, M.; Frewer, P.; Hara, I.; Scarfe, G.; Burke, W.; Schalkwijk, S.; Li, Y.; Han, D.; Goldwater, R. *Br. J. Clin. Pharmacol.* **2022**, *88* (2), 655–668.
- (4) Xiong, Y.; Guo, J.; Candelore, M. R.; Liang, R.; Miller, C.; Dallas-Yang, Q.; Jiang, G.; McCann, P. E.; Qureshi, S. A.; Tong, X.; Xu, S. S.; Shang, J.; Vincent, S. H.; Tota, L. M.; Wright, M. J.; Yang, X.; Zhang, B. B.; Tata, J. R.; Parmee, E. R. *J. Med. Chem.* **2012**, *55* (13), 6137–6148.
- (5) Ode, K. *Anaesth. Intensive Care Med.* **2019**, *20* (2), 118–125.
- (6) Shin, N.; Stubbs, M.; Koblish, H.; Yue, E. W.; Soloviev, M.; Douty, B.; Wang, K. H.; Wang, Q.; Gao, M.; Feldman, P.; Yang, G.; Hall, L.; Hansbury, M.; O'Connor, S.; Leffet, L.; Collins, R.; Katiyar, K.; He, X.; Waeltz, P.; Collier, P.; Lu, J.; Li, Y.-L.; Li, Y.; Liu, P. C. C.; Burn, T.; Covington, M.; Diamond, S.; Shuey, D.; Roberts, A.; Yeleswaram, S.; Hollis, G.; Metcalf, B.; Yao, W.; Huber, R.; Combs, A.; Newton, R.; Scherle, P. *J. Pharmacol. Exp. Ther.* **2020**, *374* (1), 211–222.
- (7) Pinto, M. M. M.; Fernandes, C.; Tiritan, M. E. *Molecules* **2020**, *25* (8), 1931.
- (8) Laha, J. K.; Cuny, G. D. *J. Org. Chem.* **2011**, *76* (20), 8477–8482.

- (9) Laha, J. K.; Bhimpuria, R. A.; Hunjan, M. K. *Chem. – Eur. J.* **2017**, *23* (9), 2044–2050.
- (10) Hilpert, L. J.; Sieger, S. V.; Haydl, A. M.; Breit, B. *Angew. Chem. Int. Ed.* **2019**, *58* (11), 3378–3381.
- (11) Ye, Y.; Kim, S.-T.; Jeong, J.; Baik, M.-H.; Buchwald, S. L. *J. Am. Chem. Soc.* **2019**, *141* (9), 3901–3909.
- (12) Jiu, A. Y.; Slocumb, H. S.; Yeung, C. S.; Yang, X.-H.; Dong, V. M. *Angew. Chem. Int. Ed.* **2021**, *60* (36), 19660–19664.
- (13) Kainz, Q. M.; Matier, C. D.; Bartoszewicz, A.; Zultanski, S. L.; Peters, J. C.; Fu, G. *C. Science*, **2016**, *351*, 681–684.
- (14) Pezzetta, C.; Bonifazi, D.; Davidson, R. W. M. *Org. Lett.* **2019**, *21* (22), 8957–8961.
- (15) Twilton, J.; Le, C.; Zhang, P.; Shaw, M. H.; Evans, R. W.; MacMillan, D. W. C. *Nat. Rev. Chem.* **2017**, *1* (7), 0052.
- (16) Milligan, J. A.; Phelan, J. P.; Badir, S. O.; Molander, G. A. *Angew. Chem. Int. Ed.* **2019**, *58* (19), 6152–6163.
- (17) Lipp, A.; Badir, S. O.; Molander, G. A. *Angew. Chem. Int. Ed.* **2021**, *60* (4), 1714–1726.
- (18) Tellis, J. C.; Primer, D. N.; Molander, G. A. *Science* **2014**, *345* (6195), 433–436.
- (19) Zuo, Z.; Cong, H.; Li, W.; Choi, J.; Fu, G. C.; MacMillan, D. W. C. *J. Am. Chem. Soc.* **2016**, *138* (6), 1832–1835.
- (20) Yasu, Y.; Koike, T.; Akita, M. *Adv. Synth. Catal.* **2012**, *354* (18), 3414–3420.
- (21) Tellis, J. C.; Primer, D. N.; Molander, G. A. *Science*, **2014**, *345*, 433–436.

- (22) Jabri, S.; Ogawa, A. K.; Sinz, C. J.; Hicks, J. D.; Cheng, A. C.; Gao, Y.-D.; Yang, S.; Bao, J.; Hayes, D. A. A. W.; Lang, S. B.; Taoka, B. M.; Tian, M.; Shearn-Nance, G. P.; Kuang, R.; Lombardo, M. J.; Wu, Z.; Zhao, Z. WO2021257353A1, 2021.
- (23) Hertzberg, R. P.; Pope, A. J. *Curr. Opin. Chem. Biol.* **2000**, *4* (4), 445–451.
- (24) Poremba, K. E.; Kadunce, N. T.; Suzuki, N.; Cherney, A. H.; Reisman, S. E. *J. Am. Chem. Soc.* **2017**, *139* (16), 5684–5687.
- (25) DeLano, T. J.; Dibrell, S. E.; Lacker, C. R.; Pancoast, A. R.; Poremba, K. E.; Cleary, L.; Sigman, M. S.; Reisman, S. E. *Chem. Sci.* **2021**, *12* (22), 7758–7762.
- (26) Feast, W. J.; Tsibouklis, J. *Polym. Int.* **1994**, *35* (1), 67–74.
- (27) Hansen, E. C.; Pedro, D. J.; Wotal, A. C.; Gower, N. J.; Nelson, J. D.; Caron, S.; Weix, D. J. *Nat. Chem.* **2016**, *8* (12), 1126–1130.
- (28) Gutierrez, O.; Tellis, J. C.; Primer, D. N.; Molander, G. A.; Kozlowski, M. C. *J. Am. Chem. Soc.* **2015**, *137* (15), 4896–4899.
- (29) Guo, L.; Yuan, M.; Zhang, Y.; Wang, F.; Zhu, S.; Gutierrez, O.; Chu, L. *J. Am. Chem. Soc.* **2020**, *142* (48), 20390–20399.
- (30) Siu, J. C.; Sauer, G. S.; Saha, A.; Macey, R. L.; Fu, N.; Chauviré, T.; Lancaster, K. M.; Lin, S. *J. Am. Chem. Soc.* **2018**, *140* (39), 12511–12520.
- (31) Newcomb, M. *Tetrahedron* **1993**, *49* (6), 1151–1176.
- (32) Huang, H.; Wu, Y.; Zhang, W.; Feng, C.; Wang, B.-Q.; Cai, W.-F.; Hu, P.; Zhao, K.-Q.; Xiang, S.-K. *J. Org. Chem.* **2017**, *82* (6), 3094–3101.
- (33) Lockner, J. W.; Dixon, D. D.; Risgaard, R.; Baran, P. S. *Org. Lett.* **2011**, *13* (20), 5628–5631.
- (34) Molander, G. A.; Colombel, V.; Braz, V. A. *Org. Lett.* **2011**, *13* (7), 1852–1855.

- (35) Miyazawa, K.; Yasu, Y.; Koike, T.; Akita, M. *Chem. Commun.* **2013**, 49 (65), 7249.
- (36) Qian, D.; Bera, S.; Hu, X. *J. Am. Chem. Soc.* **2021**, 143 (4), 1959–1967.
- (37) Krska, S. W.; DiRocco, D. A.; Dreher, S. D.; Shevlin, M. *Acc. Chem. Res.* **2017**, 50 (12), 2976–2985.
- (38) Nakamura, T.; Suzuki, K.; Yamashita, M. *J. Am. Chem. Soc.* **2017**, 139 (49), 17763–17766.
- (39) Schmidt, J.; Choi, J.; Liu, A. T.; Slusarczyk, M.; Fu, G. C. *Science* **2016**, 354 (6317), 1265–1269.

## ***Appendix 4***

*Spectra Relevant to Chapter 3:*

*Enantioselective Synthesis of N-Benzylic Heterocycles by*

*Nickel/Photoredox Dual Catalysis*

TJD-5-299-column.1.fid

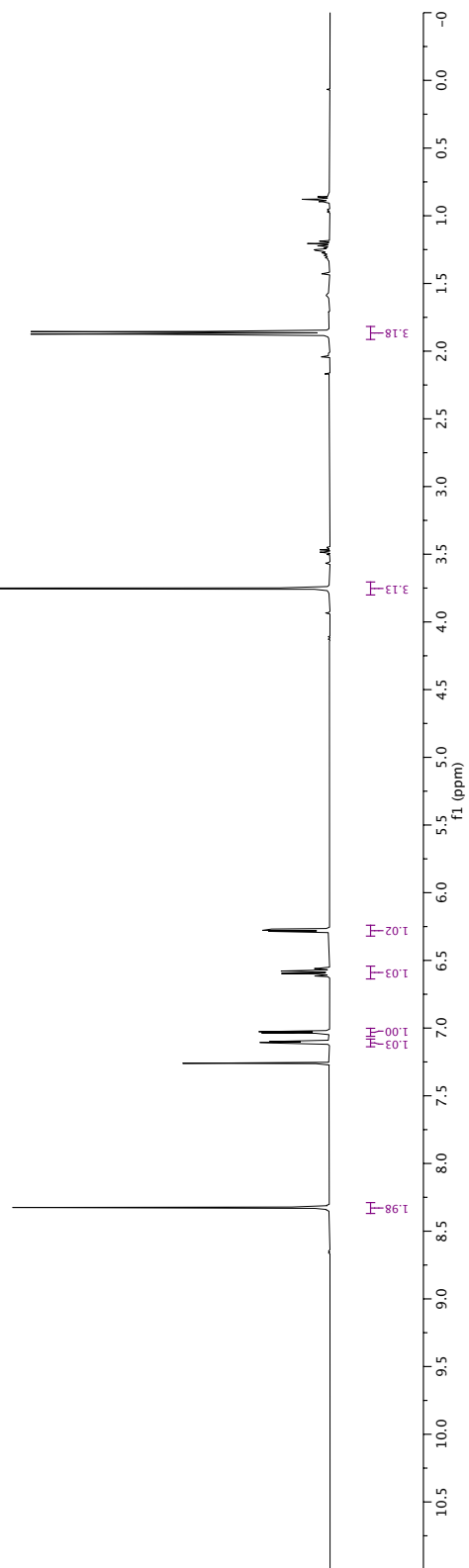
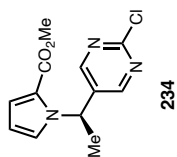
Parameter	Value
Title	TJD-5299-column.1.fid
Solvent	CDCl3
Temperature	297.1
Number of Scans	32
Receiver Gain	197.4
Relaxation Delay	1.0000
Pulse Width	12.5000
Acquisition Time	4.0894
Spectrometer Frequency	400.13
Spectral Width	8012.8
Nucleus	<sup>1</sup> H

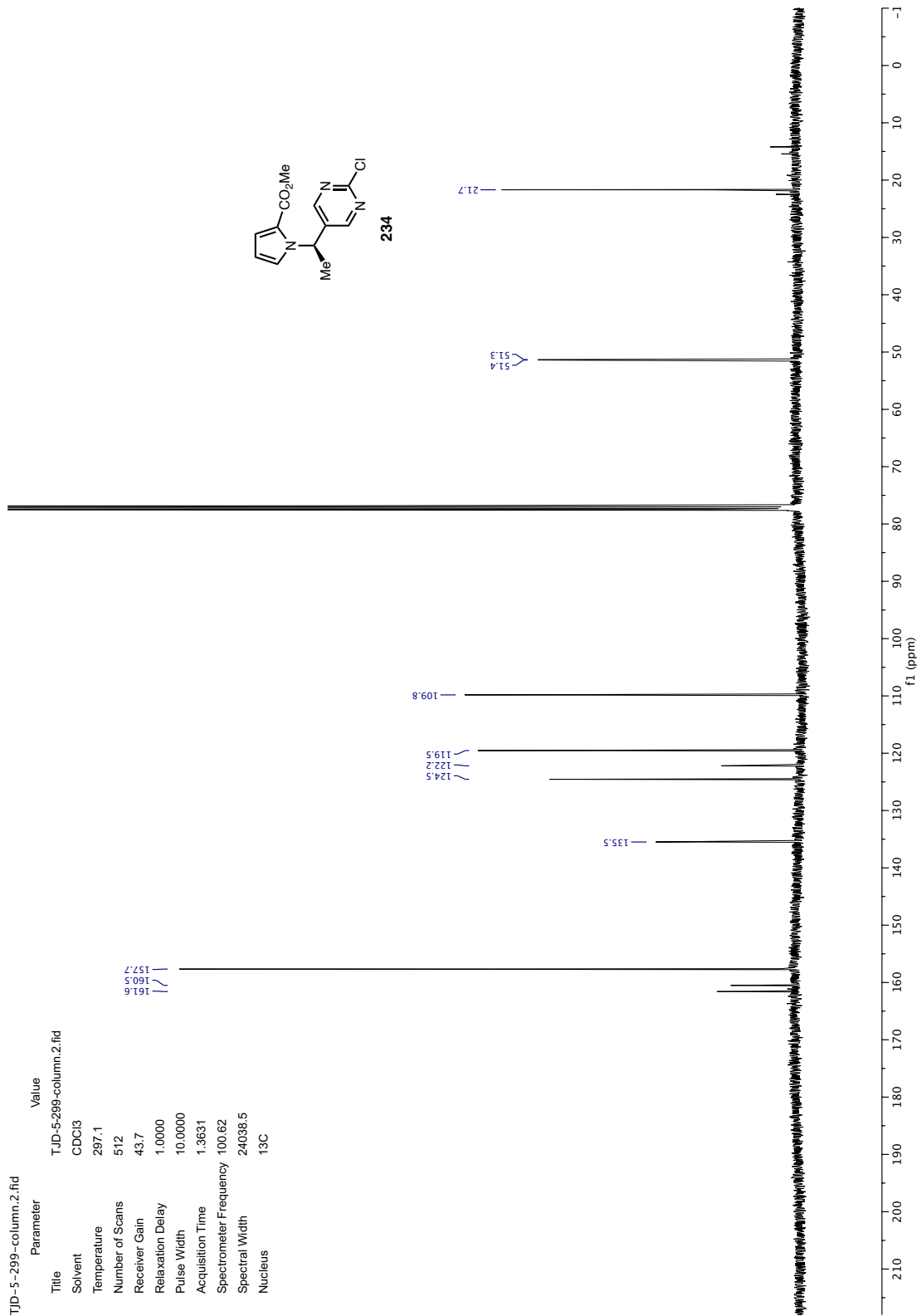
C (ddd)	7.03
B (ddf)	7.10
D (d)	6.59
E (dd)	6.28

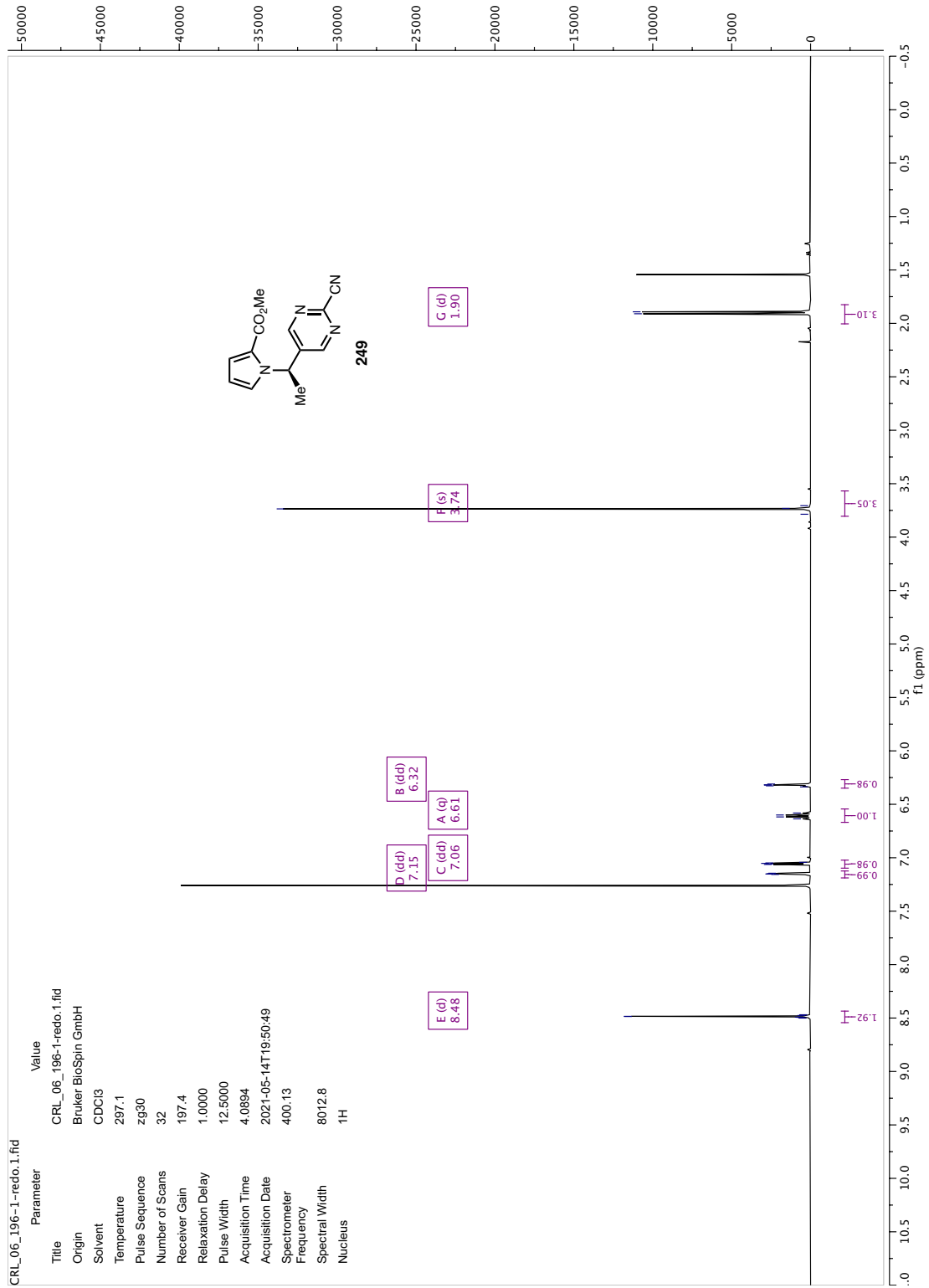
A (d)  
8.33

F (s)  
3.75

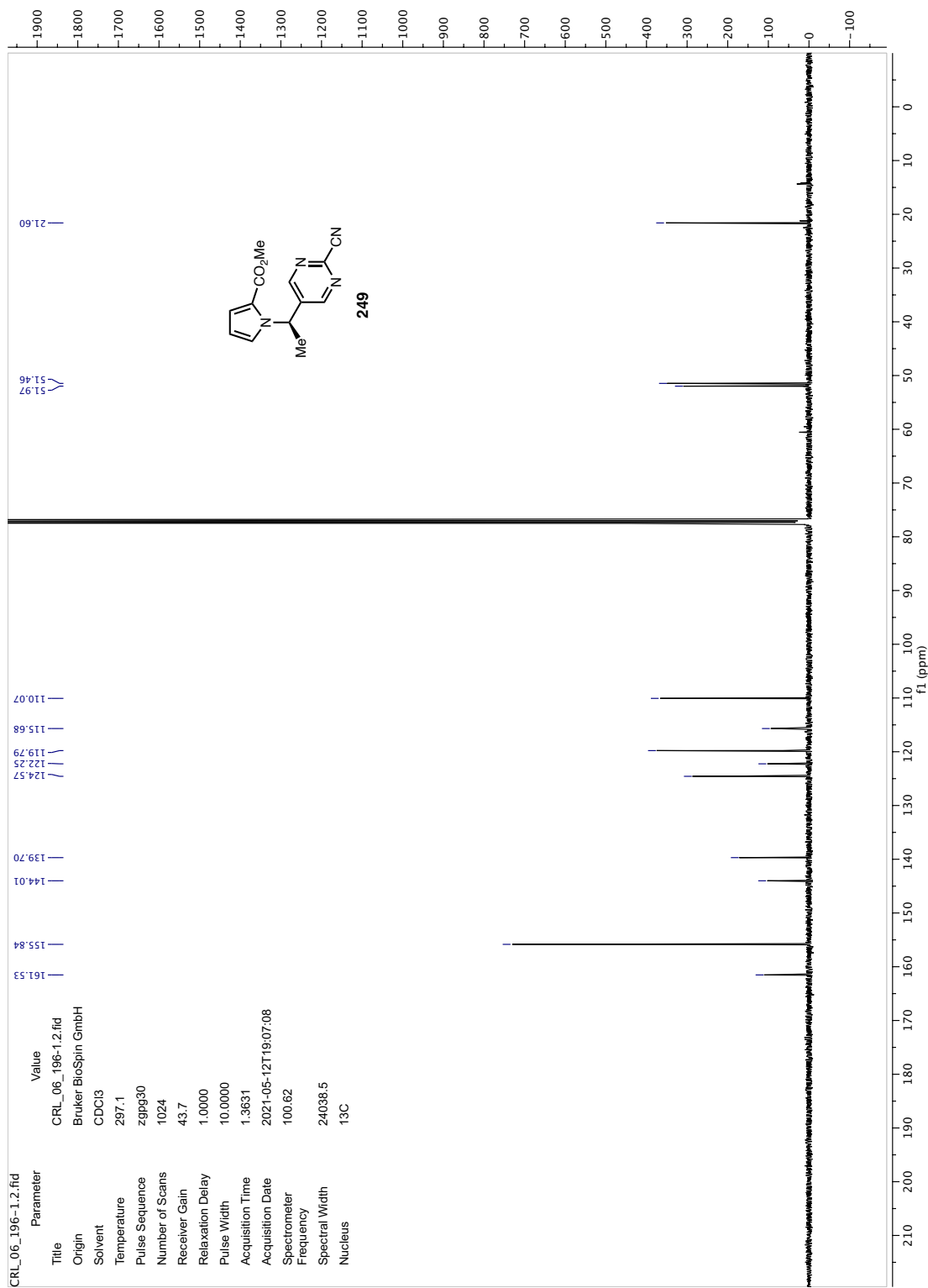
G (d)  
1.86

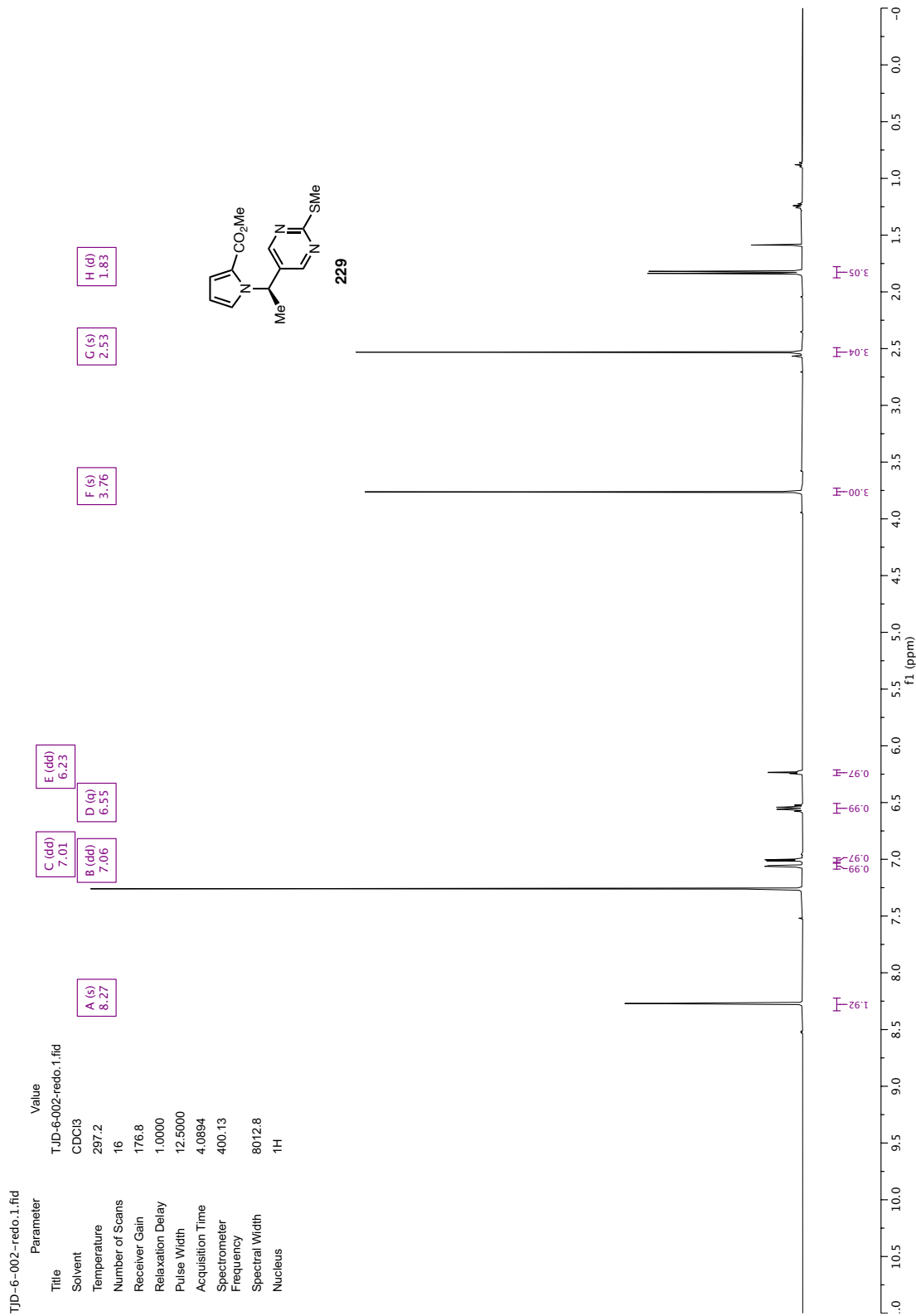


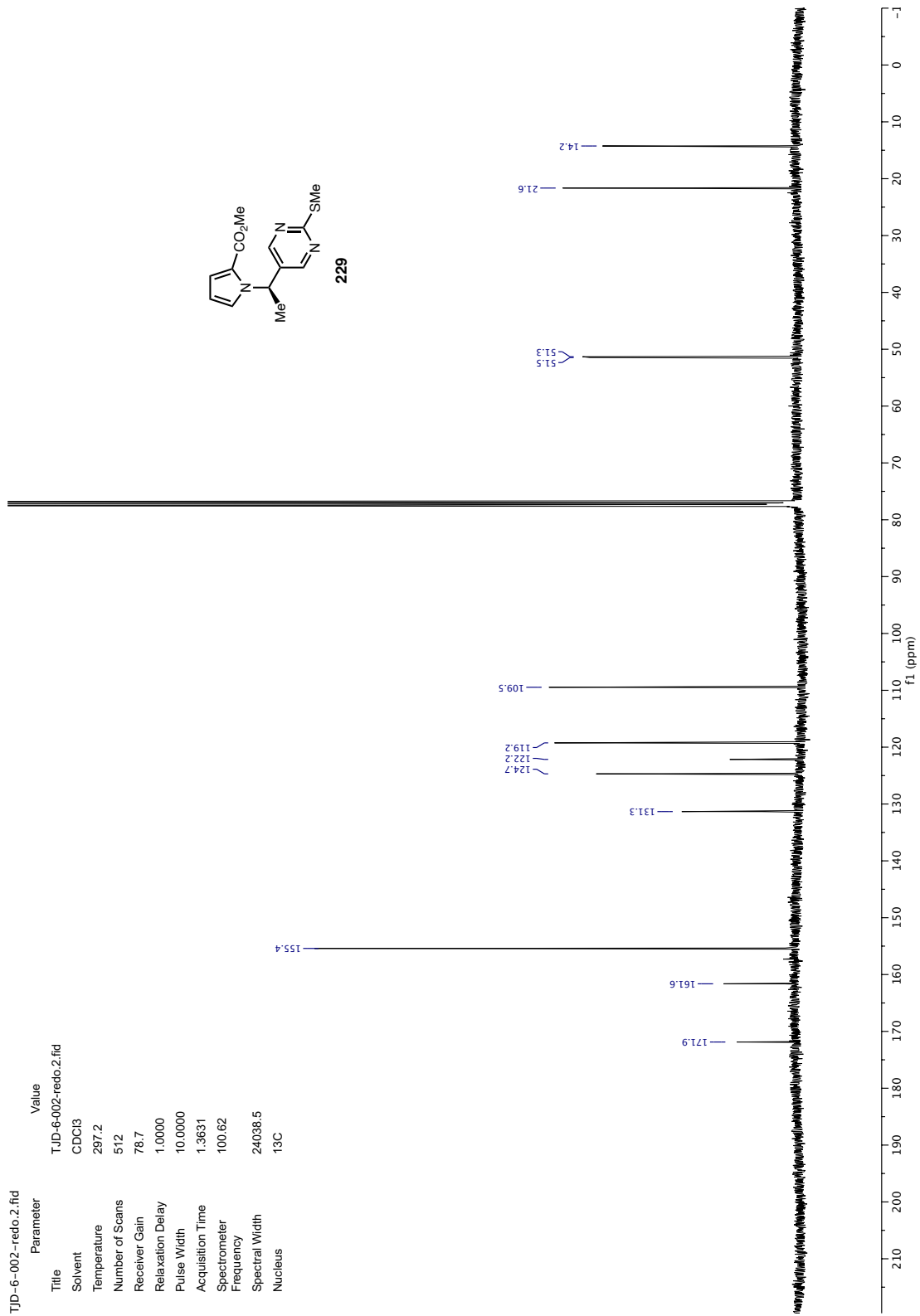


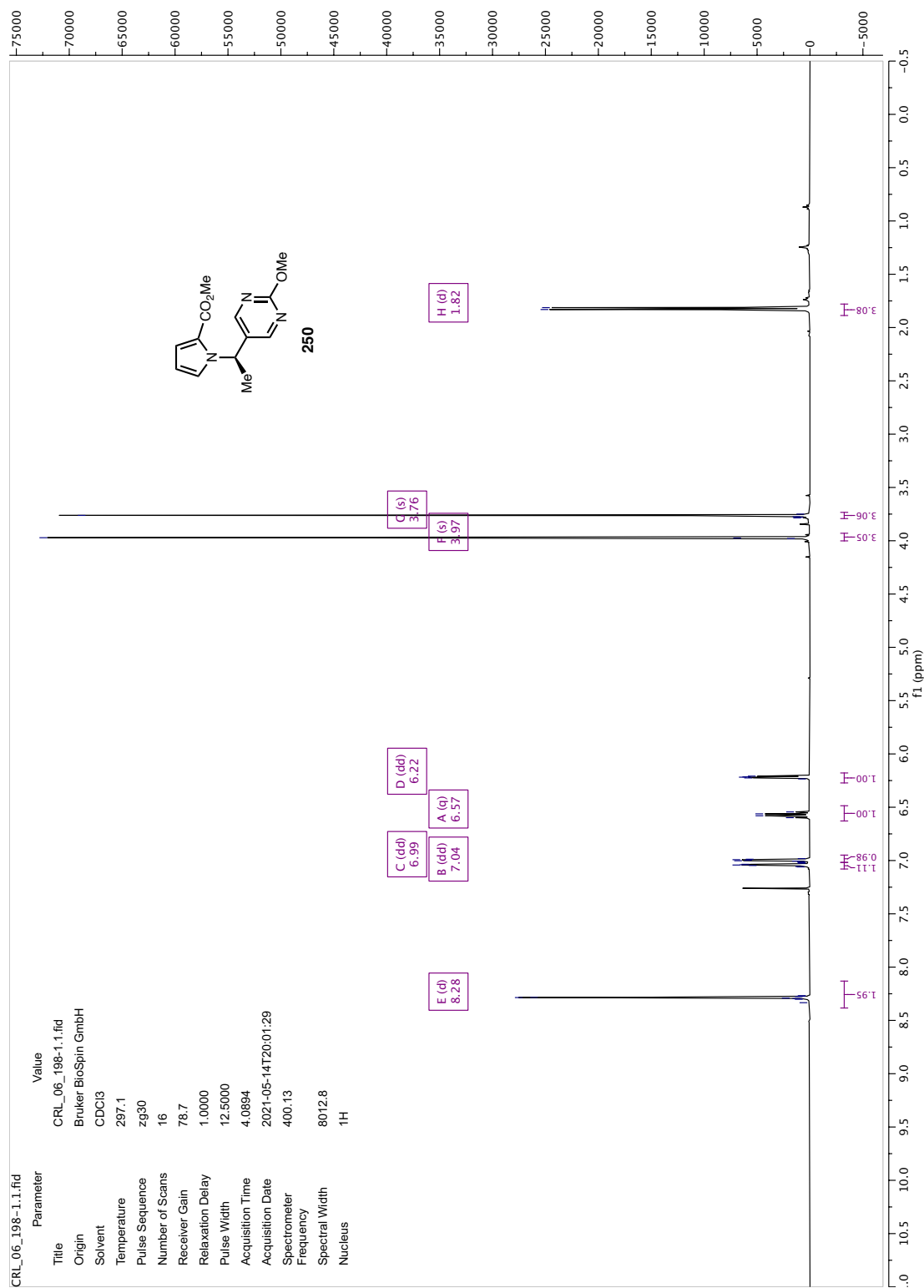


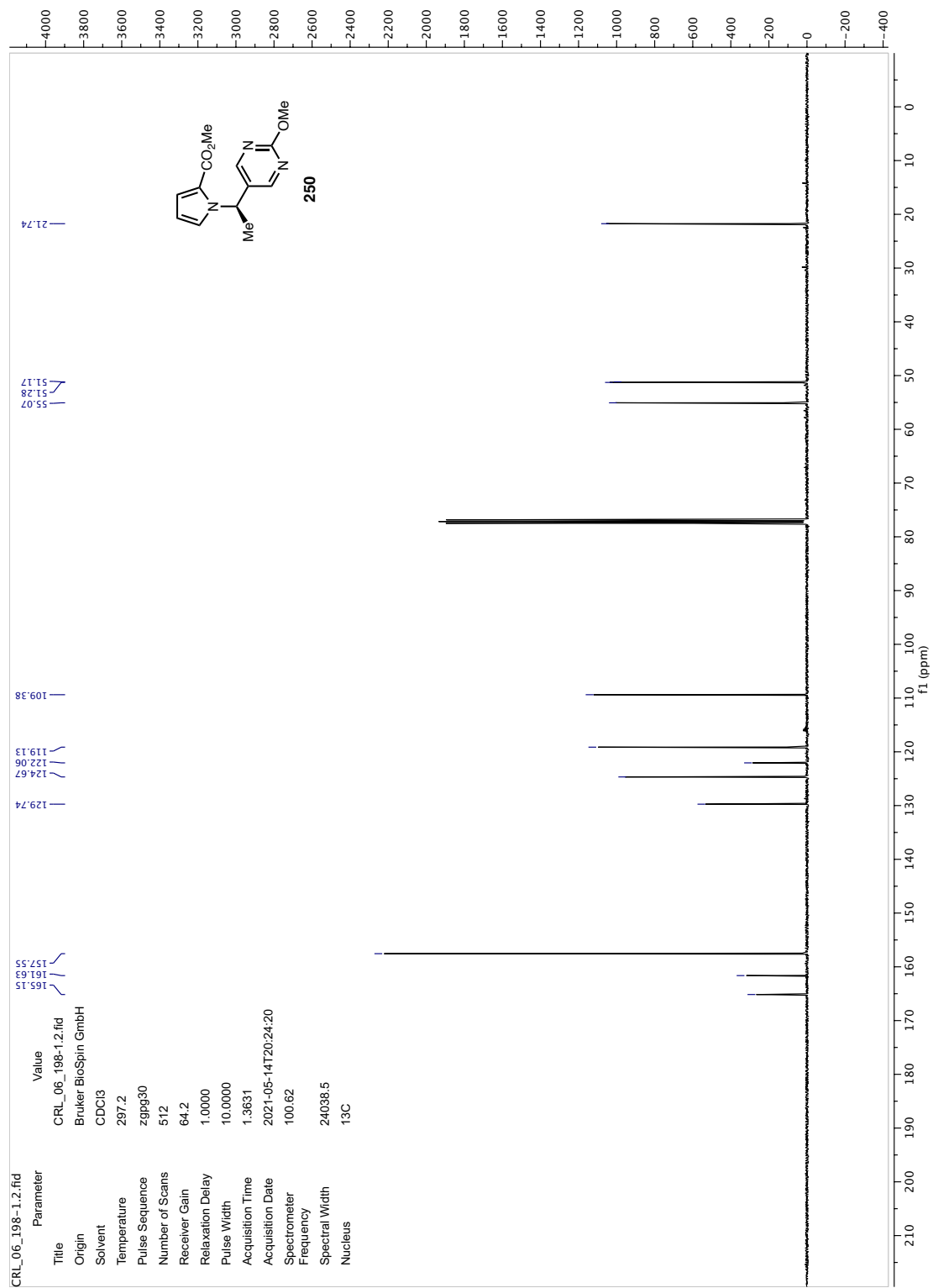


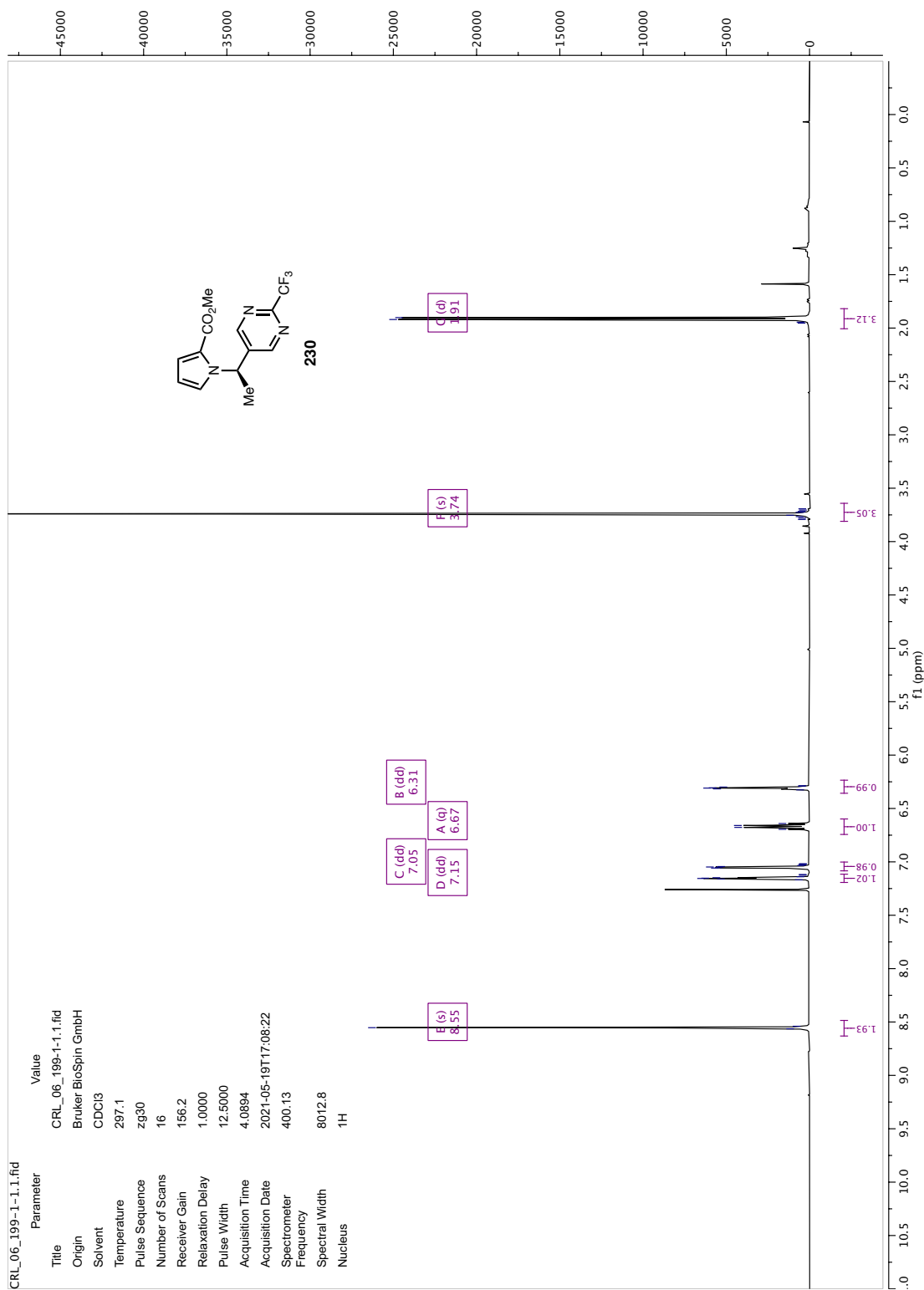


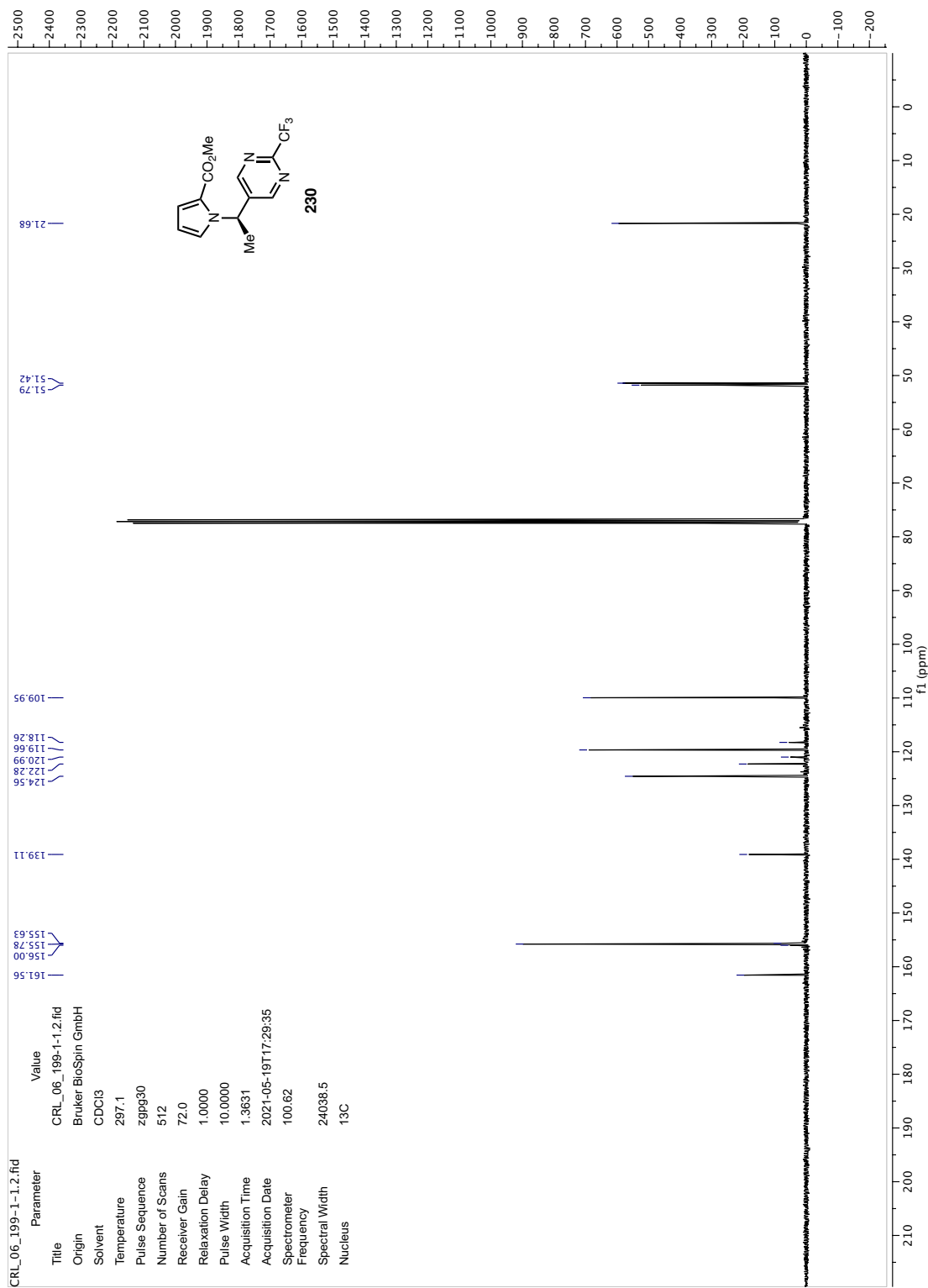


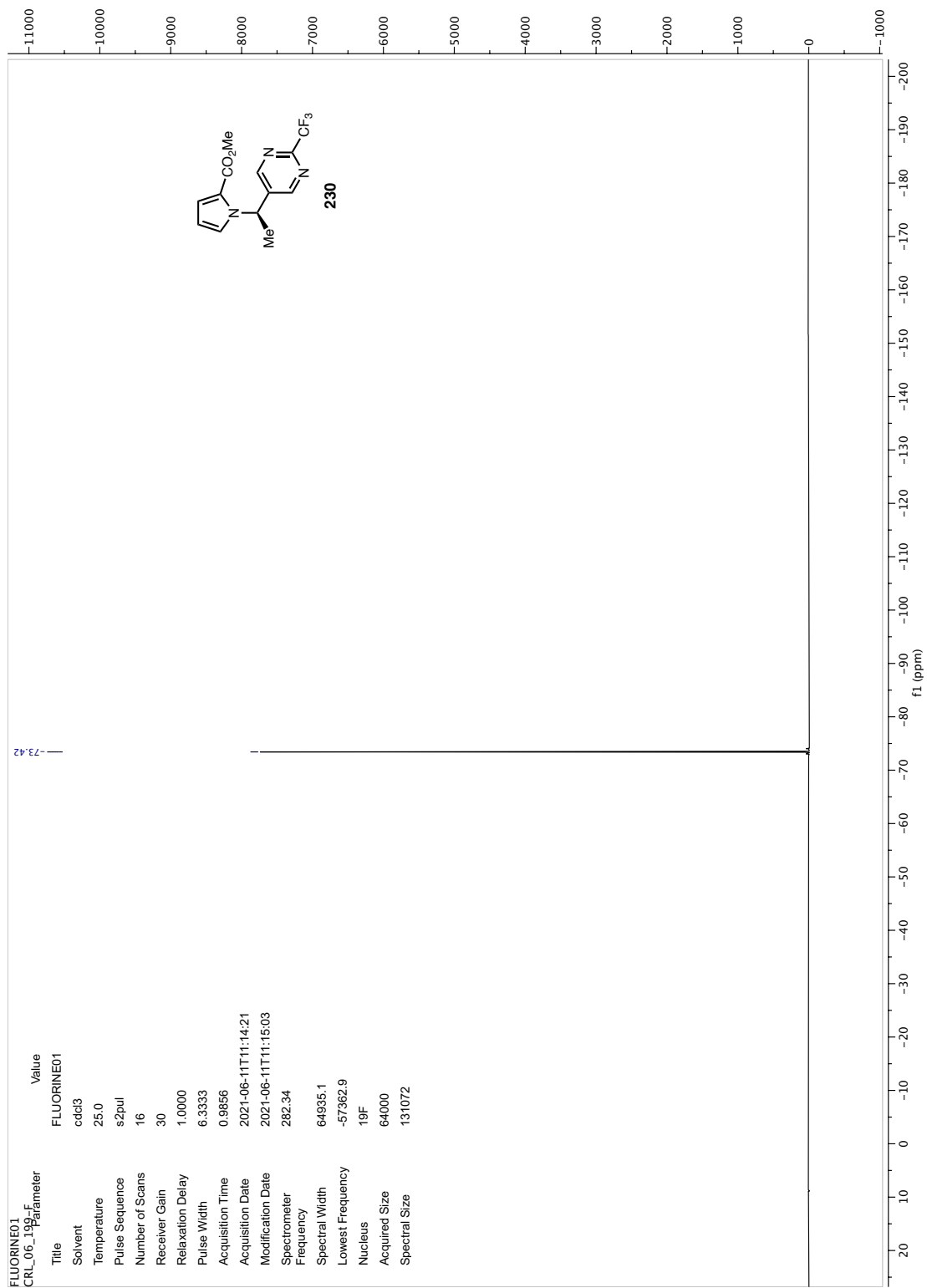




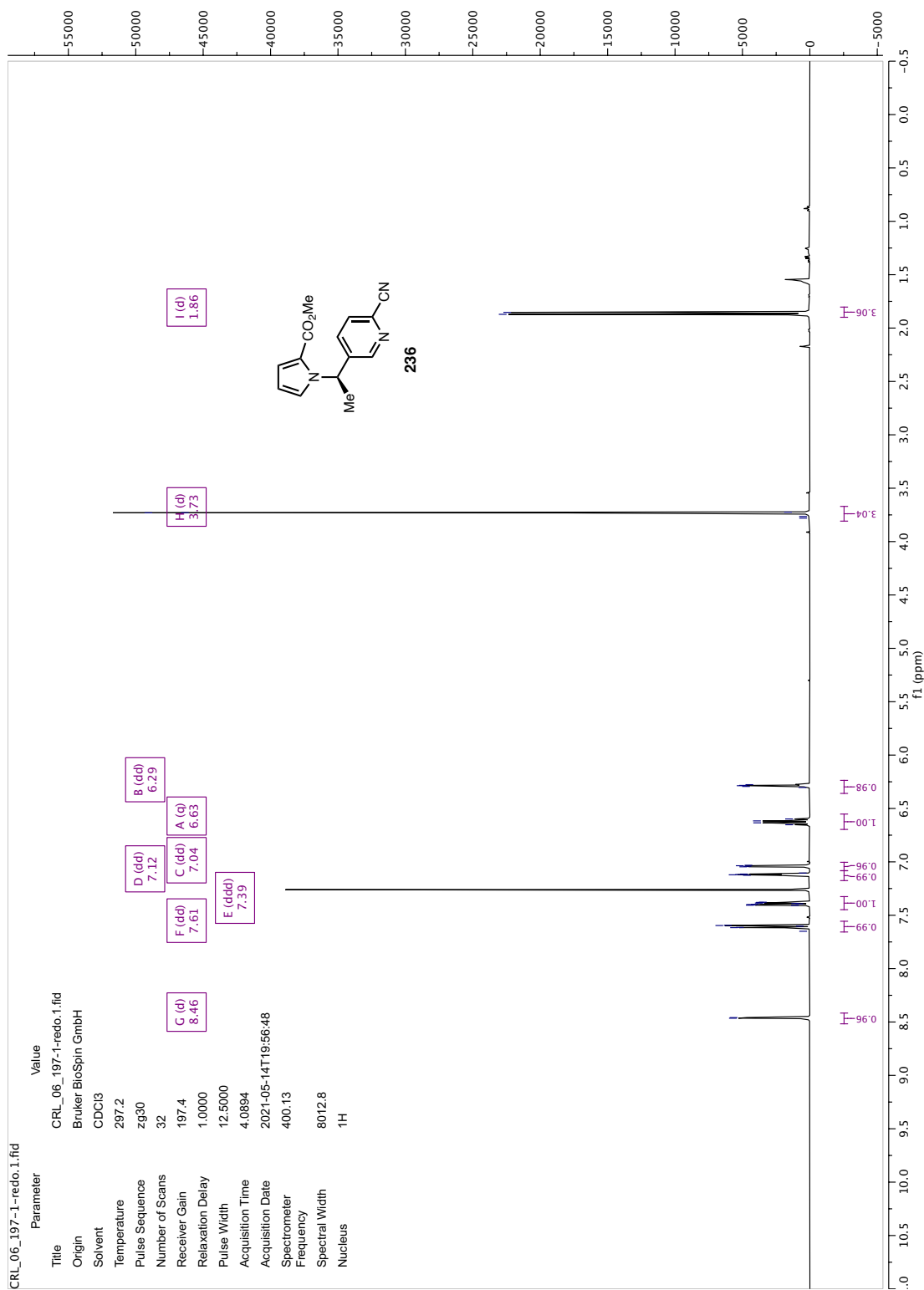


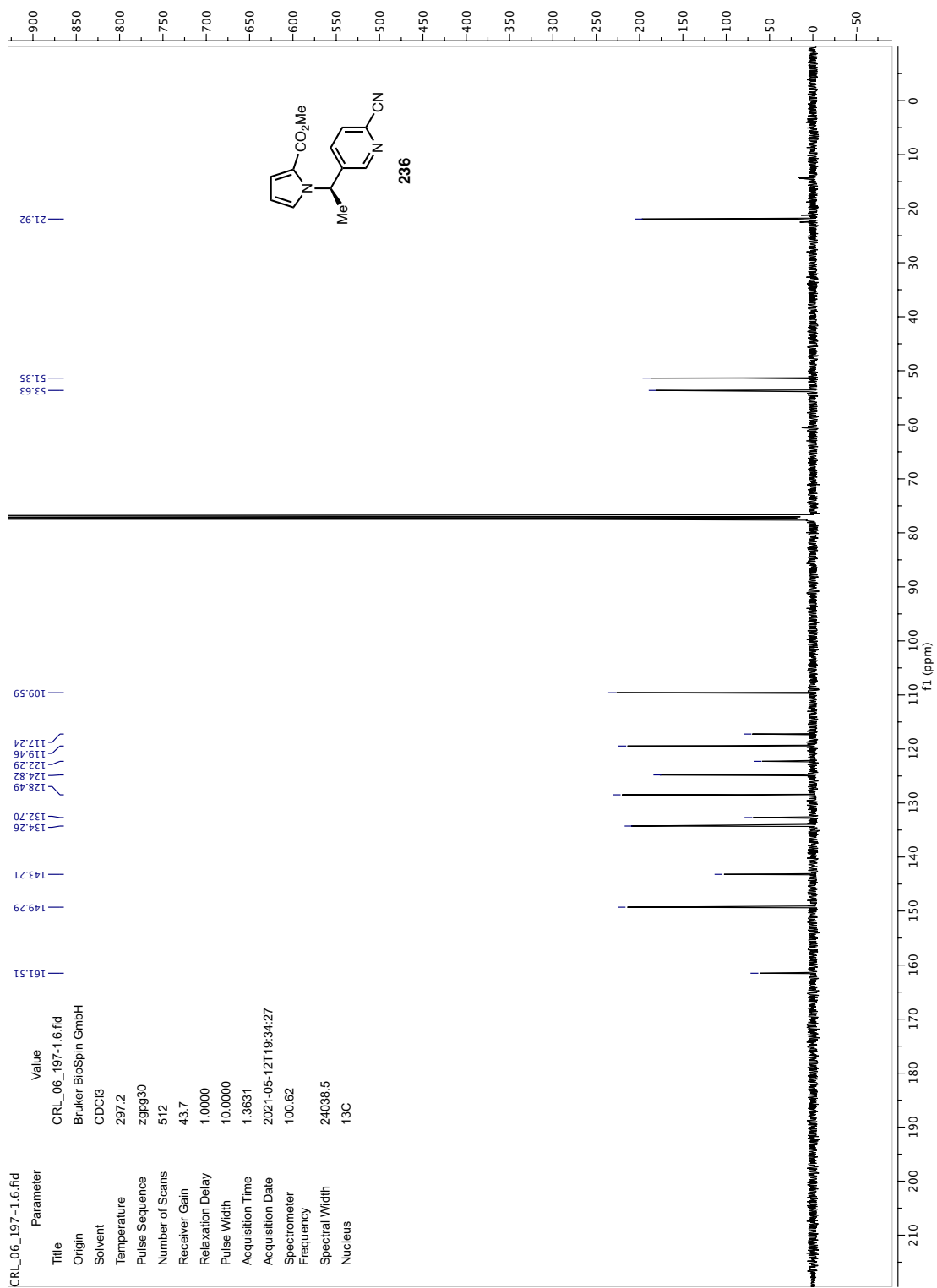








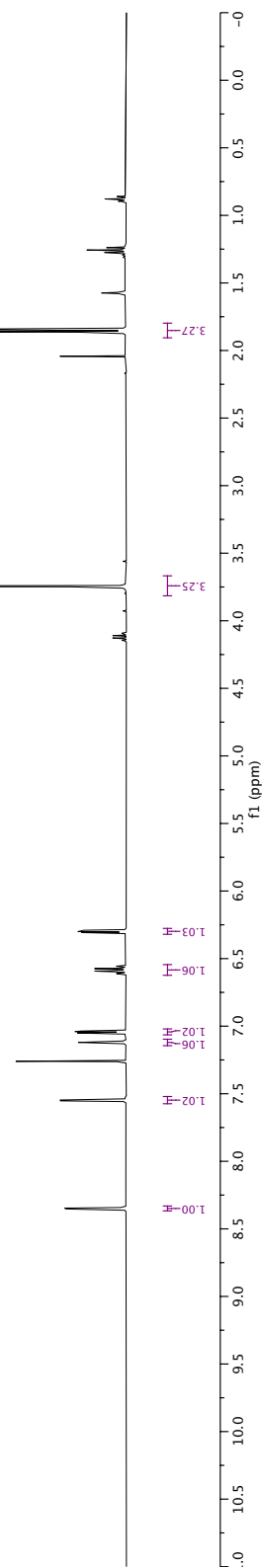
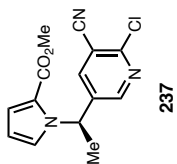


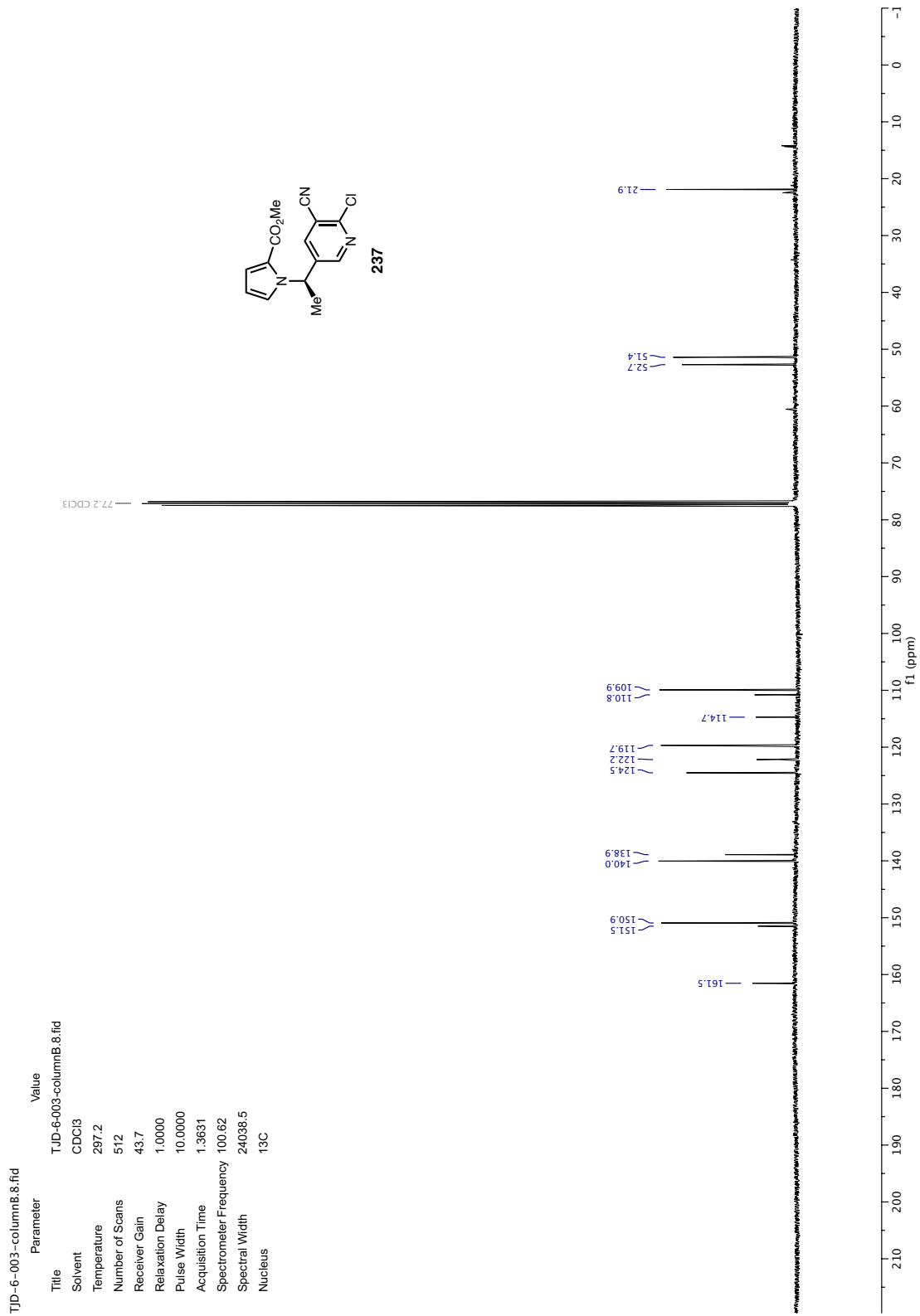


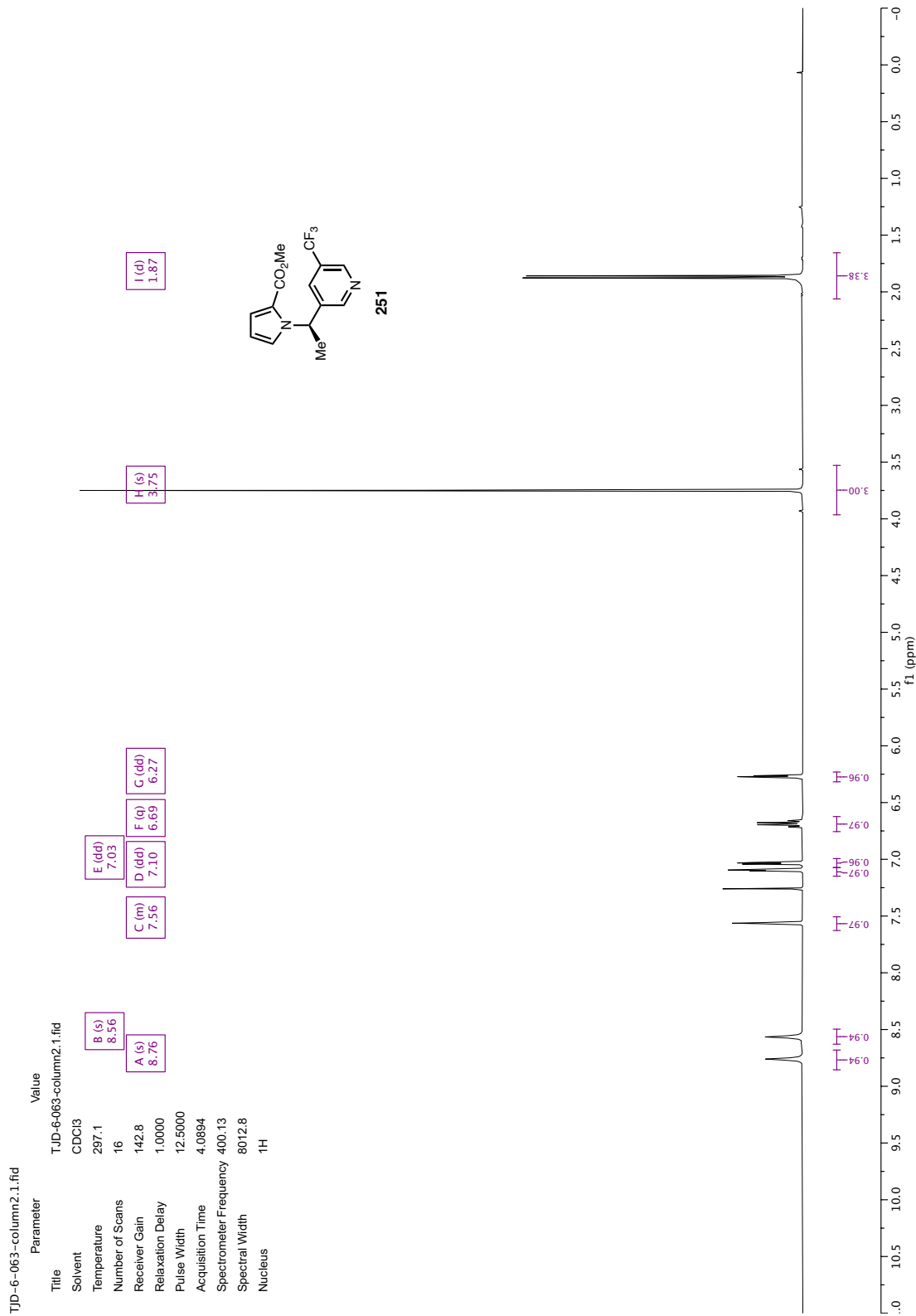
TJD-6-003-column8.7.fid

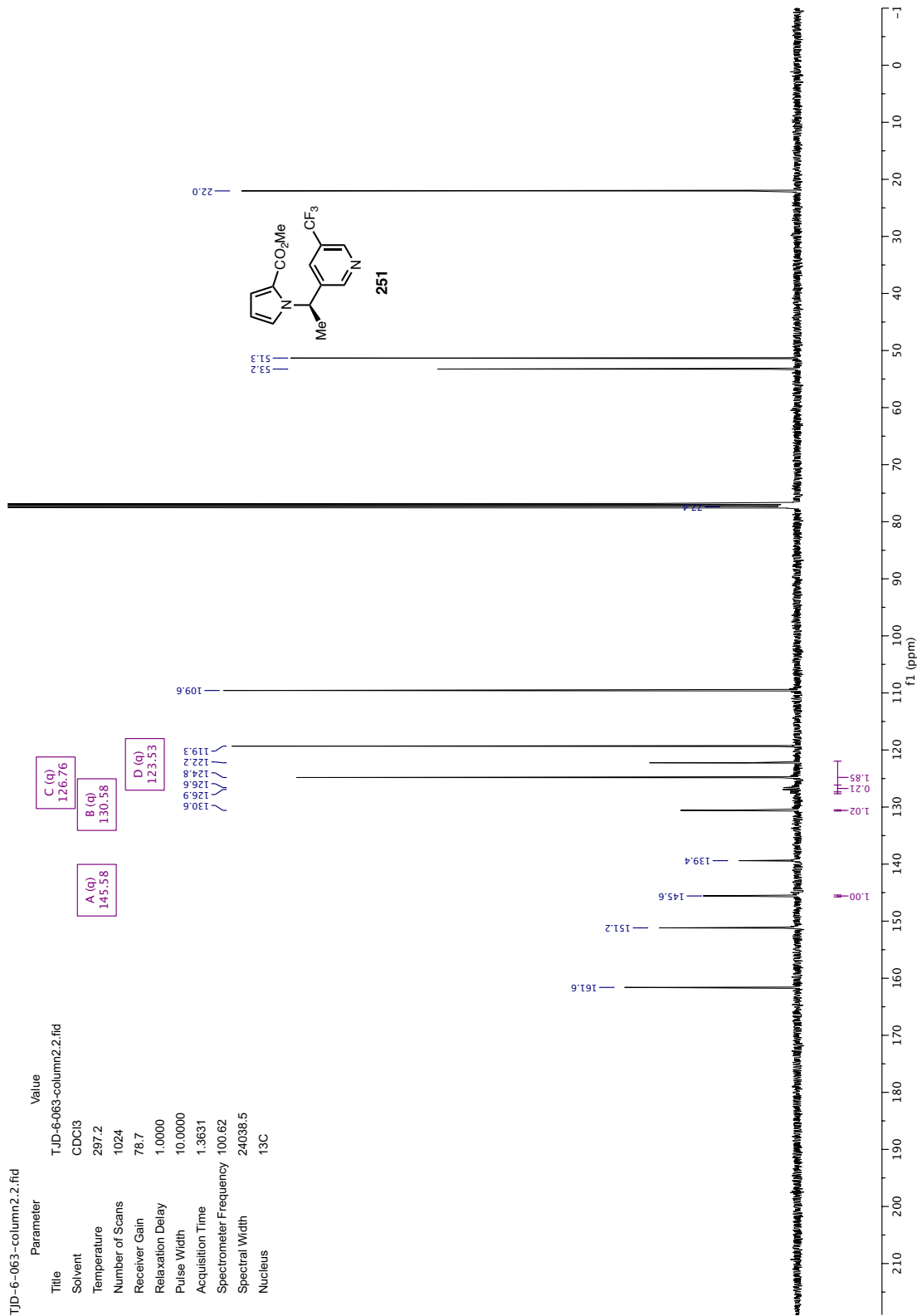
Parameter	Value
Title	TJD-6-003-column8.7.fid
Origin	Bruker BioSpin GmbH
Solvent	CDCl3
Temperature	297.1
Pulse Sequence	zg30
Number of Scans	16
Receiver Gain	197.4
Relaxation Delay	1.0000
Pulse Width	12.5000
Acquisition Time	4.0894
Acquisition Date	2021-05-13T11:36:17
Spectrometer	400.13
Spectral Width	8012.8
Nucleus	<sup>1</sup> H

A (dd)	8.55
B (dd)	7.55
C (dd)	7.12
D (dd)	7.04
E (q)	6.58
F (dd)	6.30
G (s)	3.75
H (d)	1.85

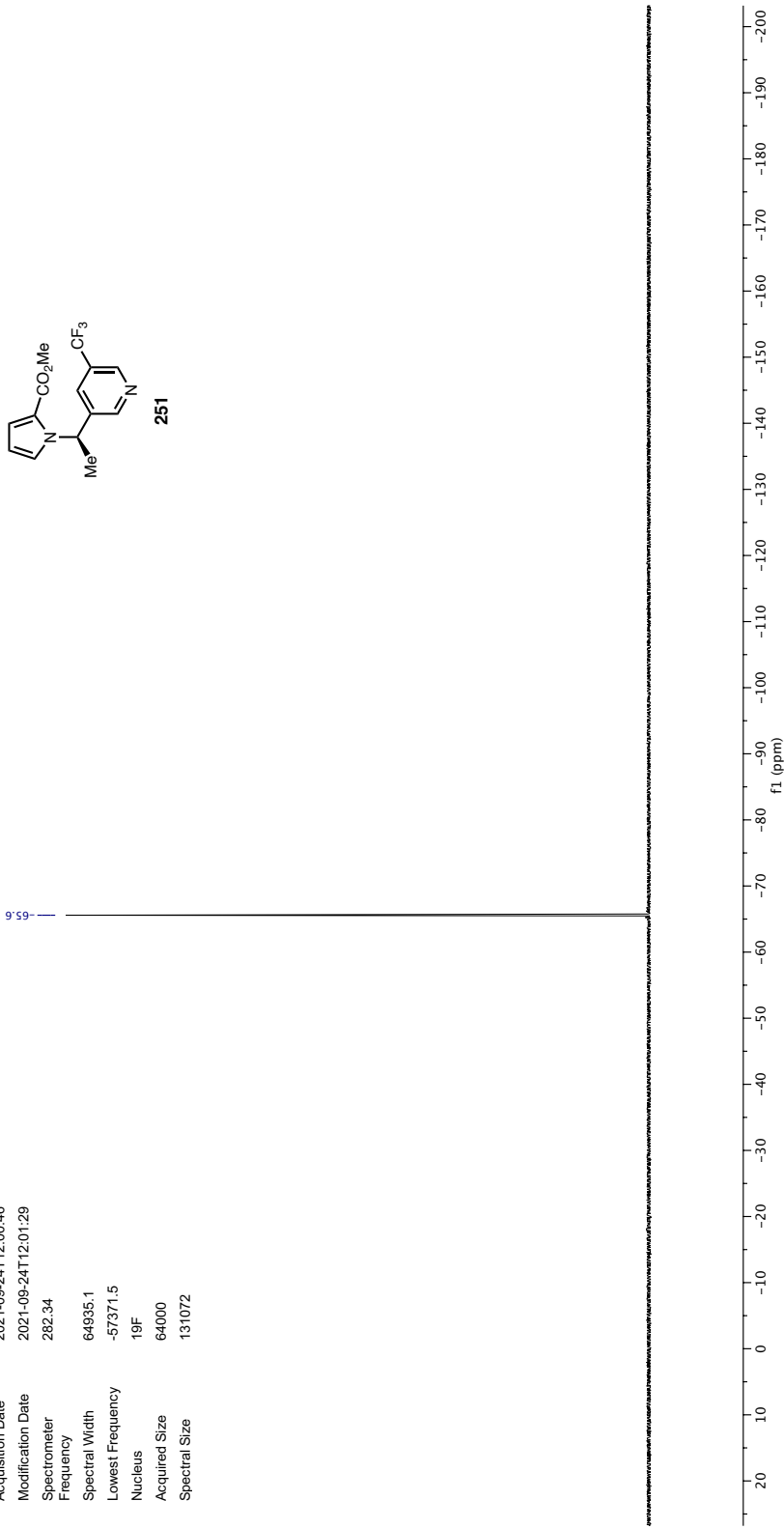
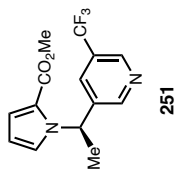


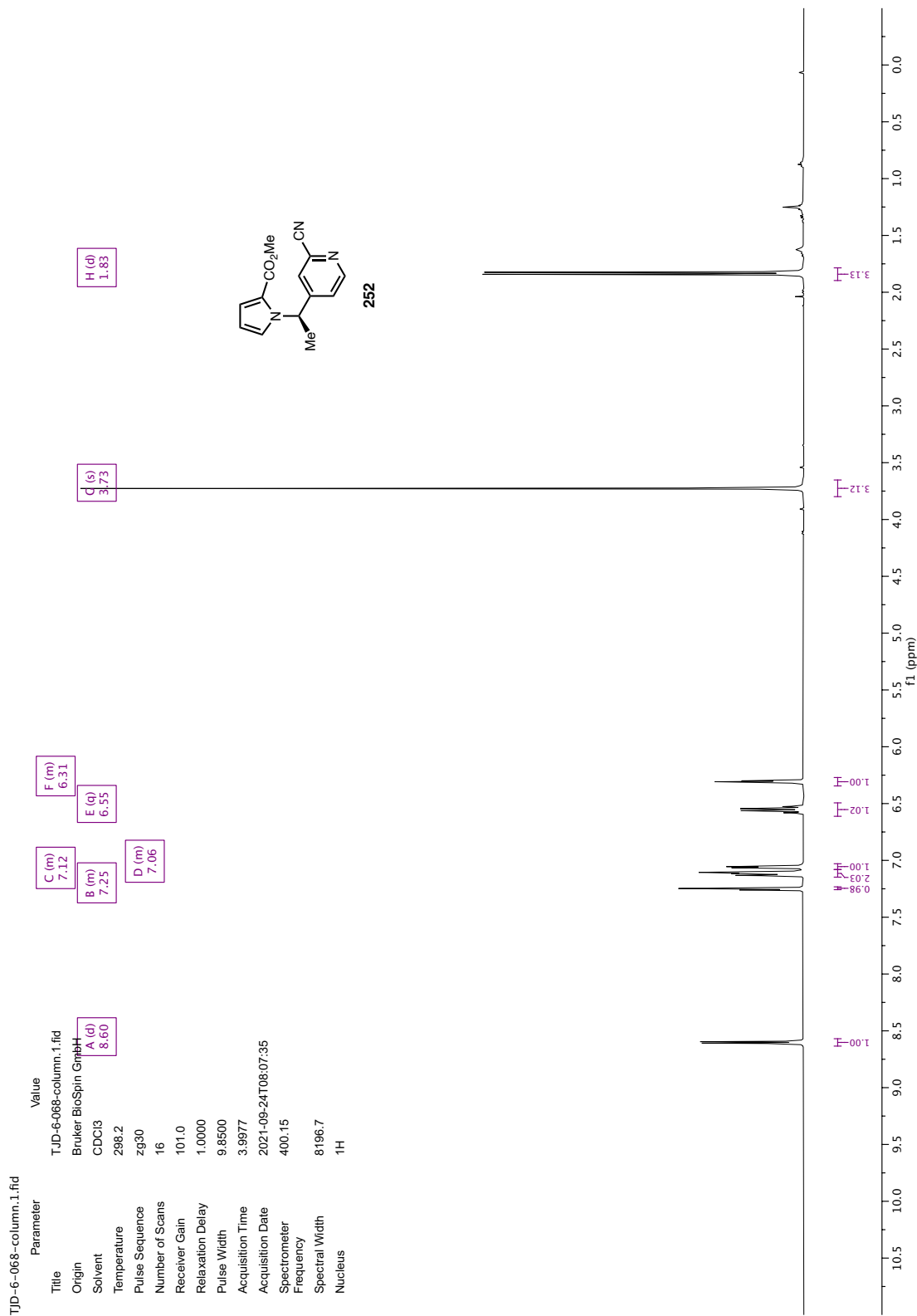




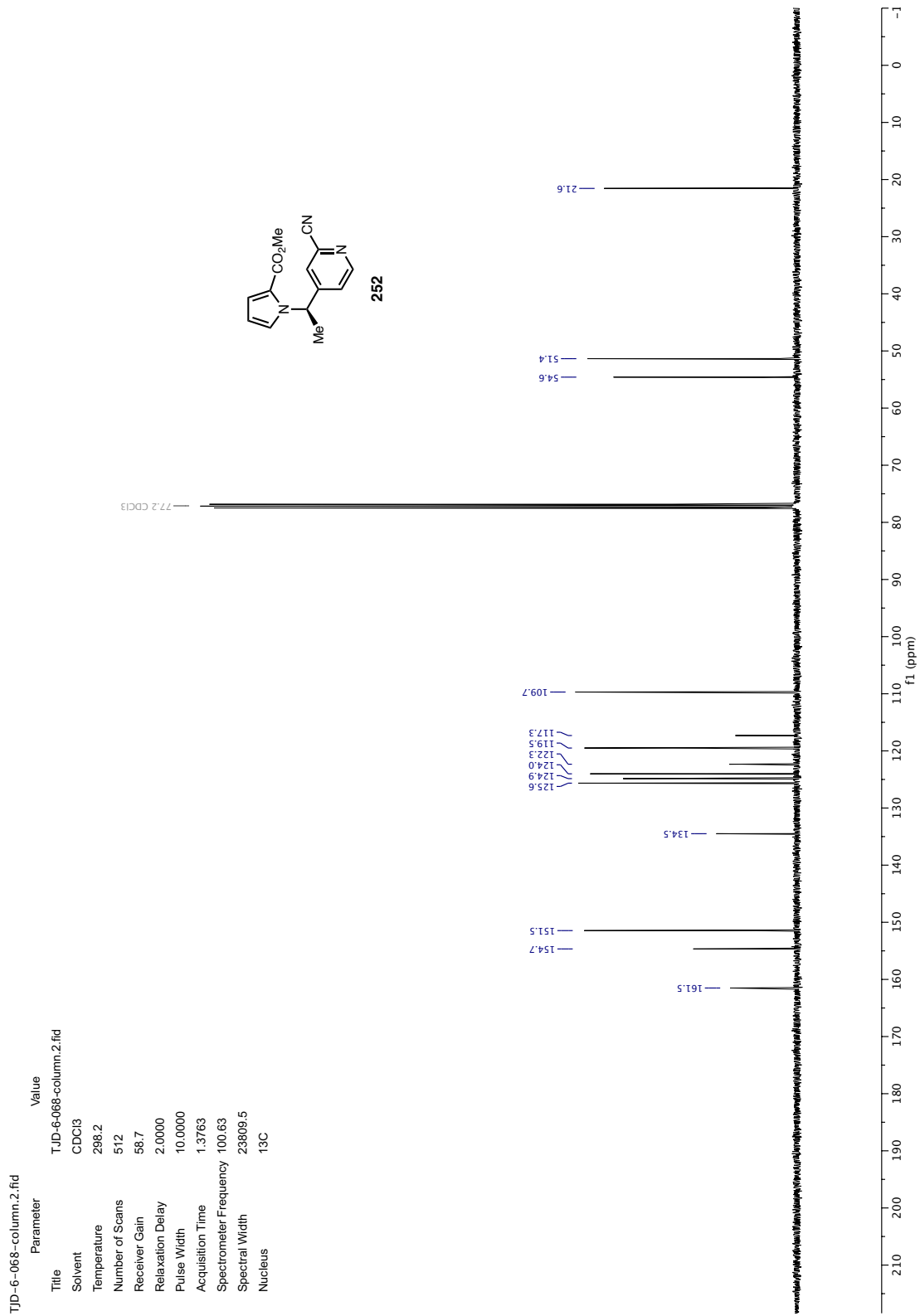


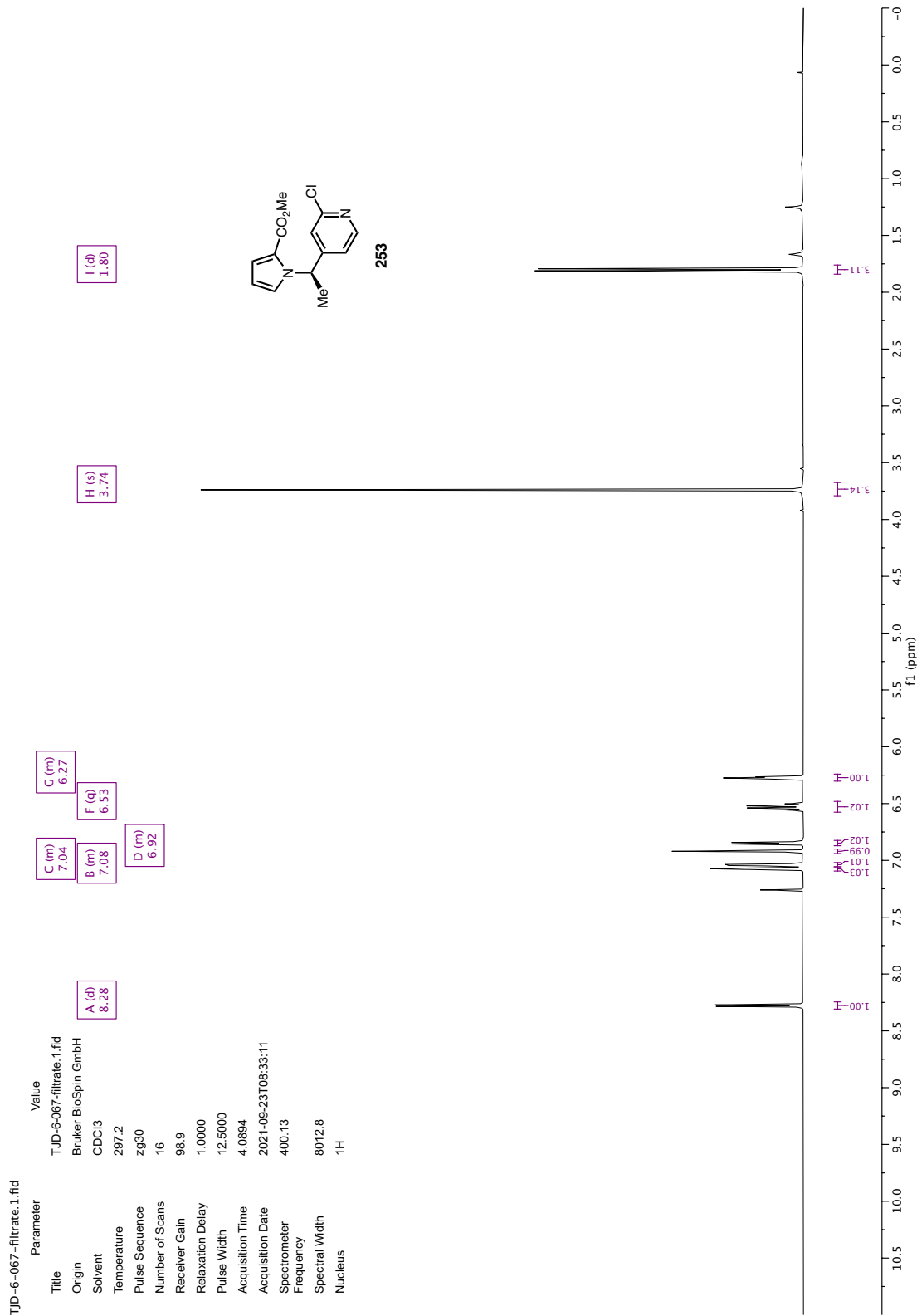
FLUORINE01 TJD-6-06-3-Parameter	Title	Value
	FLUORINE01	
	Solvent	cdcl3
	Temperature	25.0
	Pulse Sequence	s2pul
	Number of Scans	16
	Receiver Gain	30
	Relaxation Delay	1.0000
	Pulse Width	6.3333
	Acquisition Time	0.9856
	Acquisition Date	2021-09-24T12:00:46
	Modification Date	2021-09-24T12:01:29
	Spectrometer	282.34
	Spectral Width	64935.1
	Lowest Frequency	-57371.5
	Nucleus	19F
	Acquired Size	64000
	Spectral Size	131072

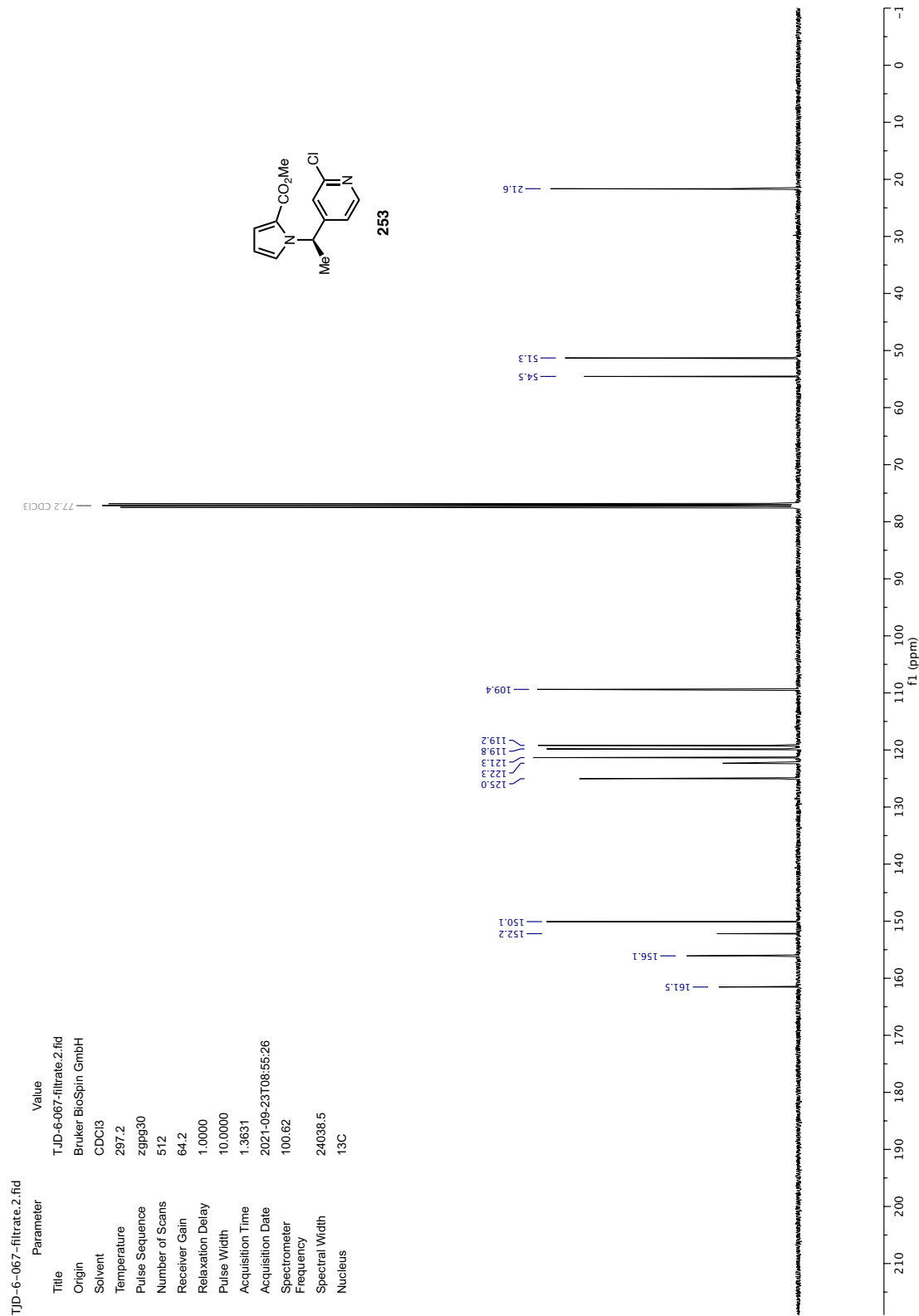


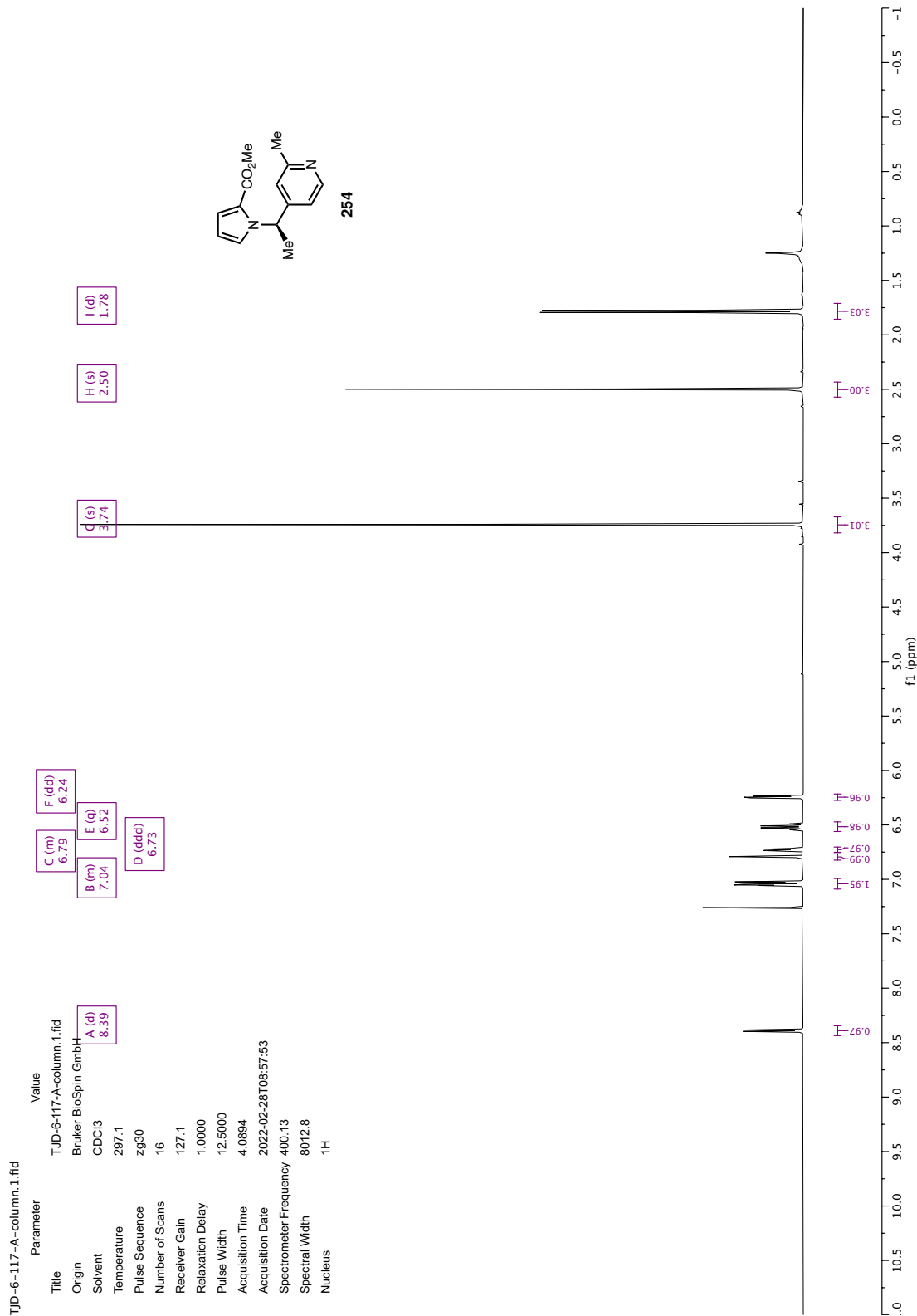


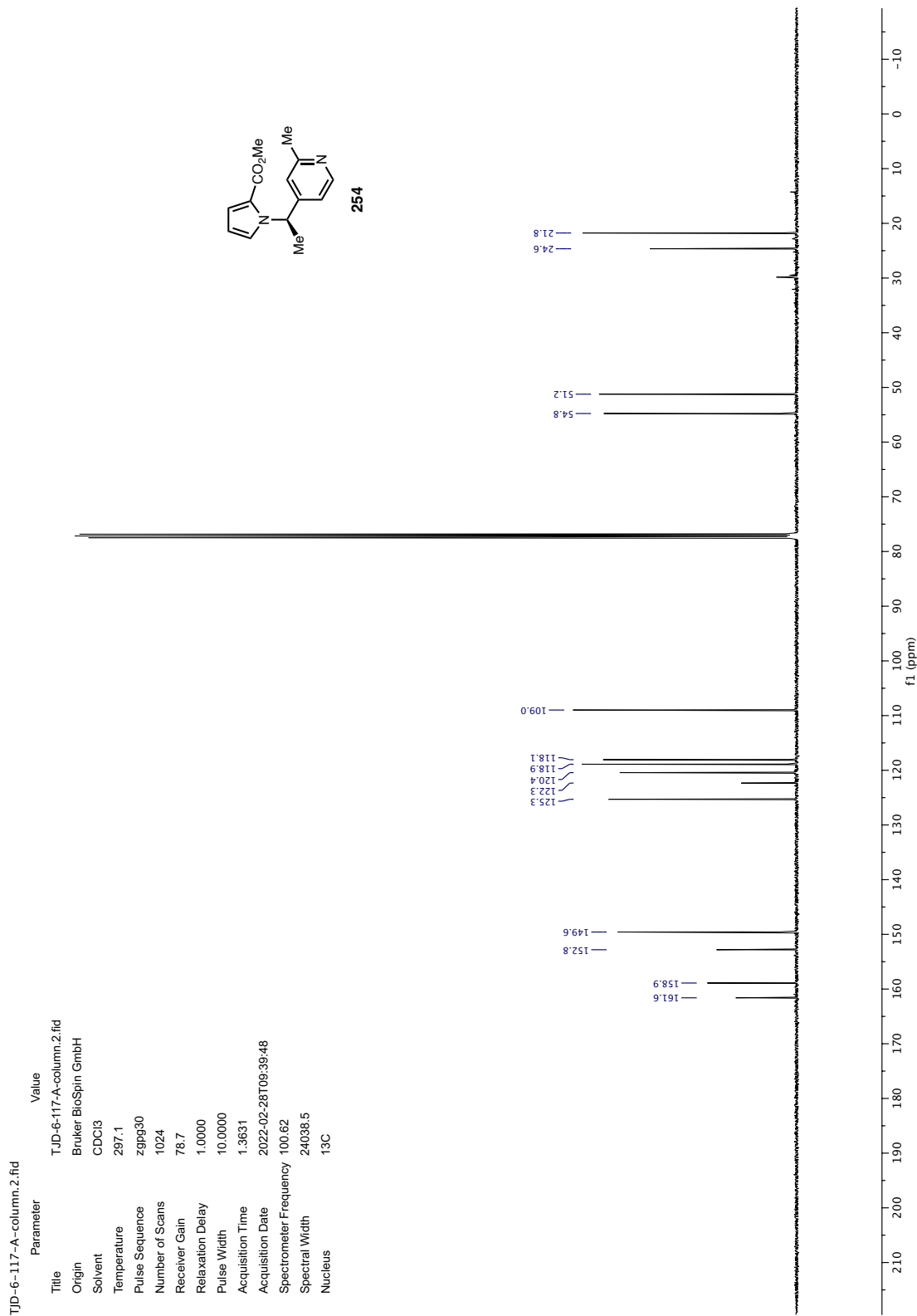








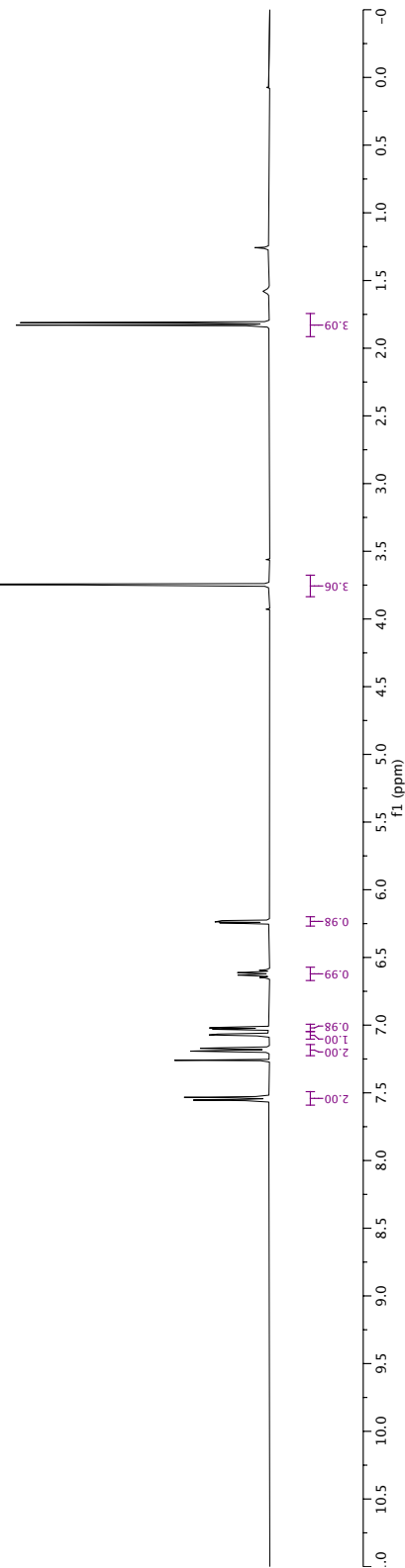
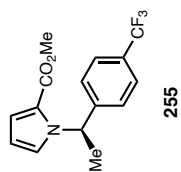


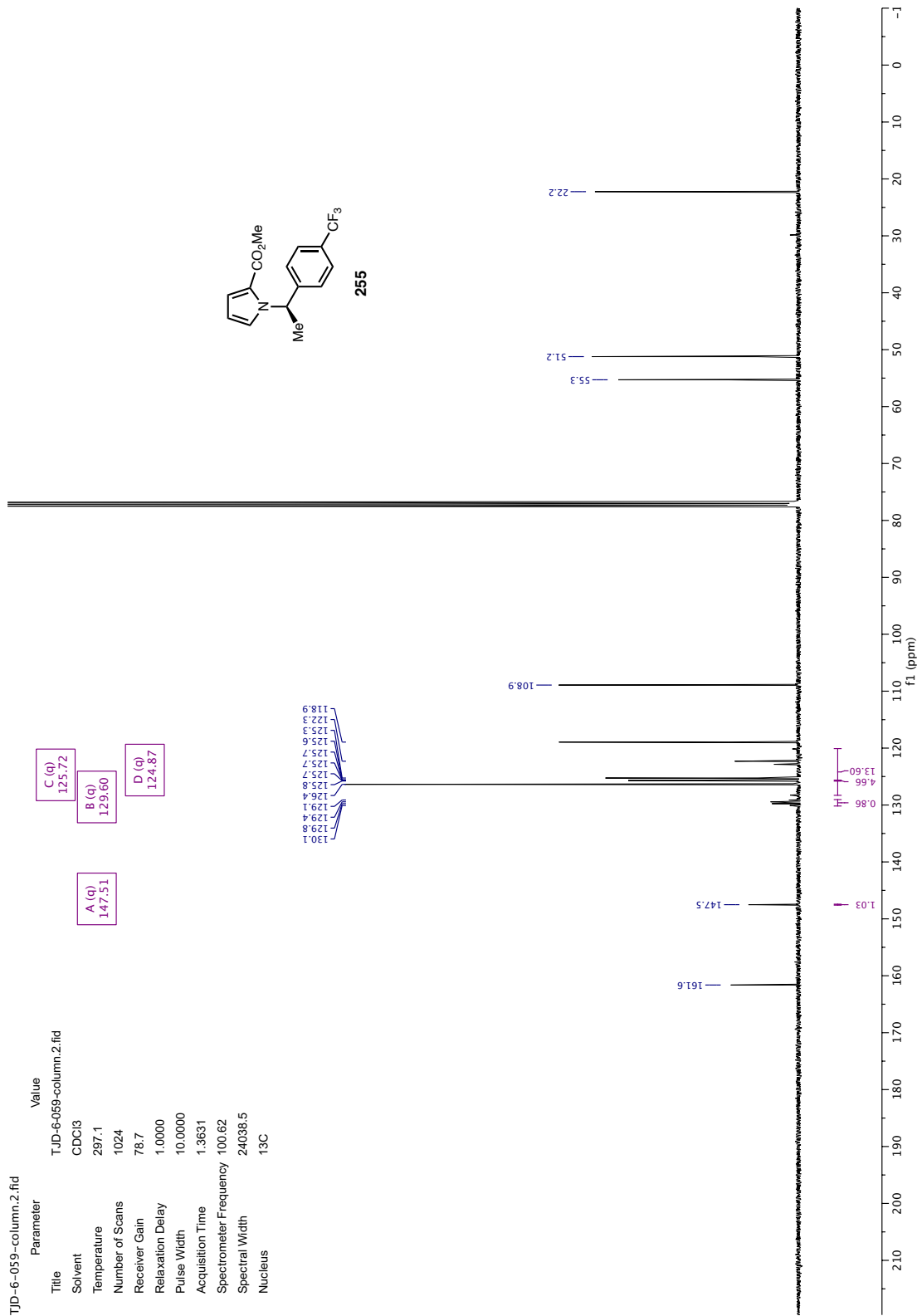


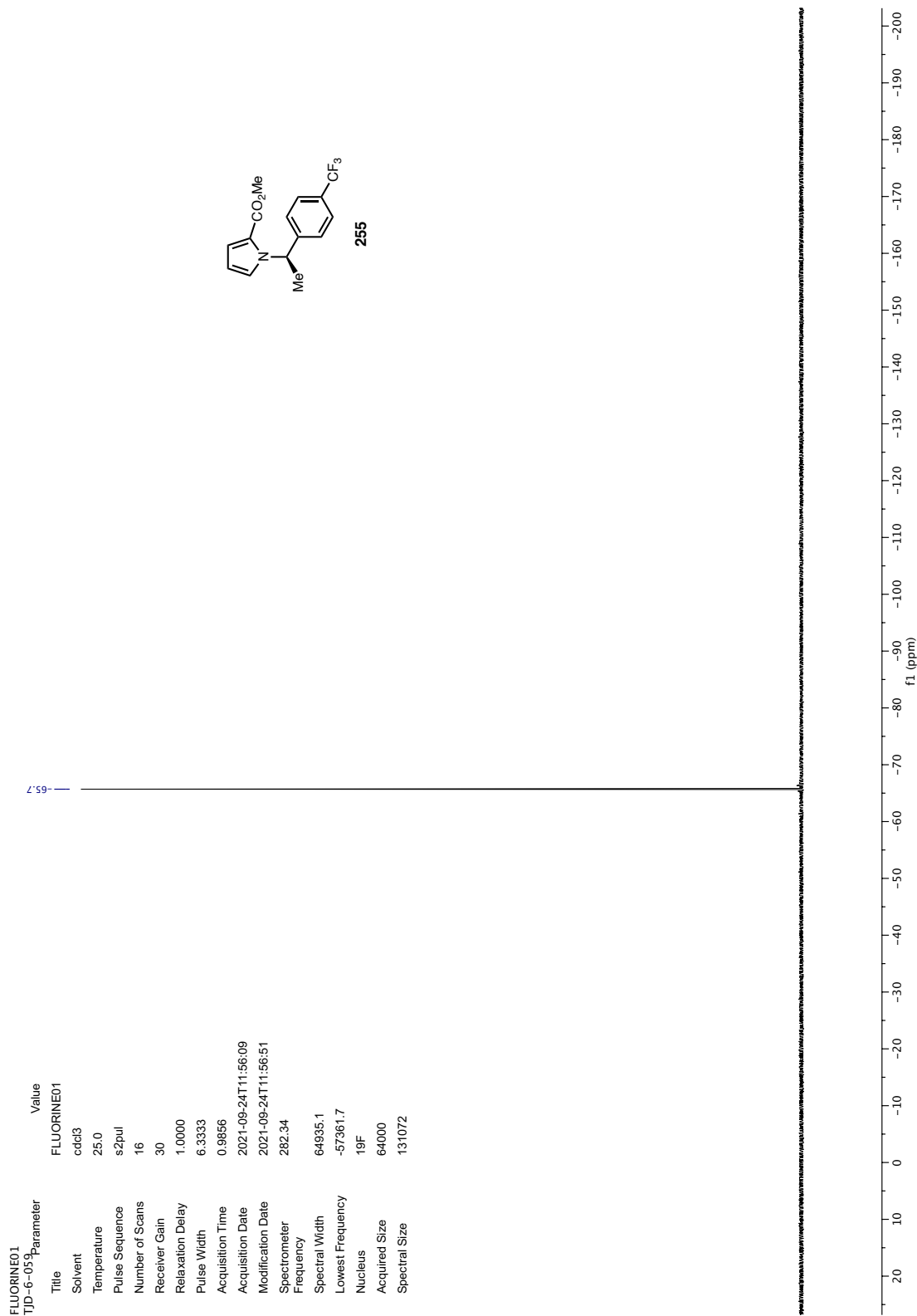
TJD-6-059-column.1.fid

Parameter	Value
Title	TJD-6-059-column.1.fid
Solvent	CDCl3
Temperature	297.2
Number of Scans	16
Receiver Gain	156.2
Relaxation Delay	1.0000
Pulse Width	12.5000
Acquisition Time	4.0894
Spectrometer Frequency	400.13
Spectral Width	8012.8
Nucleus	1H

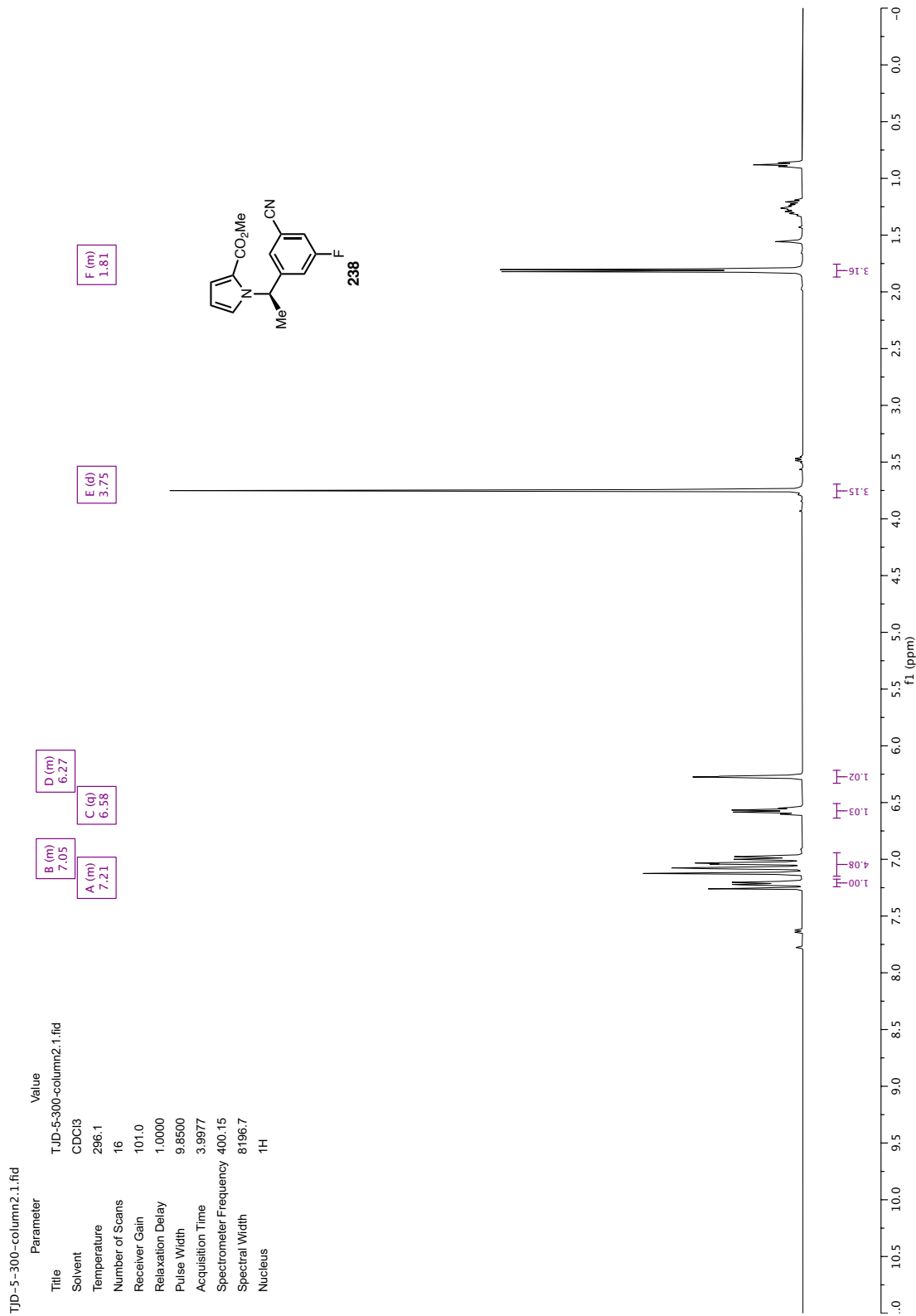
A (m)	7.54	B (m)	7.18	C (dd)	7.07
E (d)	6.62	F (dd)	6.24	G (s)	3.75
H (d)	1.82				

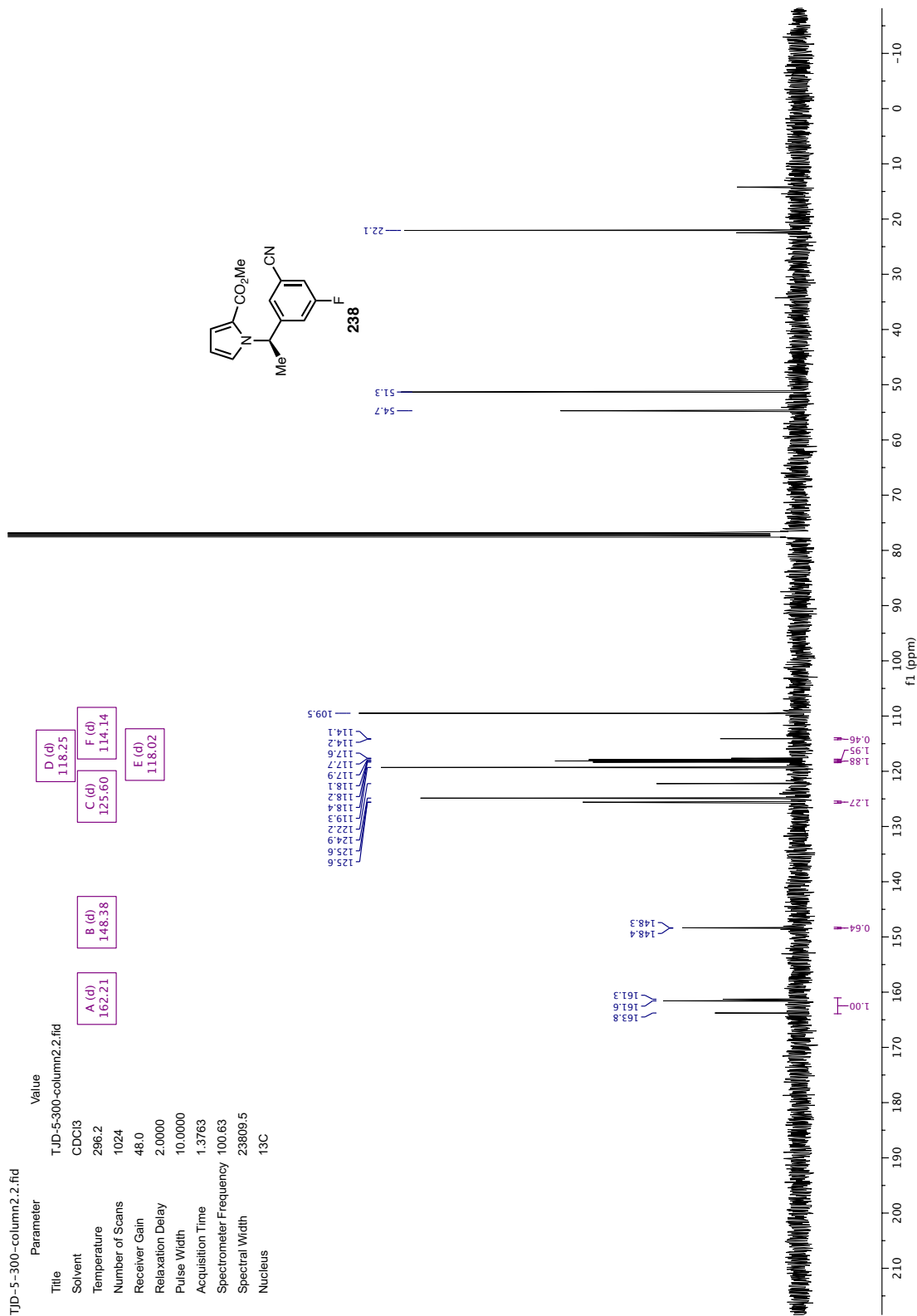






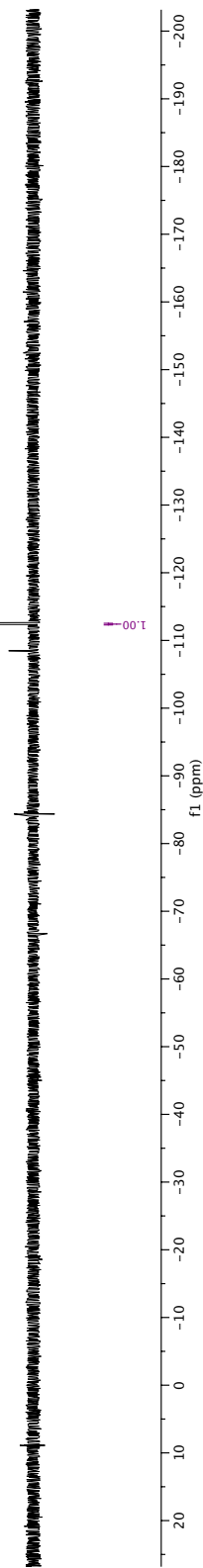
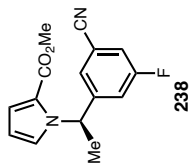


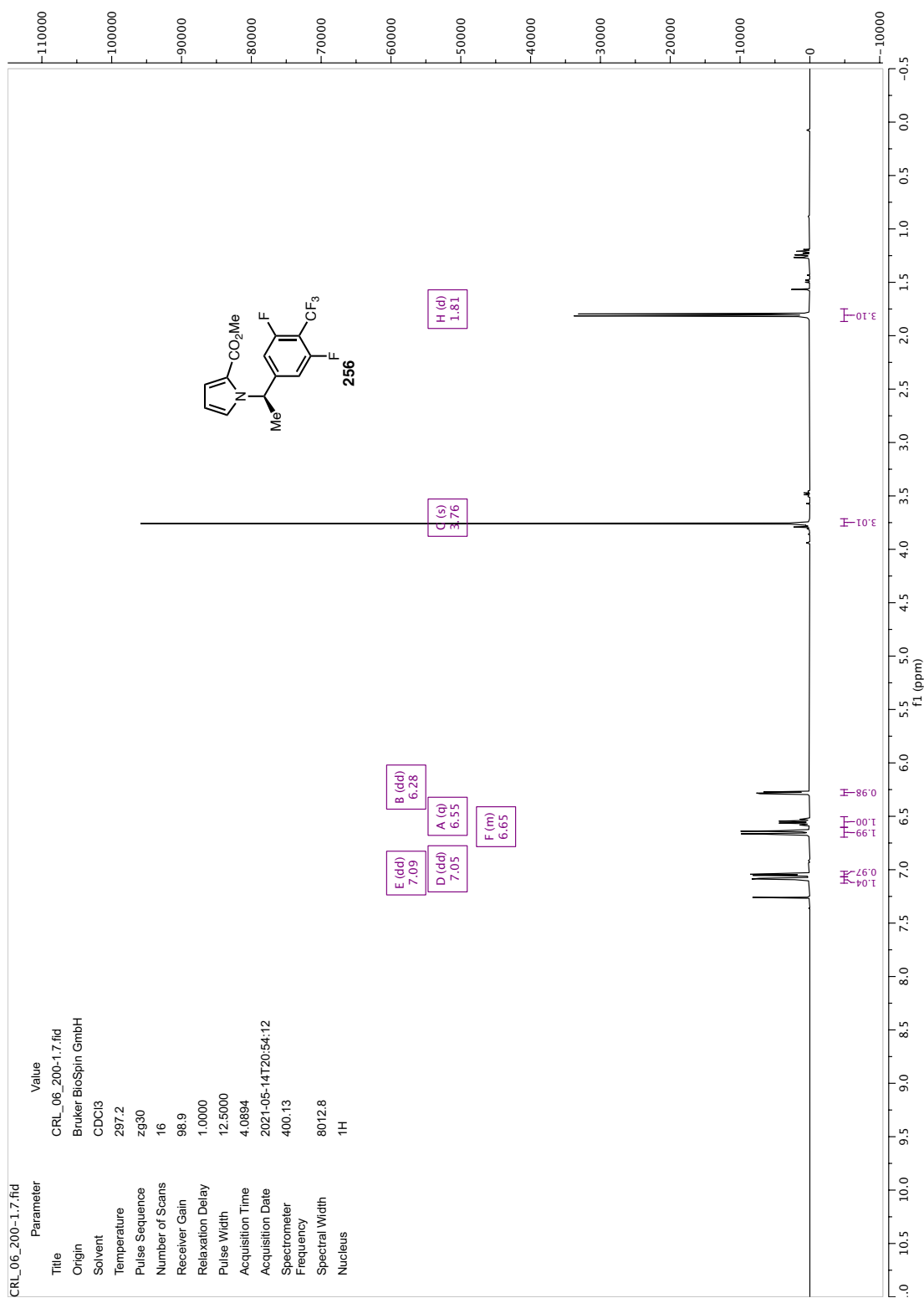


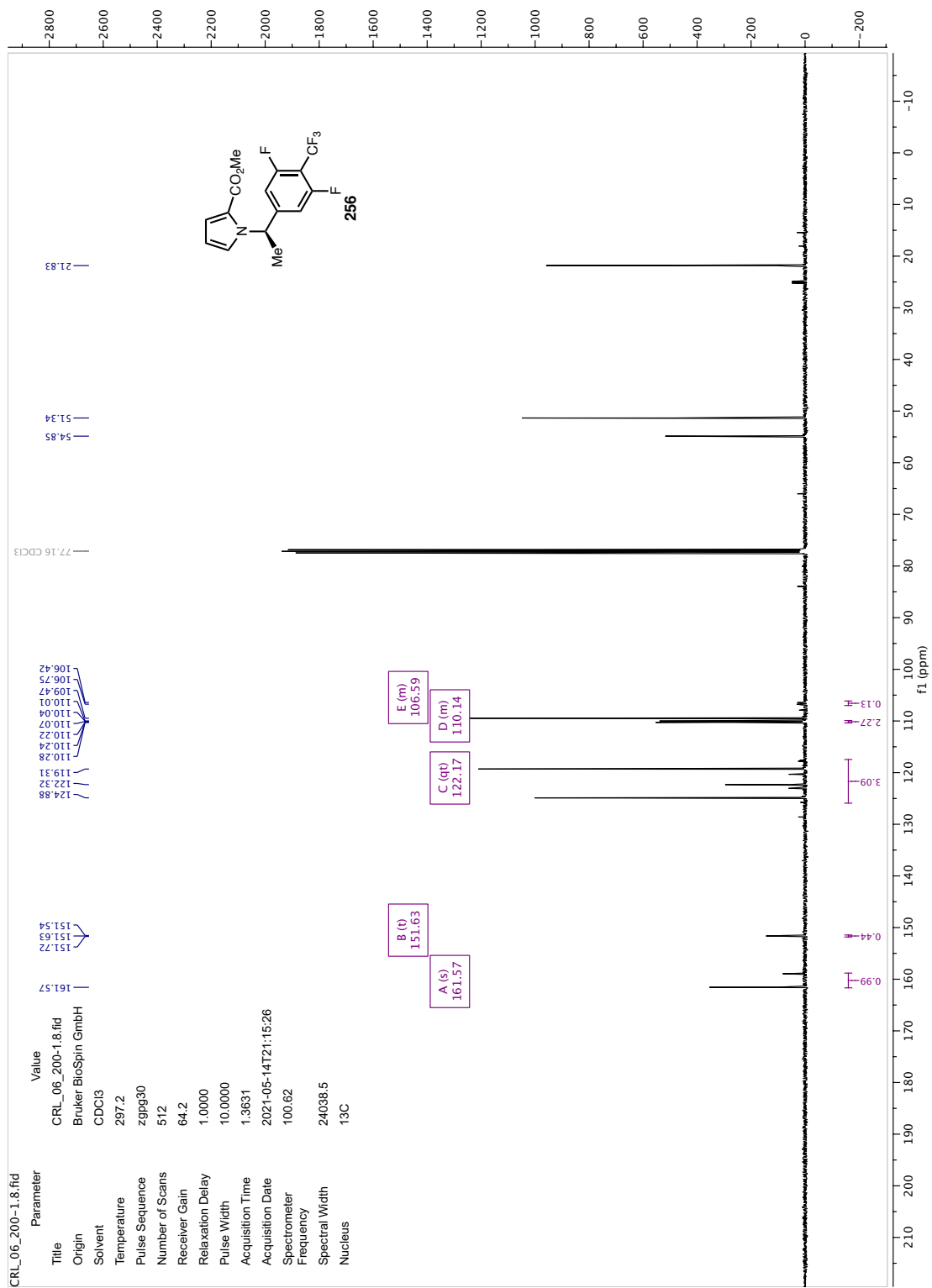


FLUORINE01 TJD-5-30 Parameter	Value
Title	FLUORINE01
Solvent	cdd3
Temperature	25.0
Pulse Sequence	s2pul
Number of Scans	16
Receiver Gain	30
Relaxation Delay	1.0000
Pulse Width	6.3333
Acquisition Time	0.9856
Acquisition Date	2021-06-18T10:17:57
Modification Date	2021-06-18T10:18:43
Spectrometer	282.34
Frequency	64935.1
Spectral Width	-57365.1
Lowest Frequency	19F
Nucleus	64000
Acquired Size	131072
Spectral Size	

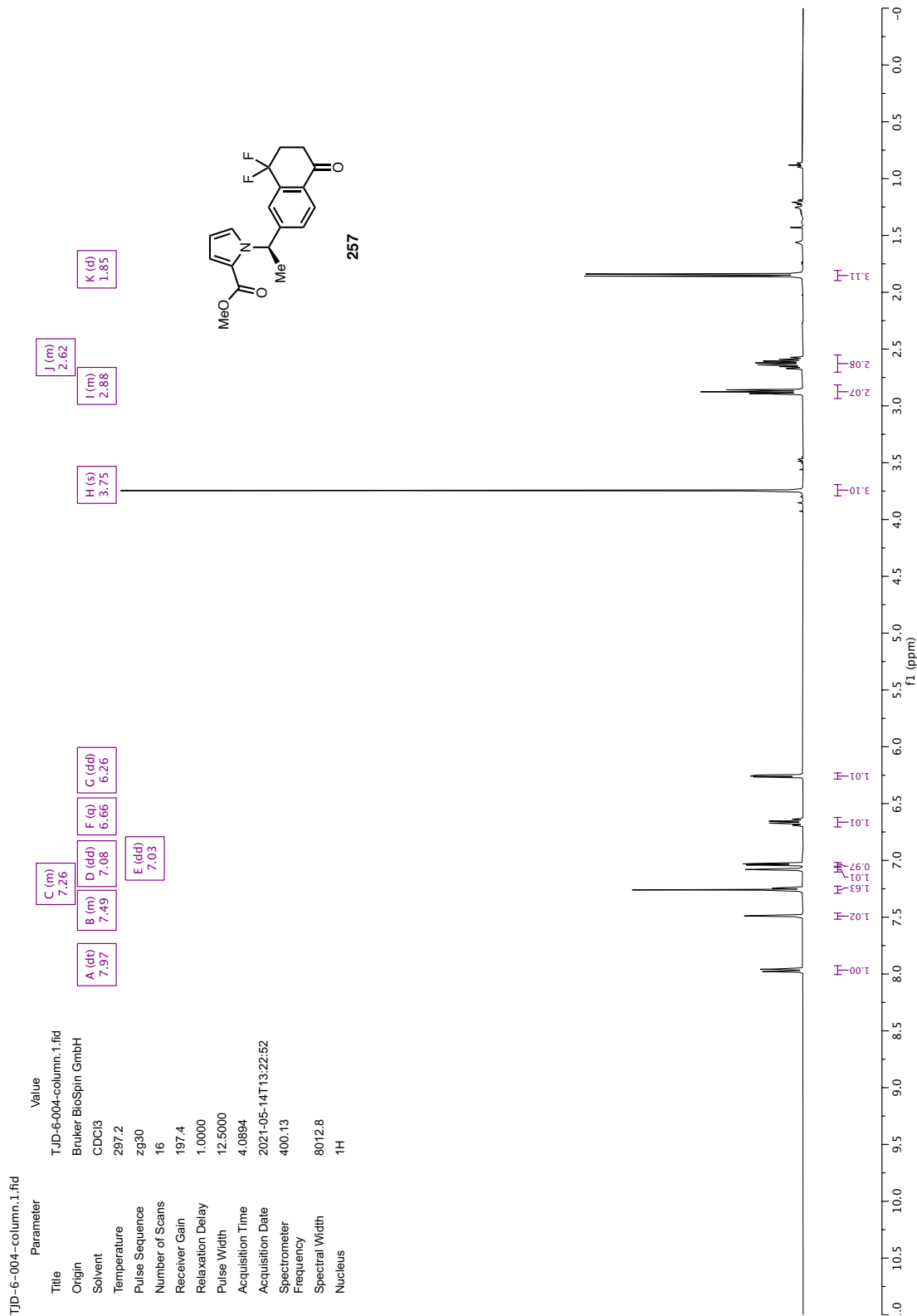
A (dd)  
-112.41

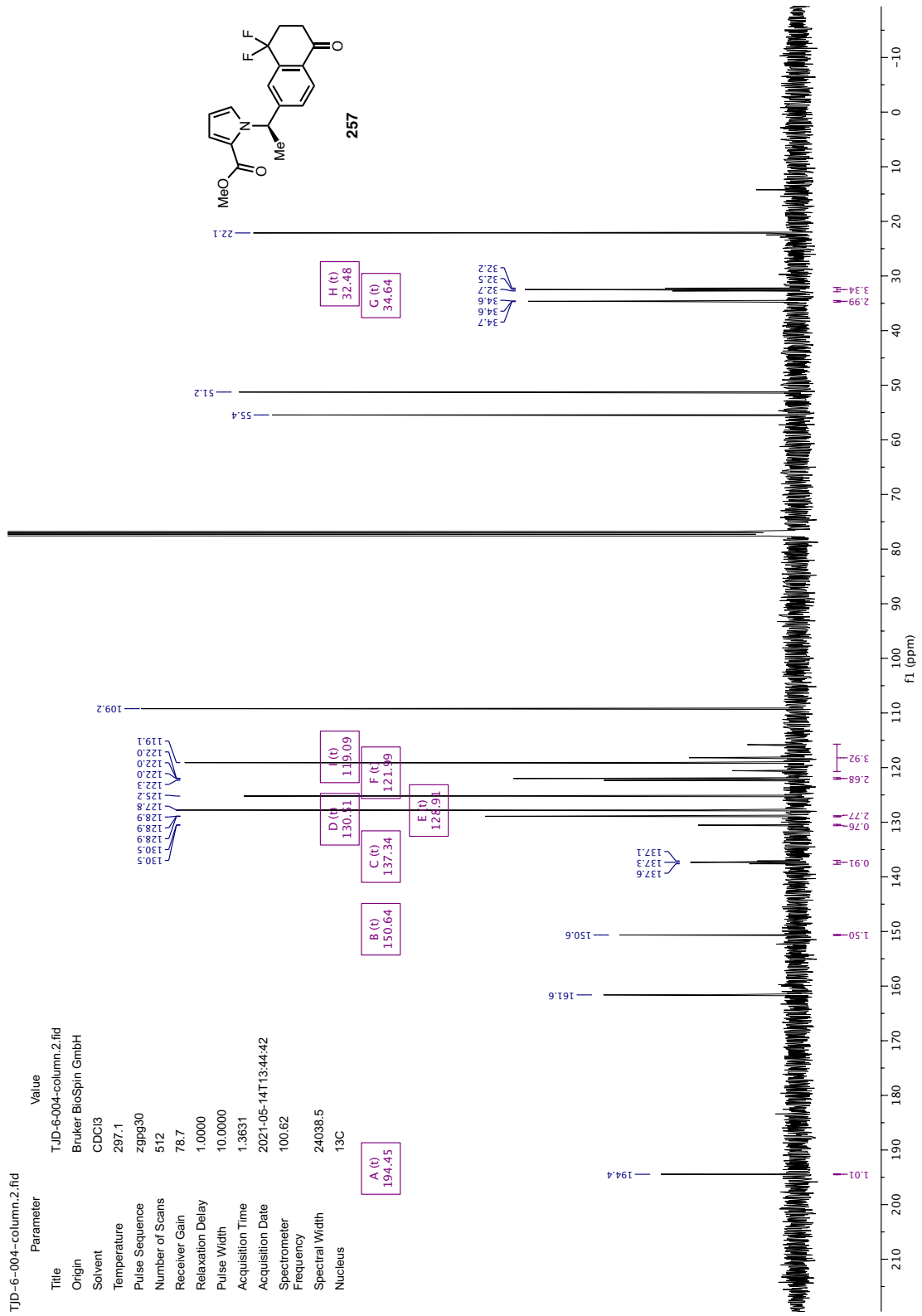








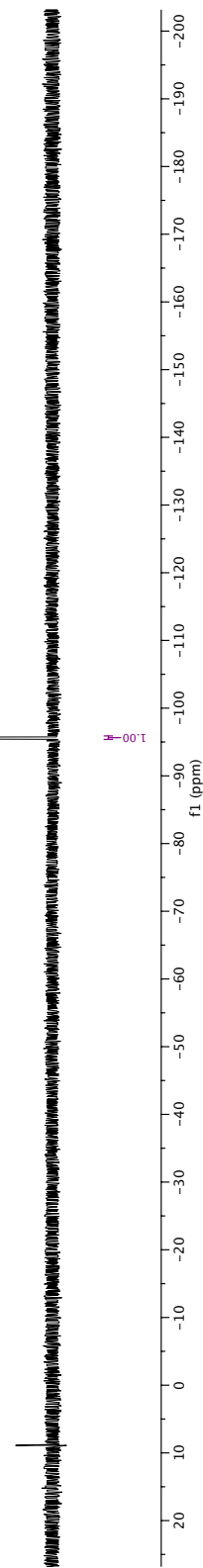
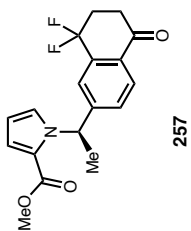


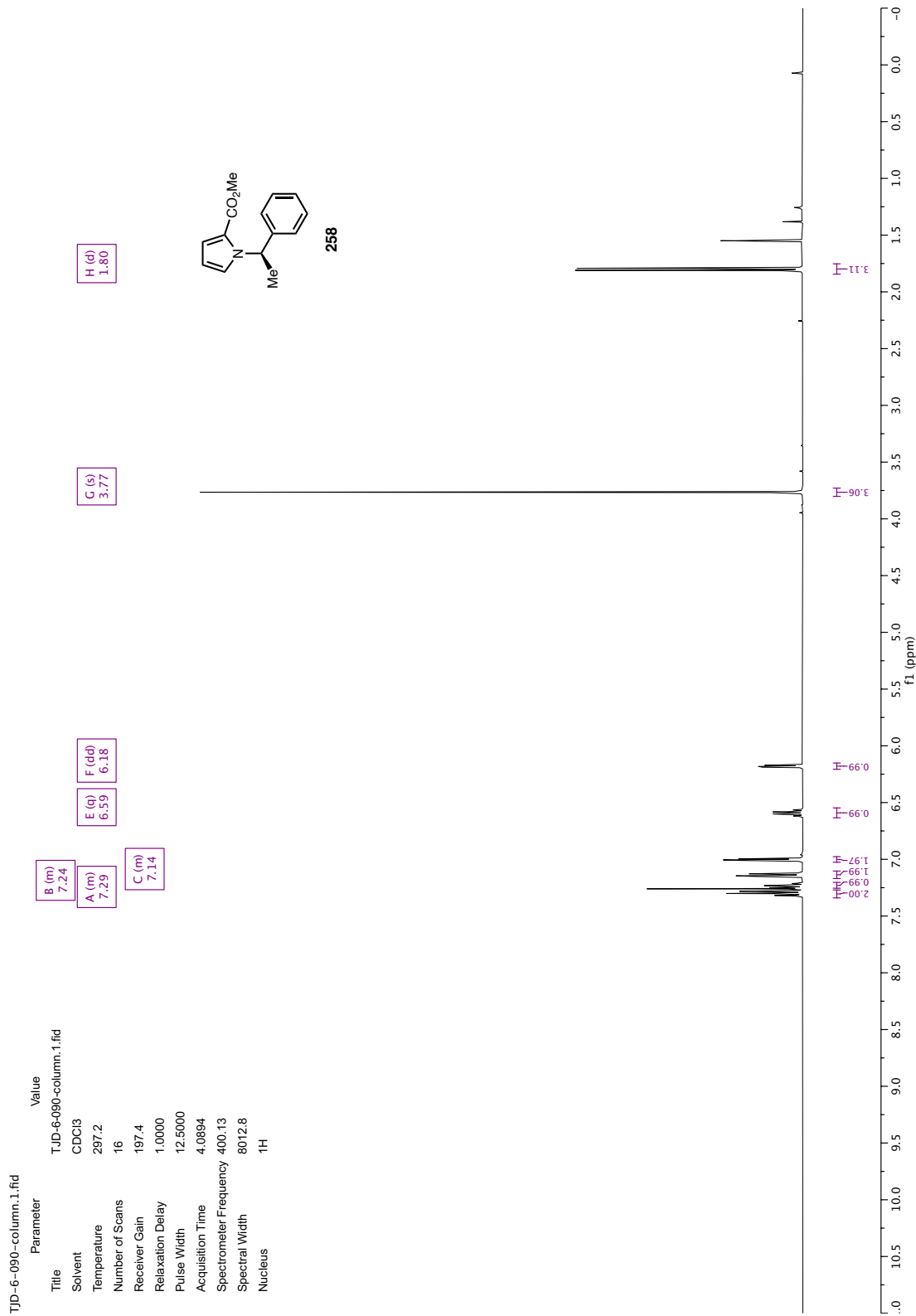


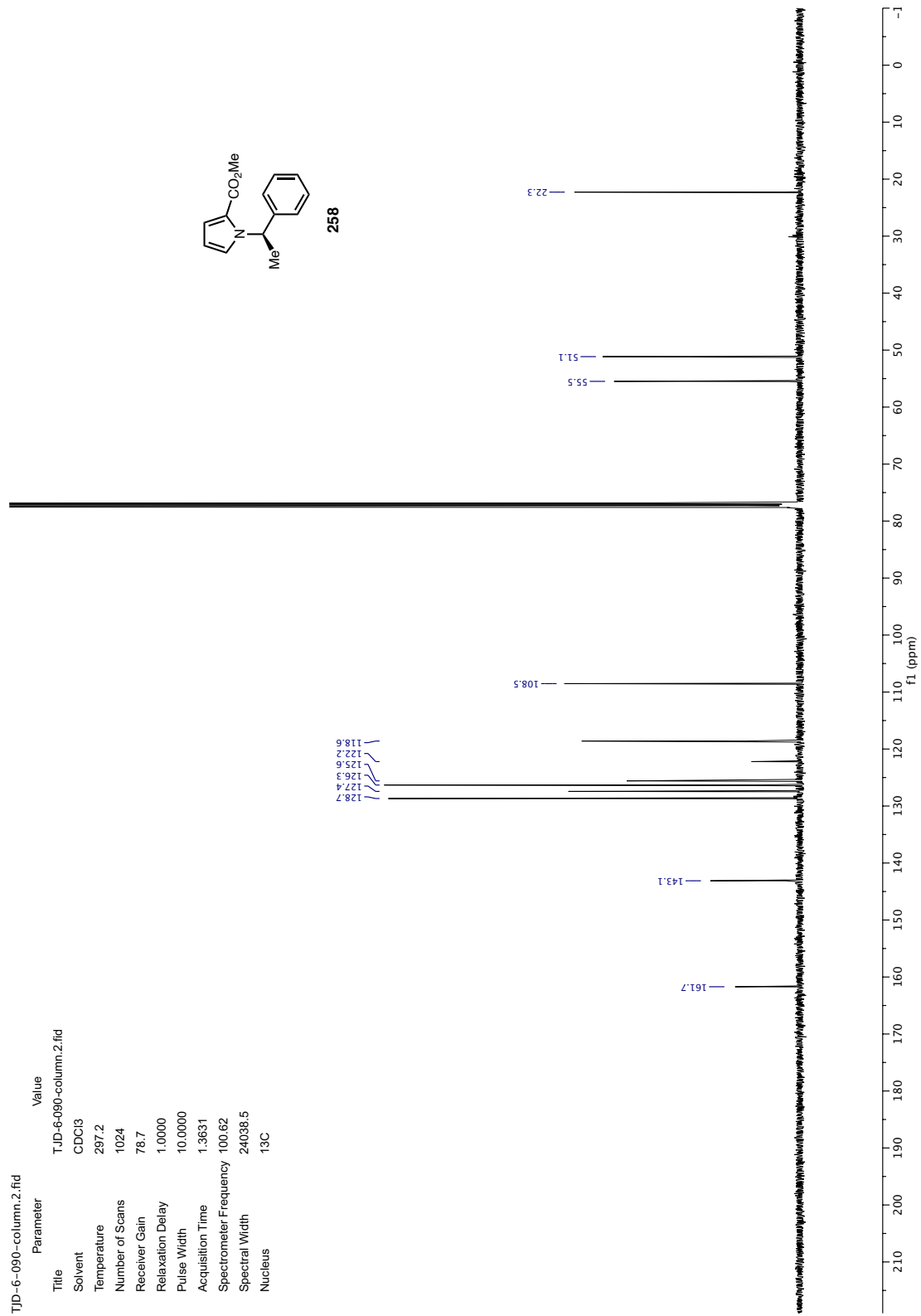


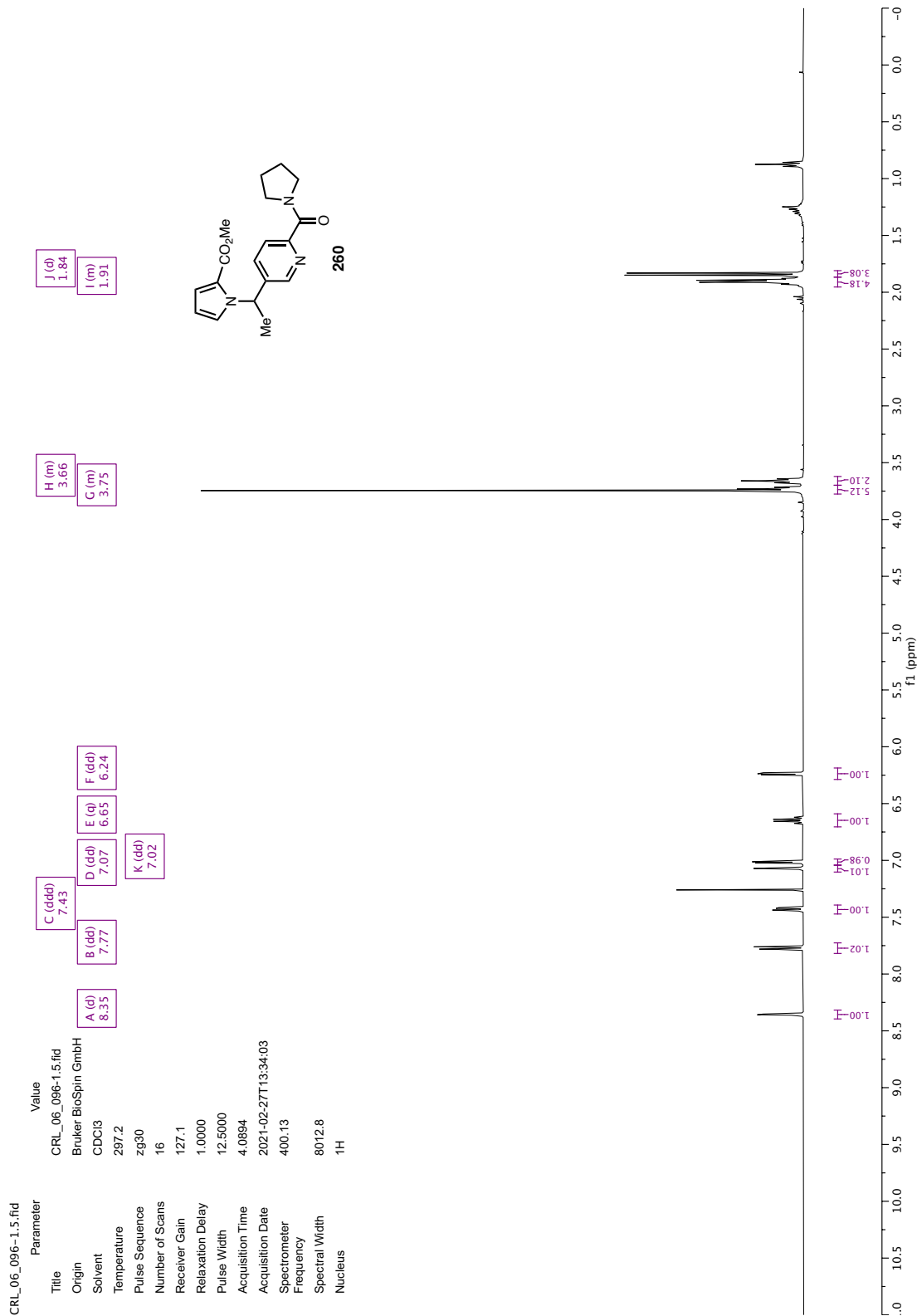
FLUORINE01	Title	Value
TJD-6-004	Parameter	FLUORINE01
	Solvent	cdcl3
	Temperature	25.0
	Pulse Sequence	s2pul
	Number of Scans	16
	Receiver Gain	30
	Relaxation Delay	1.0000
	Pulse Width	6.3333
	Acquisition Time	0.9856
	Acquisition Date	2021-06-18T10:22:07
	Modification Date	2021-06-18T10:22:49
	Spectrometer	282.34
	Spectral Width	64935.1
	Lowest Frequency	-57365.0
	Nucleus	19F
	Acquired Size	64000
	Spectral Size	131072

A (f)  
-95.60



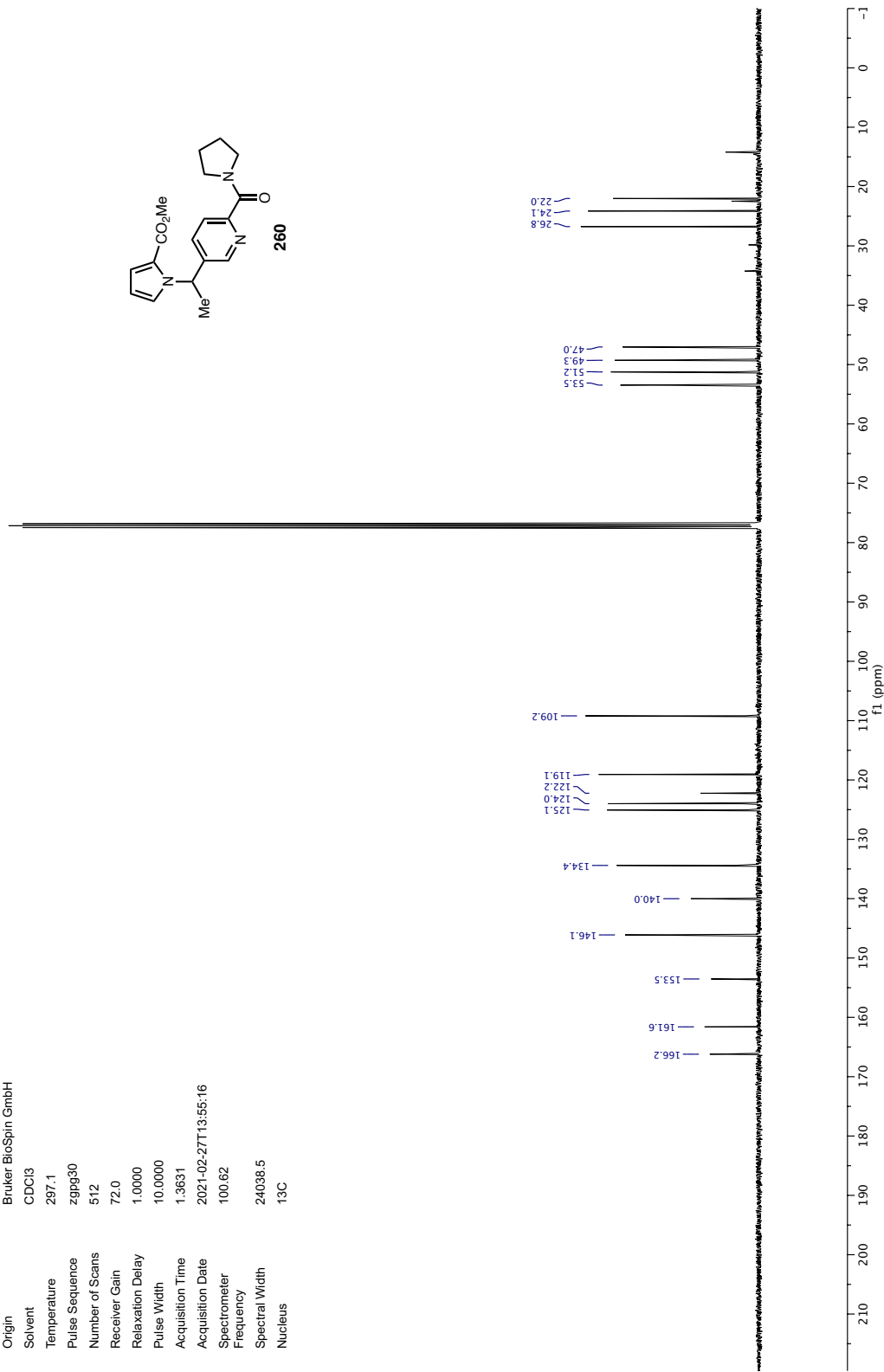
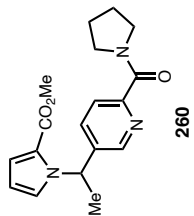


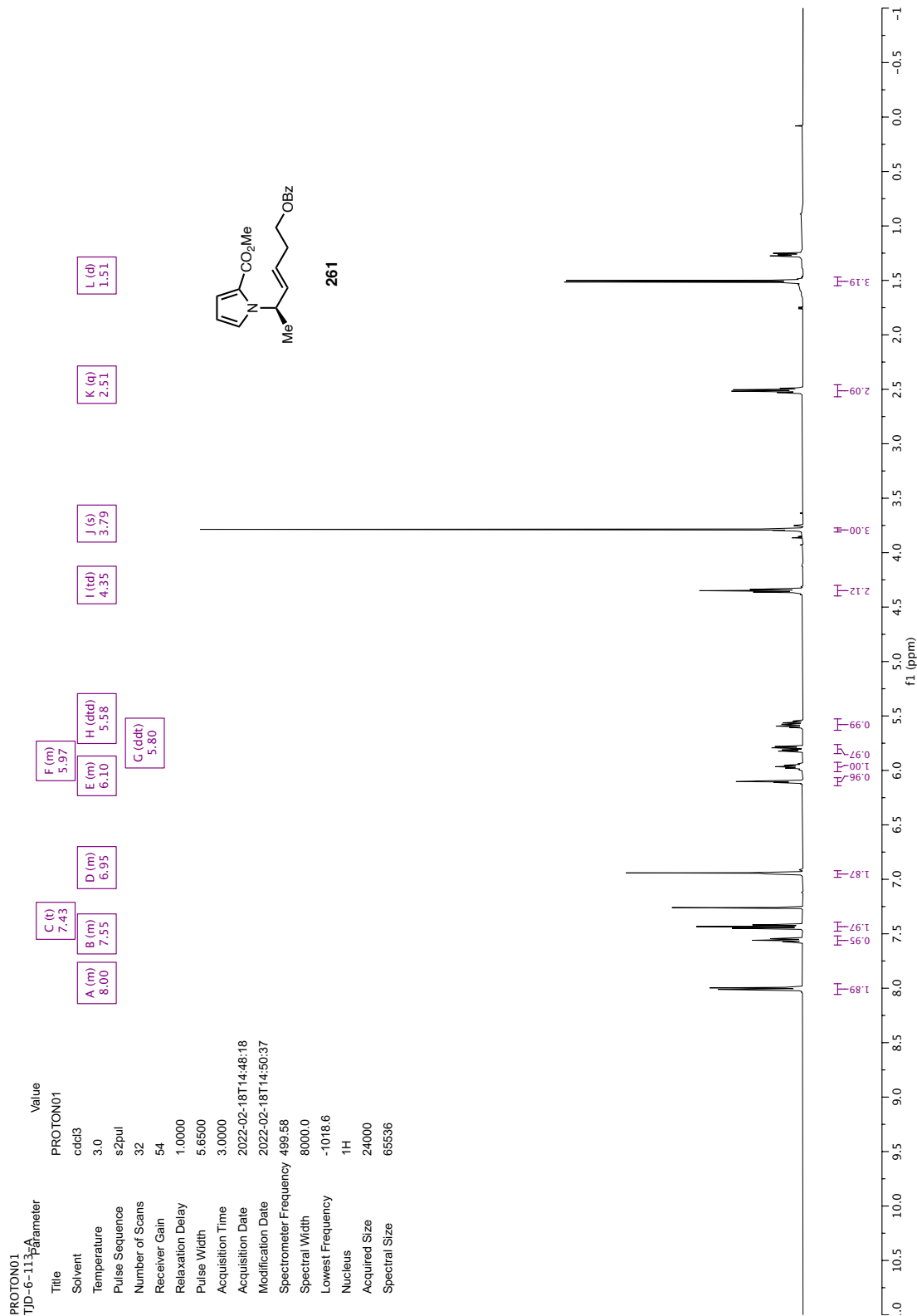


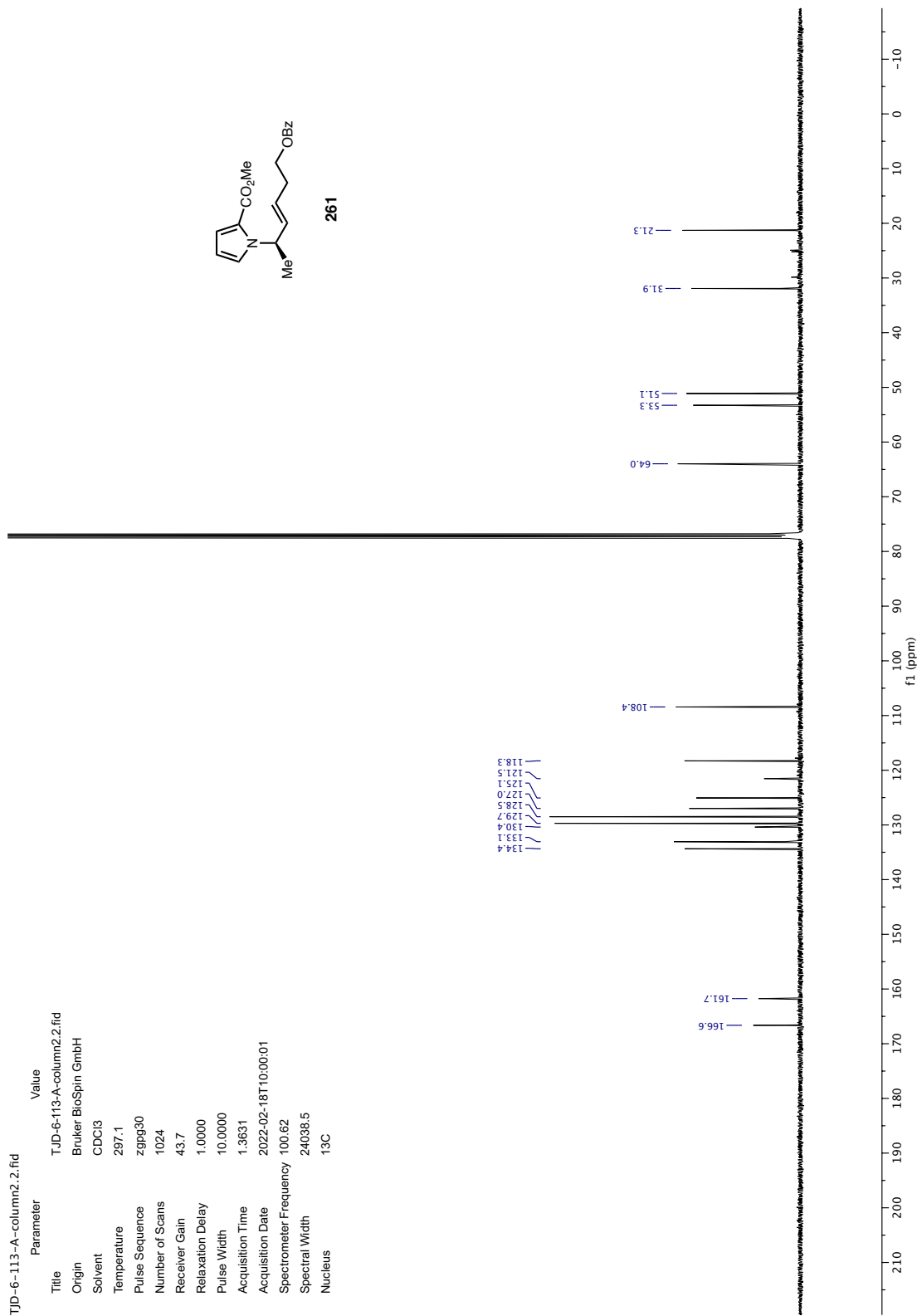


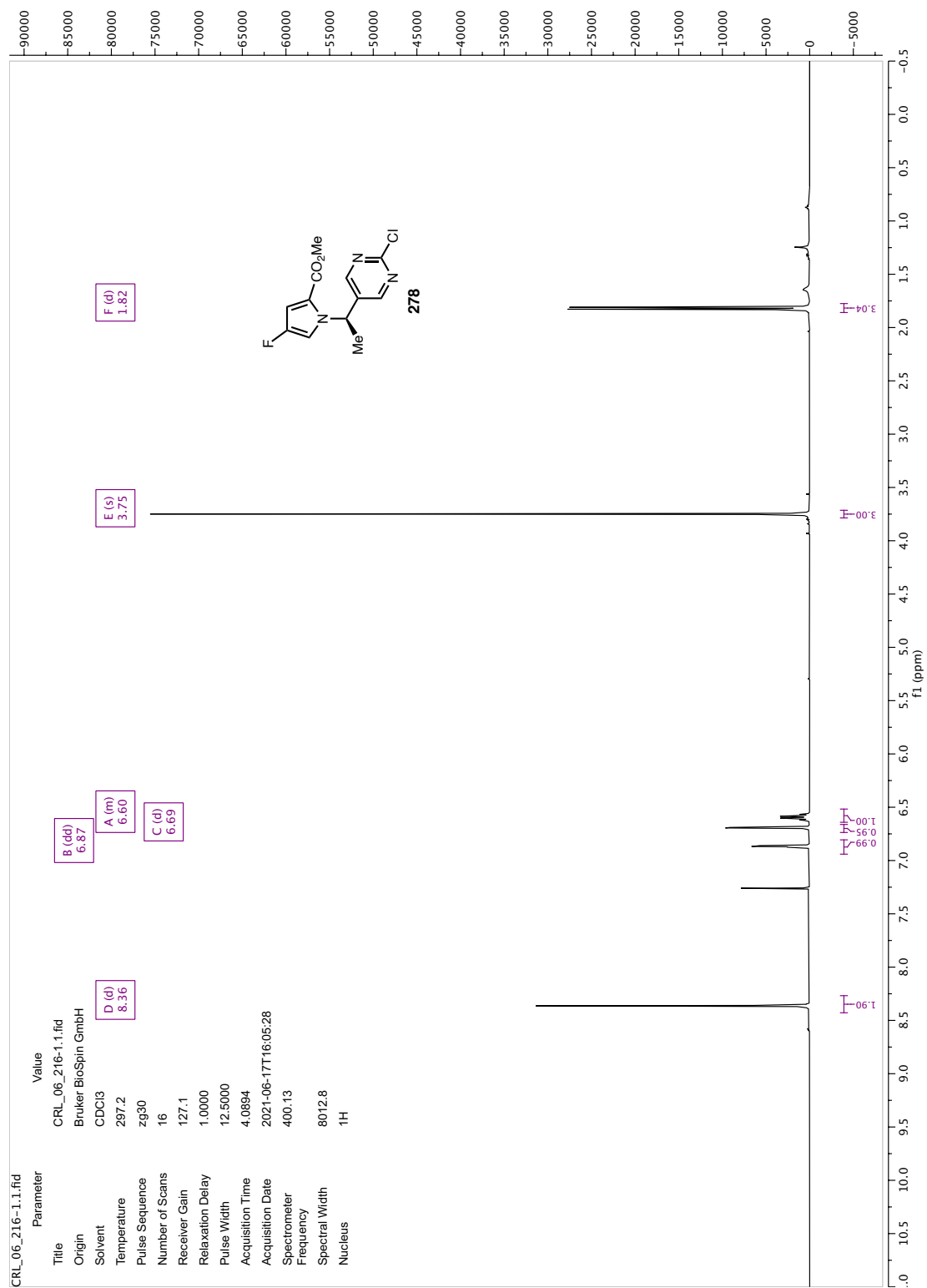
CRL\_06\_096-1.6.fid

Parameter	Value
Title	CRL_06_096-1.6.fid
Origin	Bruker BioSpin GmbH
Solvent	CDCl3
Temperature	297.1
Pulse Sequence	zgpg30
Number of Scans	512
Receiver Gain	72.0
Relaxation Delay	1.0000
Pulse Width	10.0000
Acquisition Time	1.3631
Acquisition Date	2021-02-27T13:55:16
Spectrometer	100.62
Frequency	24038.5
Spectral Width	13C
Nucleus	

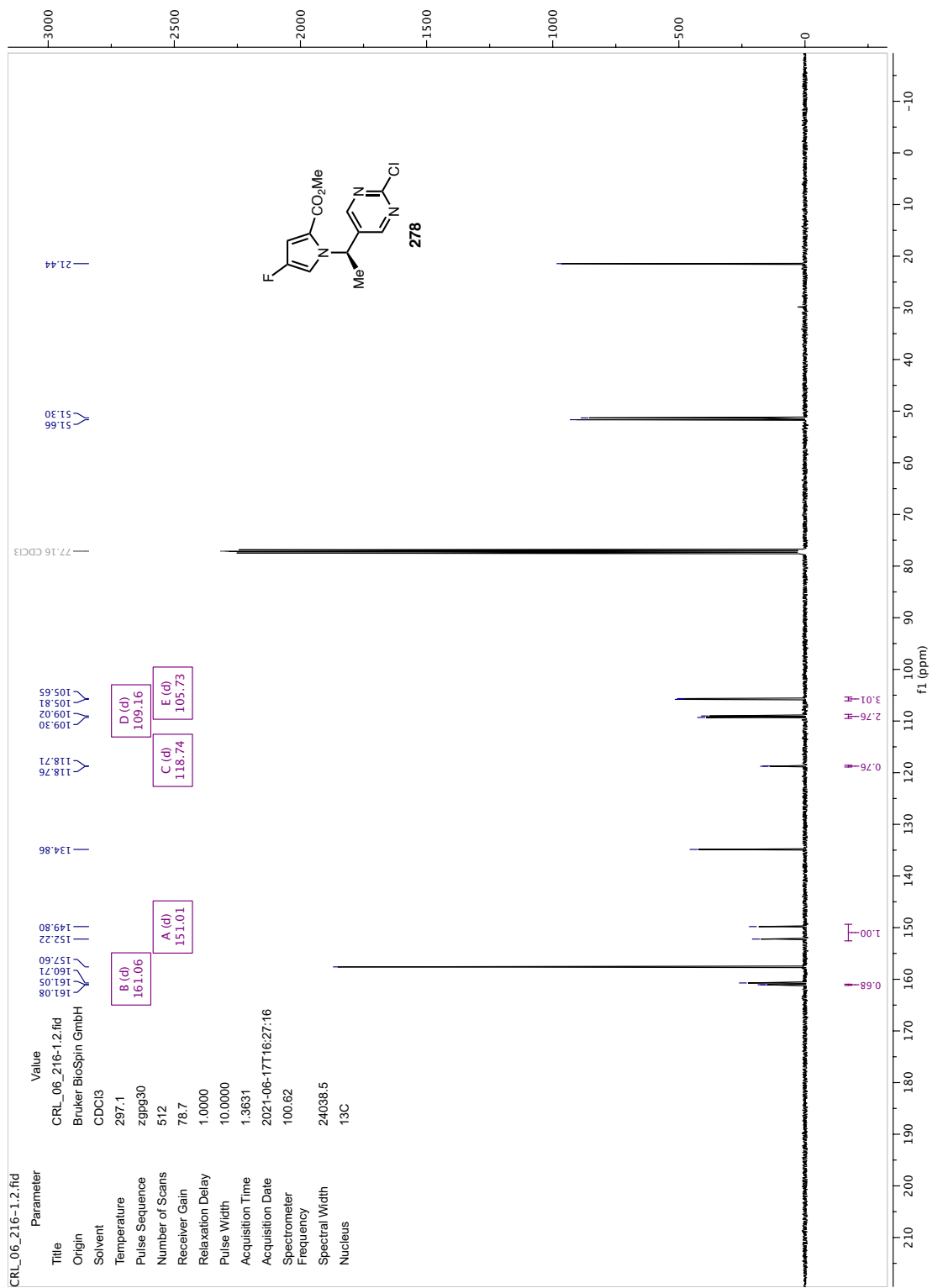


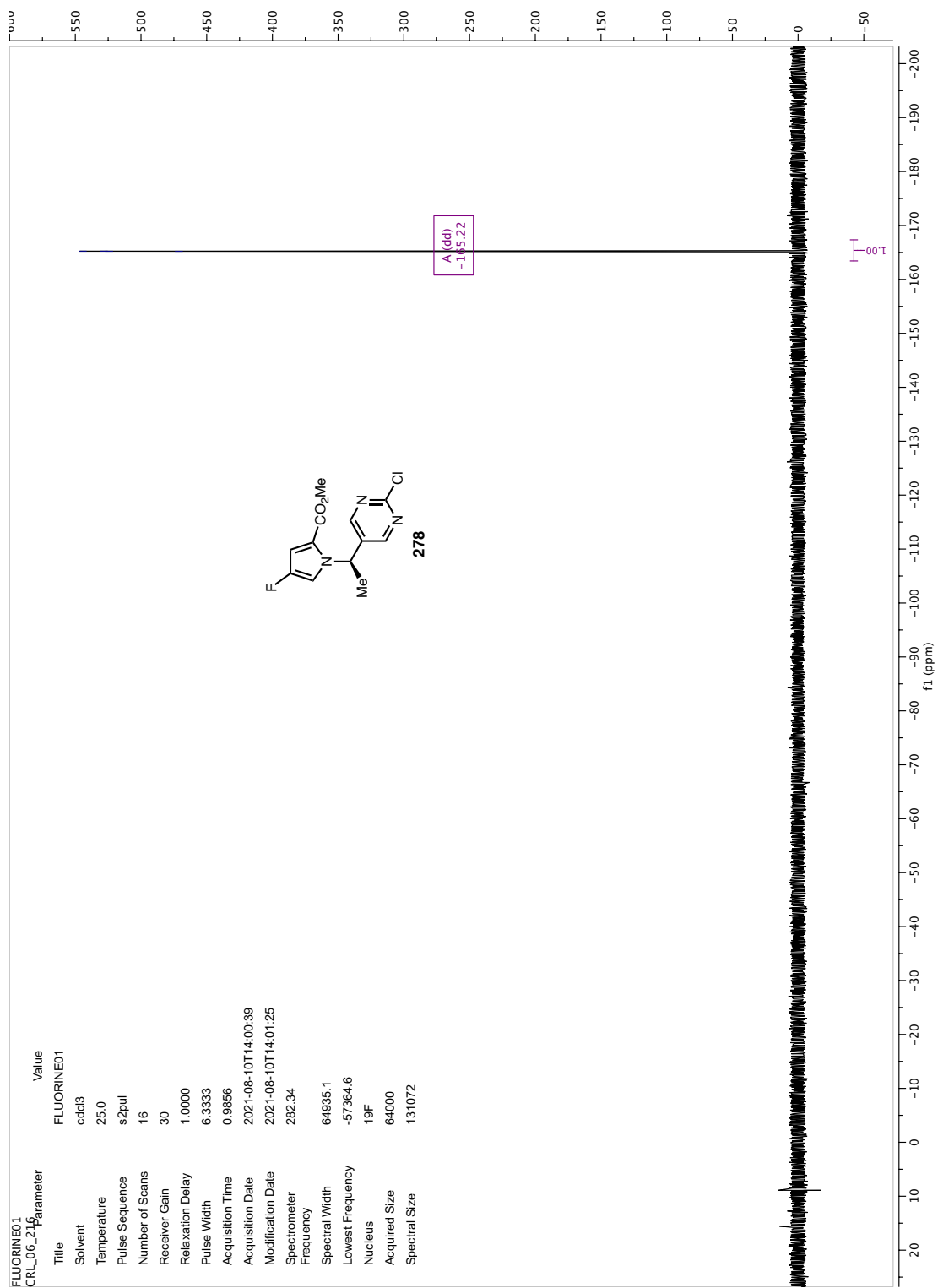


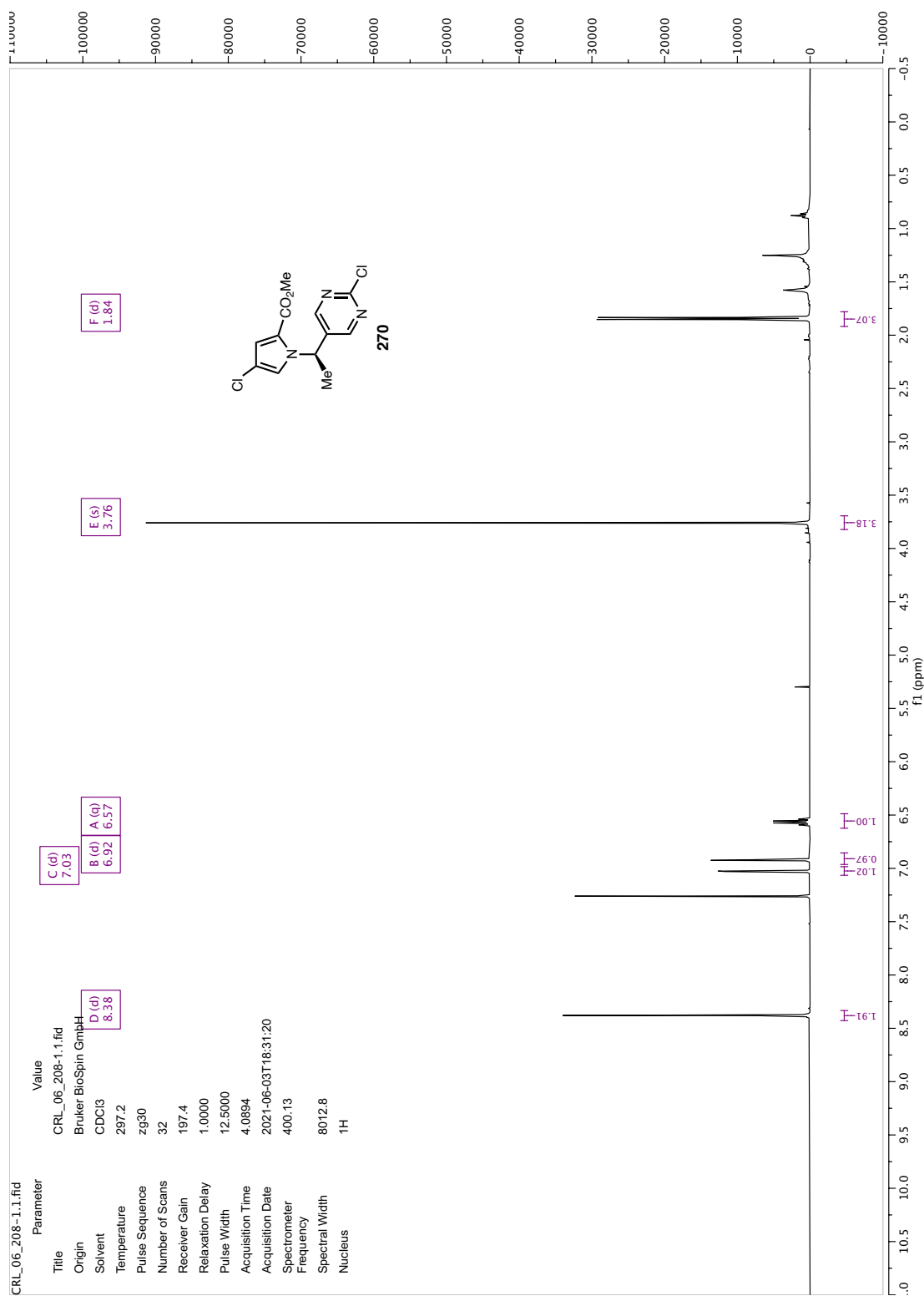


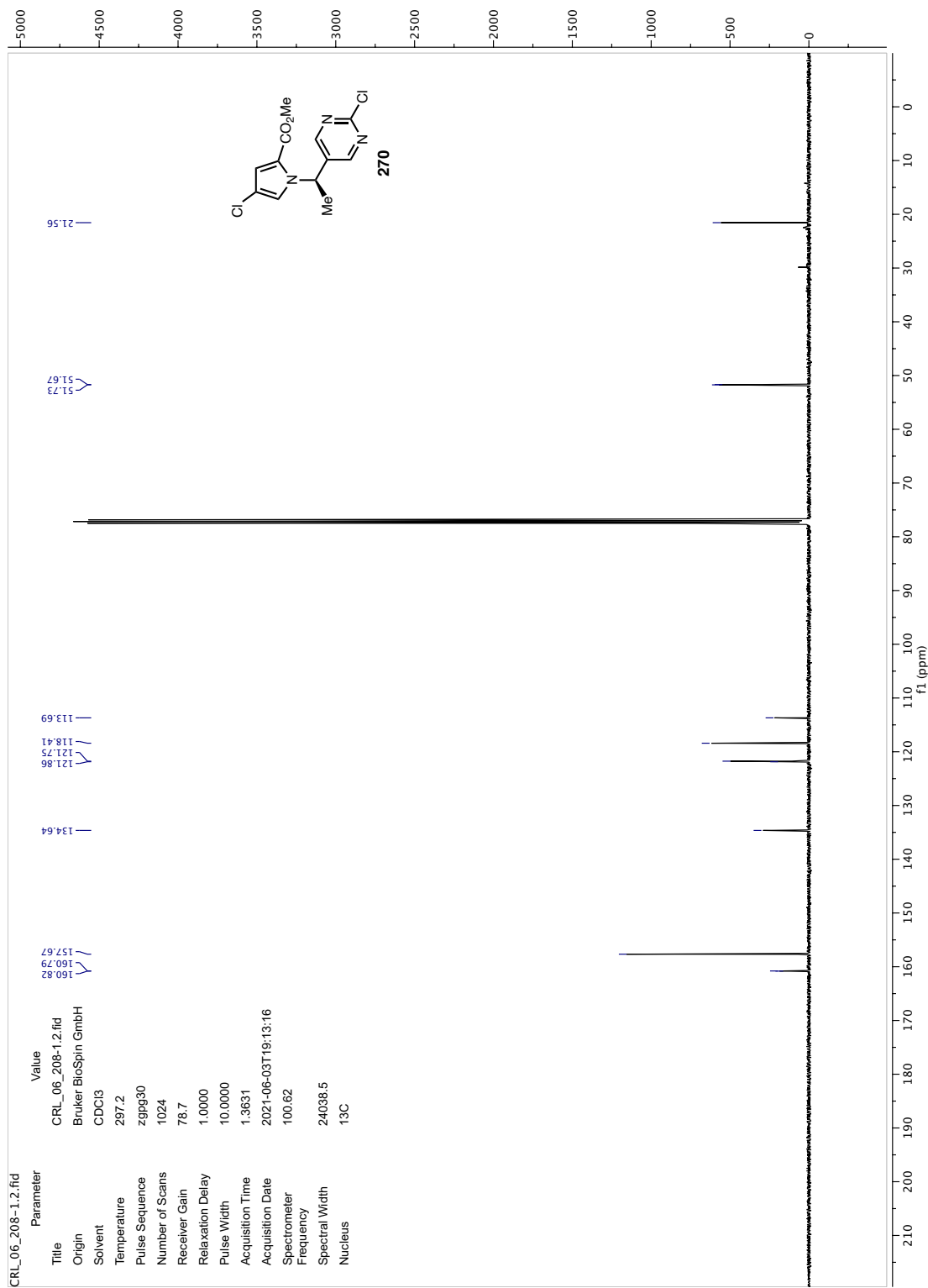








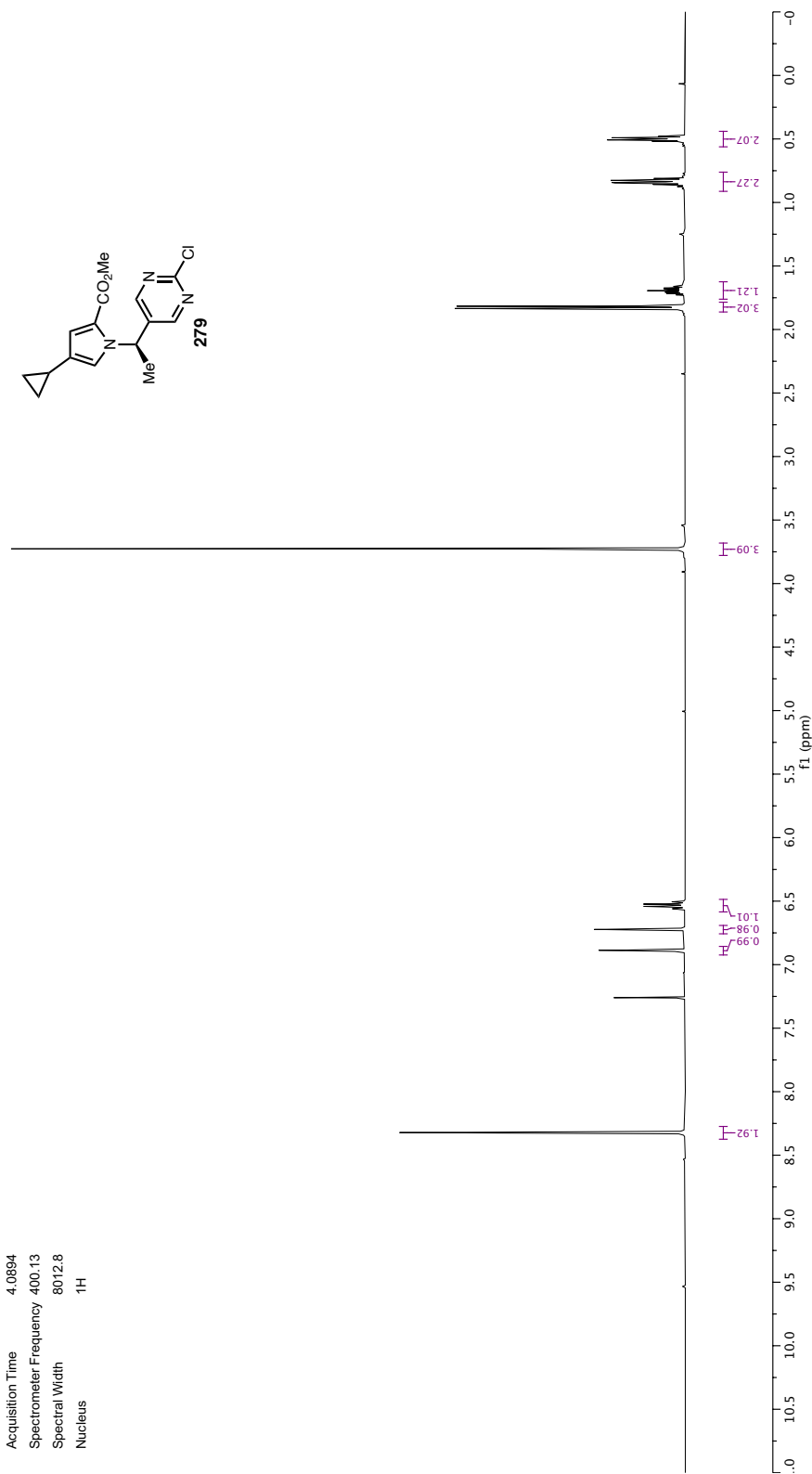
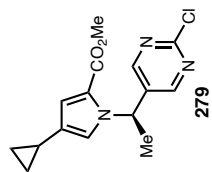




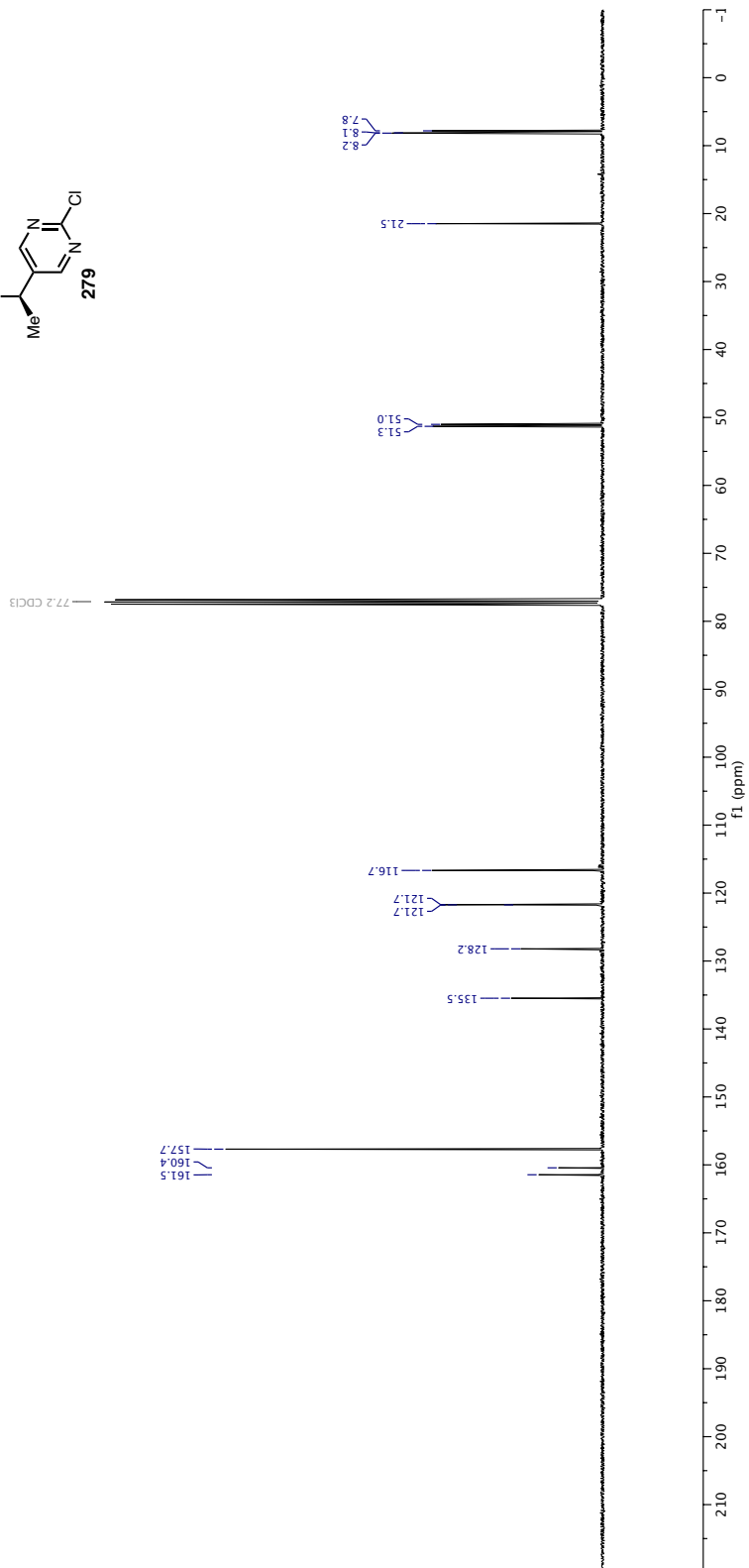
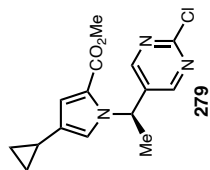
TJD-6-046--column.1.fid

Parameter	Value
Title	TJD-6-046-column.1.fid
Solvent	CDCl3
Temperature	297.2
Number of Scans	16
Receiver Gain	112.8
Relaxation Delay	1.0000
Pulse Width	12.5000
Acquisition Time	4.0894
Spectrometer Frequency	400.13
Spectral Width	8012.8
Nucleus	1H

A (s)	8.32
B (d)	6.89
C (d)	6.72
D (g)	6.53
E (s)	3.73
F (d)	1.83
G (m)	0.84
H (m)	1.69
I (m)	0.50



Parameter	Value
Title	TJD-6-046-column.2.fid
Solvent	CDCl <sub>3</sub>
Temperature	297.2
Number of Scans	512
Receiver Gain	87.8
Relaxation Delay	1.0000
Pulse Width	10.0000
Acquisition Time	1.3631
Spectrometer Frequency	100.62
Spectral Width	24038.5
Nucleus	<sup>13</sup> C



TJD-6-045-column.1.fid

Parameter Value

Title TJD-6-045-column.1.fid  
 Solvent CDCl3  
 Temperature 297.2  
 Number of Scans 16  
 Receiver Gain 112.8  
 Relaxation Delay 1.0000  
 Pulse Width 12.5000  
 Acquisition Time 4.0894  
 Spectrometer Frequency 400.13  
 Spectral Width 8012.8  
 Nucleus 1H

H (t) 0.98

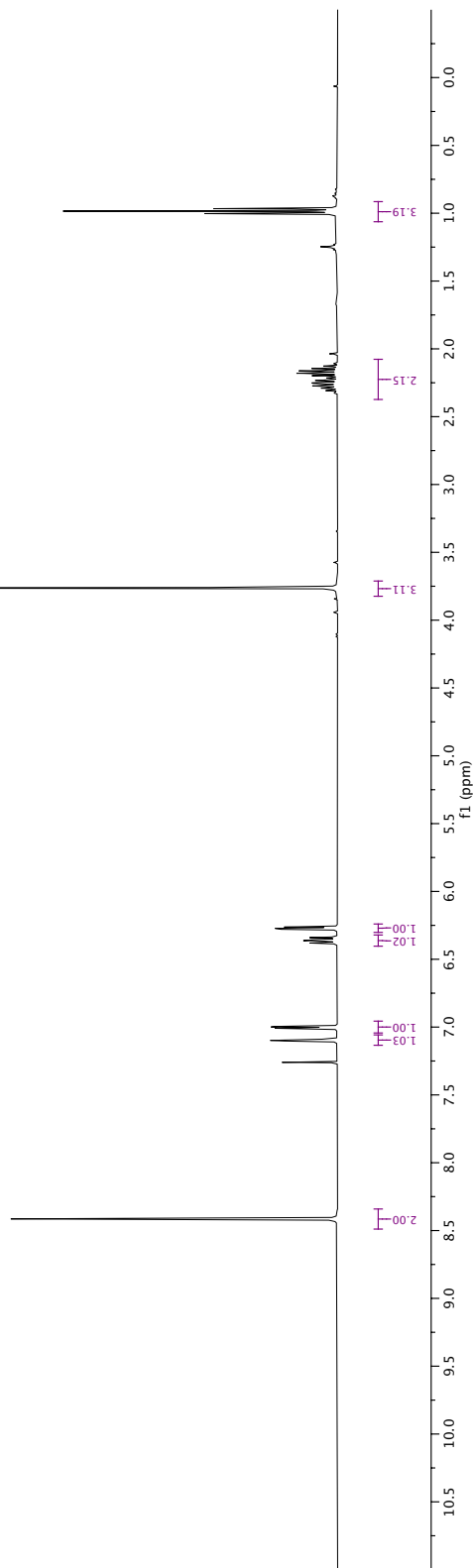
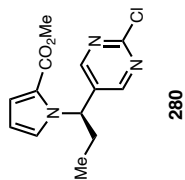
C (m) 2.22

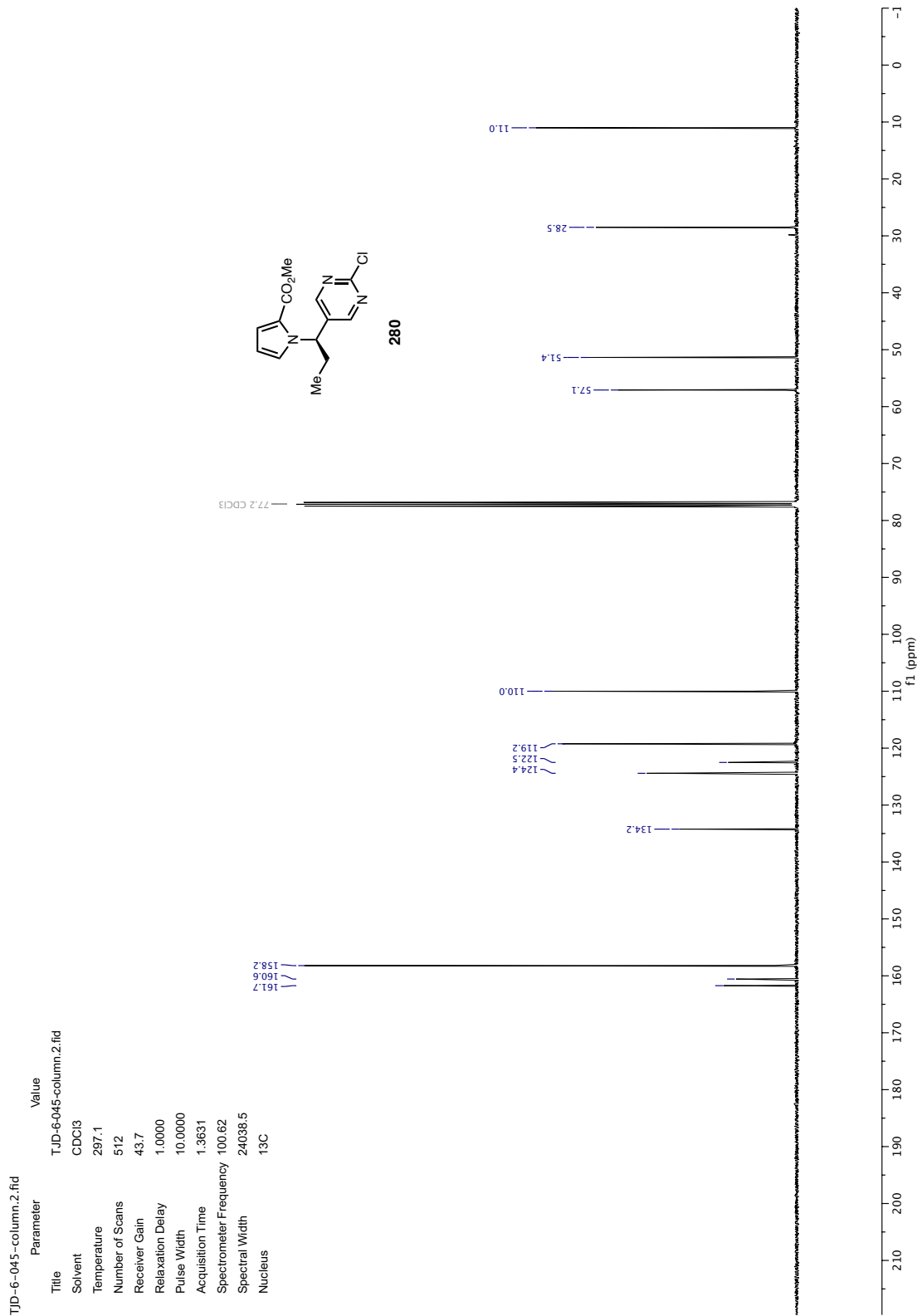
F (s) 3.76

E (dd) 6.27  
 D (dd) 6.36

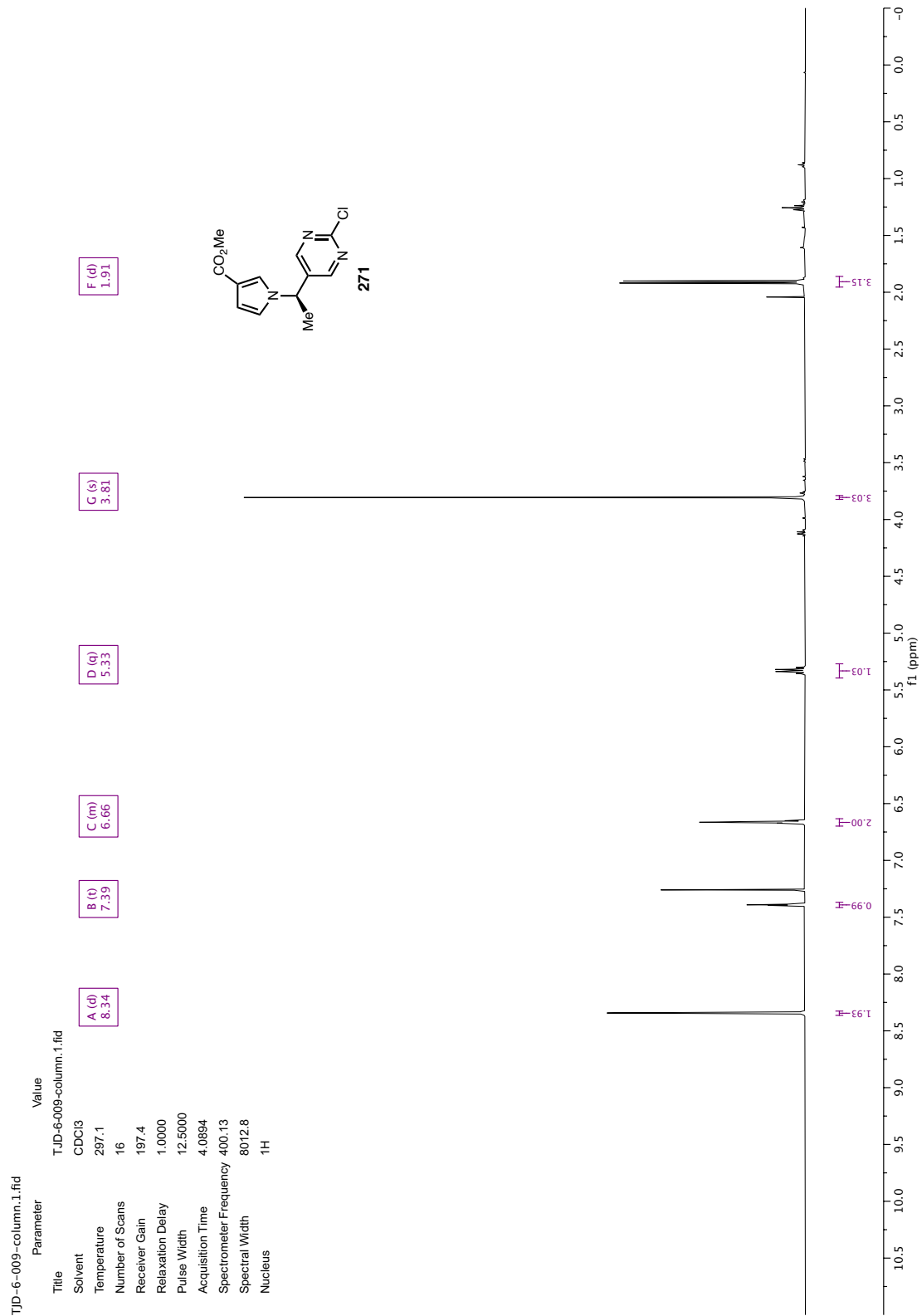
C (dd) 7.00  
 B (dd) 7.10

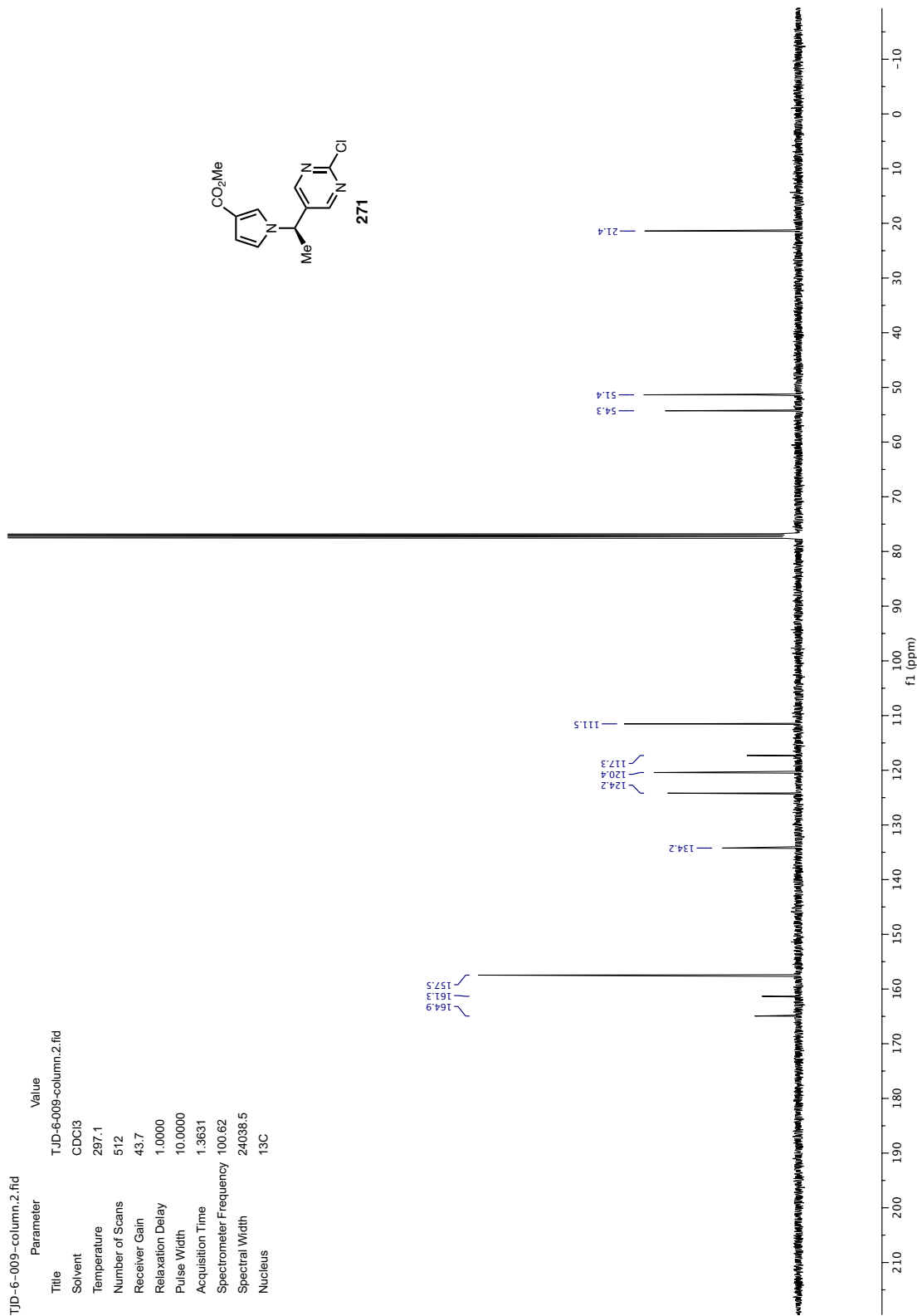
A (s) 8.41

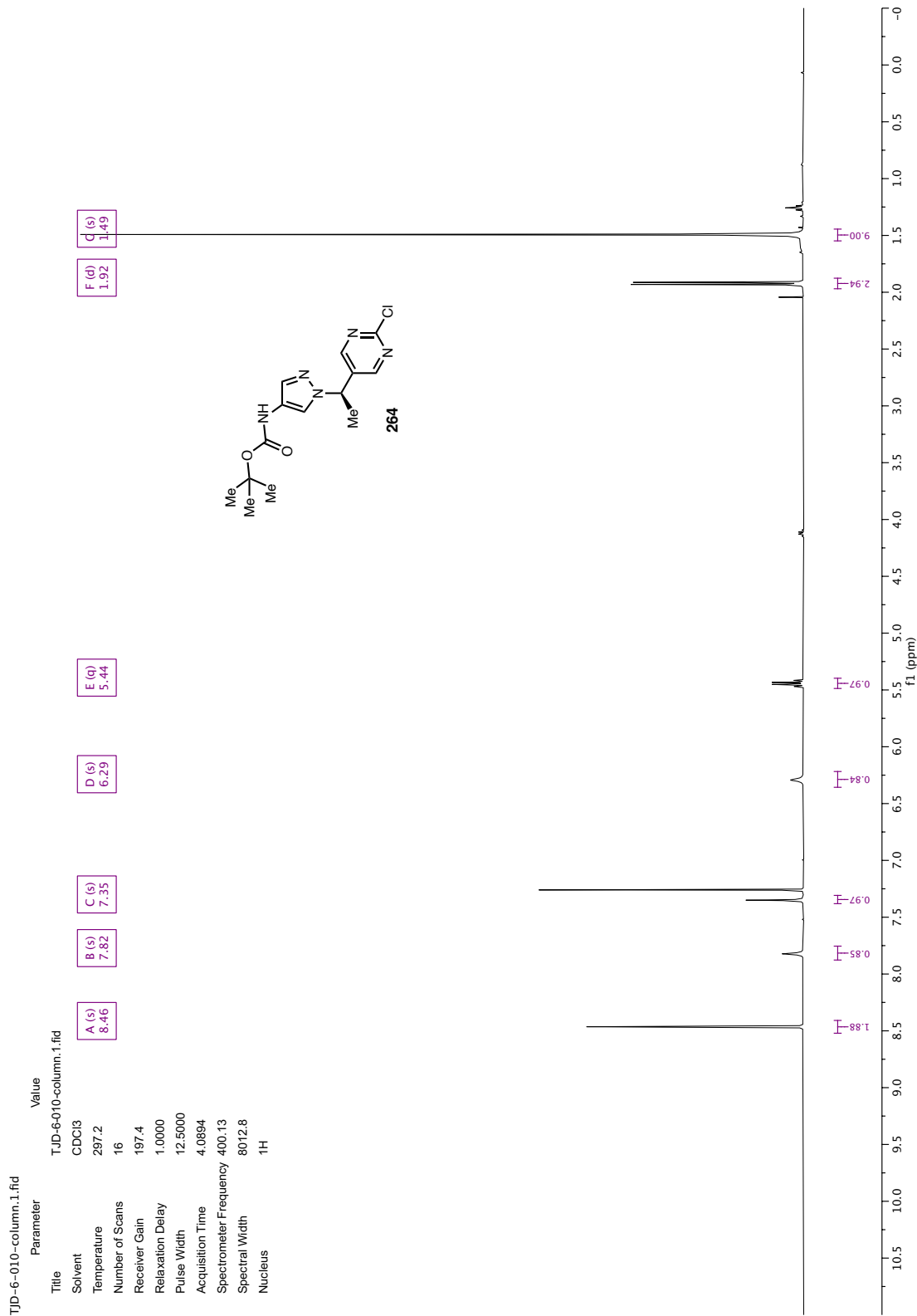


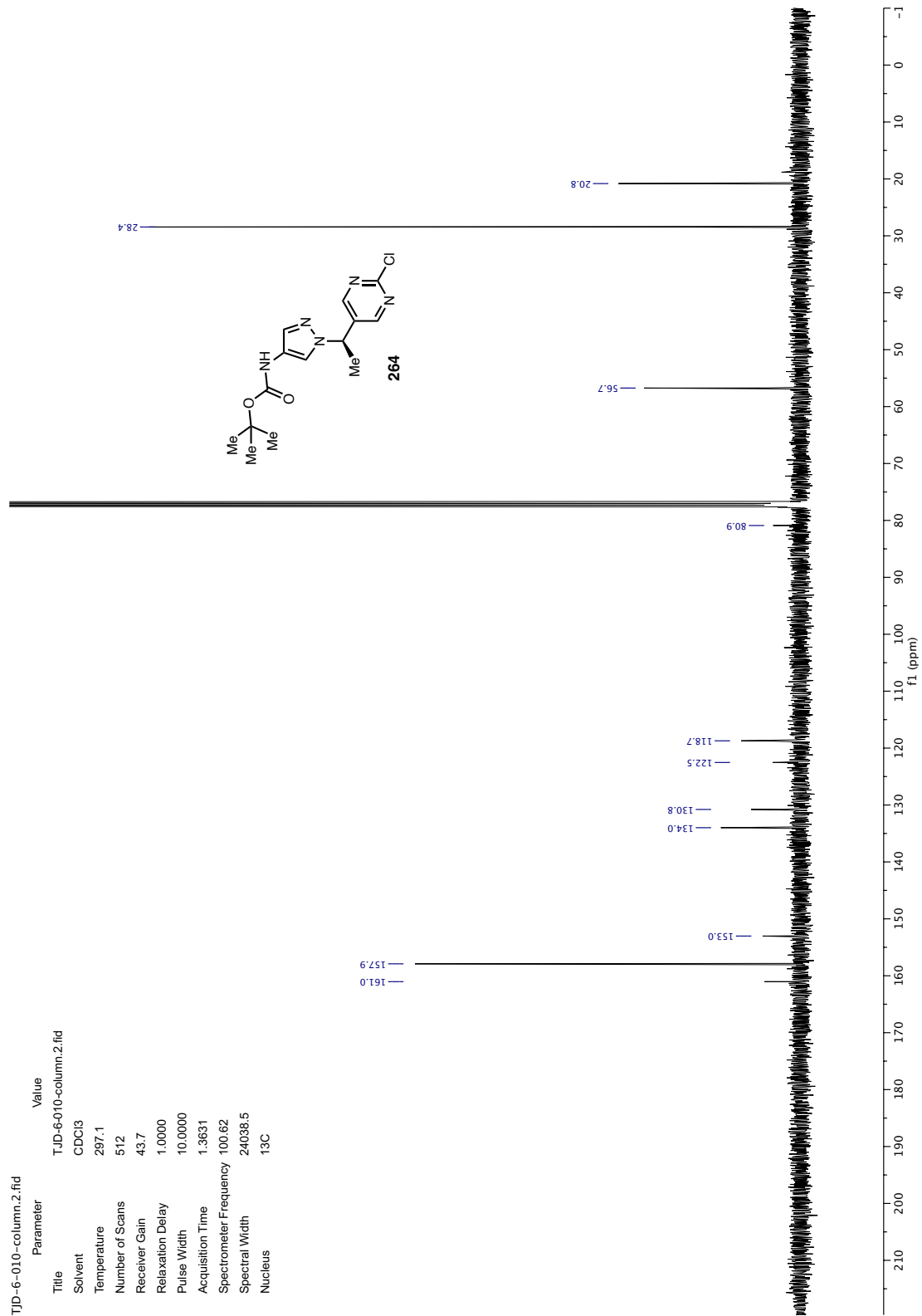


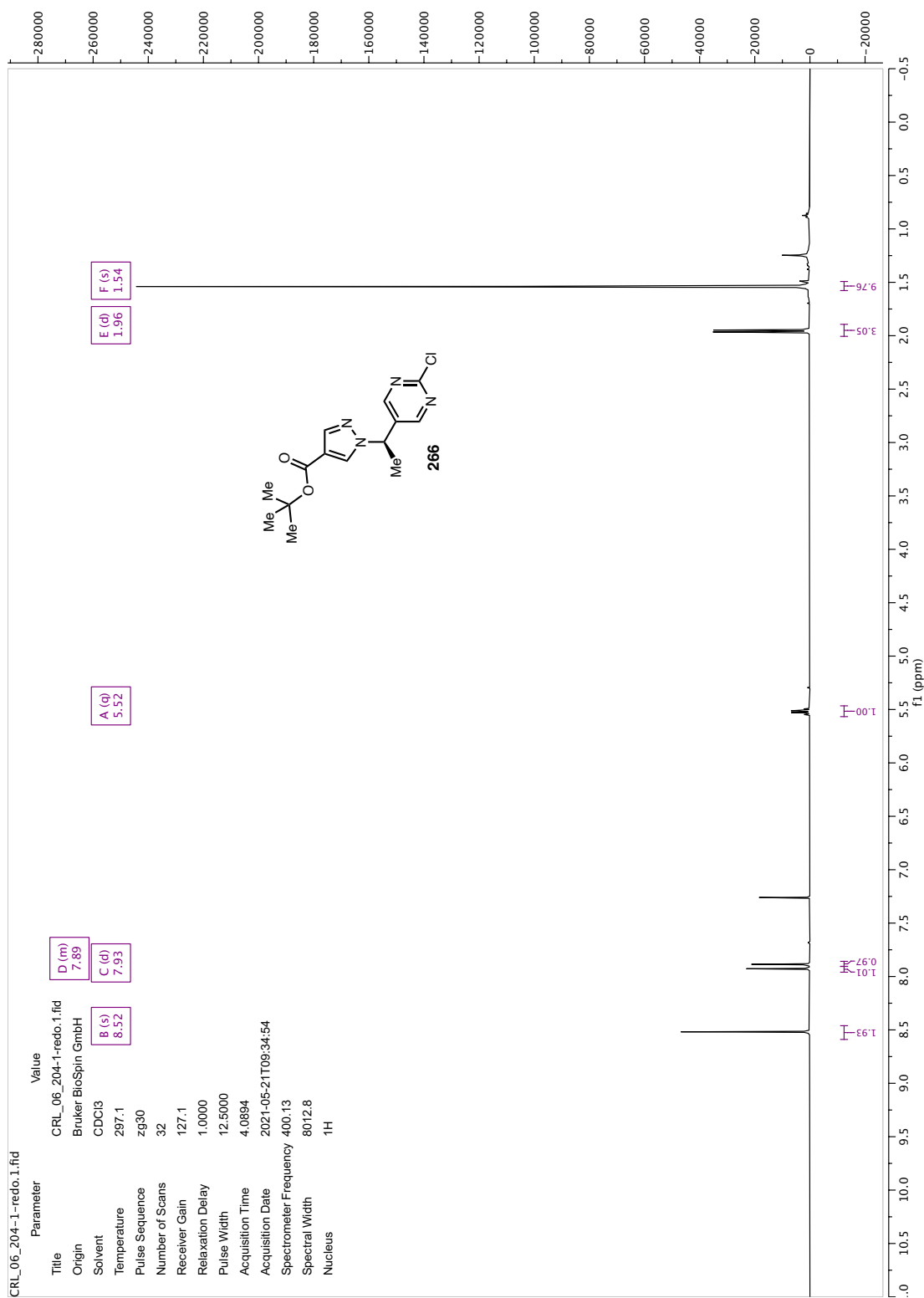


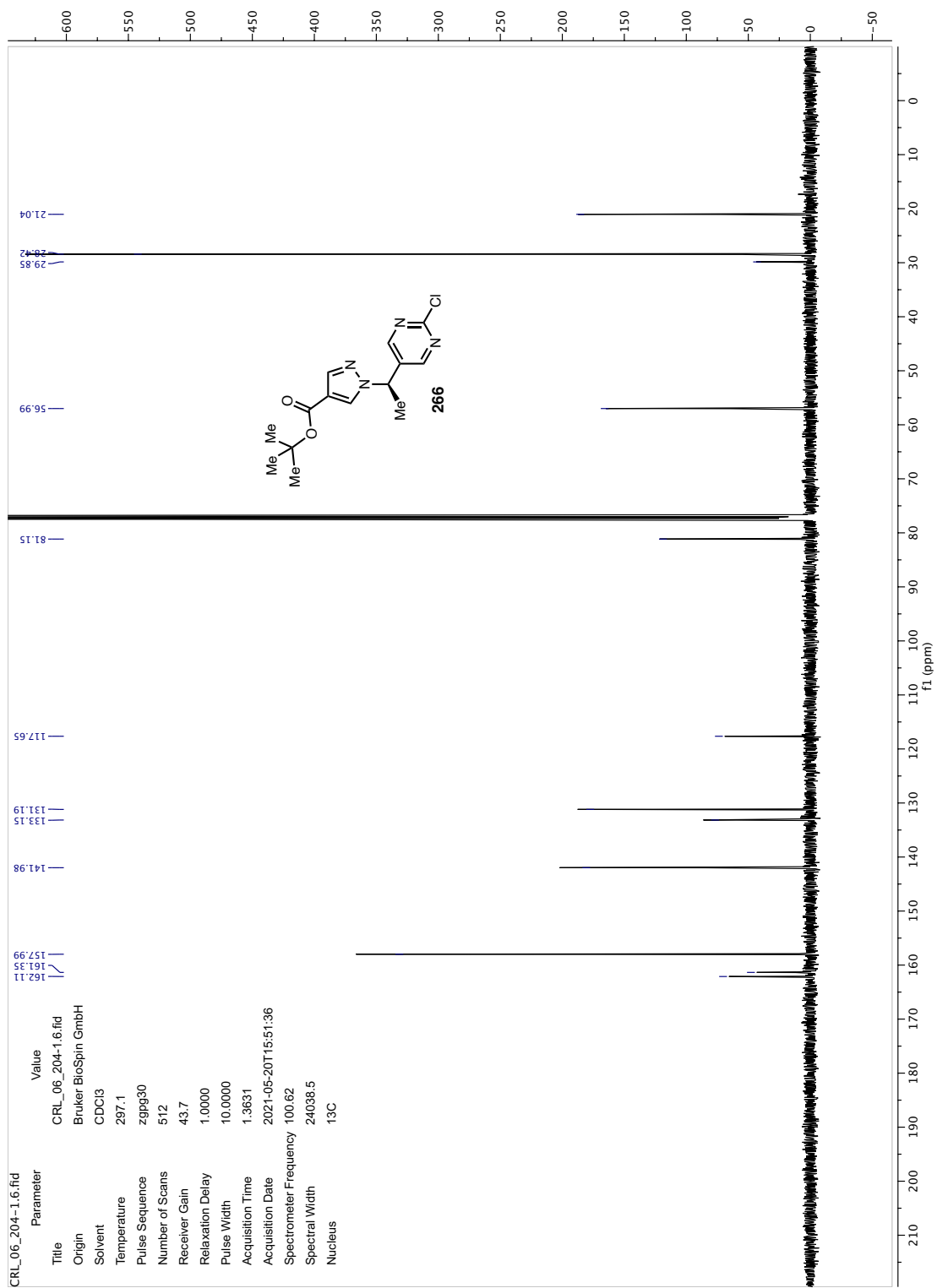


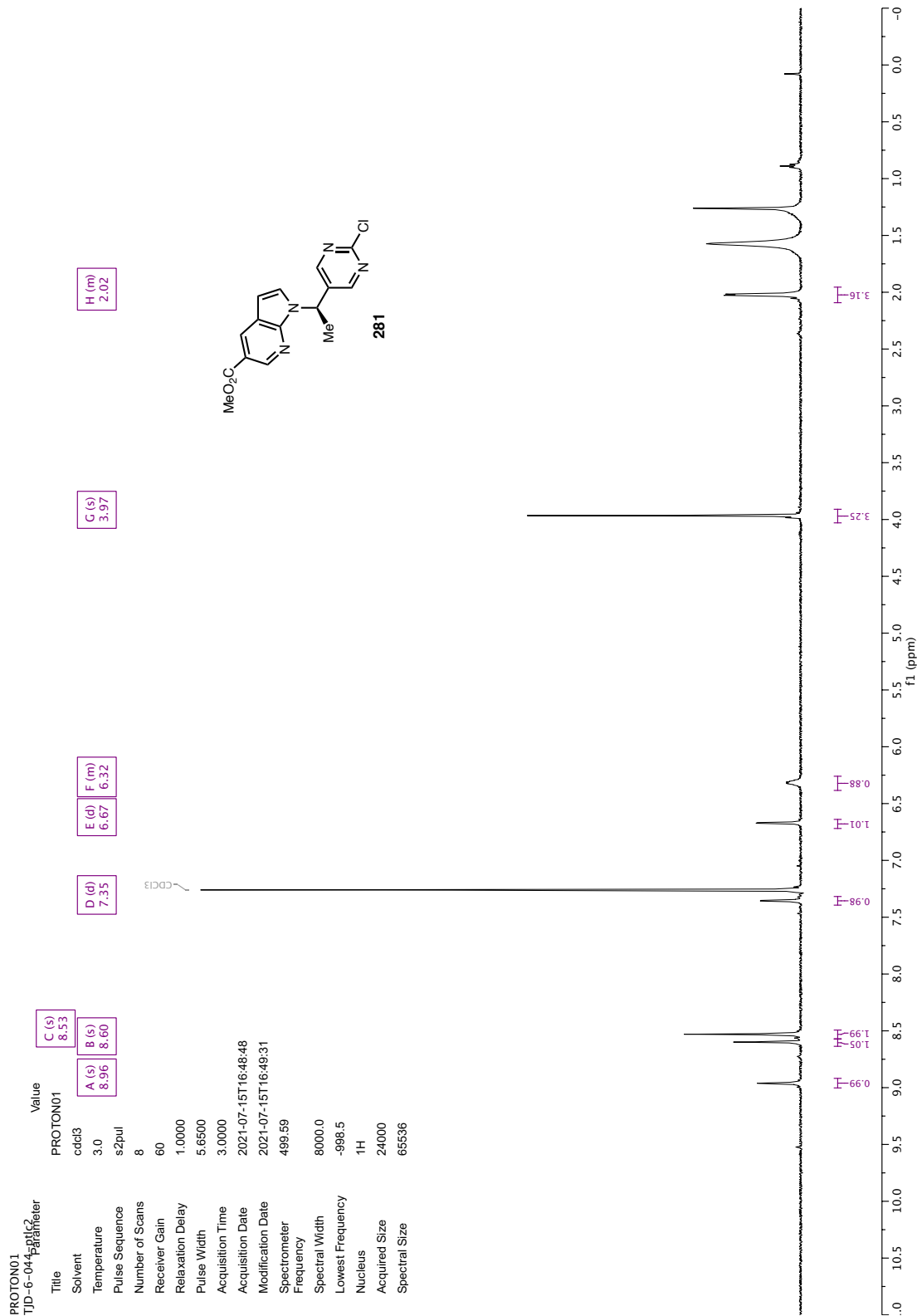


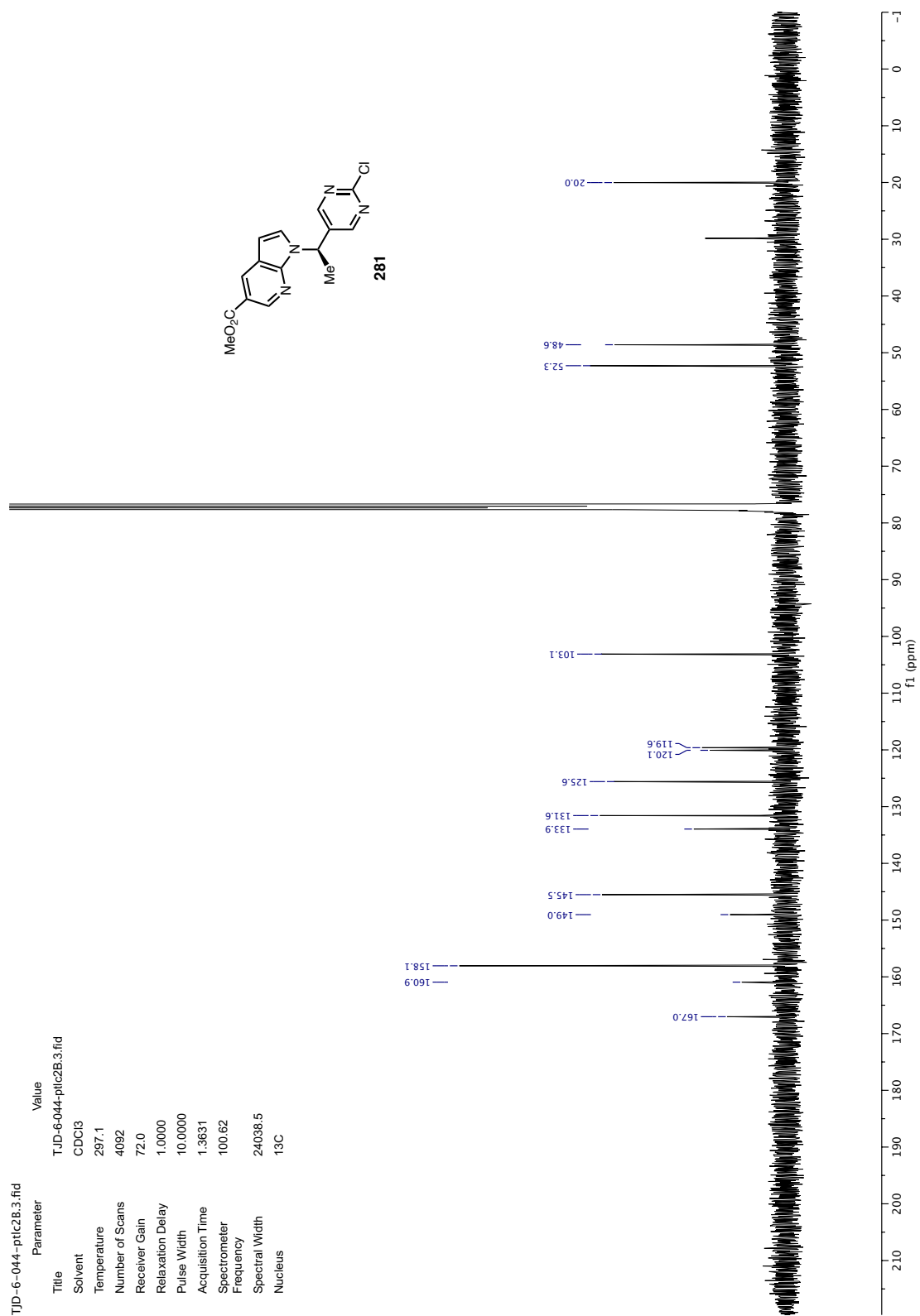




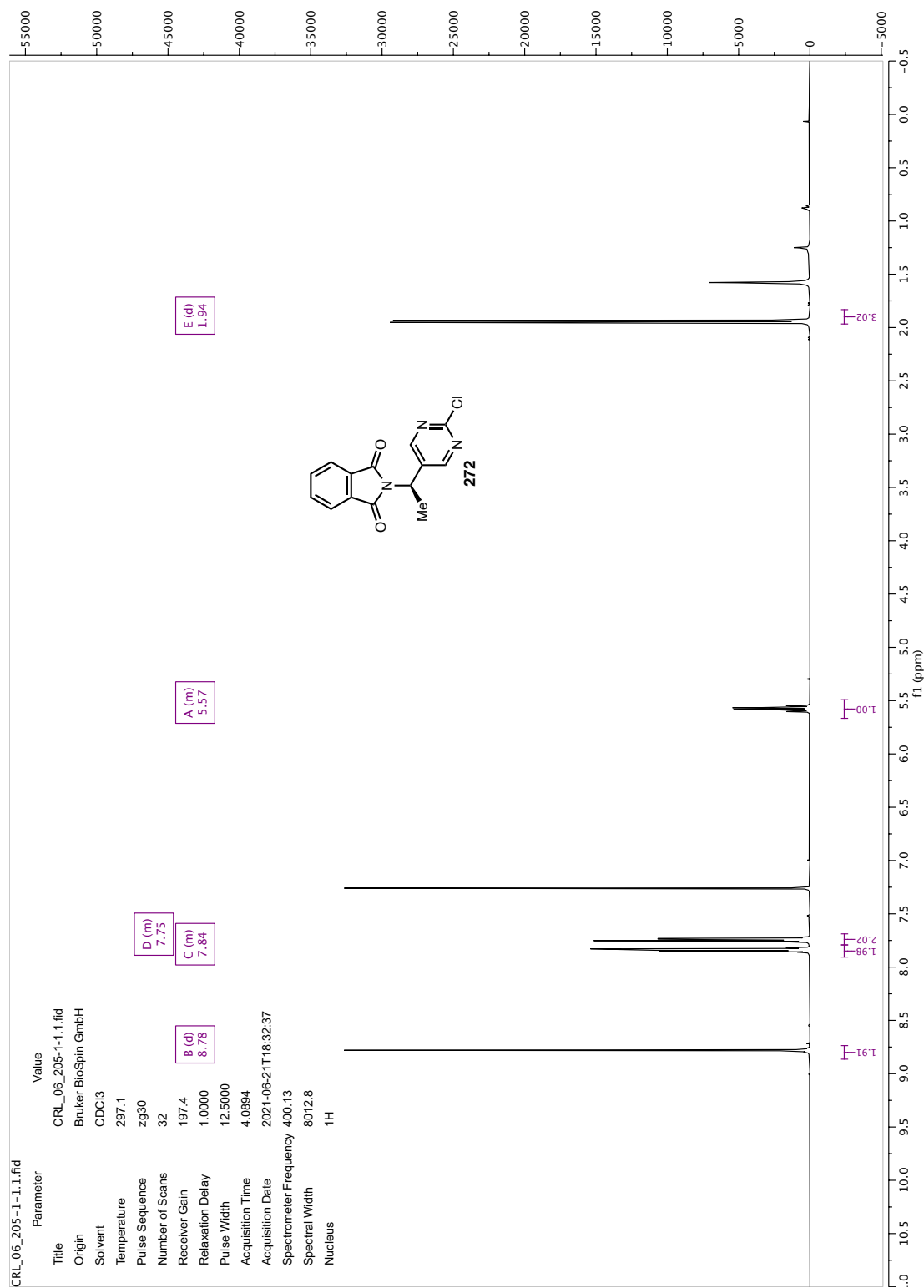


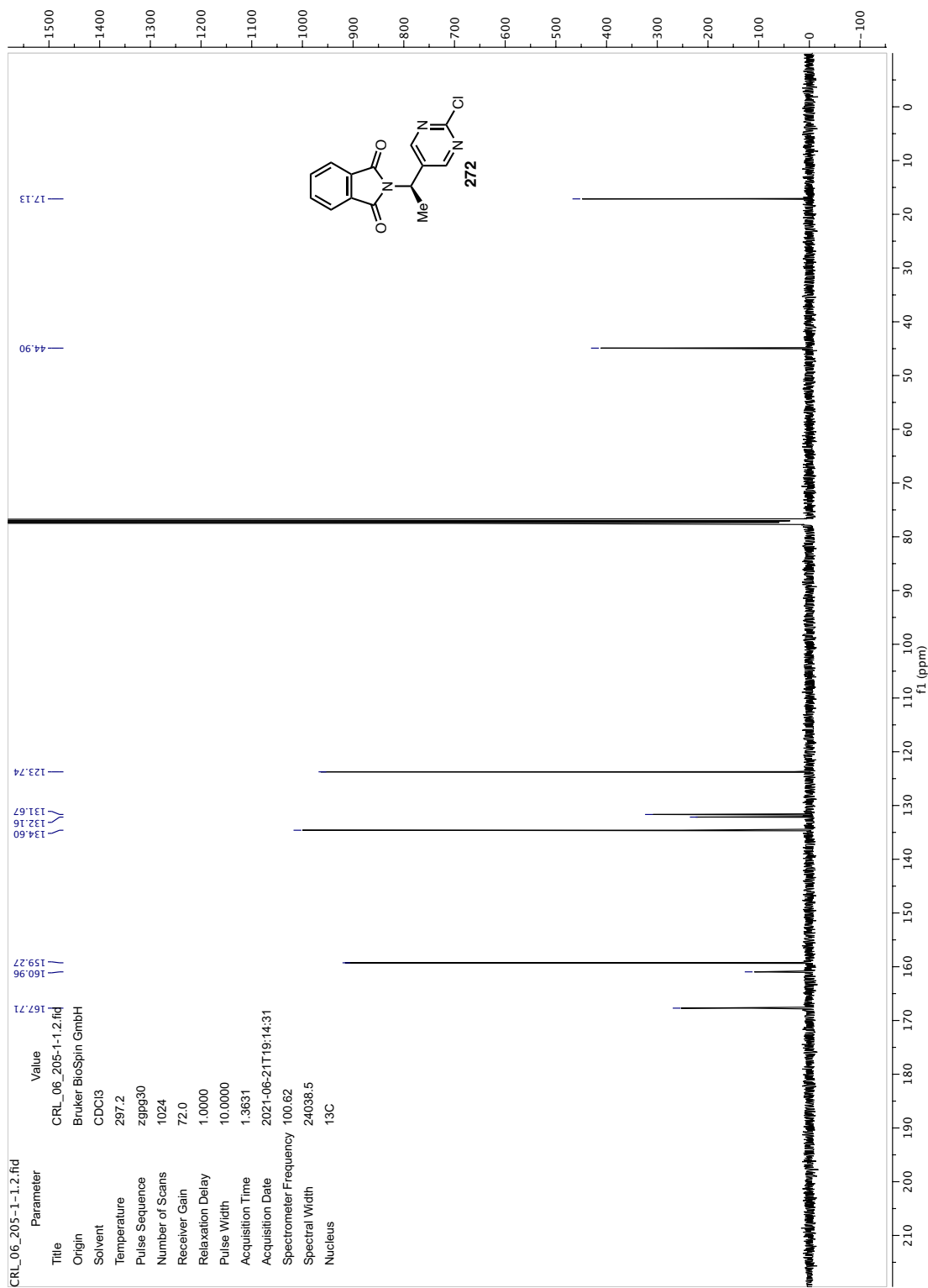


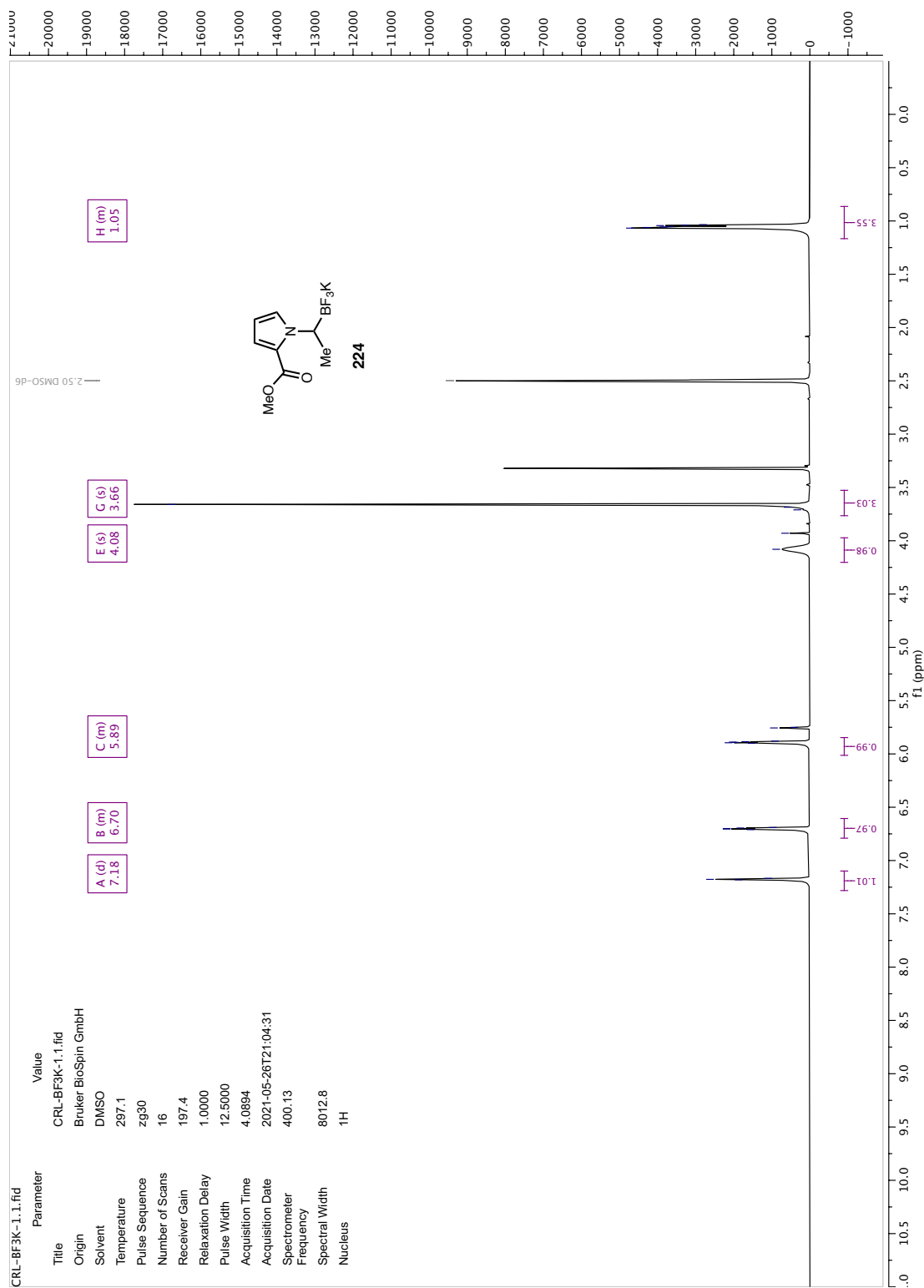


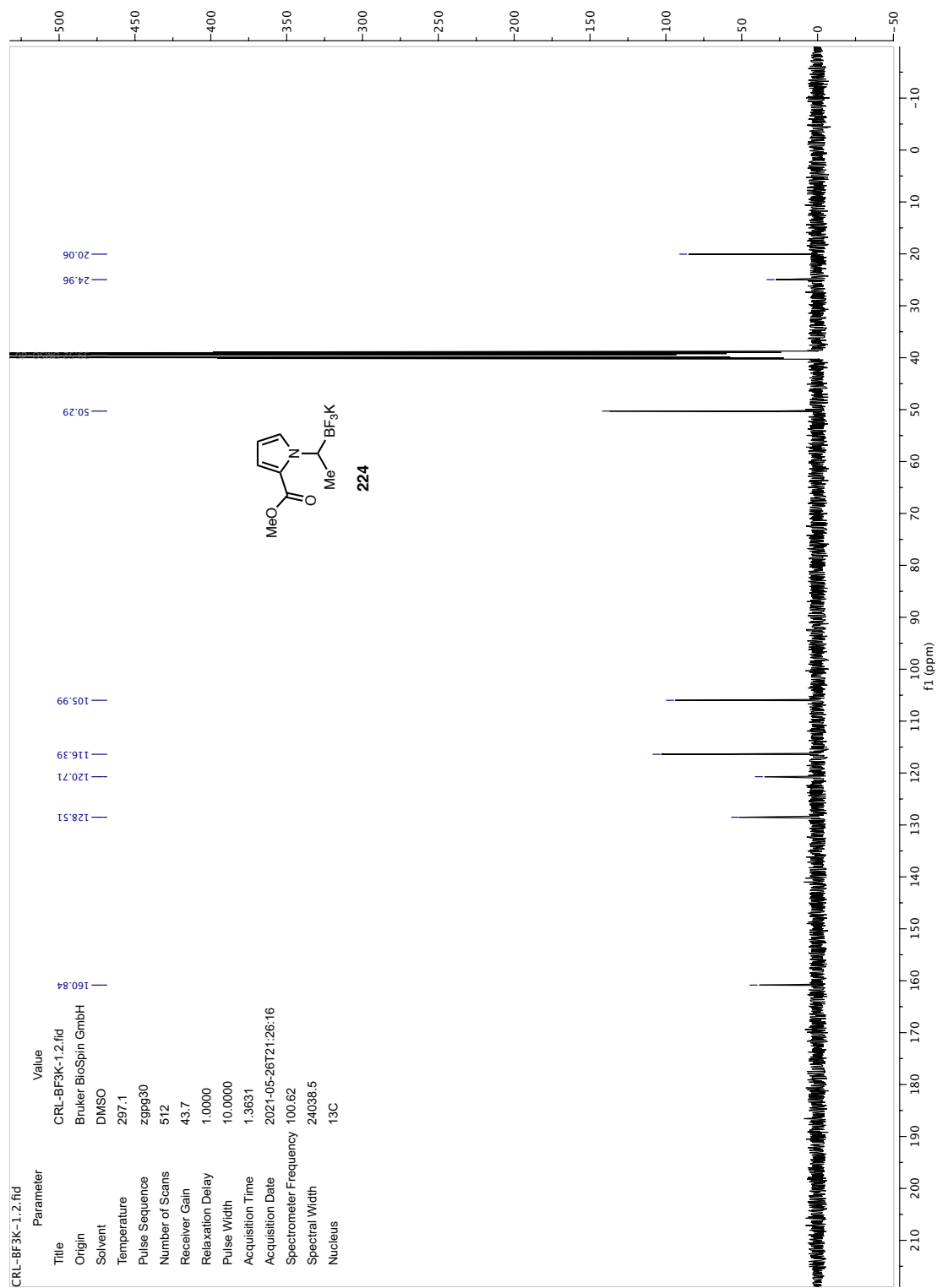


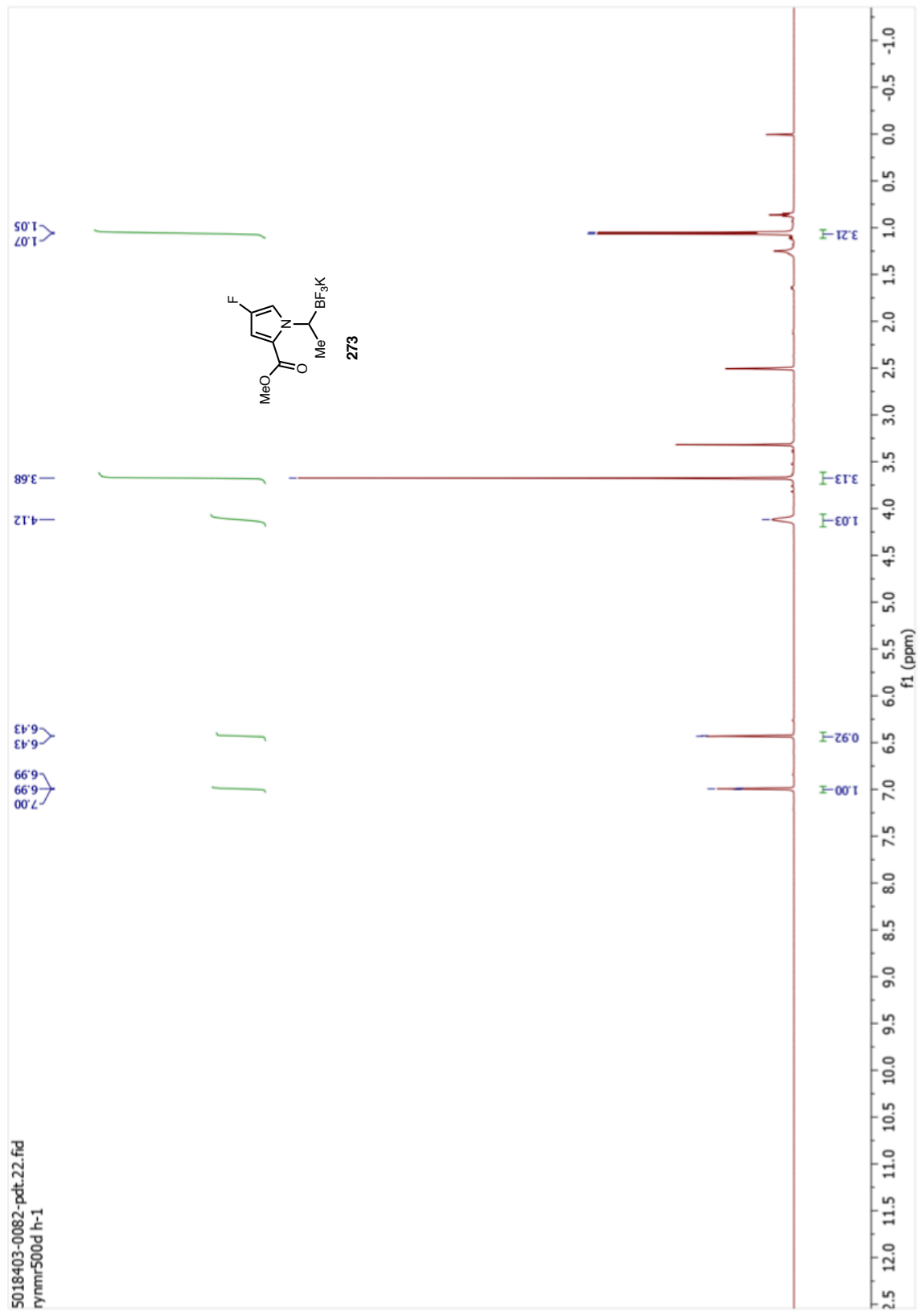


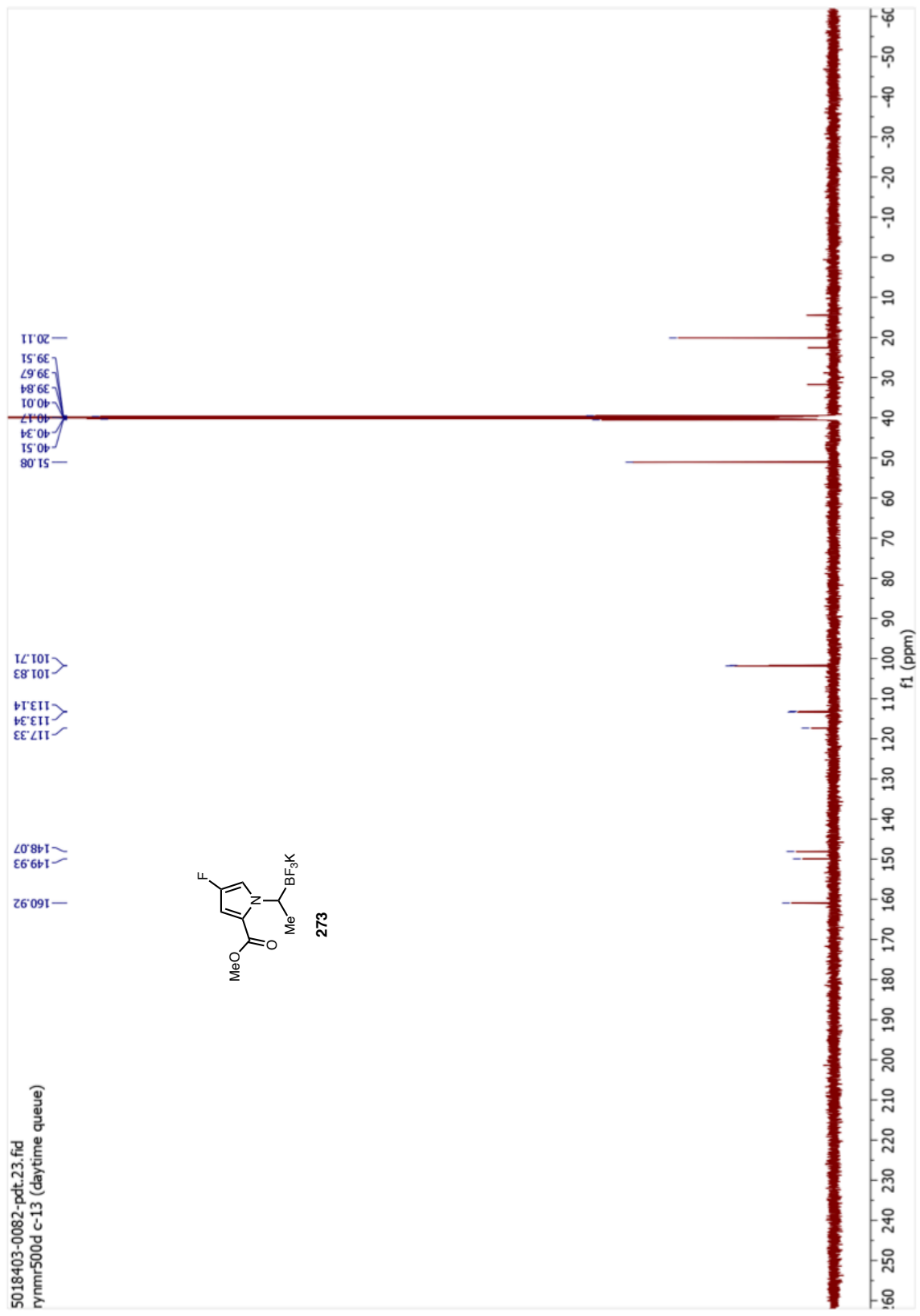


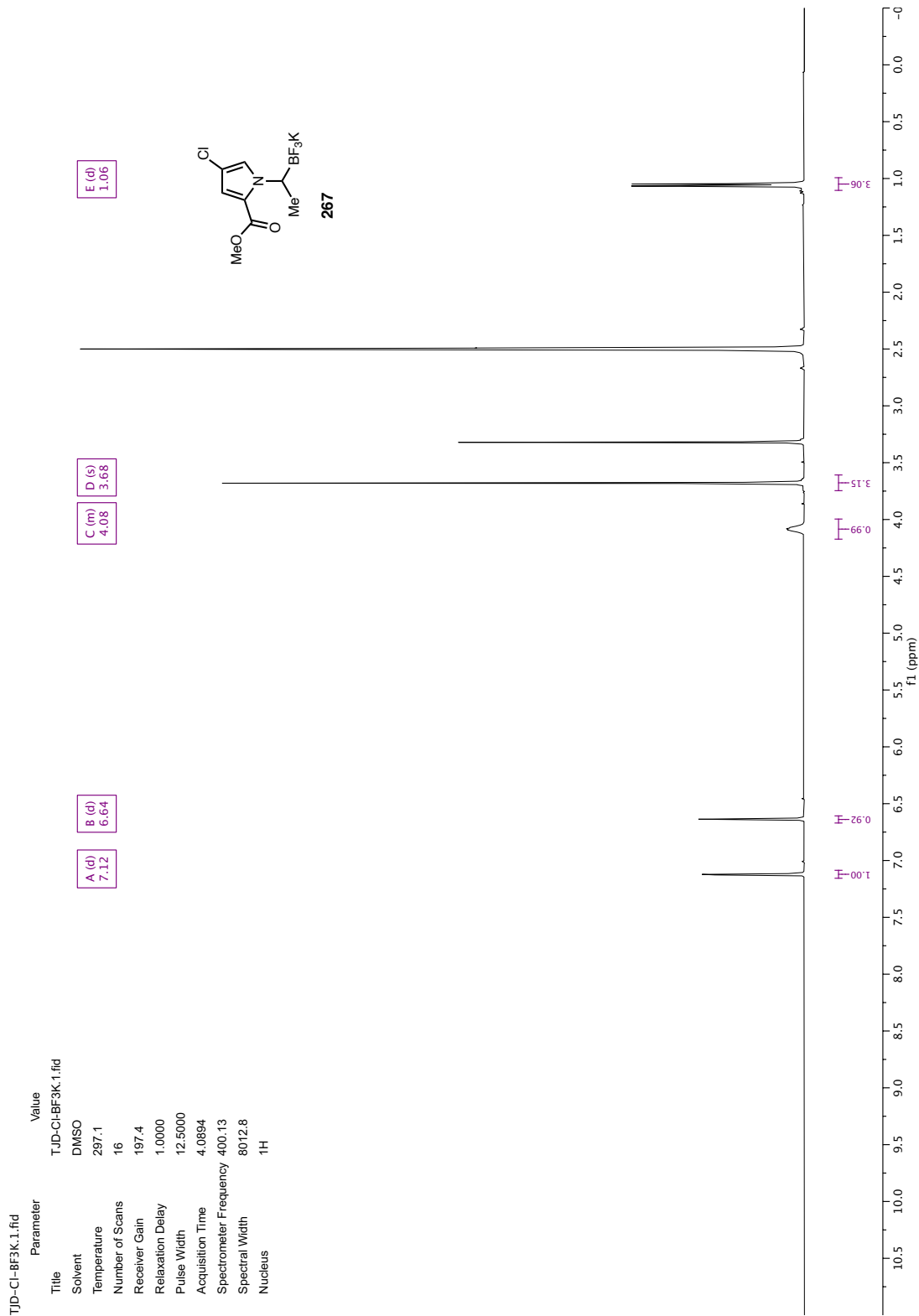


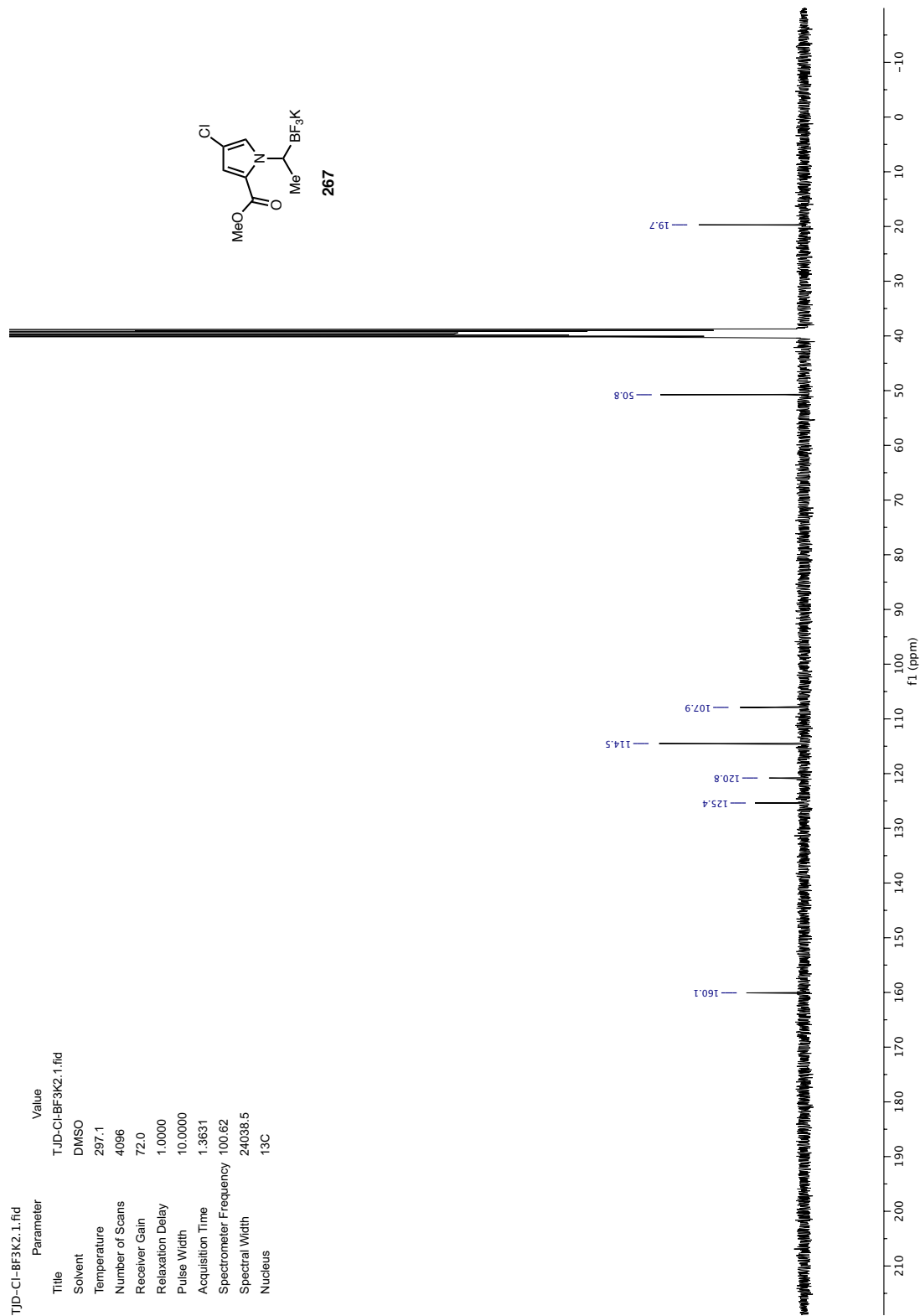




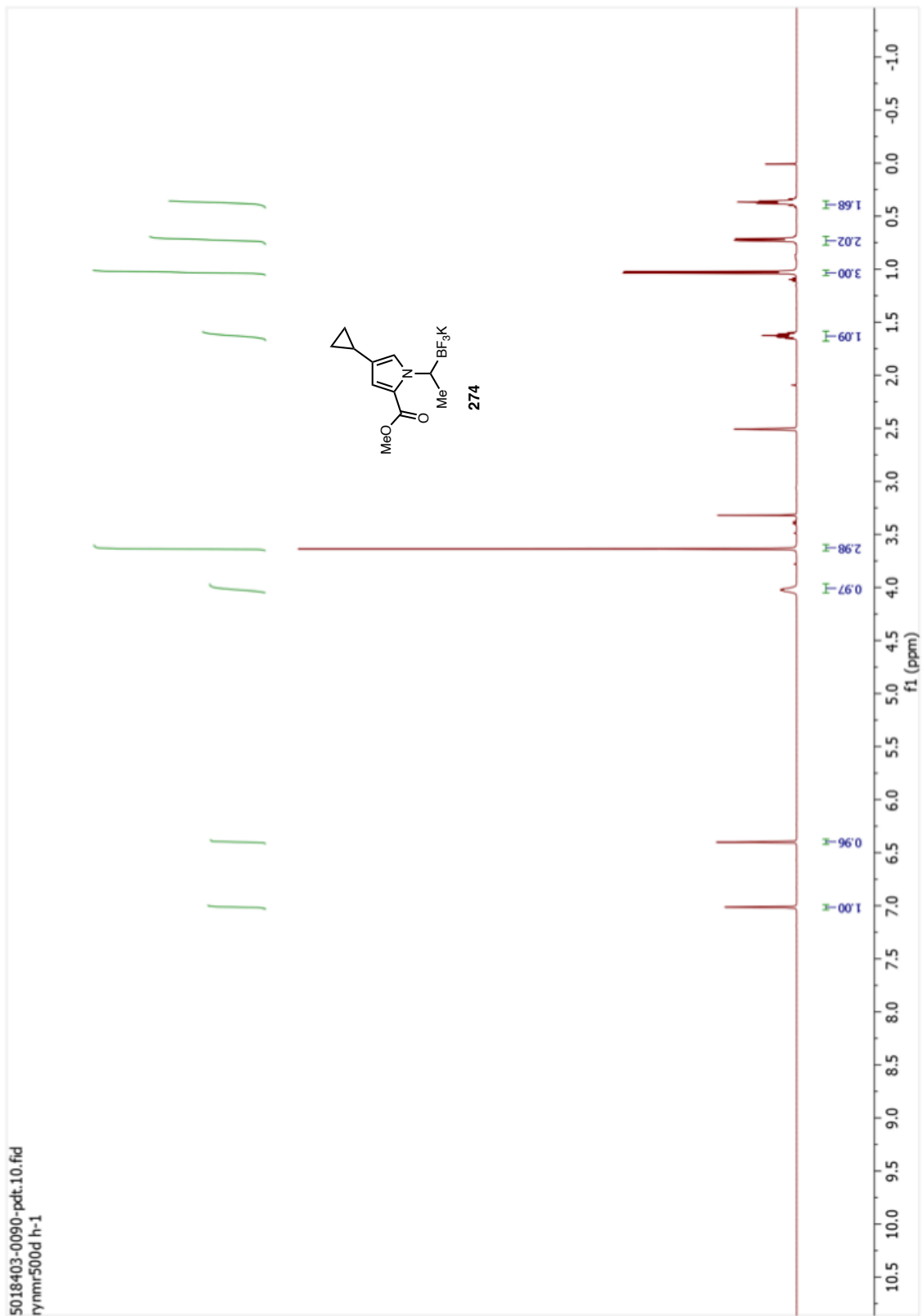


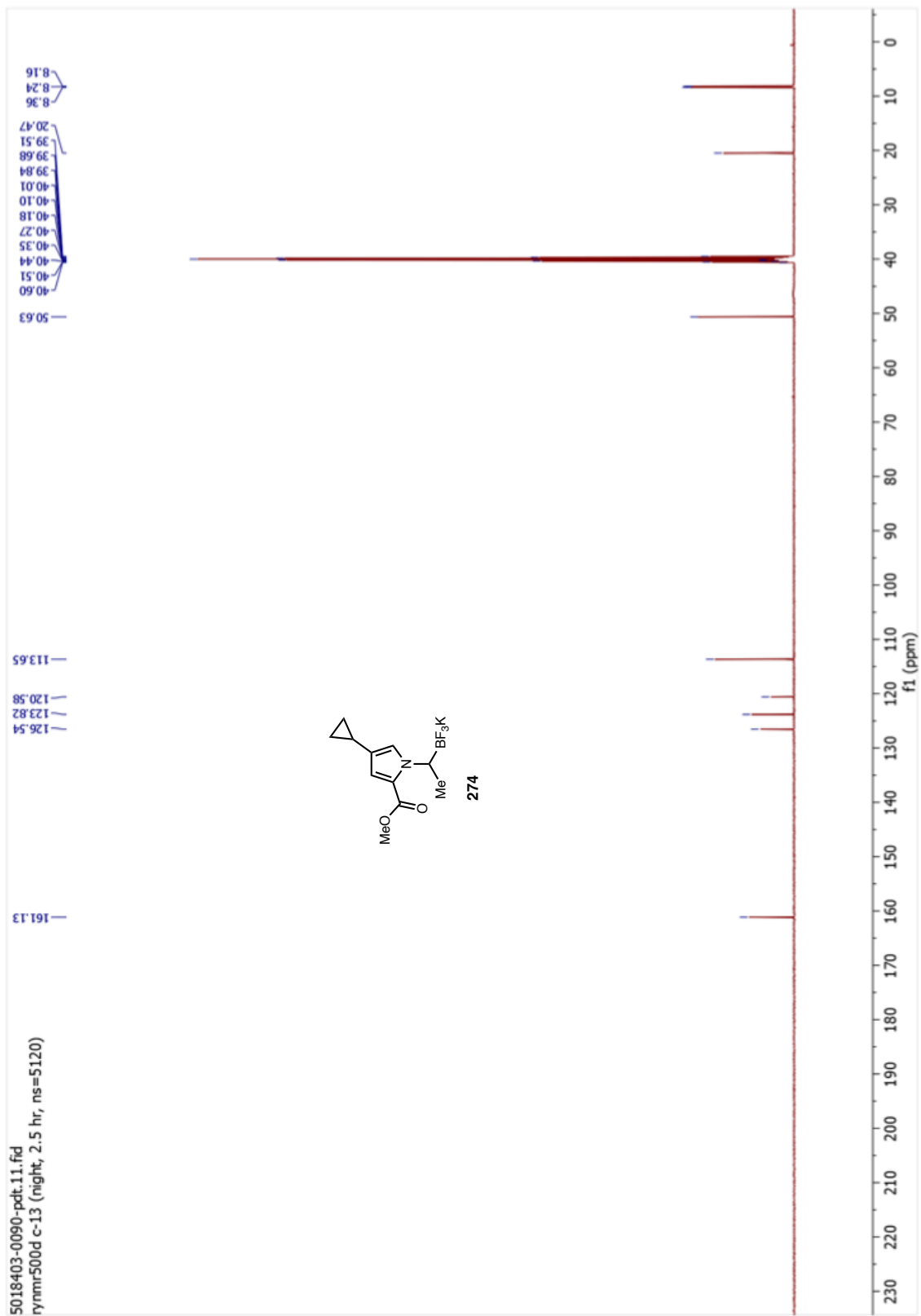


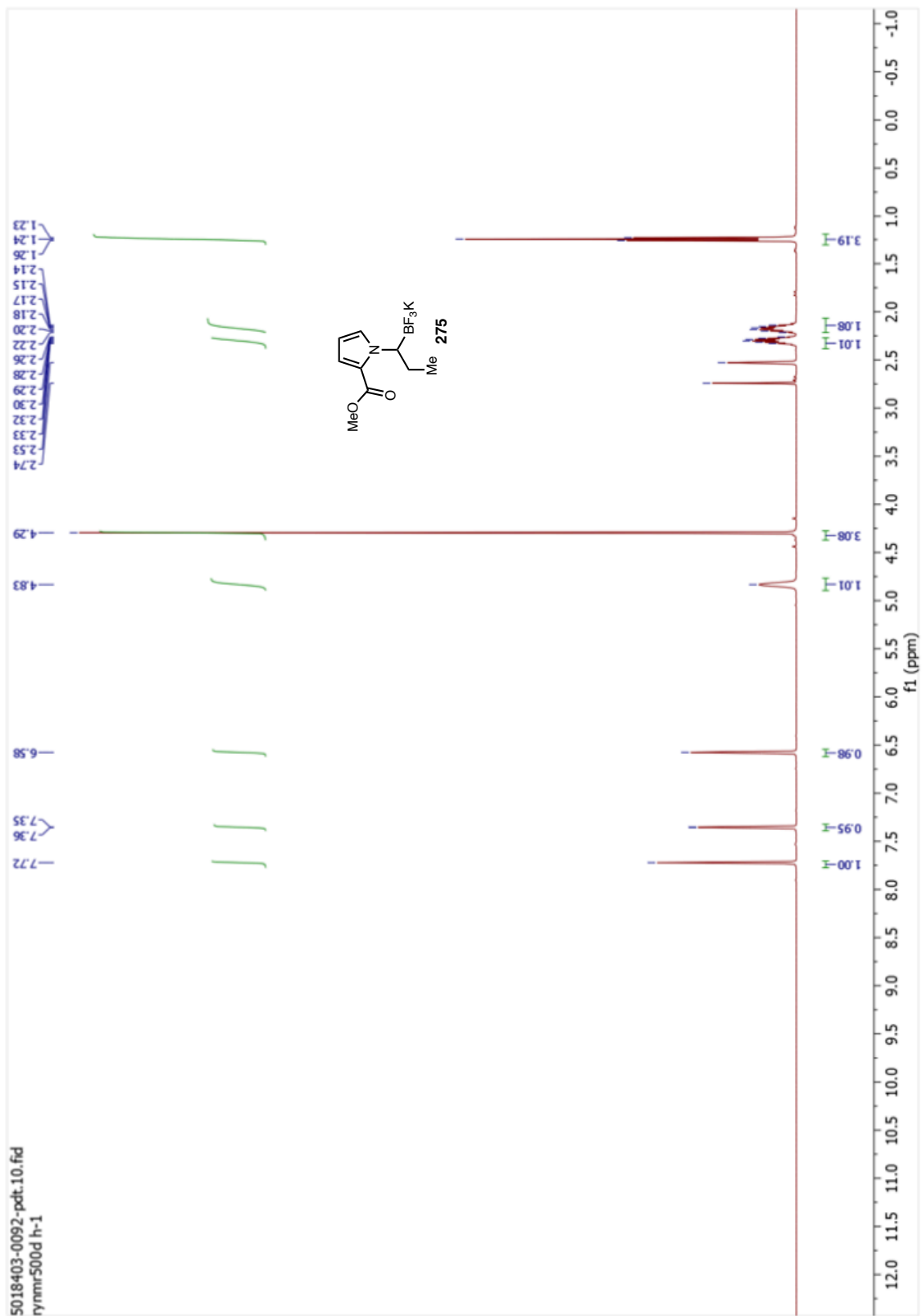


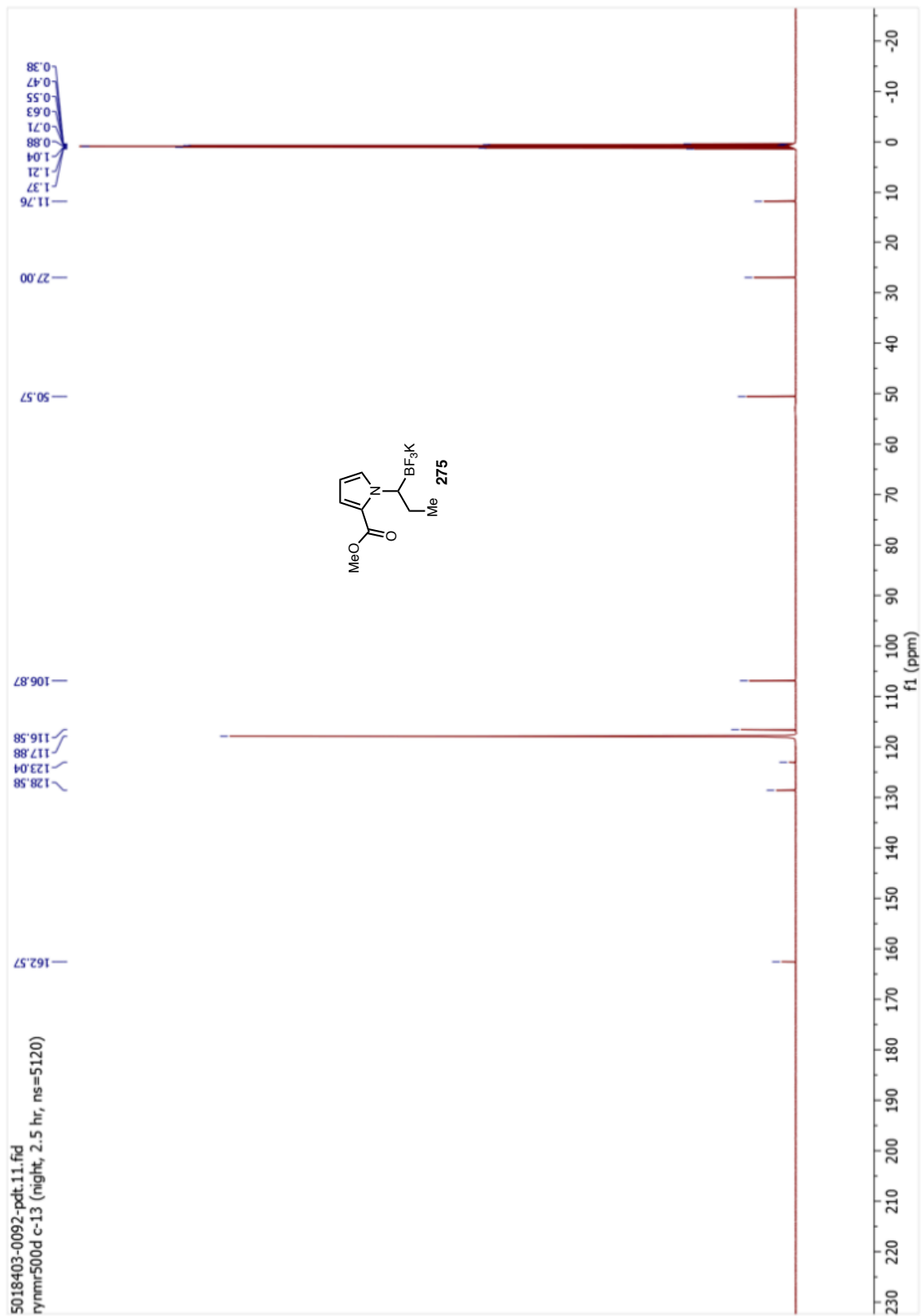


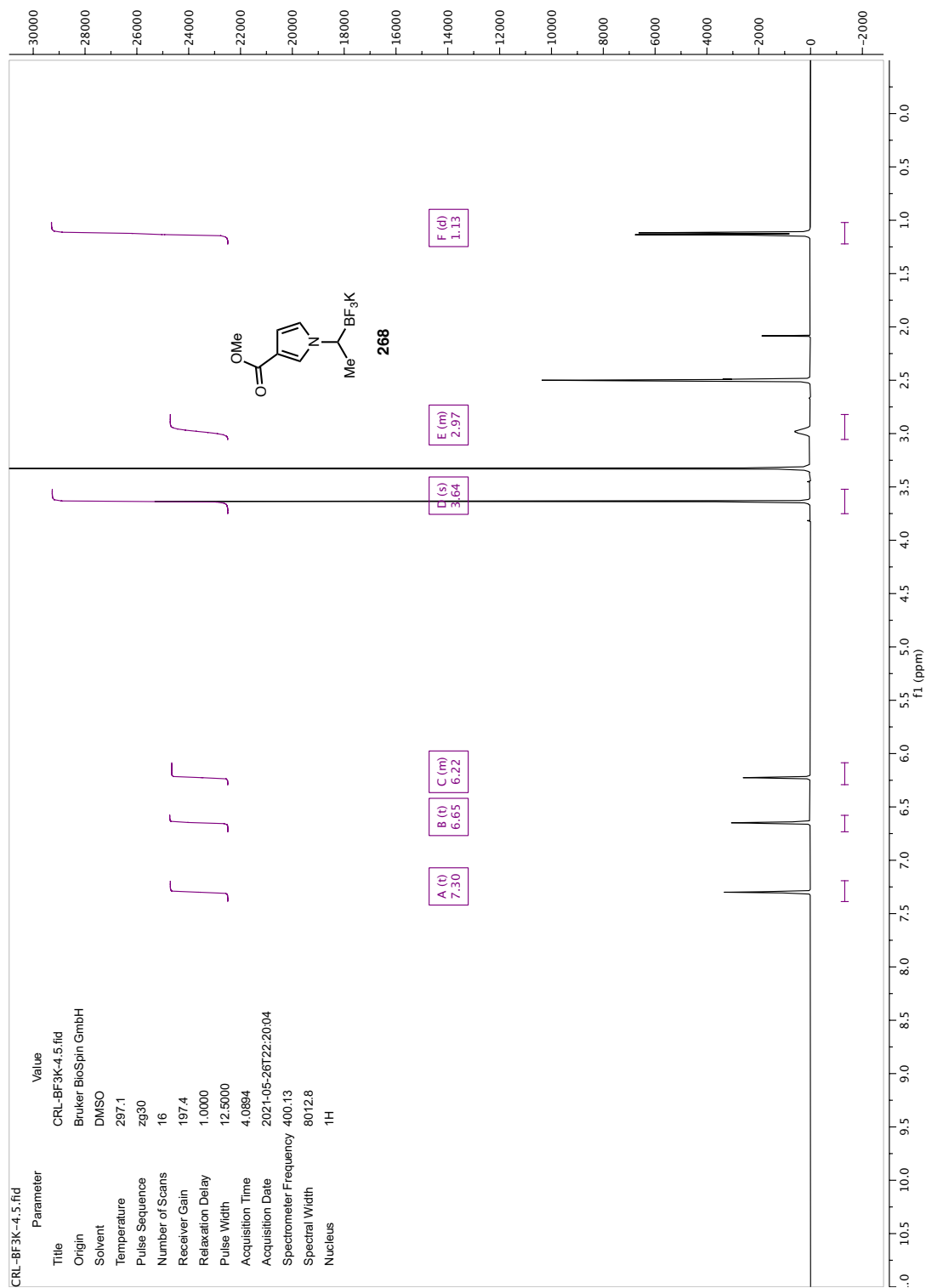


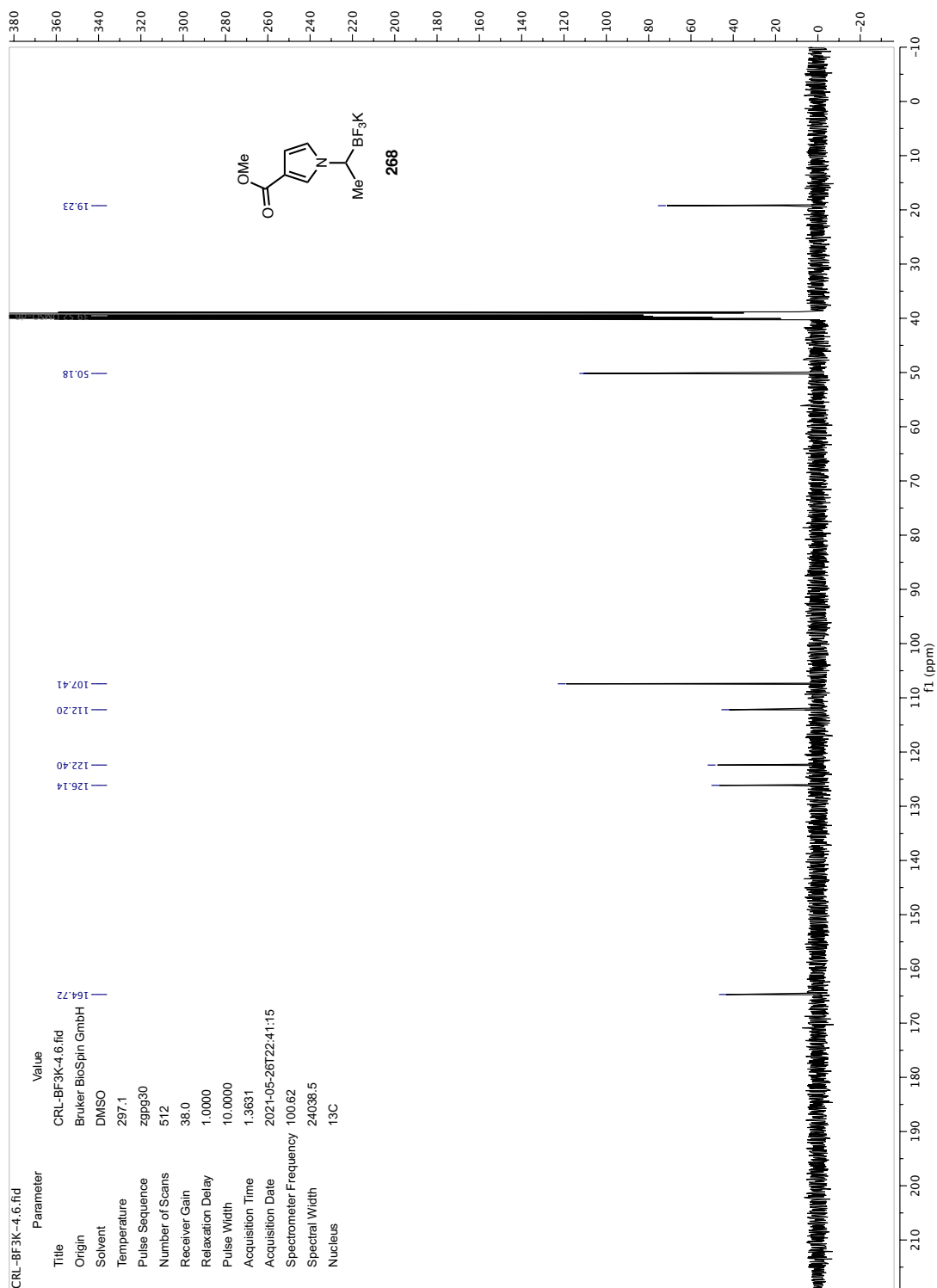


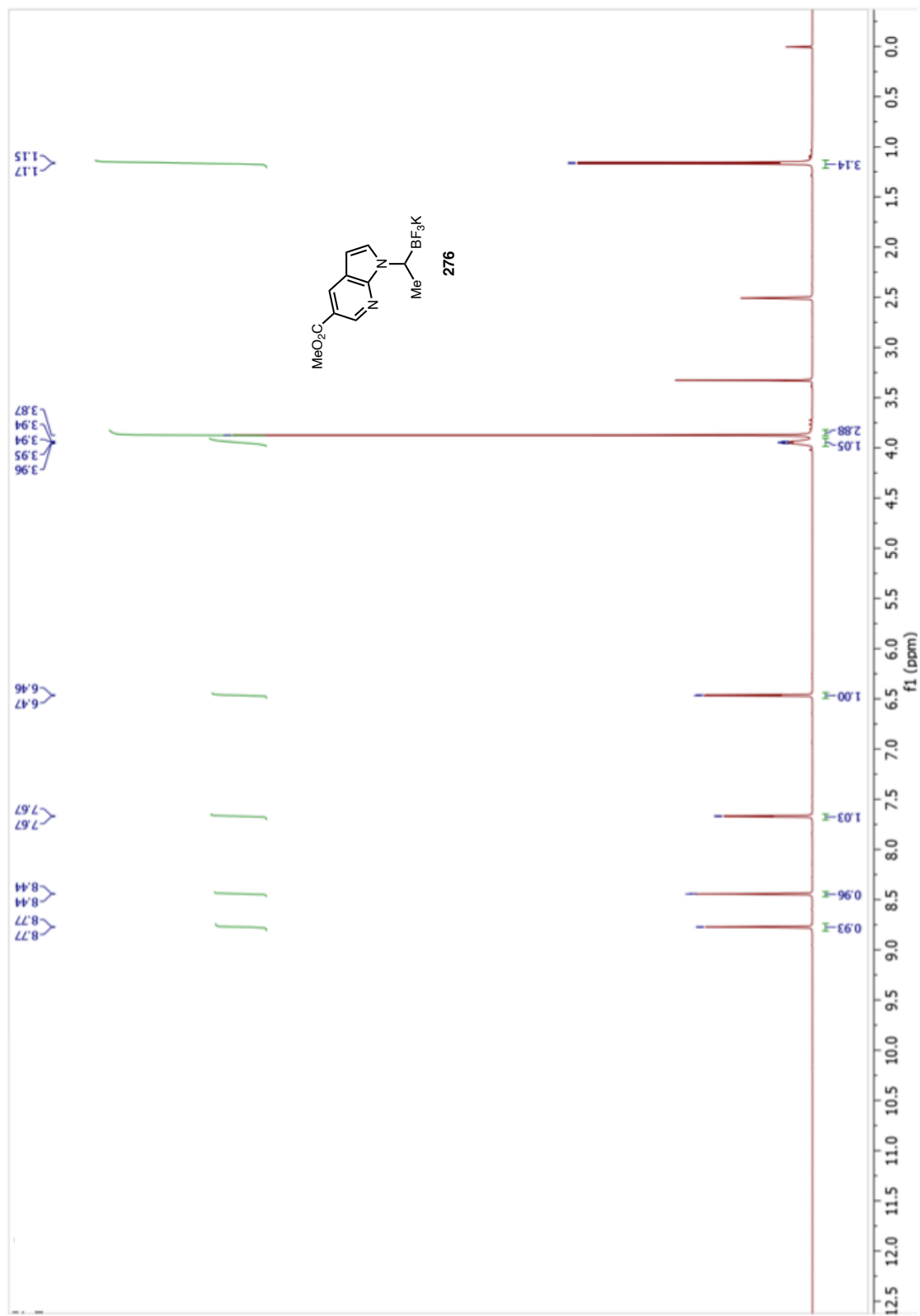


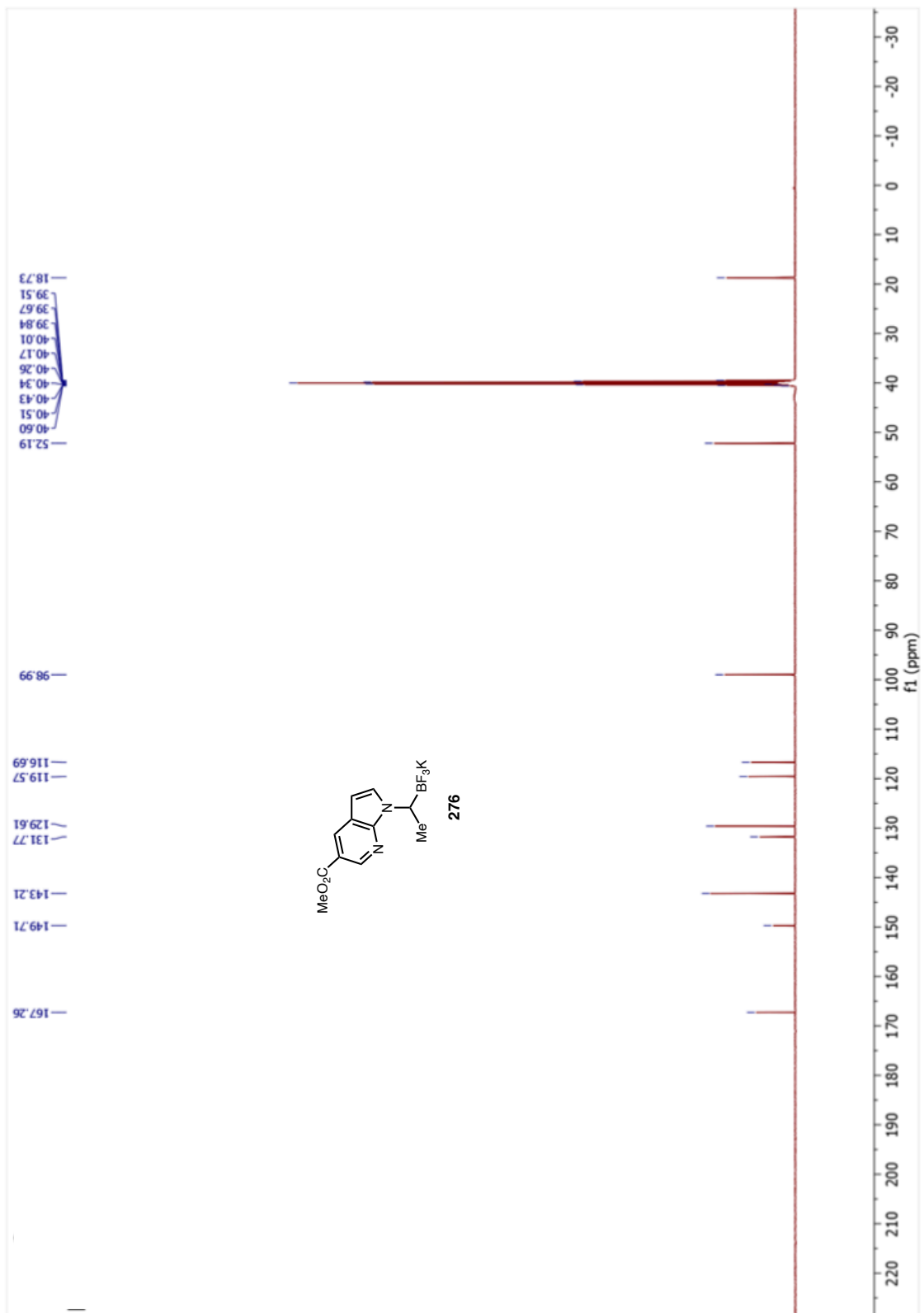




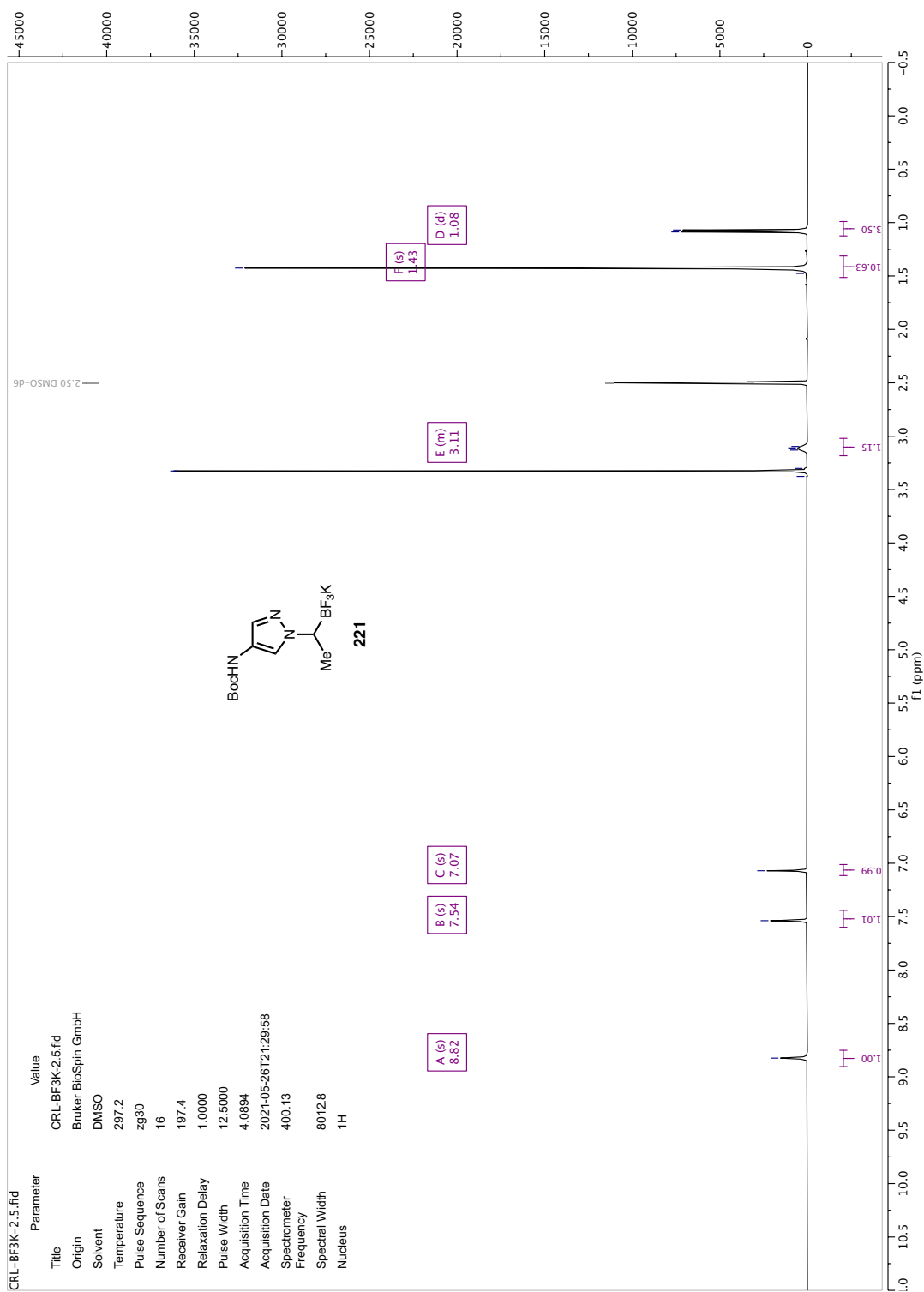


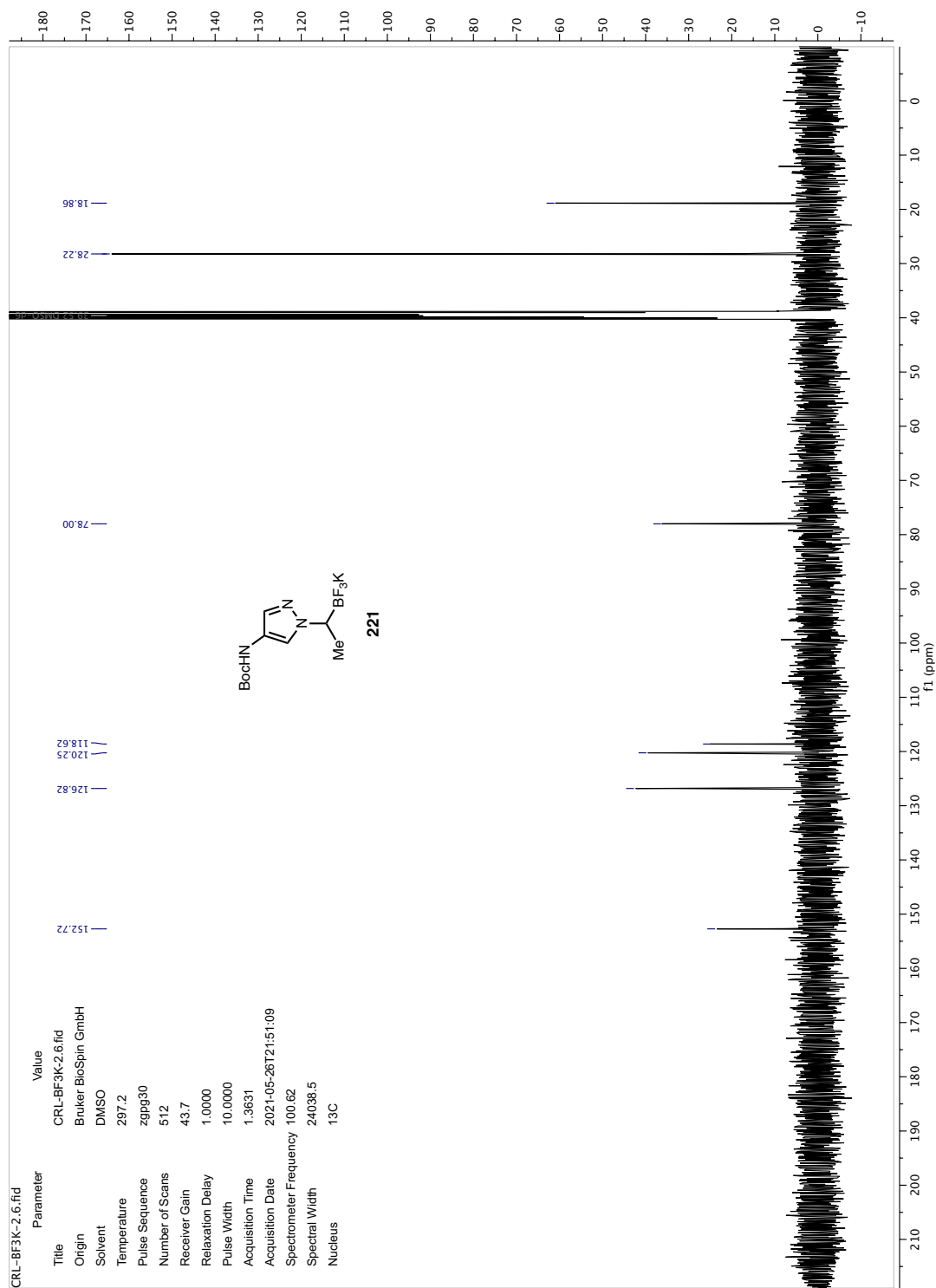


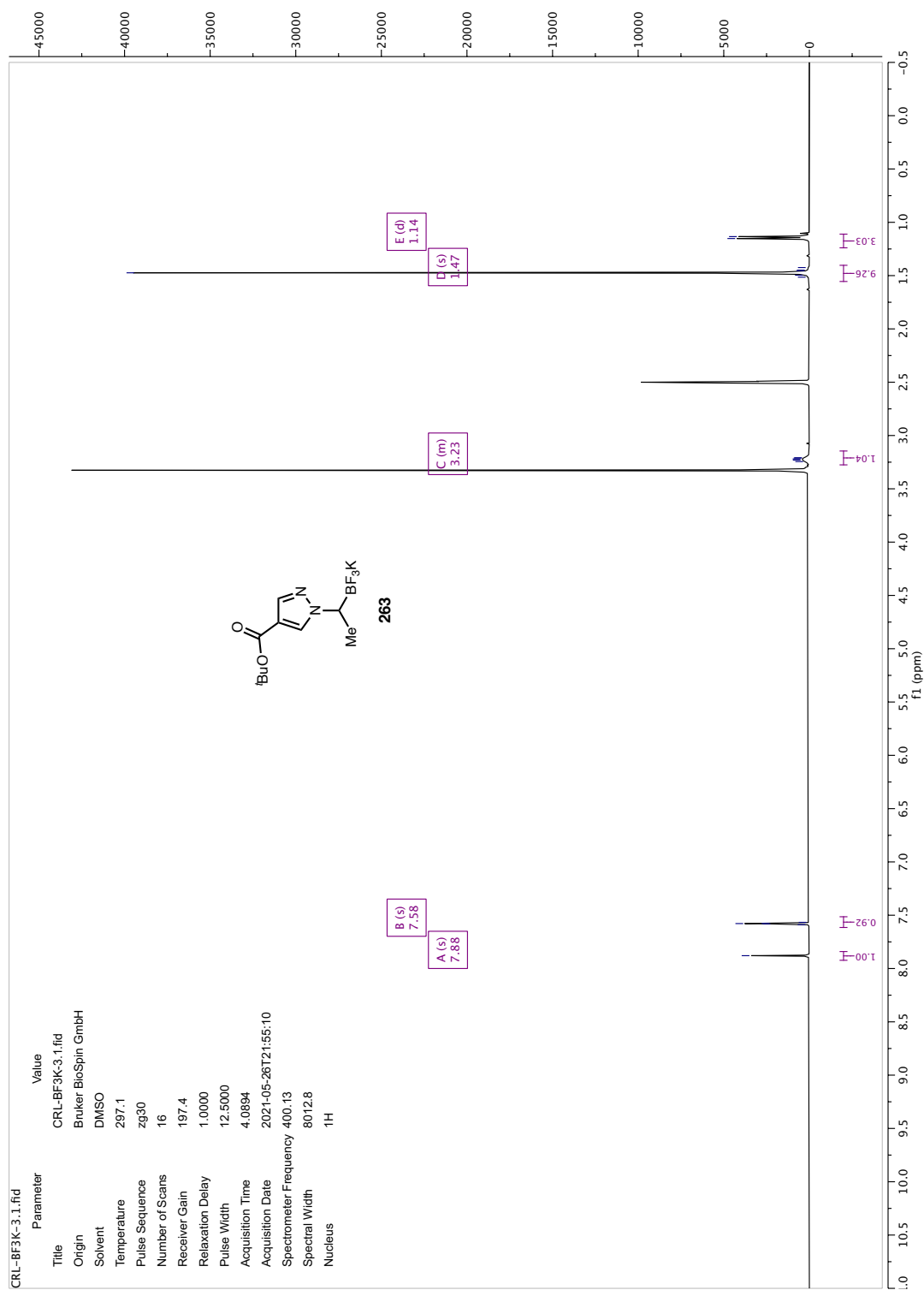


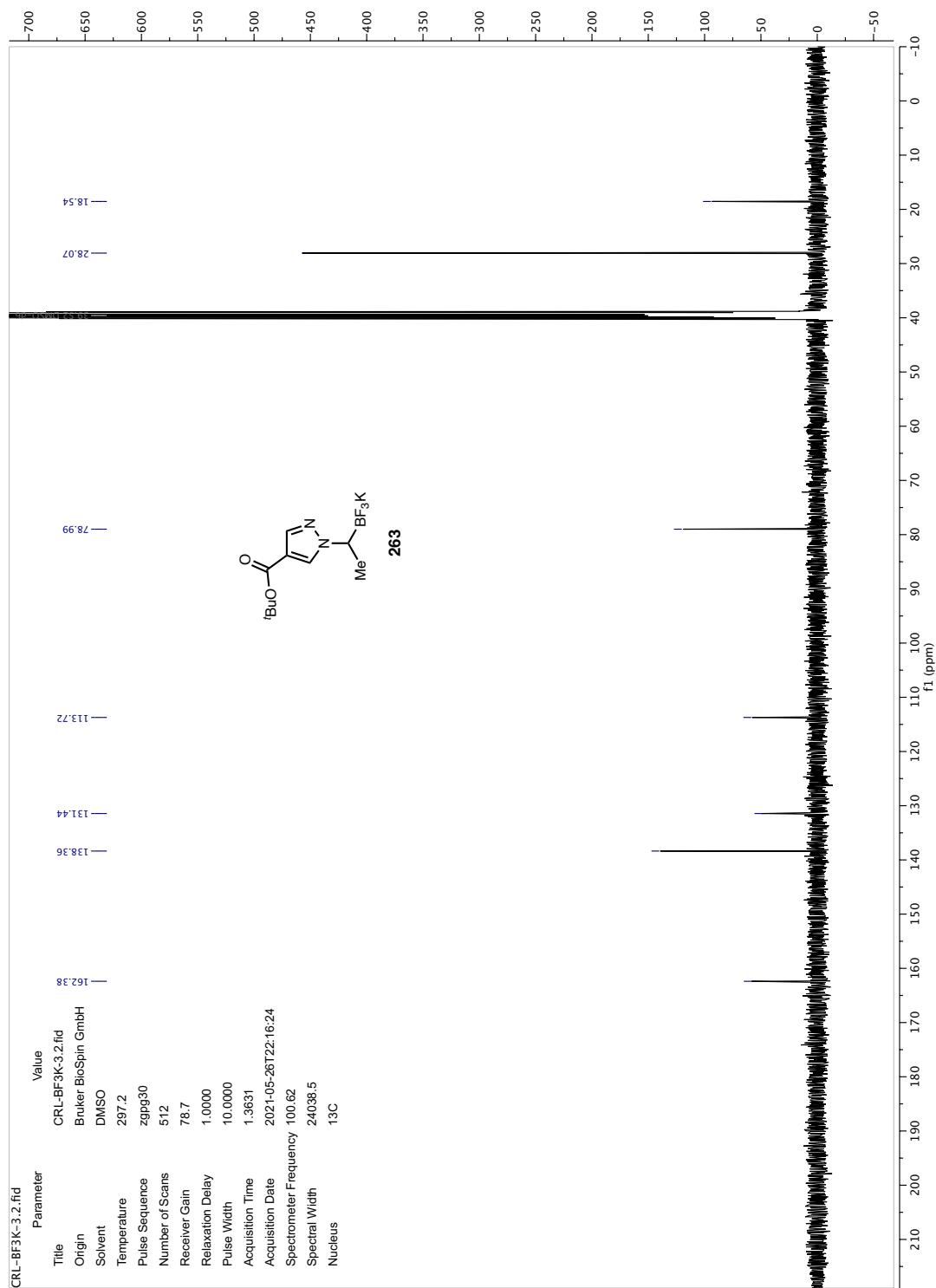


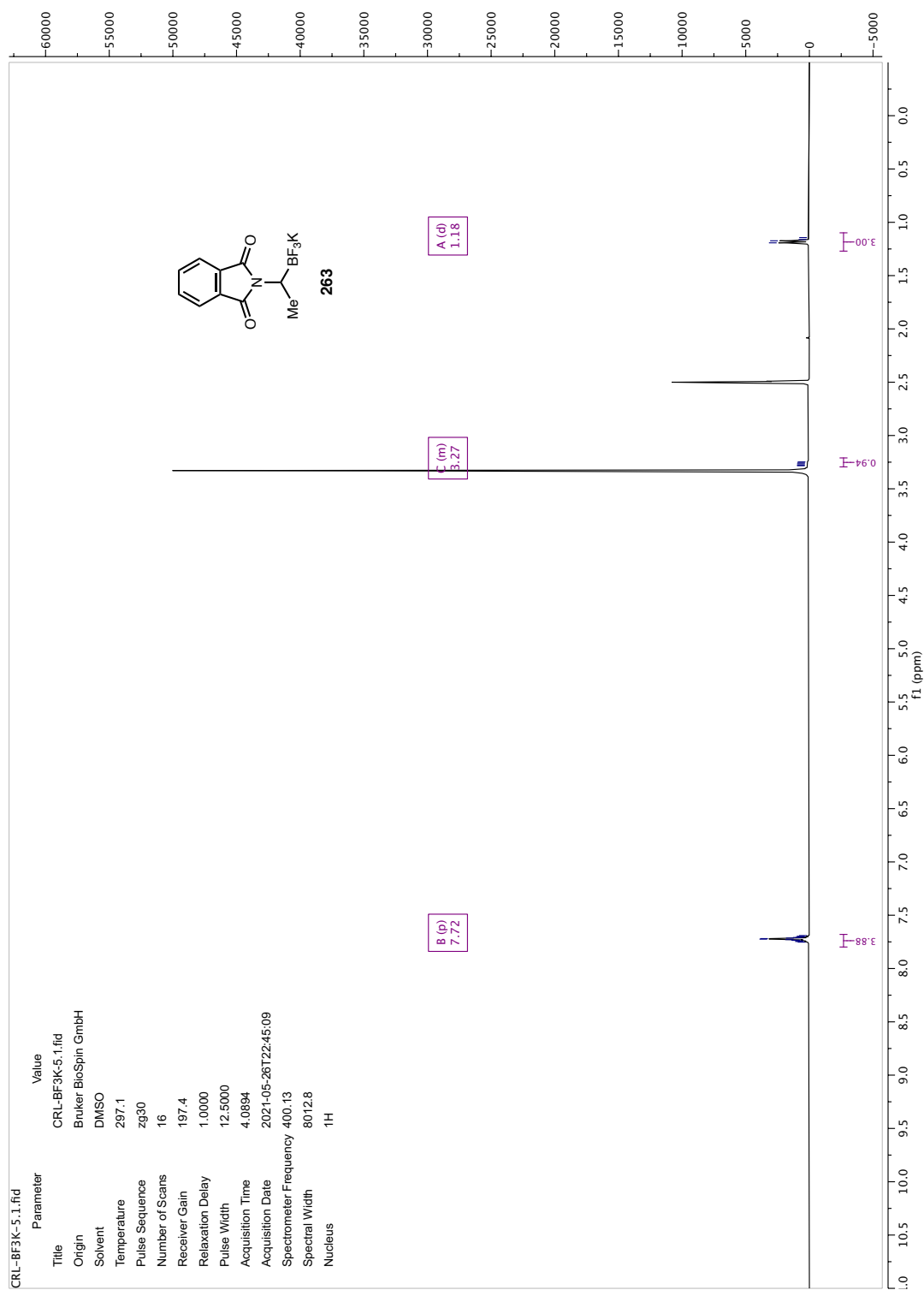


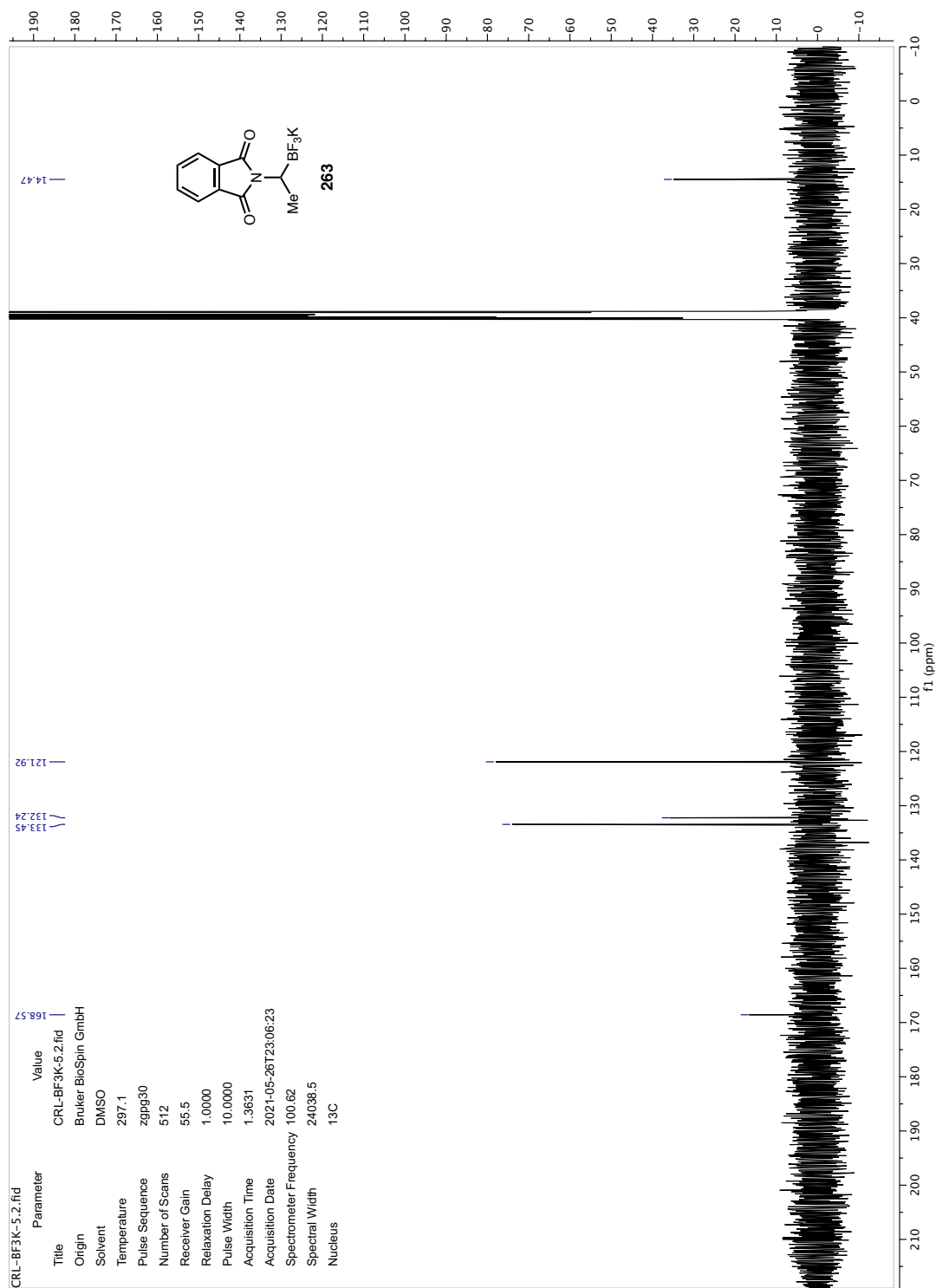






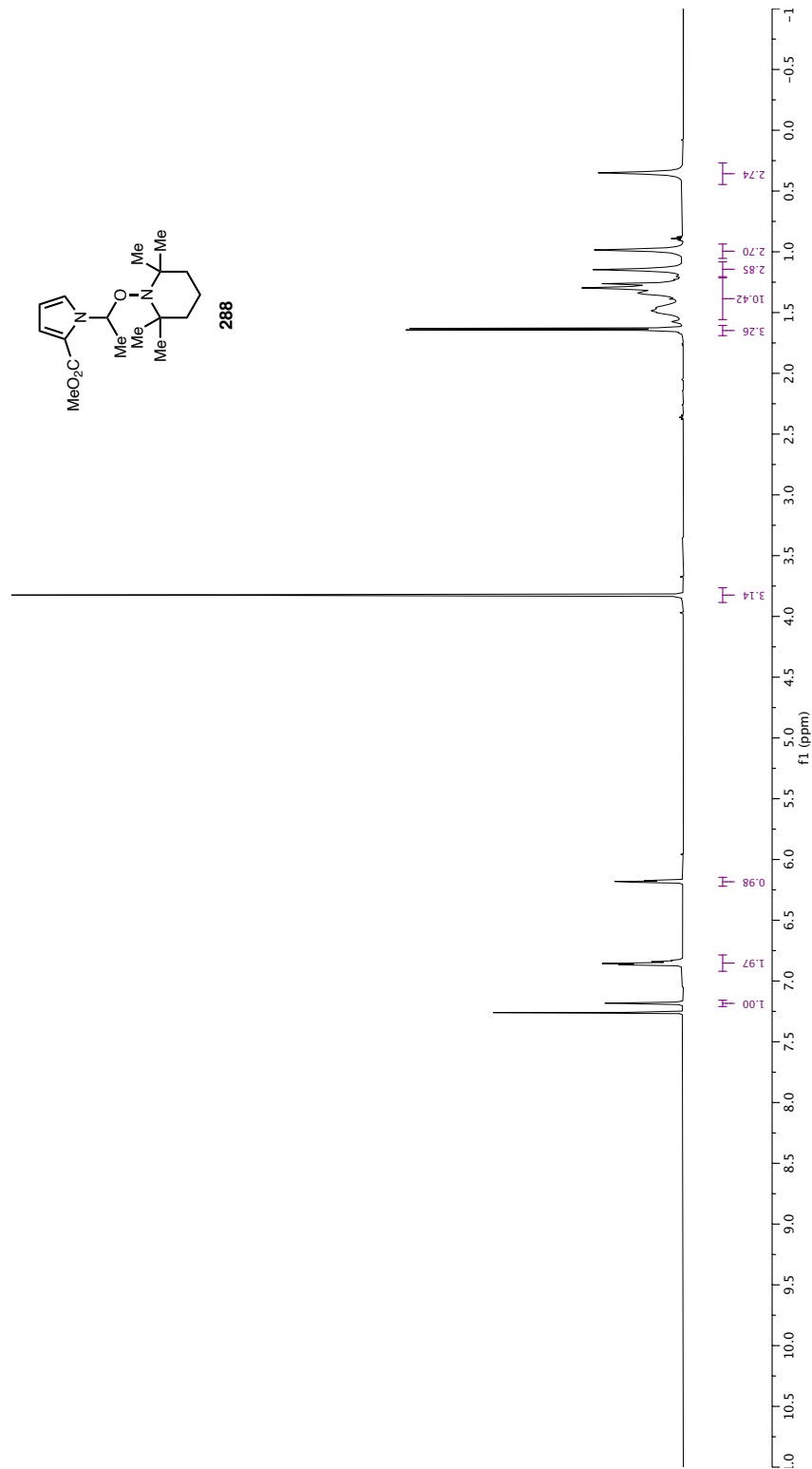




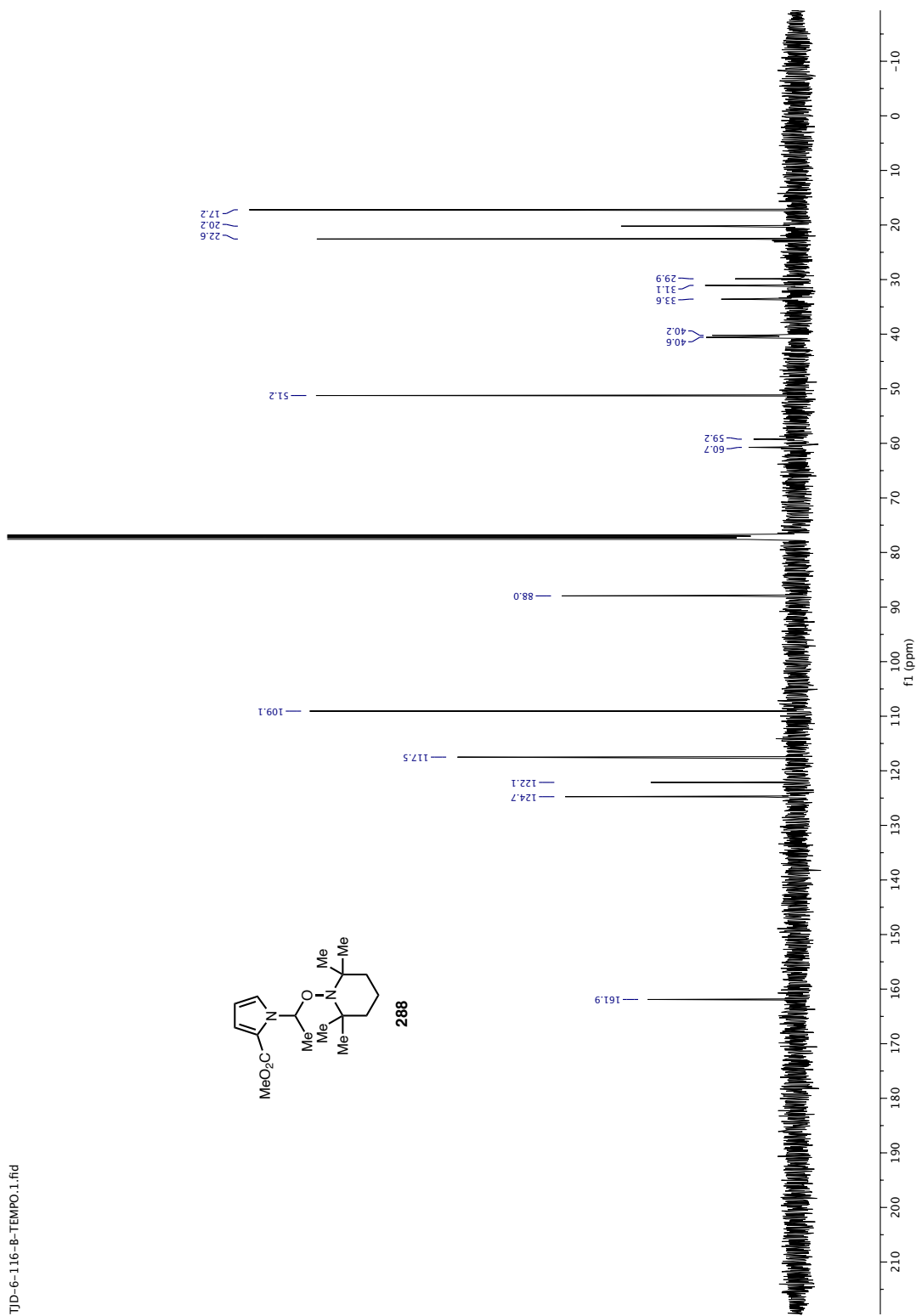
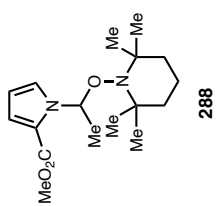


PROTON01  
TJD-6-116-B-TEMPO

B (m)	6.86	C (dd)	6.18	D (s)	3.82	E (d)	1.64	F (m)	1.35	G (s)	0.98	H (s)	1.15	I (s)	0.35
-------	------	--------	------	-------	------	-------	------	-------	------	-------	------	-------	------	-------	------



TJD-6-116-B-TEMPO.1.fid





## ABOUT THE AUTHOR

Travis Jon DeLano was born on December 14<sup>th</sup>, 1994, to Mary DeLano and Thomas J. Tomczyk in Portland, Maine. He grew up in the nearby town of Cape Elizabeth, where he spent his childhood playing with his brother Nate and his family's dogs, Allie and Maggie. He spent much of his high school years dishwashing and cooking in local restaurants and enjoying the beauty of Maine.

In 2013, Travis began his undergraduate studies at Northeastern University in Boston, MA, where he earned his B.S. in chemistry in 2017. Travis had the privilege to conduct medicinal chemistry research in Professor Michael. P. Pollastri's Laboratory for Neglected Disease Drug Discovery, under the mentorship of Dr. Dana M. Klug. While at Northeastern, Travis also had the opportunity to conduct 6-month co-op jobs at both Takeda Pharmaceuticals and Vertex Pharmaceuticals. These research experiences in undergrad solidified his passion for using organic chemistry to treat human disease.

Following his graduation from Northeastern, Travis moved across the country to Pasadena, CA to pursue his graduate studies under the direction of Professor Sarah E. Reisman at the California Institute of Technology. His graduate work focused on the development of nickel-catalyzed asymmetric cross-coupling reactions, with forays into electroorganic chemistry, photoredox catalysis, and applications of machine learning. Following the completion of his Ph.D., Travis will return to Boston to re-join the medicinal chemistry team at Vertex Pharmaceuticals.